

electromagnetic

acoustic scattering

by simple shapes

AD699859

AFCRL-70-0047

ELECTROMAGNETIC AND ACOUSTIC SCATTERING
BY SIMPLE SHAPES

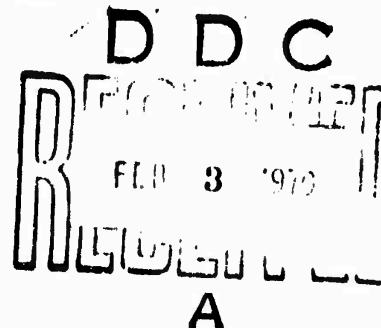
Edited by

J. J. Bowman, T. B. A. Senior, P. L. E. Uslenghi.

Radiation Laboratory
The University of Michigan
Ann Arbor, Michigan 48105

Contract No. AF19(628)-4328
Project No. 5635
Task No. 563502
Work Unit No. 56350201

FINAL REPORT
15 January 1970



This document has been approved for public
release and sale; its distribution is unlimited.

Contract Monitor: Philipp Blacksmith
Microwave Physics Laboratory

Prepared
for

AIR FORCE CAMBRIDGE RESEARCH LABORATORIES
OFFICE OF AEROSPACE RESEARCH
UNITED STATES AIR FORCE
BEDFORD, MASSACHUSETTS 01730

ELECTROMAGNETIC AND ACOUSTIC SCATTERING BY SIMPLE SHAPES

Edited by

J. J. BOWMAN, T. B. A. SENIOR, P. L. E. USLENGHI

*Radiation Laboratory,
The University of Michigan, USA*

Authors

J. S. Asvestas	D. L. Sengupta
J. J. Bowman	T. B. A. Senior
P. L. Christiansen	F. B. Sleator
O. Einarsson	P. L. E. Uslenghi
R. E. Kleinman	N. R. Zitron



1969

NORTH-HOLLAND PUBLISHING COMPANY - AMSTERDAM

© NORTH-HOLLAND PUBLISHING COMPANY, AMSTERDAM, 1969

All Rights Reserved. No part of this publication may be reproduced, stored in a retrieval system, or transmitted, in any form or by any means, electronic, mechanical, photocopying, recording or otherwise, without the prior permission of the Copyright owner.

PUBLISHERS:

NORTH-HOLLAND PUBLISHING COMPANY – AMSTERDAM

SOLE DISTRIBUTORS FOR THE WESTERN HEMISPHERE:

WILEY INTERSCIENCE DIVISION
JOHN WILEY & SONS, INC. – NEW YORK

Library of Congress Catalog Card Number: 78-97199

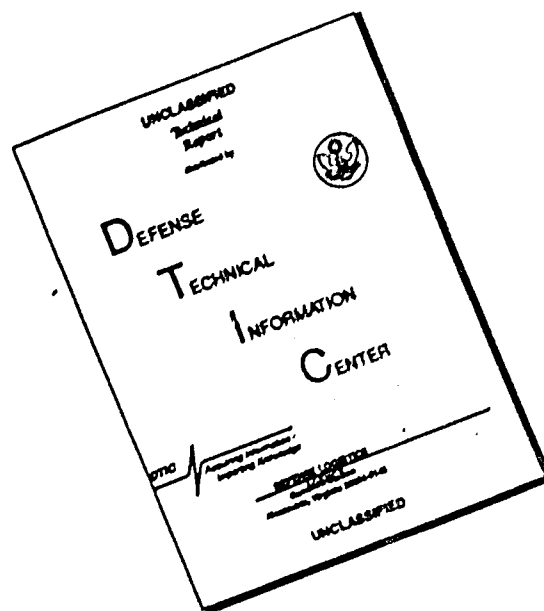
North-Holland Publishing Company SBN: 7204 0152 6

John Wiley & Sons SBN: 471 09293 2

Reproduction in whole or in part is
permitted for any purpose of the
United States Government

PRINTED IN THE NETHERLANDS

DISCLAIMER NOTICE



THIS DOCUMENT IS BEST QUALITY AVAILABLE. THE COPY FURNISHED TO DTIC CONTAINED A SIGNIFICANT NUMBER OF PAGES WHICH DO NOT REPRODUCE LEGIBLY.

PREFACE

For almost twenty years the Radiation Laboratory of The University of Michigan has been actively engaged in predicting the radar scattering behavior of a wide variety of targets, both simple and complex, and out of this work a wealth of material has grown. Much of it has been published in the open literature, but some has remained bound in the experience of the individual investigators or has appeared only in technical reports with limited distribution. The suggestion that this material be collected together and, in conjunction with an exhaustive review of the literature, be made available to a wider audience, was the factor that led to the writing of this book.

In considering the form that such a book might take, it was apparent that a rigid limitation of objectives would be necessary to keep the manuscript to manageable size. Because of the several treatments of the methods of scattering and diffraction theory that have appeared in recent years, it was felt that the main focus should be placed on the presentation of results, but even so, a further restriction on the type and material composition of the scattering body was still required to permit a reasonably complete coverage of each particular case. We therefore decided to confine ourselves to bodies which are soft or hard in the acoustical sense, or are perfectly conducting to electromagnetic waves, and fifteen geometrically simple scattering shapes were selected for the study. Except in one instance (the wire), these shapes are determined by the coordinate system in which the wave equation is separable, and are the ones for which extensive mathematical results are available.

The information about the scattering behavior of these fifteen different shapes was collected, revised and systematically organized, and is here presented in chapters divided according to the shape. Many new formulae and computations are included, especially for the wire (Chapter 12) and the cone (Chapter 18). Each section of the book is as self-contained as possible compatible with a tolerable amount of repetition, and the contents of each chapter are presented in a standard, stylized format to facilitate ready reference. Emphasis is placed on results in the form of formulae and diagrams, but a brief outline of the methods for the solution of scattering problems is given in the Introduction, together with the main properties of those special functions which are used extensively throughout the book. The bibliography is selective and critical, rather than exhaustive, and every effort has been made to correct errors in the source material. It is our hope that a handbook such as this will prove valuable to radar and antenna specialists, and to all interested in scattering theory.

We are grateful to the United States Air Force Cambridge Research Laboratories for financial support of the project under Contracts AF 19(604)-6655 and AF 19(628)-4328, and to Mr. Carlyle J. Sletten of that organization for his advice and encouragement. We acknowledge with thanks the particular assistance provided by our colleague, Dr. Ralph E. Kleinman, during the conceptual and planning stages of the book, and are indebted to Miss Catherine A. Rader and Mrs. Katherine O. McWilliams for the typing of the manuscript, and to Mr. August Antones for the art work. Finally, we wish to thank Drs. W. H. Wimmers of North-Holland Publishing Company for his continued interest during the preparation and printing of this book, and the many authors and publishers for their kind permission to reproduce copyrighted material.

JOHN J. BOWMAN
THOMAS B. A. SENIOR
PIERGIORGIO L. E. USLENGHI

Ann Arbor, June 1969

LIST OF SYMBOLS

Unless otherwise stated, the symbols most commonly used in the book have the following meaning:

ϵ = electric permittivity (dielectric constant) in vacuo.

μ = magnetic permeability in vacuo.

$1/\sqrt{\epsilon\mu}$ = velocity of light in vacuo ($\approx 2.9979 \times 10^8$ m/sec).

$Z = Y^{-1} = \sqrt{\mu/\epsilon}$ = intrinsic impedance of free space ($= 120\pi \Omega$).

ω = angular frequency.

$i = \sqrt{-1}$ = imaginary unit.

$e^{-i\omega t}$ = time-dependence factor (omitted throughout).

$k = 2\pi/\lambda = \omega\sqrt{\epsilon\mu}$ = wave number in vacuo ($k = \omega/c$ in the acoustical case, where c is the velocity of sound).

ϵ_n = Neumann symbol ($\epsilon_0 = 1$; $\epsilon_n = 2$, for $n = 1, 2, 3, \dots$).

x, y, z = rectangular Cartesian coordinates.

ρ, ϕ, z = circular cylindrical coordinates.

r, θ, ϕ = spherical polar coordinates.

\log = natural logarithm.

∇ = grad = gradient operator.

$\nabla \cdot$ = div = divergence operator.

$\nabla \wedge$ = curl = rot = curl operator.

$\nabla^2 = \nabla \cdot \nabla$ = div grad = Laplace's operator.

$R = |\mathbf{r} - \mathbf{r}_0|$ = distance between the source point \mathbf{r}_0 and the observation point \mathbf{r} .

V^i = incident velocity potential.

V^s = scattered velocity potential.

$V = V^i + V^s$ = total velocity potential.

E^i = incident electric field vector.

H^i = incident magnetic field vector.

E^s = scattered electric field vector.

H^s = scattered magnetic field vector.

$E = E^i + E^s$ = total electric field vector.

$H = H^i + H^s$ = total magnetic field vector.

P = far-field coefficient in two-dimensional problems. } see Section 1.2.4

S = far-field coefficient in three-dimensional problems. }

$\sigma(\beta)$ = bistatic radar cross section, with separation angle β }
between transmitter and receiver. } see Section 1.2.5

σ = $\sigma(0)$ = back scattering or monostatic radar cross section.

σ_t = total scattering cross section.

α_n = n -th zero of $\text{Ai}(-\gamma)$. } see Section 1.3.2.

β_n = n -th zero of $\text{Ai}(-\beta)$. }

CONTENTS

Preface	V
List of symbols	VII

Introduction

J. J. BOWMAN, I. B. A. SENIOR and P. L. E. USLENGHI

1.1. GENERAL CONSIDERATIONS	1
1.2. FUNDAMENTAL CONCEPTS	2
1.2.1. Maxwell's equations	2
1.2.2. Acoustical equations	2
1.2.3. Wave propagation	3
1.2.4. Boundary and radiation conditions	4
1.2.5. Radar cross sections	7
1.2.6. Electromagnetic potentials.	8
1.2.7. Green's functions.	11
1.2.8. Reciprocity theorem	13
1.2.9. Babinet's principle	14
1.2.10. Integral equations	15
1.2.11. Separation of variables	17
1.2.12. Low frequency methods	20
1.2.13. High frequency methods	21
1.2.13.1. Geometrical optics	22
1.2.13.2. Keller's theory.	24
1.2.13.3. Luneburg-Kline expansion	26
1.2.13.4. Physical optics.	29
1.2.13.5. Fock's theory	31
1.2.13.6. Watson's transformation	34
1.2.14. Other methods	36
1.2.14.1. Conformal mapping	36
1.2.14.2. Variational techniques	37
1.2.14.3. Function theoretic methods	41
1.2.14.4. Numerical methods.	49
1.3. SPECIAL FUNCTIONS	50
1.3.1. Bessel functions	50
1.3.2. Airy functions	60
1.3.3. Fock functions	63
1.3.4. Fresnel integrals	67
1.3.5. Legendre functions	68
Bibliography	70

PART ONE – INFINITE BODIES**Chapter 1 – General considerations****Chapter 2 – The circular cylinder**

T. B. A. SENIOR and P. L. E. USLENGHI

2.1. CIRCULAR CYLINDRICAL GEOMETRY.	92
2.2. PLANE WAVE INCIDENCE	93
2.2.1. <i>E</i> -polarization	93
2.2.1.1. Exact solutions	93
2.2.1.2. Low frequency approximations	94
2.2.1.3. High frequency approximations	99
2.2.2. <i>H</i> -polarization	103
2.2.2.1. Exact solutions	103
2.2.2.2. Low frequency approximations	108
2.2.2.3. High frequency approximations	109
2.3. LINE SOURCES.	112
2.3.1. <i>E</i> -polarization	112
2.3.1.1. Exact solutions	112
2.3.1.2. Low frequency approximations	114
2.3.1.3. High frequency approximations	114
2.3.2. <i>H</i> -polarization	115
2.3.2.1. Exact solutions	115
2.3.2.2. Low frequency approximations	117
2.3.2.3. High frequency approximations	117
2.4. DIPOLE SOURCES.	119
2.4.1. Electric dipoles.	119
2.4.1.1. Exact solutions	119
2.4.1.2. Low frequency approximations	123
2.4.1.3. High frequency approximations	123
2.4.2. Magnetic dipoles	123
2.4.2.1. Exact solutions	123
2.4.2.2. Low frequency approximations	124
2.4.2.3. High frequency approximations	125
2.5. POINT SOURCES	125
2.5.1. Acoustically soft cylinder	125
2.5.1.1. Exact solutions	125
2.5.1.2. Low frequency approximations	125
2.5.1.3. High frequency approximations	125
2.5.2. Acoustically hard cylinder	126
2.5.2.1. Exact solutions	126
2.5.2.2. Low frequency approximations	127
2.5.2.3. High frequency approximations	127
Bibliography	127

Chapter 3 – The elliptic cylinder

P. L. E. USLENGHI and N. R. ZILRON

3.1. ELLIPTIC CYLINDER GEOMETRY.	129
3.2. PLANE WAVE INCIDENCE	131
3.2.1. <i>E</i> -polarization	131
3.2.1.1. Exact solutions	131

3.2.1.2.	Low frequency approximations	134
3.2.1.3.	High frequency approximations	139
3.2.1.4.	Shape approximation	145
3.2.2.	<i>H</i> -polarization	146
3.2.2.1.	Exact solutions	146
3.2.2.2.	Low frequency approximations	150
3.2.2.3.	High frequency approximations	156
3.2.2.4.	Shape approximation	161
3.3.	LINE SOURCES	162
3.3.1.	<i>E</i> -polarization	162
3.3.1.1.	Exact solutions	162
3.3.1.2.	Low frequency approximations	163
3.3.1.3.	High frequency approximations	163
3.3.2.	<i>H</i> -polarization	167
3.3.2.1.	Exact solutions	167
3.3.2.2.	Low frequency approximations	169
3.3.2.3.	High frequency approximations	169
3.4.	DIPOLE SOURCES	171
3.4.1.	Electric dipoles	171
3.4.1.1.	Exact solutions	171
3.4.1.2.	Low frequency approximations	174
3.4.1.3.	High frequency approximations	174
3.4.2.	Magnetic dipoles	174
3.4.2.1.	Exact solutions	174
3.4.2.2.	Low frequency approximations	176
3.4.2.3.	High frequency approximations	176
3.5.	POINT SOURCES	176
3.5.1.	Acoustically soft cylinder	176
3.5.1.1.	Exact solutions	176
3.5.1.2.	Low frequency approximations	177
3.5.1.3.	High frequency approximations	177
3.5.2.	Acoustically hard cylinder	177
3.5.2.1.	Exact solutions	177
3.5.2.2.	Low frequency approximations	179
3.5.2.3.	High frequency approximations	179
	Bibliography	179

Chapter 4 – The strip

J. S. ASVESTAS and R. E. KLEINMAN

4.1.	STRIP GEOMETRY AND PRELIMINARY CONSIDERATIONS	181
4.2.	PLANE WAVE INCIDENCE	182
4.2.1.	<i>E</i> -polarization	182
4.2.1.1.	Exact solutions	182
4.2.1.2.	Low frequency approximations	188
4.2.1.3.	High frequency approximations	195
4.2.2.	<i>H</i> -polarization	203
4.2.2.1.	Exact solutions	203
4.2.2.2.	Low frequency approximations	208
4.2.2.3.	High frequency approximations	213
4.3.	LINE SOURCES	220
4.3.1.	<i>E</i> -polarization	220
4.3.1.1.	Exact solutions	220

4.3.1.2.	Low frequency approximations	223
4.3.1.3.	High frequency approximations	223
4.3.2.	<i>H</i> -polarization	226
4.3.2.1.	Exact solutions	226
4.3.2.2.	Low frequency approximations	229
4.3.2.3.	High frequency approximations	229
4.4.	DIPOLE SOURCES	230
4.4.1.	Electric dipoles	230
4.4.1.1.	Exact solutions	230
4.4.1.2.	Low frequency approximations	233
4.4.1.3.	High frequency approximations	233
4.4.2.	Magnetic dipoles	233
4.4.2.1.	Exact solutions	233
4.4.2.2.	Low frequency approximations	235
4.4.2.3.	High frequency approximations	235
4.5.	POINT SOURCES	235
4.5.1.	Acoustically soft strip	235
4.5.1.1.	Exact solutions	235
4.5.1.2.	Low frequency approximations	236
4.5.1.3.	High frequency approximations	236
4.5.2.	Acoustically hard strip	236
4.5.2.1.	Exact solutions	236
4.5.2.2.	Low frequency approximations	237
4.5.2.3.	High frequency approximations	237
	Bibliography	237

Chapter 5 – The hyperbolic cylinder

P. L. E. USLENGHI

5.1.	HYPERBOLIC CYLINDER GEOMETRY	240
5.2.	PLANE WAVE INCIDENCE	240
5.2.1.	<i>E</i> -polarization	240
5.2.2.	<i>H</i> -polarization	243
5.3.	LINE SOURCES	244
5.3.1.	<i>E</i> -polarization	244
5.3.1.1.	Exact solutions	244
5.3.1.2.	High frequency approximations	244
5.3.2.	<i>H</i> -polarization	247
5.3.2.1.	Exact solutions	247
5.3.2.2.	High frequency approximations	249
5.4.	POINT AND DIPOLE SOURCES	251
	Bibliography	251

Chapter 6 – The wedge

J. J. BOWMAN and T. B. A. SENIOR

6.1.	WEDGE GEOMETRY AND PRELIMINARY CONSIDERATIONS	252
6.2.	PLANE WAVE INCIDENCE	254
6.2.1.	<i>E</i> -polarization	254
6.2.2.	<i>H</i> -polarization	250

6.3.	LINE SOURCES	264
6.3.1.	<i>E</i> -polarization	264
6.3.2.	<i>H</i> -polarization	267
6.4.	POINT SOURCES	269
6.4.1.	Acoustically soft wedge	269
6.4.2.	Acoustically hard wedge	272
6.5.	DIPOLE SOURCES	275
6.5.1.	Electric dipoles	275
6.5.2.	Magnetic dipoles	279
	Bibliography	282

Chapter 7 – The parabolic cylinder

P. L. CHRISTIANSEN

7.1.	PARABOLIC CYLINDRICAL GEOMETRY	284
7.2.	EXTERIOR PLANE WAVE INCIDENCE	285
7.2.1.	<i>E</i> -polarization	285
7.2.1.1.	Exact solutions	285
7.2.1.2.	High frequency approximations	288
7.2.2.	<i>H</i> -polarization	290
7.2.2.1.	Exact solutions	290
7.2.2.2.	High frequency approximations	293
7.3.	EXTERIOR LINE SOURCES	296
7.3.1.	<i>E</i> -polarization	296
7.3.1.1.	Exact solutions	296
7.3.1.2.	High frequency approximations	298
7.3.2.	<i>H</i> -polarization	299
7.3.2.1.	Exact solutions	299
7.3.2.2.	High frequency approximations	301
7.4.	INTERIOR LINE SOURCES	302
7.4.1.	<i>E</i> -polarization	302
7.4.1.1.	Exact solutions	302
7.4.1.2.	High frequency approximations	304
7.4.2.	<i>H</i> -polarization	304
7.4.2.1.	Exact solutions	304
7.4.2.2.	High frequency approximations	306
7.5.	POINT AND DIPOLE SOURCES	306
	Bibliography	306

Chapter 8 – The half-plane

J. J. BOWMAN and T. B. A. SENIOR

8.1.	HALF-PLANE GEOMETRY AND PRELIMINARY CONSIDERATIONS	308
8.2.	PLANE WAVE INCIDENCE	311
8.2.1.	<i>E</i> -polarization	311
8.2.2.	<i>H</i> -polarization	316
8.3.	LINE SOURCES	323
8.3.1.	<i>E</i> -polarization	323
8.3.2.	<i>H</i> -polarization	327

8.4. POINT SOURCES	330
8.4.1. Acoustically soft half-plane	330
8.4.2. Acoustically hard half-plane	333
8.5. DIPOLE SOURCES	335
8.5.1. Electric dipoles	335
8.5.2. Magnetic dipoles	341
Bibliography	344

PART TWO – FINITE BODIES

Chapter 9 – General considerations

Chapter 10 – The sphere

D. L. SENGUPTA

10.1. SPHERICAL GEOMETRY	353
10.2. ACOUSTICALLY SOFT SPHERE	354
10.2.1. Point sources	354
10.2.1.1. Exact solutions	354
10.2.1.2. Low frequency approximations	355
10.2.1.3. High frequency approximations	355
10.2.2. Plane wave incidence	356
10.2.2.1. Exact solutions	356
10.2.2.2. Low frequency approximations	361
10.2.2.3. High frequency approximations	362
10.3. ACOUSTICALLY HARD SPHERE	369
10.3.1. Point sources	369
10.3.1.1. Exact solutions	369
10.3.1.2. Low frequency approximations	370
10.3.1.3. High frequency approximations	370
10.3.2. Plane wave incidence	374
10.3.2.1. Exact solutions	374
10.3.2.2. Low frequency approximations	376
10.3.2.3. High frequency approximations	376
10.4. PERFECTLY CONDUCTING SPHERE	380
10.4.1. Electric dipole sources	380
10.4.1.1. Exact solutions	380
10.4.1.2. Low frequency approximations	385
10.4.1.3. High frequency approximations	386
10.4.2. Magnetic dipole sources	387
10.4.2.1. Exact solutions	387
10.4.2.2. Low frequency approximations	392
10.4.2.3. High frequency approximations	392
10.4.3. Plane wave incidence	395
10.4.3.1. Exact solutions	395
10.4.3.2. Low frequency approximations	401
10.4.3.3. High frequency approximations	406
Bibliography	414

Chapter 11 – The prolate spheroid

L. B. A. SENIOR and P. L. L. USTENGU

11.1. PROLATE SPHEROIDAL GEOMETRY	416
---	-----

11.2. ACOUSTICALLY SOFT SPHEROID	417
11.2.1. Point sources	417
11.2.1.1. Exact solutions	417
11.2.1.2. Low frequency approximations	418
11.2.1.3. High frequency approximations	418
11.2.2. Plane wave incidence	422
11.2.2.1. Exact solutions	422
11.2.2.2. Low frequency approximations	430
11.2.2.3. High frequency approximations	435
11.2.2.4. Shape approximation	436
11.3. ACOUSTICALLY HARD SPHEROID	437
11.3.1. Point sources	437
11.3.1.1. Exact solutions	437
11.3.1.2. Low frequency approximations	438
11.3.1.3. High frequency approximations	438
11.3.2. Plane wave incidence	441
11.3.2.1. Exact solutions	441
11.3.2.2. Low frequency approximations	446
11.3.2.3. High frequency approximations	454
11.3.2.4. Shape approximation	458
11.4. PERFECTLY CONDUCTING SPHEROID	459
11.4.1. Dipole sources	459
11.4.1.1. Exact solutions	459
11.4.1.2. Low frequency approximations	460
11.4.1.3. High frequency approximations	461
11.4.2. Plane wave incidence	461
11.4.2.1. Exact solutions	461
11.4.2.2. Low frequency approximations	462
11.4.2.3. High frequency approximations	466
11.4.2.4. Shape approximation	468
Bibliography	469

Chapter 12 – The wire

O. EINARSSON

12.1. THIN WIRE GEOMETRY	472
12.2. THE AVERAGE BACK SCATTERING CROSS SECTION	474
12.3. THE BACK SCATTERING CROSS SECTION	475
12.4. THE BISTATIC CROSS SECTION	485
12.5. THE CURRENT DISTRIBUTION	491
12.6. SPECIAL FUNCTIONS	494
Bibliography	501

Chapter 13 – The oblate spheroid

T. B. A. SENIOR and P. L. E. USLENGHI

13.1. OBLATE SPHEROIDAL GEOMETRY	503
13.2. ACOUSTICALLY SOFT SPHEROID	504
13.2.1. Point sources	504
13.2.1.1. Exact solutions	504

13.2.1.2. Low frequency approximations	505
13.2.1.3. High frequency approximations	505
13.2.2. Plane wave incidence	507
13.2.2.1. Exact solutions	507
13.2.2.2. Low frequency approximations	508
13.2.2.3. High frequency approximations	509
13.2.2.4. Shape approximation	510
13.3. ACOUSTICALLY HARD SPHEROID	511
13.3.1. Point sources	511
13.3.1.1. Exact solutions	511
13.3.1.2. Low frequency approximations	512
13.3.1.3. High frequency approximations	512
13.3.2. Plane wave incidence	514
13.3.2.1. Exact solutions	514
13.3.2.2. Low frequency approximations	515
13.3.2.3. High frequency approximations	516
13.3.2.4. Shape approximation	517
13.4. PERFECTLY CONDUCTING SPHEROID	518
13.4.1. Dipole sources	518
13.4.1.1. Exact solutions	518
13.4.1.2. Low frequency approximations	520
13.4.1.3. High frequency approximations	520
13.4.2. Plane wave incidence	520
13.4.2.1. Exact solutions	520
13.4.2.2. Low frequency approximations	520
13.4.2.3. High frequency approximations	524
13.4.2.4. Shape approximation	524
Bibliography	526

Chapter 14 – The disc

F. B. SLEATOR

14.1. DISC GEOMETRY	528
14.2. ACOUSTICALLY SOFT DISC	528
14.2.1. Point sources	528
14.2.1.1. Exact solutions	528
14.2.1.2. Low frequency approximations	529
14.2.1.3. High frequency approximations	529
14.2.2. Plane wave incidence	534
14.2.2.1. Exact solutions	534
14.2.2.2. Low frequency approximations	535
14.2.2.3. High frequency approximations	539
14.3. ACOUSTICALLY HARD DISC	542
14.3.1. Point sources	542
14.3.1.1. Exact solutions	542
14.3.1.2. Low frequency approximations	543
14.3.1.3. High frequency approximations	544
14.3.2. Plane wave incidence	545
14.3.2.1. Exact solutions	545
14.3.2.2. Low frequency approximations	546
14.3.2.3. High frequency approximations	552
14.4. PERFECTLY CONDUCTING DISC	554

14.4.1. Dipole sources	554
14.4.1.1. Exact solutions	554
14.4.1.2. Low frequency approximations	561
14.4.1.3. High frequency approximations	564
14.4.2. Plane wave incidence	564
14.4.2.1. Exact solutions	564
14.4.2.2. Low frequency approximations	575
14.4.2.3. High frequency approximations	577
Bibliography	586

PART THREE – SEMI-INFINITE BODIES

Chapter 15 – General considerations

Chapter 16 – The paraboloid

P. L. E. USLENGHI

16.1. GEOMETRY AND EIGENFUNCTIONS FOR PARABOLOID OF REVOLUTION	593
16.2. ACOUSTICALLY SOFT CONVEX PARABOLOID	596
16.2.1. Point sources	596
16.2.1.1. Exact solutions	596
16.2.1.2. High frequency approximations	596
16.2.2. Plane wave incidence	601
16.2.2.1. Exact solutions	601
16.2.2.2. High frequency approximations	603
16.3. ACOUSTICALLY HARD CONVEX PARABOLOID	605
16.3.1. Point sources	605
16.3.1.1. Exact solutions	605
16.3.1.2. High frequency approximations	606
16.3.2. Plane wave incidence	609
16.3.2.1. Exact solutions	609
16.3.2.2. High frequency approximations	612
16.4. PERFECTLY CONDUCTING CONVEX PARABOLOID	614
16.4.1. Dipole sources	614
16.4.2. Plane wave incidence	614
16.4.2.1. Exact solutions	614
16.4.2.2. High frequency approximations	618
16.5. SURVEY OF CONCAVE PARABOLOID	620
Bibliography	621

Chapter 17 – The hyperboloid

P. L. E. USLENGHI

17.1. HYPERBOLOIDAL GEOMETRY	623
17.2. ACOUSTICALLY SOFT HYPERBOLOID	624
17.2.1. Point sources	624
17.2.2. Plane wave incidence	627
17.3. ACOUSTICALLY HARD HYPERBOLOID	629
17.3.1. Point sources	629
17.3.2. Plane wave incidence	631

17.4. PERFECTLY CONDUCTING HYPERBOLOID	632
17.4.1. Dipole sources	632
17.4.2. Plane wave incidence	634
Bibliography	636

Chapter 18 – The cone

J. J. BOWMAN

18.1. CONE GEOMETRY AND PRELIMINARY CONSIDERATIONS	637
18.2. ACOUSTICALLY SOFT CONE	639
18.2.1. Point sources	639
18.2.2. Plane wave incidence	644
18.3. ACOUSTICALLY HARD CONE	649
18.3.1. Point sources	649
18.3.2. Plane wave incidence	654
18.4. PERFECTLY CONDUCTING CONE	660
18.4.1. Electric dipole sources	660
18.4.2. Magnetic dipole sources	667
18.4.3. Plane wave incidence	671
18.5. SPECIAL FUNCTIONS	691
Bibliography	699

APPENDICES

A. SELECTED BIBLIOGRAPHY	705
B. VECTOR RELATIONS	710
C. ORTHOGONAL CURVILINEAR COORDINATES	715
Author index	722
Subject index	727

INTRODUCTION

J. J. BOWMAN, T. B. A. SENIOR and P. L. E. USLENGHI

1.1. General considerations

Various factors dictated the choice of the fifteen shapes treated in this book. Bodies such as the sphere, circular cylinder, wire, cone, wedge, half-plane, disc and paraboloid have important applications in radar and antenna theories. Others, such as the elliptic cylinder and the spheroids, have often been used for the development and testing of approximation methods of general applicability, in both the low and high frequency limits. For all except the wire, the scalar wave equation is separable in some system of orthogonal coordinates. Shapes excluded from this book are the triaxial ellipsoid (STRUTT [1897]; MÖGLICH [1927]), the elliptic cone (KRAUS and LEVINE [1961]), the quarter plane (RADLOW [1961, 1965]), the torus (WESTON [1960]), the ogive (AR [1967]), the parallel-plate waveguide and the thin-walled half-cylinder (VAJNSHTEJN [1954]), among others. Composite shapes of great practical interest, such as the cone-cylinder and the cone-sphere, are also excluded.

Acoustically soft and hard, and perfectly conducting bodies are considered. The fifteen scatterers are divided into three groups: (i) infinitely long cylinders with generators parallel to the z axis, (ii) finite and (iii) semi-infinite bodies with the z axis as axis of symmetry. The emphasis is placed on scattering rather than on radiation problems, i.e. the primary source is usually located off the surface of the scatterer. Radiating slots in the scattering surface are not considered, and although the case of a dipole on the surface is examined, no general discussion of the equivalence between dipoles and slots is given. The primary field is that of a plane wave, a point source or a dipole; in Part One, line sources parallel to the generators of the scatterer are also considered.

The choice of time-harmonic fields (with time-dependence factor $e^{-i\omega t}$ omitted throughout) is justified by the fact that this is an important case in practice, that most of the literature does indeed consider this type of field only, and that an arbitrary field can always be decomposed into the sum of monochromatic waves by Fourier analysis. It should be noted, however, that the high-frequency results quoted in this book are valid for real positive frequencies, and cannot in general be extended to the whole complex frequency plane (in particular, they cannot in general be analytically continued to negative real frequencies).

The scattered field or the total field is given at an arbitrarily located observation point. Explicit results are also exhibited for the total field at the surface of the scatterer

(especially important in antenna applications) and for the far field, from which the radar cross sections are derived.

1.2. Fundamental concepts

This section is not intended to be a comprehensive treatise on methods, but rather a brief survey of the most widely used techniques in which the reader may find some useful formulae and the most relevant bibliographical references.

1.2.1. Maxwell's equations

The electromagnetic field at a time t and at any point in a linear, homogenous and isotropic medium of electric permittivity ϵ , magnetic permeability μ and zero conductivity is described by the homogeneous Maxwell equations

$$\nabla \wedge \mathbf{H} = \epsilon \frac{\partial \mathbf{E}}{\partial t}, \quad \nabla \wedge \mathbf{E} = -\mu \frac{\partial \mathbf{H}}{\partial t}, \quad (1.1)$$

which govern the behavior of the electric field \mathbf{E} and of the magnetic field \mathbf{H} at all ordinary points in space, but do not describe the field at the source points. By taking the divergence of both sides of eqs. (1.1) and with the convention that at some time the fields may become solenoidal (which is certainly the case if, for example, $\mathbf{E}_{t=-\infty} = \mathbf{H}_{t=-\infty} = 0$) one finds the auxiliary equations

$$\nabla \cdot \mathbf{H} = \nabla \cdot \mathbf{E} = 0. \quad (1.2)$$

If a scattering body is embedded in the medium, eqs. (1.1) and (1.2) are satisfied by the incident or primary fields \mathbf{E}^i and \mathbf{H}^i , by the total (incident plus scattered) fields \mathbf{E} and \mathbf{H} , and therefore also by the secondary or scattered fields \mathbf{E}^s and \mathbf{H}^s , which represent the disturbance added to the primary fields by the scatterer.

In the following we shall consider only the particular case of monochromatic radiation. The wave number k and the intrinsic impedance Z of the medium surrounding the scatterer are given by

$$k = \omega \sqrt{\epsilon \mu} = 2\pi/\lambda, \quad Z = Y^{-1} = \sqrt{\mu/\epsilon}, \quad (1.3)$$

where ω is the angular frequency and λ the wavelength (in free space, $Z = 120 \pi$ ohm). The time dependence factor $\exp(-i\omega t)$ is suppressed throughout the book. By replacing the operator $\partial/\partial t$ with the multiplicative factor $-i\omega$, it is seen that eqs. (1.1) become:

$$\nabla \wedge \mathbf{H} = -ikY\mathbf{E}, \quad \nabla \wedge \mathbf{E} = ikZ\mathbf{H}. \quad (1.4)$$

1.2.2. Acoustical equations

If the medium surrounding the scatterer is a gas, such as air, with negligible viscosity,

in which small perturbations from the rest condition occur, the equations that describe the motion of the gas at all ordinary points in space are Newton's equation

$$\delta_0 \frac{\partial \mathbf{u}}{\partial t} = -\nabla p \quad (1.5)$$

and the continuity equation

$$\frac{\partial p}{\partial t} = -\delta_0 c^2 \nabla \cdot \mathbf{u}, \quad (c^2 = \gamma p_0 / \delta_0), \quad (1.6)$$

where δ_0 and p_0 are the density and pressure respectively of the gas at rest, γ is the ratio of the specific heat at constant pressure to that at constant volume ($\gamma = 1.4$ for air at normal temperature and pressure), \mathbf{u} is the gas particle velocity, p is the excess pressure (i.e. the difference between the actual pressure and p_0), and t is the time.

It is customary to introduce a velocity potential V such that

$$\mathbf{u} = \nabla V; \quad (1.7)$$

then from eq. (1.5) and the fact that $p = 0$ at rest:

$$p = -\delta_0 \frac{\partial V}{\partial t}. \quad (1.8)$$

The symbols V^i , V^s and $V = V^i + V^s$ will indicate the incident, scattered and total velocity potentials, respectively.

For harmonic vibrations with time dependence $\exp(-i\omega t)$, eqs. (1.5), (1.6) and (1.8) become:

$$\mathbf{u} = -\frac{i}{\omega \delta_0} \nabla p, \quad (1.9)$$

$$p = -\frac{i}{\omega} \delta_0 c^2 \nabla \cdot \mathbf{u}, \quad (1.10)$$

$$p = i\omega \delta_0 V. \quad (1.11)$$

1.2.3. Wave propagation

In the electromagnetic case, it follows from eqs. (1.1) that

$$\left(\nabla \wedge \nabla \wedge + \epsilon \mu \frac{\partial^2}{\partial t^2} \right) \mathbf{E} = 0, \quad \left(\nabla \wedge \nabla \wedge + \epsilon \mu \frac{\partial^2}{\partial t^2} \right) \mathbf{H} = 0, \quad (1.12)$$

or

$$\left(\nabla^2 - \epsilon \mu \frac{\partial^2}{\partial t^2} \right) \mathbf{E} = 0, \quad \left(\nabla^2 - \epsilon \mu \frac{\partial^2}{\partial t^2} \right) \mathbf{H} = 0, \quad (1.13)$$

where ∇^2 operates on the rectangular Cartesian components of \mathbf{E} and \mathbf{H} . For harmonic time dependence, eqs. (1.13) become

$$(\nabla^2 + k^2) \mathbf{E} = 0, \quad (\nabla^2 + k^2) \mathbf{H} = 0. \quad (1.14)$$

In the acoustical case, it follows from eqs. (I.5) and (I.6) that

$$\left(\nabla^2 - \frac{1}{c^2} \frac{\partial^2}{\partial t^2}\right) p = 0, \quad \left(\nabla^2 - \frac{1}{c^2} \frac{\partial^2}{\partial t^2}\right) \mathbf{u} = 0. \quad (\text{I.15})$$

In the following we shall work with the velocity potential V , from which p and \mathbf{u} are obtained through simple operations of differentiation as indicated in eqs. (I.7) and (I.8). We therefore consider the wave equation

$$\left(\nabla^2 - \frac{1}{c^2} \frac{\partial^2}{\partial t^2}\right) V = 0,$$

which for harmonic time dependence becomes

$$(\nabla^2 + k^2)V = 0, \quad (k = \omega/c). \quad (\text{I.17})$$

The solutions of eq. (I.17) represent sound waves of angular frequency ω and velocity c (for air at N.T.P., $c \approx 340$ m/sec). Similarly, the solutions of each of the six equations (I.14) represent waves of angular frequency ω and velocity $1/\sqrt{\epsilon\mu}$ (in vacuo, $1/\sqrt{\epsilon\mu} \approx 2.9979 \times 10^8$ m/sec). It is thus evident that a certain correspondence exists between the solutions of scalar and vector boundary value problems, and this correspondence takes a particularly simple form for two-dimensional problems (see Chapter I).

1.2.4. Boundary and radiation conditions

In the electromagnetic case we limit our considerations to perfect conductors, i.e., we require that the tangential component of the total electric field at any regular point of the scattering surface be zero:

$$\mathbf{E} - (\mathbf{E} \cdot \hat{\mathbf{n}})\hat{\mathbf{n}} = 0, \quad (\text{I.18})$$

where $\hat{\mathbf{n}}$ is the unit normal to the surface directed from the body into the surrounding medium. It is seen from Maxwell's equations that condition (I.18) implies that the normal component of the total magnetic field is zero at any regular point of the surface of the scatterer.

Some components of the electric and magnetic fields become infinite at those points of the scattering surface where the Gaussian curvature is infinite. To ensure the uniqueness of the solution one must then invoke an additional boundary condition, the Meixner integrability condition: the electromagnetic energy contained in any finite volume about the surface singularity must be finite (MEIXNER [1949]). For example, in the case of the wedge with aperture angle 2Ω shown in Fig. 6.1 ($\Omega = 0$ for the half plane), it can be shown that the components of the electric and magnetic fields parallel to the edge behave like ρ^v and those perpendicular to the edge like ρ^{v-1} as $\rho \rightarrow 0$, where ρ is the distance of the observation point from the edge of the wedge and $v = \pi/(2\pi - 2\Omega)$ (VAN BLADIE [1964]).

A generalization of the boundary condition (I.18) which is not explicitly considered

in this book and which has many practical applications is the so-called impedance boundary condition or Leontovich condition:

$$\mathbf{E} - (\mathbf{E} \cdot \hat{\mathbf{n}})\hat{\mathbf{n}} = \eta \mathbf{Z} \hat{\mathbf{n}} \wedge \mathbf{H}, \quad (1.19)$$

where η is the relative surface impedance ($\eta = 0$ for a perfect conductor). A nonzero surface impedance may account for the finite conductivity of the scatterer (see, for example, SENIOR [1960a]), for the roughness of its surface (SENIOR [1960b]), for the presence of highly absorbing coating layers (WESTON [1963]), or for an overdense plasma.

If the scatterer and all the primary sources are located within a finite distance from a fixed origin $r = 0$, the fields \mathbf{E} and \mathbf{H} are required to satisfy the Silver-Müller radiation condition

$$\begin{aligned} \lim_{r \rightarrow \infty} [r \wedge (\nabla \wedge) + ikr] \mathbf{E} &= 0 \\ \lim_{r \rightarrow \infty} [r \wedge (\nabla \wedge) + ikr] \mathbf{H} &= 0 \end{aligned} \quad \text{uniformly in } \theta. \quad (1.20)$$

In the case of plane wave incidence it is necessary to separate incident from scattered fields; the scattered fields \mathbf{E}^s and \mathbf{H}^s are required to satisfy condition (1.20).

If the scatterer is an infinitely long cylindrical body with generators parallel to the z axis ($z = r \cos \theta$) and the primary sources are at a finite distance from $r = 0$, then condition (1.20) is to be satisfied for all θ in the angular range $0 < \delta \leq \theta \leq \pi - \delta$ with δ arbitrarily small and constant. If the primary source is a line source parallel to the z axis (two-dimensional problem) condition (1.20) must be replaced by

$$\begin{aligned} \lim_{\rho \rightarrow \infty} \rho^{\frac{1}{2}} \left(\frac{\partial}{\partial \rho} - ik \right) E_z &= 0 \\ \lim_{\rho \rightarrow \infty} \rho^{\frac{1}{2}} \left(\frac{\partial}{\partial \rho} - ik \right) H_z &= 0 \end{aligned} \quad \text{uniformly in } \phi; \quad (1.21)$$

when the primary source is a plane wave at broadside incidence, only the scattered fields E_z^s and H_z^s are required to satisfy condition (1.21).

In the acoustical case we only consider scatterers that are either perfectly soft or perfectly rigid. At the surface of a soft scatterer, the excess pressure p is zero; it follows from eq. (1.11) that the boundary condition for the total velocity potential is

$$V = 0. \quad (1.22)$$

At the surface of a rigid or hard scatterer, the normal component $\mathbf{u} \cdot \hat{\mathbf{n}}$ of the particle velocity \mathbf{u} is zero; it follows from eq. (1.7) that the boundary condition for the total velocity potential is

$$\frac{\partial V}{\partial n} = 0. \quad (1.23)$$

Conditions (1.22) and (1.23) are also known as Dirichlet and Neumann boundary

conditions, respectively. A more general boundary condition is

$$\left(\frac{\partial}{\partial n} + i \frac{\omega \delta_0}{\eta} \right) V = 0, \quad (1.24)$$

where δ_0 is the density (mass per unit volume) of the medium surrounding the scatterer and η is the normal acoustic impedance, i.e. the ratio of the excess pressure to the normal component of the particle velocity at the surface of the scatterer (in particular, $\eta = 0$ for a soft body and $\eta^{-1} = 0$ for a hard body). Condition (1.24) is not considered in this book; for a noteworthy application to the scattering of sound by circular cylinders and spheres, see LAX and FESHBACH [1948].

The radiation conditions for scalar scattering problems are similar to those previously stated for vector problems; namely, that

$$\lim_{r \rightarrow \infty} r \left(\frac{\partial}{\partial r} - ik \right) V = 0 \quad \text{uniformly in } \hat{r} \quad (1.25)$$

for three-dimensional problems, and

$$\lim_{\rho \rightarrow \infty} \rho^{\frac{1}{2}} \left(\frac{\partial}{\partial \rho} - ik \right) V = 0 \quad \text{uniformly in } \phi \quad (1.26)$$

for two-dimensional problems. If the primary field is a plane wave, then V is to be replaced by V^s in eqs. (1.25) and (1.26).

If the primary sources and the scattering body are given, the boundary conditions at the surface of the scatterer and the radiation condition at infinity are sufficient to ensure the uniqueness of the solution to the (scalar or vector) wave equation.

In three-dimensional problems, the far scattered field may be written as

$$V^s \sim \frac{e^{ikr}}{kr} S \quad (r \rightarrow \infty) \quad (1.27)$$

in the acoustical case, and as

$$E^s \sim \frac{e^{ikr}}{kr} S \hat{e} \quad (r \rightarrow \infty) \quad (1.28)$$

in the electromagnetic case, so that in both cases only the expression for $S = S(\theta, \phi)$ needs to be given explicitly. Similarly, the far scattered fields in two-dimensional problems may be written as

$$P(\phi) \sqrt{\frac{2}{\pi k \rho}} e^{ik\rho - \frac{1}{4}i\pi} \quad (\rho \rightarrow \infty). \quad (1.29)$$

In the following, the use of the far field coefficients S and P is restricted to the case of plane wave incidence.

Finally, it should be pointed out that conditions (1.20) and (1.25) are sufficient but not necessary, and can be replaced by weaker requirements (WILCOX [1956a, b]).

1.2.5. Radar cross sections

The radar cross sections are defined for plane wave incidence, and are closely related to the far field coefficients S and P of the previous section.

In the three-dimensional case, the differential scattering cross section or bistatic radar cross section $\sigma(\theta, \phi)$ is defined by

$$\sigma(\theta, \phi) = \lim_{r \rightarrow \infty} 4\pi r^2 \frac{|\mathbf{E}^s|^2}{|\mathbf{E}^i|^2} \quad (1.30)$$

where $|\mathbf{E}|^2 = |E_x|^2 + |E_y|^2 + |E_z|^2$, and \mathbf{E}^s is the scattered electric field at the observation point (r, θ, ϕ) . For an incident electric field of unit amplitude, eqs. (1.28) and (1.30) yield:

$$\sigma(\theta, \phi) = \frac{4\pi}{k^2} |S(\theta, \phi)|^2. \quad (1.31)$$

The total scattering cross section σ_T is defined by the ratio of the time averaged total scattered power to the time averaged incident Poynting vector, and is related to the bistatic cross section by the equation

$$\sigma_T = \frac{1}{4\pi} \int_{\theta=0}^{\pi} \int_{\phi=0}^{2\pi} \sigma(\theta, \phi) \sin \theta d\theta d\phi. \quad (1.32)$$

A relation between σ_T and the far field coefficient $S(\hat{r})$ of eq. (1.28) is provided by the forward scattering theorem (see e.g. BORN and WOLF [1959]):

$$\sigma_T = \frac{4\pi}{k^2} \text{Im } S(\hat{r}_0)(\hat{e} \cdot \hat{e}) \quad (1.33)$$

where \hat{r}_0 is oriented in the direction of propagation of the incident wave, \hat{e} gives the direction of the incident electric field, and S is normalized to the amplitude of the incident field.

In the case of broadside incidence on an infinitely long cylindrical body with generators parallel to the z axis, the bistatic cross section $\sigma(\phi)$ per unit length is defined by

$$\sigma(\phi) = \lim_{\rho \rightarrow \infty} 2\pi\rho \frac{|V^s|^2}{|V^i|^2}, \quad (1.34)$$

where $V^s = E_z^s$ if the electric field is parallel to the z axis, while $V^s = H_z^s$ if the magnetic field is parallel to the z axis. If V^i has unit amplitude, it follows from eq. (1.29) that

$$\sigma(\phi) = \frac{4}{k} |P(\phi)|^2. \quad (1.35)$$

The total scattering cross section per unit length is defined by the ratio of the time averaged total scattered power per unit length of cylinder to the time averaged incident

Poynting vector; if $|V| = 1$, then

$$\sigma_T = -\frac{4}{k} \operatorname{Re} P(\phi_0), \quad (1.36)$$

where ϕ_0 is the azimuth of the direction of propagation of the incident wave.

The definitions of radar cross sections may be modified to take into account the polarization of the receiver. Thus, for example, the three-dimensional bistatic cross section can also be written as

$$\sigma(\theta, \phi) = \frac{4\pi}{k^2} |S(\theta, \phi)|^2 |\hat{e} \cdot \hat{f}|^2, \quad (1.37)$$

where \hat{e} is the unit vector of eq. (1.28) and \hat{f} represents the polarization of the receiver; if $|\hat{e} \cdot \hat{f}| = 1$, result (1.37) reduces to eq. (1.31).

1.2.6. Electromagnetic potentials

It is often convenient to represent the electromagnetic field in terms of a scalar potential $\Phi(\mathbf{r}, t)$ and a vector potential $\mathbf{A}(\mathbf{r}, t)$:

$$\mathbf{E} = -\nabla\Phi - \frac{\partial\mathbf{A}}{\partial t}, \quad \mathbf{H} = \frac{1}{\mu} \nabla \wedge \mathbf{A}, \quad (1.38)$$

where Φ and \mathbf{A} are required to satisfy the Lorentz condition

$$\nabla \cdot \mathbf{A} + \epsilon\mu \frac{\partial\Phi}{\partial t} = 0. \quad (1.39)$$

This condition has the advantages of assuring a relativistic covariant relation between Φ and \mathbf{A} and of making both potentials satisfy the wave equation, namely

$$\nabla^2\Phi - \epsilon\mu \frac{\partial^2\Phi}{\partial t^2} = -\frac{\rho}{\epsilon}, \quad (1.40)$$

$$\nabla^2\mathbf{A} - \epsilon\mu \frac{\partial^2\mathbf{A}}{\partial t^2} = -\mu\mathbf{J}, \quad (1.41)$$

where ρ and \mathbf{J} are the charge and current densities of the primary and/or secondary sources, depending on whether the potentials represent the primary and/or scattered fields. The particular solutions of eqs. (1.40) and (1.41) are expressible as integrals over the charge and current distributions; the retarded solutions are:

$$\Phi(\mathbf{r}, t) = \frac{1}{4\pi\epsilon} \int \frac{\rho(\mathbf{r}', t - |\mathbf{r} - \mathbf{r}'|/c)}{|\mathbf{r} - \mathbf{r}'|} d\mathbf{r}', \quad (1.42)$$

$$\mathbf{A}(\mathbf{r}, t) = \frac{\mu}{4\pi} \int \frac{\mathbf{J}(\mathbf{r}', t - |\mathbf{r} - \mathbf{r}'|/c)}{|\mathbf{r} - \mathbf{r}'|} d\mathbf{r}', \quad (1.43)$$

where $c = (\epsilon\mu)^{-1/2}$. The advanced solutions, corresponding to $(t + |\mathbf{r} - \mathbf{r}'|/c)$ in the

argument of the integrands, must be disregarded on the basis of causality. For a discussion of the dependence of Φ and A on the field sources in the time-harmonic case see, for example, VAN BLADEL [1964; Section 7.8].

For given fields E and H , the potentials Φ and A are not uniquely defined; in fact, if Φ and A satisfy eqs. (I.38) and (I.39), the same is true of all potentials Φ' and A' related to Φ and A by the gauge transformation

$$\Phi' = \Phi + \frac{\partial f}{\partial t}, \quad A' = A - \nabla f, \quad (I.44)$$

where $f(r, t)$ is any solution of the homogeneous wave equation

$$\nabla^2 f - \epsilon\mu \frac{\partial^2 f}{\partial t^2} = 0. \quad (I.45)$$

The potentials have the advantage of being "more regular" than the electric and magnetic fields. This regularity can be further enhanced by introducing other functions, the so-called superpotentials, from which the fields are obtained by higher-order differentiations. The most widely used superpotentials are the electric and magnetic Hertz vectors Π_e and Π_m , also known as polarization potentials. The vector potential Π_e originates fields

$$E = \nabla \wedge \nabla \wedge \Pi_e, \quad H = \epsilon \nabla \wedge \frac{\partial}{\partial t} \Pi_e, \quad (I.46)$$

whereas the vector potential Π_m gives rise to fields

$$E = -\mu \nabla \wedge \frac{\partial}{\partial t} \Pi_m, \quad H = \nabla \wedge \nabla \wedge \Pi_m. \quad (I.47)$$

The electric and magnetic fields in a region where ϵ and μ are constant and $\rho = J = 0$ are the sums of the partial fields of eqs. (I.46) and (I.47). Observe that E and H remain unchanged when the gradients of arbitrary functions of space and time are added to the Hertz vectors. The fields determined by eqs. (I.46) and (I.47) satisfy the Maxwell's equations (I.1) provided that

$$\begin{aligned} \left(\nabla \wedge \nabla \wedge + \epsilon\mu \frac{\partial^2}{\partial t^2} \right) \Pi_e &= \nabla f, \\ \left(\nabla \wedge \nabla \wedge + \epsilon\mu \frac{\partial^2}{\partial t^2} \right) \Pi_m &= \nabla f, \end{aligned} \quad (I.48)$$

where $f(r, t)$ is an arbitrary scalar function of position and time.

In particular, the potentials Φ and A may be derived from Hertz vectors; thus, one may choose either

$$\Phi = -\nabla \cdot \Pi_e, \quad A = \epsilon\mu \frac{\partial}{\partial t} \Pi_e \quad (I.49)$$

or

$$\Phi = 0, \quad A = \mu \nabla \wedge \Pi_m; \quad (I.50)$$

the fields are then given by eqs. (1.38), the Lorentz condition is automatically satisfied, and $f = \nabla \cdot \Pi_e$ in eq. (1.48) for Π_e .

A general theory of the Hertz vectors and of the associated gauge transformation is to be found in NISBET [1955]; see also MCCREA [1957]. For the relation of the Hertz vectors to the sources of the field see, for example, STRATTON [1941; Sections 1.11, and 8.3 to 8.6], BORN and WOLF [1959; Sections 2.2.2 and 2.2.3], PANOFSKY and PHILLIPS [1962; Sections 14.5 to 14.9] and VAN BLADEL [1964; Section 7.2]. It is here sufficient to recall that, in the time-harmonic case, an electric dipole located at the point r_0 with a moment

$$\frac{4\pi e}{k} \hat{e} \quad (1.51)$$

produces a field that can be derived from eqs. (1.46) in which

$$\Pi_e = \frac{e^{ikR}}{kR} \hat{e}, \quad (R = |r - r_0|), \quad (1.52)$$

whereas the field of a magnetic dipole located at r_0 and with a moment

$$\frac{4\pi}{k} \hat{e} \quad (1.53)$$

can be derived from eqs. (1.47) in which

$$\Pi_m = \frac{e^{ikR}}{kR} \hat{e}. \quad (1.54)$$

In the time-harmonic case, an especially important class of Hertz vectors is obtained by setting

$$\Pi_e = ur, \quad \Pi_m = vr \quad (1.55)$$

where the scalar functions of position u and v , the so-called Debye potentials, satisfy the wave equation

$$\begin{aligned} (\nabla^2 + k^2)u &= 0, \\ (\nabla^2 + k^2)v &= 0, \end{aligned} \quad (1.56)$$

and r is the radial vector from a fixed origin. Every electromagnetic field defined in a source-free region between two concentric spheres can be represented there by two Debye potentials (WILCOX [1957]); the components of the field are

$$\begin{aligned} E_r &= \left(\frac{\partial^2}{\partial r^2} + k^2 \right) (ru), \\ E_\theta &= \frac{1}{r} \frac{\partial^2}{\partial r \partial \theta} (ru) + \frac{ikZ}{\sin \theta} \frac{\partial v}{\partial \phi}, \\ E_\phi &= \frac{1}{r \sin \theta} \frac{\partial^2}{\partial r \partial \phi} (ru) - ikZ \frac{\partial v}{\partial \theta}, \end{aligned}$$

$$H_r = \left(\frac{\partial^2}{\partial r^2} + k^2 \right) (rv), \quad (1.57)$$

$$H_\theta = \frac{1}{r} \frac{\partial^2}{\partial r \partial \theta} (rv) - \frac{ikY}{\sin \theta} \frac{\partial u}{\partial \phi},$$

$$H_\phi = \frac{1}{r \sin \theta} \frac{\partial^2}{\partial r \partial \phi} (rv) + ikY \frac{\partial u}{\partial \theta}.$$

The Debye potentials can be expressed in terms of the current density distribution \mathbf{J} of the sources: see BOUWKAMP and CASIMIR [1954] and VAN BLADEL [1964; Section 7.7].

1.2.7. Green's functions

Consider the equation

$$Lf = -g \quad (1.58)$$

subject to certain boundary conditions, where L is a differential operator, $g(x)$ is a given continuous function, $f(x)$ is the unknown function, and x may be considered as a vector in an n -dimensional space. Its solution may be written as

$$f(x) = \int G(x|x') g(x') dx'; \quad (1.59)$$

here $G(x|x')$ is the so-called Green function for the boundary value problem under consideration, and satisfies the equation:

$$LG(x|x') = -\delta(x-x'), \quad (1.60)$$

where δ is the Dirac delta function. Thus, formally:

$$G(x|x') = -L^{-1}\delta(x-x') + G_0, \quad (1.61)$$

where G_0 is any solution of $LG_0 = 0$.

Green's function has the following properties: 1) it is symmetrical in x and x' :

$$G(x|x') = G(x'|x), \quad (1.62)$$

and 2) it is the solution of the homogeneous differential equation $LG = 0$ at all points except $x = x'$, where a singularity occurs. The physical meaning of eqs. (1.58) and (1.59) is that the source g originates the field f . Green's function represents the field produced at x by a source of unit intensity located at x' (here x and x' represent both space and time coordinates). Therefore, the field f is given by an integral over all the space-time positions of the source.

We wish to point out that since we are here concerned only with macroscopic phenomena, the principle of causality must be respected; this implies that time reversal must be introduced in the reciprocity relation satisfied by a time-dependent

Green function. For example, the Green function for the scalar wave equation

$$\left(\nabla^2 - \frac{1}{c^2} \frac{\partial^2}{\partial t^2} \right) V = 0$$

must satisfy the reciprocity relation

$$G(\mathbf{r}, t | \mathbf{r}', t') = G(\mathbf{r}', -t' | \mathbf{r}, -t). \quad (1.63)$$

For $t' = 0$, eq. (1.63) becomes

$$G(\mathbf{r}, t | \mathbf{r}', 0) = G(\mathbf{r}', 0 | \mathbf{r}, -t),$$

that is, the effect at the point \mathbf{r} and at the time t of an impulse started at \mathbf{r}' at time zero equals the effect produced at \mathbf{r}' at time zero by the same impulse started at \mathbf{r} at the time $-t$. For a detailed discussion of time-dependent scalar Green's functions see, for example, MORSE and FESHBACH [1953; Section 7.3].

The Green function $G(\mathbf{r} | \mathbf{r}')$ for the steady-state wave equation (1.17), i.e. the solution of

$$(\nabla^2 + k^2)G = -\delta(\mathbf{r} - \mathbf{r}'), \quad (1.64)$$

is investigated e.g. by MORSE and FESHBACH [1953; Section 7.2]; for a bounded region of space, see SOMMERFELD [1949; paragraph 27]. In free space, the solution of eq. (1.64) which obeys the radiation condition is

$$G(\mathbf{r} | \mathbf{r}') = \frac{\exp(ik|\mathbf{r} - \mathbf{r}'|)}{4\pi|\mathbf{r} - \mathbf{r}'|} \quad (1.65)$$

for three dimensions, and

$$G(\mathbf{r} | \mathbf{r}') = \frac{1}{4i} H_0^{(1)}(k|\mathbf{r} - \mathbf{r}'|) \quad (1.66)$$

in two dimensions. The corresponding free space Green function for the Laplace equation, i.e. the solution of

$$\nabla^2 G = -\delta(\mathbf{r} - \mathbf{r}'), \quad (1.67)$$

is

$$G(\mathbf{r} | \mathbf{r}') = \frac{1}{4\pi|\mathbf{r} - \mathbf{r}'|} \quad (1.68)$$

for three dimensions, and

$$G(\mathbf{r} | \mathbf{r}') = -\frac{1}{2\pi} \ln |\mathbf{r} - \mathbf{r}'| \quad (1.69)$$

for two dimensions.

Green's function technique is also applicable to the solution of vector problems such as

$$L\mathbf{f} = -\mathbf{g}. \quad (1.70)$$

Now, however, it is in general necessary to use nine scalar Green functions to express the three components of \mathbf{f} in terms of the three components of \mathbf{g} . These nine quantities constitute a tensor of rank two, the so-called dyadic Green function $\mathcal{G}(\mathbf{x}|\mathbf{x}')$, which satisfies

$$L\mathcal{G}(\mathbf{x}|\mathbf{x}') = -\delta(\mathbf{x}-\mathbf{x}')\mathcal{I}, \quad (1.71)$$

where \mathcal{I} is the identity. Thus, the solution of eq. (1.70) is:

$$\mathbf{f}(\mathbf{x}) = \int \mathcal{G}(\mathbf{x}|\mathbf{x}') \cdot \mathbf{g}(\mathbf{x}') d\mathbf{x}'. \quad (1.72)$$

The dyadic formalism enables one to discuss the solutions of vector scattering problems without actually calling into play the inevitably complicated representations of solutions of particular problems. The dyadic Green function of free space has been discussed by VAN BLADEL [1961]; also available are the dyadic Green functions for the half plane (TAI [1954a]) and for the circular and elliptic cylinders, wedge, flat ground, sphere and cone (TAI [1954b]). Some fundamental properties of dyadics are listed in Appendix B.

1.2.8. Reciprocity theorem

Equations (1.62) and (1.63) of the previous section already constitute reciprocity relations. A reciprocity theorem for time-dependent electromagnetic fields in vacuo has been given by WELCH [1960]. If Maxwell's equations are written in the form

$$\begin{aligned} \nabla \wedge \mathbf{H} &= \mathbf{J} + \epsilon \frac{\partial \mathbf{E}}{\partial t}, \\ \nabla \wedge \mathbf{E} &= -\mathbf{J}_m - \mu \frac{\partial \mathbf{H}}{\partial t}, \end{aligned} \quad (1.73)$$

where a magnetic current \mathbf{J}_m has been introduced for reasons of symmetry, then:

$$\int_{t_1}^{t_2} dt \int_{\text{all space}} [\mathbf{E}^r \cdot \mathbf{J}^a + \mathbf{H}^r \cdot \mathbf{J}_m^a] dv = - \int_{t_1}^{t_2} dt \int_{\text{all space}} [\mathbf{E}^a \cdot \mathbf{J}^r + \mathbf{H}^a \cdot \mathbf{J}_m^r] dv, \quad (1.74)$$

where $\mathbf{E}^r, \mathbf{H}^r$ are the retarded fields produced by sources \mathbf{J}^r and \mathbf{J}_m^r , and $\mathbf{E}^a, \mathbf{H}^a$ are the advanced fields produced by sources \mathbf{J}^a and \mathbf{J}_m^a ; in deriving eq. (1.74), it has been assumed that the sources were switched on at some time after t_1 . The reciprocity theorem (1.74) can be modified for time-harmonic fields, yielding (see VAN BLADEL [1964: Section 7.5]):

$$\int_{\text{all space}} [\mathbf{E}^r \cdot \mathbf{J}^a - \mathbf{H}^r \cdot \mathbf{J}_m^a] dv = \int_{\text{all space}} [\mathbf{E}^a \cdot \mathbf{J}^r - \mathbf{H}^a \cdot \mathbf{J}_m^r] dv, \quad (1.75)$$

where $\mathbf{E}^r, \mathbf{H}^r$ and $\mathbf{E}^a, \mathbf{H}^a$ are respectively generated by sources $\mathbf{J}^r, \mathbf{J}_m^r$ and $\mathbf{J}^a, \mathbf{J}_m^a$ operating at the same frequency. Reciprocity relations for propagation in a homogeneous anisotropic medium and for the scattering matrix have been respectively derived by RUMSLEY [1954] and by DE HOOP [1960]; see also VAN BLADEL [1964: Sections 8.3 and 8.7]. The relationship between transmitting and receiving properties of an antenna has been discussed by DE HOOP [1968].

I.2.9. Babinet's principle

Babinet's principle enables one to derive the electromagnetic field diffracted by a set of apertures A in an infinite metal plane of zero thickness from the field scattered by a plane metal screen S of zero thickness having the same size, shape and position as the apertures ($A = S$). Here we follow the presentation of Babinet's principle given by BOUWKAMP [1954], where a comprehensive bibliography on this subject is also to be found. An extension of Babinet's principle to screens that are not perfectly conducting has been attempted by NEUGEBAUER [1956].

Let (F, G) denote any incident electromagnetic field, where the first vector represents the electric field ($E^i = F$) and the second the magnetic field ($H^i = G$), and define the "complementary incident field" to be $(-ZG, YF)$, i.e. $E^i = -ZG$ and $H^i = YF$. For example, if the incident field is a plane wave, the complementary incident field is obtained by rotating the plane of polarization through a right angle counter-clockwise when looking in the direction of propagation. Both incident and complementary incident fields satisfy Maxwell's equations for free space.

Firstly, we consider the scattering of the field (F, G) by a perfectly conducting plane screen S of zero thickness, located in the plane $z = 0$. Secondly, we consider the "complementary diffraction problem", that is the scattering of the complementary field $(-ZG, YF)$ by the apertures A in a perfectly conducting plane screen of zero thickness located at $z = 0$, such that the apertures A in the second problem extend over that portion of the $z = 0$ plane which was occupied by the screen S in the first problem. In both problems, the sources of the primary field are supposed to be located in the half space $z > 0$, so that $z > 0$ is the "illuminated" half space, whereas $z < 0$ is the "shadowed" half space. The rigorous form of Babinet's principle states that the solution of either one of these problems can be obtained at once from the solution of the other.

In the first problem, let the total field at any point in space be given by $(F + E^s, G + H^s)$, where (E^s, H^s) is the scattered field due to the currents induced in the screen by the incident field (F, G) . In the complementary problem, we distinguish between the fields in front of and behind the aperture. Let (E_0, H_0) be the total field that would be present in the illuminated half space $z > 0$ if there were no holes A in the perfectly conducting screen $z = 0$, and let (E^d, H^d) be the diffracted field when the apertures A are present. Then the total field behind the apertures ($z < 0$) is (E^d, H^d) , whereas the total field in front of the apertures ($z > 0$) is $(E_0 + E^d, H_0 + H^d)$. According to Babinet's principle:

$$E^d = \mp ZH_0^s, \quad H^d = \pm YE_0^s, \quad (z \gtrless 0). \quad (1.76)$$

Finally, observe that in the portion of the $z = 0$ plane that is not occupied by the screen,

$$E_z^s = H_x^s = H_y^s = 0, \quad (1.77)$$

from which it follows that in the apertures the tangential magnetic field and the normal

electric field are not disturbed by the presence of the screen. Also, the components

$$E^s - E^s \cdot \hat{z}, \quad E^d - E^d \cdot \hat{z}, \quad H^s \cdot \hat{z}, \quad H^d \cdot \hat{z}$$

are even functions of z , whereas

$$H^s - \hat{H}^s \cdot \hat{z}, \quad H^d - \hat{H}^d \cdot \hat{z}, \quad E^s \cdot \hat{z}, \quad E^d \cdot \hat{z}$$

are odd functions of z .

I.2.10. Integral equations

For an acoustic or electromagnetic wave incident on a body, integral equations can be derived from which to determine the fields induced on the surface of the scatterer. Although these are capable of exact solution for only a limited number of geometries, they do form the starting point for most numerical methods (see Section I.2.14.4) and are also valuable in the derivation of low and high frequency approximations.

It is convenient to confine attention to a three-dimensional, closed and bounded body whose surface S is regular in the sense of KELLOGG [1929], and to treat successively the cases in which the body is acoustically soft or hard, or is perfectly conducting.

If V^i is the velocity potential of an incident acoustic field, the total velocity potential V at a point \mathbf{r} in the space surrounding S is

$$V(\mathbf{r}) = V^i(\mathbf{r}) + \frac{1}{4\pi} \int_S \left\{ V(\mathbf{r}_1) \frac{\partial}{\partial n_1} \left(\frac{e^{ikR}}{R} \right) - \frac{e^{ikR}}{R} \frac{\partial}{\partial n_1} V(\mathbf{r}_1) \right\} dS \quad (I.78)$$

where \mathbf{r}_1 is a variable point on S , $R = |\mathbf{r} - \mathbf{r}_1|$, and $\hat{n}_1 = \hat{n}(\mathbf{r}_1)$ is a unit vector normal to S directed out of the body and into the surrounding space. From this representation, integral equations for either the field or its normal derivative on S can be derived.

For a soft body ($V = 0$ on S), eq. (I.78) reduces to

$$V(\mathbf{r}) = V^i(\mathbf{r}) - \frac{1}{4\pi} \int_S \frac{e^{ikR}}{R} \frac{\partial}{\partial n_1} V(\mathbf{r}_1) dS \quad (I.79)$$

which in turn leads to two integral equations for the unknown surface field. The first of these follows on allowing \mathbf{r} to be a point on S and is

$$4\pi V^i(\mathbf{r}) = \int_S \frac{e^{ikR}}{R} \frac{\partial}{\partial n_1} V(\mathbf{r}_1) dS, \quad (\mathbf{r}, \mathbf{r}_1 \in S). \quad (I.80)$$

The singularity of the kernel $R^{-1}e^{ikR}$ at $\mathbf{r} = \mathbf{r}_1$ is integrable. The second equation is obtained by differentiating eq. (I.79) in the direction $\hat{n} = \hat{n}(\mathbf{r})$ of the outwards normal towards the point \mathbf{r} and then allowing \mathbf{r} to lie on S :

$$2 \frac{\partial}{\partial n} V^i(\mathbf{r}) = \frac{\partial}{\partial n} V(\mathbf{r}) + \frac{1}{2\pi} \int_S^* \frac{\partial}{\partial n_1} V(\mathbf{r}_1) \frac{\partial}{\partial n} \left(\frac{e^{ikR}}{R} \right) dS, \quad (\mathbf{r}, \mathbf{r}_1 \in S), \quad (I.81)$$

where the asterisk denotes the taking of the Cauchy principal value at $\mathbf{r} = \mathbf{r}_1$. The

kernel is no longer singular at $\mathbf{r} = \mathbf{r}_1$ and is continuous as $\mathbf{r} \rightarrow \mathbf{r}_1$. Eq. (I.81) is particularly useful for existence and uniqueness theorems (MULLER [1952]), and is also amenable to solution by iteration.

For a hard body ($\partial V/\partial n = 0$ on S), eq. (I.78) reduces to

$$V(\mathbf{r}) = V^i(\mathbf{r}) + \frac{1}{4\pi} \int_S V(\mathbf{r}_1) \frac{\partial}{\partial n_1} \left(\frac{e^{ikR}}{R} \right) dS, \quad (\text{I.82})$$

and as in the previous case, two integral equations can be derived for the unknown field on S . For the first of these, \mathbf{r} is allowed to approach S to give

$$2V^i(\mathbf{r}) = V(\mathbf{r}) - \frac{1}{2\pi} \int_S^* V(\mathbf{r}_1) \frac{\partial}{\partial n_1} \left(\frac{e^{ikR}}{R} \right) dS, \quad (\text{I.83})$$

where the asterisk again denotes the Cauchy principal value. The kernel is continuous at $\mathbf{r} = \mathbf{r}_1$. The second equation follows as in the corresponding Dirichlet case and is

$$4\pi \frac{\partial}{\partial n} V^i(\mathbf{r}) = - \frac{\partial}{\partial n} \int_S V(\mathbf{r}_1) \frac{\partial}{\partial n_1} \left(\frac{e^{ikR}}{R} \right) dS, \quad (\mathbf{r}, \mathbf{r}_1 \in S). \quad (\text{I.84})$$

Since the derivative $\partial/\partial n$ cannot be taken inside the integral, eq. (I.84) is actually an integrodifferential equation.

In the electromagnetic problem in which the field $(\mathbf{E}^i, \mathbf{H}^i)$ is incident on S , the derivation of integral equations again proceeds from a representation of the total field in the source-free region surrounding S (STRATTON [1941]):

$$\mathbf{E}(\mathbf{r}) = \mathbf{E}^i(\mathbf{r}) + \frac{1}{4\pi} \int_S \left\{ ikZ(\hat{\mathbf{n}}_1 \wedge \mathbf{H}) \frac{e^{ikR}}{R} + (\hat{\mathbf{n}}_1 \wedge \mathbf{E}) \wedge \nabla \left(\frac{e^{ikR}}{R} \right) + (\hat{\mathbf{n}}_1 \cdot \mathbf{E}) \nabla \left(\frac{e^{ikR}}{R} \right) \right\} dS \quad (\text{I.85})$$

$$\mathbf{H}(\mathbf{r}) = \mathbf{H}^i(\mathbf{r}) - \frac{1}{4\pi} \int_S \left\{ ikY(\hat{\mathbf{n}}_1 \wedge \mathbf{E}) \frac{e^{ikR}}{R} - (\hat{\mathbf{n}}_1 \wedge \mathbf{H}) \wedge \nabla \left(\frac{e^{ikR}}{R} \right) - (\hat{\mathbf{n}}_1 \cdot \mathbf{H}) \nabla \left(\frac{e^{ikR}}{R} \right) \right\} dS \quad (\text{I.86})$$

in which the differentiation is with respect to the coordinates of the surface point \mathbf{r}_1 .

If the body is perfectly conducting, an integral equation for the surface current density $\mathbf{J} = \hat{\mathbf{n}} \wedge \mathbf{H}$ follows immediately from eq. (I.86) and is (MAUE [1949]):

$$2\hat{\mathbf{n}}(\mathbf{r}) \wedge \mathbf{H}^i(\mathbf{r}) = \mathbf{J}(\mathbf{r}) - \frac{1}{2\pi} \int_S \hat{\mathbf{n}}(\mathbf{r}) \wedge \left\{ \mathbf{J}(\mathbf{r}_1) \wedge \nabla \left(\frac{e^{ikR}}{R} \right) \right\} dS, \quad (\mathbf{r}, \mathbf{r}_1 \in S). \quad (\text{I.87})$$

An alternative form of Maue's integral equation is

$$4\pi \hat{\mathbf{n}}(\mathbf{r}) \wedge \mathbf{E}^i(\mathbf{r}) = -ikZ \int_S \left\{ \hat{\mathbf{n}}(\mathbf{r}) \wedge \mathbf{J}(\mathbf{r}_1) \frac{e^{ikR}}{R} - \frac{1}{k^2} (\nabla \cdot \mathbf{J}(\mathbf{r}_1)) \hat{\mathbf{n}}(\mathbf{r}) \wedge \nabla \left(\frac{e^{ikR}}{R} \right) \right\} dS, \quad (\mathbf{r}, \mathbf{r}_1 \in S), \quad (\text{I.88})$$

where $\nabla^s \cdot$ is the surface divergence operator at \mathbf{r}_1 . Analogous equations for surfaces at which an impedance boundary condition is fulfilled have been derived by MITZNER [1967].

1.2.11. Separation of variables

The solution V of the scalar wave eq. (I.17) can be considered as a function of any system of orthogonal curvilinear coordinates u_1, u_2, u_3 . There is a limited set of coordinate systems in which one can find a set of particular solutions V that can be expressed as products of three functions:

$$V(u_1, u_2, u_3) = V_1(u_1) V_2(u_2) V_3(u_3), \quad (\text{I.89})$$

where $V_i(u_i)$ ($i = 1, 2, 3$) is a function of u_i only, and satisfies a second-order ordinary differential equation. The general solution of eq. (I.17) is a linear combination of the separated solutions (I.89). There are eleven separable coordinate systems for the scalar wave equation: the triaxial ellipsoidal coordinates and their ten degenerate forms; the coordinate surfaces are confocal quadric surfaces or their degenerate forms (for details see, for example, MORSE and FESHBACH [1953; Chapter 5]; MOON and SPENCER [1961]).

In passing from the partial differential eq. (I.17) to the three ordinary differential equations with independent variables u_1, u_2, u_3 by means of the substitution (I.89), two separation constants λ_1 and λ_2 are introduced. The separated solution takes one of the following six forms:

$$V = V_1(u_1; k, \lambda_1, \lambda_2) V_2(u_2; \lambda_1) V_3(u_3; \lambda_2) \quad (\text{I.90})$$

for rectangular Cartesian and circular cylinder coordinates;

$$V = V_1(u_1; k, \lambda_1) V_2(u_2; \lambda_1, \lambda_2) V_3(u_3; \lambda_2) \quad (\text{I.91})$$

for spherical coordinates;

$$V = V_1(u_1; k, \lambda_1) V_2(u_2; \lambda_1, \lambda_2) V_3(u_3; \lambda_1, \lambda_2) \quad (\text{I.92})$$

for parabolic cylinder coordinates;

$$V = V_1(u_1; \lambda_1) V_2(u_2; k, \lambda_1, \lambda_2) V_3(u_3; k, \lambda_1, \lambda_2) \quad (\text{I.93})$$

for elliptic cylinder, prolate spheroidal, oblate spheroidal and parabolic coordinates;

$$V = V_1(u_1; k, \lambda_1, \lambda_2) V_2(u_2; \lambda_1, \lambda_2) V_3(u_3; \lambda_1, \lambda_2) \quad (\text{I.94})$$

for conical coordinates;

$$V = V_1(u_1; k, \lambda_1, \lambda_2) V_2(u_2; k, \lambda_1, \lambda_2) V_3(u_3; k, \lambda_1, \lambda_2) \quad (\text{I.95})$$

for paraboloidal and ellipsoidal coordinates.

With respect to the separation constants, the solution V is completely separable in cases (I.90) and (I.91), due to the high degree of symmetry in the coordinate systems; it is only partially separable in cases (I.92) and (I.93), and it is nonseparable in cases (I.94) and (I.95).

The allowed values for the separation constants may form a discrete or a continuous spectrum, and are to be determined by imposing the boundary conditions for the specific problem on hand. Thus, for example, the field scattered from a circular cylinder must be periodic with period 2π in the azimuthal variable ϕ , and this requirement restricts the separation constant λ_1 to integer values $\lambda_1 = 0, \pm 1, \pm 2, \dots$. The spectrum for the other separation constant, λ_2 , is determined by the type of primary field; for a plane wave incident at an angle α with the cylinder axis, only the value $\lambda_2 = k \cos \alpha$ is allowed; for a point source, λ_2 can be any real number.

The general solution of eq. (I.17), which is a linear combination of all the separated solutions (I.89) that correspond to different values of λ_1 and λ_2 , is represented by a double infinite series if both λ_1 and λ_2 have discrete spectra, by a double integral if both λ_1 and λ_2 have continuous spectra, and by an infinite series of single integrals if one spectrum is discrete and the other continuous; only in particular cases will the general solution be represented by a single infinite series or a single definite integral.

The combination constants that appear in the general solution of eq. (I.17) are found by imposing the boundary and radiation conditions. The explicit determination of these constants is possible for all scatterers whose surface is a coordinate surface in any of the eleven separable coordinate systems, provided that the scatterer is either perfectly soft or perfectly hard. If the scatterer is penetrable to the radiation, or if it has a finite, nonzero surface impedance, then the explicit determination of the combination constants is straightforward only if the separated solutions (I.89) are completely separable for the separation constants λ_1 and λ_2 , i.e. in cases (I.90) and (I.91); for the other eight coordinate systems, the explicit solution of the boundary value problem requires the inversion of an infinite matrix or the solution of an integral equation.

The particular case in which $k = 0$ in eq. (I.17) gives the Laplace equation $\nabla^2 V = 0$. In two-dimensional problems, the Laplace equation separates in any coordinate system which is obtained by conformal mapping from the rectangular Cartesian system (x, y) . In three dimensions, the Laplace equation obviously separates in the eleven coordinate systems for which the scalar wave equation separates. In addition, however, there are some coordinate systems in which any separated solution of Laplace's equation is of the form

$$V(u_1, u_2, u_3) = \frac{V_1(u_1) V_2(u_2) V_3(u_3)}{B(u_1, u_2, u_3)}, \quad (I.96)$$

where B , the so-called modulation factor, is independent of the separation constants λ_1 and λ_2 and can therefore be factored outside the summations over the allowed values of λ_1 and λ_2 in writing the general solution of $\nabla^2 V = 0$. The Laplace equation in three dimensions separates in the sense of eq. (I.96) in all the cyclidal coordinate systems, which include the ellipsoidal coordinates and all their degenerate forms; the coordinate surfaces are confocal cyclides. In particular two important coordinate systems in which the Laplace equation separates with a modulation factor B that is not identically equal to unity are the toroidal and the bispherical coordinates.

The vector wave equation

$$(\nabla^2 + k^2)\mathbf{F} = 0 \quad (\text{I.97})$$

could be solved by taking three solutions of the scalar wave equation (I.17) as the three rectangular components of the vector \mathbf{F} , and in this sense eq. (I.97) would be separable in the same eleven coordinate systems in which eq. (I.17) is separable; in most cases, however, it would then become impossible to fit the boundary conditions. In the following, therefore, we consider the separability of eq. (I.97) only in the restricted sense of HANSEN [1935] and STRATTON [1941] (see also SENIOR [1960c]).

The solution \mathbf{F} of eq. (I.97) can always be written as the sum of a longitudinal part

$$\mathbf{L} = \nabla\Phi \quad (\text{I.98})$$

and of a transverse part

$$\mathbf{T} = \nabla \wedge \mathbf{A}. \quad (\text{I.99})$$

Consider a system of orthogonal curvilinear coordinates u_1, u_2, u_3 with metric coefficients h_1, h_2, h_3 defined as in Appendix C, and for which the scalar wave equation is separable. Suppose that the surface of the scatterer is described by $u_1 = \alpha$, where α is a constant. The transverse part \mathbf{T} can be derived from two scalar fields, and in order to satisfy the boundary conditions it is convenient to choose these two scalar functions so that the partial field derived from one scalar is tangential to the surface $u_1 = \alpha$, whereas the partial field derived from the other scalar is perpendicular to $u_1 = \alpha$. This is possible if one of the metric coefficients is unity, and if the ratio of the other two metric coefficients is independent of the coordinate corresponding to the unity metric coefficients; these conditions are met by six of the eleven coordinate systems for which eq. (I.17) is separable: rectangular Cartesian coordinates; circular, elliptic and parabolic cylinder coordinates; spherical and conical coordinates (see MORSE and FESHBACH [1953; Chapter 13]). For these six coordinate systems, the solution \mathbf{F} of eq. (I.97) may be written as the sum of three vectors $\mathbf{L}, \mathbf{M}, \mathbf{N}$, with \mathbf{L} given by eq. (I.98) and

$$\mathbf{M} = \nabla(f\Phi_1) \wedge \hat{\mathbf{u}}_1, \quad (\text{I.100})$$

$$\mathbf{N} = kf\Phi_2\hat{\mathbf{u}}_1 + k^{-1}\nabla\left[\frac{\partial}{\partial u_1}(f\Phi_2)\right], \quad (\text{I.101})$$

where Φ, Φ_1 and Φ_2 are solutions of the scalar wave equation, $f = 1$ for the rectangular and the three cylindrical coordinate systems (with u_1 as the coordinate varying along the cylinder generators), and $f = r$ ($u_1 = r$ is the radial distance from the origin of coordinates) for the spherical and conical systems.

Of course, solutions can also be found to certain vector problems which, because of their symmetry, reduce to the solution of a scalar wave equation in one of the eleven coordinate systems in which it is separable. For an extension of the Hansen-Stratton vector wave function method to spherically inhomogeneous media, see e.g. MARCUVITZ [1951], TAI [1958] and GUTMAN [1965].

Finally, we observe that for certain scatterers whose boundary extends only to a portion of a coordinate surface (such as a thin-walled semi-infinite circular pipe), a rigorous solution can be obtained by combining separation of variables and function-theoretic methods (see Section I.2.14.3).

I.2.12. *Low frequency methods*

The first attempt to obtain low-frequency solutions of the steady-state wave equation from the solutions of the corresponding static problems is due to STRUTT, Lord Rayleigh [1897]; a comprehensive survey of Strutt's contributions to scattering theory is presented by TWERSKY [1964]. In general, the term "Rayleigh scatterer" is applied to a body whose characteristic dimensions are small compared to the wavelength, but authors often disagree with one another on the precise definition. Thus, for example, to BORN and WOLF [1959] a Rayleigh scatterer is one that does not change the frequency of the incident field in forming the scattered field, whereas to other authors it is one whose scattered far field is linearly polarized, or is proportional to k^2 . For our purposes a satisfactory definition of Rayleigh scattering has been given by KLEINMAN [1965a]: for a given scatterer, the "Rayleigh region" is that range of values of k for which the quantity of interest, e.g. the scattered far field, can be expanded in convergent series in positive integral powers of k . For three-dimensional scattering by smooth finite objects, such series exist and have finite radii of convergence, as proved by KLEINMAN [1965b] in the scalar case and by WERNER [1963] in the electromagnetic case. These expansions are known as "Rayleigh series", or "quasi-static series", or "low-frequency expansions".

In keeping with Rayleigh's original work, some authors restrict the Rayleigh region to the wavelength range in which the Rayleigh series is not only convergent but is well approximated by its first term. To this order, the backscattering cross section of a thin, elongated, perfectly conducting body of revolution on which a plane electromagnetic wave is axially incident is

$$\sigma = \frac{4}{\pi} k^4 V^2, \quad (\text{I.102})$$

where V is the volume of the body. As the body is made less elongated, the approximation (I.102) becomes worse; however, it can be improved somewhat by multiplying the right-hand side of (I.102) by a shape factor (SIEGEL [1959]). and anyhow, eq. (I.102) is in error by only 27 percent for a sphere.

In the scalar case, the determination of the low-frequency expansion by the extension of Rayleigh's method consists of two steps: the terms of the expansion are found for the near field, and then they are continued into the far field. The details of this procedure may be found, for example, in NOBLE [1962] and KLEINMAN [1965a]. When applied to soft (hard) scatterers, the method consists of a series of steps which require the solution of the same Dirichlet (Neumann) potential problem, but with different boundary values at each step. This inconvenience has been eliminated in a new method developed by KLEINMAN [1965b] (see also AR and KLEINMAN [1966]),

which produces successive terms iteratively, without requiring the solution of a new problem at each step.

In both Rayleigh's and Kleinman's methods, the solution of the potential problem, i.e. the static Green's function for the scatterer under consideration, must be known. For a limited number of shapes, potential problems can be solved by separation of variables (see Section 1.2.11). DARLING (1960) has proposed a method of solving potential problems for surfaces which are intersections of separable surfaces, and DARLING and SENIOR [1965] have applied it to a spherically-capped cone.

The extension of Rayleigh's method to electromagnetic scattering by penetrable three-dimensional bodies was performed by STEVENSON [1953a]; a detailed account may be found in VAN BLADEL [1964; Sections 9.4 through 9.6]. The calculations required for obtaining each successive term in the low-frequency series, however, rapidly become so intolerable (see, for example, STEVENSON [1953b]) that Stevenson's technique does not seem to have been employed in deriving more than three terms. KLEINMAN [1965c, 1967] has achieved some simplification and removed some of the ambiguities in Stevenson's work. Low frequency electromagnetic scattering by two-dimensional bodies has been studied by VAN BLADEL [1963].

The extension of the method of KLEINMAN [1965b] to two-dimensional scalar problems as well as to electromagnetic problems might possibly be achieved by combining it with an extension of a variational approach due to SCHIFFER [1957]; however, no results are presently available. A survey of low-frequency scattering for both scalar and vector problems has been given by KLEINMAN [1965a].

1.2.13. *High frequency methods*

The relationship between ray optics and wave propagation was well understood after the works of Huygens in 1690 and of Fresnel in 1818, and the connection between electromagnetism and optics was established by Maxwell in 1873. For a rigorous and extensive discussion of these and related matters, the reader should see the books by BATEMAN [1915], LUNEBURG [1944], BAKER and COPSON [1950], BORN and WOLF [1959], SOMMERFELD [1954], and KLINE and KAY [1965].

When the wavelength is small compared with the characteristic dimensions of the scattering body, asymptotic high-frequency methods must be employed. This is true even if the solutions of scattering problems can be written exactly as series of eigenfunctions, because at high frequencies the convergence properties of these series are generally very poor.

For a given scatterer, it is intuitive that as the wave number k tends to infinity, the scattered field tends to the values predicted by the simple laws of geometrical optics. It is on this observation that the methods of geometrical and physical optics and the geometrical theory of diffraction are based. In that portion of space which is illuminated by the primary wave, one would expect the scattered field to be given by the geometric optics value plus higher-order correction terms; indeed, starting from the wave equation, it is possible to derive a complete asymptotic expansion in inverse powers of k , the so-called Luneburg-Kline expansion, whose leading term is

the geometric optics field. The transition region between light and shadow, or penumbra region, near the surface of a smooth opaque convex body has been investigated in detail by Fock. A different high-frequency method, known in its original form as the Watson transformation, is applicable to those canonical shapes for which an exact solution to the scattering problem is available. All these techniques are outlined in the following subsections; for general surveys, see also KOUYOUMJIAN [1965] and FELSEN [1964].

1.2.13.1. GEOMETRICAL OPTICS

In geometrical optics, the propagation of energy between two points Q and P occurs according to Fermat's principle that the optical distance between Q and P must be stationary; in particular, therefore, the optical rays in a homogeneous isotropic medium are straight lines. The variation of the intensity of the geometric optics field along a ray is dictated by energy conservation: the energy flux in a tube of rays must be the same at all points along the tube. Let us consider the vector case, and specifically the electric field E ; with reference to Fig. 1.1, we have that

$$|E(P)| = |E(Q)| \sqrt{\frac{dS_Q}{dS_P}}, \quad (1.103)$$

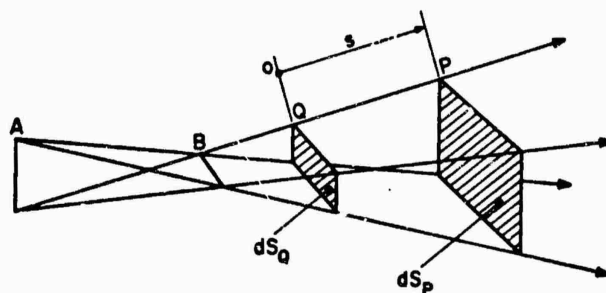


Fig. 1.1. Astigmatic tube of rays.

where dS_Q and dS_P are the cross sections of the elementary tube of rays at Q and P respectively, and are inversely proportional to the Gaussian curvature of the wavefront. Thus, if we denote by s the oriented distance of the observation point P from a fixed origin Q , and by $\rho_1 = AQ$ and $\rho_2 = BQ$ the distances of the astigmatic lines A and B from Q , and if in addition we assume that the polarization of E is unchanged along the ray, then

$$E(P) = E(Q) \sqrt{\frac{\rho_1 \rho_2}{(\rho_1 + s)(\rho_2 + s)}} e^{iks}. \quad (1.104)$$

This geometric optics result yields an infinite value of the field at the caustics A and B , where either $\rho_1 = -s$ or $\rho_2 = -s$; the field in the vicinity of a caustic has been determined by KAY and KELLER [1954]. Note, however, that formula (1.104) gives the correct phase jump of $\frac{1}{2}\pi$ that occurs when the observer passes through a caustic.

The first problem that arises when a wave is reflected at the surface of a body is the determination of the reflected field at the surface, for a given incident field; we consider the vector case only, since the scalar case is trivial. Let the incident fields be given by

$$\mathbf{E}^i = \mathbf{E}^0 e^{ik\Phi}, \quad \mathbf{H}^i = \mathbf{H}^0 e^{ik\Phi} \quad (\text{I.105})$$

where Φ obeys the eikonal equation $(\nabla\Phi)^2 = 1$, and the incident fields \mathbf{E}^0 and \mathbf{H}^0 at the surface of the body are assumed to be slowly varying functions of coordinates. Let \mathbf{E}^r and \mathbf{H}^r be the reflected fields at the surface of the body. Let $\hat{\mathbf{k}}$, $\hat{\mathbf{k}}_r$, $\hat{\mathbf{n}}$ and θ be respectively the unit vectors representing the directions of propagation along the incident and the reflected rays, the unit normal to the surface oriented from the body into the surrounding space, and the angle of incidence, such that

$$\hat{\mathbf{k}}_r \cdot \hat{\mathbf{n}} = -\hat{\mathbf{k}} \cdot \hat{\mathbf{n}} = \cos \theta. \quad (\text{I.106})$$

The reflected fields at the surface are (Fock [1965; Chapter 8]):

$$\mathbf{E}^r = \frac{-1}{\sin^2 \theta} \{R_1(\mathbf{E}^0 \cdot \hat{\mathbf{n}})(\hat{\mathbf{n}} \cos 2\theta + \hat{\mathbf{k}} \cos \theta) - ZR_2(\mathbf{H}^0 \cdot \hat{\mathbf{n}})\hat{\mathbf{n}} \wedge \hat{\mathbf{k}}\}, \quad (\text{I.107})$$

$$\mathbf{H}^r = \frac{-1}{\sin^2 \theta} \{R_2(\mathbf{H}^0 \cdot \hat{\mathbf{n}})(\hat{\mathbf{n}} \cos 2\theta + \hat{\mathbf{k}} \cos \theta) + YR_1(\mathbf{E}^0 \cdot \hat{\mathbf{n}})\hat{\mathbf{n}} \wedge \hat{\mathbf{k}}\}, \quad (\text{I.108})$$

where R_1 and R_2 are the Fresnel reflection coefficients:

$$R_1 = \frac{\varepsilon' \cos \theta - \sqrt{(\varepsilon'\mu' - \sin^2 \theta)}}{\varepsilon' \cos \theta + \sqrt{(\varepsilon'\mu' - \sin^2 \theta)}}, \quad (\text{I.109})$$

$$R_2 = \frac{\mu' \cos \theta - \sqrt{(\varepsilon'\mu' - \sin^2 \theta)}}{\mu' \cos \theta + \sqrt{(\varepsilon'\mu' - \sin^2 \theta)}}, \quad (\text{I.110})$$

and ε' and μ' are the relative electric permittivity and the relative magnetic permeability of the reflecting body. In particular, for a perfect conductor ($\mu' = 1$, $|\varepsilon'| = \infty$), $R_1 = +1$ and $R_2 = -1$.

The second problem that arises when a wave is reflected at the surface of a body is the determination of the reflected field along the reflected ray as a function of the reflected field at the surface. This problem has been solved by Fock [1965; Chapters 6 and 8] by taking into account the geometry of both the incident wavefront and the reflecting surface at the point of incidence. Fock's general results will not be repeated here; however, a simple formula which is useful in many applications is given in the following.

Consider a scalar point source located at P_0 , such that

$$V^i = \frac{e^{ik(P_0Q)}}{k(P_0Q)} \quad (\text{I.111})$$

is the field incident at Q on the surface of the scatterer. Let ρ_1 be the radius of curva-

ture of the convex scattering surface in the plane of incidence at Q , and let ρ_2 be the radius of curvature in a plane perpendicular to the plane of incidence and containing the normal to the surface at Q . The geometric optics scattered field at a point P along the reflected ray is:

$$V_{g.o.}^s = \mp \frac{\exp \{ik[(P_0 Q) + (QP)]\}}{k(P_0 Q)} \times \left\{ \left[1 + \frac{(QP)}{(P_0 Q)} + \frac{2(QP)}{\rho_1 \cos \theta} \right] \left[1 + \frac{(QP)}{(P_0 Q)} + \frac{2(QP) \cos \theta}{\rho_2} \right] \right\}^{-1}, \quad (1.112)$$

where the upper (lower) sign holds for a perfectly soft (hard) scatterer, and θ is the angle of incidence.

1.2.13.2. KELLER'S THEORY

A significant extension of classical geometrical optics was provided by KELLER [1953, 1958, 1962], who proposed and systematically developed the geometrical theory of diffraction. Keller postulates that along with the usual rays of geometrical optics there exists a class of diffracted rays which accounts for the phenomenon of diffraction. These rays are produced when incident rays hit edges, corners, or vertices of scattering surfaces, or when the incident rays impinge tangentially on smoothly curved boundaries. Diffracted rays may also arise at caustics and foci, or when total reflection takes place. Some of the diffracted rays penetrate into the shadow regions and account for the existence of fields there; other rays modify the field in the illuminated regions. The initial value of the field on a diffracted ray is obtained by multiplying the field on the incident ray at the point of diffraction by an appropriate diffraction coefficient. By hypothesis the diffraction coefficient is determined entirely by the local properties of the field, the media, and the boundary in the immediate neighborhood of the point of diffraction. Away from the diffracting surfaces, the diffracted rays behave just like the ordinary rays of geometrical optics. Since only the local properties near the diffraction points are important, the diffracted ray amplitudes may be determined from the solution of the simplest boundary value problems having these local properties. Such problems are called canonical problems, and many of them are included in this book. Alternatively, experimental measurements on canonical configurations can yield the diffraction coefficients. As in the case of classical geometrical optics, the geometrical theory of diffraction is basically a heuristic theory; nevertheless, the theory has been confirmed in a wide variety of cases by comparison with special problems for which rigorous solutions are available. Because of its similarity to geometrical optics, Keller's method can be expected to yield good results when the wavelength is small compared to the obstacle dimensions. However, it has been found that in many cases the results are useful even for wavelengths as large as the relevant dimensions of the scatterer. An important advantage of the method is that it does not depend on separation of variables or any similar procedure, and it is therefore especially useful for shapes not easily subjected to rigorous treatment.

KELLER [1958] presented his extension of geometrical optics in two equivalent forms. The first is the explicit form, in which the different species of diffracted rays are enumerated and an explicit characterization of each is provided. The second formulation is based upon an extension of Fermat's principle to include discontinuous media and classes of curves which may have arcs on discontinuity surfaces and points on edges or vertices of these surfaces. The equivalence of the two formulations follows from considerations of the calculus of variations. A comprehensive bibliography and a discussion of previous work are also contained in his paper. Later, KELLER [1962] reviewed the ray theory of diffraction with particular attention paid to specific applications and experimental confirmation of the theory. Today the literature concerning Keller's theory, its many applications and refinements, is so extensive that a complete bibliography here is precluded. A detailed summary of the theory is presented by LEWIS and KELLER [1964] with applications to representative problems involving reflection, transmission, and diffraction in homogeneous and inhomogeneous media. KELLER and HANSEN [1965] have provided an exhaustive survey of the theory of high-frequency diffraction by thin screens and other objects with edges, and have compared the results obtained by other methods with those obtained by means of the geometrical theory. For lucid treatments of the theory as applied to diffraction by smooth convex objects, consult the now classic papers of KELLER [1956] and LEVY and KELLER [1959]. In this connection it should be mentioned that diffracted rays on convex surfaces were termed "creeping waves" by FRANZ and DEPPERMAN [1952] and by FRANZ [1954], and this terminology is now widely used. The geometrical theory of diffraction as applied to smooth transparent objects of arbitrary shape is discussed by CHEN [1964], although only scalar fields and two-dimensional problems are considered explicitly. By introducing the concept of complex rays, KELLER and KARAL [1960] have dealt with the excitation of surface waves by a line source above an impedance surface, and they have checked their results against certain special configurations for which exact solutions are available. For an application concerning diffraction by an absorbing infinite strip with arbitrary face impedances, along with experimental data, see BOWMAN [1967]. Recent detailed comparisons of the theory with experiment have been made available by BECHTEL [1965] for finite cones (also included are additional corrections to KELLER's [1960, 1961a] results) and by ROSS [1966] for rectangular flat plates; in both cases the angular variations of the monostatic cross sections are evaluated. See YEE et al. [1968] and FJELSEN and YEE [1968a, b] for treatments concerning geometrical diffraction techniques and their relation to canonical problems with parallel plane-geometries (e.g. the parallel plane waveguide, which is discussed in Section 1.2.14.3).

The simple ray formulation of Keller is restricted to the calculation of fields in regions that exclude the vicinity of caustics, focal points, shadow boundaries, and other transition regions. Within such transition regions – which delimit the domains of existence of the various ray species – more elaborate procedures are required. FJELSEN [1964] has given a comprehensive review of the transition phenomena which cannot be described by simple ray optics. The analytical description of the field in

a transition zone is generally achieved by means of a uniform asymptotic solution, and boundary layer or transverse diffusion techniques, among others, have been extensively employed in this connection. For discussions involving edge diffraction see BUCHAL and KELLER [1960] and WOLFE [1966, 1967]; for treatments involving caustics see BUCHAL and KELLER [1960], KRAVTSOV [1964a, b] and LUDWIG [1966]; for diffraction by smooth convex bodies see BROWN [1966], FOCK and WAINSTAIN [1963], LEWIS et al. [1967], LUDWIG [1967] and ZANDERER [1964a, b; 1967]; and for diffraction by a smooth convex interface between two different media see RULF [1967, 1968].

1.2.13.3. LUNEBURG-RAYLINE EXPANSION

This is a method for obtaining the high-frequency field reflected by an obstacle of arbitrary shape, and can be applied to both scalar and vector problems. Assume that the scalar wave function V , which satisfies the reduced wave equation $(\nabla^2 + k^2)V = 0$, has an asymptotic expansion of the form

$$V \sim e^{ik\Phi} \sum_{n=0}^{\infty} v_n(ik)^{-n}, \quad \text{as } k \rightarrow \infty, \quad (1.113)$$

where the v_n 's are functions of the coordinates of the observation point, but are independent of k . By inserting eq. (1.113) into the wave equation and by equating to zero the coefficient of each power of k , it is found that

$$(\nabla\Phi)^2 = 1, \quad (1.114)$$

$$2\nabla v_n \cdot \nabla\Phi + v_n \nabla^2\Phi = -\nabla^2 v_{n-1}, \quad (n = 0, 1, 2, \dots; v_{-1} = 0). \quad (1.115)$$

The eiconal equation (1.114) determines the phase function Φ , whereas the v_n 's are obtained from eqs. (1.115) by iteration. If s denotes the arc length along an optical ray, that is a curve orthogonal to the wavefronts $\Phi = \text{constant}$, then the solution of eq. (1.115) can be written in the form (LUNEBURG [1944]):

$$v_n(s) = v_n(s_0) \left[\frac{G(s)}{G(s_0)} \right]^{\frac{1}{2}} - \frac{1}{2} [G(s)]^{\frac{1}{2}} \int_{s_0}^s [G(t)]^{-\frac{1}{2}} \nabla^2 v_{n-1}(t) dt, \quad (1.116)$$

where $G(s)$ denotes the Gaussian curvature or, in two dimensions, the ordinary curvature, of the wavefront $\Phi = \text{constant}$ at the point s on a ray. In particular, it is easily seen that v_0 varies along a ray as the inverse of the square root of the cross sectional area of a narrow tube of rays, as was found in Section 1.2.13.1 by energy conservation.

The construction of the asymptotic expansion (1.113) requires the determination of a phase function Φ satisfying eq. (1.114) and of the associated system of optical rays, which are the straight lines orthogonal to the surfaces $\Phi = \text{constant}$. Let us introduce the surface coordinates x_2, x_3 on the wavefront $\Phi = 0$ by means of the two families of lines of curvature of $\Phi = 0$. If s is the distance from $\Phi = 0$ along the oriented normal, then the orthogonal coordinates (s, x_2, x_3) uniquely locate a point, and we may choose $\Phi = +s$ as a solution of eq. (1.113). Thus eq. (1.116) becomes (KELLER et al. [1956]):

$$v_n(s, x_2, x_3) = v_n(s_0, x_2, x_3) \left[\frac{(\rho_2 + s_0)(\rho_3 + s_0)}{(\rho_2 + s)(\rho_3 + s)} \right]^{\frac{1}{2}} - \frac{1}{2} [(\rho_2 + s)(\rho_3 + s)]^{-\frac{1}{2}} \int_{s_0}^s [(\rho_2 + t)(\rho_3 + t)]^{\frac{1}{2}} \nabla^2 v_{n-1}(t, x_2, x_3) dt, \quad (I.117)$$

where $\rho_2(x_2, x_3)$ and $\rho_3(x_2, x_3)$ are the principal radii of curvature of the surface $s = 0$ at the point $(0, x_2, x_3)$, and

$$\begin{aligned} \nabla^2 = & \frac{\partial^2}{\partial s^2} + \left[\frac{1}{\rho_2 + s} + \frac{1}{\rho_3 + s} \right] \frac{\partial}{\partial s} + \\ & + \left(\frac{\rho_2}{\rho_2 + s} \right)^2 \left[\frac{\partial^2}{\partial x_2^2} + \frac{s}{\rho_2(\rho_2 + s)} \frac{\partial \rho_2}{\partial x_2} \frac{\partial}{\partial x_2} - \frac{s}{\rho_3(\rho_3 + s)} \frac{\partial \rho_3}{\partial x_2} \frac{\partial}{\partial x_2} \right] + \\ & + \left(\frac{\rho_3}{\rho_3 + s} \right)^2 \left[\frac{\partial^2}{\partial x_3^2} - \frac{s}{\rho_2(\rho_2 + s)} \frac{\partial \rho_2}{\partial x_3} \frac{\partial}{\partial x_3} + \frac{s}{\rho_3(\rho_3 + s)} \frac{\partial \rho_3}{\partial x_3} \frac{\partial}{\partial x_3} \right]. \end{aligned} \quad (I.118)$$

Observe that v_0 becomes infinite at the points $s = -\rho_2$ and $s = -\rho_3$ on each ray (x_2, x_3) ; the locus of these points is called the caustic surface of the system of rays. On a caustic, the expansion (I.113) is not valid and V is asymptotic to a positive fractional power of k (KAY and KELLER [1954]).

Detailed applications of eqs. (I.113) through (I.118) to various scattering bodies when the primary field is that of point sources, line sources and plane waves are given in KELLER et al. [1956]. The first two terms of the series in eq. (I.113) are given explicitly by SCHENSTED [1955] for the case of a plane wave axially incident on an acoustically hard semi-infinite body of revolution.

Results analogous to eqs. (I.113) through (I.118) have been obtained for Maxwell's equations (KLINE [1951]), and the analogues of eqs. (I.114) and (I.115) are also available for more general linear equations (KLINE [1954]). The first two terms of the asymptotic series for the field reflected by a perfectly conducting semi-infinite body of revolution when the primary field is a plane electromagnetic wave at axial incidence have been derived by SCHENSTED [1955], and are given in the following. The coordinate system is shown in Fig. I.2; s is the distance along a ray from some

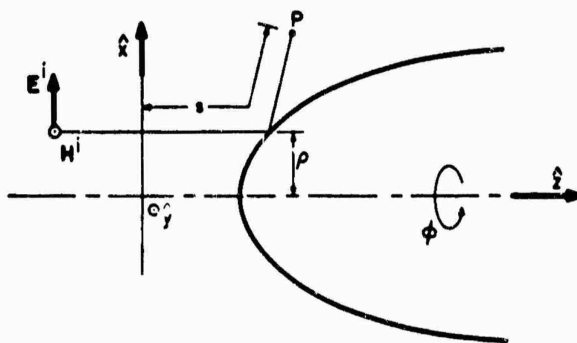


Fig. I.2. Geometry for body of revolution.

reference plane $\Phi = s = 0$ to the field point P, $x_2 = \rho$ is the distance of the incident ray from the axis of symmetry of the body, and $x_3 = \phi$ is the rotational angle about the axis. The incident electric field

$$E^i = \hat{x} e^{iks} \quad (I.119)$$

produces the scattered field

$$E^s \sim e^{iks} [E_0 + E_1 k^{-1} + O(k^{-2})], \quad (I.120)$$

where (SCHENSTED [1955]):

$$E_0 = \left[\frac{\rho}{h_\rho h_\phi} \right]^{\frac{1}{2}} (-\cos \phi \hat{\rho} + \sin \phi \hat{\phi}), \quad (I.121)$$

$$\begin{aligned} E_1 = i \left[\frac{\rho}{h_\rho h_\phi} \right]^{\frac{1}{2}} & \left\{ \left[\frac{1-h_\rho^{-1}}{2f^{(2)}} \left(\frac{1}{8\rho^2} - \frac{f^{(1)}f^{(3)}}{h_\rho(1+f^{(1)2})} \right) + \left(\frac{1-h_\rho^{-1}}{2f^{(2)}} \right)^2 \frac{2f^{(3)} + \rho f^{(4)}}{4\rho} - \right. \right. \\ & - \left. \frac{5}{6} \left(\frac{1-h_\rho^{-1}}{2f^{(2)}} \right)^3 f^{(3)2} - \frac{1}{16\rho f^{(1)}} \right] (1+f^{(1)2})(\cos \phi \hat{\rho} - \sin \phi \hat{\phi}) + \\ & + \left[\frac{f^{(2)}}{2} \left(1 + \frac{f^{(1)2}-1}{h_\rho(f^{(1)2}+1)} \right) - \frac{f^{(1)}}{2\rho} (1-h_\rho^{-1}) - \frac{(5f^{(1)2}+1)(3f^{(1)2}-1)}{16h_\phi f^{(1)}(f^{(1)2}+1)} \right] \cos \phi \hat{\rho} + \\ & + \left[\frac{f^{(2)}}{2} (1-h_\rho^{-1}) - \frac{f^{(1)}}{2\rho} (1+h_\rho^{-1}) + \frac{15f^{(1)2}-1}{16h_\phi f^{(1)}} \right] \sin \phi \hat{\phi} + \\ & + \left. \left[\frac{f^{(3)}(1-h_\rho^{-1})}{2h_\rho f^{(2)}} - \frac{1}{2\rho h_\rho} - \frac{f^{(1)}f^{(2)}}{h_\rho(f^{(1)2}+1)} + \frac{3f^{(1)2}+1}{2h_\phi(f^{(1)2}+1)} \right] \cos \phi \hat{s} \right\}, \quad (I.122) \end{aligned}$$

the equation of the body's surface is $s = f(\rho)$, $f^{(n)}$ is the n -th derivative of $f(\rho)$, the coordinates (x, y, z) and (s, ρ, ϕ) of the observation point are linked by

$$\begin{aligned} x &= \rho \cos \phi + \frac{2f^{(1)}}{f^{(1)2}+1} (s-f) \cos \phi, \\ y &= \rho \sin \phi + \frac{2f^{(1)}}{f^{(1)2}+1} (s-f) \sin \phi, \\ z &= f + \frac{f^{(1)2}-1}{f^{(1)2}+1} (s-f), \end{aligned} \quad (I.123)$$

the two sets of unit vectors are related by

$$\begin{aligned} \hat{s} &= \frac{2f^{(1)}}{f^{(1)2}+1} \cos \phi \hat{x} + \frac{2f^{(1)}}{f^{(1)2}+1} \sin \phi \hat{y} + \frac{f^{(1)2}-1}{f^{(1)2}+1} \hat{z}, \\ \hat{\rho} &= -\frac{f^{(1)2}-1}{f^{(1)2}+1} \cos \phi \hat{x} - \frac{f^{(1)2}-1}{f^{(1)2}+1} \sin \phi \hat{y} + \frac{2f^{(1)}}{f^{(1)2}+1} \hat{z}, \\ \hat{\phi} &= -\sin \phi \hat{x} + \cos \phi \hat{y}, \end{aligned} \quad (I.124)$$

and the metric coefficients are:

$$\begin{aligned} h_s &= 1, \\ h_\rho &= 1 + \frac{2f^{(2)}}{f^{(1)2} + 1} (s-f), \\ h_\phi &= \rho + \frac{2f^{(1)}}{f^{(1)2} + 1} (s-f). \end{aligned} \quad (\text{I.125})$$

When eqs. (I.120) through (I.122) are applied to the paraboloid, the exact scattered field is obtained in closed form (see Chapter 16).

1.2.13.4. PHYSICAL OPTICS

The term "physical optics" denotes an approximate method for the determination of the field scattered by an object through an assumption about the specific form of the field distribution on the surface. Explicitly, it is assumed that the field there is the geometrical optics surface field, implying that at each point on the geometrically illuminated side of the body the scattering at the surface takes place as though from an infinite tangent plane at the point, whereas over the shadowed portion of the body the surface field is zero. For a perfectly conducting body the postulated current distribution is therefore

$$\mathbf{J} = \begin{cases} 2\hat{\mathbf{n}} \wedge \mathbf{H}^i & \text{on the illuminated side, } S_i \\ 0 & \text{on the shadowed side} \end{cases} \quad (\text{I.126})$$

where $\hat{\mathbf{n}}$ is a unit vector normal drawn outwards as regards the body, and when substituted into the exact integral representation of the scattered field, the magnetic vector in (for example) the far field is (KOUYOUMJIAN [1965]).

$$\mathbf{H}^s \approx \frac{ik^2}{4\pi} \frac{e^{ikr}}{kr} \int_{S_i} \{ \hat{\mathbf{n}}(\hat{\mathbf{r}} \cdot \mathbf{H}^i) - (\hat{\mathbf{r}} \cdot \hat{\mathbf{n}})\mathbf{H}^i \} \exp(-ik\hat{\mathbf{r}} \cdot \mathbf{r}_1) dS. \quad (\text{I.127})$$

In contrast to the geometrical optics expression for the scattered field, the integral in eq. (I.127) is frequency dependent, and it is therefore possible that physical optics provides a more accurate estimate of the scattering.

For bodies which are acoustically soft or hard, physical optics is defined in a like manner. Thus, for a soft body such that $V = 0$ at the surface, the postulate of physical optics is

$$\frac{\partial V}{\partial n} = \begin{cases} 2 \frac{\partial V^i}{\partial n} & \text{on the illuminated side of the surface} \\ 0 & \text{on the shadowed side of the surface} \end{cases} \quad (\text{I.128})$$

and similarly, for a hard body such that $\partial V / \partial n = 0$ at the surface, the assumption is

$$V = \begin{cases} 2V^i & \text{on the illuminated side of the surface} \\ 0 & \text{on the shadowed side of the surface.} \end{cases} \quad (\text{I.129})$$

The extension to the case in which the surface is characterized by an impedance boundary condition, with the impedance representing an acoustic rigidity or an electromagnetic surface impedance, is obvious (see, for example, USLENGHI [1964]), and the use of physical optics as a means of estimating the scattering from a dielectric- or plasma-coated body has recently received some attention (BLORE and MUSAL [1965]).

In all of the above cases, physical optics reduces the determination of the scattered field to quadratures, and for perfectly conducting bodies at least, it is probably the most widely used of all methods for estimating the scattering. It is particularly convenient for machine computation, and because of this the recent years have seen a growing tendency to credit physical optics with an accuracy which is in no sense justifiable. It is therefore unfortunate that necessary and sufficient conditions for the validity of the method cannot be stated and, indeed, several of the most fruitful applications have been in circumstances where prior justification would be difficult.

Physical optics is a natural extension of geometrical optics (see Section I.2.13.1) and as such is a high frequency approximation. Given a finite, smooth, perfectly conducting convex body, the geometrical optics estimate of the cross section is

$$\sigma_{g.o.} = \pi R_1 R_2 \quad (I.130)$$

where R_1 and R_2 are the principal radii of curvature at the points of geometrical reflection. The corresponding physical optics integral has a saddle at this point and a steepest descents evaluation retaining only the leading term yields

$$\sigma_{p.o.} = \sigma_{g.o.} \quad (I.131)$$

which is simultaneously the correct leading term in the high frequency asymptotic expansion as derived by the Luneburg-Kline method (see Section I.2.13.3). If a more accurate evaluation of the physical optics integral is attempted, the correction terms may or may not be mathematically correct. Thus, SCHENSTED [1955] has shown that for a smooth body of revolution symmetrically illuminated the first two terms in the asymptotic evaluation of the integral for back scattering are in agreement with the Luneburg-Kline expansion for a perfectly conducting body, but only the first term agrees for a hard body. If the physical optics integral is evaluated exactly, either analytically or numerically, care must be taken to exclude any contribution resulting from the end points of the range of integration corresponding to the shadow boundary. Here, the non-physical discontinuity of the physical optics current gives rise to a contribution which is erroneous and is generally of the same order as any correction to the geometrical optics cross section.

If a body has one (or both) of its radii of curvature infinite at the specular point (as, for example, with a cylindrical section or flat plate), the geometrical optics cross section is infinite, and a particular advantage of the physical optics method is that a bounded (and wavelength dependent) estimate of the scattering cross section can now be obtained. With increasing frequency, this estimate of the specular return becomes more accurate, a fact which can be attributed to the diminishing importance

of the contribution of the current elements in the vicinity of the edges where the postulated current is seriously in error. In contrast to geometrical optics, physical optics also provides a non-zero estimate of the scattering in directions other than the specular one, and if interest is confined to directions which are not too far from specular (through, perhaps, the first side lobe of the pattern), the estimate can be valuable certainly as regards the structure of the pattern. But even here, the predicted cross-polarized component is of the same order as that provided by the error in the specification of the surface field in the vicinity of the edge, and at wider angles of scatter the entire field is erroneous. Indeed, KOUYOUMJIAN [1965] has noted that physical optics in general fails to satisfy the reciprocity theorem everywhere except in the direction of a specular return.

In spite of these shortcomings, physical optics is still an approximation technique of considerable utility that can be expected to provide an accurate estimate of the scattering whenever this arises from a portion of the surface where the actual surface field is adequately approximated by the postulated distribution. In some cases at least we can gauge this in advance. Thus, for example, the physical optics estimate of the axial back scatter from a semi-infinite cone agrees with rigorous calculations for large and small cone angles (SIEGEL et al. [1955]) in spite of the presence of a vertex, and this can be attributed to the fact that the surface within a wavelength or so of the tip contributes little to the scattering (ÜBERALL [1964]); and similarly if the cone is smoothly terminated, the estimated return from the ring singularity at the junction of the cone and the base is in excellent agreement (SENIOR [1965]) with experimental data.

Several possible extensions of the physical optics method have been proposed. It has often been suggested that the accuracy could be improved by successive iteration using the standard physical optics estimate of the scattered field as a first approximation. There seems little (if any) theoretical basis for this belief, however (see, for example, FRANZ [1949], SCHELKUNOFF [1951], BOUWKAMP [1954]), and we are not aware of any case where the numerical accuracy of the estimated scattering has been increased thereby. To remove the non-physical discontinuity in the postulated surface field distribution at the shadow boundary, which discontinuity is one of the major sources of error in the physical optics method, ADACHI [1965] has proposed that for a long thin body at axial incidence, currents be defined over the shadowed portion of the body in exactly the manner as they are for the illuminated portion. The results obtained are in reasonable agreement with experiment, but this is certainly a consequence of the fact that no deep shadow exists under the circumstances described. In cases where a deep shadow does exist, the only rigorously-justifiable continuation of the physical optics distribution is provided by Fock's theory (see Section 1.2.13.5).

1.2.13.5. FOCK'S THEORY

The principle of the local field in the penumbra region established by Fock [1946a] is basic to the analysis of the high-frequency diffraction by a convex, perfectly conducting object with continuously varying curvature. Reasoning from the exact

integral equation for the induced surface current, Fock concluded for high-frequency scattering that the current distribution in the transition region between light and shadow depends only on the local curvature of the body in the plane of incidence and on the incident (locally plane) electromagnetic wave. Fock gave, as an estimate of the width of the penumbra region, the relation

$$d = (\lambda R_0^2 / \pi)^{1/2}, \quad (\text{I.132})$$

where R_0 is the radius of curvature at the geometric optics boundary. He then proceeded to determine a "universal" function for the current near the shadow boundary of a general convex body by considering the particular case of diffraction by a paraboloid of revolution. Fock argued that by virtue of the local nature of the diffraction process, the formula obtained for this particular case would hold for any other convex body having at the point considered the same values of the principal radii of curvature, and that the paraboloid of revolution was sufficiently general to possess any prescribed radii of curvature. The current distribution was derived in terms of a contour integral involving Airy functions and asymptotically gave the physical optics current distribution in the illuminated region and a creeping wave type of current distribution in the shadow region. The Fock theory thus provides the transition from light to shadow for points on the surface of a smooth convex body whose dimensions are large compared to the incident wavelength. The "universal" current distribution in the vicinity of the shadow boundary obtained indirectly by Fock for a locally parabolic surface was later obtained directly by CULLEN [1958] who employed an asymptotic analysis of the exact integral equation.

In a second paper, FOCK [1946b] extended his results (by a different method) to give the field distribution not only on the surface of the body, but also in the neighborhood of the surface. Moreover, the body is no longer assumed to be perfectly conducting, but is regarded as a good conductor in the sense that the Leontovich impedance boundary condition (eq. (I.19)) is imposed on the surface. By means of a physical argument concerning different scales for horizontal and vertical distances, Fock gives a description of the field in the region of the geometrical shadow boundary near the surface in terms of a parabolic differential equation. Again the transition from light to shadow is provided. A collection of Fock's papers is available in English (FOCK [1965]); they are lucid and well worth reading.

In Fock's original formulation, the "universal" current distribution contains a distance parameter that measures distance along the direction of propagation of the incident field rather than along the surface of the body. The difference between these distances is small for observation points near the shadow boundary, but it may become appreciable for locations deep in the shadow region. As suggested by Keller the correct distance parameter is the actual path length measured along the geodesic on the body, and GOODRICH [1959] has provided an exposition of Fock's theory which includes the generalization required to bring the creeping wave interpretation into agreement with Fock's results. LOGAN and YEE [1962] (see also LOGAN [1959]) have performed extensive computations of the "Fock functions", and have provided a

significant unification of the theory. See LOGAN and YEE [1962] also for an extensive bibliography.

WESTON [1965] investigated, by a method akin to that of CULLEN [1958], the modification required when the surface possesses a discontinuity in curvature in the penumbra region. In particular, Weston considers the important case where a plane wave is incident on a cylindrical surface with a flat section smoothly joined to a convex parabolic section, the position of the join coinciding exactly with the shadow boundary. The electric field is assumed polarized perpendicular to the surface. By means of a high-frequency asymptotic analysis the exact integral equation is reduced to a Volterra type which is solvable by standard Laplace transform methods. When the incident plane wave is propagating along the flat portion towards the parabolic section, the surface field in the transition region between the join and deep shadow is expressed in the form of a contour integral involving Airy functions. Deep in the shadow region, the surface field is expressed in terms of the creeping waves launched onto the convex section. Due to the particular geometry near the shadow boundary, the launch weights associated with the creeping waves are different from those obtained in ordinary Fock theory. On the other hand, when the incident plane wave is travelling in the opposite direction such that the parabolic section is in the illuminated region, it is shown that far along the flat section, the total field is comprised of the incident field plus a travelling wave whose magnitude decreases as the square root of the distance from the join.

The significance of WESTON's [1965] paper is that the author has treated a new canonical problem wherein the local geometry of the penumbra region differs in an essential way from previous investigations. The treatment has been extended by HONG and WESTON [1966] to include the case where the join of the flat plane and the parabolic cylinder no longer coincides exactly with the shadow boundary. The new modified Fock function describes the current distribution as a function of two variables: one is the distance between the shadow boundary and the observation point, and the other the distance between the shadow boundary and the join. Both analytical and numerical methods are used to obtain the modified Fock function, and the results are applied to estimate the backscattering cross section of a cone-sphere.

For a smooth convex body of arbitrary shape, HONG [1967] has discussed an integral equation approach which can yield not only the leading term but also successive terms in the asymptotic expansion of the diffracted fields. Hong considers both electromagnetic and acoustic (Neumann boundary condition) diffraction and introduces a geodesic coordinate system to describe the geometry of the diffracting surface, although he assumes that the surface is symmetric with respect to the shadow boundary and that the geodesics are torsion-free (axial incidence on a body of revolution). By means of a high-frequency asymptotic analysis, the exact scalar and vector integral equations governing the surface fields are reduced to one-dimensional Volterra equations which are solved by the use of Fourier transformation. Explicit expressions for the leading and second-order terms are derived for the penumbra and shadow regions. The leading terms are the same as those of FOCK [1946a] for the penumbra

region and those of LEVY and KELLER [1959] for the shadow region. In the solution for the shadow region, the ray convergence factor for the creeping waves, usually obtained by physical reasoning in the geometrical theory of diffraction, is now justified mathematically. Except for the ray convergence factor, the leading term in the shadow is independent of the curvature in the direction transverse to the geodesic. The second order terms in the asymptotic expansion of the surface fields are the new results. These depend on both radii of curvature in a more complicated way, and the effect of transverse curvature on the electromagnetic creeping waves differs from that on the acoustic creeping waves. For an alternative approach based on boundary layer theory see ZANDERER [1964a, b] and BROWN [1966], see also LUDWIG [1967] and ZANDERER [1967].

1.2.13.6. WATSON'S TRANSFORMATION

In the early history of radio propagation, a problem of considerable importance was the determination of the field of a transmitter beyond the line of sight and into the region of geometrical shadow of the earth. The model generally adopted was that of a vertical electric dipole in the presence of a metallic sphere of radius a representing the earth, but due to the extremely large values of a/λ at all frequencies of interest, it was impractical to compute the field from its known expansion in terms of spherical harmonics because of the slow convergence. The difficulty was overcome by WATSON [1918] who used a method related to that of POINCARÉ [1910] and NICHOLSON [1910] to convert the series to a residue series and hence to a contour integral in the complex plane. He then showed that the contour could be deformed so as to enclose a new set of poles and, by evaluating the residue series associated with these new poles, was led to a series which was rapidly convergent for large a/λ . The procedure for converting the original expansion (convenient for small a/λ) to the residue series appropriate for large a/λ is now known as Watson's transformation.

The method can be illustrated by considering the problem of a plane acoustic wave incident on a soft sphere of radius a . In terms of spherical polar coordinates (r, θ, ϕ) with θ measured relative to the backscattering direction, the total field can be written as

$$V = \sum_{n=0}^{\infty} i^n (n + \frac{1}{2}) \left\{ h_n^{(2)}(kr) - \frac{h_n^{(2)}(ka)}{h_n^{(1)}(ka)} h_n^{(1)}(kr) \right\} P_n(-\cos \theta) \quad (1.133)$$

where the spherical Hankel functions and Legendre polynomial are as defined in Sections 1.3.1 and 1.3.5 respectively. The eigenfunction expansion of eq. (1.133) has the alternative representation

$$V = \frac{1}{2} \int_C \left\{ h_v^{(2)}(kr) - \frac{h_v^{(2)}(ka)}{h_v^{(1)}(ka)} h_v^{(1)}(kr) \right\} P_v(-\cos \theta) e^{-\frac{1}{2}i(v-1)\pi} \frac{(v + \frac{1}{2}) dv}{\sin v\pi} \quad (1.134)$$

where C is a path which encloses in a clockwise sense the zeros of $\sin v\pi$ on the positive real axis of the complex v plane (see Fig. 1.3). Since the integrand is an odd function of $(v + \frac{1}{2})$, the lower portion of the path may be reflected in the point $v = -\frac{1}{2}$ to give an

integral over a straight line path from $v = -\infty + i\varepsilon$ to $\infty + i\varepsilon$, $\varepsilon > 0$. If $|\theta - \pi| < \frac{1}{2}\pi - \arccos(a/r)$, i.e. within the geometrical shadow, the integrand is exponentially

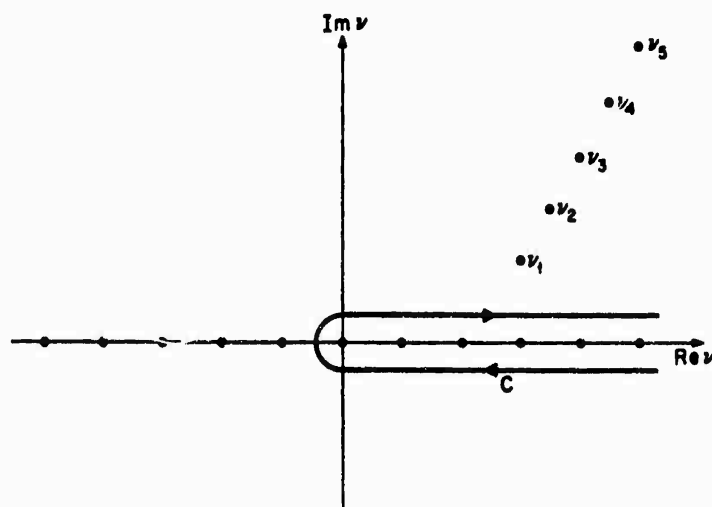


Fig. 1.3. Poles and contour in the complex v plane.

attenuated as $|v| \rightarrow \infty$, $\text{Im } v > 0$. The path can then be closed in the upper half plane and the field expressed as the residue series

$$V = \pi \sum_n \left\{ h_{v_n}^{(2)}(ka) / \left[\frac{\partial}{\partial v} \{ h_v^{(1)}(ka) \} \right]_{v=v_n} \right\} h_{v_n}^{(1)}(kr) P_{v_n}(-\cos \theta) e^{-\frac{1}{2} i v_n \pi} \frac{v_n + \frac{1}{2}}{\sin v_n \pi} \quad (\text{I.135})$$

where the v_n , $n = 1, 2, 3, \dots$ are the zeros of $h_v^{(1)}(ka)$ in the upper half v plane (see Fig. 1.3).

In respect of the dipole problem, WATSON [1918] examined the convergence of the residue series in the shadow and verified the exponential decay observed experimentally. His "proof" of convergence is incorrect in certain details and a valid proof has been given by GOODRICH and KAZARINOFF [1963]. URSELL [1968] has recently investigated the behavior of the series in the shadow region of circular and elliptic cylinders and has shown that there are portions of the shadow where later terms are exponentially large, implying a rate of convergence which is even slower than for the original eigenfunction expansion. It was verified, however, that the convergent residue series is also an asymptotic one, thereby justifying analyses of the field behavior based on the initial terms of the expansion.

When the observation point is outside the shadow region, the original contour integral must be modified before the Watson transformation is applied. The significant extension of Watson's technique necessary in this case, whereby the solution is decomposed into a contour integral (containing the reflected wave) along a path of steepest descent, plus a residue series analogous to that in eq. (I.135), has been credited to White [1922].

A method for obtaining the residue series directly, rather than by transformation

of the harmonic series, was provided by SOMMERFELD [1949]. The method is based on subjecting each radial function to the boundary condition at the surface of the scatterer as well as to the radiation condition at infinity, and was exploited by MARCUVITZ [1951] and FELSEN [1957] to provide alternative field representations for the Green's functions appropriate to various radial and angular domains. Whereas the angular eigenfunction expansion is convenient at lower frequencies, the expansion in terms of the radial eigenfunctions is effective at higher frequencies. A detailed application of the direct method to a study of propagation in radially inhomogeneous media was provided by FRIEDMAN [1951], and the validity of the method in general has been discussed by PFLUMM [1960], COHEN [1964, 1965] and FISCHER [1966]. The completeness of the (orthogonal) radial functions, and sufficient conditions for such expansions to exist, are still open questions.

As demonstrated by GOODRICH [1959], the results obtained from the Watson transformation when the zeros and residues of the Hankel functions are asymptotically approximated for large ka are equivalent to those provided by Fock theory. The application of the Watson technique to potential scattering in quantum mechanics has been considered by REGGE [1959]; see NEWTON [1964, 1966] for an extensive review and bibliography.

The complex poles of the residue series are variously named after Watson, Sommerfeld or Regge. In acoustic scattering by soft or hard bodies, or electromagnetic scattering by perfectly conducting shapes, these poles are the roots $v = v_n$, $n = 1, 2, 3, \dots$, of the equations

$$H_v(z) = 0, \quad \frac{\partial}{\partial z} H_v(z) = 0,$$

$$\frac{\partial}{\partial z} [z^{\pm \frac{1}{2}} H_v(z)] = 0,$$

where $H_v(z)$ is the cylindrical Hankel function of the first or second kind. A more general version of these equations is

$$\frac{\partial}{\partial z} H_v(z) + i\eta H_v(z) = 0$$

where, for example, η may represent a surface impedance. Detailed studies of the locations of these zeros and their trajectories in the complex plane have been made by MAGNUS and KOTIN [1960], LOGAN and YEE [1962], KELLER et al. [1963], STREIFER [1964] and COCHRAN [1965].

1.2.14. Other methods

1.2.14.1. CONFORMAL MAPPING

The exact solution of two-dimensional scattering problems is known only for a few simple shapes of the cylinder cross section, such as those treated in Part One of this book. For more general shapes, various approximation methods have been developed which, in the high frequency limit, require a certain degree of smoothness of the

boundary (usually, the continuity of the curvature). The special cases of a wedge-type singularity and of a discontinuity in the curvature were considered by KELLER [1961b] and WESTON [1962], respectively.

Certain types of singularities of the boundary can be handled by mapping that region of the plane which is external to the cylinder cross section into another region with a geometrically simpler boundary. Such a conformal transformation preserves the right angle between the direction of propagation of the wave and the wavefront. Moreover, the order of the singularity of the mapping function on the boundary is proportional to that of the geometry of the boundary itself (WARSHAWSKI [1935]). The scattered field satisfies a transformed wave equation and boundary conditions, whereas the radiation condition remains invariant; this transformed boundary value problem can be formulated in terms of a Fredholm integral equation of the second kind governing the transformed scattered field (GARABEDIAN [1955]). Detailed applications to a soft cylinder have been made by HONG and GOODRICH [1965], who have solved Garabedian's equation by successive approximations under the hypotheses that both original and transformed boundaries have continuous tangents and that the distance between the two curves is sufficiently small compared to the wavelength. HONG and GOODRICH [1965] have considered two problems: the scattering of a plane wave by an almost circular cylinder with smooth periodic corrugations, in which case they found the result previously obtained with a different method by CLEMMOW and WESTON [1961], and the scattering of a plane wave by a cylinder whose cross section has a finite number of edges, i.e. points of discontinuity in the curvature or in a derivative of the curvature of the boundary. An application of conformal mapping to the scattering by an elliptic cylinder has been given by UDAGAWA and MIYAZAKI [1965].

1.2.14.2. VARIATIONAL TECHNIQUES

The scattered field in both scalar and vector cases can always be expressed as an integral involving the value of the field at the surface of the scatterer (see Section 1.2.10). The problem is thus reduced to the solution of an integral equation for the field at the boundary; unfortunately, this does not diminish the difficulty of finding the solution. There is, however, an advantage in the integral equation formulation, in that it enables one to construct stationary expressions for many quantities of interest; thus, for example, the first-order variation of the far field coefficient is zero with respect to similar variations of the field at the surface of the scatterer.

The principle of Schwinger is based on a remark due to VOLTERRA [1884] that an integral equation can be formulated as a variational principle. Schwinger's principle can be applied to both scalar and vector problems, and is outlined in the following (see JONES [1955a]). Consider the inhomogeneous equation

$$Lg = f \quad (1.136)$$

where L is a linear symmetric operator, such as $(\nabla^2 + k^2)$, f is a function determined by the incident field, and g can be regarded as a distribution of secondary sources.

Equation (I.136) is supposed to have a unique solution. The far field coefficient S may be written as

$$S = (f_0, g) = \int f_0(r)g(r)dr \quad (\text{I.137})$$

where f_0 corresponds to a suitable incident field, and the integral is over the secondary sources, e.g. it extends to the aperture area in the scattering from an aperture in an opaque screen, or to the surface of the scatterer in the scattering from an opaque body. If g_0 is such that

$$Lg_0 = f_0 \quad (\text{I.138})$$

then one has the reciprocity theorem

$$S = (f_0, g) = (f, g_0) \quad (\text{I.139})$$

from which it follows that

$$S = \frac{(f_0, g)(f, g_0)}{(g, Lg_0)} \quad (\text{I.140})$$

it can be proven that the necessary and sufficient condition for eqs. (I.136) and (I.138) to be satisfied is that expression (I.140) be stationary for small independent variations of g and g_0 about their correct values: this is Schwinger's principle.

The essence of this method is that if a good approximation for the field is inserted in the variational expression, an improved approximation for S should result. LEVINE and SCHWINGER [1948b] expanded the field in a set of functions and solved the set of linear algebraic equations for the unknown coefficients which is obtained from the variational principle; JONES [1955a] has shown that his technique is equivalent to solving an integral equation by Galerkin's method. Another approach consists in inserting in the variational expression an approximation for the field which is mathematically simple and physically plausible. Both ways of approximation satisfy the reciprocity theorem, and it therefore appears that the main function of Schwinger's principle is to ensure that reciprocity is not violated; in fact, the analysis can be carried out directly in terms of reciprocity, without introducing the variational principle (JONES [1955a]).

Other variational principles besides Schwinger's have been developed and applied to the non-self-adjoint problems of scattering theory (see e.g. MACFARLANE [1947], KOHN [1948], ALTSHULER [1958]); often, however, the stationary points obtained are not minima and a convergence theory of successive improvement is lacking. In high-frequency scattering, for example, the works of WETZEL [1957] and KODIS [1958] proved that it is very difficult for a variational method to provide even the first correction term to geometrical optics; thus, this first correction term for the total scattering cross section of a soft circular cylinder as obtained by PAPAS [1950] with the Schwinger variational method is in error by about 30 percent. At the present time, it would appear that only the principle of GARABEDIAN [1955] rests on firm mathematical grounds. For a mathematical survey and criticism of variational methods see DOLPH [1961].

A few boundary value problems which have been solved by variational methods are listed in the following. Two variational principles for the determination of the far field diffracted by an aperture in a plane hard screen when the primary field is a plane harmonic sound wave have been given by LEVINE [1950]. The variational theorem of KORNHAUSER and STAKGOLD [1952] for the scalar wave equation in two dimensions constitutes a rigorous proof that for a perfectly conducting cylindrical wave guide of arbitrary cross section, the dominant mode is always an H -mode. A variational study of the propagation of dominant mode plane sound waves within an open-ended, semi-infinite cylindrical tube of arbitrary cross section is found in LEVINE [1954a]. A variational method for the study of the scattering of plane sound waves by soft obstacles with spherical and circular cylindrical symmetry has been developed by MONTROLL and GREENBERG [1952].

Variational methods for solving various vector boundary value problems have been given by LEVINE [1954b], whereas the case of the vector wave equation describing the field due to an arbitrary source located in the neighborhood of an inhomogeneous absorbing medium has been studied by WAGNER [1963]. New variational principles have been developed by GOBLICK and BEVENSEE [1960] for periodic structures in waveguides, and by TAO [1966] for the fundamental equations of electromagnetism. A monograph devoted to variational methods for cavities and waveguides, and for scattering and radiation problems with conducting boundaries has been published by CAIRO and KAHAN [1962]; see also MORSE and FESHBACH [1953; Section 9.4] and KODIS [1954].

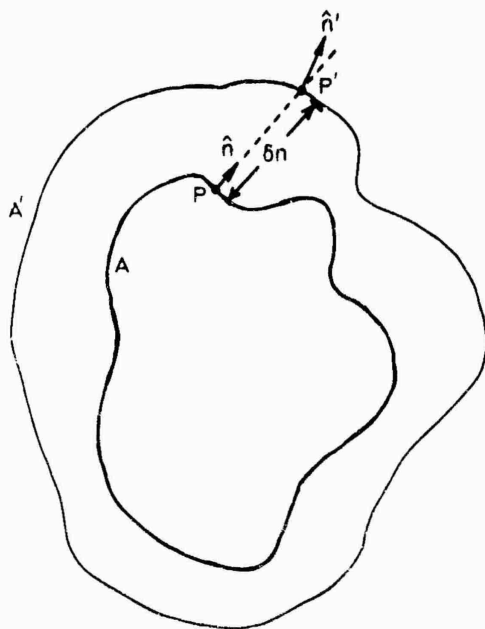
Formulas were derived by FLAMMER [1957] for the first variation of the total scattering cross section, and for the first and second variations of the electric and magnetic dyadic Green's functions under the deformation of the boundary of a conducting body from a form for which the quantities are known; the formulas for the variation of the cross section are given below. Suppose that both the total fields

$$\begin{aligned} E^{(+)} &= \hat{e} e^{i\mathbf{k} \cdot \mathbf{r}} + E^{(+)*}, \\ H^{(+)} &= -\frac{iY}{k} \nabla \wedge E^{(+)} \end{aligned} \quad (1.141)$$

due to a plane wave propagating in the direction \mathbf{k} and incident on a perfectly conducting body with surface A , and

$$\begin{aligned} E^{(-)} &= \hat{e} e^{-i\mathbf{k} \cdot \mathbf{r}} + E^{(-)*}, \\ H^{(-)} &= -\frac{iY}{k} \nabla \wedge E^{(-)} \end{aligned} \quad (1.142)$$

due to a plane wave propagating in the opposite direction $-\mathbf{k}$ and incident on the same body, are known. Suppose that the surface A is deformed by shifting each point \mathbf{P} a small amount $\delta \mathbf{n} = (\mathbf{P}' - \mathbf{P}) \cdot \hat{\mathbf{n}}$ along the outward normal $\hat{\mathbf{n}}$ to a new position \mathbf{P}' , as shown in Fig. 1.4.

Fig. I.4. Geometry for perturbation of surface A .

Such deformation of the scatterer produces a small variation $\delta\sigma_T$ in the total scattering cross section σ_T corresponding to the direction of incidence \hat{k} ; to first order, this variation is:

$$\delta\sigma_T = \text{Im} \left\{ k \iint_A [E^{(+)} \cdot E^{(-)} + Z^2 H^{(+)} \cdot H^{(-)}] \delta n dA \right\}; \quad (\text{I.143})$$

formula (I.143) is valid provided that the normal \hat{n} to A at P and the normal to the deformed surface at P' form a very small angle, and that E and H have continuous first derivatives on both A and the deformed surface. Formula (I.143) simplifies for the two-dimensional problem of broadside incidence on an infinitely long cylinder with generators parallel to an axis z . If E is parallel to z ,

$$E^{(\pm)} = \hat{z} V_e^{(\pm)}, \quad (\text{I.144})$$

then $V_e^{(\pm)} = 0$ on A (soft cylinder), whereas if H is parallel to z ,

$$H^{(\pm)} = \pm Y \hat{z} V_m^{(\pm)}, \quad (\text{I.145})$$

then $\partial V_m^{(\pm)} / \partial n = 0$ on A (hard cylinder); both $V_e^{(\pm)}$ and $V_m^{(\pm)}$ satisfy the scalar wave equation $(\nabla^2 + k^2)V = 0$. The variation $\delta\sigma_T$ of the total scattering cross section per unit length is (see also GARABEDIAN [1955])

$$(\delta\sigma_T)_{\text{soft}} = -\text{Im} \left\{ k^{-1} \int_l \frac{\partial V_e^{(+)}}{\partial n} \frac{\partial V_e^{(-)}}{\partial n} \delta n dl \right\} \quad (\text{I.146})$$

in case (I.144), and

$$(\delta\sigma_T)_{\text{hard}} = \text{Im} \left\{ k^{-1} \int_l [\nabla V_m^{(+)} \cdot \nabla V_m^{(-)} - k^2 V_m^{(+)} V_m^{(-)}] \delta n dl \right\} \quad (\text{I.147})$$

in case (I.145); the line integrals in eqs. (I.146) and (I.147) are taken along the boundary l of the cross section of the scattering cylinder in a plane perpendicular to z .

Finally, applications of variational techniques to the scattering of electromagnetic waves by thin wires of finite length are presented in Chapter 12.

1.2.14.3. FUNCTION-THEORETIC METHODS

Most of the scattering problems treated in this book yield to direct solution by separation of variables with the subsequent application of appropriate series or integral transform techniques. In these "simple" boundary value problems the application of the transform theorem immediately determines the unknown coefficients or functions by algebraic equations. There is, however, an important class of diffraction problems susceptible to closed form solution when the customary transform methods are supplemented by function-theoretic techniques. Perhaps the most widely known technique to be applied to this special class of diffraction problems, and to many other problems in mathematical physics, is that due to WIENER and HOPF [1931] for the Fourier transform in the complex domain, although it is now recognized that the more general method of singular integral equations of the Cauchy type (MUSKHELISHVILI [1953]) contains the Wiener-Hopf method as a special case. The essence of these methods is to reduce the consideration of certain integral equations to the consideration of the Hilbert boundary problem in the theory of analytic functions. The whole apparatus of complex variable theory – the basic tools being analytic continuation, Liouville's theorem, and factorization of analytic functions – thus becomes available to yield new solutions in closed form. Since the literature concerning these very powerful techniques and their application to physical problems is so extensive, we content ourselves with a brief survey of the more important contributions to diffraction theory.

An integral equation of the Wiener-Hopf type has the general form

$$a\psi(x) = f(x) + \int_0^x \psi(x')K(x-x')dx', \quad x > 0 \quad (1.148)$$

where $f(x)$ and $K(x)$ are known functions, and $\psi(x)$ is unknown. The homogeneous case $f(x) = 0$, was first examined by WIENER and HOPF [1931] (see also PALEY and WILNER [1934], TITCHMARSH [1948]), while the theory was extended to the non-homogeneous case $f(x) \neq 0$ by FOCK [1942, 1944]. Integral equations of the type in eq. (1.148) generally arise when boundary conditions are prescribed on semi-infinite structures such as semi-infinite planes or cylinders, and the formulation of such diffraction problems as Wiener-Hopf integral equations is generally attributed to Schwinger (see CARLSON and HEINS [1947]) and independently to COPSON [1946]. For reviews of the Wiener-Hopf theory and bibliography see BOUWKAMP [1954], KARP [1950], HEINS [1956], MORSE and FESHBACH [1953] and NOBLE [1958]. The Wiener-Hopf equation considered as a special case of Cauchy-type singular integral equations is discussed by SPARENBERG [1956], WESTPFAHL [1959] and HÖNL et al.

[1961]. We may note that in practical applications, systems of simultaneous Wiener-Hopf integral equations frequently occur.

The significant feature about eq. (I.148) is the convolution character of the integral. If, in addition, the range of integration and of validity of the equation were $(-\infty, \infty)$, the application of a Fourier transformation would reduce the problem to an algebraic one. Based on this observation, the usual procedure is to extend the domain of definition of eq. (I.148) to embrace all values of x by writing

$$\phi(x) + a\psi(x) = f(x) + \int_{-\infty}^{\infty} \psi(x')K(x-x') dx', \quad -\infty < x < \infty \quad (\text{I.149})$$

with the conventions

$$\begin{aligned} \psi(x) &= 0 & \text{for } x < 0, \\ \phi(x) &= 0 & \text{for } x > 0. \end{aligned} \quad (\text{I.150})$$

Fourier transformation now results in a single equation between two unknown transform functions, both of which are deduced by function-theoretic arguments (factorization, analytic continuation, Liouville's theorem). Rather than enter into these details, however, we shall indicate (following WESTPFAHL [1959]) how integral equations of the Wiener-Hopf type may be reduced to singular integral equations of the Cauchy type.

Let $\bar{K}(\alpha)$ and $\bar{\psi}(\alpha)$ be Fourier transforms defined by

$$\bar{K}(\alpha) = \int_{-\infty}^{\infty} K(x)e^{-i\alpha x} dx, \quad (\text{I.151})$$

$$\bar{\psi}(\alpha) = \int_0^{\infty} \psi(x)e^{-i\alpha x} dx, \quad (\text{I.152})$$

then eq. (I.148) will be satisfied if the *dual* integral equations (TITCHMARSH [1948])

$$\int_{-\infty}^{\infty} \bar{\psi}(\alpha)[\bar{K}(\alpha) - a]e^{i\alpha x} d\alpha = -2\pi f(x), \quad x > 0 \quad (\text{I.153})$$

$$\int_{-\infty}^x \bar{\psi}(\alpha)e^{i\alpha x} d\alpha = 0, \quad x < 0 \quad (\text{I.154})$$

are satisfied. Multiply eqs. (I.153) and (I.154) by $\exp(-i\alpha'x)$ and integrate over $0 < x < \infty$ and $-\infty < x < 0$, respectively. By means of the well-known relations

$$\begin{aligned} \int_0^x e^{-i\alpha x} dx &= 2\pi\delta_-(\alpha) = \pi\delta(\alpha) + P \frac{1}{i\alpha}, \\ \int_{-\infty}^0 e^{-i\alpha x} dx &= 2\pi\delta_+(\alpha) = \pi\delta(\alpha) - P \frac{1}{i\alpha}, \end{aligned} \quad (\text{I.155})$$

where the symbol P denotes the Cauchy principal value, we obtain two singular

integral equations of the Cauchy type

$$-L(\alpha)\bar{\psi}(\alpha) + \frac{1}{\pi i} \text{P} \int_{-\infty}^{\infty} \frac{L(\alpha')\bar{\psi}(\alpha')}{\alpha' - \alpha} d\alpha' = 2f(\alpha), \quad (\text{I.156})$$

$$\bar{\psi}(\alpha) + \frac{1}{\pi i} \text{P} \int_{-\infty}^{\infty} \frac{\bar{\psi}(\alpha')}{\alpha' - \alpha} d\alpha' = 0 \quad (\text{I.157})$$

where $L(\alpha) = \bar{K}(\alpha) - a$ and

$$f(\alpha) = \int_0^{\infty} f(x)e^{-i\alpha x} dx. \quad (\text{I.158})$$

The whole apparatus of singular integral equations (see e.g. MUSKHELISHVILI [1953], GAKHOV [1966], POGORZELSKI [1966]) is now at our disposal to achieve a solution.

We assume that $L(\alpha)$ is holomorphic and non-zero in a strip $|\text{Im } \alpha| < c$ and that the condition $\arg \log L(\alpha)|_{-\infty}^{\infty} = 0$ is satisfied. Basic to the solution is the decomposition of the function $L(\alpha)$ into factors $L^+(\alpha)$ and $L^-(\alpha)$ such that

$$L(\alpha) = L^+(\alpha)/L^-(\alpha) \quad (\text{I.159})$$

with

$$\begin{aligned} L^+(\alpha) &= \exp \left[\frac{1}{2\pi i} \int_{-\infty - ic}^{\alpha - ic} \frac{\log L(\alpha')}{\alpha' - \alpha} d\alpha' \right], \\ L^-(\alpha) &= \exp \left[\frac{1}{2\pi i} \int_{\alpha + ic}^{\infty + ic} \frac{\log L(\alpha')}{\alpha' - \alpha} d\alpha' \right]. \end{aligned} \quad (\text{I.160})$$

The factors $L^+(\alpha)$ and $L^-(\alpha)$ are analytic and non-zero in the half-planes $\text{Im } \alpha > -c$ and $\text{Im } \alpha < c$, respectively. If for $|\alpha| \rightarrow \infty$ we require

$$\begin{aligned} L^+(\alpha) &= O(\alpha^p), & |p| < 1, \\ L^-(\alpha) &= O(\alpha^q), & |q| < 1, \end{aligned} \quad (\text{I.161})$$

then the solution to eqs. (I.156) and (I.157) is (WESTPFAHL [1959]; see also FOCK [1942, 1944])

$$\bar{\psi}(\alpha) = \frac{L^-(\alpha)}{2\pi i} \oint_{-\infty}^{\infty} \frac{f(\alpha')}{L^+(\alpha')} \frac{d\alpha'}{\alpha' - \alpha} + CL^-(\alpha), \quad (\text{I.162})$$

where the "hook" on the integral sign means that the path of integration passes above the pole $\alpha' = \alpha$. By Fourier inversion,

$$\psi(x) = \frac{1}{4\pi^2 i} \int_{-\infty}^x d\alpha' \frac{f(\alpha')}{L^+(\alpha')} \oint_{-\infty}^x L^-(\alpha) e^{i\alpha x} \frac{d\alpha}{\alpha' - \alpha} + \frac{1}{2\pi} C \int_{-\infty}^x L^-(\alpha) e^{i\alpha x} d\alpha, \quad (\text{I.163})$$

where for the α integration the contour passes below the pole at $\alpha = \alpha'$. The term involving the arbitrary constant C represents the homogeneous solution corresponding to $f(x) = 0$. For $0 \leq p < 1$ or $0 \leq q < 1$, the constant C must be set equal to zero and the non-homogeneous solution is then unique.

As a simple example, consider the diffraction of a plane electromagnetic wave

$$E_z^i = \exp \{-ik(x \cos \phi_0 + y \sin \phi_0)\} \quad (\text{I.164})$$

by a perfectly conducting half plane (see Chapter 8) $y = 0, x > 0$. The integral equation for the surface current is (COPSON [1946])

$$\int_0^\infty \psi(x') H_0^{(1)}(k|x-x'|) dx' = -2i \exp(-ikx \cos \phi_0), \quad x > 0 \quad (\text{I.165})$$

and is of Wiener-Hopf type. The corresponding dual integral equations are (CLEMOW [1951])

$$\begin{aligned} \int_{-\infty}^\infty \frac{\bar{\psi}(\alpha)}{\sqrt{(k^2 - \alpha^2)}} e^{i\alpha x} d\alpha &= -2\pi i \exp(-ikx \cos \phi_0), & x > 0 \\ \int_{-\infty}^\infty \bar{\psi}(\alpha) e^{i\alpha x} d\alpha &= 0, & x < 0 \end{aligned} \quad (\text{I.166})$$

and finally we are led to the singular integral equations in eqs. (I.156) and (I.157) with (WESTFAHL [1959])

$$L(\alpha) = (k^2 - \alpha^2)^{-\frac{1}{2}}, \quad \bar{f}(\alpha) = (\alpha + k \cos \phi_0)^{-1} \quad (\text{I.167})$$

where it is assumed that $\text{Im}(\alpha + k \cos \phi_0) < 0$ in order to secure convergence of the integral in eq. (I.158). With the assumption $\text{Im} k > 0$ (later allowed to vanish) the factorization can be performed by inspection; thus

$$L^+(\alpha) = (k + \alpha)^{-\frac{1}{2}}, \quad L^-(\alpha) = (k - \alpha)^{\frac{1}{2}}. \quad (\text{I.168})$$

The branch such that $\text{Im}(k^2 - \alpha^2)^{\frac{1}{2}} > 0$ has been chosen. Since in eq. (I.161) we have $p = -\frac{1}{2}, q = \frac{1}{2}$, the constant C must be zero and the (unique) solution is

$$\bar{\psi}(\alpha) = \frac{(k - \alpha)^{\frac{1}{2}}}{2\pi i} \int_{-\infty}^\infty \frac{(k + \alpha')^{\frac{1}{2}}}{\alpha' + k \cos \phi_0} \frac{d\alpha'}{\alpha' - \alpha}, \quad (\text{I.169})$$

where the path of integration passes below the pole $\alpha' = -k \cos \phi_0$ and above the pole $\alpha' = \alpha$. The contour may be closed by a semi-circle in the upper half α' -plane (encircling the pole $\alpha' = -k \cos \phi_0$) to yield

$$\bar{\psi}(\alpha) = - \frac{(k - \alpha)^{\frac{1}{2}}(k - k \cos \phi_0)^{\frac{1}{2}}}{\alpha + k \cos \phi_0}. \quad (\text{I.170})$$

Introducing cylindrical coordinates (ρ, ϕ) , one can show that for $\rho \rightarrow \infty, \phi \neq \pi \pm \phi_0$ the diffracted field in the far zone is given by

$$E_z^d \sim \frac{\exp(ik\rho - \frac{3}{2}i\pi)}{(2\pi k\rho)^{\frac{1}{2}}} \bar{\psi}(k \cos \phi), \quad (\text{I.171})$$

where from eq. (I.170)

$$\bar{\psi}(k \cos \phi) = - \frac{2 \sin \frac{1}{2}\phi \sin \frac{1}{2}\phi_0}{\cos \phi + \cos \phi_0}. \quad (\text{I.172})$$

This result is in agreement with eq. (8.20) of Chapter 8, and illustrates how the Fourier transform $\bar{\psi}(x)$ is related to the far field amplitude.

It is significant that the method of Wiener and Hopf can be formulated from several different points of view, and many authors have solved the same diffraction problems by means of alternative approaches to the theory. In the earliest applications (e.g. COPSON [1946]) Green's theorem was employed to formulate the boundary value problem as an integral equation for the unknown surface current, and if the equation was of Wiener-Hopf type, Fourier transformation together with function-theoretic considerations in the plane of the transform variable were applied to gain a solution. The approach due to JONES [1952a], and embraced by NOBLE [1958], is to apply a Fourier transformation directly to the partial differential equation before applying the boundary conditions. The complex variable equation in the transform plane is thereby obtained directly without the necessity for formulating an integral equation, although it is then not always obvious whether the transform equations can be reduced to the Wiener-Hopf form. In still another approach, the cumbersome derivation of integral equations is circumvented by employing the method of separation of variables to formulate dual integral equations for quantities related to the far field amplitude. This separation of variables procedure was utilized to full advantage by VAJNSHTEIN [1954] and is expounded by KARP [1950] and by CLEMMOW [1951]. Finally, the method by which certain two dimensional diffraction problems are reduced to singular integral equations of the Cauchy type is treated by WESTPFAHL [1959] and HÖNL et al. [1961]. All of the techniques described here have one main feature in common. At some stage in the solution, a given function of the complex transform variable must be decomposed as in eq. (I.159). For most applications this is the difficult task and can be done by inspection only in certain cases (notably the half plane).

One of the earliest applications of the Wiener-Hopf method to diffraction theory, other than to diffraction by a half plane, concerned the problem of plane wave scattering by an infinite set of staggered, equally spaced, semi-infinite plates (CARLSON and HEINS [1947], HEINS and CARLSON [1947], HEINS [1950]). Concurrently, the radiation and transmission properties of a waveguide consisting of a pair of semi-infinite parallel plates were studied by HEINS [1948] (see also CHESTER [1950]), but a more comprehensive (and simpler) treatment is provided by VAJNSHTEIN [1954]. The problem of scattering of plane waves by a pair of semi-infinite parallel planes is treated by CLEMMOW [1951], while diffraction by a finite set of parallel half planes is investigated by IGARASHI [1964].

It is interesting to compare the field diffracted by two parallel half planes with that diffracted by a single half plane. We consider a plane electromagnetic wave given by eq. (I.164) incident upon two half planes described by $y = \pm a$, $x > 0$ as in Fig. I.5. By combining the results of CLEMMOW [1951] and VAJNSHTEIN [1954], we can write

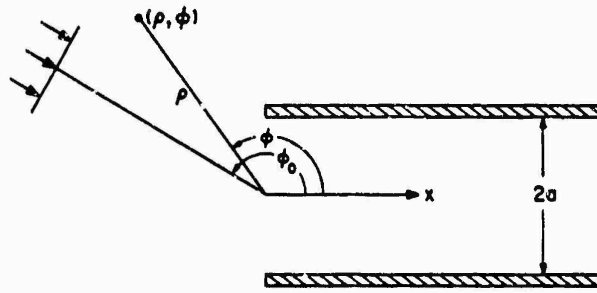


Fig. 1.5. Geometry for parallel plane waveguide.

the far diffracted field ($\rho \rightarrow \infty$) obtained from the exact solution in the following manner: for $0 < \phi_0 < \pi$ and $\phi \neq \pi \pm \phi_0$,

$$E_z^d \sim \frac{\exp(ik\rho + \frac{1}{4}i\pi)}{(2\pi k\rho)^{\frac{1}{2}}} \frac{\sin \frac{1}{2}\phi \sin \frac{1}{2}\phi_0}{\cos \phi + \cos \phi_0} [L_1^+(k \cos \phi) L_1^+(k \cos \phi_0) + \text{sgn}(\sin \phi) L_2^+(k \cos \phi) L_2^+(k \cos \phi_0)] \exp\{-ika(|\sin \phi| + \sin \phi_0)\}, \quad (1.173)$$

where $L_{1,2}^+(\alpha)$ are Wiener-Hopf factorization functions analytic with no zeros in the upper α -plane and defined by

$$\begin{aligned} L_1^+(\alpha) L_1^+(-\alpha) &= 1 + \exp[2ia(k^2 - \alpha^2)^{\frac{1}{2}}], \\ L_2^+(\alpha) L_2^+(-\alpha) &= 1 - \exp[2ia(k^2 - \alpha^2)^{\frac{1}{2}}] \end{aligned} \quad (1.174)$$

with the branch $\text{Im}(k^2 - \alpha^2)^{\frac{1}{2}} > 0$ for $\text{Im} k > 0$. The signum function $\text{sgn}(x)$ is defined as $\text{sgn}(x) = \pm 1$ for $x \gtrless 0$. Clearly eq. (1.173) yields the half plane result in eqs. (1.171) and (1.172) when the separation of the plates $2a$ shrinks to zero. We are interested, however, in the case for which $ka \gg 1$. From VAJNSHTEJN [1954] we have, for instance,

$$L_1^+(k \cos \phi) = \begin{cases} e^V, & \cos \phi > 0 \\ (1 + \exp\{2ika|\sin \phi|\})e^V, & \cos \phi < 0 \end{cases} \quad (1.175)$$

where

$$V = \frac{1}{2\pi i} \int_C \log(1 + \exp\{2ika \cos \tau\}) \frac{\cos \tau d\tau}{\sin \tau - \cos \phi}, \quad (1.176)$$

the contour C starting at $\frac{1}{2}\pi - i\infty$, passing through the origin, and ending at $-\frac{1}{2}\pi + i\infty$. For $ka \gg 1$, VAJNSHTEJN [1954] has shown that a steepest descent approximation yields

$$V \sim \frac{1}{2\pi i} \int_{-\infty}^{\infty} \log(1 + \exp\{2ika - \frac{1}{2}t^2\}) \frac{dt}{t - \sqrt{2ka}e^{i\pi} \cos \phi}, \quad (1.177)$$

and this we can expand in the form

$$V \sim \frac{1}{2} \text{sgn}(\cos \phi) \sum_{m=1}^{\infty} \frac{(-1)^m}{m} e^{2imka} G(\sqrt{\frac{1}{2}mka} |\cos \phi|) \quad (1.178)$$

where

$$G(w) = \frac{2}{\sqrt{\pi}} e^{-2iw^2} \int_{(1-i)w}^{\infty} e^{-\mu^2} d\mu, \quad (I.179)$$

$$|G(w)| < 1 \quad \text{for } w > 0, \quad G(w) = 1 \quad \text{for } w = 0. \quad (I.180)$$

Similar results are obtained for $L_2^+(k \cos \phi)$, except the $(-1)^m$ in eq. (I.178) no longer appears.

It may be noted that the results quoted so far are valid for all ϕ except in the vicinity of the geometrical optics shadow boundary $\phi = \pi + \phi_0$ and the reflection boundary $\phi = \pi - \phi_0$. In these directions the asymptotic expansion in eq. (I.173) would have to be modified, and in the region $\phi < \pi - \phi_0$ the geometrically reflected field would have to be added, to obtain the full scattered field. Let us take, for example, $\cos \phi < 0$, $\cos \phi_0 < 0$ (both source and observer confined to the left half space). Since for $w \rightarrow \infty$,

$$G(w) \sim e^{i\pi}(w\sqrt{2\pi})^{-1}, \quad (I.181)$$

it follows from eq. (I.178) that

$$e^V \sim 1 - \frac{e^{i\pi}}{\sqrt{4\pi ka \cos \theta}} \sum_{m=0}^{\infty} \frac{(-1)^m}{m^{\frac{1}{2}}} e^{2imka} + O\left(\frac{1}{ka}\right) \quad (I.182)$$

with similar results corresponding to $L_2^+(k \cos \phi)$; eq. (I.173) then yields for $ka \gg 1$:

$$\begin{aligned} E_z^d \sim & \sqrt{\frac{2}{\pi k \rho}} e^{ik\rho + i\pi} \frac{2 \sin \frac{1}{2}\phi \sin \frac{1}{2}\phi_0}{\cos \phi + \cos \phi_0} \left\{ \cos [ka(\sin \phi + \sin \phi_0)] + \right. \\ & + \frac{e^{i\pi}}{\sqrt{4\pi ka}} \left(\frac{1}{\cos \phi} + \frac{1}{\cos \phi_0} \right) \sum_{m=0}^{\infty} \frac{e^{i(2m+1)2ka}}{(2m+1)^{\frac{1}{2}}} \cos [ka(\sin \phi - \sin \phi_0)] - \\ & \left. - \frac{e^{i\pi}}{\sqrt{4\pi ka}} \left(\frac{1}{\cos \phi} + \frac{1}{\cos \phi_0} \right) \sum_{m=0}^{\infty} \frac{e^{i(2m)2ka}}{(2m)^{\frac{1}{2}}} \cos [ka(\sin \phi + \sin \phi_0)] + O\left(\frac{1}{ka}\right) \right\}. \end{aligned} \quad (I.183)$$

This result, although simple to derive, does not seem to have appeared in the literature (see, however, BOWMAN and WESTON [1968]). The first term in eq. (I.183) consists of a superposition of edge waves from the two half planes, each in the absence of the other and excited by the incident field alone. The infinite sums correspond to successive interactions between the half planes. These mutual interaction terms may be derived on the basis of ray optics as described in YEE et al. [1968]; however, when the ray optics calculation is carried out, the quantities $(2m+1)^{\frac{1}{2}}$ and $(2m)^{\frac{1}{2}}$ get replaced by $2^{2m}(2m+1)^{\frac{1}{2}}$ and $2^{2m-1}(2m)^{\frac{1}{2}}$, respectively. The simple ray optics result thus underestimates the asymptotic result in eq. (I.183) and would have to be modified to obtain more accurate expressions. For other results concerning ray optical techniques and their relation to canonical problems with parallel plane geometries see FELSEN and YEE [1968a, b].

The Wiener-Hopf method has also been applied to yield solutions to the important problems of scattering and radiation from semi-infinite circular cylinders. LEVINE and SCHWINGER [1948a] (see also JONES [1952a, 1964], MORSE and FESHBACH [1953], NOBLE [1958]) investigated the radiation and reflection of sound waves in an open-ended cylindrical tube, while VAJNSHTEIN [1954] treated the problem in more detail for both acoustic and electromagnetic radiation. The reflection and transmission properties of electromagnetic waves (H_{11} -mode) in an open-ended circular pipe has also been studied intensively by IJIMA [1952], although his report does not seem to be readily available. The problem of scattering of electromagnetic plane waves by a semi-infinite circular tube was treated by PEARSON [1953] for axial incidence and by BOWMAN [1963] for general incidence; these results may be found in the exhaustive review of EINARSSON et al. [1966]. The scattering of sound waves by a solid semi-infinite circular cylinder with a plane end surface was investigated by JONES [1955b] (also MATSUI [1960]), and the treatment was extended to include the electromagnetic case by EINARSSON et al. [1966]. In all of these problems concerning semi-infinite circular cylinders, the fundamental step is to find the split functions $L_n^+(\alpha)$ and $M_n^+(\alpha)$ ($n = 0, 1, 2, \dots$) analytic in the upper half plane and defined by

$$\begin{aligned} L_n^+(\alpha)L_n^+(-\alpha) &= \pi i J_n[a(k^2 - \alpha^2)^{\frac{1}{2}}] H_n^{(1)'}[a(k^2 - \alpha^2)^{\frac{1}{2}}], \\ M_n^+(\alpha)M_n^+(-\alpha) &= \pi i J_n'[a(k^2 - \alpha^2)^{\frac{1}{2}}] H_n^{(1)}[a(k^2 - \alpha^2)^{\frac{1}{2}}], \end{aligned} \quad (I.184)$$

where a denotes the radius of the cylinder, and $\text{Im}(k^2 - \alpha^2)^{\frac{1}{2}} > 0$ for $\text{Im} k > 0$. For $ka \gg 1$ and $ka > n$ the functions $L_n^+(k \cos \theta)$, $M_n^+(k \cos \theta)$ can be expanded asymptotically in terms of a "universal" function $V(s, q)$ closely related to V in eq. (I.177) (VAJNSHTEIN [1954], BOWMAN [1963], EINARSSON et al. [1966]). This opens the possibility, at least for axial incidence, of obtaining diffracted field expansions analogous to that in eq. (I.183) for the open-ended parallel plane waveguide. The case $ka \ll 1$ finds application in the problem of scattering by a long thin wire (Chapter 12). For a semi-infinite hollow cylinder of elliptical cross section, problems of acoustic radiation and scattering have been solved by BLASS [1951], and for tubes of arbitrary cross section an approximation technique based on the Wiener-Hopf method is discussed by LEVINE [1954a].

Another class of problems that yield to exact solution by function-theoretic methods concerns electromagnetic or acoustic diffraction in wedge shaped regions where the boundary conditions are of the mixed or impedance type (see Section 1.2.4). In connection with obstacles with a single constant impedance, solutions for diffraction by a half plane were obtained by SENIOR [1952, 1959a], WILLIAMS [1960] and MARCINKOWSKI [1961], and for the wedge by SENIOR [1959b] and WILLIAMS [1959]. More general problems were solved by MALIUZHNETS [1950; 1957a, b; 1959; 1960], who proposed and developed a method of solving diffraction problems in angular regions. This method is based on representing the field in a wedge-shaped region by a Sommerfeld integral (see Chapters 6 and 8) for which an inversion formula exists (MALIUZHNETS [1958a]), and thereby reduces the diffraction problem to a functional equation for integrands. Solutions to the functional equations were obtained in many

interesting cases by the use of integral transforms of the Fourier type or Laplace type. In particular, the problem of plane-wave diffraction by a wedge with different surface impedances on its two faces is solved in closed form (MALIUZHINETS [1959, 1960]). MALIUZHINETS [1958b] further notes that his inversion formula for the Sommerfeld integral reduces in certain cases to the inversion formula of KONTOROVICH and LEBEDEV [1939], which has also been applied to problems associated with wedges and cones (see e.g. JONES [1964], KARP [1950], KONTOROVICH and LEBEDEV [1939], LEBEDEV and SKAL'SKAYA [1962]). The solution of MALIUZHINETS [1959, 1960] for a wedge with two face impedances contains the solution of the shoreline problem (see e.g. GRÜNBERG [1942, 1943, 1944], FOCK [1944], BAZER and KARP [1952], CLEMMOW [1953]) as a special case. An alternative method suitable for wedge-shaped regions was developed by PETERS [1952], who treated a hydrodynamic problem arising in connection with water waves on a sloping beach. This method which still involves the factorization of a function into two parts with overlapping regions of regularity was later adapted by SENIOR [1959b] to the problem of diffraction by an imperfectly conducting wedge.

Many other diffraction problems have yielded to either exact or approximate solution by means of function-theoretic techniques. WESTPFAHL [1959] (see also CASE [1964]) presents an asymptotic solution to the singular integral equations arising in diffraction by a perfectly conducting strip (see Chapter 4), but his results were vastly improved by KHASKIND and VAJNSHTEIN [1964] and by FIALKOVSKIY [1966]. FAULKNER [1965] employed an asymptotic factorization theorem of KRANZER and RADLOW [1962] to treat the problem of diffraction by a wide imperfectly conducting strip, and his results were found by BOWMAN [1967] to be in agreement with the (simpler) ray-optics calculation. For diffraction by a semi-infinite plate of finite (although small) thickness, see JONES [1953], and for diffraction by a parallel plane waveguide of finite length, see JONES [1952b]. WESTPFAHL and WITTE [1967] have treated the acoustic diffraction by a large circular aperture or disc, and have also included an extensive bibliography. An interesting generalization of the Wiener-Hopf method appears in the papers by RADLOW [1961; 1964a, b; 1965], who found solutions to the diffraction problems associated with the quarter-plane and the right-angled dielectric wedge. In obtaining these solutions, a new function-theoretic technique employing two complex variables was introduced; however, the solutions are sufficiently complicated that no useful physical results, such as a diffraction coefficient, are available, and the solutions have not met with general acceptance.

1.2.14.4. NUMERICAL METHODS

The integral equations for the field at the surface of the scatterer which were presented in Section 1.2.10 have been solved exactly for a few simple scattering shapes only, and in all these cases the solution could have been obtained by some other method, such as separation of variables. For bodies of complex shape, the scattering problem can be solved numerically by dividing the scattering surface in portions over each of which the amplitude and the phase of the surface field can be considered as approxi-

mately constant, or as varying in an approximately known way. The integral equation is then replaced by a set of linear algebraic equations, to be solved numerically by a computer. Computer programs based on this method have been applied to the study of radiation and scattering from wire structures (BAGHDASARIAN and ANGELAKOS [1965], MEI [1965], RICHMOND [1965], HARRINGTON [1967]), from two-dimensional bodies (MEI and VAN BLADEL [1963], ANDREASEN [1964, 1965a]) and from three-dimensional bodies (ANDREASEN [1965b], WATERMAN [1965]).

The numerical integral equation method is well suited to problems in the low-frequency and resonance regions. If the dimensions of the scatterer are very large compared to the wavelength, also the number of linear algebraic equations becomes very large and difficult to handle by presently available computers.

Although the integral equation approach is the most logical one for numerical solutions because boundary and radiation conditions are automatically taken into account, other methods have also been applied; thus, for example, MULLIN et al. [1965] have studied the two-dimensional scattering from infinite cylinders of almost circular cross section by assuming a series expansion in terms of circular cylindrical wave-functions for the scattered field, and by imposing the boundary conditions at a finite number of points on the scattering surface.

1.3. Special functions

1.3.1. Bessel functions

Bessel functions are solutions of Bessel's differential equation

$$z^2 \frac{d^2 u}{dz^2} + z \frac{du}{dz} + (z^2 - v^2)u = 0, \quad (1.185)$$

where the parameter v is an unrestricted complex number. This differential equation has a regular singular point at $z = 0$ and an irregular singular point at $z = \infty$; all other points are ordinary points of the differential equation. In defining the solutions of Bessel's equation we shall adhere to the notations used in WATSON [1958]. Detailed properties of the Bessel functions may be found in ABRAMOWITZ and STEGUN [1964], ERDÉLYI et al. [1953], GRADSHTEYN and RYZHIK [1965], MAGNUS and OBERHETTINGER [1949], MAGNUS et al. [1966] and WATSON [1958]. For numerical tables consult ABRAMOWITZ and STEGUN [1964] and WATSON [1958].

When v is not an integer, eq. (1.185) has two independent solutions $J_v(z)$ and $J_{-v}(z)$ where

$$J_v(z) = \sum_{m=0}^{\infty} \frac{(-1)^m \left(\frac{1}{2}z\right)^{v+2m}}{m! \Gamma(v+m+1)}. \quad (1.186)$$

The function $J_v(z)$ is known as the Bessel function of the first kind and v -th order. It is single-valued throughout the z -plane cut along the negative real axis from 0 to $-\infty$ and for fixed z ($\neq 0$) it is an entire function of v , while for fixed v the function $z^{-v} J_v(z)$ is an entire function of z . When v is equal to a non-negative integer n , the

Bessel function $J_n(z)$ has no branch point and is an entire function of z ; however, because of the linear relationship

$$J_{-n}(z) = (-1)^n J_n(z), \quad (I.187)$$

a second independent solution to eq. (I.185) is now required. This second solution, known as the Bessel function of the second kind or the Neumann function, is denoted by $Y_v(z)$ and defined for all v by

$$Y_v(z) = \frac{J_v(z) \cos v\pi - J_{-v}(z)}{\sin v\pi}, \quad v \neq n$$

$$Y_n(z) = \lim_{v \rightarrow n} Y_v(z). \quad (I.188)$$

In particular, the Neumann function of non-negative integer order may be given as

$$Y_n(z) = \frac{2}{\pi} J_n(z) \log\left(\frac{1}{2}z\right) - \frac{1}{\pi} \sum_{m=0}^{n-1} \frac{(n-m-1)!}{m!} \left(\frac{1}{2}z\right)^{2m-n} -$$

$$- \frac{1}{\pi} \sum_{m=0}^{\infty} \frac{\psi(n+m) + \psi(m)}{(-1)^m m! (n+m)!} \left(\frac{1}{2}z\right)^{2m+n}, \quad (I.189)$$

where for non-negative integer m ,

$$\psi(m) = -C + \sum_{s=1}^m \frac{1}{s}, \quad \psi(0) = -C, \quad C = 0.5772 \dots \text{(Euler's constant)}. \quad (I.190)$$

The finite sum in eq. (I.189) is to be omitted if $n = 0$. The Neumann function is single-valued in the cut z -plane and for fixed $z (\neq 0)$ is an entire function of v . Equation (I.187) is also valid for $Y_n(z)$. The functions $J_v(z)$ and $Y_v(z)$ are real if v is real and z is positive.

Two functions of frequent occurrence are the Bessel functions of the third kind $H_v^{(1)}(z)$ and $H_v^{(2)}(z)$, also called the first and second Hankel functions, respectively. These are defined as the linear combinations

$$H_v^{(1)}(z) = J_v(z) + iY_v(z),$$

$$H_v^{(2)}(z) = J_v(z) - iY_v(z). \quad (I.191)$$

For $v \neq n$ where n is an integer, it follows from eqs. (I.188) and (I.191) that

$$H_v^{(1)}(z) = (i \sin v\pi)^{-1} [J_{-v}(z) - J_v(z)e^{-iv\pi}],$$

$$H_v^{(2)}(z) = (i \sin v\pi)^{-1} [J_v(z)e^{iv\pi} - J_{-v}(z)], \quad (I.192)$$

whereas for $v = n$ ($n = 0, 1, 2, \dots$) application of eq. (I.189) to eqs. (I.191) yields

$$H_n^{(1),(2)}(z) = \left[1 \pm \frac{2i}{\pi} \log\left(\frac{1}{2}z\right)\right] J_n(z) \mp \frac{i}{\pi} \sum_{m=0}^{n-1} \frac{(n-m-1)!}{m!} \left(\frac{1}{2}z\right)^{2m-n} \mp$$

$$\mp \frac{i}{\pi} \sum_{m=0}^{\infty} \frac{\psi(n+m) + \psi(m)}{(-1)^m m! (n+m)!} \left(\frac{1}{2}z\right)^{2m+n}. \quad (I.193)$$

Equation (I.187) is also valid for $H_n^{(1),(2)}(z)$.

Equation (I.185) is unchanged if ν is replaced by $-\nu$, and the following linear relations exist:

$$\begin{aligned} J_{-\nu}(z) &= J_{\nu}(z) \cos \nu\pi - Y_{\nu}(z) \sin \nu\pi, \\ Y_{-\nu}(z) &= J_{\nu}(z) \sin \nu\pi + Y_{\nu}(z) \cos \nu\pi, \\ H_{-\nu}^{(1),(2)}(z) &= e^{\pm i\nu\pi} H_{\nu}^{(1),(2)}(z), \\ 2J_{-\nu}(z) &= e^{i\nu\pi} H_{\nu}^{(1)}(z) + e^{-i\nu\pi} H_{\nu}^{(2)}(z), \\ 2iY_{-\nu}(z) &= e^{i\nu\pi} H_{\nu}^{(1)}(z) - e^{-i\nu\pi} H_{\nu}^{(2)}(z). \end{aligned} \quad (\text{I.194})$$

The Bessel functions are single-valued for all points z of the principal branch $|\arg z| < \pi$. The transition to different functional branches across the cut $(-\infty, 0)$ can be made by means of the relations

$$\begin{aligned} J_{\nu}(ze^{im\pi}) &= e^{-im\nu\pi} J_{\nu}(z), \\ Y_{\nu}(ze^{im\pi}) &= e^{-im\nu\pi} Y_{\nu}(z) + 2i \sin(m\nu\pi) \cot(\nu\pi) J_{\nu}(z), \\ -\sin(\nu\pi) H_{\nu}^{(1)}(ze^{im\pi}) &= \sin[(m-1)\nu\pi] H_{\nu}^{(1)}(z) + e^{-i\nu\pi} \sin(m\nu\pi) H_{\nu}^{(2)}(z), \\ \sin(\nu\pi) H_{\nu}^{(2)}(ze^{im\pi}) &= \sin[(m+1)\nu\pi] H_{\nu}^{(2)}(z) + e^{i\nu\pi} \sin(m\nu\pi) H_{\nu}^{(1)}(z), \end{aligned} \quad (\text{I.195})$$

where m is an integer.

Various Wronskian determinants can be derived. Define $W\{u_1(z), u_2(z)\} = u_1(z)u_2'(z) - u_2(z)u_1'(z)$ where the prime denotes (d/dz) , then

$$\begin{aligned} W\{J_{\nu}(z), J_{-\nu}(z)\} &= -2(\pi z)^{-1} \sin \nu\pi, \\ W\{J_{\nu}(z), Y_{\nu}(z)\} &= 2(\pi z)^{-1}, \\ W\{H_{\nu}^{(1)}(z), H_{\nu}^{(2)}(z)\} &= -4i(\pi z)^{-1}, \\ W\{J_{\nu}(z), H_{\nu}^{(1),(2)}(z)\} &= \pm 2i(\pi z)^{-1}. \end{aligned} \quad (\text{I.196})$$

It follows from the first Wronskian in eq. (I.196) that $J_{\nu}(z)$ and $J_{-\nu}(z)$ are not linearly independent solutions when ν is an integer; the remaining Wronskians never vanish and therefore the corresponding pairs of functions are always linearly independent. Still further Wronskians can be deduced by means of eqs. (I.194) and (I.196); for example

$$W\{Y_{\nu}(z), Y_{-\nu}(z)\} = -2(\pi z)^{-1} \sin \nu\pi,$$

indicating that $Y_{\nu}(z)$ and $Y_{-\nu}(z)$ are linearly independent except when ν is an integer.

The following recursion and differentiation formulas hold:

$$\begin{aligned} J_{\nu-1}(z) + J_{\nu+1}(z) &= \frac{2\nu}{z} J_{\nu}(z), \\ J_{\nu-1}(z) - J_{\nu+1}(z) &= 2 \frac{dJ_{\nu}(z)}{dz}, \end{aligned} \quad (\text{I.198})$$

while for $m = 0, 1, 2, \dots$,

$$\begin{aligned} \left(\frac{d}{z dz} \right)^m [z^{\nu} J_{\nu}(z)] &= z^{\nu-m} J_{\nu-m}(z), \\ \left(\frac{d}{z dz} \right)^m [z^{-\nu} J_{\nu}(z)] &= (-1)^m z^{-\nu-m} J_{\nu+m}(z). \end{aligned} \quad (\text{I.199})$$

The same relations are also valid for Bessel functions of the second and third kind. Differentiation with respect to the order leads to

$$\frac{\partial J_\nu(z)}{\partial \nu} = J_\nu(z) \log \left(\frac{1}{2}z\right) - \sum_{m=0}^{\infty} \frac{(-1)^m \psi(\nu+m) \left(\frac{1}{2}z\right)^{\nu+2m}}{m! \Gamma(\nu+m+1)}, \quad (I.200)$$

$$\frac{\partial Y_\nu(z)}{\partial \nu} = \cot(\nu\pi) \frac{\partial J_\nu(z)}{\partial \nu} - \operatorname{cosec}(\nu\pi) \left[\frac{\partial J_{-\nu}(z)}{\partial \nu} - \pi Y_{-\nu}(z) \right], \quad (I.201)$$

where ψ is the digamma function

$$\psi(\nu) = \frac{d}{d\nu} \log \Gamma(\nu+1). \quad (I.202)$$

For non-negative integer arguments in ψ see eq. (I.190).

When ν is fixed and $|z| \rightarrow \infty$ Hankel's asymptotic expansions of the various Bessel functions are

$$H_\nu^{(1)}(z) \sim \sqrt{\frac{2}{\pi z}} \exp \left[i \left(z - \frac{1}{2} \nu \pi - \frac{1}{4} \pi \right) \right] \sum_{m=0}^{\infty} \frac{(-1)^m (v, m)}{(2iz)^m}, \quad (-\pi < \arg z < 2\pi), \quad (I.203)$$

$$H_\nu^{(2)}(z) \sim \sqrt{\frac{2}{\pi z}} \exp \left[-i \left(z - \frac{1}{2} \nu \pi - \frac{1}{4} \pi \right) \right] \sum_{m=0}^{\infty} \frac{(v, m)}{(2iz)^m}, \quad (-2\pi < \arg z < \pi), \quad (I.204)$$

$$J_\nu(z) \sim \sqrt{\frac{2}{\pi z}} \left[\cos \left(z - \frac{1}{2} \nu \pi - \frac{1}{4} \pi \right) \sum_{m=0}^{\infty} \frac{(-1)^m (v, 2m)}{(2z)^{2m}} - \sin \left(z - \frac{1}{2} \nu \pi - \frac{1}{4} \pi \right) \sum_{m=0}^{\infty} \frac{(-1)^m (v, 2m+1)}{(2z)^{2m+1}} \right], \quad (|\arg z| < \pi), \quad (I.205)$$

$$Y_\nu(z) \sim \sqrt{\frac{2}{\pi z}} \left[\sin \left(z - \frac{1}{2} \nu \pi - \frac{1}{4} \pi \right) \sum_{m=0}^{\infty} \frac{(-1)^m (v, 2m)}{(2z)^m} + \cos \left(z - \frac{1}{2} \nu \pi - \frac{1}{4} \pi \right) \sum_{m=0}^{\infty} \frac{(-1)^m (v, 2m+1)}{(2z)^{2m+1}} \right], \quad (|\arg z| < \pi), \quad (I.206)$$

where (v, m) is the Hankel symbol defined by

$$(v, m) = \frac{\Gamma(\frac{1}{2} + v + m)}{m! \Gamma(\frac{1}{2} + v - m)}, \quad (I.207)$$

$$(v, 0) = 1, \quad (v, m) = \frac{[4v^2 - 1^2] \dots [4v^2 - (2m-1)^2]}{2^{2m} m!} \quad \text{for } m = 1, 2, \dots \quad (I.208)$$

For discussion of the remainders in eqs. (I.203) through (I.206) after the M -th terms see WATSON [1958] and MEIER [1932]. For real positive values of z and ν , the remainders are less in absolute value than the absolute value of the first discarded

term. If $\nu = n + \frac{1}{2}$ ($n = 0, 1, 2, \dots$) the asymptotic series in eqs. (I.203) through (I.206) terminate and the Hankel symbol becomes

$$(n + \tfrac{1}{2}, m) = \frac{(n+m)!}{m!(n-m)!}. \quad (\text{I.209})$$

In this case the Bessel functions reduce to elementary functions.

For z fixed and $|\nu| \rightarrow \infty$:

$$J_\nu(z) \sim \sqrt{\frac{1}{2\pi\nu}} \left(\frac{ez}{2\nu}\right)^\nu [1 + O(\nu^{-1})], \quad |\arg \nu| < \pi, \quad (\text{I.210})$$

$$J_{-\nu}(z) \sim \sin(\nu\pi) \sqrt{\frac{2}{\pi\nu}} \left(\frac{ez}{2\nu}\right)^{-\nu} [1 + O(\nu^{-1})], \quad |\arg \nu| < \pi. \quad (\text{I.211})$$

From these one can obtain asymptotic expansions for $Y_\nu(z)$, $H_\nu^{(1),(2)}(z)$ by means of eqs. (I.188) and (I.192); for example, if $\nu \rightarrow +\infty$ then

$$Y_\nu(z) \sim -\sqrt{\frac{2}{\pi\nu}} \left(\frac{ez}{2\nu}\right)^{-\nu} [1 + O(\nu^{-1})]. \quad (\text{I.212})$$

The DEBYE [1909, 1910] asymptotic expansions of the Bessel functions have been discussed in detail by WATSON [1958]. These are expansions valid when both ν and z are large and complex, although z is supposed to be restricted such that $|\arg z| < \frac{1}{2}\pi$. The ratio ν/z is restricted to lie in certain regions of the complex (ν/z)-plane and the results are useful only if $|\nu - z| > |\nu^{\frac{1}{2}}|$. Auxiliary angles γ , α , β are introduced by the relations

$$\frac{\nu}{z} = \cosh \gamma = \cosh(\alpha + i\beta), \quad (\text{I.213})$$

where α may have any real value and β is restricted by $0 < \beta < \frac{1}{2}\pi$. Because of Stokes' phenomenon, the complex (ν/z)-plane must be divided into separate regions as illustrated in Fig. I.6. The continuous curves that start at $\nu/z = 1$ are prescribed parametrically by the equations

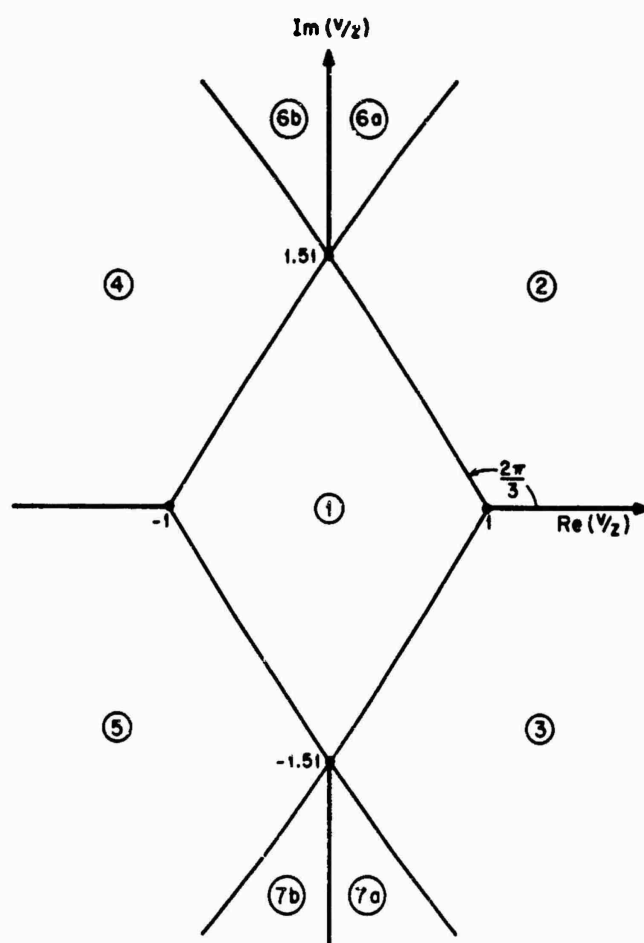
$$\begin{aligned} \operatorname{Re} \left(\frac{\nu}{z} \right) &= \cosh \alpha' \cos \beta', \\ \operatorname{Im} \left(\frac{\nu}{z} \right) &= \sinh \alpha' \sin \beta', \end{aligned} \quad (\text{I.214})$$

where α' , β' are restrained by the relation

$$1 - \alpha' \tanh \alpha' - \beta' \cot \beta' = 0, \quad (\text{I.215})$$

whereas the continuous curves that begin at $\nu/z = -1$ are determined by eqs. (I.214) except that now α' , β' are restrained by

$$1 - \alpha' \tanh \alpha' + (\pi - \beta') \cot \beta' = 0. \quad (\text{I.216})$$

Fig. 1.6. Regions in the complex (v/z) -plane (WATSON [1958]).

It is convenient to introduce the functions $S_v^{(1)}(z)$ and $S_v^{(2)}(z)$, where these are given asymptotically by the formulas

$$S_v^{(1)}(z) \sim \frac{\exp \{v(\tanh \gamma - \gamma) - \frac{1}{2}i\pi\}}{(-\frac{1}{2}iv\pi \tanh \gamma)^{\frac{1}{2}}} \sum_{m=0}^{\infty} \frac{\Gamma(m + \frac{1}{2})}{\Gamma(\frac{1}{2})} \frac{A_m}{(\frac{1}{2}v \tanh \gamma)^m}, \quad (1.217)$$

$$S_v^{(2)}(z) \sim \frac{\exp \{-v(\tanh \gamma - \gamma) + \frac{1}{2}i\pi\}}{(-\frac{1}{2}iv\pi \tanh \gamma)^{\frac{1}{2}}} \sum_{m=0}^{\infty} \frac{\Gamma(m + \frac{1}{2})}{\Gamma(\frac{1}{2})} \frac{A_m}{(-\frac{1}{2}v \tanh \gamma)^m}, \quad (1.218)$$

with

$$\arg(-\frac{1}{2}iv\pi \tanh \gamma) = \arg z + \arg(-i \sinh \gamma), \quad |\arg(-i \sinh \gamma)| < \frac{1}{2}\pi. \quad (1.219)$$

The values of A_0 , A_1 and A_2 are

$$\begin{aligned} A_0 &= 1, \quad A_1 = \frac{1}{8} - \frac{5}{24} \coth^2 \gamma, \\ A_2 &= \frac{3}{128} - \frac{7}{576} \coth^2 \gamma + \frac{3}{3456} \coth^4 \gamma. \end{aligned} \quad (1.220)$$

The asymptotic forms of the Bessel functions in the various regions of the (v/z) -plane

TABLE 1.1 (WATSON [1958])

Regions	$S_v^{(1)}(z)$
1, 3, 4	$H_v^{(1)}(z)$
2, 6a	$2J_v(z)$
5, 7b	$2e^{-iv\pi}J_{-v}(z)$
6b	$e^{iNv\pi}H_v^{(1)}(ze^{-iN\pi})$
7a	$e^{-iMv\pi}H_v^{(1)}(ze^{-iM\pi})$

TABLE 1.2 (WATSON [1958])

Regions	$S_v^{(2)}(z)$
1, 2, 5	$H_v^{(2)}(z)$
3, 7a	$2J_v(z)$
4, 6b	$2e^{iv\pi}J_{-v}(z)$
6a	$e^{iMv\pi}H_v^{(2)}(ze^{iM\pi})$
7b	$e^{-iNv\pi}H_v^{(2)}(ze^{iN\pi})$

are expressed in terms of $S_v^{(1)}(z)$ and $S_v^{(2)}(z)$ by means of Tables 1.1 and 1.2. In these tables, M and N are positive integers such that M is the smallest integer for which

$$1 - \alpha \tanh \alpha + [(M+1)\pi - \beta] \cot \beta > 0, \quad 0 < \beta < \frac{1}{2}\pi \quad (1.221)$$

and N is the smallest integer for which

$$1 - \alpha \tanh \alpha - (N\pi + \beta) \cot \beta > 0, \quad \frac{1}{2}\pi < \beta < \pi. \quad (1.222)$$

In the critical case $\beta = \frac{1}{2}\pi$, the expansions appropriate to region 1 are valid. For regions 6 and 7 the circuit relations in eqs. (1.195) can be used to express the Hankel functions in the forms given in Tables 1.3 and 1.4. For sufficiently large v , the terms

TABLE 1.3

Regions	$S_v^{(1)}(z)$
6b	$(i \sin v\pi)^{-1} [e^{2iNv\pi}J_{-v}(z) - e^{-iv\pi}J_v(z)]$
7a	$(i \sin v\pi)^{-1} [J_{-v}(z) - e^{-i(2M+1)v\pi}J_v(z)]$

TABLE 1.4

Regions	$S_v^{(2)}(z)$
6a	$(i \sin v\pi)^{-1} [e^{i(2M+1)v\pi}J_v(z) - J_{-v}(z)]$
7b	$(i \sin v\pi)^{-1} [e^{iv\pi}J_v(z) - e^{-2iMv\pi}J_{-v}(z)]$

involving M and N in Tables 1.3 and 1.4 become subdominant with the result that Tables 1.1 and 1.2 may be replaced by the simpler Tables 1.5 and 1.6. From the tables asymptotic expansions of any fundamental system of solutions of Bessel's equation

TABLE 1.5

Regions	$S_v^{(1)}(z)$
1, 3, 4	$H_v^{(1)}(z)$
2, 6a, 6b	$2J_v(z)$
5, 7a, 7b	$2e^{-iv\pi}J_{-v}(z)$

TABLE 1.6

Regions	$S_v^{(2)}(z)$
1, 2, 5	$H_v^{(2)}(z)$
3, 7a, 7b	$2J_v(z)$
4, 6a, 6b	$2e^{iv\pi}J_{-v}(z)$

can be constructed when v and z are both arbitrarily large complex numbers, the real part of z being positive. For an alternate summary of the Debye expansions see CAMPOPIANO [1957], and in the case of real positive z but complex v see HÖNL et al. [1961] (NUSSENZVEIG [1965] notes that HÖNL et al. [1961] contains several mistakes).

When v and z are both large but $|v - z| \lesssim |v|^{\frac{1}{2}}$ the Debye asymptotic expansions are no longer valid, and it is necessary to employ expansions suitable for the transitional regions. In the following, it is supposed that $z = x$, $x > 0$ and the parameters m , t are defined as

$$m = (\frac{1}{2}x)^{\frac{1}{2}}, \quad t = (v - x)/m, \quad (1.223)$$

then for $m \rightarrow \infty$:

$$J_v(x) \sim \frac{1}{m\sqrt{\pi}} \left\{ v(t) - \frac{1}{60m^2} [4tv(t) + t^2v'(t)] + \frac{1}{2520m^4} \left[\left(\frac{7}{20}t^5 + 26t^2\right)v(t) + (6t^3 + 18)v'(t) \right] + O(m^{-6}) \right\}, \quad (1.224)$$

$$J'_v(x) \sim \frac{-1}{m^2\sqrt{\pi}} \left\{ v'(t) + \frac{1}{60m^2} [4tv'(t) + (6 - t^3)v(t)] + \frac{1}{10080m^4} \left[\left(\frac{7}{3}t^5 - 76t^2\right)v'(t) + (3t^4 - 168t)v(t) \right] + O(m^{-6}) \right\}, \quad (1.225)$$

$$H_v^{(1)}(x) \sim \frac{-i}{m\sqrt{\pi}} \left\{ w_1(t) - \frac{1}{60m^2} [4tw_1(t) + t^2w_1'(t)] + \frac{1}{2520m^4} \left[\left(\frac{7}{20}t^5 + 26t^2\right)w_1(t) + (6t^3 + 18)w_1'(t) \right] + O(m^{-6}) \right\}, \quad (1.226)$$

$$H_v^{(1)'}(x) \sim \frac{i}{m^2\sqrt{\pi}} \left\{ w_1'(t) + \frac{1}{60m^2} [4tw_1'(t) + (6 - t^3)w_1(t)] + \frac{1}{10080m^4} \left[\left(\frac{7}{3}t^5 - 76t^2\right)w_1'(t) + (3t^4 - 168t)w_1(t) \right] + O(m^{-6}) \right\}, \quad (1.227)$$

where the FOCK [1945] notation for the Airy functions has been used,

$$\begin{aligned} u(t) &= \sqrt{\pi} \text{Bi}(t), & v(t) &= \sqrt{\pi} \text{Ai}(t), \\ w_1(t) &= \sqrt{\pi} [\text{Bi}(t) + i \text{Ai}(t)], \\ w_2(t) &= \sqrt{\pi} [\text{Bi}(t) - i \text{Ai}(t)]. \end{aligned} \quad (1.228)$$

See Section I.3.2 for definitions of the Airy functions. Expansions for $Y_v(x)$, $Y'_v(x)$ are obtained from $J_v(x)$, $J'_v(x)$ upon replacing $v(t)$ by $-u(t)$ in eqs. (1.224) and (1.225), while expansions for $H_v^{(2)}(x)$, $H_v^{(2)'}(x)$ are obtained from $H_v^{(1)}(x)$, $H_v^{(1)'}(x)$ upon replacing $w_1(t)$ by $-w_2(t)$ in eqs. (1.226) and (1.227). For other asymptotic expansions see the references already cited, to which may be added LANGER [1931, 1932], CHERRY [1950], OLIVER [1952, 1954] and SCHÖBL [1954].

Modified Bessel and Hankel functions, $I_\nu(z)$ and $K_\nu(z)$, respectively, are often used. They may be defined by

$$\begin{aligned} I_\nu(z) &= e^{-\frac{1}{2}i\nu\pi} J_\nu(ze^{\frac{1}{2}i\pi}), & (-\pi < \arg z \leq \tfrac{1}{2}\pi), \\ I_\nu(z) &= e^{\frac{1}{2}i\nu\pi} J_\nu(ze^{-\frac{1}{2}i\pi}), & (\tfrac{1}{2}\pi < \arg z \leq \pi), \end{aligned} \quad (1.229)$$

$$\begin{aligned} K_\nu(z) &= \tfrac{1}{2}\pi i e^{\frac{1}{2}i\nu\pi} H_\nu^{(1)}(ze^{\frac{1}{2}i\pi}), & (-\pi < \arg z \leq \tfrac{1}{2}\pi), \\ K_\nu(z) &= -\tfrac{1}{2}\pi i e^{-\frac{1}{2}i\nu\pi} H_\nu^{(2)}(ze^{-\frac{1}{2}i\pi}), & (-\tfrac{1}{2}\pi < \arg z \leq \pi). \end{aligned} \quad (1.230)$$

For all values of z , $I_\nu(z)$ and $K_\nu(z)$ are linearly independent functions. Each is single-valued throughout the z -plane cut along the negative real axis, and for fixed $z (\neq 0)$ each is an entire function of ν . When ν is equal to a non-negative integer n , the modified Bessel function $I_n(z)$ is an entire function of z . Both modified functions are real when ν is real and z is positive, and if in addition $\nu > -1$, then both functions are positive. Other properties of the modified Bessel functions can be deduced from those of ordinary Bessel functions by the application of eqs. (1.229) and (1.230). The function $K_\nu(z)$ is sometimes called the Macdonald function of ν -th order.

The spherical Bessel functions $j_\nu(z)$, $y_\nu(z)$, $h_\nu^{(1)}(z)$ and $h_\nu^{(2)}(z)$ are defined in terms of ordinary Bessel functions by the relations

$$\begin{aligned} j_\nu(z) &= \sqrt{\frac{\pi}{2z}} J_{\nu+\frac{1}{2}}(z), \\ y_\nu(z) &= \sqrt{\frac{\pi}{2z}} Y_{\nu+\frac{1}{2}}(z), \\ h_\nu^{(1),(2)}(z) &= \sqrt{\frac{\pi}{2z}} H_{\nu+\frac{1}{2}}^{(1),(2)}(z). \end{aligned} \quad (1.231)$$

These functions satisfy the differential equation

$$z^2 \frac{d^2 u}{dz^2} + 2z \frac{du}{dz} + [z^2 - \nu(\nu+1)]u = 0 \quad (1.232)$$

or

$$\left(\frac{d^2}{dz^2} + 1 \right) (zu) = \frac{\nu(\nu+1)}{z} u. \quad (1.233)$$

The properties of the spherical Bessel functions follow from those of the ordinary Bessel functions. For $\nu = n$ ($n = 0, 1, 2, \dots$) the spherical Hankel functions may be represented by the finite series expansions

$$\begin{aligned} h_n^{(1)}(z) &= i^{-n-1} z^{-1} e^{iz} \sum_{m=0}^n \frac{(n+m)!}{m!(n-m)!} (-2iz)^{-m}, \\ h_n^{(2)}(z) &= i^{n+1} z^{-1} e^{-iz} \sum_{m=0}^n \frac{(n+m)!}{m!(n-m)!} (2iz)^{-m}. \end{aligned} \quad (1.234)$$

and expansions for $j_n(z)$, $y_n(z)$ follow upon application of

$$2j_n(z) = h_n^{(1)}(z) + h_n^{(2)}(z), \quad 2iy_n(z) = h_n^{(1)}(z) - h_n^{(2)}(z). \quad (1.235)$$

The representations in eqs. (I.234) are clearly useful when $|z| \rightarrow \infty$. Alternative expressions are

$$\begin{aligned} h_n^{(1),(2)}(z) &= \mp i z^n \left(-\frac{d}{z dz} \right)^n \frac{e^{\pm iz}}{z}, \\ j_n(z) &= z^n \left(-\frac{d}{z dz} \right)^n \frac{\sin z}{z}, \\ y_n(z) &= -z^n \left(-\frac{d}{z dz} \right)^n \frac{\cos z}{z}, \end{aligned} \quad (I.236)$$

sometimes known as Rayleigh's formulas. Ascending series representations may also be obtained; in particular,

$$\begin{aligned} j_n(z) &= 2^n z^n \sum_{m=0}^{\infty} \frac{(-1)^m (n+m)! z^{2m}}{m! (2n+2m+1)!}, \\ y_n(z) &= \frac{-1}{2^n z^{n+1}} \sum_{m=0}^{\infty} \frac{\Gamma(2n-2m+1) z^{2m}}{m! \Gamma(n-m+1)}. \end{aligned} \quad (I.237)$$

Equation (I.232) is unchanged if v is replaced by $-v-1$, and the following linear relations exist:

$$\begin{aligned} j_{-v-1}(z) &= -j_v(z) \sin v\pi - y_v(z) \cos v\pi, \\ y_{-v-1}(z) &= j_v(z) \cos v\pi - y_v(z) \sin v\pi, \\ h_{-v-1}^{(1),(2)}(z) &= \pm i e^{\pm i v \pi} h_v^{(1),(2)}(z). \end{aligned} \quad (I.238)$$

It is clear that these relations simplify if v is an integer.

For the Wronskian determinant, define $W\{u_1(z), u_2(z)\}$ to mean $u_1(z)u_2'(z) - u_2(z)u_1'(z)$, then

$$\begin{aligned} W\{j_v(z), y_v(z)\} &= z^{-2}, \\ W\{h_v^{(1)}(z), h_v^{(2)}(z)\} &= -2iz^{-2}, \\ W\{j_v(z), h_v^{(1),(2)}(z)\} &= \pm iz^{-2}, \\ W\{y_v(z), h_v^{(1),(2)}(z)\} &= -z^{-2}. \end{aligned} \quad (I.239)$$

All the pairs of functions in eqs. (I.239) are linearly independent.

The recursion formulas in eqs. (I.198) become

$$\begin{aligned} j_{v-1}(z) + j_{v+1}(z) &= \frac{2v+1}{z} j_v(z), \\ v j_{v-1}(z) - (v+1) j_{v+1}(z) &= (2v+1) \frac{dj_v(z)}{dz}, \end{aligned} \quad (I.240)$$

while for $m = 0, 1, 2, \dots$ the differentiation formulas in eqs. (I.199) become

$$\begin{aligned} \left(\frac{1}{z} \frac{d}{dz} \right)^m [z^{v+m+1} j_v(z)] &= z^{v-m+1} j_{v-m}(z), \\ \left(\frac{1}{z} \frac{d}{dz} \right)^m [z^{-v} j_v(z)] &= (-1)^m z^{-v-m} j_{v+m}(z). \end{aligned} \quad (I.241)$$

The same relations are also valid for spherical Bessel functions of the second and third kind.

The functions defined by

$$\psi_\nu(z) = z j_\nu(z), \quad \zeta_\nu^{(1),(2)}(z) = z h_\nu^{(1),(2)}(z), \quad (I.242)$$

and known as Riccati-Bessel functions, are also in common usage. The properties of these functions follow directly from those of the spherical Bessel functions or of the ordinary Bessel functions. It is worthwhile here to write out the asymptotic expansions in the transitional regions corresponding to eqs. (I.224) through (I.227). In particular, for $x > 0$, $m = (\frac{1}{2}x)^{\frac{1}{2}}$, $t = (v-x)/m$ and $m \rightarrow \infty$:

$$\begin{aligned} \psi_{v-\frac{1}{2}}(x) \sim m^{\frac{1}{2}} \left\{ v(t) - \frac{1}{60m^2} [4tv(t) + t^2v'(t)] + \frac{1}{2520m^4} [(\frac{7}{20}t^5 + 26t^2)v(t) + \right. \\ \left. + (6t^3 + 18)v'(t)] + O(m^{-6}) \right\}, \end{aligned} \quad (I.243)$$

$$\begin{aligned} \psi'_{v-\frac{1}{2}}(x) \sim -m^{-\frac{1}{2}} \left\{ v'(t) + \frac{1}{60m^2} [4tv'(t) - (9+t^2)v(t)] + \right. \\ \left. + \frac{1}{10080m^4} [(\frac{7}{5}t^5 - 34t^2)v'(t) + 3t^4v(t)] + O(m^{-6}) \right\}, \end{aligned} \quad (I.244)$$

$$\begin{aligned} \zeta_{v-\frac{1}{2}}^{(1)}(x) \sim -im^{\frac{1}{2}} \left\{ w_1(t) - \frac{1}{60m^2} [4tw_1(t) + t^2w_1'(t)] + \frac{1}{2520m^4} [(\frac{7}{20}t^5 + 26t^2)w_1(t) + \right. \\ \left. + (6t^3 + 18)w_1'(t)] + O(m^{-6}) \right\}, \end{aligned} \quad (I.245)$$

$$\begin{aligned} \zeta_{v-\frac{1}{2}}^{(1)'}(x) \sim im^{-\frac{1}{2}} \left\{ w_1'(t) + \frac{1}{60m^2} [4tw_1'(t) - (9+t^2)w_1(t)] + \right. \\ \left. + \frac{1}{10080m^4} [(\frac{7}{5}t^5 - 34t^2)w_1'(t) + 3t^4w_1(t)] + O(m^{-6}) \right\}, \end{aligned} \quad (I.246)$$

where $v(t)$, $w_1(t)$ are defined in eqs. (I.228) along with $u(t)$, $w_2(t)$. Expansions for $\zeta_{v-\frac{1}{2}}^{(2)}(x)$, $\zeta_{v-\frac{1}{2}}^{(2)'}(x)$ follow those of $\zeta_{v-\frac{1}{2}}^{(1)}(x)$, $\zeta_{v-\frac{1}{2}}^{(1)'}(x)$ upon replacing $w_1(t)$ by $-w_2(t)$ in eqs. (I.245) and (I.246). It should be noted that interchanges of notations for the spherical Bessel and Riccati-Bessel functions, as well as other notations for these functions, appear in the literature.

I.3.2. Airy functions

The Airy functions $\text{Ai}(z)$ and $\text{Bi}(z)$, defined as in MULLER [1946], are linearly independent solutions of the differential equation

$$\frac{d^3 u}{dz^3} - zu = 0, \quad (I.247)$$

and may be expressed as linear combinations of Bessel functions of order $\pm \frac{1}{3}$ in

particular,

$$\text{Ai}(z) = \frac{1}{3}\sqrt{z}[I_{-\frac{1}{3}}(\frac{2}{3}z^{\frac{1}{3}}) - I_{\frac{1}{3}}(\frac{2}{3}z^{\frac{1}{3}})] = \frac{1}{\pi}\sqrt{\frac{2}{3}}K_{\frac{1}{3}}(\frac{2}{3}z^{\frac{1}{3}}), \quad (\text{I.248})$$

$$\text{Bi}(z) = \sqrt{\frac{2}{3}}z[I_{-\frac{1}{3}}(\frac{2}{3}z^{\frac{1}{3}}) + I_{\frac{1}{3}}(\frac{2}{3}z^{\frac{1}{3}})], \quad (\text{I.249})$$

where $I_\nu(z)$ and $K_\nu(z)$ are the modified Bessel functions defined in Section 1.3.1. In terms of ordinary Bessel functions:

$$\begin{aligned} \text{Ai}(-z) &= \frac{1}{3}\sqrt{z}[J_{-\frac{1}{3}}(\frac{2}{3}z^{\frac{1}{3}}) + J_{\frac{1}{3}}(\frac{2}{3}z^{\frac{1}{3}})] \\ &= \frac{1}{2}\sqrt{\frac{2}{3}}z[e^{i\pi}H_{\frac{1}{3}}^{(1)}(\frac{2}{3}z^{\frac{1}{3}}) + e^{-i\pi}H_{\frac{1}{3}}^{(2)}(\frac{2}{3}z^{\frac{1}{3}})], \end{aligned} \quad (\text{I.250})$$

$$\begin{aligned} \text{Bi}(-z) &= \sqrt{\frac{2}{3}}z[J_{-\frac{1}{3}}(\frac{2}{3}z^{\frac{1}{3}}) - J_{\frac{1}{3}}(\frac{2}{3}z^{\frac{1}{3}})] \\ &= \frac{1}{2}i\sqrt{\frac{2}{3}}z[e^{i\pi}H_{\frac{1}{3}}^{(1)}(\frac{2}{3}z^{\frac{1}{3}}) - e^{-i\pi}H_{\frac{1}{3}}^{(2)}(\frac{2}{3}z^{\frac{1}{3}})]. \end{aligned} \quad (\text{I.251})$$

The Airy functions $\text{Ai}(z)$, $\text{Bi}(z)$ are entire transcendental functions of z and are real for real values of z . Their derivatives are expressible in terms of Bessel functions of order $\pm \frac{2}{3}$:

$$\text{Ai}'(z) = \frac{2}{3}z[I_{-\frac{2}{3}}(\frac{2}{3}z^{\frac{1}{3}}) - I_{\frac{2}{3}}(\frac{2}{3}z^{\frac{1}{3}})] = \frac{z}{\pi\sqrt{3}}K_{\frac{2}{3}}(\frac{2}{3}z^{\frac{1}{3}}), \quad (\text{I.252})$$

$$\text{Bi}'(z) = \frac{z}{\sqrt{3}}[I_{-\frac{2}{3}}(\frac{2}{3}z^{\frac{1}{3}}) + I_{\frac{2}{3}}(\frac{2}{3}z^{\frac{1}{3}})], \quad (\text{I.253})$$

$$\begin{aligned} \text{Ai}'(-z) &= -\frac{1}{3}z[J_{-\frac{2}{3}}(\frac{2}{3}z^{\frac{1}{3}}) - J_{\frac{2}{3}}(\frac{2}{3}z^{\frac{1}{3}})] \\ &= \frac{z}{2\sqrt{3}}[e^{-i\pi}H_{\frac{2}{3}}^{(1)}(\frac{2}{3}z^{\frac{1}{3}}) + e^{i\pi}H_{\frac{2}{3}}^{(2)}(\frac{2}{3}z^{\frac{1}{3}})], \end{aligned} \quad (\text{I.254})$$

$$\begin{aligned} \text{Bi}'(-z) &= \frac{z}{\sqrt{3}}[J_{-\frac{2}{3}}(\frac{2}{3}z^{\frac{1}{3}}) + J_{\frac{2}{3}}(\frac{2}{3}z^{\frac{1}{3}})] \\ &= \frac{iz}{2\sqrt{3}}[e^{-i\pi}H_{\frac{2}{3}}^{(1)}(\frac{2}{3}z^{\frac{1}{3}}) - e^{-i\pi}H_{\frac{2}{3}}^{(2)}(\frac{2}{3}z^{\frac{1}{3}})]. \end{aligned} \quad (\text{I.255})$$

Other properties of the Airy functions are readily obtainable from those of the Bessel functions.

Integral representations for the Airy functions are

$$\text{Ai}(z) = \frac{1}{2\pi i} \int_{\gamma} \frac{e^{i\pi\alpha}}{e^{-i\pi\alpha}} \exp(\frac{1}{3}t^3 - zt) dt, \quad (\text{I.256})$$

$$\text{Bi}(z) = \frac{1}{2\pi} \left\{ \int_{\gamma} \frac{e^{i\pi\alpha}}{e^{-i\pi\alpha}} \exp(\frac{1}{3}t^3 - zt) dt + \int_{\gamma} \frac{e^{-i\pi\alpha}}{e^{i\pi\alpha}} \exp(\frac{1}{3}t^3 - zt) dt \right\}, \quad (\text{I.257})$$

which for $z = x$ (x real) may be written as

$$\text{Ai}(x) = \frac{1}{\pi} \int_0^\infty \cos(\frac{1}{3}t^3 + xt) dt, \quad (\text{I.258})$$

$$\text{Bi}(x) = \frac{1}{\pi} \int_0^{\infty} [\exp(-\frac{1}{3}t^3 + xt) + \sin(\frac{1}{3}t^3 + xt)] dt. \quad (\text{I.259})$$

The integral in eq. (I.258) is closely related to the integral first introduced by AIRY [1838] and thus bears his name.

An important relation between Airy functions is

$$\text{Ai}(ze^{\pm \frac{2}{3}\pi i}) = \frac{1}{2} e^{\pm \frac{2}{3}\pi i} [\text{Ai}(z) \mp i \text{Bi}(z)], \quad (\text{I.260})$$

from which it follows that

$$\text{Ai}(z) + e^{\frac{2}{3}\pi i} \text{Ai}(ze^{\frac{2}{3}\pi i}) + e^{-\frac{2}{3}\pi i} \text{Ai}(ze^{-\frac{2}{3}\pi i}) = 0, \quad (\text{I.261})$$

$$\text{Bi}(z) + e^{\frac{2}{3}\pi i} \text{Bi}(ze^{\frac{2}{3}\pi i}) + e^{-\frac{2}{3}\pi i} \text{Bi}(ze^{-\frac{2}{3}\pi i}) = 0, \quad (\text{I.262})$$

$$\text{Bi}(z) = e^{\frac{2}{3}\pi i} \text{Ai}(ze^{\frac{2}{3}\pi i}) + e^{-\frac{2}{3}\pi i} \text{Ai}(ze^{-\frac{2}{3}\pi i}). \quad (\text{I.263})$$

Various Wronskian determinants can be derived. Let $W\{u_1(z), u_2(z)\}$ denote $u_1(z)u_2'(z) - u_2(z)u_1'(z)$ where the prime means (d/dz) , then

$$W\{\text{Ai}(z), \text{Bi}(z)\} = 1/\pi,$$

$$W\{\text{Ai}(z), \text{Ai}(ze^{\pm \frac{2}{3}\pi i})\} = \frac{1}{2\pi} e^{\mp \frac{2}{3}\pi i}, \quad (\text{I.264})$$

$$W\{\text{Ai}(ze^{\frac{2}{3}\pi i}), \text{Ai}(ze^{-\frac{2}{3}\pi i})\} = \frac{i}{2\pi}.$$

All the pairs of functions in eqs. (I.264) are linearly independent.

The functions $\text{Ai}(z)$, $\text{Ai}'(z)$ have zeros, denoted $-\alpha_n$, $-\beta_n$ respectively, on the negative real axis only, while the functions $\text{Bi}(z)$, $\text{Bi}'(z)$ have zeros on the negative real axis and in the sector $\frac{1}{3}\pi < |\arg z| < \frac{2}{3}\pi$. LOGAN [1959] has tabulated the first fifty zeros of both Ai and Ai' . For real x the functions $\text{Ai}(x)$ and $\text{Bi}(x)$, their first derivatives $\text{Ai}'(x)$ and $\text{Bi}'(x)$, and also $\pm M(x)$ and $\pm N(x)$, where

$$[M(x)]^2 = \text{Ai}^2(x) + \text{Bi}^2(x), \quad [N(x)]^2 = \text{Ai}'^2(x) + \text{Bi}'^2(x),$$

are plotted in Fig. 1.7 as a function of x . Numerical tables of Airy functions may be found in MILLER [1946] and in ABRAMOWITZ and STEGUN [1964].

Normalized Airy functions as defined by FOCK [1945, 1965] are frequently used. These are:

$$\begin{aligned} u(z) &= \sqrt[3]{\pi} \text{Bi}(z), & v(z) &= \sqrt[3]{\pi} \text{Ai}(z), \\ w_1(z) &= \sqrt[3]{\pi} [\text{Bi}(z) + i \text{Ai}(z)], \\ w_2(z) &= \sqrt[3]{\pi} [\text{Bi}(z) - i \text{Ai}(z)], \end{aligned} \quad (\text{I.265})$$

and obey the Wronskian relationships

$$\begin{aligned} W\{u(z), v(z)\} &= -1, \\ W\{w_1(z), w_2(z)\} &= 2i, \\ W\{u(z), w_{1,2}(z)\} &= \mp i, \\ W\{v(z), w_{1,2}(z)\} &= 1. \end{aligned} \quad (\text{I.266})$$

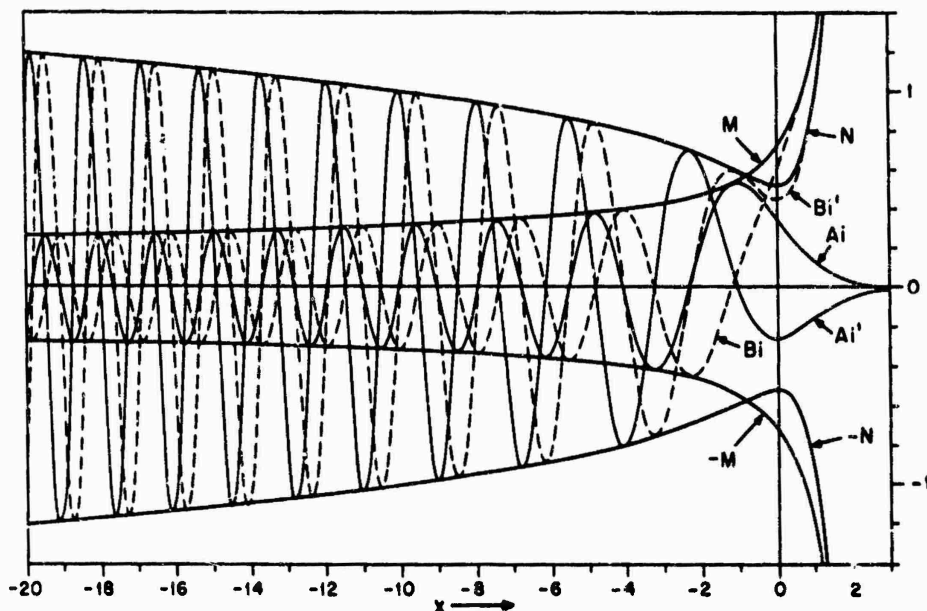


Fig. 1.7. The Airy functions (MILLER [1946]).

For x real numerical tables of $u(x)$, $v(x)$ and the derivatives $u'(x)$, $v'(x)$ are supplied by FOCK [1965].

1.3.3. Fock functions

These functions owe their first extensive application to diffraction theory to FOCK [1946], after whom they are named. Here we limit our consideration to the definitions and expansions of those Fock functions and related functions which are used in this book. An exhaustive treatment including numerical tables and diagrams is to be found in the two reports by LOGAN [1959], whose terminology is adopted; see also the survey article by LOGAN and YEE [1962].

The Fock functions are:

$$f(\xi) = f^{(0)}(\xi) = \frac{1}{\sqrt{\pi}} \int_{\Gamma} \frac{e^{i\xi t}}{w_1(t)} dt = \frac{e^{-i\pi}}{2\pi} \int_{\Gamma} \frac{e^{i\xi t}}{\text{Ai}(te^{i\pi})} dt, \quad (1.267)$$

$$g(\xi) = g^{(0)}(\xi) = \frac{1}{\sqrt{\pi}} \int_{\Gamma} \frac{e^{i\xi t}}{w_1'(t)} dt = -\frac{e^{i\pi}}{2\pi} \int_{\Gamma} \frac{e^{i\xi t}}{\text{Ai}'(te^{i\pi})} dt, \quad (1.268)$$

where Γ is a contour which starts at infinity in the angular sector $\frac{1}{2}\pi < \arg t < \pi$, passes between the origin and the pole of the integrand nearest the origin, and ends at infinity in the angular sector $-\frac{1}{2}\pi < \arg t < \frac{1}{2}\pi$. These functions can be generalized as follows (n is an integer):

$$f^{(n)}(\xi) = \frac{i^n}{\sqrt{\pi}} \int_{\Gamma} \frac{t^n e^{i\xi t}}{w_1(t)} dt, \quad (1.269)$$

$$g^{(n)}(\xi) = \frac{i^n}{\sqrt{\pi}} \int_{\Gamma} \frac{t^n e^{i\xi t}}{w_1'(t)} dt. \quad (1.270)$$

For large negative values of ξ :

$$f(\xi) \sim 2i\xi e^{-\frac{1}{2}i\xi^3} \left\{ 1 - \frac{i}{4\xi^3} + \frac{1}{2\xi^6} + \dots \right\}, \quad (1.271)$$

$$g(\xi) \sim 2e^{-\frac{1}{2}i\xi^3} \left\{ 1 + \frac{i}{4\xi^3} - \xi^{-6} + \dots \right\}. \quad (1.272)$$

For positive values of ξ , the Fock functions $f^{(n)}(\xi)$ and $g^{(n)}(\xi)$ may be expanded in series of residues:

$$f^{(n)}(\xi) = e^{-i\pi(2+7n)/6} \sum_l \frac{(\alpha_l)^n \exp(\alpha_l \xi e^{\frac{1}{2}i\pi})}{\text{Ai}'(-\alpha_l)}, \quad (1.273)$$

$$g^{(n)}(\xi) = e^{-i\pi n/6} \sum_l \frac{(\beta_l)^{n-1} \exp(\beta_l \xi e^{\frac{1}{2}i\pi})}{\text{Ai}(-\beta_l)}, \quad (1.274)$$

where α_l and β_l are the l -th roots of the equations $\text{Ai}(-x) = 0$ and $\text{Ai}'(-x) = 0$, respectively (see Section 1.3.2). Functions closely related to $f(\xi)$ and $g(\xi)$ are:

$$F(\xi) = f(\xi)e^{\frac{1}{2}i\xi^3}, \quad G(\xi) = g(\xi)e^{\frac{1}{2}i\xi^3}, \quad (1.275)$$

which have the asymptotic behavior:

$$F(\xi) \sim \begin{cases} 2i\xi, & \text{for } \xi \rightarrow -\infty, \\ 0, & \text{for } \xi \rightarrow +\infty; \end{cases} \quad (1.276)$$

$$G(\xi) \sim \begin{cases} 2, & \text{for } \xi \rightarrow -\infty, \\ 0, & \text{for } \xi \rightarrow +\infty. \end{cases} \quad (1.277)$$

Amplitude and phase of $f(\xi)$ and $g(\xi)$ are shown in Fig. 1.8.

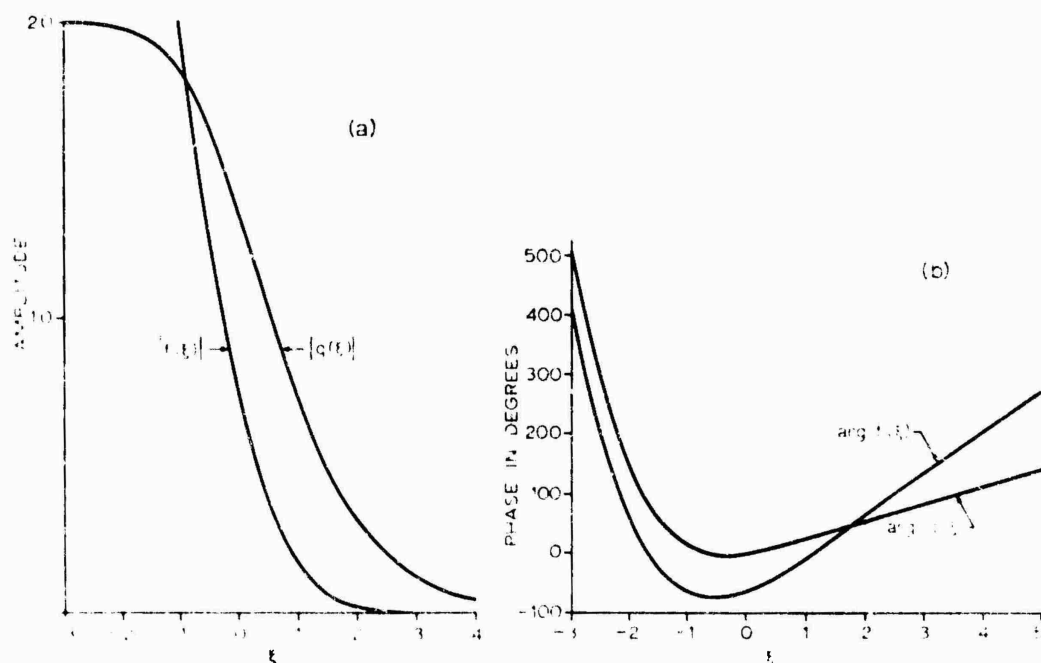


Fig. 1.8. Amplitude (a) and phase (b) of the Fock functions $f(\xi)$ and $g(\xi)$ (LOGAN [1959]).

The reflection coefficient functions $\tilde{p}(\xi)$ and $\tilde{q}(\xi)$ are defined by:

$$\tilde{p}(\xi) = \tilde{p}^{(0)}(\xi) = \frac{1}{\sqrt{\pi}} \int_r \frac{v(t)}{w_1(t)} e^{i\xi t} dt = \frac{e^{-\frac{1}{2}i\pi}}{2\sqrt{\pi}} \int_r \frac{\text{Ai}(t)}{\text{Ai}(te^{\frac{1}{2}i\pi})} e^{i\xi t} dt, \quad (1.278)$$

$$\tilde{q}(\xi) = \tilde{q}^{(0)}(\xi) = \frac{1}{\sqrt{\pi}} \int_r \frac{v'(t)}{w_1'(t)} e^{i\xi t} dt = -\frac{e^{\frac{1}{2}i\pi}}{2\sqrt{\pi}} \int_r \frac{\text{Ai}'(t)}{\text{Ai}'(te^{\frac{1}{2}i\pi})} e^{i\xi t} dt, \quad (1.279)$$

where $r(t)$ is given in the Section 1.3.2; they can be generalized as follows (n is an integer):

$$\tilde{p}^{(n)}(\xi) = \frac{i^n}{\sqrt{\pi}} \int_r t^n \frac{v(t)}{w_1(t)} e^{i\xi t} dt, \quad (1.280)$$

$$\tilde{q}^{(n)}(\xi) = \frac{i^n}{\sqrt{\pi}} \int_r t^n \frac{v'(t)}{w_1'(t)} e^{i\xi t} dt. \quad (1.281)$$

For large negative values of ξ :

$$\tilde{p}(\xi) \sim \frac{1}{2}\sqrt{-\xi} \exp \left[-i\left(\frac{1}{12}\xi^3 + \frac{1}{4}\pi\right) \right] \{1 - 2i\xi^{-3} + 20\xi^{-6} + \dots\}, \quad (1.282)$$

$$\tilde{q}(\xi) \sim -\frac{1}{2}\sqrt{-\xi} \exp \left[-i\left(\frac{1}{12}\xi^3 + \frac{1}{4}\pi\right) \right] \{1 + 2i\xi^{-3} - 28\xi^{-6} + \dots\}. \quad (1.283)$$

The amplitudes of $\tilde{p}(\xi)$ and $\tilde{q}(\xi)$ are shown in Fig. 1.9.

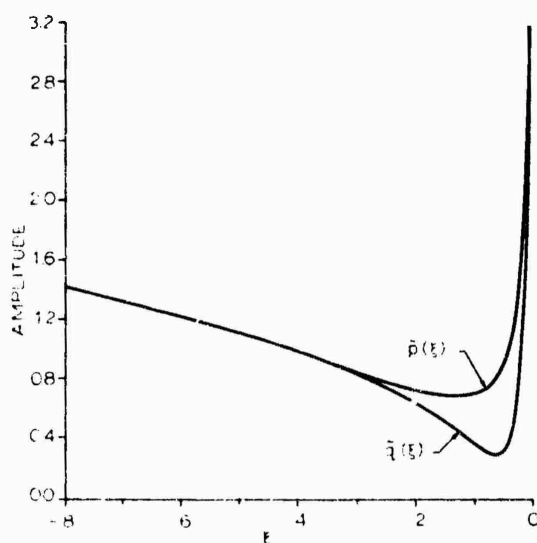


Fig. 1.9. Amplitude of the reflection coefficient functions $\tilde{p}(\xi)$ and $\tilde{q}(\xi)$ (LOGAN [1959]).

Reflection coefficient functions which are closely related to $\tilde{p}(\xi)$ and $\tilde{q}(\xi)$ and are frequently used are:

$$p(\xi) = \tilde{p}(\xi) + \frac{1}{2\sqrt{\pi}} \quad (1.284)$$

$$q(\xi) = \tilde{q}(\xi) + \frac{1}{2\sqrt{\pi}} \quad (1.285)$$

their real and imaginary parts are shown in Fig. I.10.

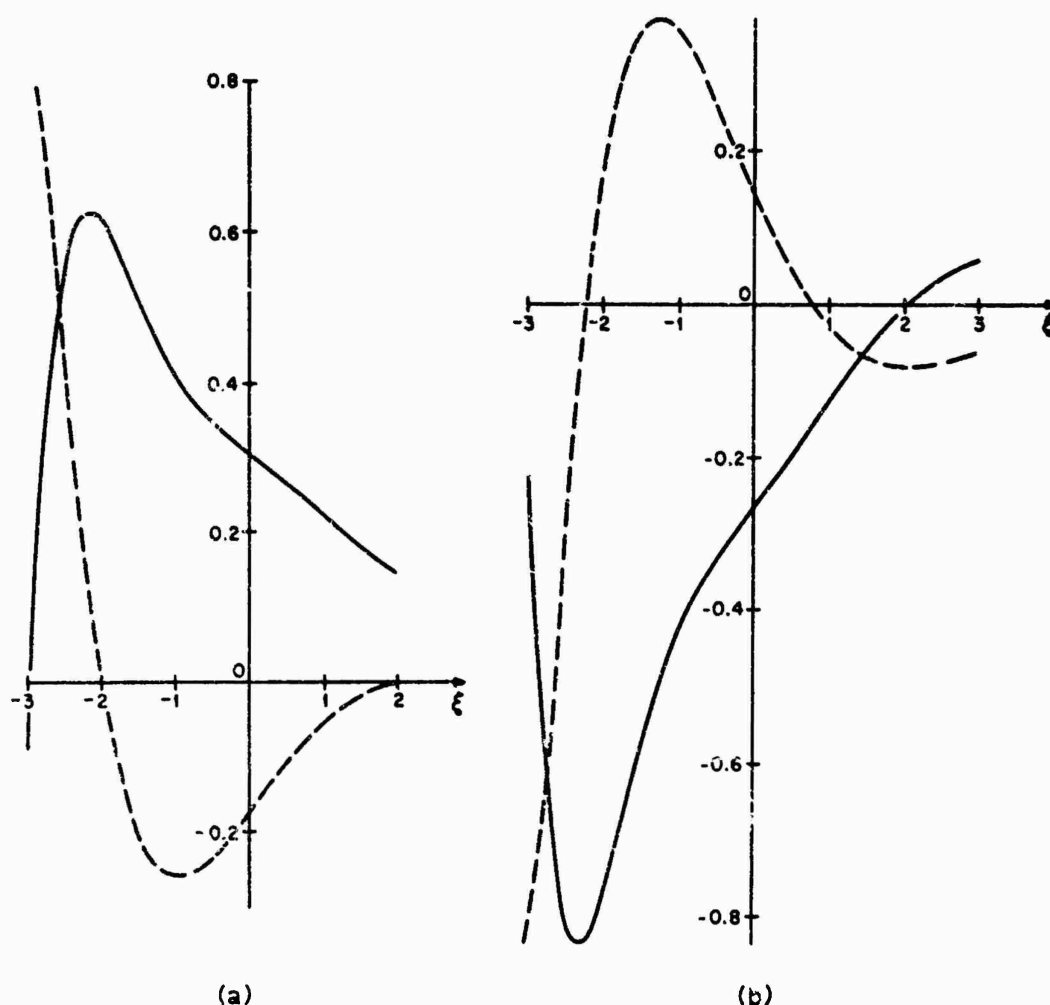


Fig. I. 10. Real (—) and imaginary (---) parts of the reflection coefficient functions $p(\xi)$ and $q(\xi)$, (a) and (b), respectively (LOGAN [1959]).

The following functions often appear in the Soviet literature (here the caret does not mean unit vector):

$$\begin{aligned} \hat{f}(\xi) &= \tilde{p}(\xi)e^{i\xi}, & \hat{q}(\xi) &= \tilde{q}(\xi)e^{i\xi}, \\ \hat{f}(\xi) &= \tilde{f}(\xi) + \frac{e^{i\xi}}{2\xi\sqrt{\pi}}, & \hat{q}(\xi) &= \tilde{q}(\xi) + \frac{e^{i\xi}}{2\xi\sqrt{\pi}}. \end{aligned} \quad (1.286)$$

The "universal" Fock function $V_1(\sigma, \tau, \eta)$ is defined as:

$$\begin{aligned} V_1(\sigma, \tau, \eta) &= \int_{\tau}^{\sigma} e^{i\sigma t} \left[e^{i\xi} \text{Ai}((t-\tau)e^{-i\xi}) + \right. \\ &\quad \left. + \frac{\text{Ai}'(te^{-i\xi}) + \eta e^{-i\xi} \text{Ai}(te^{-i\xi})}{\text{Ai}'(te^{-i\xi}) + \eta e^{i\xi} \text{Ai}(te^{i\xi})} \text{Ai}((t-\tau)e^{i\xi}) \right] dt. \end{aligned} \quad (1.287)$$

This is valuable in the treatment of bodies whose surfaces are characterised by an impedance (proportional to η), and also finds application to the perfectly conducting parabolic cylinder, where $\eta = 0$.

1.3.4. Fresnel integrals

The Fresnel integral $F(w)$, with w denoting a complex variable, is defined as

$$F(w) = \int_w^\infty e^{i\mu^2} d\mu, \quad (1.288)$$

where the path of integration is subject to the restriction $0 < \arg \mu < \frac{1}{2}\pi$ as $\mu \rightarrow \infty$. The function $F(w)$ is an entire transcendental function of w and is related to the complementary error function $\text{Erfc}(w)$ originally introduced by KRAMP [1799] (see ERDÉLYI et al. [1953]); in particular,

$$F(w) = e^{\frac{1}{2}i\pi} \text{Erfc}(e^{-\frac{1}{2}i\pi} w) \quad (1.289)$$

where

$$\text{Erfc}(w) = \int_w^\infty e^{-t^2} dt. \quad (1.290)$$

A factor $2/\sqrt{\pi}$ on the right-hand side of eq. (1.290) often appears in the definition of $\text{Erfc}(w)$. The following series representations converge everywhere in the finite w -plane:

$$F(w) = \frac{1}{2}\sqrt{\pi}e^{\frac{1}{2}i\pi} - w \sum_{n=0}^{\infty} \frac{(iw^2)^n}{n!(2n+1)}, \quad (1.291)$$

$$F(w) = \frac{1}{2}\sqrt{\pi}e^{\frac{1}{2}i\pi} - we^{iw^2} \sum_{n=0}^{\infty} \frac{(-2iw^2)^n}{1 \cdot 3 \dots (2n+1)}. \quad (1.292)$$

From these it is clear that $F(w)$ satisfies the symmetry relation

$$F(w) + F(-w) = \sqrt{\pi}e^{\frac{1}{2}i\pi}. \quad (1.293)$$

For $w \rightarrow \infty$ and $-\frac{1}{2}\pi < \arg w < \pi$, an asymptotic expansion of $F(w)$ is

$$F(w) \sim \frac{i}{2w} e^{iw^2} \left[1 + \sum_{n=1}^{\infty} \frac{1 \cdot 3 \dots (2n-1)}{(2iw^2)^n} \right]. \quad (1.294)$$

Asymptotic expansions for other ranges of $\arg w$ can be obtained from the combined use of eqs. (1.293) and (1.294).

The function $F(w)$ may be written as

$$\sqrt{\frac{2}{\pi}} F(w) = \left[\frac{1}{2} - C\left(\sqrt{\frac{2}{\pi}} w\right) \right] + i \left[\frac{1}{2} - S\left(\sqrt{\frac{2}{\pi}} w\right) \right] \quad (1.295)$$

where $C(u)$ and $S(u)$ are the FRESNEL [1821-22] integrals

$$C(u) = \int_0^u \cos\left(\frac{1}{2}\pi t^2\right) dt, \quad (1.296)$$

$$S(u) = \int_0^u \sin\left(\frac{1}{2}\pi t^2\right) dt.$$

For real u , the curve represented parametrically by

$$x = C(u), \quad y = S(u)$$

is the well-known spiral of CORNU [1874] (see e.g. SOMMERFELD [1954], ROSSI [1957]). For a list of numerical tables consult ABRAMOWITZ and STEGUN [1964] and HENSMAN and JENKINS [1957].

1.3.5. Legendre functions

The Legendre functions are solutions of the differential equation

$$(1-z^2) \frac{d^2 u}{dz^2} - 2z \frac{du}{dz} + \left[v(v+1) - \frac{\mu^2}{1-z^2} \right] u = 0 \quad (1.297)$$

where the parameters v, μ are unrestricted complex numbers. The differential equation (1.297) has regular singular points at $z = \pm 1, \infty$ and these points appear as ordinary branch points in the solutions. The variable z is therefore generally distinguished into two categories: first, the variable z may be an arbitrary point in the complex z -plane with the exception of points on the cut along the real axis from $+1$ to $-\infty$; second, the variable z is a real number x lying in the interval $-1 \leq x \leq 1$. For complex z the Legendre functions will be defined as in HOBSON [1931], whereas for real z between -1 and $+1$, we adopt a definition that differs from HOBSON [1931] but coincides with another commonly used definition (e.g. STRATTON [1941]). Many different definitions and notations for the Legendre functions have appeared in the literature and therefore, when a reference is consulted, great care should be exercised to determine what definition is employed by the author. Detailed properties of the Legendre functions may be found in ERDÉLYI et al. [1953], GRADSHTEYN and RYZHIK [1965], HOBSON [1931], MACROBERT [1948], MAGNUS and OBERHETTINGER [1949], MAGNUS et al. [1966] and ROBIN [1957-1959]. The last reference also contains an extensive list of numerical tables to which may be added ABRAMOWITZ and STEGUN [1964].

In the complex z -plane the Legendre functions $P_v^\mu(z)$ and $Q_v^\mu(z)$ of the first and second kind, respectively, are defined by

$$P_v^\mu(z) = \frac{1}{\Gamma(1-\mu)} \left(\frac{z-1}{z+1} \right)^{\frac{1}{2}\mu} F(-v, v+1; 1-\mu; \frac{1}{2}(1-z)), \quad |1-z| < 2 \quad (1.298)$$

$$Q_v^\mu(z) = \frac{e^{i\mu\pi} \sqrt{\pi} \Gamma(v+\mu+1) (z^2-1)^{\frac{1}{2}\mu}}{2^{v+1} \Gamma(v+\frac{1}{2}) z^{v+\mu+1}} F\left(\frac{1}{2}(v+\mu+2), \frac{1}{2}(v+\mu+1); v+\frac{1}{2}; \frac{1}{z^2}\right), \quad |z| > 1 \quad (1.299)$$

where

$$|\arg(z \pm 1)| < \pi, \quad |\arg z| < \pi \quad (1.300)$$

and F is the hypergeometric function defined by

$$F(a, b; c; \zeta) = \sum_{n=0}^{\infty} \frac{\Gamma(a+n)\Gamma(b+n)\Gamma(c)^n}{\Gamma(a)\Gamma(b)\Gamma(c+n)n!}, \quad |\zeta| < 1. \quad (1.301)$$

The functions defined in eqs. (I.298) and (I.299) are single-valued and regular in the z -plane cut along the real axis from $+1$ to $-\infty$. They may be uniquely continued without restriction to other complex values of z outside the cut by means of the transformation formulas for the hypergeometric function. Altogether, there are 72 different ways to represent a solution of Legendre's differential equation (I.297) in terms of the hypergeometric function with 18 different arguments.

Equation (I.297) remains unchanged if μ is replaced by $-\mu$, ν by $-\nu-1$, or z by $-z$, and the following linear relations exist:

$$P_{\nu}^{-\mu}(z) = \frac{\Gamma(\nu-\mu+1)}{\Gamma(\nu+\mu+1)} \left[P_{\nu}^{\mu}(z) - \frac{2}{\pi} e^{-i\mu\pi} \sin(\mu\pi) Q_{\nu}^{\mu}(z) \right], \quad (\text{I.302})$$

$$Q_{\nu}^{-\mu}(z) = e^{-2i\mu\pi} \frac{\Gamma(\nu-\mu+1)}{\Gamma(\nu+\mu+1)} Q_{\nu}^{\mu}(z), \quad (\text{I.303})$$

$$P_{-\nu-1}^{\mu}(z) = P_{\nu}^{\mu}(z), \quad (\text{I.304})$$

$$Q_{-\nu-1}^{\mu}(z) = \{ \sin[(\nu+\mu)\pi] Q_{\nu}^{\mu}(z) - \pi \cos(\nu\pi) e^{i\mu\pi} P_{\nu}^{\mu}(z) \} / \sin[(\nu-\mu)\pi], \quad (\text{I.305})$$

$$P_{\nu}^{\mu}(-z) = e^{\mp i\nu\pi} P_{\nu}^{\mu}(z) - \frac{2}{\pi} e^{-i\mu\pi} \sin[(\nu+\mu)\pi] Q_{\nu}^{\mu}(z), \quad (\text{I.306})$$

$$Q_{\nu}^{\mu}(-z) = -e^{\pm i\nu\pi} Q_{\nu}^{\mu}(z), \quad (\text{I.307})$$

where in the last two formulas the upper or lower sign is taken according as $\text{Im } z \gtrless 0$.

The Wronskian relation is

$$P_{\nu}^{\mu}(z) \frac{d}{dz} Q_{\nu}^{\mu}(z) - Q_{\nu}^{\mu}(z) \frac{d}{dz} P_{\nu}^{\mu}(z) = \frac{e^{i\mu\pi} \Gamma(\nu+\mu+1)}{(1-z^2) \Gamma(\nu-\mu+1)} \quad (\text{I.308})$$

and by means of eqs. (I.302) through (I.307), still further Wronskians may be derived, such as

$$P_{\nu}^{\mu}(z) \frac{d}{dz} P_{\nu}^{-\mu}(z) - P_{\nu}^{-\mu}(z) \frac{d}{dz} P_{\nu}^{\mu}(z) = \frac{2}{\pi} \frac{\sin \mu\pi}{z^2-1}, \quad (\text{I.309})$$

$$Q_{\nu}^{\mu}(z) \frac{d}{dz} P_{\nu}^{-\mu}(z) - P_{\nu}^{-\mu}(z) \frac{d}{dz} Q_{\nu}^{\mu}(z) = \frac{e^{i\mu\pi}}{z^2-1}, \quad (\text{I.310})$$

$$P_{\nu}^{\mu}(z) \frac{d}{dz} P_{\nu}^{\mu}(-z) - P_{\nu}^{\mu}(-z) \frac{d}{dz} P_{\nu}^{\mu}(z) = \frac{2}{\pi} \frac{\sin[(\nu+\mu)\pi] \Gamma(\nu+\mu+1)}{(z^2-1) \Gamma(\nu-\mu+1)}. \quad (\text{I.311})$$

From these it may be concluded that $P_{\nu}^{\mu}(z)$, $Q_{\nu}^{\mu}(z)$ are linearly independent except when $\nu-\mu$ or $\nu+\mu$ are negative integers; $P_{\nu}^{\mu}(z)$, $P_{\nu}^{-\mu}(z)$ are linearly independent except when μ is an integer; $Q_{\nu}^{\mu}(z)$, $P_{\nu}^{-\mu}(z)$ are linearly independent except when $\nu+\mu$ is a negative integer (in which case $Q_{\nu}^{\mu}(z)$ is not defined); and $P_{\nu}^{\mu}(z)$, $P_{\nu}^{\mu}(-z)$ are linearly independent except when $\mu-\nu$ or $\mu+\nu+1$ are positive integers.

The following recurrence relations are valid for both $P_v^\mu(z)$ and $Q_v^\mu(z)$. For varying order:

$$\left(\frac{d}{dz} + \frac{\mu z}{z^2 - 1}\right) P_v^\mu(z) = \frac{v(v+1) - \mu(\mu-1)}{(z^2 - 1)^{\frac{1}{2}}} P_v^{\mu-1}(z), \quad (1.312)$$

$$\left(\frac{d}{dz} - \frac{\mu z}{z^2 - 1}\right) P_v^\mu(z) = (z^2 - 1)^{-\frac{1}{2}} P_v^{\mu+1}(z), \quad (1.313)$$

and for varying degree:

$$\begin{aligned} (z^2 - 1) \frac{d}{dz} P_v^\mu(z) &= vz P_v^\mu(z) - (v + \mu) P_{v-1}^\mu(z) \\ &= -(v+1)z P_v^\mu(z) + (v - \mu + 1) P_{v+1}^\mu(z). \end{aligned} \quad (1.314)$$

Many other contiguous relations can be derived from these.

For $\mu = m$, $m = 0, 1, 2, \dots$, eqs. (I.302) and (I.303) simplify to

$$\begin{aligned} P_v^{-m}(z) &= \frac{\Gamma(v-m+1)}{\Gamma(v+m+1)} P_v^m(z), \\ Q_v^{-m}(z) &= \frac{\Gamma(v-m+1)}{\Gamma(v+m+1)} Q_v^m(z). \end{aligned} \quad (1.315)$$

Also for $\mu = m$, $m = 0, 1, 2, \dots$, we have

$$\begin{aligned} P_v^m(z) &= (z^2 - 1)^{\frac{1}{2}m} \frac{d^m}{dz^m} P_v(z) \\ Q_v^m(z) &= (z^2 - 1)^{\frac{1}{2}m} \frac{d^m}{dz^m} Q_v(z). \end{aligned} \quad (1.316)$$

For $v = n$, $n = 0, 1, 2, \dots$ and $\mu \neq 0, 1, 2, \dots$, the function $P_n^\mu(z)$ is a polynomial of degree n multiplied by an elementary function. On the other hand, for $\mu = m$, $m = 0, 1, 2, \dots$, the function $P_n^m(z)$ is a polynomial of degree $n - m$ multiplied by an elementary function, and if $m > n$ then $P_n^m(z) = 0$. The functions $P_n^m(z)$ and $Q_n^m(z)$ satisfy the relations

$$\begin{aligned} P_n^m(-z) &= (-1)^n P_n^m(z), \\ Q_n^m(-z) &= (-1)^{n+1} Q_n^m(z), \end{aligned} \quad (1.317)$$

and may be represented by

$$P_n^m(z) = \frac{(z^2 - 1)^{\frac{1}{2}m}}{2^n n!} \frac{d^{n+m}}{dz^{n+m}} (z^2 - 1)^n, \quad (1.318)$$

$$Q_n^m(z) = \frac{(-1)^n 2^{n-1} (n-1)! (z^2 - 1)^{\frac{1}{2}m}}{(2n-1)!} \frac{d^{n+m}}{dz^{n+m}} \left[(z^2 - 1)^n \int_z^1 \frac{du}{(u^2 - 1)^{n+1}} \right]. \quad (1.319)$$

For purely imaginary argument $z = \pm i\xi$, $\xi > 0$ a useful expression is

$$Q_v^\mu(\pm i\xi) = \frac{e^{i\mu\pi} \sqrt{\pi} \Gamma(v+\mu+1) (\xi^2+1)^{-\frac{1}{2}\mu} 2^{-\mu}}{e^{\pm \frac{1}{2}i(v+1)\pi} \Gamma(v+\frac{1}{2}) (\xi + \sqrt{\xi^2+1})^{v-\mu+1}} \times F\left(v-\mu+1, \frac{1}{2}-\mu; v+\frac{1}{2}; \frac{-1}{(\xi + \sqrt{\xi^2+1})^2}\right). \quad (1.320)$$

This representation also converges at $\xi = 0$ provided $\operatorname{Re} \mu \geq 0$; in particular

$$Q_v^\mu(\pm i0) = \frac{\Gamma(\frac{1}{2}(v+\mu+1)) \sqrt{\pi} 2^{\mu-1}}{\Gamma(\frac{1}{2}(v-\mu+2))} \exp\{\frac{1}{2}i(2\mu \mp v \mp 1)\pi\}, \quad (1.321)$$

$$Q_v^{\mu'}(\pm i0) = \frac{\Gamma(\frac{1}{2}(v+\mu+2)) 2^\mu \sqrt{\pi}}{\Gamma(\frac{1}{2}(v-\mu+1))} \exp\{\frac{1}{2}i(2\mu \mp v)\pi\}, \quad (1.322)$$

where the prime denotes the derivative with respect to the argument.

For Legendre functions in which $z = x = \cos \theta$, where $-1 < x < 1$ and $0 < \theta < \pi$, it is convenient to introduce slightly modified solutions of eq. (1.297) since the limits of $P_v^\mu(z)$, $Q_v^\mu(z)$ differ in general according as $z \rightarrow x+i0$ or $z \rightarrow x-i0$. These modified solutions are denoted by $P_v^\mu(x)$ and $Q_v^\mu(x)$ and defined by

$$P_v^\mu(x) = \frac{1}{2} e^{-i\mu\pi} [e^{\frac{1}{2}i\mu\pi} P_v^\mu(x+i0) + e^{-\frac{1}{2}i\mu\pi} P_v^\mu(x-i0)], \quad (1.323)$$

$$Q_v^\mu(x) = \frac{1}{2} e^{-2i\mu\pi} [e^{-\frac{1}{2}i\mu\pi} Q_v^\mu(x+i0) + e^{\frac{1}{2}i\mu\pi} Q_v^\mu(x-i0)], \quad (1.324)$$

where $f(x \pm i0)$ means $\lim_{\epsilon \rightarrow 0} f(x \pm i\epsilon)$. The function $P_v^\mu(x)$ may also be written as

$$P_v^\mu(x) = \frac{i}{\pi} e^{-2i\mu\pi} [e^{-\frac{1}{2}i\mu\pi} Q_v^\mu(x+i0) - e^{\frac{1}{2}i\mu\pi} Q_v^\mu(x-i0)]. \quad (1.325)$$

The definitions (1.323) through (1.325) for the Legendre functions $P_v^\mu(x)$, $Q_v^\mu(x)$ on the cut differ from those in HOBSON [1931]; the definitions here contain an extra factor $\exp(-i\mu\pi)$.

Convenient alternative representations for $Q_v^\mu(\cos \theta \pm i0)$ are given by

$$Q_v^\mu(\cos \theta \pm i0) = \int_0^\pi \frac{\pi}{2 \sin \theta} \frac{\Gamma(v+\mu+1)}{\Gamma(v+\frac{1}{2})} e^{i\mu\pi} \exp\{\mp i[(v+\frac{1}{2})\theta + \frac{1}{2}\pi]\} \times F\left(\frac{1}{2}+\mu, \frac{1}{2}-\mu; v+\frac{1}{2}; \frac{\pm i e^{\mp i\theta}}{2 \sin \theta}\right), \quad (1.326)$$

$$Q_v^\mu(\cos \theta \pm i0) = \sqrt{\pi} \frac{2^\mu \Gamma(v+\mu+1)}{\Gamma(v+\frac{1}{2})} \sin^\mu \theta e^{i\mu\pi} \exp\{\mp i[(v+\mu+1)\theta - \frac{1}{2}\mu\pi]\} \times F(v+\mu+1, \mu+\frac{1}{2}; v+\frac{1}{2}; e^{\mp 2i\theta}), \quad (1.327)$$

and the application of these equations to eqs. (1.324) and (1.325) leads to trigonometric expansions of $P_v^\mu(\cos \theta)$ and $Q_v^\mu(\cos \theta)$; for example, for $0 < \theta < \pi$:

$$P_v^\mu(\cos \theta) = \frac{2^{\mu+1} \Gamma(v+\mu+1)}{\sqrt{\pi} \Gamma(v+\frac{1}{2})} \sin^\mu \theta e^{-i\mu\pi} \sum_{s=0}^{\infty} \frac{(\mu+\frac{1}{2})_s (v+\mu+1)_s}{s! (v+\frac{1}{2})_s} \times \sin [(2s+v+\mu+1)\theta], \quad (I.328)$$

$$Q_v^\mu(\cos \theta) = \frac{\sqrt{\pi} 2^\mu \Gamma(v+\mu+1)}{\Gamma(v+\frac{1}{2})} \sin^\mu \theta e^{-i\mu\pi} \sum_{s=0}^{\infty} \frac{(\mu+\frac{1}{2})_s (v+\mu+1)_s}{s! (v+\frac{1}{2})_s} \times \cos [(2s+v+\mu+1)\theta] \quad (I.329)$$

where the symbol $(\alpha)_s$ means

$$(\alpha)_s = \Gamma(\alpha+s)/\Gamma(\alpha). \quad (I.330)$$

For $|x| < 1$, eq. (I.298) yields

$$P_v^\mu(x \pm i0) = \frac{e^{\mp i\mu\pi}}{\Gamma(1-\mu)} \left(\frac{1+x}{1-x} \right)^{\frac{1}{2}\mu} F(-v, v+1; 1-\mu; \frac{1}{2}(1-x)). \quad (I.331)$$

For $0 < \theta < \pi$, therefore, eqs. (I.323) and (I.331) lead to the trigonometric series

$$P_v^{-\mu}(\cos \theta) = e^{i\mu\pi} \tan^\mu(\frac{1}{2}\theta) \sum_{s=0}^{\infty} \frac{(-1)^s \Gamma(v+s+1) \sin^{2s}(\frac{1}{2}\theta)}{s! \Gamma(v-s+1) \Gamma(\mu+s+1)}, \quad (I.332)$$

$$\frac{\partial}{\partial v} P_v^{-\mu}(\cos \theta) = e^{i\mu\pi} \tan^\mu(\frac{1}{2}\theta) \sum_{s=0}^{\infty} \frac{(-1)^s \Gamma(v+s+1) \sin^{2s}(\frac{1}{2}\theta)}{s! \Gamma(v-s+1) \Gamma(\mu+s+1)} [\psi(v+s) - \psi(v-s)], \quad (I.333)$$

where

$$\psi(v) = \frac{d}{dv} \log \Gamma(v+1). \quad (I.334)$$

In particular, for $\mu = 0$:

$$P_v(\cos \theta) = \sum_{s=0}^{\infty} \frac{(-1)^s \Gamma(v+s+1) \sin^{2s}(\frac{1}{2}\theta)}{(s!)^2 \Gamma(v-s+1)}. \quad (I.335)$$

For $\theta = \pi$, $P_v(\cos \theta)$ displays a logarithmic singularity, and an expansion suitable for $\theta \approx \pi$ is

$$P_v(\cos \theta) = \frac{\sin v\pi}{\pi} \sum_{s=0}^{\infty} \frac{(-1)^s \Gamma(v+s+1) \cos^{2s}(\frac{1}{2}\theta)}{(s!)^2 \Gamma(v-s+1)} \times [\log \cot^2(\frac{1}{2}\theta) + \psi(v) + \psi(-v-1) - 2\psi(s)], \quad (I.336)$$

or alternatively

$$P_v(\cos \theta) = \frac{\sin v\pi}{\pi} \sum_{s=0}^{\infty} \frac{(-1)^s \Gamma(v+s+1) \cos^{2s}(\frac{1}{2}\theta)}{(s!)^2 \Gamma(v-s+1)} \times [\log \cos^2(\frac{1}{2}\theta) + \psi(v+s) + \psi(-v+s-1) - 2\psi(s)]. \quad (I.337)$$

For the Legendre functions on the cut, the linear relations in eqs. (I.302) through (I.307) become

$$P_v^{-\mu}(x) = e^{2i\mu\pi} \frac{\Gamma(v-\mu+1)}{\Gamma(v+\mu+1)} \left[\cos(\mu\pi) P_v^{\mu}(x) - \frac{2}{\pi} \sin(\mu\pi) Q_v^{\mu}(x) \right], \quad (\text{I.338})$$

$$Q_v^{-\mu}(x) = e^{2i\mu\pi} \frac{\Gamma(v-\mu+1)}{\Gamma(v+\mu+1)} [\cos(\mu\pi) Q_v^{\mu}(x) + \frac{1}{2}\pi \sin(\mu\pi) P_v^{\mu}(x)], \quad (\text{I.339})$$

$$P_{-v-1}^{\mu}(x) = P_v^{\mu}(x), \quad (\text{I.340})$$

$$Q_{-v-1}^{\mu}(x) = \{\sin[(v+\mu)\pi] Q_v^{\mu}(x) - \pi \cos(v\pi) \cos(\mu\pi) P_v^{\mu}(x)\} / \sin[(v-\mu)\pi], \quad (\text{I.341})$$

$$P_v^{\mu}(-x) = \cos[(v+\mu)\pi] P_v^{\mu}(x) - \frac{2}{\pi} \sin[(v+\mu)\pi] Q_v^{\mu}(x), \quad (\text{I.342})$$

$$Q_v^{\mu}(-x) = -\cos[(v+\mu)\pi] Q_v^{\mu}(x) - \frac{1}{2}\pi \sin[(v+\mu)\pi] P_v^{\mu}(x). \quad (\text{I.343})$$

The Wronskians given in eqs. (I.308) through (I.311) become

$$P_v^{\mu}(x) \frac{d}{dx} Q_v^{\mu}(x) - Q_v^{\mu}(x) \frac{d}{dx} P_v^{\mu}(x) = \frac{e^{-2i\mu\pi} \Gamma(v+\mu+1)}{(1-x^2) \Gamma(v-\mu+1)}, \quad (\text{I.344})$$

$$P_v^{\mu}(x) \frac{d}{dx} P_v^{-\mu}(x) - P_v^{-\mu}(x) \frac{d}{dx} P_v^{\mu}(x) = \frac{2}{\pi} \frac{\sin \mu\pi}{x^2-1}, \quad (\text{I.345})$$

$$Q_v^{\mu}(x) \frac{d}{dx} P_v^{-\mu}(x) - P_v^{-\mu}(x) \frac{d}{dx} Q_v^{\mu}(x) = \frac{\cos \mu\pi}{x^2-1}, \quad (\text{I.346})$$

$$P_v^{\mu}(x) \frac{d}{dx} P_v^{\mu}(-x) - P_v^{\mu}(-x) \frac{d}{dx} P_v^{\mu}(x) = \frac{2}{\pi} \frac{e^{-2i\mu\pi} \sin[(v+\mu)\pi] \Gamma(v+\mu+1)}{(x^2-1) \Gamma(v-\mu+1)} \quad (\text{I.347})$$

From these it may be concluded that $P_v^{\mu}(x)$, $Q_v^{\mu}(x)$ are linearly independent except when $v-\mu$ or $v+\mu$ are negative integers; $P_v^{\mu}(x)$, $P_v^{-\mu}(x)$ are linearly independent except when μ is an integer; $Q_v^{\mu}(x)$, $P_v^{-\mu}(x)$ are linearly independent except when $\mu+v$ is a negative integer or when μ is half an odd integer; and $P_v^{\mu}(x)$, $P_v^{\mu}(-x)$ are linearly independent except when $\mu-v$ or $\mu+v+1$ are positive integers.

The recurrence relations given in eqs. (I.312) through (I.314) become, for varying order:

$$\begin{aligned} \left(\frac{d}{d\theta} + \mu \cot \theta \right) P_v^{\mu}(\cos \theta) &= [v(v+1) - \mu(\mu-1)] P_v^{\mu-1}(\cos \theta), \\ \left(\frac{d}{d\theta} - \mu \cot \theta \right) P_v^{\mu}(\cos \theta) &= -P_v^{\mu+1}(\cos \theta), \end{aligned} \quad (\text{I.348})$$

and for varying degree:

$$\begin{aligned} \sin \theta \frac{d}{d\theta} P_v^{\mu}(\cos \theta) &= v \cos \theta P_v^{\mu}(\cos \theta) - (v+\mu) P_{v-1}^{\mu}(\cos \theta) \\ &= -(v+1) \cos \theta P_v^{\mu}(\cos \theta) + (v-\mu+1) P_{v+1}^{\mu}(\cos \theta). \end{aligned} \quad (\text{I.349})$$

The recurrence formulas (I.348) through (I.349) are also valid for $Q_v^\mu(\cos \theta)$. Many other contiguous relations can be obtained from these.

For $n = 0, 1, 2, \dots$ and arbitrary v , the function $P_{n+v}^{-v}(\cos \theta)$ is given by

$$P_{n+v}^{-v}(\cos \theta) = \frac{e^{i\nu\pi} \sin^v \theta}{2^v \Gamma(v+1)} F(-n, 2v+n+1; v+1; \sin^2 \frac{1}{2}\theta) \quad (\text{I.350})$$

and obeys the relation

$$P_{n+v}^{-v}(-\cos \theta) = (-1)^n P_{n+v}^{-v}(\cos \theta). \quad (\text{I.351})$$

An alternative representation is

$$P_{n+v}^{-v}(x) = \frac{(-1)^n e^{i\nu\pi} (1-x^2)^{-\frac{1}{2}\nu}}{2^{n+v} \Gamma(n+v+1)} \frac{d^n}{dx^n} (1-x^2)^{n+v}. \quad (\text{I.352})$$

It is clear that $(1-x^2)^{-\frac{1}{2}\nu} P_{n+v}^{-v}(x)$ is a polynomial in x of degree n and remains finite at $x = \pm 1$. For $\text{Re } v > -1$ (not necessary when v is an integer), the following orthogonality relation is satisfied:

$$\int_{-1}^1 P_{n+v}^{-v}(x) P_{n'+v}^{-v}(x) dx = \delta_{nn'} \frac{2^n! e^{2i\nu\pi}}{(2n+2v+1) \Gamma(n+2v+1)}, \quad (\text{I.353})$$

where $\delta_{nn} = 1$ and $\delta_{nn'} = 0$ for $n \neq n'$.

For $\mu = m$, $m = 0, 1, 2, \dots$, eqs. (I.338) and (I.339) simplify to

$$\begin{aligned} P_v^{-m}(x) &= (-1)^m \frac{\Gamma(v-m+1)}{\Gamma(v+m+1)} P_v^m(x), \\ Q_v^{-m}(x) &= (-1)^m \frac{\Gamma(v-m+1)}{\Gamma(v+m+1)} Q_v^m(x). \end{aligned} \quad (\text{I.354})$$

Also for $\mu = m$, $m = 0, 1, 2, \dots$, we have

$$\begin{aligned} P_v^m(x) &= (1-x^2)^{\frac{1}{2}m} \frac{d^m}{dx^m} P_v(x), \\ Q_v^m(x) &= (1-x^2)^{\frac{1}{2}m} \frac{d^m}{dx^m} Q_v(x). \end{aligned} \quad (\text{I.355})$$

It should be emphasized here that HOBSON's [1931] definition of the Legendre function on the cut results in an extra factor $(-1)^m$ on the right-hand sides in eqs. (I.355). Both forms are in common usage.

For $v = n$, $n = 0, 1, 2, \dots$ and $\mu \neq 0, 1, 2, \dots$, the function $P_n^\mu(x)$ is a polynomial of degree n multiplied by an elementary function. On the other hand, for $\mu = m$, $m = 0, 1, 2, \dots$, the function $P_n^m(x)$ is a polynomial of degree $n-m$ multiplied by an elementary function, and if $m > n$ then $P_n^m(x) = 0$. The functions $P_n^m(x)$ and $Q_n^m(x)$ satisfy the relations

$$\begin{aligned} P_n^m(-x) &= (-1)^{n-m} P_n^m(x), \\ Q_n^m(-x) &= (-1)^{n-m+1} Q_n^m(x). \end{aligned} \quad (\text{I.356})$$

and may be represented by

$$P_n^m(x) = \frac{(1-x^2)^{\frac{1}{2}m}}{2^n n!} \frac{d^{n+m}}{dx^{n+m}} (x^2-1)^n, \quad (1.357)$$

$$Q_n^m(x) = \frac{2^{n-1}(n-1)!(1-x^2)^{\frac{1}{2}m}}{(2n-1)!} \frac{d^{n+m}}{dx^{n+m}} \left[(x^2-1)^n \int_0^x \frac{du}{(1-u^2)^{n+1}} \right]. \quad (1.358)$$

The functions $P_n^m(x)$ are finite at $x = \pm 1$ whereas the functions $Q_n^m(x)$ are not. The following orthogonality relations are satisfied:

$$\int_{-1}^1 P_n^m(x) P_m^m(x) dx = \delta_{nm} \frac{2(n+m)!}{(2n+1)(n-m)!}, \quad (1.359)$$

$$\int_{-1}^1 \frac{P_n^m(x) P_m^m(x)}{1-x^2} dx = \delta_{nm} \frac{(n+m)!}{m(n-m)!}, \quad (1.360)$$

$$\int_0^\pi \left(\frac{dP_n^m}{d\theta} \frac{dP_m^m}{d\theta} + \frac{m^2}{\sin^2 \theta} P_n^m P_m^m \right) \sin \theta d\theta = \delta_{nm} \frac{2n(n+1)(n+m)!}{(2n+1)(n-m)!}. \quad (1.361)$$

For $|v| \rightarrow \infty$, $|\arg v| \leq \pi - \epsilon$, $\delta \leq \theta \leq \pi - \delta$, where $0 < (\epsilon, \delta) < \pi$:

$$P_v(\cos \theta) \sim \left(\frac{2}{\pi v \sin \theta} \right)^{\frac{1}{2}} \left\{ \left(1 - \frac{1}{4v} \right) \cos \left[(v + \frac{1}{2})\theta - \frac{1}{4}\pi \right] - \frac{\cot \theta}{8v} \sin \left[(v + \frac{1}{2})\theta - \frac{1}{4}\pi \right] + O\left(\frac{1}{v^2}\right) \right\}, \quad (1.362)$$

$$Q_v(\cos \theta) \sim \left(\frac{\pi}{2v \sin \theta} \right)^{\frac{1}{2}} \left\{ \left(1 - \frac{1}{4v} \right) \cos \left[(v + \frac{1}{2})\theta + \frac{1}{4}\pi \right] - \frac{\cot \theta}{8v} \sin \left[(v + \frac{1}{2})\theta + \frac{1}{4}\pi \right] + O\left(\frac{1}{v^2}\right) \right\}. \quad (1.363)$$

On the other hand, for $|v| \rightarrow \infty$, $\theta \rightarrow 0$, such that the product $(2v+1) \sin \frac{1}{2}\theta$ remains finite:

$$P_v(\cos \theta) \sim J_0(u) + \sin^2 \frac{1}{2}\theta \left[\frac{1}{6}u J_3(u) - J_2(u) + \frac{1}{2u} J_1(u) \right] + O(\sin^4 \frac{1}{2}\theta), \quad (1.364)$$

$$Q_v(\cos \theta) \sim -\frac{1}{2}\pi \left\{ Y_0(u) + \sin^2 \frac{1}{2}\theta \left[\frac{1}{6}u Y_3(u) - Y_2(u) + \frac{1}{2u} Y_1(u) \right] + O(\sin^4 \frac{1}{2}\theta) \right\}, \quad (1.365)$$

where $u = (2v+1) \sin \frac{1}{2}\theta$. Expressions valid for $\theta \rightarrow \pi$ may be obtained from eqs. (1.364) and (1.365) by the application of

$$\begin{aligned} P_v(\cos \theta) &= \cos(v\pi) P_v(-\cos \theta) - \frac{2}{\pi} \sin(v\pi) Q_v(-\cos \theta), \\ Q_v(\cos \theta) &= -\cos(v\pi) Q_v(-\cos \theta) - \frac{1}{2}\pi \sin(v\pi) P_v(-\cos \theta). \end{aligned} \quad (1.366)$$

A uniform asymptotic expression for $|v| \rightarrow \infty$ has been given by SZEGÖ [1934]:

$$P_v(\cos \theta) \sim \left(\frac{\theta}{\sin \theta} \right)^{\frac{1}{2}} \sum_{s=0}^{\infty} A_s(\theta) (v + \frac{1}{2})^{-s} J_s[(v + \frac{1}{2})\theta], \quad (\text{I.367})$$

$$Q_v(\cos \theta) \sim -\frac{1}{2}\pi \left(\frac{\theta}{\sin \theta} \right)^{\frac{1}{2}} \sum_{s=0}^{\infty} A_s(\theta) (v + \frac{1}{2})^{-s} Y_s[(v + \frac{1}{2})\theta], \quad (\text{I.368})$$

where the $A_s(\theta)$ are elementary functions, regular in $0 \leq \theta < \pi$. In particular, the first three coefficients are

$$A_0 = 1, \quad A_1 = \frac{1}{8} \left(\cot \theta - \frac{1}{\theta} \right), \quad A_2 = \frac{1}{128} \left(-\frac{15}{\theta^2} + \frac{6}{\theta} \cot \theta + \frac{9}{\sin^2 \theta} - 1 \right). \quad (\text{I.369})$$

The expansions (I.367) and (I.368) reduce to those in eqs. (I.362) and (I.363) when $|(v + \frac{1}{2})\theta| \rightarrow \infty$ and are also valid for $\theta \rightarrow 0$. For other asymptotic expansions see ROBIN [1957-1959] and THORNE [1957].

Bibliography

- ABRAMOWITZ, M. and I. STEGUN [1964], *Handbook of Mathematical Functions with Formulas, Graphs, and Mathematical Tables*, National Bureau of Standards Appl. Math. Series, U.S. Government Printing Office, Washington, D.C.
- ADACHI, S. [1956], The Nose-On Echo Area of Axially Symmetric Thin Bodies having Sharp Apices, *Proc. IEEE* **53**, 1067-1068.
- AIRY, G. B. [1838], On the Intensity of Light in the Neighborhood of a Caustic, *Trans. Cambridge Phil. Soc.* **6**, 379-402.
- ALTSHULER, S. [1958], Variational Principles for the Wave Function in Scattering Theory, *Phys. Rev.* **109**, 1830-1836.
- ANDREASEN, M. G. [1964], Scattering from Parallel Metallic Cylinders with Arbitrary Cross Section, *IEEE Trans.* **AP-12**, 746-754.
- ANDREASEN, M. G. [1965a], Scattering from Cylinders with Arbitrary Surface Impedance, *Proc. IEEE* **53**, 812-817.
- ANDREASEN, M. G. [1965b], Scattering from Bodies of Revolution, *IEEE Trans.* **AP-13**, 303-310.
- AR, E. [1967], On the Low Frequency Acoustical Scattering of a Plane Wave from a Soft Spindle at Nose-On Incidence, *Quart. Appl. Math.* **25**, 285-292.
- AR, E. and R. E. KLEIMAN [1966], The Exterior Neumann Problem for the Three-Dimensional Helmholtz Equation, *Arch. Rational Mech. Anal.* **23**, 218-236.
- BAGHDASARIAN, A. and D. J. ANGELAKOS [1965], Scattering from Conducting Loops and Solution of Circular Loop Antennas by Numerical Methods, *Proc. IEEE* **53**, 818-822.
- BAKER, B. B. and E. T. COPSON [1950], *The Mathematical Theory of Huygens' Principle*, Oxford University Press (2nd edition).
- BATEMAN, H. [1915], *Electrical and Optical Wave Motion*, Cambridge University Press; reprinted in 1955 by Dover Publications, New York.
- BAZER, J. and S. N. KARP [1952], Propagation of Plane Electromagnetic Waves past a Shoreline, New York University Report No. EM-46.
- BECHEL, M. E. [1965], Application of Geometric Diffraction Theory to Scattering from Cones and Disks, *Proc. IEEE* **53**, 877-882.
- BLOSS, J. [1951], The Extension of the Wiener-Hopf Technique to Radiation Problems involving Boundaries of Elliptic Cross-Section, Dissertation, Polytechnic Institute of Brooklyn. Also,

- McGill Symposium on Microwave Optics, Air Force Cambridge Research Center Report No. TR-59-118 (II), 1959.
- BLORE, W. E. and H. M. MUSAL Jr. [1965], The Radar Cross Section of Plasma-Coated Metal Bodies, *Proc. IEEE* **53**, 1122-1123.
- BORN, M. and E. WOLF [1959], *Principles of Optics*, Pergamon Press, New York.
- BOUWKAMP, C. J. [1954], Diffraction Theory, *Rep. Progr. Phys.* **17**, 25-100.
- BOUWKAMP, C. J. and H. B. G. CASIMIR [1954], On Multipole Expansions in the Theory of Electromagnetic Radiation, *Physica* **20**, 539-554.
- BOWMAN, J. J. [1963], Scattering of Plane Electromagnetic Waves from a Semi-Infinite Hollow Circular Pipe (Axial Incidence), Memorandum D0620-125-M41-10; Scattering of Plane Electromagnetic Waves from a Semi-Infinite Hollow Circular Pipe (Off-Axis Incidence), Memorandum D0620-127-M41-13; Scattering from a Semi-Infinite Quarter-Sector Duct bounded by Two Infinite Planes, Memorandum D0620-129-M41-16; On the Vajnshtejn Factorization Functions, Memorandum D0620-135-M41-20, Conduction Corporation, Ann Arbor, Michigan.
- BOWMAN, J. J. [1967], High-Frequency Backscattering from an Absorbing Infinite Strip with Arbitrary Face Impedances, *Can. J. Phys.* **45**, 2409-2430.
- BOWMAN, J. J. and V. H. WESTON [1968], Reduction of Radar Cross Section of Ducts, University of Michigan Radiation Laboratory Report No. 1492-1-Q.
- BROWN Jr., W. P. [1966], On the Asymptotic Behavior of Electromagnetic Fields scattered from Convex Cylinders near Grazing Incidence, *J. Math. Anal. Appl.* **15**, 355-385.
- BUCHAL, R. N. and J. B. KELLER [1960], Boundary Layer Problems in Diffraction Theory, *Comm. Pure Appl. Math.* **13**, 85-114.
- CAIRO, L. and T. KAHAN [1962], *Techniques variationnelles en radiodélectricité*, Dunod, Paris (in French; an English translation by G. D. Sims was published by Blackie, London in 1965).
- CARLSON, J. F. and A. E. HEINS [1947], The Reflection of an Electromagnetic Plane Wave by an Infinite Set of Plates, I, *Quart. Appl. Math.* **4**, 313-329.
- CAMPOPLANO, C. N. [1957], Summary of Asymptotic Expansions for Bessel Functions, Polytechnic Institute of Brooklyn Report No. R-582-57, PIB-502.
- CASE, K. M. [1964], An Approximation Method for Diffraction Theory, *Rev. Mod. Phys.* **36**, 669-679.
- CHEN, Y. M. [1964], Diffraction by a Smooth Transparent Object, *J. Math. Phys.* **5**, 820-832.
- CHERRY, T. M. [1950], Uniform Asymptotic Formulae for Functions with Transition Points, *Trans. Am. Math. Soc.* **68**, 224-257.
- CHESTER, W. [1950], The Propagation of Sound Waves in an Open-Ended Channel, *Phil. Mag.* **41**, 11-33.
- CLEMMOW, P. C. [1951], A Method for the Exact Solution of a Class of Two-Dimensional Diffraction Problems, *Proc. Roy. Soc. A* **205**, 286-308.
- CLEMMOW, P. C. [1953], Radio Propagation over a Flat Earth across a Boundary separating two Different Media, *Phil. Trans. Roy. Soc. A* **246**, 1-55.
- CLEMMOW, P. C. and V. H. WESTON [1961], Diffraction of a Plane Wave by an almost Circular Cylinder, *Proc. Roy. Soc. A* **264**, 246-268.
- COCHRAN, J. A. [1965], The Zeros of Hankel Functions as Functions of their Order, *Numerische Math.* **7**, 238-250.
- COHEN, D. S. [1964], Eigenfunction Expansions and Non-Selfadjoint Boundary Value Problems, *Comm. Pure Appl. Math.* **17**, 23-34.
- COHEN, D. S. [1965], New Eigenfunction Expansions and Alternative Representations for the Reduced Wave Equation, *J. Math. Mech.* **14**, 403-412.
- COPSON, E. T. [1945], On an Integral Equation arising in the Theory of Diffraction, *Quart. J. Math.* **17**, 19-34.
- CORNET, A. [1874], Méthode nouvelle pour la discussion des problèmes de diffraction dans le cas d'une onde cylindrique, *J. de Physique* **3**, 5-15, 44-52.

- CULLEN, J. A. [1958], Surface Currents induced by Short-Wavelength Radiation, *Phys. Rev.* **109**, 1863-1867.
- DARLING, D. A. [1960], Some Relations between Potential Theory and the Wave Equation, The University of Michigan Radiation Laboratory Report No. 2871-5-T, Ann Arbor, Michigan.
- DARLING, D. A. and T. B. A. SENIOR [1965], Low Frequency Expansions for Scattering by Separable and Non-Separable Bodies, *J. Acoust. Soc. Am.* **37**, 228-234.
- DEBYE, P. [1909], Näherungsformeln für die Zylinderfunktionen für grosse Werte des Arguments und unbeschränkt veränderliche Werte des Index, *Math. Ann.* **67**, 535-558.
- DEBYE, P. [1910], Semikonvergente Entwicklungen für die Zylinderfunktionen und ihre Ausdehnung in Komplexe, *Münchener Sitzungsberichte* **40**, 1-29.
- DEHOOP, A. T. [1960], A Reciprocity Theorem for the Electromagnetic Field Scattered by an Obstacle, *Appl. Sci. Res.* **B8**, 135-139.
- DEHOOP, A. T. [1968], A Reciprocity Relation between the Transmitting and the Receiving Properties of an Antenna, *Appl. Sci. Res.* **19**, 90-96.
- DOLPH, C. L. [1961], Recent Developments in some Non-Self-Adjoint Problems of Mathematical Physics, *Bull. Am. Math. Soc.* **67**, 1-69.
- EINARSSON, O., R. E. KLEINMAN, P. LAURIN and P. L. E. USLENGHI [1966], Studies in Radar Cross Sections L-Diffraction and Scattering by Regular Bodies IV: The Circular Cylinder, University of Michigan Radiation Laboratory Report No. 7133-3-T.
- ERDÉLYI, A., W. MAGNUS, F. OBERHETTINGER and F. G. TRICOMI [1953], *Higher Transcendental Functions*, Volumes I, II, III, McGraw-Hill Book Co., Inc., New York.
- FAULKNER, T. R. [1965], Diffraction of an Electromagnetic Plane-Wave by a Metallic Strip, *J. Inst. Maths. Applies.* **1**, 149-163.
- FELSEN, L. B. [1957], Alternative Field Representations in Regions bounded by Spheres, Cones, and Planes, *IRE Trans.* **AP-5**, 109-121.
- FELSEN, L. B. [1964], Quasi-Optic Diffraction, in: *Proc. Symp. Quasi Optics*, Polytechnic Press, Polytechnic Institute of Brooklyn, New York.
- FELSEN, L. B. and H. Y. YEE [1968a], Ray-Optical Techniques for Waveguide Discontinuities, *IEEE Trans.* **AP-16**, 268-269.
- FELSEN, L. B. and H. Y. YEE [1968b], Multiple Interaction by Ray Optics - Some Observations and an Example, to be published.
- FIALKOVSKIY, A. T. [1966], Diffraction of Planar Electromagnetic Wave by a Slot and a Strip, *Radio Eng. Electron.* **11**, 150-157.
- FISCHER, E. [1966], On the Watson Transformation, *Comm. Pure Appl. Math.* **19**, 287-297.
- FLAMMER, C. [1957], Variational Formulae for Domain Functionals in Electromagnetic Theory, Stanford Research Institute Technical Report No. 57 (ASTIA No. AD 110 284), Menlo Park, California.
- FOCK, V. A. [1942], Sur certaines équations intégrales de physique mathématique, *C. R. Acad. Sci. URSS* **36**, 133-136.
- FOCK, V. A. [1944], On some Integral Equations of Mathematical Physics, *Mat. Sborn.* **14**, 3-50 (in Russian).
- FOCK, V. A. [1945], Diffraction of Radio Waves around the Earth's Surface, *J. Phys. USSR* **9**, 255-266.
- FOCK, V. A. [1946a], The Distribution of Currents induced by a Plane Wave on the Surface of a Conductor, *J. Phys. USSR* **10**, 130-136.
- FOCK, V. A. [1946b], The Field of a Plane Wave near the Surface of a Conducting Body, *J. Phys. USSR* **10**, 399-409.
- FOCK, V. A. [1965], *Electromagnetic Diffraction and Propagation Problems*, Pergamon Press, New York.
- FOCK, V. A. and L. A. WAINSTEIN [1963], On the Transverse Diffusion of Short Wave Diffracted by a Convex Cylinder, in: *Electromagnetic Theory and Antennas*, Pergamon Press, New York. Also Chapter 9 of FOCK [1965].

- FRANZ, W. [1949], Zur Theorie der Beugung, *Z. Physik* **125**, 563–596.
- FRANZ, W. [1954], Über die Greenschen Funktionen des Zylinders und der Kugel, *Z. Naturforsch.* **9a**, 705–716.
- FRANZ, W. and K. DEPPERMAN [1952], Theorie der Beugung am Zylinder unter Berücksichtigung der Kriechwelle, *Ann. Physik* **10**, 361–373.
- FRESNEL, A. J. [1821–22], Mémoire sur la diffraction de la lumière, *Mém. de l'Acad. R. des Sci.* **5**, 339–476 (also *Oeuvres*, Vol. I (1866)).
- FRIEDMAN, B. [1951], Propagation in a Non-Homogeneous Atmosphere, *Comm. Pure Appl. Math.* **4**, 317–350.
- GAKHOV, F. D. [1966], *Boundary Value Problems*, Pergamon Press.
- GARABEDIAN, P. R. [1955], An Integral Equation Governing Electromagnetic Waves, *Quart. Appl. Math.* **12**, 428–433.
- GOBLICK, T. J. and R. M. BEVENSEE [1965], Variational Principles and Mode Coupling in Periodic Structures, *IRE Trans. MTT-8*, 500–509.
- GOODRICH, R. F. [1959], Fock Theory – An Appraisal and Exposition, *IRE Trans. AP-7*, S28–S36.
- GOODRICH, R. F. and N. D. KAZARINOFF [1963], Scalar Diffraction by Prolate Spheroids whose Eccentricities are almost one, *Proc. Cambridge Phil. Soc.* **59**, 167–183.
- GRADSHTEYN, I. S. and I. W. RYZHIK [1965], *Table of Integrals, Series and Products*, Academic Press, Inc., New York.
- GRÜNBERG, G. A. [1942], Theory of the Coastal Refraction of Electromagnetic Waves, *J. Phys. USSR* **6**, 187–209.
- GRÜNBERG, G. A. [1943], Suggestions for a Theory of Coastal Refraction, *Phys. Rev.* **63**, 185–189.
- GRÜNBERG, G. A. [1944], Theory of the Coastal Refraction of Electromagnetic Waves, *Zh. Eksperim. i Teor. Fiz.* **14**, 84–111 (in Russian).
- GUTMAN, A. L. [1965], Application of the Cross-Sections Method to the Solution of the Problem concerning the Diffraction of an Electromagnetic Wave by an Inhomogeneous Sphere, *Radio Eng. Electron.* **10**, 1363–1372 (translated from *Radiotechn. i Elektron.*).
- HANSEN, W. W. [1935], A New Type of Expansion in Radiation Problems, *Phys. Rev.* **47**, 139–143.
- HARRINGTON, R. F. [1967], Matrix Methods for Field Problems, *Proc. IEEE* **55**, 136–149.
- HEINS, A. E. [1948], The Radiation and Transmission Properties of a Pair of Semi-Infinite Parallel Plates, *Quart. Appl. Math.* **6**, 157–166, 215–220.
- HEINS, A. E. [1950], The Reflection of an Electromagnetic Plane Wave by an Infinite Set of Plates, III, *Quart. Appl. Math.* **8**, 281–291.
- HEINS, A. E. [1956], The Scope and Limitations of the Method of Wiener and Hopf, *Comm. Pure Appl. Math.* **9**, 447–466.
- HEINS, A. E. and J. F. CARLSON [1947], The Reflection of an Electromagnetic Plane Wave by an Infinite Set of Plates, II, *Quart. Appl. Math.* **5**, 82–88.
- HENSMAN, R. and D. P. JENKINS [1957], Tables of $(2/\sqrt{\pi}) \exp(z^2) \int_0^\infty \exp(-t^2) dt$ for Complex z , Unnumbered report, Royal Radar Establishment, Malvern, England.
- HOBSON, E. W. [1931], *The Theory of Spherical and Ellipsoidal Harmonics*, Cambridge University Press, Cambridge, England.
- HONG, S. [1967], Asymptotic Theory of Electromagnetic and Acoustic Diffraction by Smooth Convex Surfaces of Variable Curvature, *J. Math. Phys.* **8**, 1223–1232.
- HONG, S. and R. F. GOODRICH [1965], Application of Conformal Mapping to Scattering and Diffraction Problems, in: *Electromagnetic Wave Theory*, ed. J. Brown, 907–914, Pergamon Press, London (1967).
- HONG, S. and V. H. WESTON [1966], A Modified Fock Function for the Distribution of Currents in the Penumbra Region with Discontinuity in Curvature, *Radio Science* **1**, 1045–1053.
- HONL, H., A. W. MAUE and K. WESTPAHL [1961], Theorie der Beugung, in: *Handbuch der Physik* **25**, Springer-Verlag, Berlin.
- IGARASHI, A. [1964], Simultaneous Wiener-Hopf Equations and their Application to Diffraction Problems in Electromagnetic Theory, *J. Phys. Soc. Japan* **19**, 1213–1221.

- IJIMA, T. [1952], On the Electromagnetic Fields in Case of Existence of a Semi-Infinite Hollow Conductive Circular Cylinder, II, Electrotechnical Laboratory, Agency of Industrial Science and Technology, Tokyo, Report No. 531 (in Japanese).
- JONES, D. S. [1952a], A Simplifying Technique in the Solution of a Class of Diffraction Problems, *Quart. J. Math.* **3**, 189-196.
- JONES, D. S. [1952b], Diffraction by a Wave-Guide of Finite Length, *Proc. Cambridge Phil. Soc.* **48**, 118-134.
- JONES, D. S. [1953], Diffraction by a Thick Semi-Infinite Plate, *Proc. Roy. Soc.* **A217**, 153-175.
- JONES, D. S. [1955a], A Critique of the Variational Method in Scattering Problems, in: *Symposium on Electromagnetic Wave Theory*, IRE Trans. **AP-4**, 297-301 (1956).
- JONES, D. S. [1955b], The Scattering of a Scalar Wave by a Semi-Infinite Rod of Circular Cross Section, *Phil. Trans. Roy. Soc.* **A247**, 499-528.
- JONES, D. S. [1964], *The Theory of Electromagnetism*, The Macmillan Co., New York.
- KARP, S. N. [1950], Wiener-Hopf Techniques and Mixed Boundary Value Problems, *Comm. Pure Appl. Math.* **3**, 411-426.
- KAY, I. and J. B. KELLER [1954], Asymptotic Evaluation of the Field at a Caustic, *J. Appl. Phys.* **25**, 876-883.
- KELLER, J. B. [1953], The Geometric Optics Theory of Diffraction, presented at McGill Symposium on Microwave Optics. Air Force Cambridge Research Center Report No. TR-59-118 (II) 1959.
- KELLER, J. B. [1956], Diffraction by a Convex Cylinder, *Trans. IRE* **AP-4**, 312-321.
- KELLER, J. B. [1958], A Geometrical Theory of Diffraction, in: *Calculus of Variations and its Applications*, *Proc. Symp. on Appl. Math.* **8**, 27-52, McGraw-Hill Book Co., Inc., New York.
- KELLER, J. B. [1960], Backscattering from a Finite Cone, *IRE Trans.* **AP-8**, 175-182.
- KELLER, J. B. [1961a], Backscattering from a Finite Cone - Comparison of Theory and Experiment, *IRE Trans.* **AP-9**, 411-412.
- KELLER, J. B. [1961b], Diffraction by Polygonal Cylinders, in: *Electromagnetic Waves*, ed. R. E. Langer, 129-137, The University of Wisconsin Press, Madison, Wisconsin.
- KELLER, J. B. [1962], Geometric Theory of Diffraction, *J. Opt. Soc. Am.* **52**, 116-130.
- KELLER, J. B. and E. B. HANSEN [1965], Survey of the Theory of Diffraction of Short Waves by Edges, *Acta Phys. Polon.* **27**, 217-234.
- KELLER, J. B. and F. C. KARAL JR. [1960], Surface Wave Excitation and Propagation, *J. Appl. Phys.* **31**, 1039-1046.
- KELLER, J. B., R. M. LEWIS and B. D. SECKLER [1956], Asymptotic Solution of some Diffraction Problems, *Comm. Pure Appl. Math.* **9**, 207-265.
- KELLER, J. B., S. I. RUBINOW and M. GOLDSTEIN [1963], Zeros of Hankel Functions and Poles of Scattering Amplitudes, *J. Math. Phys.* **4**, 829-832.
- KELLOGG, O. D. [1929], *Foundations of Potential Theory*, Springer-Verlag OHG, Berlin.
- KHASKIND, M. D. and L. A. VAINSHTEIN [1964], Diffraction of Plane Waves by a Slit and a Tape, *Radio Eng. Electron.* **9**, 1492-1502.
- KLEINMAN, R. E. [1965a], The Rayleigh Region, *Proc. IEEE* **53**, 848-856.
- KLEINMAN, R. E. [1965b], The Dirichlet Problem for the Helmholtz Equation, *Arch. Rational Mech. Anal.* **18**, 205-229.
- KLEINMAN, R. E. [1965c], Low Frequency Solution of Electromagnetic Scattering Problems, presented at the URSI Symposium, Delft, The Netherlands; reprinted in: *Electromagnetic Wave Theory*, ed. J. Brown, 891-905, Pergamon Press, London (1967).
- KLEINMAN, R. E. [1967], Far Field Scattering at Low Frequencies, *Appl. Sci. Res.* **18**, 1-8.
- KUENE, M. [1951], An Asymptotic Solution of Maxwell's Equations, *Comm. Pure Appl. Math.* **4**, 225-263.
- KUENE, M. [1954], Asymptotic Solution of Linear Hyperbolic Partial Differential Equations, *J. Rational Mech. Anal.* **3**, 315-342.
- KUENE, M. and I. W. KAY [1965], *Electromagnetic Theory and Geometrical Optics*, Interscience, New York.

- KODIS, R. D. [1954], An Introduction to Variational Methods in Electromagnetic Scattering, J. Soc. Indust. Appl. Math. **2**, 89-112.
- KODIS, R. D. [1958], Variational Principles in High-Frequency Scattering, Proc. Cambridge Phil. Soc. **54**, 512-529.
- KOHN, W. [1948], Variational Methods in Nuclear Collision Problems, Phys. Rev. **74**, 1763-1772.
- KONTOROVICH, M. J. and N. N. LEBEDEV [1939], On a Method of Solution of some Problems of the Diffraction Theory, J. Phys. USSR **1**, 229-241.
- KORNHAUSER, E. T. and I. STAKGOLD [1952], A Variational Theorem for $\nabla^2 u : \lambda u = 0$ and its Application, J. Math. and Phys. **31**, 45-54.
- KOUYOUMJIAN, R. G. [1965], Asymptotic High-Frequency Methods, Proc. IEEE **53**, 864-876.
- KRAMP, C. [1799], *Analyse des réfractions*, Strasbourg and Leipzig.
- KRANZER, H. C. and J. RADLOW [1962], An Asymptotic Method for Solving Perturbed Wiener-Hopf Problems, J. Math. Mech. **14**, 41-59.
- KRAUS, L. and L. M. LEVINE [1961], Diffraction by an Elliptic Cone, Comm. Pure Appl. Math. **24**, 49-68.
- KRAVTSOV, YU. A. [1964a], A Modification of the Geometrical Optics Method, Radiotiz. **7**, 664-673 (in Russian).
- KRAVTSOV, YU. A. [1964b], Asymptotic Solution of Maxwell's Equations near a Caustic, Radiotiz. **7**, 1049-1056 (in Russian).
- LANGER, R. E. [1931], On the Asymptotic Solutions of Ordinary Differential Equations, Trans. Am. Math. Soc. **33**, 23-64.
- LANGER, R. E. [1932], On the Asymptotic Solutions of Ordinary Differential Equations, Trans. Am. Math. Soc. **34**, 447-480.
- LAX, M. and H. FESHBACH [1948], Absorption and Scattering for Impedance Boundary Conditions on Spheres and Circular Cylinders, J. Acoust. Soc. Am. **20**, 108-124.
- LEBEDEV, N. N. and I. P. SKAL'SKAYA [1962], A New Method for Solving the Problems of Diffraction of Electromagnetic Waves by a Wedge with Finite Conductivity, Soviet Phys.-Techn. Phys. **4**, 627-637 (translation of Zh. Tekhn. Fiz. USSR **32**, 1174-1183).
- LEVINE, H. [1950], Variational Principles in Acoustic Diffraction Theory, J. Acoust. Soc. Am. **22**, 48-55.
- LEVINE, H. [1954a], On the Theory of Sound Reflection in an Open-Ended Cylindrical Tube, J. Acoust. Soc. Am. **26**, 200-211.
- LEVINE, H. [1954b], Variational Methods for Solving Electromagnetic Boundary Value Problems, Six Lectures, Electronic Defense Laboratory, Sylvania Electronic Products, Inc., Mountain View, California.
- LEVINE, H. and J. SCHWINGER [1948a], On the Radiation of Sound from an Unflanged Circular Pipe, Phys. Rev. **73**, 383-406.
- LEVINE, H. and J. SCHWINGER [1948b], On the Theory of Diffraction by an Aperture in an Infinite Plane Screen - I, Phys. Rev. **74**, 958-974.
- LEVY, B. R. and J. B. KELLER [1959], Diffraction by a Smooth Object, Comm. Pure Appl. Math. **12**, 159-209.
- LEWIS, R. M. and J. B. KELLER [1964], Asymptotic Methods for Partial Differential Equations: The Reduced Wave Equation and Maxwell's Equations, Research Report No. EM-194, New York University.
- LEWIS, R. M., N. BERSHIN and D. LUDWIG [1967], Uniform Asymptotic Theory of Creeping Waves, Comm. Pure Appl. Math. **20**, 295-328.
- LOGAN, N. A. [1959], General Research in Diffraction Theory, Vols. 1 and 2, Lockheed Missiles and Space Division Technical Reports LMSD-288087 and LMSD-288088 - ASTIA Nos. AD241228 and AD 243182, Sunnyvale, California.
- LOGAN, N. A. and K. S. YEE [1962], A Mathematical Model for Diffraction by Convex Surfaces, in: *Electromagnetic Waves*, ed. R. L. Fanger, 139-180, The University of Wisconsin Press, Madison, Wisconsin.

- LUDWIG, D. [1966], Uniform Asymptotic Expansions at a Caustic, *Comm. Pure Appl. Math.* **19**, 215-250.
- LUDWIG, D. [1967], Uniform Asymptotic Expansions of the Field Scattered by a Convex Object at High Frequencies, *Comm. Pure Appl. Math.* **20**, 103-138.
- LUNEBURG, R. K. [1944], *The Mathematical Theory of Optics*, Brown University Press, Providence, Rhode Island; reprinted in 1964 by The University of California Press, Berkeley, California. (The author's name is misspelled in the original edition of this book, and in a number of papers and reports.)
- MACFARLANE, G. [1947], Variational Methods for Determining Eigenvalues of the Wave Equation of Anomalous Propagation, *Proc. Cambridge Phil. Soc.* **43**, 213-219.
- MACROBERT, T. M. [1948], *Spherical Harmonics*, Dover Publications, Inc., New York.
- MAGNUS, W. and L. KOTIN [1960], The Zeros of the Hankel Function as a Function of its Order, *Numerische Math.* **2**, 228-244.
- MAGNUS, W. and F. OBERHETTINGER [1949], *Formulas and Theorems for the Special Functions of Mathematical Physics*, Chelsea Publishing Co., New York.
- MAGNUS, W., F. OBERHETTINGER and R. P. SONI [1966], *Formulas and Theorems for the Special Functions of Mathematical Physics*, Springer-Verlag, New York.
- MALIUZHINETS, G. D. [1950], Generalization of the Reflection Method in the Theory of Diffraction of Sinusoidal Waves, Doctoral dissertation, Phys. Inst. Acad. Sci. USSR (in Russian).
- MALIUZHINETS, G. D. [1957a], The Radiation of Sound by the Vibrating Boundaries of an Arbitrary Wedge, Part I, *Soviet Phys. - Acoust.* **1**, 152-174 (translation of *Akust. Zh.* **1**, 144, 1955).
- MALIUZHINETS, G. D. [1957b], Radiation of Sound from Vibrating Faces of an Arbitrary Wedge, Part II, *Soviet Phys. - Acoust.* **1**, 240-248 (translation of *Akust. Zh.* **1**, 266, 1955).
- MALIUZHINETS, G. D. [1958a], Inversion Formula for the Sommerfeld Integral, *Soviet Phys. - Doklady* **3**, 52-56 (translation of *Dokl. Akad. Nauk. SSSR* **118**, 1099, 1958).
- MALIUZHINETS, G. D. [1958b], Relation between the Inversion Formulas for the Sommerfeld Integral and the Formulas of Kontorovich-Lebedev, *Soviet Phys. Doklady* **3**, 226-268 (translation of *Dokl. Akad. Nauk. SSSR* **118**, 1958).
- MALIUZHINETS, G. D. [1959], Excitation, Reflection and Emission of Surface Waves from a Wedge with Given Face Impedances, *Soviet Phys. Doklady* **3**, 752-755 (translation of *Dokl. Akad. Nauk. SSSR* **121**, 436-439, 1958).
- MALIUZHINETS, G. D. [1960], Das Sommerfeldsche Integral und die Lösung von Beugungsaufgaben in Winkelgebieten, *Ann. Physik* **6**, 107-112.
- MARCINKOWSKI, C. J. [1961], Some Diffraction Patterns of an Absorbing Half-Plane, *Appl. Sci. Res.* **B9**, 189-198.
- MARCUVITZ, N. [1951], Field Representations in Spherically Stratified Regions, in: *The Theory of Electromagnetic Waves*, ed. M. Kline, S263-S315, Dover, New York.
- MATSUI, E. [1960], On the Free-Field Correction for Laboratory Standard Microphones on a Semi-Infinite Rod, *Nat. Bur. St., Appl. Math. Ser. Report No.* 7035.
- MAUE, A. W. [1949], Zur Formulierung eines Allgemeinen Beugungsproblems durch eine Integralgleichung, *Z. Physik* **126**, 601-618.
- MCCREA, W. H. [1957], Hertzian Electromagnetic Potentials, *Proc. Roy. Soc.* **A240**, 447-457.
- MEI, K. K. [1965], On the Integral Equations for Thin-Wire Antennas, *IEEE Trans.* **AP-13**, 374-378.
- MEI, K. K. and J. VAN BLADEL [1963], Low-Frequency Scattering by Rectangular Cylinders, *IEEE Trans.* **AP-11**, 52-56.
- MEIJER, C. S. [1932], Asymptotische Entwicklungen von Besselschen, Hankelschen und verwandten Funktionen, *Ned. Akad. Wetensch. Proc.* **35**, 656-667, 852-866, 948-958, 1079-1090.
- MEIXNER, J. [1949], Die Kantenbedingung in der Theorie der Beugung elektromagnetischer Wellen an vollkommen leitenden ebenen Schirmen, *Ann. Physik* **441**, 2-9.
- MILLER, J. C. P. [1946], The Airy Integral, *British Assoc. Adv. Sci. Mathematical Tables*, Part-Vol. B, Cambridge University Press, Cambridge, England.
- MILTZNER, K. M. [1967], An Integral Equation Approach to Scattering from a Body of Finite Con-

- ductivity, *Radio Science* **2**, 1459-1470.
- MÖGLICH, F. [1927], Beugungserscheinungen an Körpern von ellipsoidischer Gestalt, *Ann. Physik* **83**, 609-734.
- MONTROLL, E. W. and J. M. GREENBERG [1952], Scattering of Plane Waves by Soft Obstacles, III. Scattering by Obstacles with Spherical and Circular Cylindrical Symmetry, *Phys. Rev.* **86**, 889-898.
- MOON, P. H. and D. E. SPENCER [1961], *Field Theory Handbook*, Springer, Berlin.
- MORSE, P. M. and H. FESHBACH [1953], *Methods of Theoretical Physics*, Vols. 1 and 2, McGraw-Hill Book Co., Inc., New York.
- MULLER, C. [1952], Zur Methode der Strahlungskapazität von H. Weyl, *Math. Z.* **56**, 80-83.
- MULLIN, C. R., R. SANDBURG and C. O. VELLINE [1965], A Numerical Technique for the Determination of Scattering Cross Sections of Infinite Cylinders of arbitrary Geometrical Cross Section, *IEEE Trans. AP-13*, 141-149.
- MUSKHELISHVILI, N. I. [1953], *Singular Integral Equations*, P. Noordhoff, Groningen, Holland.
- NEUGEBAUER, H. E. J. [1956], Diffraction of Electromagnetic Waves caused by Apertures in Absorbing Plane Screens, *IRE Trans. AP-4*, 115-119.
- NEWTON, R. G. [1964], *The Complex- i -Plane*, Benjamin, New York.
- NEWTON, R. G. [1966], *Scattering Theory of Waves and Particles*, McGraw-Hill Book Co., Inc., New York.
- NICHOLSON, J. W. [1910], On the Bending of Light Waves Round a Large Sphere, I, *Phil. Mag.* **19**, 516-537.
- NISBET, A. [1955], Hertzian Electromagnetic Potentials and Associated Gauge Transformations, *Proc. Roy. Soc. A231*, 250-263.
- NOBLE, B. [1958], *Methods based on the Wiener-Hopf Technique*, Pergamon Press, London.
- NOBLE, B. [1962], Integral Equation Perturbation Methods in Low Frequency Diffraction, in: *Electromagnetic Waves*, ed. R. E. Langer, 323-360, The University of Wisconsin Press, Madison, Wisconsin.
- NUSSENZVEIG, H. M. [1965], High-Frequency Scattering by an Impenetrable Sphere, *Ann. Phys.* **34**, 23-95.
- OLVER, F. W. J. [1952], Some New Asymptotic Expansions for Bessel Functions of Large Orders, *Proc. Cambridge Phil. Soc.* **48**, 414-427.
- OLVER, F. W. J. [1954], The Asymptotic Expansion of Bessel Functions of Large Order, *Phil. Trans. Roy. Soc. A247*, 328-368.
- PALEY, R. E. A. C. and N. WIENER [1934], *The Fourier Transform in the Complex Domain*, Am. Math. Soc. Colloquium Publication **19**.
- PANOFSKY, K. H. and M. PHILLIPS [1962], *Classical Electricity and Magnetism*, second edition, Addison-Wesley Publishing Co., Inc., Reading, Mass.
- PAPAS, C. H. [1950], Diffraction by a Cylindrical Obstacle, *J. Appl. Phys.* **21**, 318-325.
- PEARSON, J. D. [1953], Diffraction of Electromagnetic Waves by a Semi-Infinite Circular Waveguide, *Proc. Cambridge Phil. Soc.* **49**, 659-667.
- PETERS, A. S. [1925], Water Waves Over Sloping Beaches and the Solution of a Mixed Boundary Value Problem for $\nabla^2\phi - k^2\phi = 0$ in a Sector, *Comm. Pure Appl. Math.* **5**, 87-108.
- PELUMM, E. [1960], Expansion Problems arising from the Watson Transformation, New York University Research Report No. BR-35.
- POGORZELSKI, W. [1966], *Integral Equations and their Applications*, Pergamon Press.
- POINCARÉ, H. [1910], *Palermo Rendiconti* **29**, 169-260.
- RADIOW, J. [1961], Diffraction by a Quarter-Plane, *Arch. Rational Mech. Anal.* **8**, 139-158.
- RADIOW, J. [1964a], Diffraction by a Right-Angled Dielectric Wedge, *Intern. J. Eng. Sci.* **2**, 275-290.
- RADIOW, J. [1964b], A Two-Dimensional Singular Integral Equation of Diffraction Theory, *Bull. Am. Math. Soc.* **70**, 596-599.
- RADIOW, J. [1965], Note on the Diffraction at a Corner, *Arch. Rational Mech. Anal.* **19**, 62-70.
- REGGE, T. [1959], Introduction to Complex Orbital Momenta, *Nuovo Cimento* **14**, 951-976.

- RICHMOND, J. H. [1965], Computer Solutions of Scattering Problems, *Proc. IEEE* **53**, 796-804.
- ROBIN, L. [1957-1959], *Fonctions sphériques de Legendre et fonctions sphéroïdales*, Tome I, II, III, Gauthier-Villars, Paris, France.
- ROSS, R. A. [1966], Radar Cross Section of Rectangular Flat Plates as a Function of Aspect Angle, *IEEE Trans.* **AP-14**, 329-335.
- ROSSI, B. [1957], *Optics*, Addison-Wesley Publishing Co., Inc., Reading, Mass.
- RULE, B. [1967], Relation between Creeping Waves and Lateral Waves on a Curved Interface, *J. Math. Phys.* **8**, 1785-1793.
- RULE, B. [1968], Uniform Asymptotic Theory of Diffraction at an Interface, *Comm. Pure Appl. Math.* **21**, 67-76.
- RUMSEY, V. H. [1954], Reaction Concept in Electromagnetic Theory, *Phys. Rev.* **94**, 1483-1491.
- SCHIELKUNOFF, S. A. [1951], Kirchhoff's Formula, its Vector Analogue, and other Field Equivalents, *Comm. Pure Appl. Math.* **4**, 43-59.
- SCHENSTED, C. F. [1955], Electromagnetic and Acoustical Scattering by a Semi-Infinite Body of Revolution, *J. Appl. Phys.* **26**, 306-308.
- SCHIFFER, M. M. [1957], Partial Differential Equations of the Elliptic Type, Symposium on Partial Differential Equations, University of Kansas Press, Lawrence, Kansas.
- SCHÖBE, W. [1954], Eine an die Nicholsonformel Anschliessende Asymptotische Entwicklung für Zylinderfunktionen, *Acta Math.* **92**, 265-307.
- SENIOR, T. B. A. [1952], Diffraction by a Semi-Infinite Metallic Sheet, *Proc. Roy. Soc.* **A213**, 436-458.
- SENIOR, T. B. A. [1959a], Diffraction by an Imperfectly Conducting Half-Plane at Oblique Incidence, *Appl. Sci. Res.* **B8**, 35-61.
- SENIOR, T. B. A. [1959b], Diffraction by an Imperfectly Conducting Wedge, *Comm. Pure Appl. Math.* **12**, 337-372.
- SENIOR, T. B. A. [1960a], Impedance Boundary Conditions for Imperfectly Conducting Surfaces, *Appl. Sci. Res.* **B8**, 418-436.
- SENIOR, T. B. A. [1960b], Impedance Boundary Conditions for Statistically Rough Surfaces, *Appl. Sci. Res.* **B8**, 437-462.
- SENIOR, T. B. A. [1960c], A Note on Hansen's Vector Wave Functions, *Can. J. Phys.* **38**, 1702-1705.
- SENIOR, T. B. A. [1965], The Backscattering Cross Section of a Cone-Sphere, *IEEE Trans.* **AP-13**, 271-277.
- SIEGEL, K. M. [1959], Far Field Scattering from Bodies of Revolution, *Appl. Sci. Res.* **B7**, 293-328.
- SIEGEL, K. M., J. W. CRISPIN and C. L. SCHENSTED [1955], Electromagnetic and Acoustical Scattering from a Semi-Infinite Cone, *J. Appl. Phys.* **26**, 309-313.
- SOMMERFELD, A. [1949], *Partial Differential Equations in Physics*, Academic Press, Inc., New York.
- SOMMERFELD, A. [1954], *Optics*, Academic Press, Inc., New York.
- SPÄRBERG, J. A. [1956], Application of the Theory of Sectionally Holomorphic Functions to Wiener-Hopf Type Integral Equations, *Koninkl. Ned. Akad. Wetenschap.* **A59**, 29-34.
- STEVENSON, A. F. [1953a], Solution of Electromagnetic Scattering Problems as Power Series in the Ratio (Dimension of Scatterer) Wavelength, *J. Appl. Phys.* **24**, 1134-1142.
- STEVENSON, A. F. [1953b], Electromagnetic Scattering by an Ellipsoid in the Third Approximation, *J. Appl. Phys.* **24**, 1143-1151.
- STRATTON, J. A. [1941], *Electromagnetic Theory*, McGraw-Hill Book Co., Inc., New York.
- STREIBER, W. [1964], Creeping Wave Propagation Constants for Impedance Boundary Conditions, *IEEE Trans.* **AP-12**, 764-766.
- STROUT, J. W., Lord Rayleigh [1897], On the Incidence of Aerial and Electric Waves upon Small Obstacles in the Form of Ellipsoids or Elliptic Cylinders, and on the Passage of Electric Waves through a Circular Aperture in a Conducting Screen, *Phil. Mag.* **44**, 28-52.
- SZEGÖ, G. [1934], Über einige asymptotische Entwicklungen der Legendreschen Funktionen, *Proc. London Math. Soc.* **36**, 427-450.
- LEE, C. T. [1954a], Radiation from Current Elements and Apertures in the Presence of a Perfectly Conducting Half Plane Sheet, Stanford Research Institute Technical Report No. 45, Stanford.

- California.
- TAI, C. T. [1954b], A Glossary of Dyadic Green's Functions, Stanford Research Institute Technical Report No. 46, Stanford, California.
- TAI, C. T. [1958], The Electromagnetic Theory of the Spherical Luneberg Lens, Appl. Sci. Res. **B7** 113-130.
- TAO, L. N. [1966], On Variational Principles for Electromagnetic Theory, J. Math. Phys. **7**, 526-530.
- THORNE, R. C. [1957], The Asymptotic Expansion of Legendre Functions of Large Degree and Order, Phil. Trans. Roy. Soc. **249**, 597-620.
- TITCHMARSH, E. C. [1948], *Theory of Fourier Integrals*, Oxford University Press.
- TWERSKY, V. [1964], Rayleigh Scattering, Appl. Opt. **3**, 1150-1162.
- ÜBERALL, H. [1964], Radar Scattering from Coated Perfect Conductors: Application to the Semi-Infinite Cone and Use of Exact Eikonal, J. Res. NBS **68D**, 749-766.
- UDAGAWA, K. and Y. MIYAZAKI [1965], Diffraction of a Plane Wave by a Perfectly Conducting Elliptic Cylinder - A Study of Conformal Mapping Technique, J. Inst. Elec. Comm. Eng. Japan **48**, 43-53.
- URSELL, F. [1968], Creeping Modes in a Shadow, Proc. Cambridge Phil. Soc. **64**, 171-191.
- USLENGHI, P. [1964], Radar Cross Section of Imperfectly Conducting Bodies at Small Wavelengths, Alta Frequenza **33**, 541-546.
- VAJNSHTEIN, L. A. [1954], Propagation in Semi-Infinite Waveguides, NYU Research Report EM-63, Institute of Mathematical Sciences, New York University (six papers translated from Russian by J. Shmoys).
- The six original papers are:
- (1) Rigorous Solution of the Problem of an Open-Ended Parallel-Plate Waveguide, Izv. Akad. Nauk. SSSR, Ser. Fiz. **12**, 144-165, 1948.
 - (2) On the Theory of Diffraction by Two Parallel Half-Planes, Izv. Akad. Nauk. SSSR, Ser. Fiz. **12**, 166-180, 1948.
 - (3) Theory of Symmetric Waves in a Cylindrical Waveguide with an Open End, Zh. Tekhn. Fiz. **18**, 1543-1564, 1948.
 - (4) The Theory of Sound Waves in Open Tubes, Zh. Tekhn. Fiz. **19**, 911-930, 1949.
 - (5) Radiation of Asymmetric Electromagnetic Waves from the Open End of a Circular Waveguide, Dokl. Akad. Nauk. SSSR **74**, 485-488, 1950.
 - (6) Diffraction at the Open End of a Circularly Cylindrical Waveguide whose Diameter is much Greater than Wavelength, Dokl. Akad. Nauk. SSSR **74**, 909-912, 1950.
- VAN BLADEL, J. [1961], Some Remarks on Green's Dyadic for Infinite Space, IRE Trans. **AP-9**, 563-566.
- VAN BLADEL, J. [1963], Low-Frequency Scattering by Cylindrical Bodies, Appl. Sci. Res. **B10**, 195-202.
- VAN BLADEL, J. [1964], *Electromagnetic Fields*, McGraw-Hill Book Co., Inc., New York.
- VOLTERRA, V. [1884], Sopra un Problema di Elettrostatica, Nuovo Cimento **16**, 49-57.
- WAGNER, R. J. [1963], Variational Principles for Electromagnetic Potential Scattering, Phys. Rev. **131**, 423-434.
- WARSHAWSKI, S. I. [1935], On the Higher Derivatives at the Boundary in Conformal Mapping, Trans. Am. Math. Soc. **38**, 310-340.
- WATERMAN, P. C. [1965], Matrix Formulation of Electromagnetic Scattering, Proc. IEEE **53**, 805-812.
- WATSON, G. N. [1928], The Diffraction of Electric Waves by the Earth, Proc. Roy. Soc. **A95**, 83-99.
- WATSON, G. N. [1958], *A Treatise on the Theory of Bessel Functions*, Cambridge University Press, Cambridge, England.
- WELCH, W. J. [1960], Reciprocity Theorems for Electromagnetic Fields whose Time Dependence is Arbitrary, IRE Trans. **AP-8**, 68-73.
- WERNER, P. [1963], On the Exterior Boundary Value Problem of Perfect Reflection for Stationary Electromagnetic Wave Fields, J. Math. Anal. Appl. **7**, 348-396.
- WESTON, A. H. [1960], On Toroidal Wave Functions, J. Math. Phys. **39**, 64-71.

- WESTON, V. H. [1962], The Effect of a Discontinuity in Curvature in High-Frequency Scattering, *IRE Trans. AP-10*, 775-780 (see also *IEEE Trans. AP-13*, 611-613).
- WESTON, V. H. [1963], Theory of Absorbers in Scattering, *IEEE Trans. AP-11*, 578-584.
- WESTON, V. H. [1965], Extension of Fock Theory for Currents in the Penumbra Region, *Radio Science* **69D**, 1257-1270.
- WESTPFAHL, K. [1959], Zur Theorie einer Klasse von Beugungsproblemen mittels singulärer Integralgleichungen, I, *Ann. Physik* **4**, 283-351.
- WESTPFAHL, K. and H. H. WITTE [1967], Beugung skalarer hochfrequenter Wellen an einer Kreisblende, *Ann. Physik* **20**, 14-28.
- WETZEL, L. [1957], High Frequency Current Distributions on Conducting Obstacles, Scientific Report No. 10, Cruft Laboratory, Harvard University, Cambridge, Mass.
- WHITE, F. P. [1922], The Diffraction of Plane Electromagnetic Waves by a Perfectly Reflecting Sphere, *Proc. Roy. Soc. A100*, 505-525.
- WIENER, N. and E. HOPF [1931], Über eine Klasse singulärer Integralgleichungen, *Sitz. Berlin. Preuss. Akad. Wiss.*, 696-706.
- WILCOX, C. H. [1956a], An Expansion Theorem for Electromagnetic Fields, *Comm. Pure Appl. Math.* **9**, 115-134.
- WILCOX, C. H. [1956b], A Generalization of Theorems of Rellich and Atkinson, *Proc. Am. Math. Soc.* **7**, 271-276.
- WILCOX, C. H. [1957], Debye Potentials, *J. Math. Mech.* **6**, 167-201.
- WILLIAMS, W. E. [1959], Diffraction of an E-Polarized Plane Wave by an Imperfectly Conducting Wedge, *Proc. Roy. Soc. A252*, 376-393.
- WILLIAMS, W. E. [1960], Diffraction of an Electromagnetic Plane Wave by a Metallic Sheet, *Proc. Roy. Soc. A257*, 413-419.
- WOLFE, P. [1966], Diffraction of a Scalar Wave by a Plane Screen, *J. Soc. Indust. Appl. Math.* **14**, 577-599.
- WOLFE, P. [1967], A New Approach to Edge Diffraction, *J. Soc. Indust. Appl. Math.* **15**, 1434-1469.
- YEE, H. Y., L. B. FELSEN and J. B. KELLER [1968], Ray Theory of Reflection from the Open End of a Waveguide, *J. Soc. Indust. Appl. Math.* **16**, 268-300.
- ZANDERER, E. [1964a], Wave Propagation Around a Convex Cylinder, *J. Math. Mech.* **13**, 171-186.
- ZANDERER, E. [1964b], Wave Propagation around a Smooth Object, *J. Math. Mech.* **13**, 187-200.
- ZANDERER, E. [1967], An Integral Representation Approach to Diffraction by a Smooth Object, *J. Math. Anal. Appl.* **18**, 17-37.

PART ONE

INFINITE BODIES

CHAPTER I

GENERAL CONSIDERATIONS

The following seven chapters are devoted to infinite bodies which are two-dimensional in the sense that their surfaces are described by an equation of the form

$$\rho = f(\phi), \quad 0 \leq \phi < 2\pi \quad (1.1)$$

independently of z , where (ρ, ϕ, z) are cylindrical polar coordinates. As such, the bodies are cylinders formed by the motion of a generator parallel to the z axis, and comprise the largest class of shapes included in this volume.

Although the bodies are two-dimensional, the ability to characterize the associated scattering problem as two-dimensional depends on the nature of the source: in particular, on whether the excitation field is independent of the z coordinate. Four types of sources will be treated: plane waves whose directions of propagation are perpendicular to the z axis, and which are polarized with either the electric vector parallel to this axis (E polarization, or TM waves) or the magnetic vector parallel (H polarization, or TE waves); electric and magnetic line sources parallel to the z axis with strengths independent of z ; electric and magnetic dipole sources arbitrarily oriented, and point sources.

Consider an E -polarized plane wave propagating in a plane perpendicular to the z axis and incident on a perfectly conducting body whose surface is defined by eq. (1.1). The incident field is therefore

$$\mathbf{E}^i = \hat{z}E_z^i, \quad \mathbf{H}^i = -\frac{iY}{k} \left(\hat{x} \frac{\partial E_z^i}{\partial y} - \hat{y} \frac{\partial E_z^i}{\partial x} \right) \quad (1.2)$$

with E_z^i independent of z , and since the boundary conditions on the scattered field are likewise independent of z , the scattered field must also be E -polarized and of the form

$$\mathbf{E}^s = \hat{z}E_z^s, \quad \mathbf{H}^s = -\frac{iY}{k} \left(\hat{x} \frac{\partial E_z^s}{\partial y} - \hat{y} \frac{\partial E_z^s}{\partial x} \right). \quad (1.3)$$

The solution of the scattering problem now reduces to the determination of a scalar function E_z^s satisfying the wave equation, the radiation condition at infinity, the boundary condition

$$E_z^s = -E_z^i \quad \text{at} \quad \rho = f(\phi), \quad (1.4)$$

and, in the case of a body whose radius of curvature can be zero, an edge condition

PRECEDING PAGE BLANK

at this point (see Section I.2.4). These are identical to the conditions imposed on the velocity potential of an acoustic field scattered by a soft body, and accordingly the axial component of the electric vector for an E -polarized electromagnetic wave incident on a perfectly conducting cylinder in a plane perpendicular to the axis also represents the velocity potential for the analogous acoustic wave incident on a soft cylinder. Similarly, the axial component of the magnetic vector for an H -polarized electromagnetic wave incident on a perfectly conducting cylinder represents the velocity potential for the analogous acoustic wave incident on a hard cylinder, and it is trivial to show that this correspondence between vector and scalar problems extends to the fields arising from electric and magnetic line sources parallel to the z axis.

Although the only type of plane wave excitation that we shall treat explicitly is incidence in the plane normal to the z axis, the solutions for oblique incidence involving arbitrary three-dimensional plane waves are deducible from the results for normal incidence. To see this, we note that any two-dimensional solution of the wave equation gives rise to a three-dimensional solution on replacing k by $k \sin \theta_0$ and multiplying by $\exp(-ikz \cos \theta_0)$. If V is such a three-dimensional solution, an electromagnetic field can be derived from it by taking V as the z component of an electric or magnetic Hertz vector whose x and y components are zero. In this way we obtain two fundamental types of field:

(i) E -polarized in which $H_z = 0$,

$$\mathbf{E}^{(1)} = -\frac{i}{k} \cos \theta_0 \left(\frac{\partial V}{\partial x} \hat{x} + \frac{\partial V}{\partial y} \hat{y} \right) + \sin^2 \theta_0 V \hat{z}, \quad \mathbf{H}^{(1)} = -\frac{iY}{k} \left(\frac{\partial V}{\partial y} \hat{x} - \frac{\partial V}{\partial x} \hat{y} \right). \quad (1.5)$$

(ii) H -polarized in which $E_z = 0$,

$$\mathbf{E}^{(2)} = -\frac{iZ}{k} \left(\frac{\partial V}{\partial y} \hat{x} - \frac{\partial V}{\partial x} \hat{y} \right), \quad \mathbf{H}^{(2)} = \frac{i}{k} \cos \theta_0 \left(\frac{\partial V}{\partial x} \hat{x} + \frac{\partial V}{\partial y} \hat{y} \right) - \sin^2 \theta_0 V \hat{z}. \quad (1.6)$$

The solution of the wave equation which corresponds in the above manner to $\exp\{-ik(x \cos \phi_0 + y \sin \phi_0)\}$ is $\exp\{-ik(x \cos \phi_0 \sin \theta_0 + y \sin \phi_0 \sin \theta_0 + z \cos \theta_0)\}$ in terms of which

$$\begin{aligned} \mathbf{E}^{(1)} &= -\sin \theta_0 (\cos \phi_0 \cos \theta_0 \hat{x} + \sin \phi_0 \cos \theta_0 \hat{y} - \sin \theta_0 \hat{z}) \\ &\quad \times \exp\{-ik(x \cos \phi_0 \sin \theta_0 + y \sin \phi_0 \sin \theta_0 + z \cos \theta_0)\}, \\ \mathbf{H}^{(1)} &= -Y \sin \theta_0 (\sin \phi_0 \hat{x} - \cos \phi_0 \hat{y}) \\ &\quad \times \exp\{-ik(x \cos \phi_0 \sin \theta_0 + y \sin \phi_0 \sin \theta_0 + z \cos \theta_0)\}. \end{aligned} \quad (1.7)$$

$$\begin{aligned} \mathbf{E}^{(2)} &= -Z \sin \theta_0 (\sin \phi_0 \hat{x} - \cos \phi_0 \hat{y}) \\ &\quad \times \exp\{-ik(x \cos \phi_0 \sin \theta_0 + y \sin \phi_0 \sin \theta_0 + z \cos \theta_0)\}, \\ \mathbf{H}^{(2)} &= \sin \theta_0 (\cos \phi_0 \cos \theta_0 \hat{x} + \sin \phi_0 \cos \theta_0 \hat{y} - \sin \theta_0 \hat{z}) \\ &\quad \times \exp\{-ik(x \cos \phi_0 \sin \theta_0 + y \sin \phi_0 \sin \theta_0 + z \cos \theta_0)\}. \end{aligned} \quad (1.8)$$

When $\theta_0 = \frac{1}{2}\pi$ these reduce respectively to E - and H -polarized fields in two dimen-

sions, suggesting that for a two-dimensional body the solutions of the scattering problems for the incident fields of eqs. (1.7) and (1.8) can be deduced from those in the case $\theta_0 = \frac{1}{2}\pi$. This proves to be so when the body is perfectly conducting. Thus, in the two-dimensional solution for E_z , replace k by $k \sin \theta_0$ and multiply by $\exp(-ikz \cos \theta_0)$. When substituted for V in eq. (1.5), this forms the solution of the scattering problem for the incident field of eq. (1.7). And similarly for H polarization.

There are several features of the above technique for deriving oblique incidence solutions from those for normal incidence that should be noted. In the first place, the method breaks down for $\theta_0 = 0$ when the direction of propagation is along the z axis and when the physical realizability of an incident plane wave is in question anyhow. This case apart, it may be used to deduce the solution for an incident plane wave of arbitrary direction and polarization by appropriate combination of the basic E - and H -polarized fields, and hence, by superposition, to build up the solution for a point or dipole source (see, for example, SENIOR [1953]). The applicability of the method is, however, limited to those cases in which no coupling between the E - and H -polarized waves (i.e. between the TM and TE modes) arises as a result of the presence of the scattering body; i.e. to two-dimensional scatterers which are (i) perfectly conducting, or (ii) inhomogeneous with no discontinuities in refractive index in $0 < \rho < \infty$ (USLENGHI [1967]). In general, such coupling does occur and the two- and three-dimensional solutions are no longer directly related.

Bibliography

- SENIOR, T. B. A. [1953], The Diffraction of a Dipole Field by a Perfectly Conducting Half-plane, *Quart. J. Mech. Appl. Math.* 6, 101-114.
- USLENGHI, P. L. E. [1967], Mode Uncoupling in Oblique Scattering from Radially Inhomogeneous Cylinders, *Electron. Letters* 3, 400.

CHAPTER 2

THE CIRCULAR CYLINDER

T. B. A. SENIOR and P. L. E. USLENGHI

Among the two-dimensional structures considered in this Part, the circular cylinder is undoubtedly the simplest and, perhaps for this reason, has received the most intensive study. It has, in particular, proved valuable as a model for the development of high frequency techniques applicable to more general shapes.

2.1. Circular cylindrical geometry

The circular cylindrical coordinates (ρ, ϕ, z) shown in Fig. 2.1 are related to the rectangular Cartesian coordinates (x, y, z) by the transformation

$$\begin{aligned}x &= \rho \cos \phi, \\y &= \rho \sin \phi, \\z &= z,\end{aligned}\tag{2.1}$$

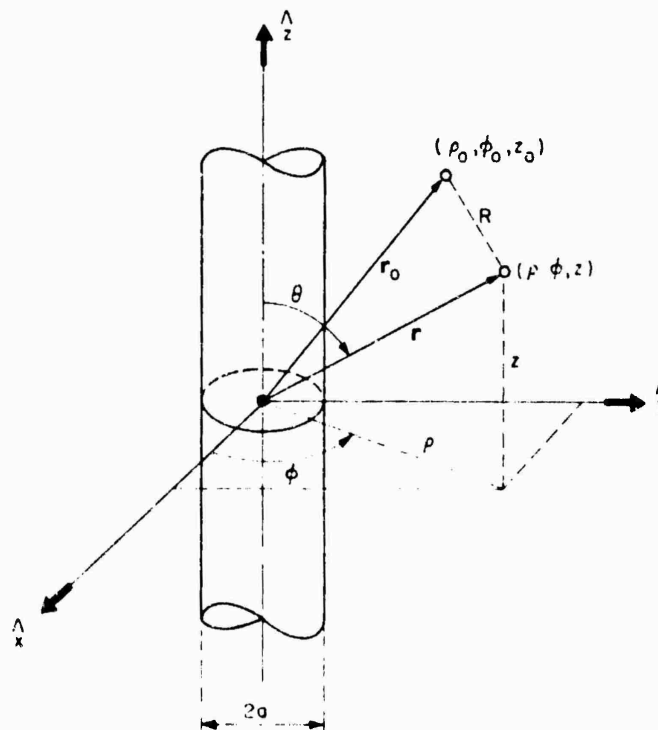


Fig. 2.1. Circular cylindrical geometry.

where $0 \leq \rho < \infty$, $0 \leq \phi < 2\pi$, and $-\infty < z < +\infty$. The z -axis is the axis of symmetry, and the surfaces $\rho = \text{constant}$, $\phi = \text{constant}$ and $z = \text{constant}$ are respectively coaxial circular cylinders of radius ρ , semi-planes originating in the z -axis, and planes perpendicular to the z -axis. Instead of the azimuthal angle ϕ , it is sometimes convenient to introduce the angle ψ , $-\pi < \psi \leq \pi$, related to ϕ by:

$$\psi = \begin{cases} \phi, & \text{for } 0 \leq \phi \leq \pi, \\ \phi - 2\pi, & \text{for } \pi < \phi \leq 2\pi. \end{cases} \quad (2.2)$$

The scattering body is the cylinder with surface $\rho = a$, and the primary source is a plane wave propagating along the negative x -axis (and therefore perpendicularly to the axis z of the cylinder), or a line source parallel to the z -axis and located at $(\rho_0 \geq a, \phi_0 = 0)$, or a point or dipole source located at $(\rho_0 \geq a, \phi_0 = 0, z_0 = 0)$.

Definitions, notation and bibliographical references to numerical tables for Bessel and Hankel functions, and for the various functions which occur in the asymptotic developments, are given in the Introduction. In particular, the quantity m which appears in the high-frequency approximation formulae is given by:

$$m = (\frac{1}{2}ka)^{\frac{1}{2}}. \quad (2.3)$$

The infinite series representing the exact eigenfunction expansions of the fields are numerically useful only if ka is not too large compared to unity. If ka is very large (e.g. $ka = 100$), at least the first ka terms of the infinite series are needed in order to obtain a result with a relative error of the order of one percent.

2.2. Plane wave incidence

2.2.1. *E*-polarization

2.2.1.1. EXACT SOLUTIONS

For a plane wave incident in the direction of the negative x -axis, such that

$$E^i = \hat{z}e^{-ikx}, \quad H^i = \hat{y}Ye^{-ikx}, \quad (2.4)$$

then

$$E_z^s = - \sum_{n=0}^{\infty} \epsilon_n (-i)^n \frac{J_n(ka)}{H_n^{(1)}(ka)} H_n^{(1)}(k\rho) \cos n\phi. \quad (2.5)$$

KODIS [1952] and KING and WU [1959] have computed E_z^s in amplitude and phase for $ka = 3.1, 6.3$ and 10 , at various positions of the field point. Additional data have been published by ADEY [1958] and are shown in Fig. 2.2.

On the surface $\rho = a$:

$$H_\phi^i + H_\phi^s = \frac{2Y}{\pi ka} \sum_{n=0}^{\infty} \epsilon_n \frac{(-i)^n}{H_n^{(1)}(ka)} \cos n\phi. \quad (2.6)$$

This expression has been computed as a function of ϕ for selected values of ka , and its amplitude and phase are shown in Fig. 2.3.

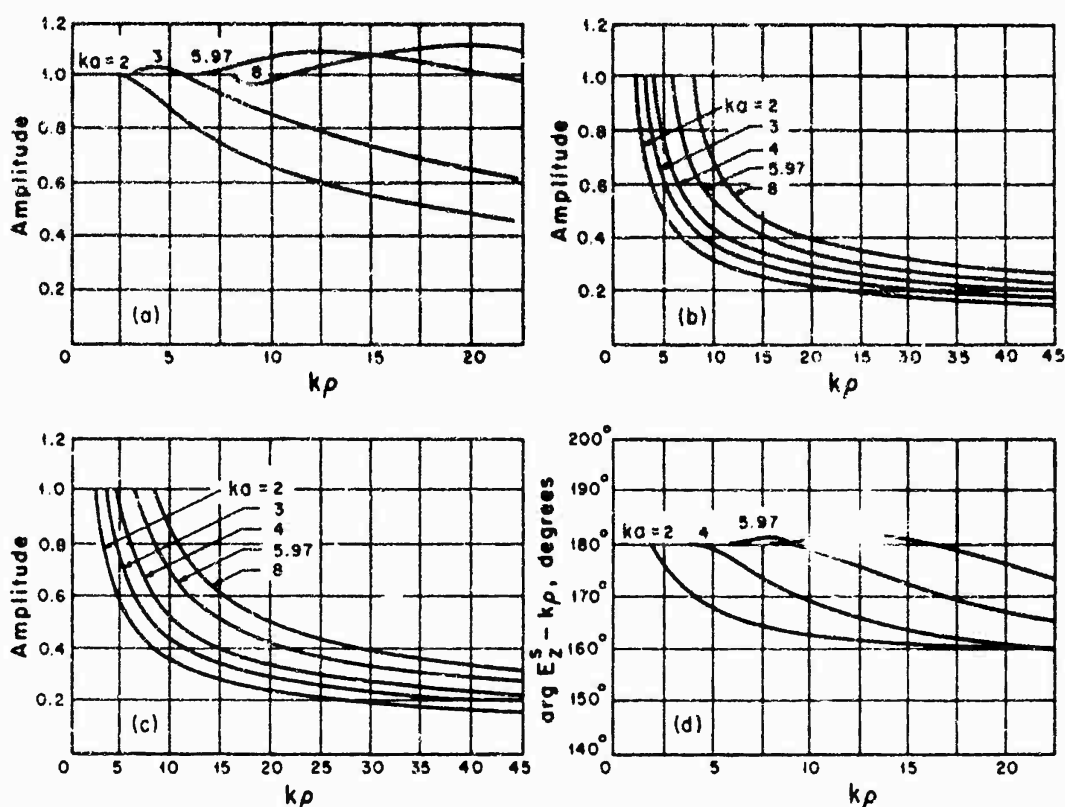


Fig. 2.2. Scattered field E_z^s produced by a plane wave with E^i parallel to the cylinder axis. Amplitude $|E_z^s|$ at (a) $\phi = \pi$, (b) $\phi = \frac{1}{2}\pi$, (c) $\phi = 0$; (d) phase at $\phi = \pi$ (ADEY [1958]).

In the far field ($\rho \rightarrow \infty$):

$$P = - \sum_{n=0}^{\infty} c_n (-1)^n \frac{J_n(ka)}{H_n^{(1)}(ka)} \cos n\phi. \quad (2.7)$$

Amplitude and phase of P as functions of ϕ for three different values of ka are shown in Fig. 2.4. For the particular case of back scattering ($\phi = 0$), $\arg P$ is plotted as a function of ka in Fig. 2.5. The normalized back scattering cross section is shown as a function of ka in Fig. 2.6. In the case of forward scattering ($\phi = \pi$), $\arg P$ is plotted as a function of ka in Fig. 2.7, and the normalized forward scattering cross section is given in Fig. 2.8. The total scattering cross section per unit length is

$$\sigma_T = 4 \sum_{n=0}^{\infty} c_n^2 \frac{J_n^2(ka)}{H_n^{(1)}(ka)}. \quad (2.8)$$

The quantity $\sigma_T/(4a)$ is plotted in Fig. 2.9.

2.2.1.2. LOW FREQUENCY APPROXIMATIONS

For a plane wave incident in the direction of the negative x -axis, such that

$$E^i = \hat{z}e^{-ikx}, \quad H^i = \hat{y}\gamma e^{-ikx}, \quad (2.9)$$

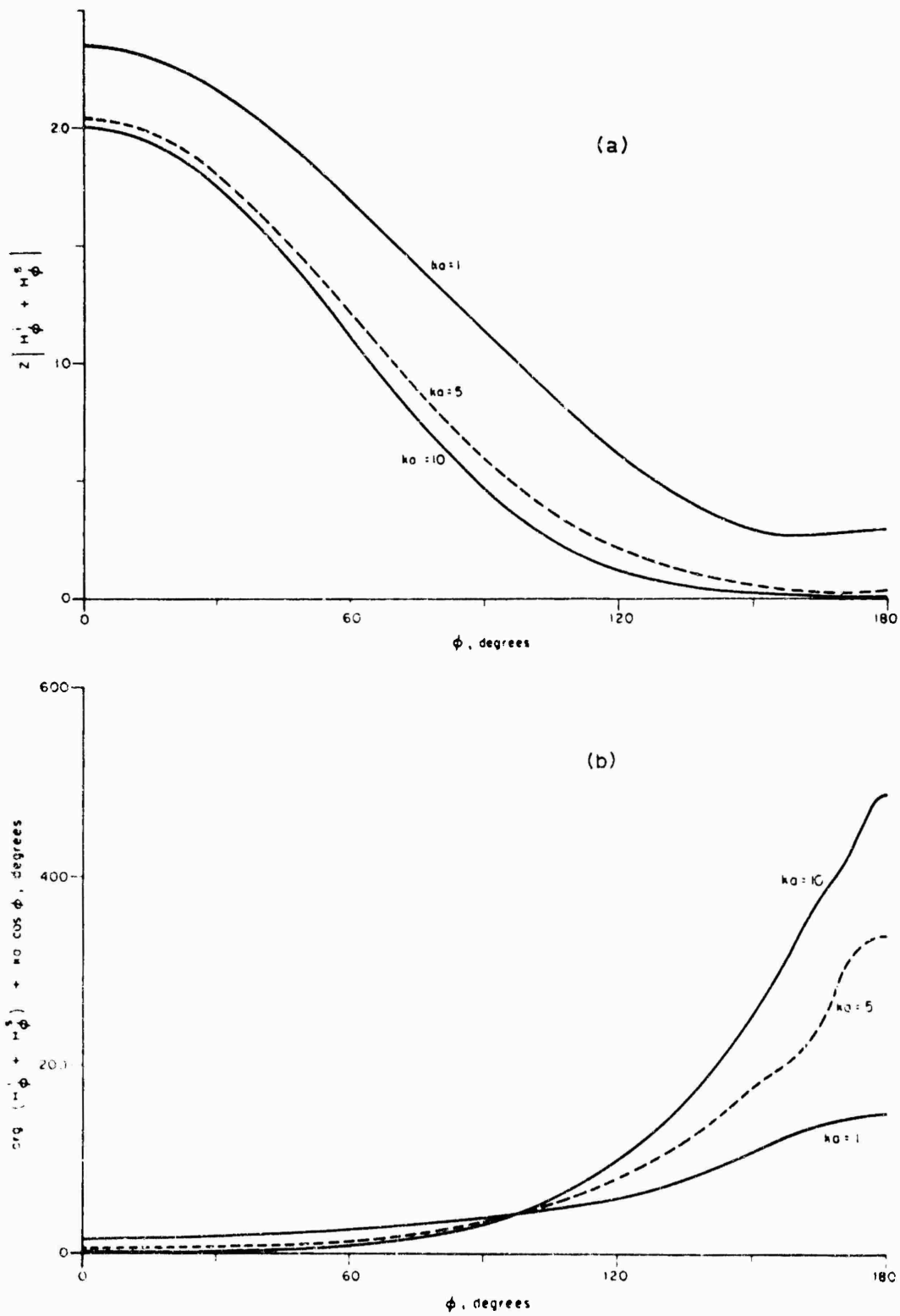


Fig. 2.3. Amplitude (a) and phase (b) of surface field produced by a plane wave with E^i parallel to the cylinder axis.

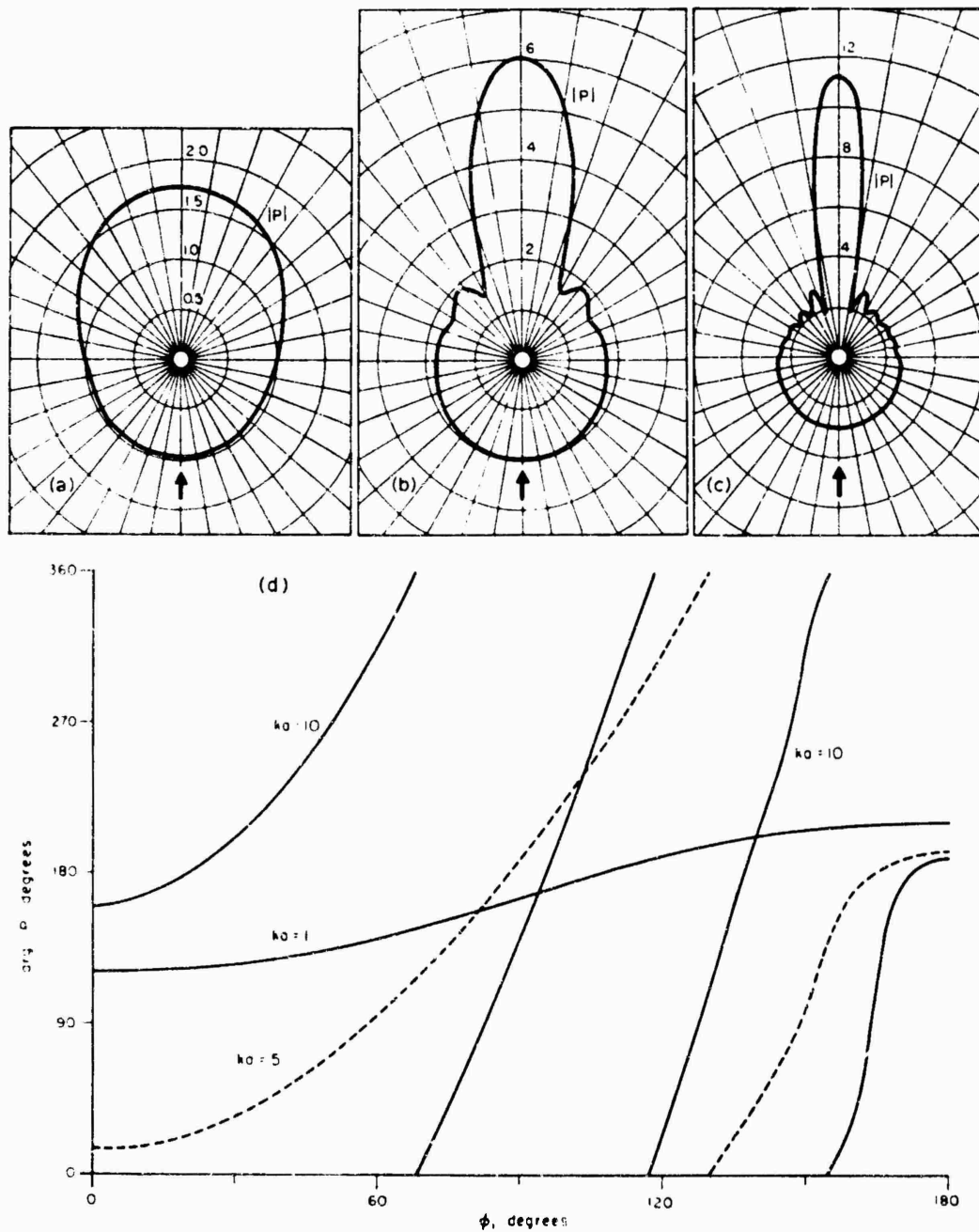


Fig. 2.4. Amplitude for (a) $ka = 1$, (b) $ka = 5$, (c) $ka = 10$ and (d) phase of bistatic far field coefficient P , for plane wave incidence with E^i parallel to the cylinder axis.

low frequency expansions may be obtained either directly (STRUTT [1897]; NOBLE [1962]; VAN BLADIE [1963]) or by power series developments of the radial cylindrical functions appearing in the exact solutions. In particular, in the far field ($\rho \rightarrow \infty$):

$$P \sim \frac{1}{2} i \pi \gamma^{-1} \log \{ka (2i)\}^{\frac{1}{2}}, \quad (2.10)$$

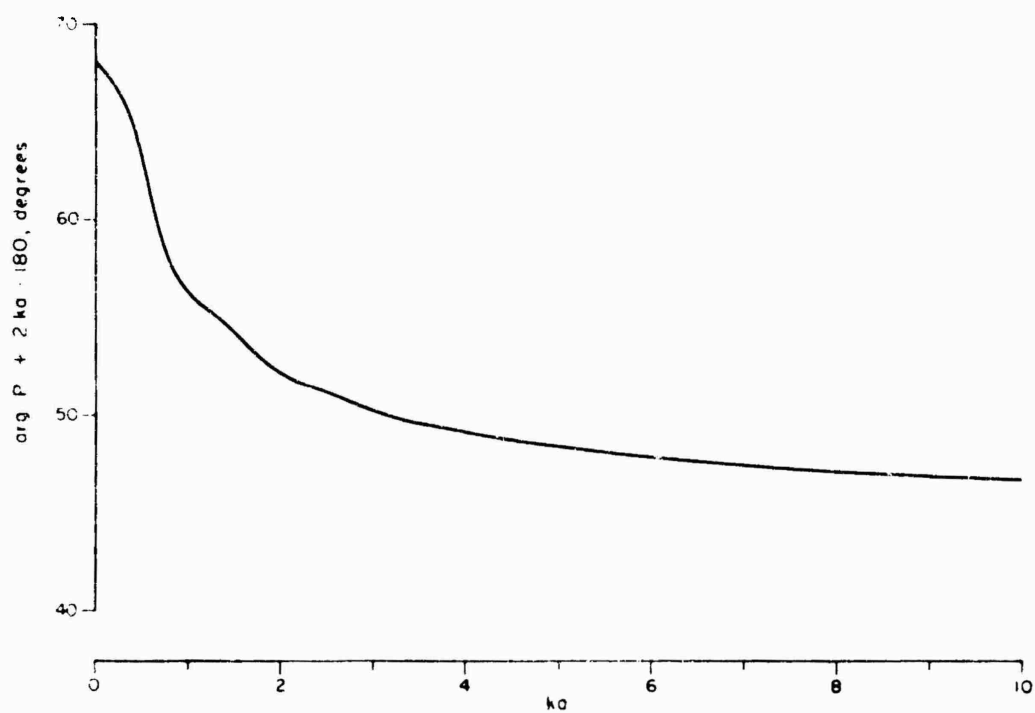


Fig. 2.5. Phase of back scattering coefficient P for E^i parallel to the cylinder axis.

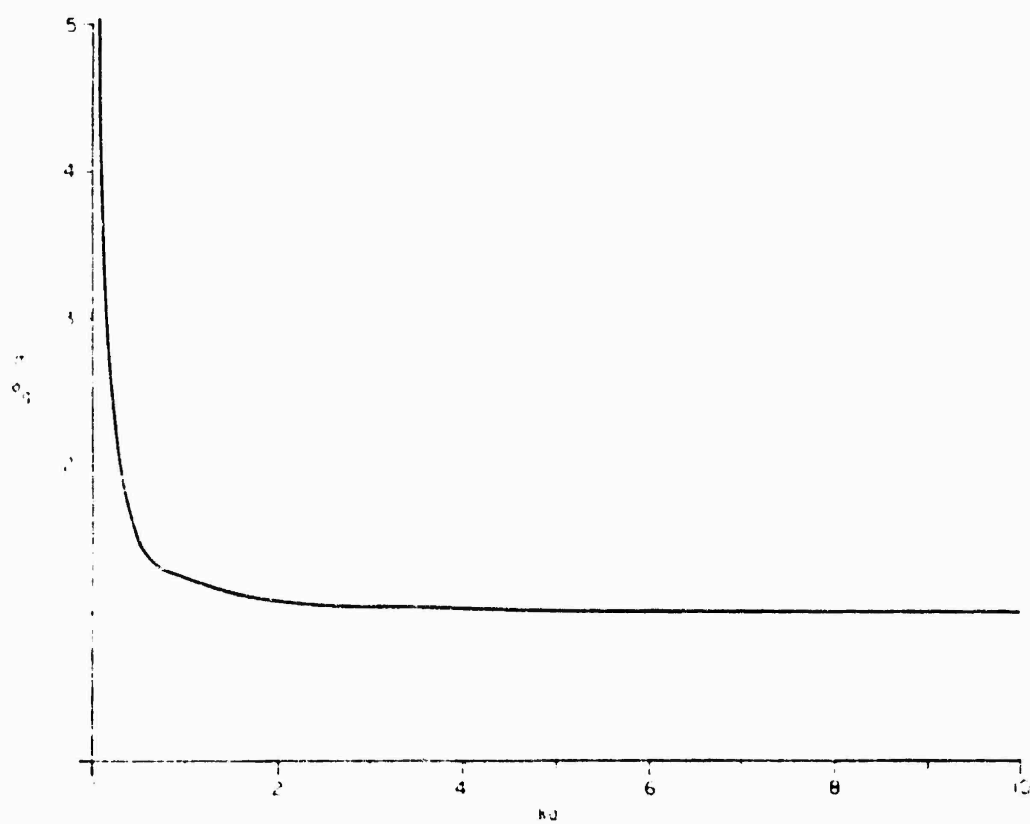


Fig. 2.6. Normalized back scattering cross section for E^i parallel to the cylinder axis.

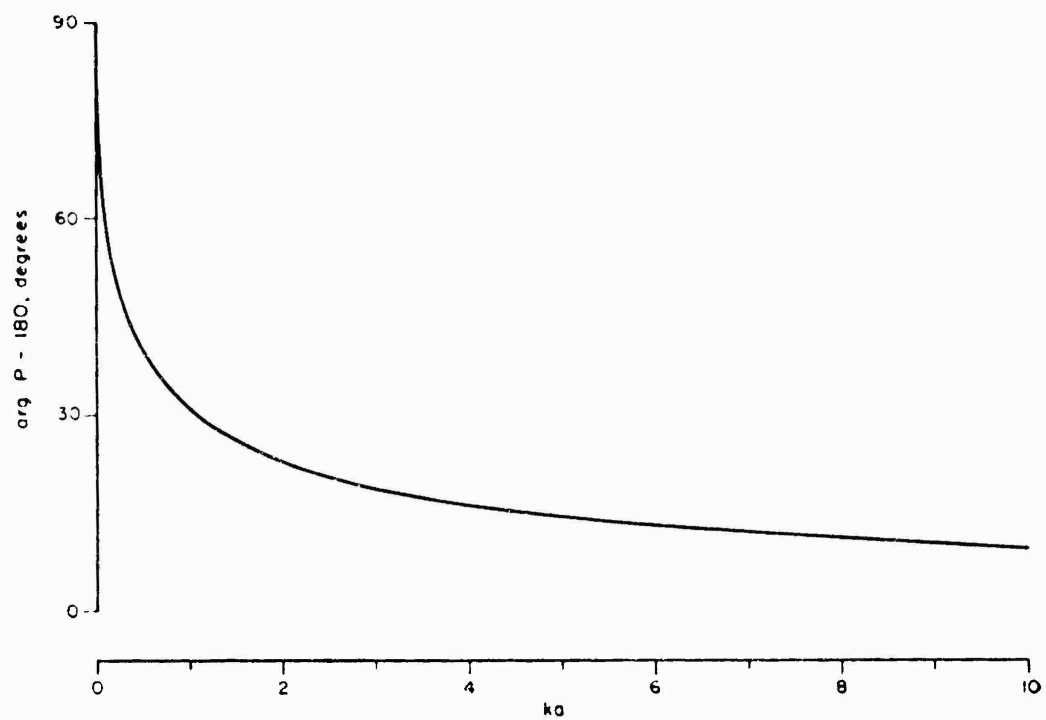


Fig. 2.7. Phase of forward scattering coefficient P for E^i parallel to the cylinder axis.

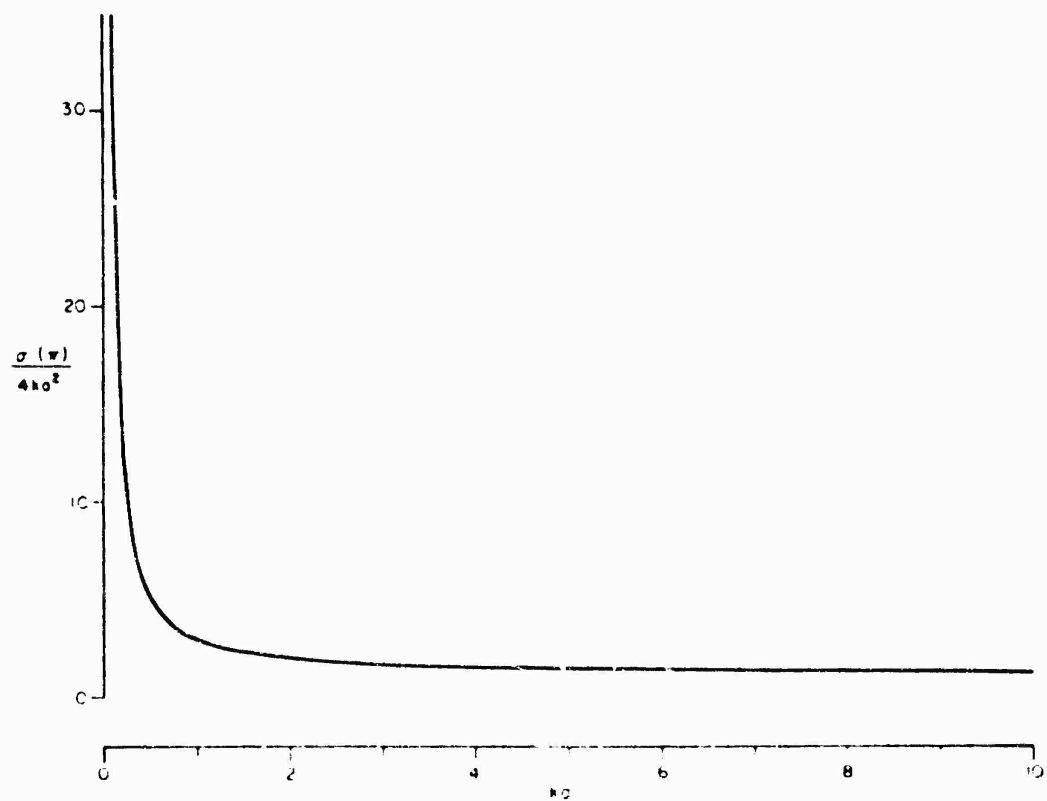


Fig. 2.8. Normalized forward scattering cross section for E^i parallel to the cylinder axis.

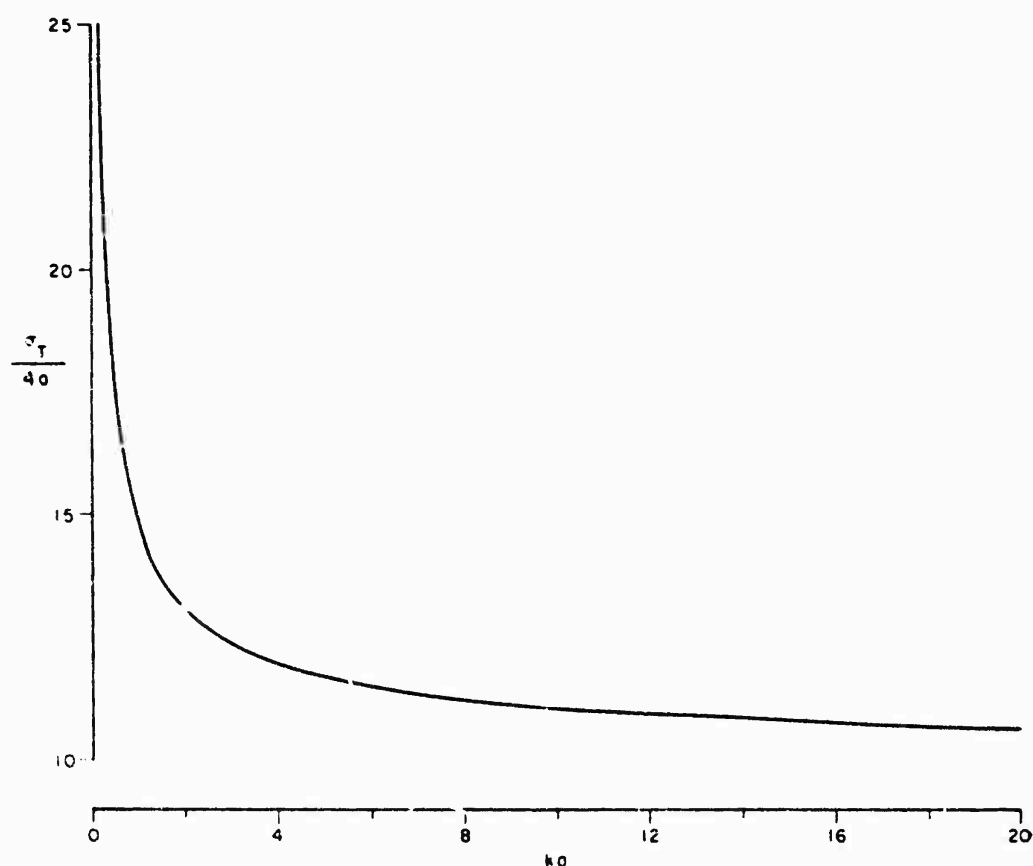


Fig. 2.9. Normalized total scattering cross section $\sigma_T/(4a)$ for E^i parallel to the cylinder axis (KING and WU [1959]).

where $\gamma = 0.5772157 \dots$ is Euler's constant. To this order, the scattering cross section is independent of ϕ ; as $ka \rightarrow 0$:

$$\sigma \sim \sigma_T \sim \frac{\pi^2}{k(\log ka)^2}. \quad (2.11)$$

Low frequency expansions of P through $O[(ka)^4]$ are given by STRUTT [1907].

2.2.1.3. HIGH FREQUENCY APPROXIMATIONS

For a plane wave incident in the direction of the negative x -axis, such that

$$E^i = \hat{z}e^{-ikx}, \quad H^i = \hat{y}e^{-ikx}, \quad (2.12)$$

high frequency expansions may be obtained either directly, e.g. by the Luneburg-Kline method (KELLER et al. [1956]), or by asymptotic evaluations of contour integral representations of the exact solution.

The complete asymptotic expansion of the reflected portion of the scattered field at a point located in the illuminated region is (KELLER et al. [1956]):

$$(E_z^*)_{\text{refl.}} \sim \frac{1}{2} \sqrt{\frac{a}{2s}} \cos \psi_1 \exp [ik(s - \frac{1}{2}a \cos \psi_1)] \\ \times \sum_{n=0}^{\infty} \sum_{h=0}^{3n} \sum_{l=0}^n a_{hln} (16ika \cos \psi_1)^{-n} \left(\frac{a}{2s}\right)^h (\cos \psi_1)^{h-2l}, \quad (2.13)$$

where:

$$a_{hln} = h^{-1} \{ (2h+4l+2n-3)(6h-4l-2n-1)a_{h-1,l,n-1} + \\ + (2h-4l-2n+5)(2h-4l-2n+3)a_{h-1,l-1,n-1} + \\ + [24(h-1)(h-2l-n)-6]a_{h-2,l,n-1} + \\ + 12(1-h)(2h-4l-2n+3)a_{h-2,l-1,n-1} + \\ + 9(2h-5)(1-2h)(a_{h-3,l,n-1} - a_{h-3,l-1,n-1}) \}, \quad \text{for } h \neq 0, \quad (2.14)$$

$$a_{0ln} = - \sum_{h=1}^{3n} a_{hln}, \quad a_{000} = -2, \quad (2.15)$$

$$s = P_1 P + \frac{1}{2}a \cos \psi_1, \quad (2.16)$$

and $P_1 P$ is the distance between the reflection point $P_1(a, \psi_1)$ of the optical ray and

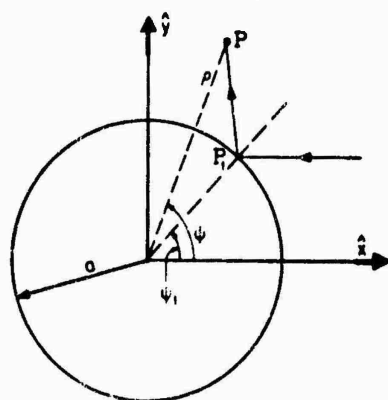


Fig. 2.10. Geometry for the reflected field.

the observation point $P(\rho, \psi)$ (see Fig. 2.10). Explicitly, the first few terms of the series (2.13) are:

$$(E_z^*)_{\text{refl.}} \sim - \sqrt{\frac{a}{2s}} \cos \psi_1 \exp [ik(s - \frac{1}{2}a \cos \psi_1)] \left\{ 1 + \frac{i}{16ka} \left[\frac{8}{\cos^3 \psi_1} - \frac{3}{\cos \psi_1} + \right. \right. \\ \left. \left. + \frac{a}{2s} \left(\frac{1}{\cos^2 \psi_1} - 3 \right) + \left(\frac{a}{2s} \right)^2 \left(\frac{6}{\cos \psi_1} - 9 \cos \psi_1 \right) + \right. \right. \\ \left. \left. + \left(\frac{a}{2s} \right)^3 (15 \cos^2 \psi_1 - 15) \right] + \dots \right\}. \quad (2.17)$$

In particular, in the far field ($\rho \rightarrow \infty$):

$$(E_z^*)_{\text{refl.}} \sim A \sqrt{\frac{a}{2\rho}} \cos \frac{1}{2}\psi \exp [ik(\rho - 2a \cos \frac{1}{2}\psi)], \quad (2.18)$$

where (KELLER et al. [1956]):

$$|A| \sim 1 + \frac{1}{(16ka)^2} \left(\frac{3477}{\cos^2 \frac{1}{2}\psi} - \frac{72i8}{\cos^4 \frac{1}{2}\psi} + \frac{3817}{\cos^6 \frac{1}{2}\psi} \right) + \dots \quad (2.19)$$

The leading term in eq. (2.18) is the geometrical optics far field:

$$(E_z^s)_{g.o.} = - \sqrt{\frac{a}{2\rho}} \cos \frac{1}{2}\psi \exp \{ik(\rho - 2a \cos \frac{1}{2}\psi)\}. \quad (2.20)$$

The creeping wave contribution is not included in eqs. (2.13) to (2.20), but is accounted for in all formulac in the rest of this section.

On the illuminated portion of the surface ($\rho = a$, $|\psi| < \frac{1}{2}\pi$) (FRANZ and GALLE [1955]):

$$H_\phi^i + H_\phi^s \sim 2Y \cos \psi \exp(-ika \cos \psi) \left[1 + \frac{i}{2ka \cos^3 \psi} + \frac{1+3 \sin^2 \psi}{2(ka \cos^3 \psi)^2} + \dots \right] + Y e^{i\pi} m^{-1} \sum_n D_n \frac{\exp [iv_n(\frac{3}{2}\pi - \psi)] + \exp [iv_n(\frac{3}{2}\pi + \psi)]}{1 - \exp(2i\pi v_n)}, \quad (2.21)$$

where

$$v_n \sim ka + e^{i\pi} \alpha_n m - e^{-i\pi} \frac{\alpha_n^2}{60} m^{-1} - \frac{1}{140} \left(1 - \frac{\alpha_n^3}{10} \right) m^{-3} + e^{i\pi} \frac{1}{12600} (29\alpha_n - \frac{281}{360}\alpha_n^4) m^{-5} + \dots, \quad (2.22)$$

$$D_n \sim \frac{1}{A i'(-\alpha_n)} \left[1 + e^{i\pi} \frac{\alpha_n}{10} m^{-2} + e^{-i\pi} \frac{59\alpha_n^2}{12600} m^{-4} + \frac{1}{12600} (37 - \frac{223}{18}\alpha_n^3) m^{-6} + \dots \right]. \quad (2.23)$$

The first group of terms in eq. (2.21) represents the optics contribution to the surface field, and the first term itself is the geometrical optics field; this development is numerically useful only if $ka \cos^3 \phi \gg 1$. The summation over n represents the creeping wave contribution to the surface field.

On the shadowed portion of the surface ($\rho = a$, $|\phi - \pi| < \frac{1}{2}\pi$) (FRANZ and GALLE [1955]):

$$H_\phi^i + H_\phi^s \sim Y e^{i\pi} m^{-1} \sum_n D_n \frac{\exp [iv_n(\phi - \frac{1}{2}\pi)] + \exp [iv_n(\frac{3}{2}\pi - \phi)]}{1 - \exp(2i\pi v_n)}, \quad (2.24)$$

where v_n and D_n are given by eqs. (2.22) and (2.23). Near the shadow boundary, the creeping wave series (2.24) is no longer useful for computational purposes.

An alternative representation of the surface field, which is appropriate in the transition region about the shadow boundary, i.e.

$$||\psi| - \frac{1}{2}\pi| \lesssim m^{-1}, \quad (2.25)$$

where the creeping wave series of eq. (2.24) fails, is the following (GORIAINOV [1958]):

$$H_{\phi}^i + H_{\phi}^s \sim iYm^{-1} \sum_{l=0}^{\infty} [f^{(0)}(m\eta_l) e^{ika\eta_l} + f^{(0)}(m\bar{\eta}_l) e^{ika\bar{\eta}_l}], \quad (2.26)$$

where

$$\eta_l = \phi - \frac{1}{2}\pi + 2\pi l, \quad \bar{\eta}_l = \frac{1}{2}\pi - \phi + 2\pi l, \quad (2.27)$$

and the function $f^{(0)}(\xi)$ is described in the Introduction (Section I.3.3).

A representation of the surface field, which provides results less accurate than those obtained from eqs. (2.21) and (2.26), but which is useful in the entire range $0 \leq \phi < \frac{1}{2}\pi$, is the following (GORIAINOV [1958]):

$$H_{\phi}^i + H_{\phi}^s \sim iYm^{-1} [f^{(0)}(m\bar{\eta}_0) \exp \{ika\bar{\eta}_0\} + F(m \cos(\pi - \phi)) \exp \{ika \cos(\pi - \phi)\}], \quad (2.28)$$

where the function $F(\xi)$ is described in the Introduction (Section I.3.3).

At large distances from the surface ($\rho \gg a$) (FRANZ and GALLE [1955]):

$$\begin{aligned} E_z^s \sim & -\sqrt{\frac{a}{2\rho}} \cos \frac{1}{2}\psi \exp \{ik(\rho - 2a \cos \frac{1}{2}\psi)\} \left[1 + i \frac{(2ka \sin \frac{1}{2}\psi)^2 - 1}{8k\rho} - \frac{3i}{16ka \cos \frac{1}{2}\psi} + \right. \\ & + \frac{i}{2ka \cos^3 \frac{1}{2}\psi} + \frac{15}{512(ka \cos \frac{1}{2}\psi)^2} - \frac{33}{32(ka \cos^2 \frac{1}{2}\psi)^2} + \frac{5}{4(ka \cos^3 \frac{1}{2}\psi)^2} + \dots \left. \right] + \\ & + m(2\pi k\rho)^{-1} \exp \{i(k\rho + \frac{1}{2}\pi)\} \sum_n C_n \frac{\exp [iv_n(\pi + \psi)] + \exp [iv_n(\pi - \psi)]}{1 - \exp(i2\pi v_n)} \\ & \times \left(1 + i \frac{4v_n^2 - 1}{8k\rho} + \dots \right), \end{aligned} \quad (2.29)$$

where

$$\begin{aligned} C_n \sim & [Ai'(-x_n)]^{-2} \left[1 + e^{i\pi x_n} \frac{x_n}{30} m^{-2} + e^{-i\pi x_n} \frac{3x_n^2}{1400} m^{-4} + \right. \\ & \left. + \frac{1}{12600} (29 - \frac{281}{90} x_n^2) m^{-6} + \dots \right], \end{aligned} \quad (2.30)$$

and v_n is given by eq. (2.22). The first group of terms in eq. (2.29) represents the optics contribution to the far field, and the first term itself is the geometrical optics field of eq. (2.20); this development is numerically useful only if $ka \cos^3 \frac{1}{2}\psi \gg 1$. The summation over n represents the creeping wave contribution to the far scattered field, and is practically applicable only for $|\phi - \pi| \gg m^{-1}$ (but see eq. (2.33)).

In the far field ($\rho \rightarrow \infty$) and in the back scattering direction ($\phi = 0$):

$$\begin{aligned} P \sim & -\frac{1}{2} \sqrt{\pi ka} \exp(-2ika + \frac{1}{2}i\pi) \left(1 + \frac{5i}{16ka} + \frac{127}{512(ka)^2} + \dots \right) + \\ & + \frac{1}{2} m e^{i\pi} \sum_n \frac{C_n}{\sin(\pi v_n)}. \end{aligned} \quad (2.31)$$

In particular, the geometrical optics back scattering cross section per unit length is:

$$\sigma_{g.o.} = \pi a. \quad (2.32)$$

In the far field ($\rho \rightarrow \infty$) and in the angular region $|\phi - \pi| \ll m^{-1}$, the dominant contribution to the scattered field is (GORIAINOV [1958]):

$$P \sim -\frac{\sin[ka(\phi - \pi)]}{\phi - \pi} - i\pi^{\frac{1}{2}} m [p(m(\phi - \pi))e^{ika(\phi - \pi)} + p(m(\pi - \phi))e^{ika(\pi - \phi)}], \quad (2.33)$$

where the reflection coefficient function $p(\xi)$ is described in the Introduction (Section I.3.3). For the particular case of forward scattering ($\phi = \pi$), a more refined approximation is (WU [1956]):

$$P \sim -ka - M_0 m - \frac{1}{30} M_1 m^{-1} + \frac{1}{140} (1 + \frac{3}{10} M_2) m^{-3} - \frac{1}{12600} (29M_0 + \frac{281}{90} M_3) m^{-5} + \\ + \frac{1}{5821200} (7361M_1 + \frac{73769}{360} M_4) m^{-7} + \dots \quad (2.34)$$

where

$$\begin{aligned} M_0 &= 1.25507437e^{3i\pi}, & M_1 &= 0.53225036e^{3i\pi}, \\ M_2 &= 0.0935216, & M_3 &= 0.772793e^{3i\pi}, \\ M_4 &= 1.0992e^{3i\pi}. \end{aligned} \quad (2.35)$$

Thus, the total scattering cross section σ_T per unit length is (WU [1956]):

$$\sigma_T \sim 4a[1 + 0.49807659(ka)^{-2/3} - 0.01117656(ka)^{-4/3} - 0.01468652(ka)^{-2} + \\ + 0.00488945(ka)^{-8/3} + 0.00179345(ka)^{-10/3} + \dots]. \quad (2.36)$$

The first three terms in (2.36) give an excellent approximation to the exact value of σ_T for all $ka \geq 1$. Various authors have attempted to derive approximate expressions for σ_T by variational methods; the results obtained have not been satisfactory.

2.2.2. *H-polarization*

2.2.2.1. EXACT SOLUTIONS

For a plane wave incident in the direction of the negative x -axis, such that

$$E^i = -\hat{y}Ze^{-ikx}, \quad H^i = \hat{z}e^{-ikx}, \quad (2.37)$$

then

$$H_z^s = -\sum_{n=0}^{\infty} \epsilon_n (-i)^n \frac{J_n'(ka)}{H_n^{(1)'}(ka)} H_n^{(1)}(k\rho) \cos n\phi. \quad (2.38)$$

KING and WU [1959] have computed H_z^s in amplitude and phase for $ka = 3.1$ at various positions of the field point.

On the surface $\rho = a$:

$$H_z^i + H_z^s = \frac{2}{\pi ka} \sum_{n=0}^{\infty} \epsilon_n \frac{(-i)^{n-1}}{H_n^{(1)'}(ka)} \cos n\phi. \quad (2.39)$$

This expression has been computed as a function of ϕ for selected values of ka , and its amplitude and phase are shown in Fig. 2.11.

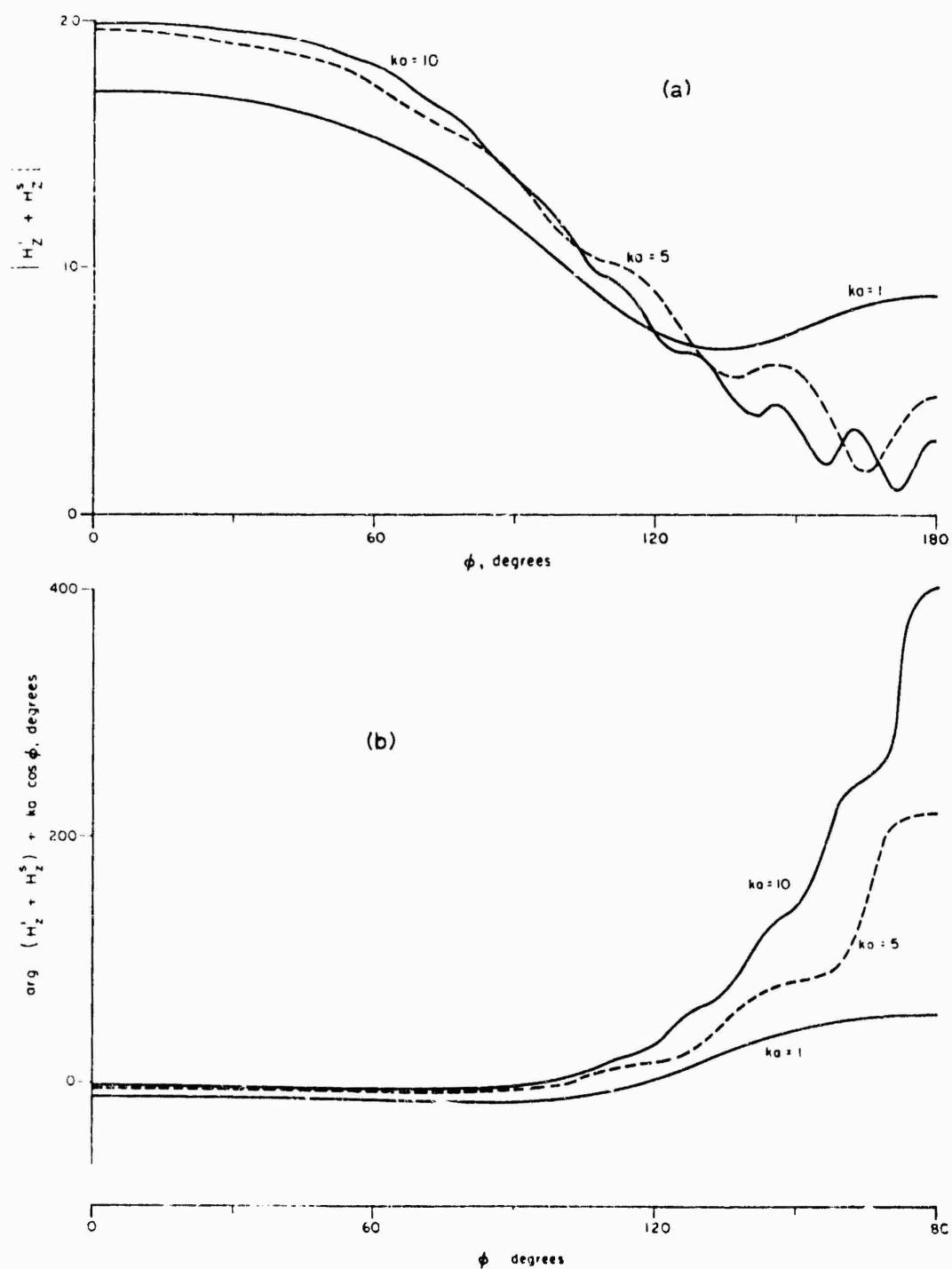


Fig. 2.11. Amplitude (a) and phase (b) of surface field produced by a plane wave with H^i parallel to the cylinder axis.

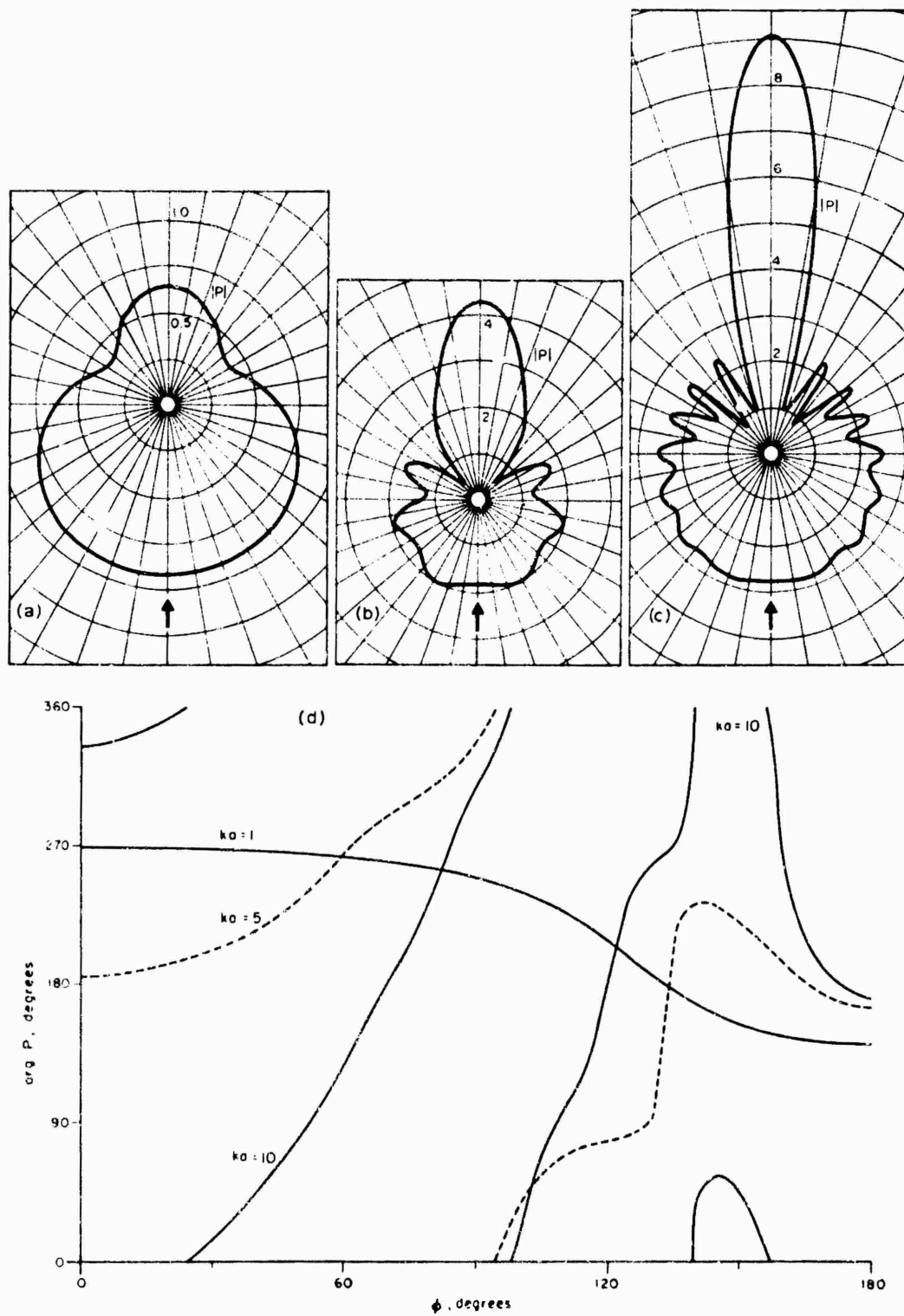


Fig. 2.12. Amplitude for (a) $ka = 1$, (b) $ka = 5$, (c) $ka = 10$ and (d) phase of bistatic far field coefficient P , for plane wave incidence with H parallel to the cylinder axis.

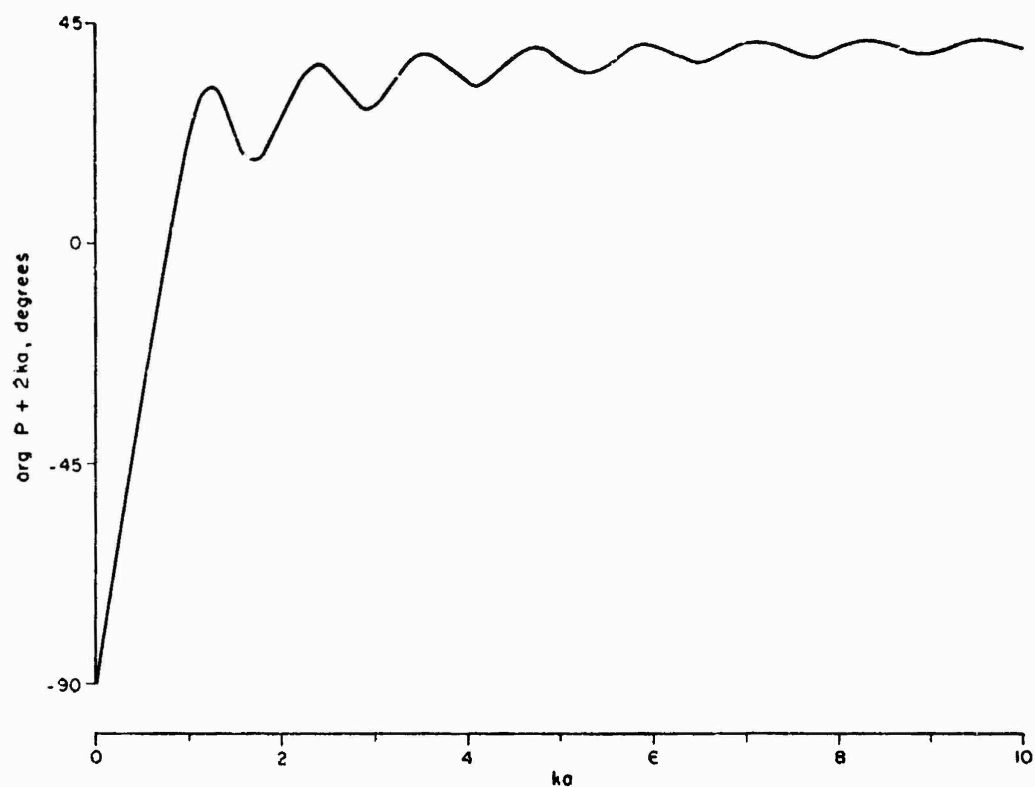


Fig. 2.13. Phase of back scattering coefficient P for H^i parallel to the cylinder axis.

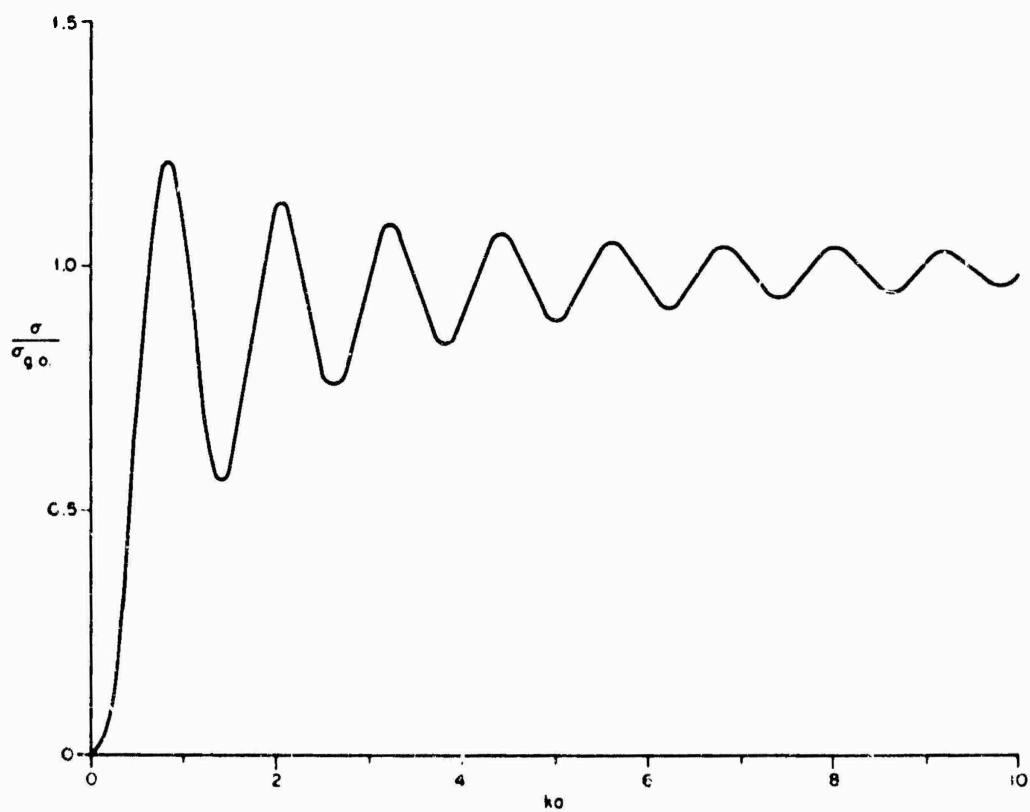


Fig. 2.14. Normalized back scattering cross section for H^i parallel to the cylinder axis.

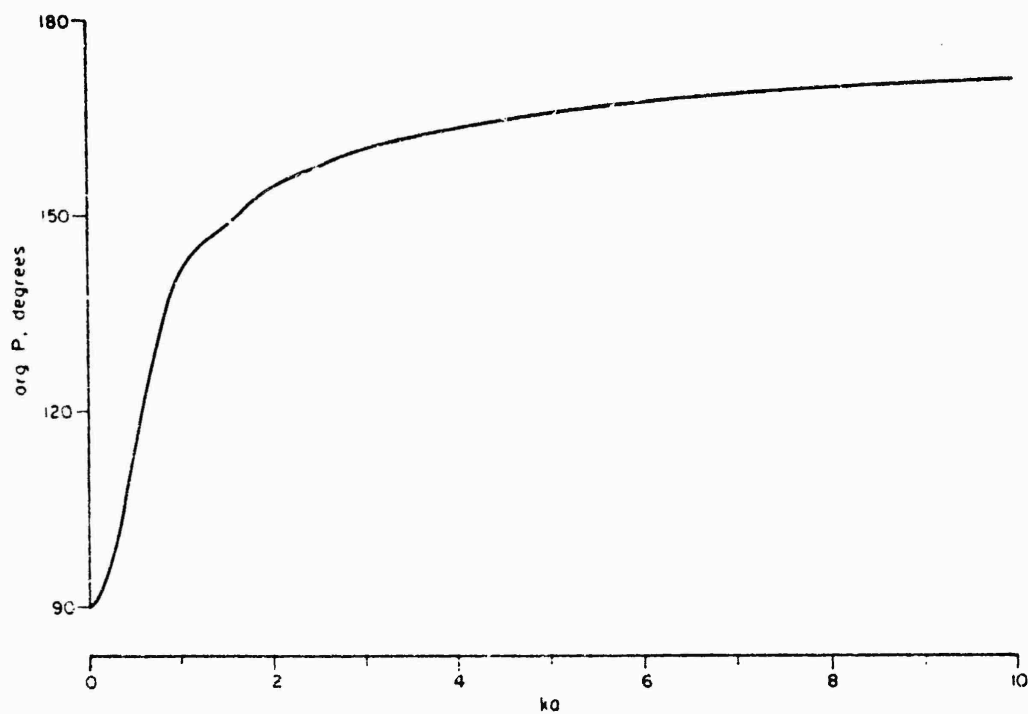


Fig. 2.15. Phase of forward scattering coefficient P for H^i parallel to the cylinder axis.

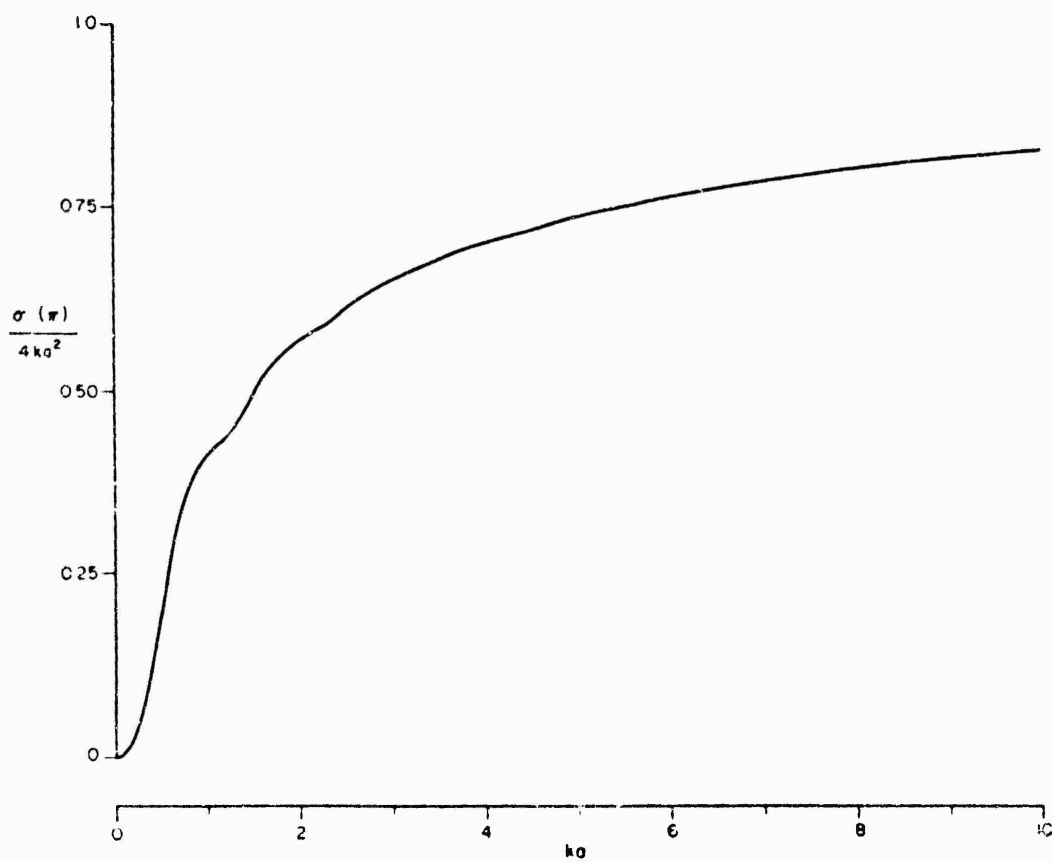


Fig. 2.16. Normalized forward scattering cross section for H^i parallel to the cylinder axis.

In the far field ($\rho \rightarrow \infty$):

$$P = - \sum_{n=0}^{\infty} \epsilon_n (-1)^n \frac{J'_n(ka)}{H_n^{(1)'}(ka)} \cos n\phi. \quad (2.40)$$

The amplitude and phase of P as functions of ϕ for three different values of ka are shown in Fig. 2.12. For the particular case of back scattering ($\phi = 0$), $\arg P$ is plotted as a function of ka in Fig. 2.13. The normalized back scattering cross section is shown as a function of ka in Fig. 2.14. In the case of forward scattering ($\phi = \pi$), $\arg P$ is plotted as a function of ka in Fig. 2.15, and the normalized forward scattering cross section is given in Fig. 2.16. The total scattering cross section per unit length is:

$$\sigma_T = \frac{4}{k} \sum_{n=0}^{\infty} \epsilon_n \left[\frac{J'_n(ka)}{H_n^{(1)'}(ka)} \right]^2. \quad (2.41)$$

The quantity $\sigma_T/(4a)$ is plotted in Fig. 2.17.

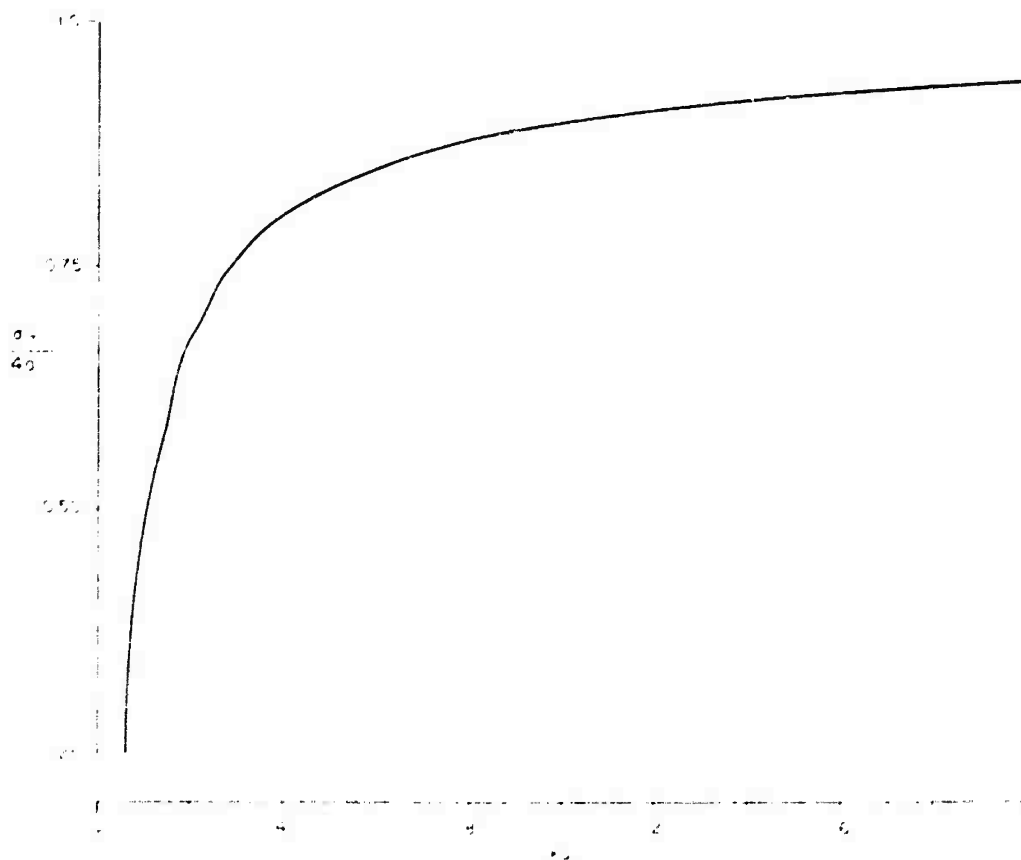


Fig. 2.17. Normalized total scattering cross section $\sigma_T/(4a)$ for H^i parallel to the cylinder axis (KING and WU [1959]).

2.2.2.2. LOW FREQUENCY APPROXIMATIONS

For a plane wave incident in the direction of the negative x -axis, such that

$$E^i = -\hat{y}Ze^{-ikx}, \quad H^i = \hat{z}e^{-ikx}, \quad (2.42)$$

low frequency expansions may be obtained either directly (STRUTT [1897]; NOBLE [1962]; VAN BLADEL [1963]) or by power series developments of the radial cylindrical functions appearing in the exact solutions. In particular, in the far field ($\rho \rightarrow \infty$):

$$P \sim -\frac{1}{4}\pi(ka)^2(1+2\cos\phi), \quad (2.43)$$

and to this order, the back scattering cross section σ and the total scattering cross section σ_T per unit length are:

$$\sigma \sim \frac{9\pi^2}{4k}(ka)^4, \quad (2.44)$$

$$\sigma_T \sim \frac{3\pi^2}{4k}(ka)^4. \quad (2.45)$$

Low frequency expansions of P through $O[(ka)^4]$ are given by STRUTT [1907].

2.2.2.3. HIGH FREQUENCY APPROXIMATIONS

For a plane wave incident in the direction of the negative x -axis, such that

$$\mathbf{E}^i = -\mathbf{j}Ze^{-ikx}, \quad \mathbf{H}^i = \hat{\mathbf{z}}e^{-ikx}, \quad (2.46)$$

high frequency expansions may be obtained either directly, i.e. by the Luneburg-Kline method (KELLER et al. [1956]), or by asymptotic evaluations of contour integral representations of the exact solution.

The complete asymptotic expansion of the reflected portion of the scattered field at a point located in the illuminated region is (KELLER et al. [1956]):

$$(H_z)_{\text{refl}} \sim \frac{1}{2} \sqrt{\frac{a}{2s}} \cos\psi_1 \exp[ik(s - \frac{1}{2}a \cos\psi_1)] \\ \times \sum_{n=0}^{\infty} \sum_{h=0}^{3n} \sum_{l=0}^n a_{hln} (16ika \cos\psi_1)^{-n} \left(\frac{a}{2s}\right)^h (\cos\psi_1)^{h-2l}, \quad (2.47)$$

where a_{hln} is given by eq. (2.14) for $h \neq 0$.

$$a_{0ln} = - \sum_{h=1}^{3n} [a_{hln} + 16(2l+n-1)a_{h-1,l,n-1} + 16(4-2l-n-2h)a_{h-1,l-1,n-1}], \quad (2.48)$$

$$a_{000} = +2, \quad (2.49)$$

the distance s is given by eq. (2.16) and the angle ψ_1 is shown in Fig. 2.10. Explicitly, the first few terms of the series (2.47) are:

$$(H_z)_{\text{refl}} \sim \frac{1}{2} \sqrt{\frac{a}{2s}} \cos\psi_1 \exp[ik(s - \frac{1}{2}a \cos\psi_1)] \left\{ 1 - \frac{i}{16ka} \left[\frac{8}{\cos^3\psi_1} + \frac{3}{\cos\psi_1} + \right. \right. \\ \left. \left. + \frac{a}{2s} \left(3 - \frac{1}{\cos^2\psi_1} \right) + \left(\frac{a}{2s}\right)^2 \left(9\cos\psi_1 - \frac{6}{\cos\psi_1} \right) + \left(\frac{a}{2s}\right)^3 (15 - 15\cos^2\psi_1) \right] + \dots \right\}. \quad (2.50)$$

In particular, in the far field ($\rho \rightarrow \infty$):

$$(H_z^s)_{\text{refl.}} \sim B \sqrt{\frac{a}{2\rho}} \cos \frac{1}{2}\psi \exp \{ik(\rho - 2a \cos \frac{1}{2}\psi)\}, \quad (2.51)$$

where (KELLER et al. [1956]):

$$|B| \sim 1 + \frac{1}{(16ka)^2} \left(\frac{3477}{\cos^2 \frac{1}{2}\psi} - \frac{6642}{\cos^4 \frac{1}{2}\psi} + \frac{3049}{\cos^6 \frac{1}{2}\psi} \right) + \dots \quad (2.52)$$

The leading term in eq. (2.51) is the geometrical optics far field:

$$(H_z^s)_{\text{g.o.}} = \sqrt{\frac{a}{2\rho}} \cos \frac{1}{2}\psi \exp \{ik(\rho - 2a \cos \frac{1}{2}\psi)\}. \quad (2.53)$$

The creeping wave contribution is not included in eqs. (2.47) to (2.53), but is accounted for in all formulae in the rest of this section.

On the illuminated portion of the surface ($\rho = a$, $|\psi| < \frac{1}{2}\pi$) (FRANZ and GALLE [1955]):

$$\begin{aligned} H_z^i + H_z^r \sim 2 \exp(-iku \cos \psi) \left[1 - \frac{i}{2ka \cos^3 \psi} - \frac{1 + 3 \sin^2 \psi}{(ka \cos^3 \psi)^2} + \dots \right] + \\ + \sum_n \bar{D}_n \frac{\exp[i\bar{v}_n(\frac{1}{2}\pi - \psi)] + \exp[i\bar{v}_n(\frac{1}{2}\pi + \psi)]}{1 - \exp(2i\pi\bar{v}_n)}, \end{aligned} \quad (2.54)$$

where

$$\begin{aligned} \bar{v}_n \sim ka + e^{i\pi} \beta_n m - e^{-i\pi} \frac{1}{10} (\beta_n^{-1} + \frac{1}{6} \beta_n^2) m^{-1} + \frac{1}{200} (\beta_n^{-3} + 4 + \frac{1}{7} \beta_n^3) m^{-3} - \\ - e^{i\pi} \frac{1}{2000} (\beta_n^{-5} - \frac{2}{3} \beta_n^{-2} + \frac{6}{63} \beta_n + \frac{281}{2268} \beta_n^4) m^{-5} + \dots \end{aligned} \quad (2.55)$$

$$\begin{aligned} \bar{D}_n \sim \frac{1}{\beta_n \text{Ai}(-\beta_n)} \left[i - e^{i\pi} \left(\frac{1}{10\beta_n^2} + \frac{1}{30} \beta_n \right) m^{-2} + e^{-i\pi} \frac{1}{200} (-3\beta_n^{-4} + \beta_n^{-1} - \frac{6}{63} \beta_n^2) m^{-4} + \right. \\ \left. + \frac{1}{100} (\frac{1}{4} \beta_n^{-6} - \frac{3}{20} \beta_n^{-3} - \frac{3}{315} + \frac{1}{12} \beta_n^3) m^{-6} + \dots \right]. \end{aligned} \quad (2.56)$$

The first group of terms in eq. (2.54) represents the optics contribution to the surface field, and the first term itself is the geometrical optics field; this development is numerically useful only if $ka \cos^3 \psi \gg 1$. The summation over n represents the creeping wave contribution to the surface field.

On the shadowed portion of the surface ($\rho = a$, $|\phi - \pi| < \frac{1}{2}\pi$) (FRANZ and GALLE [1955]):

$$H_z^i + H_z^r \sim \sum_n \bar{D}_n \frac{\exp[i\bar{v}_n(\phi - \frac{1}{2}\pi)] + \exp[i\bar{v}_n(\frac{1}{2}\pi - \phi)]}{1 - \exp(2i\pi\bar{v}_n)}, \quad (2.57)$$

where \bar{v}_n and \bar{D}_n are given by eqs. (2.55) and (2.56). Near the shadow boundary, the creeping wave series (2.57) is no longer useful for computational purposes.

An alternative representation of the surface field, which is appropriate in the transition region about the shadow boundary, i.e.

$$||\psi| - \frac{1}{2}\pi| \leq m^{-1}, \quad (2.58)$$

where the creeping wave series of eq. (2.57) fails, is the following [GORIAINOV [1958]]:

$$H_z^i + H_z^s \sim \sum_{l=0}^{\infty} [g^{(0)}(m\eta_l)e^{ika\eta_l} + g^{(0)}(m\bar{\eta}_l)e^{ika\bar{\eta}_l}], \quad (2.59)$$

where η_l and $\bar{\eta}_l$ are given by eqs. (2.27) and the function $g^{(0)}(\xi)$ is described in the Introduction (Section I.3.3).

A representation of the surface field, which provides results less accurate than those obtained from eqs. (2.54) and (2.59), but which is useful in the entire range $0 \leq \phi < \frac{1}{2}\pi$, is the following (GORIAINOV [1958]):

$$H_z^i + H_z^s \sim g^{(0)}(m\bar{\eta}_0) \exp(ika\bar{\eta}_0) + G(m \cos(\pi - \phi)) \exp\{ika \cos(\pi - \phi)\}, \quad (2.60)$$

where the function $G(\xi)$ is described in the Introduction (Section I.3.3).

At large distances from the surface ($\rho \gg a$) (FRANZ and GALLE [1955]):

$$\begin{aligned} H_z^s \sim & \sqrt{\frac{a}{2\rho}} \cos \frac{1}{2}\psi \exp\{ik(\rho - 2a \cos \frac{1}{2}\psi)\} \\ & \times \left[1 + i \frac{(2ka \sin \frac{1}{2}\psi)^2 - 1}{8k\rho} - \frac{3i}{16ka \cos \frac{1}{2}\psi} - \frac{i}{2ka \cos^3 \frac{1}{2}\psi} + \right. \\ & + \frac{15}{512(ka \cos \frac{1}{2}\psi)^2} + \frac{33}{32(ka \cos^2 \frac{1}{2}\psi)^2} - \frac{7}{4(ka \cos^3 \frac{1}{2}\psi)^2} + \dots \left. \right] + \\ & + m(2\pi k\rho)^{-\frac{1}{2}} \exp\{i(k\rho + \frac{1}{2}\pi)\} \sum_n \bar{C}_n \frac{\exp[i\bar{v}_n(\pi + \psi)] + \exp[i\bar{v}_n(\pi - \psi)]}{1 - \exp(2i\pi\bar{v}_n)} \\ & \times \left(1 + i \frac{4\bar{v}_n^2 - 1}{8k\rho} + \dots \right), \end{aligned} \quad (2.61)$$

where

$$\begin{aligned} \bar{C}_n \sim & \beta_n^{-1} [\text{Ai}(-\beta_n)]^{-2} [1 + e^{i\pi} {}_1^1_0(\frac{1}{3}\beta_n - \beta_n^{-2})m^{-2} + \\ & + e^{-i\pi} {}_2^3_0(\frac{1}{3}\beta_n^2 - \beta_n^{-4})m^{-4} + {}_1^1_0(\frac{1}{3}\beta_n^{-6} - \frac{1}{5}\beta_n^{-3} - \frac{6}{25}\frac{1}{\beta_n} - \frac{2}{3}\frac{1}{\beta_n^4}\beta_n^3)m^{-6} + \dots], \end{aligned} \quad (2.62)$$

and \bar{v}_n is given by eq. (2.55). The first group of terms in eq. (2.61) represents the optics contribution to the far field, and the first term itself is the geometrical optics field of eq. (2.53); this development is numerically useful only if $ka \cos^3 \frac{1}{2}\psi \gg 1$. The summation over n represents the creeping wave contribution to the far scattered field, and is practically applicable only for $|\phi - \pi| \leq m^{-1}$ (but see eq. (2.65)).

In the far field ($\rho \rightarrow \infty$) and in the back scattering direction ($\phi = 0$):

$$\begin{aligned} P \sim & \frac{1}{2} \sqrt{\pi k a} \exp\{-2ika + \frac{1}{2}i\pi\} \left(1 - \frac{11i}{16ka} - \frac{353}{512(ka)^2} + \dots \right) + \\ & + \frac{1}{2} m e^{i\pi} \sum_n \frac{\bar{C}_n}{\sin(\pi\bar{v}_n)}. \end{aligned} \quad (2.63)$$

In particular, the geometrical optics back scattering cross section per unit length is:

$$\sigma_{g.o.} = \pi a. \quad (2.64)$$

In the far field ($\rho \rightarrow \infty$) and in the angular region $|\phi - \pi| \ll m^{-1}$, the dominant contribution to the scattered field is (GORIAINOV [1958]):

$$P \sim - \frac{\sin [ka(\phi - \pi)]}{\phi - \pi} - i\pi^{\frac{1}{2}} m [q(m(\phi - \pi)) \exp \{ika(\phi - \pi)\} + q(m(\pi - \phi)) \exp \{ika(\pi - \phi)\}], \quad (2.65)$$

where the reflection coefficient function $q(\xi)$ is described in the Introduction.

For the particular case of forward scattering ($\phi = \pi$), a more refined approximation is (WU [1956]):

$$P \sim -ka - \bar{M}_0 m - \frac{1}{10}(\bar{M}_{-2} + \frac{1}{3}\bar{M}_1)m^{-1} + \frac{1}{50}(1 - \frac{1}{3}\bar{M}_{-4} + \frac{3}{28}\bar{M}_2)m^{-3} - \frac{1}{100}(\frac{281}{11340}\bar{M}_3 - \frac{611}{1260}\bar{M}_0 + \frac{1}{15}\bar{M}_{-3} + \frac{1}{4}\bar{M}_{-6})m^{-5} + \frac{1}{400}(\frac{73769}{5239080}\bar{M}_4 - \frac{56299}{31185}\bar{M}_1 + \frac{1679}{2772}\bar{M}_{-2} - \frac{7}{75}\bar{M}_{-5} - \frac{7}{40}\bar{M}_{-8})m^{-7} + \dots \quad (2.66)$$

where:

$$\begin{aligned} \bar{M}_0 &= -1.088874119e^{+i\pi}, & \bar{M}_1 &= -0.93486491e^{+i\pi}, \\ \bar{M}_2 &= -0.1070199, & \bar{M}_3 &= -0.757663e^{+i\pi}, \\ \bar{M}_4 &= -1.1574e^{+i\pi}, & \bar{M}_{-2} &= -3.70409389e^{-+i\pi}, \\ \bar{M}_{-3} &= 0.41682138e^{-+i\pi}, & \bar{M}_{-4} &= 3.17579652, \\ \bar{M}_{-5} &= 2.55965945 + 3.12247506e^{-+i\pi}, & \bar{M}_{-6} &= 2.06575721e^{-+i\pi}, \\ \bar{M}_{-8} &= -1.36515171 - 2.94764528e^{-+i\pi}. \end{aligned} \quad (2.67)$$

Thus, the total scattering cross section σ_T per unit length is (WU [1956]):

$$\sigma_T \sim 4a[1 - 0.43211998(ka)^{-2.3} - 0.21371236(ka)^{-4.3} + 0.05573255(ka)^{-2} - 0.00055534(ka)^{-8.3} + 0.02324932(ka)^{-10.3} + \dots]. \quad (2.68)$$

The first three terms in eq. (2.68) give a very good approximation to the exact value of σ_T for all $ka \geq 4$. Various authors have attempted to derive approximate expressions for σ_T by variational methods; the results obtained have not been satisfactory.

2.3. Line sources

2.3.1. E-polarization

2.3.1.1. EXACT SOLUTIONS

For an electric line source parallel to the axis z of the cylinder and located at $(\rho_0, \phi_0 = 0)$, such that

$$E^i = \hat{z}H_0^{(1)}(kR), \quad (2.69)$$

the total electric field is

$$E_z^i + E_z^s = \sum_{n=0}^{\infty} \epsilon_n \left[J_n(k\rho_<) - \frac{J_n(ka)}{H_n^{(1)}(ka)} H_n^{(1)}(k\rho_<) \right] H_n^{(1)}(k\rho_>) \cos n\phi. \quad (2.70)$$

On the surface $\rho = a$:

$$H_\phi^i + H_\phi^s = \frac{2Y}{\pi ka} \sum_{n=0}^{\infty} \epsilon_n \frac{H_n^{(1)}(k\rho_0)}{H_n^{(1)}(ka)} \cos n\phi, \quad (2.71)$$

whereas in the far field ($\rho \rightarrow \infty$):

$$E_z^i + E_z^s = \sqrt{\frac{2}{\pi k\rho}} \exp(ik\rho - \frac{1}{4}\pi) \times \left[\exp(-ik\rho_0 \cos \phi) - \sum_{n=0}^{\infty} \epsilon_n (-i)^n \frac{J_n(ka)}{H_n^{(1)}(ka)} H_n^{(1)}(k\rho_0) \cos n\phi \right]. \quad (2.72)$$

If the line source is on the surface ($\rho_0 = a$), the field is identically zero everywhere.

ZITRON and DAVIS [1963] have computed a quantity proportional to the amplitude of the summation over n in eq. (2.72), as a function of ϕ and for $ka = 1.0$ with $k\rho_0 = 2, 5, 10, 20$; $ka = 3.4$ with $k\rho_0 = 6.8, 13.6, 17, 68$; and $ka = 10.0$ with $k\rho_0 = 100, 200, 500$. Some of their results are displayed in Fig. 2.18.

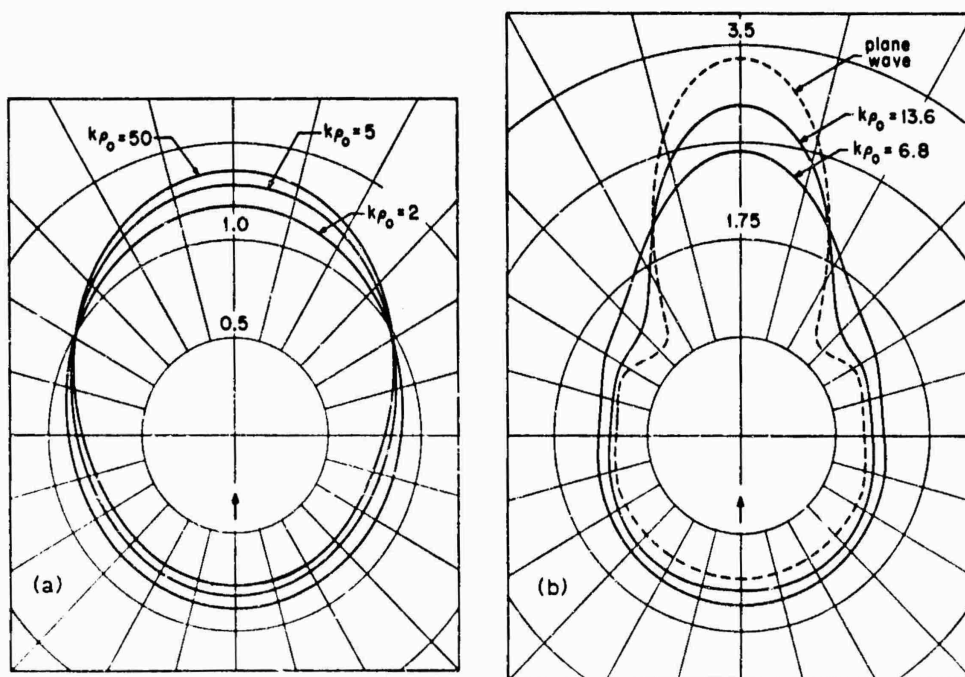


Fig. 2.18. Far scattered field amplitude (product of $\sqrt{k\rho_0}$ and modulus of summation over n in eq. (2.72)) for electric line source and (a) $ka = 1.0$, (b) $ka = 3.4$ (ZITRON and DAVIS [1963]).

2.3.1.2. LOW FREQUENCY APPROXIMATIONS

For an electric line source parallel to the z -axis and located at $(\rho_0, \phi_0 = 0)$, such that

$$E^i = \hat{z} H_0^{(1)}(kR), \quad (2.73)$$

low frequency expansions are trivially obtained from the exact solution. In particular, in the far field ($\rho \rightarrow \infty$):

$$P \sim \frac{\frac{1}{2}i\pi}{\gamma + \log \{ka/(2i)\}} H_0^{(1)}(k\rho_0), \quad (2.74)$$

where $\gamma = 0.5772157 \dots$ is Euler's constant; if, also, $k\rho_0 \ll 1$:

$$P \sim -\frac{\gamma + \log \{k\rho_0/(2i)\}}{\gamma + \log \{ka/(2i)\}}. \quad (2.75)$$

2.3.1.3. HIGH FREQUENCY APPROXIMATIONS

For an electric line source parallel to the z -axis and located at $(\rho_0, \phi_0 = 0)$, such that

$$E^i = \hat{z} H_0^{(1)}(kR), \quad (2.76)$$

high frequency approximations may be obtained by Watson-type transformations of the exact series solution (FRANZ [1954]). The total electric field at a point (ρ, ϕ) is:

$$\begin{aligned} E_z^i + E_z^s \sim & \frac{1}{2} \int_C \left[H_v^{(2)}(k\rho_<) - \frac{H_v^{(2)}(ka)}{H_v^{(1)}(ka)} H_v^{(1)}(k\rho_<) \right] H_v^{(1)}(k\rho_>) e^{iv\psi} dv + \\ & + \frac{1}{2} m e^{i\pi} \sum_n C_n H_{v_n}^{(1)}(k\rho_0) H_{v_n}^{(1)}(k\rho) \frac{\exp [iv_n(2\pi - \psi)] + \exp [iv_n(2\pi + \psi)]}{1 - \exp(2i\pi v_n)}, \end{aligned} \quad (2.77)$$

where C_n and v_n are given by eqs. (2.17) and (2.11), respectively, and the contour C of integration runs from minus infinity to plus infinity just above the real v -axis. Equation (2.77) is valid for all $|\psi| < \pi$, but in the shadow region, a more rapidly convergent expression is:

$$E_z^i + E_z^s \sim \frac{1}{2} m e^{i\pi} \sum_n C_n H_{v_n}^{(1)}(k\rho_0) H_{v_n}^{(1)}(k\rho) \frac{\exp(iv_n\phi) + \exp [iv_n(2\pi - \phi)]}{1 - \exp(2i\pi v_n)}. \quad (2.78)$$

On the illuminated portion of the surface $\rho = a$:

$$\begin{aligned} H_\phi^i + H_\phi^s \sim & \frac{2Y}{\pi ka} \int_C \frac{H_v^{(1)}(k\rho_0)}{H_v^{(1)}(ka)} e^{iv\psi} dv + \\ & + m^{-1} Y e^{i\pi} \sum_n D_n H_{v_n}^{(1)}(k\rho_0) \frac{\exp [iv_n(2\pi - \psi)] + \exp [iv_n(2\pi + \psi)]}{1 - \exp(2i\pi v_n)}, \end{aligned} \quad (2.79)$$

where D_n is given by eq. (2.23), and on the shadowed portion,

$$H_\phi^i + H_\phi^s \sim m^{-1} Y e^{i\pi} \sum_n D_n H_{v_n}^{(1)}(k\rho_0) \frac{\exp(iv_n\phi) + \exp [iv_n(2\pi - \phi)]}{1 - \exp(2i\pi v_n)}. \quad (2.80)$$

A less refined approximation, in which only the physical optics surface field is retained, is:

$$(H_{\phi}^i + H_{\phi}^s)_{p.o.} = -2iYH_1^{(1)}(kR_1) \frac{a - \rho_0 \cos \phi}{R_1} \quad (2.81)$$

with

$$R_1 = (\rho_0^2 + a^2 - 2a\rho_0 \cos \phi)^{1/2}, \quad (2.82)$$

on the illuminated portion of the surface $\rho = a$, and $(H_{\phi}^i + H_{\phi}^s)_{p.o.} = 0$ on the shadowed portion.

In the far field ($\rho \rightarrow \infty$) and in the illuminated region:

$$E_z^i + E_z^s \sim \frac{\exp(ik\rho - \frac{1}{2}i\pi)}{\sqrt{(2\pi k\rho)}} \left\{ \int_C \left[H_v^{(2)}(k\rho_0) - \frac{H_v^{(2)}(ka)}{H_v^{(1)}(ka)} H_v^{(1)}(k\rho_0) \right] \exp\{iv(\psi - \frac{1}{2}\pi)\} dv + \right. \\ \left. + me^{i\pi} \sum_n C_n H_{v_n}^{(1)}(k\rho_0) \frac{\exp[iv_n(\frac{3}{2}\pi - \psi)] + \exp[iv_n(\frac{3}{2}\pi + \psi)]}{1 - \exp(2i\pi v_n)} \right\}, \quad (2.83)$$

whereas in the shadowed region:

$$E_z^i + E_z^s \sim \frac{\exp(ik\rho + \frac{1}{2}i\pi)}{\sqrt{(2\pi k\rho)}} m \sum_n C_n H_{v_n}^{(1)}(k\rho_0) \frac{\exp[iv_n(\phi - \frac{1}{2}\pi)] + \exp[iv_n(\frac{3}{2}\pi - \phi)]}{1 - \exp(2i\pi v_n)}. \quad (2.84)$$

If the line source is located at a large distance from the surface ($\rho_0 \gg a$), the following approximation may be introduced in the preceding formulae of this section:

$$H_v^{(1), (2)}(k\rho_0) \sim \sqrt{\frac{2}{\pi k\rho_0}} \exp[\pm i(k\rho_0 - \frac{1}{2}v\pi - \frac{1}{4}\pi)] \left\{ 1 \pm i \frac{4v^2 - 1}{8k\rho_0} + O[(k\rho_0)^{-2}] \right\}. \quad (2.85)$$

If the line source is on the surface ($\rho_0 = a$), the field is identically zero everywhere.

2.3.2. H-polarization

2.3.2.1. EXACT SOLUTIONS

For a magnetic line source parallel to the axis z of the cylinder and located at $(\rho_0, \phi_0 = 0)$, such that

$$H^i = \hat{z} H_0^{(1)}(kR), \quad (2.86)$$

the total magnetic field is

$$H_z^i + H_z^s = \sum_{n=0}^{\infty} \epsilon_n \left[J_n(k\rho_0) - \frac{J'_n(ka)}{H_n^{(1)'}(ka)} H_n^{(1)}(k\rho_0) \right] H_n^{(1)}(k\rho) \cos n\phi. \quad (2.87)$$

On the surface $\rho = a$:

$$H_z^i + H_z^s = \frac{2i}{\pi ka} \sum_{n=0}^{\infty} \epsilon_n \frac{H_n^{(1)}(k\rho_0)}{H_n^{(1)'}(ka)} \cos n\phi, \quad (2.88)$$

whereas in the far field ($\rho \rightarrow \infty$):

$$H_z^i + H_z^s = \sqrt{\frac{2}{\pi k \rho}} \exp(ik\rho - \frac{1}{4}i\pi) \times \left[\exp(-ik\rho_0 \cos \phi) - \sum_{n=0}^{\infty} \epsilon_n (-i)^n \frac{J_n'(ka)}{H_n^{(1)'}(ka)} H_n^{(1)}(k\rho_0) \cos n\phi \right]. \quad (2.89)$$

If the line source is on the surface ($\rho_0 = a$):

$$H_z^i + H_z^s = \frac{2i}{\pi ka} \sum_{n=0}^{\infty} \frac{\epsilon_n}{H_n^{(1)'}(ka)} H_n^{(1)}(k\rho) \cos n\phi, \quad (2.90)$$

and in the far field ($\rho \rightarrow \infty$):

$$H_z^i + H_z^s = \frac{2i}{\pi ka} \sqrt{\frac{2}{\pi k \rho}} \exp(ik\rho - \frac{1}{4}i\pi) \sum_{n=0}^{\infty} \epsilon_n \frac{(-i)^n}{H_n^{(1)'}(ka)} \cos n\phi. \quad (2.91)$$

ZITRON and DAVIS [1963] have computed a quantity proportional to the amplitude of the summation over n in eq. (2.89), as a function of ϕ and for $ka = 1.0$ with $k\rho_0 = 2, 5, 10, 20$; $ka = 3.4$ with $k\rho_0 = 6.8, 13.6, 17, 68$; and $ka = 10.0$ with $k\rho_0 = 100, 200, 500$. Some of their results are displayed in Fig. 2.19. A diagram of the far field amplitude as a function of ϕ for $ka = 3.4$ and $k\rho_0 = 6.8, 10, 50$ has been given by FARAN [1953]. SHENDEROV [1961] has plotted amplitudes of both scattered and total far fields as functions of ϕ for $ka = 2, 6, 10$ and $\rho_0 = 1.2a$, and has compared

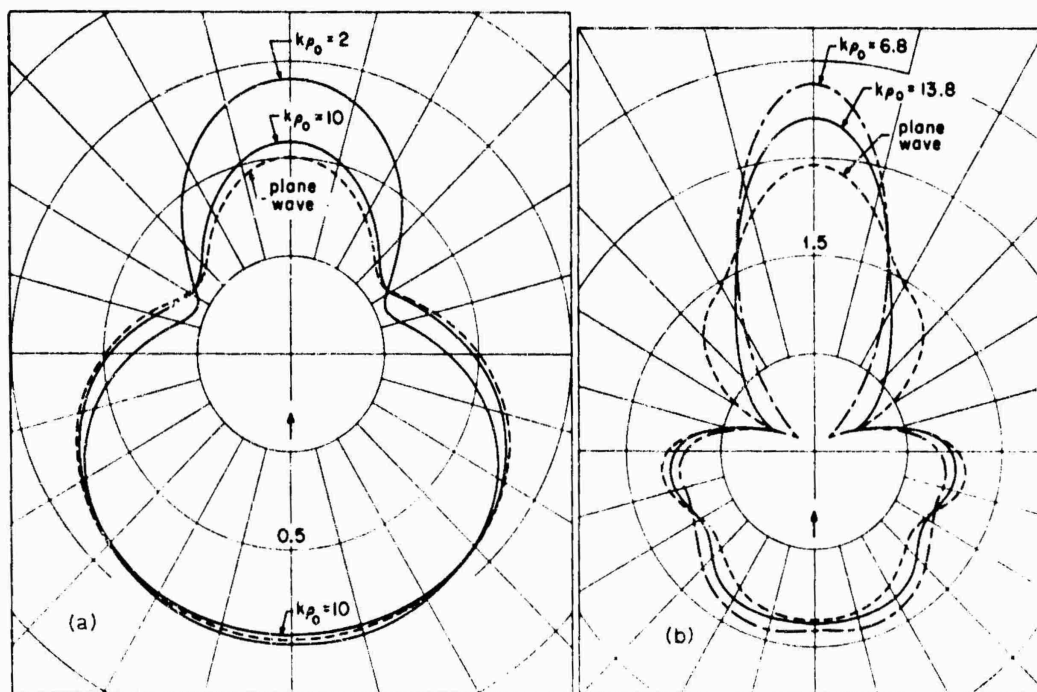


Fig. 2.19. Far scattered field amplitude (product of $\sqrt{k\rho_0}$ and modulus of summation over n in eq. (2.89)) for magnetic line source and (a) $ka = 1.0$, (b) $ka = 3.4$ (ZITRON and DAVIS [1963]).

numerical and experimental diagrams of the amplitude of the total far field for $ka = 6$, 10 and $\rho_0 = 5.2a$.

2.3.2.2. LOW FREQUENCY APPROXIMATIONS

For a magnetic line source parallel to the z -axis and located at $(\rho_0, \phi_0 = 0)$, such that

$$H^i = \hat{z} H_0^{(1)}(kR), \quad (2.92)$$

low frequency expansions are trivially obtained from the exact solution. In particular, in the far field ($\rho \rightarrow \infty$):

$$P \sim -\frac{1}{4}i\pi(ka)^2 [H_0^{(1)}(k\rho_0) + 2iH_1^{(1)}(k\rho_0) \cos \phi]; \quad (2.93)$$

if, also, $k\rho_0 \ll 1$:

$$P \sim \frac{1}{2}(ka)^2 \left[\gamma + \log \left(\frac{k\rho_0}{2i} \right) \right], \quad (2.94)$$

which is independent of ϕ .

2.3.2.3. HIGH FREQUENCY APPROXIMATIONS

For a magnetic line source parallel to the z -axis and located at $(\rho_0, \phi_0 = 0)$, such that

$$H^i = \hat{z} H_0^{(1)}(kR), \quad (2.95)$$

high frequency approximations may be obtained by Watson-type transformations of the exact series solution (FRANZ [1954]). The total magnetic field at a point (ρ, ϕ) is:

$$H_z^i + H_z^s \sim \frac{1}{2} \int_C \left[H_v^{(2)}(k\rho_<) - \frac{H_v^{(2)}(ka)}{H_v^{(1)}(ka)} H_v^{(1)}(k\rho_<) \right] H_v^{(1)}(k\rho_>) e^{iv\psi} dv + \\ + \frac{1}{2} me^{i\pi} \sum_n \bar{C}_n H_{\bar{v}_n}^{(1)}(k\rho_0) H_{\bar{v}_n}^{(1)}(k\rho) \frac{\exp[i\bar{v}_n(2\pi - \psi)] + \exp[i\bar{v}_n(2\pi + \psi)]}{1 - \exp(2i\pi\bar{v}_n)}, \quad (2.96)$$

where \bar{C}_n and \bar{v}_n are given by eqs. (2.62) and (2.55), respectively, and the contour C of integration runs from minus infinity to plus infinity just above the real v -axis. Equation (2.96) is valid for all $|\psi| < \pi$, but in the shadow region, a more rapidly convergent expression is:

$$H_z^i + H_z^s \sim \frac{1}{2} me^{i\pi} \sum_n \bar{C}_n H_{\bar{v}_n}^{(1)}(k\rho_0) H_{\bar{v}_n}^{(1)}(k\rho) \frac{\exp(i\bar{v}_n\phi) + \exp[i\bar{v}_n(2\pi - \phi)]}{1 - \exp(2i\pi\bar{v}_n)}. \quad (2.97)$$

In particular, if the source is located on the surface ($\rho_0 = a$):

$$H_z^i + H_z^s \sim \sum_n \bar{D}_n H_{\bar{v}_n}^{(1)}(k\rho) \frac{\exp(i\bar{v}_n\phi) + \exp[i\bar{v}_n(2\pi - \phi)]}{1 - \exp(2i\pi\bar{v}_n)}, \quad (2.98)$$

where \bar{D}_n is given by eq. (2.56) (see also the literature on axial slots, e.g. SENSIPER [1957], WAIT [1959], HASSERJIAN and ISHIMARU [1962]).

On the illuminated portion of the surface $\rho = a$:

$$H_z^i + H_z^s \sim \frac{2i}{\pi ka} \int_C \frac{H_v^{(1)}(k\rho_0)}{H_v^{(1)'}(ka)} e^{iv\psi} dv + \sum_n \bar{D}_n H_{v_n}^{(1)}(k\rho_0) \frac{\exp[i\bar{v}_n(2\pi - \psi)] + \exp[i\bar{v}_n(2\pi + \psi)]}{1 - \exp(2i\pi\bar{v}_n)}, \quad (2.98)$$

and on the shadowed portion:

$$H_z^i + H_z^s \sim \sum_n \bar{D}_n H_{v_n}^{(1)}(k\rho_0) \frac{\exp(i\bar{v}_n\phi) + \exp[i\bar{v}_n(2\pi - \phi)]}{1 - \exp(2i\pi\bar{v}_n)}. \quad (2.99)$$

In particular, if also the source is on the surface ($\rho = \rho_0 = a$):

$$H_z^i + H_z^s \sim \frac{2}{m} e^{-\frac{1}{2}i\pi} \sum_n \bar{E}_n \frac{\exp(i\bar{v}_n\phi) + \exp[i\bar{v}_n(2\pi - \phi)]}{1 - \exp(2i\pi\bar{v}_n)}, \quad (2.100)$$

where:

$$\bar{E}_n \sim \beta_n^{-1} [1 - e^{\frac{1}{2}i\pi} \frac{1}{10} (\beta_n + \beta_n^{-2}) m^{-2} - e^{-\frac{1}{2}i\pi} \frac{1}{200} (3\beta_n^{-4} + \frac{1}{3}\beta_n^{-1} + \frac{1}{7}\beta_n^2 - \frac{1}{30}\beta_n^5) m^{-4} + \frac{1}{100} (\beta_n^{-6} - \frac{1}{2}\beta_n^{-3} - \frac{1}{4}\frac{9}{2} + \frac{1}{56}\frac{9}{70}\beta_n^3 - \frac{4}{90}\frac{5}{7}\frac{1}{20}\beta_n^6) m^{-6} + \dots]. \quad (2.101)$$

A less refined approximation, in which only the physical optics surface field is retained, is:

$$(H_z^i + H_z^s)_{p.o.} = 2H_0^{(1)}(kR_1) \quad (2.102)$$

with R_1 given by eq. (2.82), on the illuminated portion of the surface $\rho = a$, and $(H_z^i + H_z^s)_{p.o.} = 0$ on the shadowed portion.

In the far field ($\rho \rightarrow \infty$) and in the illuminated region:

$$H_z^i + H_z^s \sim \frac{\exp(ik\rho - \frac{1}{2}i\pi)}{\sqrt{(2\pi k\rho)}} \left\{ \int_C \left[H_v^{(2)}(k\rho_0) - \frac{H_v^{(2)'}(ka)}{H_v^{(1)'}(ka)} H_v^{(1)}(k\rho_0) \right] \exp\{iv(\psi - \frac{1}{2}\pi)\} dv + me^{\frac{1}{2}i\pi} \sum_n \bar{C}_n H_{v_n}^{(1)}(k\rho_0) \frac{\exp[i\bar{v}_n(\frac{3}{2}\pi - \psi)] + \exp[i\bar{v}_n(\frac{3}{2}\pi + \psi)]}{1 - \exp(2i\pi\bar{v}_n)} \right\}, \quad (2.103)$$

whereas in the shadowed region:

$$H_z^i + H_z^s \sim \frac{\exp(ik\rho + \frac{1}{2}i\pi)}{\sqrt{(2\pi k\rho)}} m \sum_n \bar{C}_n H_{v_n}^{(1)}(k\rho_0) \frac{\exp[i\bar{v}_n(\phi - \frac{1}{2}\pi)] + \exp[i\bar{v}_n(\frac{3}{2}\pi - \phi)]}{1 - \exp(2i\pi\bar{v}_n)}. \quad (2.104)$$

In particular, if the source is on the surface ($\rho_0 = a$):

$$H_z^i + H_z^s \sim \sqrt{\frac{2}{\pi k\rho}} \exp(ik\rho - \frac{1}{2}i\pi) \left\{ \frac{2i}{\pi ka} \int_C \frac{\exp[iv(\psi - \frac{1}{2}\pi)]}{H_v^{(1)'}(ka)} dv + \sum_n \bar{D}_n \frac{\exp[i\bar{v}_n(\frac{3}{2}\pi - \psi)] + \exp[i\bar{v}_n(\frac{3}{2}\pi + \psi)]}{1 - \exp(2i\pi\bar{v}_n)} \right\} \quad (2.105)$$

in the illuminated region, and

$$H_z^i + H_z^s \sim \sqrt{\frac{2}{\pi k \rho}} \exp(ik\rho - \frac{1}{4}i\pi) \sum_n \bar{D}_n \frac{\exp[i\bar{v}_n(\phi - \frac{1}{2}\pi)] + \exp[i\bar{v}_n(\frac{3}{2}\pi - \phi)]}{1 - \exp(2i\pi\bar{v}_n)} \quad (2.106)$$

in the shadowed region.

If the line source is located at a large distance from the surface ($\rho_0 \gg a$), the approximation of eq. (2.85) may be introduced in the preceding formulae of this section.

2.4. Dipole sources

2.4.1. Electric dipoles

2.4.1.1. EXACT SOLUTIONS

For an arbitrarily oriented electric dipole located at $\mathbf{r}_0 \equiv (\rho_0 \geq a, \phi_0, z_0)$ with moment $(4\pi\epsilon/k)\hat{\mathbf{c}}$, the total electric field is:

$$\mathbf{E}^i(\mathbf{r}) + \mathbf{E}^s(\mathbf{r}) = 4\pi k \mathcal{G}_e(\mathbf{r}|\mathbf{r}_0) \cdot \hat{\mathbf{c}}, \quad (2.107)$$

where $\mathcal{G}_e(\mathbf{r}|\mathbf{r}_0)$ is the electric dyadic Green's function for the circular cylinder (TAR [1954]):

$$\begin{aligned} \mathcal{G}_e(\mathbf{r}|\mathbf{r}_0) = & \frac{i}{8\pi} \int_{-\infty}^{\infty} dt \sum_{n=0}^{\infty} \frac{\epsilon_n}{k^2 - t^2} \{ \mathbf{M}_{en}^{(3)}(t, \mathbf{r}) [\mathbf{M}_{en}^{(1)}(-t, \mathbf{r}_0) + a_n \mathbf{M}_{en}^{(3)}(-t, \mathbf{r}_0)] + \\ & + \mathbf{M}_{0n}^{(3)}(t, \mathbf{r}) [\mathbf{M}_{0n}^{(1)}(-t, \mathbf{r}_0) + a_n \mathbf{M}_{0n}^{(3)}(-t, \mathbf{r}_0)] + \\ & + \mathbf{N}_{en}^{(3)}(t, \mathbf{r}) [\mathbf{N}_{en}^{(1)}(-t, \mathbf{r}_0) + b_n \mathbf{N}_{en}^{(3)}(-t, \mathbf{r}_0)] + \\ & + \mathbf{N}_{0n}^{(3)}(t, \mathbf{r}) [\mathbf{N}_{0n}^{(1)}(-t, \mathbf{r}_0) + b_n \mathbf{N}_{0n}^{(3)}(-t, \mathbf{r}_0)] \}, \quad \text{for } \rho > \rho_0, \end{aligned} \quad (2.108)$$

$$\begin{aligned} \mathcal{G}_e(\mathbf{r}|\mathbf{r}_0) = & \frac{i}{8\pi} \int_{-\infty}^{\infty} dt \sum_{n=0}^{\infty} \frac{\epsilon_n}{k^2 - t^2} \{ [\mathbf{M}_{en}^{(1)}(t, \mathbf{r}) + a_n \mathbf{M}_{en}^{(3)}(t, \mathbf{r})] \mathbf{M}_{en}^{(3)}(-t, \mathbf{r}_0) + \\ & + [\mathbf{M}_{0n}^{(1)}(t, \mathbf{r}) + a_n \mathbf{M}_{0n}^{(3)}(t, \mathbf{r})] \mathbf{M}_{0n}^{(3)}(-t, \mathbf{r}_0) + \\ & + [\mathbf{N}_{en}^{(1)}(t, \mathbf{r}) + b_n \mathbf{N}_{en}^{(3)}(t, \mathbf{r})] \mathbf{N}_{en}^{(3)}(-t, \mathbf{r}_0) + \\ & + [\mathbf{N}_{0n}^{(1)}(t, \mathbf{r}) + b_n \mathbf{N}_{0n}^{(3)}(t, \mathbf{r})] \mathbf{N}_{0n}^{(3)}(-t, \mathbf{r}_0) \}, \quad \text{for } \rho < \rho_0, \end{aligned} \quad (2.109)$$

with

$$a_n = - \frac{J'_n(a\sqrt{k^2 - t^2})}{H_n^{(1)}(a\sqrt{k^2 - t^2})}, \quad b_n = - \frac{J_n(a\sqrt{k^2 - t^2})}{H_n^{(1)}(a\sqrt{k^2 - t^2})}, \quad (2.110)$$

$$\mathbf{M}_{en}^{(j)}(t, \mathbf{r}) = e^{iz} \left[\mp \frac{n}{\rho} Z_n^{(j)}(\rho\sqrt{k^2 - t^2}) \frac{\sin n\phi \hat{\rho}}{\cos n\phi \hat{\phi}} - \frac{\partial Z_n^{(j)}(\rho\sqrt{k^2 - t^2})}{\partial \rho} \frac{\cos n\phi \hat{\rho}}{\sin n\phi \hat{\phi}} \right], \quad (2.111)$$

$$N_{\epsilon_n}^{(j)}(t, r) = \frac{1}{k} e^{iuz} \left[i t \frac{\partial Z_n^{(j)}(\rho \sqrt{(k^2 - t^2)})}{\partial \rho} \frac{\cos n\phi \hat{\rho}}{\sin n\phi \hat{\rho}} \mp \frac{i n t}{\rho} Z_n^{(j)}(\rho \sqrt{(k^2 - t^2)}) \frac{\sin n\phi \hat{\phi}}{\cos n\phi \hat{\phi}} + \right. \\ \left. + (k^2 - t^2) Z_n^{(j)}(\rho \sqrt{(k^2 - t^2)}) \frac{\cos n\phi \hat{z}}{\sin n\phi \hat{z}} \right], \quad (2.112)$$

$$j = 1, 3 \quad \text{and} \quad Z_n^{(1)}(x) = J_n(x), \quad Z_n^{(3)}(x) = H_n^{(1)}(x).$$

For a longitudinal electric dipole at $(\rho_0, \phi_0 = 0, z_0 = 0)$ with moment $(4\pi\epsilon/k)\hat{z}$, corresponding to an incident electric Hertz vector $(e^{ikR}/kR)\hat{z}$, such that (EINARSSON et al. [1966]):

$$\begin{aligned} E_\rho^i &= -k^2 \frac{e^{ikR}}{kR} \left(1 + \frac{3i}{kR} - \frac{3}{k^2 R^2} \right) \frac{z(\rho - \rho_0 \cos \phi)}{R^2}, \\ E_\phi^i &= -k^2 \frac{e^{ikR}}{kR} \left(1 + \frac{3i}{kR} - \frac{3}{k^2 R^2} \right) \frac{z\rho_0 \sin \phi}{R^2}, \\ E_z^i &= k^2 \frac{e^{ikR}}{kR} \left[\frac{\rho^2}{R^2} \left(1 + \frac{\rho_0^2}{\rho^2} - 2 \frac{\rho_0}{\rho} \cos \phi \right) + \frac{i}{kR} \left(1 + \frac{i}{kR} \right) \left(1 - \frac{3z^2}{R^2} \right) \right], \\ H_\rho^i &= k^2 Y \frac{e^{ikR}}{kR} \left(1 + \frac{i}{kR} \right) \frac{\rho_0 \sin \phi}{R}, \\ H_\phi^i &= -k^2 Y \frac{e^{ikR}}{kR} \left(1 + \frac{i}{kR} \right) \frac{\rho - \rho_0 \cos \phi}{R}, \\ H_z^i &= 0, \end{aligned} \quad (2.113)$$

the total electromagnetic field components can be derived from the total electric Hertz vector (OBERHETTINGER [1943]; WAIT [1959])

$$\begin{aligned} \Pi_\epsilon &= \Pi_\epsilon \hat{z} = \hat{z} \frac{i}{2k} \sum_{n=0}^{\infty} \epsilon_n \cos(n\phi) \int_{-\infty}^{\infty} H_n^{(1)}(\rho \sqrt{(k^2 - t^2)}) \\ &\times \left[J_n(\rho \sqrt{(k^2 - t^2)}) - \frac{J_n(a \sqrt{(k^2 - t^2)})}{H_n^{(1)}(a \sqrt{(k^2 - t^2)})} H_n^{(1)}(\rho \sqrt{(k^2 - t^2)}) \right] e^{iuz} dt \end{aligned} \quad (2.114)$$

by the relations:

$$\begin{aligned} E_\rho &= \frac{\partial^2 \Pi_\epsilon}{\partial \rho \partial z}, \quad E_\phi = \frac{1}{\rho} \frac{\partial^2 \Pi_\epsilon}{\partial \phi \partial z}, \quad E_z = \left(\frac{\partial^2}{\partial z^2} + k^2 \right) \Pi_\epsilon, \\ H_\rho &= -\frac{ikY}{\rho} \frac{\partial \Pi_\epsilon}{\partial \phi}, \quad H_\phi = ikY \frac{\partial \Pi_\epsilon}{\partial \rho}, \quad H_z = 0. \end{aligned} \quad (2.115)$$

On the surface $\rho = a$:

$$H_\phi^i + H_\phi^s = \frac{iY}{\pi a} \sum_{n=0}^{\infty} \epsilon_n \cos(n\phi) \int_{-\infty}^{\infty} \frac{H_n^{(1)}(\rho_0 \sqrt{(k^2 - t^2)})}{H_n^{(1)}(a \sqrt{(k^2 - t^2)})} e^{iuz} dt. \quad (2.116)$$

In the far field ($\rho \rightarrow \infty$):

$$E_\theta^i + E_\theta^s = -\frac{e^{ikr}}{kr} k^2 \sin \theta \left[\exp(-ik\rho_0 \sin \theta \cos \phi) - \sum_{n=0}^{\infty} \epsilon_n (-i)^n \frac{J_n(ka \sin \theta)}{H_n^{(1)}(ka \sin \theta)} H_n^{(1)}(k\rho_0 \sin \theta) \cos n\phi \right], \quad (2.117)$$

$$E_\phi^i + E_\phi^s = 0, \quad (2.118)$$

where the spherical polar coordinates (r, θ, ϕ) are shown in Fig. 2.1. A quantity proportional to the amplitude of the summation in eq. (2.117) has been plotted as a function of ϕ and for $\theta = \frac{1}{2}\pi$ by LUCKE [1951] for $ka = 0.5$ and $k\rho_0 = 1.5$, by CARTER [1943] for $\rho_0 = 0.24\lambda$ with $a/\lambda = 0.0016, 0.16, 0.24, 0.318, 0.8$, and $\rho_0 = 0.878\lambda$ with $a/\lambda = 0.383$, and by OBERHETTINGER [1943] for $a = \lambda$ and $\rho_0/\lambda = \frac{5}{4}, \frac{3}{2}, \frac{7}{4}, 2$.

If the longitudinal dipole is on the surface ($\rho_0 = a$), the field is identically zero everywhere.

For a circumferential dipole at ($\rho_0, \phi_c = 0, z_0 = 0$) with moment $(4\pi\epsilon/k)\hat{y}$, the far field ($\rho \rightarrow \infty$) in the plane $z = 0$ is:

$$E_\phi^i + E_\phi^s = -k^2 \frac{e^{ik\rho}}{k\rho} \left[\cos \phi \exp(-ik\rho_0 \cos \phi) - \sum_{n=0}^{\infty} \epsilon_n (-i)^{n-1} \frac{J'_n(ka)}{H_n^{(1)'}(ka)} H_n^{(1)'}(k\rho_0) \cos n\phi \right], \quad (2.119)$$

$$E_z^i + E_z^s = 0. \quad (2.120)$$

If the circumferential dipole is on the surface ($\rho_0 = a$), the field is identically zero everywhere. CARTER [1943] has plotted a quantity proportional to the amplitude of the far field of eq. (2.119) as a function of ϕ , for $a = 0.16\lambda$ and $\rho_0 = 0.24\lambda$.

For a radial dipole at ($\rho_0, \phi_0 = 0, z_0 = 0$) with moment $(4\pi\epsilon/k)\hat{x}$, the far field ($\rho \rightarrow \infty$) in the plane $z = 0$ is:

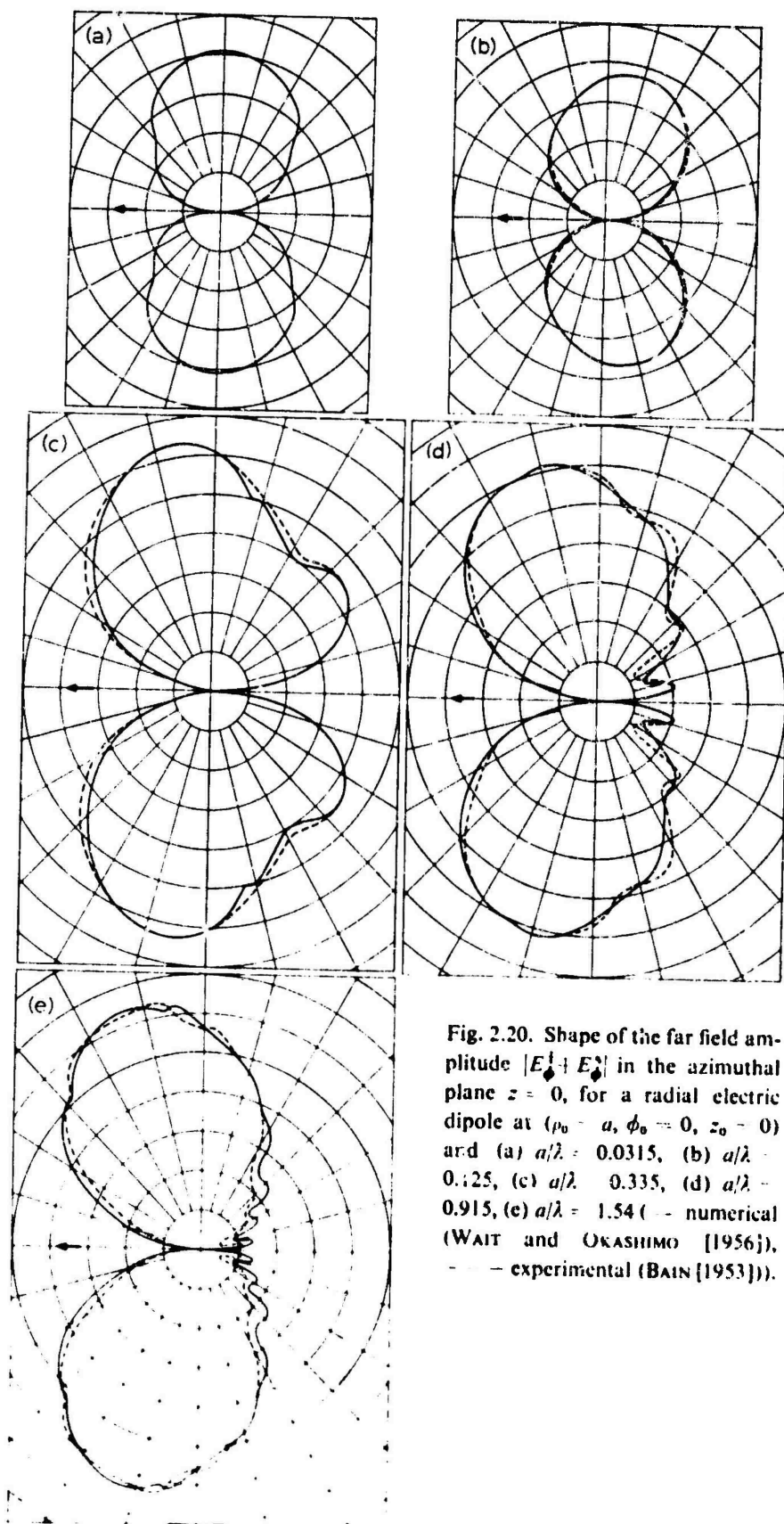
$$E_z^i + E_z^s = 0, \quad (2.121)$$

$$E_\phi^i + E_\phi^s = -k^2 \frac{e^{ik\rho}}{k\rho} \left[\sin \phi \exp(-ik\rho_0 \cos \phi) - 2 \sum_{n=1}^{\infty} (-i)^{n-1} \frac{J'_n(ka)}{H_n^{(1)'}(ka)} \frac{n}{k\rho_0} H_n^{(1)'}(k\rho_0) \sin n\phi \right], \quad (2.122)$$

and, in particular, if the dipole is on the surface ($\rho_0 = a$):

$$E_\phi^i + E_\phi^s = -\frac{4}{\pi a^2} \frac{e^{ik\rho}}{k\rho} \sum_{n=1}^{\infty} \frac{n(-i)^n}{H_n^{(1)'}(ka)} \sin n\phi \quad (2.123)$$

WAIT and OKASHIMO [1956] have computed a quantity proportional to the amplitude of the far field of eq. (2.123) as a function of ϕ for five values of ka , and have compared it with the experimental values of BAIN [1953]; these results are shown in Fig. 2.20.



LEVIS [1959] has published numerical tables of the real part, imaginary part and amplitude of the two components of the far electric field as functions of θ and ϕ for the case of a radial dipole on the surface of the cylinder and for $a/\lambda = 0.05(0.05) 0.50$; some of his results have been plotted for comparison with experimental data (LEVIS [1959; 1960]).

The far field in the plane $z = 0$ due to an arbitrarily oriented electric dipole at $(\rho_0, \phi_0 = 0, z_0 = 0)$ can be easily derived from eqs. (2.117) to (2.122).

2.4.1.2. LOW FREQUENCY APPROXIMATIONS

No specific results are available; however, low frequency approximations for the far field can be easily derived from the exact results of the preceding section.

2.4.1.3. HIGH FREQUENCY APPROXIMATIONS

No specific results are available.

2.4.2. Magnetic dipoles

2.4.2.1. EXACT SOLUTIONS

For an arbitrarily oriented magnetic dipole located at $\mathbf{r}_0 \equiv (\rho_0 \geq a, \phi_0, z_0)$ with moment $(4\pi/k)\hat{\mathbf{c}}$, the total magnetic field is:

$$\mathbf{H}^i(\mathbf{r}) + \mathbf{H}^s(\mathbf{r}) = 4\pi k \mathcal{G}_m(\mathbf{r}|\mathbf{r}_0) \cdot \hat{\mathbf{c}}, \quad (2.124)$$

where $\mathcal{G}_m(\mathbf{r}|\mathbf{r}_0)$ is the magnetic dyadic Green's function for the circular cylinder, which is related to the electric dyadic Green's function of eqs. (2.108) and (2.109) by (TAI [1954]):

$$\mathcal{G}_m(\mathbf{r}|\mathbf{r}_0) = \frac{1}{k^2} \nabla \wedge \{ [\nabla_0 \wedge \mathcal{G}_e(\mathbf{r}_0|\mathbf{r})]^T \}; \quad (2.125)$$

here $\nabla_0 \wedge$ operates on \mathbf{r}_0 , and T indicates the transposed matrix.

For a longitudinal magnetic dipole at $(\rho_0, \phi_0 = 0, z_0 = 0)$ with moment $(4\pi/k)\hat{\mathbf{z}}$, corresponding to an incident magnetic Hertz vector $(e^{ikR}/kR)\hat{\mathbf{z}}$, such that (EINARSSON et al. [1966]):

$$\begin{aligned} H_\rho^i &= -k^2 \frac{e^{ikR}}{kR} \left(1 + \frac{3i}{kR} - \frac{3}{k^2 R^2} \right) \frac{z(\rho - \rho_0 \cos \phi)}{R^2}, \\ H_\phi^i &= -k^2 \frac{e^{ikR}}{kR} \left(1 + \frac{3i}{kR} - \frac{3}{k^2 R^2} \right) \frac{z\rho_0 \sin \phi}{R^2}, \\ H_z^i &= k^2 \frac{e^{ikR}}{kR} \left[\frac{\rho^2}{R^2} \left(1 + \frac{\rho_0^2}{\rho^2} - 2 \frac{\rho_0}{\rho} \cos \phi \right) + \frac{i}{kR} \left(1 + \frac{i}{kR} \right) \left(1 - \frac{3z^2}{R^2} \right) \right], \\ E_\rho^i &= -k^2 Z \frac{e^{ikR}}{kR} \left(1 + \frac{i}{kR} \right) \frac{\rho_0 \sin \phi}{R}, \\ E_\phi^i &= k^2 Z \frac{e^{ikR}}{kR} \left(1 + \frac{i}{kR} \right) \frac{\rho - \rho_0 \cos \phi}{R}, \\ E_z^i &= 0, \end{aligned} \quad (2.126)$$

the total electromagnetic field components can be derived from the total magnetic Hertz vector (WAIT [1959])

$$\begin{aligned} \Pi_m = \Pi_m \hat{z} = \hat{z} \frac{i}{2k} \sum_{n=0}^{\infty} \epsilon_n \cos(n\phi) \int_{-\infty}^{\infty} H_n^{(1)}(\rho > \sqrt{(k^2 - t^2)}) \\ \times \left[J_n(\rho < \sqrt{(k^2 - t^2)}) - \frac{J'_n(a\sqrt{(k^2 - t^2)})}{H_n^{(1)'}(a\sqrt{(k^2 - t^2)})} H_n^{(1)}(\rho < \sqrt{(k^2 - t^2)}) \right] e^{itz} dt \end{aligned} \quad (2.127)$$

by the relations:

$$\begin{aligned} H_\rho = \frac{\partial^2 \Pi_m}{\partial \rho \partial z}, \quad H_\phi = \frac{1}{\rho} \frac{\partial^2 \Pi_m}{\partial \phi \partial z}, \quad H_z = \left(\frac{\partial^2}{\partial z^2} + k^2 \right) \Pi_m, \\ E_\rho = \frac{ikZ}{\rho} \frac{\partial \Pi_m}{\partial \phi}, \quad E_\phi = -ikZ \frac{\partial \Pi_m}{\partial \rho}, \quad E_z = 0. \end{aligned} \quad (2.128)$$

On the surface $\rho = a$:

$$H_\phi^i + H_\phi^s = -\frac{2i}{\pi ka^2} \sum_{n=1}^{\infty} n \sin(n\phi) \int_{-\infty}^{\infty} \frac{H_n^{(1)}(\rho_0 \sqrt{(k^2 - t^2)})}{H_n^{(1)'}(a\sqrt{(k^2 - t^2)})} \frac{te^{itz}}{\sqrt{(k^2 - t^2)}} dt, \quad (2.129)$$

$$H_z^i + H_z^s = -\frac{1}{\pi ka} \sum_{n=0}^{\infty} \epsilon_n \cos(n\phi) \int_{-\infty}^{\infty} \frac{H_n^{(1)}(\rho_0 \sqrt{(k^2 - t^2)})}{H_n^{(1)'}(a\sqrt{(k^2 - t^2)})} \sqrt{(k^2 - t^2)} e^{itz} dt. \quad (2.130)$$

in the far field ($\rho \rightarrow \infty$):

$$\begin{aligned} E_\phi^i + E_\phi^s = \frac{e^{ikr}}{kr} k^2 Z \sin \theta \left[\exp(-ik\rho_0 \sin \theta \cos \phi) - \right. \\ \left. - \sum_{n=0}^{\infty} \epsilon_n (-i)^n \frac{J'_n(ka \sin \theta)}{H_n^{(1)'}(ka \sin \theta)} H_n^{(1)}(k\rho_0 \sin \theta) \cos n\phi \right]. \end{aligned} \quad (2.131)$$

If the longitudinal dipole is on the surface ($\rho_0 = a$):

$$\Pi_m = -\frac{1}{\pi ka} \sum_{n=0}^{\infty} \epsilon_n \cos(n\phi) \int_{-\infty}^{\infty} \frac{H_n^{(1)}(\rho \sqrt{(k^2 - t^2)})}{H_n^{(1)'}(a\sqrt{(k^2 - t^2)})} \frac{e^{itz}}{\sqrt{(k^2 - t^2)}} dt, \quad (2.132)$$

and, in particular, in the far field ($\rho \rightarrow \infty$):

$$E_\phi^i + E_\phi^s = \frac{e^{ikr}}{kr} \frac{2ik^2 Z}{\pi ka} \sum_{n=0}^{\infty} \epsilon_n \frac{(-i)^n}{H_n^{(1)'}(ka \sin \theta)} \cos n\phi. \quad (2.133)$$

A longitudinal magnetic dipole at $\rho_0 = a$ is equivalent to a narrow axial slot (see, for example, WAIT [1959]).

Apart from the general formulation of eq. (2.124), no specific results are available for circumferential and radial magnetic dipoles.

2.4.2.2. LOW FREQUENCY APPROXIMATIONS

No specific results are available; however, low frequency approximations for the far field can be easily derived from the exact results of the preceding section.

2.4.2.3. HIGH FREQUENCY APPROXIMATIONS

No specific results are available.

2.5. Point sources

2.5.1. Acoustically soft cylinder

2.5.1.1. EXACT SOLUTIONS

For a point source at $(\rho_0, \phi_0 = 0, z_0 = 0)$, such that

$$V^i = \frac{e^{ikR}}{kR}, \quad (2.134)$$

then

$$V^i + V^s = \frac{i}{2k} \sum_{n=0}^{\infty} \varepsilon_n \cos(n\phi) \int_{-\infty}^{\infty} \left[J_n(\rho < \sqrt{(k^2 - t^2)}) - \frac{J_n(a\sqrt{(k^2 - t^2)})}{H_n^{(1)}(a\sqrt{(k^2 - t^2)})} H_n^{(1)}(\rho < \sqrt{(k^2 - t^2)}) \right] H_n^{(1)}(\rho > \sqrt{(k^2 - t^2)}) e^{itz} dt. \quad (2.135)$$

On the surface $\rho = a$:

$$\frac{\partial}{\partial \rho} (V^i + V^s) = \frac{1}{\pi k a} \sum_{n=0}^{\infty} \varepsilon_n \cos(n\phi) \int_{-\infty}^{\infty} \frac{H_n^{(1)}(\rho_0 \sqrt{(k^2 - t^2)})}{H_n^{(1)}(a\sqrt{(k^2 - t^2)})} e^{itz} dt. \quad (2.136)$$

In the far field ($\rho \rightarrow \infty$):

$$V^i + V^s = \frac{e^{ikr}}{kr} \left[\exp(-ik\rho_0 \sin \theta \cos \phi) - \sum_{n=0}^{\infty} \varepsilon_n (-i)^n \frac{J_n(ka \sin \theta)}{H_n^{(1)}(ka \sin \theta)} \times H_n^{(1)}(k\rho_0 \sin \theta) \cos n\phi \right], \quad (2.137)$$

where the spherical polar coordinates (r, θ, ϕ) are shown in Fig. 2.1. If the point source is on the surface ($\rho_0 = a$), the field is identically zero everywhere.

2.5.1.2. LOW FREQUENCY APPROXIMATIONS

No specific results are available; however, low frequency approximations for the far field can be easily derived from the exact result of eq. (2.137).

2.5.1.3. HIGH FREQUENCY APPROXIMATIONS

For a point source at $(\rho_0, \phi_0 = 0, z_0 = 0)$, such that

$$V^i = \frac{e^{ikR}}{kR}, \quad (2.138)$$

asymptotic evaluations of the exact solution are not available. The geometrical optics

scattered field at a point $(\rho, \phi < \pi, z)$ located in the illuminated region is:

$$V_{s.o.}^s = -\frac{1}{k} \left\{ (F^2 + z_1^2)(1 + \sqrt{G/F}) \left[1 + \frac{G}{F} + \frac{2G}{a \cos(\phi_1 + \alpha)} \right] \right\}^{-\frac{1}{2}} \times \exp \{ ik[\sqrt{(F^2 + z_1^2)} + \sqrt{\{G^2 + (z - z_1)^2\}}] \}, \quad (2.139)$$

where

$$\alpha = \arcsin \left(\frac{a}{F} \sin \phi_1 \right), \quad (2.140)$$

$$z_1 = z(1 + \sqrt{G/F})^{-1}, \quad (2.141)$$

$$F = (\rho_0^2 + a^2 - 2a\rho_0 \cos \phi_1)^{\frac{1}{2}}, \quad G = [\rho^2 + a^2 - 2a\rho \cos(\phi_1 - \phi)]^{\frac{1}{2}}, \quad (2.142)$$

and ϕ_1 is that root of

$$\frac{\rho_0}{F} \sin \phi_1 + \frac{\rho}{G} \sin(\phi_1 - \phi) = 0, \quad (2.143)$$

which is less than $\frac{1}{2}\pi$.

The geometrical optics field is zero in the shadowed region, i.e. at all points such that

$$|\psi| > \arccos \frac{a}{\rho_0}, \quad (2.144)$$

$$\rho < \rho_0 [\cos \psi + \sqrt{\{(\rho_0/a)^2 - 1\} \sin |\psi|}]^{-1}. \quad (2.145)$$

2.5.2. Acoustically hard cylinder

2.5.2.1. EXACT SOLUTIONS

For a point source at $(\rho_0, \phi_0 = 0, z_0 = 0)$, such that

$$V^i = \frac{e^{ikR}}{kR}, \quad (2.146)$$

then

$$V^i + V^s = \frac{i}{2k} \sum_{n=0}^{\infty} \varepsilon_n \cos(n\phi) \int_{-\infty}^{\infty} \left[J_n(\rho < \sqrt{(k^2 - t^2)}) - \frac{J'_n(a\sqrt{(k^2 - t^2)})}{H_n^{(1)}(a\sqrt{(k^2 - t^2)})} H_n^{(1)}(\rho < \sqrt{(k^2 - t^2)}) \right] H_n^{(1)}(\rho > \sqrt{(k^2 - t^2)}) e^{itz} dt. \quad (2.147)$$

On the surface $\rho = a$:

$$V^i + V^s = -\frac{1}{\pi k a} \sum_{n=0}^{\infty} \varepsilon_n \cos(n\phi) \int_{-\infty}^{\infty} \frac{H_n^{(1)}(\rho_0 \sqrt{(k^2 - t^2)})}{H_n^{(1)}(a\sqrt{(k^2 - t^2)})} \frac{e^{itz}}{\sqrt{(k^2 - t^2)}} dt. \quad (2.148)$$

In the far field ($\rho \rightarrow \infty$):

$$V^i + V^s = \frac{e^{ikr}}{kr} \left[\exp \{ -ik\rho_0 \sin \theta \cos \phi \} - \sum_{n=0}^{\infty} \varepsilon_n (-i)^n \frac{J'_n(ka \sin \theta)}{H_n^{(1)'}(ka \sin \theta)} H_n^{(1)}(k\rho_0 \sin \theta) \cos n\phi \right]. \quad (2.149)$$

If the point source is on the surface ($\rho_0 = a$):

$$V^i + V^s = -\frac{1}{\pi ka} \sum_{n=0}^{\infty} \varepsilon_n \cos(n\phi) \int_{-\infty}^{\infty} \frac{H_n^{(1)}(\rho\sqrt{(k^2 - t^2)})}{H_n^{(1)'}(a\sqrt{(k^2 - t^2)})} \frac{e^{itz}}{\sqrt{(k^2 - t^2)}} dt, \quad (2.150)$$

and, in particular, in the far field ($\rho \rightarrow \infty$):

$$V^i + V^s = \frac{e^{ikr}}{kr} \frac{2i}{\pi ka \sin \theta} \sum_{n=0}^{\infty} \varepsilon_n \frac{(-i)^n}{H_n^{(1)'}(ka \sin \theta)} \cos n\phi. \quad (2.151)$$

2.5.2.2. LOW FREQUENCY APPROXIMATIONS

No specific results are available; however, low frequency approximations for the far field can be easily derived from the exact results of eqs. (2.149) and (2.151).

2.5.2.3. HIGH FREQUENCY APPROXIMATIONS

For a point source at ($\rho_0, \phi_0 = 0, z_0 = 0$), such that

$$V^i = \frac{e^{ikR}}{kR}, \quad (2.152)$$

asymptotic evaluations of the exact solution are not available.

The geometrical optics scattered field at a point ($\rho, \phi < \pi, z$) located in the illuminated region is:

$$V_{g.o.}^s = \frac{1}{k} \left\{ (F^2 + z_1^2) (1 + \sqrt{G/F}) \left[1 + \frac{G}{F} + \frac{2G}{a \cos(\phi_1 + \alpha)} \right] \right\}^{-\frac{1}{2}} \times \exp \{ ik[\sqrt{(F^2 + z_1^2)} + \sqrt{G^2 + (z - z_1)^2}] \}, \quad (2.153)$$

where α, z_1, F, G and ϕ_1 are given by eqs. (2.140) to (2.143). The geometrical optics field is zero in the shadowed region, i.e. at all points for which the inequalities (2.144) and (2.145) are satisfied.

Bibliography

- ADEY, A. W. [1958], Scattering of Electromagnetic Waves by Long Cylinders, *Electron. and Radio Eng.* **35**, 149-158.
- BAIN, J. D. [1953], Radiation Pattern Measurements of Stub and Slot Antennas on Spheres and Cylinders, Stanford Research Institute Technical Report No. 42, Stanford, California.
- CARTER, P. S. [1943], Antenna Arrays Around Cylinders, *Proc. IRE* **31**, 671-693. The formulae have numerous errors.
- EINARSSON, O., R. E. KLEINMAN, P. LAURIN and P. L. E. USLENGHI [1966], Studies in Radar Cross Sections I. Diffraction and Scattering by Regular Bodies IV: The Circular Cylinder, The

- University of Michigan Radiation Laboratory Report 7133-3-T, Ann Arbor, Michigan.
- FARAN, J. J. [1953], Scattering of Cylindrical Waves by a Cylinder, *J. Acoust. Soc. Am.* **25**, 155-156.
- The diagram for $k\rho_0 = 6.8$ is incorrect (see ZITRON and DAVIS [1963]).
- FRANZ, W. [1954], Über die Greensche Funktionen des Zylinders und der Kugel, *Z. Naturforsch.* **9a**, 705-716.
- FRANZ, W. and R. GALLI [1955], Semiasymptotische Reihen für die Beugung einer ebenen Welle an Zylinder, *Z. Naturforsch.* **10a**, 374-378. Formula (17a) has an error in the denominator of \tilde{O}_1 , where the factor 3×6 should be replaced by $3\sqrt{6}$.
- GORIAINOV, A. S. [1958], An Asymptotic Solution of the Problem of Diffraction of a Plane Electromagnetic Wave by a Conducting Cylinder, *Radio Eng. Electron. (USSR)* **3**, 23-39 (English transl. of *Radiotekhn. i Elektron.* **3**). The sign of the right-hand side of formulae (4) and (5) is incorrect, a misprint appears in the first equation of (32), and the diagram of $\tilde{g}(\zeta)$ in Fig. 3 has a phase error of 180° .
- HASSERJIAN, G. and A. ISHIMARU [1962], Currents induced on the Surface of a Conducting Circular Cylinder by a Slot, *J. Res. Nat. Bur. St. D* **66**, 335-365.
- KELLER, J. B., R. M. LEWIS and B. D. SECKLER [1956], Asymptotic Solution of Some Diffraction Problems, *Comm. Pure Appl. Math.* **9**, 207-265.
- KING, R. W. P. and T. T. WU [1959], *The Scattering and Diffraction of Waves*, Harvard University Press, Cambridge, Massachusetts.
- KODIS, R. D. [1952], Diffraction Measurements at 1.25 Centimeters, *J. Appl. Phys.* **23**, 249-255.
- LEVIS, C. A. [1959], Patterns of a Radial Dipole on an Infinite Circular Cylinder: Numerical Values, Ohio State University Antenna Laboratory Report 667-51, Columbus, Ohio.
- LEVIS, C. A. [1960], Patterns of a Radial Dipole on an Infinite Circular Cylinder: Numerical Values, *IRE Trans. AP-8*, 218-222.
- LUCKE, W. S. [1951], Electric Dipoles in the Presence of Elliptic and Circular Cylinders, *J. Appl. Phys.* **22**, 15-19.
- NOBLE, B. [1962], Integral Equation Perturbation Methods in Low-Frequency Diffraction, in: *Electromagnetic Waves*, ed. R. E. Langer, 323-360, University of Wisconsin Press, Madison, Wisconsin.
- OBERHETTINGER, F. [1943], Über ein Randwertproblem der Wellengleichung in Zylinderkoordinaten, *Ann. Physik* **43**, 136-160.
- SENSIPER, S. [1957], Cylindrical Radio Waves, *IRE Trans. AP-5*, 56-70.
- SHENDEROV, E. L. [1961], Diffraction of a Cylindrical Sound Wave by a Cylinder, *Soviet Phys. Acoust.* **7**, 293-296 (English transl. of *Akust. Zh.* **7**).
- STRUTT, J. W., Lord Rayleigh [1897], On the Incidence of Aerial and Electric Waves Upon Small Obstacles in the Form of Ellipsoids or Elliptic Cylinders, and on the Passage of Electric Waves through a Circular Aperture in a Conducting Screen, *Phil. Mag.* **44**, 28-52.
- STRUTT, J. W., Lord Rayleigh [1907], On the Light Dispersed from Fine Lines Ruled upon Reflecting Surfaces or Transmitted by Very Narrow Slits, *Phil. Mag.* **14**, 350-359.
- TAI, C. T. [1954], A Glossary of Dyadic Green's Functions, Stanford Research Institute Technical Report 46, Stanford, California. Formula (16) is misprinted.
- VAN BLADEL, J. [1963], Low-Frequency Scattering by Cylindrical Bodies, *Appl. Sci. Res. B10*, 195-202.
- WAIT, J. R. [1959], *Electromagnetic Radiation from Cylindrical Structures*, Pergamon Press, New York. The right-hand side of formula (62) has the wrong sign.
- WAIT, J. R. and K. OKASHIMO [1956], Patterns of Stub Antennas on Cylindrical Structures, *Can. J. Phys.* **34**, 190-202.
- WU, T. T. [1956], High-Frequency Scattering, *Phys. Rev.* **104**, 1201-1212.
- ZITRON, N. and J. DAVIS [1963], A Numerical Investigation of Scattering of Radiation for an Asymmetric Source by Circular Cylinder, Mathematics Research Center Technical Summary Report 365, University of Wisconsin, Madison, Wisconsin. [See also *Can. J. Phys.* **44**, 2941-2944.]

CHAPTER 3

THE ELLIPTIC CYLINDER

P. L. E. USLENGHI and N. R. ZITRON

The elliptic cylinder is the most general scatterer of bounded cross section for which the exterior boundary-value problem for the two-dimensional wave equation can be solved by separation of variables.

The fat elliptic cylinder is an obvious generalization of the circular cylinder, whereas the thin elliptic cylinder may be used as a model for the strip. In general, the elliptic cylinder is a means for testing approximation techniques applicable to convex cylinders with variable curvature.

3.1. Elliptic cylinder geometry

The elliptic cylindrical coordinates (u, v, z) shown in Fig. 3.1 are related to the rectangular Cartesian coordinates (x, y, z) by the transformation

$$\begin{aligned} x &= \frac{1}{2}d \cosh u \cos v, \\ y &= \frac{1}{2}d \sinh u \sin v, \\ z &= z, \end{aligned} \tag{3.1}$$

where $0 \leq u < \infty$, $0 \leq v < 2\pi$, and $-\infty < z < \infty$. Instead of u and v , it is often convenient to use the quantities

$$\xi = \cosh u, \quad \eta = \cos v, \tag{3.2}$$

with $1 \leq \xi < \infty$ and $-1 \leq \eta \leq 1$. The (x, z) and (y, z) planes are planes of symmetry and the surfaces $\xi = \text{constant}$, $|\eta| = \text{constant}$ and $z = \text{constant}$ are respectively confocal elliptic cylinders of interfocal distance d , eccentricity ξ^{-1} , major axis $d\xi$ and minor axis $d\sqrt{(\xi^2 - 1)}$; confocal hyperbolic cylinders of two sheets with interfocal distance d , and planes perpendicular to the z axis.

The scattering body is the elliptic cylinder with surface $u = u_1$, and the primary source is a plane wave whose direction of propagation is perpendicular to the axis z of the cylinder and forms the angle ϕ_0 with the negative x axis, or a line source parallel to the z axis and located at $(u_0 \geq u_1, v_0)$, or a point or dipole source located at $(u_0 \geq u_1, v_0, z_0)$. Unless otherwise stated, it is assumed that the coordinates x_0 and y_0 of the source are non-negative; thus, in the case of plane wave incidence one has that $0 \leq \phi_0 \leq \frac{1}{2}\pi$. The ratio between major and minor axes of the elliptical cross section of the scatterer in a plane $z = \text{constant}$ is equal to $\xi_1/\sqrt{(\xi_1^2 - 1)}$; values of

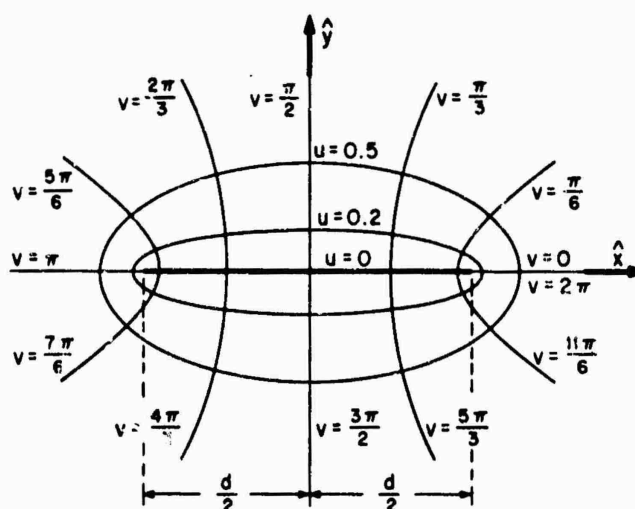


Fig. 3.1. Elliptic cylindrical geometry.

$\xi_1 = \cosh u_1$ corresponding to a few typical ratios are tabulated in the following:

major axis minor axis	100:1	10:1	5:1	2:1
ξ_1	1.000 050 0	1.005 037 8	1.020 620 7	1.154 700 5

The definitions and notation for the Mathieu functions are those of STRATTON [1941]. Thus, the even and odd radial functions of the first, second and third kinds are indicated by $Re_m^{(j)}(c, \xi)$, where $j = 1, 2$ and 3 respectively, whereas the symbols

$Se_m(c, \eta)$ are used for the angular functions; $m \geq 0$ is an integer, and $So_0(c, \eta) = 0$,

so that all the terms in the summations over m of the following sections which contain functions So_m are to be taken equal to zero for $m = 0$. The parameter c is the product of wave number and semi-focal distance: $c = \frac{1}{2}kd$. The quantities $N_m^{(e), (o)}$ which appear in the following sections are functions of m and c , and are defined by STRATTON [1941]. Numerical tables for Mathieu functions and related quantities with notations which at least partially agree with that adopted in this chapter are given by STRATTON et al. [1941], WILTSE and KING [1958a, b] and the National Bureau of Standards (1951). A list of numerical tables, and a comparison of notations used by different authors, are given by BLANCH [1964]. Recent results on asymptotic expansions are found, for example, in DINGLE and MÜLLER [1962], in MÜLLER [1962] and in SHARPLES [1967].

Although no precise information on the rapidity of convergence of the infinite eigenfunction series representing the exact solutions seems to be available, it is probable that the series converge at least as rapidly as the corresponding eigenfunction series for a circular cylinder of diameter $d\xi_1$.

3.2. Plane wave incidence

3.2.1. E-Polarization

3.2.1.1. EXACT SOLUTIONS

For a plane wave whose direction of propagation is perpendicular to the z -axis, and forms the angle ϕ_0 with the negative x -axis and the angle $(\frac{1}{2}\pi - \phi_0)$ with the negative y -axis ($0 \leq \phi_0 \leq \frac{1}{2}\pi$), such that

$$\begin{aligned} E^i &= \hat{z} \exp \{-ik(x \cos \phi_0 + y \sin \phi_0)\}, \\ H^i &= Y(-\sin \phi_0 \hat{x} + \cos \phi_0 \hat{y}) \exp \{-ik(x \cos \phi_0 + y \sin \phi_0)\}, \end{aligned} \quad (3.3)$$

then

$$\begin{aligned} E_z^s &= -\sqrt{8\pi} \sum_{m=0}^{\infty} (-i)^m \left[\frac{1}{N_m^{(e)}} \frac{Re_m^{(1)}(c, \xi_1)}{Re_m^{(3)}(c, \xi_1)} Re_m^{(3)}(c, \xi) Se_m(c, \cos \phi_0) Se_m(c, \eta) + \right. \\ &\quad \left. + \frac{1}{N_m^{(o)}} \frac{Ro_m^{(1)}(c, \xi_1)}{Ro_m^{(3)}(c, \xi_1)} Ro_m^{(3)}(c, \xi) So_m(c, \cos \phi_0) So_m(c, \eta) \right]. \end{aligned} \quad (3.4)$$

On the surface $\xi = \xi_1$:

$$\begin{aligned} H_v &= \frac{Y}{c} \sqrt{\frac{8\pi}{\xi_1^2 - \eta^2}} \sum_{m=0}^{\infty} (-i)^m \left[\frac{1}{N_m^{(e)} Re_m^{(3)}(c, \xi_1)} Se_m(c, \cos \phi_0) Se_m(c, \eta) + \right. \\ &\quad \left. + \frac{1}{N_m^{(o)} Ro_m^{(3)}(c, \xi_1)} So_m(c, \cos \phi_0) So_m(c, \eta) \right]. \end{aligned} \quad (3.5)$$

In the far field ($\xi \rightarrow \infty$):

$$\begin{aligned} P &= -2\pi \sum_{m=0}^{\infty} (-1)^m \left[\frac{1}{N_m^{(e)}} \frac{Re_m^{(1)}(c, \xi_1)}{Re_m^{(3)}(c, \xi_1)} Se_m(c, \cos \phi_0) Se_m(c, \eta) + \right. \\ &\quad \left. + \frac{1}{N_m^{(o)}} \frac{Ro_m^{(1)}(c, \xi_1)}{Ro_m^{(3)}(c, \xi_1)} So_m(c, \cos \phi_0) So_m(c, \eta) \right]. \end{aligned} \quad (3.6)$$

The total scattering cross section per unit length is:

$$\begin{aligned} \sigma_T &= \frac{8\pi}{k} \sum_{m=0}^{\infty} \left[\frac{1}{N_m^{(e)}} \frac{Re_m^{(1)}(c, \xi_1)}{Re_m^{(3)}(c, \xi_1)} Se_m(c, \cos \phi_0) \right]^2 + \\ &\quad + \frac{1}{N_m^{(o)}} \frac{Ro_m^{(1)}(c, \xi_1)}{Ro_m^{(3)}(c, \xi_1)} So_m(c, \cos \phi_0) \right]^2. \end{aligned} \quad (3.7)$$

For incidence along the major axis ($\phi_0 = 0$):

$$E_z^s = -\sqrt{8\pi} \sum_{m=0}^{\infty} \frac{(-i)^m}{N_m^{(e)}} \frac{Re_m^{(1)}(c, \xi_1)}{Re_m^{(3)}(c, \xi_1)} Re_m^{(3)}(c, \xi) Se_m(c, \eta). \quad (3.8)$$

On the surface $\xi = \xi_1$:

$$H_v = \frac{Y}{c} \sqrt{\frac{8\pi}{\xi_1^2 - \eta^2}} \sum_{m=0}^{\infty} \frac{(-i)^m}{N_m^{(e)}} \frac{1}{Re_m^{(3)}(c, \xi_1)} Se_m(c, \eta). \quad (3.9)$$

Amplitude and phase of the surface current density have been plotted by MANDRAZHI [1962] for $c = 2\sqrt{2}$ and axes ratio $\xi_1/\sqrt{(\xi_1^2-1)} = 6.7$. The normalized amplitude of H_v given by eq. (3.9) has been computed as a function of v by BARAKAT [1969] for $c = 1$ and four different values of ξ_1 , and is shown in Fig. 3.2.

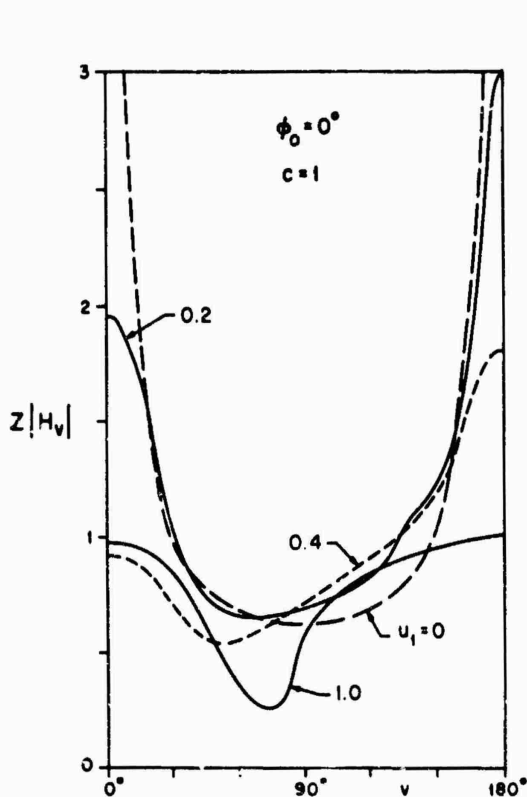


Fig. 3.2. Amplitude of surface field produced by a plane wave with E^i parallel to the cylinder axis; case $\phi_0 = 0$ (BARAKAT [1969]).

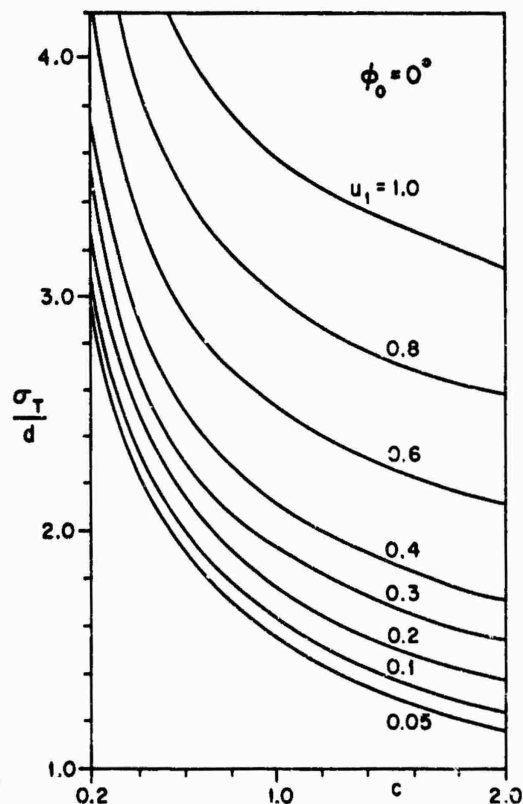


Fig. 3.3. Normalized total scattering cross section for E^i parallel to the cylinder axis and incidence along the major axis (BARAKAT [1963]).

In the far field ($\xi \rightarrow \infty$):

$$P = -2\pi \sum_{m=0}^{\infty} \frac{(-1)^m}{N_m^{(c)}} \frac{\text{Re}_m^{(1)}(c, \xi_1)}{\text{Re}_m^{(3)}(c, \xi_1)} S e_m(c, \eta). \quad (3.10)$$

The total scattering cross section per unit length is:

$$\sigma_T = \frac{8\pi}{k} \sum_{m=0}^{\infty} \frac{1}{N_m^{(c)}} \left| \frac{\text{Re}_m^{(1)}(c, \xi_1)}{\text{Re}_m^{(3)}(c, \xi_1)} \right|^2. \quad (3.11)$$

The normalized cross section σ_T/d has been computed as a function of c and for eight different values of ξ_1 by BARAKAT [1963], and is shown in Fig. 3.3.

For incidence along the minor axis ($\phi_0 = \frac{1}{2}\pi$):

$$E_z^s = -\sqrt{8\pi} \sum_{m=0}^{\infty} (-1)^m \left[\frac{Se_{2m}(c, 0)}{N_{2m}^{(e)}} \frac{Re_{2m}^{(1)}(c, \xi_1)}{Re_{2m}^{(3)}(c, \xi_1)} Re_{2m}^{(3)}(c, \xi) Se_{2m}(c, \eta) - \right. \\ \left. -i \frac{So_{2m+1}(c, 0)}{N_{2m+1}^{(o)}} \frac{Ro_{2m+1}^{(1)}(c, \xi_1)}{Ro_{2m+1}^{(3)}(c, \xi_1)} Ro_{2m+1}^{(3)}(c, \xi) So_{2m+1}(c, \eta) \right]. \quad (3.12)$$

On the surface $\xi = \xi_1$:

$$H_v = \frac{Y}{c} \sqrt{\frac{8\pi}{\xi_1^2 - \eta^2}} \sum_{m=0}^{\infty} (-1)^m \left[\frac{Se_{2m}(c, 0)}{N_{2m}^{(e)}} \frac{1}{Re_{2m}^{(3)}(c, \xi_1)} Se_{2m}(c, \eta) - \right. \\ \left. -i \frac{So_{2m+1}(c, 0)}{N_{2m+1}^{(o)}} \frac{1}{Ro_{2m+1}^{(3)}(c, \xi_1)} So_{2m+1}(c, \eta) \right]. \quad (3.13)$$

For axes ratio $\xi_1/\sqrt{(\xi_1^2 - 1)} = 6.7$, MANDRAZHI [1962] has plotted the amplitude of the surface current density for $c = \frac{4}{3}$, and the phase for $c = 2\sqrt{2}$; 2; $\sqrt{2}$; $\frac{4}{3}$. The normalized amplitude of H_v given by eq. (3.13) has been computed as a function of v by BARAKAT [1969] for $c = 1$ and four different values of ξ_1 , and is shown in Fig. 3.4.

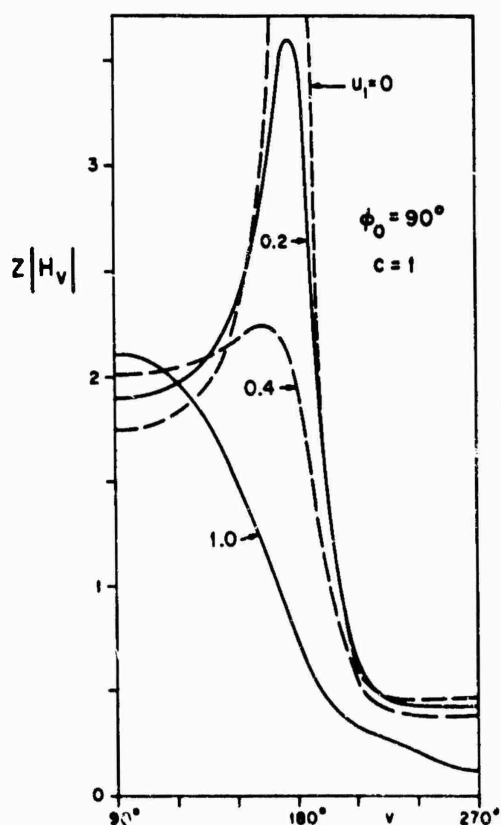


Fig. 3.4. Amplitude of surface field produced by a plane wave with E^i parallel to the cylinder axis; case $\phi_0 = \frac{1}{2}\pi$ (BARAKAT [1969]).

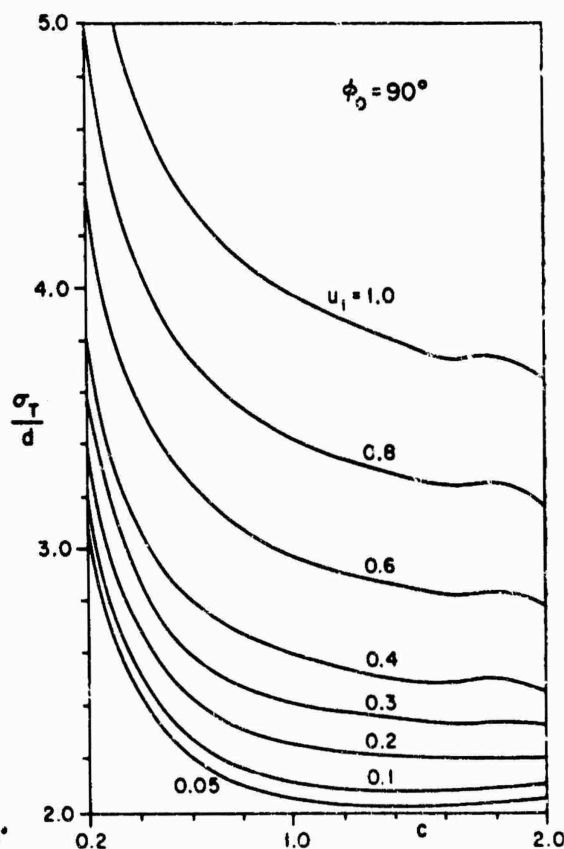


Fig. 3.5. Normalized total scattering cross section for E^i parallel to the cylinder axis and incidence along the minor axis (BARAKAT [1963]).

In the far field ($\xi \rightarrow \infty$):

$$P = -2\pi \sum_{m=0}^{\infty} \left[\frac{Se_{2m}(c, 0)}{N_{2m}^{(e)}} \frac{Re_{2m}^{(1)}(c, \xi_1)}{Re_{2m}^{(3)}(c, \xi_1)} Se_{2m}(c, \eta) - \frac{So_{2m+1}(c, 0)}{N_{2m+1}^{(o)}} \frac{Ro_{2m+1}^{(1)}(c, \xi_1)}{Ro_{2m+1}^{(3)}(c, \xi_1)} So_{2m+1}(c, \eta) \right]. \quad (3.14)$$

The total scattering cross section per unit length is:

$$\sigma_T = \frac{8\pi}{k} \sum_{m=0}^{\infty} \left[\frac{1}{N_{2m}^{(e)}} \left| \frac{Re_{2m}^{(1)}(c, \xi_1)}{Re_{2m}^{(3)}(c, \xi_1)} Se_{2m}(c, 0) \right|^2 + \frac{1}{N_{2m+1}^{(o)}} \left| \frac{Ro_{2m+1}^{(1)}(c, \xi_1)}{Ro_{2m+1}^{(3)}(c, \xi_1)} So_{2m+1}(c, 0) \right|^2 \right]. \quad (3.15)$$

The normalized cross section σ_T/d has been computed as a function of c and for eight different values of ξ_1 by BARAKAT [1963], and is shown in Fig. 3.5.

3.2.1.2. LOW FREQUENCY APPROXIMATIONS

For a plane wave whose direction of propagation is perpendicular to the z -axis, and forms the angle ϕ_0 with the negative x -axis and the angle $(\frac{1}{2}\pi - \phi_0)$ with the negative y -axis ($0 \leq \phi_0 \leq \frac{1}{2}\pi$), such that

$$\begin{aligned} E^i &= \hat{z} \exp \{-ik(x \cos \phi_0 + y \sin \phi_0)\}, \\ H^i &= Y(-\sin \phi_0 \hat{x} + \cos \phi_0 \hat{y}) \exp \{-ik(x \cos \phi_0 + y \sin \phi_0)\}, \end{aligned} \quad (3.16)$$

low frequency expansions may be obtained either directly (STRUTT [1897]; NOBLE [1962]; VAN BLADEL [1963]) or by power series developments of the Mathieu functions appearing in the exact solutions (BURKE and TWERSKY [1964]; BURKE et al. [1964]).

In the far field ($\xi \rightarrow \infty$; $v = \phi$) and through $O(c^2)$ (BURKE and TWERSKY [1964]):

$$\begin{aligned} P \sim D \left(-1 + \frac{2iL}{\pi} \right) + (\frac{1}{2}c\xi_1)^2 \left\{ \left[\frac{4\sqrt{(\xi_1^2 - 1)}}{\xi_1 L} (1 - D) + \xi_1^{-2} (\cos 2\phi + \cos 2\phi_0) \right] \frac{1}{2}D - \right. \\ \left. - i \left[\frac{2D}{\pi \xi_1} (1 - 2D) \sqrt{(\xi_1^2 - 1)} + \frac{LD}{\pi \xi_1^2} (\cos 2\phi + \cos 2\phi_0) - \right. \right. \\ \left. \left. - \pi(1 + \xi_1^{-1} \sqrt{(\xi_1^2 - 1)}) (\cos \phi \cos \phi_0 + \xi_1^{-1} \sqrt{\xi_1^2 - 1} \sin \phi \sin \phi_0) \right] \right\}. \end{aligned} \quad (3.17)$$

where

$$D = \left(1 + \frac{4L^2}{\pi^2} \right)^{-1}, \quad (3.18)$$

$$L = \gamma + \log [\frac{1}{2}c(\xi_1 + \sqrt{(\xi_1^2 - 1)})], \quad (3.19)$$

and $\gamma = 0.5772157 \dots$ is Euler's constant. BURKE and TWERSKY [1964] have derived a closed form for P correct through $O(c^6)$, and have expanded it through $O(c^6)$ (BURKE and TWERSKY [1960]). The normalized bistatic cross section per unit length for

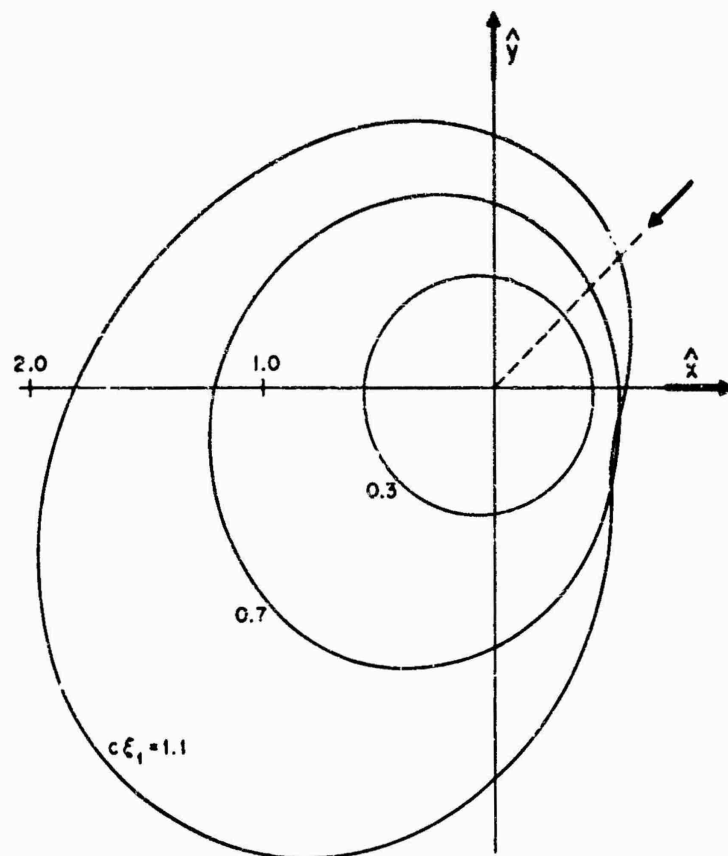


Fig. 3.6. Normalized bistatic cross section $\frac{1}{4}k\sigma(\phi)$ for E^I parallel to the cylinder axis with $\phi_0 = 45^\circ$ and axes ratio $\xi_1/\sqrt{(\xi_1^2-1)} = 2$ (BURKE and TWERSKY [1964]).

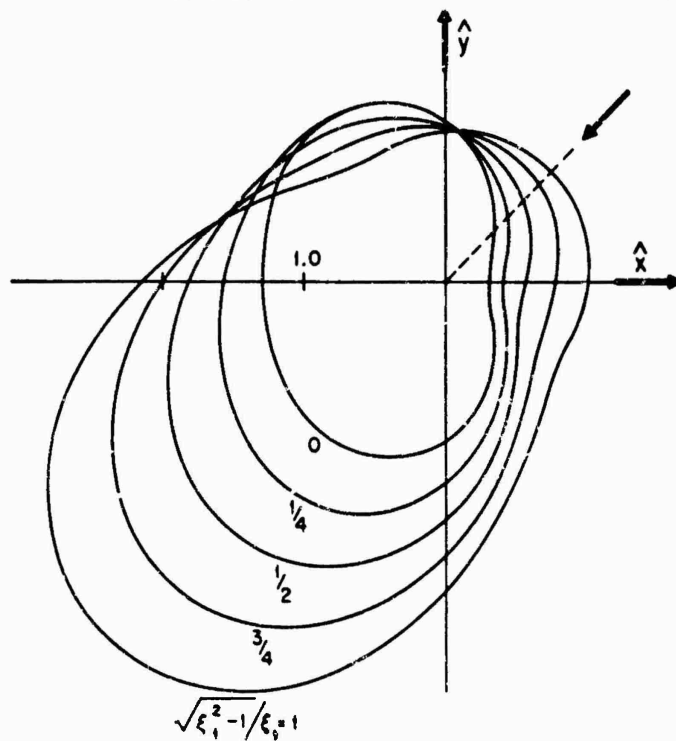


Fig. 3.7. Normalized bistatic cross section $\frac{1}{4}k\sigma(\phi)$ for E^I parallel to the cylinder axis with $\phi_0 = 45^\circ$ and $c\xi_1 = 1.1$ (BURKE and TWERSKY [1964]).

$\phi_0 = \frac{1}{2}\pi$ and different values of the axes ratio and of $c\xi_1$ is plotted as a function of ϕ in Figs. 3.6 and 3.7. BURKE et al. [1964] have plotted the normalized bistatic cross section per unit length $\frac{1}{4}k\sigma(\phi)$ as a function of ϕ for $\phi_0 = \frac{1}{2}\pi$; $c\xi_1 = 0.3, 0.7, 1.1$ and axes ratio $\sqrt{\xi_1^2 - 1}/\xi_1 = 0, \frac{1}{4}, \frac{1}{2}, \frac{3}{4}, 1$. The normalized back scattering cross section per unit length is shown in Fig. 3.8 as a function of ϕ_0 for $c\xi_1 = 1.1$ and in Fig. 3.9 as a function of $c\xi_1$ for $\phi_0 = \frac{1}{2}\pi$, for five different values of the axes ratio.

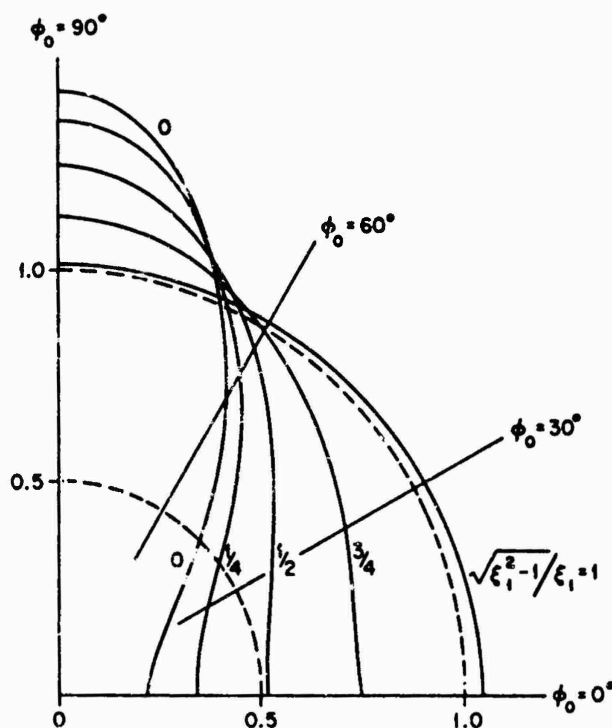


Fig. 3.8. Normalized back scattering cross section $\frac{1}{4}k\sigma$ for E^i parallel to the cylinder axis and $c\xi_1 = 1.1$ (BURKE and TWERSKY [1964]).

The total scattering cross section per unit length is

$$\sigma_T \sim \frac{4}{k} D \left\{ 1 - (\frac{1}{2}c\xi_1)^2 \left[\frac{2\sqrt{(\xi_1^2 - 1)}}{\xi_1 L} (1 - D) + \xi_1^{-2} \cos 2\phi_0 \right] \right\}. \quad (3.20)$$

The normalized total scattering cross section per unit length corresponding to the closed form derived by BURKE and TWERSKY [1964] is shown as a function of ϕ_0 for $c\xi_1 = 1.1$ and different values of the axes ratio in Fig. 3.10.

For incidence along the major axis ($\phi_0 = 0$), in the far field ($\xi \rightarrow \infty$; $v = \phi$) and through $O(c^2)$:

$$P \sim D \left(-1 + \frac{2iL}{\pi} \right) + (\frac{1}{2}c\xi_1)^2 \left\{ \left[\frac{4\sqrt{(\xi_1^2 - 1)}}{\xi_1 L} (1 - D) + \xi_1^{-2} (1 + \cos 2\phi) \right] \frac{1}{2} D - \right. \\ \left. - i \left[\frac{2D}{\pi\xi_1} (1 - 2D) \sqrt{(\xi_1^2 - 1)} + \frac{LD}{\pi\xi_1^2} (1 + \cos 2\phi) - \pi(1 + \xi_1^{-1} \sqrt{(\xi_1^2 - 1)}) \cos \phi \right] \right\}. \quad (3.21)$$

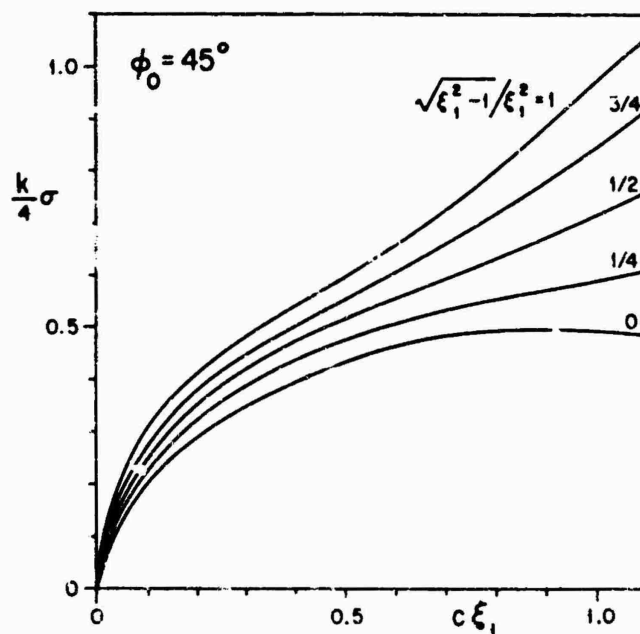


Fig. 3.9. Normalized back scattering cross section for E^i parallel to the cylinder axis (BURKE and TWERSKY [1964]).

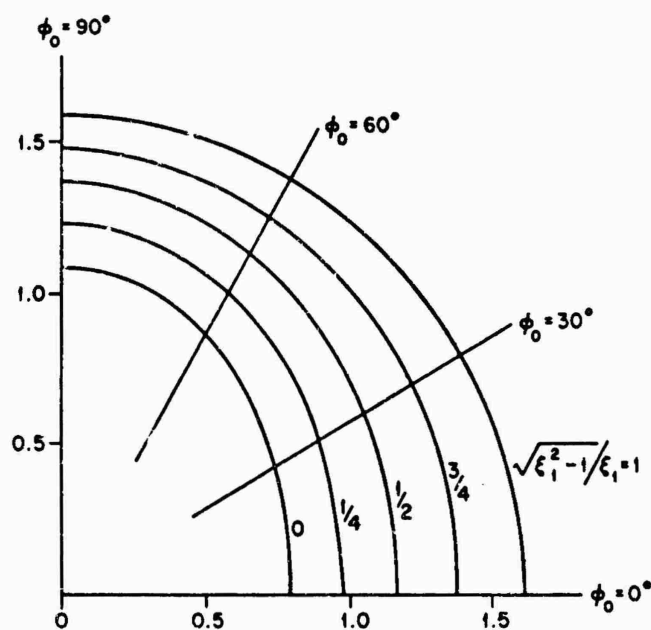


Fig. 3.10. Normalized total scattering cross section $\frac{1}{4}k\sigma_T$ for E^i parallel to the cylinder axis and $c\xi_1 = 1.1$ (BURKE and TWERSKY [1964]).

BURKE et al. [1964] have published diagrams of the normalized bistatic cross section per unit length $\frac{1}{4}k\sigma(\phi)$ as a function of ϕ for $c\xi_1 = 0.3, 0.7, 1.1$ and axes ratio $\sqrt{\xi_1^2 - 1}/\xi_1 = 0, \frac{1}{4}, \frac{1}{2}, \frac{3}{4}, 1$.

The normalized back scattering cross section per unit length as a function of $c\xi_1$ and for different values of the axes ratio is shown in Fig. 3.11.

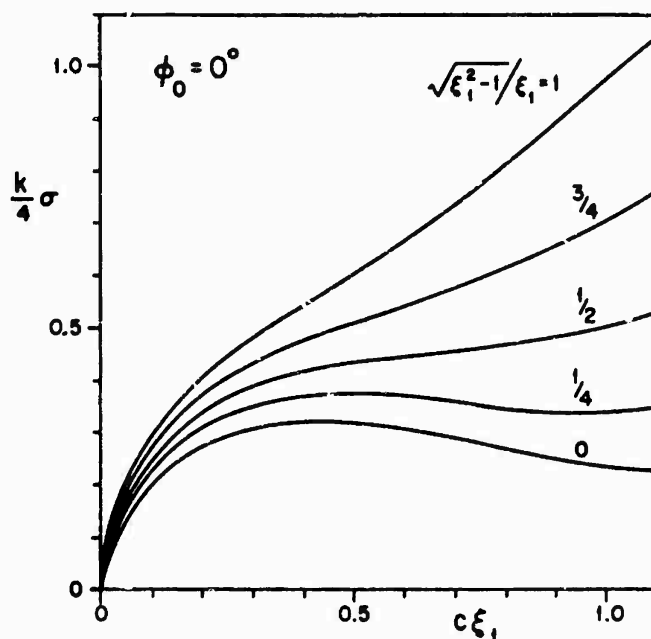


Fig. 3.11. Normalized back scattering cross section for E^1 parallel to the cylinder axis, and incidence along the major axis (BURKE and TWERSKY [1964]).

The total scattering cross section per unit length is:

$$\sigma_T \sim \frac{4}{k} D \left\{ 1 - \left(\frac{1}{2} c \xi_1 \right)^2 \left[\frac{2\sqrt{(\xi_1^2 - 1)}}{\xi_1 L} (1 - D) + \xi_1^{-2} \right] \right\}. \quad (3.22)$$

For incidence along the minor axis ($\phi_0 = \frac{1}{2}\pi$), in the far field ($\xi \rightarrow \infty$, $v = \phi$) and through $O(c^2)$:

$$\begin{aligned} P \sim D \left(-1 + \frac{2iL}{\pi} \right) + \left(\frac{1}{2} c \xi_1 \right)^2 \left\{ \left[\frac{4\sqrt{(\xi_1^2 - 1)}}{\xi_1 L} (1 - D) - \xi_1^{-2} (1 - \cos 2\phi) \right] \frac{1}{2} D - \right. \\ \left. - i \left[\frac{2D}{\pi \xi_1} (1 - 2D) \sqrt{(\xi_1^2 - 1)} - \frac{LD}{\pi \xi_1^2} (1 - \cos 2\phi) - \pi (1 - \xi_1^{-2} + \xi_1^{-1} \sqrt{(\xi_1^2 - 1)}) \sin \phi \right] \right\}. \end{aligned} \quad (3.23)$$

BURKE et al. [1964] have published diagrams of the normalized bistatic cross section per unit length $\frac{1}{4}k\sigma(\phi)$ as a function of ϕ for $c\xi_1 = 0.3, 0.7, 1.1$ and axes ratio $\sqrt{\xi_1^2 - 1}/\xi_1 = 0, \frac{1}{4}, \frac{1}{2}, \frac{3}{4}, 1$.

The normalized back scattering cross section per unit length as a function of $c\xi_1$ and for different values of the axes ratio is shown in Fig. 3.12.

The total scattering cross section per unit length is:

$$\sigma_T \sim \frac{4}{k} D \left\{ 1 - \left(\frac{1}{2} c \xi_1 \right)^2 \left[\frac{2\sqrt{(\xi_1^2 - 1)}}{\xi_1 L} (1 - D) - \xi_1^{-2} \right] \right\}. \quad (3.24)$$

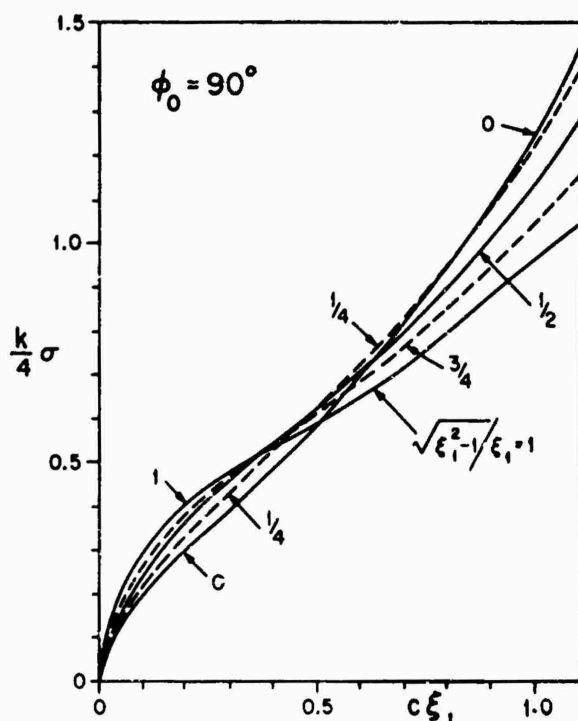


Fig. 3.12. Normalized back scattering cross section for E^i parallel to the cylinder axis, and incidence along the minor axis (BURKE and TWERSKY [1964]).

3.2.1.3. HIGH FREQUENCY APPROXIMATIONS

For a plane wave whose direction of propagation is perpendicular to the z -axis, and forms the angle ϕ_0 with the negative x -axis and the angle $(\frac{1}{2}\pi - \phi_0)$ with the negative y -axis ($0 \leq \phi_0 \leq \frac{1}{2}\pi$), such that

$$\begin{aligned} E^i &= \hat{z} \exp \{-ik(x \cos \phi_0 + y \sin \phi_0)\}, \\ H^i &= Y(-\sin \phi_0 \hat{x} + \cos \phi_0 \hat{y}) \exp \{-ik(x \cos \phi_0 + y \sin \phi_0)\}, \end{aligned} \quad (3.25)$$

the geometrical optics scattered field at a point P located in the illuminated region is

$$(E_z^s)_{g.o.} = - \left[1 + \frac{2(P_1 P)}{D \cos \phi_1} \right]^{-\frac{1}{2}} \exp \{ik[(P_1 P) - x_1 \cos \phi_0 - y_1 \sin \phi_0]\}, \quad (3.26)$$

where $(P_1 P)$ is the distance between the reflection point $P_1 \equiv (x_1, y_1, z) \equiv (\xi_1, \eta_1, z)$ and the observation point $P \equiv (x, y, z) \equiv (\xi, \eta, z)$,

$$(P_1 P) = [(x - x_1)^2 + (y - y_1)^2]^{\frac{1}{2}}, \quad (3.27)$$

D is the radius of curvature of the scatterer at P_1 :

$$D = \frac{1}{2} d \frac{(\xi_1^2 - \eta_1^2)^{\frac{1}{2}}}{\xi_1 \sqrt{(\xi_1^2 - 1)}}, \quad (3.28)$$

the reflection angle ϕ_1 of Fig. 3.13 is given by:

$$\cos \phi_1 = \frac{1}{\sqrt{(\xi_1^2 - \eta_1^2)}} [\eta_1 \sqrt{\xi_1^2 - 1} \cos \phi_0 \pm \xi_1 \sqrt{1 - \eta_1^2} \sin \phi_0], \quad (\pm \text{ for } y_1 \gtrless 0), \quad (3.29)$$

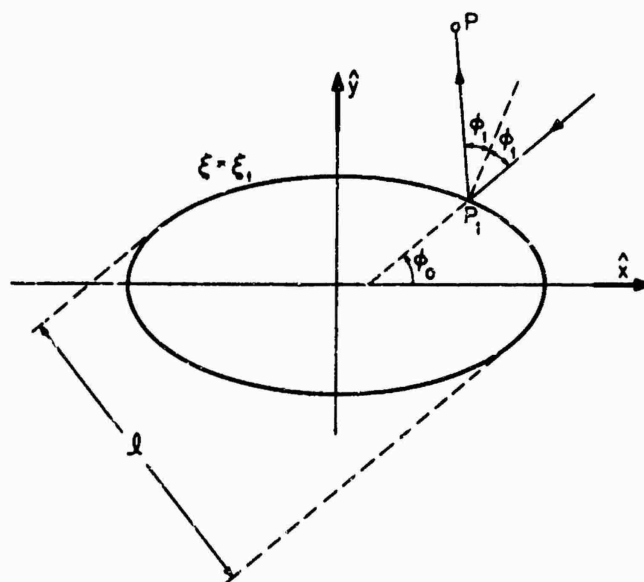


Fig. 3.13. Geometry for reflected field with plane wave incidence.

and η_1 is a root of:

$$\frac{a}{2(P_1 P)} = \frac{\eta_1 \sqrt{\xi_1^2 - 1} \cos \phi_0 + \alpha \xi_1 \sqrt{1 - \eta_1^2} \sin \phi_0}{(\xi \eta \eta_1 - \xi_1) \sqrt{(\xi_1^2 - 1)} + \beta \xi_1 \sqrt{(\xi^2 - 1)(1 - \eta^2)(1 - \eta_1^2)}},$$

where

$$\begin{aligned} \alpha &= \pm 1, \text{ for } y_1 \gtrless 0; \\ \beta &= \begin{cases} +1, & \text{if } y \text{ and } y_1 \text{ have the same sign;} \\ -1, & \text{if } y \text{ and } y_1 \text{ have the opposite sign.} \end{cases} \end{aligned} \quad (3.30)$$

In the shadowed region, $(E_z)_{\text{g.o.}} = 0$.

Formula (3.26) is a good approximation if $kD \gg 1$; this condition is satisfied a fortiori if:

$$c(\xi_1 - \xi_1^{-1}) \gg 1. \quad (3.31)$$

For incidence along the major axis ($\phi_0 = 0$) and in the illuminated region:

$$(E_z)_{\text{g.o.}} = - \left[\frac{\xi_1^2 - 1}{2\xi\xi_1 - \xi_1^2 - 1} \right]^{\frac{1}{2}} \exp \{ic(\xi - 2\xi_1)\}, \quad (3.32)$$

and the back scattering cross section per unit length is:

$$\sigma_{\text{g.o.}} = \frac{\pi c}{k} (\xi_1 - \xi_1^{-1}). \quad (3.33)$$

For incidence along the minor axis ($\phi_0 = \frac{1}{2}\pi$) and in the illuminated region:

$$(E_z)_{\text{g.o.}} = -\xi_1 [2 - \xi_1^2 + 2\sqrt{(\xi^2 - 1)(\xi_1^2 - 1)}]^{-\frac{1}{2}} \exp \{ic(\sqrt{(\xi^2 - 1)} - 2\sqrt{(\xi_1^2 - 1)})\}, \quad (3.34)$$

and the back scattering cross section per unit length is:

$$\sigma_{\text{b.o.}} = \frac{\pi c}{k} \frac{\xi_1^2}{\sqrt{(\xi_1^2 - 1)}}. \quad (3.35)$$

In the physical optics approximation, the total magnetic field at a point $P_1(\xi_1, \eta_1, z)$ on the surface $\xi = \xi_1$ is:

$$(H_v)_{\text{p.o.}} \begin{cases} = \frac{2Y}{\sqrt{(\xi_1^2 - \eta_1^2)}} (\eta_1 \sqrt{\xi_1^2 - 1} \cos \phi_0 \pm \xi_1 \sqrt{1 - \eta_1^2} \sin \phi_0) \\ \quad \times \exp \{ -ic[\xi_1 \eta_1 \cos \phi_0 \pm \sqrt{(\xi_1^2 - 1)(1 - \eta_1^2)} \sin \phi_0] \}. \quad (\pm \text{ if } y_1 \gtrless 0), \\ \quad \text{in the illuminated region,} \\ = 0, \text{ in the shadowed region.} \end{cases} \quad (3.36)$$

In the far field ($\xi \rightarrow \infty$) (BURKE and TWERSKY [1960]):

$$P_{\text{p.o.}} = -\sqrt{\frac{1}{4}\pi c(\xi_1 - \xi_1^{-1})} |\cos \frac{1}{2}(v - \phi_0)| [1 - \xi_1^{-2} \sin^2(\frac{1}{2}(v + \phi_0))]^{-\frac{1}{2}} \\ \times \exp [\frac{1}{4}i\pi + 2ic\xi_1 \sqrt{1 - \xi_1^{-2}} \sin^2 \frac{1}{2}(v + \phi_0) \cos \frac{1}{2}(v - \phi_0)] + \\ + \frac{1}{2}cA [\cos(v - \gamma) - \cos(\phi_0 - \gamma)] \frac{\sin [2cA \sin(\frac{1}{2}(v + \phi_0) - \gamma) \cos \frac{1}{2}(v - \phi_0)]}{2cA \sin(\frac{1}{2}(v + \phi_0) - \gamma) \cos \frac{1}{2}(v - \phi_0)}. \quad (3.37)$$

where:

$$\gamma = \arctan \left[\frac{\tan \phi_0}{1 - \xi_1^{-2}} \right], \quad (3.38)$$

$$A = \xi_1 \sqrt{\frac{\tan^2 \phi_0 + (1 - \xi_1^{-2})^2}{\tan^2 \phi_0 + 1 - \xi_1^{-2}}}. \quad (3.39)$$

The total scattering cross section per unit length is (BURKE and TWERSKY [1960]):

$$(\sigma_T)_{\text{p.o.}} = 2Ad \cos(\phi_0 - \gamma) = 2l, \quad (3.40)$$

where l is the distance between the two rays at grazing incidence, i.e. the "thickness" of the cylinder $\xi = \xi_1$ as seen from the direction of incidence (see Fig. 3.13). In particular, for incidence along the major axis,

$$[(\sigma_T)_{\text{p.o.}}]_{\phi_0=0} = \frac{4c}{k} \sqrt{(\xi_1^2 - 1)}, \quad (3.41)$$

whereas for incidence along the minor axis,

$$[(\sigma_T)_{\text{p.o.}}]_{\phi_0=90} = \frac{4c}{k} \xi_1. \quad (3.42)$$

A better approximation for the total scattering cross section per unit length is available for incidence along the major and minor axes (WU [1956]):

$$(\sigma_T)_{\phi_0=0^\circ} \sim 2d\sqrt{\xi_1^2-1}\{1+0.498\,076\,595[c(\xi_1-\xi_1^{-1})]^{-\frac{1}{2}}+\dots\}, \quad (3.43)$$

$$(\sigma_T)_{\phi_0=90^\circ} \sim 2d\xi_1 \left\{ 1+0.498\,076\,595 \left[\frac{c\xi_1^2}{\sqrt{(\xi_1^2-1)}} \right]^{-\frac{1}{2}} + \dots \right\}. \quad (3.44)$$

An approximation in which an expression for the diffracted field is retained, may be obtained either by an asymptotic expansion of the exact solution or by Keller's geometrical theory of diffraction. In the latter case, the scattered electric field is written as:

$$E_z^s = (E_z^s)_{\text{g.o.}} + (E_z^s)_d. \quad (3.45)$$

The diffracted field $(E_z^s)_d$ at a point $P(\xi, \eta, z)$ away from the surface $\xi = \xi_1$ is (KELLER [1956]):

$$\begin{aligned} (E_z^s)_d \sim \sum_n \left[\left\{ (P_2 P)^{-\frac{1}{2}} B_n(P_1) B_n(P_2) \right. \right. \\ \times \exp \left[ik \{ (P_2 P) - x_{P_1} \cos \phi_0 - y_{P_1} \sin \phi_0 \} + \int_{P_1}^{P_2} (ik + \delta_n) dl \right] + \\ \left. + (Q_2 P)^{-\frac{1}{2}} B_n(Q_1) B_n(Q_2) \right. \\ \times \exp \left[ik \{ (Q_2 P) - x_{Q_1} \cos \phi_0 - y_{Q_1} \sin \phi_0 \} + \int_{Q_1}^{Q_2} (ik + \delta_n) dl \right] \Big\} \\ \times \left\{ 1 - \exp \left[\oint (ik + \delta_n) dl \right] \right\}^{-1} \Big], \quad (3.46) \end{aligned}$$

where the points P_1, P_2, Q_1 and Q_2 on the surface $\xi = \xi_1$ are shown in Fig. 3.14,

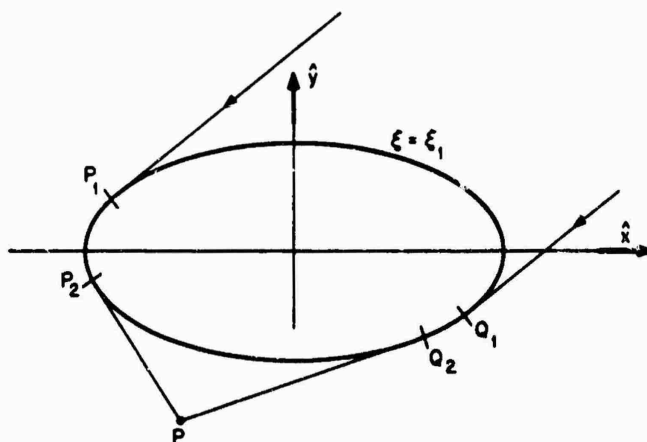


Fig. 3.14. Geometry for diffracted field.

the line integrals $\int_{P_1}^{P_2}$, $\int_{Q_1}^{Q_2}$, and \oint are evaluated along the optical rays from P_1 to P_2 and from Q_1 to Q_2 , and around the entire ellipse $\xi = \xi_1$, respectively. The arclength element dl is given by

$$(dl)^2 = \frac{\xi_1^2 - \eta^2}{1 - \eta^2} d^2(\eta)^2. \quad (3.47)$$

The decay exponents δ_n and the diffraction coefficients B_n may be written in the forms

$$\delta_n = \delta_{0n} \mu_n, \quad B_n = B_{0n} \gamma_n, \quad (3.48)$$

where

$$\delta_{0n}(\eta) = \frac{1}{2}k \left[\frac{c}{2\xi_1 \sqrt{(\xi_1^2 - 1)}} \right]^{-\frac{1}{2}} \exp \left\{ \frac{5}{8}i\pi \right\} \alpha_n (\xi_1^2 - \eta^2)^{-1}, \quad (3.49)$$

$$B_{0n}(\eta) = \left[\frac{c}{2\xi_1 \sqrt{(\xi_1^2 - 1)}} \right]^{\frac{1}{2}} \exp \left\{ \frac{1}{24}i\pi \right\} \left(\frac{\xi_1^2 - \eta^2}{2\pi k} \right)^{\frac{1}{2}} [\text{Ai}'(-\alpha_n)]^{-1}, \quad (3.50)$$

and μ_n and γ_n may be taken equal to unity in the first approximation, whereas in a second approximation (KELLER and LEVY [1959]):

$$\mu_n(\eta) = 1 + \frac{e^{11\pi}}{60} \alpha_n \left[\frac{c}{2\xi_1 \sqrt{(\xi_1^2 - 1)}} \right]^{-\frac{1}{2}} (\xi_1^2 - \eta^2)^{-1} \left[1 + 8 \frac{\eta^2(1 - \eta^2)}{\xi_1^2(\xi_1^2 - 1)} \right], \quad (3.51)$$

$$\gamma_n(\eta) = \exp \left\{ \frac{1}{5} \alpha_n^2 e^{11\pi} \left[\frac{1}{2} c \xi_1^2 (\xi_1^2 - 1) \right]^{-\frac{1}{2}} \frac{\sin v \cos v}{\sqrt{(\xi_1^2 - \eta^2)}} \right\}. \quad (3.52)$$

The diffracted field near the surface $\xi = \xi_1$ is of the order $c^{\frac{1}{2}}$ greater than the field of eq. (3.46) (see KELLER [1956]).

A rigorous asymptotic expansion for the field at $\xi = \xi_1$ is (WEINSTEIN and FEDOROV [1961]):

$$H_v \sim \frac{iY}{c \sqrt{(\xi_1^2 - \eta^2)}} \sum_{j=-\infty}^{\infty} B(v + 2\pi j; \phi_0), \quad (3.53)$$

where

$$B(\alpha; \phi_0) = [2c^2 \xi_1 \sqrt{(\xi_1^2 - 1)}]^{\frac{1}{2}} \left[\frac{\xi_1^2 - \cos^2 v_{1\mu}}{\xi_1^2 - \cos^2 \alpha} \right]^{\frac{1}{2}} f[(-1)^\mu (\zeta_{1\mu} - \zeta)] \\ \times \exp \{ -i[k\Delta_\mu + (-1)^\mu (\tau - \tau_{1\mu})] \}, \quad (3.54)$$

$$\Delta_\mu = \frac{d}{2\xi_1} \cos \phi_0 \cos v_{1\mu}, \quad (3.55)$$

$$\tau = c \int^{\alpha} \sqrt{(\xi_1^2 - \cos^2 v)} dv, \quad \tau_{1\mu} = c \int^{v_{1\mu}} \sqrt{(\xi_1^2 - \cos^2 v)} dv, \quad (3.56)$$

$$\zeta = \frac{1}{2}c \left[\frac{c}{2\xi_1 \sqrt{(\xi_1^2 - 1)}} \right]^{-\frac{1}{2}} \int^{\alpha} \frac{dv}{\sqrt{(\xi_1^2 - \cos^2 v)}}, \quad (3.57)$$

$$\zeta_{1\mu} = \frac{1}{2}c \left[\frac{c}{2\xi_1 \sqrt{(\xi_1^2 - 1)}} \right]^{-\frac{1}{2}} \int^{v_{1\mu}} \frac{dv}{\sqrt{(\xi_1^2 - \cos^2 v)}},$$

$$\mu = \begin{cases} 1, & \text{for } \alpha > \phi_0, \\ 2, & \text{for } \alpha < \phi_0, \end{cases} \quad (3.58)$$

the Fock function $f[\zeta]$ is defined in the Introduction, and v_{11} and v_{12} are the angular coordinates of the points of grazing incidence, as shown in Fig. 3.15.

where v_1 is given by:

$$\begin{aligned}\cos \frac{1}{2}(v + \phi_0) &= \frac{\sqrt{\xi_1^2 - 1} \cos v_1}{\sqrt{(\xi_1^2 - \cos^2 v_1)}}, \\ \sin \frac{1}{2}(v + \phi_0) &= \frac{\xi_1 \sin v_1}{\sqrt{(\xi_1^2 - \cos^2 v_1)}}.\end{aligned}\quad (3.63)$$

An approximation for the surface field which is sufficiently accurate for practical purposes may be obtained by an extension of Fock's method (WETZEL [1957]; GOODRICH [1958]; KING and WU [1959]).

A series which may be of some usefulness in numerical computations can be derived by substituting the appropriate asymptotic representations for the angular and radial Mathieu functions directly into the exact series solution. If the direction of propagation of the incident wave forms the angle α with the *positive* x -axis, so that

$$E^i = \hat{z} \exp \{ik(x \cos \alpha + y \sin \alpha)\} \quad (3.64)$$

then at a point $P(u, v)$ (ROBIN [1965]):

$$\begin{aligned}E_z \sim & \sqrt{\frac{2}{\cosh u}} e^{-2c} \sum_{n=0}^{\infty} \frac{2^{5n+2} (ic)^n}{n! \cos^{n+1} \alpha \cos^{n+1} \psi} \\ & \times [\cos^{2n+1} (\tfrac{1}{2}\alpha + \tfrac{1}{4}\pi) \sin^{2n+1} (\tfrac{1}{2}\psi + \tfrac{1}{4}\pi) + \sin^{2n+1} (\tfrac{1}{2}\alpha + \tfrac{1}{4}\pi) \cos^{2n+1} (\tfrac{1}{2}\psi + \tfrac{1}{4}\pi)] \\ & \times \{ \exp [-ic \sinh u + i(2n+1) \arctan (\tanh \tfrac{1}{2}u)] - \\ & - \exp [ic(\sinh u - 2 \sinh u_1) - i(2n+1)\gamma] \},\end{aligned}\quad (3.65)$$

where

$$\gamma = \arctan \left(\frac{\tanh \tfrac{1}{2}u - \sinh u_1}{1 + \sinh u_1 \tanh \tfrac{1}{2}u} \right), \quad (3.66)$$

$$\psi = \begin{cases} v, & \text{for } 0 \leq v < \tfrac{1}{2}\pi, \\ v - 2\pi, & \text{for } \tfrac{1}{2}\pi < v \leq 2\pi; \end{cases} \quad (3.67)$$

formula (3.65) is valid in the angular sectors:

$$-\tfrac{1}{2}\pi < \alpha < \tfrac{1}{2}\pi, \quad -\tfrac{1}{2}\pi < \psi < \tfrac{1}{2}\pi. \quad (3.68)$$

3.2.1.4. SHAPE APPROXIMATION

For an elliptic cylinder whose surface $\xi = \xi_1$ is defined in terms of the circular cylindrical coordinates (ρ_1, ϕ_1, z) by the equation

$$\rho_1 = u \left(1 - \frac{\sin^2 \phi_1}{2\xi_1^2} \right), \quad (3.69)$$

where

$$\xi_1^{-2} \ll 1, \quad (3.70)$$

i.e. the elliptic cylinder departs only infinitesimally from the circular cylinder

$\rho_1 = a$, the scattered field may be expressed as a perturbation of the solution for this circular cylinder.

For incidence at an angle ϕ_0 with respect to the negative x -axis and $(\frac{1}{2}\pi - \phi_0)$ with respect to the negative y -axis, such that

$$E^i = \hat{z} \exp \{-ik(x \cos \phi_0 + y \sin \phi_0)\}, \quad (3.71)$$

the scattered field at a point $P(\rho, \phi, z)$ is:

$$E_z^s \sim - \sum_{n=0}^{\infty} \varepsilon_n (-i)^n \left[\frac{J_n(ka)}{H_n^{(1)}(ka)} + a_n(\phi_0) \xi_1^{-2} \right] H_n^{(1)}(k\rho) \cos [n(\phi - \phi_0)] + O(\xi_1^{-4}), \quad (3.72)$$

where

$$a_n(\phi_0) = \frac{i}{2\pi} [H_n^{(1)}(ka)]^{-2} \left[1 + \frac{H_n^{(1)}(ka)}{2H_{n-2}^{(1)}(ka)} e^{2i\phi_0} + \frac{H_n^{(1)}(ka)}{2H_{n+2}^{(1)}(ka)} e^{-2i\phi_0} \right]. \quad (3.73)$$

In the far field ($\rho \rightarrow \infty$):

$$P \sim - \sum_{n=0}^{\infty} \varepsilon_n (-1)^n \left[\frac{J_n(ka)}{H_n^{(1)}(ka)} + a_n(\phi_0) \xi_1^{-2} \right] \cos [n(\phi - \phi_0)] + O(\xi_1^{-4}). \quad (3.74)$$

The previous formulas may also be obtained as particular cases of the results of HONG and GOODRICH [1965] and CLEMMOW and WESTON [1961]; in the latter paper and in a paper by UDAGAWA and MIYAZAKI [1965], high-frequency expansions are also given.

3.2.2. *H*-Polarization

3.2.2.1. EXACT SOLUTIONS

For a plane wave whose direction of propagation is perpendicular to the z -axis, and forms the angle ϕ_0 with the negative x -axis and the angle $(\frac{1}{2}\pi - \phi_0)$ with the negative y -axis ($0 \leq \phi_0 \leq \frac{1}{2}\pi$), such that

$$\begin{aligned} H^i &= \hat{z} \exp \{-ik(x \cos \phi_0 + y \sin \phi_0)\}, \\ E^i &= Z(\sin \phi_0 \hat{x} - \cos \phi_0 \hat{y}) \exp \{-ik(x \cos \phi_0 + y \sin \phi_0)\}, \end{aligned} \quad (3.75)$$

then

$$\begin{aligned} H_z^s &= -\sqrt{8\pi} \sum_{m=0}^{\infty} (-i)^m \left[\frac{1}{N_m^{(e)}} \frac{Re_m^{(1)'}(c, \xi_1)}{Re_m^{(3)'}(c, \xi_1)} Re_m^{(3)}(c, \xi) Se_m(c, \cos \phi_0) Se_m(c, \eta) + \right. \\ &\quad \left. + \frac{1}{N_m^{(o)}} \frac{Ro_m^{(1)'}(c, \xi_1)}{Ro_m^{(3)'}(c, \xi_1)} Ro_m^{(3)}(c, \xi) So_m(c, \cos \phi_0) So_m(c, \eta) \right]. \end{aligned} \quad (3.76)$$

On the surface $\xi = \xi_1$:

$$\begin{aligned} H_z &= \sqrt{\frac{8\pi}{\xi_1^2 - 1}} \sum_{m=0}^{\infty} (-i)^{m-1} \left[\frac{1}{N_m^{(e)}(\partial/\partial \xi_1)} Re_m^{(3)}(c, \xi_1) Se_m(c, \cos \phi_0) Se_m(c, \eta) + \right. \\ &\quad \left. + \frac{1}{N_m^{(o)}(\partial/\partial \xi_1)} Ro_m^{(3)}(c, \xi_1) So_m(c, \cos \phi_0) So_m(c, \eta) \right]. \end{aligned} \quad (3.77)$$

In the far field ($\xi \rightarrow \infty$):

$$P = -2\pi \sum_{m=0}^{\infty} (-1)^m \left[\frac{1}{N_m^{(e)}} \frac{Re_m^{(1)'}(c, \xi_1)}{Re_m^{(3)'}(c, \xi_1)} Se_m(c, \cos \phi_0) Se_m(c, \eta) + \frac{1}{N_m^{(o)}} \frac{Ro_m^{(1)'}(c, \xi_1)}{Ro_m^{(3)'}(c, \xi_1)} So_m(c, \cos \phi_0) So_m(c, \eta) \right]. \quad (3.78)$$

The total scattering cross section per unit length is:

$$\sigma_T = \frac{8\pi}{k} \sum_{m=0}^{\infty} \left[\frac{1}{N_m^{(e)}} \left| \frac{Re_m^{(1)'}(c, \xi_1)}{Re_m^{(3)'}(c, \xi_1)} Se_m(c, \cos \phi_0) \right|^2 + \frac{1}{N_m^{(o)}} \left| \frac{Ro_m^{(1)'}(c, \xi_1)}{Ro_m^{(3)'}(c, \xi_1)} So_m(c, \cos \phi_0) \right|^2 \right]. \quad (3.79)$$

For incidence along the major axis ($\phi_0 = 0$):

$$H_z^s = -\sqrt{8\pi} \sum_{m=0}^{\infty} \frac{(-i)^m}{N_m^{(e)}} \frac{Re_m^{(1)'}(c, \xi_1)}{Re_m^{(3)'}(c, \xi_1)} Re_m^{(3)}(c, \xi) Se_m(c, \eta). \quad (3.80)$$

On the surface $\xi = \xi_1$:

$$H_z = \sqrt{\frac{8\pi}{\xi_1^2 - 1}} \sum_{m=0}^{\infty} \frac{(-i)^{m-1}}{N_m^{(e)}} \frac{1}{(\partial/\partial \xi_1) Re_m^{(3)}(c, \xi_1)} Se_m(c, \eta). \quad (3.81)$$

The amplitude of H_z given by eq. (3.81) has been computed as a function of ν by BARAKAT [1969] for $c = 1$ and four different values of ξ_1 , and for $c = 2$ and $u_1 = 0.4$, and is shown in Fig. 3.16.

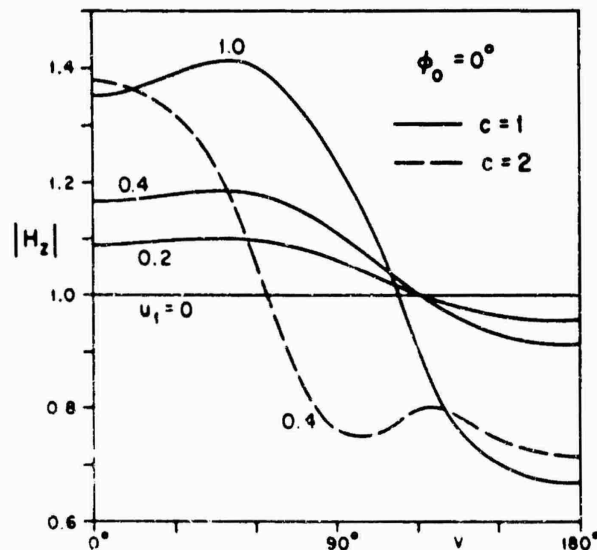


Fig. 3.16. Amplitude of surface field produced by a plane wave with H^i parallel to the cylinder axis; case $\phi_0 = 0$ (BARAKAT [1969]).

In the far field ($\xi \rightarrow \infty$):

$$P = -2\pi \sum_{m=0}^{\infty} \frac{(-1)^m}{N_m^{(e)}} \frac{Re_m^{(1)'}(c, \xi_1)}{Re_m^{(3)'}(c, \xi_1)} Se_m(c, \eta). \quad (3.82)$$

The total scattering cross section per unit length is:

$$\sigma_T = \frac{8\pi}{k} \sum_{m=0}^{\infty} \frac{1}{N_m^{(e)}} \left| \frac{Re_m^{(1)'}(c, \xi_1)}{Re_m^{(3)'}(c, \xi_1)} \right|^2. \quad (3.83)$$

The normalized cross section σ_T/d has been computed as a function of c and for eight different values of ξ_1 by BARAKAT [1963], and is shown in Fig. 3.17.

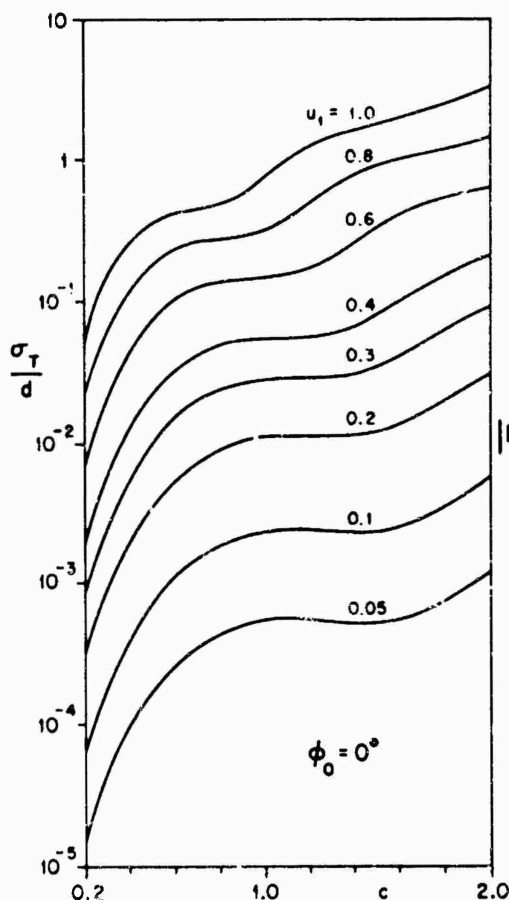


Fig. 3.17. Normalized total scattering cross section for H^i parallel to the cylinder axis and incidence along the major axis (BARAKAT [1963]).

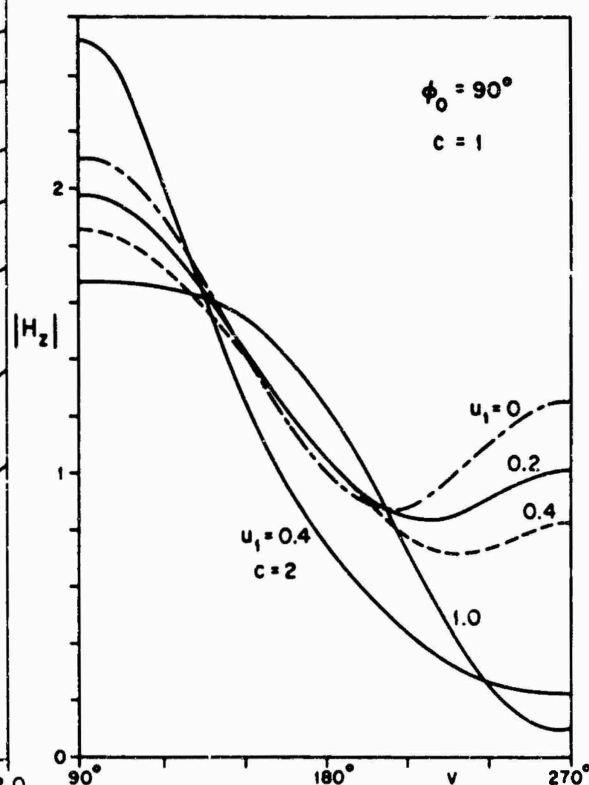


Fig. 3.18. Amplitude of surface field produced by a plane wave with H^i parallel to the cylinder axis; case $\phi_0 = \frac{1}{2}\pi$ (BARAKAT [1969]).

For incidence along the minor axis ($\phi_0 = \frac{1}{2}\pi$):

$$H_z^i = -\sqrt{8\pi} \sum_{m=0}^{\infty} (-1)^m \left[\frac{Se_{2m}(c, 0)}{N_{2m}^{(e)}} \frac{Re_{2m}^{(1)'}(c, \xi_1)}{Re_{2m}^{(3)'}(c, \xi_1)} Re_{2m}^{(3)}(c, \xi) Se_{2m}(c, \eta) - \right. \\ \left. -i \frac{So_{2m+1}(c, 0)}{N_{2m+1}^{(o)}} \frac{Ro_{2m+1}^{(1)'}(c, \xi_1)}{Ro_{2m+1}^{(3)'}(c, \xi_1)} Ro_{2m+1}^{(3)}(c, \xi) So_{2m+1}(c, \eta) \right]. \quad (3.84)$$

On the surface $\xi = \xi_1$:

$$H_z = \sqrt{\frac{8\pi}{\xi_1^2 - 1}} \sum_{m=0}^{\infty} (-1)^m \left[\frac{i \text{Se}_{2m}(c, 0)}{N_{2m}^{(e)}} \frac{1}{(\partial/\partial \xi_1) \text{Re}_{2m}^{(3)}(c, \xi_1)} \text{Se}_{2m}(c, \eta) + \frac{\text{So}_{2m+1}(c, 0)}{N_{2m+1}^{(o)}} \frac{1}{(\partial/\partial \xi_1) \text{Ro}_{2m+1}^{(3)}(c, \xi_1)} \text{So}_{2m+1}(c, \eta) \right]. \quad (3.85)$$

The amplitude of H_z given by eq. (3.85) has been computed as a function of η by BARAKAT [1969] for $c = 1$ and four different values of ξ_1 , and for $c = 2$ and $u_1 = 0.4$, and is shown in Fig. 3.18.

In the far field ($\xi \rightarrow \infty$):

$$P = -2\pi \sum_{m=0}^{\infty} \left[\frac{\text{Se}_{2m}(c, 0)}{N_{2m}^{(e)}} \frac{\text{Re}_{2m}^{(1)'}(c, \xi_1)}{\text{Re}_{2m}^{(3)'}(c, \xi_1)} \text{Se}_{2m}(c, \eta) - \frac{\text{So}_{2m+1}(c, 0)}{N_{2m+1}^{(o)}} \frac{\text{Ro}_{2m+1}^{(1)'}(c, \xi_1)}{\text{Ro}_{2m+1}^{(3)'}(c, \xi_1)} \text{So}_{2m+1}(c, \eta) \right]. \quad (3.86)$$

The total scattering cross section per unit length is:

$$\sigma_T = \frac{8\pi}{k} \sum_{m=0}^{\infty} \left[\frac{1}{N_{2m}^{(e)}} \left| \frac{\text{Re}_{2m}^{(1)'}(c, \xi_1)}{\text{Re}_{2m}^{(3)'}(c, \xi_1)} \text{Se}_{2m}(c, 0) \right|^2 + \frac{1}{N_{2m+1}^{(o)}} \left| \frac{\text{Ro}_{2m+1}^{(1)'}(c, \xi_1)}{\text{Ro}_{2m+1}^{(3)'}(c, \xi_1)} \text{So}_{2m+1}(c, 0) \right|^2 \right]. \quad (3.87)$$

The normalized cross section σ_T/d has been computed as a function of c and for eight different values of ξ_1 by BARAKAT [1963], and is shown in Fig. 3.19.

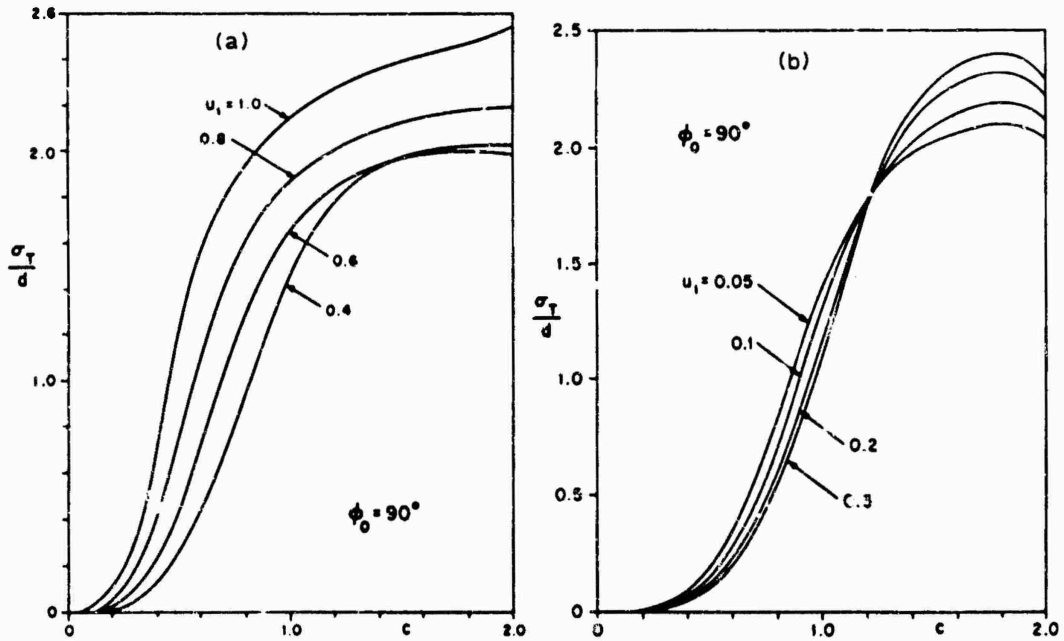


Fig. 3.19. Normalized total scattering cross section for H^i parallel to the cylinder axis and incidence along the minor axis (BARAKAT [1963]).

3.2.2.2. LOW FREQUENCY APPROXIMATIONS

For a plane wave whose direction of propagation is perpendicular to the z -axis, and forms the angle ϕ_0 with the negative x -axis and the angle $(\frac{1}{2}\pi - \phi_0)$ with the negative y -axis ($0 \leq \phi_0 \leq \frac{1}{2}\pi$), such that

$$\begin{aligned} H^i &= \hat{z} \exp \{-ik(x \cos \phi_0 + y \sin \phi_0)\}, \\ E^i &= Z(\sin \phi_0 \hat{x} - \cos \phi_0 \hat{y}) \exp \{-ik(x \cos \phi_0 + y \sin \phi_0)\}, \end{aligned} \quad (3.88)$$

low frequency expansions may be obtained either directly (STRUTT [1897]; NOBLE [1962]; VAN BLADEL [1963]) or by power series developments of the Mathieu functions appearing in the exact solutions (BURKE and TWERSKY [1964]; BURKE et al. [1964]).

In the far field ($\xi \rightarrow \infty$; $v = \phi$) and through $O(c^4)$ (BURKE and TWERSKY [1964]):

$$\begin{aligned} P \sim & -i\pi(\frac{1}{2}c\xi_1)^2[\xi_1^{-1}\sqrt{(\xi_1^2-1)} + (1+\xi_1^{-1}\sqrt{(\xi_1^2-1)}) \\ & \times (\xi_1^{-1}\sqrt{\xi_1^2-1} \cos \phi \cos \phi_0 + \sin \phi \sin \phi_0)] + \\ & + \pi(\frac{1}{2}c\xi_1)^4 \left\{ -\pi(1-\xi_1^{-2}) + \pi \left(1 - \frac{1}{2\xi_1^2} + \xi_1^{-1}\sqrt{(\xi_1^2-1)} \right) \right. \\ & \times [(1-\xi_1^{-2}) \cos \phi \cos \phi_0 + \sin \phi \sin \phi_0] + \\ & + \frac{1}{2}i \left[\frac{\sqrt{(\xi_1^2-1)}}{2\xi_1} (6-3\xi_1^{-2}-8L\xi_1^{-1}\sqrt{(\xi_1^2-1)}) + \frac{\sqrt{(\xi_1^2-1)}}{\xi_1^3} (\cos 2\phi + \cos 2\phi_0) + \right. \\ & + \frac{1+\xi_1^{-1}\sqrt{(\xi_1^2-1)}}{4\xi_1^2} \\ & \times \{ \xi_1^{-1}\sqrt{\xi_1^2-1}(\cos \phi \cos 3\phi_0 + \cos 3\phi \cos \phi_0) + \sin \phi \sin 3\phi_0 + \sin 3\phi \sin \phi_0 \} + \\ & + \left(1 - \frac{1}{2\xi_1^2} + \xi_1^{-1}\sqrt{(\xi_1^2-1)} \right) \left\{ \xi_1^{-1}\sqrt{\xi_1^2-1}[7+2\xi_1^{-1}\sqrt{\xi_1^2-1}(2L-1)] \cos \phi \cos \phi_0 + \right. \\ & + (7\xi_1^{-1}\sqrt{(\xi_1^2-1)}-2+4L) \sin \phi \sin \phi_0 + \xi_1^{-1}\sqrt{\xi_1^2-1} \cos 2\phi \cos 2\phi_0 + \\ & \left. \left. + \left(1 - \frac{1}{2\xi_1^2} \right) \sin 2\phi \sin 2\phi_0 \right\} \right\}, \end{aligned} \quad (3.89)$$

where

$$L = \gamma + \log [\frac{1}{2}c(\xi_1 + \sqrt{(\xi_1^2-1)})], \quad (3.90)$$

and $\gamma = 0.5772157 \dots$ is Euler's constant. BURKE and TWERSKY [1964] have derived the closed form for P which yields the explicit expansion correct through terms $O(c^8)$ (BURKE and TWERSKY [1960]). The normalized bistatic cross section per unit length for $\phi_0 = \frac{1}{2}\pi$ and different values of the axes ratio and of $c\xi_1$ is plotted as a function of ϕ in Figs. 3.20 and 3.21. BURKE et al. [1964] have plotted the normalized bistatic cross section per unit length $\frac{1}{2}k\sigma(\phi)$ as a function of ϕ for $\phi_0 = \frac{1}{2}\pi$; $c\xi_1 = 0.3, 0.7, 1.1$ and axes ratio $\sqrt{\xi_1^2-1}$; $\xi_1 = 0, \frac{1}{4}, \frac{1}{2}, \frac{3}{4}, 1$.

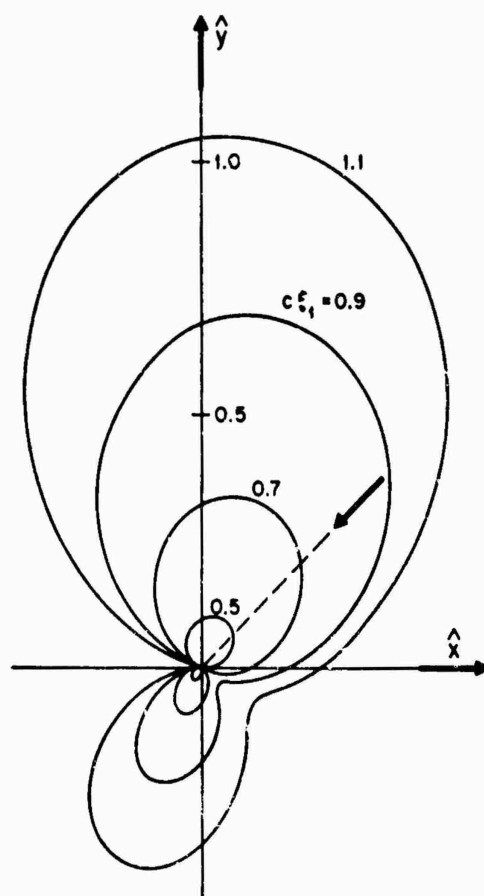


Fig. 3.20. Normalized bistatic cross section $\frac{1}{4}k\sigma(\phi)$ for H^1 parallel to the cylinder axis with $\phi_0 = 45^\circ$ and axes ratio $\xi_1/\sqrt{\xi_1^2 - 1} = 2$ (BURKE and TWERSKY [1964]).

The normalized back scattering cross section per unit length is shown in Fig. 3.22 as a function of ϕ_0 for $c\xi_1 = 1.1$ and in Fig. 3.23 as a function of $c\xi_1$ for $\phi_0 = \frac{1}{4}\pi$, for five different values of the axes ratio.

The total scattering cross section per unit length is:

$$\sigma_T \sim \frac{4\pi^2}{k} (\frac{1}{2}c\xi_1)^4 \left[1 - \xi_1^{-2} + \left(1 - \frac{1}{2\xi_1^2} + \xi_1^{-1}\sqrt{(\xi_1^2 - 1)} \right) (1 - \xi_1^{-2} \cos^2 \phi_0) \right]. \quad (3.91)$$

The normalized total scattering cross section per unit length corresponding to the closed form derived by BURKE and TWERSKY [1964] is shown as a function of ϕ_0 for $c\xi_1 = 1.1$ and different values of the axes ratio in Fig. 3.24.

For incidence along the major axis ($\phi_0 = 0$), in the far field ($\xi \rightarrow \infty$; $r = \phi$) and through $O(c^4)$:

$$P \sim -i\pi(\frac{1}{2}c\xi_1)^2 \xi_1^{-1} \sqrt{\xi_1^2 - 1} [1 + (1 + \xi_1^{-1} \sqrt{(\xi_1^2 - 1)}) \cos \phi] + \\ + \pi(\frac{1}{2}c\xi_1)^4 \left\{ -\pi(1 - \xi_1^{-2}) \left[1 - \left(1 - \frac{1}{2\xi_1^2} + \xi_1^{-1} \sqrt{(\xi_1^2 - 1)} \right) \cos \phi \right] + \right.$$

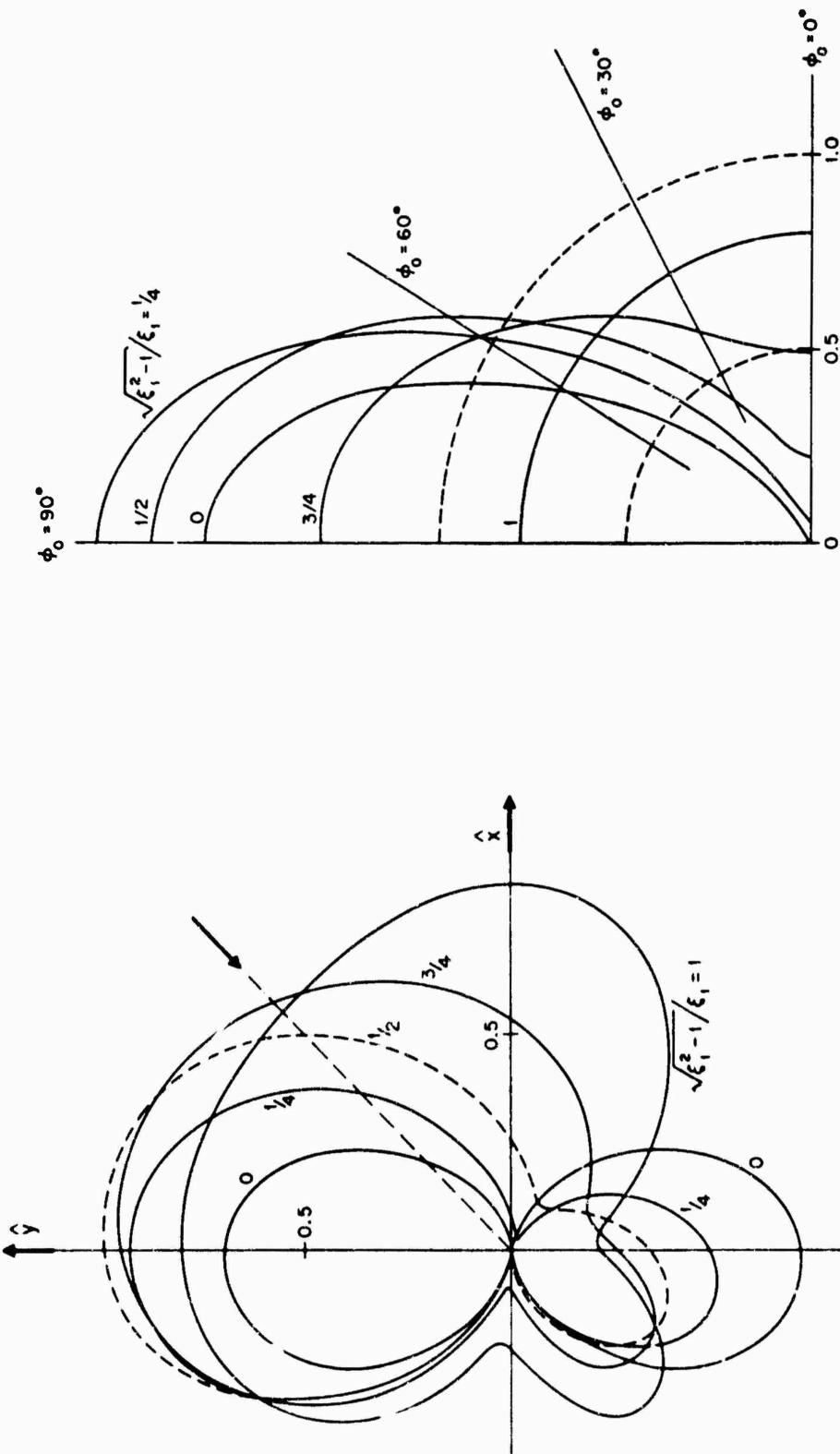


Fig. 3.22. Normalized back scattering cross section $\{k\sigma$ for H^1 parallel to the cylinder axis and $\epsilon_1^2 = 1.1$ (BURKE and TWEESKY [1964]).

Fig. 3.21. Normalized bistatic cross section $\{k\sigma(\phi)$ for H^1 parallel to the cylinder axis with $\phi_0 = 45^\circ$ and $\epsilon_1^2 = 1.1$ (BURKE and TWEESKY [1964]).

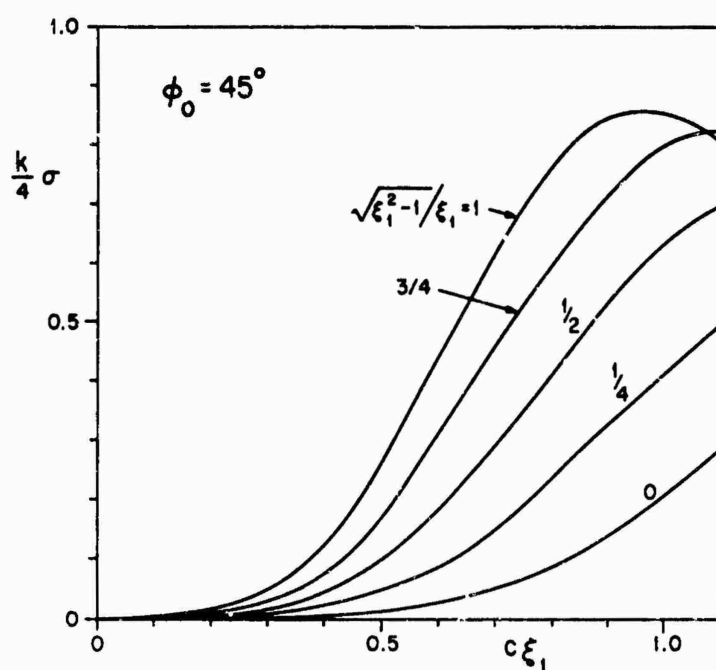


Fig. 3.23. Normalized back scattering cross section for H^1 parallel to the cylinder axis (BURKE and TWERSKY [1964]).

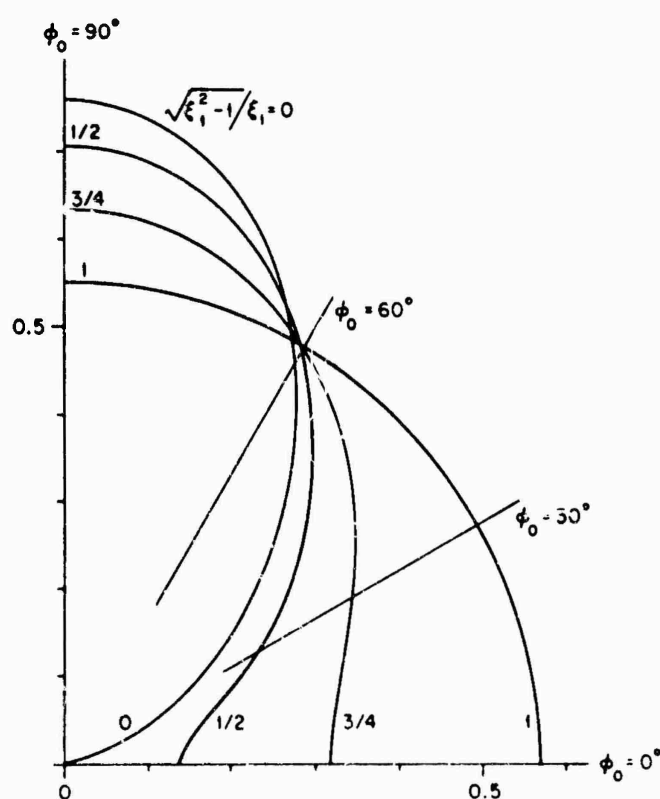


Fig. 3.24. Normalized total scattering cross section $k\sigma_T$ for H^1 parallel to the cylinder axis and $c\xi_1 = 1.1$ (BURKE and TWERSKY [1964]).

$$\begin{aligned}
& + \frac{i\sqrt{(\xi_1^2-1)}}{2\xi_1} \left[3 - \frac{1}{2\xi_1^2} - 4L\xi_1^{-1}\sqrt{(\xi_1^2-1)} + \xi_1^{-2} \cos 2\phi + \right. \\
& + \frac{1 + \xi_1^{-1}\sqrt{(\xi_1^2-1)}}{4\xi_1^2} (\cos \phi + \cos 3\phi) + \left. \left(1 - \frac{1}{2\xi_1^2} + \xi_1^{-1}\sqrt{(\xi_1^2-1)} \right) \right. \\
& \quad \left. \times \{ \cos 2\phi + [7 + 2\xi_1^{-1}\sqrt{\xi_1^2-1}(2L-1)] \cos \phi \} \right] \}. \quad (3.92)
\end{aligned}$$

BURKE et al. [1964] have published diagrams of the normalized bistatic cross section per unit length $\frac{1}{4}k\sigma(\phi)$ as a function of ϕ for $c\xi_1 = 0.3, 0.7, 1.1$ and axes ratio $\sqrt{\xi_1^2-1}/\xi_1 = 0, \frac{1}{4}, \frac{1}{2}, \frac{3}{4}, 1$.

The normalized back scattering cross section per unit length as a function of $c\xi_1$ and for different values of the axes ratio is shown in Fig. 3.25.

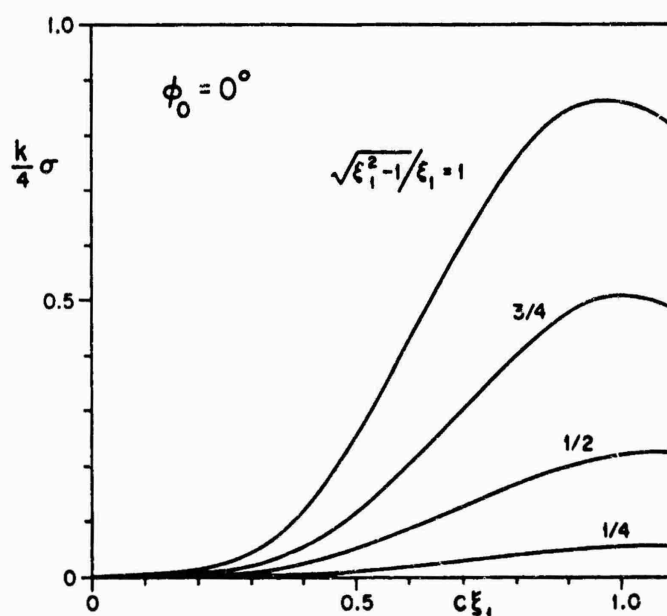


Fig. 3.25. Normalized back scattering cross section for H^1 parallel to the cylinder axis, and incidence along the major axis (BURKE and TWERSKY [1964]).

The total scattering cross section per unit length is:

$$\sigma_T \sim \frac{4\pi^2}{k} (\frac{1}{2}c\xi_1)^4 (1 - \xi_1^{-2}) \left(2 - \frac{1}{2\xi_1^2} + \xi_1^{-1}\sqrt{(\xi_1^2-1)} \right). \quad (3.93)$$

For incidence along the minor axis ($\phi_0 = \frac{1}{2}\pi$), in the far field ($\xi \rightarrow \infty$; $r = \phi$) and through $O(c^4)$:

$$\begin{aligned}
P \sim & -i\pi(\frac{1}{2}c\xi_1)^2 [\xi_1^{-1}\sqrt{(\xi_1^2-1)} + (1 + \xi_1^{-1}\sqrt{(\xi_1^2-1)}) \sin \phi] + \\
& + \pi(\frac{1}{2}c\xi_1)^4 \left\{ -\pi(1 - \xi_1^{-2}) + \pi \left(1 - \frac{1}{2\xi_1^2} + \xi_1^{-1}\sqrt{(\xi_1^2-1)} \right) \sin \phi + \right.
\end{aligned}$$

$$\begin{aligned}
& + \frac{1}{2}i \left[\frac{\sqrt{(\xi_1^2 - 1)}}{2\xi_1} (6 - 5\xi_1^{-2} - 8L\xi_1^{-1}\sqrt{(\xi_1^2 - 1)}) + \xi_1^{-3}\sqrt{\xi_1^2 - 1} \cos 2\phi + \right. \\
& + \frac{1 + \xi_1^{-1}\sqrt{(\xi_1^2 - 1)}}{4\xi_1^2} (\sin 3\phi - \sin \phi) + \left. \left(1 - \frac{1}{2\xi_1^2} + \xi_1^{-1}\sqrt{(\xi_1^2 - 1)} \right) \right. \\
& \quad \left. \times \{ (7\xi_1^{-1}\sqrt{(\xi_1^2 - 1)} - 2 + 4L) \sin \phi - \xi_1^{-1}\sqrt{\xi_1^2 - 1} \cos 2\phi \} \right] \}. \quad (3.94)
\end{aligned}$$

BURKE et al. [1964] have published diagrams of the normalized bistatic cross section per unit length $\frac{1}{4}k\sigma(\phi)$ as a function of ϕ for $c\xi_1 = 0.3, 0.7, 1.1$ and axes ratio $\sqrt{\xi_1^2 - 1}/\xi_1 = 0, \frac{1}{4}, \frac{1}{2}, \frac{3}{4}, 1$.

The normalized back scattering cross section per unit length as a function of $c\xi_1$ and for different values of the axes ratio is shown in Fig. 3.26.

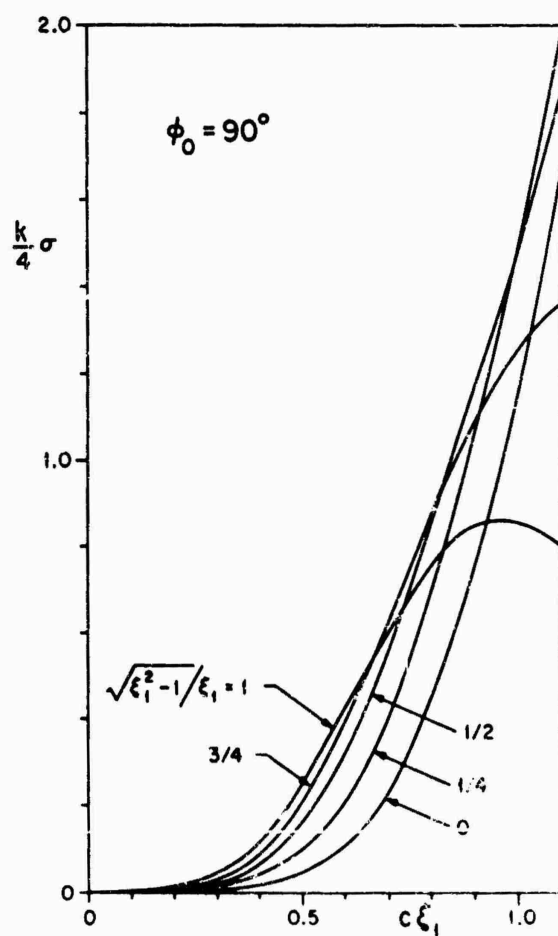


Fig. 3.26. Normalized back scattering cross section for H^1 parallel to the cylinder axis, and incidence along the minor axis (BURKE and TWERSKY [1964]).

The total scattering cross section per unit length is:

$$\sigma_T \sim \frac{4\pi^2}{k} (\frac{1}{2}c\xi_1)^4 (2 - \frac{1}{2}\xi_1^{-2} + \xi_1^{-1}\sqrt{(\xi_1^2 - 1)}). \quad (3.95)$$

3.2.2.3. HIGH FREQUENCY APPROXIMATIONS

For a plane wave whose direction of propagation is perpendicular to the z -axis, and forms the angle ϕ_0 with the negative x -axis and the angle $(\frac{1}{2}\pi - \phi_0)$ with the negative y -axis ($0 \leq \phi_0 \leq \frac{1}{2}\pi$), such that

$$\begin{aligned} H^i &= \hat{z} \exp \{-ik(x \cos \phi_0 + y \sin \phi_0)\}, \\ E^i &= Z(\sin \phi_0 \hat{x} - \cos \phi_0 \hat{y}) \exp \{-ik(x \cos \phi_0 + y \sin \phi_0)\}, \end{aligned} \quad (3.96)$$

the geometrical optics scattered field at a point P located in the illuminated region is (see Fig. 3.13):

$$(H_z^s)_{g.o.} = \left[1 + \frac{2(P_1 P)}{D \cos \phi_1}\right]^{-\frac{1}{2}} \exp \{ik[(P_1 P) - x_1 \cos \phi_0 - y_1 \sin \phi_0]\}, \quad (3.97)$$

where $(P_1 P)$ is the distance between the reflection point $P \equiv (x_1, y_1, z) \equiv (\xi_1, \eta_1, z)$ and the observation point $P \equiv (x, y, z) \equiv (\xi, \eta, z)$, and D, ϕ_1, η_1 are given by eqs. (3.28), (3.29), (3.30) respectively.

In the shadowed region, $(H_z^s)_{g.o.} = 0$.

Formula (3.97) is a good approximation if $kD \gg 1$; this condition is satisfied a fortiori if:

$$c(\xi_1 - \xi_1^{-1}) \gg 1. \quad (3.98)$$

For incidence along the major axis ($\phi_0 = 0$) and in the illuminated region:

$$(H_z^s)_{g.o.} = \left[\frac{\xi_1^2 - 1}{2\xi\xi_1 - \xi_1^2 - 1}\right]^{\frac{1}{2}} \exp \{ic(\xi - 2\xi_1)\}, \quad (3.99)$$

and the back scattering cross section per unit length is:

$$\sigma_{g.o.} = \frac{\pi c}{k} (\xi_1 - \xi_1^{-1}). \quad (3.100)$$

For incidence along the minor axis ($\phi_0 = \frac{1}{2}\pi$) and in the illuminated region:

$$(H_z^s)_{g.o.} = \xi_1 [2 - \xi_1^2 + 2\sqrt{(\xi^2 - 1)(\xi_1^2 - 1)}]^{-\frac{1}{2}} \exp \{ic(\sqrt{(\xi^2 - 1)} - 2\sqrt{(\xi_1^2 - 1)})\}, \quad (3.101)$$

and the back scattering cross section per unit length is:

$$\sigma_{g.o.} = \frac{\pi c}{k} \frac{\xi_1^2}{\sqrt{(\xi_1^2 - 1)}}. \quad (3.102)$$

In the physical optics approximation, the total magnetic field at a point $P(\xi_1, \eta_1, z)$ on the surface $\xi = \xi_1$ is:

$$(H_z)_{p.o.} = \begin{cases} 2 \exp \{-ic[\xi_1 \eta_1 \cos \phi_0 \pm \sqrt{(\xi_1^2 - 1)(1 - \eta_1^2)} \sin \phi_0]\}, \\ \quad (\pm \text{ if } y_1 \lessgtr 0), \text{ in the illuminated region,} \\ 0, \quad \text{in the shadowed region.} \end{cases} \quad (3.103)$$

In the far field ($\xi \rightarrow \infty$) (BURKE and TWERSKY [1960]).

$$P_{p.o.} = \sqrt{\{ \frac{1}{4} \pi c (\xi_1 - \xi_1^{-1}) | \cos \frac{1}{2} (v - \phi_0) | \} [1 - \xi_1^{-2} \sin^2 (\frac{1}{2} (v + \phi_0))]^{-\frac{1}{2}} \\ \times \exp [\frac{1}{4} i \pi + 2 i c \xi_1 \sqrt{1 - \xi_1^{-2} \sin^2 (\frac{1}{2} (v + \phi_0))} \cos \frac{1}{2} (v - \phi_0)] + \\ + \frac{1}{2} c A [\cos (v - \gamma) - \cos (\phi_0 - \gamma)] \frac{\sin [2 c A \sin (\frac{1}{2} (v + \phi_0) - \gamma) \cos \frac{1}{2} (v - \phi_0)]}{2 c A \sin (\frac{1}{2} (v + \phi_0) - \gamma) \cos \frac{1}{2} (v - \phi_0)}, \quad (3.104)$$

where γ and A are given by eqs. (3.38) and (3.39).

The total scattering cross section per unit length is (BURKE and TWERSKY [1960]):

$$(\sigma_T)_{p.o.} = 2 A d \cos (\phi_0 - \gamma) = 2 l, \quad (3.105)$$

where l is the distance between the two rays at grazing incidence (see Fig. 3.13). In particular, for incidence along the major axis,

$$[(\sigma_T)_{p.o.}]_{\phi_0=0} = \frac{4c}{k} \sqrt{(\xi_1^2 - 1)}, \quad (3.106)$$

whereas for incidence along the minor axis,

$$[(\sigma_T)_{p.o.}]_{\phi_0=90} = \frac{4c}{k} \xi_1. \quad (3.107)$$

A better approximation for the total scattering cross section per unit length is available for incidence along the major and minor axes (WU [1956]):

$$(\sigma_T)_{\phi_0=0} \sim 2 d \sqrt{\xi_1^2 - 1} \{ 1 - 0.43211998 [c(\xi_1 - \xi_1^{-1})]^{-\frac{1}{3}} + \dots \}, \quad (3.108)$$

$$(\sigma_T)_{\phi_0=90} \sim 2 d \xi_1 \left\{ 1 - 0.43211998 \left[\frac{c \xi_1^2}{\sqrt{(\xi_1^2 - 1)}} \right]^{-\frac{1}{3}} + \dots \right\}. \quad (3.109)$$

An approximation in which an expression for the diffracted field is retained, may be obtained either by an asymptotic expansion of the exact solution or by Keller's geometrical theory of diffraction. In the latter case, the scattered magnetic field is written as

$$H_z^s = (H_z^s)_{p.o.} + (H_z^s)_d. \quad (3.110)$$

The diffracted field $(H_z^s)_d$ at a point $P(\xi, \eta, z)$ away from the surface $\xi = \xi_1$ is (KELLER [1955]):

$$(H_z^s)_d \sim \sum_n \left[\left\{ (P_2 P)^{-\frac{1}{2}} \bar{B}_n(P_1) \bar{B}_n(P_2) \right. \right. \\ \times \exp \left[i k \{ (P_2 P) - x_{P_1} \cos \phi_0 - y_{P_1} \sin \phi_0 \} + \int_{P_1}^{P_2} (i k + \delta_n) d l \right] + \\ + (Q_2 P)^{-\frac{1}{2}} \bar{B}_n(Q_1) \bar{B}_n(Q_2) \\ \times \exp \left[i k \{ (Q_2 P) - x_{Q_1} \cos \phi_0 - y_{Q_1} \sin \phi_0 \} + \int_{Q_1}^{Q_2} (i k + \delta_n) d l \right] \Big\} \\ \times \left[1 - \exp \left[\oint (i k + \delta_n) d l \right] \right]^{-1} \Big], \quad (3.111)$$

where the points P_1 , P_2 , Q_1 and Q_2 on the surface $\xi = \xi_1$ are shown in Fig. 3.14, and the line integrals $\int_{P_1}^{P_2}$, $\int_{Q_1}^{Q_2}$ and \oint are evaluated along the optical rays from P_1 to P_2 and from Q_1 to Q_2 , and around the entire ellipse $\xi = \xi_1$, respectively. The arclength element dl is given by eq. (3.47). The decay exponents δ_n and the diffraction coefficients \bar{B}_n may be written in the forms

$$\delta_n = \delta_{0n} \bar{\mu}_n, \quad \bar{B}_n = \bar{B}_{0n} \bar{\gamma}_n, \quad (3.112)$$

where

$$\delta_{0n}(\eta) = \frac{1}{2}k \left[\frac{c}{2\xi_1 \sqrt{(\xi_1^2 - 1)}} \right]^{-\frac{1}{2}} \exp \left\{ \frac{1}{8}i\pi \right\} \beta_n (\xi_1^2 - \eta^2)^{-\frac{1}{2}}, \quad (3.113)$$

$$\bar{B}_{0n}(\eta) = \left[\frac{c}{2\xi_1 \sqrt{(\xi_1^2 - 1)}} \right]^{\frac{1}{2}} \exp \left\{ \frac{1}{24}i\pi \right\} \left(\frac{\xi_1^2 - \eta^2}{2\pi k} \right)^{\frac{1}{2}} [\beta_n^{\frac{1}{2}} \text{Ai}(-\beta_n)]^{-1}, \quad (3.114)$$

and $\bar{\mu}_n$ and $\bar{\gamma}_n$ may be taken equal to unity in the first approximation, whereas in a second approximation (KELLER and LEVY [1959]):

$$\begin{aligned} \bar{\mu}_n(\eta) = 1 + \frac{1}{80}e^{i\pi} \beta_n \left[\frac{c}{2\xi_1 \sqrt{(\xi_1^2 - 1)}} \right]^{-\frac{1}{2}} (\xi_1^2 - \eta^2)^{-\frac{1}{2}} \left\{ 1 + 8 \frac{\eta^2(1 - \eta^2)}{\xi_1^2(\xi_1^2 - 1)} + \right. \\ \left. + 6\beta_n^{-3} \left[1 + \frac{\eta^2(1 - \eta^2)}{2\xi_1^2(\xi_1^2 - 1)} \right] \right\}, \end{aligned} \quad (3.115)$$

$$\bar{\gamma}_n(\eta) = \exp \left\{ \frac{1}{3}\beta_n^2 e^{i\pi} \left(1 + \frac{1}{4\beta_n^3} \right) \left[\frac{1}{2}c\xi_1^2(\xi_1^2 - 1) \right]^{-\frac{1}{2}} \frac{\sin v \cos v}{\sqrt{(\xi_1^2 - \eta^2)}} \right\}. \quad (3.116)$$

The diffracted field on the surface $\xi = \xi_1$ is (KELLER and LEVY [1959]):

$$\begin{aligned} (H_z^d)_d \sim \left[\frac{c}{2\xi_1 \sqrt{(\xi_1^2 - 1)}} \right]^{-\frac{1}{2}} \exp \left\{ -\frac{1}{2}i\pi \right\} \left(\frac{2\pi k}{\xi_1^2 - \eta^2} \right)^{\frac{1}{2}} \sum_n \text{Ai}(-\beta_n) \bar{B}_n(P) \\ \times \left\{ \bar{B}_n(P_1) \exp \left[\int_{P_1}^P (ik + \delta_n) dl - ik(x_{P_1} \cos \phi_0 + y_{P_1} \sin \phi_0) \right] + \right. \\ \left. + \bar{B}_n(Q_1) \exp \left[\int_{Q_1}^P (ik + \delta_n) dl - ik(x_{Q_1} \cos \phi_0 + y_{Q_1} \sin \phi_0) \right] \right\} \\ \times \left\{ 1 - \exp \left[\oint (ik + \delta_n) dl \right] \right\}^{-1}. \end{aligned} \quad (3.117)$$

A rigorous asymptotic expansion for the field at $\xi = \xi_1$ is (WEINSTEIN and FEDOROV [1961]):

$$H_z \sim \sum_{j=-\infty}^{\infty} \bar{B}(v + 2\pi j; \phi_0), \quad (3.118)$$

where

$$\bar{B}(x; \phi_0) = \left[\frac{\xi_1^2 - \cos^2 \tau_{1\mu}}{\xi_1^2 - \cos^2 x} \right]^{\frac{1}{2}} g[(-1)^\mu (\zeta_{1\mu} - \zeta)] \exp \{ -i[kA_\mu + (-1)^\mu (\tau - \tau_{1\mu})] \}, \quad (3.119)$$

A_μ , τ , $\tau_{1\mu}$, ζ , $\zeta_{1\mu}$ and μ are given by eqs. (3.55) to (3.58), the Fock function $g[\zeta]$ is

defined in the Introduction, and v_{11} and v_{12} are the angular coordinates of the points of grazing incidence, as shown in Fig. 3.15. If the argument $(-1)^{\mu}(\zeta_{1\mu} - \zeta)$ of g is large and negative, eq. (3.119) must be replaced by:

$$B(x; \phi_0) = 2 \exp[-ic(\xi_1 \cos \alpha \cos \phi_0 + \sqrt{\xi_1^2 - 1} \sin \alpha \sin \phi_0)]. \quad (3.120)$$

A rigorous asymptotic expansion for the far field coefficient ($\xi \rightarrow \infty$) is (WEINSTEIN and FEDOROV [1961]):

$$P = \sqrt{\frac{1}{2}\pi} e^{i\pi/4} \sum_{j=-\infty}^{\infty} \tilde{r}(v + 2\pi j; \phi_0), \quad (3.121)$$

where

$$\begin{aligned} \tilde{r}(x; \phi_0) = & -\sqrt{\frac{c}{2\xi_1 \sqrt{(\xi_1^2 - 1)}}} \left[\frac{c}{2\xi_1 \sqrt{(\xi_1^2 - 1)}} \right]^{\frac{1}{2}} [(\xi_1^2 - \cos^2 v_{1\mu})(\xi_1^2 - \cos^2 \bar{v}_{1\mu})]^{\frac{1}{2}} \\ & \times g[(-1)^{\mu}(\zeta_{1\mu} - \bar{\zeta}_{1\mu})] \exp[-ik(\Delta_{\mu} + \bar{\Delta}_{\mu}) + i(-1)^{\mu}(\tau_{1\mu} - \bar{\tau}_{1\mu})], \end{aligned} \quad (3.122)$$

$\bar{\Delta}_{\mu}$, $\bar{\tau}_{1\mu}$ and $\bar{\zeta}_{1\mu}$ are obtained from Δ_{μ} , $\tau_{1\mu}$ and $\zeta_{1\mu}$ respectively, by replacing $v_{1\mu}$ with $\bar{v}_{1\mu}$ in eqs. (3.55) to (3.57); μ is given by eq. (3.58); the function $g[\xi]$ is defined in the Introduction (Section I.3.3); the angular coordinates v_{11} and v_{12} of the points of grazing incidence, and \bar{v}_{11} and \bar{v}_{12} of the points at which the rays leave the scattering surface, are shown in Fig. 3.15.

If $(-1)^{\mu}(\zeta_{1\mu} - \bar{\zeta}_{1\mu})$ is large and negative, eq. (3.122) must be replaced by:

$$\begin{aligned} \tilde{r}(x; \phi_0) = & \sqrt{\frac{c}{2\xi_1 \sqrt{(\xi_1^2 - 1)}}} [(\xi_1^2 - \cos^2 v_1)]^{\frac{1}{2}} \sqrt{\cos \frac{1}{2}(v - \phi_0)} \\ & \times \exp\{-ic[\xi_1 \cos v_1 (\cos v + \cos \phi_0) + \sqrt{\xi_1^2 - 1} \sin v_1 (\sin v + \sin \phi_0)]\}, \end{aligned} \quad (3.123)$$

where v_1 is given by eqs. (3.63).

An approximation for the surface field which is sufficiently accurate for all practical purposes may be obtained by an extension of Fock's method (WETZEL [1957]; GOODRICH [1958]; KING and WU [1959]). In particular, the surface field ($\xi = \xi_1$) in the shadow region for incidence along the minor axis ($\phi_0 = \frac{1}{2}\pi$) is (GOODRICH [1958]):

$$H_z \sim e^{ikL} g(A) + e^{ikL'} g(A'), \quad (3.124)$$

where

$$L = \frac{1}{2} d \xi_1 [E(\frac{1}{2}\pi, \xi_1) - E(\frac{1}{2}\pi - \beta, \xi_1)], \quad (3.125)$$

$$L' = \frac{1}{2} d \xi_1 [E(\frac{1}{2}\pi, \xi_1) + E(\frac{1}{2}\pi - \beta, \xi_1)], \quad (3.126)$$

$$A = [\frac{1}{2} c (\xi_1 - \xi_1^{-1})]^{\frac{1}{2}} [F(\frac{1}{2}\pi, \xi_1) - F(\frac{1}{2}\pi - \beta, \xi_1)], \quad (3.127)$$

$$A' = [\frac{1}{2} c (\xi_1 - \xi_1^{-1})]^{\frac{1}{2}} [F(\frac{1}{2}\pi, \xi_1) + F(\frac{1}{2}\pi - \beta, \xi_1)], \quad (3.128)$$

$$\beta = \begin{cases} 2\pi - v, & \text{if } \frac{1}{2}\pi \leq v \leq 2\pi, \\ v - \pi, & \text{if } \pi \leq v \leq \frac{1}{2}\pi. \end{cases} \quad (3.129)$$

the elliptic functions E and F are

$$E(\alpha, \xi_1) = \int_0^\alpha \sqrt{1 - \xi_1^{-2} \sin^2 u} du, \quad (3.130)$$

$$F(\alpha, \xi_1) = \int_0^\alpha \frac{du}{\sqrt{1 - \xi_1^{-2} \sin^2 u}}, \quad (3.131)$$

the function $g(\xi)$ is defined in the Introduction, and L and L' are the path lengths measured along the ellipse $\xi = \xi_1$ from the shadow lines to the observation point $P(\xi_1, \eta)$ (see Fig. 3.27).

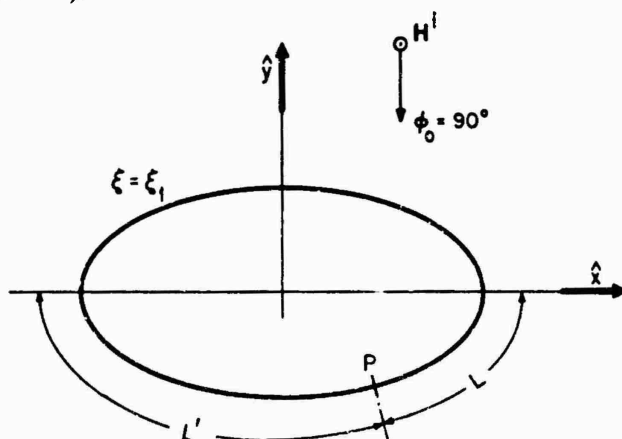


Fig. 3.27. Geometry for the Fock-Goodrich approximation.

For incidence along the minor axis ($\phi_0 = \frac{1}{2}\pi$), the surface field amplitude $|H_z|$ and phase ($\arg H_z + c \sqrt{(\xi_1^2 - 1)}$) have been plotted as functions of the arc distance from the center ($u = u_1$, $v = \frac{1}{2}\pi$) of the illuminated side by KING and WU [1959], who compared the experimental results of Wetzel with the Fock, Fock-Goodrich and Wetzel approximations for $c\xi_1 = 12$ and $\xi_1/\sqrt{(\xi_1^2 - 1)} = 1.2$ and 1.6, and by WETZEL and BRICK [1960], who compared their experimental results with the Fock approximation for $c(\xi_1 - \xi_1^{-1}) = 8.3$ with $\xi_1^{-1} = 0.552$, $c(\xi_1 - \xi_1^{-1}) = 4.7$ with $\xi_1^{-1} = 0.780$, and $c(\xi_1 - \xi_1^{-1}) = 2.2$ with $\xi_1^{-1} = 0.910$.

A series which may be of some usefulness in numerical computations can be derived by substituting the appropriate asymptotic representations for the angular and radial Mathieu functions directly into the exact series solution. If the direction of propagation of the incident waves forms the angle α with the *positive* x -axis, so that

$$H^i = \hat{z} \exp \{ik(x \cos \alpha + y \sin \alpha)\}, \quad (3.132)$$

then at a point $P(u, v)$ (ROBIN [1965]):

$$\begin{aligned} H_z \sim & \frac{2^{-n}}{\cosh u} e^{-2c} \sum_{n=0}^{\infty} \frac{2^{5n+2} (ic)^n}{n! \cos^{n+1} \alpha \cos^{n+1} \psi} \\ & \times [\cos^{2n+1} (\tfrac{1}{2}\alpha + \tfrac{1}{4}\pi) \sin^{2n+1} (\tfrac{1}{2}\psi + \tfrac{1}{4}\pi) + \sin^{2n+1} (\tfrac{1}{2}\alpha + \tfrac{1}{4}\pi) \cos^{2n+1} (\tfrac{1}{2}\psi + \tfrac{1}{4}\pi)] \\ & \times \{\exp [-ic \sinh u + i(2n+1) \arctan (\tanh \tfrac{1}{2}u)] + \\ & + \exp [ic(\sinh u - 2 \sinh u_1) - i(2n+1)\gamma]\}, \end{aligned} \quad (3.133)$$

where

$$\gamma = \arctan \left(\frac{\tanh \frac{1}{2}u - \sinh u_1}{1 + \sinh u_1 \tanh \frac{1}{2}u} \right), \quad (3.134)$$

$$\psi = \begin{cases} v, & \text{for } 0 \leq v < \frac{1}{2}\pi, \\ v-2\pi, & \text{for } \frac{1}{2}\pi < v \leq 2\pi; \end{cases} \quad (3.135)$$

formula (3.133) is valid in the angular sectors:

$$-\frac{1}{2}\pi < \alpha < \frac{1}{2}\pi, \quad -\frac{1}{2}\pi < \psi < \frac{1}{2}\pi. \quad (3.136)$$

3.2.2.4. SHAPE APPROXIMATION

For an elliptic cylinder whose surface $\xi = \xi_1$ is defined in terms of the circular cylindrical coordinates (ρ_1, ϕ_1, z) by the equation

$$\rho_1 = a \left(1 - \frac{\sin^2 \phi_1}{2\xi_1^2} \right), \quad (3.137)$$

where

$$\xi_1^2 \gg 1, \quad (3.138)$$

i.e. the elliptic cylinder departs only infinitesimally from the circular cylinder $\rho_1 = a$, the scattered field may be expressed as a perturbation of the solution for this circular cylinder.

For incidence at an angle ϕ_0 with respect to the negative x -axis and $(\frac{1}{2}\pi - \phi_0)$ with respect to the negative y -axis, such that

$$H^i = \hat{z} \exp \{ -ik(x \cos \phi_0 + y \sin \phi_0) \}, \quad (3.139)$$

the scattered field at a point $P(\rho, \phi, z)$ is:

$$H_z^s \sim - \sum_{n=0}^{\infty} \varepsilon_n (-i)^n \left[\frac{J'_n(ka)}{H_n^{(1)'}(ka)} + b_n(\phi_0) \xi_1^{-2} \right] H_n^{(1)'}(k\rho) \cos [n(\phi - \phi_0)] + O(\xi_1^{-4}), \quad (3.140)$$

where

$$b_n(\phi_0) = \frac{i}{2\pi} [H_n^{(1)'}(ka)]^{-2} \left\{ 1 - \frac{n^2}{(ka)^2} + \frac{H_n^{(1)'}(ka)}{2H_{n-2}^{(1)'}(ka)} \left[1 - \frac{(n-1)(n-2)}{(ka)^2} \right] e^{2i\phi_0} + \right. \\ \left. + \frac{H_n^{(1)'}(ka)}{2H_{n+2}^{(1)'}(ka)} \left[1 - \frac{(n+1)(n+2)}{(ka)^2} \right] e^{-2i\phi_0} \right\}. \quad (3.141)$$

In the far field ($\rho \rightarrow \infty$):

$$P \sim - \sum_{n=0}^{\infty} \varepsilon_n (-i)^n \left[\frac{J'_n(ka)}{H_n^{(1)'}(ka)} + b_n(\phi_0) \xi_1^{-2} \right] \cos [n(\phi - \phi_0)] + O(\xi_1^{-4}). \quad (3.142)$$

3.3. Line sources

3.3.1. E-Polarization

3.3.1.1. EXACT SOLUTIONS

For an electric line source parallel to the axis z of the cylinder and located at (ξ_0, η_0) , such that

$$E^i = \hat{z} H_0^{(1)}(kR), \quad (3.143)$$

the total electric field is

$$E_z = 4 \sum_{m=0}^{\infty} \left\{ \frac{1}{N_m^{(e)}} \left[\text{Re}_m^{(1)}(c, \xi_<) - \frac{\text{Re}_m^{(1)}(c, \xi_1)}{\text{Re}_m^{(3)}(c, \xi_1)} \text{Re}_m^{(3)}(c, \xi_<) \right] \right. \\ \left. \times \text{Re}_m^{(3)}(c, \xi_>) \text{Se}_m(c, \eta_0) \text{Se}_m(c, \eta) + \right. \\ \left. + \frac{1}{N_m^{(o)}} \left[\text{Ro}_m^{(1)}(c, \xi_<) - \frac{\text{Ro}_m^{(1)}(c, \xi_1)}{\text{Ro}_m^{(3)}(c, \xi_1)} \text{Ro}_m^{(3)}(c, \xi_<) \right] \right. \\ \left. \times \text{Ro}_m^{(3)}(c, \xi_>) \text{So}_m(c, \eta_0) \text{So}_m(c, \eta) \right\}. \quad (3.144)$$

On the surface $\xi = \xi_1$:

$$H_v = \frac{4Y}{c\sqrt{(\xi_1^2 - \eta^2)}} \sum_{m=0}^{\infty} \left[\frac{1}{N_m^{(e)}} \frac{\text{Re}_m^{(3)}(c, \xi_0)}{\text{Re}_m^{(3)}(c, \xi_1)} \text{Se}_m(c, \eta_0) \text{Se}_m(c, \eta) + \right. \\ \left. + \frac{1}{N_m^{(o)}} \frac{\text{Ro}_m^{(3)}(c, \xi_0)}{\text{Ro}_m^{(3)}(c, \xi_1)} \text{So}_m(c, \eta_0) \text{So}_m(c, \eta) \right]. \quad (3.145)$$

In the far field ($\xi \rightarrow \infty$):

$$E_z = \sqrt{\frac{2}{\pi c \xi}} e^{ic\xi - \frac{1}{2}i\pi} \sqrt{8\pi} \sum_{m=0}^{\infty} (-i)^m \left\{ \frac{1}{N_m^{(e)}} \left[\text{Re}_m^{(1)}(c, \xi_0) - \frac{\text{Re}_m^{(1)}(c, \xi_1)}{\text{Re}_m^{(3)}(c, \xi_1)} \text{Re}_m^{(3)}(c, \xi_0) \right] \right. \\ \left. \times \text{Se}_m(c, \eta_0) \text{Se}_m(c, \eta) + \right. \\ \left. + \frac{1}{N_m^{(o)}} \left[\text{Ro}_m^{(1)}(c, \xi_0) - \frac{\text{Ro}_m^{(1)}(c, \xi_1)}{\text{Ro}_m^{(3)}(c, \xi_1)} \text{Ro}_m^{(3)}(c, \xi_0) \right] \text{So}_m(c, \eta_0) \text{So}_m(c, \eta) \right\}. \quad (3.146)$$

If the line source is in the plane $y = 0$ at $(\xi_0, \eta_0 = 1)$:

$$E_z = 4 \sum_{m=0}^{\infty} \frac{1}{N_m^{(e)}} \left[\text{Re}_m^{(1)}(c, \xi_<) - \frac{\text{Re}_m^{(1)}(c, \xi_1)}{\text{Re}_m^{(3)}(c, \xi_1)} \text{Re}_m^{(3)}(c, \xi_<) \right] \text{Re}_m^{(3)}(c, \xi_>) \text{Se}_m(c, \eta). \quad (3.147)$$

On the surface $\xi = \xi_1$:

$$H_v = \frac{4Y}{c\sqrt{(\xi_1^2 - \eta^2)}} \sum_{m=0}^{\infty} \frac{1}{N_m^{(e)}} \frac{\text{Re}_m^{(3)}(c, \xi_0)}{\text{Re}_m^{(3)}(c, \xi_1)} \text{Se}_m(c, \eta). \quad (3.148)$$

In the far field ($\xi \rightarrow \infty$):

$$E_z = \sqrt{\frac{2}{\pi c \xi}} e^{ic\xi - \frac{1}{2}i\pi} \sqrt{8\pi} \sum_{m=0}^{\infty} \frac{(-i)^m}{N_m^{(e)}} \left[\text{Re}_{2m}^{(1)}(c, \xi_0) - \frac{\text{Re}_{2m}^{(1)}(c, \xi_1)}{\text{Re}_{2m}^{(3)}(c, \xi_1)} \text{Re}_{2m}^{(3)}(c, \xi_0) \right] \text{Se}_{2m}(c, \eta). \quad (3.149)$$

If the line source is in the plane $x = 0$ at $(\xi_0, \eta_0 = 0)$:

$$E_z = 4 \sum_{m=0}^{\infty} \left\{ \frac{\text{Se}_{2m}(c, 0)}{N_{2m}^{(e)}} \left[\text{Re}_{2m}^{(1)}(c, \xi_0) - \frac{\text{Re}_{2m}^{(1)}(c, \xi_1)}{\text{Re}_{2m}^{(3)}(c, \xi_1)} \text{Re}_{2m}^{(3)}(c, \xi_0) \right] \right. \\ \left. \times \text{Re}_{2m}^{(3)}(c, \xi_0) \text{Se}_{2m}(c, \eta) + \right. \\ \left. + \frac{\text{So}_{2m+1}(c, 0)}{N_{2m+1}^{(o)}} \left[\text{Ro}_{2m+1}^{(1)}(c, \xi_0) - \frac{\text{Ro}_{2m+1}^{(1)}(c, \xi_1)}{\text{Ro}_{2m+1}^{(3)}(c, \xi_1)} \text{Ro}_{2m+1}^{(3)}(c, \xi_0) \right] \right. \\ \left. \times \text{Ro}_{2m+1}^{(3)}(c, \xi_0) \text{So}_{2m+1}(c, \eta) \right\}. \quad (3.150)$$

On the surface $\xi = \xi_1$:

$$H_v = \frac{4Y}{c\sqrt{(\xi_1^2 - \eta^2)}} \sum_{m=0}^{\infty} \left[\frac{\text{Se}_{2m}(c, 0)}{N_{2m}^{(e)}} \frac{\text{Re}_{2m}^{(3)}(c, \xi_0)}{\text{Re}_{2m}^{(3)}(c, \xi_1)} \text{Se}_{2m}(c, \eta) + \right. \\ \left. + \frac{\text{So}_{2m+1}(c, 0)}{N_{2m+1}^{(o)}} \frac{\text{Ro}_{2m+1}^{(3)}(c, \xi_0)}{\text{Ro}_{2m+1}^{(3)}(c, \xi_1)} \text{So}_{2m+1}(c, \eta) \right]. \quad (3.151)$$

For axes ratio $\xi_1/\sqrt{(\xi_1^2 - 1)} = 6.7$ and $u_0 = 0.7213$, MANDRAZHI [1962] has plotted the amplitude of the surface current density for $c = 2\sqrt{2}$, and the phase for $c = 2\sqrt{2}$; 2 ; $\sqrt{2}$; $\frac{4}{3}$.

In the far field ($\xi \rightarrow \infty$):

$$E_z = \sqrt{\frac{2}{\pi c \xi}} e^{ic\xi - \frac{1}{2}i\pi} \sqrt{8\pi} \sum_{m=0}^{\infty} (-1)^m \\ \times \left\{ \frac{\text{Se}_{2m}(c, 0)}{N_{2m}^{(e)}} \left[\text{Re}_{2m}^{(1)}(c, \xi_0) - \frac{\text{Re}_{2m}^{(1)}(c, \xi_1)}{\text{Re}_{2m}^{(3)}(c, \xi_1)} \text{Re}_{2m}^{(3)}(c, \xi_0) \right] \text{Se}_{2m}(c, \eta) - \right. \\ \left. - i \frac{\text{So}_{2m+1}(c, 0)}{N_{2m+1}^{(o)}} \left[\text{Ro}_{2m+1}^{(1)}(c, \xi_0) - \frac{\text{Ro}_{2m+1}^{(1)}(c, \xi_1)}{\text{Ro}_{2m+1}^{(3)}(c, \xi_1)} \text{Ro}_{2m+1}^{(3)}(c, \xi_0) \right] \text{So}_{2m+1}(c, \eta) \right\}. \quad (3.152)$$

3.3.1.2. LOW FREQUENCY APPROXIMATIONS

No specific results are available; however, low frequency approximations can be easily derived either from the exact formulas of the previous section or by general methods (see, e.g., NOBLE [1962]).

3.3.1.3. HIGH FREQUENCY APPROXIMATIONS

For an electric line source parallel to the z -axis and located at (ξ_0, η_0) , such that

$$E^i = \hat{z} H_0^{(1)}(kR), \quad (3.153)$$

and so far from the surface $\xi = \xi_1$ that at the surface

$$E^i \sim \hat{z} \sqrt{\frac{2}{\pi k R}} e^{ikR - \frac{1}{2}i\pi}, \quad (3.154)$$

the geometric optics scattered field at a point P located in the illuminated region is

$$(E_z)_{g.o.} \sim - \sqrt{\frac{2}{\pi k(P_0 P_1)}} \left[1 + \frac{2(P_1 P)}{D \cos \phi_1} + \frac{(P_1 P)}{(P_0 P_1)} \right]^{-\frac{1}{2}} \exp \{ik[(P_0 P_1) + (P_1 P)] - \frac{1}{2}i\pi\}, \quad (3.155)$$

where $(P_0 P_1)$ and $(P_1 P)$ are, respectively, the distances between the source P_0 and the reflection point $P_1(\xi_1, \eta_1, z)$ and between P_1 and the observation point P ,

$$D = \frac{1}{2}d \frac{(\xi_1^2 - \eta_1^2)^{\frac{1}{2}}}{\xi_1 \sqrt{(\xi_1^2 - 1)}}, \quad (3.156)$$

the coordinate η_1 is determined as a function of ξ_0, η_0, ξ, η and ξ_1 by the relation

$$\frac{\partial}{\partial \eta_1} [(P_0 P_1) + (P_1 P)] = 0, \quad (3.157)$$

and the reflection angle ϕ_1 by

$$\cos \phi_1 = \frac{(\xi_0 \eta_0 \eta_1 - \xi_1) \sqrt{\xi_1^2 - 1} + \xi_1 \sqrt{\xi_0^2 - 1} \sin v_0 \sin v_1}{\sqrt{\xi_1^2 - \eta_1^2} [(\xi_0 \eta_0 - \xi_1 \eta_1)^2 + (\sqrt{\xi_0^2 - 1} \sin v_0 - \sqrt{\xi_1^2 - 1} \sin v_1)^2]^{\frac{1}{2}}}. \quad (3.158)$$

Formula (3.155) is applicable if $kD \gg 1$; this condition is satisfied a fortiori if

$$c(\xi_1 - \xi_1^{-1}) \gg 1. \quad (3.159)$$

In the shadowed region, $(E_z)_{g.o.} = 0$.

In the physical optics approximation, the total magnetic field at a point P_1 on the illuminated portion of the surface $\xi = \xi_1$ due to the source of eq. (3.153) is

$$(H_v)_{p.o.} = 2iYH_1^{(1)}(k(P_0 P_1)) \cos \phi_1, \quad (3.160)$$

where ϕ_1 is the angle of incidence; on the shadowed portion of the surface, $(H_v)_{p.o.} = 0$.

If the approximation (3.154) applies, then the surface field (3.160) becomes

$$(H_v)_{p.o.} \sim 2Y \sqrt{\frac{2}{\pi k(P_0 P_1)}} \exp \{ik(P_0 P_1) - \frac{1}{2}i\pi\} \cos \phi_1. \quad (3.161)$$

An approximation in which an expression for the diffracted field is retained, may be obtained either by an asymptotic expansion of the exact solution (LEVY [1960]; WEINSTEIN and FEDOROV [1961]) or by Keller's geometrical theory of diffraction. In the latter case, the scattered electric field is written as:

$$E_z^s = (E_z^s)_{g.o.} + (E_z^s)_d. \quad (3.162)$$

The diffracted field $(E_z^s)_d$ at a point $P(\xi, \eta, z)$ away from the surface $\xi = \xi_1$ and corresponding to the incident field of eq. (3.154) is (KELLER [1956]):

$$\begin{aligned} (E_z^s)_d \sim & \sqrt{\frac{2}{\pi k(P_0 P_1)(P_2 P)}} \sum_n B_n(P_1) B_n(P_2) \\ & \times \exp \left[-\frac{1}{4} i \pi + i k \{ (P_0 P_1) + (P_2 P) \} + \int_{P_1}^{P_2} (i k + \delta_n) dl \right] + \\ & + \sqrt{\frac{2}{\pi k(P_0 Q_1)(Q_2 P)}} \sum_n B_n(Q_1) B_n(Q_2) \\ & \times \exp \left[-\frac{1}{4} i \pi + i k \{ (P_0 Q_1) + (Q_2 P) \} + \int_{Q_1}^{Q_2} (i k + \delta_n) dl \right] \left\{ 1 - \exp \left[\oint (i k + \delta_n) dl \right] \right\}^{-1}, \end{aligned} \quad (3.163)$$

where the points P_1, P_2, Q_1 and Q_2 on the surface $\xi = \xi_1$ are those shown in Fig. 3.14 (but now the incident rays originate at the point $P_0(\xi_0, \eta_0)$ and no longer at infinity), and the line integrals $\int_{P_1}^{P_2}, \int_{Q_1}^{Q_2}$ and \oint are evaluated along the optical rays from P_1 to P_2 and from Q_1 to Q_2 , and around the entire ellipse $\xi = \xi_1$, respectively. The arclength element dl is given by eq. (3.47), and the decay exponents δ_n and the diffraction coefficients B_n by eqs. (3.48) through (3.52). The diffracted field near the surface $\xi = \xi_1$ is of the order $c^{\frac{1}{2}}$ greater than the field of eq. (3.163) (see KELLER [1956]).

In the particular case of a thin elliptic cylinder for which

$$c\xi_1 \gg 1, \quad [c(\xi_1 - \xi_1^{-1})]^{\frac{1}{2}} \ll 1, \quad (3.164)$$

the total magnetic field on the surface $\xi = \xi_1$, due to a line source located at a large distance from the scatterer ($u_0 \gg 1$) and of strength proportional to $(kR)^{-\frac{1}{2}}$, is (GOODRICH and KAZARINOFF [1963]):

$$H_v \sim -Y \sqrt{\frac{8c}{\pi}} \frac{(\xi_1^2 - \eta^2)^{-\frac{1}{2}}}{(\xi_0^2 - 1)^{\frac{1}{2}}} e^{ic(\xi_0 - 1)} \sum_{n=0}^N \frac{(-c)^n}{n! 2^n} G(r, v_0; -c\sigma_n^{(1)}), \quad (3.165)$$

where N is a non-negative integer much smaller than $c\xi_1$ but otherwise unspecified, and

$$\sigma_n^{(1)} = -i(4n+3) + \frac{8c^{\frac{1}{2}}u_1}{n! \Gamma(-n-\frac{1}{2})} (-1)^n e^{-\frac{1}{2}i\pi}. \quad (3.166)$$

If

$$v_0 = 0, \quad v > 0, \quad c \sin v \gg 1, \quad (3.167)$$

then

$$\begin{aligned} G(r, 0; -c\sigma) \sim & \frac{i}{8cT_1^2} (1 - R_1^2 e^{4ic})^{-1} \\ & \times \left| \frac{\exp \{ic(1 - \cos r)\}}{\sin \frac{1}{2}r} (\tan \frac{1}{2}r)^{-\frac{1}{2}} + R_1 \frac{\exp \{ic(3 + \cos r)\}}{\cos \frac{1}{2}r} (\tan \frac{1}{2}r)^{\frac{1}{2}} \right|. \end{aligned} \quad (3.168)$$

if

$$v_0 = 0, \quad |v - \pi| \ll 1, \quad c|\sin v| \ll 1, \quad (3.169)$$

then

$$G(v, 0; -c\sigma) \sim \frac{i}{8cT_1^2} (1 - R_1^2 e^{4ic})^{-1} e^{ic(1 - \cos v)}; \quad (3.170)$$

if

$$0 < v_0 \leq \frac{1}{2}\pi, \quad -\pi < \psi < 0, \quad c|\sin v| \gg 1, \quad (3.171)$$

then

$$\begin{aligned} G(v, v_0; -c\sigma) \sim & \frac{i(R_{II} - R_I)e^{ic(1 - \xi_0)}}{8c(1 - R_I^2 e^{4ic})(1 - R_{II}^2 e^{4ic})} \\ & \times \left\{ (1 + R_I R_{II} e^{4ic}) \left[\frac{e^{ic(1 + \cos \psi)}}{\cos \frac{1}{2}\psi} \frac{e^{ic(\xi_0 + \eta_0)}}{\cos \frac{1}{2}\beta_2} (\tan \frac{1}{2}\beta_2 \tan \frac{1}{2}\psi)^\alpha - \right. \right. \\ & \quad \left. - \frac{e^{ic(1 - \cos \psi)}}{\sin \frac{1}{2}\psi} \frac{e^{ic(\xi_0 - \eta_0)}}{\cos \frac{1}{2}\beta_1} (\tan \frac{1}{2}\beta_1)^\alpha (\tan \frac{1}{2}\psi)^{-\alpha} \right] + \\ & + (R_I + R_{II})e^{2ic} \left[\frac{e^{ic(1 + \cos \psi)}}{\cos \frac{1}{2}\psi} \frac{e^{ic(\xi_0 - \eta_0)}}{\cos \frac{1}{2}\beta_1} (\tan \frac{1}{2}\beta_1 \tan \frac{1}{2}\psi)^\alpha - \right. \\ & \quad \left. - \frac{e^{ic(1 - \cos \psi)}}{\sin \frac{1}{2}\psi} \frac{e^{ic(\xi_0 + \eta_0)}}{\cos \frac{1}{2}\beta_2} (\tan \frac{1}{2}\beta_2)^\alpha (\tan \frac{1}{2}\psi)^{-\alpha} \right] \Big\}, \quad (3.172) \end{aligned}$$

and in particular, for $v_0 = \frac{1}{2}\pi$:

$$\begin{aligned} G(v, \frac{1}{2}\pi; -c\sigma) \sim & \frac{i(K_{II} - R_I)e^{ic}}{2^{\frac{1}{2}}c(1 - R_I e^{2ic})(1 - R_{II} e^{2ic})} \\ & \times \left[\frac{\exp \{ic(1 + \cos \psi)\}}{\cos \frac{1}{2}\psi} (\tan \frac{1}{2}\psi)^\alpha - \frac{\exp \{ic(1 - \cos \psi)\}}{\sin \frac{1}{2}\psi} (\tan \frac{1}{2}\psi)^{-\alpha} \right]; \quad (3.173) \end{aligned}$$

if

$$v_0 = \frac{1}{2}\pi, \quad |\psi| \ll 1, \quad c|\sin v| \ll 1, \quad (3.174)$$

then

$$G(v, \frac{1}{2}\pi; -c\sigma) \sim \frac{i \exp \{ic(1 + \cos \psi)\}}{2^{\frac{1}{2}}c} \left[\frac{1}{T_I(1 - R_I e^{2ic})} + \frac{2 \sin \frac{1}{2}\psi}{T_{II}(1 - R_{II} e^{2ic})} \right]; \quad (3.175)$$

where

$$T_I = \frac{\pi^{\frac{1}{2}}(4c)^{\frac{1}{2}}e^{-\frac{1}{2}i\pi}}{\Gamma(\frac{1}{2}(1 + \alpha))}, \quad (3.176)$$

$$R_I = \frac{\Gamma(\frac{1}{2}(1 + \alpha))e^{-\frac{1}{2}i\pi}}{2^{2\alpha+1}c^{\alpha+\frac{1}{2}}\Gamma(-\frac{1}{2}\alpha)}, \quad (3.177)$$

$$T_{II} = \frac{\pi^{\frac{1}{2}}(4c)^{\frac{1}{2}}e^{\frac{1}{2}i(1-\alpha)\pi}}{2c^{\frac{1}{2}}\Gamma(1 + \frac{1}{2}\alpha)}. \quad (3.178)$$

$$R_{11} = \frac{\Gamma(1 + \frac{1}{2}\alpha)e^{-\frac{1}{2}i\pi}}{4^{\alpha}c^{\alpha+\frac{1}{2}}\Gamma(\frac{1}{2}(1-\alpha))}, \quad (3.179)$$

$$\psi = \begin{cases} v, & \text{for } v < \pi, \\ v - 2\pi, & \text{for } v > \pi, \end{cases} \quad (3.180)$$

$$\alpha = \frac{1}{2}(i\sigma - 1), \quad (3.181)$$

$$\cos \beta_1 = \frac{\xi_0 \eta_0 - 1}{\xi_0 - \eta_0}, \quad (\beta_1 \sim v_0), \quad (3.182)$$

$$\cos \beta_2 = -\frac{\xi_0 \eta_0 + 1}{\xi_0 + \eta_0}, \quad (\beta_2 \sim \pi - v_0). \quad (3.183)$$

GOODRICH and KAZARINOFF [1963] also give a physical interpretation, in terms of traveling waves, of the first term $n = 0$ of eq. (3.165) for $v_0 = 0$ and $v_0 = \frac{1}{2}\pi$.

3.3.2. *H*-polarization

3.3.2.1. EXACT SOLUTIONS

For a magnetic line source parallel to the axis z of the cylinder and located at (ξ_0, η_0) , such that

$$H^i = \hat{z}H_0^{(1)}(kR), \quad (3.184)$$

the total magnetic field is

$$\begin{aligned} H_z = 4 \sum_{m=0}^{\infty} \left\{ \frac{1}{N_m^{(e)}} \left[\text{Re}_m^{(1)}(c, \xi_<) - \frac{\text{Re}_m^{(1)'}(c, \xi_1)}{\text{Re}_m^{(3)'}(c, \xi_1)} \text{Re}_m^{(3)}(c, \xi_<) \right] \right. \\ \times \text{Re}_m^{(3)}(c, \xi_>) \text{Se}_m(c, \eta_0) \text{Se}_m(c, \eta) + \\ \left. + \frac{1}{N_m^{(o)}} \left[\text{Ro}_m^{(1)}(c, \xi_<) - \frac{\text{Ro}_m^{(1)'}(c, \xi_1)}{\text{Ro}_m^{(3)'}(c, \xi_1)} \text{Ro}_m^{(3)}(c, \xi_<) \right] \right. \\ \left. \times \text{Ro}_m^{(3)}(c, \xi_>) \text{So}_m(c, \eta_0) \text{So}_m(c, \eta) \right\}. \quad (3.185) \end{aligned}$$

On the surface $\xi = \xi_1$:

$$\begin{aligned} H_z = \frac{4i}{(\xi_1^2 - 1)} \sum_{m=0}^{\infty} \left[\frac{1}{N_m^{(e)}} \frac{\text{Re}_m^{(3)}(c, \xi_0)}{(\partial/\partial \xi_1) \text{Re}_m^{(3)}(c, \xi_1)} \text{Se}_m(c, \eta_0) \text{Se}_m(c, \eta) + \right. \\ \left. + \frac{1}{N_m^{(o)}} \frac{\text{Ro}_m^{(3)}(c, \xi_0)}{(\partial/\partial \xi_1) \text{Ro}_m^{(3)}(c, \xi_1)} \text{So}_m(c, \eta_0) \text{So}_m(c, \eta) \right]. \quad (3.186) \end{aligned}$$

In the far field ($\xi \rightarrow \infty$):

$$H_z = \sqrt{\frac{2}{\pi c \xi}} e^{ic\xi - \frac{1}{2}i\pi} \sqrt{8\pi} \sum_{m=0}^{\infty} \frac{(-i)^m}{N_m^{(e)}} \left\{ \frac{1}{N_m^{(e)}} \left[\operatorname{Re}_m^{(1)}(c, \xi_0) - \frac{\operatorname{Re}_m^{(1)'}(c, \xi_1)}{\operatorname{Re}_m^{(3)'}(c, \xi_1)} \operatorname{Re}_m^{(3)}(c, \xi_0) \right] \right. \\ \left. \times \operatorname{Se}_m(c, \eta_0) \operatorname{Se}_m(c, \eta) + \right. \\ \left. + \frac{1}{N_m^{(o)}} \left[\operatorname{Ro}_m^{(1)}(c, \xi_0) - \frac{\operatorname{Ro}_m^{(1)'}(c, \xi_1)}{\operatorname{Ro}_m^{(3)'}(c, \xi_1)} \operatorname{Ro}_m^{(3)}(c, \xi_0) \right] \operatorname{So}_m(c, \eta_0) \operatorname{So}_m(c, \eta) \right\}. \quad (3.187)$$

If the line source is in the plane $y = 0$ at $(\xi_0, \eta_0 = 1)$:

$$H_z = 4 \sum_{m=0}^{\infty} \frac{1}{N_m^{(e)}} \left[\operatorname{Re}_m^{(1)}(c, \xi_0) - \frac{\operatorname{Re}_m^{(1)'}(c, \xi_1)}{\operatorname{Re}_m^{(3)'}(c, \xi_1)} \operatorname{Re}_m^{(3)}(c, \xi_0) \right] \operatorname{Re}_m^{(3)}(c, \xi_0) \operatorname{Se}_m(c, \eta). \quad (3.188)$$

On the surface $\xi = \xi_1$:

$$H_z = \frac{4i}{\sqrt{(\xi_1^2 - 1)}} \sum_{m=0}^{\infty} \frac{1}{N_m^{(e)}} \frac{\operatorname{Re}_m^{(3)}(c, \xi_0)}{(\partial/\partial \xi_1) \operatorname{Re}_m^{(3)}(c, \xi_1)} \operatorname{Se}_m(c, \eta). \quad (3.189)$$

In the far field ($\xi \rightarrow \infty$):

$$H_z = \sqrt{\frac{2}{\pi c \xi}} e^{ic\xi - \frac{1}{2}i\pi} \sqrt{8\pi} \sum_{m=0}^{\infty} \frac{(-i)^m}{N_m^{(e)}} \left[\operatorname{Re}_m^{(1)}(c, \xi_0) - \frac{\operatorname{Re}_m^{(1)'}(c, \xi_1)}{\operatorname{Re}_m^{(3)'}(c, \xi_1)} \operatorname{Re}_m^{(3)}(c, \xi_0) \right] \operatorname{Se}_m(c, \eta). \quad (3.190)$$

If the line source is in the plane $x = 0$ at $(\xi_0, \eta_0 = 0)$:

$$H_z = 4 \sum_{m=0}^{\infty} \left\{ \frac{\operatorname{Se}_{2m}(c, 0)}{N_{2m}^{(e)}} \left[\operatorname{Re}_{2m}^{(1)}(c, \xi_0) - \frac{\operatorname{Re}_{2m}^{(1)'}(c, \xi_1)}{\operatorname{Re}_{2m}^{(3)'}(c, \xi_1)} \operatorname{Re}_{2m}^{(3)}(c, \xi_0) \right] \right. \\ \left. \times \operatorname{Re}_{2m}^{(3)}(c, \xi_0) \operatorname{Se}_{2m}(c, \eta) + \right. \\ \left. + \frac{\operatorname{So}_{2m+1}(c, 0)}{N_{2m+1}^{(o)}} \left[\operatorname{Ro}_{2m+1}^{(1)}(c, \xi_0) - \frac{\operatorname{Ro}_{2m+1}^{(1)'}(c, \xi_1)}{\operatorname{Ro}_{2m+1}^{(3)'}(c, \xi_1)} \operatorname{Ro}_{2m+1}^{(3)}(c, \xi_0) \right] \right. \\ \left. \times \operatorname{Ro}_{2m+1}^{(3)}(c, \xi_0) \operatorname{So}_{2m+1}(c, \eta) \right\}. \quad (3.191)$$

On the surface $\xi = \xi_1$:

$$H_z = \frac{4i}{\sqrt{(\xi_1^2 - 1)}} \sum_{m=0}^{\infty} \left[\frac{\operatorname{Se}_{2m}(c, 0)}{N_{2m}^{(e)}} \frac{\operatorname{Re}_{2m}^{(3)}(c, \xi_0)}{(\partial/\partial \xi_1) \operatorname{Re}_{2m}^{(3)}(c, \xi_1)} \operatorname{Se}_{2m}(c, \eta) + \right. \\ \left. + \frac{\operatorname{So}_{2m+1}(c, 0)}{N_{2m+1}^{(o)}} \frac{\operatorname{Ro}_{2m+1}^{(3)}(c, \xi_0)}{(\partial/\partial \xi_1) \operatorname{Ro}_{2m+1}^{(3)}(c, \xi_1)} \operatorname{So}_{2m+1}(c, \eta) \right]. \quad (3.192)$$

In the far field ($\xi \rightarrow \infty$):

$$H_z = \sqrt{\frac{2}{\pi c \xi}} e^{ic\xi - \frac{1}{2}i\pi} \sqrt{8\pi} \sum_{m=0}^{\infty} \frac{(-i)^m}{N_m^{(e)}} \left\{ \frac{\operatorname{Se}_{2m}(c, 0)}{N_{2m}^{(e)}} \left[\operatorname{Re}_{2m}^{(1)}(c, \xi_0) - \right. \right.$$

$$\begin{aligned}
& - \frac{Re_{2m}^{(1)'}(c, \xi_1)}{Re_{2m}^{(3)'}(c, \xi_1)} Re_{2m}^{(3)}(c, \xi_0) \Big] Se_{2m}(c, \eta) - \\
& - i \frac{So_{2m+1}(c, 0)}{N_{2m+1}^{(o)}} \left[Ro_{2m+1}^{(1)}(c, \xi_0) - \frac{Ro_{2m+1}^{(1)'}(c, \xi_1)}{Ro_{2m+1}^{(3)'}(c, \xi_1)} Ro_{2m+1}^{(3)}(c, \xi_0) \right] So_{2m+1}(c, \eta) \Big\}.
\end{aligned}
\tag{3.193}$$

3.3.2.2. LOW FREQUENCY APPROXIMATIONS

No specific results are available; however, low frequency approximations can be easily derived either from the exact formulas of the previous section or by general methods (see, e.g., NOBLE [1962]).

3.3.2.3. HIGH FREQUENCY APPROXIMATIONS

For a magnetic line source parallel to the z -axis and located at (ξ_0, η_0) such that

$$H^i = \hat{z} H_0^{(1)}(kR), \tag{3.194}$$

and so far from the surface $\xi = \xi_1$ that at the surface

$$H^i \sim \hat{z} \sqrt{\frac{2}{\pi k R}} e^{ikR - \frac{1}{2}i\pi}, \tag{3.195}$$

the geometric optics scattered field at a point P located in the illuminated region is

$$(H_z)_{g.o.} \sim \sqrt{\frac{2}{\pi k (P_0 P_1)}} \left[1 + \frac{2(P_1 P)}{D \cos \phi_1} + \frac{(P_1 P)}{(P_0 P_1)} \right]^{-\frac{1}{2}} \exp \{ ik[(P_0 P_1) + (P_1 P)] - \frac{1}{2}i\pi \},
\tag{3.196}$$

where $(P_0 P_1)$ and $(P_1 P)$ are, respectively, the distances between the source P_0 and the reflection point $P_1(\xi_1, \eta_1, z)$, and between P_1 and the observation point P ; D , η_1 and ϕ_1 are given by eqs. (3.156) to (3.158). Formula (3.196) is applicable if $kD \gg 1$, and this condition is satisfied a fortiori if $c(\xi_1 - \xi_1^{-1}) \gg 1$.

In the shadowed region, $(H_z)_{g.o.} = 0$.

In the physical optics approximation, the total magnetic field at a point P_1 on the surface $\xi = \xi_1$ due to the source of eq. (3.194) is

$$(H_z)_{p.o.} = \begin{cases} 2H_0^{(1)}(k(P_0 P_1)), & \text{in the illuminated region,} \\ 0, & \text{in the shadow.} \end{cases} \tag{3.197}$$

An approximation in which an expression for the diffracted field is retained, may be obtained either by an asymptotic expansion of the exact solution (KAZARINOFF and RITT [1959]; LIVY [1960]; WEINSTEIN and FEDOROV [1961]) or by Keller's geometrical theory of diffraction. In the latter case, the scattered magnetic field is written as:

$$H_z = (H_z)_{g.o.} + (H_z)_d. \tag{3.198}$$

The diffracted field $(H_z^d)_d$ at a point $P(\xi, \eta, z)$ away from the surface $\xi = \xi_1$ and corresponding to the incident field of eq. (3.195) is (KELLER [1956]):

$$\begin{aligned} (H_z^d)_d \sim & \left\{ \sqrt{\frac{2}{\pi k(P_0 P_1)(P_2 P)}} \sum_n \bar{B}_n(P_1) \bar{B}_n(P_2) \right. \\ & \times \exp \left[-\frac{1}{2} i \pi + i k \{ (P_0 P_1) + (P_2 P) \} + \int_{P_1}^{P_2} (i k + \delta_n) d l \right] + \\ & + \sqrt{\frac{2}{\pi k(P_0 Q_1)(Q_2 P)}} \sum_n \bar{B}_n(Q_1) \bar{B}_n(Q_2) \\ & \times \exp \left[-\frac{1}{2} i \pi + i k \{ (P_0 Q_1) + (Q_2 P) \} + \int_{Q_1}^{Q_2} (i k + \delta_n) d l \right] \left\{ 1 - \exp \left[\oint (i k + \delta_n) d l \right] \right\}^{-1}, \end{aligned} \quad (3.199)$$

where the points P_1, P_2, Q_1 and Q_2 on the surface $\xi = \xi_1$ are those shown in Fig. 3.14 (but now the incident rays originate at the point $P_0(\xi_0, \eta_0)$ and no longer at infinity), the line integrals $\int_{P_1}^{P_2}, \int_{Q_1}^{Q_2}$ and \oint are evaluated along the optical rays from P_1 to P_2 and from Q_1 to Q_2 , and around the entire ellipse $\xi = \xi_1$, respectively. The arclength element $d l'$ is given by eq. (3.47), and the decay exponents δ_n and the diffraction coefficients \bar{B}_n by eqs. (3.112) through (3.116).

The diffracted field on the surface $\xi = \xi_1$ is (LEVY and KELLER [1959]):

$$\begin{aligned} (H_z^d)_d \sim & \left[\frac{c}{2 \xi_1 \sqrt{(\xi_1^2 - 1)}} \right]^{-\frac{1}{2}} e^{-\frac{1}{2} i \pi} \left(\frac{2 \pi k}{\xi_1^2 - \eta^2} \right)^{\frac{1}{2}} \sum_n \text{Ai}(-\beta_n) \bar{B}_n(P) \times \\ & \times \left\{ \sqrt{\frac{2}{\pi k(P_0 P_1)}} \bar{B}_n(P_1) \exp \left[i k (P_0 P_1) + \int_{P_1}^P (i k + \delta_n) d l \right] + \right. \\ & + \sqrt{\frac{2}{\pi k(P_0 Q_1)}} \bar{B}_n(Q_1) \exp \left[i k (P_0 Q_1) + \int_{Q_1}^P (i k + \delta_n) d l \right] \left\{ 1 - \exp \left[\oint (i k + \delta_n) d l \right] \right\}^{-1}. \end{aligned} \quad (3.200)$$

In the particular case of a thin elliptic cylinder for which

$$c \xi_1 \gg 1, \quad [c(\xi_1 - \xi_1^{-1})]^{\frac{1}{2}} \ll 1, \quad (3.201)$$

the total magnetic field on the surface $\xi = \xi_1$, due to a line source located at a large distance from the scatterer ($u_0 \gg 1$) and of strength proportional to $(kR)^{-\frac{1}{2}}$, is (GOODRICH and KAZARINOFF [1963]):

$$H_z \sim 8i \sqrt{\frac{c}{\pi}} \frac{e^{i c (\xi_0 - 1)}}{\sqrt{(\xi_0^2 - 1)}} \sum_{n=0}^N \frac{(-c)^n}{n! 2^n} G(v, v_0; -c \sigma_n^{(2)}), \quad (3.202)$$

where N is a non-negative integer much smaller than $c \xi_1$ but otherwise unspecified, and

$$\sigma_n^{(2)} = -i(4n+1) \left[1 + \frac{2c^{\frac{1}{2}} u_1}{n! \Gamma(-n-\frac{1}{2})} (-1)^n e^{-\frac{1}{2} i \pi} \right], \quad (3.203)$$

and G is given by eqs. (3.167) through (3.183). GOODRICH and KAZARINOFF (1963) also give a physical interpretation, in terms of traveling waves, of the first term $n = 0$ of eq. (3.202) for $v_0 = 0$ and $v_0 = \frac{1}{2}\pi$.

3.4. Dipole sources

3.4.1. Electric dipoles

3.4.1.1. EXACT SOLUTIONS

For an arbitrarily oriented electric dipole located at $r_0 \equiv (\xi_0 \geq \xi_1, \eta_0, z_0)$ with moment $(4\pi\epsilon/k)\hat{c}$, the total electric field at $r \equiv (\xi, \eta, z)$ is:

$$E(r) = 4\pi k \mathcal{G}_e(r|r_0) \cdot \hat{c}, \quad (3.204)$$

where $\mathcal{G}_e(r|r_0)$ is the electric dyadic Green's function for the elliptic cylinder (TAI [1954]):

$$\begin{aligned} \mathcal{G}_e(r|r_0) = & \frac{i}{2\pi} \int_{-\infty}^{\infty} \frac{dt}{k^2 - t^2} \sum_{m=0}^{\infty} \left[\frac{1}{\Omega_m^{(e)}} \{ M_{em}^{(3)}(t, r) [M_{em}^{(1)}(-t, r_0) + a_{em} M_{em}^{(3)}(-t, r_0)] + \right. \\ & + N_{em}^{(3)}(t, r) [N_{em}^{(1)}(-t, r_0) + b_{em} N_{em}^{(3)}(-t, r_0)] \} + \\ & + \frac{1}{\Omega_m^{(o)}} \{ M_{om}^{(3)}(t, r) [M_{om}^{(1)}(-t, r_0) + a_{om} M_{om}^{(3)}(-t, r_0)] + \\ & \left. + N_{om}^{(3)}(t, r) [N_{om}^{(1)}(-t, r_0) + b_{om} N_{om}^{(3)}(-t, r_0)] \} \right], \quad \text{for } \xi > \xi_0, \quad (3.205) \end{aligned}$$

$$\begin{aligned} \mathcal{G}_e(r|r_0) = & \frac{i}{2\pi} \int_{-\infty}^{\infty} \frac{dt}{k^2 - t^2} \sum_{m=0}^{\infty} \left[\frac{1}{\Omega_m^{(e)}} \{ [M_{em}^{(1)}(t, r) + a_{em} M_{em}^{(3)}(t, r)] M_{em}^{(3)}(-t, r_0) + \right. \\ & + [N_{em}^{(1)}(t, r) + b_{em} N_{em}^{(3)}(t, r)] N_{em}^{(3)}(-t, r_0) \} + \\ & + \frac{1}{\Omega_m^{(o)}} \{ [M_{om}^{(1)}(t, r) + a_{om} M_{om}^{(3)}(t, r)] M_{om}^{(3)}(-t, r_0) + \\ & \left. + [N_{om}^{(1)}(t, r) + b_{om} N_{om}^{(3)}(t, r)] N_{om}^{(3)}(-t, r_0) \} \right], \quad \text{for } \xi < \xi_0, \quad (3.206) \end{aligned}$$

with

$$a_{em} = -\frac{Re_m^{(1)'(\gamma, \xi_1)}}{Re_m^{(3)'(\gamma, \xi_1)}}, \quad a_{om} = -\frac{Ro_m^{(1)'(\gamma, \xi_1)}}{Ro_m^{(3)'(\gamma, \xi_1)}}, \quad (3.207)$$

and the prime indicates the derivative with respect to ξ_1 ,

$$b_{em} = -\frac{Re_m^{(1)}(\gamma, \xi_1)}{Re_m^{(3)}(\gamma, \xi_1)}, \quad b_{om} = -\frac{Ro_m^{(1)}(\gamma, \xi_1)}{Ro_m^{(3)}(\gamma, \xi_1)}, \quad (3.208)$$

$$\Omega_m^{(e)} = \int_0^{2\pi} [Se_m(\gamma, \cos v)]^2 dv, \quad \Omega_m^{(o)} = \int_0^{2\pi} [So_m(\gamma, \cos v)]^2 dv, \quad (3.209)$$

$$\gamma = c\sqrt{1 - t^2/k^2}, \quad (3.210)$$

(therefore, in particular, $[\Omega_m^{(e), (o)}]_{t=0} = N_m^{(e), (o)}$),

$$M_{\epsilon_m}^{(j)}(t, r) = \frac{ke^{itz}}{c\sqrt{(\xi^2 - \eta^2)}} \left[\hat{u} Re_m^{(j)}(\gamma, \xi) \frac{\partial}{\partial v} Se_m(\gamma, \eta) - \hat{v} Se_m(\gamma, \eta) \frac{\partial}{\partial u} Re_m^{(j)}(\gamma, \xi) \right], \quad (3.211)$$

$$N_{\epsilon_m}^{(j)}(t, r) = \frac{ite^{itz}}{c\sqrt{(\xi^2 - \eta^2)}} \left[\hat{u} Se_m(\gamma, \eta) \frac{\partial}{\partial u} Re_m^{(j)}(\gamma, \xi) + \hat{v} Re_m^{(j)}(\gamma, \xi) \frac{\partial}{\partial v} Se_m(\gamma, \eta) \right] + \frac{k^2 - t^2}{k} e^{itz} \hat{z} Re_m^{(j)}(\gamma, \xi) Se_m(\gamma, \eta), \quad (3.212)$$

$j = 1$ or 3 , and the unit vectors \hat{u} and \hat{v} are given by:

$$\hat{u} = (\xi^2 - \eta^2)^{-1/2} (\sqrt{\xi^2 - 1} \cos v \hat{x} + \xi \sin v \hat{y}), \quad (3.213)$$

$$\hat{v} = (\xi^2 - \eta^2)^{-1/2} (\sqrt{\xi^2 - 1} \cos v \hat{y} - \xi \sin v \hat{x}). \quad (3.214)$$

In particular, for a longitudinal electric dipole at (ξ_0, η_0, z_0) with moment $(4\pi e/k)\hat{z}$, corresponding to an incident electric Hertz vector $(e^{ikR}/kR)\hat{z}$, the total electromagnetic field components can be derived from the total electric Hertz vector

$$\begin{aligned} \Pi_{\epsilon} = \Pi_{\epsilon} \hat{z} = \hat{z} \frac{2i}{k} \int_{-\infty}^{\infty} dt e^{it(z-z_0)} \sum_{m=0}^{\infty} \left\{ \frac{1}{\Omega_m^{(e)}} Re_m^{(3)}(\gamma, \xi_0) \right. \\ \times \left[Re_m^{(1)}(\gamma, \xi_0) - \frac{Re_m^{(1)}(\gamma, \xi_1)}{Re_m^{(3)}(\gamma, \xi_1)} Re_m^{(3)}(\gamma, \xi_0) \right] Se_m(\gamma, \eta_0) Se_m(\gamma, \eta) + \\ \left. + \frac{1}{\Omega_m^{(o)}} Ro_m^{(3)}(\gamma, \xi_0) \left[Ro_m^{(1)}(\gamma, \xi_0) - \frac{Ro_m^{(1)}(\gamma, \xi_1)}{Ro_m^{(3)}(\gamma, \xi_1)} Ro_m^{(3)}(\gamma, \xi_0) \right] So_m(\gamma, \eta_0) So_m(\gamma, \eta) \right\}, \end{aligned} \quad (3.215)$$

by the relations:

$$\begin{aligned} E_u = \frac{k}{c\sqrt{(\xi^2 - \eta^2)}} \frac{\partial^2 \Pi_{\epsilon}}{\partial u \partial z}, \quad E_v = \frac{k}{c\sqrt{(\xi^2 - \eta^2)}} \frac{\partial^2 \Pi_{\epsilon}}{\partial v \partial z}, \quad E_z = \left(\frac{\partial^2}{\partial z^2} + k^2 \right) \Pi_{\epsilon}, \\ H_u = -\frac{ik^2 Y}{c\sqrt{(\xi^2 - \eta^2)}} \frac{\partial \Pi_{\epsilon}}{\partial v}, \quad H_v = \frac{ik^2 Y}{c\sqrt{(\xi^2 - \eta^2)}} \frac{\partial \Pi_{\epsilon}}{\partial u}, \quad H_z = 0. \end{aligned} \quad (3.216)$$

On the surface $\xi = \xi_1$:

$$\begin{aligned} H_v = \frac{2ikY}{c\sqrt{(\xi_1^2 - \eta^2)}} \int_{-\infty}^{\infty} dt e^{it(z-z_0)} \sum_{m=0}^{\infty} \left\{ \frac{1}{\Omega_m^{(e)}} \frac{Re_m^{(3)}(\gamma, \xi_0)}{Re_m^{(3)}(\gamma, \xi_1)} Se_m(\gamma, \eta_0) Se_m(\gamma, \eta) + \right. \\ \left. + \frac{1}{\Omega_m^{(o)}} \frac{Ro_m^{(3)}(\gamma, \xi_0)}{Ro_m^{(3)}(\gamma, \xi_1)} So_m(\gamma, \eta_0) So_m(\gamma, \eta) \right\}. \end{aligned} \quad (3.217)$$

If the longitudinal dipole is on the surface ($\xi_0 = \xi_1$), the field is identically zero everywhere.

If the longitudinal dipole is at $(\xi_0, \eta_0, z_0 = 0)$, the total far field ($\xi \rightarrow \infty$) is:

$$\begin{aligned}
 E_\theta = & -2\sqrt{2\pi} \frac{e^{ikr}}{kr} k^2 \sin \theta \sum_{m=0}^{\infty} (-i)^m \left(\frac{1}{\bar{\Omega}_m^{(e)}} \left[\text{Re}_m^{(1)}(c \sin \theta, \xi_0) \dots \right. \right. \\
 & - \frac{\text{Re}_m^{(1)}(c \sin \theta, \xi_1)}{\text{Re}_m^{(3)}(c \sin \theta, \xi_1)} \text{Re}_m^{(3)}(c \sin \theta, \xi_0) \left. \right] \text{Se}_m(c \sin \theta, \eta_0) \text{Se}_m(c \sin \theta, \eta) + \\
 & + \frac{1}{\bar{\Omega}_m^{(o)}} \left[\text{Ro}_m^{(1)}(c \sin \theta, \xi_0) - \frac{\text{Ro}_m^{(1)}(c \sin \theta, \xi_1)}{\text{Ro}_m^{(3)}(c \sin \theta, \xi_1)} \text{Ro}_m^{(3)}(c \sin \theta, \xi_0) \right] \\
 & \times \text{So}_m(c \sin \theta, \eta_0) \text{So}_m(c \sin \theta, \eta), \quad (3.218)
 \end{aligned}$$

where

$$\bar{\Omega}_m^{(e), (o)} = [\Omega_m^{(e), (o)}]_{\gamma=c \sin \theta} \quad (3.219)$$

(therefore, in particular, $[\bar{\Omega}_m^{(e), (e)}]_{\theta=\frac{1}{2}\pi} = N_m^{(e), (o)}$), and r and θ are spherical polar coordinates; r is the distance of the observation point from the origin, and θ is the angle that the straight line from the dipole to the observation point forms with the z -axis. The shape of $|E_\theta|$ as a function of v has been computed by LUCKE [1951] for $\theta = \frac{1}{2}\pi$ and special values of the other parameters, and is shown in Fig. 3.28. Radiation patterns in the azimuthal plane $\theta = \frac{1}{2}\pi$ have been published by KOCHERZHEVSKI [1955] for longitudinal dipoles located at $v_0 = 0$ and $v_0 = \frac{1}{2}\pi$, with various values of c , ξ_1 and ξ_0 .

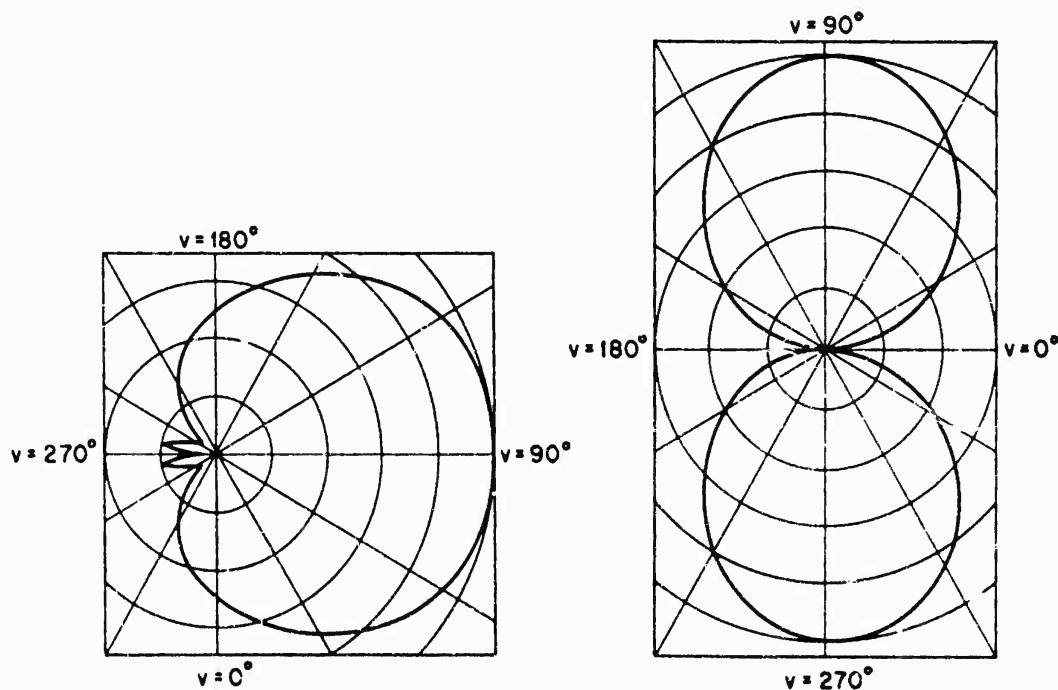


Fig. 3.28. Shape of the far field amplitude $|E_\theta|$ in the azimuthal plane $z = 0$, for a longitudinal electric dipole located at $(c\sqrt{\xi_0^2 - 1} = 1.50$; $v_0 = 90^\circ$; $z_0 = 0$), with $c\xi_1 = 1.12$ and axes ratio $\xi_1/\sqrt{\xi_1^2 - 1} = 2.24$ (LUCKE [1951]).

Fig. 3.29. Shape of the far field amplitude $|H_\theta|$ in the azimuthal plane $z = 0$, for a radial electric dipole located at $(\xi_0 = \xi_1$; $v_0 = 0$; $z_0 = 0$), with $c\xi_1 = 1.20$ and axes ratio $\xi_1/\sqrt{\xi_1^2 - 1} = 1.79$ (LUCKE [1951]).

The total electromagnetic field components for an electric dipole parallel to \hat{u} (radial dipole) or to \hat{v} (transverse or circumferential dipole) can be derived from the general result (3.204). The far field patterns may also be obtained from the results for plane wave incidence by using the reciprocity theorem (SINCLAIR [1951]).

The shape of the far field amplitude $|H_z|$ as a function of v in the azimuthal plane $z = z_0$ has been computed by LUCKE [1951] for a radial dipole at $(\xi_0 = \xi_1, v_0 = 0)$ and for a particular cylinder, and is shown in Fig. 3.29. A comparison between theoretical and experimental radiation patterns in the plane $z = z_0$ has been given by SINCLAIR [1951] for a radial dipole at $(\xi_0 = \xi_1, v_0 = 0 \text{ or } \frac{1}{2}\pi)$ with $c\xi_1 = 1.274\pi$, $c\sqrt{(\xi_1^2 - 1)} = 0.780\pi$, and a frequency of 1500 MHz. Radiation patterns in the azimuthal plane $z = z_0$ have been computed by KOCHERZHEVSKI [1955] for transverse dipoles located at $v_0 = 0$ and $v_0 = \frac{1}{2}\pi$, with various values of c , ξ_1 and ξ_0 .

3.4.1.2. LOW FREQUENCY APPROXIMATIONS

No specific results are available; however, low frequency expansions can be derived from the exact results of the previous section.

3.4.1.3. HIGH FREQUENCY APPROXIMATIONS

Although the geometrical and physical optics approximations to the scattered field are derivable by standard techniques, no specific results are available.

3.4.2. Magnetic dipoles

3.4.2.1. EXACT SOLUTIONS

For an arbitrarily oriented magnetic dipole located at $\mathbf{r}_0 \equiv (\xi_0, \eta_0, z_0)$ with moment $(4\pi/k)\hat{\mathbf{z}}$, the total magnetic field at $\mathbf{r} \equiv (\xi, \eta, z)$ is:

$$\mathbf{H}(\mathbf{r}) = 4\pi k \mathcal{G}_m(\mathbf{r}|\mathbf{r}_0) \cdot \hat{\mathbf{z}}, \quad (3.220)$$

where $\mathcal{G}_m(\mathbf{r}|\mathbf{r}_0)$ is the magnetic dyadic Green's function for the elliptic cylinder, which is related to the electric dyadic Green's function of eqs. (3.205) and (3.206) by (TAI [1954]):

$$\mathcal{G}_m(\mathbf{r}|\mathbf{r}_0) = \frac{1}{k^2} \nabla \wedge \{[\nabla_0 \wedge \mathcal{G}_e(\mathbf{r}_0|\mathbf{r})]^T\}; \quad (3.221)$$

here $\nabla_0 \wedge$ operates on \mathbf{r}_0 , and T indicates the transposed matrix.

In particular, for a longitudinal magnetic dipole at (ξ_0, η_0, z_0) with moment $(4\pi/k)\hat{\mathbf{z}}$, corresponding to an incident magnetic Hertz vector $(e^{ikR}/kR)\hat{\mathbf{z}}$, the total electromagnetic field components can be derived from the total magnetic Hertz vector

$$\begin{aligned} \Pi_m = \Pi_m^{\hat{\mathbf{z}}} = \hat{\mathbf{z}} \frac{2i}{k} \int_{-\infty}^{\infty} dt e^{it(z-z_0)} \sum_{m=0}^{\infty} \left\{ \frac{1}{\Omega_m^{(e)}} \operatorname{Re}_m^{(3)}(\gamma, \xi_0) \right. \\ \left. \times \left[\operatorname{Re}_m^{(1)}(\gamma, \xi_0) - \frac{\operatorname{Re}_m^{(1)}(\gamma, \xi_1)}{\operatorname{Re}_m^{(3)}(\gamma, \xi_1)} \operatorname{Re}_m^{(3)}(\gamma, \xi_0) \right] \operatorname{Se}_m(\gamma, \eta_0) \operatorname{Se}_m(\gamma, \eta) + \right. \end{aligned}$$

$$+ \frac{1}{\Omega_m^{(0)}} \text{Ro}_m^{(3)}(\gamma, \xi_0) \left[\text{Ro}_m^{(1)}(\gamma, \xi_0) - \frac{R_m^{(1)' }(\gamma, \xi_1)}{\text{Ro}_m^{(3)' }(\gamma, \xi_1)} \text{Ro}_m^{(3)}(\gamma, \xi_0) \right] \text{So}_m(\gamma, \eta_0) \text{So}_m(\gamma, \eta) \Bigg\}, \quad (3.222)$$

by the relations:

$$E_u = \frac{ik^2 Z}{c\sqrt{(\xi^2 - \eta^2)}} \frac{\partial \Pi_m}{\partial v}, \quad E_v = -\frac{ik^2 Z}{c\sqrt{(\xi^2 - \eta^2)}} \frac{\partial \Pi_m}{\partial u}, \quad E_z = 0, \quad (3.223)$$

$$H_u = \frac{k}{c\sqrt{(\xi^2 - \eta^2)}} \frac{\partial^2 \Pi_m}{\partial u \partial z}, \quad H_v = \frac{k}{c\sqrt{(\xi^2 - \eta^2)}} \frac{\partial^2 \Pi_m}{\partial v \partial z}, \quad H_z = \left(\frac{\partial^2}{\partial z^2} + k^2 \right) \Pi_m.$$

On the surface $\xi = \xi_1$:

$$H_v = -\frac{2i}{c\sqrt{(\xi_1^2 - \eta^2)}} \int_{-\infty}^{\infty} t dt e^{it(z-z_0)} \sum_{m=0}^{\infty} \left\{ \frac{1}{\Omega_m^{(e)}} \frac{\text{Re}_m^{(3)}(\gamma, \xi_0)}{(\partial/\partial u_1) \text{Re}_m^{(3)}(\gamma, \xi_1)} \right. \\ \left. \times \text{Se}_m(\gamma, \eta_0) \frac{\partial}{\partial v} \text{Se}_m(\gamma, \eta) + \frac{1}{\Omega_m^{(o)}} \frac{\text{Ro}_m^{(3)}(\gamma, \xi_0)}{(\partial/\partial u_1) \text{Ro}_m^{(3)}(\gamma, \xi_1)} \text{So}_m(\gamma, \eta_0) \frac{\partial}{\partial v} \text{So}_m(\gamma, \eta) \right\}, \quad (3.224)$$

$$H_z = -\frac{2}{k} \int_{-\infty}^{\infty} dt (k^2 - t^2) e^{it(z-z_0)} \sum_{m=0}^{\infty} \left\{ \frac{1}{\Omega_m^{(e)}} \frac{\text{Re}_m^{(3)}(\gamma, \xi_0)}{(\partial/\partial u_1) \text{Re}_m^{(3)}(\gamma, \xi_1)} \text{Se}_m(\gamma, \eta_0) \text{Se}_m(\gamma, \eta) + \right. \\ \left. + \frac{1}{\Omega_m^{(o)}} \frac{\text{Ro}_m^{(3)}(\gamma, \xi_0)}{(\partial/\partial u_1) \text{Ro}_m^{(3)}(\gamma, \xi_1)} \text{So}_m(\gamma, \eta_0) \text{So}_m(\gamma, \eta) \right\}. \quad (3.225)$$

If $z_0 = 0$, in the far field ($\xi \rightarrow \infty$):

$$E_v = 2\sqrt{2\pi} k^2 Z \sin \theta \frac{e^{ikr}}{kr} \sum_{m=0}^{\infty} (-i)^m \left\{ \frac{1}{\Omega_m^{(e)}} \left[\text{Re}_m^{(1)}(c \sin \theta, \xi_0) - \right. \right. \\ \left. \left. - \frac{\text{Re}_m^{(1)' }(c \sin \theta, \xi_1)}{\text{Re}_m^{(3)' }(c \sin \theta, \xi_1)} \text{Re}_m^{(3)}(c \sin \theta, \xi_0) \right] \text{Se}_m(c \sin \theta, \eta_0) \text{Se}_m(c \sin \theta, \eta) + \right. \\ \left. + \frac{1}{\Omega_m^{(o)}} \left[\text{Ro}_m^{(1)}(c \sin \theta, \xi_0) - \frac{\text{Ro}_m^{(1)' }(c \sin \theta, \xi_1)}{\text{Ro}_m^{(3)' }(c \sin \theta, \xi_1)} \text{Ro}_m^{(3)}(c \sin \theta, \xi_0) \right] \right. \\ \left. \times \text{So}_m(c \sin \theta, \eta_0) \text{So}_m(c \sin \theta, \eta) \right\}, \quad (3.226)$$

where $\bar{\Omega}_m^{(e),(o)}$ are given by eq. (3.219), and r and θ are spherical polar coordinates; r is the distance of the observation point from the origin, and θ is the angle that the straight line from the source point to the observation point forms with the z -axis. If the longitudinal dipole is on the surface ($\xi_0 = \xi_1$):

$$\Pi_m = -\frac{2}{k} \int_{-\infty}^{\infty} dt e^{it(z-z_0)} \sum_{m=0}^{\infty} \left\{ \frac{1}{\Omega_m^{(e)}} \frac{\text{Re}_m^{(3)}(\gamma, \xi)}{(\partial/\partial u_1) \text{Re}_m^{(3)}(\gamma, \xi_1)} \text{Se}_m(\gamma, \eta_0) \text{Se}_m(\gamma, \eta) + \right. \\ \left. + \frac{1}{\Omega_m^{(o)}} \frac{\text{Ro}_m^{(3)}(\gamma, \xi)}{(\partial/\partial u_1) \text{Ro}_m^{(3)}(\gamma, \xi_1)} \text{So}_m(\gamma, \eta_0) \text{So}_m(\gamma, \eta) \right\}, \quad (3.227)$$

and, in particular, in the far field ($\xi \rightarrow \infty$) with $z_0 = 0$:

$$E_v = 2i\sqrt{2\pi}k^2Z \sin \theta \frac{e^{ikr}}{kr} \sum_{m=0}^{\infty} (-i)^m \left\{ \frac{Se_m(c \sin \theta, \eta_0) Se_m(c \sin \theta, \eta)}{\Omega_m^{(e)}(\partial/\partial u_1) Re_m^{(3)}(c \sin \theta, \xi_1)} + \frac{So_m(c \sin \theta, \eta_0) So_m(c \sin \theta, \eta)}{\Omega_m^{(o)}(\partial/\partial u_1) Ro_m^{(3)}(c \sin \theta, \xi_1)} \right\}. \quad (3.228)$$

The total electromagnetic field components for a magnetic dipole parallel to $\hat{\theta}$ (radial dipole) or to $\hat{\phi}$ (transverse or circumferential dipole) can be derived from the general result (3.220). The far field patterns may also be obtained from the results for plane wave incidence by using the reciprocity theorem (SINCLAIR [1951]).

A comparison between theoretical and experimental radiation patterns in the plane $z = z_0$ has been given by SINCLAIR [1951] for a longitudinal and a transverse dipole at ($\xi_0 = \xi_1, \nu_0 = 0$) with $c\xi_1 = 1.274\pi$, $c\sqrt{(\xi_1^2 - 1)} = 0.780\pi$, and a frequency of 1500 MHz.

The equivalence between magnetic dipoles at $\xi_0 = \xi_1$ and slots is not discussed here; the reader interested in radiation from slots is referred, for example, to WAIT [1959] chapter 13.

3.4.2.2. LOW FREQUENCY APPROXIMATIONS

No specific results are available; however, low frequency expansions can be derived from the exact results of the previous section.

3.4.2.3. HIGH FREQUENCY APPROXIMATIONS

Although the geometrical and physical optics approximations to the scattered field are derivable by standard techniques, no specific results are available.

3.5. Point sources

3.5.1. Acoustically soft cylinder

3.5.1.1. EXACT SOLUTIONS

For a point source at ($\xi_0 \geq \xi_1, \eta_0, z_0$) such that

$$V^i = \frac{e^{ikR}}{kR}, \quad (3.229)$$

then

$$V^i + V^s = \frac{2i}{k} \int_{-\infty}^{\infty} dt e^{it(z-z_0)} \sum_{m=0}^{\infty} \left\{ \frac{1}{\Omega_m^{(e)}} Re_m^{(3)}(\gamma, \xi_>) \times \left[Re_m^{(1)}(\gamma, \xi_<) - \frac{Re_m^{(1)}(\gamma, \xi_1)}{Re_m^{(3)}(\gamma, \xi_1)} Re_m^{(3)}(\gamma, \xi_<) \right] Se_m(\gamma, \eta_0) Se_m(\gamma, \eta) + \frac{1}{\Omega_m^{(o)}} Ro_m^{(3)}(\gamma, \xi_>) \left[Ro_m^{(1)}(\gamma, \xi_<) - \frac{Ro_m^{(1)}(\gamma, \xi_1)}{Ro_m^{(3)}(\gamma, \xi_1)} Ro_m^{(3)}(\gamma, \xi_<) \right] So_m(\gamma, \eta_0) So_m(\gamma, \eta) \right\}, \quad (3.230)$$

where $\Omega_m^{(e), (o)}$ and γ are given by eqs. (3.209) and (3.210); observe that $(V^i + V^s)$ equals Π_e of eq. (3.215).

On the surface $\xi = \xi_1$:

$$\begin{aligned} \frac{\partial}{\partial u} (V^i + V^s) = & \frac{2}{k} \int_{-\infty}^{\infty} dt e^{it(z-z_0)} \sum_{m=0}^{\infty} \left\{ \frac{1}{\Omega_m^{(e)}} \frac{Re_m^{(3)}(\gamma, \xi_0)}{Re_m^{(3)}(\gamma, \xi_1)} Se_m(\gamma, \eta_0) Se_m(\gamma, \eta) + \right. \\ & \left. + \frac{1}{\Omega_m^{(o)}} \frac{Ro_m^{(3)}(\gamma, \xi_0)}{Ro_m^{(3)}(\gamma, \xi_1)} So_m(\gamma, \eta_0) So_m(\gamma, \eta) \right\}. \end{aligned} \quad (3.231)$$

If the point source is at $(\xi_0, \eta_0, z_0 = 0)$, the total far field ($\xi \rightarrow \infty$) is:

$$\begin{aligned} V^i + V^s = & 2\sqrt{2\pi} \frac{e^{ikr}}{kr} \sum_{m=0}^{\infty} (-i)^m \left\{ \frac{1}{\Omega_m^{(e)}} \left[Re_m^{(1)}(c \sin \theta, \xi_0) - \right. \right. \\ & \left. \left. - \frac{Re_m^{(1)}(c \sin \theta, \xi_1)}{Re_m^{(3)}(c \sin \theta, \xi_1)} Re_m^{(3)}(c \sin \theta, \xi_0) \right] Se_m(c \sin \theta, \eta_0) Se_m(c \sin \theta, \eta) + \right. \\ & \left. + \frac{1}{\Omega_m^{(o)}} \left[Ro_m^{(1)}(c \sin \theta, \xi_0) - \frac{Ro_m^{(1)}(c \sin \theta, \xi_1)}{Ro_m^{(3)}(c \sin \theta, \xi_1)} Ro_m^{(3)}(c \sin \theta, \xi_0) \right] \right. \\ & \left. \times So_m(c \sin \theta, \eta_0) So_m(c \sin \theta, \eta) \right\}, \end{aligned} \quad (3.232)$$

where $\bar{\Omega}_m^{(e), (o)}$ are given by eq. (3.219), and r and θ are spherical polar coordinates; r is the distance of the observation point from the origin, and θ is the angle that the straight line from the source point to the observation point forms with the z -axis.

If the point source is on the surface ($\xi_0 = \xi_1$), the total field is identically zero everywhere.

3.5.1.2. LOW FREQUENCY APPROXIMATIONS

No specific results are available; however, low frequency expansions can be derived from the exact results of the previous section.

3.5.1.3. HIGH FREQUENCY APPROXIMATIONS

Although the geometrical optics approximation to the scattered field is derivable by standard techniques, no specific results are available.

3.5.2. Acoustically hard cylinder

3.5.2.1. EXACT SOLUTIONS

For a point source at $(\xi_0 \geq \xi_1, \eta_0, z_0)$, such that

$$V^i = \frac{e^{ikR}}{kR}, \quad (3.233)$$

then

$$\begin{aligned}
V^i + V^s = & \frac{2i}{k} \int_{-\infty}^{\infty} dt e^{it(z-z_0)} \sum_{m=0}^{\infty} \left\{ \frac{1}{\Omega_m^{(e)}} \operatorname{Re}_m^{(3)}(\gamma, \xi_0) \right. \\
& \times \left[\operatorname{Re}_m^{(1)}(\gamma, \xi_0) - \frac{\operatorname{Re}_m^{(1)' }(\gamma, \xi_1)}{\operatorname{Re}_m^{(3)' }(\gamma, \xi_1)} \operatorname{Re}_m^{(3)}(\gamma, \xi_0) \right] \operatorname{Se}_m(\gamma, \eta_0) \operatorname{Se}_m(\gamma, \eta) + \\
& \left. + \frac{1}{\Omega_m^{(o)}} \operatorname{Ro}_m^{(3)}(\gamma, \xi_0) \left[\operatorname{Ro}_m^{(1)}(\gamma, \xi_0) - \frac{\operatorname{Ro}_m^{(1)' }(\gamma, \xi_1)}{\operatorname{Ro}_m^{(3)' }(\gamma, \xi_1)} \operatorname{Ro}_m^{(3)}(\gamma, \xi_0) \right] \operatorname{So}_m(\gamma, \eta_0) \operatorname{So}_m(\gamma, \eta) \right\},
\end{aligned} \quad (3.234)$$

where $\Omega_m^{(e), (o)}$ and γ are given by eqs. (3.209) and (3.210); observe that $(V^i + V^s)$ equals Π_m of eq. (3.222).

On the surface $\xi = \xi_1$:

$$\begin{aligned}
V^i + V^s = & -\frac{2}{k} \int_{-\infty}^{\infty} dt e^{it(z-z_0)} \sum_{m=0}^{\infty} \left\{ \frac{1}{\Omega_m^{(e)}} \frac{\operatorname{Re}_m^{(3)}(\gamma, \xi_0)}{(\partial/\partial u_1) \operatorname{Re}_m^{(3)}(\gamma, \xi_1)} \operatorname{Se}_m(\gamma, \eta_0) \operatorname{Se}_m(\gamma, \eta) + \right. \\
& \left. + \frac{1}{\Omega_m^{(o)}} \frac{\operatorname{Ro}_m^{(3)}(\gamma, \xi_0)}{(\partial/\partial u_1) \operatorname{Ro}_m^{(3)}(\gamma, \xi_1)} \operatorname{So}_m(\gamma, \eta_0) \operatorname{So}_m(\gamma, \eta) \right\}.
\end{aligned} \quad (3.235)$$

If $z_0 = 0$, the total far field ($\xi \rightarrow \infty$) is:

$$\begin{aligned}
V^i + V^s = & 2\sqrt{2\pi} \frac{e^{ikr}}{kr} \sum_{m=0}^{\infty} (-i)^m \left\{ \frac{1}{\Omega_m^{(e)}} \left[\operatorname{Re}_m^{(1)}(c \sin \theta, \xi_0) - \right. \right. \\
& - \frac{\operatorname{Re}_m^{(1)' }(c \sin \theta, \xi_1)}{\operatorname{Re}_m^{(3)' }(c \sin \theta, \xi_1)} \operatorname{Re}_m^{(3)}(c \sin \theta, \xi_0) \left. \right] \operatorname{Se}_m(c \sin \theta, \eta_0) \operatorname{Se}_m(c \sin \theta, \eta) + \\
& + \frac{1}{\Omega_m^{(o)}} \left[\operatorname{Ro}_m^{(1)}(c \sin \theta, \xi_0) - \frac{\operatorname{Ro}_m^{(1)' }(c \sin \theta, \xi_1)}{\operatorname{Ro}_m^{(3)' }(c \sin \theta, \xi_1)} \operatorname{Ro}_m^{(3)}(c \sin \theta, \xi_0) \right] \\
& \times \operatorname{So}_m(c \sin \theta, \eta_0) \operatorname{So}_m(c \sin \theta, \eta) \left. \right\}, \quad (3.236)
\end{aligned}$$

where $\bar{\Omega}_m^{(e), (o)}$ are given by eq. (3.219), and r and θ are spherical polar coordinates; r is the distance of the observation point from the origin, and θ is the angle that the straight line from the source point to the observation point forms with the z -axis.

If the point source is on the surface ($\xi_0 = \xi_1$):

$$\begin{aligned}
V^i + V^s = & -\frac{2}{k} \int_{-\infty}^{\infty} dt e^{it(z-z_0)} \sum_{m=0}^{\infty} \left\{ \frac{1}{\Omega_m^{(e)}} \frac{\operatorname{Re}_m^{(3)}(\gamma, \xi)}{(\partial/\partial u_1) \operatorname{Re}_m^{(3)}(\gamma, \xi_1)} \operatorname{Se}_m(\gamma, \eta_0) \operatorname{Se}_m(\gamma, \eta) + \right. \\
& \left. + \frac{1}{\Omega_m^{(o)}} \frac{\operatorname{Ro}_m^{(3)}(\gamma, \xi)}{(\partial/\partial u_1) \operatorname{Ro}_m^{(3)}(\gamma, \xi_1)} \operatorname{So}_m(\gamma, \eta_0) \operatorname{So}_m(\gamma, \eta) \right\}, \quad (3.237)
\end{aligned}$$

and, in particular, in the far field ($\xi \rightarrow \infty$) with $z_0 = 0$:

$$\begin{aligned}
V^i + V^s = & 2i\sqrt{2\pi} \frac{e^{ikr}}{kr} \sum_{m=0}^{\infty} (-i)^m \left\{ \operatorname{Se}_m(c \sin \theta, \eta_0) \operatorname{Se}_m(c \sin \theta, \eta) + \right. \\
& + \frac{\operatorname{So}_m(c \sin \theta, \eta_0) \operatorname{So}_m(c \sin \theta, \eta)}{\bar{\Omega}_m^{(o)} (\partial/\partial u_1) \operatorname{Ro}_m^{(3)}(c \sin \theta, \xi_1)} \left. \right\}. \quad (3.238)
\end{aligned}$$

3.5.2.2. LOW FREQUENCY APPROXIMATIONS

No specific results are available; however, low frequency expansions can be derived from the exact results of the previous section.

3.5.2.3. HIGH FREQUENCY APPROXIMATIONS

Although the geometrical optics approximation to the scattered field is derivable by standard techniques, no specific results are available.

Bibliography

- BARAKAT, R. [1963], Diffraction of Plane Waves by an Elliptic Cylinder, *J. Acoust. Soc. Am.* **35**, 1990–1996. Formulas (23) and (34) have a misprint.
- BARAKAT, R. [1969], Surface Currents on Perfectly Conducting Elliptic Cylinders in Plane-Wave Fields, to be published.
- BLANCH, G. [1964], Mathieu Functions, in: *Handbook of Mathematical Functions with Formulas, Graphs, and Mathematical Tables*, eds. M. Abramowitz and I. A. Stegun, 721–750, N.B.S. Applied Mathematics Series No. 55, U.S. Government Printing Office, Washington, D.C.
- BURKE, J. E. and V. TWERSKY [1960], On Scattering of Waves by an Elliptic Cylinder and by a Semi-Elliptic Protuberance on a Ground Plane, Sylvania Electronic Defense Laboratories Report EDL-M266, Mountain View, California.
- BURKE, J. E. and V. TWERSKY [1964], On Scattering of Waves by an Elliptic Cylinder and by a Semielliptic Protuberance on a Ground Plane, *J. Opt. Soc. Am.* **54**, 732–744.
- BURKE, J. E., E. J. CHRISTENSEN and S. B. LYTLE [1964], Scattering Patterns for Elliptic Cylinders, *J. Opt. Soc. Am.* **54**, 1065–1066.
- CLEMMOW, P. C. and V. H. WESTON [1961], Diffraction of a Plane Wave by an Almost Circular Cylinder, *Proc. Roy. Soc.* **A264**, 246–268.
- DINGLE, R. B. and H. J. W. MÜLLER [1962], Asymptotic Expansions of Mathieu Functions and their Characteristic Numbers, *J. Reine Angew. Math.* **211**, 11–32.
- GOODRICH, R. F. [1958], Studies in Radar Cross Sections XXVI – Fock Theory, The University of Michigan Research Institute Report No. 2591-3-T (ASTIA Document No. AD-160790), Ann Arbor, Michigan.
- GOODRICH, R. F. and N. D. KAZARINOFF [1963], Diffraction by Thin Elliptic Cylinders, *Michigan Math. J.* **10**, 105–127. A few formulas and Fig. 1 have misprints.
- HONG, S. and R. F. GOODRICH [1965], Application of Conformal Mapping to Scattering and Diffraction Problems presented at the URSI Symp. on Electromagnetic Wave Theory, Delft, the Netherlands; reprinted in: *Electromagnetic Wave Theory*, ed. J. Brown, 907–914, Pergamon Press, London.
- KAZARINOFF, N. D. and R. K. RIFT [1959], Scalar Diffraction by an Elliptic Cylinder, *IRE Trans.* **AP-7**, S21–S27.
- KELLER, J. B. [1956], Diffraction by a Convex Cylinder, *IRE Trans.* **AP-4**, 312–321. Formula (25) has a misprint.
- KELLER, J. B. and B. R. LEVY [1959], Decay Exponents and Diffraction Coefficients for Surface Waves on Surfaces of Nonconstant Curvature, *IRE Trans.* **AP-7**, S52–S61. A few formulas have misprints.
- KING, R. W. P. and T. T. WU [1959], *The Scattering and Diffraction of Waves*, Harvard University Press, Cambridge, Mass.
- KOCHERZHEVSKI, G. N. [1955], Radiation of Electric Dipoles Situated Near a Perfectly Conducting Elliptic Cylinder, *Zh. Tekhn. Fiz.* **25**, 1140–1154. A 90° rotation of the radiation pattern with respect to the figure caption occurs in Figs. 6, 11, 12 and 13.

- LEVY, B. R. [1960], Diffraction by an Elliptic Cylinder, *J. Math. Mech.* **9**, 147-165.
- LUCKE, W. S. [1951], Electric Dipoles in the Presence of Elliptic and Circular Cylinders, *J. Appl. Phys.* **22**, 14-19.
- MANDRAZHI, V. P. [1962], Properties of the Current Density Distribution at the Surface of a Thin Strip and of an Elliptic Cylinder in the Diffraction of Cylindrical Electromagnetic Waves, *Telecommunications and Radio Engineering*, 33-46.
- MÜLLER, H. J. W. [1962], On Asymptotic Expansions of Mathieu Functions, *J. Reine Angew. Math.* **211**, 179-190.
- National Bureau of Standards [1951], *Tables Relating to Mathieu Functions*, Columbia University Press, New York.
- NOBLE, B. [1962], Integral Equation Perturbation Methods in Low-Frequency Diffraction, in: *Electromagnetic Waves*, ed. R. E. Langer, 323-360, University of Wisconsin Press, Madison, Wis.
- ROBIN, L. [1965], Diffraction d'une onde électromagnétique plane par un cylindre elliptique parfaitement conducteur. Cas où la longueur d'onde est petite par rapport à la distance focale de l'ellipse de section droite, *C. R. Acad. Sci. Paris* **260**, 435-438.
- SHARPLES, A. [1967], Uniform Asymptotic Forms of Modified Mathieu Functions, *Quart. J. Mech. Appl. Math.* **20**, 365-380.
- SINCLAIR, G. [1951], The Patterns of Antennas located near Cylinders of Elliptical Cross Section, *Proc. IRE* **39**, 660-668.
- STRATTON, J. A. [1941], *Electromagnetic Theory*, McGraw-Hill Book Company, New York.
- STRATTON, J. A., P. M. MORSE, L. J. CHU and R. A. HUTNER [1941], *Elliptic Cylinder and Spheroidal Wave Functions*, John Wiley and Sons, Inc., New York.
- STRUTT, J. W., Lord Rayleigh [1897], On the incidence of Aerial and Electric Waves upon Small Obstacles in the Form of Ellipsoids or Elliptic Cylinders, and on the Passage of Electric Waves through a Circular Aperture in a Conducting Screen, *Philos. Mag.* **44**, 28-52.
- TAI, C. T. [1954], A Glossary of Dyadic Green's Functions, Stanford Research Institute Technical Report No. 46, Stanford, California. Formula (16) is misprinted.
- UDAGAWA, K. and Y. MIYAZAKI [1965], Diffraction of a Plane Wave by a Perfectly Conducting Elliptic Cylinder - A Study by Conformal Mapping Technique, *J. Inst. Elec. Comm. Engrs. Japan* **48**, 43-53.
- VAN BLADEL, J. [1963], Low-Frequency Scattering by Cylindrical Bodies, *Appl. Sci. Res.* **B10**, 195-202.
- WAIT, J. R. [1959], *Electromagnetic Radiation from Cylindrical Structures*, Pergamon Press, New York.
- WEINSTEIN, L. A. and A. A. FEDOROV [1961], Scattering of Plane and Cylindrical Waves on an Elliptical Cylinder and Conception of Diffraction of Rays, *Radio Eng. Electron. (USSR)* **6**, 41-64 (translated from *Radiotekhn. i Elektron.*).
- WETZEL, L. [1957], High-Frequency Current Distributions on Conducting Obstacles, Cruft Laboratory Scientific Report No. 10 (ASTIA Document No. AD-117101), Harvard University, Cambridge, Mass.
- WETZEL, L. and D. B. BRICK [1960], An Experimental Investigation of the Fock Approximation for Conducting Cylinders, *IRE Trans.* **AP-8**, 599-602.
- WILSE, J. C. and M. J. KING [1958a], Values of the Mathieu Functions, The Johns Hopkins University Radiation Laboratory Technical Report AF-53, Baltimore, Maryland.
- WILSE, J. C. and M. J. KING [1958b], Derivatives, Zeros, and Other Data Pertaining to Mathieu Functions, The Johns Hopkins University Radiation Laboratory Technical Report AF-57, Baltimore, Maryland.
- WU, T. T. [1956], High Frequency Scattering, *Phys. Rev.* **104**, 1201-1212.

CHAPTER 4

THE STRIP

J. S. ASVESTAS and R. E. KLEINMAN

The strip is the limit of an elliptic cylinder as the eccentricity tends to unity and, as such, the exact results for the elliptic cylinder apply directly. Because the strip is the simplest shape which exhibits multiple diffraction by (or mutual coupling between) edges, it has been the object of intensive study (e.g. BOUWKAMP [1954]; HÖNL et al. [1961]; KELLER and HANSEN [1965]). Of the many attempts to achieve a closed form solution comparable to the elegant integral representations for solutions of the half plane problem, none has been successful to date.

4.1. Strip geometry and preliminary considerations

The strip, of width d , is defined in terms of rectangular Cartesian coordinates (x, y, z) as $y = 0$, $|x| \leq \frac{1}{2}d$. The edges are therefore parallel to the z -axis. In terms

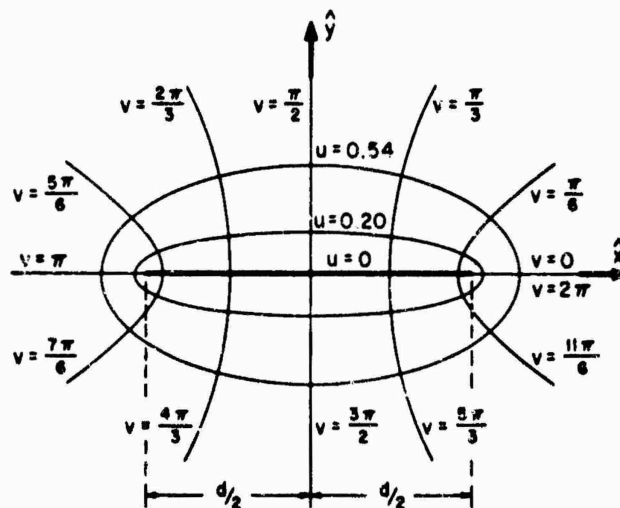


Fig. 4.1. Geometry for the strip.

of the elliptic cylindrical coordinates (u, v, z) shown in Fig. 4.1 and related to the rectangular Cartesian coordinates (x, y, z) by

$$\begin{aligned} x &= \frac{1}{2}d \cosh u \cos v, \\ y &= \frac{1}{2}d \sinh u \sin v, \\ z &= z, \end{aligned} \quad (4.1)$$

where $0 \leq u < \infty$, $0 \leq v < 2\pi$ and $-\infty < z < \infty$, the strip is the coordinate surface $u = 0$; $0 < v < \pi$ designates the upper face and $\pi < v < 2\pi$ designates the lower. Instead of u and v , it is often convenient to use the quantities

$$\xi = \cosh u, \quad \eta = \cos v, \quad (4.2)$$

with $1 \leq \xi < \infty$ and $-1 \leq \eta \leq 1$. In addition to the circular cylindrical coordinates (ρ, ϕ, z) , used for expressing the far field behavior ($u \rightarrow \infty, v \rightarrow \phi$, and $\frac{1}{2}d \sinh u \sim \frac{1}{2}d \cosh u \sim \rho$), it sometimes proves convenient to introduce a pair of cylindrical coordinates with origins at the edges of the strip (see Section 4.2.1.3).

The primary source is a plane wave propagating in the plane perpendicular to the z -axis and in a direction making an angle $\pi + \phi_0$ with the positive x -axis, or a line source parallel to the z -axis and located at (ρ_0, ϕ_0) [or (u_0, v_0) or (x_0, y_0)] or a point or dipole source located at (ρ_0, ϕ_0, z_0) [or (u_0, v_0, z_0)]. For convenience and without loss of generality it is assumed that $0 \leq \phi_0 \leq \frac{1}{2}\pi$.

The elliptic cylinder coordinates and Mathieu function notation are the same as employed in Chapter 3 and discussed in Section 3.1. This discussion will not be repeated here except to note that the parameter c is the product of wave number and half strip width, i.e.

$$c = \frac{1}{2}kd.$$

The results presented for the perfectly conducting strip for plane wave or line source excitation may be used to obtain the fields scattered by a slit (of width equal to that of the strip) in a perfectly conducting infinite screen through Babinet's principle (see Introduction).

It has been the experience of the authors that errors in transforming formulae for the strip are minimized by avoiding the use of trigonometric identities involving half angles. Thus, $\sqrt{1 + \cos \phi}$ appears consistently in place of $\sqrt{2}|\cos \frac{1}{2}\phi|$, and this is in contrast to the terminology adopted in Chapter 8.

4.2. Plane wave incidence

4.2.1 *E*-polarization

4.2.1.1. EXACT SOLUTIONS

For a plane wave whose direction of propagation is perpendicular to the z -axis, and forms the angle ϕ_0 with the negative x -axis and the angle $(\frac{1}{2}\pi - \phi_0)$ with the negative y -axis ($0 \leq \phi_0 \leq \frac{1}{2}\pi$), such that

$$\begin{aligned} E^i &= \hat{z} \exp \{ -ik(x \cos \phi_0 + y \sin \phi_0) \}, \\ H^i &= Y(-\sin \phi_0 \hat{x} + \cos \phi_0 \hat{y}) \exp \{ -ik(x \cos \phi_0 + y \sin \phi_0) \}, \end{aligned} \quad (4.3)$$

the scattered electric field is:

$$E_z^s = -\sqrt{8\pi} \sum_{m=0}^{\infty} \frac{(-i)^m}{N_m^{(c)}} \frac{Re_m^{(1)}(c, 1)}{Re_m^{(3)}(c, 1)} Re_m^{(3)}(c, \xi) Sc_m(c, \cos \phi_0) Sc_m(c, \eta). \quad (4.4)$$

An alternate expression for the scattered field is (GRINBERG [1958]):

$$E_z^s(x, y) = \begin{cases} \frac{1}{2i} \frac{\partial}{\partial y} \left\{ \int_{-\infty}^{-\frac{1}{2}d} E_z^s(\gamma, 0) H_0^{(1)}(kR) d\gamma + \int_{\frac{1}{2}d}^{\infty} E_z^s(\gamma, 0) H_0^{(1)}(kR) d\gamma - \right. \\ \left. - \int_{-\frac{1}{2}d}^{\frac{1}{2}d} e^{-ik\gamma \cos \phi_0} H_0^{(1)}(kR) d\gamma \right\}, & \text{for } y \geq 0, \\ E_z^s(x, -y), & \text{for } y \leq 0, \end{cases} \quad (4.5)$$

where

$$R = \sqrt{\{(x-\gamma)^2 + y^2\}}, \quad (4.6)$$

$$E_z^s(x, 0) = \begin{cases} \frac{1}{2} e^{ikx} \sqrt{\frac{2x}{d} - 1} \left[\omega_+ \left(\frac{2x}{d} - 1 \right) + \omega_- \left(\frac{2x}{d} - 1 \right) \right], & \text{for } x \geq \frac{1}{2}d, \\ \frac{1}{2} e^{-ikx} \sqrt{-\frac{2x}{d} - 1} \left[\omega_+ \left(-\frac{2x}{d} - 1 \right) - \omega_- \left(-\frac{2x}{d} - 1 \right) \right], & \text{for } x \leq -\frac{1}{2}d, \end{cases} \quad (4.7)$$

$$\omega_{\pm}(\tau) = \lim_{n \rightarrow \infty} \omega_{\pm}^{(n)}(\tau), \quad (\tau \geq 0), \quad (4.8)$$

with

$$\omega_{\pm}^{(0)}(\tau) = -\frac{1}{\pi} \int_{-1}^1 \frac{e^{ic\rho} [e^{ic\rho \cos \phi_0} \pm e^{-ic\rho \cos \phi_0}]}{(\tau + \rho + 1)\sqrt{(\rho + 1)}} d\rho, \quad (4.9)$$

and

$$\omega_{\pm}^{(n)}(\tau) = \omega_{\pm}^{(0)}(\tau) \pm \frac{e^{2ic}}{\pi} \int_0^{\infty} \frac{e^{2ic\rho} \sqrt{\rho} \omega_{\pm}^{(n-1)}(\rho) d\rho}{(\tau + \rho + 2)\sqrt{(\rho + 2)}}, \quad (n \geq 1). \quad (4.10)$$

On the portions of the $y = 0$ plane not occupied by the strip, the scattered electric field is given by eq. (4.7), whereas the scattered magnetic field is zero. On the strip ($u = 0$) the total magnetic field is:

$$H_v = -\text{sgn}(\sin v) H_x \\ = \frac{Y}{c} \sqrt{\frac{8\pi}{1-\eta^2}} \sum_{m=0}^{\infty} (-i)^m \left[\frac{Se_m(c, \cos \phi_0) Se_m(c, \eta)}{N_m^{(e)} Re_m^{(3)}(c, 1)} + \frac{So_m(c, \cos \phi_0) So_m(c, \eta)}{N_m^{(o)} Ro_m^{(3)}(c, 1)} \right]. \quad (4.11)$$

In the far field ($\xi \rightarrow \infty$):

$$P = -2\pi \sum_{m=0}^{\infty} \frac{(-1)^m Re_m^{(1)}(c, 1)}{N_m^{(e)} Re_m^{(3)}(c, 1)} Se_m(c, \cos \phi_0) Se_m(c, \eta). \quad (4.12)$$

WATERMAN [1963] has computed $|P|^2$ and $\arg P$ as functions of ϕ for $\phi_0 = \frac{1}{4}\pi$ with $c = 1, 2, 5$ and 10 . Typical results are shown in Fig. 4.2.

The total scattering cross section per unit length is:

$$\sigma_T = \frac{8\pi}{k} \sum_{m=0}^{\infty} \frac{1}{N_m^{(e)}} \left| \frac{Re_m^{(1)}(c, 1)}{Re_m^{(3)}(c, 1)} Se_m(c, \cos \phi_0) \right|^2, \quad (4.13)$$

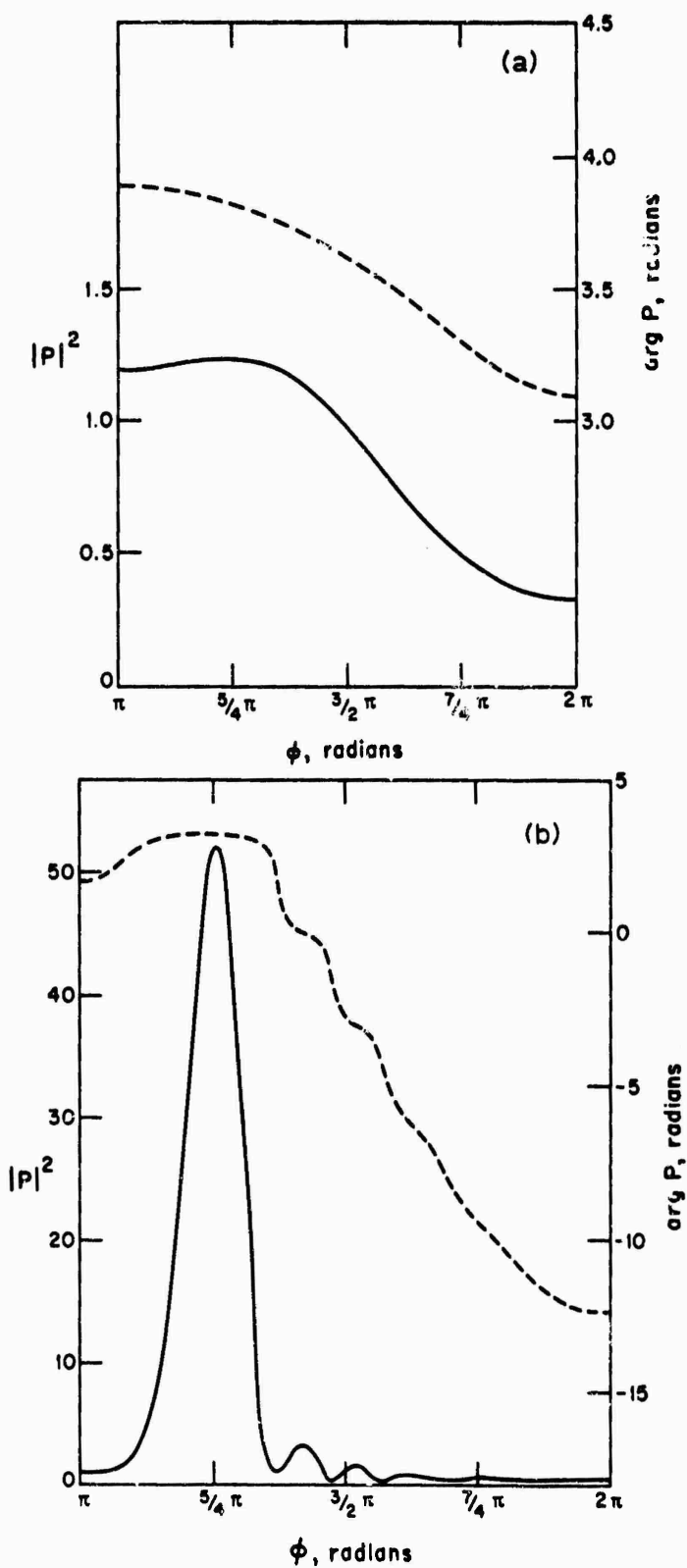


Fig. 4.2. Far field amplitude (—) and phase (---) as a function of ϕ for E -polarization with $\phi_0 = \frac{1}{4}\pi$ (WATERMAN [1963]); (a) $c = 1$, (b) $c = 10$.

and some numerical results based on this formula are shown in Fig. 4.3.

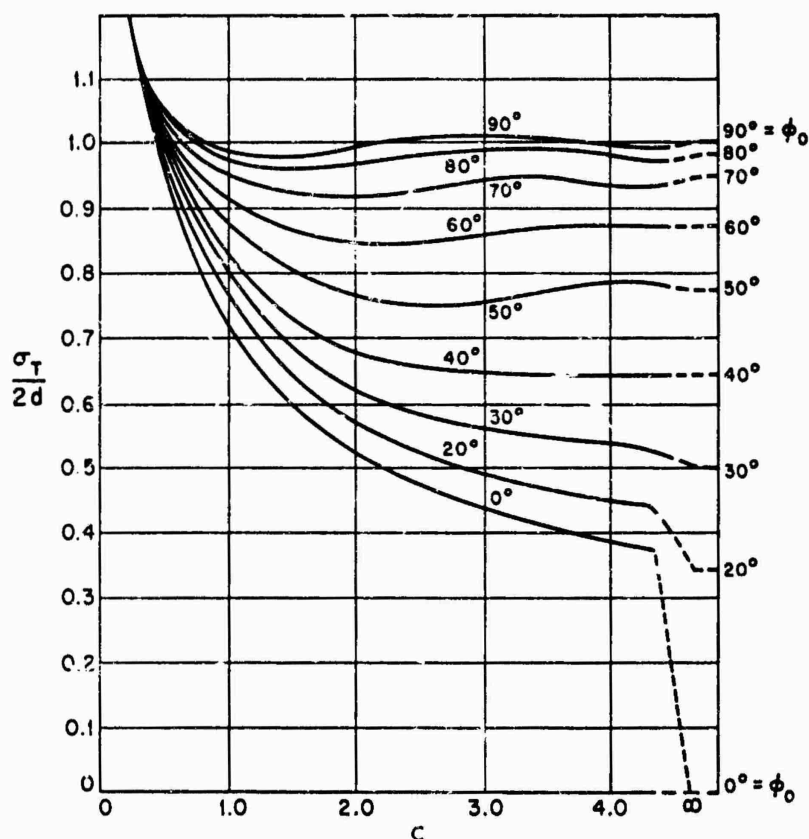


Fig. 4.3. Normalized total scattering cross section per unit length as a function of c for E -polarization (MORSE and RUBENSTEIN [1938]).

At grazing incidence ($\phi_0 = 0$):

$$E_z^s = -\sqrt{8\pi} \sum_{m=0}^{\infty} \frac{(-i)^m}{N_m^{(e)}} \frac{\text{Re}_m^{(1)}(c, 1)}{\text{Re}_m^{(3)}(c, 1)} \text{Re}_m^{(3)}(c, \xi) \text{Se}_m(c, \eta), \quad (4.14)$$

and on the strip ($u = 0$):

$$H_v = \frac{Y}{c} \sqrt{\frac{8\pi}{1-\eta^2}} \sum_{m=0}^{\infty} \frac{(-i)^m}{N_m^{(e)} \text{Re}_m^{(3)}(c, 1)} \text{Se}_m(c, \eta). \quad (4.15)$$

MANDRAZHI [1962] has plotted the amplitude and phase of the surface current density for $c = \frac{1}{2}, \sqrt{2}, 2$ and $2\sqrt{2}$. The normalized amplitude of H_v has been computed as a function of v for $c = 1$ by BARAI ET [1969] and is shown in Fig. 4.4.

In the far field ($\xi \rightarrow \infty$):

$$P = -2\pi \sum_{m=0}^{\infty} \frac{(-1)^m}{N_m^{(e)}} \frac{\text{Re}_m^{(1)}(c, 1)}{\text{Re}_m^{(3)}(c, 1)} \text{Se}_m(c, \eta). \quad (4.16)$$

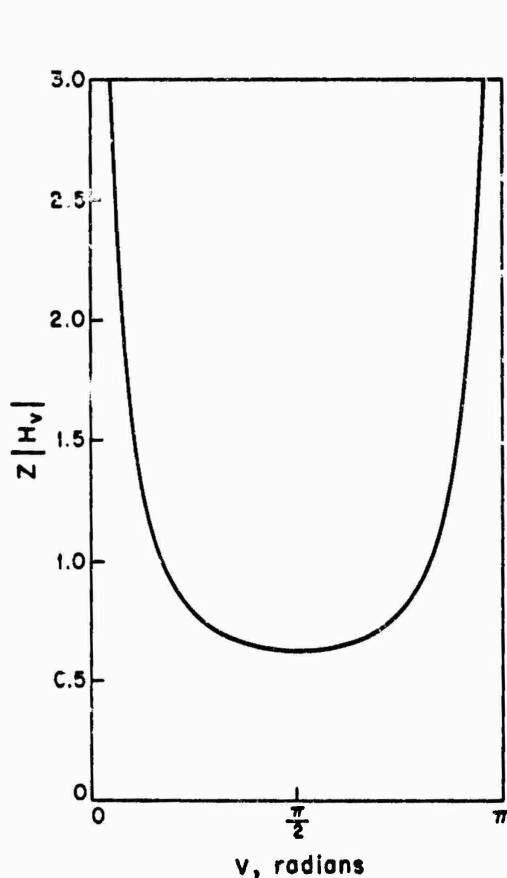


Fig. 4.4. Normalized amplitude of the surface field for E -polarization with $\phi_0 = 0$ and $c = 1$ (BARAKAT [1969]).

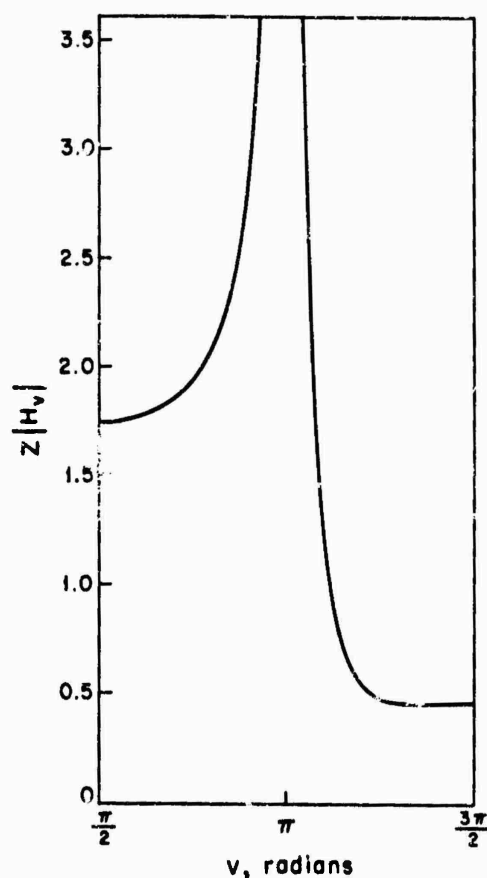


Fig. 4.5. Normalized amplitude of the surface field for E -polarization with $\phi_0 = \frac{1}{2}\pi$ and $c = 1$ (BARAKAT [1969]).

The total scattering cross section per unit length is:

$$\sigma_T = \frac{8\pi}{k} \sum_{m=0}^{\infty} \frac{1}{N_m^{(\epsilon)}} \left| \frac{\text{Re}_m^{(1)}(c, 1)}{\text{Re}_m^{(3)}(c, 1)} \right|^2, \quad (4.17)$$

and some numerical results based on this formula are shown in Fig. 4.3.

For broadside incidence ($\phi_0 = \frac{1}{2}\pi$):

$$E_z = -\sqrt{8\pi} \sum_{m=0}^{\infty} \frac{(-1)^m \text{Se}_{2m}(c, 0)}{N_{2m}^{(\epsilon)}} \frac{\text{Re}_{2m}^{(1)}(c, 1)}{\text{Re}_{2m}^{(3)}(c, 1)} \text{Re}_{2m}^{(3)}(c, \xi) \text{Se}_{2m}(c, \eta), \quad (4.18)$$

and on the strip ($u = 0$):

$$H_v = \frac{Y}{c} \sqrt{\frac{8\pi}{1-\eta^2}} \sum_{m=0}^{\infty} (-1)^m \left[\frac{\text{Se}_{2m}(c, 0)}{N_{2m}^{(\epsilon)} \text{Re}_{2m}^{(3)}(c, 1)} \text{Se}_{2m}(c, \eta) - \right. \\ \left. -i \frac{\text{So}_{2m+1}(c, 0)}{N_{2m+1}^{(\text{o})} \text{Ro}_{2m+1}^{(3)}(c, 1)} \text{So}_{2m+1}(c, \eta) \right] \quad (4.19)$$

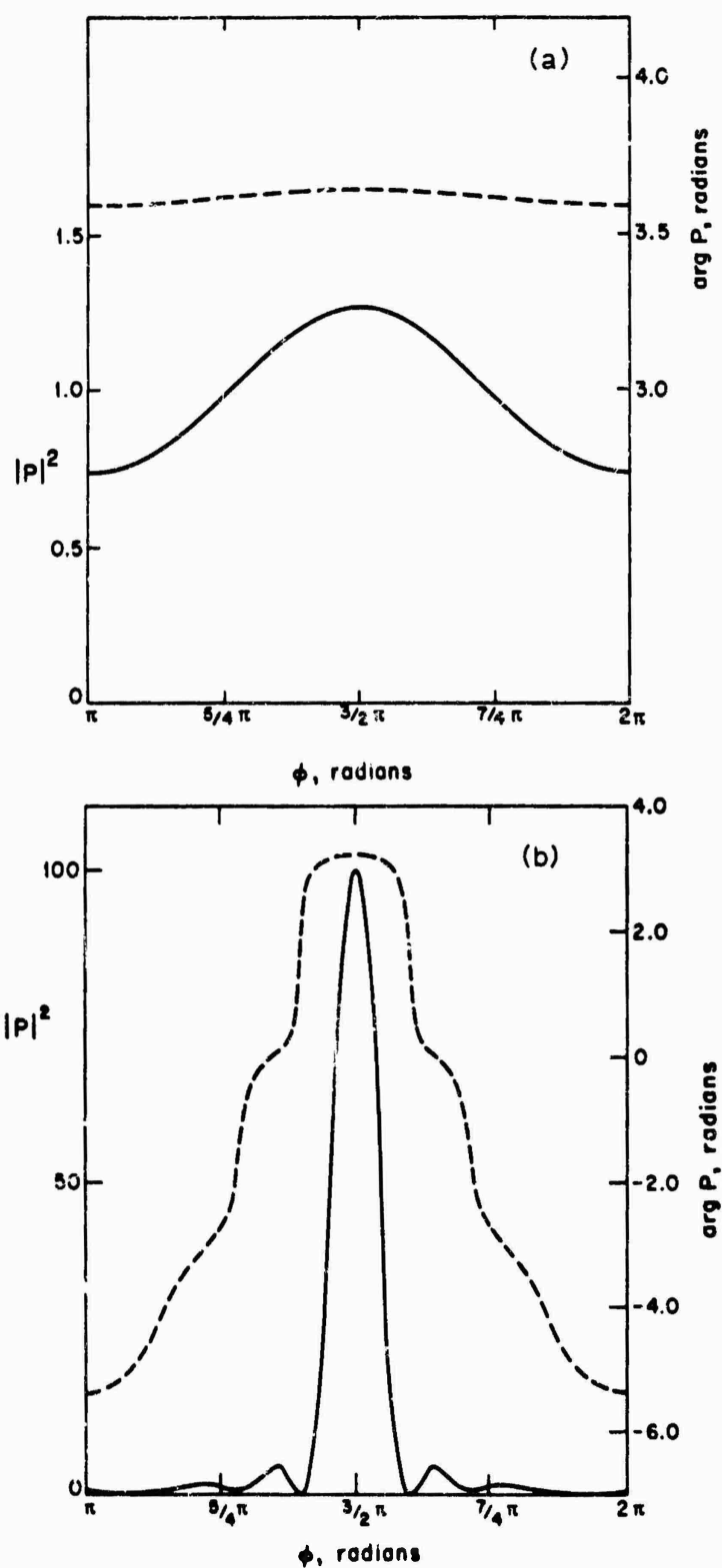


Fig. 4.6. Far field amplitude (—) and phase (---) as functions of ϕ for E-polarization with $\phi_0 = \frac{1}{2}\pi$ (WATERMAN [1963]); (a) $c = 1$, (b) $c = 10$.

MANDRAZHI [1962] has plotted the amplitude of the surface current density for $c = \frac{4}{3}$, and the phase for $c = \frac{4}{3}, \sqrt{2}, 2$ and $2\sqrt{2}$. BARAKAT [1969] has computed the normalized amplitude of H_v as a function of v for $c = 1$ and the results are shown in Fig. 4.5.

In the far field ($\xi \rightarrow \infty$):

$$P = -2\pi \sum_{m=0}^{\infty} \frac{Se_{2m}(c, 0)Re_{2m}^{(1)}(c, 1)}{N_{2m}^{(e)} Re_{2m}^{(3)}(c, 1)} Se_{2m}(c, \eta). \quad (4.20)$$

WATERMAN [1963] has computed $|P|^2$ and $\arg P$ as functions of ϕ for $\phi_0 = \frac{1}{2}\pi$ with $c = 1, 2, 5$ and 10 . Typical results are shown in Fig. 4.6.

The total scattering cross section per unit length is:

$$\sigma_T = \frac{8\pi}{k} \sum_{m=0}^{\infty} \frac{1}{N_{2m}^{(e)}} \left| \frac{Re_{2m}^{(1)}(c, 1)}{Re_{2m}^{(3)}(c, 1)} Se_{2m}(c, 0) \right|^2, \quad (4.21)$$

and some numerical results based on this formula are shown in Fig. 4.3.

4.2.1.2. LOW FREQUENCY APPROXIMATIONS

For a plane wave whose direction of propagation is perpendicular to the z -axis, and forms an angle ϕ_0 with the negative x -axis and an angle $(\frac{1}{2}\pi - \phi_0)$ with the negative y -axis ($0 \leq \phi_0 \leq \frac{1}{2}\pi$), such that

$$\begin{aligned} E^i &= \hat{z} \exp \{-ik(x \cos \phi_0 + y \sin \phi_0)\}, \\ H^i &= Y(-\sin \phi_0 \hat{x} + \cos \phi_0 \hat{y}) \exp \{-ik(x \cos \phi_0 + y \sin \phi_0)\}, \end{aligned} \quad (4.22)$$

low frequency expansions have been obtained either directly (STRUTT [1897a,b, 1913]; MILES [1949]; JONL and ZIMMER [1953]; MÜLLER and WESTPFAHL [1953]; SOMMERFELD [1954]; BOUWKAMP [1954]; DE HOOP [1955]; PIMENOV [1959]; MILLAR [1960]) or by expansion of the Mathieu functions appearing in the exact series solution (JONES and NOBLE [1961]; BURKE and TWERSKY [1964]; BURKE et al. [1964]).

For arbitrary incidence the total magnetic field on the strip ($u = 0$) is (MILLAR [1960]):

$$\begin{aligned} H_x &= -\operatorname{sgn}(\sin v)H_v \\ &= -Y \sin \phi_0 \exp \{-ic \cos v \cos \phi_0\} + \frac{iY}{c \sin v} \left[\sum_{n=0}^6 f_n c^n + o(c^6) \right], \end{aligned} \quad (4.23)$$

where

$$p = \log \frac{1}{2}c + \gamma - \frac{1}{2}i\pi, \quad (4.24)$$

$\gamma = 0.5772157 \dots$ is Euler's constant,

and

$$f_0 = \frac{1}{p} \quad (4.25)$$

$$f_1 = i \cos \phi_0 \cos v, \quad (4.26)$$

$$f_2 = \frac{\sin^2 \phi_0}{4p} + \frac{1}{2} \left[\cos^2 \phi_0 - \frac{1}{2} \left(1 + \frac{1}{2p} \right) \right] \cos 2v, \quad (4.27)$$

$$f_3 = -\frac{1}{4}i \left[\frac{1}{2} \cos^3 \phi_0 - (p + \frac{1}{4}) \cos \phi_0 \right] \cos v - \frac{1}{8}i \left[\cos^3 \phi_0 - \frac{1}{2} \cos \phi_0 \right] \cos 3v, \quad (4.28)$$

$$\begin{aligned} f_4 = & \frac{\cos^4 \phi_0}{64p} + \frac{1}{32} \left(1 - \frac{3}{2p} \right) \cos^2 \phi_0 + \frac{1}{128} \left(\frac{1}{p^2} + \frac{3}{2p} - 2 \right) + \\ & + \frac{1}{8} \left[-\frac{1}{3} \cos^4 \phi_0 + \frac{1}{2} \left(\frac{1}{3} + \frac{1}{2p} \right) \cos^2 \phi_0 + \frac{1}{2} \left(\frac{1}{3} - \frac{1}{2p} \right) \right] \cos 2v + \\ & + \frac{1}{48} \left[-\cos^4 \phi_0 + \frac{1}{2} \cos^2 \phi_0 + \frac{1}{8} \left(1 + \frac{3}{4p} \right) \right] \cos 4v, \end{aligned} \quad (4.29)$$

$$\begin{aligned} f_5 = & \frac{1}{15}i \left[\frac{1}{3} \cos^5 \phi_0 - \frac{1}{2} (p + \frac{1}{3}) \cos^3 \phi_0 + (p^2 - \frac{1}{4}p + \frac{1}{48}) \cos \phi_0 \right] \cos v + \\ & + \frac{1}{128}i \left[\cos^5 \phi_0 - \frac{1}{2} \cos^3 \phi_0 - (p + \frac{3}{8}) \cos \phi_0 \right] \cos 3v + \\ & + \frac{1}{384}i \left[\cos^5 \phi_0 - \frac{1}{2} \cos^3 \phi_0 - \frac{1}{8} \cos \phi_0 \right] \cos 5v, \end{aligned} \quad (4.30)$$

$$\begin{aligned} f_6 = & -\frac{\cos^6 \phi_0}{2304p} - \frac{1}{384} \left(1 - \frac{1}{p} \right) \cos^4 \phi_0 + \frac{1}{768} \left(1 + \frac{3}{4p} - \frac{3}{2p^2} \right) \cos^2 \phi_0 + \\ & + \frac{1}{768} \left(1 - \frac{29}{12p} + \frac{3}{2p^2} \right) + \\ & + \frac{1}{256} \left[\frac{1}{3} \cos^6 \phi_0 - \frac{1}{2} \left(\frac{1}{p} + \frac{1}{3} \right) \cos^4 \phi_0 + \left(p - \frac{49}{24} + \frac{3}{2p} \right) \cos^2 \phi_0 - \right. \\ & \left. - \frac{1}{2} \left(p - \frac{13}{8} + \frac{5}{16p} + \frac{1}{2p^2} \right) \right] \cos 2v + \\ & + \frac{1}{64} \left[\frac{1}{15} \cos^6 \phi_0 - \frac{1}{30} \cos^4 \phi_0 - \right. \\ & \left. - \frac{1}{32} \left(\frac{1}{p} + \frac{4}{15} \right) \cos^2 \phi_0 + \frac{1}{32} \left(\frac{1}{p} - \frac{4}{5} \right) \right] \cos 4v + \\ & + \frac{1}{3840} \left[\cos^6 \phi_0 - \frac{1}{2} \cos^4 \phi_0 - \frac{1}{8} \cos^2 \phi_0 - \frac{5}{96p} - \frac{1}{16} \right] \cos 6v. \end{aligned} \quad (4.31)$$

In the far field ($\xi \rightarrow \infty$) and for arbitrary incidence (MILLAR [1960]):

$$F = i\pi \sum_{n=0}^3 T_{2n}(\phi, \phi_0; p) c^{2n} + o(c^7), \quad (4.32)$$

where

$$T_0 = \frac{1}{2p}, \quad (4.33)$$

$$T_2 = -\frac{1}{4} \left[\frac{\cos^2 \phi}{2p} - \cos \phi_0 \cos \phi - \frac{\sin^2 \phi_0}{2p} \right], \quad (4.34)$$

$$T_4 = \frac{\cos^4 \phi}{128p} - \frac{1}{32} \cos \phi_0 \cos^3 \phi - \frac{1}{32} \left(\frac{\sin^2 \phi_0}{p} + \cos^2 \phi_0 - \frac{1}{2} - \frac{1}{4p} \right) \cos^2 \phi +$$

$$+ \frac{1}{128} \left[-\frac{1}{2} \cos^3 \phi_0 + (p + \frac{1}{2}) \cos \phi_0 \right] \cos \phi + \left[\frac{\cos^4 \phi_0}{128p} + \frac{1}{64} \left(1 - \frac{3}{2p} \right) \cos^2 \phi_0 + \right.$$

$$\left. + \frac{1}{256} \left(\frac{1}{p^2} + \frac{3}{2p} - 2 \right) \right], \quad (4.35)$$

$$T_6 = -\frac{\cos^6 \phi}{4608p} + \frac{1}{768} \cos \phi_0 \cos^5 \phi + \frac{1}{384} \left(\frac{3 \sin^2 \phi_0}{4p} + \cos^2 \phi_0 - \frac{1}{4p} - \frac{1}{2} \right) \cos^4 \phi -$$

$$- \frac{1}{192} \left[-\cos^3 \phi_0 + \frac{1}{2}(3p+1) \cos \phi_0 \right] \cos^3 \phi - \frac{1}{128} \left[\left(\frac{1}{4p} - \frac{1}{3} \right) \cos^4 \phi_0 + \right.$$

$$\left. + \frac{1}{2} \left(\frac{4}{3} - \frac{1}{p} \right) \cos^2 \phi_0 + \frac{1}{4} \left(\frac{1}{2p^2} - \frac{1}{4p} - \frac{1}{3} \right) \right] \cos^2 \phi +$$

$$+ \frac{1}{64} \left[\frac{1}{2} \cos^5 \phi_0 - \frac{1}{2}(p + \frac{1}{2}) \cos^3 \phi_0 + (p^2 - \frac{1}{2}p + \frac{1}{8}) \cos \phi_0 \right] \cos \phi +$$

$$+ \frac{1}{768} \left[-\frac{\cos^6 \phi_0}{6p} - \left(1 - \frac{1}{p} \right) \cos^4 \phi_0 + \frac{1}{2} \left(1 + \frac{3}{4p} - \frac{3}{2p^2} \right) \cos^2 \phi_0 + \right.$$

$$\left. + \frac{1}{2} \left(1 - \frac{29}{12p} + \frac{3}{2p^2} \right) \right]. \quad (4.36)$$

An expression equivalent to eq. (4.32) was used by BURKE and TWERSKY [1960] to compute the bistatic cross section per unit length as a function of ϕ , as shown in Fig. 4.7.

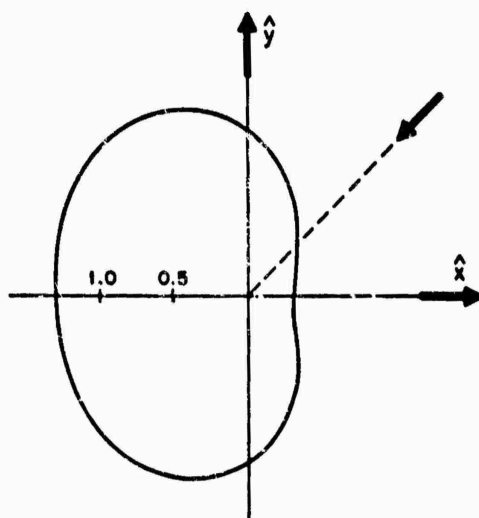


Fig. 4.7. Normalized bistatic cross section per unit length, $1/k\sigma$, for E -polarization with $\phi_0 = \frac{1}{2}\pi$ and $c = 1.1$ (BURKE and TWERSKY [1964]).

Additional computations for $\phi_0 = 0, \frac{1}{2}\pi$ and $\frac{3}{2}\pi$, and $c = 0.3, 0.7$ and 1.1 are given

by BURKE et al. [1964]. The normalized back scattering cross section per unit length is shown in Fig. 4.8 as a function of ϕ_0 for $c = 1.1$ and in Fig. 4.9 as a function of c for $\phi_0 = 0, \frac{1}{2}\pi$ and $\frac{3}{2}\pi$.

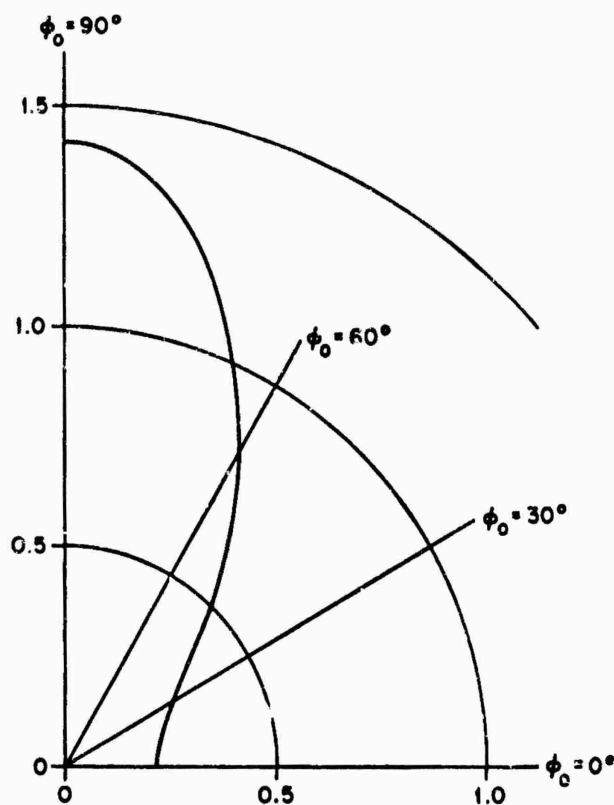


Fig. 4.8. Normalized back scattering cross section per unit length, $\frac{1}{4}k\alpha$, as a function of ϕ_0 for E -polarization with $c = 1.1$ (BURKE and TWERSKY [1964]).

The normalized total scattering cross section per unit length is (MILLAR [1960]):

$$\begin{aligned} \frac{\sigma_T}{2d} = \frac{\pi^2}{cq} \left\{ 1 - \frac{1}{4}c^2 \cos 2\phi_0 + \frac{3}{256}c^4 \left[1 + \frac{16}{3} \frac{\delta}{q} + \frac{8}{3}(q-3) \cos^2 \phi_0 + 8 \cos^4 \phi_0 \right] - \right. \\ \left. - \frac{1}{64}c^6 \left[\frac{29}{144} - \frac{\delta}{q} + \left(\frac{q-1}{8} - \left(q - \frac{2}{q} \right) \delta \right) \cos^2 \phi_0 + \frac{1}{2}(q - \frac{5}{3}) \cos^4 \phi_0 + \right. \right. \\ \left. \left. + \frac{5}{9} \cos^6 \phi_0 \right] \right\} + o(c^6), \quad (4.37) \end{aligned}$$

where:

$$\delta = p + \frac{1}{2}i\pi, \quad q = \pi^2 + 4\delta^2. \quad (4.38)$$

The normalized cross section given by eq. (4.37) is plotted in Fig. 4.10; the discrepancy between these curves and the exact ones of Fig. 4.3 is less than 5 percent for $0.5 < c < 1$, and increases as c decreases below 0.5. An independent calculation based

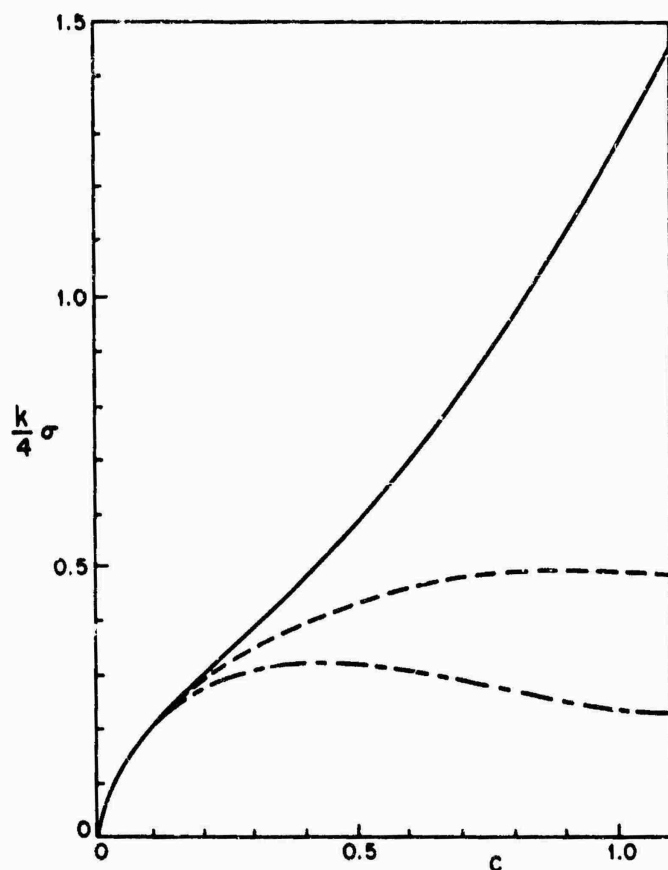


Fig. 4.9. Normalized back scattering cross section per unit length, $\frac{k}{4}\sigma$, as a function of c for E -polarization with $\phi_0 = 0$ (—), $\phi_0 = \frac{1}{2}\pi$ (---), and $\phi_0 = \pi$ (— · —) (BURKE and TWERSKY [1964]).

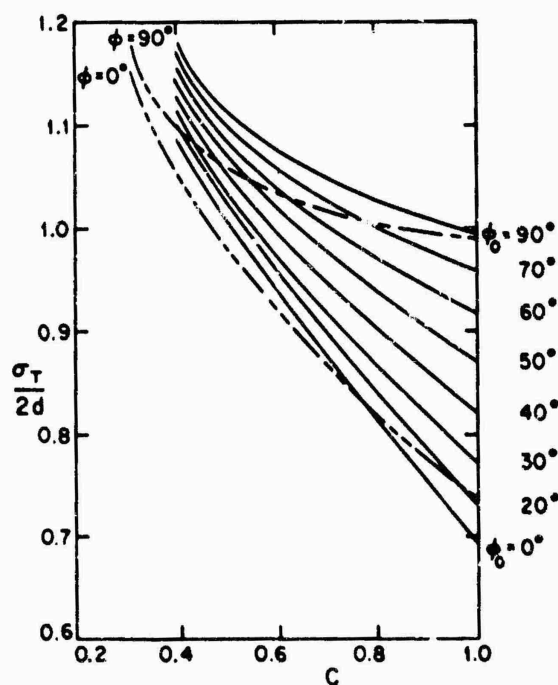


Fig. 4.10. Normalized total scattering cross section per unit length as a function of c for E -polarization; — MILLAR [1960], --- MORSE and RUBENSTEIN [1938].

on an exact analysis for broadside incidence (SKAVLEM [1951]) gives results which are in better agreement with those of MILLAR [1960].

For grazing incidence ($\phi_0 = 0$), the total magnetic field on the strip is (MILLAR [1960]):

$$H_x = -\operatorname{sgn}(\sin v)H_v = \frac{iY}{c \sin v} \left[\sum_{n=0}^6 f_n c^n + o(c^6) \right], \quad (4.39)$$

where:

$$f_0 = \frac{1}{p}, \quad (4.40)$$

$$f_1 = i \cos v, \quad (4.41)$$

$$f_2 = \frac{1}{4} \left(1 - \frac{1}{4p} \right) \cos 2v, \quad (4.42)$$

$$f_3 = -\frac{1}{4}i \left(\frac{1}{4} - p \right) \cos v - \frac{1}{16}i \cos 3v, \quad (4.43)$$

$$f_4 = \frac{1}{64} \left(1 - \frac{5}{4}p + \frac{1}{2p^2} \right) + \frac{1}{128} \left(-1 + \frac{3}{4p} \right) \cos 4v, \quad (4.44)$$

$$f_5 = \frac{1}{16}i \left(\frac{7}{16} - \frac{3}{4}p + p^2 \right) \cos v + \frac{1}{128}i \left(\frac{1}{8} - p \right) \cos 3v + \frac{1}{1024}i \cos 5v, \quad (4.45)$$

$$f_6 = \frac{1}{512} \left(p - \frac{17}{8} + \frac{27}{16p} - \frac{1}{2p^2} \right) \cos 2v + \frac{1}{12288} \left(1 - \frac{1}{6p} \right) \cos 6v. \quad (4.46)$$

In the far field ($\xi \rightarrow \infty$) and for grazing incidence (MILLAR [1960]):

$$P = i\pi \sum_{n=0}^3 T_{2n}(\phi, 0; p) c^{2n} + o(c^7), \quad (4.47)$$

where:

$$T_0 = \frac{1}{2p}, \quad (4.48)$$

$$T_2 = \frac{1}{4} \left(\cos \phi - \frac{\cos^2 \phi}{2p} \right), \quad (4.49)$$

$$T_4 = \frac{\cos^4 \phi}{128p} - \frac{1}{32} \cos^3 \phi + \frac{1}{64} \left(\frac{1}{2p} - 1 \right) \cos^2 \phi + \frac{1}{16} (p - \frac{1}{4}) \cos \phi + \frac{1}{128} \left(\frac{1}{2p^2} - \frac{5}{4p} + 1 \right), \quad (4.50)$$

$$T_6 = -\frac{\cos^6 \phi}{4608p} + \frac{1}{768} \cos^5 \phi + \frac{1}{768} \left(1 - \frac{1}{2p} \right) \cos^4 \phi + \frac{1}{384} (1 - 3p) \cos^3 \phi - \frac{1}{512} \left(\frac{1}{2p^2} - \frac{5}{4p} + 1 \right) \cos^2 \phi + \frac{1}{64} (p^2 - \frac{3}{4}p + \frac{3}{16}) \cos \phi. \quad (4.51)$$

BURKE et al. [1964] have plotted the normalized bistatic cross section per unit length, $\frac{1}{4}k\sigma(\phi)$, as a function of ϕ for $c = 0.3, 0.7$ and 1.1 . The normalized back scattering cross section per unit length as a function of c is shown in Fig. 4.9. The normalized total scattering cross section per unit length is (MILLAR [1960]):

$$\frac{\sigma_T}{2d} = \frac{\pi^2}{cq} \left\{ 1 - \frac{1}{4}c^2 + \frac{3}{256}c^4 \left(1 + \frac{16}{3} \frac{\delta}{q} + \frac{8}{3}q \right) + \right. \\ \left. + \frac{1}{64}c^6 \left[\frac{29}{144} - \frac{5}{8}q + \left(q - \frac{1}{q} \right) \delta \right] \right\} + o(c^6). \quad (4.52)$$

At broadside incidence ($\phi_0 = \frac{1}{2}\pi$), the total magnetic field on the strip is (MILLAR [1960]):

$$H_x = -\text{sgn}(\sin v)H_v = -Y + \frac{iY}{c \sin v} \left[\sum_{n=0}^3 f_{2n} c^{2n} + o(c^7) \right], \quad (4.53)$$

where:

$$f_0 = \frac{1}{p}, \quad (4.54)$$

$$f_2 = \frac{1}{4p} - \frac{1}{4} \left(1 + \frac{1}{2p} \right) \cos 2v, \quad (4.55)$$

$$f_4 = \frac{1}{128} \left(\frac{1}{p^2} + \frac{3}{2p} - 2 \right) + \frac{1}{16} \left(\frac{1}{3} - \frac{1}{2p} \right) \cos 2v + \frac{1}{384} \left(1 + \frac{3}{4p} \right) \cos 4v, \quad (4.56)$$

$$f_6 = \frac{1}{768} \left(1 - \frac{29}{12p} + \frac{3}{2p^2} \right) - \frac{1}{512} \left(p - \frac{13}{8} + \frac{5}{16p} + \frac{1}{2p^2} \right) \cos 2v + \\ + \frac{1}{2048} \left(\frac{1}{p} - \frac{4}{5} \right) \cos 4v - \frac{1}{61440} \left(\frac{5}{6p} - 1 \right) \cos 6v. \quad (4.57)$$

In the far field ($\xi \rightarrow \infty$) (MILLAR [1960]):

$$P = i\pi \sum_{n=0}^3 T_{2n}(\phi, \frac{1}{2}\pi; p) c^{2n} + o(c^7), \quad (4.58)$$

with

$$T_0 = \frac{1}{2p}, \quad (4.59)$$

$$T_2 = \frac{1}{8p}, \quad (4.60)$$

$$T_4 = \frac{\cos^4 \phi}{128p} + \frac{1}{64} \left(1 - \frac{3}{2p} \right) \cos^2 \phi + \frac{1}{256} \left(\frac{1}{p^2} + \frac{3}{2p} - 2 \right), \quad (4.61)$$

$$T_6 = -\frac{\cos^6 \phi}{4608p} + \frac{1}{768} \left(\frac{1}{p} - 1 \right) \cos^4 \phi + \frac{1}{512} \left(\frac{1}{3} + \frac{1}{4p} - \frac{1}{2p^2} \right) \cos^2 \phi + \frac{1}{1536} \left(1 - \frac{29}{12p} + \frac{3}{2p^2} \right). \quad (4.62)$$

BURKE et al. [1964] have plotted the normalized bistatic cross section per unit length, $\frac{1}{4}k\sigma(\phi)$, as a function of ϕ for $c = 0.3, 0.7$ and 1.1 . The normalized back scattering cross section per unit length as a function of c appears in Fig. 4.9. The normalized total scattering cross section per unit length is (MILLAR [1960]):

$$\frac{\sigma_T}{2d} = \frac{\pi^2}{cq} \left\{ 1 + \frac{1}{4}c^2 + \frac{3}{256}c^4 \left(1 + \frac{16}{3} \frac{\delta}{q} \right) - \frac{1}{64}c^6 \left(\frac{29}{144} - \frac{\delta}{q} \right) \right\} + o(c^6). \quad (4.63)$$

4.2.1.3. HIGH FREQUENCY APPROXIMATIONS

For a plane wave whose direction of propagation is perpendicular to the z -axis and forms the angle ϕ_0 with the negative x -axis and the angle $(\frac{1}{2}\pi - \phi_0)$ with the negative y -axis ($0 \leq \phi_0 \leq \frac{1}{2}\pi$), such that

$$\begin{aligned} E^i &= \hat{z} \exp \{ -ik(x \cos \phi_0 + y \sin \phi_0) \}, \\ H^i &= Y(-\sin \phi_0 \hat{x} + \cos \phi_0 \hat{y}) \exp \{ -ik(x \cos \phi_0 + y \sin \phi_0) \}, \end{aligned} \quad (4.64)$$

the scattered electric field is (KARP and KELLER [1961])

$$\begin{aligned} E_z^s &= -\frac{1}{2}i \sqrt{\frac{2}{\pi k \rho_1}} \frac{\sqrt{\{(1 + \cos \psi_1)(1 + \cos \phi_0)\}}}{\cos \psi_1 + \cos \phi_0} \exp \{ ik\rho_1 - \frac{1}{4}i\pi - ic \cos \phi_0 \} \\ &\quad \times \left\{ 1 - \frac{i}{2k\rho_1} \frac{1 + \cos \psi_1 \cos \phi_0}{(\cos \psi_1 + \cos \phi_0)^2} + O[(k\rho_1)^{-2}] \right\} + \\ &\quad + \frac{1}{2}i \sqrt{\frac{2}{\pi k \rho_2}} \frac{\sqrt{\{(1 - \cos \psi_2)(1 - \cos \phi_0)\}}}{\cos \psi_2 + \cos \phi_0} \exp \{ ik\rho_2 - \frac{1}{4}i\pi + ic \cos \phi_0 \} \\ &\quad \times \left\{ 1 - \frac{i}{2k\rho_2} \frac{1 + \cos \psi_2 \cos \phi_0}{(\cos \psi_2 + \cos \phi_0)^2} + O[(k\rho_2)^{-2}] \right\}, \end{aligned} \quad (4.65)$$

where:

$$\rho_{1,2} \gg d, \quad \psi_{1,2} \neq \pi \pm \phi_0, \quad \phi_0 \neq 0, \quad (4.66)$$

and the geometric variables are defined as:

$$\begin{aligned} \rho_1 \cos \psi_1 &= \frac{1}{2}d(\cosh u \cos v - 1) = \rho \cos \phi - \frac{1}{2}d, \\ \rho_1 \sin \psi_1 &= \frac{1}{2}d \sinh u \sin v = \rho \sin \phi, \\ \rho_2 \cos \psi_2 &= \frac{1}{2}d(\cosh u \cos v + 1) = \rho \cos \phi + \frac{1}{2}d, \\ \rho_2 \sin \psi_2 &= \frac{1}{2}d \sinh u \sin v = \rho \sin \phi, \end{aligned} \quad (4.67)$$

as illustrated in Fig. 4.11.

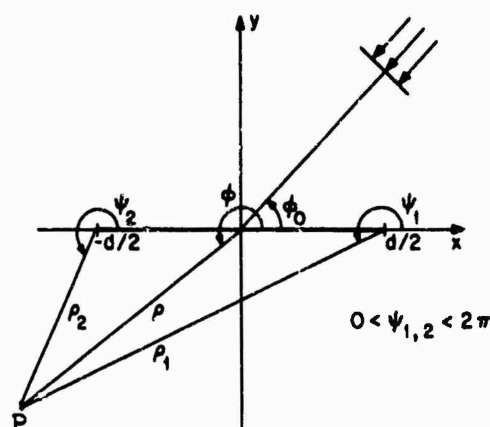


Fig. 4.11. Strip geometry for the geometrical theory of diffraction.

The expression in eq. (4.65) is based on analysis of singly diffracted rays only. An expression of the scattered field which includes contributions from multiply diffracted rays but to a lower order in $k\rho_{1,2}$ is (KARP and KELLER [1961]):

$$\begin{aligned}
 E_z^s = & \sqrt{\frac{2}{\pi k \rho_1}} e^{ik\rho_1 - \frac{1}{2}i\pi} \left\{ -\frac{1}{2}ie^{-ic \cos \phi_0} \frac{\sqrt{\{(1 + \cos \psi_1)(1 + \cos \phi_0)\}}}{\cos \psi_1 + \cos \phi_0} + \right. \\
 & + \frac{1}{32c} \sqrt{\frac{2}{\pi c}} e^{2ic + \frac{1}{2}i\pi} \left(1 + \frac{ie^{4ic}}{256\pi c^3} \right)^{-1} \frac{\sqrt{(1 + \cos \psi_1)}}{1 - \cos \psi_1} \left(\frac{\sin \frac{1}{2}\phi_0}{\cos^2 \frac{1}{2}\phi_0} e^{ic \cos \phi_0} - \right. \\
 & \left. \left. - \frac{\cos \frac{1}{2}\phi_0}{\sin^2 \frac{1}{2}\phi_0} \frac{\exp \{2ic - \frac{1}{2}i\pi - ic \cos \phi_0\}}{16c\sqrt{\pi c}} \right) + O\left(\frac{1}{k\rho_1}\right) \right\} + \\
 & + \sqrt{\frac{2}{\pi k \rho_2}} e^{ik\rho_2 - \frac{1}{2}i\pi} \left\{ \frac{1}{2}ie^{ic \cos \phi_0} \frac{\sqrt{\{(1 - \cos \psi_2)(1 - \cos \phi_0)\}}}{\cos \psi_2 + \cos \phi_0} + \right. \\
 & + \frac{1}{32c} \sqrt{\frac{2}{\pi c}} e^{2ic + \frac{1}{2}i\pi} \left(1 + \frac{ie^{4ic}}{256\pi c^3} \right)^{-1} \frac{\sqrt{(1 - \cos \psi_2)}}{1 + \cos \psi_2} \left(\frac{\cos \frac{1}{2}\phi_0}{\sin^2 \frac{1}{2}\phi_0} e^{-ic \cos \phi_0} - \right. \\
 & \left. \left. - \frac{\sin \frac{1}{2}\phi_0}{\cos^2 \frac{1}{2}\phi_0} \frac{\exp \{2ic - \frac{1}{2}i\pi + ic \cos \phi_0\}}{16c\sqrt{\pi c}} \right) + O\left(\frac{1}{k\rho_2}\right) \right\}, \quad (4.68)
 \end{aligned}$$

where

$$\rho_{1,2} \gg d, \quad \psi_{1,2} \neq \pi \pm \phi_0, 0, \pi, 2\pi; \quad \phi_0 \neq 0. \quad (4.69)$$

On the strip ($u = 0$) the total magnetic field for non-grazing ($c \sin \phi \gg 1$) but otherwise arbitrary incidence is (LÜNEBURG and WESTPFAHL [1968]):

$$\begin{aligned}
 H_x = & -Y \sin \phi_0 e^{-ic\eta \cos \phi_0} + Y \operatorname{sgn}(\sin v) \{ -\sin \phi_0 e^{-ic\eta \cos \phi_0} + \\
 & + \sum_{n=0}^3 [h_n(\cos \phi_0, \eta) + h_n(-\cos \phi_0, \eta)] c^{-1n} + O(c^{-i}) \}, \quad (4.70)
 \end{aligned}$$

where

$$h_0(\cos \phi_0, \eta) = -\sqrt{1 - \cos \phi_0} e^{ic \cos \phi_0} A[-\cos \phi_0, c(1 + \eta)], \quad (4.71)$$

$$h_1(\cos \phi_0, \eta) = \frac{1}{8\sqrt{\pi}} \frac{\sqrt{(1 + \cos \phi_0)}}{1 - \cos \phi_0} \exp \{2ic - ic \cos \phi_0 + \frac{1}{2}i\pi\} A[-1, c(1 + \eta)], \quad (4.72)$$

$$h_2(\cos \phi_0, \eta) = 0, \quad (4.73)$$

$$h_3(\cos \phi_0, \eta) = \frac{3}{32\sqrt{\pi}} \frac{\sqrt{(1 + \cos \phi_0)}}{1 - \cos \phi_0} \exp \{2ic - ic \cos \phi_0 - \frac{1}{2}i\pi\} \times \left\{ \left(\frac{1}{4} + \frac{1}{1 - \cos \phi_0} \right) A[-1, c(1 + \eta)] + B[-1, c(1 + \eta)] \right\}, \quad (4.74)$$

$$A[\alpha, \beta] = \frac{e^{i\beta + \frac{1}{2}i\pi}}{\sqrt{\pi\beta}} - \frac{2}{\pi} e^{i\alpha\beta - \frac{1}{2}i\pi} \sqrt{1 - \alpha} F(\sqrt{\beta(1 - \alpha)}), \quad (4.75)$$

$$B[-1, \beta] = -(\beta/\pi)^{\frac{1}{2}} e^{i\beta - \frac{1}{2}i\pi} + \frac{(1 - 4i\beta)}{\sqrt{2\pi}} e^{-i\beta - \frac{1}{2}i\pi} F(\sqrt{2\beta}), \quad (4.76)$$

and $F(\tau)$ is the Fresnel integral defined in the Introduction. Neglecting the summation in eq. (4.70), the geometric optics approximation to the magnetic field is obtained. The above expressions are valid uniformly in η ; however, they may be simplified in restricted regions of the surface. In particular, away from the edges, such that $c|\sin v| \gg 1$ (LÜNEBURG and WESTPFAHL [1968]), the magnetic field on the surface is given by eq. (4.70) with the summation replaced by:

$$\sum_{n=0}^3 [\bar{h}_n(\cos \phi_0, \eta) + \bar{h}_n(-\cos \phi_0, -\eta)] c^{-\frac{1}{2}(n+3)} + O(c^{-\frac{5}{2}}), \quad (4.77)$$

where:

$$\bar{h}_0(\cos \phi_0, \eta) = \frac{e^{-\frac{1}{2}i\pi}}{2\sqrt{\pi}} \frac{\sqrt{1 - \cos \phi_0} \exp \{ic(1 + \cos \phi_0 + \eta)\}}{(1 + \cos \phi_0)(1 + \eta)^{\frac{1}{2}}}, \quad (4.78)$$

$$\bar{h}_1(\cos \phi_0, \eta) = 0, \quad (4.79)$$

$$\bar{h}_2(\cos \phi_0, \eta) = \frac{-3e^{\frac{1}{2}i\pi}}{4\sqrt{\pi}} \frac{\sqrt{1 - \cos \phi_0} \exp \{ic(1 + \cos \phi_0 + \eta)\}}{(1 + \cos \phi_0)(1 + \eta)^{\frac{1}{2}}}, \quad (4.80)$$

$$\bar{h}_3(\cos \phi_0, \eta) = \frac{e^{\frac{1}{2}i\pi}}{32\pi} \frac{\sqrt{1 + \cos \phi_0} \exp \{-ic(3 + \cos \phi_0 - \eta)\}}{(1 - \cos \phi_0)(1 + \eta)^{\frac{1}{2}}}. \quad (4.81)$$

On the other hand, near the edges, such that $c(1 \pm \eta) \ll 1$, the magnetic field on the surface is (LÜNEBURG and WESTPFAHL [1968]):

$$H_x = -Y \sin \phi_0 e^{-ic\eta \cos \phi_0} + Y \operatorname{sgn}(\sin v) h, \quad (4.82)$$

where

$$h = \frac{i}{c} \left[\frac{\psi_1(\cos \phi_0)}{\sqrt{1+\eta}} + \psi_2(\cos \phi_0) \sqrt{1+\eta} \right], \quad \text{for } c(1+\eta) \ll 1 \text{ and } c \gg 1, \quad (4.83)$$

$$h = \frac{i}{c} \left[\frac{\psi_1(\cos \phi_0)}{\sqrt{1-\eta}} + \psi_2(\cos \phi_0) \sqrt{1-\eta} \right], \quad \text{for } c(1-\eta) \ll 1 \text{ and } c \gg 1, \quad (4.84)$$

with

$$\begin{aligned} \psi_1(\cos \phi_0) = & \sqrt{\frac{c}{\pi}} (1 - \cos \phi_0) \exp \{ic \cos \phi_0 + \frac{1}{2}i\pi\} - \frac{i\sqrt{(1 + \cos \phi_0)}}{8\pi c(1 - \cos \phi_0)} \\ & \times \exp \{ic(2 - \cos \phi_0)\} \left[1 - \frac{3i}{4c} \left(\frac{1}{4} + \frac{1}{1 - \cos \phi_0} \right) \right], \end{aligned} \quad (4.85)$$

$$\begin{aligned} \psi_2(\cos \phi_0) = & -c \sqrt{\frac{c}{\pi}} (1 - \cos \phi_0) \exp \{ic \cos \phi_0 + \frac{1}{2}i\pi\} [1 - 2(1 + \cos \phi_0)^{\frac{1}{2}}] - \\ & - \frac{1}{8\pi} \frac{\sqrt{(1 + \cos \phi_0)}}{1 - \cos \phi_0} \exp \{ic(2 - \cos \phi_0)\} \\ & \times \left\{ 4\sqrt{2} - 1 - \frac{3i}{4c} \left[(4\sqrt{2} - 1) \left(\frac{1}{4} + \frac{1}{1 - \cos \phi_0} \right) - 2 \right] \right\}. \end{aligned} \quad (4.86)$$

Alternate but equivalent representations of the surface field are given by MILLAR [1953b].

For arbitrary incidence, the scattered electric field on the portions of the plane $y = 0$ outside the strip ($|x| > \frac{1}{2}d$) is (GRINBERG [1958]):

$$\begin{aligned} E_z^s = & \frac{1}{2} e^{ic\xi} \sqrt{\xi^2 - 1} [\omega_+(\xi - 1) \pm \omega_-(\xi - 1)], \quad \left[\begin{array}{l} + \text{ for } v = 0, (x > \frac{1}{2}d); \\ - \text{ for } v = \pi, (x < -\frac{1}{2}d); \end{array} \right] \end{aligned} \quad (4.87)$$

where

$$\omega_{\pm}(\tau) \sim \omega_{\pm}^{(0)}(\tau) \pm \frac{e^{2ic} \int_0^{\infty} e^{2ic\rho} \sqrt{\rho/(\rho+2)} \omega_{\pm}^{(0)}(\rho) d\rho}{\pi(-+2) [1 \mp \{(\frac{1}{2}i + 2c)H_0^{(1)}(2c) - 2icH_1^{(1)}(2c)\}]}, \quad (4.88)$$

with

$$\omega_+^{(0)}(\tau) = -\frac{2}{\pi} \int_{-1}^1 \frac{e^{ic\rho} \cos(c\rho \cos \phi_0)}{(\tau + \rho + 1)\sqrt{(\rho+1)}} d\rho, \quad (4.89)$$

$$\omega_-^{(0)}(\tau) = -\frac{2i}{\pi} \int_{-1}^1 \frac{e^{ic\rho} \sin(c\rho \cos \phi_0)}{(\tau + \rho + 1)\sqrt{(\rho+1)}} d\rho. \quad (4.90)$$

The order of the approximation in eq. (4.88) is difficult to assess, but the error is at least $O(c^{-\frac{1}{2}})$.

In the far field ($\xi \rightarrow \infty$) and for arbitrary incidence (FIALKOVSKIY [1966]):

$$P = \frac{i}{2(\cos \phi + \cos \phi_0)} \left\{ \exp \{ic(\cos \phi_0 + \cos \phi)\} / \{(1 - \cos \phi_0)(1 - \cos \phi)\} \right. \\ \times [1 + \Gamma(c, \cos \phi)][1 + \Gamma(c, \cos \phi_0)] - \exp \{-ic(\cos \phi_0 + \cos \phi)\} \sqrt{1 + \cos \phi_0} \\ \times \sqrt{1 + \cos \phi} [1 + \Gamma(c, -\cos \phi)][1 + \Gamma(c, -\cos \phi_0)] \left. \right\} + O(c^{-2}), \quad (4.91)$$

where:

$$\Gamma(c, \cos \phi_0) = K(c, \cos \phi_0) - 2c \sqrt{\frac{1 + \cos \phi_0}{1 - \cos \phi_0}} e^{-2ic \cos \phi_0} [H_0^{(1)}(2c) - iH_1^{(1)}(2c)], \quad (4.92)$$

$$K(c, \cos \phi_0) = \sqrt{1 - \cos^2 \phi_0} \int_0^c H_0^{(1)}(2t) e^{-2it \cos \phi_0} dt, \quad (4.93)$$

and

$$K(c, 1) = -1, \quad K(c, -1) = 0. \quad (4.94)$$

The far field result of eq. (4.91) is valid uniformly in ϕ and ϕ_0 . Computations of the backscattered far field have been made by UFIMTSEV [1958] for $c = \sqrt{28}$ and $c = \sqrt{80}$ using a cruder version of eq. (4.91), in which the quantity Γ differed from the value of eq. (4.92) by a factor varying monotonically from 1 for $\phi_0 = 0$ to $2\sqrt{2}$ for $\phi_0 = \frac{1}{2}\pi$. The results are shown in Fig. 4.12.

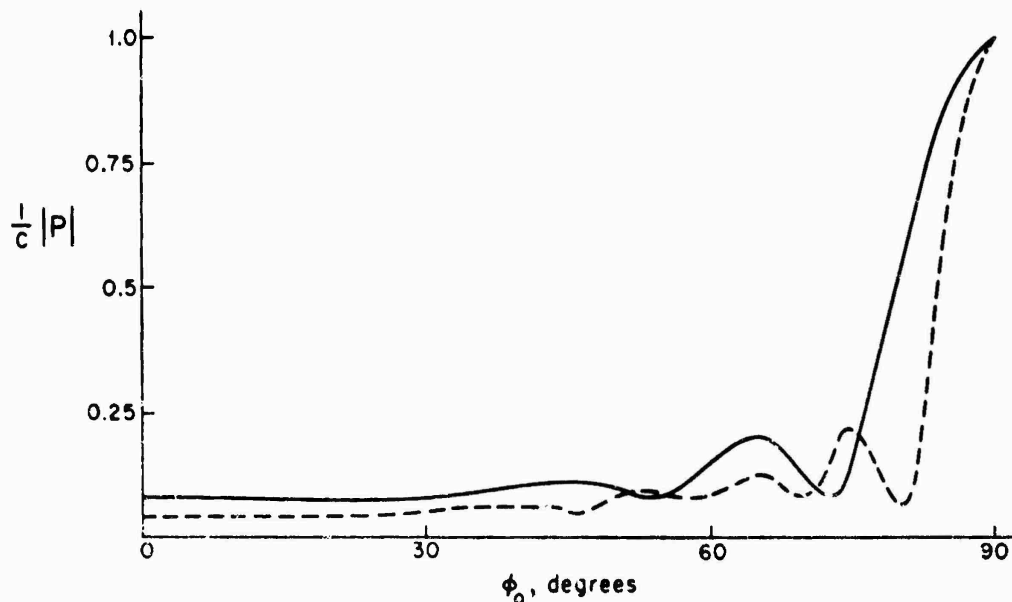


Fig. 4.12. Normalized back scattered far field coefficient as a function of ϕ_0 for E -polarization with $c = \sqrt{28}$ (—) and $c = \sqrt{80}$ (---) (UFIMTSEV [1958]).

Away from grazing angles, ($c|\sin \phi| \gg 1$, $c \sin \phi_0 \gg 1$), the far field is (LÜNEBURG and WESTPAHL [1968]):

$$P = p_0 + c^{-1}p_1 + c^{-2}p_2 + c^{-3}p_3 + O(c^{-4}), \quad (4.95)$$

where:

$$p_0 = \frac{i}{2(\cos \phi + \cos \phi_0)} \left\{ \sqrt{\{(1 - \cos \phi)(1 - \cos \phi_0)\}} \exp \{ic(\cos \phi + \cos \phi_0)\} - \sqrt{\{(1 + \cos \phi)(1 + \cos \phi_0)\}} \exp \{-ic(\cos \phi + \cos \phi_0)\} \right\}, \quad (4.96)$$

$$p_1 = \frac{e^{2ic - \frac{1}{2}i\pi}}{16\sqrt{\pi}} \left\{ \frac{\sqrt{\{(1 - \cos \phi)(1 + \cos \phi_0)\}}}{(1 + \cos \phi)(1 - \cos \phi_0)} \exp \{ic(\cos \phi - \cos \phi_0)\} + \frac{\sqrt{\{(1 + \cos \phi)(1 - \cos \phi_0)\}}}{(1 - \cos \phi)(1 + \cos \phi_0)} \exp \{-ic(\cos \phi - \cos \phi_0)\} \right\}, \quad (4.97)$$

$$p_2 = \frac{3e^{2ic + \frac{1}{2}i\pi}}{64\sqrt{\pi}} \left\{ \frac{\sqrt{\{(1 - \cos \phi)(1 + \cos \phi_0)\}}}{(1 + \cos \phi)(1 - \cos \phi_0)} \left(\frac{1}{4} + \frac{1}{1 + \cos \phi} + \frac{1}{1 - \cos \phi_0} \right) \exp \{ic(\cos \phi - \cos \phi_0)\} + \frac{\sqrt{\{(1 + \cos \phi)(1 - \cos \phi_0)\}}}{(1 - \cos \phi)(1 + \cos \phi_0)} \right. \\ \left. \times \left(\frac{1}{4} + \frac{1}{1 - \cos \phi} + \frac{1}{1 + \cos \phi_0} \right) \exp \{-ic(\cos \phi - \cos \phi_0)\} \right\}, \quad (4.98)$$

$$p_3 = \frac{e^{4ic}}{256\pi} \left\{ \frac{\sqrt{\{(1 - \cos \phi)(1 - \cos \phi_0)\}}}{(1 + \cos \phi)(1 + \cos \phi_0)} \exp \{ic(\cos \phi + \cos \phi_0)\} + \frac{\sqrt{\{(1 + \cos \phi)(1 + \cos \phi_0)\}}}{(1 - \cos \phi)(1 - \cos \phi_0)} \exp \{-ic(\cos \phi + \cos \phi_0)\} \right\}. \quad (4.99)$$

A result equivalent to that of eq. (4.95) was given by MILLAR [1958b]. The first term, p_0 , was obtained by KELLER [1957] using singly diffracted rays.

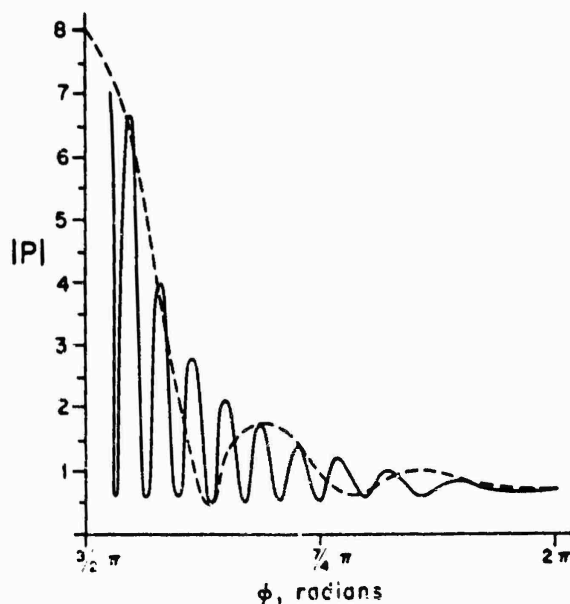


Fig. 4.13. First order far field coefficient as a function of ϕ at broadside incidence ($\phi_0 = \frac{1}{2}\pi$) for E -polarization with $c = 8$ (---) and $c = 10\pi$ (—) (KELLER [1957]).

The second and fourth terms p_1 and p_3 , were given by KARP and KELLER [1961] using multiply diffracted rays; however, their treatment did not produce the third term p_2 . The amplitude of p_0 is shown as a function of ϕ for broadside incidence ($\phi_0 = \frac{1}{2}\pi$) with $c = 8$ and $c = 10\pi$ in Fig. 4.13.

In particular, for backscattering ($\phi = \phi_0$) and non-grazing incidence ($c \sin \phi_0 \gg 1$), the coefficients in eq. (4.95) become:

$$p_0 = -\frac{\sin(2c \cos \phi_0)}{2 \cos \phi_0} - \frac{1}{2}i \cos(2c \cos \phi_0), \quad (4.100)$$

$$p_1 = \frac{e^{2ic - \frac{1}{2}i\pi}}{8\sqrt{\pi} \sin \phi_0}, \quad (4.101)$$

$$p_2 = \frac{3e^{2ic + \frac{1}{2}i\pi}}{32\sqrt{\pi} \sin \phi_0} \left(\frac{1}{4} + \frac{2}{\sin^2 \phi_0} \right), \quad (4.102)$$

$$p_3 = \frac{e^{4ic}}{256\pi} \left[\frac{1 - \cos \phi_0}{(1 + \cos \phi_0)^2} e^{2ic \cos \phi_0} + \frac{1 + \cos \phi_0}{(1 - \cos \phi_0)^2} e^{-2ic \cos \phi_0} \right], \quad (4.103)$$

which for broadside incidence ($\phi_0 = \frac{1}{2}\pi$) reduce to:

$$p_0 = -c - \frac{1}{2}i, \quad (4.104)$$

$$p_1 = \frac{e^{2ic - \frac{1}{2}i\pi}}{8\sqrt{\pi}}, \quad (4.105)$$

$$p_2 = \frac{27e^{2ic + \frac{1}{2}i\pi}}{128\sqrt{\pi}}, \quad (4.106)$$

$$p_3 = \frac{e^{4ic}}{128\pi}. \quad (4.107)$$

On the other hand, for forward scattering ($\phi = \phi_0 + \pi$) and non-grazing incidence ($c \sin \phi_0 \gg 1$), the coefficients in eq. (4.95) become:

$$p_0 = -c \sin \phi_0 - \frac{i}{2 \sin \phi_0}, \quad (4.108)$$

$$p_1 = \frac{e^{2ic - \frac{1}{2}i\pi}}{16\sqrt{\pi}} \left[\frac{1 + \cos \phi_0}{(1 - \cos \phi_0)^2} e^{-2ic \cos \phi_0} + \frac{1 - \cos \phi_0}{(1 + \cos \phi_0)^2} e^{2ic \cos \phi_0} \right], \quad (4.109)$$

$$p_2 = \frac{3e^{2ic + \frac{1}{2}i\pi}}{64\sqrt{\pi}} \left[\frac{1 + \cos \phi_0}{(1 - \cos \phi_0)^2} \left(\frac{1}{4} + \frac{2}{1 - \cos \phi_0} \right) e^{-2ic \cos \phi_0} + \frac{1 - \cos \phi_0}{(1 + \cos \phi_0)^2} \left(\frac{1}{4} + \frac{2}{1 + \cos \phi_0} \right) e^{2ic \cos \phi_0} \right], \quad (4.110)$$

$$p_3 = \frac{e^{4ic}}{128\pi \sin \phi_0}, \quad (4.111)$$

which for broadside ($\phi_0 = \frac{1}{2}\pi$) reduce to the values given in eqs. (4.104) through (4.107).

The physical optics approximation to the far field coefficient is:

$$P = - \frac{\sin \phi_0 \sin [c(\cos \phi + \cos \phi_0)]}{\cos \phi + \cos \phi_0}, \quad (4.112)$$

which differs from p_0 of eq. (4.95) except for forward scattering, and for back scattering at broadside incidence.

The normalized total scattering cross section per unit length for non-grazing incidence ($c \sin \phi_0 \gg 1$) is (SESHADRI [1958b]):

$$\frac{\sigma_T}{2d} = \sigma_0 + \sigma_1 c^{-\frac{1}{2}} + \sigma_2 c^{-\frac{3}{2}} + \sigma_3 c^{-4} + O(c^{-1}), \quad (4.113)$$

where:

$$\sigma_0 = \sin \phi_0, \quad (4.114)$$

$$\sigma_1 = \frac{\sin^2 \phi_0}{16\sqrt{\pi}} \left\{ \frac{\cos [2c(1 + \cos \phi_0) + \frac{1}{4}\pi]}{(1 + \cos \phi_0)^3} + \frac{\cos [2c(1 - \cos \phi_0) + \frac{1}{4}\pi]}{(1 - \cos \phi_0)^3} \right\}, \quad (4.115)$$

$$\begin{aligned} \sigma_2 = \frac{3 \sin^2 \phi_0}{32\sqrt{\pi}} & \left\{ \frac{(9 + \cos \phi_0)}{8(1 + \cos \phi_0)^4} \cos [2c(1 + \cos \phi_0) - \frac{1}{4}\pi] + \right. \\ & \left. + \frac{(9 - \cos \phi_0)}{8(1 - \cos \phi_0)^4} \cos [2c(1 - \cos \phi_0) - \frac{1}{4}\pi] \right\}, \end{aligned} \quad (4.116)$$

$$\sigma_3 = - \frac{\cos 4c}{128\pi \sin \phi_0}. \quad (4.117)$$

The factor $\sin \phi_0$ in the denominator of the coefficient σ_3 of eq. (4.116) represents a correction due to LÜNEBURG and WESTPFAHL [1968]. Results of computations based on eq. (4.113) are shown in Fig. 4.14; although the incorrect expression for σ_3 was used, the error does not affect the curves appreciably.

In particular, for broadside incidence ($\phi_0 = \frac{1}{2}\pi$), eq. (4.113) reduces to:

$$\frac{\sigma_T}{2d} = 1 + \frac{\cos (2c + \frac{1}{4}\pi)}{8c^2 \sqrt{c\pi}} + \frac{27 \cos (2c - \frac{1}{4}\pi)}{128c^3 \sqrt{c\pi}} - \frac{\cos 4c}{128\pi c^4} + O(c^{-\frac{5}{2}}). \quad (4.118)$$

Extensive computations of $\sigma_T/2d$, including terms through $c^{-\frac{5}{2}}$, have been given by WU [1958]; however, Wu's term in $c^{-\frac{3}{2}}$ disagrees with that in eq. (4.118), which was also independently derived by MILLAR [1957] and LÜNEBURG and WESTPFAHL [1968].

On the other hand, for grazing incidence ($\phi_0 = 0$) the normalized total scattering cross section is (SESHADRI and WU [1960]):

$$\frac{\sigma_T}{2d} = \sqrt{\frac{2}{\pi c}} \left\{ 1 - \frac{1}{2^4 c} + \frac{3}{2^9 c^2} + \frac{1}{2^7 c^3} \left[\frac{15}{2^6} - \frac{\sin(4c + \frac{1}{4}\pi)}{\pi\sqrt{2}} \right] - \frac{1}{2^{11} c^4} \left[\frac{525}{2^8} - \frac{21 \cos(4c + \frac{1}{4}\pi)}{\pi\sqrt{2}} \right] - \frac{1}{2^{16} c^5} \left[\frac{6615}{2^7} - \frac{861 \sin(4c + \frac{1}{4}\pi)}{\pi\sqrt{2}} \right] + O(c^{-6}) \right\}. \quad (4.119)$$

The curve for grazing incidence ($\phi_0 = 0$) in Fig. 4.14 has been computed using the first five terms in eq. (4.119) (KING and WU [1959]).

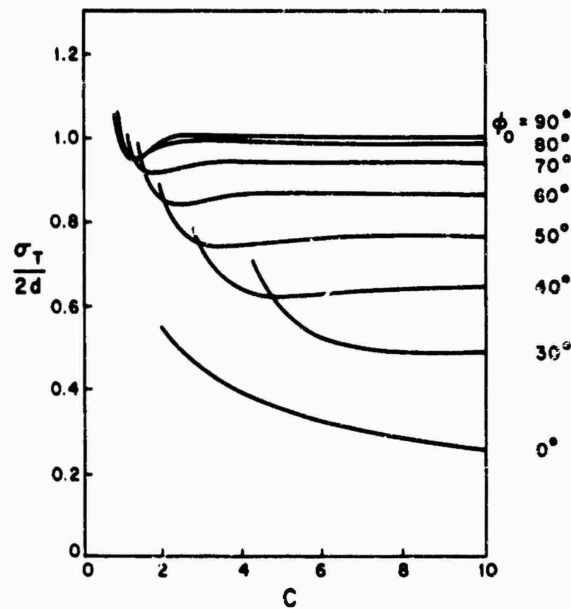


Fig. 4.14. Normalized total scattering cross section per unit length, $\sigma_T/2d$, for E -polarization as a function of c for various angles of incidence (KING and WU [1959]).

4.2.2. H -polarization

4.2.2.1. EXACT SOLUTIONS

For a plane wave whose direction of propagation is perpendicular to the z -axis, and forms the angle ϕ_0 with the negative x -axis and the angle $(\frac{1}{2}\pi - \phi_0)$ with the negative y -axis ($0 \leq \phi_0 \leq \frac{1}{2}\pi$) such that

$$\begin{aligned} H^i &= \hat{z} \exp \{ -ik(x \cos \phi_0 + y \sin \phi_0) \}, \\ E^i &= Z(\sin \phi_0 \hat{x} - \cos \phi_0 \hat{y}) \exp \{ -ik(x \cos \phi_0 + y \sin \phi_0) \}, \end{aligned} \quad (4.120)$$

the scattered magnetic field is:

$$H_z^s = -\sqrt{8\pi} \sum_{m=0}^{\infty} \frac{(-i)^m}{N_m^{(0)}} \frac{Ro_m^{(1)'}(c, 1)}{Ro_m^{(3)'}(c, 1)} Ro_m^{(3)}(c, \xi) So_m(c, \cos \phi_0) So_m(c, \eta). \quad (4.121)$$

An alternate expression for the scattered field is (GRINBERG [1957]):

$$H_z^s(x, y) = \begin{cases} \left[\frac{1}{2i} \int_{-\infty}^{-\frac{1}{2}d} \frac{\partial}{\partial \delta} H_z^s(\gamma, \delta) \right]_{\delta=0^+} H_0^{(1)}(kR) d\gamma + \frac{1}{2i} \int_{\frac{1}{2}d}^{\infty} \frac{\partial}{\partial \delta} H_z^s(\gamma, \delta) \Big|_{\delta=0^+} H_0^{(1)}(kR) d\gamma - \\ - \frac{1}{2} k \sin \phi_0 \int_{-\frac{1}{2}d}^{\frac{1}{2}d} H_0^{(1)}(kR) e^{-ik\gamma \cos \phi_0} d\gamma, & \text{for } y \geq 0, \\ -H_z^s(x, -y), & \text{for } y \leq 0, \end{cases} \quad (4.122)$$

where

$$R = \sqrt{\{(x-\gamma)^2 + y^2\}}, \quad (4.123)$$

$$\begin{aligned} \frac{\partial H_z^s(\gamma, \delta)}{\partial \delta} \Big|_{\delta=0} &= \\ &= \begin{cases} \frac{e^{iky}}{2\sqrt{(2\gamma/d-1)}} \left[\omega_+ \left(\frac{2\gamma}{d} - 1 \right) + \omega_- \left(\frac{2\gamma}{d} - 1 \right) \right], & \text{for } \gamma \geq \frac{1}{2}d, \\ \frac{e^{-iky}}{2\sqrt{(-2\gamma/d-1)}} \left[\omega_+ \left(-\frac{2\gamma}{d} - 1 \right) - \omega_- \left(-\frac{2\gamma}{d} - 1 \right) \right], & \text{for } \gamma \leq -\frac{1}{2}d, \end{cases} \end{aligned} \quad (4.124)$$

$$\omega_{\pm}(\tau) = \lim_{n \rightarrow \infty} \omega_{\pm}^{(n)}(\tau), \quad (\tau \geq 0), \quad (4.125)$$

$$\omega_{\pm}^{(0)}(\tau) = \frac{-ik \sin \phi_0}{\pi} \int_{-1}^1 \frac{e^{ic\rho} \sqrt{(\rho+1)}}{\tau + \rho + 1} [e^{ic\rho \cos \phi_0} \pm e^{-ic\rho \cos \phi_0}] d\rho, \quad (4.126)$$

and

$$\omega_{\pm}^{(n)}(\tau) = \omega_{\pm}^{(0)}(\tau) \mp \frac{e^{2ic}}{\pi} \int_0^{\infty} \frac{e^{2ic\rho}}{(\tau + \rho + 2)} \sqrt{\frac{\rho+2}{\rho}} \omega_{\pm}^{(n-1)}(\rho) d\rho, \quad (n \geq 1). \quad (4.127)$$

For normal incidence, $\omega_- \equiv 0$. In this case GRINBERG [1957] has calculated the first two iterates in eq. (4.127) for $c = \pi$. The results appear in Fig. 4.15.

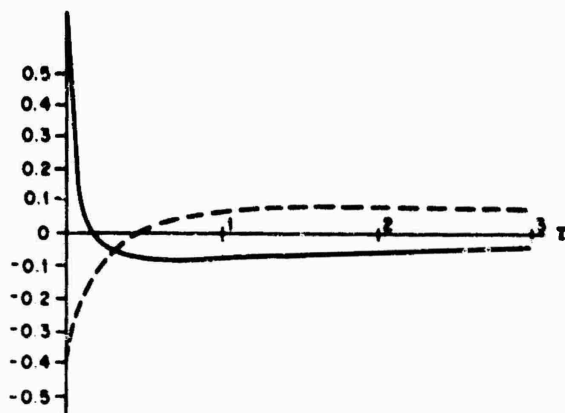


Fig. 4.15. Real (---) and imaginary (—) parts of $(\tau/2k)\omega_+(\tau)$ for $\phi_0 = \frac{1}{2}\pi$ and $c = \pi$ (GRINBERG [1957]).

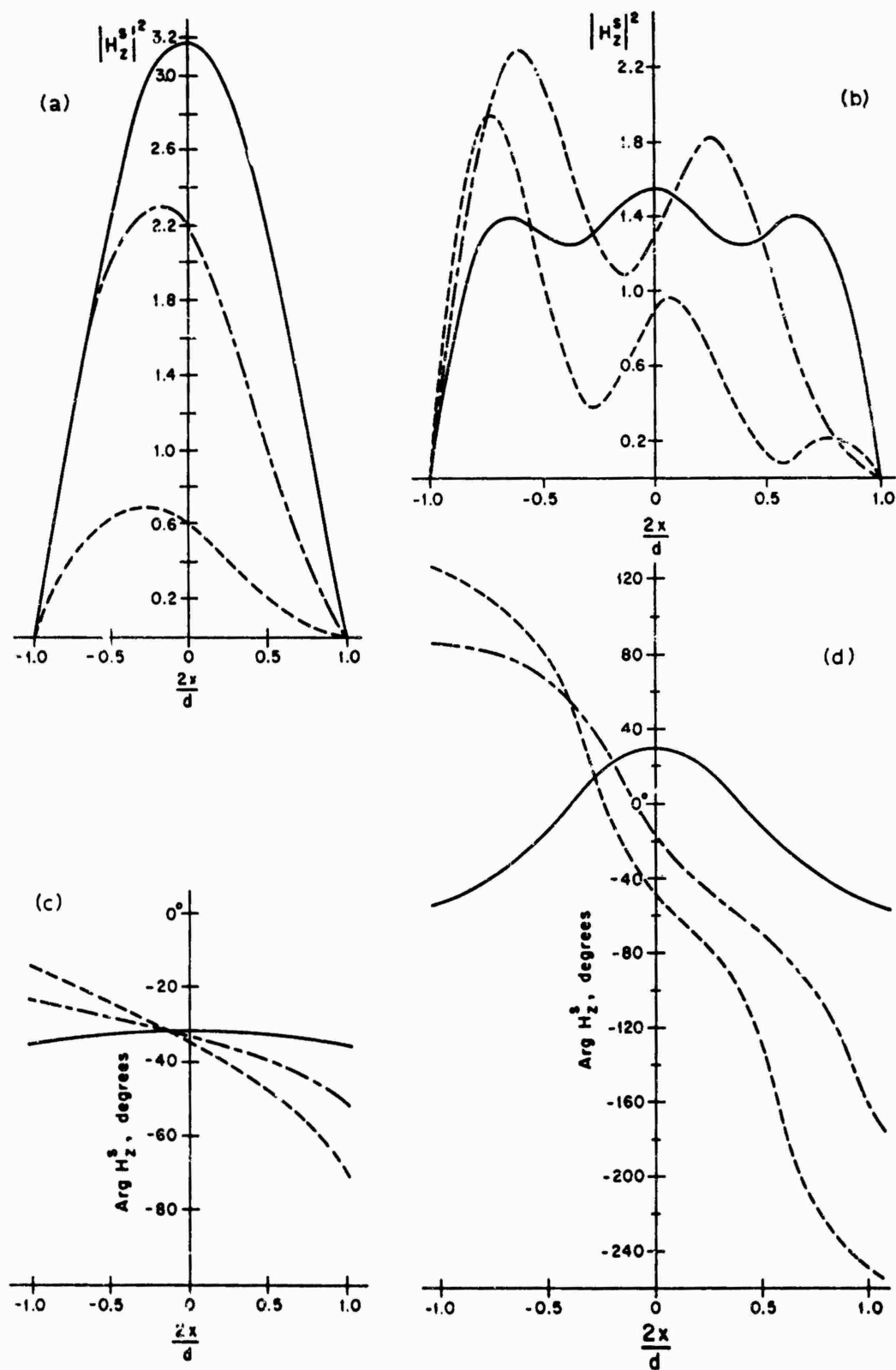


Fig. 4.16. Scattered magnetic field, $H_z^s(x)$, on the strip as a function of x for H -polarization for $\phi_0 = \frac{1}{2}\pi$ (---), $\phi_0 = \frac{1}{4}\pi$ (- - -), $\phi_0 = \frac{1}{2}\pi$ (—) (Hsu [1959]).
 (a) $|H_z^s|^2$ for $d = 0.45\lambda$; (b) $|H_z^s|^2$ for $d = 1.27\lambda$; (c) $\text{arg } H_z^s$ for $d = 0.45\lambda$; (d) $\text{arg } H_z^s$ for $d = 1.27\lambda$.

Since

$$\left. \frac{\partial H_z^s(x, y)}{\partial y} \right|_{y=0} = -ikYE_x^s(x, 0), \quad (4.128)$$

the scattered electric field on the portions of the $y = 0$ plane not occupied by the strip is given by eq. (4.124), whereas the scattered magnetic field is zero. On the strip ($u = 0$) the total magnetic field is:

$$H_z = \sqrt{8\pi} \sum_{m=0}^{\infty} (-i)^{m-1} \left[\frac{Se_m(c, \cos \phi_0) Se_m(c, \eta)}{N_m^{(e)} \frac{\partial}{\partial u} Re_m^{(3)}(c, \cosh u) \Big|_{u=0}} + \frac{So_m(c, \cos \phi_0) So_m(c, \eta)}{N_m^{(o)} \frac{\partial}{\partial u} Ro_m^{(3)}(c, \cosh u) \Big|_{u=0}} \right]. \quad (4.129)$$

Hsu [1959, 1960] has computed $|H_z^s|^2$ and $\arg H_z^s$ on the strip for $c = 0.45\pi, 1.27\pi$ and 2.21π , and $\phi_0 = \frac{1}{6}\pi, \frac{1}{3}\pi$ and $\frac{1}{2}\pi$. Some of these results for the upper face ($y = 0^+$) are shown in Fig. 4.16; on the lower face ($y = 0^-$), $|H_z^s|^2$ is the same as that shown, whereas $\arg H_z^s$ is obtained by adding 180° to the values in Fig. 4.16.

In the far field ($\xi \rightarrow \infty$):

$$P = -2\pi \sum_{m=0}^{\infty} \frac{(-1)^m}{N_m^{(o)}} \frac{Ro_m^{(1)'}(c, 1)}{Ro_m^{(3)'}(c, 1)} So_m(c, \cos \phi_0) So_m(c, \eta). \quad (4.130)$$

The total scattering cross section per unit length is:

$$\sigma_T = \frac{8\pi}{k} \sum_{m=0}^{\infty} \frac{1}{N_m^{(o)}} \left| \frac{Ro_m^{(1)'}(c, 1)}{Ro_m^{(3)'}(c, 1)} So_m(c, \cos \phi_0) \right|^2. \quad (4.131)$$

The normalized total cross section is shown as a function of c for various values of ϕ_0 in Fig. 4.17.

For grazing incidence ($\phi_0 = 0$):

$$H_z^s = 0, \quad (4.132)$$

thus

$$H_z = H_z^i = e^{-ikx} = \sqrt{8\pi} \sum_{m=0}^{\infty} (-i)^m \frac{Re_m^{(1)}(c, 1)}{N_m^{(e)}} Se_m(c, \eta). \quad (4.133)$$

For broadside incidence ($\phi_0 = \frac{1}{2}\pi$) the scattered magnetic field is:

$$H_z^s = i\sqrt{8\pi} \sum_{m=0}^{\infty} (-1)^m \frac{So_{2m+1}(c, 0)}{N_{2m+1}^{(o)}} \frac{Ro_{2m+1}^{(1)'}(c, 1)}{Ro_{2m+1}^{(3)'}(c, 1)} Ro_{2m+1}^{(3)}(c, \xi) So_{2m+1}(c, \eta). \quad (4.134)$$

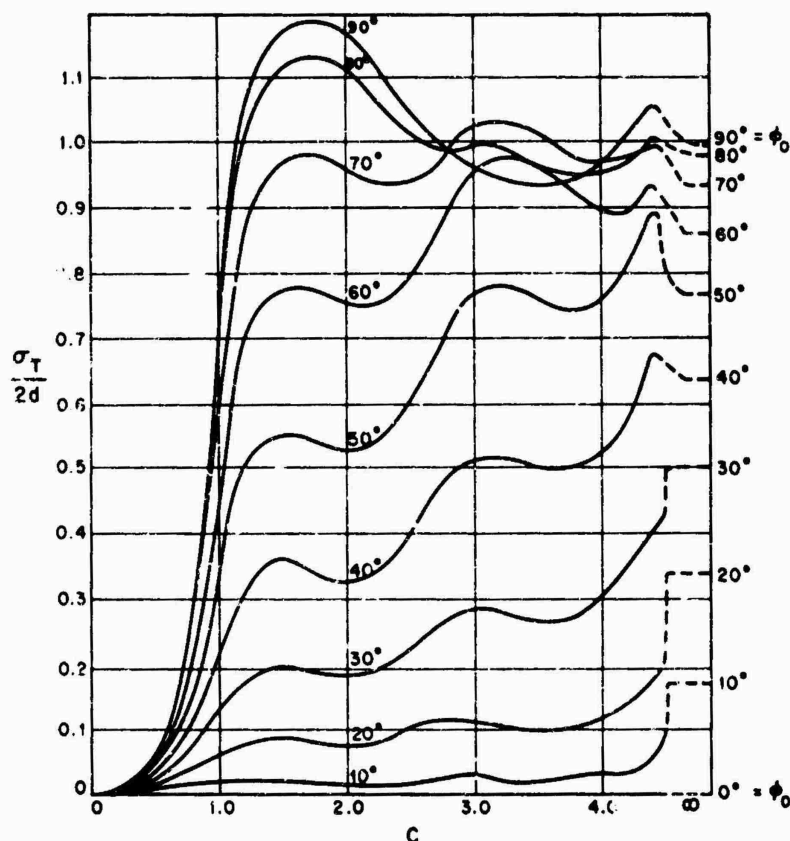


Fig. 4.17. Normalized total scattering cross section per unit length, $\sigma_T/2d$, as a function of c for H -polarization (MORSE and RUBENSTEIN [1938]).

while on the strip ($u = 0$) the total magnetic field is:

$$H_z = \sqrt{8\pi} \sum_{m=0}^{\infty} (-1)^m \left[i \frac{Se_{2m}(c, 0)Se_{2m}(c, \eta)}{N_{2m}^{(e)} \frac{\partial}{\partial u} Re_{2m}^{(3)}(c, \cosh u)} \Big|_{u=0} + \frac{So_{2m+1}(c, 0)So_{2m+1}(c, \eta)}{N_{2m+1}^{(o)} \frac{\partial}{\partial u} Ro_{2m+1}^{(3)}(c, \cosh u)} \Big|_{u=0} \right]. \quad (4.135)$$

The amplitude and phase of H_z^s on the strip are shown in Fig. 4.16 for $c = 0.45\pi$ and 1.27π . The amplitude of the total magnetic field H_z is shown in Fig. 4.18 for various values of c .

In the far field ($\xi \rightarrow \infty$):

$$P = 2\pi \sum_{m=0}^{\infty} \frac{1}{N_{2m+1}^{(o)}} \frac{Ro_{2m+1}^{(1)}(c, 1)}{Ro_{2m+1}^{(3)}(c, 1)} So_{2m+1}(c, \eta). \quad (4.136)$$

The total scattering cross section per unit length is:

$$\sigma_i = \frac{8\pi}{k} \sum_{m=0}^{\infty} \frac{1}{N_{2m+1}^{(o)}} \frac{Ro_{2m+1}^{(1)}(c, 1)}{Ro_{2m+1}^{(3)}(c, 1)} So_{2m+1}(c, 0)^2. \quad (4.137)$$

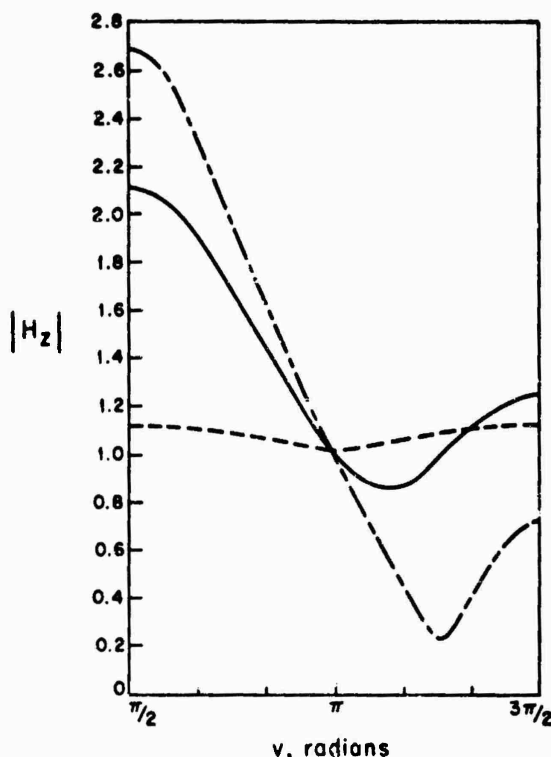


Fig. 4.18. Amplitude of the total magnetic field, $|H_z|$, on the strip as a function of v for H -polarization at broadside incidence ($\phi_0 = \frac{1}{2}\pi$) and $c = 0.5$ (---), $c = 1.0$ (—), $c = 2.0$ (- · -) (BARAKAT [1969]).

and some numerical results based on this formula are shown in Fig. 4.17.

4.2.2.2. LOW FREQUENCY APPROXIMATIONS

For a plane wave whose direction of propagation is perpendicular to the z -axis, and forms the angle ϕ_0 with the negative x -axis and the angle $(\frac{1}{2}\pi - \phi_0)$ with the negative y -axis ($0 \leq \phi_0 \leq \frac{1}{2}\pi$), such that

$$\begin{aligned} H^i &= \hat{z} \exp \{-ik(x \cos \phi_0 + y \sin \phi_0)\}, \\ E^i &= Z(\sin \phi_0 \hat{x} - \cos \phi_0 \hat{y}) \exp \{-ik(x \cos \phi_0 + y \sin \phi_0)\}, \end{aligned} \quad (4.138)$$

low frequency expansions have been obtained either directly (STRUTT [1897a, b, 1913]; GROSCHWITZ and HÖNL [1952]; HÖNL and ZIMMER [1953]; MÜLLER and WESTPFAHL [1953]; BOUWKAMP [1954]; SOMMERFELD [1954]; TRANTER [1954]; DE HOOP [1955]; PIMENOV [1959]; MILLAR [1960]) or by expansion of the Mathieu functions appearing in the exact series solution (BURKE and TWERSKY [1964]; BURKE et al. [1964]).

For arbitrary incidence, the scattered magnetic field on the strip ($u = 0$) is (MILLAR [1960]):

$$H_z^s = c \sum_{n=0}^6 g_n c^n + o(c^6), \quad (4.139)$$

where:

$$p = \log \frac{1}{4}c + \gamma - \frac{1}{2}i\pi, \quad (4.140)$$

$\gamma = 0.5772157 \dots$ is Euler's constant,

and

$$g_0 = -i \sin \phi_0 \sin v, \quad (4.141)$$

$$g_1 = -\frac{1}{8} \sin 2\phi_0 \sin 2v, \quad (4.142)$$

$$g_2 = \frac{1}{4} i \sin \phi_0 (p - \frac{3}{4} + \frac{1}{2} \cos^2 \phi_0) \sin v + \frac{1}{24} i \sin \phi_0 (\frac{1}{2} + \cos^2 \phi_0) \sin 3v, \quad (4.143)$$

$$g_3 = -\frac{1}{48} \sin^3 \phi_0 \cos \phi_0 \sin 2v + \frac{1}{384} \sin 2\phi_0 (\frac{1}{2} + \cos^2 \phi_0) \sin 4v, \quad (4.144)$$

$$g_4 = -\frac{1}{16} i \sin \phi_0 [p^2 - \frac{1}{2} p (\frac{5}{2} - \cos^2 \phi_0) + \frac{7}{16} - \frac{1}{3} \cos^2 \phi_0 + \frac{1}{12} \cos^4 \phi_0] \sin v - \\ - \frac{1}{128} i \sin \phi_0 (p - \frac{5}{8} + \frac{1}{6} \cos^2 \phi_0 + \frac{1}{3} \cos^4 \phi_0) \sin 3v - \\ - \frac{1}{5120} i \sin \phi_0 (1 + \frac{4}{3} \cos^2 \phi_0 + \frac{8}{3} \cos^4 \phi_0) \sin 5v, \quad (4.145)$$

$$g_5 = \frac{1}{1024} \sin 2\phi_0 (p - \frac{9}{8} + \frac{5}{6} \cos^2 \phi_0 - \frac{1}{3} \cos^4 \phi_0) \sin 2v + \\ + \frac{1}{15360} \sin 2\phi_0 (3 - \cos^2 \phi_0 - 2 \cos^4 \phi_0) \sin 4v - \\ - \frac{1}{46080} \sin 2\phi_0 (\frac{3}{8} + \frac{1}{2} \cos^2 \phi_0 + \cos^4 \phi_0) \sin 6v, \quad (4.146)$$

$$g_6 = \frac{1}{256} i \sin \phi_0 [4p^3 - 7p^2 + \frac{1}{24} p - \frac{6}{376} p + (2p^2 - \frac{9}{4} p + \frac{23}{32}) \cos^2 \phi_0 + \\ + (\frac{1}{3} p - \frac{5}{24}) \cos^4 \phi_0 + \frac{1}{36} \cos^6 \phi_0] \sin v + \frac{1}{512} i \sin \phi_0 [p^2 - \frac{9}{8} p + \frac{29}{96} + \\ + (\frac{1}{2} p - \frac{1}{80}) \cos^2 \phi_0 + \frac{1}{60} \cos^4 \phi_0 + \frac{1}{30} \cos^6 \phi_0] \sin 3v + \\ + \frac{1}{61440} i \sin \phi_0 (5p - \frac{35}{12} + \frac{1}{2} \cos^2 \phi_0 + \frac{2}{3} \cos^4 \phi_0 + \frac{4}{3} \cos^6 \phi_0) \sin 5v + \\ + \frac{1}{322560} i \sin \phi_0 (\frac{5}{16} + \frac{3}{8} \cos^2 \phi_0 + \frac{1}{2} \cos^4 \phi_0 + \cos^6 \phi_0) \sin 7v. \quad (4.147)$$

In the far field ($\xi \rightarrow \infty$) and for arbitrary incidence (MILLAR [1960]):

$$P = i\pi c^2 \sum_{n=0}^3 T_{2n}(\phi, \phi_0; p) c^{2n} + o(c^8), \quad (4.148)$$

where

$$T_0 = -\frac{1}{4} \sin \phi_0 \sin \phi, \quad (4.149)$$

$$T_2 = \frac{1}{16} \sin \phi_0 \sin \phi [\frac{1}{2} \cos^2 \phi + \frac{1}{2} \cos \phi_0 \cos \phi + (p - \frac{3}{4} + \frac{1}{2} \cos^2 \phi_0)], \quad (4.150)$$

$$T_4 = -\frac{1}{64} \sin \phi_0 \sin \phi \{ \frac{1}{12} \cos^4 \phi + \frac{1}{6} \cos \phi_0 \cos^3 \phi + [\frac{1}{3} \cos^2 \phi_0 + \frac{1}{2} p - \frac{1}{3}] \cos^2 \phi - \\ - \frac{1}{6} \sin^2 \phi_0 \cos \phi_0 \cos \phi + [p^2 - p(\frac{5}{4} - \frac{1}{2} \cos^2 \phi_0) + \\ + \frac{7}{16} - \frac{1}{3} \cos^2 \phi_0 + \frac{1}{12} \cos^4 \phi_0] \}, \quad (4.151)$$

$$T_6 = \frac{1}{256} \sin \phi_0 \sin \phi \{ \frac{1}{144} \cos^6 \phi + \frac{1}{48} \cos \phi_0 \cos^5 \phi + \\ + \frac{1}{4} (\frac{1}{3} p - \frac{5}{24} + \frac{1}{4} \cos^2 \phi_0) \cos^4 \phi - \\ - \frac{1}{18} [\sin^2 \phi_0 \cos \phi_0 - \frac{1}{8} \cos \phi_0 (\frac{1}{2} + \cos^2 \phi_0)] \cos^3 \phi + \\ + \frac{1}{2} [p^2 - \frac{1}{2} p (\frac{9}{4} - \cos^2 \phi_0) + \frac{23}{64} - \frac{5}{16} \cos^2 \phi_0 + \frac{1}{8} \cos^4 \phi_0] \cos^2 \phi - \\ - \frac{1}{16} \cos \phi_0 (p - \frac{9}{8} + \frac{5}{6} \cos^2 \phi_0 - \frac{1}{3} \cos^4 \phi_0) \cos \phi + \frac{1}{4} [4p^3 - 7p^2 + \\ + \frac{1}{24} p - \frac{6}{376} p + (2p^2 - \frac{9}{4} p + \frac{23}{32}) \cos^2 \phi_0 + \frac{1}{3} (p - \frac{5}{8}) \cos^4 \phi_0 + \frac{1}{36} \cos^6 \phi_0] \}. \quad (4.152)$$

An expression equivalent to eq. (4.148) was used by BURKE and TWERSKY [1960, 1964] to compute the bistatic cross section per unit length as a function of ϕ as shown in Fig. 4.19. Additional computations for $\phi_0 = 0, \frac{1}{4}\pi$ and $\frac{1}{2}\pi$ with $c = 0.3, 0.7$ and 1.1 are given by BURKE et al. [1964]. The normalized back scattering cross

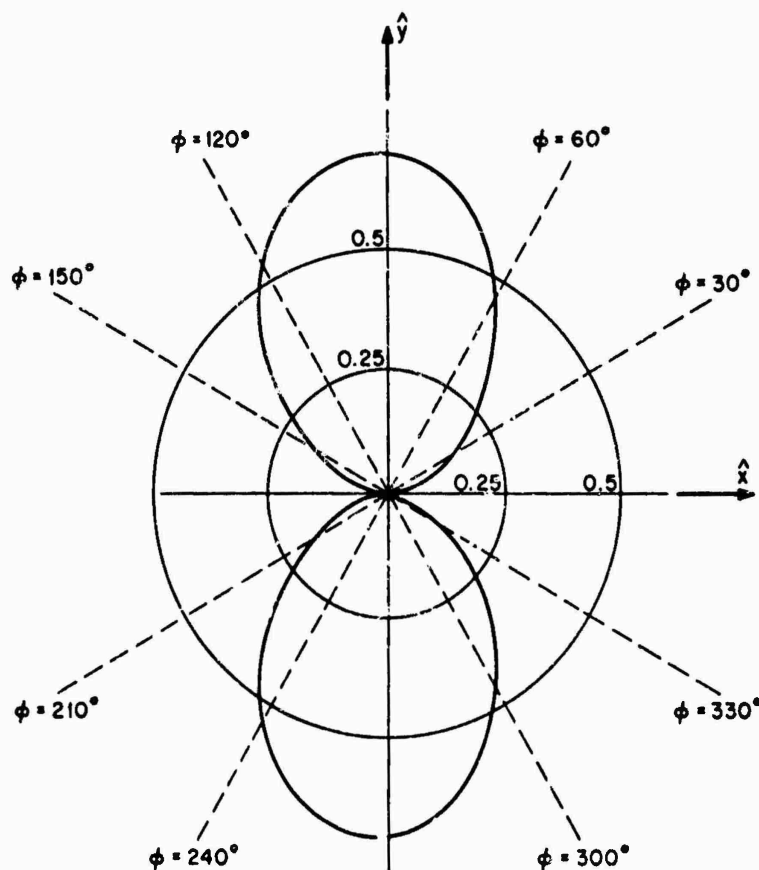


Fig. 4.19. Normalized bistatic cross section per unit length, $\frac{1}{4}k\sigma$, as a function of ϕ for H -polarization with $\phi_0 = \frac{1}{4}\pi$ and $c = 1.1$ (BURKE and TWERSKY [1964]).

section per unit length is shown in Fig. 4.20 as a function of ϕ_0 for $c = 1.1$ and in Fig. 4.21 as a function of c for $\phi_0 = \frac{1}{4}\pi$ and $\frac{1}{2}\pi$.

The normalized total scattering cross section per unit length is (BOERSMA [1964]):

$$\begin{aligned} \frac{\sigma_T}{2d} = & \frac{1}{32}\pi^2 c^3 \sin^2 \phi_0 \left\{ 1 + \frac{5}{16}c^2 \left(1 - \frac{8}{3}\delta - \frac{4}{3}\cos^2 \phi_0 \right) + \right. \\ & + \frac{1}{8}c^4 \left[\frac{5}{24}\cos^4 \phi_0 - \left(\frac{1}{32} - \delta \right) \cos^2 \phi_0 + \frac{1}{160}(109 - 336\delta + 288\delta^2 - 24\pi^2) \right] + \\ & + c^6 \left[-\frac{1}{16}\delta^3 + \frac{2}{35}\delta^2 - \frac{4}{144}\delta + \frac{1}{64}\pi^2\delta + \frac{4}{294}\frac{\pi^2}{12} - \frac{9}{1024}\pi^2 + \right. \\ & + \left(-\frac{3}{64}\delta^2 + \frac{1}{256}\delta - \frac{1}{128}\frac{\pi^2}{8} + \frac{1}{256}\pi^2 \right) \cos^2 \phi_0 + \\ & \left. \left. + \left(-\frac{5}{384}\delta + \frac{3}{64}\pi^2 \right) \cos^4 \phi_0 - \frac{7}{4608}\cos^6 \phi_0 \right] \right\} + O(c^{10}), \end{aligned} \quad (4.153)$$

where

$$\delta = p + \frac{1}{2}i\pi. \quad (4.154)$$

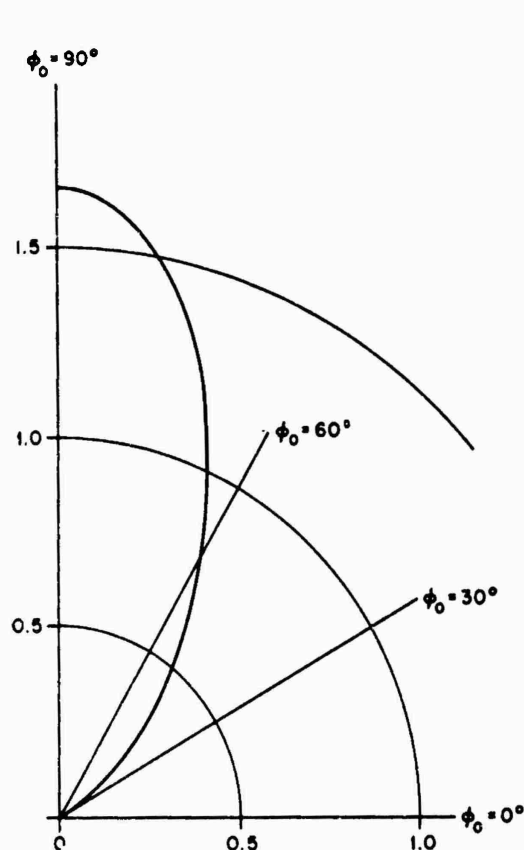


Fig. 4.20. Normalized back scattering cross section per unit length, $\frac{1}{4}k\sigma$, as a function of ϕ_0 for H -polarization with $c = 1.1$ (BURKE and TWERSKY [1964]).

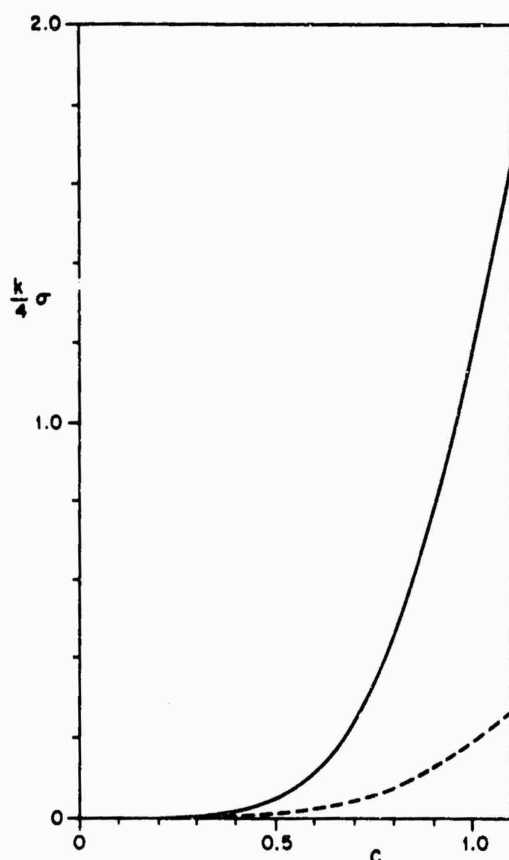


Fig. 4.21. Normalized back scattering cross section per unit length, $\frac{1}{4}k\sigma$, as a function of c for H -polarization with $\phi_0 = \frac{1}{2}\pi$ (—) and $\phi_0 = \frac{1}{4}\pi$ (---) (BURKE and TWERSKY [1964]).

The normalized total scattering cross section calculated using the first three terms (including $O(c^7)$) of eq. (4.153) is shown in Fig. 4.22 as a function of c for various values of ϕ_0 whereas the closed form results of BURKE and TWERSKY [1964] are shown in Fig. 4.23 as a function of ϕ_0 for $c = 1.1$.

For grazing incidence ($\phi_0 = 0$), no scattering occurs: $H_z^s \equiv 0$.

At broadside incidence ($\phi_0 = \frac{1}{2}\pi$), the scattered magnetic field on the strip ($u = 0$) is given by eq. (4.139) in which the coefficients g_{2n+1} are identically zero and

$$g_0 = -i \sin v, \quad (4.155)$$

$$g_2 = \frac{1}{4}i(p - \frac{1}{4}) \sin v + \frac{1}{8}i \sin 3v, \quad (4.156)$$

$$g_4 = -\frac{1}{16}i(p^2 - \frac{5}{4}p + \frac{7}{16}) \sin v - \frac{1}{8}i(p - \frac{5}{8}) \sin 3v - \frac{1}{128}i \sin 5v, \quad (4.157)$$

$$g_6 = \frac{1}{256}i(4p^3 - 7p^2 + \frac{109}{24}p - \frac{607}{96}) \sin v + \frac{1}{512}i(p^2 - \frac{9}{8}p + \frac{29}{64}) \sin 3v + \frac{1}{12288}i(p - \frac{7}{2}) \sin 5v + \frac{1}{1032192}i \sin 7v. \quad (4.158)$$

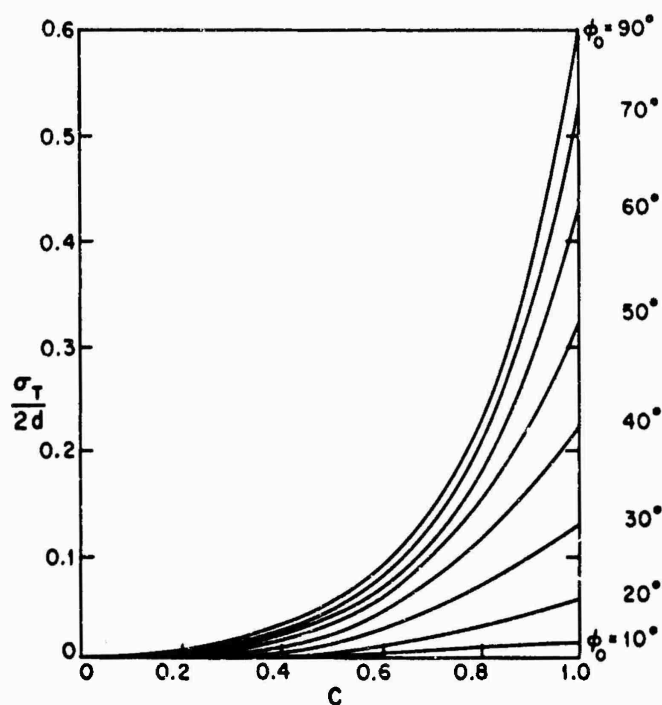


Fig. 4.22. Normalized total scattering cross section per unit length, $\sigma_T/2d$, as a function of c for H -polarization (MILLAR [1960]).

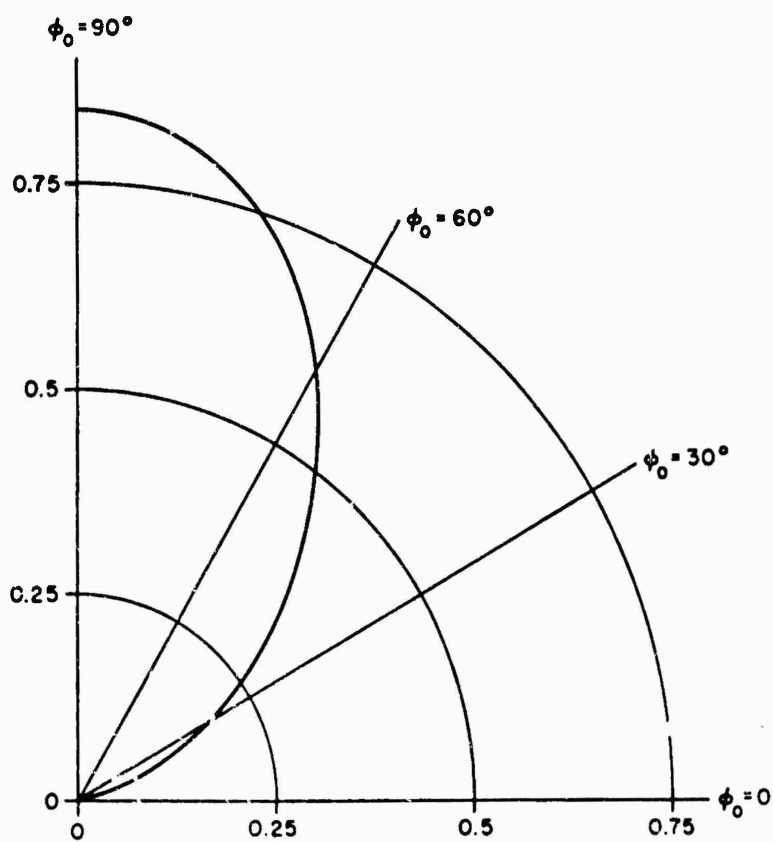


Fig. 4.23. Normalized total scattering cross section per unit length, $\sigma_T/2d$, as a function of ϕ_0 for H -polarization with $c = 1.1$ (BURKE and TWERSKY [1964]).

In the far field ($\xi \rightarrow \infty$) (MILLAR [1960]):

$$P = i\pi c^2 \sum_{n=0}^3 T_{2n}(\phi, \frac{1}{2}\pi; p) c^{2n} + o(c^8), \quad (4.159)$$

with

$$T_0 = -\frac{1}{4} \sin \phi, \quad (4.160)$$

$$T_2 = \frac{1}{16} \sin \phi \left(\frac{1}{2} \cos^2 \phi + p - \frac{3}{4} \right), \quad (4.161)$$

$$T_4 = -\frac{1}{64} \sin \phi \left[\frac{1}{12} \cos^4 \phi + \left(\frac{1}{2} p - \frac{1}{3} \right) \cos^2 \phi + \left(p^2 - \frac{5}{4} p + \frac{7}{16} \right) \right], \quad (4.162)$$

$$T_6 = \frac{1}{256} \sin \phi \left[\frac{1}{44} \cos^6 \phi + \frac{1}{12} \left(p - \frac{5}{8} \right) \cos^4 \phi + \frac{1}{2} \left(p^2 - \frac{9}{8} p + \frac{23}{64} \right) \cos^2 \phi + \frac{1}{4} \left(4p^3 - 7p^2 + \frac{109}{24} p - \frac{607}{576} \right) \right]. \quad (4.163)$$

BURKE et al. [1964] have plotted the normalized bistatic cross section per unit length, $\frac{1}{4}k\sigma(\phi)$, as a function of ϕ for $c = 0.3, 0.7$ and 1.1 . The normalized back scattering cross section per unit length as a function of c is shown in Fig. 4.21. The normalized total scattering cross section per unit length is (BOERSMA [1964]):

$$\begin{aligned} \frac{\sigma_T}{2d} = & \frac{1}{2} \pi^2 c^3 \left\{ 1 + \frac{5}{16} c^2 \left(1 - \frac{8}{3} \delta \right) + \frac{1}{1536} c^4 (109 - 336\delta + 288\delta^2 - 24\pi^2) + \right. \\ & \left. + c^6 \left(-\frac{1}{16} \delta^3 + \frac{27}{256} \delta^2 - \frac{401}{6144} \delta + \frac{1}{64} \pi^2 \delta + \frac{4391}{294912} - \frac{9}{1024} \pi^2 \right) \right\} + O(c^{10}). \end{aligned} \quad (4.164)$$

A plot of the first three terms of this expression appears in Fig. 4.22.

4.2.2.3. HIGH FREQUENCY APPROXIMATIONS

For a plane wave whose direction of propagation is perpendicular to the z -axis, and forms the angle ϕ_0 with the negative x -axis and the angle $(\frac{1}{2}\pi - \phi_0)$ with the negative y -axis ($0 \leq \phi_0 \leq \frac{1}{2}\pi$), such that

$$\begin{aligned} H^i &= \hat{z} \exp \{ -ik(x \cos \phi_0 + y \sin \phi_0) \}, \\ E^i &= Z(\sin \phi_0 \hat{x} - \cos \phi_0 \hat{y}) \exp \{ -ik(x \cos \phi_0 + y \sin \phi_0) \}, \end{aligned} \quad (4.165)$$

the scattered magnetic field is (KARP and KELLER [1961]):

$$\begin{aligned} H_z^s = & \frac{1}{2} i \operatorname{sgn}(\sin \psi_1) \left\{ \int_{-\infty}^{\infty} \frac{2}{\pi k \rho_1} \exp \{ ik\rho_1 - \frac{1}{2} i\pi - ic \cos \phi_0 \} \sqrt{\frac{(1 - \cos \psi_1)(1 - \cos \phi_0)}{\cos \psi_1 + \cos \phi_0}} \right. \\ & \times \left[1 - \frac{i}{2k\rho_1} \frac{1 + \cos \psi_1 \cos \phi_0}{(\cos \psi_1 + \cos \phi_0)^2} + O\{(k\rho_1)^{-2}\} \right] - \\ & - \int_{-\infty}^{\infty} \frac{2}{\pi k \rho_2} \exp \{ ik\rho_2 - \frac{1}{2} i\pi + ic \cos \phi_0 \} \sqrt{\frac{(1 + \cos \psi_2)(1 + \cos \phi_0)}{\cos \psi_2 + \cos \phi_0}} \\ & \times \left[1 - \frac{i}{2k\rho_2} \frac{1 + \cos \psi_2 \cos \phi_0}{(\cos \psi_2 + \cos \phi_0)^2} + O\{(k\rho_2)^{-2}\} \right] \Bigg\}, \end{aligned} \quad (4.166)$$

where:

$$\rho_{1,2} \rightarrow d, \quad \psi_{1,2} \neq \pi \pm \phi_0, \quad \phi_0 \neq 0. \quad (4.167)$$

and the geometric variables are defined in eqs. (4.67) and illustrated in Fig. 4.11. The expression in eq. (4.166) is based on analysis of singly diffracted rays only. An expression of the scattered magnetic field which includes contributions from multiply diffracted rays but to a lower order in $k\rho_{1,2}$ is (KARP and KELLER [1961]):

$$\begin{aligned}
 H_z^s = & \operatorname{sgn}(\sin \psi_1) \left[\sqrt{\frac{2}{\pi k \rho_1}} e^{ik\rho_1 - \frac{1}{2}i\pi} \left\{ -\frac{1}{2}ie^{-ic \cos \phi_0} \frac{\sqrt{\{(1 - \cos \psi_1)(1 - \cos \phi_0)\}}}{\cos \psi_1 + \cos \phi_0} + \right. \right. \\
 & + \frac{1}{4} \sqrt{\frac{2}{\pi c}} e^{2ic - \frac{1}{2}i\pi} \left(1 - \frac{ie^{4ic}}{16\pi c} \right)^{-1} (1 - \cos \psi_1)^{-\frac{1}{2}} \\
 & \times \left(\frac{e^{ic \cos \phi_0}}{\cos \frac{1}{2}\phi_0} - \frac{\exp \{2ic + \frac{1}{2}i\pi - ic \cos \phi_0\}}{4\sqrt{\pi c} \sin \frac{1}{2}\phi_0} \right) + O\left(\frac{1}{k\rho_1}\right) \Big\} + \\
 & + \sqrt{\frac{2}{\pi k \rho_2}} e^{ik\rho_2 - \frac{1}{2}i\pi} \left\{ \frac{1}{2}ie^{ic \cos \phi_0} \frac{\sqrt{\{(1 + \cos \psi_2)(1 + \cos \phi_0)\}}}{\cos \psi_2 + \cos \phi_0} + \right. \\
 & + \frac{1}{4} \sqrt{\frac{2}{\pi c}} e^{2ic - \frac{1}{2}i\pi} \left(1 - \frac{ie^{4ic}}{16\pi c} \right)^{-1} (1 + \cos \psi_2)^{-\frac{1}{2}} \\
 & \times \left(\frac{e^{-ic \cos \phi_0}}{\sin \frac{1}{2}\phi_0} - \frac{\exp \{2ic + \frac{1}{2}i\pi + ic \cos \phi_0\}}{4\sqrt{\pi c} \cos \frac{1}{2}\phi_0} \right) + O\left(\frac{1}{k\rho_2}\right) \Big\}, \quad (4.168)
 \end{aligned}$$

where:

$$\rho_{1,2} \gg d; \quad \psi_{1,2} \neq \pi \pm \phi_0, 0, \pi, 2\pi; \quad \phi_0 \neq 0. \quad (4.169)$$

An expression which is still approximate but includes terms of all orders in $k\rho_{1,2}$ based on successive interactions of half plane fields, is (KARP and RUSSEK [1956]):

$$H_z^s = \begin{cases} \exp \{-ik\rho \cos(\phi + \phi_0)\} + V_{1i} + V_{2i} + C_1 V_{12} + C_2 V_{21}, \\ \text{for } 0 \leq \phi \leq \pi \text{ } (0 \leq \psi_{1,2} \leq \pi), \end{cases} \quad (4.170)$$

$$\begin{cases} -H_z^s(2\pi - \phi, 2\pi - \psi_1, 2\pi - \psi_2), \\ \text{for } \pi \leq \phi \leq 2\pi \text{ } (\pi \leq \psi_{1,2} \leq 2\pi), \end{cases} \quad (4.171)$$

where:

$$\begin{aligned}
 V_{1i} = & \frac{e^{\frac{1}{2}i\pi}}{\sqrt{\pi}} \left[\exp \{-ik\rho \cos(\phi - \phi_0)\} F(\sqrt{2k\rho_1} \cos \frac{1}{2}(\psi_1 - \phi_0)) + \right. \\
 & + \exp \{-ik\rho \cos(\phi + \phi_0)\} F(-\sqrt{2k\rho_1} \cos \frac{1}{2}(\psi_1 + \phi_0)) \Big], \quad (0 \leq \psi_1 \leq \pi), \quad (4.172)
 \end{aligned}$$

$$\begin{aligned}
 V_{2i} = & \frac{e^{\frac{1}{2}i\pi}}{\sqrt{\pi}} \left[\exp \{-ik\rho \cos(\phi - \phi_0)\} F(\sqrt{2k\rho_2} \cos \frac{1}{2}(\psi_2 - \phi_0)) + \right. \\
 & + \exp \{-ik\rho \cos(\phi + \phi_0)\} F(\sqrt{2k\rho_2} \cos \frac{1}{2}(\psi_2 + \phi_0)) \Big], \quad (0 \leq \psi_2 \leq \pi). \quad (4.173)
 \end{aligned}$$

$$V_{12} = -2e^{ik\rho_2} \int_m^{\infty} \frac{e^{i\mu^2} d\mu}{\sqrt{(\mu^2 + 2k\rho_2)}}, \quad m = 2 \sqrt{\frac{c\rho_1(1 - \cos \psi_1)}{\rho_1 + \rho_2 + d}}, \quad (4.174)$$

$$V_{21} = -2e^{ik\rho_1} \int_{m'}^{\infty} \frac{e^{i\mu^2} d\mu}{\sqrt{(\mu^2 + 2k\rho_1)}}, \quad m' = 2 \sqrt{\frac{c\rho_2(1 + \cos \psi_2)}{\rho_1 + \rho_2 + d}}, \quad (4.175)$$

$$C_1 = -\frac{1}{\pi} \left[1 - \frac{ie^{4ic}}{4\pi c} \right]^{-1} \left\{ \frac{\exp \{ic \cos \phi_0\}}{\cos \frac{1}{2}\phi_0} - \frac{\exp \{2ic + \frac{1}{2}i\pi - ic \cos \phi_0\}}{2\sqrt{\pi c} \sin \frac{1}{2}\phi_0} \right\}, \quad (4.176)$$

$$C_2 = -\frac{1}{\pi} \left[1 - \frac{ie^{4ic}}{4\pi c} \right]^{-1} \left\{ \frac{\exp \{-ic \cos \phi_0\}}{\sin \frac{1}{2}\phi_0} - \frac{\exp \{2ic + \frac{1}{2}i\pi + ic \cos \phi_0\}}{2\sqrt{\pi c} \cos \frac{1}{2}\phi_0} \right\}, \quad (4.177)$$

and $F(\tau)$ is the Fresnel integral defined in the Introduction. The geometric variables are given by eqs. (4.67) and illustrated in Fig. 4.11. Eqs. (4.170) and (4.171) are not valid for grazing incidence. On the strip ($u = 0$) the total magnetic field for arbitrary incidence is (MILLAR [1958a]):

$$H_z = \exp \{-ic\eta \cos \phi_0\} + \operatorname{sgn}(\sin v) \{ \exp \{-ic\eta \cos \phi_0\} + \sin \phi_0 \sum_{n=0}^3 [h_n(\cos \phi_0, \eta) + h_n(-\cos \phi_0, -\eta)] c^{1(3-n)} + O(c^{-1}) \}, \quad (4.178)$$

where:

$$h_0(\cos \phi_0, \eta) = -\frac{2 \exp \{-\frac{1}{2}i\pi - ic\eta \cos \phi_0\}}{\sqrt{\pi} \sin \phi_0} F[\sqrt{\{c(1 - \cos \phi_0)(1 - \eta)\}}], \quad (4.179)$$

$$h_1(\cos \phi_0, \eta) = \frac{\exp \{2ic + ic \cos \phi_0\}}{\pi \sqrt{c}} \left\{ 2A_0[2c(1 + \cos \phi_0)] F[\sqrt{\{2c(1 - \eta)\}}] + \frac{1}{c} \left[\left(\frac{2}{1 - \cos \phi_0} - 1 \right) \frac{F[\sqrt{\{2c(1 - \eta)\}}]}{1 + \cos \phi_0} + \frac{1}{2} A_1[2c(1 + \cos \phi_0)] G(\eta) \right] \right\}, \quad (4.180)$$

$$h_2(\cos \phi_0, \eta) = \frac{-\exp \{\frac{1}{2}i\pi + 4ic - ic \cos \phi_0\}}{\pi \sqrt{\pi c}} \left\{ A_0[2c(1 - \cos \phi_0)] F[\sqrt{\{2c(1 - \eta)\}}] + \frac{A_0[2c(1 - \cos \phi_0)] G(\eta)}{4c} + \frac{1}{c} F[\sqrt{\{2c(1 - \eta)\}}] \left[\frac{1}{2(1 - \cos \phi_0)} \left(\sqrt{\frac{2}{1 + \cos \phi_0}} - 1 \right) + \frac{1}{8} A_1[2c(1 - \cos \phi_0)] - \frac{1}{16} A_3[2c(1 - \cos \phi_0)] \right] \right\}, \quad (4.181)$$

$$h_3(\cos \phi_0, \eta) = \frac{i \exp \{6ic + ic \cos \phi_0\}}{2\pi^2 \sqrt{c}} A_0[2c(1 + \cos \phi_0)] F[\sqrt{\{2c(1 - \eta)\}}], \quad (4.182)$$

$$G(\eta) = [c(1 - \eta) - \frac{1}{2}] F[\sqrt{\{2c(1 - \eta)\}}] e^{-ic(1 - \eta)} - i 2^{-\frac{1}{2}} \sqrt{1 - \eta} e^{ic(1 - \eta)}, \quad (4.183)$$

$$A_0(x) = -2ix^{-\frac{1}{2}} e^{-ix^2} F[\sqrt{x}], \quad (4.184)$$

$$A_1(x) = -2 - 4ix^{\frac{1}{2}} e^{-ix^2} F[\sqrt{x}], \quad (4.185)$$

and $F(\tau)$ is the Fresnel integral defined in the Introduction. Higher order terms may be derived following MILLAR [1958a]. By neglecting the summation in eq. (4.178), the

geometric optics approximation to the magnetic field is obtained. The above expressions are valid uniformly in η ; however, they may be simplified in restricted regions of the surface. In particular, away from the edges, such that $c|\sin v| \gg 1$, the field on the surface is given by eq. (4.178) with the quantity $\sin \phi_0 \sum_{n=1}^3$ replaced by:

$$\begin{aligned} & \frac{e^{-\frac{1}{2}i\pi+ic}}{\sqrt{\pi c}} \left[\frac{\exp\{ic(\cos \phi_0 + \eta)\}}{\sqrt{\{(1 + \cos \phi_0)(1 + \eta)\}}} + \frac{\exp\{-ic(\cos \phi_0 + \eta)\}}{\sqrt{\{(1 - \cos \phi_0)(1 - \eta)\}}} \right] + \\ & + \frac{i \sin \phi_0 e^{4ic}}{2\pi c} \left[\frac{\exp\{ic(\cos \phi_0 - 2\eta)\}}{(1 + \cos \phi_0)\sqrt{\{(1 - \cos \phi_0)(1 - \eta)\}}} + \right. \\ & \left. + \frac{\exp\{-ic(\cos \phi_0 - 2\eta)\}}{(1 - \cos \phi_0)\sqrt{\{(1 + \cos \phi_0)(1 + \eta)\}}} \right] + O(c^{-1}). \end{aligned} \quad (4.186)$$

For arbitrary incidence, the scattered electric field on the portions of the plane $y = 0$ outside of the strip ($|x| > \frac{1}{2}d$) is (GRINBERG [1957]):

$$\begin{aligned} E_x^s = \frac{iZ}{k} \frac{\partial H_z^s}{\partial y} \Big|_{y=0} &= Z \frac{e^{ic\xi}}{\sqrt{(\xi-1)}} [\omega_+(\xi-1) \pm \omega_-(\xi-1)], \\ & (+ \text{ for } v = 0, (x \geq \tfrac{1}{2}d); - \text{ for } v = \pi, (x \leq -\tfrac{1}{2}d)), \end{aligned} \quad (4.187)$$

where:

$$\omega_{\pm}(\tau) \sim \omega_{\pm}^{(0)}(\tau) \mp \frac{\sqrt{2}e^{2ic} \int_0^{\infty} \omega_{\pm}^{(0)}(\rho) e^{2ic\rho} \rho^{-\frac{1}{2}} d\rho}{\pi(\tau+2)(1 \pm 2\pi^{-\frac{1}{2}} e^{-2ic-4i\pi} F[2\sqrt{c}])}, \quad (4.188)$$

$$\omega_+^{(0)}(\tau) = \frac{\sin \phi_0}{\pi} \int_{-1}^1 \frac{e^{ic\rho}}{\tau + \rho + 1} \sqrt{\rho+1} \cos(c\rho \cos \phi_0) d\rho, \quad (4.189)$$

$$\omega_-^{(0)}(\tau) = \frac{i \sin \phi_0}{\pi} \int_{-1}^1 \frac{e^{ic\rho}}{\tau + \rho + 1} \sqrt{\rho+1} \sin(c\rho \cos \phi_0) d\rho, \quad (4.190)$$

and $F[\tau]$ is the Fresnel integral defined in the Introduction. The order of the approximation in eq. (4.187) is not known.

In the far field ($\xi \rightarrow \infty$) and for arbitrary incidence (KHASKIND and VAKINSHTEYN [1964]):

$$\begin{aligned} P = & \frac{-i \operatorname{sgn}(\sin \phi)}{2(\cos \phi + \cos \phi_0)} \left\{ \exp\{ic(\cos \phi + \cos \phi_0)\} \sqrt{\{(1 + \cos \phi)(1 + \cos \phi_0)\}} \right. \\ & \times [1 + \Gamma(c, \cos \phi)][1 + \Gamma(c, \cos \phi_0)] - \\ & - \exp\{-ic(\cos \phi + \cos \phi_0)\} \sqrt{\{(1 - \cos \phi)(1 - \cos \phi_0)\}} \\ & \left. \times [1 + \Gamma(c, -\cos \phi)][1 + \Gamma(c, -\cos \phi_0)] \right\} + O(c^{-1}), \end{aligned} \quad (4.191)$$

where:

$$\Gamma(c, x) = \sqrt{1-x^2} \int_x^c H_0^{(1)}(2t) e^{-2ixt} dt, \quad (4.192)$$

and

$$\Gamma(c, 1) = -1, \quad \bar{\Gamma}(c, -1) = 0. \quad (4.193)$$

The expression in eq. (4.191) is uniformly valid in ϕ and ϕ_0 and equivalent results are given by MILLAR [1958a]. Computations of $|P|$ as a function of ϕ for $\phi_0 = \frac{1}{4}\pi$

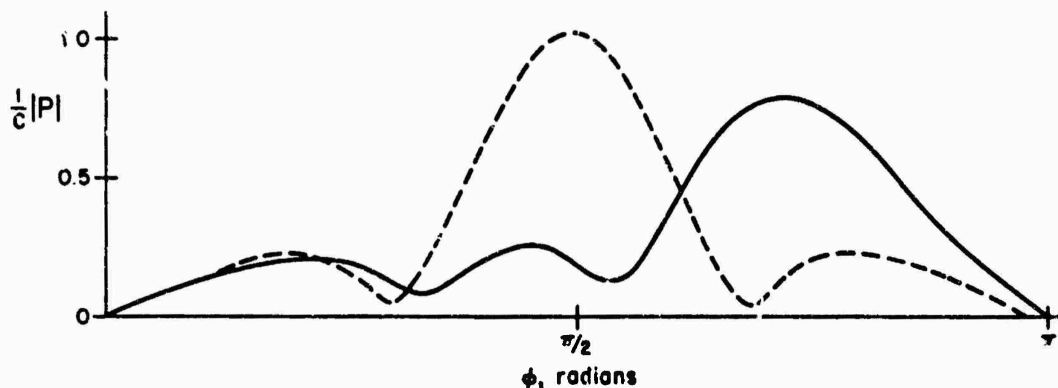


Fig. 4.24. Normalized far field amplitude, $|P|/c$, as a function ϕ for H -polarization with $c = \sqrt{28}$, $\phi_0 = \frac{1}{4}\pi$ (—) and $\phi_0 = \frac{1}{2}\pi$ (---) (UFIMTSEV [1958]).

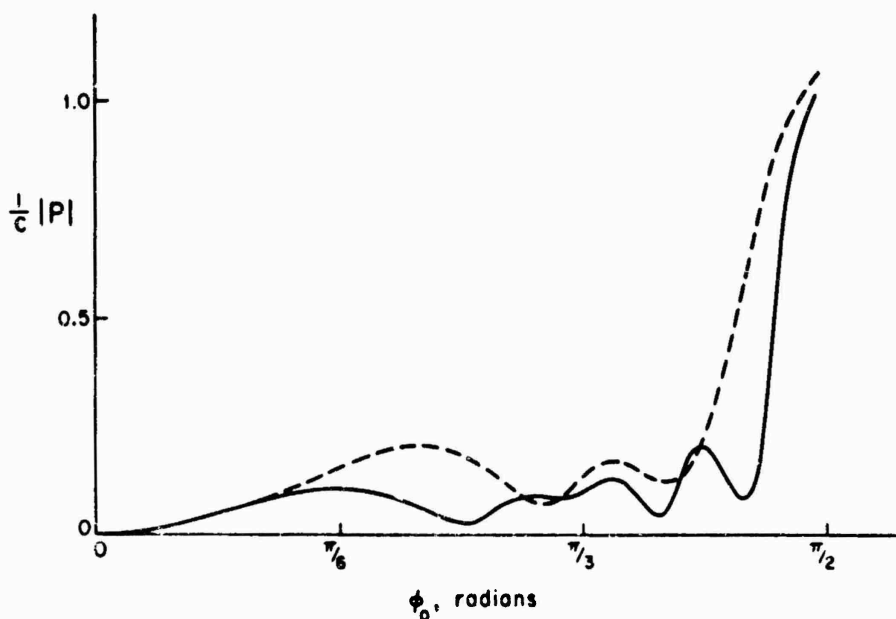


Fig. 4.25. Normalized back scattered far field, $|P|/c$ as a function of ϕ_0 for H -polarization with $c = \sqrt{28}$ (—) and $c = \sqrt{80}$ (---) (UFIMTSEV [1958]).

and $\frac{1}{2}\pi$ and $c = \sqrt{28}$ are shown in Fig. 4.24, whereas Fig. 4.25 presents the backscattered field as a function of ϕ_0 for $c = \sqrt{28}$ and $c = \sqrt{80}$. These results are rigorous (UFIMTSEV [1958]); however, the method of derivation has not been indicated. Away from grazing angles ($c|\sin \phi| \gg 1$, $c \sin \phi_0 \gg 1$), the far field is:

$$\begin{aligned}
 P = & -\operatorname{sgn}(\sin \phi) \left\{ \frac{i}{2(\cos \phi + \cos \phi_0)} \right. \\
 & \times [\exp \{i c (\cos \phi + \cos \phi_0)\} \sqrt{\{(1 + \cos \phi)(1 + \cos \phi_0)\}} - \\
 & \quad \left. - \exp \{-i c (\cos \phi + \cos \phi_0)\} \sqrt{\{(1 - \cos \phi)(1 - \cos \phi_0)\}}] + \right. \\
 & \left. + \frac{e^{2ic - \frac{1}{2}i\pi}}{2\sqrt{\pi c}} \left[\frac{\exp \{i c (\cos \phi_0 - \cos \phi)\}}{\sqrt{\{(1 - \cos \phi)(1 + \cos \phi_0)\}}} + \frac{\exp \{-i c (\cos \phi_0 - \cos \phi)\}}{\sqrt{\{(1 - \cos \phi_0)(1 + \cos \phi)\}}} \right] + O(c^{-1}) \right\}.
 \end{aligned}
 \tag{4.194}$$

The first term, $O(c^0)$, in this expression was obtained by KELLER [1957] using singly diffracted rays; its amplitude is the same as the corresponding term for E -polarization (eq. (4.96)), which is plotted for $\phi_0 = \frac{1}{2}\pi$ and $c = 8$ and $c = 10\pi$ in Fig. 4.13. The second term in eq. (4.194) of order $c^{-\frac{1}{2}}$ has been obtained by KARP and KELLER [1961],

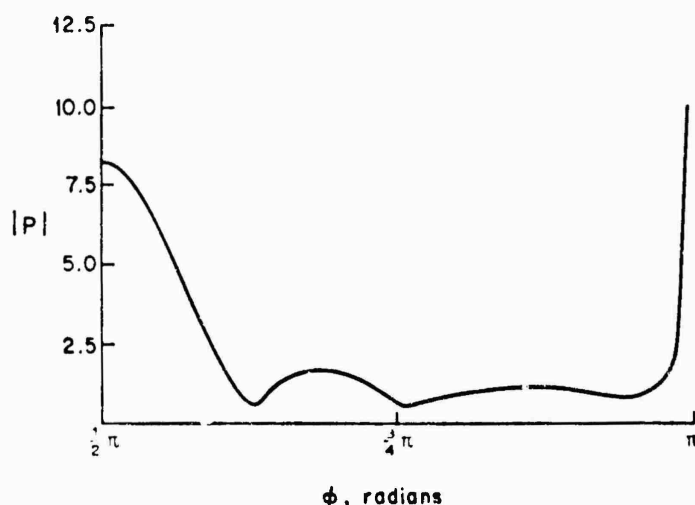


Fig. 4.26. Amplitude of the far field coefficient, $|P|$, as a function of ϕ for H -polarization with $c = 8$ (KELLER [1957]).

and it can also be obtained by specializing the results of either eq. (4.170) or eq. (4.191). The amplitude of P for broadside incidence, computed from an expression which agrees with that of eq. (4.194) to order c^{-1} , is shown in Fig. 4.26. In particular, for back scattering ($\phi = \phi_0$) and non-grazing incidence ($c \sin \phi_0 \gg 1$), the far field is:

$$P = \frac{\sin(2c \cos \phi_0)}{2 \cos \phi_0} - \frac{1}{2} i \cos(2c \cos \phi_0) - \frac{e^{2ic - \frac{1}{2}i\pi}}{\sqrt{\pi c} \sin \phi_0} + O(c^{-1}), \tag{4.195}$$

which for broadside incidence reduces to:

$$P = c - \frac{1}{2} i - \frac{e^{2ic - \frac{1}{2}i\pi}}{\sqrt{\pi c}} + O(c^{-1}). \tag{4.196}$$

On the other hand, for forward scattering ($\phi = \phi_0 + \pi$) and non-grazing incidence

($c \sin \phi_0 \gg 1$), the far field is:

$$P = -c \sin \phi_0 + \frac{i}{2 \sin \phi_0} + \frac{e^{2ic - \frac{1}{2}i\pi}}{2\sqrt{\pi c}} \left[\frac{e^{2ic \cos \phi_0}}{1 + \cos \phi_0} + \frac{e^{-2ic \cos \phi_0}}{1 - \cos \phi_0} \right] + O(c^{-1}), \quad (4.197)$$

which for broadside incidence ($\phi_0 = \frac{1}{2}\pi$) reduces to the negative of the result of eq. (4.196).

The physical optics approximation to the far field coefficient is:

$$P = \text{sgn}(\sin \phi) \sin \phi_0 \frac{\sin [c(\cos \phi + \cos \phi_0)]}{\cos \phi + \cos \phi_0}, \quad (4.198)$$

which differs from the leading term in eq. (4.194) except for forward scattering, and for back scattering at broadside incidence.

The normalized total scattering cross section per unit length for non-grazing incidence ($c \sin \phi_0 \gg 1$) is (SESHADRI [1958a]; KIEBURTZ [1965]):

$$\begin{aligned} \frac{\sigma_T}{2d} = & \sin \phi_0 - \frac{1}{2c\sqrt{\pi c}} \left\{ \frac{\cos [2c(1 + \cos \phi_0) - \frac{1}{2}\pi]}{1 + \cos \phi_0} + \frac{\cos [2c(1 - \cos \phi_0) - \frac{1}{2}\pi]}{1 - \cos \phi_0} \right\} + \\ & + \frac{\cos 4c}{2\pi c^2 \sin \phi_0} - \frac{1}{8\pi c^2 \sqrt{\pi c}} \left\{ \frac{\cos [2c(3 + \cos \phi_0) + \frac{1}{2}\pi]}{1 + \cos \phi_0} + \frac{\cos [2c(3 - \cos \phi_0) + \frac{1}{2}\pi]}{1 - \cos \phi_0} \right\} - \\ & - \frac{\pi(7 - \cos \phi_0) \cos [2c(1 + \cos \phi_0) + \frac{1}{2}\pi]}{4(1 + \cos \phi_0)^2} - \frac{\pi(7 + \cos \phi_0) \cos [2c(1 - \cos \phi_0) + \frac{1}{2}\pi]}{4(1 - \cos \phi_0)^2} \Bigg\} + \\ & + O(c^{-3}). \quad (4.199) \end{aligned}$$

Results of computations based on eq. (4.199) are shown in Fig. 4.27.

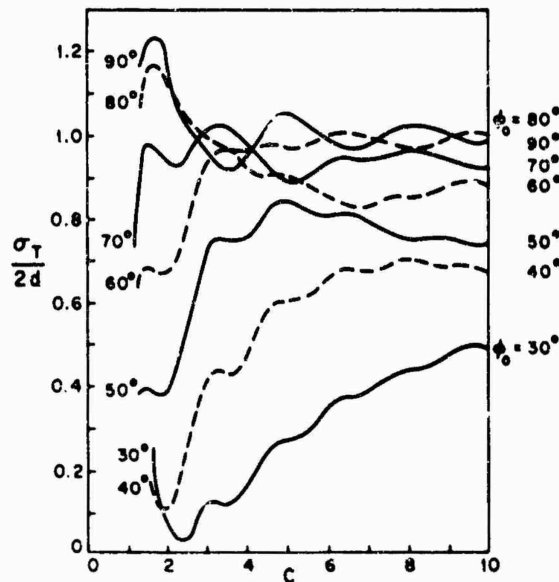


Fig. 4.27. Normalized total scattering cross section per unit length, $\sigma_T/2d$, as a function of c for H -polarization and various angles of incidence (KING and WU [1959]).

For broadside incidence ($\phi_0 = \frac{1}{2}\pi$), a higher order approximation is (MILLAR [1958a]):

$$\frac{\sigma_T}{2d} = 1 - \frac{\cos(2c - \frac{1}{4}\pi)}{c\sqrt{\pi c}} + \frac{\cos 4c}{2\pi c^2} - \frac{1}{4\pi c^2\sqrt{\pi c}} [\cos(6c + \frac{1}{4}\pi) - \frac{7}{4}\pi \cos(2c + \frac{1}{4}\pi)] - \frac{1}{8\pi^2 c^3} [\sin 8c - \frac{5}{2}\pi \sin 4c] + O(c^{-\frac{5}{2}}). \quad (4.200)$$

Near grazing incidence, conflicting expressions for the total scattering cross section have been obtained by MILLAR [1958a] and KIEBURTZ [1965].

4.3. Line sources

4.3.1. E-polarization

4.3.1.1. EXACT SOLUTIONS

For an electric line source parallel to the z -axis and located at (u_0, v_0) , such that

$$E^i = \hat{z}H_0^{(1)}(kR), \quad (4.201)$$

the total electric field is:

$$E_z = 4 \sum_{m=0}^{\infty} \left\{ \frac{1}{N_m^{(e)}} \left[\text{Re}_m^{(1)}(c, \xi_-) - \frac{\text{Re}_m^{(1)}(c, 1)}{\text{Re}_m^{(3)}(c, 1)} \text{Re}_m^{(3)}(c, \xi_-) \right] \right. \\ \left. \times \text{Re}_m^{(3)}(c, \xi_+) \text{Se}_m(c, \eta_0) \text{Se}_m(c, \eta) + \right. \\ \left. + \frac{1}{N_m^{(o)}} \text{Ro}_m^{(1)}(c, \xi_-) \text{Rc}_m^{(3)}(c, \xi_+) \text{So}_m(c, \eta_0) \text{So}_m(c, \eta) \right\}. \quad (4.202)$$

An alternate expression for the scattered field is (GRINBERG [1958]):

$$E_z^s(x, y) = \begin{cases} \frac{1}{2i} \frac{\partial}{\partial y} \left\{ \int_{-x}^{-\frac{1}{2}d} E_z^i(\gamma, 0) H_0^{(1)}(kR) d\gamma + \int_{\frac{1}{2}d}^{\infty} E_z^i(\gamma, 0) H_0^{(1)}(kR) d\gamma - \right. \\ \left. - \int_{-\frac{1}{2}d}^{\frac{1}{2}d} H_0^{(1)}(kR_0) H_0^{(1)}(kR) d\gamma \right\}, & \text{for } y \geq 0, \\ E_z^i(x, -y), & \text{for } y \leq 0, \end{cases} \quad (4.203)$$

where:

$$R = \sqrt{\{(x-\gamma)^2 + y^2\}}, \quad (4.204)$$

$$R_0 = \sqrt{\{(x_0-\gamma)^2 + y_0^2\}}, \quad (4.205)$$

$$E_z^i(x, 0) = \begin{cases} \left(\frac{1}{2} e^{ikx} \right)^{\frac{2x}{d} - 1} \left[\omega_+ \left(\frac{2x}{d} - 1 \right) + \omega_- \left(\frac{2x}{d} - 1 \right) \right], & \text{for } x \geq \frac{1}{2}d, \\ \left(\frac{1}{2} e^{-ikx} \right)^{\frac{-2x}{d} - 1} \left[\omega_+ \left(\frac{-2x}{d} - 1 \right) - \omega_- \left(\frac{-2x}{d} - 1 \right) \right], & \text{for } x \leq -\frac{1}{2}d, \end{cases} \quad (4.206)$$

$$\omega_{\pm}(\tau) = \lim_{n \rightarrow \infty} \omega_{\pm}^{(n)}(\tau), \quad (4.207)$$

$$\omega_{\pm}^{(0)}(\tau) = -\frac{1}{\pi} \int_{-1}^1 \frac{e^{ic\rho}}{(\tau + \rho + 1)\sqrt{(\rho + 1)}} [H_0^{(1)}(k\sqrt{\{(\frac{1}{2}d\rho + x_0)^2 + y_0^2\}}) \pm H_0^{(1)}(k\sqrt{\{(\frac{1}{2}d\rho - x_0)^2 + y_0^2\}})] d\rho, \quad (4.208)$$

and

$$\omega_{\pm}^{(n)}(\tau) = \omega_{\pm}^{(0)}(\tau) \pm \frac{e^{2ic}}{\pi} \int_0^{\infty} \frac{e^{2ic\rho}}{\tau + \rho + 2} \sqrt{\frac{\rho}{\rho + 2}} \omega_{\pm}^{(n-1)}(\rho) d\rho. \quad (4.209)$$

The quantity $E_z(x, 0)$ given in eq. (4.206) is the scattered electric field on the portions of the $y = 0$ plane not occupied by the strip, whereas the scattered magnetic field is zero there.

On the strip ($u = 0$):

$$H_v = \frac{4Y}{c|\sin v|} \sum_{m=0}^{\infty} \left[\frac{1}{N_m^{(e)}} \frac{Re_m^{(3)}(c, \xi_0)}{Re_m^{(3)}(c, 1)} Se_m(c, \eta_0) Se_m(c, \eta) + \frac{1}{N_m^{(o)}} \frac{Ro_m^{(3)}(c, \xi_0)}{Ro_m^{(3)}(c, 1)} So_m(c, \eta_0) So_m(c, \eta) \right]. \quad (4.210)$$

In the far field ($\xi \rightarrow \infty$):

$$E_z = \sqrt{\frac{2}{\pi c \xi}} e^{ic\xi - \frac{1}{2}i\pi} \sqrt{8\pi} \sum_{m=0}^{\infty} (-i)^m \left\{ \frac{1}{N_m^{(e)}} \left[Re_m^{(1)}(c, \xi_0) - \frac{Re_m^{(1)}(c, 1)}{Re_m^{(3)}(c, 1)} Re_m^{(3)}(c, \xi_0) \right] Se_m(c, \eta_0) Se_m(c, \eta) + \frac{1}{N_m^{(o)}} Ro_m^{(1)}(c, \xi_0) So_m(c, \eta_0) So_m(c, \eta) \right\}. \quad (4.211)$$

If the line source lies on either portion of the $y = 0$ plane not occupied by the strip then:

$$E_z = 4 \sum_{m=0}^{\infty} \frac{1}{N_m^{(e)}} \left[Re_m^{(1)}(c, \xi_0) - \frac{Re_m^{(1)}(c, 1)}{Re_m^{(3)}(c, 1)} Re_m^{(3)}(c, \xi_0) \right] Re_m^{(3)}(c, \xi_0) Se_m(c, \eta), \quad (4.212)$$

and on the strip ($u = 0$):

$$H_v = \frac{4Y}{c|\sin v|} \sum_{m=0}^{\infty} \frac{1}{N_m^{(e)}} \frac{Re_m^{(3)}(c, \xi_0)}{Re_m^{(3)}(c, 1)} Se_m(c, \eta). \quad (4.213)$$

MANDRAZHI [1962] has plotted the amplitude of the surface current density for $c = 2$ and the phase for $c = \frac{4}{3}, \sqrt{2}, 2, 2\sqrt{2}$, with $u_0 = 0.4$. For a line source at ($|x_0| > \frac{1}{2}d, y_0 = 0$), the scattered magnetic field on the strip is (GRINBERG [1960]):

$$H_x^s = \begin{cases} \pm \frac{Y}{ik} j(x + \frac{1}{2}d, -x_0 - \frac{1}{2}d), & \text{for } x_0 < -\frac{1}{2}d, \\ \pm \frac{Y}{ik} j(-x + \frac{1}{2}d, x_0 - \frac{1}{2}d), & \text{for } x_0 > \frac{1}{2}d, \end{cases} \quad (4.214)$$

where the plus sign is to be used for the upper face of the strip, the minus sign for the lower, and

$$j(\gamma, R) = \lim_{n \rightarrow \infty} j^{(n)}(\gamma, R), \quad (0 \leq \gamma \leq d; R > 0), \quad (4.215)$$

where:

$$j^{(0)}(\gamma, R) = -\frac{2i}{\pi} \sqrt{\frac{R}{\gamma}} \frac{e^{ik(R+\gamma)}}{R+\gamma}, \quad (4.216)$$

$$j^{(n)}(\gamma, R) = j^{(0)}(\gamma, R) + \frac{1}{\pi} \int_0^{\infty} j^{(n-1)}(d-\gamma, R) \sqrt{\frac{R}{\rho+d}} \frac{e^{ik(R+\rho+d)}}{R+\rho+d} d\rho. \quad (4.217)$$

In the far field ($\xi \rightarrow \infty$):

$$E_z = \sqrt{\frac{2}{\pi c \xi}} e^{ic\xi - \frac{1}{2}i\pi} \sqrt{8\pi} \sum_{m=0}^{\infty} \frac{(-i)^m}{N_{2m}^{(e)}} \left[\frac{Re_{2m}^{(1)}(c, \xi_0) - \frac{Re_{2m}^{(1)}(c, 1)}{Re_{2m}^{(3)}(c, 1)} Re_{2m}^{(3)}(c, \xi_0) \right] Se_{2m}(c, \eta). \quad (4.218)$$

If the line source lies in the half plane $v_0 = \frac{1}{2}\pi$ (i.e. $x_0 = 0, y_0 > 0$), then:

$$E_z = 4 \sum_{m=0}^{\infty} \left\{ \frac{Se_{2m}(c, 0)}{N_{2m}^{(e)}} \left[\frac{Re_{2m}^{(1)}(c, \xi_0) - \frac{Re_{2m}^{(1)}(c, 1)}{Re_{2m}^{(3)}(c, 1)} Re_{2m}^{(3)}(c, \xi_0) \right] Se_{2m}(c, \eta) + \right. \\ \left. + \frac{So_{2m+1}(c, 0)}{N_{2m+1}^{(o)}} \frac{Ro_{2m+1}^{(1)}(c, \xi_0) Ro_{2m+1}^{(3)}(c, \xi_0)}{Ro_{2m+1}^{(3)}(c, 1)} So_{2m+1}(c, \eta) \right\}. \quad (4.219)$$

On the strip ($u = 0$):

$$H_r = \frac{4Y}{c|\sin v|} \sum_{m=0}^{\infty} \left[\frac{Se_{2m}(c, 0)}{N_{2m}^{(e)}} \frac{Re_{2m}^{(3)}(c, \xi_0)}{Re_{2m}^{(3)}(c, 1)} Se_{2m}(c, \eta) + \right. \\ \left. + \frac{So_{2m+1}(c, 0)}{N_{2m+1}^{(o)}} \frac{Ro_{2m+1}^{(3)}(c, \xi_0)}{Ro_{2m+1}^{(3)}(c, 1)} So_{2m+1}(c, \eta) \right]. \quad (4.220)$$

MANDRAZHI [1962] has plotted the amplitude of the surface current density for $c = 2\sqrt{2}$ and the phase for $c = \frac{4}{3}$ and $2\sqrt{2}$, with $u_0 = 0.7213$. In the far field ($\xi \rightarrow \infty$):

$$E_z = \sqrt{\frac{2}{\pi c \xi}} e^{ic\xi - \frac{1}{2}i\pi} \sqrt{8\pi} \sum_{m=0}^{\infty} (-1)^m \left\{ \frac{Se_{2m}(c, 0)}{N_{2m}^{(e)}} \left[\frac{Re_{2m}^{(1)}(c, \xi_0) - \frac{Re_{2m}^{(1)}(c, 1)}{Re_{2m}^{(3)}(c, 1)} Re_{2m}^{(3)}(c, \xi_0) \right] Se_{2m}(c, \eta) - \right. \\ \left. - \frac{So_{2m+1}(c, 0)}{N_{2m+1}^{(o)}} \frac{Ro_{2m+1}^{(1)}(c, \xi_0) Ro_{2m+1}^{(3)}(c, \xi_0)}{Ro_{2m+1}^{(3)}(c, 1)} So_{2m+1}(c, \eta) \right\}. \quad (4.221)$$

4.3.1.2. LOW FREQUENCY APPROXIMATIONS

For an electric line source parallel to the z -axis and located at (u_0, v_0) , such that

$$E^i = 2H_0^{(1)}(kR), \quad (4.222)$$

the total electric field in the static limit $k \rightarrow 0$ is:

$$E_z = \frac{i}{\pi} \log \frac{\cosh(u - u_0) - \cos(v - v_0)}{\cosh(u + u_0) - \cos(v - v_0)} + o(k^0). \quad (4.223)$$

No other explicit results are available; however, low frequency approximations can be obtained either from the exact results of the previous section or by established techniques (MILLAR [1960]; NOBLE [1962]; PIMENOV [1959]).

4.3.1.3. HIGH FREQUENCY APPROXIMATIONS

For an electric line source parallel to the z -axis, located at (u_0, v_0) , and sufficiently removed from the strip so that near its surface

$$E^i = 2H_0^{(1)}(kR) \quad (4.224)$$

can be approximated by

$$E^i \sim 2 \sqrt{\frac{2}{\pi k R}} e^{ikR - \frac{1}{2}i\pi}, \quad (4.225)$$

then, for non-grazing incidence ($c \sin v_0 \gg 1$), the total field derived using Keller's geometrical theory of diffraction and taking into account only singly diffracted rays is:

$$E_z = \begin{cases} H_0^{(1)}(kR) + G, & \text{in regions } I_a \text{ and } I_b, \\ H_0^{(1)}(kR) - H_0^{(1)}(kR') + G, & \text{in region II,} \\ G, & \text{in region III,} \end{cases} \quad (4.226)$$

where

$$G = \frac{e^{ik(\rho_2 + \rho_2^0)}}{\pi k \sqrt{\rho_2 \rho_2^0}} \sqrt{\frac{(1 - \cos \psi_2)(1 - \cos \phi_2^0)}{(\cos \psi_2 + \cos \phi_2^0)}} - \frac{e^{ik(\rho_1 + \rho_1^0)}}{\pi k \sqrt{\rho_1 \rho_1^0}} \sqrt{\frac{(1 + \cos \psi_1)(1 + \cos \phi_1^0)}{(\cos \psi_1 + \cos \phi_1^0)}} + O(k^{-\frac{1}{2}}), \quad (4.227)$$

the regions are defined as (see Fig. 4.28):

$$\begin{aligned} \text{region } I_a: & \quad \pi + \phi_1^0 < \psi_1 < 2\pi & \text{or} & \quad \pi < \psi_2 < \pi + \phi_2^0, \\ \text{region } I_b: & \quad 0 < \psi_1 < \pi - \phi_1^0 & \text{or} & \quad \pi - \phi_2^0 < \psi_2 < \pi, \\ \text{region II:} & \quad \pi - \phi_1^0 < \psi_1 < \pi & \text{and} & \quad 0 < \psi_2 < \pi - \phi_2^0, \\ \text{region III:} & \quad \pi < \psi_1 < \pi + \phi_1^0 & \text{and} & \quad \pi + \phi_2^0 < \psi_2 < 2\pi. \end{aligned} \quad (4.228)$$

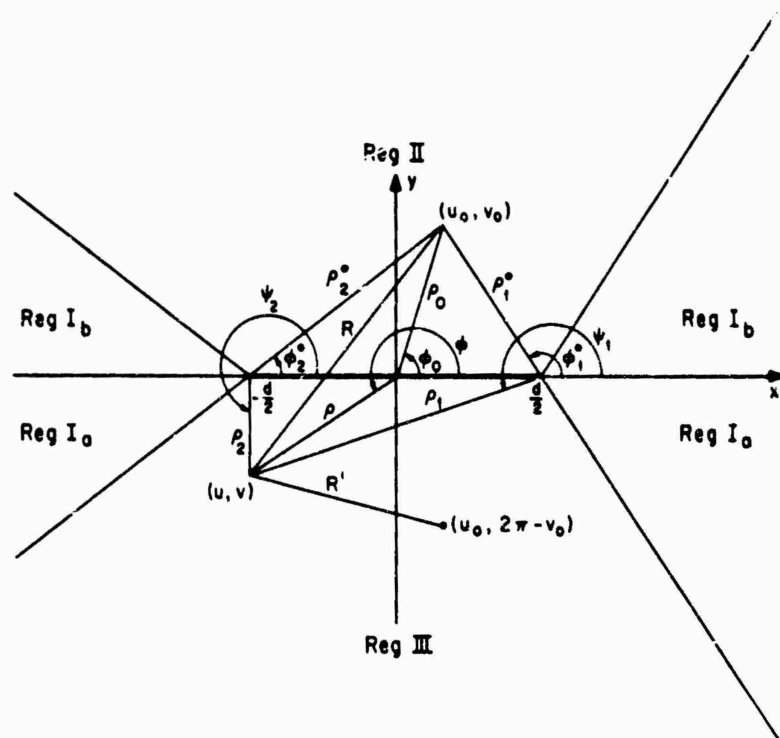


Fig. 4.28. Strip geometry for a line source.

and the geometric variables are given by:

$$\begin{aligned} \rho_1 \cos \psi_1 &= \rho \cos \phi - \frac{1}{2}d, & \rho_1^0 \cos \phi_1^0 &= \rho_0 \cos \phi_0 - \frac{1}{2}d, \\ \rho_1 \sin \psi_1 &= \rho \sin \phi, & \rho_1^0 \sin \phi_1^0 &= \rho_0 \sin \phi_0, \\ \rho_2 \cos \psi_2 &= \rho \cos \phi + \frac{1}{2}d, & \rho_2^0 \cos \phi_2^0 &= \rho_0 \cos \phi_0 + \frac{1}{2}d, \\ \rho_2 \sin \psi_2 &= \rho \sin \phi, & \rho_2^0 \sin \phi_2^0 &= \rho_0 \sin \phi_0, \end{aligned} \quad (4.229)$$

$$R = \sqrt{\rho^2 + \rho_0^2 - 2\rho\rho_0 \cos(\phi - \phi_0)}, \quad R' = \sqrt{\rho^2 + \rho_0^2 - 2\rho\rho_0 \cos(\phi + \phi_0)},$$

as illustrated in Fig. 4.28. HANSEN [1962] has shown eq. (4.227) to be the leading term in an asymptotic expansion of the field in the geometrical shadow (region III). In the far field ($\xi \rightarrow \infty$):

$$\begin{aligned} G \sim \frac{e^{ik(\rho + \rho_0)}}{\pi k \sqrt{\rho \rho_0}} & \left[\frac{\sqrt{\{(1 - \cos \phi)(1 - \cos \phi_0)\}}}{\cos \phi + \cos \phi_0} \exp \{ic(\cos \phi + \cos \phi_0)\} - \right. \\ & \left. - \frac{\sqrt{\{(1 + \cos \phi)(1 + \cos \phi_0)\}}}{\cos \phi + \cos \phi_0} \exp \{-ic(\cos \phi + \cos \phi_0)\} \right] + O(k^{-1}). \end{aligned} \quad (4.230)$$

For an incident field given by eq. (4.225), the total magnetic field on the surface of the strip is (GOODRICH and KAZARINOFF [1963]):

$$H_r \sim -Y \sqrt{\frac{8c}{\pi}} \frac{e^{ic(\xi_0 - 1)}}{|\sin v| \sqrt{(\xi_0^2 - 1)}} \sum_{n=0}^N \frac{(-c)^n}{n! 2^n} G(v, v_0; -c\sigma_n^{(1)}). \quad (4.231)$$

where N is a non-negative integer much smaller than c but otherwise unspecified, and

$$\sigma_n^{(1)} = -i(4n+3). \quad (4.232)$$

If

$$v_0 = 0, \quad v > 0, \quad c \sin v \gg 1, \quad (4.233)$$

then

$$G(v, 0; -c\sigma) \sim \frac{i}{8cT_1^2} (1 - R_1^2 e^{4ic})^{-1} \times \left\{ \frac{\exp \{ic(1 - \cos v)\}}{\sin \frac{1}{2}v} (\tan \frac{1}{2}v)^{-\alpha} + R_1 \frac{\exp \{ic(3 + \cos v)\}}{\cos \frac{1}{2}v} (\tan \frac{1}{2}v)^{\alpha} \right\}; \quad (4.234)$$

if

$$v_0 = 0, \quad |v - \pi| \ll 1, \quad c|\sin v| \ll 1, \quad (4.235)$$

then

$$G(v, 0; -c\sigma) \sim \frac{1}{8cT_1^2} (1 - R_1^2 e^{4ic})^{-1} \exp \{ic(1 - \cos v)\}; \quad (4.236)$$

if

$$0 < v_0 \leq \frac{1}{2}\pi, \quad -\pi < \psi < 0, \quad c|\sin v| \gg 1, \quad (4.237)$$

then

$$G(v, v_0; -c\sigma) \sim \frac{i(R_{II} - R_I) \exp \{ic(1 - \xi_0)\}}{8c(1 - R_1^2 e^{4ic})(1 - R_{II}^2 e^{4ic})} \left\{ (1 + R_I R_{II} e^{4ic}) \times \left[\frac{\exp \{ic(1 + \cos \psi)\}}{\cos \frac{1}{2}\psi} \frac{\exp \{ic(\xi_0 + \eta_0)\}}{\cos \frac{1}{2}\beta_2} (\tan \frac{1}{2}\beta_2 \tan \frac{1}{2}\psi)^{\alpha} - \frac{\exp \{ic(1 - \cos \psi)\}}{\sin \frac{1}{2}\psi} \frac{\exp \{ic(\xi_0 - \eta_0)\}}{\cos \frac{1}{2}\beta_1} (\tan \frac{1}{2}\beta_1)^{\alpha} (\tan \frac{1}{2}\psi)^{-\alpha} \right] + (R_I + R_{II}) e^{2ic} \left[\frac{\exp \{ic(1 + \cos \psi)\}}{\cos \frac{1}{2}\psi} \frac{\exp \{ic(\xi_0 - \eta_0)\}}{\cos \frac{1}{2}\beta_1} (\tan \frac{1}{2}\beta_1 \tan \frac{1}{2}\psi)^{\alpha} - \frac{\exp \{ic(1 - \cos \psi)\}}{\sin \frac{1}{2}\psi} \frac{\exp \{ic(\xi_0 - \eta_0)\}}{\cos \frac{1}{2}\beta_2} (\tan \frac{1}{2}\beta_2)^{\alpha} (\tan \frac{1}{2}\psi)^{-\alpha} \right] \right\}, \quad (4.238)$$

and, in particular, for $v_0 = \frac{1}{2}\pi$:

$$G(v, \frac{1}{2}\pi; -c\sigma) \sim \frac{i(R_{II} - R_I) e^{ic}}{2ic(1 - R_I e^{2ic})(1 - R_{II} e^{2ic})} \times \left[\frac{\exp \{ic(1 + \cos \psi)\}}{\cos \frac{1}{2}\psi} (\tan \frac{1}{2}\psi)^{\alpha} - \frac{\exp \{ic(1 - \cos \psi)\}}{\sin \frac{1}{2}\psi} (\tan \frac{1}{2}\psi)^{-\alpha} \right]; \quad (4.239)$$

if

$$v_0 = \frac{1}{2}\pi, \quad \psi = 1, \quad c|\sin v| \gg 1, \quad (4.240)$$

then

$$G(v, \frac{1}{2}\pi; -c\sigma) \sim \frac{i \exp \{ic(1 + \cos \psi)\}}{2^{\frac{1}{2}}c} \left[\frac{1}{T_I(1 - R_I e^{2ic})} + \frac{2 \sin \frac{1}{2}\psi}{T_{II}(1 - R_{II} e^{2ic})} \right]; \quad (4.241)$$

where

$$T_I = \frac{\pi^{\frac{1}{2}}(4c)^{\frac{1}{2}\alpha} e^{-\frac{1}{2}i\alpha\pi}}{\Gamma(\frac{1}{2}(1 + \alpha))}, \quad (4.242)$$

$$R_I = \frac{\Gamma(\frac{1}{2}(1 + \alpha)) e^{-\frac{1}{2}i\pi}}{2^{2\alpha+1} c^{\alpha+\frac{1}{2}} \Gamma(-\frac{1}{2}\alpha)}, \quad (4.243)$$

$$T_{II} = \frac{\pi^{\frac{1}{2}}(4c)^{\frac{1}{2}\alpha} e^{\frac{1}{2}i(1-\alpha)\pi}}{2c^{\frac{1}{2}} \Gamma(1 + \frac{1}{2}\alpha)} \quad (4.244)$$

$$R_{II} = \frac{\Gamma(1 + \frac{1}{2}\alpha) e^{-\frac{1}{2}i\pi}}{4^{\alpha} c^{\alpha+\frac{1}{2}} \Gamma(\frac{1}{2}(1 - \alpha))}, \quad (4.245)$$

$$\psi = \begin{cases} v, & \text{for } v < \pi, \\ v - 2\pi, & \text{for } v > \pi, \end{cases} \quad (4.246)$$

$$\alpha = \frac{1}{2}(i\sigma - 1), \quad (\sigma = \sigma_n^{(1)}), \quad (4.247)$$

$$\cos \beta_1 = \frac{\xi_0 \eta_0 - 1}{\xi_0 - \eta_0}, \quad (\beta_1 \sim v_0), \quad (4.248)$$

$$\cos \beta_2 = -\frac{\xi_0 \eta_0 + 1}{\xi_0 + \eta_0}, \quad (\beta_2 \sim \pi - v_0). \quad (4.249)$$

For an incident field given by eq. (4.224), the scattered electric field is given by eqs. (4.203) through (4.209), where now all quantities $\omega_{\pm}^{(n)}(\tau)$ can be approximated by (GRINBERG [1958]):

$$\omega_{\pm}^{(n)}(\tau) \sim \omega_{\pm}(\tau) = \omega_{\pm}^{(0)}(\tau) \pm \frac{e^{2ic} \int_0^{\infty} \sqrt{\rho/(c+2)} e^{2ic\rho} \omega_{\pm}^{(0)}(\rho) d\rho}{\pi(\tau+2) \{1 \mp [(\frac{1}{2}i+2c)H_0^{(1)}(2c) - 2icH_1^{(1)}(2c)]\}}, \quad (r \geq 1), \quad (4.250)$$

which is independent of n . The order of the approximation is not known.

4.3.2. *H-polarization*

4.3.2.1. EXACT SOLUTIONS

For a magnetic line source parallel to the z -axis and located at (u_0, v_0) , such that

$$H^i = 2H_0^{(1)}(kR), \quad (4.251)$$

the total magnetic field is:

$$H_z = 4 \sum_{m=0}^{\infty} \left\{ \frac{1}{N_m^{(e)}} \operatorname{Re}_m^{(1)}(c, \xi_<) \operatorname{Re}_m^{(3)}(c, \xi_>) \operatorname{Se}_m(c, \eta_0) \operatorname{Se}_m(c, \eta) + \right. \\ \left. + \frac{1}{N_m^{(o)}} \left[\operatorname{Ro}_m^{(1)}(c, \xi_<) - \frac{\operatorname{Ro}_m^{(1)'}(c, 1)}{\operatorname{Ro}_m^{(3)'}(c, 1)} \operatorname{Ro}_m^{(3)}(c, \xi_<) \right] \operatorname{Ro}_m^{(3)}(c, \xi_>) \operatorname{So}_m(c, \eta_0) \operatorname{So}_m(c, \eta) \right\}. \quad (4.252)$$

An alternate expression for the scattered magnetic field is (GRINBERG [1957]):

$$H_z^s(x, y) = \begin{cases} \frac{1}{2i} \int_{-x}^{-\frac{1}{2}d} \frac{\partial}{\partial \delta} H_z^s(\gamma, \delta) \Big|_{\delta=0^+} H_0^{(1)}(kR) d\gamma + \frac{1}{2i} \int_{\frac{1}{2}d}^{\infty} \frac{\partial}{\partial \delta} H_z^s(\gamma, \delta) \Big|_{\delta=0^+} H_0^{(1)}(kR) d\gamma + \\ + \frac{1}{2i} \int_{-\frac{1}{2}d}^{\frac{1}{2}d} H_0^{(1)}(kR) \frac{\partial}{\partial y_0} H_0^{(1)}(kR_0) d\gamma, & \text{for } y \geq 0, \\ -H_z^s(x, -y), & \text{for } y \leq 0, \end{cases} \quad (4.253)$$

where:

$$R = \sqrt{\{(x-\gamma)^2 + y^2\}}, \quad (4.254)$$

$$R_0 = \sqrt{\{(x_0-\gamma)^2 + y_0^2\}}, \quad (4.255)$$

$$\frac{\partial H_z^s(x, \delta)}{\partial \delta} \Big|_{\delta=0^+} = \\ = \begin{cases} 2 \sqrt{\{(2x/d)-1\}} \left[\omega_+ \left(\frac{2x}{d} - 1 \right) + \omega_- \left(\frac{2x}{d} - 1 \right) \right], & \text{for } x \geq \frac{1}{2}d, \\ 2 \sqrt{\{(-2x/d)-1\}} \left[\omega_+ \left(-\frac{2x}{d} - 1 \right) - \omega_- \left(-\frac{2x}{d} - 1 \right) \right], & \text{for } x \leq -\frac{1}{2}d, \end{cases} \quad (4.256)$$

$$\omega_{\pm}(\tau) = \lim_{n \rightarrow \infty} \omega_{\pm}^{(n)}(\tau), \quad (4.257)$$

$$\omega_{\pm}^{(0)}(\tau) = - \frac{1}{\pi} \int_{-\frac{1}{2}}^{\frac{1}{2}} \frac{e^{i\tau\rho}}{\tau + \rho + 1} \sqrt{\rho+1} \left[\frac{\partial}{\partial y_0} H_0^{(1)}(k\sqrt{\{(\frac{1}{2}d\rho + x_0)^2 + y_0^2\}}) \pm \right. \\ \left. \pm \frac{\partial}{\partial y_0} H_0^{(1)}(k\sqrt{\{(\frac{1}{2}d\rho - x_0)^2 + y_0^2\}}) \right] d\rho, \quad (4.258)$$

and

$$\omega_{\pm}^{(n)}(\tau) = \omega_{\pm}^{(0)}(\tau) + \frac{1}{\pi} \int_0^{\infty} \frac{e^{2i\tau(\rho+1)}}{(\tau + \rho + 2)} \sqrt{\frac{\rho+2}{\rho}} \omega_{\pm}^{(n-1)}(\rho) d\rho. \quad (4.259)$$

Since

$$\frac{\partial H_z^s(x, \delta)}{\partial \delta} \Big|_{\delta=0^+} = -ikYE_z^s(x, 0), \quad (4.260)$$

the quantity in eq. (4.256) is proportional to the scattered electric field on the portions

of the $y = 0$ plane not occupied by the strip; in contrast, the scattered magnetic field is zero there.

On the strip ($u = 0$):

$$H_z = 4i \sum_{m=0}^{\infty} \left[\frac{1}{N_m^{(e)}} \frac{Re_m^{(3)}(c, \xi_0)}{(\partial/\partial u)Re_m^{(3)}(c, \cosh u)|_{u=0}} Se_m(c, \eta_0)Se_m(c, \eta) + \right. \\ \left. + \frac{1}{N_m^{(o)}} \frac{Ro_m^{(3)}(c, \xi_0)}{(\partial/\partial u)Ro_m^{(3)}(c, \cosh u)|_{u=0}} So_m(c, \eta_0)So_m(c, \eta) \right]. \quad (4.261)$$

In the far field ($\xi \rightarrow \infty$):

$$H_z = \sqrt{\frac{2}{\pi c \xi}} e^{ic\xi - \frac{1}{2}i\pi} \sqrt{8\pi} \sum_{m=0}^{\infty} (-i)^m \left\{ \frac{1}{N_m^{(e)}} Re_m^{(1)}(c, \xi_0) Se_m(c, \eta_0) Se_m(c, \eta) + \right. \\ \left. + \frac{1}{N_m^{(o)}} \left[Ro_m^{(1)}(c, \xi_0) - \frac{Ro_m^{(1)'}(c, 1)}{Ro_m^{(3)'}(c, 1)} Ro_m^{(3)}(c, \xi_0) \right] So_m(c, \eta_0) So_m(c, \eta) \right\}. \quad (4.262)$$

If the line source lies on either portion of the $y = 0$ plane not occupied by the strip then:

$$H_z = 4 \sum_{m=0}^{\infty} \frac{1}{N_m^{(e)}} Re_m^{(1)}(c, \xi_<) Re_m^{(3)}(c, \xi_>) Se_m(c, \eta), \quad (4.263)$$

and on the strip ($u = 0$):

$$H_z = 4 \sum_{m=0}^{\infty} \frac{Re_m^{(1)}(c, 1)}{N_m^{(e)}} Re_m^{(3)}(c, \xi_0) Se_m(c, \eta). \quad (4.264)$$

In the far field ($\xi \rightarrow \infty$):

$$H_z = \sqrt{\frac{2}{\pi c \xi}} e^{ic\xi - \frac{1}{2}i\pi} \sqrt{8\pi} \sum_{m=0}^{\infty} \frac{(-i)^m}{N_m^{(e)}} Re_m^{(1)}(c, \xi_0) Se_m(c, \eta). \quad (4.265)$$

If the line source lies in the half plane $v_0 = \frac{1}{2}\pi$ (i.e. $x_0 = 0, y_0 > 0$), then:

$$H_z = 4 \sum_{m=0}^{\infty} \left\{ \frac{Se_{2m}(c, 0)}{N_{2m}^{(e)}} Re_{2m}^{(1)}(c, \xi_<) Re_{2m}^{(3)}(c, \xi_>) Se_{2m}(c, \eta) + \right. \\ \left. + \frac{So_{2m+1}(c, 0)}{N_{2m+1}^{(o)}} \left[Ro_{2m+1}^{(1)}(c, \xi_<) - \frac{Ro_{2m+1}^{(1)'}(c, 1)}{Ro_{2m+1}^{(3)'}(c, 1)} Ro_{2m+1}^{(3)}(c, \xi_<) \right] \right. \\ \left. \times Ro_{2m+1}^{(3)}(c, \xi_>) So_{2m+1}(c, \eta) \right\}. \quad (4.266)$$

On the strip ($u = 0$):

$$H_z = 4i \sum_{m=0}^{\infty} \left[\frac{Se_{2m}(c, 0)}{N_{2m}^{(e)}} \frac{Re_{2m}^{(3)}(c, \xi_0)}{(\partial/\partial u)Re_{2m}^{(3)}(c, \cosh u)|_{u=0}} Se_{2m}(c, \eta) + \right. \\ \left. + \frac{So_{2m+1}(c, 0)}{N_{2m+1}^{(o)}} \frac{Ro_{2m+1}^{(3)}(c, \xi_0)}{(\partial/\partial u)Ro_{2m+1}^{(3)}(c, \cosh u)|_{u=0}} So_{2m+1}(c, \eta) \right]. \quad (4.267)$$

and in the far field ($\xi \rightarrow \infty$):

$$H_z = \sqrt{\frac{2}{\pi c \xi}} e^{ic\xi - \frac{1}{2}i\pi} \sqrt{8\pi} \sum_{m=0}^{\infty} (-1)^m \left\{ \frac{Se_{2m}(c, 0)}{N_{2m}^{(e)}} Re_{2m}^{(1)}(c, \xi_0) Se_{2m}(c, \eta) - \right. \\ \left. - i \frac{So_{2m+1}(c, 0)}{N_{2m+1}^{(o)}} \left[Ro_{2m+1}^{(1)}(c, \xi_0) - \frac{Ro_{2m+1}^{(1)'}(c, 1)}{Ro_{2m+1}^{(3)'}(c, 1)} Ro_{2m+1}^{(3)}(c, \xi_0) \right] So_{2m+1}(c, \eta) \right\}. \quad (4.268)$$

4.3.2.2. LOW FREQUENCY APPROXIMATIONS

No explicit results are available; however, low frequency approximations can be obtained either from the exact solutions of the previous section or by established techniques (MILLAR [1960]; NOBLE [1962]; PIMENOV [1959]).

4.3.2.3. HIGH FREQUENCY APPROXIMATIONS

For a magnetic line source parallel to the z -axis, located at (u_0, v_0) , and sufficiently removed from the strip so that near its surface

$$H^i = 2H_0^{(1)}(kR) \quad (4.269)$$

can be approximated by

$$H^i \sim 2 \sqrt{\frac{2}{\pi k R}} e^{ikR - \frac{1}{2}i\pi}, \quad (4.270)$$

then, for non-grazing incidence ($c \sin v_0 \gg 1$), the total magnetic field derived using Keller's geometrical theory of diffraction and taking into account only singly diffracted rays is:

$$H_z = \begin{cases} H_0^{(1)}(kR) + G, & \text{in region I}_a, \\ H_0^{(1)}(kR) - G, & \text{in region I}_b, \\ H_0^{(1)}(kR) + H_0^{(1)}(kR') - G, & \text{in region II}, \\ G, & \text{in region III}, \end{cases} \quad (4.271)$$

where

$$G = - \frac{\exp \{ik(\rho_1 + \rho_1^0)\}}{\pi k \sqrt{\rho_1 \rho_1^0}} \sqrt{\frac{(1 - \cos \psi_1)(1 - \cos \phi_1^0)}{\cos \psi_1 + \cos \phi_1^0}} + \\ + \frac{\exp \{ik(\rho_2 + \rho_2^0)\}}{\pi k \sqrt{\rho_2 \rho_2^0}} \sqrt{\frac{(1 + \cos \psi_2)(1 + \cos \phi_2^0)}{\cos \psi_2 + \cos \phi_2^0}} + O(k^{-3/2}), \quad (4.272)$$

the various regions and the geometric variables are defined in eqs. (4.228) and (4.229), and are illustrated in Fig. 4.28. HANSEN [1962] has shown eq. (4.272) to be the leading term in an asymptotic expansion of the field in the geometrical shadow (region III).

In the far field ($\xi \rightarrow \infty$):

$$G \sim \frac{\exp \{ik(\rho + \rho_0)\}}{\pi k \sqrt{\rho \rho_0}} \left[\frac{\sqrt{\{(1 + \cos \phi)(1 + \cos \phi_0)\}}}{\cos \phi + \cos \phi_0} \exp \{ic(\cos \phi + \cos \phi_0)\} - \frac{\sqrt{\{(1 - \cos \phi)(1 - \cos \phi_0)\}}}{\cos \phi + \cos \phi_0} \exp \{-ic(\cos \phi + \cos \phi_0)\} \right] + O(k^{-1/2}). \quad (4.273)$$

For an incident field given by eq. (4.270), the total magnetic field on the surface of the strip is (GOODRICH and KAZARINOFF [1963]):

$$H_z \sim 8i \sqrt{\frac{c}{\pi}} \frac{\exp \{ic(\xi_0 - 1)\}}{\sqrt{(\xi_0^2 - 1)}} \sum_{n=0}^N \frac{(-c)^n}{n! 2^n} G(v, v_0; -c\sigma_n^{(2)}), \quad (4.274)$$

where N is a non-negative integer much smaller than c but otherwise unspecified,

$$\sigma_n^{(2)} = -i(4n + 1), \quad (4.275)$$

and G is given by eqs. (4.233) through (4.249) with $\sigma = \sigma_n^{(2)}$.

For an incident field given by eq. (4.269), the scattered magnetic field is given by eqs. (4.253) through (4.260), where now all quantities $\omega_{\pm}^{(n)}(\tau)$ can be approximated by (GRINBERG [1957]):

$$\omega_{\pm}^{(n)}(\tau) \sim \omega_{\pm}(\tau) = \omega_{\pm}^{(0)}(\tau) \mp \frac{\sqrt{2}e^{2ic} \int_0^{\tau} \omega_{\pm}^{(0)}(\rho) \rho^{-1/2} e^{2ic\rho} d\rho}{\pi(c+2)(1 \pm 2\pi^{-1/2} e^{-2ic-4i\pi} F[2\sqrt{c}])}, \quad (n \geq 1) \quad (4.276)$$

which is independent of n . $F(\tau)$ is the Fresnel integral defined in the Introduction. The order of the approximation is not known.

4.4. Dipole sources

4.4.1. Electric dipoles

4.4.1.1. EXACT SOLUTIONS

For an arbitrarily oriented electric dipole located at $r_0 \equiv (u_0, v_0, z_0)$ with moment $(4\pi\epsilon/k)\hat{e}$, the total electric field at $r \equiv (u, v, z)$ is:

$$E(r) = 4\pi k \mathcal{G}_e(r|r_0) \cdot \hat{e}, \quad (4.277)$$

where $\mathcal{G}_e(r|r_0)$ is the electric dyadic Green's function for the strip (TAI [1954]):

$$\begin{aligned} \mathcal{G}_e(r|r_0) = & \frac{i}{2\pi\epsilon} \int_{-\infty}^{+\infty} \frac{dt}{k^2 - t^2} \sum_{m=0}^{\infty} \left[\frac{1}{\Omega_m^{(e)}} \{ M_{em}^{(3)}(t, r) M_{em}^{(1)}(-t, r_0) + \right. \\ & \left. + N_{em}^{(3)}(t, r) [N_{em}^{(1)}(-t, r_0) + h_{em} N_{em}^{(3)}(-t, r_0)] \} + \right. \\ & \left. + \frac{1}{\Omega_m^{(o)}} \{ M_{om}^{(3)}(t, r) [M_{om}^{(1)}(-t, r_0) + a_{om} M_{om}^{(3)}(-t, r_0)] + \right. \\ & \left. + N_{om}^{(3)}(t, r) N_{om}^{(1)}(-t, r_0) \} \right], \quad \text{for } u > u_0. \quad (4.278) \end{aligned}$$

$$\begin{aligned} \mathcal{G}_e(\mathbf{r}|\mathbf{r}_0) = & \frac{i}{2\pi} \int_{-\infty}^{+\infty} \frac{dt}{k^2 - t^2} \sum_{m=0}^{\infty} \left[\frac{1}{\Omega_m^{(e)}} \{ M_{em}^{(1)}(t, \mathbf{r}) M_{em}^{(3)}(-t, \mathbf{r}_0) + \right. \\ & \left. + [N_{em}^{(1)}(t, \mathbf{r}) + b_{em} N_{em}^{(3)}(t, \mathbf{r})] N_{em}^{(3)}(-t, \mathbf{r}_0) \} + \right. \\ & \left. + \frac{1}{\Omega_m^{(o)}} \{ [M_{om}^{(1)}(t, \mathbf{r}) + a_{om} M_{em}^{(3)}(t, \mathbf{r})] M_{om}^{(3)}(-t, \mathbf{r}_0) + \right. \\ & \left. + N_{om}^{(1)}(t, \mathbf{r}) N_{om}^{(3)}(-t, \mathbf{r}_0) \} \right], \quad \text{for } u < u_0, \quad (4.279) \end{aligned}$$

with

$$a_{om} = -\frac{Ro_m^{(1)}(\gamma, 1)}{Ro_m^{(3)}(\gamma, 1)}, \quad b_{em} = -\frac{Re_m^{(1)}(\gamma, 1)}{Re_m^{(3)}(\gamma, 1)}, \quad (4.280)$$

$$\Omega_m^{(o)} = \int_0^{2\pi} [So_m(\gamma, \cos v)]^2 dv, \quad \Omega_m^{(e)} = \int_0^{2\pi} [Se_m(\gamma, \cos v)]^2 dv, \quad (4.281)$$

$$\gamma = c \sqrt{1 - \frac{t^2}{k^2}}, \quad (4.282)$$

$$M_{om}^{(j)}(t, \mathbf{r}) = \frac{ke^{itz}}{c\sqrt{(\xi^2 - \eta^2)}} \left[\hat{u} Re_m^{(j)}(\gamma, \xi) \frac{\partial}{\partial v} Se_m(\gamma, \cos v) - \hat{v} Se_m(\gamma, \eta) \frac{\partial}{\partial u} Re_m^{(j)}(\gamma, \cosh u) \right], \quad (4.283)$$

$$\begin{aligned} N_{em}^{(j)}(t, \mathbf{r}) = & \frac{ite^{itz}}{c\sqrt{(\xi^2 - \eta^2)}} \left[\hat{u} Se_m(\gamma, \eta) \frac{\partial}{\partial u} Re_m^{(j)}(\gamma, \cosh u) + \hat{v} Re_m^{(j)}(\gamma, \xi) \frac{\partial}{\partial v} Se_m(\gamma, \cos v) \right] + \\ & + \hat{z} \frac{k^2 - t^2}{k} e^{itz} Re_m^{(j)}(\gamma, \xi) Se_m(\gamma, \eta), \quad (4.284) \end{aligned}$$

$j = 1$ or 3 , and the unit vectors \hat{u} and \hat{v} are given by:

$$\hat{u} = \frac{1}{\sqrt{(\xi^2 - \eta^2)}} (\sqrt{\xi^2 - 1} \cos v \hat{x} + \xi \sin v \hat{y}), \quad (4.285)$$

$$\hat{v} = \frac{1}{\sqrt{(\xi^2 - \eta^2)}} (\sqrt{\xi^2 - 1} \cos v \hat{y} - \xi \sin v \hat{x}). \quad (4.286)$$

In particular, for a longitudinal electric dipole at (u_0, v_0, z_0) with moment $(4\pi\epsilon/k)\hat{z}$, corresponding to an incident electric Hertz vector $(e^{ikr}/kr)\hat{z}$, the total electromagnetic field components can be derived from the total electric Hertz vector

$$\begin{aligned} \Pi_e = \Pi_e \hat{z} = & \hat{z} \frac{2i}{k} \int_{-\infty}^{+\infty} dt e^{it(z-z_0)} \sum_{m=0}^{\infty} \left\{ \frac{1}{\Omega_m^{(e)}} Re_m^{(3)}(\gamma, \xi_0) \right. \\ & \times \left[Re_m^{(1)}(\gamma, \xi_0) - \frac{Re_m^{(1)}(\gamma, 1)}{Re_m^{(3)}(\gamma, 1)} Re_m^{(3)}(\gamma, \xi_0) \right] Se_m(\gamma, \eta_0) Se_m(\gamma, \eta) + \\ & \left. + \frac{1}{\Omega_m^{(o)}} Ro_m^{(3)}(\gamma, \xi_0) Ro_m^{(1)}(\gamma, \xi_0) So_m(\gamma, \eta_0) So_m(\gamma, \eta) \right\} \quad (4.287) \end{aligned}$$

by the relations,

$$E_u = \frac{k}{c\sqrt{(\xi^2 - \eta^2)}} \frac{\partial^2 \Pi_\epsilon}{\partial u \partial z}, \quad E_v = \frac{k}{c\sqrt{(\xi^2 - \eta^2)}} \frac{\partial^2 \Pi_\epsilon}{\partial v \partial z}, \quad E_z = \left(\frac{\partial^2}{\partial z^2} + k^2 \right) \Pi_\epsilon, \quad (4.288)$$

$$H_u = -\frac{ik^2 Y}{c\sqrt{(\xi^2 - \eta^2)}} \frac{\partial \Pi_\epsilon}{\partial v}, \quad H_v = \frac{ik^2 Y}{c\sqrt{(\xi^2 - \eta^2)}} \frac{\partial \Pi_\epsilon}{\partial u}, \quad H_z = 0.$$

On the surface $u = 0$:

$$H_v = \frac{2ikY}{c|\sin v|} \int_{-\infty}^{+\infty} dt e^{it(z-z_0)} \sum_{m=0}^{\infty} \left\{ \frac{1}{\Omega_m^{(e)}} \frac{Re_m^{(3)}(\gamma, \xi_0)}{Re_m^{(3)}(\gamma, 1)} Se_m(\gamma, \eta_0) Se_m(\gamma, \eta) + \right. \\ \left. + \frac{1}{\Omega_m^{(o)}} \frac{Ro_m^{(3)}(\gamma, \xi_0)}{Ro_m^{(3)}(\gamma, 1)} So_m(\gamma, \eta_0) So_m(\gamma, \eta) \right\}. \quad (4.289)$$

If the longitudinal dipole lies on the strip ($u_0 = 0$) both the electric and the magnetic fields are zero everywhere. If the longitudinal dipole is at ($u_0, v_0, z_0 = 0$), the total far field ($\xi \rightarrow \infty$) is:

$$E_\theta = -2\sqrt{2\pi} \frac{e^{ikr}}{kr} k^2 \sin \theta \sum_{m=0}^{\infty} (-i)^m \left\{ \frac{1}{\Omega_m^{(e)}} \left[Re_m^{(1)}(c \sin \theta, \xi_0) - \right. \right. \\ \left. \left. - \frac{Re_m^{(1)}(c \sin \theta, 1)}{Re_m^{(3)}(c \sin \theta, 1)} Re_m^{(3)}(c \sin \theta, \xi_0) \right] Se_m(c \sin \theta, \eta_0) Se_m(c \sin \theta, \eta) + \right. \\ \left. + \frac{1}{\Omega_m^{(o)}} Ro_m^{(1)}(c \sin \theta, \xi_0) So_m(c \sin \theta, \eta_0) So_m(c \sin \theta, \eta) \right\}, \quad (4.290)$$

where

$$\bar{\Omega}_m^{(e), (o)} = [\Omega_m^{(e), (o)}]_{\gamma = c \sin \theta}, \quad (4.291)$$

and r and θ are spherical polar coordinates: r is the distance from the origin to the point of observation and θ the angle measured from the positive z -axis to the line between the origin and the observation point. Radiation patterns in the azimuthal plane $\theta = \frac{1}{2}\pi$ have been published by LUCKE [1951] for a longitudinal dipole at $v_0 = \frac{1}{2}\pi$ and by KOCHERZHEVSKI [1955] for longitudinal dipoles at $v_0 = 0$ and $v_0 = \frac{1}{2}\pi$ and special values of c and u_0 . [There appears to be a discrepancy between Lucke's figure and Fig. 8 of Kocherzhevski; the source of the error can only be determined by computation of eq. (4.290).]

The total electromagnetic field components for an electric dipole parallel to \hat{u} (radial dipole) or to \hat{v} (transverse or circumferential dipole) can be derived from eq. (4.277). The far field patterns may also be obtained by using the reciprocity theorem.

The shape of the far field amplitude pattern, $|H_z|$ as a function of v , in the azimuthal plane $\theta = \frac{1}{2}\pi$ has been computed by LUCKE [1951] for a radial dipole with $u_0 = 0$, $v_0 = \frac{1}{2}\pi$ and $c = 0.2, 1.0, 2.5$ and 4.5 . The shape of the far field amplitude pattern,

$|E_v|$ as a function of v , in the azimuthal plane $\theta = \frac{1}{2}\pi$ has been computed by KOCHERZHEVSKI [1955] for a transverse dipole with $v_0 = 0$ and $\frac{1}{2}\pi$, and special values of c and u_0 .

4.4.1.2. LOW FREQUENCY APPROXIMATIONS

No specific results are available; low frequency expansions, however, can be derived from the results of the previous section.

4.4.1.3. HIGH FREQUENCY APPROXIMATIONS

No specific results are available although geometrical and physical optics approximations are derivable by standard techniques.

4.4.2. Magnetic dipoles

4.4.2.1. EXACT SOLUTIONS

For an arbitrarily oriented magnetic dipole located at $\mathbf{r}_0 \equiv (u_0, v_0, z_0)$ with moment $(4\pi/k)\hat{\mathbf{c}}$, the total magnetic vector at $\mathbf{r} \equiv (u, v, z)$ is:

$$\mathbf{H}(\mathbf{r}) = 4\pi k \mathcal{G}_m(\mathbf{r}|\mathbf{r}_0) \cdot \hat{\mathbf{c}}, \quad (4.292)$$

where $\mathcal{G}_m(\mathbf{r}|\mathbf{r}_0)$ is the magnetic dyadic Green's function for the strip, and is related to the electric dyadic Green's function of eqs. (4.278) and (4.279) by (TAI [1954]):

$$\mathcal{G}_m(\mathbf{r}|\mathbf{r}_0) = \frac{1}{k^2} \nabla \wedge \{[\nabla_0 \wedge \mathcal{G}_e(\mathbf{r}|\mathbf{r}_0)]^T\}; \quad (4.293)$$

here $\nabla_0 \wedge$ operates on \mathbf{r}_0 and T indicates the transposed dyadic.

In particular, for a longitudinal magnetic dipole at (u_0, v_0, z_0) with moment $(4\pi/k)\hat{\mathbf{z}}$, corresponding to an incident Hertz vector $(e^{ikr}/kr)\hat{\mathbf{z}}$, the total electromagnetic field components can be derived from the total magnetic Hertz vector

$$\begin{aligned} \Pi_m = \Pi_m \hat{\mathbf{z}} = \hat{\mathbf{z}} \frac{2i}{k} \int_{-\infty}^{+\infty} dt e^{it(z-z_0)} \sum_{m=0}^{\infty} \left\{ \frac{1}{\Omega_m^{(e)}} \text{Re}_m^{(3)}(\gamma, \xi_+) \right. \\ \times \text{Re}_m^{(1)}(\gamma, \xi_-) \text{Se}_m(\gamma, \eta_0) \text{Se}_m(\gamma, \eta) + \frac{1}{\Omega_m^{(o)}} \text{Ro}_m^{(3)}(\gamma, \xi_+) \\ \times \left[\text{Ro}_m^{(1)}(\gamma, \xi_-) - \frac{\text{Ro}_m^{(1)}(c, 1)}{\text{Ro}_m^{(3)}(c, 1)} \text{Ro}_m^{(3)}(\gamma, \xi_-) \right] \text{So}_m(\gamma, \eta_0) \text{So}_m(\gamma, \eta) \Big\} \end{aligned} \quad (4.294)$$

by the relations:

$$\begin{aligned} E_u = \frac{ik^2 Z}{c \sqrt{(\xi^2 - \eta^2)}} \frac{\partial \Pi_m}{\partial v}, \quad E_v = \frac{-ik^2 Z}{c \sqrt{(\xi^2 - \eta^2)}} \frac{\partial \Pi_m}{\partial u}, \quad E_z = 0, \\ H_u = \frac{k}{c \sqrt{(\xi^2 - \eta^2)}} \frac{\partial^2 \Pi_m}{\partial u \partial z}, \quad H_v = \frac{k}{c \sqrt{(\xi^2 - \eta^2)}} \frac{\partial^2 \Pi_m}{\partial v \partial z}, \quad H_z = \left(\frac{\partial^2}{\partial z^2} + k^2 \right) \Pi_m. \end{aligned} \quad (4.295)$$

On the surface $u = 0$:

$$H_v = -\frac{2i}{c|\sin v|} \int_{-\infty}^{+\infty} t dt e^{it(z-z_0)} \sum_{m=0}^{\infty} \left\{ \frac{1}{\Omega_m^{(e)}} \frac{Re_m^{(3)}(\gamma, \xi_0)}{(\partial/\partial u)Re_m^{(3)}(\gamma, \cosh u)|_{u=0}} \right. \\ \times Se_m(\gamma, \eta_0) \frac{\partial}{\partial v} Se_m(\gamma, \cos v) + \frac{1}{\Omega_m^{(o)}} \frac{Ro_m^{(3)}(\gamma, \xi_0)}{(\partial/\partial u)Ro_m^{(3)}(\gamma, \cosh u)|_{u=0}} \\ \left. \times So_m(\gamma, \eta_0) \frac{\partial}{\partial v} So_m(\gamma, \cos v) \right\}, \quad (4.296)$$

$$H_z = -\frac{2}{k} \int_{-\infty}^{+\infty} dt (k^2 - t^2) e^{it(z-z_0)} \sum_{m=0}^{\infty} \left\{ \frac{1}{\Omega_m^{(e)}} \frac{Re_m^{(3)}(\gamma, \xi_0)}{(\partial/\partial u)Re_m^{(3)}(\gamma, \cosh u)|_{u=0}} \right. \\ \times Se_m(\gamma, \eta_0) Se_m(\gamma, \eta) + \frac{1}{\Omega_m^{(o)}} \frac{Ro_m^{(3)}(\gamma, \xi_0)}{(\partial/\partial u)Ro_m^{(3)}(\gamma, \cosh u)|_{u=0}} \\ \left. \times So_m(\gamma, \eta_0) So_m(\gamma, \eta) \right\}. \quad (4.297)$$

If $z_0 = 0$, in the far field ($\xi \rightarrow \infty$):

$$E_v = 2\sqrt{2\pi k^2 Z} \sin \theta \frac{e^{ikr}}{kr} \sum_{m=0}^{\infty} (-i)^m \left\{ \frac{1}{\Omega_m^{(e)}} Re_m^{(1)}(c \sin \theta, \xi_0) \right. \\ \times Se_m(c \sin \theta, \eta_0) Se_m(c \sin \theta, \eta) + \frac{1}{\Omega_m^{(o)}} \left[Ro_m^{(1)}(c \sin \theta, \xi_0) - \right. \\ \left. - \frac{Ro_m^{(1)}(c \sin \theta, 1)}{Ro_m^{(3)}(c \sin \theta, 1)} Ro_m^{(3)}(c \sin \theta, \xi_0) \right] So_m(c \sin \theta, \eta_0) So_m(c \sin \theta, \eta) \Big\}, \quad (4.298)$$

where $\bar{\Omega}_m^{(e),(o)}$ are given by eq. (4.291) and r and θ are spherical polar coordinates: r is the distance from the origin to the point of observation and θ the angle measured from the positive z -axis to the line between the origin and the observation point. If the longitudinal dipole is on the surface ($u_0 = 0$):

$$\Pi_m = -\frac{2}{k} \int_{-\infty}^{+\infty} dt e^{it(z-z_0)} \sum_{m=0}^{\infty} \left\{ \frac{1}{\Omega_m^{(e)}} \frac{Re_m^{(3)}(\gamma, \xi)}{(\partial/\partial u)Re_m^{(3)}(\gamma, \cosh u)|_{u=0}} Se_m(\gamma, \eta_0) Se_m(\gamma, \eta) + \right. \\ \left. + \frac{1}{\Omega_m^{(o)}} \frac{Ro_m^{(3)}(\gamma, \xi)}{(\partial/\partial u)Ro_m^{(3)}(\gamma, \cosh u)|_{u=0}} So_m(\gamma, \eta_0) So_m(\gamma, \eta) \right\}, \quad (4.299)$$

and, in particular, in the far field ($\xi \rightarrow \infty$) with $z_0 = 0$:

$$E_r = 2i\sqrt{2\pi k^2 Z} \sin \theta \frac{e^{ikr}}{kr} \sum_{m=0}^{\infty} (-i)^m \left\{ \frac{Se_m(c \sin \theta, \eta_0) Se_m(c \sin \theta, \eta)}{\bar{\Omega}_m^{(e)} (\partial/\partial u) Re_m^{(3)}(c \sin \theta, \cosh u)|_{u=0}} + \right. \\ \left. + \frac{So_m(c \sin \theta, \eta_0) So_m(c \sin \theta, \eta)}{\Omega_m^{(o)} (\partial/\partial u) Ro_m^{(3)}(c \sin \theta, \cosh u)|_{u=0}} \right\}. \quad (4.300)$$

The total electromagnetic field components for a magnetic dipole parallel to \hat{u} (radial dipole) or to $\hat{\phi}$ (transverse or circumferential dipole) can be derived from the

general result of eq. (4.292). The far field patterns may also be obtained by using the reciprocity theorem.

4.4.2.2. LOW FREQUENCY APPROXIMATIONS

No specific results are available; low frequency expansions, however, can be derived from the results of the previous section.

4.4.2.3. HIGH FREQUENCY APPROXIMATIONS

No specific results are available although geometrical and physical optics approximations are derivable by standard techniques.

4.5. Point sources

4.5.1. Acoustically soft strip

4.5.1.1. EXACT SOLUTIONS

For a point source at (u_0, v_0, z_0) , such that

$$V^i = \frac{e^{ikR}}{kR}, \quad (4.301)$$

then

$$\begin{aligned} V^i + V^s = & \frac{2i}{k} \int_{-\tau}^{+\tau} dt e^{it(z-z_0)} \sum_{m=0}^{\tau} \left\{ \frac{1}{\Omega_m^{(e)}} \operatorname{Re}_m^{(3)}(\gamma, \xi_0) \right. \\ & \times \left[\operatorname{Re}_m^{(1)}(\gamma, \xi_0) - \frac{\operatorname{Re}_m^{(1)}(\gamma, 1)}{\operatorname{Re}_m^{(3)}(\gamma, 1)} \operatorname{Re}_m^{(3)}(\gamma, \xi_0) \right] \operatorname{Se}_m(\gamma, \eta_0) \operatorname{Se}_m(\gamma, \eta) + \\ & \left. + \frac{1}{\Omega_m^{(o)}} \operatorname{Ro}_m^{(3)}(\gamma, \xi_0) \operatorname{Ro}_m^{(1)}(\gamma, \xi_0) \operatorname{So}_m(\gamma, \eta_0) \operatorname{So}_m(\gamma, \eta) \right\}, \end{aligned} \quad (4.302)$$

where $\Omega_m^{(e),(o)}$ and γ are given by eqs. (4.281) and (4.282).

On the surface $u = 0$:

$$\begin{aligned} \frac{\partial}{\partial u} (V^i + V^s) = & \frac{2}{k} \int_{-\tau}^{+\tau} dt e^{it(z-z_0)} \sum_{m=0}^{\tau} \left\{ \frac{1}{\Omega_m^{(e)}} \frac{\operatorname{Re}_m^{(3)}(\gamma, \xi_0)}{\operatorname{Re}_m^{(3)}(\gamma, 1)} \operatorname{Se}_m(\gamma, \eta_0) \operatorname{Se}_m(\gamma, \eta) + \right. \\ & \left. + \frac{1}{\Omega_m^{(o)}} \frac{\operatorname{Ro}_m^{(3)}(\gamma, \xi_0)}{\operatorname{Ro}_m^{(3)}(\gamma, 1)} \operatorname{So}_m(\gamma, \eta_0) \operatorname{So}_m(\gamma, \eta) \right\}. \end{aligned} \quad (4.303)$$

If the point source is at $(u_0, v_0, z_0 = 0)$, the total far field ($\xi \rightarrow \infty$) is:

$$\begin{aligned} V^i + V^s = & 2\sqrt{2\pi} \frac{e^{ikr}}{kr} \sum_{m=0}^{\tau} (-i)^m \left\{ \frac{1}{\Omega_m^{(e)}} \left[\operatorname{Re}_m^{(1)}(c \sin \theta, \xi_0) - \right. \right. \\ & \left. \left. - \frac{\operatorname{Re}_m^{(1)}(c \sin \theta, 1)}{\operatorname{Re}_m^{(3)}(c \sin \theta, 1)} \operatorname{Re}_m^{(3)}(c \sin \theta, \xi_0) \right] \operatorname{Se}_m(c \sin \theta, \eta_0) \operatorname{Se}_m(c \sin \theta, \eta) + \right. \\ & \left. + \frac{1}{\Omega_m^{(o)}} \operatorname{Ro}_m^{(1)}(c \sin \theta, \xi_0) \operatorname{So}_m(c \sin \theta, \eta_0) \operatorname{So}_m(c \sin \theta, \eta) \right\}, \end{aligned} \quad (4.304)$$

where $\bar{\Omega}_m^{(\epsilon), (o)}$ are given by eq. (4.291) and r and θ are spherical polar coordinates: r is the distance from the origin to the observation point and θ the angle measured from the positive z -axis to the line between the origin and the observation point. If the point source is on the surface ($u_0 = 0$), the total field is identically zero everywhere.

4.5.1.2. LOW FREQUENCY APPROXIMATIONS

No specific results are available; low frequency expansions, however, can be derived from the results of the previous section.

4.5.1.3. HIGH FREQUENCY APPROXIMATIONS

No specific results are available although the geometrical optics approximation is derivable by standard techniques.

4.5.2. Acoustically hard strip

4.5.2.1. EXACT SOLUTIONS

For a point source at (u_0, v_0, z_0) , such that

$$V^i = \frac{e^{ikR}}{kR}, \quad (4.305)$$

then

$$\begin{aligned} V^i + V^s = & \frac{2i}{k} \int_{-\infty}^{+\infty} dt e^{it(z-z_0)} \sum_{m=0}^{\infty} \left\{ \frac{1}{\Omega_m^{(\epsilon)}} \operatorname{Re}_m^{(3)}(\gamma, \xi_0) \operatorname{Re}_m^{(1)}(\gamma, \xi_0) \operatorname{Se}_m(\gamma, \eta_0) \operatorname{Se}_m(\gamma, \eta) + \right. \\ & \left. + \frac{1}{\Omega_m^{(o)}} \operatorname{Ro}_m^{(3)}(\gamma, \xi_0) \left[\operatorname{Ro}_m^{(1)}(\gamma, \xi_0) - \frac{\operatorname{Ro}_m^{(1)}(\gamma, 1)}{\operatorname{Ro}_m^{(3)}(\gamma, 1)} \operatorname{Ro}_m^{(3)}(\gamma, \xi_0) \right] \operatorname{So}_m(\gamma, \eta_0) \operatorname{So}_m(\gamma, \eta) \right\}, \end{aligned} \quad (4.306)$$

where $\Omega_m^{(\epsilon), (o)}$ and γ are given by eqs. (4.281) and (4.282).

On the surface $u = 0$:

$$\begin{aligned} V^i + V^s = & -\frac{2}{k} \int_{-\infty}^{+\infty} dt e^{it(z-z_0)} \sum_{m=0}^{\infty} \left\{ \frac{1}{\Omega_m^{(\epsilon)}} \frac{\operatorname{Re}_m^{(3)}(\gamma, \xi_0)}{(\partial/\partial u) \operatorname{Re}_m^{(3)}(\gamma, \cosh u)} \Big|_{u=0} \right. \\ & \left. \times \operatorname{Se}_m(\gamma, \eta_0) \operatorname{Se}_m(\gamma, \eta) + \frac{1}{\Omega_m^{(o)}} \frac{\operatorname{Ro}_m^{(3)}(\gamma, \xi_0)}{(\partial/\partial u) \operatorname{Ro}_m^{(3)}(\gamma, \cosh u)} \Big|_{u=0} \operatorname{So}_m(\gamma, \eta_0) \operatorname{So}_m(\gamma, \eta) \right\}. \end{aligned} \quad (4.307)$$

If the point source is at $(u_0, v_0, z_0 = 0)$, the total far field ($\xi \rightarrow \infty$) is:

$$\begin{aligned}
V^i + V^s = & 2\sqrt{\frac{2\pi}{kr}} \sum_{m=0}^{\infty} (-i)^m \left\{ \frac{1}{\bar{\Omega}_m^{(e)}} \operatorname{Re}_m^{(1)}(c \sin \theta, \xi_0) \operatorname{Se}_m(c \sin \theta, \eta_0) \operatorname{Se}_m(c \sin \theta, \eta) + \right. \\
& + \frac{1}{\bar{\Omega}_m^{(o)}} \left[\operatorname{Ro}_m^{(1)}(c \sin \theta, \xi_0) - \frac{\operatorname{Ro}_m^{(1)'}(c \sin \theta, 1)}{\operatorname{Ro}_m^{(3)'}(c \sin \theta, 1)} \operatorname{Ro}_m^{(3)}(c \sin \theta, \xi_0) \right] \\
& \left. \times \operatorname{So}_m(c \sin \theta, \eta_0) \operatorname{So}_m(c \sin \theta, \eta) \right\}, \quad (4.308)
\end{aligned}$$

where $\bar{\Omega}_m^{(e), (o)}$ are given by eq. (4.291) and r and θ are spherical polar coordinates: r is the distance from the origin to the observation point and θ the angle measured from the positive z -axis to the line between the origin and the observation point. If the point source is on the surface ($u_0 = 0$):

$$\begin{aligned}
V^i + V^s = & -\frac{2}{k} \int_{-x_0}^{+x_0} dt e^{it(z-z_0)} \sum_{m=0}^{\infty} \left\{ \frac{1}{\bar{\Omega}_m^{(e)}} \frac{\operatorname{Re}_m^{(3)}(\gamma, \xi)}{(\partial/\partial u) \operatorname{Re}_m^{(3)}(\gamma, \cosh u)|_{u=0}} \operatorname{Se}_m(\gamma, \eta_0) \right. \\
& \left. \times \operatorname{Se}_m(\gamma, \eta) + \frac{1}{\bar{\Omega}_m^{(o)}} \frac{\operatorname{Ro}_m^{(3)}(\gamma, \xi)}{(\partial/\partial u) \operatorname{Ro}_m^{(3)}(\gamma, \cosh u)|_{u=0}} \operatorname{So}_m(\gamma, \eta_0) \operatorname{So}_m(\gamma, \eta) \right\}, \quad (4.309)
\end{aligned}$$

and, in particular, in the far field ($\xi \rightarrow \infty$) with $z_0 = 0$:

$$\begin{aligned}
V^i + V^s = & 2i\sqrt{\frac{2\pi}{kr}} \sum_{m=0}^{\infty} (-i)^m \left\{ \frac{\operatorname{Se}_m(c \sin \theta, \eta_0) \operatorname{Se}_m(c \sin \theta, \eta)}{\bar{\Omega}_m^{(e)} (\partial/\partial u) \operatorname{Re}_m^{(3)}(c \sin \theta, \cosh u)|_{u=0}} + \right. \\
& \left. + \frac{\operatorname{So}_m(c \sin \theta, \eta_0) \operatorname{So}_m(c \sin \theta, \eta)}{\bar{\Omega}_m^{(o)} (\partial/\partial u) \operatorname{Ro}_m^{(3)}(c \sin \theta, \cosh u)|_{u=0}} \right\}. \quad (4.310)
\end{aligned}$$

4.5.2.2. LOW FREQUENCY APPROXIMATIONS

No specific results are available; low frequency expansions, however, can be derived from the results of the previous section.

4.5.2.3. HIGH FREQUENCY APPROXIMATIONS

No specific results are available although the geometrical optics approximation is derivable by standard techniques.

Bibliography

- BARAKAT, R. [1969], Surface Currents on Perfectly Conducting Elliptic Cylinders in Plane-Wave Fields, to be published.
- BOERSMA, J. [1964], Boundary Value Problems in Diffraction Theory and Lifting Surface Theory, Thesis, Groningen University.
- BOUWKAMP, C. J. [1954], Diffraction Theory, Rept. Progr. Phys. **17**, 35-100.
- BURKE, J. F. and V. TWERSKY [1960], On Scattering of Waves by an Elliptic Cylinder and by a Semielliptic Protuberance on a Ground Plane, Sylvania Electronic Defense Laboratory Report EDL-M266, Mountain View, California.
- BURKE, J. F. and V. TWERSKY [1964], On Scattering of Waves by an Elliptic Cylinder and by a Semielliptic Protuberance on a Ground Plane, J. Opt. Soc. Am. **54**, 732-744.

- BURKL, J. E., E. J. CHRISTENSEN and S. B. LITTLE [1964], Scattering Patterns for Elliptic Cylinders, *J. Opt. Soc. Am.* **54**, 1065-1066.
- DE HOOP, A. T. [1955], Variational Formulation of Two-Dimensional Diffraction Problems with Application to Diffraction by a Slit, *Ned. Akad. Wetensch. Proc. Ser. B* **58**, 401-411.
- FIALKOVSKIY, A. T. [1966], Diffraction of Planar Electromagnetic Waves by a Slot and a Strip, *Radio Eng. Electron.* **2**, 150-157.
- GOODRICH, R. F. and N. D. KAZARINOFF [1963], Diffraction by Thin Elliptic Cylinders, *Michigan Math. J.* **10**, 105-127. A few formulas and Fig. 1 have misprints.
- GRINBERG, G. A. [1957], A New Method for Solving Problems Related to the Diffraction of Electromagnetic Waves by a Plane with an Unbounded Straight Slit, *Zh. Tekhn. Fiz.* **27**, 2410-2419.
- GRINBERG, G. A. [1958], A Method for Solving Problems of the Diffraction of Electromagnetic Waves by Ideally Conducting Plane Screens Based on the Study of the Currents Induced on the Shaded Side of the Screen, *Soviet Phys.-Techn. Phys.* **3**, 521-534.
- GRINBERG, G. A. [1960], Diffraction of Electromagnetic Waves by a Strip of Finite Width, *Soviet Phys. Doklady* **4**, 1222-1225.
- GROSHWITZ, E. and H. HÖNL [1952], Die Beugung elektromagnetischer Wellen am Spalt. I, *Z. Physik* **131**, 305-319. For a criticism of this paper see BOUWKAMP [1954], MÜLLER and WESTPFAHL [1953] and TRANIER [1954].
- HANSEN, E. B. [1962], Scalar Diffraction by an Infinite Strip and a Circular Disk, *J. Math. Phys.* **41**, 229-245.
- HÖNL, H., A. W. MAUE and K. WESTPFAHL [1961], Theorie der Beugung, in: *Handbuch der Physik*, Vol. XXV/1, Springer-Verlag, Berlin.
- HÖNL, H. and E. ZIMMER [1953], Intensität und Polarisation bei der Beugung elektromagnetischer Wellen am Spalt. II, *Z. Physik* **135**, 196-218.
- HSU, H. P. [1959], Study of Aperture Fields in the Diffraction by a Slit, Case Institute of Technology Science Report No. 5.
- HSU, H. P. [1960], Aperture Fields in the Diffraction by a Slit, *J. Appl. Phys.* **31**, 1742-1746.
- JONES, D. S. and B. NOBLE [1961], The Low-frequency Scattering by a Perfectly Conducting Strip, *Proc. Cambridge Phil. Soc.* **57**, 364-366.
- KARP, S. N. and J. B. KELLER [1961], Multiple Diffraction by an Aperture in a Hard Screen, *Optica Acta* **8**, 61-72. There are misprints in eqs. (7) and (25).
- KARP, S. N. and A. RUSSEK [1965], Diffraction by a Wide Slit, *J. Appl. Phys.* **27**, 886-894.
- KELLER, J. B. [1957], Diffraction by an Aperture, *J. Appl. Phys.* **28**, 426-444.
- KELLER, J. B. and E. B. HANSEN [1965], Survey of the Theory of Diffraction of Short Waves by Edges, *Acta Phys. Polon.* **27**, 217-234.
- KHASKIND, M. D. and L. A. VAINSHTEYN [1964], Diffraction of Plane Waves by a Slit and a Tape, *Radio Eng. Electron.* **10**, 1492-1502.
- KILBURTZ, R. B. [1965], Construction of Asymptotic Solutions to Scattering Problems in the Fourier Transform Representation, *Appl. Sci. Res.* **B12**, 221-234. Eq. (25) has been misprinted.
- KING, R. W. P. and T. T. WU [1959], *The Scattering and Diffraction of Waves*, Harvard Univ. Press, Cambridge, Mass.
- KOCHERZINSKI, G. N. [1955], Radiation of Electric Dipoles Situated Near a Perfectly Conducting Elliptic Cylinder, *Zh. Tekhn. Fiz.* **25**, 1140-1154. A 90° rotation of the radiation pattern with respect to the figure caption occurs in Figs. 6, 11, 12 and 13.
- LUCKE, W. S. [1951], Electric Dipoles in the Presence of Elliptic and Circular Cylinders, *J. Appl. Phys.* **22**, 15-19.
- LUNEBURG, E. and K. WESTPFAHL [1968], Beugung am Streifen: Hochfrequenz-Asymptotik und Kleinman'sche Lösung, *Ann. Physik* **21**, 12-25.
- MANDRAZHIL, V. P. [1962], Properties of the Current Density Distribution at the Surface of a Thin Strip and of an Elliptic Cylinder in the Diffraction of Cylindrical Electromagnetic Waves, *Telecommunications and Radio Engineering*, 33-46.

- MILES, J. W. [1949], On the Diffraction of an Electromagnetic Wave through a Plane Screen, *J. Appl. Phys.* **20**, 760-771.
- MILLAR, R. F. [1957], Dissertation, Cambridge.
- MILLAR, R. F. [1958a], Diffraction by a Wide Slit and Complementary Strip. I, *Proc. Cambridge Phil. Soc.* **54**, 479-496. There is a minor error on p. 489, eq. (41).
- MILLAR, R. F. [1958b], Diffraction by a Wide Slit and Complementary Strip. II, *Proc. Cambridge Phil. Soc.* **54**, 497-511. There are minor errors on pp. 499, 502, 503, 504 and 506.
- MILLAR, R. F. [1960], A Note on Diffraction by an Infinite Slit, *Can. J. Phys.* **38**, 38-47. There are minor errors on pp. 41, 42 and 47.
- MORSE, P. M. and P. J. RUBENSTEIN [1938], The Diffraction of Waves by Ribbons and by Slits, *Phys. Rev.* **54**, 895-898.
- MÜLLER, R. and K. WESTPFAHL [1953], Eine strenge Behandlung der Beugung elektromagnetischer Wellen am Spalt, *Z. Physik* **134**, 245-263.
- NOBLE, B. [1962], Integral Equation Perturbation Methods in Low Frequency Diffraction, in: *Electromagnetic Waves*, ed. R. Langer, 323-360, University of Wisconsin Press, Madison, Wis.
- PIMENOV, YU. V. [1959], The Plane Problem of Diffraction of Electromagnetic Waves by an Ideally Conducting Strip of Finite Width, *Soviet Phys.-Techn. Phys.* **4**, 532-538.
- SESHADRI, S. R. [1958a], High-Frequency Transmission Coefficient of an Infinite Slit in a Plane Screen, *Sci. Report No. 17*, Cruft Laboratory, Harvard University.
- SESHADRI, S. R. [1958b], High-Frequency Diffraction of Plane Waves by an Infinite Slit, *Sci. Report No. 20*, Cruft Laboratory, Harvard University.
- SESHADRI, S. R. and T. T. WU [1960], High-Frequency Diffraction of Plane Waves by an Infinite Slit for Grazing Incidence, *IRE Trans. Antennas Propagation* **AP-8**, 37-42.
- SKAVLEM, S. [1951], On the Diffraction of Scalar Plane Waves by a Slit of Infinite Length, *Arch. for Mat. og Naturv.* **B 51**, 61-80.
- SOMMERFELD, A. [1954], *Lectures in Theoretical Physics, Vol. IV: Optics*, 274-289, Academic Press, Inc., New York.
- STRUTT, J. W., Lord Rayleigh [1897a], On the Passage of Waves Through Apertures in Plane Screens and Allied Problems, *Phil. Mag.* **43**, 259-272.
- STRUTT, J. W., Lord Rayleigh [1897b], On the Incidence of Aerial and Electric Waves upon Small Obstacles in the Form of Ellipsoids or Elliptic Cylinders and on the Passage of Electric Waves through a Circular Aperture in a Conducting Screen, *Phil. Mag.* **44**, 28-52.
- STRUTT, J. W., Lord Rayleigh [1913], On the Passage of Waves through Fine Slits in Thin Opaque Screens, *Proc. Roy. Soc. A* **89**, 194-219.
- TAI, C. T. [1954], A Glossary of Dyadic Green's Functions, Stanford Research Institute Technical Report 46, Stanford, California. Formula (16) is misprinted.
- TRANIER, C. J. [1954], A Further Note on Dual Integral Equations and an Application to the Diffraction of Electromagnetic Waves, *Quart. J. Mech. Appl. Math.* **7**, 317-325.
- UFIMISEV, P. Ia. [1958], Secondary Diffraction of Electromagnetic Waves by a Strip, *Soviet Phys.-Techn. Phys.* **3**, 535-548.
- WATERMAN, P. C. [1963], Exact Theory of Scattering by Conducting Strips, Avco Corporation Res. Report RAD-TM-63-78.
- WU, T. T. [1958], High-Frequency Diffraction by an Infinite Slit, Technical Report No. 281, Cruft Laboratory, Harvard University.

CHAPTER 5

THE HYPERBOLIC CYLINDER

P. L. E. USLENGHI

The only exact result presently known for the hyperbolic cylinder is for the field produced by a line source parallel to the generators of a convex hard cylinder. A few high-frequency approximation formulas are available; numerical data are non-existent.

The hyperbolic cylinder becomes a wedge in the limiting case of an interfocal distance equal to zero.

5.1. Hyperbolic cylinder geometry

The elliptic cylindrical coordinates have already been introduced in Chapter 3, and are shown in Fig. 3.1. The reader is referred to Section 3.1 for the definitions of the coordinate systems and of the primary sources, and for definitions, notation and bibliography on the Mathieu functions. However, the only Mathieu functions needed in this chapter are non-periodic in the angular variable, and their definitions and notation are explicitly given in Section 5.3.2.1.

The scattering body is the hyperbolic cylinder of one sheet with surface $\eta = \eta_1 \geq 0$. The primary source is usually located on the convex side of the cylinder ($\eta_0 \leq \eta_1$); thus, in the case of plane wave incidence one has that $\nu_1 < \phi_0 \leq \pi$, where $\phi = \nu_1$ is the angle that the asymptotes to the hyperbola $\eta = \eta_1$ form with the x -axis. An exception is made for the case of a concave hyperbolic mirror with a line source at the focus ($x_0 = \frac{1}{2}d, y_0 = 0$). Without loss of generality, it will be assumed that $y_0 \geq 0$. We shall depart from this notation only in Section 5.3.2.1.

5.2. Plane wave incidence

5.2.1. *E*-polarization

No exact results are available. For incidence at an angle ϕ_0 with respect to the negative x -axis, such that

$$E^i = \hat{z} \exp \{ -ik(x \cos \phi_0 + y \sin \phi_0) \}, \quad (5.1)$$

the geometrical optics scattered field at a point P located in the illuminated region is

$$(E_z)_{g.o.} = - \left[1 + \frac{2(P_1 P)}{D \cos \phi_1} \right]^{-\frac{1}{2}} \exp \{ ik[(P_1 P) - x_1 \cos \phi_0 - y_1 \sin \phi_0] \}, \quad (5.2)$$

where (P_1P) is the distance between the reflection point $P_1(x_1, y_1, z)$ and the observation point $P(x, y, z)$,

$$(P_1P) = [(x-x_1)^2 + (y-y_1)^2]^{\frac{1}{2}}, \quad (5.3)$$

the reflection angle ϕ_1 of Fig. 5.1 is given by

$$x-x_1 = (P_1P) \cos(\phi_0 + 2\phi_1), \quad y-y_1 = (P_1P) \sin(\phi_0 + 2\phi_1), \quad (5.4)$$

and D is the radius of curvature of the scatterer at P_1 :

$$D = \frac{1}{2}d \frac{(\xi_1^2 - \eta_1^2)^{\frac{1}{2}}}{\eta_1 \sqrt{1 - \eta_1^2}}. \quad (5.5)$$

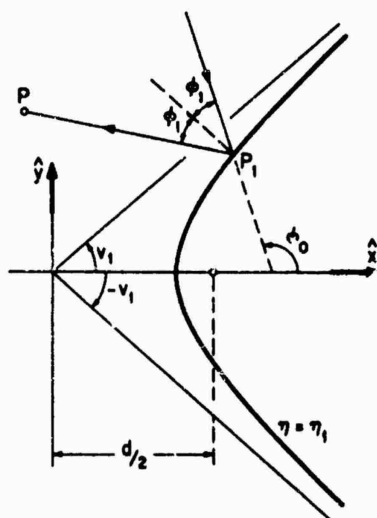


Fig. 5.1. Geometry for the reflected field with plane wave incidence.

Formula (5.2) is applicable if $kD \gg 1$. In the shadowed region, $(E_z)_{g.o.} = 0$. If $\phi_0 \geq \pi - v_1$, there is no shadowed region.

In particular, for incidence along the positive x -axis ($\phi_0 = \pi$) the back scattered field ($y = 0$) is

$$(E_z^s)_{g.o.} = - \left[\frac{1 - \eta_1^2}{1 + \eta_1^2 + (4\eta_1/d)|x|} \right]^{\frac{1}{2}} \exp(-ikx + 2ic\eta_1). \quad (5.6)$$

In the physical optics approximation, the total magnetic field at the surface $\eta = \eta_1$ is

$$(H_z)_{p.o.} = \begin{cases} \frac{2Y}{\sqrt{(\xi^2 - \eta_1^2)}} (\pm \xi \sqrt{1 - \eta_1^2} \cos \phi_0 - \eta_1 \sqrt{\xi^2 - 1} \sin \phi_0) \\ \quad \times \exp \{ -ic[\xi \eta_1 \cos \phi_0 \pm \sqrt{(\xi^2 - 1)(1 - \eta_1^2)} \sin \phi_0] \}, & \text{in the illuminated region, } (\pm \text{ if } y_1 \gtrless 0), \\ 0, & \text{in the shadowed region.} \end{cases} \quad (5.7)$$

A more refined approximation, in which an asymptotic expression for the diffracted field in the shadowed region is retained, can be derived from the results of KELLER [1956]. The total electric field at a point $P(x, y, z)$ located in the shadowed region away from the surface $\eta = \eta_1$ is:

$$\begin{aligned}
 E_z \sim & \frac{1}{\sqrt{(2\pi k(P_2 P))}} \left[\frac{c}{2n_1 \sqrt{(1-\eta_1^2)}} \right]^{\frac{1}{2}} [(\xi_1^2 - \eta_1^2)(\xi_2^2 - \eta_1^2)]^{\frac{1}{4}} \\
 & \times \exp \left\{ \frac{1}{i^{\frac{1}{2}}} i\pi + ik[(P_2 P) - x_1 \cos \phi_0 - y_1 \sin \phi_0] + ic \int_{(P_1 P_2)} d\xi \sqrt{\frac{\xi^2 - \eta_1^2}{\xi^2 - 1}} \right\} \\
 & \times \sum_{n=1}^{\infty} [\text{Ai}'(-\alpha_n)]^{-2} \exp \left\{ \alpha_n \left(\frac{1}{2} c \right)^{\frac{1}{2}} (\eta_1 \sqrt{(1-\eta_1^2)})^{\frac{1}{2}} \exp \left\{ \frac{5}{6} i\pi \right\} \int_{(P_1 P_2)} \frac{d\xi}{\sqrt{\{(\xi^2 - 1)(\xi^2 - \eta_1^2)\}}} \right\},
 \end{aligned} \tag{5.8}$$

where $P_1 \equiv (x_1, y_1, z) \equiv (\xi_1, \eta_1, z)$ and $P_2 \equiv (x_2, y_2, z) \equiv (\xi_2, \eta_1, z)$ are the points of Fig. 5.2 at which the incident ray, and the diffracted ray passing through P ,

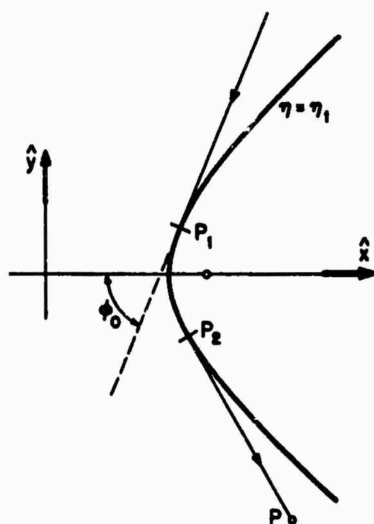


Fig. 5.2. Geometry for the diffracted field with plane wave incidence.

are tangent to the scatterer $\eta = \eta_1$; α_n are the zeros of the Airy function ($\text{Ai}(-\alpha_n) = 0$),

$$(P_2 P) = [(x - x_2)^2 + (y - y_2)^2]^{\frac{1}{2}}, \tag{5.9}$$

and

$$\int_{(P_1 P_2)} = \begin{cases} \int_{\xi_1}^{\xi_2}, & \text{if } y_1 \text{ and } y_2 \text{ have the same sign,} \\ \int_1^{\xi_1} + \int_1^{\xi_2}, & \text{if } y_1 \text{ and } y_2 \text{ have opposite signs,} \end{cases}$$

where $\xi_<(\xi_>)$ is the smaller (greater) of ξ_1 and ξ_2 . A correction to the leading term (5.8) that depends upon the derivative of the curvature has been found by

KELLER and LEVY [1959]. The total field in the shadowed region near the surface $\eta = \eta_1$ is of the order $k^{\frac{1}{2}}$ greater than the field of eq. (5.8) (see KELLER [1956]).

5.2.2. *H-polarization*

No exact results are available. For incidence at an angle ϕ_0 with respect to the negative x -axis, such that

$$H^i = \hat{z} \exp \{-ik(x \cos \phi_0 + y \sin \phi_0)\}, \quad (5.10)$$

the geometrical optics scattered field at a point P located in the illuminated region is

$$(H_z^s)_{g.o.} = \left[1 + \frac{2(P_1 P)}{D \cos \phi_1}\right]^{-\frac{1}{2}} \exp \{ik[(P_1 P) - x_1 \cos \phi_0 - y_1 \sin \phi_0]\}, \quad (5.11)$$

where the distance $(P_1 P)$ between the reflection point $P_1(x_1, y_1, z)$ and the observation point $P(x, y, z)$, the angle ϕ_1 of Fig. 5.1 and the radius D of curvature of the scatterer at P_1 are given by eqs. (5.3), (5.4) and (5.5), respectively. Formula (5.11) is applicable if $kD \gg 1$. In the shadowed region, $(H_z^s)_{g.o.} = 0$. If $\phi_0 \geq \pi - \nu_1$, there is no shadowed region.

In particular, for incidence along the positive x -axis ($\phi_0 = \pi$) the back scattered field ($y = 0$) is:

$$(H_z^s)_{g.o.} = \left[\frac{1 - \eta_1^2}{1 + \eta_1^2 + (4\eta_1/d)|x|}\right]^{\frac{1}{2}} \exp(-ikx + 2ic\eta_1). \quad (5.12)$$

In the physical optics approximation, the total magnetic field at the surface $\eta = \eta_1$ is

$$(H_z)_{p.o.} = \begin{cases} 2 \exp \{-ic[\xi \eta_1 \cos \phi_0 \pm \sqrt{(\xi^2 - 1)(1 - \eta_1^2)}] \sin \phi_0\}, \\ \quad \text{in the illuminated region, } (\pm \text{ if } y_1 \gtrless 0), \\ 0, \quad \text{in the shadowed region.} \end{cases} \quad (5.13)$$

A more refined approximation, in which an asymptotic expression for the diffracted field in the shadowed region is retained, can be derived from the results of KELLER [1956]. The total magnetic field at a point $P(x, y, z)$ located in the shadowed region away from the surface $\eta = \eta_1$ is:

$$\begin{aligned} H_z \sim & \frac{1}{\sqrt{\{2\pi k(P_2 P)\}}} \left[\frac{c}{2\eta_1 \sqrt{(1 - \eta_1^2)}} \right]^{\frac{1}{2}} [(\xi_1^2 - \eta_1^2)(\xi_2^2 - \eta_1^2)]^{\frac{1}{4}} \\ & \times \exp \left\{ \frac{1}{2} i\pi + ik[(P_2 P) - x_1 \cos \phi_0 - y_1 \sin \phi_0] + ic \int_{(P_1 P_2)} d\xi \sqrt{\frac{\xi^2 - \eta_1^2}{\xi^2 - 1}} \right\} \\ & \times \sum_{n=1}^{\infty} \frac{\exp \left\{ \beta_n \left(\frac{1}{2} c \right) (\eta_1 \sqrt{(1 - \eta_1^2)})^{\frac{1}{2}} \exp \left\{ \frac{5}{6} i\pi \right\} \int_{(P_1 P_2)} \frac{d\xi}{\sqrt{(\xi^2 - 1)(\xi^2 - \eta_1^2)}} \right\}}{\beta_n [Ai(-\beta_n)]^2}, \end{aligned} \quad (5.14)$$

where $P_1 \equiv (x_1, y_1, z) \equiv (\xi_1, \eta_1, z)$ and $P_2 \equiv (x_2, y_2, z) \equiv (\xi_2, \eta_1, z)$ are the points of Fig. 5.2 at which the incident ray, and the diffracted ray passing through P , are tangent to the scatterer $\eta = \eta_1$; β_n are the zeros of the derivative of the Airy function ($\text{Ai}'(-\beta_n) = 0$), (P_2P) is given by eq. (5.9), and $\int_{(P,P_2)}$ must be computed as indicated in Section 5.2.1. A correction to the leading term (5.14) that depends upon the derivative of the curvature has been found by KELLER and LEVY [1959]. Information on the damping of the diffracted waves on the scatterer's surface can also be obtained from the general results that FRANZ and KLANTÉ [1959] derived for an arbitrary convex cylinder. In addition to the well-known damping factor depending on the radius of curvature D , a first-order correction term yields an amplitude factor $D^{-1/4}$, while the second-order correction term results in a change in damping depending on D , $\partial D/\partial \xi$ and $\partial^2 D/\partial \xi^2$. The results of Franz and Klante are valid if $(\frac{1}{3}kD)^{1/3} > \frac{1}{37}$, and if the relative variations of $1/D$ and $(\partial/\partial \xi)(1/D)$ are small within an arc-length of the order D .

5.3. Line sources

5.3.1. *E*-polarization

5.3.1.1. EXACT SOLUTIONS

Although a method similar to that used by BLOOM [1964] for the hard cylinder is applicable to this case, no specific results are available.

5.3.1.2. HIGH FREQUENCY APPROXIMATIONS

For an electric line source parallel to the z -axis, located at (ξ_0, η_0) on the convex side of the cylinder, such that

$$E^i = \hat{z} H_0^{(1)}(kR), \quad (5.15)$$

and so far from the surface $\eta = \eta_1$ that at the surface

$$E^i \sim \hat{z} \sqrt{\frac{2}{\pi k R}} e^{ikR - \frac{1}{4}i\pi}, \quad (5.16)$$

the geometric optics scattered field at a point P located in the illuminated region is

$$(E_s^i)_{g.o.} \sim - \sqrt{\frac{2}{\pi k (P_0 P_1)}} \left[1 + \frac{2(P_1 P)}{D \cos \phi_1} + \frac{(P_1 P)}{(P_0 P_1)} \right]^{-1/4} \exp \{ ik[(P_0 P_1) + (P_1 P)] - \frac{1}{4}i\pi \}, \quad (5.17)$$

where $(P_0 P_1)$ and $(P_1 P)$ are, respectively, the distances between the source P_0 and the reflection point P_1 , and between P_1 and the observation point P ; D is given by eq. (5.5), the coordinate ξ_1 by the relations

$$\frac{\partial}{\partial u_1} [(P_0 P_1) + (P_1 P)] = 0, \quad \frac{\partial^2}{\partial u_1^2} [(P_0 P_1) + (P_1 P)] > 0, \quad (5.18)$$

and the reflection angle ϕ_1 by

$$\phi_1 = \arcsin \left\{ \frac{d}{2(P_0 P_1) \sqrt{(\xi_1^2 - \eta_1^2)}} \left| (\xi_0 \eta_0 \eta_1 - \xi_1) \sqrt{(\xi_1^2 - 1)} \pm \xi_1 \sqrt{((\xi_0^2 - 1)(1 - \eta_0^2)(1 - \eta_1^2))} \right| \right\},$$

(\pm if $y_1 \geq 0$). (5.19)

Formula (5.17) is applicable if $kD \gg 1$. In the shadowed region, $(E_z)_{\text{g.o.}} = 0$. If the line source is in the angular sector

$$x_0 \leq 0, \quad |y_0| \leq |x_0| \tan v_1,$$

there is no shadowed region.

For a line source of strength (5.15) located at the focal line ($x_0 = -\frac{1}{2}d, y_0 = 0$), the scattered electric field is given by the Luneburg-Kline expansion (KELLER et al. [1956]):

$$E_z^s \sim \frac{\exp \{i[k(QP) + 2c\eta_1 - \frac{1}{4}\pi]\}}{\sqrt{(k(QP)w)}} \sum_{n=0}^{\infty} (2ic\eta_1)^{-n} \sum_{j=0}^n \left[\frac{2c\eta_1}{k(QP)w} \right]^j \sum_{t=0}^{2n-j} a_{jtn} w^{-t}, \quad (5.20)$$

where QP is the distance between the focal line ($\frac{1}{2}d, 0$) and the observation point P (see Fig. 5.3),

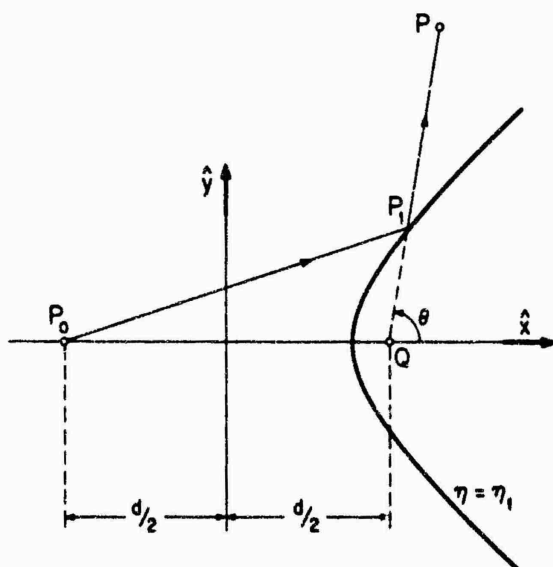


Fig. 5.3. Geometry for the reflected field with a line source at $P_0(-\frac{1}{2}d, 0)$.

$$w = 1 + \frac{2\eta_1}{1 - \eta_1^2} (\eta_1 - \cos \theta), \quad (5.21)$$

θ is the angle that the reflected ray $P_1 P$ forms with the positive x -axis,

$$a_{jtn} = \frac{1}{2j} \left[-(2j+t)(t+1)a_{j-1, t+1, n-1} + \right. \\ \left. + 2 \frac{1+\eta_1^2}{1-\eta_1^2} (j+t-\frac{1}{2})(t+j)a_{j-1, t, n-1} - (j+t-\frac{1}{2})(j+t-\frac{1}{2})a_{j-1, t-1, n-1} \right],$$

($1 \leq j \leq n; 0 \leq t \leq 2n-j$). (5.22)

$$a_{0in} = \sqrt{\frac{2}{\pi}} \frac{[(2n)!]^2}{2^{5n}(n!)^3} (-1)^{i+1} \binom{n}{i} - \sum_{j=1}^n \sum_{s=0}^{2n-j} a_{jsn} \binom{j}{i-s} (-1)^{i-s},$$

$$(0 \leq i \leq 2n; n \geq 1), \quad (5.23)$$

$$a_{000} = -\sqrt{\frac{2}{\pi}}, \quad (5.24)$$

and the binomial coefficients $\binom{\alpha}{\beta}$ in eq. (5.23) are understood to be zero unless $0 \leq \beta \leq \alpha$. The first few terms of the expansion (5.20) are:

$$E_z^s \sim -\sqrt{\frac{2}{\pi k(QP)w}} \exp \{i[k(QP) + 2c\eta_1 - \frac{1}{4}\pi]\}$$

$$\times \left[1 + \frac{i}{16c\eta_1} \left(1 - \frac{1}{w} \right) \left(\frac{3+5\eta_1^2}{1-\eta_1^2} - \frac{3}{w} \right) - \frac{i}{8k(QP)w} \left(4 \frac{1+\eta_1^2}{1-\eta_1^2} - \frac{3}{w} \right) + \dots \right]. \quad (5.25)$$

In the physical optics approximation, the total magnetic field at a point P_1 on the illuminated portion of the surface $\eta = \eta_1$ is

$$(H_z)_{p.o.} = -2iYH_1^{(1)}(k(P_0P_1)) \cos \phi_1, \quad (5.26)$$

where ϕ_1 is the angle of incidence; on the shadowed portion of the surface, $(H_z)_{p.o.} = 0$.

A more refined approximation, in which an asymptotic expression for the diffracted field in the shadowed region is retained, is easily obtained from the results of KELLER [1956]. For the line source (5.16), the total electric field at a point P located in the shadowed region away from the surface $\eta = \eta_1$ is:

$$E_z \sim \frac{1}{\pi k \sqrt{\{(P_0P_1)(P_2P)\}}} \left[\frac{c}{2\eta_1 \sqrt{(1-\eta_1^2)}} \right]^{\frac{1}{2}} [(\xi_1^2 - \eta_1^2)(\xi_2^2 - \eta_1^2)]^{\frac{1}{4}}$$

$$\times \exp \left\{ -\frac{1}{8}i\pi + ik[(P_0P_1) + (P_2P)] + ic \int_{(P_1P_2)} d\xi \sqrt{\frac{\xi^2 - \eta_1^2}{\xi^2 - 1}} \right\}$$

$$\times \sum_{n=1}^{\infty} [Ai'(-\alpha_n)]^{-2} \exp \left\{ \alpha_n \left(\frac{1}{2}c \right)^{\frac{1}{2}} (\eta_1 \sqrt{(1-\eta_1^2)})^{\frac{1}{2}} \exp \left\{ \frac{5}{8}i\pi \right\} \int_{(P_1P_2)} \sqrt{\frac{d\xi}{(\xi^2 - 1)(\xi^2 - \eta_1^2)}} \right\}, \quad (5.27)$$

where the various quantities have the same meaning as in eq. (5.8). A correction to the leading term (5.27) that depends upon the derivative of the curvature has been found by KELLER and LEVY [1959]. The total field in the shadowed region near the surface $\eta = \eta_1$ is of the order $k^{\frac{1}{2}}$ greater than the field of eq. (5.27) (see KELLER [1956]).

Finally, a line source of strength (5.16) located at $P_0(x_0 = \frac{1}{2}d, y_0 = 0)$ on the concave side of the cylinder originates a geometric optics scattered field:

$$(E_z)_{g.o.} \sim -\sqrt{\frac{2}{\pi k(P_0P_1)}} \left[1 - \frac{2(P_1P)}{D \cos \phi_1} + \frac{(P_1P)}{(P_0P_1)} \right]^{-\frac{1}{2}} \exp \{ik[(P_0P_1) + (P_1P)] - \frac{1}{4}i\pi\}, \quad (5.28)$$

where P_1 is the reflection point and ϕ_1 is the angle of incidence at P_1 (see Fig. 5.4).

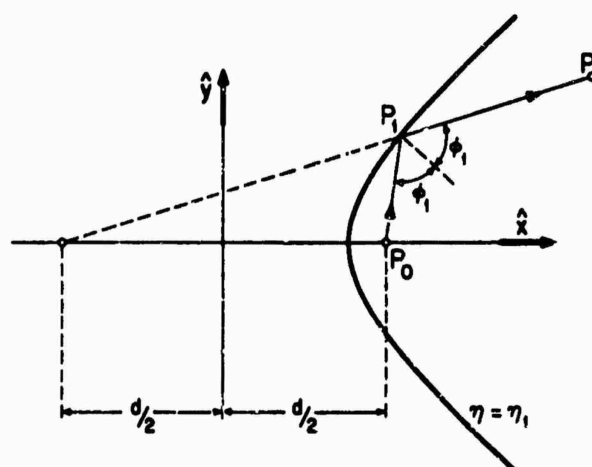


Fig. 5.4. Geometry for the reflected field with a line source at $P_0(\frac{1}{2}d, 0)$.

5.3.2. *H*-polarization

5.3.2.1. EXACT SOLUTIONS

In this section, the notation of BLOOM [1964] is used. We introduce the angular variable

$$\psi = \begin{cases} v, & \text{for } 0 \leq v \leq \pi, \\ v - 2\pi, & \text{for } \pi < v \leq 2\pi, \end{cases}$$

and the scatterer's surface $\psi = \pm\psi_1$, with $\frac{1}{2}\pi < \psi_1 < \pi$, as shown in Fig. 5.5.

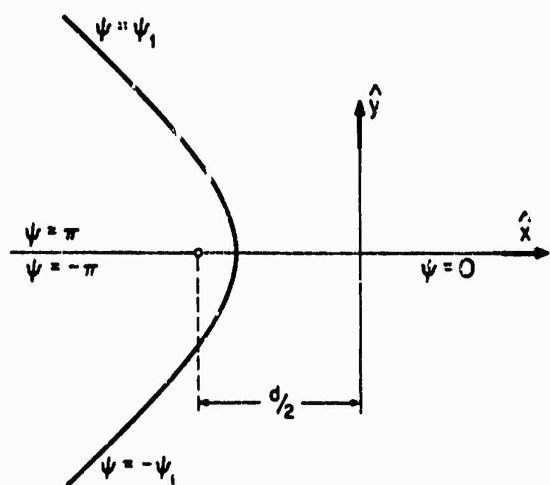


Fig. 5.5. Geometry for exact solution with a magnetic line source.

For a magnetic line source parallel to the z -axis and located at (u_0, ψ_0) on the convex side of the cylinder, such that

$$H^i = \hat{z}H_0^{(1)}(kR), \quad (5.29)$$

the total magnetic field in the region ($u \geq 0$, $-\psi_1 \leq \psi \leq \psi_1$) is (BLOOM [1964]):

$$\begin{aligned}
 H_z = & -4i \sum_{m=1}^{\infty} \tau_1(m) P^{(1)}(iu_<; \tau_1(m)) \frac{H^{(1)}(u_>; \tau_1(m))}{[(\partial/\partial u)H^{(1)}(u; \tau_1(m))]_{u=0}} \\
 & \times \left[\frac{(\partial/\partial \psi)P^{(2)}(\psi; \tau)}{(\partial^2/\partial \psi \partial \tau)P^{(1)}(\psi; \tau)} \right]_{\substack{\psi=\psi_1 \\ \tau=\tau_1(m)}} P^{(1)}(\psi_0; \tau_1(m)) P^{(1)}(\psi; \tau_1(m)) - \\
 & -4 \sum_{m=1}^{\infty} \tau_2(m) P^{(2)}(iu_<; \tau_2(m)) \frac{H^{(1)}(u_>; \tau_2(m))}{H^{(1)}(0; \tau_2(m))} \\
 & \times \left[\frac{(\partial/\partial \psi)P^{(1)}(\psi; \tau)}{(\partial^2/\partial \psi \partial \tau)P^{(2)}(\psi; \tau)} \right]_{\substack{\psi=\psi_1 \\ \tau=\tau_2(m)}} P^{(2)}(\psi_0; \tau_2(m)) P^{(2)}(\psi; \tau_2(m)). \quad (5.30)
 \end{aligned}$$

The equality in eq. (5.30) is valid in the sense of $L^2(-\psi_1, \psi_1)$. The angular functions $P^{(1)}(\psi; \tau)$ and $P^{(2)}(\psi; \tau)$ are, respectively, the even and odd principal solutions of

$$\frac{\partial^2 P}{\partial \psi^2} + (\tau^2 - c^2 \cos^2 \psi) P = 0$$

normalized as follows:

$$P^{(1)}(0; \tau) = 1, \quad \left[\frac{\partial P^{(2)}(\psi; \tau)}{\partial \psi} \right]_{\psi=0} = 1.$$

The eigenvalues $\tau_1(m)$ and $\tau_2(m)$ are the roots of the transcendental equations

$$\left[\frac{\partial}{\partial \psi} P^{(1)}(\psi; \tau_1(m)) \right]_{\psi=\psi_1} = 0, \quad \left[\frac{\partial}{\partial \psi} P^{(2)}(\psi; \tau_2(m)) \right]_{\psi=\psi_1} = 0, \quad (m = 1, 2, \dots). \quad (5.31)$$

The functions $H^{(1)}(u, \tau)$ are those solutions of the associated Mathieu equation

$$\frac{\partial^2 H}{\partial u^2} + (c^2 \cosh^2 u - \tau^2) H = 0$$

which are analogous to Hankel functions of the first kind.

The total magnetic field of eq. (5.30) has the following integral representations (BLOOM [1964]):

$$\begin{aligned}
 H_z = & -\frac{2}{\pi} \int_c \tau P(\pm iu_<; \tau) \\
 & \times \frac{H^{(1)}(u_>; \tau) P(\pm \psi_<; \tau) P(\psi_>; \tau)}{[(\partial/\partial u)H^{(1)}(u; \tau)]_{u=0} [(\partial/\partial \psi)P^{(1)}(\psi; \tau)(\partial/\partial \psi)P^{(2)}(\psi; \tau)]_{\psi=\psi_1}} d\tau, \quad (5.32)
 \end{aligned}$$

where either both upper signs or both lower signs must be chosen,

$$\psi_< = \max_{\min} (\psi, \psi_0). \quad (5.33)$$

$$P(\psi; \tau) = P^{(1)}(\psi; \tau) \left[\frac{\partial}{\partial \psi} P^{(2)}(\psi; \tau) \right]_{\psi=\psi_1} - P^{(2)}(\psi; \tau) \left[\frac{\partial}{\partial \psi} P^{(1)}(\psi; \tau) \right]_{\psi=\psi_1}, \quad (5.34)$$

and the path C of integration is either a straight line running parallel to the real τ -axis and just above it from minus infinity to plus infinity, or a contour that encircles the positive real τ -axis in the clockwise sense.

If source and observation points are both on the surface ($\psi_0 = \pm\psi_1$; $\psi = \psi_1$), the total magnetic field is

$$H_z = -\frac{2}{\pi} \int_C \frac{H^{(1)}(u_>; \tau)}{[(\partial/\partial u)H^{(1)}(u; \tau)]_{u=i\psi_1}} \frac{\tau P(\pm iu_<; \tau)}{[(\partial/\partial \psi)P^{(1)}(\psi; \tau)(\partial/\partial \psi)P^{(2)}(\psi; \tau)]_{\psi=\psi_1}} d\tau, \quad (5.35)$$

which has the residue series representation (BLOOM [1964]):

$$H_z = 4 \sum_{m=1}^{\infty} \tau(m) \frac{H^{(1)}(\mp u_<; \tau(m))}{[(\partial/\partial u)H^{(1)}(u; \tau(m))]_{u=0}} \frac{H^{(1)}(u_>; \tau(m))}{H^{(1)}(0; \tau(m))} \frac{H^{(1)}(i\psi_1; \tau(m))}{[(\partial^2/\partial u \partial \tau)H^{(1)}(u; \tau)]_{u=i\psi_1, \tau=\tau(m)}}, \quad (5.36)$$

where $\tau(m)$ are those roots of

$$\left[\frac{\partial}{\partial u} H^{(1)}(u; \tau) \right]_{u=i\psi_1} = 0 \quad (5.37)$$

that lie in the upper half of the τ plane. The series (5.36) was derived under the assumption that the roots $\tau(m)$ are all simple; it is uniformly convergent with respect to u_0 and u in every closed region $0 \leq (u_0, u) \leq M < \infty$, $|u - u_0| \geq \delta > 0$.

If source and observation points are not both on the surface $\pm\psi_1$, the residue series representations for H_z do not, in general, converge to H_z ; however, they are asymptotic expansions of H_z as $c \rightarrow \infty$ in the geometrical shadow (for details, see BLOOM [1964]).

5.3.2.2. HIGH FREQUENCY APPROXIMATIONS

For a magnetic line source parallel to the z -axis, located at (ξ_0, η_0) on the convex side of the cylinder, such that

$$H^i = 2H_0^{(1)}(kR), \quad (5.38)$$

and so far from the surface $\eta = \eta_1$ that at the surface

$$H^s \sim 2 \sqrt{\frac{2}{\pi k R}} e^{ikR - \frac{1}{2}i\pi}, \quad (5.39)$$

the geometric optics scattered field at a point P located in the illuminated region is

$$(H_z)_{\text{sc}} \sim \sqrt{\frac{2}{\pi k (\rho_0 P_1)}} \left[1 + \frac{2(P_1 P)}{D \cos \phi_1} + \frac{(P_1 P)}{(P_0 P_1)} \right]^{-\frac{1}{2}} \exp \{ ik[(P_0 P_1) + (P_1 P)] - \frac{1}{2}i\pi \}. \quad (5.40)$$

where $(P_0 P_1)$ and $(P_1 P)$ are, respectively, the distances between the source P_0 and the reflection point P_1 , and between P_1 and the observation point P ; D is given by eq. (5.5), the coordinate ξ_1 by eqs. (5.18), and the reflection angle ϕ_1 by eq. (5.19). Formula (5.40) is applicable if $kD \gg 1$. In the shadowed region, $(H_z)_{s.c.} = 0$. If the line source is in the angular sector

$$x_0 \leq 0, \quad |y_0| \leq |x_0| \tan \nu_1,$$

there is no shadowed region.

For a line source of strength (5.38) located at the focal line ($x_0 = -\frac{1}{2}d, y_0 = 0$), the scattered magnetic field is given by the Luneburg-Kline expansion (KELLER et al. [1956]):

$$H_z^s \sim \frac{\exp \{i[k(QP) + 2c\eta_1 - \frac{1}{4}\pi]\}}{\sqrt{\{k(QP)w\}}} \sum_{n=0}^{\infty} (2ic\eta_1)^{-n} \sum_{j=0}^n \left[\frac{2c\eta_1}{k(QP)w} \right]^j \sum_{t=0}^{2n-j} a_{jtn} w^{-t}, \quad (5.41)$$

where (QP) is the distance between the focal line ($\frac{1}{2}d, 0$) and the observation point P (see Fig. 5.3), w is given by eq. (5.21), θ is the angle that the reflected ray forms with the positive x -axis, a_{jtn} is given by eq. (5.22) for $j \geq 1$, whereas

$$\begin{aligned} a_{0tn} = & (-1)^t \binom{n}{t} \left\{ \frac{[(2n)!]^2}{(n!)^3} + 32(n - \frac{1}{2}) \frac{[2(n-1)!]^2}{[(n-1)!]^3} \right\} 2^{-5n} \sqrt{\frac{2}{\pi}} - \\ & - \sum_{j=1}^n \sum_{s=0}^{2n-j} a_{jsn} \binom{j}{t-s} (-1)^{t-s} + \sum_{j=0}^{n-1} \sum_{s=0}^{2n-j-2} a_{j,s,n-1} (-1)^{t-s} \\ & \times \left\{ (2j+2s+1) \left[\frac{1+\eta_1^2}{1-\eta_1^2} \binom{j}{t-s} + \binom{j}{t-s-1} \right] - (j+\frac{1}{2}) \binom{j+1}{t-s+1} \right\}, \\ & (0 \leq t \leq 2n; n \geq 1), \end{aligned} \quad (5.42)$$

$$a_{000} = +\sqrt{2/\pi}. \quad (5.43)$$

The first few terms of the expansion (5.41) are:

$$\begin{aligned} H_z^s \sim & \sqrt{\frac{2}{\pi k(QP)w}} \exp \{i[k(QP) + 2c\eta_1 - \frac{1}{4}\pi]\} \\ & \times \left[1 - \frac{i}{16c\eta_1} \left(\frac{5-3\eta_1^2}{1-\eta_1^2} + \frac{10\eta_1^2-2}{w(1-\eta_1^2)} - \frac{3}{w^2} \right) - \frac{i}{8k(QP)w} \left(4 \frac{1+\eta_1^2}{1-\eta_1^2} - \frac{3}{w} \right) + \dots \right]. \end{aligned} \quad (5.44)$$

In the physical optics approximation, the total magnetic field at a point P_1 on the surface $\eta = \eta_1$ is

$$(H_z)_{p.o.} = \begin{cases} 2H_0^{(1)}(k(P_0 P_1)), & \text{in the illuminated region,} \\ 0, & \text{in the shadow.} \end{cases} \quad (5.45)$$

A more refined approximation, in which an asymptotic expression for the diffracted field in the shadowed region is retained, is easily obtained from the results of KELLER

[1956]. For the line source (5.39), the total magnetic field at a point P located in the shadowed region away from the surface $\eta = \eta_1$ is:

$$H_z \sim \frac{1}{\pi k \sqrt{\{(P_0 P_1)(P_2 P)\}}} \left[\frac{c}{2\eta_1 \sqrt{(1-\eta_1^2)}} \right]^{\frac{1}{2}} [(\xi_1^2 - \eta_1^2)(\xi_2^2 - \eta_1^2)]^{\frac{1}{4}} \\ \times \exp \left\{ -\frac{1}{8}i\pi + ik[(P_0 P_1) + (P_2 P)] + ic \int_{(P_1 P_2)} \frac{d\xi}{\sqrt{\frac{\xi^2 - \eta_1^2}{\xi^2 - 1}}} \right\} \\ \times \sum_{n=1}^{\infty} \frac{\exp \left\{ \beta_n (\frac{1}{2}c)^{\frac{1}{2}} (\eta_1 \sqrt{(1-\eta_1^2)})^{\frac{1}{2}} \exp \left\{ \frac{5}{6}i\pi \right\} \int_{(P_1 P_2)} \frac{d\xi}{\sqrt{\{(\xi^2 - 1)(\xi^2 - \eta_1^2)\}}} \right\}}{\beta_n [\text{Ai}(-\beta_n)]^2}, \quad (5.46)$$

where the various quantities have the same meaning as in eq. (5.14). A correction to the leading term (5.46) that depends upon the derivative of the curvature has been found by KELLER and LEVY [1959] (see also FRANZ and KLANTÉ [1959]).

Finally, a line source of strength (5.39) located at $P_0(x_0 = \frac{1}{2}d, y_0 = 0)$ on the concave side of the cylinder originates a geometric optics scattered field:

$$(H_z^s)_{g.o.} \sim \sqrt{\frac{2}{\pi k(P_0 P_1)}} \left[i - \frac{2(P_1 P)}{D \cos \phi_1} + \frac{(P_1 P)}{(P_0 P_1)} \right]^{-\frac{1}{2}} \exp \{ ik[(P_0 P_1) + (P_1 P)] - \frac{1}{4}i\pi \}, \quad (5.47)$$

where P_1 is the reflection point and ϕ_1 is the angle of incidence at P_1 (see Fig. 5.4).

5.4. Point and dipole sources

Although geometrical and physical optics approximations are easily obtainable, no explicit results are available.

Bibliography

- BLOOM, C. O. [1964], Diffraction by a Hyperbola, Doctoral Dissertation, New York University, New York. (Also available through University Microfilms, Inc., Ann Arbor, Michigan.) Equations (1.11) are incorrect.
- FRANZ, W. and K. KLANTÉ [1959], Diffraction by Surfaces of Variable Curvature, IRE Trans. AP-7, S68-S70.
- KELLER, J. B. [1956], Diffraction by a Convex Cylinder, IRE Trans. AP-4, 312-321. Formula (25) has a misprint in the second line.
- KELLER, J. B., R. M. LEWIS and B. D. SECKLER [1956], Asymptotic Solution of some Diffraction Problems, Comm. Pure Appl. Math. 9, 207-265.
- KELLER, J. B. and B. R. LEVY [1959], Decay Exponents and Diffraction Coefficients for Surface Waves on Surfaces of Nonconstant Curvature, IRE Trans. AP-7, S52-S61.

CHAPTER 6

THE WEDGE

J. J. BOWMAN and T. B. A. SENIOR

The boundary value problem for the wedge of arbitrary angle can be analysed in a variety of coordinate systems including hyperbolic (elliptic) cylinder coordinates, but the consideration of the wedge as the limit of a hyperbolic cylinder as the inter-focal distance shrinks to zero proves to be of little use. The solution, originally obtained as a generalization of that for the half-plane (see Chapter 8), has many applications to problems involving edge phenomena and other diffraction effects.

6.1. Wedge geometry and preliminary considerations

The wedge is defined in terms of the rectangular Cartesian coordinates (x, y, z) by the equation $|y| = x \tan \Omega$, $x > 0$, where 2Ω is the closed angle of the wedge. The edge is therefore coincident with the z -axis. The wedge is also defined in terms of both the circular cylindrical coordinates (ρ, ϕ, z) and the spherical coordinates (r, θ, ϕ) by the equations $\phi = \Omega$ (upper surface) and $\phi = 2\pi - \Omega$ (lower surface). It is convenient to introduce a parameter ν related to the open angle of the wedge and defined by:

$$\nu\pi = 2\pi - 2\Omega. \quad (6.1)$$

The primary source is a plane wave propagating in the plane perpendicular to the z -axis and in a direction making an angle $\pi + \phi_0$ with the positive x -axis (and therefore making an angle $\pi + \phi_0 - \Omega$ with the upper face of the wedge), or a line source parallel to the z -axis and located at (ρ_0, ϕ_0) , or a point or dipole source located at (ρ_0, ϕ_0, z_0) . These configurations are illustrated in Fig. 6.1. In each case both E - and H -polarized excitations are considered, and, in addition, the dipole source may be of arbitrary orientation. For convenience, and without loss of generality, it is assumed that $\Omega \leq \phi_0 \leq \pi$.

The distance from the point of observation to the source is denoted by R , so that, for a line source,

$$R = \sqrt{\rho^2 + \rho_0^2 - 2\rho\rho_0 \cos(\phi - \phi_0)} = \sqrt{(x - x_0)^2 + (y - y_0)^2}, \quad (6.2)$$

whereas for a point or dipole source,

$$\begin{aligned} R &= \sqrt{\rho^2 + \rho_0^2 - 2\rho\rho_0 \cos(\phi - \phi_0) + (z - z_0)^2} \\ &= \sqrt{(x - x_0)^2 + (y - y_0)^2 + (z - z_0)^2}. \end{aligned} \quad (6.3)$$

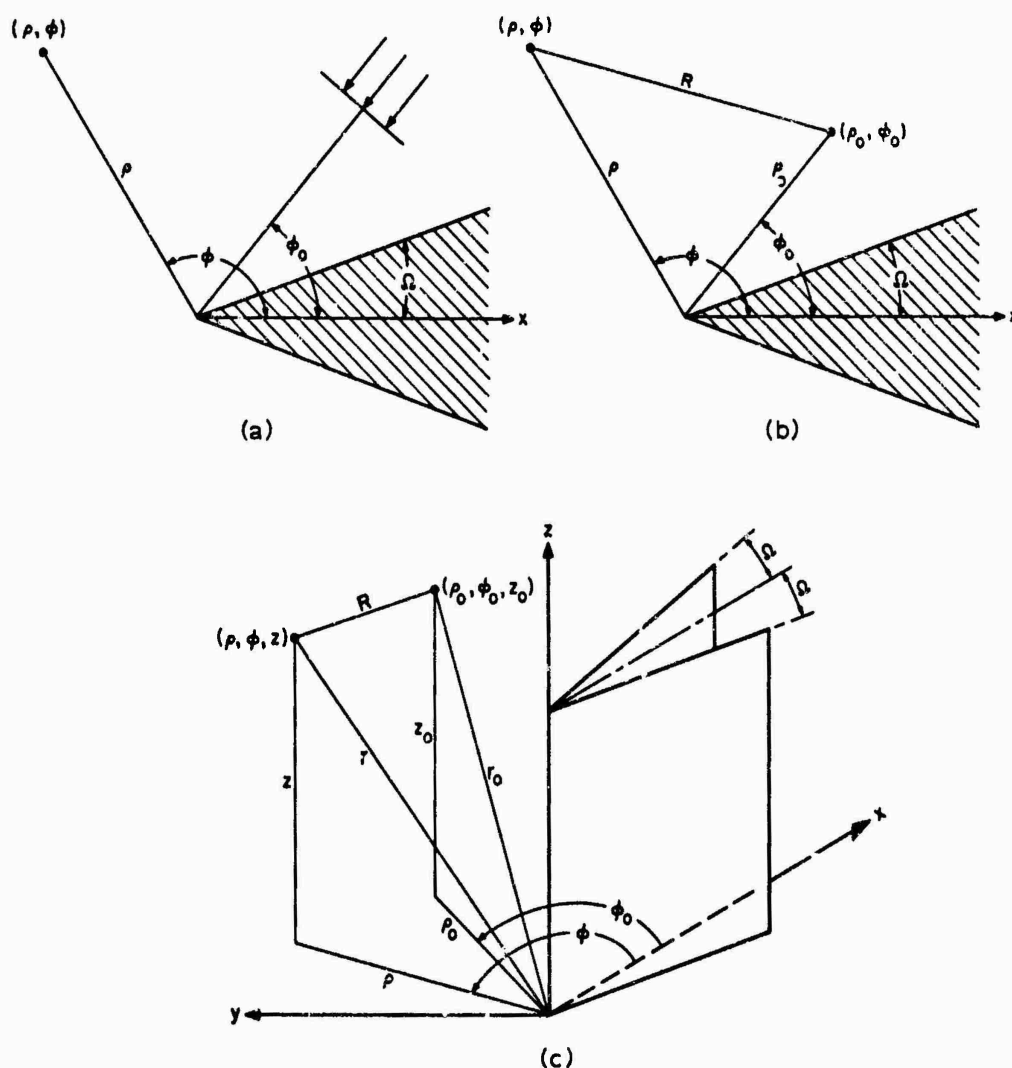


Fig. 6.1. Geometry for (a) plane wave illumination, (b) line sources and (c) point sources.

We also introduce the parameter R_1 associated with the edge diffraction where, for a line source,

$$R_1 = \rho + \rho_0, \quad (6.4)$$

and for a point or dipole source,

$$R_1 = \sqrt{(\rho + \rho_0)^2 + (z - z_0)^2}. \quad (6.5)$$

Two step functions of frequent occurrence in the sequel are the Heaviside step function $\eta(\psi)$, where

$$\eta(\psi) = \begin{cases} 1 & \text{for } \psi > 0 \\ 0 & \text{for } \psi < 0 \end{cases},$$

and the signum function $\text{sgn}(\psi) = \pm 1$ for $\psi \gtrless 0$.

For any type of source the complete field can be expressed as a contour integral of

the form

$$\int_{C_1+C_2} G(\alpha)s(\alpha+\phi)d\alpha$$

(see, for example, TUZHILIN [1963]), where C_1 and C_2 are known as the Sommerfeld contours in recognition of the original contribution of SOMMERFELD [1896]. In the integrand $s(\alpha+\phi)$ is proportional to the sum (or difference) of two cotangents, and the kernel $G(\alpha)$ is determined by the source. The contours C_1 and C_2 are shown in Fig. 6.2, where the shading indicates those regions where $G(\alpha)$ vanishes exponentially

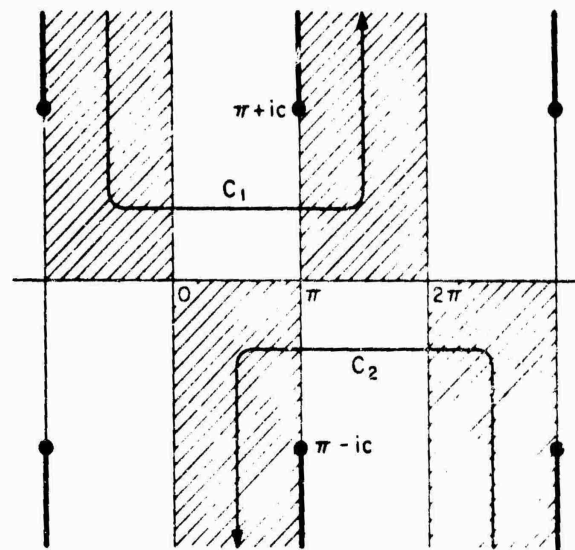


Fig. 6.2. Sommerfeld contours.

as $|\operatorname{Im}\alpha| \rightarrow \infty$ on the upper Riemann sheet. When the source is at a finite distance, the kernel has branch points at $\alpha = (2n+1)\pi \pm ic$, $n = 0, \pm 1, \pm 2, \dots$, where

$$c = 2 \cosh^{-1} \frac{R_1}{2\sqrt{\rho\rho_0}}.$$

Except in the case of plane wave incidence (when $c = \infty$), the α -plane then has branch cuts extending to infinity as shown in Fig. 6.2.

For wedge angles such that $\nu = 1/n$, where n is a positive integer, the above contour integral can be evaluated as a sum of $2n$ residues. The resultant field is a superposition of the field due to the primary source and its $2n-1$ images, and therefore consists entirely of geometrical optics contributions. An experimental verification of this fact has been provided by GRANNEMANN and WATSON [1955].

6.2. Plane wave incidence

6.2.1. *E*-polarization

For incidence at an angle ϕ_0 with respect to the negative x -axis, such that

$$E^i = \hat{z} \exp \{-ik\rho \cos(\phi - \phi_0)\}, \quad (6.6)$$

a contour integral representation of the total electric field is (MACDONALD [1902]; WIEGREFE [1912]; CARSLAW [1920]):

$$E_z = \frac{1}{4i\pi v} \int_{C_1+C_2} e^{ik\rho \cos \alpha} \left\{ \cot \frac{\pi - \alpha - \phi + \phi_0}{2v} - \cot \frac{\pi - \alpha - \phi - \phi_0 + 2\Omega}{2v} \right\} d\alpha, \quad (6.7)$$

where C_1 and C_2 are the Sommerfeld contours shown in Fig. 6.2. An alternative representation of the total field as an eigenfunction expansion is:

$$E_z = 2 \sum_{n=0}^{\infty} \varepsilon_n \sin \frac{n(\phi - \Omega)}{v} \sin \frac{n(\phi_0 - \Omega)}{v} S_{n/v}, \quad (6.8)$$

where (MACDONALD [1902]):

$$S_r = e^{-\frac{1}{2}i\pi r} J_r(k\rho). \quad (6.9)$$

For $\Omega = 22\frac{1}{2}^\circ$ with $\phi_0 = 67\frac{1}{2}^\circ$ and $112\frac{1}{2}^\circ$, and $\Omega = 45^\circ$ with $\phi_0 = 90^\circ$ and 135° , HEDGEcock and MCLAY [1959] have given schematic presentations of $|E_z|^2$ as measured using probes moving along 8 trajectories 7.5λ in length spaced λ apart in the direction of propagation. The region of space probed is approximately rectangular in shape with the upper right hand corner of the rectangle at the vertex of the wedge. Additional data has been obtained by WATSON and HORTON [1950] for the case $\Omega = 11\frac{1}{4}^\circ$ and $\phi_0 = 78\frac{1}{4}^\circ$ with $\rho = 11.9\lambda$ (approx.), and the measured pattern is reproduced in Fig. 6.3.

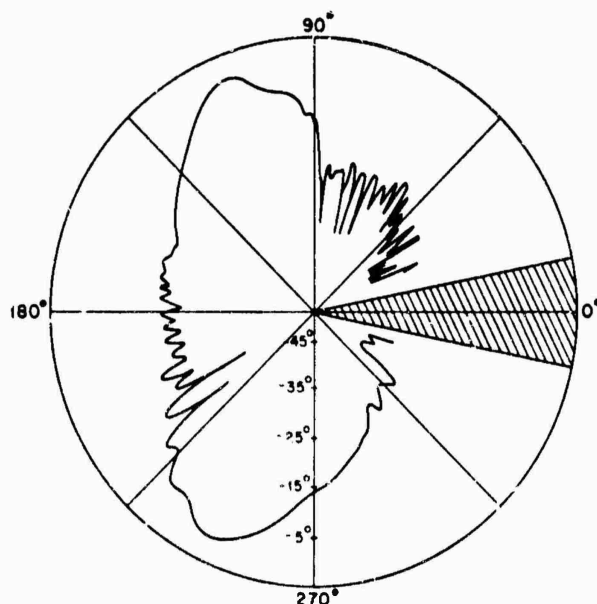


Fig. 6.3. Measured amplitude of the total electric field E_z for $\Omega = 11\frac{1}{4}^\circ$ and $\phi_0 = 78\frac{1}{4}^\circ$ with $\rho = 11.9\lambda$ (WATSON and HORTON [1950]).

Expressions for the surface field H_p are trivially obtainable from the above, and simplified forms of the contour integral representation are possible for certain values

of v . In particular, for a right-angled wedge ($v = \frac{1}{2}$), the field on the upper surface, $\phi = \frac{1}{2}\pi$, is (LEBEDEV and SKAL'SKAYA [1960]):

$$\begin{aligned}
 H_\rho = & -2 \sin(\phi_0 - \frac{1}{2}\pi) \exp\{-ik\rho \cos(\phi_0 - \frac{1}{2}\pi)\} - \\
 & - \frac{2}{\sqrt{3}} e^{-\frac{1}{2}i\pi} \left\{ \sin \frac{1}{2}(\phi_0 - \frac{1}{2}\pi) \left[\cos(\phi_0 - \frac{1}{2}\pi) H_{\frac{1}{2}}^{(1)}(k\rho) + \right. \right. \\
 & + \sin^2(\phi_0 - \frac{1}{2}\pi) \int_{k\rho}^{\infty} \sin\{(\xi - k\rho) \cos(\phi_0 - \frac{1}{2}\pi)\} H_{\frac{1}{2}}^{(1)}(\xi) d\xi \Big] - \\
 & \left. - \frac{1}{2} \cos \frac{1}{2}(\phi_0 - \frac{1}{2}\pi) \sin(\phi_0 - \frac{1}{2}\pi) \int_{k\rho}^{\infty} \cos\{(\xi - k\rho) \cos(\phi_0 - \frac{1}{2}\pi)\} H_{\frac{1}{2}}^{(1)}(\xi) \frac{d\xi}{\xi} \right\}, \quad (6.10)
 \end{aligned}$$

and on the lower surface, $\phi = \frac{3}{2}\pi$,

$$\begin{aligned}
 H_\rho = & -2 \sin(\phi_0 - \frac{3}{2}\pi) \cos(\phi_0 - \frac{1}{2}\pi) \exp\{ik\rho \sin(\phi_0 - \frac{1}{2}\pi)\} - \frac{2}{\sqrt{3}} e^{-\frac{1}{2}i\pi} \left\{ \cos \frac{1}{2}(\phi_0 - \frac{1}{2}\pi) \right. \\
 & \times \left[\sin(\phi_0 - \frac{1}{2}\pi) H_{\frac{1}{2}}^{(1)}(k\rho) + \cos^2(\phi_0 - \frac{1}{2}\pi) \int_{k\rho}^{\infty} \sin\{(\xi - k\rho) \sin(\phi_0 - \frac{1}{2}\pi)\} H_{\frac{1}{2}}^{(1)}(\xi) d\xi \right] - \\
 & \left. - \frac{1}{2} \sin \frac{1}{2}(\phi_0 - \frac{1}{2}\pi) \cos(\phi_0 - \frac{1}{2}\pi) \int_{k\rho}^{\infty} \cos\{(\xi - k\rho) \sin(\phi_0 - \frac{1}{2}\pi)\} H_{\frac{1}{2}}^{(1)}(\xi) \frac{d\xi}{\xi} \right\}. \quad (6.11)
 \end{aligned}$$

For grazing incidence on the lower face (that is, for $\phi_0 = \frac{3}{2}\pi$), eqs. (6.10) and (6.11) reduce to

$$H_\rho = -2 + \frac{1}{2} e^{-\frac{1}{2}i\pi} \int_{k\rho}^{\infty} H_{\frac{1}{2}}^{(1)}(\xi) \frac{d\xi}{\xi} \quad (6.12)$$

and

$$H_\rho = -e^{-\frac{1}{2}i\pi} H_{\frac{1}{2}}^{(1)}(k\rho), \quad (6.13)$$

respectively.

If $k\rho \ll 1$, a small argument expansion of the Bessel functions in eq. (6.8) gives:

$$E_z = \frac{4}{\Gamma(1/v)} (\frac{1}{2}k\rho)^{1/v} e^{-\frac{1}{2}i\pi/v} \sin \frac{\phi - \Omega}{v} \sin \frac{\phi_0 - \Omega}{v} + O[(k\rho)^{\min(2/v, 2+1/v)}], \quad (6.14)$$

which makes explicit the edge behavior.

For $k\rho \gg 1$ a convenient decomposition of the field is

$$E_z = E_z^{g.o.} + E_z^d, \quad (6.15)$$

where $E_z^{g.o.}$ and E_z^d are the geometrical optics and diffracted fields respectively. The geometrical optics field is

$$E_z^{g.o.} = \sum_{n_1} \exp(ik\rho \cos \alpha_{n_1}) - \sum_{n_2} \exp(ik\rho \cos \alpha_{n_2}), \quad (6.16)$$

where

$$\begin{aligned}\alpha_{n_1} &= \pi - \phi + \phi_0 - 2n_1 v\pi, \\ \alpha_{n_2} &= \pi - \phi - \phi_0 + 2\Omega - 2n_2 v\pi,\end{aligned}\quad (6.17)$$

and the summations extend over all integers n_1 and n_2 satisfying the inequalities

$$\begin{aligned}|\phi - \phi_0 + 2n_1 v\pi| &< \pi, \\ |\phi + \phi_0 - 2\Omega + 2n_2 v\pi| &< \pi,\end{aligned}\quad (6.18)$$

respectively. The diffracted field E_z^d can be written as (OBERHETTINGER [1956, 1958]):

$$E_z^d = \{V_d(-\pi - \phi + \phi_0) - V_d(\pi - \phi + \phi_0)\} - \{V_d(-\pi - \phi - \phi_0 + 2\Omega) - V_d(\pi - \phi - \phi_0 + 2\Omega)\}, \quad (6.19)$$

with

$$V_d(\beta) = \frac{1}{2\pi v} \int_0^\infty \exp(ik\rho \cosh t) \frac{\sin(\beta/v)}{\cosh(t/v) - \cos(\beta/v)} dt. \quad (6.20)$$

For β near $2nv\pi$ where n is an integer (TUZHILIN [1963]; but see also OBERHETTINGER [1956], for the case $n = 0$):

$$V_d(\beta) \sim \sum_{m=0}^{\infty} \{A_m(\beta, v) - a_m(\beta - 2nv\pi)\} f_m + \operatorname{sgn}(\beta - 2nv\pi) I, \quad (6.21)$$

where

$$f_m = \frac{i^m \Gamma(m + \frac{1}{2})}{\sqrt{2(k\rho)^{m+\frac{1}{2}}}} e^{i(k\rho + \frac{1}{2}\pi)}, \quad (6.22)$$

$$I = \frac{e^{-\frac{1}{2}i\pi}}{\sqrt{\pi}} \exp\{ik\rho \cos(\beta - 2nv\pi)\} F[\sqrt{2k\rho} |\sin \frac{1}{2}(\beta - 2nv\pi)|], \quad (6.23)$$

and $F(\tau)$ is the Fresnel integral

$$F(\tau) = \int_0^\tau e^{i\mu^2} d\mu \quad (6.24)$$

whose properties are described in the Introduction. The coefficients $a_m(\beta - 2nv\pi)$ are

$$a_m(\beta - 2nv\pi) = \frac{(-1)^m}{2^{m+1} \pi \{\sin \frac{1}{2}(\beta - 2nv\pi)\}^{2m+1}} \quad (6.25)$$

and the coefficients $A_m(\beta, v)$ are (TUZHILIN [1963]):

$$A_m(\beta, v) = \frac{1}{2\pi v} \cot \frac{\beta}{2v} \sum_{k=0}^m \left(\sin \frac{\beta}{2v}\right)^{-2k} \sum_{l=k}^m C_{k,l}^m v^{-2l}, \quad (6.26)$$

where the expression for the $C_{k,l}^m$ given by TUZHILIN [1963] can be further reduced to

$$\begin{aligned}C_{k,l}^m &= \frac{(-1)^k 2l}{(2l)! 2^{2k+m}} \sum_{p=0}^{2k} (-1)^p \binom{2k}{p} (2k-2p)^{2l} \sum_{s=0}^{m-l} \binom{-\frac{1}{2}}{m-l-s} \frac{(4s+2l)!}{(2s+2l)!} \\ &\times \sum_{q=0}^{2s} \frac{(-1)^q}{2s+2l+q} \frac{2^{-q}}{(2s-q)!(2s+q)!} \sum_{r=0}^q \frac{(-1)^r}{r!} \frac{(q-2r)^{2s+q}}{(q-r)!}.\end{aligned}\quad (6.27)$$

Explicitly, the first coefficients $A_m(\beta, \nu)$ are (OBERHETTINGER [1956]):

$$\begin{aligned} A_0(\beta, \nu) &= \frac{1}{2\pi\nu} \cot \frac{\beta}{2\nu}, \\ A_1(\beta, \nu) &= -\frac{1}{4\pi\nu} \cot \frac{\beta}{2\nu} \left\{ \frac{1}{2} + \frac{1}{\nu^2} \left(\sin \frac{\beta}{2\nu} \right)^{-2} \right\}, \\ A_2(\beta, \nu) &= \frac{1}{8\pi\nu} \cot \frac{\beta}{2\nu} \left\{ \frac{3}{8} + \left(\frac{5}{6\nu^2} - \frac{1}{3\nu^4} \right) \left(\sin \frac{\beta}{2\nu} \right)^{-2} + \frac{1}{\nu^4} \left(\sin \frac{\beta}{2\nu} \right)^{-4} \right\}, \\ A_3(\beta, \nu) &= -\frac{1}{16\pi\nu} \cot \frac{\beta}{2\nu} \left\{ \frac{5}{16} + \left(\frac{259}{360\nu^2} - \frac{7}{18\nu^4} + \frac{2}{45\nu^6} \right) \left(\sin \frac{\beta}{2\nu} \right)^{-2} + \right. \\ &\quad \left. + \left(\frac{7}{6\nu^2} - \frac{2}{3\nu^4} \right) \left(\sin \frac{\beta}{2\nu} \right)^{-4} + \frac{1}{\nu^6} \left(\sin \frac{\beta}{2\nu} \right)^{-6} \right\}. \end{aligned} \quad (6.28)$$

The representation given in eq. (6.21) describes the asymptotic behavior of $V_d(\beta)$ in the vicinity of the geometrical optics boundary $\beta = 2\nu\pi$, and displays the discontinuity in $V_d(\beta)$ necessary to compensate for the corresponding discontinuity in $E_z^{g.o.}$. Of the four values of β implicit in eq. (6.19), not more than two can correspond to a geometrical optics boundary. An alternative but less convenient description of the diffracted field in the vicinity of a boundary has been given by PAULI [1938] using confluent hypergeometric functions.

For values of β away from a geometrical optics boundary such that the argument of the Fresnel integral in eq. (6.23) is large compared with unity,

$$V_d(\beta) \sim \sum_{m=0}^{\infty} A_m(\beta, \nu) f_m, \quad (6.29)$$

and from the leading term in this expansion,

$$E_z^d \sim \frac{e^{i(k\rho + \frac{1}{2}\pi)}}{\sqrt{(2\pi k\rho)}} \frac{1}{\nu} \sin \frac{\pi}{\nu} \left\{ \left(\cos \frac{\pi}{\nu} - \cos \frac{\phi - \phi_0}{\nu} \right)^{-1} - \left(\cos \frac{\pi}{\nu} + \cos \frac{2\pi - \phi - \phi_0}{\nu} \right)^{-1} \right\}. \quad (6.30)$$

This has the appearance of a cylindrical wave with

$$P = \frac{i}{2\nu} \sin \frac{\pi}{\nu} \left\{ \left(\cos \frac{\pi}{\nu} - \cos \frac{\phi - \phi_0}{\nu} \right)^{-1} - \left(\cos \frac{\pi}{\nu} + \cos \frac{2\pi - \phi - \phi_0}{\nu} \right)^{-1} \right\} \quad (6.31)$$

emanating from the edge. Computed values of $|P|$ for $\nu = \frac{1}{2}$ and three different ϕ_0 are shown in Fig. 6.4.

On the geometrical optics boundaries the total electric field has the following asymptotic representations where, for simplicity, it has been assumed that $\Omega < \frac{1}{2}\pi$.

(i) $\phi = \pi - \phi_0 + 2\Omega$ with $\Omega < \phi_0 < \pi$ (boundary for geometrical reflection from the upper face):

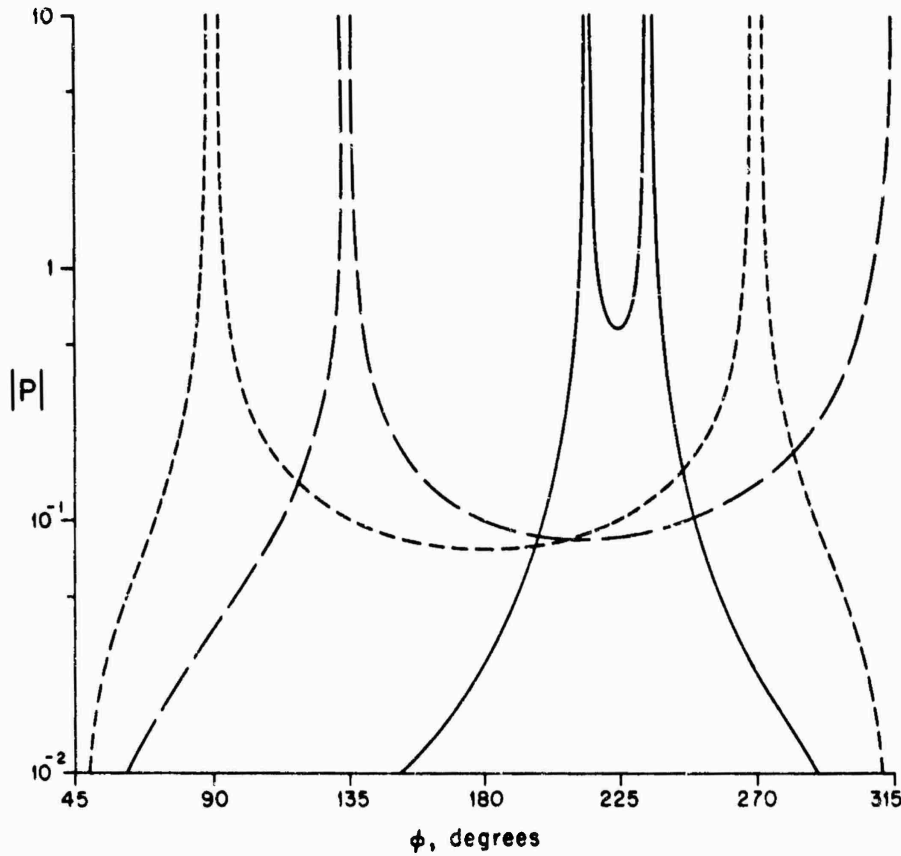


Fig. 6.4. Far field amplitude of the diffracted wave for $\phi_0 = 55^\circ$ (—), $\phi_0 = 135^\circ$ (---) and $\phi_0 = 180^\circ$ (- - -).

$$E_z \sim \exp \{ik\rho \cos 2(\phi_0 - \Omega)\} - \frac{1}{2}e^{ik\rho} + \frac{1}{v} \frac{e^{i(k\rho + \frac{1}{2}\pi)}}{\sqrt{(2\pi k\rho)}} \left\{ \frac{\sin(\pi/v)}{\cos(\pi/v) + \cos[(3\pi - 2\phi_0)/v]} + \frac{1}{2} \cot \frac{\pi}{v} \right\}. \quad (6.32)$$

(ii) $\phi = 3\pi - \phi_0 - 2\Omega$ with $\pi - \Omega < \phi_0 < \pi$ (boundary for geometrical reflection from the lower face):

$$E_z \sim \exp \{ik\rho \cos 2(\phi_0 + \Omega)\} - \frac{1}{2}e^{ik\rho} + \frac{1}{v} \frac{e^{i(k\rho + \frac{1}{2}\pi)}}{\sqrt{(2\pi k\rho)}} \left\{ \frac{\sin(\pi/v)}{\cos(\pi/v) + \cos[(\pi - 2\phi_0)/v]} + \frac{1}{2} \cot \frac{\pi}{v} \right\}. \quad (6.33)$$

Eqs. (6.32) and (6.33) are also valid when $\phi_0 = \pi$ provided $\Omega > 0$.

(iii) $\phi = \pi + \phi_0$ with $\Omega < \phi_0 < \pi - \Omega$ (boundary of the geometrical shadow):

$$E_z \sim \frac{1}{2}e^{ik\rho} - \frac{1}{v} \frac{e^{i(k\rho + \frac{1}{2}\pi)}}{\sqrt{(2\pi k\rho)}} \left\{ \frac{\sin(\pi/v)}{\cos(\pi/v) + \cos[(\pi - 2\phi_0)/v]} + \frac{1}{2} \cot \frac{\pi}{v} \right\}. \quad (6.34)$$

For the particular case of a right-angled wedge ($v = \frac{3}{2}$) an expression for E_z^d alternative to that given in eqs. (6.19) and (6.20) has been provided by REICHE

[1912], and can be written as

$$E_z^d = v_d(\phi - \phi_0) - v_d(\phi + \phi_0 - \frac{1}{2}\pi), \quad (6.35)$$

where

$$v_d(\beta) = -\frac{e^{i\pi}}{\sqrt{3}} \left[\sin \beta \sin \frac{1}{3}\beta \int_{k\rho}^{\infty} \cos \{(\xi - k\rho) \cos \beta\} H_{\frac{1}{3}}^{(1)}(\xi) d\xi + \cos \frac{1}{3}\beta \int_{k\rho}^{\infty} \sin \{(\xi - k\rho) \cos \beta\} H_{\frac{1}{3}}^{(1)}(\xi) \frac{d\xi}{\xi} \right]. \quad (6.36)$$

The function $v_d(\beta)$ is discontinuous at the geometrical optics boundaries in order to compensate for the discontinuities in $E_z^{(0)}$, and its behavior on the boundaries $\beta = \pi, 2\pi$ is determined by the relations

$$\begin{aligned} v_d(\pi + \varepsilon) &= \frac{1}{2} \operatorname{sgn}(\xi) e^{ik\rho} + O(\varepsilon), \\ v_d(2\pi + \varepsilon) &= -\frac{1}{2} \operatorname{sgn}(\xi) e^{ik\rho} + O(\varepsilon). \end{aligned} \quad (6.37)$$

6.2.2. *H-polarization*

For incidence at an angle ϕ_0 with respect to the negative x -axis, such that

$$H^i = 2 \exp \{-ik\rho \cos(\phi - \phi_0)\} \quad (6.38)$$

a contour integral representation of the total magnetic field is (MACDONALD [1902]; WIEGREFE [1921]; CARSLAW [1920]):

$$H_z = \frac{1}{4i\pi\nu} \int_{C_1 + C_2} e^{ik\rho \cos \alpha} \left\{ \cot \frac{\pi - \alpha - \phi + \phi_0}{2\nu} + \cot \frac{\pi - \alpha - \phi - \phi_0 + 2\Omega}{2\nu} \right\} d\alpha, \quad (6.39)$$

where C_1 and C_2 are the Sommerfeld contours shown in Fig. 6.2. An alternative representation of the total field as an eigenfunction expansion is

$$H_z = \sum_{n=0}^{\infty} \varepsilon_n \cos \frac{n(\phi - \Omega)}{\nu} \cos \frac{n(\phi_0 - \Omega)}{\nu} S_{n/\nu}, \quad (6.40)$$

where (MACDONALD [1902]):

$$S_{\tau} = e^{-\frac{1}{2}i\pi\tau} J_{\tau}(k\rho). \quad (6.41)$$

WATSON and HORTON [1950] have measured $|H_z|^2$ for $\Omega = 11\frac{1}{2}^\circ$ and $\phi_0 = 78\frac{1}{2}^\circ$ with $\rho = 11.9\lambda$ (approx.), and their data is reproduced in Fig. 6.5.

Expressions for the total magnetic field on the surface are trivially obtainable from the above, and simplified forms of the contour integral representation are possible for certain values of ν . In particular, for a right-angled wedge ($\nu = \frac{1}{2}$), the field on the upper surface, $\phi = \frac{1}{2}\pi$, is

$$\begin{aligned} H_z = 2 \exp \{-ik\rho \cos(\phi_0 - \frac{1}{2}\pi)\} - \frac{2}{\sqrt{3}} e^{i\pi} \left[\sin(\phi_0 - \frac{1}{2}\pi) \sin \frac{1}{3}(\phi_0 - \frac{1}{2}\pi) \right. \\ \times \int_{k\rho}^{\infty} \cos \{(\xi - k\rho) \cos(\phi_0 - \frac{1}{2}\pi)\} H_{\frac{1}{3}}^{(1)}(\xi) d\xi + \\ \left. + \cos \frac{1}{3}(\phi_0 - \frac{1}{2}\pi) \int_{k\rho}^{\infty} \sin \{(\xi - k\rho) \cos(\phi_0 - \frac{1}{2}\pi)\} H_{\frac{1}{3}}^{(1)}(\xi) \frac{d\xi}{\xi} \right] \end{aligned} \quad (6.42)$$

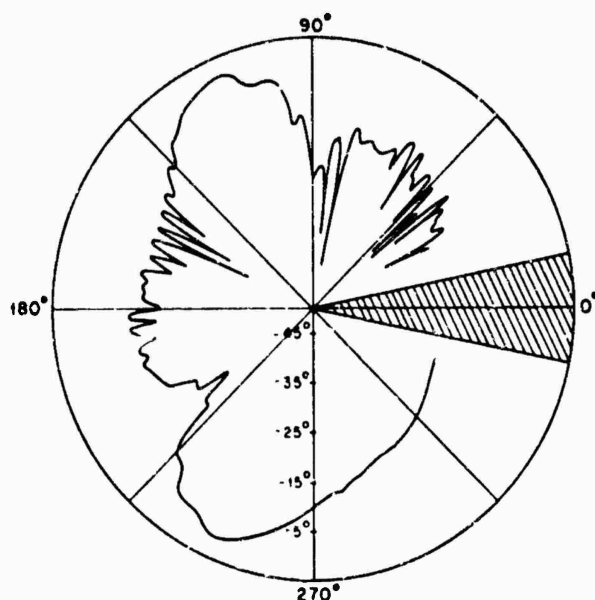


Fig. 6.5. Measured amplitude of the total magnetic field H_z for $\Omega = 11\frac{1}{4}^\circ$ and $\phi_0 = 78\frac{1}{4}^\circ$ with $\rho = 11.9\lambda$ (WATSON AND HORTON [1950]).

and on the lower surface, $\phi = \frac{7}{4}\pi$,

$$H_z = 2\eta(\phi_0 - \frac{1}{4}\pi) \exp \{ik\rho \sin(\phi_0 - \frac{1}{4}\pi)\} - \frac{2}{\sqrt{3}} e^{i\pi} \left[\cos(\phi_0 - \frac{1}{4}\pi) \cos \frac{1}{2}(\phi_0 - \frac{1}{4}\pi) \right. \\ \times \int_{k\rho}^{\infty} \cos \{(\xi - k\rho) \sin(\phi_0 - \frac{1}{4}\pi)\} H_{\frac{1}{2}}^{(1)}(\xi) d\xi - \\ \left. - \sin \frac{1}{2}(\phi_0 - \frac{1}{4}\pi) \int_{k\rho}^{\infty} \sin \{(\xi - k\rho) \sin(\phi_0 - \frac{1}{4}\pi)\} H_{\frac{1}{2}}^{(1)}(\xi) \frac{d\xi}{\xi} \right]. \quad (6.43)$$

For grazing incidence on the lower face (that is, for $\phi_0 = \frac{3}{4}\pi$), eqs. (6.42) and (6.43) reduce to

$$H_z = 2 - \frac{1}{\sqrt{3}} e^{i\pi} \int_{k\rho}^{\infty} H_{\frac{1}{2}}^{(1)}(\xi) d\xi \quad (6.44)$$

and

$$H_z = 1 + \frac{1}{\sqrt{3}} e^{i\pi} \int_{k\rho}^{\infty} \sin(\xi - k\rho) H_{\frac{1}{2}}^{(1)}(\xi) \frac{d\xi}{\xi}, \quad (6.45)$$

respectively, where, in the derivation of eq. (6.45), the "jump" discontinuity of the first integral in eq. (6.43) must be taken into account.

If $k\rho \ll 1$, a small argument expansion of the Bessel functions in eq. (6.40) gives:

$$H_z = \frac{2}{v} + \frac{4}{\Gamma(1/v)} (\frac{1}{2}k\rho)^{1/v} e^{-\frac{1}{2}i\pi/v} \cos \frac{\phi - \Omega}{v} \cos \frac{\phi_0 - \Omega}{v} + O[(k\rho)^{\min(2/v, 2)}] \quad (6.46)$$

which makes explicit the edge behavior.

For $k\rho \gg 1$ a convenient decomposition of the field is

$$H_z = H_z^{s.o.} + H_z^d \quad (6.47)$$

where $H_z^{s.o.}$ and H_z^d are the geometrical optics and diffracted fields respectively.

The geometrical optics field is

$$H_z^{s.o.} = \sum_{n_1} \exp(ik\rho \cos \alpha_{n_1}) + \sum_{n_2} \exp(ik\rho \cos \alpha_{n_2}), \quad (6.48)$$

where

$$\begin{aligned} \alpha_{n_1} &= \pi - \phi + \phi_0 - 2n_1 v\pi, \\ \alpha_{n_2} &= \pi - \phi - \phi_0 + 2\Omega - 2n_2 v\pi, \end{aligned} \quad (6.49)$$

and the summations extend over all integers n_1 and n_2 satisfying the inequalities

$$\begin{aligned} |\phi - \phi_0 + 2n_1 v\pi| &< \pi, \\ |\phi + \phi_0 - 2\Omega + 2n_2 v\pi| &< \pi, \end{aligned} \quad (6.50)$$

respectively. The diffracted field H_z^d can be written as (OBERHETTINGER [1956, 1958]):

$$\begin{aligned} H_z^d &= \{V_d(-\pi - \phi + \phi_0) - V_d(\pi - \phi + \phi_0)\} + \\ &\quad + \{V_d(-\pi - \phi - \phi_0 + 2\Omega) - V_d(\pi - \phi - \phi_0 + 2\Omega)\}, \end{aligned} \quad (6.51)$$

with

$$V_d(\beta) = \frac{1}{2\pi v} \int_0^\infty e^{ik\rho \cosh t} \frac{\sin(\beta/v)}{\cosh(t/v) - \cos(\beta/v)} dt. \quad (6.52)$$

For β near $2nv\pi$ where n is an integer (TUZHILIN [1963]; but see also OBERHETTINGER, [1956], for the case $n = 0$):

$$V_d(\beta) \sim \sum_{m=0}^{\infty} \{A_m(\beta, v) - a_m(\beta - 2nv\pi)\} f_m + \operatorname{sgn}(\beta - 2nv\pi) I \quad (6.53)$$

where f_m and I are as defined in eqs. (6.22) and (6.23) respectively, and $a_m(\beta - 2nv\pi)$ and $A_m(\beta, v)$ as defined in eqs. (6.25) through (6.28). The above representation describes the asymptotic behavior of $V_d(\beta)$ in the vicinity of the geometrical optics boundary $\beta = 2nv\pi$, and displays the discontinuity in $V_d(\beta)$ necessary to compensate for the corresponding discontinuity in $H_z^{s.o.}$. Of the four values of β implicit in eq. (6.51), not more than two can correspond to a geometrical optics boundary. An alternative but less convenient description of the diffracted field in the vicinity of a boundary has been given by PAULI [1938] using confluent hypergeometric functions.

For values of β away from a geometrical optics boundary such that the argument of the Fresnel integral in the expression for I (see eq. (6.23)) is large compared with unity,

$$V_d(\beta) \sim \sum_{m=0}^{\infty} A_m(\beta, v) f_m, \quad (6.54)$$

and from the leading term in this expansion,

$$H_z^d \sim \frac{e^{i(k\rho + \frac{1}{2}\pi)}}{\sqrt{(2\pi k\rho)}} \frac{1}{v} \sin \frac{\pi}{v} \left| \left(\cos \frac{\pi}{v} - \cos \frac{\phi - \phi_0}{v} \right)^{-1} + \left(\cos \frac{\pi}{v} + \cos \frac{2\pi - \phi - \phi_0}{v} \right)^{-1} \right|. \quad (6.55)$$

This has the appearance of a cylindrical wave with

$$P = \frac{i}{2v} \sin \frac{\pi}{v} \left\{ \left(\cos \frac{\pi}{v} - \cos \frac{\phi - \phi_0}{v} \right)^{-1} + \left(\cos \frac{\pi}{v} + \cos \frac{2\pi - \phi - \phi_0}{v} \right)^{-1} \right\} \quad (6.56)$$

emanating from the edge. Computed values of $|F|$ for $v = \frac{1}{2}$ and three different ϕ_0 are shown in Fig. 6.6.

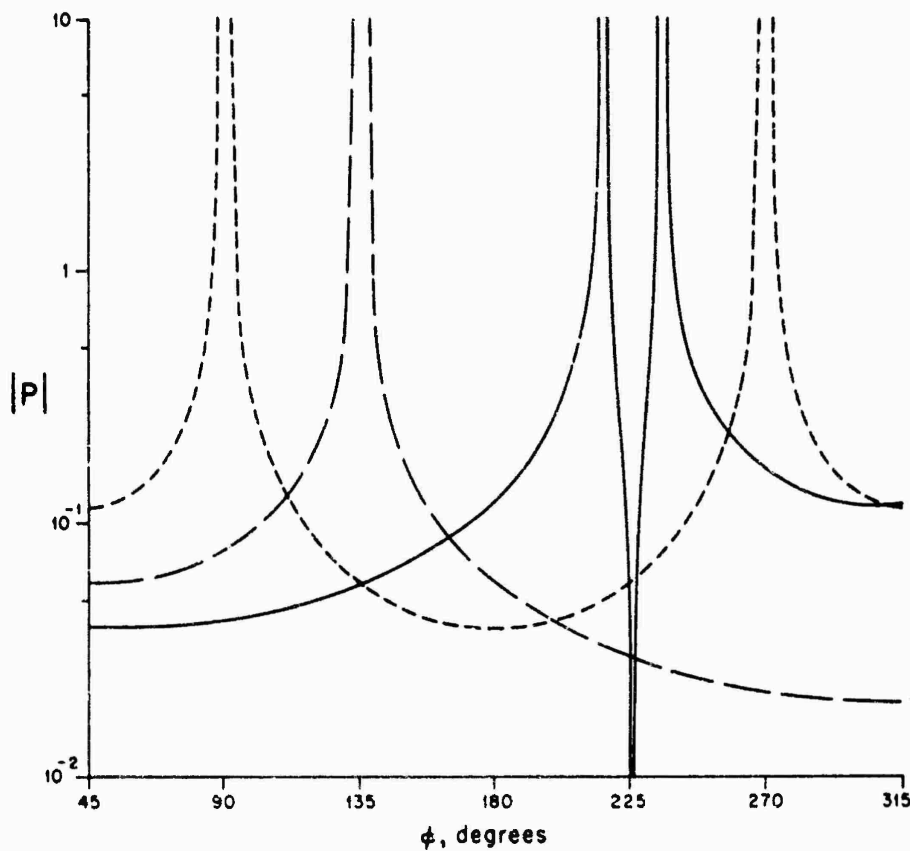


Fig. 6.6. Far field amplitude of the diffracted wave for $\phi_0 = 55^\circ$ (—), $\phi_0 = 135^\circ$ (---) and $\phi_0 = 180^\circ$ (-.-).

On the geometrical optics boundaries, the total magnetic field has the following asymptotic representations where, for simplicity, it has been assumed that $\Omega < \frac{1}{2}\pi$.

(i) $\phi = \pi - \phi_0 + 2\Omega$ with $\Omega < \phi_0 < \pi$ (boundary for geometrical reflection from the upper face):

$$H_z \sim \exp \{ik\rho \cos 2(\phi_0 - \Omega)\} + \frac{1}{2}e^{ik\rho} + \frac{1}{v} \frac{e^{i(k\rho + \frac{1}{2}\pi)}}{\sqrt{(2\pi k\rho)}} \left\{ \frac{\sin(\pi/v)}{\cos(\pi/v) + \cos[(3\pi - 2\phi_0)/v]} - \frac{1}{2} \cot \frac{\pi}{v} \right\}. \quad (6.57)$$

(ii) $\phi = 3\pi - \phi_0 - 2\Omega$ with $\pi - \Omega < \phi_0 < \pi$ (boundary for geometrical reflection from the lower face):

$$H_z \sim \exp \{ik\rho \cos 2(\phi_0 + \Omega)\} + \frac{1}{2}e^{ik\rho} + \frac{1}{v} \frac{e^{i(k\rho + \frac{1}{2}\pi)}}{\sqrt{(2\pi k\rho)}} \left\{ \frac{\sin(\pi/v)}{\cos(\pi/v) + \cos[(\pi - 2\phi_0)/v]} - \frac{1}{2} \cot \frac{\pi}{v} \right\}. \quad (6.58)$$

Eqs. (6.57) and (6.58) are also valid when $\phi_0 = \pi$ provided $\Omega > 0$.

(iii) $\phi = \pi + \phi_0$ with $\Omega < \phi_0 < \pi - \Omega$ (boundary of the geometrical shadow):

$$H_z \sim \frac{1}{2}e^{ik\rho} + \frac{1}{v} \frac{e^{i(k\rho + \frac{1}{2}\pi)}}{\sqrt{(2\pi k\rho)}} \left\{ \frac{\sin(\pi/v)}{\cos(\pi/v) + \cos[(\pi - 2\phi_0)/v]} - \frac{1}{2} \cot \frac{\pi}{v} \right\}. \quad (6.59)$$

When $\phi_0 = \pi - \Omega$ (grazing incidence on the lower face) and $\phi = 2\pi - \Omega$ (observation point on the lower face) the last two equations are replaced by:

$$H_z \sim e^{ik\rho} - \frac{e^{i(k\rho + \frac{1}{2}\pi)}}{\sqrt{(2\pi k\rho)}} \frac{1}{v} \cot \frac{\pi}{v}, \quad (6.60)$$

and this is also valid when $\Omega = 0$. By reciprocity it is further valid for $\phi_0 = \Omega$ and $\phi = \pi + \Omega$.

For the particular case of a right-angled wedge ($v = \frac{1}{2}$) an expression for H_z^d alternative to that given in eqs. (6.51) and (6.52) has been provided by REICHE [1912], and can be written as

$$H_z^d = v_d(\phi - \phi_0) + v_d(\phi + \phi_0 - \frac{1}{2}\pi), \quad (6.61)$$

where

$$v_d(\beta) = -\frac{e^{i\pi}}{\sqrt{3}} \left[\sin \beta \sin \frac{1}{2}\beta \int_{k\rho}^{\infty} \cos \{(\xi - k\rho) \cos \beta\} H_{\frac{1}{2}}^{(1)}(\xi) d\xi + \cos \frac{1}{2}\beta \int_{k\rho}^{\infty} \sin \{(\xi - k\rho) \cos \beta\} H_{\frac{1}{2}}^{(1)}(\xi) \frac{d\xi}{\xi} \right]. \quad (6.62)$$

The function $v_d(\beta)$ is discontinuous at the geometrical optics boundaries in order to compensate for the discontinuities in $H_z^{g.o.}$, and its behavior on the boundaries $\beta = \pi, 2\pi$ is indicated in eq. (6.37).

6.3. Line sources

6.3.1. E-polarization

For an electric line source parallel to the edge and located at (ρ_0, ϕ_0) such that

$$E^i = 2H_0^{(1)}(kR), \quad (6.63)$$

a contour integral representation of the total electric field is (MACDONALD [1962]; WIEGREFE [1912]; CARSLAW [1920]):

$$E_z = \frac{1}{4i\pi v} \int_{C_1 + C_2} H_0^{(1)}[kR(x)] \left\{ \cot \frac{\pi - \alpha - \phi + \phi_0}{2v} - \cot \frac{\pi - \alpha - \phi - \phi_0 + 2\Omega}{2v} \right\} dx, \quad (6.64)$$

where

$$R(\alpha) = (\rho^2 + \rho_0^2 + 2\rho\rho_0 \cos \alpha)^{1/2} \quad (6.65)$$

and C_1 and C_2 are the Sommerfeld contours shown in Fig. 6.2. An alternative representation of the total field as an eigenfunction expansion is

$$E_z = \frac{2}{v} \sum_{n=0}^{\infty} \varepsilon_n \sin \frac{n(\phi - \Omega)}{v} \sin \frac{n(\phi_0 - \Omega)}{v} S_{n/v}, \quad (6.66)$$

where (MACDONALD [1902]):

$$S_\tau = J_\tau(k\rho_<)H_\tau^{(1)}(k\rho_>), \quad (6.67)$$

which may also be written (TUZHILIN [1963]):

$$S_\tau = \sum_{s=0}^{\infty} \frac{(\frac{1}{2}k\rho\rho_0)^{2s+\tau}}{s!\Gamma(s+\tau+1)} \frac{H_{2s+\tau}^{(1)}(k\sqrt{(\rho^2 + \rho_0^2)})}{[\sqrt{(\rho^2 + \rho_0^2)}]^{2s+\tau}}. \quad (6.68)$$

Using a simulated line source and wedge angles $\Omega = 22\frac{1}{2}^\circ, 45^\circ$, Row [1953] has measured $|E_z|$ along a trajectory parallel to the upper face of the wedge.

Expressions for the surface field H_ρ are trivially obtainable from the above; no simplified forms of the contour integral representation are available.

If $k\rho_< \ll 1$ the eigenfunction expansion (6.66) is rapidly convergent. In particular, for $k\rho \ll 1$:

$$E_z = \frac{4}{\Gamma(1/v)} (\frac{1}{2}k\rho\rho_0)^{1/v} \frac{H_{1/v}^{(1)}(k\sqrt{(\rho^2 + \rho_0^2)})}{[\sqrt{(\rho^2 + \rho_0^2)}]^{1/v}} \sin \frac{\phi - \Omega}{v} \sin \frac{\phi_0 - \Omega}{v} + O[(k\rho)^{\min(2/v, 2+1/v)}], \quad (6.69)$$

which makes explicit the edge behavior.

For $k\rho\rho_0/R_1 \gg 1$ (source and observation point far from the edge), a convenient decomposition of the field is

$$E_z = E_z^{g.o.} + E_z^d, \quad (6.70)$$

where $E_z^{g.o.}$ and E_z^d are the geometrical optics and diffracted fields respectively. The geometrical optics field is

$$E_z^{g.o.} = \sum_{n_1} H_0^{(1)}[kR(\alpha_{n_1})] - \sum_{n_2} H_0^{(1)}[kR(\alpha_{n_2})], \quad (6.71)$$

where

$$\begin{aligned} \alpha_{n_1} &= \pi - \phi + \phi_0 - 2n_1 v\pi, \\ \alpha_{n_2} &= \pi - \phi - \phi_0 + 2\Omega - 2n_2 v\pi, \end{aligned} \quad (6.72)$$

and the summations extend over all integers n_1 and n_2 satisfying the inequalities

$$\begin{aligned} |\phi - \phi_0 + 2n_1 v\pi| &< \pi, \\ |\phi + \phi_0 - 2\Omega + 2n_2 v\pi| &< \pi, \end{aligned} \quad (6.73)$$

respectively. The diffracted field E_z^d can be written as

$$E_z^d = \{V_d(-\pi - \phi + \phi_0) - V_d(\pi - \phi + \phi_0)\} - \{V_d(-\pi - \phi - \phi_0 + 2\Omega) - V_d(\pi - \phi - \phi_0 + 2\Omega)\}, \quad (6.74)$$

with

$$V_d(\beta) = \frac{1}{2\pi\nu} \int_0^\infty H_0^{(1)}[kR(it)] \frac{\sin(\beta/\nu)}{\cosh(t/\nu) - \cos(\beta/\nu)} dt. \quad (6.75)$$

For β near $2n\nu\pi$ where n is an integer (TUZHILIN [1963]):

$$V_d(\beta) \sim \sum_{m=0}^{\infty} \{A_m(\beta, \nu) - a_m(\beta - 2n\nu\pi)\} f_m + \operatorname{sgn}(\beta - 2n\nu\pi) I, \quad (6.76)$$

where $a_m(\beta - 2n\nu\pi)$ and $A_m(\beta, \nu)$ are defined in eqs. (6.25) through (6.28), and

$$f_m = \frac{i(-1)^m \Gamma(m + \frac{1}{2})}{\sqrt{2}} \left(\frac{R_1}{k\rho\rho_0} \right)^{m+\frac{1}{2}} H_{m+\frac{1}{2}}^{(1)}(kR_1), \quad (6.77)$$

$$I = -\frac{2i}{\pi} e^{ikR(\beta - 2n\nu\pi)} \int_{|M|}^{\infty} \frac{e^{i\mu^2}}{\sqrt{\{\mu^2 + 2kR(\beta - 2n\nu\pi)\}}} d\mu, \quad (6.78)$$

with

$$M = \frac{2\sqrt{(k\rho\rho_0)} \sin \frac{1}{2}(\beta - 2n\nu\pi)}{\sqrt{\{R_1 + R(\beta - 2n\nu\pi)\}}}. \quad (6.79)$$

Eq. (6.76) describes the asymptotic behavior of $V_d(\beta)$ in the vicinity of the geometrical optics boundary specified by the integer n , and displays the discontinuity in $V_d(\beta)$ necessary to compensate for the corresponding discontinuity in $E_z^{g.o.}$. For $|M| \gg 1$, i.e. away from the boundary,

$$V_d(\beta) \sim \sum_{m=0}^{\infty} A_m(\beta, \nu) f_m \quad (6.80)$$

and from the leading term of this expansion,

$$E_z^d \sim \frac{e^{ik\rho_0}}{\sqrt{(\pi k\rho_0)}} \frac{e^{ik\rho}}{\sqrt{(\pi k\rho)}} \frac{1}{\nu} \sin \frac{\pi}{\nu} \times \left\{ \left(\cos \frac{\pi}{\nu} - \cos \frac{\phi - \phi_0}{\nu} \right)^{-1} - \left(\cos \frac{\pi}{\nu} + \cos \frac{2\pi - \phi - \phi_0}{\nu} \right)^{-1} \right\}. \quad (6.81)$$

This has the appearance of a cylindrical wave diverging from the edge.

On the geometrical optics boundaries, the total field has the following asymptotic representations, where, for simplicity, it has been assumed that $\Omega < \frac{1}{2}\pi$.

(i) $\phi = \pi - \phi_0 + 2\Omega$ with $\Omega < \phi_0 < \pi$ (boundary for geometrical reflection from the upper face):

$$E_z \sim H_0^{(1)}(kR) - \frac{1}{2} H_0^{(1)}(kR_1) + \frac{1}{\nu} \frac{e^{ik(\rho + \rho_0)}}{\pi k \sqrt{(\rho\rho_0)}} \left\{ \frac{\sin(\pi/\nu)}{\cos(\pi/\nu) + \cos[(3\pi - 2\phi_0)/\nu]} + \frac{1}{2} \cot \frac{\pi}{\nu} \right\}. \quad (6.82)$$

(ii) $\phi = 3\pi - \phi_0 - 2\Omega$ with $\pi - \Omega < \phi_0 < \pi$ (boundary for geometrical reflection from the lower face):

$$E_z \sim H_0^{(1)}(kR) - \frac{1}{2} H_0^{(1)}(kR_1) + \frac{1}{v} \frac{e^{ik(\rho + \rho_0)}}{\pi k \sqrt{(\rho \rho_0)}} \left\{ \frac{\sin(\pi/v)}{\cos(\pi/v) + \cos[(\pi - 2\phi_0)/v]} + \frac{1}{2} \cot \frac{\pi}{v} \right\}. \quad (6.83)$$

Eqs. (6.82) and (6.83) are also valid when $\phi_0 = \pi$ provided $\Omega > 0$.

(iii) $\phi = \pi + \phi_0$ with $\Omega < \phi_0 < \pi - \Omega$ (boundary of the geometrical shadow):

$$E_z \sim \frac{1}{2} H_0^{(1)}(kR_1) - \frac{1}{v} \frac{e^{ik(\rho + \rho_0)}}{\pi k \sqrt{(\rho \rho_0)}} \left\{ \frac{\sin(\pi/v)}{\cos(\pi/v) + \cos[(\pi - 2\phi_0)/v]} + \frac{1}{2} \cot \frac{\pi}{v} \right\}. \quad (6.84)$$

6.3.2. *H*-polarization

For a magnetic line source parallel to the edge and located at (ρ_0, ϕ_0) such that

$$H^i = \hat{z} H_0^{(1)}(kR), \quad (6.85)$$

a contour integral representation of the total magnetic field is (MACDONALD [1902]; WIEGREFE [1912]; CARSLAW [1920]):

$$H_z = \frac{1}{4i\pi v} \int_{C_1 + C_2} H_0^{(1)}[kR(\alpha)] \left\{ \cot \frac{\pi - \alpha - \phi + \phi_0}{2v} + \cot \frac{\pi - \alpha - \phi - \phi_0 + 2\Omega}{2v} \right\} d\alpha, \quad (6.86)$$

where

$$R(\alpha) = (\rho^2 + \rho_0^2 + 2\rho\rho_0 \cos \alpha)^{\frac{1}{2}} \quad (6.87)$$

and C_1 and C_2 are the Sommerfeld contours shown in Fig. 6.2. An alternative representation of the total field as an eigenfunction expansion is

$$H_z = \frac{2}{v} \sum_{n=0}^{\infty} \epsilon_n \cos \frac{n(\phi - \Omega)}{v} \cos \frac{n(\phi_0 - \Omega)}{v} S_{n/v}, \quad (6.88)$$

where (MACDONALD [1902]):

$$S_\tau = J_\tau(k\rho_<) H_\tau^{(1)}(k\rho_>), \quad (6.89)$$

which may also be written (TUZHILIN [1963]):

$$S_\tau = \sum_{s=0}^{\tau} \frac{(\frac{1}{2}k\rho\rho_0)^{2s+\tau}}{s! \Gamma(s+\tau+1)} \frac{H_{2s+\tau}^{(1)}(k\sqrt{(\rho^2 + \rho_0^2)})}{[\sqrt{(\rho^2 + \rho_0^2)}]^{2s+\tau}}. \quad (6.90)$$

Expressions for the total magnetic field on the surface are trivially obtainable from the above; no simplified forms of the contour integral representation are available.

If $k\rho_< \ll 1$ the eigenfunction expansion (6.88) is rapidly convergent. In particular, for $k\rho_< \ll 1$:

$$H_z = \frac{2}{v} H_0^{(1)}(k\sqrt{(\rho^2 + \rho_0^2)}) + \frac{4}{\Gamma(1/v)} (\frac{1}{2}k\rho\rho_0)^{1/v} \times \frac{H_{1/v}^{(1)}(k\sqrt{(\rho^2 + \rho_0^2)})}{[\sqrt{(\rho^2 + \rho_0^2)}]^{1/v}} \cos \frac{\phi - \Omega}{v} \cos \frac{\phi_0 - \Omega}{v} + O[(k\rho)^{\min(2/v, 2)}], \quad (6.91)$$

which makes explicit the edge behavior.

For $k\rho\rho_0/R_1 \gg 1$ (source and observation point far from the edge), a convenient decomposition of the field is

$$H_z = H_z^{g.o.} + H_z^d, \quad (6.92)$$

where $H_z^{g.o.}$ and H_z^d are the geometrical optics and diffracted fields respectively. The geometrical optics field is

$$H_z^{g.o.} = \sum_{n_1} H_0^{(1)}[kR(\alpha_{n_1})] + \sum_{n_2} H_0^{(1)}[kR(\alpha_{n_2})], \quad (6.93)$$

where

$$\begin{aligned} \alpha_{n_1} &= \pi - \phi + \phi_0 - 2n_1 v\pi, \\ \alpha_{n_2} &= \pi - \phi - \phi_0 + 2\Omega - 2n_2 v\pi, \end{aligned} \quad (6.94)$$

and the summations extend over all integers n_1 and n_2 satisfying the inequalities

$$\begin{aligned} |\phi - \phi_0 + 2n_1 v\pi| &< \pi, \\ |\phi + \phi_0 - 2\Omega + 2n_2 v\pi| &< \pi, \end{aligned} \quad (6.95)$$

respectively. The diffracted field H_z^d can be written as

$$H_z^d = \{V_d(-\pi - \phi + \phi_0) - V_d(\pi - \phi + \phi_0)\} + \{V_d(-\pi - \phi - \phi_0 + 2\Omega) - V_d(\pi - \phi - \phi_0 + 2\Omega)\}, \quad (6.96)$$

with

$$V_d(\beta) = \frac{1}{2\pi v} \int_0^\infty H_0^{(1)}[kR(it)] \frac{\sin(\beta/v)}{\cosh(t/v) - \cos(\beta/v)} dt. \quad (6.97)$$

For β near $2nv\pi$ where n is an integer (TUZHILIN [1963]):

$$V_d(\beta) \sim \sum_{m=0}^{\infty} \{A_m(\beta, v) - a_m(\beta - 2nv\pi)\} f_m + \operatorname{sgn}(\beta - 2nv\pi) I, \quad (6.98)$$

where f_m and I are as defined in eqs. (6.77) and (6.78) respectively, and $a_m(\beta - 2nv\pi)$ and $A_m(\beta, v)$ as defined in eqs. (6.25) through (6.28). The above representation describes the asymptotic behavior of $V_d(\beta)$ in the vicinity of the geometrical optics boundary $\beta = 2nv\pi$, and displays the discontinuity in $V_d(\beta)$ necessary to compensate for the corresponding discontinuity in $H_z^{g.o.}$. For values of β away from a geometrical optics boundary such that the lower limit of integration in the integral expression for I (see eq. (6.78)) is large compared with unity,

$$V_d(\beta) \sim \sum_{m=0}^{\infty} A_m(\beta, v) f_m. \quad (6.99)$$

and from the leading term of this expansion,

$$H_z^d \sim \frac{e^{ik\rho_0}}{\sqrt{(\pi k \rho_0)}} \frac{e^{ik\rho}}{\sqrt{(\pi k \rho)}} \frac{1}{v} \sin \frac{\pi}{v} \times \left\{ \left(\cos \frac{\pi}{v} - \cos \frac{\phi - \phi_0}{v} \right)^{-1} + \left(\cos \frac{\pi}{v} + \cos \frac{2\pi - \phi - \phi_0}{v} \right)^{-1} \right\}. \quad (6.100)$$

This has the appearance of a cylindrical wave diverging from the edge.

On the geometrical optics boundaries, the total magnetic field has the following asymptotic representations where, for simplicity, it has been assumed that $\Omega < \frac{1}{2}\pi$.

(i) $\phi = \pi - \phi_0 + 2\Omega$ with $\Omega < \phi_0 < \pi$ (boundary for geometrical reflection from the upper face):

$$H_z \sim H_0^{(1)}(kR) + \frac{1}{2} H_0^{(1)}(kR_1) + \frac{1}{v} \frac{e^{ik(\rho + \rho_0)}}{\pi k \sqrt{(\rho \rho_0)}} \left\{ \frac{\sin(\pi/v)}{\cos(\pi/v) + \cos[(3\pi - 2\phi_0)/v]} - \frac{1}{2} \cot \frac{\pi}{v} \right\}. \quad (6.101)$$

(ii) $\phi = 3\pi - \phi_0 - 2\Omega$ with $\pi - \Omega < \phi_0 < \pi$ (boundary for geometrical reflection from the lower face):

$$H_z \sim H_0^{(1)}(kR) + \frac{1}{2} H_0^{(1)}(kR_1) + \frac{1}{v} \frac{e^{ik(\rho + \rho_0)}}{\pi k \sqrt{(\rho \rho_0)}} \left\{ \frac{\sin(\pi/v)}{\cos(\pi/v) + \cos[(\pi - 2\phi_0)/v]} - \frac{1}{2} \cot \frac{\pi}{v} \right\}. \quad (6.102)$$

Eqs. (6.101) and (6.102) are also valid when $\phi_0 = \pi$ provided $\Omega > 0$.

(iii) $\phi = \pi + \phi_0$ with $\Omega < \phi_0 < \pi - \Omega$ (boundary of the geometrical shadow):

$$H_z \sim \frac{1}{2} H_0^{(1)}(kR_1) + \frac{1}{v} \frac{e^{ik(\rho + \rho_0)}}{\pi k \sqrt{(\rho \rho_0)}} \left\{ \frac{\sin(\pi/v)}{\cos(\pi/v) + \cos[(\pi - 2\phi_0)/v]} - \frac{1}{2} \cot \frac{\pi}{v} \right\}. \quad (6.103)$$

When $\phi_0 = \pi - \Omega$ (grazing incidence on the lower face) and $\phi = 2\pi - \Omega$ (observation point on the lower face) the last two equations are replaced by

$$H_z \sim H_0^{(1)}(kR_1) - \frac{e^{ik(\rho + \rho_0)}}{\pi k \sqrt{(\rho \rho_0)}} \frac{1}{v} \cot \frac{\pi}{v}, \quad (6.104)$$

and this is also valid when $\Omega = 0$. By reciprocity it is further valid for $\phi_0 = \Omega$ and $\phi = \pi + \Omega$.

6.4. Point sources

6.4.1. Acoustically soft wedge

For a point source at (ρ_0, ϕ_0, z_0) such that

$$V^i = \frac{e^{ikR}}{kR}, \quad (6.105)$$

a contour integral representation of the total field is (WIEGREFE [1912]; MACDONALD [1915]; CARSLAW [1920]):

$$V = \frac{1}{4i\pi\nu} \int_{C_1+C_2} \frac{e^{ikR(\alpha)}}{kR(\alpha)} \left\{ \cot \frac{\pi - \alpha - \phi + \phi_0}{2\nu} - \cot \frac{\pi - \alpha - \phi - \phi_0 + 2\Omega}{2\nu} \right\} d\alpha, \quad (6.106)$$

where

$$R(\alpha) = \{\rho^2 + \rho_0^2 + 2\rho\rho_0 \cos \alpha + (z - z_0)^2\}^{\frac{1}{2}} \quad (6.107)$$

and C_1 and C_2 are the Sommerfeld contours shown in Fig. 6.2. An alternative representation of the total field as an eigenfunction expansion is

$$V = \frac{2}{\nu} \sum_{n=0}^{\infty} \varepsilon_n \sin \frac{n(\phi - \Omega)}{\nu} \sin \frac{n(\phi_0 - \Omega)}{\nu} S_{n/\nu}, \quad (6.108)$$

where (OBERHETTINGER [1954]):

$$S_\tau = \frac{i}{2k} \int_{-\infty}^{\infty} e^{it(z-z_0)} J_\tau(\rho < \sqrt{(k^2 - t^2)}) H_\tau^{(1)}(\rho > \sqrt{(k^2 - t^2)}) dt, \quad (6.109)$$

which may be written as (TUZHILIN [1963]):

$$S_\tau = i \sum_{s=0}^{\infty} \frac{(\frac{1}{2}k\rho\rho_0)^{2s+\tau}}{s! \Gamma(s+\tau+1)} \frac{h_{2s+\tau}^{(1)}(k\sqrt{\{\rho^2 + \rho_0^2 + (z-z_0)^2\}})}{(\sqrt{\{\rho^2 + \rho_0^2 + (z-z_0)^2\}})^{2s+\tau}}, \quad (6.110)$$

and may further be written (MACDONALD [1915]):

$$S_\tau = ie^{-2i\tau\pi} \sum_{s=0}^{\infty} \frac{\Gamma(s+2\tau+1)}{s!} (2s+2\tau+1) j_{s+\tau}(kr_<) h_{s+\tau}^{(1)}(kr_>) P_{s+\tau}^{-\tau}(\cos \theta) P_{s+\tau}^{-\tau}(\cos \theta_0). \quad (6.111)$$

Expressions for the surface field $\partial V / \partial \phi$ are trivially obtainable from the above; no simplified forms of the contour integral representation are available.

If $k\rho_< \ll 1$ the eigenfunction expansion (6.108) is rapidly convergent. In particular, for $k\rho \ll 1$:

$$V = i \frac{4}{\Gamma(1/\nu)} (\frac{1}{2}k\rho\rho_0)^{1/\nu} \frac{h_{1/\nu}^{(1)}(k\sqrt{\{\rho^2 + \rho_0^2 + (z-z_0)^2\}})}{(\sqrt{\{\rho^2 + \rho_0^2 + (z-z_0)^2\}})^{1/\nu}} \sin \frac{\phi - \Omega}{\nu} \sin \frac{\phi_0 - \Omega}{\nu} + O[(k\rho)^{\min(2/\nu, 2+1/\nu)}], \quad (6.112)$$

which makes explicit the edge behavior.

For $k\rho\rho_0/R_1 \gg 1$ (source and observation point far from the edge), a convenient decomposition of the field is

$$V = V^{\text{g.o.}} + V^{\text{d}} \quad (6.113)$$

where $V^{\text{g.o.}}$ and V^{d} are the geometrical optics and diffracted fields respectively. The geometrical optics field is

$$V^{\text{g.o.}} = \sum_{n_1} \frac{\exp \{ikR(x_{n_1})\}}{kR(x_{n_1})} - \sum_{n_2} \frac{\exp \{ikR(x_{n_2})\}}{kR(x_{n_2})}, \quad (6.114)$$

where

$$\begin{aligned}\alpha_{n_1} &= \pi - \phi + \phi_0 - 2n_1 v\pi, \\ \alpha_{n_2} &= \pi - \phi - \phi_0 + 2\Omega - 2n_2 v\pi,\end{aligned}\quad (6.115)$$

and the summations extend over all integers n_1 and n_2 satisfying the inequalities

$$\begin{aligned}|\phi - \phi_0 + 2n_1 v\pi| &< \pi, \\ |\phi + \phi_0 - 2\Omega + 2n_2 v\pi| &< \pi,\end{aligned}\quad (6.116)$$

respectively. The diffracted field V^d can be written as

$$\begin{aligned}V^d &= \{V_d(-\pi - \phi + \phi_0) - V_d(\pi - \phi + \phi_0)\} - \\ &\quad - \{V_d(-\pi - \phi - \phi_0 + 2\Omega) - V_d(\pi - \phi - \phi_0 + 2\Omega)\},\end{aligned}\quad (6.117)$$

with

$$V_d(\beta) = \frac{1}{2\pi v} \int_0^\infty \frac{e^{ikR(it)}}{kR(it)} \frac{\sin(\beta/v)}{\cosh(t/v) - \cos(\beta/v)} dt. \quad (6.118)$$

For β near $2nv\pi$, where n is an integer (TUZHILIN [1963]):

$$V_d(\beta) \sim \sum_{m=0}^\infty \{A_m(\beta, v) - a_m(\beta - 2nv\pi)\} f_m + \operatorname{sgn}(\beta - 2nv\pi) I, \quad (6.119)$$

where $a_m(\beta - 2nv\pi)$ and $A_m(\beta, v)$ are defined in eqs. (6.25) through (6.28), and

$$f_m = \frac{i(-1)^m \Gamma(m + \frac{1}{2})}{2k} \sqrt{\frac{\pi}{\rho\rho_0}} \left(\frac{R_1}{k\rho\rho_0}\right)^m H_m^{(1)}(kR_1), \quad (6.120)$$

$$I = i \int_{|M|}^\infty \frac{H_1^{(1)}[\mu^2 + kR(\beta - 2nv\pi)]}{\sqrt{\{\mu^2 + 2kR(\beta - 2nv\pi)\}}} d\mu, \quad (6.121)$$

with

$$M = \frac{2\sqrt{(k\rho\rho_0) \sin \frac{1}{2}(\beta - 2nv\pi)}}{\sqrt{\{R_1 + R(\beta - 2nv\pi)\}}}. \quad (6.122)$$

Eq. (6.119) describes the asymptotic behavior of $V_d(\beta)$ in the vicinity of the geometrical optics boundary specified by the integer n , and displays the discontinuity in $V_d(\beta)$ necessary to compensate for the corresponding discontinuity in $V^{R,0}$. For $|M| \gg 1$, i.e. away from the boundary,

$$V_d(\beta) \sim \sum_{m=0}^\infty A_m(\beta, v) f_m, \quad (6.123)$$

and from the leading term of this expansion,

$$\begin{aligned}V^d &\sim \frac{e^{i(kR_1 + \frac{1}{2}\pi)}}{\sqrt{(2\pi k R_1)}} \frac{1}{k\sqrt{(\rho\rho_0)}} \frac{1}{v} \sin \frac{\pi}{v} \\ &\quad \times \left\{ \left(\cos \frac{\pi}{v} - \cos \frac{\phi - \phi_0}{v} \right)^{-1} - \left(\cos \frac{\pi}{v} + \cos \frac{2\pi - \phi - \phi_0}{v} \right)^{-1} \right\}.\end{aligned}\quad (6.124)$$

On the geometrical optics boundaries, the total field has the following asymptotic representations, where, for simplicity, it has been assumed that $\Omega < \frac{1}{2}\pi$.

(i) $\phi = \pi - \phi_0 + 2\Omega$ with $\Omega < \phi_0 < \pi$ (boundary for geometrical reflection from the upper face):

$$V \sim \frac{e^{ikR}}{kR} - \frac{1}{2} \frac{e^{ikR_1}}{kR_1} + \frac{1}{v} \frac{e^{i(kR_1 + \frac{1}{2}\pi)}}{\sqrt{(2\pi kR_1)}} \frac{1}{k\sqrt{(\rho\rho_0)}} \times \left\{ \frac{\sin(\pi/v)}{\cos(\pi/v) + \cos[(3\pi - 2\phi_0)/v]} + \frac{1}{2} \cot \frac{\pi}{v} \right\}. \quad (6.125)$$

(ii) $\phi = 3\pi - \phi_0 - 2\Omega$ with $\pi - \Omega < \phi_0 < \pi$ (boundary for geometrical reflection from the lower face):

$$V \sim \frac{e^{ikR}}{kR} - \frac{1}{2} \frac{e^{ikR_1}}{kR_1} + \frac{1}{v} \frac{e^{i(kR_1 + \frac{1}{2}\pi)}}{\sqrt{(2\pi kR_1)}} \frac{1}{k\sqrt{(\rho\rho_0)}} \left\{ \frac{\sin(\pi/v)}{\cos(\pi/v) + \cos[(\pi - 2\phi_0)/v]} + \frac{1}{2} \cot \frac{\pi}{v} \right\}. \quad (6.126)$$

Eqs. (6.125) and (6.126) are also valid when $\phi_0 = \pi$ provided $\Omega > 0$.

(iii) $\phi = \pi + \phi_0$ with $\Omega < \phi_0 < \pi - \Omega$ (boundary of the geometrical shadow):

$$V \sim \frac{1}{2} \frac{e^{ikR_1}}{kR_1} - \frac{1}{v} \frac{e^{i(kR_1 + \frac{1}{2}\pi)}}{\sqrt{(2\pi kR_1)}} \frac{1}{k\sqrt{(\rho\rho_0)}} \left\{ \frac{\sin(\pi/v)}{\cos(\pi/v) + \cos[(\pi - 2\phi_0)/v]} + \frac{1}{2} \cot \frac{\pi}{v} \right\}. \quad (6.127)$$

6.4.2. Acoustically hard wedge

For a point source at (ρ_0, ϕ_0, z_0) such that

$$V^i = \frac{e^{ikR}}{kR}, \quad (6.128)$$

a contour integral representation of the total field is (WIEGREFE [1912]; MACDONALD [1915]; CARSLAW [1920]):

$$V = \frac{1}{4i\pi v} \int_{C_1 + C_2} \frac{e^{ikR(x)}}{kR(x)} \left\{ \cot \frac{\pi - \alpha - \phi + \phi_0}{2v} + \cot \frac{\pi - \alpha - \phi - \phi_0 + 2\Omega}{2v} \right\} dx, \quad (6.129)$$

where

$$R(x) = \{\rho^2 + \rho_0^2 + 2\rho\rho_0 \cos x + (z - z_0)^2\}^{\frac{1}{2}} \quad (6.130)$$

and C_1 and C_2 are the Sommerfeld contours shown in Fig. 6.2. An alternative representation of the total field as an eigenfunction expansion is

$$V = \frac{2}{v} \sum_{n=0}^{\infty} \epsilon_n \cos \frac{n(\phi - \Omega)}{v} \cos \frac{n(\phi_0 - \Omega)}{v} S_{n/v}, \quad (6.131)$$

where (OBERHETTINGER [1954]):

$$S_r = \frac{i}{2k} \int_{-\infty}^{\infty} e^{it(z-z_0)} J_r[\rho \sqrt{(k^2 - t^2)}] H_r^{(1)}[\rho_0 \sqrt{(k^2 - t^2)}] dt, \quad (6.132)$$

which may be written as (TUZHILIN [1963]):

$$S_\tau = i \sum_{s=0}^{\infty} \frac{(\frac{1}{2}k\rho\rho_0)^{2s+\tau}}{s! \Gamma(s+\tau+1)} \frac{h_{2s+\tau}^{(1)}(k\sqrt{\{\rho^2 + \rho_0^2 + (z-z_0)^2\}})}{(\sqrt{\{\rho^2 + \rho_0^2 + (z-z_0)^2\}})^{2s+\tau}} \quad (6.133)$$

and may further be written (MACDONALD [1915]):

$$S_\tau = ie^{-2i\tau\pi} \sum_{s=0}^{\infty} \frac{\Gamma(s+2\tau+1)}{s!} (2s+2\tau+1) j_{s+\tau}(kr_<) h_{s+\tau}^{(1)}(kr_>) P_{s+\tau}^{-\tau}(\cos \theta) P_{s+\tau}^{-\tau}(\cos \theta_0). \quad (6.134)$$

Expressions for the total field on the surface are trivially obtainable from the above; no simplified forms of the contour integral representations are available.

If $k\rho_< \ll 1$ the eigenfunction expansion (6.131) is rapidly convergent. In particular, for $k\rho \ll 1$

$$V = \frac{2i}{v} h_0^{(1)}(k\sqrt{\{\rho^2 + \rho_0^2 + (z-z_0)^2\}}) + \frac{4i}{\Gamma(1/v)} (\frac{1}{2}k\rho\rho_0)^{1/v} \times \frac{h_1^{(1)}(k\sqrt{\{\rho^2 + \rho_0^2 + (z-z_0)^2\}})}{(\sqrt{\{\rho^2 + \rho_0^2 + (z-z_0)^2\}})^{1/v}} \cos \frac{\phi - \Omega}{v} \cos \frac{\phi_0 - \Omega}{v} + O[(k\rho)^{\min(2/v, 2)}], \quad (6.135)$$

which makes explicit the edge behavior.

For $k\rho\rho_0/R_1 \gg 1$ (source and observation point far from the edge), a convenient decomposition of the field is

$$V = V^{s.o.} + V^d \quad (6.136)$$

where $V^{s.o.}$ and V^d are the geometrical optics and diffracted fields respectively. The geometrical optics field is

$$V^{s.o.} = \sum_{n_1} \frac{\exp \{ikR(\alpha_{n_1})\}}{kR(\alpha_{n_1})} + \sum_{n_2} \frac{\exp \{ikR(\alpha_{n_2})\}}{kR(\alpha_{n_2})}, \quad (6.137)$$

where

$$\begin{aligned} \alpha_{n_1} &= \pi - \phi + \phi_0 - 2n_1 v\pi, \\ \alpha_{n_2} &= \pi - \phi - \phi_0 + 2\Omega - 2n_2 v\pi, \end{aligned} \quad (6.138)$$

and the summations extend over all integers n_1 and n_2 satisfying the inequalities

$$\begin{aligned} |\phi - \phi_0 + 2n_1 v\pi| &< \pi, \\ |\phi + \phi_0 - 2\Omega + 2n_2 v\pi| &< \pi, \end{aligned} \quad (6.139)$$

respectively. The diffracted field V^d can be written as

$$\begin{aligned} V^d &= \{V_d(-\pi - \phi + \phi_0) - V_d(\pi - \phi + \phi_0)\} + \\ &+ \{V_d(-\pi - \phi - \phi_0 + 2\Omega) - V_d(\pi - \phi - \phi_0 + 2\Omega)\}. \end{aligned} \quad (6.140)$$

with

$$V_d(\beta) = \frac{1}{2\pi v} \int_0^\infty \frac{e^{ikR(it)}}{kR(it)} \frac{\sin(\beta/v)}{\cosh(t/v) - \cos(\beta/v)} dt. \quad (6.141)$$

For β near $2nv\pi$ where n is an integer (TUZHILIN [1963]):

$$V_d(\beta) \sim \sum_{m=0}^{\infty} \{A_m(\beta, v) - a_m(\beta - 2nv\pi)\} f_m + \operatorname{sgn}(\beta - 2nv\pi) I, \quad (6.142)$$

where f_m and I are as defined in eqs. (6.120) and (6.121) respectively, and $a_m(\beta - 2nv\pi)$ and $A_m(\beta, v)$ as defined in eqs. (6.25) through (6.28). The above representation describes the asymptotic behavior of $V_d(\beta)$ in the vicinity of the geometrical optics boundary $\beta = 2nv\pi$, and displays the discontinuity in $V_d(\beta)$ necessary to compensate for the corresponding discontinuity in $V^{E,0}$. For values of β away from a geometrical optics boundary such that the lower limit of integration in the integral expression for I (see eq. (6.121)) is large compared to unity,

$$V_d(\beta) \sim \sum_{m=0}^{\infty} A_m(\beta, v) f_m, \quad (6.143)$$

and from the leading term of this expansion,

$$V^d \sim \frac{e^{i(kR_1 + \frac{1}{2}\pi)}}{\sqrt{(2\pi kR_1)}} \frac{1}{k\sqrt{(\rho\rho_0)}} \frac{1}{v} \sin \frac{\pi}{v} \times \left\{ \left(\cos \frac{\pi}{v} - \cos \frac{\phi - \phi_0}{v} \right)^{-1} + \left(\cos \frac{\pi}{v} + \cos \frac{2\pi - \phi - \phi_0}{v} \right)^{-1} \right\}. \quad (6.144)$$

On the geometrical optics boundaries, the total field has the following asymptotic representations, where, for simplicity, it has been assumed that $\Omega < \frac{1}{2}\pi$.

(i) $\phi = \pi - \phi_0 + 2\Omega$ with $\Omega < \phi_0 < \pi$ (boundary for geometrical reflection from the upper face):

$$V \sim \frac{e^{ikR}}{kR} + \frac{1}{2} \frac{e^{ikR_1}}{kR_1} + \frac{1}{v} \frac{e^{i(kR_1 + \frac{1}{2}\pi)}}{\sqrt{(2\pi kR_1)}} \frac{1}{k\sqrt{(\rho\rho_0)}} \left\{ \frac{\sin(\pi/v)}{\cos(\pi/v) + \cos[(3\pi - 2\phi_0)/v]} - \frac{1}{2} \cot \frac{\pi}{v} \right\}. \quad (6.145)$$

(ii) $\phi = 3\pi - \phi_0 - 2\Omega$ with $\pi - \Omega < \phi_0 < \pi$ (boundary for geometrical reflection from the lower face):

$$V \sim \frac{e^{ikR}}{kR} + \frac{1}{2} \frac{e^{ikR_1}}{kR_1} + \frac{1}{v} \frac{e^{i(kR_1 + \frac{1}{2}\pi)}}{\sqrt{(2\pi kR_1)}} \frac{1}{k\sqrt{(\rho\rho_0)}} \left\{ \frac{\sin(\pi/v)}{\cos(\pi/v) + \cos[(\pi - 2\phi_0)/v]} - \frac{1}{2} \cot \frac{\pi}{v} \right\}. \quad (6.146)$$

Eqs. (6.145) and (6.146) are also valid when $\phi_0 = \pi$ provide $\Omega > 0$.

(iii) $\phi = \pi + \phi_0$ with $\Omega < \phi_0 < \pi - \Omega$ (boundary of the geometrical shadow):

$$V \sim \frac{1}{2} \frac{e^{ikR_1}}{kR_1} + \frac{1}{v} \frac{e^{i(kR_1 + \frac{1}{2}\pi)}}{\sqrt{(2\pi kR_1)}} \frac{1}{k\sqrt{(\rho\rho_0)}} \left\{ \frac{\sin(\pi/v)}{\cos(\pi/v) + \cos[(\pi - 2\phi_0)/v]} - \frac{1}{2} \cot \frac{\pi}{v} \right\}. \quad (6.147)$$

When $\phi_0 = \pi - \Omega$ (grazing incidence on the lower face) and $\phi = 2\pi - \Omega$ (observation point on the lower face) the last two equations are replaced by

$$V \sim \frac{e^{ikR_1}}{kR_1} - \frac{e^{i(kR_1 + \frac{1}{2}\pi)}}{\sqrt{(2\pi kR_1)}} \frac{1}{k\sqrt{(\rho\rho_0)}} \frac{1}{v} \cot \frac{\pi}{v}, \quad (6.148)$$

and this is also valid when $\Omega = 0$. By reciprocity it is further valid for $\phi_0 = \Omega$ and $\phi = \pi + \Omega$.

6.5. Dipole sources

6.5.1. Electric dipoles

For an arbitrarily oriented electric dipole at (ρ_0, ϕ_0, z_0) with moment $(4\pi\epsilon/k)\hat{e}$, corresponding to an electric Hertz vector

$$\Pi^1 = \hat{e} \frac{e^{ikR}}{kR} \quad (6.149)$$

where

$$\hat{e} = \hat{x} \sin \Theta \cos \Phi + \hat{y} \sin \Theta \sin \Phi + \hat{z} \cos \Theta, \quad (6.150)$$

a contour integral representation of the total electric Hertz vector is (MALYUZHINETS and TUZHILIN [1963]):

$$\begin{aligned} \Pi = \frac{1}{4iv\pi} \int_{C_1+C_2} \frac{e^{ikR(\alpha)}}{kR(\alpha)} \left\{ \hat{e}(\pi - \alpha - \phi + \phi_0 - \Phi) \cot \frac{\pi - \alpha - \phi + \phi_0}{2v} - \right. \\ \left. - \hat{e}(\pi - \alpha - \phi - \phi_0 + \Phi) \cot \frac{\pi - \alpha - \phi - \phi_0 + 2\Omega}{2v} \right\} d\alpha, \end{aligned} \quad (6.151)$$

where

$$R(\alpha) = \{\rho^2 + \rho_0^2 + 2\rho\rho_0 \cos \alpha + (z - z_0)^2\}^{\frac{1}{2}}, \quad (6.152)$$

$$\hat{e}(\alpha) = \hat{x} \sin \Theta \cos \alpha - \hat{y} \sin \Theta \sin \alpha + \hat{z} \cos \Theta, \quad (6.153)$$

and C_1 and C_2 are the Sommerfeld contours shown in Fig. 6.2. Expressions for the total electric and magnetic fields can be obtained from eq. (6.151) by application of the usual differential operators in Cartesian coordinates to Π (MALYUZHINETS and TUZHILIN [1963]). Alternative expressions for the fields have also been given by TEISSEYRE [1955a, b, c; 1956]. In the case of a \hat{z} oriented dipole, Π reduces to $\hat{z}V^s$, where V^s is the point source solution for an acoustically soft wedge (see Section 6.4.1).

A representation for the total electric field as an eigenfunction expansion is

$$E(\mathbf{r}) = 4\pi k \mathcal{G}_e(\mathbf{r}|\mathbf{r}_0) \cdot \hat{e}. \quad (6.154)$$

where $\mathcal{G}_e(\mathbf{r}|\mathbf{r}_0)$ is the electric dyadic Green function for the wedge. In circular cylindrical coordinates (TAT [1954]):

$$\begin{aligned} \frac{4\pi}{k} \mathcal{G}_e(r|r_0) = & \left\{ \frac{\hat{\rho}}{\rho} \frac{\partial}{\partial \phi} - \hat{\phi} \frac{\partial}{\partial \rho} \right\} \left\{ \frac{\hat{\rho}_0}{\rho_0} \frac{\partial}{\partial \phi_0} - \hat{\phi}_0 \frac{\partial}{\partial \rho_0} \right\} \bar{U} + \\ & + \left\{ \hat{\rho} \frac{\partial^2}{\partial \rho \partial z} + \frac{\hat{\phi}}{\rho} \frac{\partial^2}{\partial \phi \partial z} + \hat{z} \left(\frac{\partial^2}{\partial z^2} + k^2 \right) \right\} \left\{ \hat{\rho}_0 \frac{\partial^2}{\partial \rho_0 \partial z_0} + \right. \\ & \left. + \frac{\hat{\phi}_0}{\rho_0} \frac{\partial^2}{\partial \phi_0 \partial z_0} + \hat{z}_0 \left(\frac{\partial^2}{\partial z_0^2} + k^2 \right) \right\} \frac{U}{k^2}, \quad (6.155) \end{aligned}$$

where

$$\bar{U} = \frac{2}{v} \sum_{n=0}^{\infty} \varepsilon_n \cos \frac{n(\phi - \Omega)}{v} \cos \frac{n(\phi_0 - \Omega)}{v} T_{n/v}, \quad (6.156)$$

$$U = \frac{2}{v} \sum_{n=0}^{\infty} \varepsilon_n \sin \frac{n(\phi - \Omega)}{v} \sin \frac{n(\phi_0 - \Omega)}{v} T_{n/v}, \quad (6.157)$$

$$T_\tau = \frac{i}{2k} \int_{-\infty}^{\infty} \frac{dt}{k^2 - t^2} e^{it(z - z_0)} J_\tau[\rho < \sqrt{(k^2 - t^2)}] H_\tau^{(1)}[\rho > \sqrt{(k^2 - t^2)}]. \quad (6.158)$$

Since

$$\left(\frac{\partial^2}{\partial z_0^2} + k^2 \right) U = V^s, \quad (6.159)$$

the solution for a \hat{z} oriented dipole (that is, $\hat{e} = \hat{z}$) again follows immediately from the point source solution. On the other hand, in spherical coordinates (TILSTON [1952]):

$$\begin{aligned} \frac{4\pi}{k} \mathcal{G}_e(r|r_0) = & \left\{ \frac{\hat{\theta}}{\sin \theta} \frac{\partial}{\partial \phi} - \hat{\phi} \frac{\partial}{\partial \theta} \right\} \left\{ \frac{\hat{\theta}_0}{\sin \theta_0} \frac{\partial}{\partial \phi_0} - \hat{\phi}_0 \frac{\partial}{\partial \theta_0} \right\} \bar{U} + \\ & + \left\{ \hat{\rho} \left(\frac{\partial^2}{\partial r^2} + k^2 \right) + \frac{\hat{\theta}}{r} \frac{\partial^2}{\partial r \partial \theta} + \frac{\hat{\phi}}{r \sin \theta} \frac{\partial^2}{\partial r \partial \phi} \right\} \left\{ \hat{\rho}_0 \left(\frac{\partial^2}{\partial r_0^2} + k^2 \right) + \right. \\ & \left. + \frac{\hat{\theta}_0}{r_0} \frac{\partial^2}{\partial r_0 \partial \theta_0} + \frac{\hat{\phi}_0}{r_0 \sin \theta_0} \frac{\partial^2}{\partial r_0 \partial \phi_0} \right\} \frac{r r_0 U}{k^2}, \quad (6.160) \end{aligned}$$

where \bar{U} and U are as given in eqs. (6.156) and (6.157) respectively, but with eq. (6.158) replaced by

$$\begin{aligned} T_\tau = i e^{-2i\tau\pi} \sum_{s=0}^{\infty} \frac{\Gamma(s+2\tau+1)}{s!} \frac{2s+2\tau+1}{(s+\tau)(s+\tau+1)} \\ \times j_{s+\tau}(kr <) h_{s+\tau}^{(1)}(kr >) P_{s+\tau}^{-\tau}(\cos \theta) P_{s+\tau}^{-\tau}(\cos \theta_0). \quad (6.161) \end{aligned}$$

Since

$$r_0 \left(\frac{\partial^2}{\partial r_0^2} + k^2 \right) (r_0 U) = V^s, \quad (6.162)$$

the solution for a radial dipole (that is, $\hat{\mathbf{e}} = \hat{\mathbf{r}}_0$) now follows immediately from the point source solution.

If $kr \ll 1$ and $kr_0 \gg 1$, the representation in equation (6.160) is rapidly convergent and leads to (FELSEN [1957])

$$\begin{aligned} E = & \frac{2ik}{v\Gamma(1/v)} \frac{\exp(ikr_0 - \frac{1}{2}i\pi/v)}{r_0} (\frac{1}{2}k\rho \sin \theta_0)^{1/v-1} \left\{ \hat{\rho} \sin \frac{\phi - \Omega}{v} + \hat{\phi} \cos \frac{\phi - \Omega}{v} \right\} \\ & \times \left\{ (\hat{\theta}_0 \cdot \hat{\mathbf{e}}) \cos \theta_0 \sin \frac{\phi_0 - \Omega}{v} + (\hat{\phi}_0 \cdot \hat{\mathbf{e}}) \cos \frac{\phi_0 - \Omega}{v} \right\} + \\ & + O[(kr_0)^{-1}(kr)^{\min(2/v-1, 1/v, 1)}, (kr_0)^{-2}], \end{aligned} \quad (6.163)$$

$$\begin{aligned} H = & \frac{2ikY}{v\Gamma(1/v)} \frac{\exp(ikr_0 - \frac{1}{2}i\pi/v)}{r_0} (\frac{1}{2}k\rho \sin \theta_0)^{1/v-1} \left\{ \hat{\rho} \cos \frac{\phi - \Omega}{v} - \hat{\phi} \sin \frac{\phi - \Omega}{v} \right\} \\ & \times \left\{ (\hat{\theta}_0 \cdot \hat{\mathbf{e}}) \sin \frac{\phi_0 - \Omega}{v} + (\hat{\phi}_0 \cdot \hat{\mathbf{e}}) \cos \theta_0 \cos \frac{\phi_0 - \Omega}{v} \right\} - \frac{2kY}{v} \frac{e^{ikr_0}}{r_0} \hat{\mathbf{z}} (\hat{\phi}_0 \cdot \hat{\mathbf{e}}) \sin \theta_0 + \\ & + O[(kr_0)^{-1}(kr)^{\min(2/v-1, 1/v, 1)}, (kr_0)^{-2}], \end{aligned} \quad (6.164)$$

where

$$\begin{aligned} \hat{\theta}_0 \cdot \hat{\mathbf{e}} &= \cos \theta_0 \sin \Theta \cos(\phi_0 - \Phi) - \sin \theta_0 \cos \Theta, \\ \hat{\phi}_0 \cdot \hat{\mathbf{e}} &= -\sin \Theta \sin(\phi_0 - \Phi). \end{aligned} \quad (6.165)$$

The above equations make explicit the behavior of the electromagnetic fields near to the edge.

For $k\rho\rho_0/R_1 \gg 1$ (source and observation point far from the edge), a convenient decomposition of the total electric Hertz vector is

$$\Pi = \Pi^{s.o.} + \Pi^d \quad (6.166)$$

where $\Pi^{s.o.}$ and Π^d are the geometrical optics and diffracted contributions respectively. The geometrical optics contribution is

$$\Pi^{s.o.} = \sum_{n_1} \frac{\exp\{ikR(\alpha_{n_1})\}}{kR(\alpha_{n_1})} \hat{\mathbf{e}}(-\Phi + 2n_1 v\pi) - \sum_{n_2} \frac{\exp\{ikR(\alpha_{n_2})\}}{kR(\alpha_{n_2})} \hat{\mathbf{e}}(\Phi - 2\Omega + 2n_2 v\pi), \quad (6.167)$$

where

$$\begin{aligned} \alpha_{n_1} &= \pi - \phi + \phi_0 - 2n_1 v\pi, \\ \alpha_{n_2} &= \pi - \phi - \phi_0 + 2\Omega - 2n_2 v\pi, \end{aligned} \quad (6.168)$$

and the summations extend over all integers n_1 and n_2 satisfying the inequalities

$$\begin{aligned} |\phi - \phi_0 + 2n_1 v\pi| &< \pi, \\ |\phi + \phi_0 - 2\Omega + 2n_2 v\pi| &< \pi, \end{aligned} \quad (6.169)$$

respectively. The diffracted contribution Π^d can be written as (TUZHILIN [1964]):

$$\Pi^d = \{\Pi_d^{(1)}(-\pi - \phi + \phi_0) - \Pi_d^{(1)}(\pi - \phi + \phi_0)\} - \{\Pi_d^{(2)}(-\pi - \phi - \phi_0 + 2\Omega) - \Pi_d^{(2)}(\pi - \phi - \phi_0 + 2\Omega)\}, \quad (6.170)$$

where

$$\Pi_d^{(1)}(\beta) = \frac{1}{2\pi v} \int_0^\infty \frac{e^{ikR(it)}}{kR(it)} \left[\sin \frac{\beta}{v} \{ \hat{e}(\beta - \Phi) + (\cosh t - 1)[\hat{z} \wedge \hat{e}(\beta - \Phi) \wedge \hat{z}] \} - \sinh \frac{t}{v} \sinh t [\hat{z} \wedge \hat{e}(\beta - \Phi)] \right] \frac{dt}{\cosh(t/v) - \cos(\beta/v)} \quad (6.171)$$

and $\Pi_d^{(2)}(\beta)$ is obtained from $\Pi_d^{(1)}(\beta)$ by replacing $\hat{e}(\beta - \Phi)$ by $\hat{e}(\beta + \Phi - 2\Omega)$. For β near $2nv\pi$ where n is an integer (TUZHILIN [1964]):

$$\Pi_d^{(1)}(\beta) \sim \sum_{m=0}^{\infty} \{ \pi_m^{(1)}(\beta, v) - a_m(\beta - 2nv\pi) \hat{e}(2nv\pi - \Phi) \} f_m + \hat{e}(2nv\pi - \Phi) \operatorname{sgn}(\beta - 2nv\pi) I, \quad (6.172)$$

with

$$\pi_0^{(1)} = A_0(\beta, v) \hat{e}(\beta - \Phi), \quad (6.173)$$

and, for $m \geq 1$,

$$\pi_m^{(1)} = A_m(\beta, v) \hat{e}(\beta - \Phi) + A_{m-1}(\beta, v) [\hat{z} \wedge \hat{e}(\beta - \Phi) \wedge \hat{z}] + \frac{2}{2m-1} \frac{\partial A_{m-1}(\beta, v)}{\partial \beta} [\hat{z} \wedge \hat{e}(\beta - \Phi)]. \quad (6.174)$$

In the above equations $a_m(\beta - 2nv\pi)$ and $A_m(\beta, v)$ are as defined in eqs. (6.25) through (6.28), and f_m and I are as given in eqs. (6.120) and (6.121) respectively. Similarly,

$$\Pi_d^{(2)}(\beta) \sim \sum_{m=0}^{\infty} \{ \pi_m^{(2)}(\beta, v) - a_m(\beta - 2nv\pi) \hat{e}(2nv\pi + \Phi - 2\Omega) \} f_m + \hat{e}(2nv\pi + \Phi - 2\Omega) \operatorname{sgn}(\beta - 2nv\pi) I, \quad (6.175)$$

where $\pi_m^{(2)}(\beta, v)$ is obtained from $\pi_m^{(1)}(\beta, v)$ by replacing $\hat{e}(\beta - \Phi)$ by $\hat{e}(\beta + \Phi - 2\Omega)$. Eqs. (6.172) and (6.175) describe the asymptotic behavior of $\Pi_d^{(1)}(\beta)$ or $\Pi_d^{(2)}(\beta)$ in the vicinity of the geometrical optics boundary specified by the integer n , and display the discontinuity in $\Pi_d^{(1)}(\beta)$ or $\Pi_d^{(2)}(\beta)$ necessary to compensate for the corresponding discontinuity in $\Pi^{s.o.}$. Away from the boundary such that $|M| \gg 1$ in the expression for I given in eq. (6.121),

$$\Pi_d^{(1),(2)}(\beta) \sim \sum_{m=0}^{\infty} \pi_m^{(1),(2)}(\beta, v) f_m, \quad (6.176)$$

and from the leading term in this expansion,

$$\Pi^d \sim \frac{e^{i(kR_1 + \frac{1}{2}\pi)}}{\sqrt{(2\pi k R_1)}} \frac{1}{k\sqrt{(\rho\rho_0)}} \frac{1}{v} \sin \frac{\pi}{v} \times \left| \frac{\hat{e}(\pi - \phi + \phi_0 - \Phi)}{\cos(\pi/v) - \cos[(\phi - \phi_0)/v]} - \frac{\hat{e}(\pi - \phi - \phi_0 + \Phi)}{\cos(\pi/v) + \cos[(2\pi - \phi - \phi_0)/v]} \right|. \quad (6.177)$$

6.5.2. Magnetic dipoles

For an arbitrarily oriented magnetic dipole at (ρ_0, ϕ_0, z_0) with moment $(4\pi/k)\hat{\mathbf{e}}$ corresponding to a magnetic Hertz vector

$$\tilde{\mathbf{H}}^i = \hat{\mathbf{e}} \frac{e^{ikR}}{kR} \quad (6.178)$$

where

$$\hat{\mathbf{e}} = \hat{\mathbf{x}} \sin \Theta \cos \Phi + \hat{\mathbf{y}} \sin \Theta \sin \Phi + \hat{\mathbf{z}} \cos \Theta, \quad (6.179)$$

a contour integral representation of the total magnetic Hertz vector is (TUZHILIN [1964]):

$$\tilde{\mathbf{H}} = \frac{1}{4i\pi v} \int_{C_1+C_2} \frac{e^{ikR(\alpha)}}{kR(\alpha)} \left\{ \hat{\mathbf{e}}(\pi - \alpha - \phi + \phi_0 - \Phi) \cot \frac{\pi - \alpha - \phi + \phi_0}{2v} + \right. \\ \left. + \hat{\mathbf{e}}(\pi - \alpha - \phi - \phi_0 + \Phi) \cot \frac{\pi - \alpha - \phi - \phi_0 + 2\Omega}{2v} \right\} d\alpha, \quad (6.180)$$

where

$$R(\alpha) = \{\rho^2 + \rho_0^2 + 2\rho\rho_0 \cos \alpha + (z - z_0)^2\}^{\frac{1}{2}}, \quad (6.181)$$

$$\hat{\mathbf{e}}(\alpha) = \hat{\mathbf{x}} \sin \Theta \cos \alpha - \hat{\mathbf{y}} \sin \Theta \sin \alpha + \hat{\mathbf{z}} \cos \Theta, \quad (6.182)$$

and C_1 and C_2 are the Sommerfeld contours shown in Fig. 6.2. Expressions for the total electric and magnetic fields can be obtained from eq. (6.180) by application of the usual differential operators in Cartesian coordinates to $\tilde{\mathbf{H}}$. Alternative expressions for the fields have been given by TEISSEYRE [1955a, b, c; 1956]. In the case of a $\hat{\mathbf{z}}$ oriented dipole, $\tilde{\mathbf{H}}$ reduces to $\hat{\mathbf{z}}V^h$, where V^h is the point source solution for an acoustically hard wedge (see Section 6.4.2).

A representation for the total magnetic field as an eigenfunction expansion is

$$\mathbf{H}(\mathbf{r}) = 4\pi k \mathcal{G}_m(\mathbf{r}|\mathbf{r}_0) \cdot \hat{\mathbf{e}}, \quad (6.183)$$

where $\mathcal{G}_m(\mathbf{r}|\mathbf{r}_0)$ is the magnetic dyadic Green function for the wedge. In circular cylindrical coordinates (TAI [1954]):

$$\frac{4\pi}{k} \mathcal{G}_m(\mathbf{r}|\mathbf{r}_0) = \left\{ \frac{\hat{\rho}}{\rho} \frac{\partial}{\partial \phi} - \hat{\phi} \frac{\partial}{\partial \rho} \right\} \left\{ \frac{\hat{\rho}_0}{\rho_0} \frac{\partial}{\partial \phi_0} - \hat{\phi}_0 \frac{\partial}{\partial \rho_0} \right\} U + \\ + \left\{ \hat{\rho} \frac{\partial^2}{\partial \rho \partial z} + \frac{\hat{\phi}}{\rho} \frac{\partial^2}{\partial \phi \partial z} + \hat{\mathbf{z}} \left(\frac{\partial^2}{\partial z^2} + k^2 \right) \right\} \left\{ \hat{\rho}_0 \frac{\partial^2}{\partial \rho_0 \partial z_0} + \right. \\ \left. + \frac{\hat{\phi}_0}{\rho_0} \frac{\partial^2}{\partial \phi_0 \partial z_0} + \hat{\mathbf{z}}_0 \left(\frac{\partial^2}{\partial z_0^2} + k^2 \right) \right\} \frac{\tilde{U}}{k^2}, \quad (6.184)$$

where \tilde{U} and U are defined by eqs. (6.156) through (6.158). Since

$$\left(\frac{\partial^2}{\partial z_0^2} + k^2 \right) \tilde{U} = V^h, \quad (6.185)$$

the solution for a \hat{z} oriented dipole (that is, $\hat{e} = \hat{z}$) again follows immediately from the point source solution. On the other hand, in spherical coordinates (TILSTON [1952]):

$$\begin{aligned} \frac{4\pi}{k} \mathcal{G}_m(\mathbf{r}|\mathbf{r}_0) = & \left\{ \frac{\hat{n}}{\sin \theta} \frac{\partial}{\partial \phi} - \hat{\phi} \frac{\partial}{\partial \theta} \right\} \left\{ \frac{\hat{\theta}_0}{\sin \theta_0} \frac{\partial}{\partial \phi_0} - \hat{\phi}_0 \frac{\partial}{\partial \theta_0} \right\} U + \\ & + \left\{ \hat{\rho} \left(\frac{\partial^2}{\partial r^2} + k^2 \right) + \frac{\hat{\theta}}{r} \frac{\partial^2}{\partial r \partial \theta} + \frac{\hat{\phi}}{r \sin \theta} \frac{\partial^2}{\partial r \partial \phi} \right\} \left\{ \hat{\rho}_0 \left(\frac{\partial^2}{\partial r_0^2} + k^2 \right) + \right. \\ & \left. + \frac{\hat{\theta}_0}{r_0} \frac{\partial^2}{\partial r_0 \partial \theta_0} + \frac{\hat{\phi}_0}{r_0 \sin \theta_0} \frac{\partial^2}{\partial r_0 \partial \phi_0} \right\} \frac{r r_0 \tilde{U}}{k^2}, \quad (6.186) \end{aligned}$$

where \tilde{U} and U are as given in eqs. (6.156) and (6.157) respectively, but with eq. (6.158) replaced by (6.161). Since

$$r_0 \left(\frac{\partial^2}{\partial r_0^2} + k^2 \right) (r_0 \tilde{U}) = V^h, \quad (6.187)$$

the solution for a radial dipole (that is, $\hat{e} = \hat{\rho}_0$) now follows immediately from the point source solution.

If $kr \ll 1$ and $kr_0 \gg 1$, the representation in eq. (6.186) is rapidly convergent and leads to

$$\begin{aligned} H = & \frac{2ik}{v\Gamma(1/v)} \frac{\exp(ikr_0 - \frac{1}{2}i\pi/v)}{r_0} (\frac{1}{2}k\rho \sin \theta_0)^{1/v-1} \left\{ \hat{\rho} \cos \frac{\phi - \Omega}{v} - \hat{\phi} \sin \frac{\phi - \Omega}{v} \right\} \\ & \times \left\{ (\hat{\theta}_0 \cdot \hat{e}) \cos \theta_0 \cos \frac{\phi_0 - \Omega}{v} - (\hat{\phi}_0 \cdot \hat{e}) \sin \frac{\phi_0 - \Omega}{v} \right\} - \\ & - \frac{2k}{v} \frac{e^{ikr_0}}{r_0} \hat{z} (\hat{\theta}_0 \cdot \hat{e}) \sin \theta_0 + O[(kr_0)^{-1} (kr)^{\min(2/v-1, 1/v, 1)}, (kr_0)^{-2}], \quad (6.188) \end{aligned}$$

$$\begin{aligned} E = & \frac{2ikZ}{v\Gamma(1/v)} \frac{\exp(ikr_0 - \frac{1}{2}i\pi/v)}{r_0} (\frac{1}{2}k\rho \sin \theta_0)^{1/v-1} \left\{ \hat{\rho} \sin \frac{\phi - \Omega}{v} + \hat{\phi} \cos \frac{\phi - \Omega}{v} \right\} \\ & \times \left\{ (\hat{\theta}_0 \cdot \hat{e}) \cos \frac{\phi_0 - \Omega}{v} - (\hat{\phi}_0 \cdot \hat{e}) \cos \theta_0 \sin \frac{\phi_0 - \Omega}{v} \right\} + \\ & + O[(kr_0)^{-1} (kr)^{\min(2/v-1, 1/v, 1)}, (kr_0)^{-2}], \quad (6.189) \end{aligned}$$

where $(\hat{\theta}_0 \cdot \hat{e})$ and $(\hat{\phi}_0 \cdot \hat{e})$ are given in eq. (6.165). The above equations make explicit the behavior of the electromagnetic fields near the edge.

For $k\rho\rho_0/R_1 \gg 1$ (source and observation point far from the edge), a convenient decomposition of the total magnetic Hertz vector is

$$\tilde{\mathbf{H}} = \tilde{\mathbf{H}}^{s.o.} + \tilde{\mathbf{H}}^d \quad (6.190)$$

where $\tilde{\Pi}^{s.o.}$ and $\tilde{\Pi}^d$ are the geometrical optics and diffracted contributions respectively. The geometrical optics contribution is

$$\tilde{\Pi}^{s.o.} = \sum_{n_1} \frac{\exp \{ikR(\alpha_{n_1})\}}{kR(\alpha_{n_1})} \hat{e}(-\Phi + 2n_1 v\pi) + \sum_{n_2} \frac{\exp \{ikR(\alpha_{n_2})\}}{kR(\alpha_{n_2})} \hat{e}(\Phi - 2\Omega + 2n_2 v\pi), \quad (6.191)$$

where

$$\begin{aligned} \alpha_{n_1} &= \pi - \phi + \phi_0 - 2n_1 v\pi, \\ \alpha_{n_2} &= \pi - \phi - \phi_0 + 2\Omega - 2n_2 v\pi, \end{aligned} \quad (6.192)$$

and the summations extend over all integers n_1 and n_2 satisfying the inequalities

$$\begin{aligned} |\phi - \phi_0 + 2n_1 v\pi| &< \pi, \\ |\phi + \phi_0 - 2\Omega + 2n_2 v\pi| &< \pi, \end{aligned} \quad (6.193)$$

respectively. The diffracted contribution $\tilde{\Pi}^d$ can be written as (TUZHILIN [1964]):

$$\begin{aligned} \tilde{\Pi}^d &= \{\Pi_d^{(1)}(-\pi - \phi + \phi_0) - \Pi_d^{(1)}(\pi - \phi + \phi_0)\} + \\ &\quad + \{\Pi_d^{(2)}(-\pi - \phi - \phi_0 + 2\Omega) - \Pi_d^{(2)}(\pi - \phi - \phi_0 + 2\Omega)\}, \end{aligned} \quad (6.194)$$

where

$$\begin{aligned} \Pi_d^{(1)}(\beta) &= \frac{1}{2\pi v} \int_0^\infty \frac{e^{ikR(it)}}{kR(it)} \left[\sin \frac{\beta}{v} \{ \hat{e}(\beta - \Phi) + (\cosh t - 1) [\hat{z} \wedge \hat{e}(\beta - \Phi) \wedge \hat{z}] \} - \right. \\ &\quad \left. - \sinh \frac{t}{v} \sinh t [\hat{z} \wedge \hat{e}(\beta - \Phi)] \right] \frac{dt}{\cosh(t/v) - \cos(\beta/v)} \end{aligned} \quad (6.195)$$

and $\Pi_d^{(2)}(\beta)$ is obtained from $\Pi_d^{(1)}(\beta)$ by replacing $\hat{e}(\beta - \Phi)$ by $\hat{e}(\beta + \Phi - 2\Omega)$. For β near $2nv\pi$, where n is an integer (TUZHILIN [1964]):

$$\Pi_d^{(1)}(\beta) \sim \sum_{m=0}^{\infty} \{ \pi_m^{(1)}(\beta, v) - a_m(\beta - 2nv\pi) \hat{e}(2nv\pi - \Phi) \} f_m + \hat{e}(2nv\pi - \Phi) \operatorname{sgn}(\beta - 2nv\pi) I, \quad (6.196)$$

with

$$\pi_0^{(1)} = A_0(\beta, v) \hat{e}(\beta - \Phi), \quad (6.197)$$

and, for $m \geq 1$,

$$\begin{aligned} \pi_m^{(1)} &= A_m(\beta, v) \hat{e}(\beta - \Phi) + A_{m-1}(\beta, v) [\hat{z} \wedge \hat{e}(\beta - \Phi) \wedge \hat{z}] + \\ &\quad + \frac{2}{2m-1} \frac{\partial A_{m-1}(\beta, v)}{\partial \beta} [\hat{z} \wedge \hat{e}(\beta - \Phi)]. \end{aligned} \quad (6.198)$$

In the above equations $a_m(\beta - 2nv\pi)$ and $A_m(\beta, v)$ are as defined in eqs. (6.25) through (6.28), and f_m and I are as given in eqs. (6.120) and (6.121) respectively. Similarly,

$$\begin{aligned} \Pi_d^{(2)}(\beta) &\sim \sum_{m=0}^{\infty} \{ \pi_m^{(2)}(\beta, v) - a_m(\beta - 2nv\pi) \hat{e}(2nv\pi + \Phi - 2\Omega) \} f_m + \\ &\quad + \hat{e}(2nv\pi + \Phi - 2\Omega) \operatorname{sgn}(\beta - 2nv\pi) I, \end{aligned} \quad (6.199)$$

where $\pi_m^{(2)}(\beta, \nu)$ is obtained from $\pi_m^{(1)}(\beta, \nu)$ by replacing $\hat{e}(\beta - \Phi)$ by $\hat{e}(\beta + \Phi - 2\Omega)$. Eqs. (6.196) and (6.199) describe the asymptotic behavior of $\Pi_d^{(1)}(\beta)$ or $\Pi_d^{(2)}(\beta)$ in the vicinity of the geometrical optics boundary specified by the integer n , and display the discontinuity in $\Pi_d^{(1)}(\beta)$ or $\Pi_d^{(2)}(\beta)$ necessary to compensate for the corresponding discontinuity in $\Pi^{g.o.}$.

Away from the boundary such that $|M| \gg 1$ in the expression for I given in eq. (6.121),

$$\Pi_d^{(1),(2)}(\beta) \sim \sum_{m=0}^{\infty} \pi_m^{(1),(2)}(\beta, \nu) f_m, \quad (6.200)$$

and from the leading term in this expansion,

$$\begin{aligned} \tilde{\Pi}^d \sim & \frac{e^{i(kR_1 + \frac{1}{2}\pi)}}{\sqrt{(2\pi k R_1)}} \frac{1}{k\sqrt{(\rho\rho_0)}} \frac{1}{\nu} \sin \frac{\pi}{\nu} \\ & \times \left\{ \frac{\hat{e}(\pi - \phi + \phi_0 - \Phi)}{\cos(\pi/\nu) - \cos[(\phi - \phi_0)/\nu]} + \frac{\hat{e}(\pi - \phi - \phi_0 + \Phi)}{\cos(\pi/\nu) + \cos[(2\pi - \phi - \phi_0)/\nu]} \right\}. \end{aligned} \quad (6.201)$$

Bibliography

- CARSLAW, H. S. [1920], Diffraction of Waves by a Wedge of any Angle, *Proc. London Math. Soc.* **18**, 291-306.
- FELSEN, L. B. [1957], Alternative Field Representations in Regions Bounded by Spheres, Cones and Planes, *IRE Trans. AP-5*, 109-121. Note that in eq. (54) the components \mathcal{I}_θ and \mathcal{I}_ϕ must be evaluated at the source point.
- GRANNEMANN, W. W. and R. B. WATSON [1955], Diffraction of Electromagnetic Waves by a Metallic Wedge of Acute Dihedral Angle, *J. Appl. Phys.* **26**, 392-393.
- HEDGE COCK, N. E. and A. B. McLAY [1959], Diffraction of Nearly Plane 3.2 cm EM Waves by 45° and 90° Conducting Wedges. Comparison with Theory, *IRE Trans. AP-7*, S284-S287.
- LEBEDEV, N. N. and I. P. SKAL'SKAYA [1960], Distribution of Current Densities on the Edges of an Ideally Conducting Rectangular Wedge Placed in the Field of a Plane Electromagnetic Wave, *Soviet Phys.* **4**, 841-845.
- MACDONALD, H. M. [1902], *Electric Waves*, Cambridge University Press, Cambridge, England.
- MACDONALD, H. M. [1915], A Class of Diffraction Problems, *Proc. London Math. Soc.* **14**, 410-427.
- MALYUZHINETS, G. D. and A. A. TUZHILIN [1963], The Electromagnetic Field excited by an Electric Dipole in a Wedge-Shaped Region, *Soviet Phys.-Doklady* **7**, 879-882 (English translation of *Dokl. Akad. Nauk SSSR* **146** (1962) 1039-1042). In eq. (8), replace -2ψ by 2ψ .
- OBERHETTINGER, F. [1954], Diffraction of Waves by a Wedge, *Commun. Pure Appl. Math.* **7**, 551-563. The first term on the right hand side of eq. (20) should be multiplied by $\frac{1}{2}$.
- OBERHETTINGER, F. [1956], On Asymptotic Series for Functions Occurring in the Theory of Diffraction of Waves by Wedges, *J. Math. Phys.* **34**, 245-255. The expression for $A_1(\delta, \alpha)$ in eq. (23) should be multiplied by $\frac{1}{2}$.
- OBERHETTINGER, F. [1958], On the Diffraction and Reflection of Waves and Pulses by Wedges and Corners, *J. Res. Nat. Bur. Std.* **61**, 343-365.
- PAULI, W. [1938], On Asymptotic Series for Functions in the Theory of Diffraction of Light, *Phys. Rev.* **54**, 924-931.
- REICHE, F. [1912], Die Beugung des Lichtes an einem ebenen, rechteckigen Keil von unendlicher Leitfähigkeit, *Ann. Physik* **37**, 131-156.

- ROW, R. V. [1953], Microwave Diffraction Measurements in a Parallel-Plate Region, *J. Appl. Phys.* **24**, 1448-1452.
- SOMMERFELD, A. [1896], Mathematische Theorie der Diffraction, *Math. Ann.* **47**, 317-374.
- TAI, C. T. [1954], A Glossary of Dyadic Green's Functions, Technical Report 46, Stanford Research Institute, Stanford, California. On p. 13, the factor λ in the denominator of the last term in the expression for M should be deleted.
- TEISSEYRE, R. [1955a], The Diffraction of a Dipole Field by a Perfectly Conducting Wedge, *Bull. Acad. Polon. Sci., Theor. Phys.* **3**, 157-172.
- TEISSEYRE, R. [1955b], General Solutions for the Diffraction of a Dipole Field by a Perfectly Conducting Wedge, *Bull. Acad. Polon. Sci., Theor. Phys.* **3**, 523-526.
- TEISSEYRE, R. [1955c], The Diffraction on a Conducting Wedge: The General Solutions for Dipole Field, *Nuovo Cimento* **2**, 869-871.
- TEISSEYRE, R. [1956], New Method of Solving the Diffraction Problem for a Dipole Field, *Bull. Acad. Polon. Sci., Theor. Phys.* **4**, 433-438.
- TILSTON, W. V. [1952], Contributions to the Theory of Antennas, Technical Report, Antenna Laboratory, Dept. of Electrical Engineering, University of Toronto, Toronto, Ontario (October). Due to normalization errors in both the θ and ϕ integrations, a factor $2\pi/\phi_0$ is omitted and $\Gamma(2m\pi/\phi_0 + 2n + 1)$ should be replaced by $(2m\pi/\phi_0 + 2n + 1)$ throughout. Further $mB\sin(m\pi\phi/\phi_0)$ should read $(m\pi B/\phi_0) \sin(m\pi\phi/\phi_0)$ whenever it appears (pp. 32, 33, 37). On the same pages replace C by $-C$ and on pp. 36, 37 replace A, B, C by $-A, -B, -C$ respectively. In eq. (3.48) multiply the right hand side by -1 , and in eq. (3.59) divide the summand by $n!((m\pi/\phi_0) + n) \cdot ((m\pi/\phi_0) + n + 1)$.
- TUZHILIN, A. A. [1963], New Representations of Diffraction Fields in Wedge-Shaped Regions with Ideal Boundaries, *Sov. Phys. -Acoustics* **9**, 168-172 (English translation of *Akust. Zh.* **9** (1963) 209-214. In the expression for $s(x)$ on p. 168, \pm should be replaced by \mp , and in the table on p. 169, the right hand side of the equation for I in the case of plane wave incidence should be multiplied by $-i$.
- TUZHILIN, A. A. [1964], Short-Wave Asymptotic Representation of Electromagnetic Diffraction Fields produced by Arbitrarily Oriented Dipoles in a Wedge-Shaped Region with Ideally Conducting Sides, Annotation of Reports of the Third All-Union Symposium on Wave Diffraction, *Acad. Sci. USSR*, 93-95 (in Russian). In the line following eq. (8), replace ϕ by Φ . The integral in eq. (10) should be multiplied by $\text{sgn}(\beta - 4n\Phi)$. In eq. (14) replace ϕ_n by $4n$, and in the line following, the first Π_m^1 should read Π_m^2 .
- WATSON, R. B. and C. W. HORTON [1950], On the Diffraction of a Radio Wave by a Conducting Wedge, *J. Appl. Phys.* **21**, 802-804.
- WIEGREFE, A. [1912], Über einige mehrwertige Lösungen der Wellengleichung $\Delta u + k^2 u = 0$ und ihre Anwendung in der Beugungstheorie, *Ann. Physik* **39**, 449-484.

CHAPTER 7

THE PARABOLIC CYLINDER

P. L. CHRISTIANSEN

The parabolic cylinder is the simplest shape of varying curvature for which the exterior and interior boundary value problems for the two-dimensional wave equation can be solved by separation of variables. As a consequence, the parabolic cylinder has been used for testing approximation techniques applicable to smooth cylinders of arbitrary shape. For low frequencies where the wave length is large compared to the focal distance, no specific results are available. The limit of the parabolic cylinder as the latus rectum tends to zero is the half plane.

7.1. Parabolic cylindrical geometry

The parabolic cylindrical coordinates (ξ, η, z) shown in Fig. 7.1 are related to the rectangular Cartesian coordinates (x, y, z) by the transformation

$$x = \frac{1}{2}(\xi^2 - \eta^2), \quad y = \xi\eta, \quad z = z, \quad (7.1)$$

where $-\infty < \xi < \infty$, $0 \leq \eta < \infty$ and $-\infty < z < \infty$. The z -axis is the focal line for all the parabolic cylindrical surfaces $|\xi| = \text{constant}$ and $\eta = \text{constant}$.

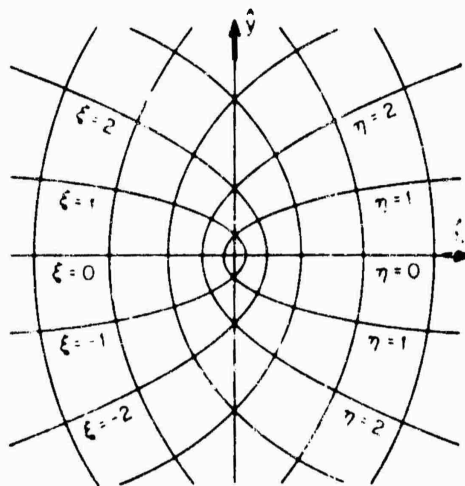


Fig. 7.1. Parabolic cylindrical geometry.

The scattering body is the parabolic cylinder with surface $\eta = \eta_1$, and the primary source is either a plane wave propagating in the plane perpendicular to the z -axis and

in a direction making an angle $\pi + \phi_0$ with the positive x -axis, or a line source parallel to the z -axis and located at $(\xi_0, \eta_0 \geq \eta_1)$. Interior plane wave incidence occurs when $\phi_0 = 0$. In this case the high frequency approximation can be obtained by application of the reciprocity theorem to the high frequency approximation of the solution for a line source placed at the focal line. Although the primary field due to a point source can be expressed in terms of parabolic cylinder functions (MAGNUS [1941-42]), the scattered field has not been studied in this case.

For convenience the following notation is introduced:

$$\xi_{>} = \begin{cases} \xi_0 & \text{for } |\xi_0| > |\xi| \\ \xi & \text{for } |\xi| > |\xi_0| \end{cases} \quad (7.2)$$

$$\xi_{<} = \begin{cases} \frac{\xi_{>}}{|\xi_{>}|} \xi_0 & \text{for } |\xi_0| < |\xi| \\ \frac{\xi_{>}}{|\xi_{>}|} \xi & \text{for } |\xi| < |\xi_0| \end{cases}, \quad (7.3)$$

$$\eta_{>} = \begin{cases} \eta & \text{for } \eta > \eta_0 \\ \eta_0 & \text{for } \eta_0 > \eta \end{cases} \quad (7.4)$$

$$\eta_{<} = \begin{cases} \eta & \text{for } \eta < \eta_0 \\ \eta_0 & \text{for } \eta_0 < \eta \end{cases} \quad (7.5)$$

The results are given in terms of the Weber-Hermite function $D_\nu(z)$ (ERDÉLYI et al. [1953]). If $\nu = n$ is a non-negative integer

$$D_n(z) = 2^{-\frac{1}{2}n} e^{-\frac{1}{2}z^2} H_n(2^{-\frac{1}{2}}z), \quad (7.6)$$

where $H_n(\tau)$ is the Hermite polynomial of n 'th degree. If $\nu = -n-1$ is a negative integer

$$D_{-n-1}(z) = \sqrt{2} e^{-\frac{1}{2}z^2} \frac{(-1)^n}{n!} e^{-\frac{1}{2}z^2} \frac{d^n}{dz^n} [e^{\frac{1}{2}z^2} F(2^{-\frac{1}{2}}e^{\frac{1}{2}z^2}z)], \quad (7.7)$$

where $F(\tau)$ is the Fresnel integral defined in the Introduction. For $z = 0$:

$$D_\nu(0) = \frac{\sqrt{\pi} 2^{\frac{1}{2}\nu}}{\Gamma(\frac{1}{2}(1-\nu))}, \quad D'_\nu(0) = -\frac{\sqrt{\pi} 2^{\frac{1}{2}(\nu+1)}}{\Gamma(-\frac{1}{2}\nu)}. \quad (7.8)$$

Numerical tables for Weber-Hermite functions $U(a, x)$, $V(a, x)$ and $W(a, x)$ are given by ABRAMOWITZ and STEGUN [1966]. The relationship between these functions and $D_\nu(z)$ is also found in this reference.

7.2. Exterior plane wave incidence

7.2.1. E-polarization

7.2.1.1. EXACT SOLUTIONS

For incidence at an angle ϕ_0 ($0 < \phi_0 \leq \pi$) with respect to the negative x -axis,

such that

$$E^i = \hat{z} \exp \{-ik(x \cos \phi_0 + y \sin \phi_0)\}, \quad (7.9)$$

a contour integral representation of the total electric field is:

$$E_z = \frac{i}{\sqrt{8\pi}} \frac{1}{\sin \frac{1}{2}\phi_0} \int_{c-i\infty}^{c+i\infty} (\cot \frac{1}{2}\phi_0)^v D_v(-\xi e^{-\frac{1}{2}i\pi} \sqrt{2k}) \left[D_{-v-1}(-\eta_1 e^{-\frac{1}{2}i\pi} \sqrt{2k}) - \frac{D_{-v-1}(-\eta_1 e^{-\frac{1}{2}i\pi} \sqrt{2k})}{D_{-v-1}(\eta_1 e^{-\frac{1}{2}i\pi} \sqrt{2k})} D_{-v-1}(\eta e^{-\frac{1}{2}i\pi} \sqrt{2k}) \right] \frac{dv}{\sin v\pi}, \quad (7.10)$$

where $-1 < c < 0$. An alternative representation of the total electric field is

$$E_z = \frac{e^{-\frac{1}{2}i\pi}}{\sqrt{\pi}} \exp \{-ik\rho \cos(\phi - \phi_0)\} F(-\sqrt{2k\rho} \cos \frac{1}{2}(\phi - \phi_0)) - \frac{i}{\sqrt{8\pi}} \frac{1}{\sin \frac{1}{2}\phi_0} \int_{c-i\infty}^{c+i\infty} (\cot \frac{1}{2}\phi_0)^v \times D_v(-\xi e^{-\frac{1}{2}i\pi} \sqrt{2k}) D_{-v-1}(\eta e^{-\frac{1}{2}i\pi} \sqrt{2k}) \frac{D_{-v-1}(-\eta_1 e^{-\frac{1}{2}i\pi} \sqrt{2k})}{D_{-v-1}(\eta_1 e^{-\frac{1}{2}i\pi} \sqrt{2k})} \frac{dv}{\sin v\pi}, \quad (7.11)$$

where $F(\tau)$ is the Fresnel integral defined in the Introduction. The circular cylindrical coordinates of the observation point are denoted by ρ and ϕ . On the surface $\eta = \eta_1$:

$$H_z = \frac{e^{-\frac{1}{2}i\pi} Y}{\sqrt{2\pi} \sin \frac{1}{2}\phi_0} \frac{1}{\sqrt{\{k(\xi^2 + \eta_1^2)\}}} \int_{c-i\infty}^{c+i\infty} (\cot \frac{1}{2}\phi_0)^v \frac{D_v(-\xi e^{-\frac{1}{2}i\pi} \sqrt{2k})}{D_{-v-1}(\eta_1 e^{-\frac{1}{2}i\pi} \sqrt{2k})} \Gamma(-v) dv. \quad (7.12)$$

In the far field ($\rho \rightarrow \infty$):

$$P = \frac{1}{8 \sin \frac{1}{2}\phi_0 \sin \frac{1}{2}\phi} \int_{c-i\infty}^{c+i\infty} (-\cot \frac{1}{2}\phi_0 \cot \frac{1}{2}\phi)^v \frac{D_{-v-1}(-\eta_1 e^{-\frac{1}{2}i\pi} \sqrt{2k})}{D_{-v-1}(\eta_1 e^{-\frac{1}{2}i\pi} \sqrt{2k})} \frac{dv}{\sin v\pi}. \quad (7.13)$$

For $\frac{1}{2}\pi < \phi_0 \leq \pi$ the total electric field can be written as a harmonic series (F'ANOV [1963]):

$$E_z = \frac{1}{\sin \frac{1}{2}\phi_0} \sum_{n=0}^{\infty} \frac{(i \cot \frac{1}{2}\phi_0)^n}{n!} L_n(-\xi e^{-\frac{1}{2}i\pi} \sqrt{2k}) \left[D_n(\eta e^{\frac{1}{2}i\pi} \sqrt{2k}) - \frac{D_n(\eta_1 e^{\frac{1}{2}i\pi} \sqrt{2k})}{D_{-n-1}(\eta_1 e^{-\frac{1}{2}i\pi} \sqrt{2k})} D_{-n-1}(\eta e^{-\frac{1}{2}i\pi} \sqrt{2k}) \right], \quad (7.14)$$

and, in particular, on the surface $\eta = \eta_1$:

$$H_z = \frac{\sqrt{2} e^{\frac{1}{2}i\pi} Y}{\sin \frac{1}{2}\phi_0} \frac{1}{\sqrt{\{k(\xi^2 + \eta_1^2)\}}} \sum_{n=0}^{\infty} \frac{(-\cot \frac{1}{2}\phi_0)^n}{n!} \frac{D_n(-\xi e^{-\frac{1}{2}i\pi} \sqrt{2k})}{D_{-n-1}(\eta_1 e^{-\frac{1}{2}i\pi} \sqrt{2k})}. \quad (7.15)$$

For axial incidence ($\phi_0 = \pi$) eq. (7.14) reduces to (LAMB [1906]):

$$E_z = e^{ikx} \left[1 - \frac{F(\eta_1 \sqrt{k})}{F(\eta_1 \sqrt{k})} \right]. \quad (7.16)$$

where $x = \frac{1}{2}(\xi^2 - \eta^2)$; in particular, on the surface $\eta = \eta_1$:

$$H_z = \frac{Y \exp \{ \frac{1}{2} i k (\xi^2 + \eta_1^2) \}}{\sqrt{\{k(\xi^2 + \eta_1^2)\}} F(\eta_1 \sqrt{k})} \quad (7.17)$$

and in the far field ($\rho \rightarrow \infty$) (KELLER et al. [1956]):

$$P = \frac{1}{\sqrt{\pi}} \frac{e^{-\frac{1}{2} i \pi}}{\sin \frac{1}{2} \phi} \frac{1}{F(\eta_1 \sqrt{k})}, \quad (7.18)$$

where $F(\tau)$ is the Fresnel integral defined in the Introduction. KELLER et al. [1956] have plotted a function related to the far field of eq. (7.18).

For $0 < \phi_0 < \frac{1}{2}\pi$, or $\phi_0 = \frac{1}{2}\pi$ with $-\xi > \eta$, the total electric field can be written as (RICE [1954]):

$$E_z = -\frac{1}{\sin \frac{1}{2} \phi_0} \sum_{r=1}^{\infty} \Gamma(-v_r) (-i \cot \frac{1}{2} \phi_0)^{v_r} D_{v_r}(-\xi e^{-\frac{1}{2} i \pi} \sqrt{2k}) \\ \times \frac{D_{v_r}(\eta_1 e^{\frac{1}{2} i \pi} \sqrt{2k})}{(\partial/\partial v) D_{-v-1}(\eta_1 e^{-\frac{1}{2} i \pi} \sqrt{2k})|_{v=v_r}} D_{-v_r-1}(\eta e^{-\frac{1}{2} i \pi} \sqrt{2k}), \quad (7.19)$$

where v_r ($r = 1, 2, \dots$) are solutions of

$$D_{-v_r-1}(\eta_1 e^{-\frac{1}{2} i \pi} \sqrt{2k}) = 0. \quad (7.20)$$

On the surface $\eta = \eta_1$:

$$H_z = \frac{\sqrt{2} e^{\frac{1}{2} i \pi} Y}{\sin \frac{1}{2} \phi_0} \frac{1}{\sqrt{\{k(\xi^2 + \eta_1^2)\}}} \sum_{r=1}^{\infty} \Gamma(-v_r) (\cot \frac{1}{2} \phi_0)^{v_r} \frac{D_{v_r}(-\xi e^{-\frac{1}{2} i \pi} \sqrt{2k})}{(\partial/\partial v) D_{-v-1}(\eta_1 e^{-\frac{1}{2} i \pi} \sqrt{2k})|_{v=v_r}}. \quad (7.21)$$

In the limiting case $\eta_1 = 0$:

$$(E_z)_{\eta_1=0} = \frac{1}{\sqrt{2\pi}} \{ D_0[(\xi \sin \frac{1}{2} \phi_0 - \eta \cos \frac{1}{2} \phi_0) e^{-\frac{1}{2} i \pi} \sqrt{2k}] \\ \times D_{-1}[(-\xi \cos \frac{1}{2} \phi_0 - \eta \sin \frac{1}{2} \phi_0) e^{-\frac{1}{2} i \pi} \sqrt{2k}] - \\ - D_0[(\xi \sin \frac{1}{2} \phi_0 + \eta \cos \frac{1}{2} \phi_0) e^{-\frac{1}{2} i \pi} \sqrt{2k}] \\ \times D_{-1}[(-\xi \cos \frac{1}{2} \phi_0 + \eta \sin \frac{1}{2} \phi_0) e^{-\frac{1}{2} i \pi} \sqrt{2k}] \}, \quad (7.22)$$

which is identical with the total electric field of eq. (8.10) for the half plane. For $\frac{1}{2}\pi < \phi_0 \leq \pi$, the total electric field can be written as a harmonic series:

$$(E_z)_{\eta_1=0} = \frac{1}{\sqrt{2\pi} \sin \frac{1}{2} \phi_0} \sum_{n=0}^{\infty} (-\cot \frac{1}{2} \phi_0)^n D_n(-\xi e^{-\frac{1}{2} i \pi} \sqrt{2k}) \\ \times [D_{-n-1}(-\eta e^{-\frac{1}{2} i \pi} \sqrt{2k}) - D_{-n-1}(\eta e^{-\frac{1}{2} i \pi} \sqrt{2k})], \quad (7.23)$$

and on the surface $\eta = 0$:

$$(H_z)_{\eta_1=0} = \frac{2e^{\frac{1}{2} i \pi} Y}{\sqrt{k}} \frac{1}{|\xi| \sin \frac{1}{2} \phi_0} \sum_{n=0}^{\infty} \frac{1}{\Gamma(\frac{1}{2}(n+1))} \left(\frac{-\cot \frac{1}{2} \phi_0}{\sqrt{2}} \right)^n D_n(-\xi e^{-\frac{1}{2} i \pi} \sqrt{2k}). \quad (7.24)$$

For $0 < \phi_0 < \frac{1}{2}\pi$, or $\phi_0 = \frac{1}{2}\pi$ with $-\xi > \eta$, the total electric field can be written as a harmonic series:

$$(E_z)_{\eta_1=0} = \sqrt{\frac{2}{\pi}} \frac{1}{\sin \frac{1}{2}\phi_0} \sum_{n=1}^{\infty} (\cot \frac{1}{2}\phi_0)^{-2n} D_{-2n}(-\xi e^{-\frac{1}{2}i\pi} \sqrt{2k}) D_{2n-1}(\eta e^{-\frac{1}{2}i\pi} \sqrt{2k}) \quad (7.25)$$

and on the surface $\eta = 0$:

$$(H_z)_{\eta_1=0} = -\frac{2e^{\frac{1}{2}i\pi} Y}{\sqrt{k|\xi|}} \frac{1}{\sin \frac{1}{2}\phi_0} \sum_{n=1}^{\infty} \Gamma(n+\frac{1}{2}) \left(\frac{i}{\sqrt{2}} \cot \frac{1}{2}\phi_0\right)^{-2n} D_{-2n}(-\xi e^{-\frac{1}{2}i\pi} \sqrt{2k}). \quad (7.26)$$

7.2.1.2. HIGH FREQUENCY APPROXIMATIONS

The complete asymptotic expansion of the scattered electric field for incidence in the direction of the positive x -axis ($\phi_0 = \pi$) is (KELLER et al. [1956]):

$$E_z^s \sim e^{ik(\rho-2\rho_1)} \sum_{n=0}^{\infty} (ik\rho_1)^{-n} \sum_{j=0}^n a_{j,n} \left[\frac{\rho_1}{\rho \sin^2 \frac{1}{2}\phi} \right]^{j+\frac{1}{2}}, \quad (7.27)$$

where:

$$a_{j,n} = \frac{1}{2}(j-\frac{1}{2})a_{j-1,n-1}, \quad (j > 0, n > 0); \quad (7.28)$$

$$a_{0,n} = -\sum_{j=1}^n a_{j,n}, \quad (n > 0); \quad a_{0,0} = -1, \quad (7.29)$$

$\rho = \frac{1}{2}(\xi^2 + \eta^2)$, and the focal length $\rho_1 = \frac{1}{2}\eta_1^2$. Explicitly, the first few terms of the series are

$$E_z^s \sim -\sqrt{\frac{\rho_1}{\rho}} \frac{1}{\sin \frac{1}{2}\phi} e^{ik(\rho-2\rho_1)} \left[1 + \frac{i}{4k\rho_1} \left(1 - \frac{\rho_1}{\rho} \frac{1}{\sin^2 \frac{1}{2}\phi} \right) + \dots \right], \quad (7.30)$$

of which the first term is the geometric optics approximation. KELLER et al. [1956] have plotted a function related to the far field which can be derived from eq. (7.30) when $\rho \rightarrow \infty$. The case of arbitrary incidence ($\phi_0 \neq \pi$) has been examined by HOCHSTADT [1959].

For arbitrary incidence and on the illuminated portion of the surface $\eta = \eta_1$, such that $(\xi \sin \phi_0 - \eta_1 \cos \phi_0) > (\eta_1/k)^{\frac{1}{2}}$ (IVANOV [1963]):

$$H_z \sim 2Y \cos \psi \exp \{ -ik(d_0)_z \} + \dots, \quad (7.31)$$

where the angle of incidence ψ and the distance $(d_0)_z$ in the exponent of the incident plane wave at the point of incidence are given by

$$\cos \psi = \frac{\eta_1 \cos \phi_0 - \xi \sin \phi_0}{\sqrt{(\xi^2 + \eta_1^2)}} \quad (7.32)$$

and

$$(d_0)_z = \xi \eta_1 \sin \phi_0 + \frac{1}{2}(\xi^2 - \eta_1^2) \cos \phi_0. \quad (7.33)$$

On the shadowed portion of the surface $\eta = \eta_1$, such that $(-\xi \sin \phi_0 + \eta_1 \cos \phi_0) > (\eta_1/k)^{1/2}$ (IVANOV [1960]):

$$H_\xi \sim \frac{2^{1/2} \exp \{ \frac{1}{6} i \pi \} \eta_1^{1/2} Y}{k^{1/2} \sqrt{\sin \phi_0 (\xi^2 + \eta_1^2)^{1/2}}} \exp \{ i k (s_{\eta_1 \cot \phi_0}^\xi - (d_0)_{\eta_1 \cot \phi_0}) \} \\ \times \sum_{r=1}^{\infty} \frac{1}{\text{Ai}'(-\alpha_r)} \exp \left\{ \exp \{ \frac{5}{6} i \pi \} (k \rho_1)^{1/2} \alpha_r \log \left(\frac{-\xi + \sqrt{(\xi^2 + \eta_1^2)}}{\eta_1} \cot \frac{1}{2} \phi_0 \right) \right\} + \dots, \quad (7.34)$$

where $\text{Ai}(\tau)$ is the Airy function defined in the Introduction. The phase of the incident plane wave at the point of tangential incidence is $-k(d_0)_{\eta_1 \cot \phi_0}$ and the arc length from the point of incidence to the observation point is $s_{\eta_1 \cot \phi_0}^\xi$. As a consequence

$$s_{\eta_1 \cot \phi_0}^\xi - (d_0)_{\eta_1 \cot \phi_0} = \rho_1 \log \left(\frac{-\xi + \sqrt{(\xi^2 + \eta_1^2)}}{\eta_1} \cot \frac{1}{2} \phi_0 \right) - \frac{1}{2} \xi \sqrt{(\xi^2 + \eta_1^2)}. \quad (7.35)$$

In eq. (7.34), $\eta_1^{1/2} \log [\eta_1^{-1} (-\xi + \sqrt{(\xi^2 + \eta_1^2)}) \cot \frac{1}{2} \phi_0]$ is the radius of curvature to the power $-\frac{1}{2}$ integrated along the path $s_{\eta_1 \cot \phi_0}^\xi$. An alternative representation, which is also valid in the transition region about the shadow boundary ($\eta = \eta_1$, $|\xi \sin \phi_0 - \eta_1 \cos \phi_0| \leq k^{-1/2} \eta_1^{1/2}$), is (IVANOV [1963]):

$$H_\xi \sim \left(\frac{2}{k} \right)^{1/2} \frac{i Y \eta_1^{1/2}}{\sqrt{\sin \phi_0 (\xi^2 + \eta_1^2)^{1/2}}} \exp \{ i k (s_{\eta_1 \cot \phi_0}^\xi - (d_0)_{\eta_1 \cot \phi_0}) \} \\ \times f \left[(k \rho_1)^{1/2} \log \left(\frac{-\xi + \sqrt{(\xi^2 + \eta_1^2)}}{\eta_1} \cot \frac{1}{2} \phi_0 \right) \right] + \dots, \quad (7.36)$$

where the modified Fock function $f(\tau)$ is described in the Introduction.

Near the cylinder surface ($\frac{1}{2} \eta^2 - \rho_1 \leq (\rho_1/k^2)^{1/2}$) and in the shadow region, such that $(-\xi \sin \phi_0 + \eta \cos \phi_0) > (\eta_1/k)^{1/2}$, the total electric field is (IVANOV [1960]):

$$E_z \sim \frac{\sqrt{\eta_1}}{\sqrt{\sin \phi_0 (\xi^2 + \eta_1^2)^{1/2}}} \exp \{ i k (s_{\eta_1 \cot \phi_0}^\xi - (d_0)_{\eta_1 \cot \phi_0}) \} \\ \times \sum_{r=1}^{\infty} [\text{Ai}'(-\alpha_r)]^{-2} \exp \left\{ \exp \{ \frac{5}{6} i \pi \} (k \rho_1)^{1/2} \alpha_r \log \left(\frac{-\xi + \sqrt{(\xi^2 + \eta_1^2)}}{\eta_1} \cot \frac{1}{2} \phi_0 \right) \right\} \\ \times \text{Ai} \{ -\alpha_r + e^{-i\pi} (k^2/\rho_1)^{1/2} (\frac{1}{2} \eta^2 - \rho_1) \} + \dots \quad (7.37)$$

An alternative representation, which is also valid in the transition region about the shadow boundary ($\frac{1}{2} \eta^2 - \rho_1 \leq (\rho_1/k^2)^{1/2}$, $|\xi \sin \phi_0 - \eta \cos \phi_0| \leq (\eta_1/k)^{1/2}$), is (IVANOV [1963]):

$$E_z \sim \frac{\sqrt{\eta_1}}{\sqrt{\sin \phi_0 (\xi^2 + \eta_1^2)^{1/2}}} \exp \{ i k (s_{\eta_1 \cot \phi_0}^\xi - (d_0)_{\eta_1 \cot \phi_0}) \} \\ \times V_1 \left[(k \rho_1)^{1/2} \log \left(\frac{-\xi + \sqrt{(\xi^2 + \eta_1^2)}}{\eta_1} \cot \frac{1}{2} \phi_0 \right), \left(\frac{k^2}{\rho_1} \right)^{1/2} (\frac{1}{2} \eta^2 - \rho_1), \infty \right] + \dots \quad (7.38)$$

where the function $V_1(\sigma, \tau, q)$ is described in the Introduction.

At observation points not asymptotically near the surface in the umbra region ($\xi\eta + \sqrt{(\xi^2 + \eta_1^2)(\eta^2 - \eta_1^2)} < \eta_1^2 \cot \phi_0$), the total electric field is (IVANOV [1963]):

$$E_z \sim \frac{\exp\{\frac{1}{2}i\pi\}}{\sqrt{2\pi k}} \frac{(k\rho_1)^{\frac{1}{2}}}{\sqrt{\sin \phi_0 [(\xi^2 + \eta_1^2)(\eta^2 - \eta_1^2)]^{\frac{1}{2}}}} \exp\{ik[s_{\eta_1 \cot \phi_0}^{\xi_d} - (d_0)_{\eta_1 \cot \phi_0} + (d)_{\xi_d}]\} \\ \times \sum_{r=1}^{\infty} [Ai'(-\alpha_r)]^{-2} \exp\left\{\exp\left\{\frac{5}{8}i\pi\right\}(k\rho_1)^{\frac{1}{2}}\alpha_r \right. \\ \left. \times \log\left(\frac{-\xi + \sqrt{(\xi^2 + \eta_1^2)}}{\eta + \sqrt{(\eta^2 - \eta_1^2)}} \cot \frac{1}{2}\phi_0\right)\right\} + \dots \quad (7.39)$$

The phase of the incident plane wave at the point of incidence is $-k(d_0)_{\eta_1 \cot \phi_0}$ and the arc length from here to the point where the diffracted ray leaves the surface is $s_{\eta_1 \cot \phi_0}^{\xi_d}$ where the ξ -coordinate of the diffraction point is

$$\xi_d = \frac{1}{\eta_1} (\xi\eta + \sqrt{(\xi^2 + \eta_1^2)(\eta^2 - \eta_1^2)}). \quad (7.40)$$

The distance from the diffraction point to the observation point is

$$(d)_{\xi_d} = \eta_1^{-2} \sqrt{(\xi^2 + \eta_1^2)(\eta^2 - \eta_1^2)} (\eta \sqrt{(\xi^2 + \eta_1^2)} + \xi \sqrt{(\eta^2 - \eta_1^2)}). \quad (7.41)$$

As a consequence

$$s_{\eta_1 \cot \phi_0}^{\xi_d} - (d_0)_{\eta_1 \cot \phi_0} + (d)_{\xi_d} = \\ = \rho_1 \log\left(\frac{-\xi + \sqrt{(\xi^2 + \eta_1^2)}}{\eta + \sqrt{(\eta^2 - \eta_1^2)}} \cot \frac{1}{2}\phi_0\right) - \frac{1}{2}\xi \sqrt{(\xi^2 + \eta_1^2)} + \frac{1}{2}\eta \sqrt{(\eta^2 - \eta_1^2)}. \quad (7.42)$$

In eq. (7.39),

$$\eta_1^{\frac{1}{2}} \log\left(\frac{-\xi + \sqrt{(\xi^2 + \eta_1^2)}}{\eta + \sqrt{(\eta^2 - \eta_1^2)}} \cot \frac{1}{2}\phi_0\right)$$

is the radius of curvature to the power $-\frac{1}{2}$ integrated along the path $s_{\eta_1 \cot \phi_0}^{\xi_d}$. An alternative representation, which is also valid in the penumbra region ($\xi\eta + \sqrt{(\xi^2 + \eta_1^2)(\eta^2 - \eta_1^2)} \approx \eta_1^2 \cot \phi_0$), is (IVANOV [1963]):

$$E_z \sim -e^{i\pi} \sqrt{\frac{2}{k}} \frac{(k\rho_1)^{\frac{1}{2}}}{\sqrt{\sin \phi_0 [(\xi^2 + \eta_1^2)(\eta^2 - \eta_1^2)]^{\frac{1}{2}}}} \exp\{ik[s_{\eta_1 \cot \phi_0}^{\xi_d} - (d_0)_{\eta_1 \cot \phi_0} + (d)_{\xi_d}]\} \\ \times \tilde{p}\left[(k\rho_1)^{\frac{1}{2}} \log\left(\frac{-\xi + \sqrt{(\xi^2 + \eta_1^2)}}{\eta + \sqrt{(\eta^2 - \eta_1^2)}} \cot \frac{1}{2}\phi_0\right)\right] + \dots \quad (7.43)$$

where the function $\tilde{p}(\tau)$ is described in the Introduction (see eq. (I.278)).

7.2.2. *H-polarization*

7.2.2.1. EXACT SOLUTIONS

For incidence at an angle ϕ_0 ($0 < \phi_0 \leq \pi$) with respect to the negative x -axis,

such that

$$H^i = \hat{z} \exp \{-ik(x \cos \phi_0 + y \sin \phi_0)\}, \quad (7.44)$$

a contour integral representation of the total magnetic field is:

$$H_z = \frac{i}{\sqrt{8\pi}} \frac{1}{\sin \frac{1}{2}\phi_0} \int_{c-i\infty}^{c+i\infty} (\cot \frac{1}{2}\phi_0)^v D_v(-\xi e^{-\frac{1}{2}i\pi} \sqrt{2k}) \left[D_{-v-1}(-\eta e^{-\frac{1}{2}i\pi} \sqrt{2k}) + \frac{D'_{-v-1}(-\eta_1 e^{-\frac{1}{2}i\pi} \sqrt{2k})}{D'_{-v-1}(\eta_1 e^{-\frac{1}{2}i\pi} \sqrt{2k})} D_{-v-1}(\eta e^{-\frac{1}{2}i\pi} \sqrt{2k}) \right] \frac{dv}{\sin v\pi}, \quad (7.45)$$

where $-1 < c < 0$. An alternative representation of the total magnetic field is

$$H_z = \frac{e^{-\frac{1}{2}i\pi}}{\sqrt{\pi}} \exp \{-ik\rho \cos(\phi - \phi_0)\} F(-2k\rho \cos \frac{1}{2}(\phi - \phi_0)) + \frac{i}{\sqrt{8\pi}} \frac{1}{\sin \frac{1}{2}\phi_0} \int_{c-i\infty}^{c+i\infty} (\cot \frac{1}{2}\phi_0)^v \times D_v(-\xi e^{-\frac{1}{2}i\pi} \sqrt{2k}) D_{-v-1}(\eta e^{-\frac{1}{2}i\pi} \sqrt{2k}) \frac{D'_{-v-1}(-\eta_1 e^{-\frac{1}{2}i\pi} \sqrt{2k})}{D'_{-v-1}(\eta_1 e^{-\frac{1}{2}i\pi} \sqrt{2k})} \frac{dv}{\sin v\pi}, \quad (7.46)$$

where $F(\tau)$ is the Fresnel integral defined in the Introduction. The circular cylindrical coordinates of the observation point are denoted by ρ and ϕ .

On the surface $\eta = \eta_1$:

$$H_z = \frac{i}{2\pi \sin \frac{1}{2}\phi_0} \int_{c-i\infty}^{c+i\infty} (\cot \frac{1}{2}\phi_0)^v \frac{D_v(-\xi e^{-\frac{1}{2}i\pi} \sqrt{2k})}{D'_{-v-1}(\eta_1 e^{-\frac{1}{2}i\pi} \sqrt{2k})} \Gamma(-v) dv. \quad (7.47)$$

In the far field ($\rho \rightarrow \infty$):

$$P = - \frac{1}{8 \sin \frac{1}{2}\phi_0 \sin \frac{1}{2}\phi} \int_{c-i\infty}^{c+i\infty} (-\cot \frac{1}{2}\phi_0 \cot \frac{1}{2}\phi)^v \frac{D'_{-v-1}(-\eta_1 e^{-\frac{1}{2}i\pi} \sqrt{2k})}{D'_{-v-1}(\eta_1 e^{-\frac{1}{2}i\pi} \sqrt{2k})} \frac{dv}{\sin v\pi}. \quad (7.48)$$

For $\frac{1}{2}\pi < \phi_0 \leq \pi$ the total magnetic field can be written as a harmonic series (IVANOV [1963]):

$$H_z = \frac{1}{\sin \frac{1}{2}\phi_0} \sum_{n=0}^{\infty} \frac{(i \cot \frac{1}{2}\phi_0)^n}{n!} D_n(-\xi e^{-\frac{1}{2}i\pi} \sqrt{2k}) \left[D_n(\eta e^{\frac{1}{2}i\pi} \sqrt{2k}) - i \frac{D'_n(\eta_1 e^{\frac{1}{2}i\pi} \sqrt{2k})}{D'_{-n-1}(\eta_1 e^{-\frac{1}{2}i\pi} \sqrt{2k})} D_{-n-1}(\eta e^{-\frac{1}{2}i\pi} \sqrt{2k}) \right], \quad (7.49)$$

and, in particular, on the surface $\eta = \eta_1$:

$$H_z = - \frac{1}{\sin \frac{1}{2}\phi_0} \sum_{n=0}^{\infty} \frac{(-\cot \frac{1}{2}\phi_0)^n}{n!} \frac{D_n(-\xi e^{-\frac{1}{2}i\pi} \sqrt{2k})}{D'_{-n-1}(\eta_1 e^{-\frac{1}{2}i\pi} \sqrt{2k})}. \quad (7.50)$$

For axial incidence ($\phi_0 = \pi$) eq. (7.49) reduces to (LAMB [1906]):

$$H_z = e^{ikx} \left[1 - \frac{F(\eta\sqrt{k})}{F(\eta_1\sqrt{k}) - \frac{i}{\eta_1\sqrt{k}} \exp(ik\eta_1^2)} \right], \quad (7.51)$$

where $x = \frac{1}{2}(\xi^2 - \eta^2)$; in particular, on the surface $\eta = \eta_1$:

$$H_z = \frac{1}{i\eta_1\sqrt{k}} \exp\{\frac{1}{2}ik(\xi^2 + \eta_1^2)\} \left[F(\eta_1\sqrt{k}) - \frac{i}{\eta_1\sqrt{k}} \exp(ik\eta_1^2) \right]^{-1} \quad (7.52)$$

and in the far field ($\rho \rightarrow \infty$) (KELLER et al. [1956]):

$$P = \frac{1}{2}\sqrt{\pi} \frac{e^{-\frac{1}{2}i\pi}}{\sin \frac{1}{2}\phi} \left[F(\eta_1\sqrt{k}) - \frac{i}{\eta_1\sqrt{k}} \exp(ik\eta_1^2) \right]^{-1}. \quad (7.53)$$

KELLER et al. [1956] have plotted a function related to the far field of eq. (7.53).

For $0 < \phi_0 < \frac{1}{2}\pi$, or $\phi_0 = \frac{1}{2}\pi$ with $-\xi > \eta$, the total magnetic field can be written as (RICE [1954]):

$$H_z = -\frac{i}{\sin \frac{1}{2}\phi_0} \sum_{r=1}^{\infty} \Gamma(-v'_r) (-i \cot \frac{1}{2}\phi_0)^{v'_r} D_{v'_r}(-\xi e^{-\frac{1}{2}i\pi} \sqrt{2k}) \\ \times \frac{D'_{v'_r}(\eta_1 e^{\frac{1}{2}i\pi} \sqrt{2k})}{(\partial/\partial v) D'_{-v-1}(\eta_1 e^{-\frac{1}{2}i\pi} \sqrt{2k})|_{v=v'_r}} D_{-v'_r-1}(\eta e^{-\frac{1}{2}i\pi} \sqrt{2k}), \quad (7.54)$$

where v'_r ($r = 1, 2, \dots$) are solutions of

$$D'_{-v'_r-1}(\eta_1 e^{-\frac{1}{2}i\pi} \sqrt{2k}) = 0. \quad (7.55)$$

On the surface $\eta = \eta_1$:

$$H_z = -\frac{1}{\sin \frac{1}{2}\phi_0} \sum_{r=1}^{\infty} \Gamma(-v'_r) (\cot \frac{1}{2}\phi_0)^{v'_r} \frac{D_{v'_r}(-\xi e^{-\frac{1}{2}i\pi} \sqrt{2k})}{(\partial/\partial v) D'_{-v-1}(\eta_1 e^{-\frac{1}{2}i\pi} \sqrt{2k})|_{v=v'_r}}. \quad (7.56)$$

In the limiting case $\eta_1 = 0$:

$$(H_z)_{\eta_1=0} = \frac{1}{\sqrt{2\pi}} \{ D_0[(\xi \sin \frac{1}{2}\phi_0 - \eta \cos \frac{1}{2}\phi_0) e^{-\frac{1}{2}i\pi} \sqrt{2k}] D_{-1}[(-\xi \cos \frac{1}{2}\phi_0 - \\ - \eta \sin \frac{1}{2}\phi_0) e^{-\frac{1}{2}i\pi} \sqrt{2k}] + D_0[(\xi \sin \frac{1}{2}\phi_0 + \eta \cos \frac{1}{2}\phi_0) e^{-\frac{1}{2}i\pi} \sqrt{2k}] \\ \times D_{-1}[(-\xi \cos \frac{1}{2}\phi_0 + \eta \sin \frac{1}{2}\phi_0) e^{-\frac{1}{2}i\pi} \sqrt{2k}] \}, \quad (7.57)$$

which is identical with the total magnetic field of eq. (8.28) for the half plane. For $\frac{1}{2}\pi < \phi_0 \leq \pi$ the total magnetic field can be written as a harmonic series:

$$(H_z)_{\eta_1=0} = \frac{1}{\sqrt{2\pi}} \frac{1}{\sin \frac{1}{2}\phi_0} \sum_{n=0}^{\infty} (-\cot \frac{1}{2}\phi_0)^n D_n(-\xi e^{-\frac{1}{2}i\pi} \sqrt{2k}) \\ \times [D_{-n-1}(-\eta e^{-\frac{1}{2}i\pi} \sqrt{2k}) + D_{-n-1}(\eta e^{-\frac{1}{2}i\pi} \sqrt{2k})] \quad (7.58)$$

and on the surface $\eta = 0$:

$$(H_z)_{\eta=0} = \frac{1}{\sin \frac{1}{2}\phi_0} \sum_{n=0}^{\infty} \frac{1}{\Gamma(\frac{1}{2}n+1)} \left(\frac{-\cot \frac{1}{2}\phi_0}{\sqrt{2}} \right)^n D_n(-\xi e^{-\frac{1}{2}i\pi} \sqrt{2k}). \quad (7.59)$$

For $0 < \phi_0 < \frac{1}{2}\pi$, or $\phi_0 = \frac{1}{2}\pi$ with $-\xi > \eta$, the total magnetic field can be written as a harmonic series:

$$(H_z)_{\eta=0} = \sqrt{\frac{2}{\pi}} \frac{1}{\sin \frac{1}{2}\phi_0} \sum_{n=1}^{\infty} (\cot \frac{1}{2}\phi_0)^{-2n+1} D_{-2n+1}(-\xi e^{-\frac{1}{2}i\pi} \sqrt{2k}) D_{2n-2}(\eta e^{-\frac{1}{2}i\pi} \sqrt{2k}) \quad (7.60)$$

and on the surface $\eta = 0$:

$$(H_z)_{\eta=0} = \frac{i}{\pi \sin \frac{1}{2}\phi_0} \sum_{n=1}^{\infty} \Gamma(n-\frac{1}{2}) \left(\frac{i}{\sqrt{2}} \cot \frac{1}{2}\phi_0 \right)^{-2n+1} D_{-2n+1}(-\xi e^{-\frac{1}{2}i\pi} \sqrt{2k}). \quad (7.61)$$

7.2.2.2. HIGH FREQUENCY APPROXIMATIONS

The complete asymptotic expansion of the scattered magnetic field for incidence in the direction of the positive x -axis ($\phi_0 = \pi$) is (KELLER et al. [1956]):

$$H_z^s \sim e^{ik(\rho-2\rho_1)} \sum_{n=0}^{\infty} (ik\rho_1)^{-n} \sum_{j=0}^n a_{j,n} \left[\frac{\rho_1}{\rho \sin^2 \frac{1}{2}\phi} \right]^{j+\frac{1}{2}}, \quad (7.62)$$

where:

$$a_{j,n} = \frac{1}{2}(j-\frac{1}{2})a_{j-1,n-1}, \quad (j > 0, n > 0); \quad (7.63)$$

$$a_{0,n} = \sum_{j=1}^n a_{j,n}, \quad (n > 0); \quad a_{0,0} = 1, \quad (7.64)$$

$\rho = \frac{1}{2}(\xi^2 + \eta^2)$ and the focal length $\rho_1 = \frac{1}{2}\eta_1^2$. Explicitly, the first few terms of the series are

$$H_z^s \sim \left[\frac{\rho_1}{\rho \sin^2 \frac{1}{2}\phi} - \frac{1}{\rho} \right] e^{ik(\rho-2\rho_1)} \left[1 - \frac{i}{4k\rho_1} \left(1 + \frac{\rho_1}{\rho} \frac{1}{\sin^2 \frac{1}{2}\phi} \right) + \dots \right], \quad (7.65)$$

of which the first term is the geometric optics approximation. KELLER et al. [1956] have plotted a function related to the far field which can be derived from eq. (7.65) when $\rho \rightarrow \infty$.

For arbitrary incidence and ϵ , the illuminated portion of the surface $\eta = \eta_1$, such that $(\xi \sin \phi_0 - \eta_1 \cos \phi_0) > (\eta_1 k)^{\frac{1}{2}}$ (IVANOV [1963]):

$$H_z \sim 2 \exp\{-ik(d_0)_z\} + \dots, \quad (7.66)$$

where the distance $(d_0)_z$ in the exponent of the incident plane wave at the point of incidence is given by

$$(d_0)_z = \xi \eta_1 \sin \phi_0 + \frac{1}{2}(\xi^2 - \eta_1^2) \cos \phi_0. \quad (7.67)$$

On the shadowed portion of the surface $\eta = \eta_1$, such that $(-\xi \sin \phi_0 + \eta_1 \cos \phi_0) > (\eta_1/k)^{1/2}$ (IVANOV [1960]):

$$H_z \sim \frac{\sqrt{\eta_1}}{\sqrt{\sin \phi_0 (\xi^2 + \eta_1^2)^{1/2}}} \exp \{ik[s_{\eta_1 \cot \phi_0}^{\xi} - (d_0)_{\eta_1 \cot \phi_0}]\} \\ \times \sum_{r=1}^{\infty} \frac{1}{\beta_r \text{Ai}(-\beta_r)} \exp \left\{ \exp \left\{ \frac{5}{6} i\pi \right\} (k\rho_1)^{1/2} \beta_r \log \left(\frac{-\xi + \sqrt{(\xi^2 + \eta_1^2)} \cot \frac{1}{2} \phi_0}{\eta_1} \right) \right\} + \dots, \quad (7.68)$$

where $\text{Ai}(\tau)$ is the Airy function defined in the Introduction. The phase of the incident plane wave at the point of tangential incidence is $-k(d_0)_{\eta_1 \cot \phi_0}$ and the arc length from the point of incidence to the observation point is $s_{\eta_1 \cot \phi_0}^{\xi}$. As a consequence

$$s_{\eta_1 \cot \phi_0}^{\xi} - (d_0)_{\eta_1 \cot \phi_0} = \rho_1 \log \left(\frac{-\xi + \sqrt{(\xi^2 + \eta_1^2)} \cot \frac{1}{2} \phi_0}{\eta_1} \right) - \frac{1}{2} \xi \sqrt{(\xi^2 + \eta_1^2)}. \quad (7.69)$$

In eq. (7.68), $\eta_1^{1/2} \log [\eta_1^{-1/2} (-\xi + \sqrt{(\xi^2 + \eta_1^2)}) \cot \frac{1}{2} \phi_0]$ is the radius of curvature to the power $-1/2$ integrated along the path $s_{\eta_1 \cot \phi_0}^{\xi}$. For $\phi_0 = \frac{1}{2}\pi$ (KELLER and LEVY [1959]):

$$H_z \sim \left[\frac{\eta_1}{\xi^2 + \eta_1^2} \right]^{1/2} \exp \{ik(s_{\eta_1}^{\xi} - (d_0)_{\eta_1})\} \sum_{r=1}^{\infty} \frac{1}{\beta_r \text{Ai}(-\beta_r)} \\ \times \exp \left\{ \exp \left\{ \frac{5}{6} i\pi \right\} (k\rho_1)^{1/2} \beta_r \log \frac{-\xi + \sqrt{(\xi^2 + \eta_1^2)}}{\eta_1} + \right. \\ \left. + \frac{1}{2} e^{i\pi} (k\rho_1)^{-1/2} \left[\frac{1}{2} \beta_r^2 \int_0^{\xi} (t^2 + \eta_1^2)^{-3/2} (8t^2 - 7\eta_1^2) dt + \frac{1}{\beta_r} \int_0^{\xi} \frac{dt}{\sqrt{(t^2 + \eta_1^2)}} \right] + \dots \right\} + \dots \quad (7.70)$$

An alternative representation, which is also valid in the transition region about the shadow boundary ($\eta = \eta_1$, $|\xi \sin \phi_0 - \eta_1 \cos \phi_0| \leq (\eta_1/k)^{1/2}$), is (IVANOV [1963]):

$$H_z \sim \frac{\sqrt{\eta_1}}{\sqrt{\sin \phi_0 (\xi^2 + \eta_1^2)^{1/2}}} \exp \{ik(s_{\eta_1 \cot \phi_0}^{\xi} - (d_0)_{\eta_1 \cot \phi_0})\} \\ \times g \left[(k\rho_1)^{1/2} \log \left(\frac{-\xi + \sqrt{(\xi^2 + \eta_1^2)} \cot \frac{1}{2} \phi_0}{\eta_1} \right) \right] + \dots \quad (7.71)$$

where the modified Fock function $g(\tau)$ is described in the Introduction.

Near the cylinder surface ($\frac{1}{2}\eta^2 - \rho_1 \leq (\rho_1/k^2)^{1/2}$) and in the shadow region, such that $(-\xi \sin \phi_0 + \eta \cos \phi_0) > (\eta_1/k)^{1/2}$, the total magnetic field is:

$$H_z \sim \frac{\sqrt{\eta_1}}{\sqrt{\sin \phi_0 (\xi^2 + \eta_1^2)^{1/2}}} \exp \{ik(s_{\eta_1 \cot \phi_0}^{\xi} - (d_0)_{\eta_1 \cot \phi_0})\} \\ \times \sum_{r=1}^{\infty} \frac{1}{\beta_r [\text{Ai}(-\beta_r)]^2} \exp \left\{ \exp \left\{ \frac{5}{6} i\pi \right\} (k\rho_1)^{1/2} \beta_r \log \left(\frac{-\xi + \sqrt{(\xi^2 + \eta_1^2)} \cot \frac{1}{2} \phi_0}{\eta_1} \right) \right\} \\ \times \text{Ai}(-\beta_r + e^{-i\pi} (k^2/\rho_1)^{1/2} (\frac{1}{2}\eta^2 - \rho_1)) + \dots \quad (7.72)$$

An alternative representation, which is also valid in the transition region about the shadow boundary $(\frac{1}{2}\eta^2 - \rho_1 \leq (\rho_1/k^2)^{\frac{1}{2}}, |\xi \sin \phi_0 - \eta \cos \phi_0| \leq (\eta_1/k)^{\frac{1}{2}})$, is (IVANOV [1963]):

$$H_z \sim \frac{\sqrt{\eta_1}}{\sqrt{\sin \phi_0 (\xi^2 + \eta_1^2)^{\frac{1}{2}}}} \exp \{ik(s_{\eta_1 \cot \phi_0}^{\xi} - (d_0)_{\eta_1 \cot \phi_0})\} \\ \times V_1 \left[(k\rho_1)^{\frac{1}{2}} \log \left(\frac{-\xi + \sqrt{(\xi^2 + \eta_1^2)}}{\eta_1} \cot \frac{1}{2}\phi_0 \right), \left(\frac{k^2}{\rho_1} \right)^{\frac{1}{2}} (\frac{1}{2}\eta^2 - \rho_1), 0 \right] + \dots, \quad (7.73)$$

where the function $V_1(\sigma, \tau, q)$ is described in the Introduction (see eq. (1.287)).

At observation points not asymptotically near the surface in the umbra region $(\xi\eta + \sqrt{(\xi^2 + \eta_1^2)(\eta^2 - \eta_1^2)}) < \eta_1^2 \cot \phi_0$, the total magnetic field is (IVANOV [1963]):

$$H_z \sim \frac{\exp \{ \frac{1}{2}i\pi \}}{\sqrt{2\pi k}} \frac{(k\rho_1)^{\frac{1}{2}}}{\sqrt{\sin \phi_0 [(\xi^2 + \eta_1^2)(\eta^2 - \eta_1^2)]^{\frac{1}{2}}}} \exp \{ik(s_{\eta_1 \cot \phi_0}^{\xi_d} - (d_0)_{\eta_1 \cot \phi_0} + (d)_{\xi_d})\} \\ \times \sum_{r=1}^{\infty} \frac{1}{\beta_r [\text{Ai}(-\beta_r)]^2} \exp \left\{ \exp \{ \frac{5}{6}i\pi \} (k\rho_1)^{\frac{1}{2}} \log \left(\frac{-\xi + \sqrt{(\xi^2 + \eta_1^2)}}{\eta + \sqrt{(\eta^2 - \eta_1^2)}} \cot \frac{1}{2}\phi_0 \right) \right\} + \dots \quad (7.74)$$

The phase of the incident plane wave at the point of incidence is $-k(d_0)_{\eta_1 \cot \phi_0}$ and the arc length from here to the point where the diffracted ray leaves the surface is $s_{\eta_1 \cot \phi_0}^{\xi_d}$ where the ξ -coordinate of the diffraction point is

$$\xi_d = \frac{1}{\eta_1} (\xi\eta + \sqrt{(\xi^2 + \eta_1^2)(\eta^2 - \eta_1^2)}). \quad (7.75)$$

The distance from the diffraction point to the observation point is

$$(d)_{\xi_d} = \eta_1^{-2} \sqrt{(\xi^2 + \eta_1^2)(\eta^2 - \eta_1^2)} \{ \eta \sqrt{(\xi^2 + \eta_1^2)} + \xi \sqrt{(\eta^2 - \eta_1^2)} \}. \quad (7.76)$$

As a consequence

$$s_{\eta_1 \cot \phi_0}^{\xi_d} - (d_0)_{\eta_1 \cot \phi_0} + (d)_{\xi_d} = \rho_1 \log \left(\frac{-\xi + \sqrt{(\xi^2 + \eta_1^2)}}{\eta + \sqrt{(\eta^2 - \eta_1^2)}} \cot \frac{1}{2}\phi_0 \right) - \\ - \frac{1}{2}\xi \sqrt{(\xi^2 + \eta_1^2)} + \frac{1}{2}\eta \sqrt{(\eta^2 - \eta_1^2)}. \quad (7.77)$$

In eq. (7.74),

$$\eta_1^{\frac{1}{2}} \log \left(\frac{-\xi + \sqrt{(\xi^2 + \eta_1^2)}}{\eta + \sqrt{(\eta^2 - \eta_1^2)}} \cot \frac{1}{2}\phi_0 \right)$$

is the radius of curvature to the power $-\frac{1}{2}$ integrated along the path $s_{\eta_1 \cot \phi_0}^{\xi_d}$. An alternative representation, which is also valid in the penumbra region $(\xi\eta + \sqrt{(\xi^2 + \eta_1^2)(\eta^2 - \eta_1^2)}) \approx \eta_1^2 \cot \phi_0$, is (IVANOV [1963]):

$$H_z \sim -e^{i\frac{1}{2}\pi} \int_0^{\frac{1}{2}} \frac{(k\rho_1)^{\frac{1}{2}}}{k \sqrt{\sin \phi_0 [(\xi^2 + \eta_1^2)(\eta^2 - \eta_1^2)]^{\frac{1}{2}}}} \exp \{ik(s_{\eta_1 \cot \phi_0}^{\xi_d} - (d_0)_{\eta_1 \cot \phi_0} + (d)_{\xi_d})\} \\ \times \tilde{q} \left[(k\rho_1)^{\frac{1}{2}} \log \left(\frac{-\xi + \sqrt{(\xi^2 + \eta_1^2)}}{\eta + \sqrt{(\eta^2 - \eta_1^2)}} \cot \frac{1}{2}\phi_0 \right) \right] + \dots \quad (7.78)$$

where the function $\tilde{q}(\tau)$ is described in the Introduction (see eq. (I.279)).

7.3. Exterior line sources

7.3.1. E-polarization

7.3.1.1. EXACT SOLUTIONS

For an exterior electric line source parallel to the axis z of the cylinder and located at $(\xi_0 \geq 0, \eta_0 > \eta_1)$, such that

$$E^i = 2H_0^{(1)}(kR), \quad (7.79)$$

a contour integral representation of the total electric field is (ROBIN [1964]):

$$E_z = \frac{1}{\pi} \int_{c-i\infty}^{c+i\infty} D_v(|\xi_0| e^{-\frac{1}{2}i\pi} \sqrt{2k}) D_{-v-1}(\eta_0 e^{-\frac{1}{2}i\pi} \sqrt{2k}) \frac{D_v(-\xi_0 e^{-\frac{1}{2}i\pi} \sqrt{2k})}{D_{-v-1}(\eta_1 e^{-\frac{1}{2}i\pi} \sqrt{2k})} \\ \times [D_{-v-1}(\eta_1 e^{-\frac{1}{2}i\pi} \sqrt{2k}) D_{-v-1}(-\eta_0 e^{-\frac{1}{2}i\pi} \sqrt{2k}) - \\ - D_{-v-1}(-\eta_1 e^{-\frac{1}{2}i\pi} \sqrt{2k}) D_{-v-1}(\eta_0 e^{-\frac{1}{2}i\pi} \sqrt{2k})] \frac{dv}{\sin v\pi}, \quad (7.80)$$

where $-1 < c < 0$. On the surface $\eta = \eta_1$:

$$H_z = -\frac{2e^{\frac{1}{2}i\pi}}{\pi} \frac{Y}{\sqrt{\{\pi k(\xi^2 + \eta_1^2)\}}} \int_{c-i\infty}^{c+i\infty} D_v(|\xi_0| e^{-\frac{1}{2}i\pi} \sqrt{2k}) D_{-v-1}(\eta_0 e^{-\frac{1}{2}i\pi} \sqrt{2k}) \\ \times \frac{D_v(-\xi_0 e^{-\frac{1}{2}i\pi} \sqrt{2k})}{D_{-v-1}(\eta_1 e^{-\frac{1}{2}i\pi} \sqrt{2k})} \Gamma(-v) dv. \quad (7.81)$$

The far field amplitude for the total electric field can be obtained from eq. (7.80) upon letting $\rho \rightarrow \infty$. The result is identical to the plane wave solution given in eq. (7.10) with ξ , η and $\cos \frac{1}{2}\phi_0$ replaced with ξ_0 , η_0 and $|\cos \frac{1}{2}\phi|$, respectively.

In the particular case $|\xi_0| - \xi_0 < \eta_0 - \eta_1$, the total electric field can be written as a harmonic series:

$$E_z = -\frac{2i}{\pi} \sum_{n=0}^{\infty} (-1)^n D_n(|\xi_0| e^{-\frac{1}{2}i\pi} \sqrt{2k}) D_{-n-1}(\eta_0 e^{-\frac{1}{2}i\pi} \sqrt{2k}) \frac{D_n(-\xi_0 e^{-\frac{1}{2}i\pi} \sqrt{2k})}{D_{-n-1}(\eta_1 e^{-\frac{1}{2}i\pi} \sqrt{2k})} \\ \times [D_{-n-1}(\eta_1 e^{-\frac{1}{2}i\pi} \sqrt{2k}) D_{-n-1}(-\eta_0 e^{-\frac{1}{2}i\pi} \sqrt{2k}) - \\ - D_{-n-1}(-\eta_1 e^{-\frac{1}{2}i\pi} \sqrt{2k}) D_{-n-1}(\eta_0 e^{-\frac{1}{2}i\pi} \sqrt{2k})], \quad (7.82)$$

and on the surface $\eta = \eta_1$:

$$H_z = \frac{4e^{-\frac{1}{2}i\pi} Y}{\sqrt{\{\pi k(\xi^2 + \eta_1^2)\}}} \sum_{n=0}^{\infty} \frac{(-1)^n}{n!} D_n(|\xi_0| e^{-\frac{1}{2}i\pi} \sqrt{2k}) D_{-n-1}(\eta_0 e^{-\frac{1}{2}i\pi} \sqrt{2k}) \\ \times \frac{D_n(-\xi_0 e^{-\frac{1}{2}i\pi} \sqrt{2k})}{D_{-n-1}(\eta_1 e^{-\frac{1}{2}i\pi} \sqrt{2k})}. \quad (7.83)$$

Alternatively, in the case $|\xi_>| - \xi_< > \eta_> + \eta_< - 2\eta_1$, the total electric field can be written as the series (ROBIN [1964]):

$$E_z = -2i \sum_{r=1}^{\infty} D_{v_r}(|\xi_>| e^{-\frac{1}{2}i\pi} \sqrt{2k}) D_{-v_r-1}(\eta_> e^{-\frac{1}{2}i\pi} \sqrt{2k}) D_{v_r}(-\xi_< e^{-\frac{1}{2}i\pi} \sqrt{2k}) \\ \times D_{-v_r-1}(\eta_< e^{-\frac{1}{2}i\pi} \sqrt{2k}) \frac{D_{-v_r-1}(-\eta_1 e^{-\frac{1}{2}i\pi} \sqrt{2k})}{(\partial/\partial v) D_{-v-1}(\eta_1 e^{-\frac{1}{2}i\pi} \sqrt{2k})|_{v=v_r}} \frac{1}{\sin v_r \pi}, \quad (7.84)$$

where v_r is defined in eq. (7.20). On the surface $\eta = \eta_1$:

$$H_z = \frac{4e^{-\frac{1}{2}i\pi} Y}{\sqrt{\{\pi k(\xi^2 + \eta_1^2)\}}} \sum_{r=1}^{\infty} D_{v_r}(|\xi_>| e^{-\frac{1}{2}i\pi} \sqrt{2k}) D_{-v_r-1}(\eta_0 e^{-\frac{1}{2}i\pi} \sqrt{2k}) \\ \times \frac{D_{v_r}(-\xi_< e^{-\frac{1}{2}i\pi} \sqrt{2k})}{(\partial/\partial v) D_{-v-1}(\eta_1 e^{-\frac{1}{2}i\pi} \sqrt{2k})|_{v=v_r}} \Gamma(-v_r). \quad (7.85)$$

In the limiting case $\eta_1 = 0$ (ROBIN [1964]):

$$(E_z)_{\eta_1=0} = \frac{1}{\pi} \int_{c-i\infty}^{c+i\infty} D_v(|\xi_>| e^{-\frac{1}{2}i\pi} \sqrt{2k}) D_{-v-1}(\eta_> e^{-\frac{1}{2}i\pi} \sqrt{2k}) D_v(-\xi_< e^{-\frac{1}{2}i\pi} \sqrt{2k}) \\ \times [D_{-v-1}(-\eta_< e^{-\frac{1}{2}i\pi} \sqrt{2k}) - D_{-v-1}(\eta_< e^{-\frac{1}{2}i\pi} \sqrt{2k})] \frac{dv}{\sin v\pi}, \quad (7.86)$$

which is an alternative representation of the total electric field of eq. (8.46) for the half plane. On the surface $\eta = 0$:

$$(H_z)_{\eta_1=0} = \frac{2e^{\frac{1}{2}i\pi} Y}{|\xi|} \sqrt{\frac{2}{\pi k}} \int_{c-i\infty}^{c+i\infty} D_v(|\xi_>| e^{-\frac{1}{2}i\pi} \sqrt{2k}) D_{-v-1}(\eta_0 e^{-\frac{1}{2}i\pi} \sqrt{2k}) \\ \times D_v(-\xi_< e^{-\frac{1}{2}i\pi} \sqrt{2k}) \frac{2^{-\frac{1}{2}v}}{\Gamma(\frac{1}{2}(v+1)) \sin v\pi} dv. \quad (7.87)$$

In the particular case $|\xi_>| - \xi_< < \eta_> - \eta_<$, the total electric field can be written as a harmonic series:

$$(E_z)_{\eta_1=0} = -\frac{2i}{\pi} \sum_{n=0}^{\infty} (-1)^n D_n(|\xi_>| e^{-\frac{1}{2}i\pi} \sqrt{2k}) D_{-n-1}(\eta_> e^{-\frac{1}{2}i\pi} \sqrt{2k}) \\ \times D_n(-\xi_< e^{-\frac{1}{2}i\pi} \sqrt{2k}) [D_{-n-1}(-\eta_< e^{-\frac{1}{2}i\pi} \sqrt{2k}) - D_{-n-1}(\eta_< e^{-\frac{1}{2}i\pi} \sqrt{2k})], \quad (7.88)$$

and on the surface $\eta = 0$:

$$(H_z)_{\eta_1=0} = \frac{4e^{-\frac{1}{2}i\pi} Y}{|\xi|} \left\{ \frac{2}{\pi k} \sum_{n=0}^{\infty} \left(-\frac{2}{\xi} \right)^{-n} D_n(|\xi_>| e^{-\frac{1}{2}i\pi} \sqrt{2k}) \right. \\ \left. \times D_{-n-1}(\eta_0 e^{-\frac{1}{2}i\pi} \sqrt{2k}) D_n(-\xi_< e^{-\frac{1}{2}i\pi} \sqrt{2k}) \right\}. \quad (7.89)$$

Alternatively, in the case $|\xi_>| - \xi_< > \eta_> + \eta_<$, the total electric field can be written

as the harmonic series (ROBIN [1964]):

$$(E_z)_{\eta_1=0} = -\frac{4i}{\pi} \sum_{n=1}^{\infty} D_{-2n}(|\xi_0| e^{-\frac{1}{2}i\pi} \sqrt{2k}) D_{2n-1}(\eta_0 e^{-\frac{1}{2}i\pi} \sqrt{2k}) \\ \times D_{-2n}(-\xi_0 e^{-\frac{1}{2}i\pi} \sqrt{2k}) D_{2n-1}(\eta_0 e^{-\frac{1}{2}i\pi} \sqrt{2k}), \quad (7.90)$$

and on the surface $\eta = 0$:

$$(H_z)_{\eta_1=0} = -\frac{4e^{-\frac{1}{2}i\pi} Y}{\xi_1} \sqrt{\frac{2}{\pi k}} \sum_{n=1}^{\infty} \frac{2^n}{\Gamma(\frac{1}{2}-n)} D_{-2n}(|\xi_0| e^{-\frac{1}{2}i\pi} \sqrt{2k}) \\ \times D_{2n-1}(\eta_0 e^{-\frac{1}{2}i\pi} \sqrt{2k}) D_{-2n}(-\xi_0 e^{-\frac{1}{2}i\pi} \sqrt{2k}). \quad (7.91)$$

7.3.1.2. HIGH FREQUENCY APPROXIMATIONS

For a line source off the surface and in the umbra region

$$\xi_0 \eta_0 \pm \sqrt{\{(\xi_0^2 + \eta_1^2)(\eta_0^2 - \eta_1^2)\}} \lesssim \xi \mp \sqrt{\{(\xi^2 + \eta_1^2)(\eta^2 - \eta_1^2)\}}, \quad \text{for } \xi_0 \lesssim \xi,$$

the total electric field is (KELLER [1956]):

$$E_z \sim \frac{e^{-\frac{1}{2}i\pi}}{\pi k} \frac{(k\rho_1)^{\frac{1}{2}}}{[(\xi_0^2 + \eta_1^2)(\eta_0^2 - \eta_1^2)(\xi^2 + \eta_1^2)(\eta^2 - \eta_1^2)]^{\frac{1}{4}}} \exp\{ik[s_{\xi_1}^{\xi_0} + (d_0)_{\xi_1} + (d)_{\xi_d}]\} \\ \times \sum_{r=1}^{\infty} [\text{Ai}'(-\alpha_r)]^{-2} \\ \times \exp\left\{\exp\left\{\frac{5}{6}i\pi\right\}(k\rho_1)^{\frac{1}{2}}\alpha_r \log\left[\left(\frac{\mp \xi_0 + \sqrt{(\xi_0^2 + \eta_1^2)}}{\eta_0 + \sqrt{(\eta_0^2 - \eta_1^2)}}\right)\left(\frac{\pm \xi + \sqrt{(\xi^2 + \eta_1^2)}}{\eta + \sqrt{(\eta^2 - \eta_1^2)}}\right)\right]\right\} + \dots \quad (7.92)$$

with the upper or lower signs according as $\xi_0 \lesssim \xi$ respectively. The focal length is $\rho_1 = \frac{1}{2}\eta_1^2$. The Airy function $\text{Ai}(\tau)$ is defined in the Introduction. The arc length from the point of incidence where the incoming ray strikes the surface tangentially to the point where the diffracted ray leaves the surface is $s_{\xi_1}^{\xi_0}$, where the ξ -coordinates of the point of incidence and the diffraction point are

$$\xi_i = \frac{1}{\eta_1} (\xi_0 \eta_0 \pm \sqrt{\{(\xi_0^2 + \eta_1^2)(\eta_0^2 - \eta_1^2)\}}) \quad (7.93)$$

and

$$\xi_d = \frac{1}{\eta_1} (\xi \mp \sqrt{\{(\xi^2 + \eta_1^2)(\eta^2 - \eta_1^2)\}}), \quad (7.94)$$

respectively. The distance from the source point to the point of incidence is

$$(d_0)_{\xi_1} = \eta_1^{-2} \sqrt{\{(\xi_0^2 + \eta_1^2)(\eta_0^2 - \eta_1^2)\}} \{\eta_0 \sqrt{(\xi_0^2 + \eta_1^2)} \pm \xi_0 \sqrt{(\eta_0^2 - \eta_1^2)}\}. \quad (7.95)$$

This distance from the diffraction point to the observation point is

$$(d)_{\xi_d} = \eta_1^{-2} \sqrt{\{(\xi^2 + \eta_1^2)(\eta^2 - \eta_1^2)\}} \{\eta \sqrt{(\xi^2 + \eta_1^2)} \mp \xi \sqrt{(\eta^2 - \eta_1^2)}\}. \quad (7.96)$$

As a consequence

$$s_{\xi_1}^{\xi_0} + (d_0)_{\xi_1} + (a)_{\xi_1} = \rho_1 \log \left[\left(\frac{\mp \xi_0 + \sqrt{(\xi_0^2 + \eta_1^2)}}{\eta_0 + \sqrt{(\eta_0^2 - \eta_1^2)}} \right) \left(\frac{\pm \xi + \sqrt{(\xi^2 + \eta_1^2)}}{\eta + \sqrt{(\eta^2 - \eta_1^2)}} \right) \right] \mp \\ \mp \frac{1}{2} \xi_0 \sqrt{(\xi_0^2 + \eta_1^2)} + \frac{1}{2} \eta_0 \sqrt{(\eta_0^2 - \eta_1^2)} \pm \frac{1}{2} \xi \sqrt{(\xi^2 + \eta_1^2)} + \frac{1}{2} \eta \sqrt{(\eta^2 - \eta_1^2)}. \quad (7.97)$$

In eq. (7.92),

$$\eta_1^{\frac{1}{2}} \log \left[\left(\frac{\mp \xi_0 + \sqrt{(\xi_0^2 + \eta_1^2)}}{\eta_0 + \sqrt{(\eta_0^2 - \eta_1^2)}} \right) \left(\frac{\pm \xi + \sqrt{(\xi^2 + \eta_1^2)}}{\eta + \sqrt{(\eta^2 - \eta_1^2)}} \right) \right]$$

is the radius of curvature to the power $-\frac{1}{2}$ integrated along the path $s_{\xi_1}^{\xi_0}$.

7.3.2. *H*-polarization

7.3.2.1. EXACT SOLUTIONS

For an exterior magnetic line source parallel to the axis z of the cylinder and located at $(\xi_0 \geq 0, \eta_0 > \eta_1)$, such that

$$H^i = 2H_0^{(1)}(kR), \quad (7.98)$$

a contour integral representation of the total magnetic field is (ROBIN [1964]):

$$H_z = \frac{1}{\pi} \int_{c-i\infty}^{c+i\infty} D_v(|\xi_0| e^{-\frac{1}{2}i\pi} \sqrt{2k}) D_{-v-1}(\eta_0 e^{-\frac{1}{2}i\pi} \sqrt{2k}) \frac{D_v(-\xi_0 e^{-\frac{1}{2}i\pi} \sqrt{2k})}{D'_{-v-1}(\eta_1 e^{-\frac{1}{2}i\pi} \sqrt{2k})} \\ \times [D'_{-v-1}(\eta_1 e^{-\frac{1}{2}i\pi} \sqrt{2k}) D_{-v-1}(-\eta_0 e^{-\frac{1}{2}i\pi} \sqrt{2k}) + D'_{-v-1}(-\eta_1 e^{-\frac{1}{2}i\pi} \sqrt{2k}) \\ \times D_{-v-1}(\eta_0 e^{-\frac{1}{2}i\pi} \sqrt{2k})] \frac{dv}{\sin v\pi}, \quad (7.99)$$

where $-1 < c < 0$. On the surface $\eta = \eta_1$:

$$H_z = \frac{1}{\pi} \int_{c-i\infty}^{c+i\infty} D_v(|\xi_0| e^{-\frac{1}{2}i\pi} \sqrt{2k}) D_{-v-1}(\eta_0 e^{-\frac{1}{2}i\pi} \sqrt{2k}) \\ \times \frac{D_v(-\xi_0 e^{-\frac{1}{2}i\pi} \sqrt{2k})}{D'_{-v-1}(\eta_1 e^{-\frac{1}{2}i\pi} \sqrt{2k})} \Gamma(-v) dv. \quad (7.100)$$

The far field amplitude for the total magnetic field can be obtained from eq. (7.99) upon letting $\rho \rightarrow \infty$. The result is identical to the plane wave solution given in eq. (7.45) with ξ, η and $\cos \frac{1}{2}\phi_0$ replaced with ξ_0, η_0 and $|\cos \frac{1}{2}\phi|$, respectively.

In the particular case $|\xi_0| - \xi_0 < \eta_0 - \eta_1$, the total magnetic field can be written as a harmonic series:

$$H_z = \frac{-2i}{\pi} \sum_{n=0}^{\infty} (-1)^n D_n(|\xi_0| e^{-\frac{1}{2}i\pi} \sqrt{2k}) D_{-n-1}(\eta_0 e^{-\frac{1}{2}i\pi} \sqrt{2k}) \frac{D_n(-\xi_0 e^{-\frac{1}{2}i\pi} \sqrt{2k})}{D'_{-n-1}(\eta_1 e^{-\frac{1}{2}i\pi} \sqrt{2k})} \\ \times [D'_{-n-1}(\eta_1 e^{-\frac{1}{2}i\pi} \sqrt{2k}) D_{-n-1}(-\eta_0 e^{-\frac{1}{2}i\pi} \sqrt{2k}) + \\ + D'_{-n-1}(-\eta_1 e^{-\frac{1}{2}i\pi} \sqrt{2k}) D_{-n-1}(\eta_0 e^{-\frac{1}{2}i\pi} \sqrt{2k})], \quad (7.101)$$

and on the surface $\eta = \eta_1$:

$$H_z = \gamma \sqrt{\frac{2}{\pi}} \sum_{n=0}^{\infty} \frac{(-1)^n}{n!} D_n(|\xi_>| e^{-\frac{1}{2}i\pi} \sqrt{2k}) D_{-n-1}(\eta_0 e^{-\frac{1}{2}i\pi} \sqrt{2k}) \frac{D_n(-\xi_< e^{-\frac{1}{2}i\pi} \sqrt{2k})}{D'_{-n-1}(\eta_1 e^{-\frac{1}{2}i\pi} \sqrt{2k})}. \quad (7.102)$$

Alternatively, in the case $|\xi_>| - \xi_< > \eta_> + \eta_< - 2\eta_1$, the total magnetic field can be written as the series (ROBIN [1964]):

$$H_z = 2i \sum_{r=1}^{\infty} D_{v'_r}(|\xi_>| e^{-\frac{1}{2}i\pi} \sqrt{2k}) D_{-v'_r-1}(\eta_> e^{-\frac{1}{2}i\pi} \sqrt{2k}) D_{v'_r}(-\xi_< e^{-\frac{1}{2}i\pi} \sqrt{2k}) \\ \times D_{-v'_r-1}(\eta_< e^{-\frac{1}{2}i\pi} \sqrt{2k}) \frac{D'_{-v'_r-1}(-\eta_1 e^{-\frac{1}{2}i\pi} \sqrt{2k})}{(\partial/\partial v) D'_{-v-1}(\eta_1 e^{-\frac{1}{2}i\pi} \sqrt{2k})|_{v=v'_r}} \frac{1}{\sin v'_r \pi}, \quad (7.103)$$

where v'_r is defined in eq. (7.55). On the surface $\eta = \eta_1$:

$$H_z = 2i \sqrt{\frac{2}{\pi}} \sum_{r=1}^{\infty} D_{v'_r}(|\xi_>| e^{-\frac{1}{2}i\pi} \sqrt{2k}) D_{-v'_r-1}(\eta_0 e^{-\frac{1}{2}i\pi} \sqrt{2k}) \\ \times \frac{D_{v'_r}(-\xi_< e^{-\frac{1}{2}i\pi} \sqrt{2k})}{(\partial/\partial v) D'_{-v-1}(\eta_1 e^{-\frac{1}{2}i\pi} \sqrt{2k})|_{v=v'_r}} \Gamma(-v'_r). \quad (7.104)$$

In the limiting case $\eta_1 = 0$ (ROBIN [1964]):

$$(H_z)_{\eta_1=0} = \frac{1}{\pi} \int_{c-i\infty}^{c+i\infty} D_v(|\xi_>| e^{-\frac{1}{2}i\pi} \sqrt{2k}) D_{-v-1}(\eta_> e^{-\frac{1}{2}i\pi} \sqrt{2k}) D_v(-\xi_< e^{-\frac{1}{2}i\pi} \sqrt{2k}) \\ \times [D_{-v-1}(-\eta_< e^{-\frac{1}{2}i\pi} \sqrt{2k}) + D_{-v-1}(\eta_< e^{-\frac{1}{2}i\pi} \sqrt{2k})] \frac{dv}{\sin v\pi}, \quad (7.105)$$

which is an alternative representation of the total magnetic field of eq. (8.68) for the half plane. On the surface $\eta = 0$:

$$(H_z)_{\eta_1=0} = \sqrt{\frac{2}{\pi}} \int_{c-i\infty}^{c+i\infty} D_v(|\xi_>| e^{-\frac{1}{2}i\pi} \sqrt{2k}) D_{-v-1}(\eta_0 e^{-\frac{1}{2}i\pi} \sqrt{2k}) \\ \times D_v(-\xi_< e^{-\frac{1}{2}i\pi} \sqrt{2k}) \frac{2^{-\frac{1}{2}v}}{\Gamma(\frac{1}{2}v+1)} \frac{dv}{\sin v\pi}, \quad (7.106)$$

In the particular case $|\xi_>| - \xi_< < \eta_> - \eta_<$, the total magnetic field can be written as a harmonic series:

$$(H_z)_{\eta_1=0} = \frac{-2i}{\pi} \sum_{n=0}^{\infty} (-1)^n D_n(|\xi_>| e^{-\frac{1}{2}i\pi} \sqrt{2k}) D_{-n-1}(\eta_> e^{-\frac{1}{2}i\pi} \sqrt{2k}) D_n(-\xi_< e^{-\frac{1}{2}i\pi} \sqrt{2k}) \\ \times [D_{-n-1}(-\eta_< e^{-\frac{1}{2}i\pi} \sqrt{2k}) + D_{-n-1}(\eta_< e^{-\frac{1}{2}i\pi} \sqrt{2k})], \quad (7.107)$$

and on the surface $\eta = 0$:

$$(H_z)_{\eta_1=0} = -2i \sqrt{\frac{2}{\pi}} \sum_{n=0}^{\infty} \frac{(-\sqrt{2})^{-n}}{\Gamma(\frac{1}{2}n+1)} D_n(|\xi_>| e^{-\frac{1}{2}i\pi} \sqrt{2k}) D_{-n-1}(\eta_0 e^{-\frac{1}{2}i\pi} \sqrt{2k}) \\ \times D_n(-\xi_< e^{-\frac{1}{2}i\pi} \sqrt{2k}). \quad (7.108)$$

Alternatively, in the case $|\xi_>| - \xi_< > \eta_> + \eta_<$, the total magnetic field can be written as the harmonic series (ROBIN [1964]):

$$(H_z)_{\eta_1=0} = \frac{-4i}{\pi} \sum_{n=1}^{\infty} D_{-2n+1}(|\xi_>| e^{-\frac{1}{2}i\pi} \sqrt{2k}) D_{2n-2}(\eta_> e^{-\frac{1}{2}i\pi} \sqrt{2k}) \\ \times D_{-2n+1}(-\xi_< e^{-\frac{1}{2}i\pi} \sqrt{2k}) D_{2n-2}(\eta_< e^{-\frac{1}{2}i\pi} \sqrt{2k}), \quad (7.109)$$

and on the surface $\eta = 0$:

$$(H_z)_{\eta_1=0} = \frac{-2i}{\sqrt{\pi}} \sum_{n=1}^{\infty} \frac{2^n}{\Gamma(\frac{1}{2}-n)} D_{-2n+1}(|\xi_>| e^{-\frac{1}{2}i\pi} \sqrt{2k}) D_{2n-2}(\eta_0 e^{-\frac{1}{2}i\pi} \sqrt{2k}) \\ \times D_{-2n+1}(-\xi_< e^{-\frac{1}{2}i\pi} \sqrt{2k}). \quad (7.110)$$

7.3.2.2. HIGH FREQUENCY APPROXIMATIONS

For a line source off the surface and in the umbra region

$$\xi_0 \eta_0 \pm \sqrt{(\xi_0^2 + \eta_1^2)(\eta_0^2 - \eta_1^2)} \leq \xi \eta \mp \sqrt{(\xi^2 + \eta_1^2)(\eta^2 - \eta_1^2)}, \quad \text{for } \xi_0 \leq \xi,$$

the total magnetic field is (KELLER [1956]):

$$H_z \sim \frac{e^{-\frac{1}{2}i\pi}}{\pi k} \frac{(k\rho_1)^{\frac{1}{2}}}{[(\xi_0^2 + \eta_1^2)(\eta_0^2 - \eta_1^2)(\xi^2 + \eta_1^2)(\eta^2 - \eta_1^2)]^{\frac{1}{4}}} \exp \{ik[s_{\xi_1}^{\xi_0} + (d_0)_{\xi_1} + (d)_{\xi_d}]\} \\ \times \sum_{r=1}^{\infty} \frac{1}{\beta_r [\text{Ai}(-\beta_r)]^2} \exp \left\{ \exp \left\{ \frac{5}{6}i\pi \right\} (k\rho_1)^{\frac{1}{2}} \beta_r \log \left[\left(\frac{\mp \xi_0 + \sqrt{(\xi_0^2 + \eta_1^2)}}{\eta_0 + \sqrt{(\eta_0^2 - \eta_1^2)}} \right) \right. \right. \\ \left. \left. \times \left(\frac{\pm \xi + \sqrt{(\xi^2 + \eta_1^2)}}{\eta + \sqrt{(\eta^2 - \eta_1^2)}} \right) \right] \right\} + \dots \quad (7.111)$$

with the upper or lower signs according as $\xi_0 \leq \xi$ respectively. The focal length is $\rho_1 = \frac{1}{2}\eta_1^2$. The Airy function $\text{Ai}(\tau)$ is defined in the Introduction. The arc length from the point of incidence where the incoming ray strikes the surface tangentially to the point where the diffracted ray leaves the surface is $s_{\xi_1}^{\xi_0}$, where the ξ -coordinates of the point of incidence and the diffraction point are

$$\xi_1 = \frac{1}{\eta_1} (\xi_0 \eta_0 \pm \sqrt{(\xi_0^2 + \eta_1^2)(\eta_0^2 - \eta_1^2)}) \quad (7.112)$$

and

$$\xi_d = \frac{1}{\eta_1} (\xi \eta \mp \sqrt{(\xi^2 + \eta_1^2)(\eta^2 - \eta_1^2)}), \quad (7.113)$$

respectively. The distance from the source point to the point of incidence is

$$(d_0)_{\xi_1} = \eta_1^{-2} \sqrt{(\xi_0^2 + \eta_1^2)(\eta_0^2 - \eta_1^2)} \{ \eta_0 \sqrt{(\xi_0^2 + \eta_1^2)} \pm \xi_0 \sqrt{(\eta_0^2 - \eta_1^2)} \}. \quad (7.114)$$

The distance from the diffraction point to the observation point is

$$(d)_{\xi_d} = \eta_1^{-2} \sqrt{(\xi^2 + \eta_1^2)(\eta^2 - \eta_1^2)} \{ \eta \sqrt{(\xi^2 + \eta_1^2)} \mp \xi \sqrt{(\eta^2 - \eta_1^2)} \}. \quad (7.115)$$

As a consequence

$$s_{\xi_1}^{\xi_0} + (d_0/\xi_1 + (d)_{\xi_0}) = \rho_1 \log \left[\left(\frac{\mp \xi_0 + \sqrt{(\xi_0^2 + \eta_1^2)}}{\eta_0 + \sqrt{(\eta_0^2 - \eta_1^2)}} \right) \left(\frac{\pm \xi + \sqrt{(\xi^2 + \eta_1^2)}}{\eta + \sqrt{(\eta^2 - \eta_1^2)}} \right) \right] \mp \\ \mp \frac{1}{2} \xi_0 \sqrt{(\xi_0^2 + \eta_1^2)} + \frac{1}{2} \eta_0 \sqrt{(\eta_0^2 - \eta_1^2)} \pm \frac{1}{2} \xi \sqrt{(\xi^2 + \eta_1^2)} + \frac{1}{2} \eta \sqrt{(\eta^2 - \eta_1^2)}. \quad (7.116)$$

In eq. (7.111),

$$\eta_1^{\frac{1}{2}} \log \left[\left(\frac{\mp \xi_0 + \sqrt{(\xi_0^2 + \eta_1^2)}}{\eta_0 + \sqrt{(\eta_0^2 - \eta_1^2)}} \right) \left(\frac{\pm \xi + \sqrt{(\xi^2 + \eta_1^2)}}{\eta + \sqrt{(\eta^2 - \eta_1^2)}} \right) \right]$$

is the radius of curvature to the power $-\frac{1}{2}$ integrated along the path $s_{\xi_1}^{\xi_0}$.

7.4. Interior line sources

7.4.1. E-polarization

7.4.1.1. EXACT SOLUTIONS

For an interior electric line source parallel to the axis z of the cylinder and located at $(\xi_0 \geq 0, \eta_0 < \eta_1)$, such that

$$E^i = 2H_0^{(1)}(kR), \quad (7.117)$$

a contour integral representation of the total electric field is (HOCHSTADT [1957]):

$$E_z = \frac{1}{\pi} \int_{c_1 - i\infty}^{c_1 + i\infty} D_\nu(|\xi| e^{-\frac{1}{2}i\pi} \sqrt{2k}) \\ \times [D_{-\nu-1}(\eta_0 e^{-\frac{1}{2}i\pi} \sqrt{2k}) D_{-\nu-1}(-\eta_1 e^{-\frac{1}{2}i\pi} \sqrt{2k}) - D_{-\nu-1}(-\eta_0 e^{-\frac{1}{2}i\pi} \sqrt{2k}) \\ \times D_{-\nu-1}(\eta_1 e^{\frac{1}{2}i\pi} \sqrt{2k})] \{ [D_{-\nu-1}(\eta_1 e^{-\frac{1}{2}i\pi} \sqrt{2k}) + D_{-\nu-1}(-\eta_1 e^{-\frac{1}{2}i\pi} \sqrt{2k})] \\ \times [D_{-\nu-1}(\eta_1 e^{-\frac{1}{2}i\pi} \sqrt{2k}) - D_{-\nu-1}(-\eta_1 e^{-\frac{1}{2}i\pi} \sqrt{2k})] \}^{-1} \\ \times \{ D_\nu(\xi_0 e^{-\frac{1}{2}i\pi} \sqrt{2k}) [D_{-\nu-1}(-\eta_0 e^{-\frac{1}{2}i\pi} \sqrt{2k}) D_{-\nu-1}(\eta_1 e^{-\frac{1}{2}i\pi} \sqrt{2k}) - \\ - D_{-\nu-1}(\eta_0 e^{-\frac{1}{2}i\pi} \sqrt{2k}) D_{-\nu-1}(-\eta_1 e^{-\frac{1}{2}i\pi} \sqrt{2k})] + \\ + D_\nu(-\xi_0 e^{-\frac{1}{2}i\pi} \sqrt{2k}) [D_{-\nu-1}(\eta_0 e^{-\frac{1}{2}i\pi} \sqrt{2k}) \\ \times D_{-\nu-1}(\eta_1 e^{-\frac{1}{2}i\pi} \sqrt{2k}) - D_{-\nu-1}(-\eta_0 e^{-\frac{1}{2}i\pi} \sqrt{2k}) D_{-\nu-1}(-\eta_1 e^{-\frac{1}{2}i\pi} \sqrt{2k})] \} \frac{d\nu}{\sin \nu\pi}, \quad (7.118)$$

where $-\frac{1}{2} < c_1 < 0$. On the surface $\eta = \eta_1$:

$$H_z = \frac{2e^{\frac{1}{2}i\pi}}{\pi} \frac{Y}{\sqrt{\{\pi k(\xi^2 + \eta_1^2)\}}} \int_{c_1 - i\infty}^{c_1 + i\infty} D_\nu(|\xi| e^{-\frac{1}{2}i\pi} \sqrt{2k}) \{ [D_{-\nu-1}(\eta_1 e^{-\frac{1}{2}i\pi} \sqrt{2k}) + \\ + D_{-\nu-1}(-\eta_1 e^{-\frac{1}{2}i\pi} \sqrt{2k})] [D_{-\nu-1}(\eta_1 e^{-\frac{1}{2}i\pi} \sqrt{2k}) - D_{-\nu-1}(-\eta_1 e^{-\frac{1}{2}i\pi} \sqrt{2k})] \}^{-1} \\ \times \{ D_\nu(\xi_0 e^{-\frac{1}{2}i\pi} \sqrt{2k}) [D_{-\nu-1}(-\eta_0 e^{-\frac{1}{2}i\pi} \sqrt{2k}) D_{-\nu-1}(\eta_1 e^{-\frac{1}{2}i\pi} \sqrt{2k}) - \\ - D_{-\nu-1}(\eta_0 e^{-\frac{1}{2}i\pi} \sqrt{2k}) D_{-\nu-1}(-\eta_1 e^{-\frac{1}{2}i\pi} \sqrt{2k})] +$$

$$+ D_\nu(-\xi_< e^{-\frac{1}{2}i\pi}\sqrt{2k})[D_{-\nu-1}(\eta_0 e^{-\frac{1}{2}i\pi}\sqrt{2k})D_{-\nu-1}(\eta_1 e^{-\frac{1}{2}i\pi}\sqrt{2k}) - D_{-\nu-1}(-\eta_0 e^{-\frac{1}{2}i\pi}\sqrt{2k})D_{-\nu-1}(-\eta_1 e^{-\frac{1}{2}i\pi}\sqrt{2k})]\Gamma(-\nu)d\nu. \quad (7.119)$$

In the particular case where the two conditions $|\xi_>| + \xi_< < \eta_> + \eta_<$ and $|\xi_>| - \xi_< < \eta_> - \eta_<$ are both fulfilled, the total electric field can be written as a harmonic series:

$$E_z = \frac{-2i}{\pi} \sum_{n=0}^{\infty} (-1)^n D_n(|\xi_>| e^{-\frac{1}{2}i\pi}\sqrt{2k}) \{ [D_{-n-1}(\eta_1 e^{-\frac{1}{2}i\pi}\sqrt{2k}) + D_{-n-1}(-\eta_1 e^{-\frac{1}{2}i\pi}\sqrt{2k})] \times [D_{-n-1}(\eta_1 e^{-\frac{1}{2}i\pi}\sqrt{2k}) - D_{-n-1}(-\eta_1 e^{-\frac{1}{2}i\pi}\sqrt{2k})] \}^{-1} \times [D_{-n-1}(\eta_> e^{-\frac{1}{2}i\pi}\sqrt{2k})D_{-n-1}(-\eta_1 e^{-\frac{1}{2}i\pi}\sqrt{2k}) - D_{-n-1}(-\eta_> e^{-\frac{1}{2}i\pi}\sqrt{2k})D_{-n-1}(\eta_1 e^{-\frac{1}{2}i\pi}\sqrt{2k})] \times \{ D_n(\xi_< e^{-\frac{1}{2}i\pi}\sqrt{2k})[D_{-n-1}(-\eta_< e^{-\frac{1}{2}i\pi}\sqrt{2k})D_{-n-1}(\eta_1 e^{-\frac{1}{2}i\pi}\sqrt{2k}) - D_{-n-1}(\eta_< e^{-\frac{1}{2}i\pi}\sqrt{2k})D_{-n-1}(-\eta_1 e^{-\frac{1}{2}i\pi}\sqrt{2k})] + D_n(-\xi_< e^{-\frac{1}{2}i\pi}\sqrt{2k}) \times [D_{-n-1}(\eta_< e^{-\frac{1}{2}i\pi}\sqrt{2k})D_{-n-1}(\eta_1 e^{-\frac{1}{2}i\pi}\sqrt{2k}) - D_{-n-1}(-\eta_< e^{-\frac{1}{2}i\pi}\sqrt{2k})D_{-n-1}(-\eta_1 e^{-\frac{1}{2}i\pi}\sqrt{2k})] \}, \quad (7.120)$$

which is a generalization of a result by GRINBERG et al. [1957], and on the surface $\eta = \eta_1$:

$$H_z = - \frac{4e^{-\frac{1}{2}i\pi}Y}{\sqrt{\pi k(\xi^2 + \eta_1^2)}} \sum_{n=0}^{\infty} \frac{(-1)^n}{n!} D_n(|\xi_>| e^{-\frac{1}{2}i\pi}\sqrt{2k}) \{ [D_{-n-1}(\eta_1 e^{-\frac{1}{2}i\pi}\sqrt{2k}) + D_{-n-1}(-\eta_1 e^{-\frac{1}{2}i\pi}\sqrt{2k})] [D_{-n-1}(\eta_1 e^{-\frac{1}{2}i\pi}\sqrt{2k}) - D_{-n-1}(-\eta_1 e^{-\frac{1}{2}i\pi}\sqrt{2k})] \}^{-1} \times \{ D_n(\xi_< e^{-\frac{1}{2}i\pi}\sqrt{2k}) [D_{-n-1}(-\eta_0 e^{-\frac{1}{2}i\pi}\sqrt{2k})D_{-n-1}(\eta_1 e^{-\frac{1}{2}i\pi}\sqrt{2k}) - D_{-n-1}(\eta_0 e^{-\frac{1}{2}i\pi}\sqrt{2k})D_{-n-1}(-\eta_1 e^{-\frac{1}{2}i\pi}\sqrt{2k})] + D_n(-\xi_< e^{-\frac{1}{2}i\pi}\sqrt{2k}) \times [D_{-n-1}(\eta_0 e^{-\frac{1}{2}i\pi}\sqrt{2k})D_{-n-1}(\eta_1 e^{-\frac{1}{2}i\pi}\sqrt{2k}) - D_{-n-1}(-\eta_0 e^{-\frac{1}{2}i\pi}\sqrt{2k})D_{-n-1}(-\eta_1 e^{-\frac{1}{2}i\pi}\sqrt{2k})] \}. \quad (7.121)$$

An alternative representation of the total electric field of eq. (7.118) is:

$$E_z = \frac{e^{-\frac{1}{2}i\pi}}{\sqrt{\pi k}} \sum_{r=1}^{\infty} D_{\mu_r}(|\xi_>| e^{-\frac{1}{2}i\pi}\sqrt{2k}) [D_{-\mu_r-1}(\eta_> e^{-\frac{1}{2}i\pi}\sqrt{2k}) + D_{-\mu_r-1}(-\eta_> e^{-\frac{1}{2}i\pi}\sqrt{2k})] \times [D_{\mu_r}(\xi_< e^{-\frac{1}{2}i\pi}\sqrt{2k}) + D_{\mu_r}(-\xi_< e^{-\frac{1}{2}i\pi}\sqrt{2k})] \times [D_{-\mu_r-1}(\eta_< e^{-\frac{1}{2}i\pi}\sqrt{2k}) + D_{-\mu_r-1}(-\eta_< e^{-\frac{1}{2}i\pi}\sqrt{2k})] \times \left\{ \int_0^{\eta_1} [D_{-\mu_r-1}(\eta e^{-\frac{1}{2}i\pi}\sqrt{2k}) + D_{-\mu_r-1}(-\eta e^{-\frac{1}{2}i\pi}\sqrt{2k})]^2 d\eta \right\}^{-1} \Gamma(-\mu_r), \quad (7.122)$$

where μ_r ($r = 1, 2, \dots$) are solutions of

$$D_{-\mu_r-1}(\eta_1 e^{-\frac{1}{2}i\pi}\sqrt{2k}) + D_{-\mu_r-1}(-\eta_1 e^{-\frac{1}{2}i\pi}\sqrt{2k}) = 0; \quad (7.123)$$

all solutions have $\text{Re } \mu_r = -\frac{1}{2}$ (MAGNUS [1940, 1941-42]). On the surface $\eta = \eta_1$:

$$H_z = \frac{2Y}{k\sqrt{(\xi^2 + \eta_1^2)}} \sum_{r=1}^{\infty} D_{\mu_r}(|\xi| e^{-\frac{1}{2}i\pi} \sqrt{2k}) \\ \times [D_{-\mu_r-1}(\eta_0 e^{-\frac{1}{2}i\pi} \sqrt{2k}) + D_{-\mu_r-1}(-\eta_0 e^{-\frac{1}{2}i\pi} \sqrt{2k})] \\ \times [D_{\mu_r}(\xi e^{-\frac{1}{2}i\pi} \sqrt{2k}) + D_{\mu_r}(-\xi e^{-\frac{1}{2}i\pi} \sqrt{2k})] \left\{ D_{-\mu_r-1}(\eta_1 e^{-\frac{1}{2}i\pi} \sqrt{2k}) \right. \\ \left. \times \int_0^{\eta_1} [D_{-\mu_r-1}(\eta e^{-\frac{1}{2}i\pi} \sqrt{2k}) + D_{-\mu_r-1}(-\eta e^{-\frac{1}{2}i\pi} \sqrt{2k})]^2 d\eta \right\}^{-1} \frac{\Gamma(-\mu_r)}{\Gamma(1+\mu_r)}. \quad (7.124)$$

7.4.1.2. HIGH FREQUENCY APPROXIMATIONS

The complete asymptotic expansion of the scattered electric field when the line source is at the focal line ($\xi_0 = \eta_0 = 0$) has been examined by KELLER et al. [1956]. Explicitly, the first term of the series is

$$E_z^s \sim -\sqrt{\frac{2}{\pi k}} \frac{e^{-\frac{1}{2}i\pi}}{\sqrt{\{y^2/(4\rho_1) + \rho_1\}}} e^{ik(x+2\rho_1)} + \dots, \quad (7.125)$$

which is the geometric optics approximation. The focal length is $\rho_1 = \frac{1}{2}\eta_1^2$. The more general problem of a line source in the focal plane off the focal line has been considered by HOCHSTADT [1957] and EPSTEIN [1956].

7.4.2. H-polarization

7.4.2.1. EXACT SOLUTIONS

For an interior magnetic line source parallel to the axis z of the cylinder and located at ($\xi_0 \geq 0, \eta_0 < \eta_1$), such that

$$H^i = \hat{z} H_0^{(1)}(kR), \quad (7.126)$$

a contour integral representation of the total magnetic field is (HOCHSTADT [1957]):

$$H_z = -\frac{1}{\pi} \int_{c_1-i\infty}^{c_1+i\infty} D_\nu(|\xi| e^{-\frac{1}{2}i\pi} \sqrt{2k}) [D_{-\nu-1}(\eta_0 e^{-\frac{1}{2}i\pi} \sqrt{2k}) D'_{-\nu-1}(-\eta_1 e^{-\frac{1}{2}i\pi} \sqrt{2k}) + \\ + D_{-\nu-1}(-\eta_0 e^{-\frac{1}{2}i\pi} \sqrt{2k}) D'_{-\nu-1}(\eta_1 e^{-\frac{1}{2}i\pi} \sqrt{2k})] \\ \times \{ [D'_{-\nu-1}(\eta_1 e^{-\frac{1}{2}i\pi} \sqrt{2k}) - D'_{-\nu-1}(-\eta_1 e^{-\frac{1}{2}i\pi} \sqrt{2k})] \\ \times [D'_{-\nu-1}(\eta_1 e^{-\frac{1}{2}i\pi} \sqrt{2k}) + D'_{-\nu-1}(-\eta_1 e^{-\frac{1}{2}i\pi} \sqrt{2k})] \}^{-1} \\ \times \{ D_\nu(\xi e^{-\frac{1}{2}i\pi} \sqrt{2k}) [D_{-\nu-1}(-\eta_0 e^{-\frac{1}{2}i\pi} \sqrt{2k}) D'_{-\nu-1}(\eta_1 e^{-\frac{1}{2}i\pi} \sqrt{2k}) + \\ + D_{-\nu-1}(\eta_0 e^{-\frac{1}{2}i\pi} \sqrt{2k}) D'_{-\nu-1}(-\eta_1 e^{-\frac{1}{2}i\pi} \sqrt{2k})] + \\ + D_\nu(-\xi e^{-\frac{1}{2}i\pi} \sqrt{2k}) [D_{-\nu-1}(\eta_0 e^{-\frac{1}{2}i\pi} \sqrt{2k}) D'_{-\nu-1}(\eta_1 e^{-\frac{1}{2}i\pi} \sqrt{2k}) + \\ + D_{-\nu-1}(-\eta_0 e^{-\frac{1}{2}i\pi} \sqrt{2k}) D'_{-\nu-1}(-\eta_1 e^{-\frac{1}{2}i\pi} \sqrt{2k})] \} \frac{d\nu}{\sin \nu\pi}. \quad (7.127)$$

where $-\frac{1}{2} < c_1 < 0$. On the surface $\eta = \eta_1$:

$$\begin{aligned}
 H_z = & -\frac{1}{\pi} \int_{c_1-i\infty}^{c_1+i\infty} D_v(|\xi| e^{-\frac{1}{2}i\pi} \sqrt{2k}) \\
 & \times \{ [D'_{-v-1}(\eta_1 e^{-\frac{1}{2}i\pi} \sqrt{2k}) - D'_{-v-1}(-\eta_1 e^{-\frac{1}{2}i\pi} \sqrt{2k})] \\
 & \times [D'_{-v-1}(\eta_1 e^{-\frac{1}{2}i\pi} \sqrt{2k}) + D'_{-v-1}(-\eta_1 e^{-\frac{1}{2}i\pi} \sqrt{2k})] \}^{-1} \\
 & \times \{ D_v(\xi e^{-\frac{1}{2}i\pi} \sqrt{2k}) [D_{-v-1}(-\eta_0 e^{-\frac{1}{2}i\pi} \sqrt{2k}) D'_{-v-1}(\eta_1 e^{-\frac{1}{2}i\pi} \sqrt{2k}) + \\
 & + D_{-v-1}(\eta_0 e^{-\frac{1}{2}i\pi} \sqrt{2k}) D'_{-v-1}(-\eta_1 e^{-\frac{1}{2}i\pi} \sqrt{2k})] + \\
 & + D_v(-\xi e^{-\frac{1}{2}i\pi} \sqrt{2k}) [D_{-v-1}(\eta_0 e^{-\frac{1}{2}i\pi} \sqrt{2k}) D'_{-v-1}(\eta_1 e^{-\frac{1}{2}i\pi} \sqrt{2k}) + \\
 & + D_{-v-1}(-\eta_0 e^{-\frac{1}{2}i\pi} \sqrt{2k}) D'_{-v-1}(-\eta_1 e^{-\frac{1}{2}i\pi} \sqrt{2k})] \} \Gamma(-v) dv. \quad (7.128)
 \end{aligned}$$

In the particular case where the two conditions $|\xi| + \xi < \eta_+ + \eta_-$ and $|\xi| - \xi < \eta_+ - \eta_-$ are both fulfilled, the total magnetic field can be written as a harmonic series:

$$\begin{aligned}
 H_z = & \frac{2i}{\pi} \sum_{n=0}^{\infty} (-1)^n D_n(|\xi| e^{-\frac{1}{2}i\pi} \sqrt{2k}) \{ [D'_{-n-1}(\eta_1 e^{-\frac{1}{2}i\pi} \sqrt{2k}) - D'_{-n-1}(-\eta_1 e^{-\frac{1}{2}i\pi} \sqrt{2k})] \\
 & \times [D'_{-n-1}(\eta_1 e^{-\frac{1}{2}i\pi} \sqrt{2k}) + D'_{-n-1}(-\eta_1 e^{-\frac{1}{2}i\pi} \sqrt{2k})] \}^{-1} \\
 & \times [D_{-n-1}(\eta_+ e^{-\frac{1}{2}i\pi} \sqrt{2k}) D'_{-n-1}(-\eta_1 e^{-\frac{1}{2}i\pi} \sqrt{2k}) + \\
 & + D_{-n-1}(-\eta_+ e^{-\frac{1}{2}i\pi} \sqrt{2k}) D'_{-n-1}(\eta_1 e^{-\frac{1}{2}i\pi} \sqrt{2k})] \\
 & \times \{ D_n(\xi e^{-\frac{1}{2}i\pi} \sqrt{2k}) [D_{-n-1}(-\eta_- e^{-\frac{1}{2}i\pi} \sqrt{2k}) D'_{-n-1}(\eta_1 e^{-\frac{1}{2}i\pi} \sqrt{2k}) + \\
 & + D_{-n-1}(\eta_- e^{-\frac{1}{2}i\pi} \sqrt{2k}) D'_{-n-1}(-\eta_1 e^{-\frac{1}{2}i\pi} \sqrt{2k})] + \\
 & + D_n(-\xi e^{-\frac{1}{2}i\pi} \sqrt{2k}) [D_{-n-1}(\eta_- e^{-\frac{1}{2}i\pi} \sqrt{2k}) D'_{-n-1}(\eta_1 e^{-\frac{1}{2}i\pi} \sqrt{2k}) + \\
 & + D_{-n-1}(-\eta_- e^{-\frac{1}{2}i\pi} \sqrt{2k}) D'_{-n-1}(-\eta_1 e^{-\frac{1}{2}i\pi} \sqrt{2k})] \}, \quad (7.129)
 \end{aligned}$$

and on the surface $\eta = \eta_1$:

$$\begin{aligned}
 H_z = & -2i \int_{c_1-i\infty}^{c_1+i\infty} \sum_{n=0}^{\infty} \frac{(-1)^n}{n!} D_n(|\xi| e^{-\frac{1}{2}i\pi} \sqrt{2k}) \\
 & \times \{ [D'_{-n-1}(\eta_1 e^{-\frac{1}{2}i\pi} \sqrt{2k}) - D'_{-n-1}(-\eta_1 e^{-\frac{1}{2}i\pi} \sqrt{2k})] \\
 & \times [D'_{-n-1}(\eta_1 e^{-\frac{1}{2}i\pi} \sqrt{2k}) + D'_{-n-1}(-\eta_1 e^{-\frac{1}{2}i\pi} \sqrt{2k})] \}^{-1} \\
 & \times \{ D_n(\xi e^{-\frac{1}{2}i\pi} \sqrt{2k}) [D_{-n-1}(-\eta_0 e^{-\frac{1}{2}i\pi} \sqrt{2k}) D'_{-n-1}(\eta_1 e^{-\frac{1}{2}i\pi} \sqrt{2k}) + \\
 & + D_{-n-1}(\eta_0 e^{-\frac{1}{2}i\pi} \sqrt{2k}) D'_{-n-1}(-\eta_1 e^{-\frac{1}{2}i\pi} \sqrt{2k})] + \\
 & + D_n(-\xi e^{-\frac{1}{2}i\pi} \sqrt{2k}) [D_{-n-1}(\eta_0 e^{-\frac{1}{2}i\pi} \sqrt{2k}) D'_{-n-1}(\eta_1 e^{-\frac{1}{2}i\pi} \sqrt{2k}) + \\
 & + D_{-n-1}(-\eta_0 e^{-\frac{1}{2}i\pi} \sqrt{2k}) D'_{-n-1}(-\eta_1 e^{-\frac{1}{2}i\pi} \sqrt{2k})] \}. \quad (7.130)
 \end{aligned}$$

An alternative representation of the total magnetic field of eq. (7.127) is

$$\begin{aligned}
H_z = & \frac{e^{-\frac{1}{2}i\pi}}{\sqrt{\pi k}} \sum_{r=1}^{\infty} D_{\mu'_r}(|\xi| e^{-\frac{1}{2}i\pi} \sqrt{2k}) \\
& \times [D_{-\mu'_r-1}(\eta_0 e^{-\frac{1}{2}i\pi} \sqrt{2k}) + D_{-\mu'_r-1}(-\eta_0 e^{-\frac{1}{2}i\pi} \sqrt{2k})] \\
& \times [D_{\mu'_r}(\xi e^{-\frac{1}{2}i\pi} \sqrt{2k}) + D_{\mu'_r}(-\xi e^{-\frac{1}{2}i\pi} \sqrt{2k})] \\
& \times [D_{-\mu'_r-1}(\eta_1 e^{-\frac{1}{2}i\pi} \sqrt{2k}) + D_{-\mu'_r-1}(-\eta_1 e^{-\frac{1}{2}i\pi} \sqrt{2k})] \\
& \times \left\{ \int_0^{\eta_1} [D_{-\mu'_r-1}(\eta e^{-\frac{1}{2}i\pi} \sqrt{2k}) + D_{-\mu'_r-1}(-\eta e^{-\frac{1}{2}i\pi} \sqrt{2k})]^2 d\eta \right\}^{-1} \Gamma(-\mu'_r), \quad (7.131)
\end{aligned}$$

where μ'_r ($r = 1, 2, \dots$) are solutions of

$$D'_{-\mu'_r-1}(\eta_1 e^{-\frac{1}{2}i\pi} \sqrt{2k}) - D'_{-\mu'_r-1}(-\eta_1 e^{-\frac{1}{2}i\pi} \sqrt{2k}) = 0; \quad (7.132)$$

all solutions have $\text{Re } \mu'_r = -\frac{1}{2}$. On the surface $\eta = \eta_1$:

$$\begin{aligned}
H_z = & -e^{-\frac{1}{2}i\pi} \sqrt{\frac{2}{k}} \sum_{r=1}^{\infty} D_{\mu'_r}(|\xi| e^{-\frac{1}{2}i\pi} \sqrt{2k}) \\
& \times [D_{-\mu'_r-1}(\eta_0 e^{-\frac{1}{2}i\pi} \sqrt{2k}) + D_{-\mu'_r-1}(-\eta_0 e^{-\frac{1}{2}i\pi} \sqrt{2k})] \\
& \times [D_{\mu'_r}(\xi e^{-\frac{1}{2}i\pi} \sqrt{2k}) + D_{\mu'_r}(-\xi e^{-\frac{1}{2}i\pi} \sqrt{2k})] \left\{ D'_{-\mu'_r-1}(\eta_1 e^{-\frac{1}{2}i\pi} \sqrt{2k}) \right. \\
& \times \left. \int_0^{\eta_1} [D_{-\mu'_r-1}(\eta e^{-\frac{1}{2}i\pi} \sqrt{2k}) + D_{-\mu'_r-1}(-\eta e^{-\frac{1}{2}i\pi} \sqrt{2k})]^2 d\eta \right\}^{-1} \frac{\Gamma(-\mu'_r)}{\Gamma(\mu'_r+1)}. \quad (7.133)
\end{aligned}$$

7.4.2.2. HIGH FREQUENCY APPROXIMATIONS

The complete asymptotic expansion of the scattered magnetic field when the line source is located at the focal line ($\xi_0 = \eta_0 = 0$) has been examined by KELLER et al. [1956]. Explicitly, the first term of the series is

$$H_z \sim \sqrt{\frac{2}{\pi k}} \frac{e^{-\frac{1}{2}i\pi}}{\sqrt{\{y^2/(4\rho_1) + \rho_1\}}} e^{ik(x+2\rho_1)} + \dots, \quad (7.134)$$

which is the geometric optics approximation. The focal length is $\rho_1 = \frac{1}{2}\eta_1^2$. The more general problem of a line source in the focal plane off the focal line has been considered by HOCHSTADT [1957].

7.5. Point and dipole sources

No explicit results are available.

Bibliography

- ABRAMOWITZ, M. and I. A. STEGUN [1956], *Handbook of Mathematical Functions*, National Bureau of Standards, Washington, D.C.
 LEPSHIN, D. I. [1956], On the Functions of the Parabolic Cylinder, New York University, Institute of Mathematical Sciences, Report BR-19.

- ERDÉLYI, A., W. MAGNUS, F. OBERHETTINGER and F. G. TRICOMI [1953], *Higher Transcendental Functions*, McGraw-Hill Book Co., New York.
- GRINBERG, G. A., N. N. LEBEDEV, I. P. SKALSKAYA and Ya. S. UFLYAND [1957], The Electromagnetic Field of a Line Source Located in the Interior of an Ideally Conducting Parabolic Screen, New York University, Institute of Mathematical Sciences, Report EM-103. (English translation of Zh. Eksperim. i Teor. Fiz. **30** (1956) 528-543.)
- HOCHSTADT, H. [1957], Asymptotic Formulas for Diffraction by Parabolic Surfaces, *Comm. Pure Appl. Math.* **10**, 311-329.
- HOCHSTADT, H. [1959], Some Diffraction by Convex Bodies, *Arch. Rat. Mech. Anal.* **3**, 422-438.
- IVANOV, V. I. [1960], Shortwave Asymptotic Diffraction Field in the Shadow of an Ideal Parabolic Cylinder, *Radio Eng. Electron.* **5**, 54-68. (English translation of *Radiotekhn. i Elektron.* **5** (1960) 393-402.)
- IVANOV, V. I. [1963], Diffraction of Short Plane Waves on a Parabolic Cylinder, *USSR Comp. Math. and Math. Phys.* **2**, 255-271. (English translation of *Zh. vych. mat.* **2** (1962) 241-254.) The substitution on p. 262 should read $t = (\frac{1}{2}x^2)^{-\frac{1}{2}}(\mu - \frac{1}{2}x^2)$.
- KELLER, J. B. [1956], Diffraction by a Convex Cylinder, *IRE Trans. AP-4*, 312-321.
- KELLER, J. B. and B. R. LEVY [1959], Decay Exponents and Diffraction Coefficients for Surface Waves on Surfaces of Non-Constant Curvature, *IRE Trans. AP-7*, S52-S61.
- KELLER, J. B., R. M. LEWIS and B. D. SECKLER [1956], Asymptotic Solution of Some Diffraction Problems, *Comm. Pure Appl. Math.* **9**, 207-265.
- LAMB, H. [1906], On Sommerfeld's Diffraction Problem; and on Reflection by a Parabolic Mirror, *Proc. London Math. Soc.* **4**, 190-203.
- MAGNUS, W. [1940], Übereine Randwertaufgabe der Wellengleichung für den parabolischen Zylinder, *Jahresber. deutsch. Math. Verein* **50**, 140-161.
- MAGNUS, W. [1941-42], Zur Theorie des zylindrisch-parabolischen Spiegels, *Z. Physik* **118**, 343-356.
- RICE, S. O. [1954], Diffraction of Plane Radio Waves by a Parabolic Cylinder, *Bell System Tech. J.* **33**, 417-504. KELLER [1956] and IVANOV [1960] have pointed out an error in the asymptotic estimate of the n^{th} zero of the parabolic cylinder function.
- ROBIN, L. [1964], Diffraction d'une onde cylindrique (ou plane) par un cylindre parabolique de génératrices parallèles à l'onde, *Ann. Télécommun.* **19**, 257-269.

CHAPTER 8

THE HALF-PLANE

J. J. BOWMAN and T. B. A. SENIOR

The half-plane is the limit of a parabolic cylinder as the latus rectum tends to zero and is also the limit of a wedge as the interior wedge angle vanishes. It was one of the earliest structures for which an exact solution of the boundary value problem was obtained, and has since been subject to a variety of analytical treatments. The solution, notable for the comparative simplicity of its representation in terms of the Fresnel integral, has formed the basis for many studies of edge phenomena and diffraction effects in general.

8.1. Half-plane geometry and preliminary considerations

The half-plane is defined in terms of the rectangular Cartesian coordinates (x, y, z) by the equation $y = 0, x \geq 0$. The edge is therefore coincident with the z -axis. The half-plane is also defined in terms of the circular cylindrical coordinates (ρ, ϕ, z) by the equations $\phi = 0$ (upper surface) and $\phi = 2\pi$ (lower surface), and in terms of the parabolic cylindrical coordinates (ξ, η, z) where

$$\begin{aligned}\xi &= \sqrt{2\rho} \cos \frac{1}{2}\phi, & -\infty < \xi < \infty, \\ \eta &= \sqrt{2\rho} \sin \frac{1}{2}\phi, & 0 \leq \eta < \infty;\end{aligned}$$

the half-plane is the complete coordinate surface $\eta = 0$. This last coordinate system is not employed in this chapter, but in addition to the rectangular and circular cylindrical coordinates, we shall also use the spherical coordinates (r, θ, ϕ) , where $\rho = r \sin \theta$ and $z = r \cos \theta$.

The primary source is a plane wave propagating in the plane perpendicular to the z -axis and in a direction making an angle $\pi + \phi_0$ with the positive x -axis, or a line source parallel to the z -axis and located at (ρ_0, ϕ_0) , or a point or dipole source located at (ρ_0, ϕ_0, z_0) . These configurations are illustrated in Fig. 8.1. In each case both E - and H -polarized excitations are considered, and, in addition, the dipole source may be of arbitrary orientation. For convenience, and without loss of generality, it is assumed that $0 \leq \phi_0 \leq \pi$.

The distances from the point of observation to the source, and to the image of the source in the plane $y = 0$, are denoted by R and R' respectively. Thus, for a line source,

$$R = \sqrt{\rho^2 + \rho_0^2 - 2\rho\rho_0 \cos(\phi - \phi_0)} = \sqrt{(x - x_0)^2 + (y - y_0)^2}, \quad (8.1)$$

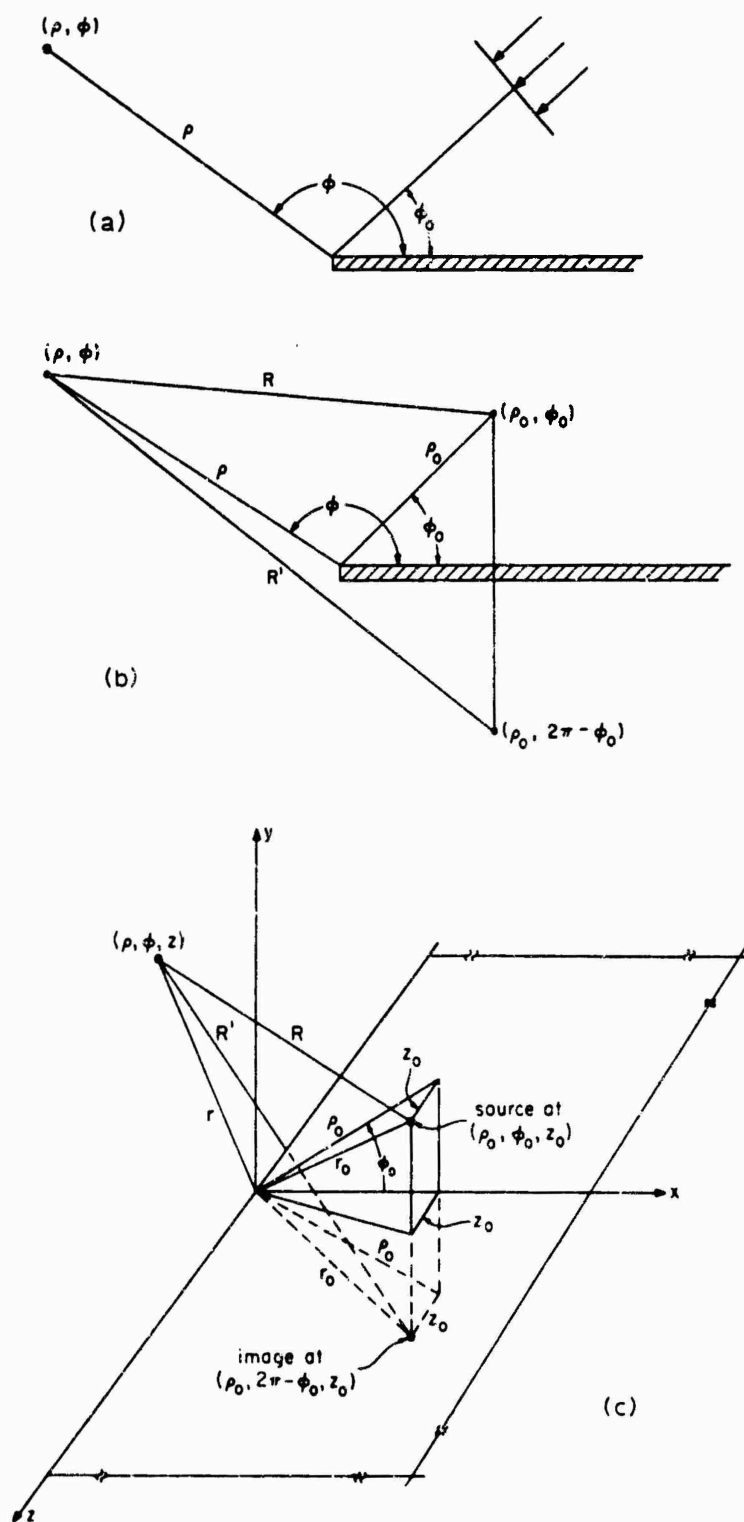


Fig. 8.1. Geometry for (a) plane wave illumination, (b) line sources and (c) point sources.

$$R' = \sqrt{\{\rho^2 + \rho_0^2 - 2\rho\rho_0 \cos(\phi + \phi_0)\}} = \sqrt{\{(x-x_0)^2 + (y+y_0)^2\}}, \quad (8.2)$$

whereas for a point or dipole source,

$$\begin{aligned} R &= \sqrt{\{\rho^2 + \rho_0^2 - 2\rho\rho_0 \cos(\phi - \phi_0) + (z-z_0)^2\}} \\ &= \sqrt{\{(x-x_0)^2 + (y-y_0)^2 + (z-z_0)^2\}}, \end{aligned} \quad (8.3)$$

$$\begin{aligned} R' &= \sqrt{\{\rho^2 + \rho_0^2 - 2\rho\rho_0 \cos(\phi + \phi_0) + (z-z_0)^2\}} \\ &= \sqrt{\{(x-x_0)^2 + (y+y_0)^2 + (z-z_0)^2\}}. \end{aligned} \quad (8.4)$$

We also introduce the parameter R_1 associated with the edge diffraction where, for a line source,

$$R_1 = \rho + \rho_0, \quad (8.5)$$

and for a point or dipole source

$$R_1 = \sqrt{\{(\rho + \rho_0)^2 + (z-z_0)^2\}}. \quad (8.6)$$

A function of particular importance in the sequel is the Fresnel integral

$$F(\tau) = \int_{\tau}^{\infty} e^{i\mu^2} d\mu \quad (8.7)$$

whose properties are discussed in the Introduction, and we also make use of the Heaviside step function, $\eta(\psi)$, where

$$\eta(\psi) = \begin{cases} 1 & \text{for } \psi > 0 \\ 0 & \text{for } \psi < 0 \end{cases}$$

and the signum function $\text{sgn}(\psi) = \pm 1$ for $\psi \gtrless 0$.

For any type of source the complete field can be expressed as a contour integral of the form

$$\int_{C_1 + C_2} G(z) s(z + \phi) dz$$

(see, for example, TUZHILIN [1963]), where C_1 and C_2 are known as the Sommerfeld contours. In the integrand $s(z + \phi)$ is proportional to the sum (or difference) of two cotangents, and the kernel $G(z)$ is determined by the source. The contours C_1 and C_2 are shown in Fig. 8.2, where the shading indicates those regions where $G(z)$ vanishes exponentially as $|\text{Im } z| \rightarrow \infty$ on the upper Riemann sheet. When the source is at a finite distance, the kernel has branch points at $z = (2n+1)\pi \pm ic$, $n = 0, \pm 1, \pm 2, \dots$, where

$$c = 2 \cosh^{-1} \frac{R_1}{2\sqrt{\rho\rho_0}}.$$

Except in the case of plane wave incidence (when $c = \infty$), the z -plane then has branch cuts extending to infinity as shown in Fig. 8.2. Complete uniform asymptotic expansions of the above contour integral may be obtained as special cases of the results given in Chapter 6 and will not be repeated in the present chapter.

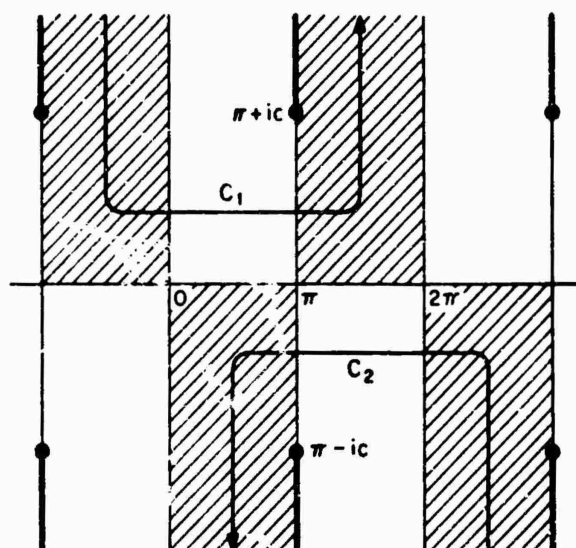


Fig. 8.2. Sommerfeld contours.

8.2. Plane wave incidence

8.2.1. *E*-polarization

For incidence at an angle ϕ_0 with respect to the negative x -axis, such that

$$E^i = \hat{z} \exp \{-ik\rho \cos(\phi - \phi_0)\}, \quad (8.8)$$

a contour integral representation of the total electric field is (SOMMERFELD [1896], CARSLAW [1899]):

$$E_z = \frac{1}{8i\pi} \int_{C_1 + C_2} e^{ik\rho \cos \alpha} \{\cot \tfrac{1}{4}(\pi - \alpha - \phi + \phi_0) - \cot \tfrac{1}{4}(\pi - \alpha - \phi - \phi_0)\} d\alpha \quad (8.9)$$

where C_1 and C_2 are the Sommerfeld contours shown in Fig. 8.2. The above expression reduces to (SOMMERFELD [1896], CLEMMOW [1951])

$$E_z = \frac{e^{-\frac{1}{2}i\pi}}{\sqrt{\pi}} \left\{ \exp \{-ik\rho \cos(\phi - \phi_0)\} F[-\sqrt{2k\rho} \cos \tfrac{1}{2}(\phi - \phi_0)] - \exp \{-ik\rho \cos(\phi + \phi_0)\} F[-\sqrt{2k\rho} \cos \tfrac{1}{2}(\phi + \phi_0)] \right\}. \quad (8.10)$$

An alternative representation for E_z in terms of parabolic cylinder functions follows from the eigenfunction expansions in Chapter 7, and still another representation is MACDONALD [1902]):

$$E_z = \sum_{n=0}^{\infty} \varepsilon_n \sin(\tfrac{1}{2}n\phi) \sin(\tfrac{1}{2}n\phi_0) S_{\frac{1}{2}n}, \quad (8.11)$$

where

$$S_v = e^{-\frac{1}{2}i\pi v} J_v(k\rho). \quad (8.12)$$

A symmetry relation that holds is

$$E_z(\phi) - E_z(2\pi - \phi) = \exp\{-ik\rho \cos(\phi - \phi_0)\} - \exp\{-ik\rho \cos(\phi + \phi_0)\}. \quad (8.13)$$

Field calculations based on eq. (8.10) are easy to perform using tabulations of the Fresnel integral. Typical of the results available are the amplitude and phase curves shown in Figs. 8.3 and 8.4 respectively.

On the surface

$$H_x = Y \sqrt{\frac{2}{\pi kx}} e^{\pm i\pi} \sin \frac{1}{2}\phi_0 \{ \mp e^{ikx} + 2i\sqrt{2kx} \cos \frac{1}{2}\phi_0 \exp(-ikx \cos \phi_0) \\ \times F[\mp \sqrt{2kx} \cos \frac{1}{2}\phi_0] \} \quad (8.14)$$

with the upper or lower sign for $\phi = 0$ or 2π respectively. If $\sqrt{2kx} \cos \frac{1}{2}\phi_0 \ll 1$ (which includes the immediate vicinity of the edge), insertion of the small argument expansion of the Fresnel integral gives

$$H_x = Y \sqrt{\frac{2}{\pi kx}} e^{\pm i\pi} \sin \frac{1}{2}\phi_0 \{ \mp e^{ikx} - \sqrt{2\pi kx} e^{-\frac{1}{2}i\pi} \cos \frac{1}{2}\phi_0 \exp(-ikx \cos \phi_0) \pm \\ \pm 4ik \cos^2 \frac{1}{2}\phi_0 e^{ikx} + O[(2kx \cos^2 \frac{1}{2}\phi_0)^2] \}. \quad (8.15)$$

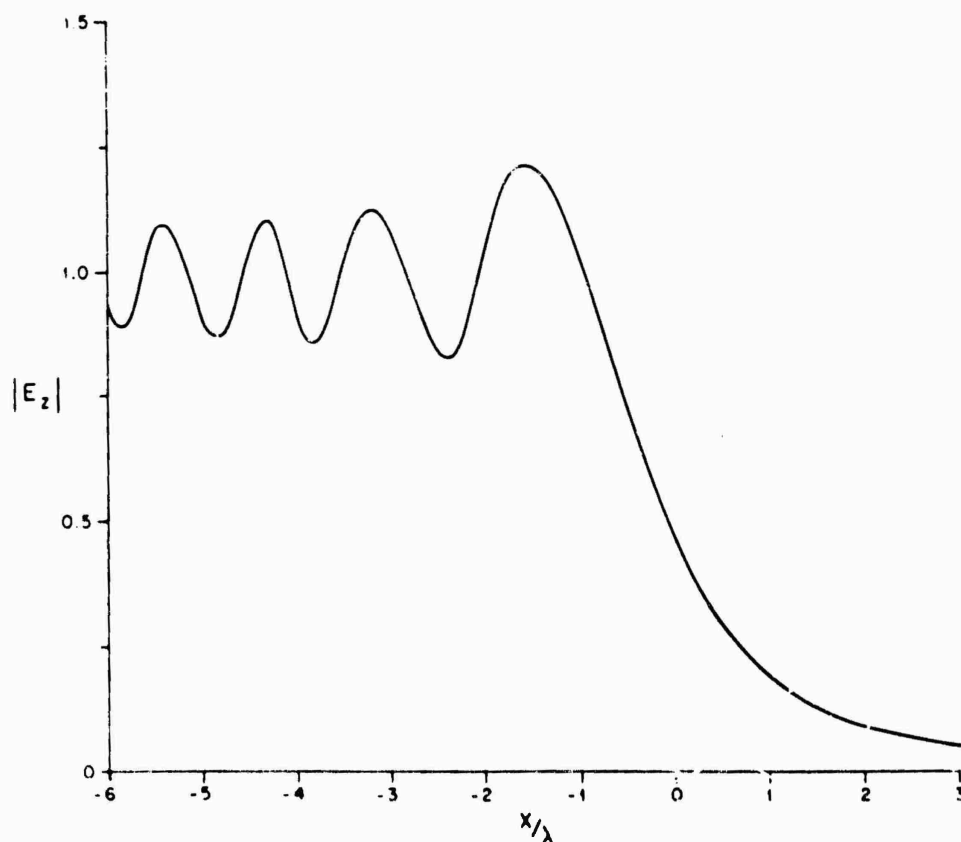


Fig. 8.3. Amplitude of total electric field E_z for $\phi_0 = \frac{1}{2}\pi$ and $y = -3\lambda$ (CLEMMOW [1959]).

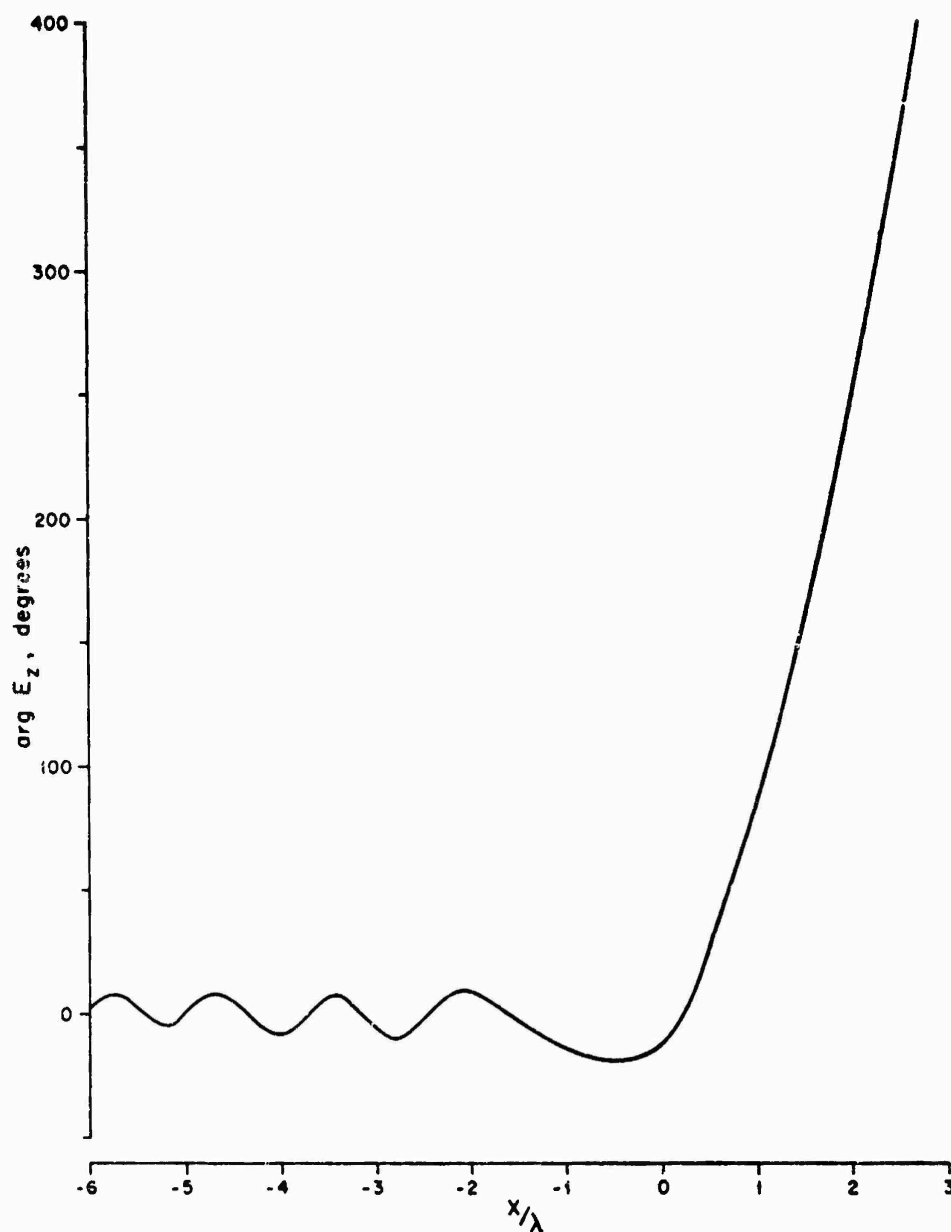


Fig. 8.4. Phase of total electric field E_z for $\phi_0 = \frac{1}{2}\pi$ and $y = -3\lambda$ (HARDEN [1952]).

The singularity at the edge is here made explicit. On the other hand, if $\sqrt{2kx} \cos \frac{1}{2}\phi_0 \gg 1$ (far from the edge)

$$H_x \sim \begin{cases} -2Y \sin \phi_0 \exp(-ikx \cos \phi_0) + \\ \quad + \frac{Y e^{i(kx - \frac{1}{2}\pi)} \sin \frac{1}{2}\phi_0}{2kx \sqrt{2\pi kx} \cos^2 \frac{1}{2}\phi_0} \{1 + O[(2kx \cos^2 \frac{1}{2}\phi_0)^{-1}]\}, & (\phi = 0) \\ - \frac{Y e^{i(kx - \frac{1}{2}\pi)} \sin \frac{1}{2}\phi_0}{2kx \sqrt{2\pi kx} \cos^2 \frac{1}{2}\phi_0} \{1 + O[(2kx \cos^2 \frac{1}{2}\phi_0)^{-1}]\}, & (\phi = 2\pi). \end{cases} \quad (8.16)$$

The amplitude and phase of the surface field component H_x , normalized to H_x^i and computed from eq. (8.14), are shown in Figs. 8.5 and 8.6 for $\phi_0 = \frac{1}{2}\pi$ and $\phi = 0, 2\pi$.

If $k\rho \ll 1$, a small argument expansion of the Fresnel integrals in eq. (8.10), or of the Bessel functions in eq. (8.11) gives

$$E_z = 2 \sqrt{\frac{2k\rho}{\pi}} e^{-\frac{1}{2}i\pi} \sin \frac{1}{2}\phi \sin \frac{1}{2}\phi_0 + O(k\rho \sin \phi \sin \phi_0). \quad (8.17)$$

If $k\rho \gg 1$, a convenient decomposition of the field is

$$E_z = E_z^{s.o.} + E_z^d, \quad (8.18)$$

where $E_z^{s.o.}$ is the geometrical optics field given by

$$E_z^{s.o.} = \eta(\pi + \phi_0 - \phi) \exp \{-ik\rho \cos(\phi - \phi_0)\} - \eta(\pi - \phi_0 - \phi) \exp \{-ik\rho \cos(\phi + \phi_0)\} \quad (8.19)$$

and E_z^d is the diffracted field, which is discontinuous at $\phi = \pi \pm \phi_0$ in order to compensate for the discontinuities in $E_z^{s.o.}$. In the immediate vicinity of these directions, the actual transitional behavior of E_z is provided by the Fresnel integrals in eq. (8.10). For $k\rho \gg 1$ and ϕ not too close to $\pi \pm \phi_0$,

$$E_z^d \sim \sqrt{\frac{2}{\pi k\rho}} e^{i(k\rho + \frac{1}{2}\pi)} \frac{\sin \frac{1}{2}\phi \sin \frac{1}{2}\phi_0}{\cos \phi + \cos \phi_0}. \quad (8.20)$$

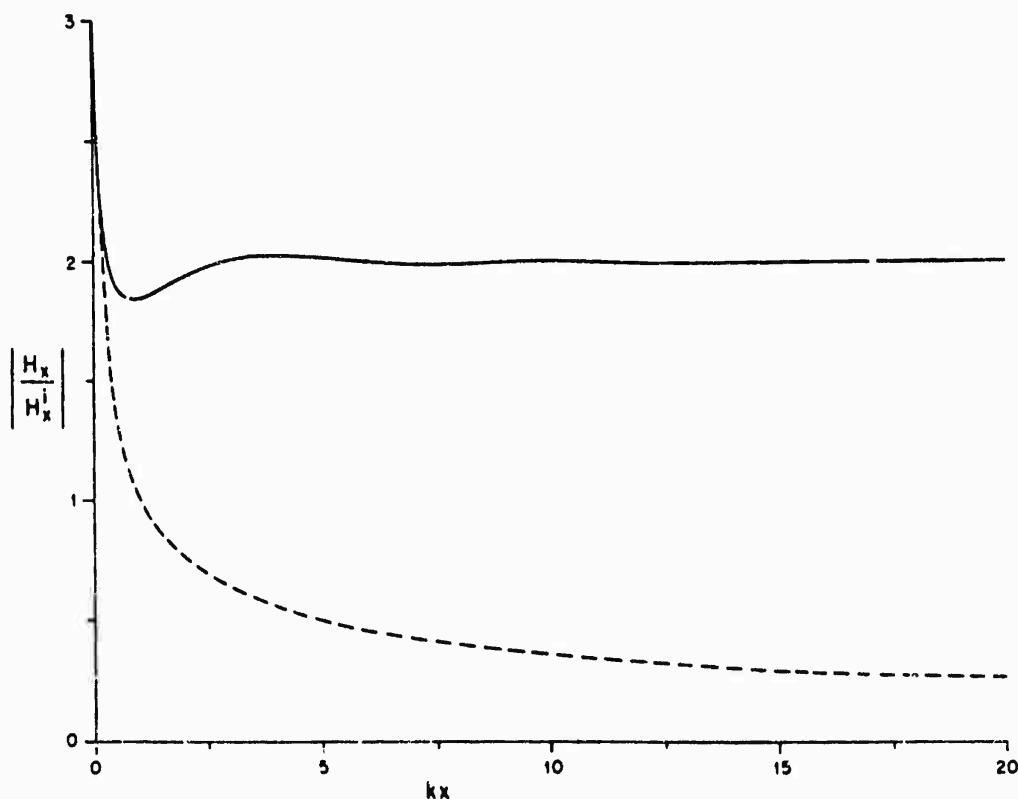


Fig. 8.5. Amplitude of normalized surface field for $\phi_0 = \frac{1}{2}\pi$ and $\phi = 0$ (—), $\phi = 2\pi$ (---).

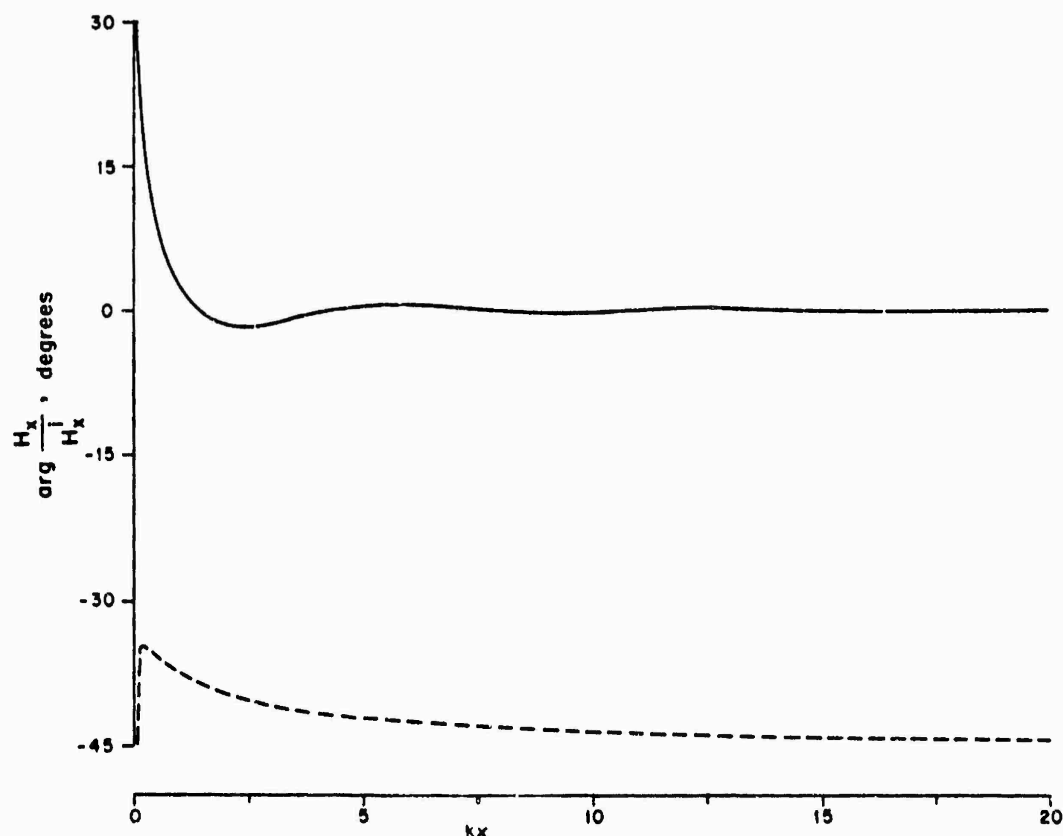


Fig. 8.6. Phase of normalized surface field for $\phi_0 = \frac{1}{2}\pi$ and $\phi = 0$ (—), $\phi = 2\pi$ (---). Note that a phase term kx has been subtracted from the phase computed for the lower surface ($\phi = 2\pi$).

This has the appearance of a cylindrical wave with

$$P = i \frac{\sin \frac{1}{2}\phi \sin \frac{1}{2}\phi_0}{\cos \phi + \cos \phi_0} \quad (8.21)$$

emanating from the edge. SAVORNIN [1939] has computed $16|P|^2$ as a function of ϕ , $\pi < \phi < 2\pi$, for $\phi_0 = \frac{1}{2}\pi$. Similar computations, but for a variety of ϕ_0 , have been made by MARCINKOWSKI [1959] and TAVENNER [1960], and some of the data is reproduced in Fig. 8.7.

As ϕ approaches $\pi \pm \phi_0$, the approximation implied by eq. (8.20) breaks down. Eq. (8.10), however, indicates that for $\phi = \pi - \phi_0$

$$E_z = \exp(ik\rho \cos 2\phi_0) - \frac{1}{2}e^{ik\rho} - \frac{e^{-\frac{1}{2}i\pi}}{\sqrt{\pi}} \exp(ik\rho \cos 2\phi_0)F[\sqrt{2k\rho} \sin \phi_0], \quad (8.22)$$

whereas for $\phi = \pi + \phi_0$,

$$E_z = \frac{1}{2}e^{ik\rho} - \frac{e^{-\frac{1}{2}i\pi}}{\sqrt{\pi}} \exp(ik\rho \cos 2\phi_0)F[\sqrt{2k\rho} \sin \phi_0]. \quad (8.23)$$

For edge-on incidence ($\phi_0 = \pi$), eq. (8.10) reduces to

$$E_z = e^{ik\rho \cos \phi} \left\{ 1 - 2 \frac{e^{-\frac{1}{2}i\pi}}{\sqrt{\pi}} F[\sqrt{2k\rho} \sin \frac{1}{2}\phi] \right\}, \quad (8.24)$$

and on the surface in this case:

$$H_x = \mp Y \sqrt{\frac{2}{\pi kx}} e^{i(kx + \frac{1}{2}\pi)}, \quad \mp \text{ for } \phi = 0, 2\pi. \quad (8.25)$$

For grazing incidence ($\phi_0 = 0$), $E_z = 0$ everywhere.

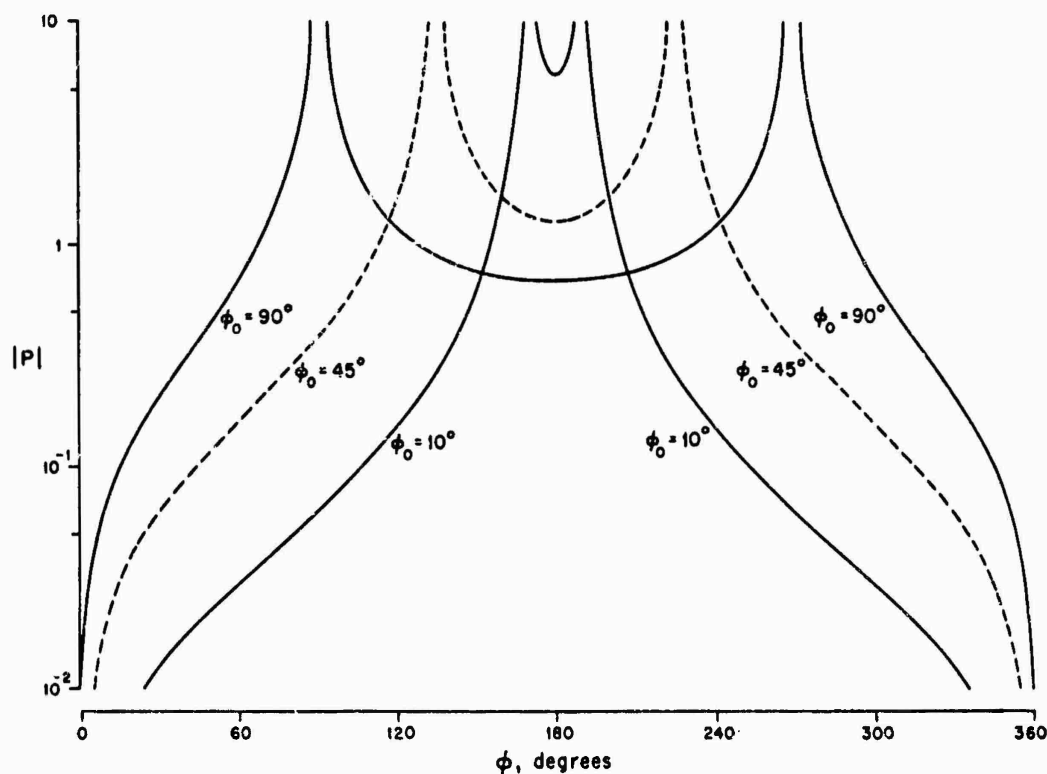


Fig. 8.7. Far field amplitude of the diffracted wave (MARCINKOWSKI [1959]).

8.2.2. *H-polarization*

For incidence at an angle ϕ_0 with respect to the negative x -axis, such that

$$\mathbf{H}^i = \hat{\mathbf{z}} \exp \{-ik\rho \cos(\phi - \phi_0)\}, \quad (8.26)$$

a contour integral representation of the total magnetic field is (SOMMERFELD [1896], CARSLAW [1899]):

$$H_z = \frac{1}{8i\pi} \int_{C_1 + C_2} e^{ik\rho \cos \alpha} \{ \cot \frac{1}{4}(\pi - \alpha - \phi + \phi_0) + \cot \frac{1}{4}(\pi - \alpha - \phi - \phi_0) \} d\alpha \quad (8.27)$$

where C_1 and C_2 are the Sommerfeld contours shown in Fig. 8.2. The above expres-

sion reduces to (SOMMERFELD [1896], CLEMMOW [1951]):

$$H_z = \frac{e^{-\frac{1}{2}i\pi}}{\sqrt{\pi}} \left\{ \exp \{ -ik\rho \cos(\phi - \phi_0) \} F[-\sqrt{2k\rho} \cos \frac{1}{2}(\phi - \phi_0)] + \right. \\ \left. + \exp \{ -ik\rho \cos(\phi + \phi_0) \} F[-\sqrt{2k\rho} \cos \frac{1}{2}(\phi + \phi_0)] \right\}. \quad (8.28)$$

An alternative representation for H_z in terms of parabolic cylinder functions follows from the eigenfunction expansions in Chapter 7, and still another representation is (MACDONALD [1902]):

$$H_z = \sum_{n=0}^{\infty} c_n \cos(\frac{1}{2}n\phi) \cos(\frac{1}{2}n\phi_0) S_{\frac{1}{2}n}, \quad (8.29)$$

where S_v is given in eq. (8.12). A symmetry relation that holds is

$$H_z(\phi) + H_z(2\pi - \phi) = \exp \{ -ik\rho \cos(\phi - \phi_0) \} + \exp \{ -ik\rho \cos(\phi + \phi_0) \}. \quad (8.30)$$

Field calculations based on eq. (8.28) are easy to perform using tabulations of the Fresnel integral. Typical of the results available are the amplitude and phase curves shown in Figs. 8.8. and 8.9 respectively. BRAUNBEK and LAUKIEN [1952] have computed the equi-amplitude and equi-phase contours and lines of average energy flow within a

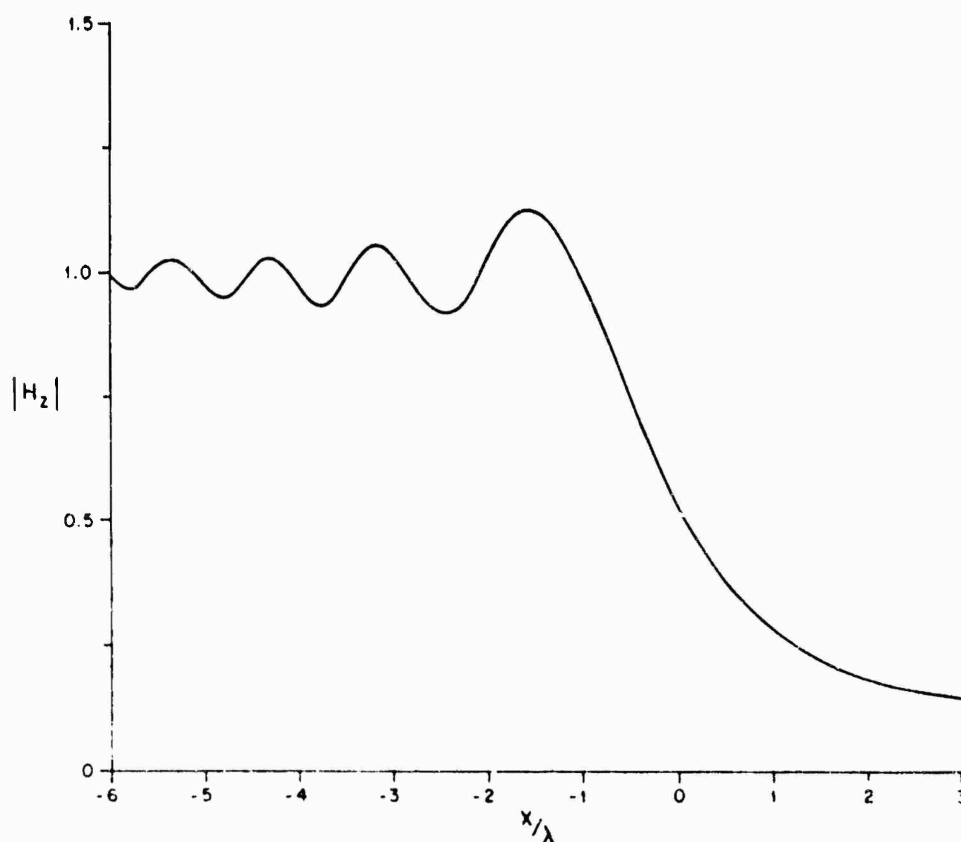


Fig. 8.8. Amplitude of total magnetic field H_z for $\phi_0 = \frac{1}{2}\pi$ and $y = -3\lambda$.

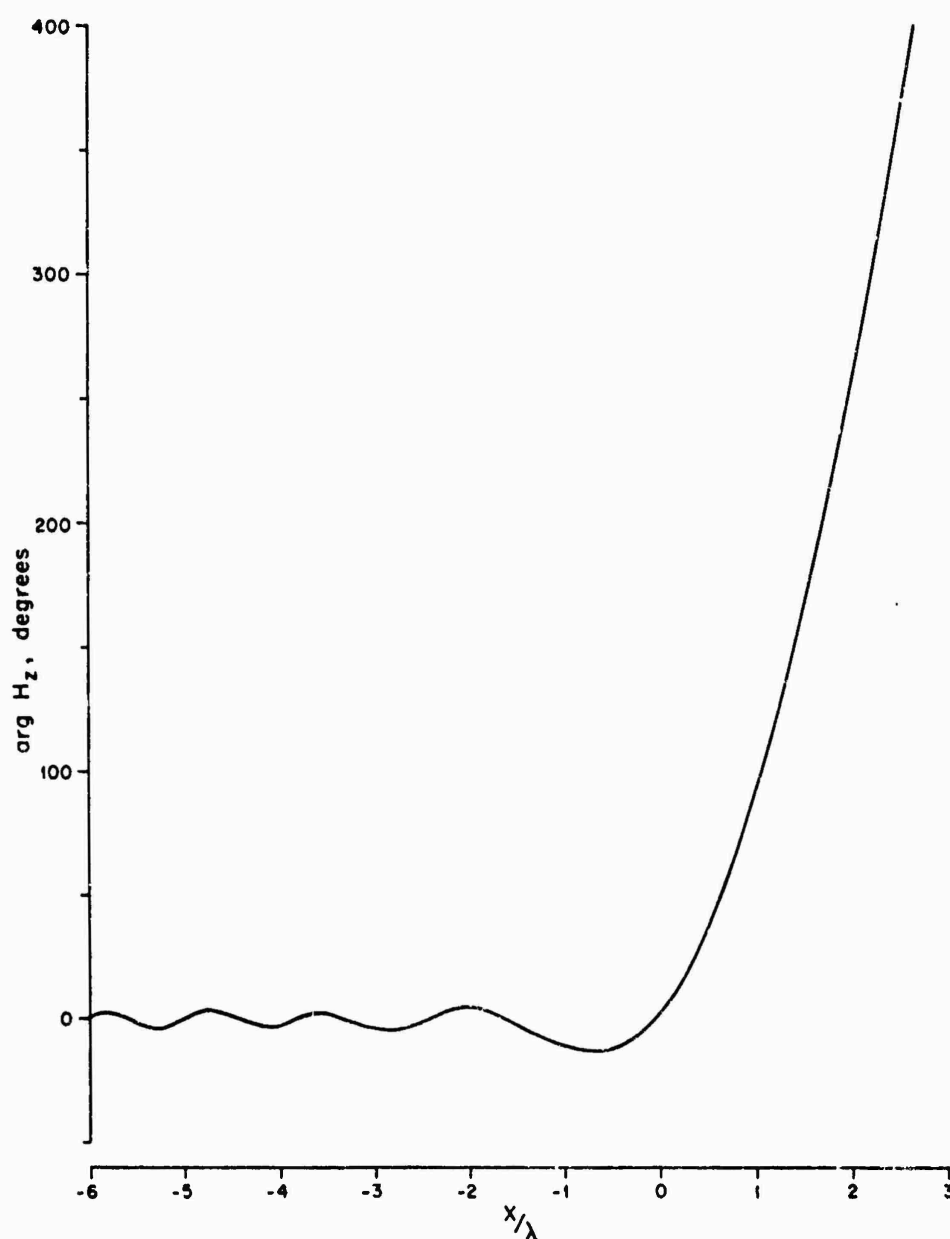


Fig. 8.9. Phase of total magnetic field H_z for $\phi_0 = \frac{1}{2}\pi$ and $y = -3\lambda$.

region bounded by a square of side 2λ centered on the edge for the case $\phi_0 = \frac{1}{2}\pi$. The first two plots are reproduced in Figs. 8.10 and 8.11.

On the surface

$$H_z = 2 \frac{e^{-\frac{1}{2}i\pi}}{\sqrt{\pi}} \exp(-ikx \cos \phi_0) F[\mp \sqrt{2kx} \cos \frac{1}{2}\phi_0] \quad (8.31)$$

with the upper or lower sign for $\phi = 0$ or 2π respectively. If $\sqrt{2kx} \cos \frac{1}{2}\phi_0 \ll 1$ (which includes the immediate vicinity of the edge), insertion of the small argument

expansion of the Fresnel integral gives

$$H_z = \exp(-ikx \cos \phi_0) \pm 2 \sqrt{\frac{2kx}{\pi}} e^{-\frac{1}{2}i\pi} \cos \frac{1}{2}\phi_0 e^{ikx} + O[(2kx \cos^2 \frac{1}{2}\phi_0)^{\frac{1}{2}}]. \quad (8.32)$$

On the other hand, if $\sqrt{2kx} \cos \frac{1}{2}\phi_0 \gg 1$ (far from the edge)

$$H_z \sim \begin{cases} 2 \exp(-ikx \cos \phi_0) - \frac{e^{i(kx + \frac{1}{2}\pi)}}{\sqrt{2\pi kx}} \sec \frac{1}{2}\phi_0 \{1 + O[(2kx \cos^2 \frac{1}{2}\phi_0)^{-1}]\}, & (\phi = 0), \\ \frac{e^{i(kx + \frac{1}{2}\pi)}}{\sqrt{2\pi kx}} \sec \frac{1}{2}\phi_0 \{1 + O[(2kx \cos^2 \frac{1}{2}\phi_0)^{-1}]\}, & (\phi = 2\pi). \end{cases} \quad (8.33)$$

The amplitude and phase of the surface field component H_z computed from eq. (8.31)

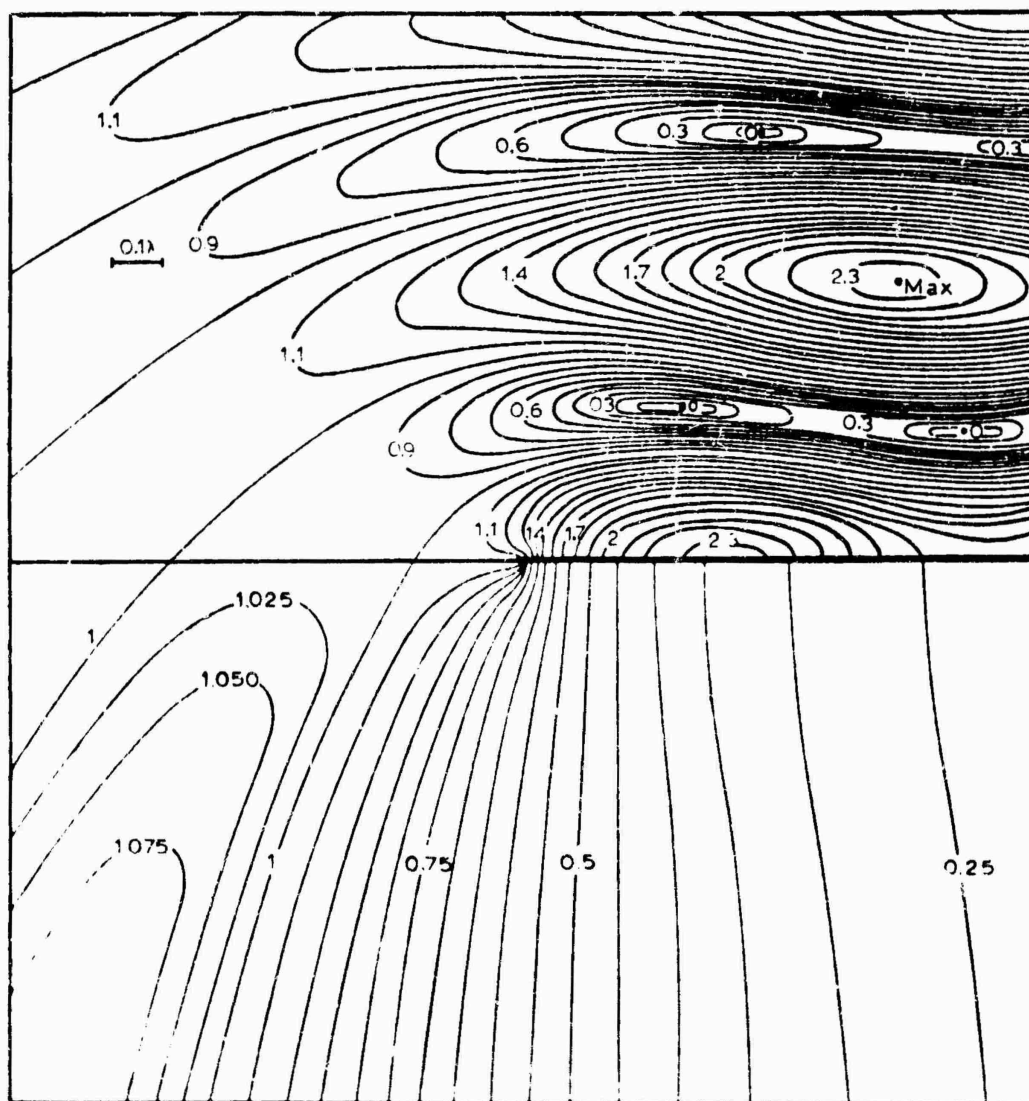


Fig. 8.10. Equi-amplitude contours of H_z for $\phi_0 = \frac{1}{2}\pi$ (BRAUNBEK and LAUKIEN [1952]).

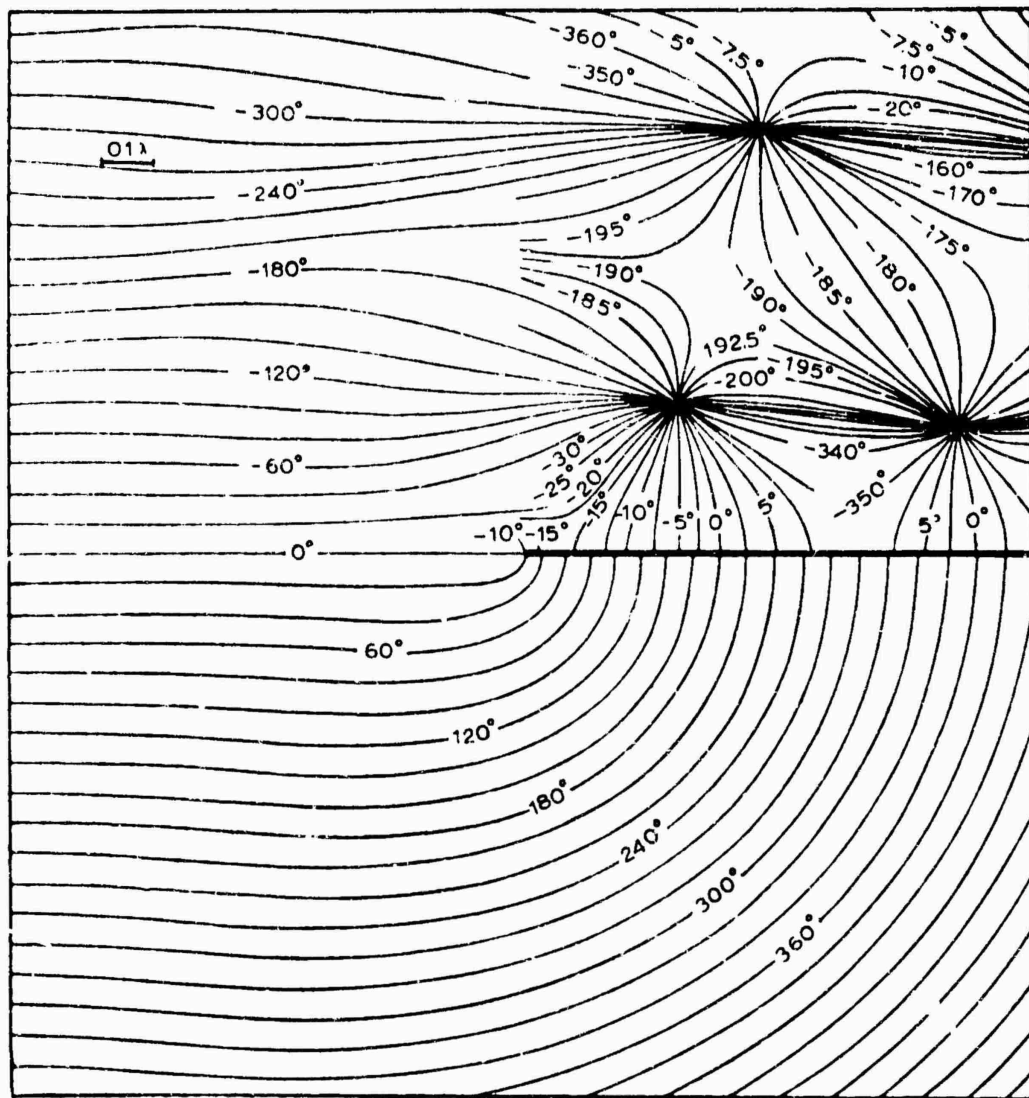


Fig. 8.11. Equi-phase contours of H_z for $\phi_0 = \frac{1}{2}\pi$ (BRAUNBEK and LAUKIEN [1952]).

are shown in Figs. 8.12 and 8.13 for $\phi_0 = \frac{1}{2}\pi$ and $\phi = 0, 2\pi$.

If $k\rho \ll 1$, a small argument expansion of the Fresnel integral in eq. (8.28), or of the Bessel functions in eq. (8.29), gives

$$H_z = 1 + 2 \sqrt{\frac{2k\rho}{\pi}} e^{-i\pi/4} \cos \frac{1}{2}\phi \cos \frac{1}{2}\phi_0 + O(k\rho \cos \phi \cos \phi_0). \quad (8.34)$$

If $k\rho \gg 1$, a convenient decomposition of the field is

$$H_z = H_z^{e.o.} + H_z^d, \quad (8.35)$$

where $H_z^{e.o.}$ is the geometrical optics field given by

$$H_z^{e.o.} = \eta(\pi + \phi_0 - \phi) \exp \{ -ik\rho \cos(\phi - \phi_0) \} + \eta(\pi - \phi_0 - \phi) \exp \{ -ik\rho \cos(\phi + \phi_0) \} \quad (8.36)$$

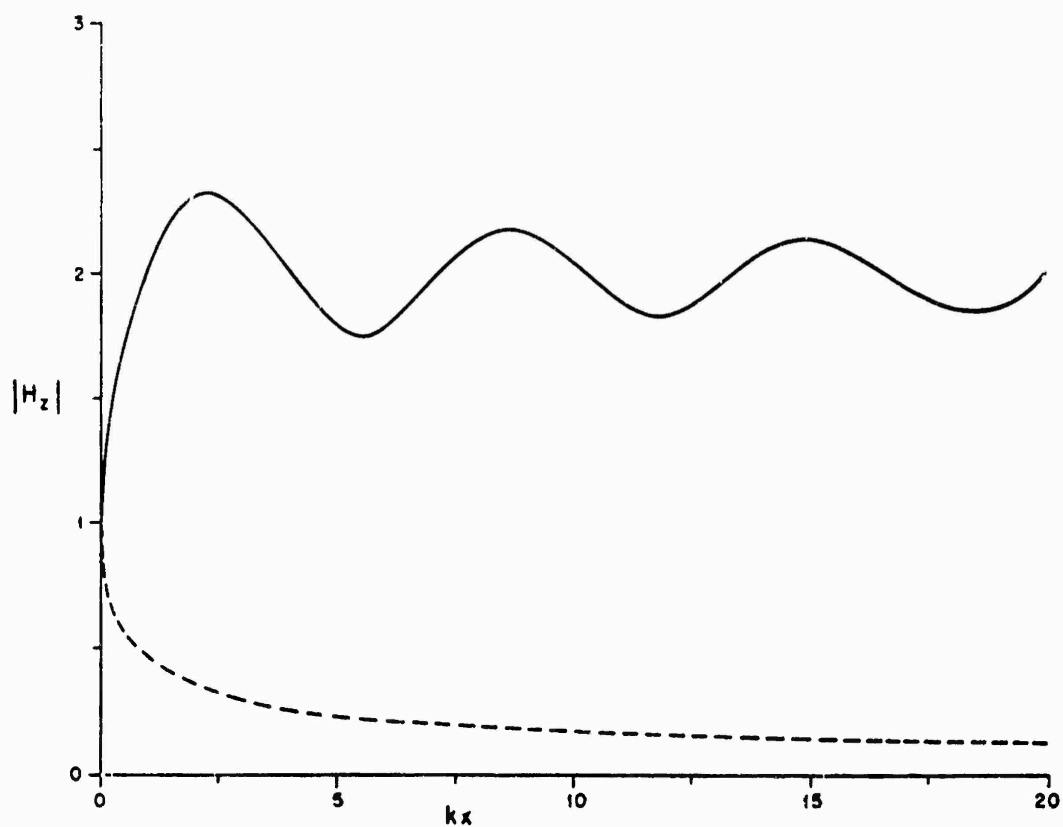


Fig. 8.12. Amplitude of surface field for $\phi_0 = \frac{1}{2}\pi$ and $\phi = 0$ (—), $\phi = 2\pi$ (---).

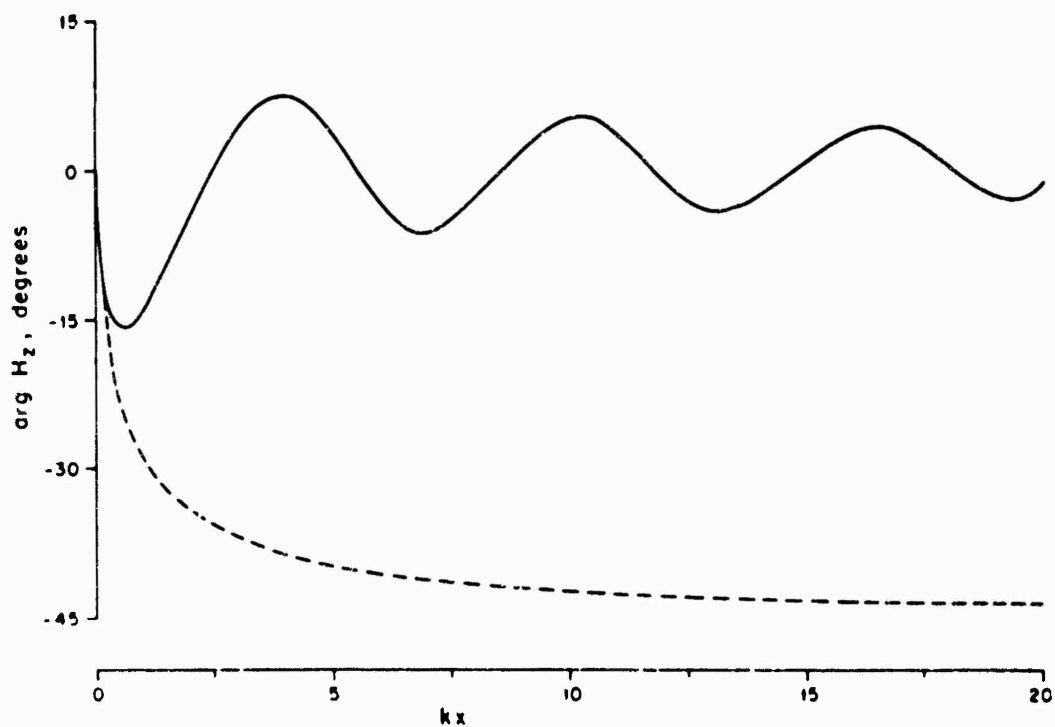


Fig. 8.13. Phase of surface field for $\phi_0 = \frac{1}{2}\pi$ and $\phi = 0$ (—), $\phi = 2\pi$ (---). Note that a phase term kx has been subtracted from the phase computed for the lower surface ($\phi = 2\pi$).

and H_z^d is the diffracted field, which is discontinuous at $\phi = \pi \pm \phi_0$ in order to compensate for the discontinuities in $H_z^{s.o.}$. In the immediate vicinity of these directions the actual transitional behavior of H_z is provided by the Fresnel integrals in eq. (8.28). For $k\rho \gg 1$ and ϕ not too close to $\pi \pm \phi_0$,

$$H_z^d \sim -\sqrt{\frac{2}{\pi k\rho}} e^{i(k\rho + \frac{1}{2}\pi)} \frac{\cos \frac{1}{2}\phi \cos \frac{1}{2}\phi_0}{\cos \phi + \cos \phi_0}. \quad (8.37)$$

This has the appearance of a cylindrical wave with

$$P = -i \frac{\cos \frac{1}{2}\phi \cos \frac{1}{2}\phi_0}{\cos \phi + \cos \phi_0} \quad (8.38)$$

emanating from the edge. SAVORNIN [1939] has computed $16|P|^2$ as a function of ϕ , $\pi < \phi < 2\pi$, for $\phi_0 = \frac{1}{2}\pi$. Similar computations, but for a variety of ϕ_0 , have been made by MARCINKOWSKI [1959] and TAVENNER [1960], and some of the data are reproduced in Fig. 8.14.

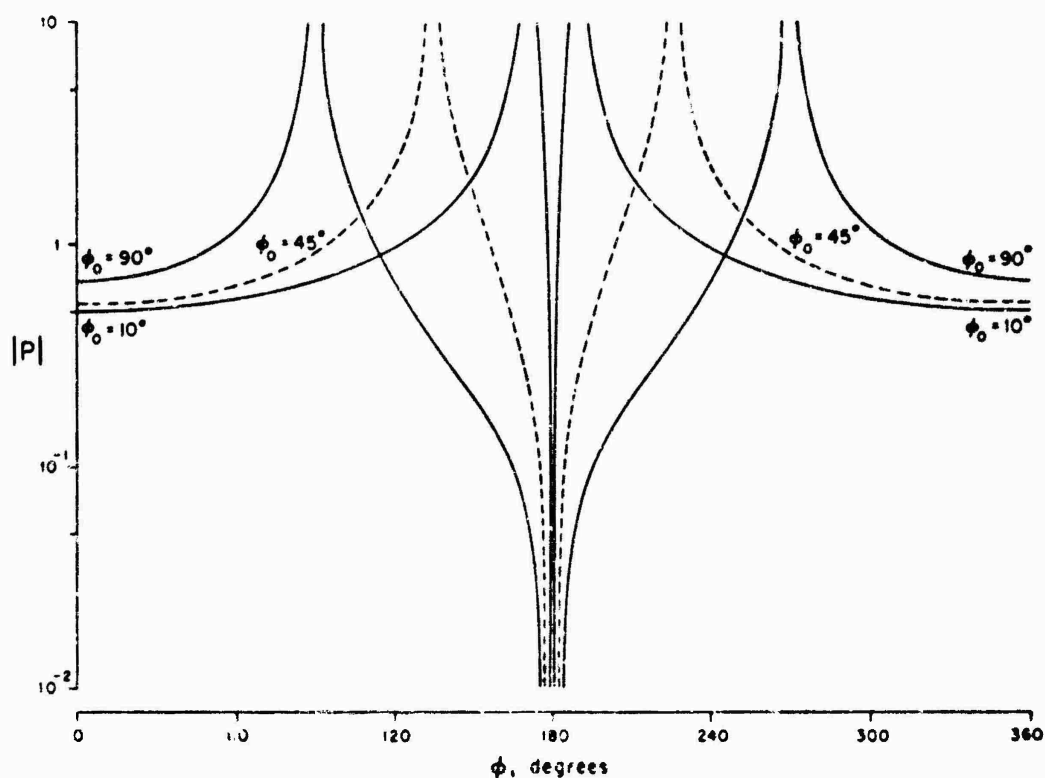


Fig. 8.14. Far field amplitude of the diffracted wave (MARCINKOWSKI [1959]).

As ϕ approaches $\pi \pm \phi_0$, the approximation implied by eq. (8.37) breaks down. Equation (8.28), however, indicates that for $\phi = \pi - \phi_0$

$$H_z = \exp(ik\rho \cos 2\frac{1}{2}\phi) + \frac{1}{2}e^{ik\rho} - \frac{e^{-\frac{1}{2}i\pi}}{\sqrt{\pi}} \exp(ik\rho \cos 2\phi_0) F[\sqrt{2k\rho} \sin \phi_0], \quad (8.39)$$

whereas for $\phi = \pi + \phi_0$,

$$H_z = \frac{1}{2}e^{ik\rho} + \frac{e^{-\frac{1}{2}i\pi}}{\sqrt{\pi}} \exp(ik\rho \cos 2\phi_0) F[\sqrt{2k\rho} \sin \phi_0]. \quad (8.40)$$

For edge-on incidence ($\phi_0 = \pi$), eq. (8.28) reduces to

$$H_z = e^{ik\rho \cos \phi}, \quad (8.41)$$

so that the scattered field is zero everywhere. For grazing incidence ($\phi_0 = 0$),

$$H_z = 2 \frac{e^{-\frac{1}{2}i\pi}}{\sqrt{\pi}} e^{-ik\rho \cos \phi} F[-\sqrt{2k\rho} \cos \frac{1}{2}\phi]. \quad (8.42)$$

8.3. Line sources

8.3.1. E-polarization

For an electric line source parallel to the edge and located at (ρ_0, ϕ_0) such that

$$E^i = 2H_0^{(1)}(kR), \quad (8.43)$$

a contour integral representation of the total electric field is (CARSLAW [1899]):

$$E_z = \frac{1}{8i\pi} \int_{C_1+C_2} H_0^{(1)}[kR(\alpha)] \{ \cot \frac{1}{4}(\pi - \alpha - \phi + \phi_0) - \cot \frac{1}{4}(\pi - \alpha - \phi - \phi_0) \} d\alpha \quad (8.44)$$

where

$$R(\alpha) = (\rho^2 + \rho_0^2 + 2\rho\rho_0 \cos \alpha)^{\frac{1}{2}} \quad (8.45)$$

and C_1 and C_2 are the Sommerfeld contours shown in Fig. 8.2. The above expression reduces to (CLEMMOW [1950]):

$$E_z = -\frac{2i}{\pi} \left\{ e^{ikR} \int_{-m}^{\infty} \frac{e^{i\mu^2}}{\sqrt{(\mu^2 + 2kR)}} d\mu - e^{ikR'} \int_{-m'}^{\infty} \frac{e^{i\mu^2}}{\sqrt{(\mu^2 + 2kR')}} d\mu \right\} \quad (8.46)$$

with

$$m = 2 \sqrt{\frac{k\rho\rho_0}{R_1 + R}} \cos \frac{1}{2}(\phi - \phi_0) = \pm \sqrt{k(R_1 - R)}, \quad \pm \text{ for } \cos \frac{1}{2}(\phi - \phi_0) \geq 0,$$

$$m' = 2 \sqrt{\frac{k\rho\rho_0}{R_1 + R'}} \cos \frac{1}{2}(\phi + \phi_0) = \pm \sqrt{k(R_1 - R')}, \quad \pm \text{ for } \cos \frac{1}{2}(\phi + \phi_0) \geq 0.$$

The form of solution given by MACDONALD [1915] can be obtained from eq. (8.46) by a change of integration variable:

$$\mu = \sqrt{2kS} \sinh \frac{1}{2}\xi, \quad S = R \text{ or } R'.$$

An alternative representation which has found some use is

$$E_z = \sum_{n=0}^{\infty} \varepsilon_n \sin(\frac{1}{2}n\phi) \sin(\frac{1}{2}n\phi_0) S_{\frac{1}{2}n} \quad (8.47)$$

where (MACDONALD [1902]):

$$S_v = J_v(k\rho_<)H_v^{(1)}(k\rho_>), \quad (8.48)$$

which may also be written (TUZHILIN [1963]):

$$S_v = \sum_{s=0}^{\infty} \frac{(\frac{1}{2}k\rho\rho_0)^{2s+v}}{s!\Gamma(s+v+1)} \frac{H_{2s+v}^{(1)}[k\sqrt{(\rho^2+\rho_0^2)}]}{[\sqrt{(\rho^2+\rho_0^2)}]^{2s+v}}. \quad (8.49)$$

The following symmetry relation holds:

$$E_z(\phi) - E_z(2\pi - \phi) = H_0^{(1)}(kR) - H_0^{(1)}(kR'). \quad (8.50)$$

If the observation point is on the surface (implying $R' = R$)

$$H_x = \frac{2Y}{\pi k} \frac{R_1}{R^2} \sqrt{\frac{\rho_0}{x}} \sin \frac{1}{2}\phi_0 \times \left\{ \mp e^{ikR_1} + 2i \frac{\sqrt{(R_1^2 - R^2)}}{R_1} e^{ikR} \int_{\pm\sqrt{(k(R_1 - R))}}^{\infty} \frac{\mu^2 + kR}{\sqrt{(\mu^2 + 2kR)}} e^{i\mu^2} d\mu \right\} \quad (8.51)$$

with the upper or lower sign for $\phi = 0$ or 2π respectively. An alternative (series) form is easily derived from eq. (8.47), and MOULLIN [1949] has used this to compute the real and imaginary parts (in-phase and quadrature components) of the normalized total current

$$\pi Z\{H_x(0) - H_x(2\pi)\} \quad (8.52)$$

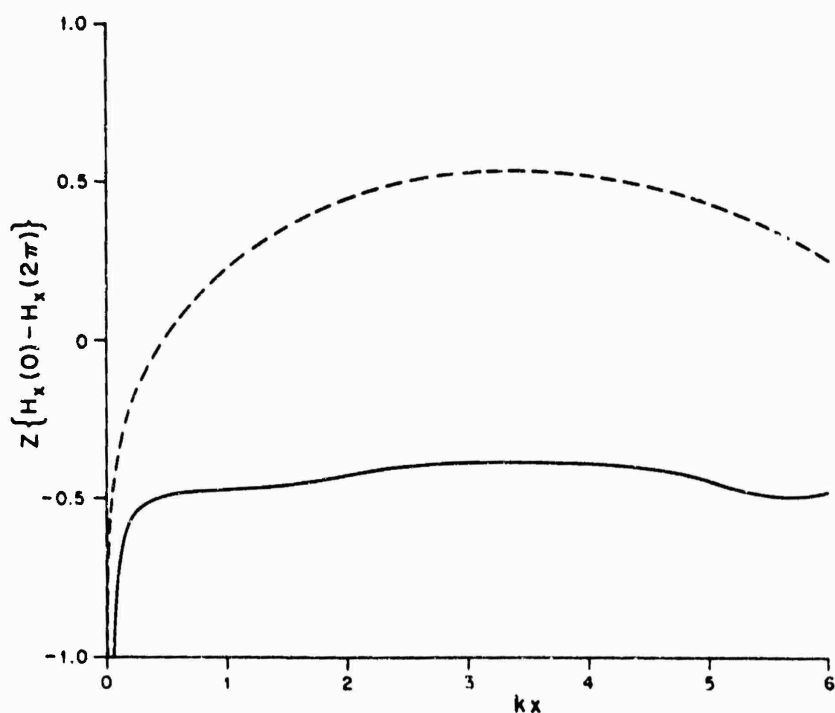


Fig. 8.15. Real (—) and imaginary (---) parts of the normalized total current for $k\rho_0 = 7$, $\phi_0 = 60^\circ$.

borne by the half-plane as functions of kx , $0 \leq kx \leq 4$, for $ky_0 = 0.603$ and $kx_0 = 0, 0.804$ and 1.95 . Similar computations, but for $1/\pi$ times the above quantities are given for other values of kx_0 and ky_0 by MOULLIN [1954]. The results of a recomputation of one of the latter cases are shown in Fig. 8.15.

If $k(R_1 - R) \ll 1$, a Taylor expansion of the integral in eq. (8.52) gives

$$H_x = \frac{2Y}{\pi k} \frac{R_1}{R^2} \sqrt{\frac{\rho_0}{x}} \sin \frac{1}{2} \phi_0 \left\{ \mp e^{ikR_1} - \frac{1}{2} i \pi k \frac{R}{R_1} \sqrt{R_1^2 - R^2} H_1^{(1)}(kR_1) \pm \right. \\ \left. \pm 2ik(R_1 - R)e^{ikR_1} + O[k^2(R_1 - R)^2] \right\} \quad (8.53)$$

which makes explicit the field singularity at the edge. If, on the other hand, $k(R_1 - R) \gg 1$,

$$H_x \sim \begin{cases} -2iY \frac{\rho_0}{R} H_1^{(1)}(kR) \sin \phi_0 - i \frac{Y}{kx} \frac{e^{ik\rho_0}}{\sqrt{(2\pi k\rho_0)}} \frac{e^{ikx}}{\sqrt{(2\pi kx)}} \frac{\sin \frac{1}{2} \phi_0}{\cos^2 \frac{1}{2} \phi_0} \\ \quad \times \{1 + O[k^{-1}(R_1 - R)^{-1}]\}, & (\phi = 0), \\ i \frac{Y}{kx} \frac{e^{ik\rho_0}}{\sqrt{(2\pi k\rho_0)}} \frac{e^{ikx}}{\sqrt{(2\pi kx)}} \frac{\sin \frac{1}{2} \phi_0}{\cos^2 \frac{1}{2} \phi_0} \{i + O[k^{-1}(R_1 - R)^{-1}]\}, & (\phi = 2\pi), \end{cases} \quad (8.54)$$

and the modification to the infinite sheet result now has the character of a cylindrical wave.

If $k(R_1 - R)$, $k(R_1 - R') \ll 1$, a small argument expansion of the integrals in eq. (8.46) gives

$$E_z = -\frac{4i}{\pi} \frac{e^{ikR_1}}{R_1} \sqrt{\rho\rho_0} \sin \frac{1}{2} \phi \sin \frac{1}{2} \phi_0 + O[k(R_1 - R)H_1^{(1)}(kR_1), k(R_1 - R')H_1^{(1)}(kR_1)] \quad (8.55)$$

and this holds for either the source or observation point, or both, near to the edge. For $k(R_1 - R)$, $k(R_1 - R') \gg 1$, a convenient decomposition of the field is

$$E_z = E_z^{g.o.} + E_z^d, \quad (8.56)$$

where $E_z^{g.o.}$ is the geometrical optics field given by

$$E_z^{g.o.} = \eta(\pi + \phi_0 - \phi) H_0^{(1)}(kR) - \eta(\pi - \phi_0 - \phi) H_0^{(1)}(kR') \quad (8.57)$$

and E_z^d is the diffracted field, which is discontinuous at $\phi = \pi \pm \phi_0$ in order to compensate for the discontinuities in $E_z^{g.o.}$. In the immediate vicinity of these directions, the actual transitional behavior of E_z is provided by the integrals in eq. (8.46). If $kR_1 \gg 1$, a first order approximation to E_z^d is (CLEMMOW [1950]):

$$E_z^d \sim \frac{2i}{\pi} \left\{ \operatorname{sgn}(\pi + \phi_0 - \phi) \frac{e^{ikR}}{\sqrt{\{k(R_1 + R)\}}} F[\sqrt{\{k(R_1 - R)\}}] - \right. \\ \left. - \operatorname{sgn}(\pi - \phi_0 - \phi) \frac{e^{ikR'}}{\sqrt{\{k(R_1 + R')\}}} F[\sqrt{\{k(R_1 - R')\}}] \right\}. \quad (8.58)$$

If, in addition, $k(R_1 - R), k(R_1 - R') \gg 1$, asymptotic expansion of the Fresnel integral gives

$$E_z^d \sim \frac{e^{ik\rho_0}}{\sqrt{(\pi k\rho_0)}} \frac{e^{ik\rho}}{\sqrt{(\pi k\rho)}} \frac{2 \sin \frac{1}{2}\phi \sin \frac{1}{2}\phi_0}{\cos \phi + \cos \phi_0}, \quad (8.59)$$

and this has the appearance of a cylindrical wave diverging from the edge.

The far field amplitude for the total electric field can be obtained from either eq. (8.46) or eq. (8.47) upon letting $k\rho \rightarrow \infty$. The result is identical to the plane wave solution given in eq. (8.10) or eq. (8.11) with ρ replaced by ρ_0 . MOULLIN [1949] has used the representation

$$P = \sum_{n=0}^{\infty} c_n e^{-\frac{1}{2}in\pi} J_{\frac{1}{2}n}(k\rho_0) \sin(\frac{1}{2}n\phi) \sin(\frac{1}{2}n\phi_0) \quad (8.60)$$

to compute the far field amplitude as a function of ϕ for a variety of $k\rho_0$ and ϕ_0 . Some results are shown in Fig. 8.16.

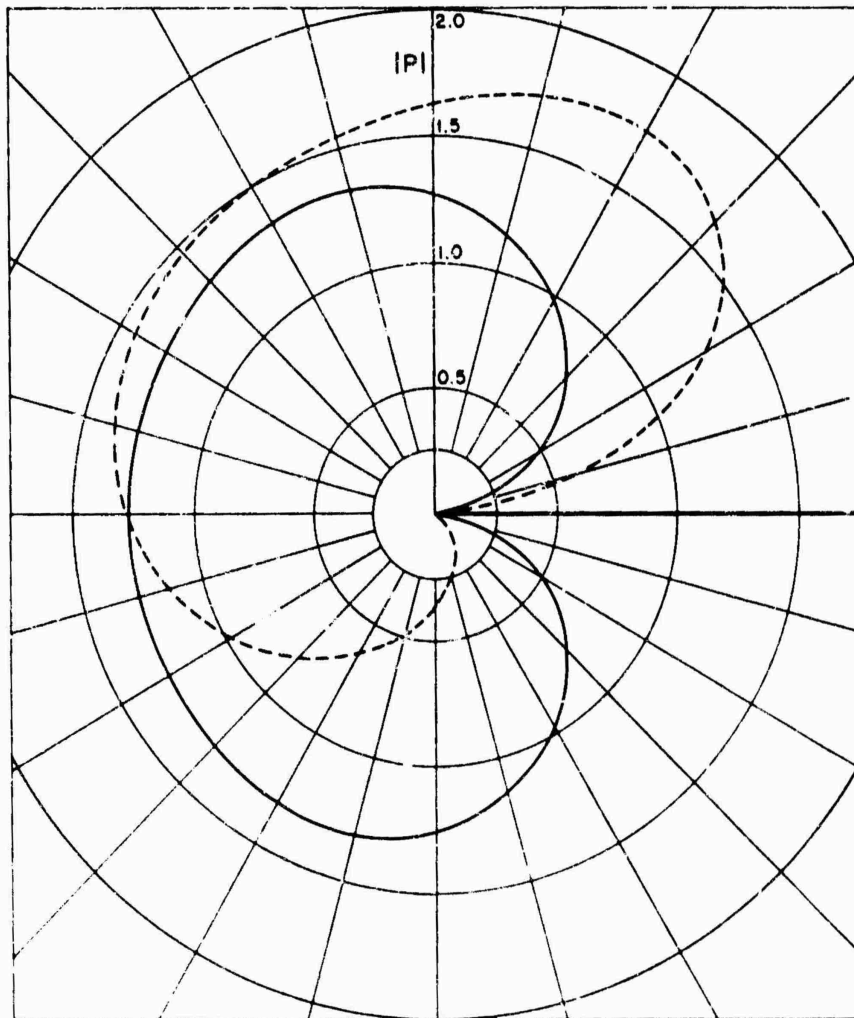


Fig. 8.16. Far field amplitude for $x_0 = \frac{1}{2}\lambda, y_0 = 0$ (—) and $x_0 = 0, y_0 = \frac{1}{2}\lambda$ (---).

On the boundaries $\phi = \pi \pm \phi_0$ of the geometrical optics regions, eq. (8.46) assumes the following forms: when $\phi = \pi - \phi_0$,

$$E_z = H_0^{(1)}(kR) - \frac{1}{2}H_0^{(1)}(kR_1) + \frac{2i}{\pi} e^{ikR} \int_{\sqrt{k(R_1-R)}}^{\infty} \frac{e^{i\mu^2}}{\sqrt{(\mu^2 + 2kR)}} d\mu, \quad (8.61)$$

whereas for $\phi = \pi + \phi_0$,

$$E_z = \frac{1}{2}H_0^{(1)}(kR_1) + \frac{2i}{\pi} e^{ikR'} \int_{\sqrt{k(R_1-R')}}^{\infty} \frac{e^{i\mu^2}}{\sqrt{(\mu^2 + 2kR')}} d\mu. \quad (8.62)$$

For the line source on the continuation of the half-plane (i.e. $\phi_0 = \pi$), eq. (8.45) reduces to

$$E_z = H_0^{(1)}(kR) + \frac{4i}{\pi} e^{ikR} \int_{\sqrt{k(R_1-R)}}^{\infty} \frac{e^{i\mu^2}}{\sqrt{(\mu^2 + 2kR)}} d\mu, \quad (8.63)$$

and if the observation point is on the surface in this case

$$H_x = \mp \frac{2Y}{\pi kR} \sqrt{\frac{\rho_0}{x}} e^{ikR}, \quad \mp \text{ for } \phi = 0, 2\pi. \quad (8.64)$$

For a line source on the half-plane itself ($\phi_0 = 0$), $E_z = 0$ everywhere.

8.3.2. *H-polarization*

For a magnetic line source parallel to the edge and located at (ρ_0, ϕ_0) such that

$$H^i = 2H_0^{(1)}(kR), \quad (8.65)$$

a contour integral representation of the total magnetic field is (CARSLAW [1899]):

$$H_z = \frac{1}{8i\pi} \int_{C_1+C_2} H_0^{(1)}[kR(\alpha)] \{ \cot \frac{1}{4}(\pi - \alpha - \phi + \phi_0) + \cot \frac{1}{4}(\pi - \alpha - \phi - \phi_0) \} d\alpha \quad (8.66)$$

where

$$R(\alpha) = (\rho^2 + \rho_0^2 + 2\rho\rho_0 \cos \alpha)^{\frac{1}{2}} \quad (8.67)$$

and C_1 and C_2 are the Sommerfeld contours shown in Fig. 8.2. The above expression reduces to (CLEMMOW [1950]):

$$H_z = -\frac{2i}{\pi} \left\{ e^{ikR} \int_{-m}^{\infty} \frac{e^{i\mu^2}}{\sqrt{(\mu^2 + 2kR)}} d\mu + e^{ikR'} \int_{-m'}^{\infty} \frac{e^{i\mu^2}}{\sqrt{(\mu^2 + 2kR')}} d\mu \right\} \quad (8.68)$$

with

$$m = 2 \sqrt{\frac{k\rho\rho_0}{R_1+R}} \cos \frac{1}{2}(\phi - \phi_0) = \pm \sqrt{k(R_1 - R)}, \quad \pm \text{ for } \cos \frac{1}{2}(\phi - \phi_0) \gtrless 0,$$

$$m' = 2 \sqrt{\frac{k\rho\rho_0}{R_1+R}} \cos \frac{1}{2}(\phi + \phi_0) = \pm \sqrt{k(R_1 - R')}, \quad \pm \text{ for } \cos \frac{1}{2}(\phi + \phi_0) \gtrless 0.$$

The form of solution given by MACDONALD [1915] can be obtained from eq. (8.61) by a change of integration variable:

$$\mu = \sqrt{2kS} \sinh \frac{1}{2}\xi, \quad S = R \quad \text{or} \quad R'.$$

An alternative representation which has found some use is

$$H_z = \sum_{n=0}^{\infty} \varepsilon_n \cos(\frac{1}{2}n\phi) \cos(\frac{1}{2}n\phi_0) S_{\frac{1}{2}n} \quad (8.69)$$

where S_n is given in eq. (8.48) or equivalently in eq. (8.49). The following symmetry relation holds:

$$H_z(\phi) + H_z(2\pi - \phi) = H_0^{(1)}(kR) + H_0^{(1)}(kR'). \quad (8.70)$$

If the observation point is on the surface (implying $R' = R$)

$$H_z = -\frac{4i}{\pi} e^{ikR} \int_0^{\infty} \frac{e^{i\mu^2}}{\mp \sqrt{k(R_1 - R)} \sqrt{(\mu^2 + 2kR)}} d\mu \quad (8.71)$$

with the upper or lower sign for $\phi = 0$ or 2π respectively. An alternative (series) form follows immediately from eq. (8.69), and this has been used to compute the real

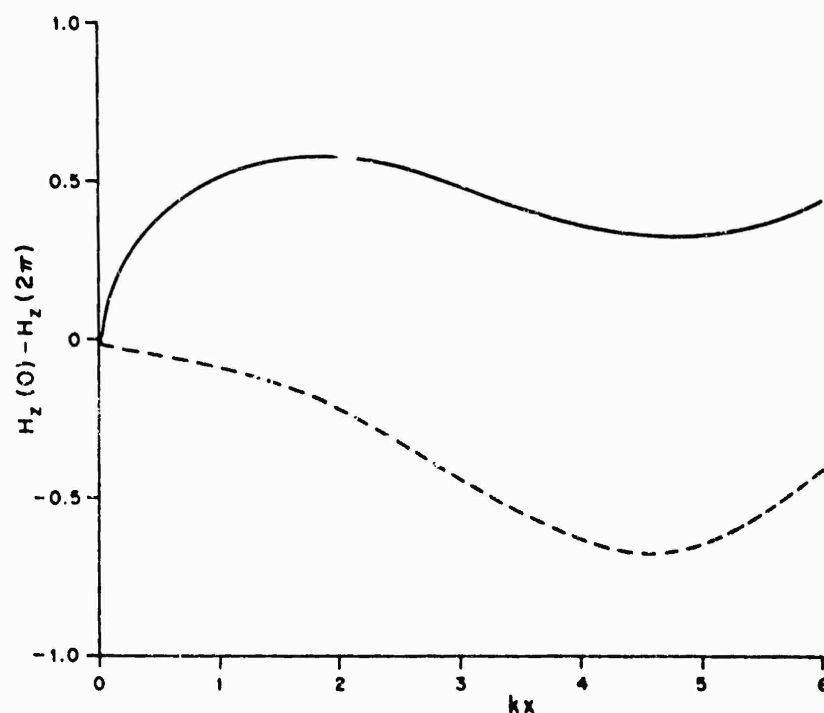


Fig. 8.17. Real (—) and imaginary (---) parts of the normalized total current for $k\rho_0 = 7$, $\phi_0 = 60^\circ$.

and imaginary parts (in-phase and quadrature components) of the total current shown in Fig. 8.17. If $k(R_1 - R) \ll 1$, a Taylor expansion of the integral in eq. (8.71) gives

$$H_z = H_0^{(1)}(kR) \mp \frac{4i}{\pi} \sqrt{\frac{R_1 - R}{R_1 + R}} e^{ikR_1} \{1 + O[k(R_1 - R)]\}. \quad (8.72)$$

If, on the other hand, $k(R_1 - R) \gg 1$,

$$H_z \sim \begin{cases} 2H_0^{(1)}(kR) - \frac{e^{ik\rho_0}}{\sqrt{(\pi k\rho_0)}} \frac{e^{ikx}}{\sqrt{(\pi kx)}} \sec \frac{1}{2}\phi_0 \{1 + O[k^{-1}(R_1 - R)^{-1}]\}, & (\phi = 0), \\ \frac{e^{ik\rho_0}}{\sqrt{(\pi k\rho_0)}} \frac{e^{ikx}}{\sqrt{(\pi kx)}} \sec \frac{1}{2}\phi_0 \{1 + O[k^{-1}(R_1 - R)^{-1}]\}, & (\phi = 2\pi), \end{cases} \quad (8.73)$$

and the modification to the infinite sheet result now has the character of a cylindrical wave.

If $k(R_1 - R)$, $k(R_1 - R') \ll 1$, a small argument expansion of the integrals in eq. (8.68) gives

$$H_z = H_0^{(1)}(kR_1) - \frac{4i}{\pi} \frac{e^{ikR_1}}{R_1} \sqrt{\rho\rho_0} \cos \frac{1}{2}\phi \cos \frac{1}{2}\phi_0 + O[k(R_1 - R)H_1^{(1)}(kR_1), k(R_1 - R')H_1^{(1)}(kR_1)] \quad (8.74)$$

and this holds for either the source or observation point, or both, near to the edge. For $k(R_1 - R)$, $k(R_1 - R') \gg 1$, a convenient decomposition of the field is

$$H_z = H_z^{g.o.} + H_z^d, \quad (8.75)$$

where $H_z^{g.o.}$ is the geometrical optics field given by

$$H_z^{g.o.} = \eta(\pi + \phi_0 - \phi)H_0^{(1)}(kR) + \eta(\pi - \phi_0 - \phi)H_0^{(1)}(kR') \quad (8.76)$$

and H_z^d is the diffracted field, which is discontinuous at $\phi = \pi \pm \phi_0$ in order to compensate for the discontinuities in $H_z^{g.o.}$. In the immediate vicinity of these directions, the actual transitional behavior of H_z is provided by the integrals in eq. (8.68). If $kR_1 \gg 1$, a first order approximation to H_z^d is (CLEMMOW [1950]):

$$H_z^d \sim \frac{2i}{\pi} \left\{ \operatorname{sgn}(\pi + \phi_0 - \phi) \frac{e^{ikR}}{\sqrt{\{k(R_1 + R)\}}} F[\sqrt{\{k(R_1 - R)\}}] + \operatorname{sgn}(\pi - \phi_0 - \phi) \frac{e^{ikR'}}{\sqrt{\{k(R_1 + R')\}}} F[\sqrt{\{k(R_1 - R')\}}] \right\}. \quad (8.77)$$

If, in addition, $k(R_1 - R)$, $k(R_1 - R') \gg 1$, asymptotic expansion of the Fresnel integrals gives

$$H_z^d \sim - \frac{e^{ik\rho_0}}{\sqrt{(\pi k\rho_0)}} \frac{e^{ik\rho}}{\sqrt{(\pi k\rho)}} \frac{2 \cos \frac{1}{2}\phi \cos \frac{1}{2}\phi_0}{\cos \phi + \cos \phi_0} \quad (8.78)$$

and this has the appearance of a cylindrical wave diverging from the edge.

The far field amplitude for the total magnetic field can be obtained from either eq. (8.68) or eq. (8.69) upon letting $k\rho \rightarrow \infty$. The result is identical to the plane wave solution given in eq. (8.28) or eq. (8.29) with ρ replaced by ρ_0 .

On the boundaries $\phi = \pi \pm \phi_0$ of the geometrical optics regions, eq. (8.68) assumes the following forms: when $\phi = \pi - \phi_0$,

$$H_z = H_0^{(1)}(kR) + \frac{1}{2} H_0^{(1)}(kR_1) + \frac{2i}{\pi} e^{ikR} \int_{\sqrt{k(R_1-R)}}^{\infty} \frac{e^{i\mu^2}}{\sqrt{(\mu^2 + 2kR)}} d\mu, \quad (8.79)$$

whereas for $\phi = \pi + \phi_0$,

$$H_z = \frac{1}{2} H_0^{(1)}(kR_1) - \frac{2i}{\pi} e^{ikR'} \int_{\sqrt{k(R_1-R')}}^{\infty} \frac{e^{i\mu^2}}{\sqrt{(\mu^2 + 2kR')}} d\mu. \quad (8.80)$$

For the line source on the continuation of the half-plane (i.e. $\phi_0 = \pi$), eq. (8.68) reduces to

$$H_z = H_0^{(1)}(kR), \quad (8.81)$$

so that the scattered field is zero everywhere. For the line source on the half-plane ($\phi_0 = 0$),

$$H_z = -\frac{4i}{\pi} e^{ikR} \int_{-\sqrt{k(R_1-R)}}^{\infty} \frac{e^{i\mu^2}}{\sqrt{(\mu^2 + 2kR)}} d\mu. \quad (8.82)$$

8.4. Point sources

8.4.1. Acoustically soft half-plane

For a point source at (ρ_0, ϕ_0, z_0) such that

$$V^i = \frac{e^{ikR}}{kR}, \quad (8.83)$$

a contour integral representation of the total field is (CARSLAW [1899]):

$$V = \frac{1}{8i\pi} \int_{C_1+C_2} \frac{e^{ikR(\alpha)}}{kR(\alpha)} \{ \cot \frac{1}{2}(\pi - \alpha - \phi + \phi_0) - \cot \frac{1}{2}(\pi - \alpha - \phi - \phi_0) \} d\alpha \quad (8.84)$$

where

$$R(\alpha) = \{ \rho^2 + \rho_0^2 + 2\rho\rho_0 \cos \alpha + (z - z_0)^2 \}^{\frac{1}{2}} \quad (8.85)$$

and C_1 and C_2 are the Sommerfeld contours shown in Fig. 8.2. The above expression reduces to

$$V = i \int_{-m}^{\infty} \frac{H_1^{(1)}(\mu^2 + kR)}{\sqrt{(\mu^2 + 2kR)}} d\mu - i \int_{-m'}^{\infty} \frac{H_1^{(1)}(\mu^2 + kR')}{\sqrt{(\mu^2 + 2kR')}} d\mu \quad (8.86)$$

with

$$m = 2 \sqrt{\frac{k\rho\rho_0}{R_1 + R}} \cos \frac{1}{2}(\phi - \phi_0) = \pm \sqrt{k(R_1 - R)}, \quad \pm \text{ for } \cos \frac{1}{2}(\phi - \phi_0) \gtrless 0,$$

$$m' = 2 \sqrt{\frac{k\rho\rho_0}{R_1 - R'}} \cos \frac{1}{2}(\phi + \phi_0) = \pm \sqrt{k(R_1 - R')}, \quad \pm \text{ for } \cos \frac{1}{2}(\phi + \phi_0) \gtrless 0.$$

The form of solution given by MACDONALD [1915] can be obtained from eq. (8.86) by a change of integration variable:

$$\mu = \sqrt{2kS} \sinh \frac{1}{2}\xi, \quad S = R \text{ or } R'.$$

An alternative representation of the total field as an eigenfunction expansion is

$$V = \sum_{n=0}^{\infty} \varepsilon_n \sin(\frac{1}{2}n\phi) \sin(\frac{1}{2}n\phi_0) S_{\frac{1}{2}n} \quad (8.87)$$

where (VANDAKUROV [1954]):

$$S_v = \frac{i}{2k} \int_{-\infty}^{\infty} dt e^{it(z-z_0)} J_v[\rho < \sqrt{(k^2 - t^2)}] H_v^{(1)}[\rho > \sqrt{(k^2 - t^2)}], \quad (8.88)$$

which may be written in the form (TUZHILIN [1963]):

$$S_v = i \sum_{s=0}^{\infty} \frac{(\frac{1}{2}k\rho\rho_0)^{2s+v}}{s! \Gamma(s+v+1)} \frac{h_{2s+v}^{(1)}(k\sqrt{\{\rho^2 + \rho_0^2 + (z-z_0)^2\}})}{(\sqrt{\{\rho^2 + \rho_0^2 + (z-z_0)^2\}})^{2s+v}} \quad (8.89)$$

and may further be written (MACDONALD [1915]):

$$S_v = ie^{-2iv\pi} \sum_{s=0}^{\infty} \frac{\Gamma(s+2v+1)}{s!} (2s+2v+1) j_{s+v}(kr_<) h_{s+v}^{(1)}(kr_>) P_{s+v}^{-v}(\cos \theta) P_{s+v}^{-v}(\cos \theta_0). \quad (8.90)$$

The following symmetry relation holds:

$$V(\phi) - V(2\pi - \phi) = \frac{e^{ikR}}{kR} - \frac{e^{ikR'}}{kR'}. \quad (8.91)$$

If the observation point is on the surface (implying $R' = R$)

$$\begin{aligned} \frac{\partial V}{\partial y} = i \frac{R_1}{R^2} \sqrt{\frac{\rho_0}{x}} \sin \frac{1}{2}\phi_0 \left\{ \pm H_1^{(1)}(kR_1) - 2 \frac{\sqrt{(R_1^2 - R^2)}}{R_1} \right. \\ \left. \times \int_{\mp \sqrt{k(R_1 - R)}}^r \frac{\mu^2 + kR}{\sqrt{(\mu^2 + 2kR)}} H_1^{(1)'}(\mu^2 + kR) d\mu \right\} \quad (8.92) \end{aligned}$$

with the upper or lower sign for $\phi = 0$ or 2π respectively. If $k(R_1 - R) \ll 1$, a Taylor expansion of the integral in eq. (8.92) gives

$$\begin{aligned} \frac{\partial V}{\partial y} = i \frac{R_1}{R^2} \sqrt{\frac{\rho_0}{x}} \sin \frac{1}{2}\phi_0 \left\{ \pm H_1^{(1)}(kR_1) - \left(1 + \frac{i}{kR}\right) \frac{\sqrt{(R_1^2 - R^2)}}{R_1} e^{ikR} \mp \right. \\ \left. \mp 2k(R_1 - R) H_1^{(1)'}(kR_1) + O[k^2(R_1 - R)^2] \right\} \quad (8.93) \end{aligned}$$

which makes explicit the field singularity at the edge. If, on the other hand, $k(R_1 - R) \gg 1$,

$$\frac{\partial V}{\partial y} \sim \begin{cases} -2i \frac{\rho_0}{R^2} \left(1 + \frac{i}{kR}\right) e^{ikR} \sin \phi_0 + \frac{i}{4kx} \frac{H_0^{(1)}(kR_1)}{\sqrt{(\rho_0 x)}} \frac{\sin \frac{1}{2}\phi_0}{\cos^2 \frac{1}{2}\phi_0} \\ \quad \times \{1 + O[k^{-1}(R_1 - R)^{-1}]\}, \quad (\phi = 0), \\ -\frac{i}{4kx} \frac{H_0^{(1)}(kR_1)}{\sqrt{(\rho_0 x)}} \frac{\sin \frac{1}{2}\phi_0}{\cos^2 \frac{1}{2}\phi_0} \{1 + O[k^{-1}(R_1 - R)^{-1}]\}, \quad (\phi = 2\pi). \end{cases} \quad (8.94)$$

If $k(R_1 - R)$, $k(R_1 - R') \ll 1$, a small argument expansion of the integrals in eq. (8.86) gives

$$V = 2iH_1^{(1)}(kR_1) \frac{\sqrt{(\rho\rho_0)}}{R_1} \sin \frac{1}{2}\phi \sin \frac{1}{2}\phi_0 + O[k(R_1 - R)h_1^{(1)}(kR_1), k(R_1 - R')h_1^{(1)}(kR_1)] \quad (8.95)$$

and this holds for either the source or observation point, or both, near to the edge. For $k(R_1 - R)$, $k(R_1 - R') \gg 1$, a convenient decomposition of the field is

$$V = V^{s.o.} + V^d, \quad (8.96)$$

where $V^{s.o.}$ is the geometrical optics field given by

$$V = \eta(\pi + \phi_0 - \phi) \frac{e^{ikR}}{kR} - \eta(\pi - \phi_0 - \phi) \frac{e^{ikR'}}{kR'} \quad (8.97)$$

and V^d is the diffracted field, which is discontinuous at $\phi = \pi \pm \phi_0$ in order to compensate for the discontinuities in $V^{s.o.}$. In the immediate vicinity of these directions, the actual transitional behavior of V is provided by the integrals in eq. (8.86). If $kR_1 \gg 1$, a first order approximation to V^d is (MACDONALD [1915]),

$$V^d \sim -\sqrt{\frac{2}{\pi k R_1}} e^{-i\pi} \left\{ \operatorname{sgn}(\pi + \phi_0 - \phi) \frac{e^{ikR}}{\sqrt{\{k(R_1 + R)\}}} F[\sqrt{\{k(R_1 - R)\}}] - \operatorname{sgn}(\pi - \phi_0 - \phi) \frac{e^{ikR'}}{\sqrt{\{k(R_1 + R')\}}} F[\sqrt{\{k(R_1 - R')\}}] \right\}. \quad (8.98)$$

If, in addition, $k(R_1 - R)$, $k(R_1 - R') \gg 1$, asymptotic expansion of the Fresnel integrals gives

$$V^d \sim \sqrt{\frac{2}{\pi k R_1}} e^{i(\pi R_1 + \frac{1}{2}\pi)} \frac{1}{\sqrt{(k\rho_0)}} \frac{1}{\sqrt{(k\rho)}} \frac{\sin \frac{1}{2}\phi \sin \frac{1}{2}\phi_0}{\cos \phi + \cos \phi_0}. \quad (8.99)$$

On the boundaries $\phi = \pi \pm \phi_0$ of the geometrical optics regions, eq. (8.86) assumes the following forms: when $\phi = \pi - \phi_0$,

$$V = \frac{e^{ikR}}{kR} - \frac{1}{2} \frac{e^{ikR_1}}{kR_1} - i \int_{\sqrt{\{k(R_1 - R)\}}}^{\infty} \frac{H_1^{(1)}(\mu^2 + kR)}{\sqrt{(\mu^2 + 2kR)}} d\mu, \quad (8.100)$$

whereas for $\phi = \pi + \phi_0$,

$$V = \frac{1}{2} \frac{e^{ikR_1}}{kR_1} - i \int_{\sqrt{k(R_1 - R')}}^{\infty} \frac{H_1^{(1)}(\mu^2 + kR')}{\sqrt{(\mu^2 + 2kR')}} d\mu. \quad (8.101)$$

For the point source on the continuation of the half-plane (i.e. $\phi_0 = \pi$), eq. (8.86) reduces to

$$V = \frac{e^{ikR}}{kR} - 2i \int_{\sqrt{k(R_1 - R)}}^{\infty} \frac{H_1^{(1)}(\mu^2 + kR)}{\sqrt{(\mu^2 + 2kR)}} d\mu, \quad (8.102)$$

and if the observation point is on the surface in this case

$$\frac{\partial V}{\partial y} = \pm \frac{i}{R} \sqrt{\frac{\rho_0}{x}} H_1^{(1)}(kR), \quad \pm \text{ for } \phi = 0, 2\pi. \quad (8.103)$$

For a point source on the half-plane itself ($\phi_0 = 0$), $V = 0$ everywhere.

8.4.2. Acoustically hard half-plane

For a point source at (ρ_0, ϕ_0, z_0) such that

$$V^i = \frac{e^{ikR}}{kR}, \quad (8.104)$$

a contour integral representation of the total field is (CARSLAW [1899]):

$$V = \frac{1}{8i\pi} \int_{C_1 + C_2} \frac{e^{ikR(\alpha)}}{kR(\alpha)} \{ \cot \frac{1}{4}(\pi - \alpha - \phi + \phi_0) + \cot \frac{1}{4}(\pi - \alpha - \phi - \phi_0) \} d\alpha \quad (8.105)$$

where

$$R(\alpha) = \{ \rho^2 + \rho_0^2 + 2\rho\rho_0 \cos \alpha + (z - z_0)^2 \}^{\frac{1}{2}} \quad (8.106)$$

and C_1 and C_2 are the Sommerfeld contours shown in Fig. 8.2. The above expression reduces to

$$V = i \int_{-m}^{\infty} \frac{H_1^{(1)}(\mu^2 + kR)}{\sqrt{(\mu^2 + 2kR)}} d\mu + i \int_{-m'}^{\infty} \frac{H_1^{(1)}(\mu^2 + kR')}{\sqrt{(\mu^2 + 2kR')}} d\mu \quad (8.107)$$

with

$$m = 2 \sqrt{\frac{k\rho\rho_0}{R_1 + R}} \cos \frac{1}{2}(\phi - \phi_0) = \pm \sqrt{k(R_1 - R)}, \quad \pm \text{ for } \cos \frac{1}{2}(\phi - \phi_0) \geq 0,$$

$$m' = 2 \sqrt{\frac{k\rho\rho_0}{R_1 + R'}} \cos \frac{1}{2}(\phi + \phi_0) = \pm \sqrt{k(R_1 - R')}, \quad \pm \text{ for } \cos \frac{1}{2}(\phi + \phi_0) \geq 0.$$

The form of solution given by MACDONALD [1915] can be obtained from eq. (8.107) by a change of integration variable:

$$\mu = \sqrt{2kS} \sinh \frac{1}{2}\xi, \quad S = R \text{ or } R'.$$

An alternative representation of the total field as an eigenfunction expansion is

$$V = \sum_{n=0}^{\infty} \varepsilon_n \cos(\tfrac{1}{2}n\phi) \cos(\tfrac{1}{2}n\phi_0) S_{\frac{1}{2}n} \quad (8.108)$$

where S_n is given in three equivalent forms by eqs. (8.88) through (8.90). The following symmetry relation holds:

$$V(\phi) + V(2\pi - \phi) = \frac{e^{ikR}}{kR} + \frac{e^{ikR'}}{kR'}. \quad (8.109)$$

If the observation point is on the surface (implying $R' = R$)

$$V = 2i \int_{\mp \sqrt{k(R_1 - R)}}^{\infty} \frac{H_1^{(1)}(\mu^2 + kR)}{\sqrt{(\mu^2 + 2kR)}} d\mu \quad (8.110)$$

with the upper or lower sign for $\phi = 0$ or 2π respectively. If $k(R_1 - R) \ll 1$, a Taylor expansion of the integral in eq. (8.110) gives

$$V = \frac{e^{ikR}}{kR} \pm 2i \sqrt{\frac{R_1 - R}{R_1 + R}} H_1^{(1)}(\sqrt{kR_1}) \{1 + O[k(R_1 - R)]\}. \quad (8.111)$$

If, on the other hand, $k(R_1 - R) \gg 1$,

$$V \sim \begin{cases} 2 \frac{e^{ikR}}{kR} + i \frac{H_0^{(1)}(kR_1)}{2k\sqrt{(\rho_0 x)}} \sec \tfrac{1}{2}\phi_0 \{1 + O[k^{-1}(R_1 - R)^{-1}]\}, & (\phi = 0), \\ i \frac{H_0^{(1)}(kR_1)}{2k\sqrt{(\rho_0 x)}} \sec \tfrac{1}{2}\phi_0 \{1 + O[k^{-1}(R_1 - R)^{-1}]\}, & (\phi = 2\pi). \end{cases} \quad (8.112)$$

If $k(R_1 - R)$, $k(R_1 - R') \ll 1$, a small argument expansion of the integrals in eq. (8.107) gives

$$V = \frac{e^{ikR_1}}{kR_1} + 2iH_1^{(1)}(kR_1) \frac{\sqrt{(\rho\rho_0)}}{R_1} \cos \tfrac{1}{2}\phi \cos \tfrac{1}{2}\phi_0 + \\ + O[k(R_1 - R)h_1^{(1)}(kR_1), k(R_1 - R')h_1^{(1)}(kR_1)] \quad (8.113)$$

and this holds for either the source or observation point, or both, near to the edge. For $k(R_1 - R)$, $k(R_1 - R') \gg 1$, a convenient decomposition of the field is

$$V = V^{g.o.} + V^d, \quad (8.114)$$

where $V^{g.o.}$ is the geometrical optics field given by

$$V = \eta(\pi + \phi_0 - \phi) \frac{e^{ikR}}{kR} + \eta(\pi - \phi_0 - \phi) \frac{e^{ikR'}}{kR'} \quad (8.115)$$

and V^d is the diffracted field, which is discontinuous at $\phi = \pi \pm \phi_0$ in order to compensate for the discontinuities in $V^{g.o.}$. In the immediate vicinity of these directions, the actual transitional behavior of V is provided by the integrals in eq. (8.107). If

$kR_1 \gg 1$, a first order approximation to V^d is (MACDONALD [1915]):

$$V^d \sim - \sqrt{\frac{2}{\pi k R_1}} e^{-\frac{1}{2}i\pi} \left\{ \operatorname{sgn}(\pi + \phi_0 - \phi) \frac{e^{ikR}}{\sqrt{\{k(R_1 + R)\}}} F[\sqrt{\{k(R_1 - R)\}}] + \right. \\ \left. + \operatorname{sgn}(\pi - \phi_0 - \phi) \frac{e^{ikR'}}{\sqrt{\{k(R_1 + R')\}}} F[\sqrt{\{k(R_1 - R')\}}] \right\}. \quad (8.116)$$

If, in addition, $k(R_1 - R)$, $k(R_1 - R') \gg 1$, asymptotic expansion of the Fresnel integrals gives

$$V^d \sim - \sqrt{\frac{2}{\pi k R_1}} e^{i(kR_1 + \frac{1}{2}\pi)} \frac{1}{\sqrt{(k\rho_0)}} \frac{1}{\sqrt{(k\rho)}} \frac{\cos \frac{1}{2}\phi \cos \frac{1}{2}\phi_0}{\cos \phi + \cos \phi_0}. \quad (8.117)$$

On the boundaries $\phi = \pi \pm \phi_0$ of the geometrical optics regions, eq. (8.107) assumes the following forms: when $\phi = \pi - \phi_0$,

$$V = \frac{e^{ikR}}{kR} + \frac{1}{2} \frac{e^{ikR_1}}{kR_1} - i \int_{\sqrt{\{k(R_1 - R)\}}}^{\infty} \frac{H_1^{(1)}(\mu^2 + kR)}{\sqrt{(\mu^2 + 2kR)}} d\mu, \quad (8.118)$$

whereas for $\phi = \pi + \phi_0$,

$$V = \frac{1}{2} \frac{e^{ikR_1}}{kR_1} + i \int_{\sqrt{\{k(R_1 - R')\}}}^{\infty} \frac{H_1^{(1)}(\mu^2 + kR')}{\sqrt{(\mu^2 + 2kR')}} d\mu. \quad (8.119)$$

For a point source on the continuation of the half-plane (i.e. $\phi_0 = \pi$), eq. (8.107) reduces to

$$V = \frac{e^{ikR}}{kR}, \quad (8.120)$$

so that the scattered field is zero everywhere. For the point source on the half-plane itself ($\phi_0 = 0$),

$$V = 2i \int_{-\sqrt{\{k(R_1 - R)\}}}^{\infty} \frac{H_1^{(1)}(\mu^2 + kR)}{\sqrt{(\mu^2 + 2kR^2)}} d\mu. \quad (8.121)$$

8.5. Dipole sources

8.5.1. Electric dipoles

For an arbitrarily oriented electric dipole at (ρ_0, ϕ_0, z_0) with moment $(4\pi\epsilon k)\hat{c}$, corresponding to an electric Hertz vector

$$\Pi^i = \hat{c} \frac{e^{ikR}}{kR} \quad (8.122)$$

where

$$\hat{c} = \hat{x} \sin \Theta \cos \Phi + \hat{y} \sin \Theta \sin \Phi + \hat{z} \cos \Theta, \quad (8.123)$$

a contour integral representation of the total electric Hertz vector is (MALYUZHINSKY)

and TUZHILIN [1963]):

$$\Pi = \frac{1}{8i\pi} \int_{C_1+C_2} \frac{e^{ikR(x)}}{kR(x)} \{ \hat{e}(\pi - \alpha - \phi + \phi_0 - \Phi) \cot \frac{1}{4}(\pi - \alpha - \phi + \phi_0) - \\ - \hat{e}(\pi - \alpha - \phi - \phi_0 + \Phi) \cot \frac{1}{4}(\pi - \alpha - \phi - \phi_0) \} dx \quad (8.124)$$

where

$$R(x) = \{ \rho^2 + \rho_0^2 + 2\rho\rho_0 \cos \alpha + (z - z_0)^2 \}^{\frac{1}{2}}, \quad (8.125)$$

$$\hat{e}(x) = \hat{x} \sin \Theta \cos \alpha - \hat{y} \sin \Theta \sin \alpha + \hat{z} \cos \Theta, \quad (8.126)$$

and C_1 and C_2 are the Sommerfeld contours shown in Fig. 8.2. The above expression may be reduced to (BOWMAN and SENIOR [1967]):

$$\Pi = \hat{x} \left[lV^s + \frac{i}{k\sqrt{(\rho\rho_0)}} H_0^{(1)}(kR_1)(l \sin \frac{1}{2}\phi_0 - m \cos \frac{1}{2}\phi_0) \sin \frac{1}{2}\phi \right] + \\ + \hat{y} \left[mV^h - \frac{i}{k\sqrt{(\rho\rho_0)}} H_0^{(1)}(kR_1)(l \sin \frac{1}{2}\phi_0 - m \cos \frac{1}{2}\phi_0) \cos \frac{1}{2}\phi \right] + \hat{z}nV^s, \quad (8.127)$$

where $l = \sin \Theta \cos \Phi$, $m = \sin \Theta \sin \Phi$, $n = \cos \Theta$ are the directional cosines of \hat{e} , and V^s and V^h are, respectively, the acoustically soft and acoustically hard point source solutions in Sec. 8.4. The following symmetry relation holds:

$$\Pi(\phi) - \Pi(2\pi - \phi) = \hat{e}(-\Phi) \frac{e^{ikR}}{kR} - \hat{e}(\Phi) \frac{e^{ikR'}}{kR'}. \quad (8.128)$$

The form of solution (8.127) is remarkable in that the previously-derived scalar solutions V^s and V^h are explicitly involved along with certain additive correction terms which obey the source-free wave equations. If $l = m \cot \frac{1}{2}\phi_0$, these additive terms vanish and the electromagnetic field is determined by V^s and V^h alone. If, furthermore, $l = m = 0$, the field is determined by V^s only. In the case of other dipole orientations, however, the additive terms are necessary to provide the correct edge behavior. In general, all the functions Π , E and H are of order $\rho^{-\frac{1}{2}}$ as $\rho \rightarrow 0$. The additive terms for the Hertz potential are equivalent to those derived by VANDAKUROV [1954] and are analogous, but not equivalent, to those presented for the electromagnetic field quantities by SENIOR [1953] in the case of the vertical (y-oriented) dipole and by WOODS [1957], WILLIAMS [1957] and JONLS [1965] in the case of the arbitrarily oriented dipole. In these last references, the electromagnetic field quantities are expressed as derivatives with respect to both source and observer coordinates, and the consequent additive correction terms are not immediately derivable from a Hertz potential.

The components of the total magnetic field derived by vector operations on Π are

$$H_x = k^3 Y \left\{ [m(z - z_0) - n(y - y_0)] I_R + [m(z - z_0) + n(y + y_0)] I_{R'} - \right. \\ \left. - 2 \frac{H_1^{(1)}(kR_1)}{kR_1 \sqrt{(\rho\rho_0)}} [(z - z_0)(l \sin \frac{1}{2}\phi_0 - m \cos \frac{1}{2}\phi_0) - \rho_0 n \sin \frac{1}{2}\phi_0] \cos \frac{1}{2}\phi \right\}, \quad (8.129)$$

$$H_y = k^3 Y \left\{ [n(x-x_0) - l(z-z_0)]I_F - [n(x-x_0) - l(z-z_0)]I_{R'} - \right. \\ \left. - 2 \frac{H_1^{(1)}(kR_1)}{kR_1 \sqrt{(\rho\rho_0)}} [(z-z_0)(l \sin \frac{1}{2}\phi_0 - m \cos \frac{1}{2}\phi_0) - \rho_0 n \sin \frac{1}{2}\phi_0] \sin \frac{1}{2}\phi \right\}, \quad (8.130)$$

$$H_z = k^3 Y \left\{ [l(y-y_0) - m(x-x_0)]I_R - [l(y+y_0) + m(x-x_0)]I_{R'} + \right. \\ \left. + 2 \frac{H_1^{(1)}(kR_1)}{kR_1 \sqrt{(\rho\rho_0)}} \rho(l \sin \frac{1}{2}\phi_0 - m \cos \frac{1}{2}\phi_0) \cos \frac{1}{2}\phi \right\}, \quad (8.131)$$

where

$$I_R = \int_{-m}^{\infty} \frac{H_2^{(1)}(\mu^2 + kR)d\mu}{(\mu^2 + kR)\sqrt{(\mu^2 + 2kR)}}, \quad (8.132)$$

$$I_{R'} = \int_{-m'}^{\infty} \frac{H_2^{(1)}(\mu^2 + kR')d\mu}{(\mu^2 + kR')\sqrt{(\mu^2 + 2kR')}} \quad (8.133)$$

and

$$m = 2 \sqrt{\frac{k\rho\rho_0}{R_1 + R}} \cos \frac{1}{2}(\phi - \phi_0) = \pm \sqrt{\{k(R_1 - R)\}}, \quad \pm \text{ for } \cos \frac{1}{2}(\phi - \phi_0) \gtrless 0,$$

$$m' = 2 \sqrt{\frac{k\rho\rho_0}{R_1 + R'}} \cos \frac{1}{2}(\phi + \phi_0) = \pm \sqrt{\{k(R_1 - R')\}}, \quad \pm \text{ for } \cos \frac{1}{2}(\phi + \phi_0) \gtrless 0.$$

The above result, with a slight modification of the integrals, has been given by VANDAKUROV [1954] in the case $n = 0$, $z_0 = 0$. The corresponding expression for the total electric field is considerably more complicated in form and will be omitted. It may be noted, however, that the integrals appearing in the result are of the type

$$\int_{-m}^{\infty} \frac{H_3^{(1)}(\mu^2 + kR)d\mu}{(\mu^2 + kR)^2 \sqrt{(\mu^2 + 2kR)}}. \quad (8.134)$$

A representation of the total electric field as an eigenfunction expansion is

$$\mathbf{E}(\mathbf{r}) = 4\pi k \mathcal{G}_e(\mathbf{r}|\mathbf{r}_0) \cdot \hat{\mathbf{c}} \quad (8.135)$$

where $\mathcal{G}_e(\mathbf{r}|\mathbf{r}_0)$ is the electric dyadic Green function for the half-plane. In circular cylindrical coordinates (TAI [1954]):

$$\frac{4\pi}{k} \mathcal{G}_e(\mathbf{r}|\mathbf{r}_0) = \left\{ \frac{\hat{\rho}}{\rho} \frac{\partial}{\partial \phi} - \hat{\phi} \frac{\partial}{\partial \rho} \right\} \left\{ \frac{\hat{\rho}_0}{\rho_0} \frac{\partial}{\partial \phi_0} - \hat{\phi}_0 \frac{\partial}{\partial \rho_0} \right\} \tilde{U} + \left\{ \frac{\hat{\rho}}{\rho} \frac{\partial^2}{\partial \rho \partial z} + \frac{\hat{\phi}}{\rho} \frac{\partial^2}{\partial \phi \partial z} + \right. \\ \left. + \frac{\partial^2}{\partial z^2} + k^2 \right\} \left\{ \frac{\hat{\rho}_0}{\rho_0} \frac{\partial^2}{\partial \rho_0 \partial z_0} + \frac{\hat{\phi}_0}{\rho_0} \frac{\partial^2}{\partial \phi_0 \partial z_0} + \frac{\partial^2}{\partial z_0^2} + k^2 \right\} \frac{U}{k^2}, \quad (8.136)$$

where

$$\tilde{U} = \sum_{n=0}^{\infty} \varepsilon_n \cos \left(\frac{1}{2}n\phi\right) \cos \left(\frac{1}{2}n\phi_0\right) T_{\frac{1}{2}n}, \tag{8.137}$$

$$U = \sum_{n=0}^{\infty} \varepsilon_n \sin \left(\frac{1}{2}n\phi\right) \sin \left(\frac{1}{2}n\phi_0\right) T_{\frac{1}{2}n}, \tag{8.138}$$

$$T_r = \frac{i}{2k} \int_{-\infty}^{\infty} \frac{dt}{k^2 - t^2} e^{it(z-z_0)} J_r[\rho < \sqrt{(k^2 - t^2)}] H_r^{(1)}[\rho > \sqrt{(k^2 - t^2)}]. \tag{8.139}$$

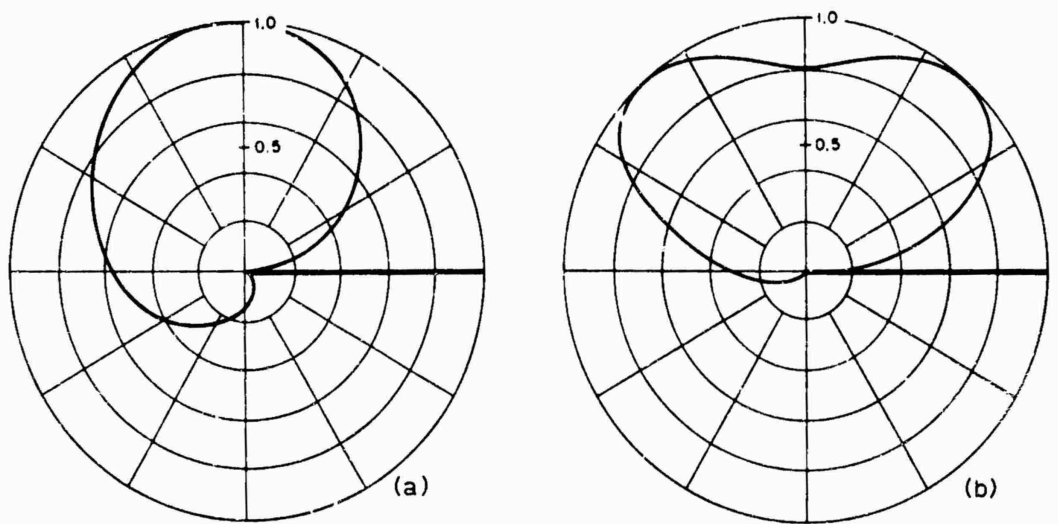


Fig. 8.18. Normalized radiation patterns in plane $z = z_0$ for \hat{x} -oriented electric dipoles with $\phi_0 = 10^\circ$ and (a) $\rho_0 = \frac{1}{10}\lambda$, (b) $\rho_0 = 2\lambda$ (TAT [1954]).

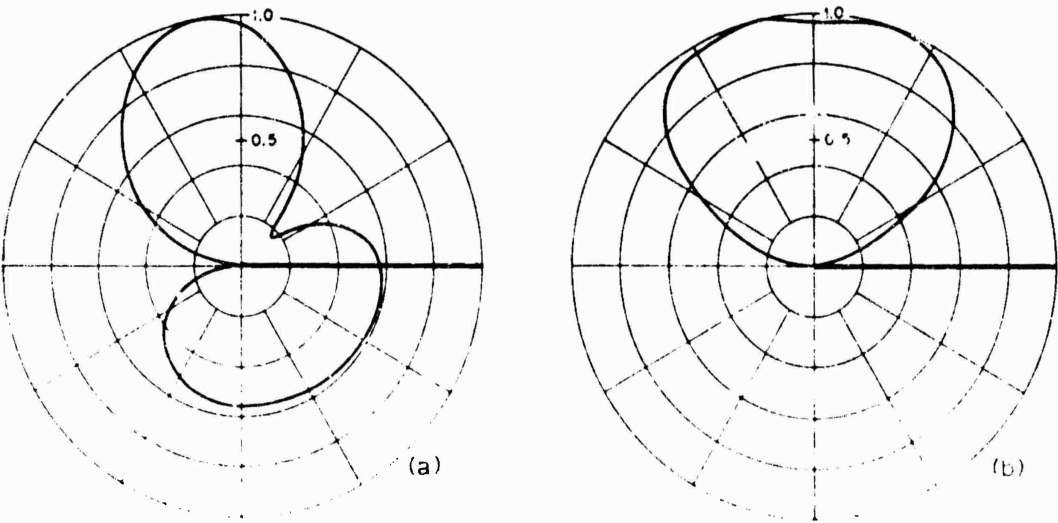


Fig. 8.19. Normalized radiation patterns in plane $z = z_0$ for \hat{y} -oriented electric dipoles with $\phi_0 = 10^\circ$ and (a) $\rho_0 = \frac{1}{10}\lambda$, (b) $\rho_0 = 2\lambda$ (TAT [1954]).

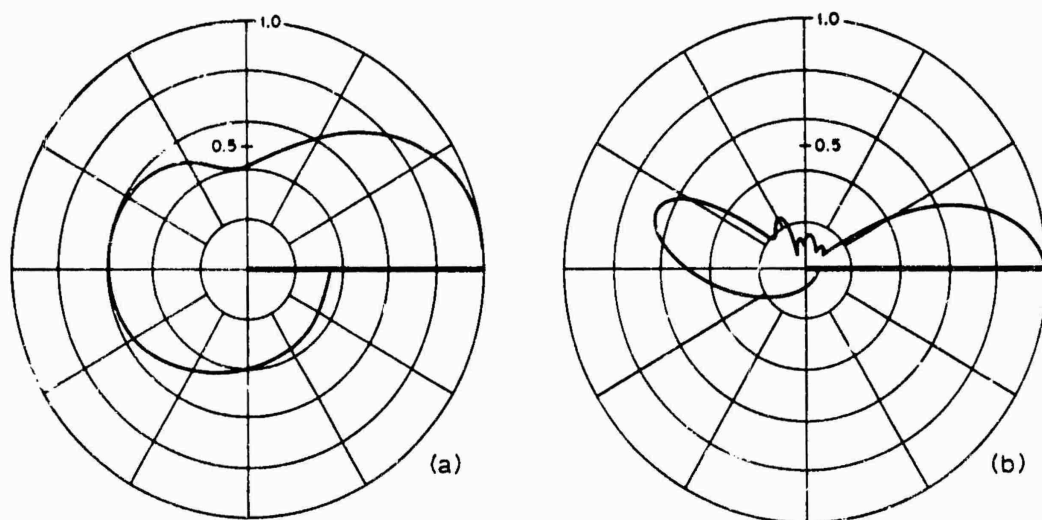


Fig. 8.20. Normalized radiation patterns in plane $z = z_0$ for \hat{z} -oriented electric dipoles with $\phi_0 = 10^\circ$ and (a) $\rho_0 = \frac{1}{10}\lambda$, (b) $\rho_0 = 2\lambda$ (TAI [1954]).

Since

$$\left(\frac{\partial^2}{\partial z_0^2} + k^2\right) U = V^s, \quad (8.140)$$

the solution for a z oriented dipole (that is, $\hat{e} = \hat{z}$) again follows immediately from the point source solution. On the basis of eq. (8.136), TAI [1954] has computed normalized radiation patterns in the principal plane $z = z_0$ for x , y and z oriented dipoles with a variety of values of $k\rho_0$ and ϕ_0 . A selection of the data is reproduced in Figs. 8.18 through 8.20.

In spherical coordinates (TILSTON [1952]):

$$\begin{aligned} \frac{4\pi}{k} \mathcal{G}_e(\mathbf{r}|\mathbf{r}_0) = & \left\{ \frac{\hat{\theta}}{\sin \theta} \frac{\partial}{\partial \phi} - \hat{\phi} \frac{\partial}{\partial \theta} \right\} \left\{ \frac{\hat{\theta}_0}{\sin \theta_0} \frac{\partial}{\partial \phi_0} - \hat{\phi}_0 \frac{\partial}{\partial \theta_0} \right\} \bar{U} + \left\{ \rho \left(\frac{\partial^2}{\partial r^2} + k^2 \right) + \right. \\ & + \frac{\hat{\theta}}{r} \frac{\partial^2}{\partial r \partial \theta} + \frac{\hat{\phi}}{r \sin \theta} \frac{\partial^2}{\partial r \partial \phi} \left. \right\} \rho_0 \left(\frac{\partial^2}{\partial r_0^2} + k^2 \right) + \frac{\hat{\theta}_0}{r_0} \frac{\partial^2}{\partial r_0 \partial \theta_0} + \\ & + \frac{\hat{\phi}_0}{r_0 \sin \theta_0} \frac{\partial^2}{\partial r_0 \partial \phi_0} \left. \right\} \frac{r r_0 U}{k^2}, \quad (8.141) \end{aligned}$$

where \bar{U} and U are as given in eqs. (8.137) and (8.138), respectively, but with eq. (8.139) replaced by

$$\begin{aligned} T_\tau = i e^{-2i\pi\tau} \sum_{s=0}^{\infty} \frac{\Gamma(s+2\tau+1)}{s!} \frac{2s+2\tau+1}{(s+\tau)(s+\tau+1)} \\ \times J_{s+\tau+\frac{1}{2}}(kr) H_{s+\tau+\frac{1}{2}}^{(1)}(kr) P_{s+\tau+\frac{1}{2}}^{-\tau}(\cos \theta) P_{s+\tau+\frac{1}{2}}^{-\tau}(\cos \theta_0). \quad (8.142) \end{aligned}$$

Since

$$r_0 \left(\frac{\partial^2}{\partial r_0^2} + k^2 \right) (r_0 U) = 1, \quad (8.143)$$

the solution for a radial dipole (that is, $\hat{\mathbf{e}} = \hat{\mathbf{p}}_0$) now follows immediately from the point source solution.

If $kr \ll 1$ and $kr_0 \gg 1$, the representation in eq. (8.141) is rapidly convergent and the dominant term leads to (FELSEN [1957]):

$$E \sim \frac{e^{ikr_0 + \frac{1}{2}i\pi}}{r} \sqrt{\frac{2k}{\pi\rho \sin \theta_0}} \{ \hat{\mathbf{p}} \sin \frac{1}{2}\phi + \hat{\boldsymbol{\phi}} \cos \frac{1}{2}\phi \} \\ \times \{ (\hat{\boldsymbol{\theta}}_0 \cdot \hat{\mathbf{e}}) \cos \theta_0 \sin \frac{1}{2}\phi_0 + (\hat{\boldsymbol{\phi}}_0 \cdot \hat{\mathbf{e}}) \cos \frac{1}{2}\phi_0 \}, \quad (8.144)$$

$$H \sim Y \frac{e^{ikr_0 + \frac{1}{2}i\pi}}{r_0} \sqrt{\frac{2k}{\pi\rho \sin \theta_0}} \{ \hat{\mathbf{p}} \cos \frac{1}{2}\phi - \hat{\boldsymbol{\phi}} \sin \frac{1}{2}\phi \} \\ \times \{ (\hat{\boldsymbol{\theta}}_0 \cdot \hat{\mathbf{e}}) \sin \frac{1}{2}\phi_0 + (\hat{\boldsymbol{\phi}}_0 \cdot \hat{\mathbf{e}}) \cos \theta_0 \cos \frac{1}{2}\phi_0 \}, \quad (8.145)$$

where

$$\hat{\boldsymbol{\theta}}_0 \cdot \hat{\mathbf{e}} = \cos \theta_0 \sin \Theta \cos (\phi_0 - \Phi) - \sin \theta_0 \cos \Theta, \\ \hat{\boldsymbol{\phi}}_0 \cdot \hat{\mathbf{e}} = -\sin \Theta \sin (\phi_0 - \Phi). \quad (8.146)$$

The above equations make explicit the behavior of the electromagnetic fields near to the edge.

For $k\rho\rho_0/R_1 \gg 1$ (source and observation point far from the edge), a convenient decomposition of the total electric Hertz vector is

$$\Pi = \Pi^{s.o.} + \Pi^d \quad (8.147)$$

where $\Pi^{s.o.}$ is the geometrical optics contribution given by

$$\Pi^{s.o.} = \eta(\pi + \phi_0 - \phi) \hat{\mathbf{e}}(-\Phi) \frac{e^{ikR}}{kR} - \eta(\pi - \phi_0 - \phi) \hat{\mathbf{e}}(\Phi) \frac{e^{ikR'}}{kR'}, \quad (8.148)$$

and Π^d is the diffracted contribution, which is discontinuous at $\phi = \pi \pm \phi_0$ in order to compensate for the discontinuities in $\Pi^{s.o.}$. If $kR_1 \gg 1$, a first order approximation to Π^d is obtained by combining the results of TUZHILIN [1964] and MACDONALD [1915]:

$$\Pi^d \sim \frac{e^{i(kR_1 + \frac{1}{2}\pi)}}{\sqrt{(2\pi k R_1)}} \frac{1}{2k\sqrt{(\rho\rho_0)}} \left\{ \frac{\hat{\mathbf{e}}(-\Phi) - \hat{\mathbf{e}}(\pi + \phi_0 - \phi - \Phi)}{\cos \frac{1}{2}(\phi - \phi_0)} - \frac{\hat{\mathbf{e}}(\Phi) - \hat{\mathbf{e}}(\pi - \phi_0 - \phi + \Phi)}{\cos \frac{1}{2}(\phi + \phi_0)} \right\} \\ - \sqrt{\frac{2}{\pi k R_1}} e^{-\frac{1}{2}i\pi} \left\{ \operatorname{sgn}(\pi + \phi_0 - \phi) \frac{\hat{\mathbf{e}}(-\Phi) e^{ikR}}{\sqrt{\{k(R_1 + R)\}}} F[\sqrt{\{k(R_1 - R)\}}] - \right. \\ \left. - \operatorname{sgn}(\pi - \phi_0 - \phi) \frac{\hat{\mathbf{e}}(\Phi) e^{ikR'}}{\sqrt{\{k(R_1 + R')\}}} F[\sqrt{\{k(R_1 - R')\}}] \right\}. \quad (8.149)$$

If, in addition, $k(R_1 - R)$, $k(R_1 - R') \gg 1$, asymptotic expansion of the Fresnel integrals gives

$$\Pi^d \sim - \frac{e^{i(kR_1 + \frac{1}{2}\pi)}}{\sqrt{(2\pi k R_1)}} \frac{1}{2k\sqrt{(\rho\rho_0)}} \left\{ \frac{\hat{\mathbf{e}}(\pi + \phi_0 - \phi - \Phi)}{\cos \frac{1}{2}(\phi - \phi_0)} - \frac{\hat{\mathbf{e}}(\pi - \phi_0 - \phi + \Phi)}{\cos \frac{1}{2}(\phi + \phi_0)} \right\}. \quad (8.150)$$

8.5.2. Magnetic dipoles

For an arbitrarily oriented magnetic dipole at (ρ_0, ϕ_0, z_0) with moment $(4\pi/k)\hat{e}$, corresponding to a magnetic Hertz vector

$$\tilde{\mathbf{H}}^i = \hat{e} \frac{e^{ikR}}{kR} \quad (8.151)$$

where

$$\hat{e} = \hat{x} \sin \Theta \cos \Phi + \hat{y} \sin \Theta \sin \Phi + \hat{z} \cos \Theta, \quad (8.152)$$

a contour integral representation of the total magnetic Hertz vector is

$$\begin{aligned} \tilde{\mathbf{H}} = \frac{1}{8i\pi} \int_{C_1+C_2} \frac{e^{ikR(\alpha)}}{kR(\alpha)} \{ & \hat{e}(\pi-\alpha-\phi+\phi_0-\Phi) \cot \frac{1}{4}(\pi-\alpha-\phi+\phi_0) + \\ & + \hat{e}(\pi-\alpha-\phi-\phi_0+\Phi) \cot \frac{1}{4}(\pi-\alpha-\phi-\phi_0) \} d\alpha \end{aligned} \quad (8.153)$$

where

$$R(\alpha) = \{\rho^2 + \rho_0^2 + 2\rho\rho_0 \cos \alpha + (z-z_0)^2\}^{1/2}, \quad (8.154)$$

$$\hat{e}(\alpha) = \hat{x} \sin \Theta \cos \alpha - \hat{y} \sin \Theta \sin \alpha + \hat{z} \cos \Theta, \quad (8.155)$$

and C_1 and C_2 are the Sommerfeld contours shown in Fig. 8.2. The above expression may be reduced to (BOWMAN and SENIOR [1967]):

$$\begin{aligned} \tilde{\mathbf{H}} = \hat{x} \left[lV^h + \frac{i}{k\sqrt{(\rho\rho_0)}} H_0^{(1)}(kR_1)(l \cos \frac{1}{2}\phi_0 + m \sin \frac{1}{2}\phi_0) \cos \frac{1}{2}\phi \right] + \\ + \hat{y} \left[mV^s + \frac{i}{k\sqrt{(\rho\rho_0)}} H_0^{(1)}(kR_1)(l \cos \frac{1}{2}\phi_0 + m \sin \frac{1}{2}\phi_0) \sin \frac{1}{2}\phi \right] + \hat{z} nV^h, \end{aligned} \quad (8.156)$$

where $l = \sin \Theta \cos \Phi$, $m = \sin \Theta \sin \Phi$, $n = \cos \Theta$ are the directional cosines of \hat{e} , and V^s and V^h are, respectively, the acoustically soft and acoustically hard point source solutions in Sec. 8.4. The following symmetry relation holds:

$$\tilde{\mathbf{H}}(\phi) + \tilde{\mathbf{H}}(2\pi - \phi) = \hat{e}(-\phi) \frac{e^{ikR}}{kR} + \hat{e}(\phi) \frac{e^{ikR'}}{kR'}. \quad (8.157)$$

The form of solution (8.156) is remarkable in that the previously derived scalar solutions V^s and V^h are explicitly involved along with certain additive correction terms which obey the source-free wave equation. If $l = -m \tan \frac{1}{2}\phi_0$, these additive terms vanish and the electromagnetic field is determined by V^s and V^h alone. If, furthermore, $l = m = 0$, the field is determined by V^h only. In the case of other dipole orientations, however, the additive terms are necessary to provide the correct edge behavior. All the functions $\tilde{\mathbf{H}}$, \mathbf{E} and \mathbf{H} are of order $\rho^{-1/2}$ as $\rho \rightarrow 0$.

The components of the total electric field derived by vector operations on $\tilde{\mathbf{H}}$ are

$$E_x = -k^3 Z \left\{ [m(z-z_0) - n(y-y_0)]I_R - [m(z-z_0) + n(y+y_0)]I_{R'} + \right. \\ \left. + 2 \frac{H_1^{(1)}(kR_1)}{kR_1 \sqrt{(\rho\rho_0)}} [(z-z_0)(l \cos \frac{1}{2}\phi_0 + m \sin \frac{1}{2}\phi_0) + \rho_0 n \cos \frac{1}{2}\phi_0] \sin \frac{1}{2}\phi \right\}, \quad (8.158)$$

$$E_y = -k^3 Z \left\{ [n(x-x_0) - l(z-z_0)]I_R + [n(x-x_0) - l(z-z_0)]I_{R'} - \right. \\ \left. - 2 \frac{H_1^{(1)}(kR_1)}{kR_1 \sqrt{(\rho\rho_0)}} [(z-z_0)(l \cos \frac{1}{2}\phi_0 + m \sin \frac{1}{2}\phi_0) + \rho_0 n \cos \frac{1}{2}\phi_0] \cos \frac{1}{2}\phi \right\}, \quad (8.159)$$

$$E_z = -k^3 Z \left\{ [l(y-y_0) - m(x-x_0)]I_R + [l(y+y_0) + m(x-x_0)]I_{R'} + \right. \\ \left. + 2 \frac{H_1^{(1)}(kR_1)}{kR_1 \sqrt{(\rho\rho_0)}} \rho(l \cos \frac{1}{2}\phi + m \sin \frac{1}{2}\phi) \sin \frac{1}{2}\phi \right\}, \quad (8.160)$$

where

$$I_R = \int_{-m}^{\infty} \frac{H_2^{(1)}(\mu^2 + kR) d\mu}{(\mu^2 + kR) \sqrt{(\mu^2 + 2kR)}}, \quad (8.161)$$

$$I_{R'} = \int_{-m'}^{\infty} \frac{H_2^{(1)}(\mu^2 + kR') d\mu}{(\mu^2 + kR') \sqrt{(\mu^2 + 2kR')}} \quad (8.162)$$

and

$$m = 2 \sqrt{\frac{k\rho\rho_0}{R_1 + R}} \cos \frac{1}{2}(\phi - \phi_0) = \pm \sqrt{\{k(R_1 - R)\}}, \quad \pm \text{ for } \cos \frac{1}{2}(\phi - \phi_0) \geq 0,$$

$$m' = 2 \sqrt{\frac{k\rho\rho_0}{R_1 + R'}} \cos \frac{1}{2}(\phi + \phi_0) = \pm \sqrt{\{k(R_1 - R')\}}, \quad \pm \text{ for } \cos \frac{1}{2}(\phi + \phi_0) \geq 0.$$

The above result, with a slight modification of the integrals, has been given by VANDAKUROV [1954] in the case $n = 0$, $z_0 = 0$. The corresponding expression for the total magnetic field is considerably more complicated in form and will be omitted. It may be noted, however, that the integrals appearing in the result are of the type

$$\int_{-m}^{\infty} \frac{H_3^{(1)}(\mu^2 + kR) d\mu}{(\mu^2 + kR)^2 \sqrt{(\mu^2 + 2kR)}}. \quad (8.163)$$

A representation for the total magnetic field as an eigenfunction expansion is

$$H(\mathbf{r}) = 4\pi k \mathcal{G}_m(\mathbf{r}|\mathbf{r}_0) \cdot \hat{\mathbf{c}} \quad (8.164)$$

where $\mathcal{G}_m(\mathbf{r}|\mathbf{r}_0)$ is the magnetic dyadic Green function for the half-plane. In circular cylindrical coordinates (TAT [1954]):

$$\begin{aligned} \frac{4\pi}{k} \mathcal{G}_m(\mathbf{r}|\mathbf{r}_0) = & \left\{ \hat{\rho} \frac{\partial}{\partial \phi} - \hat{\phi} \frac{\partial}{\partial \rho} \right\} \left\{ \hat{\rho}_0 \frac{\partial}{\partial \phi_0} - \hat{\phi}_0 \frac{\partial}{\partial \rho_0} \right\} U + \left\{ \hat{\rho} \frac{\partial^2}{\partial \rho \partial z} + \frac{\hat{\phi}}{\rho} \frac{\partial}{\partial \phi \partial z} + \right. \\ & \left. + \hat{z} \left(\frac{\partial^2}{\partial z^2} + k^2 \right) \right\} \left\{ \hat{\rho}_0 \frac{\partial^2}{\partial \rho_0 \partial z_0} + \frac{\hat{\phi}_0}{\rho_0} \frac{\partial^2}{\partial \phi_0 \partial z_0} + \hat{z}_0 \left(\frac{\partial^2}{\partial z_0^2} + k^2 \right) \right\} \frac{\tilde{U}}{k^2}, \end{aligned} \quad (8.165)$$

where \tilde{U} and U are defined by eqs. (8.137) through (8.139). Since

$$\left(\frac{\partial^2}{\partial z_0^2} + k^2 \right) \tilde{U} = V^h, \quad (8.166)$$

the solution for a z oriented dipole (that is, $\hat{e} = \hat{z}$) again follows immediately from the point source solution. On the other hand, in spherical coordinates (TILSTON [1952]):

$$\begin{aligned} \frac{4\pi}{k} \mathcal{G}_m(\mathbf{r}|\mathbf{r}_0) = & \left\{ \frac{\hat{\theta}}{\sin \theta} \frac{\partial}{\partial \phi} - \hat{\phi} \frac{\partial}{\partial \theta} \right\} \left\{ \frac{\hat{\theta}_0}{\sin \theta_0} \frac{\partial}{\partial \phi_0} - \hat{\phi}_0 \frac{\partial}{\partial \theta_0} \right\} U + \left\{ \hat{\rho} \left(\frac{\partial^2}{\partial r^2} + k^2 \right) + \right. \\ & + \frac{\hat{\theta}}{r} \frac{\partial^2}{\partial r \partial \theta} + \frac{\hat{\phi}}{r \sin \theta} \frac{\partial^2}{\partial r \partial \phi} \left\{ \hat{\rho}_0 \left(\frac{\partial^2}{\partial r_0^2} + k^2 \right) + \frac{\hat{\theta}_0}{r_0} \frac{\partial^2}{\partial r_0 \partial \theta_0} + \right. \\ & \left. \left. + \frac{\hat{\phi}_0}{r_0 \sin \theta_0} \frac{\partial^2}{\partial r_0 \partial \phi_0} \right\} \frac{r r_0 \tilde{U}}{k^2}, \end{aligned} \quad (8.167)$$

where \tilde{U} and U are as given in eqs. (8.137) and (8.138) respectively, but with eq. (8.139) replaced by (8.142). Since

$$r_0 \left(\frac{\partial^2}{\partial r_0^2} + k^2 \right) (r_0 \tilde{U}) = V^h, \quad (8.168)$$

the solution for a radial dipole (that is, $\hat{e} = \hat{\rho}_0$) now follows immediately from the point source solution.

If $kr \ll 1$ and $kr_0 \gg 1$, the representation in eq. (8.167) is rapidly convergent and the dominant term leads to

$$\begin{aligned} H \sim & \frac{e^{ikr_0 + \frac{1}{2}i\pi}}{r_0} \sqrt{\frac{2k}{\pi \rho \sin \theta_0}} \{ \hat{\rho} \cos \frac{1}{2}\phi - \hat{\phi} \sin \frac{1}{2}\phi \} \\ & \times \{ (\hat{\theta}_0 \cdot \hat{e}) \cos \theta_0 \cos \frac{1}{2}\phi_0 - (\hat{\phi}_0 \cdot \hat{e}) \sin \frac{1}{2}\phi_0 \}, \end{aligned} \quad (8.169)$$

$$\begin{aligned} E \sim & Z \frac{e^{ikr_0 + \frac{1}{2}i\pi}}{r_0} \sqrt{\frac{2k}{\pi \rho \sin \theta_0}} \{ \hat{\rho} \sin \frac{1}{2}\phi + \hat{\phi} \cos \frac{1}{2}\phi \} \\ & \times \{ (\hat{\theta}_0 \cdot \hat{e}) \cos \frac{1}{2}\phi_0 - (\hat{\phi}_0 \cdot \hat{e}) \cos \theta_0 \sin \frac{1}{2}\phi_0 \}, \end{aligned} \quad (8.170)$$

where $(\hat{\theta}_0 \cdot \hat{e})$ and $(\hat{\phi}_0 \cdot \hat{e})$ are given in eq. (8.146). The above equations make explicit the behavior of the electromagnetic fields near to the edge.

For $k\rho\rho_0, R_1 \gg 1$ (source and observation point far from the edge), a convenient decomposition of the total magnetic Hertz vector is

$$\tilde{\mathbf{H}} = \tilde{\mathbf{H}}^{e.o.} + \tilde{\mathbf{H}}^d \quad (8.171)$$

where $\tilde{\Pi}^{s.o.}$ is the geometrical optics contribution given by

$$\tilde{\Pi}^{s.o.} = \eta(\pi + \phi_0 - \phi) \hat{e}(-\Phi) \frac{e^{ikR}}{kR} + \eta(\pi - \phi_0 - \phi) \hat{e}(\Phi) \frac{e^{ikR'}}{kR'} \quad (8.172)$$

and $\tilde{\Pi}^d$ is the diffracted contribution, which is discontinuous at $\phi = \pi \pm \phi_0$ in order to compensate for the discontinuities in $\tilde{\Pi}^{s.o.}$. If $kR_1 \gg 1$, a first order approximation to $\tilde{\Pi}^d$ is obtained by combining the results of TUZHILIN [1964] and MACDONALD [1915]:

$$\begin{aligned} \tilde{\Pi}^d \sim & \frac{e^{i(kR_1 + \frac{1}{2}\pi)}}{\sqrt{(2\pi k R_1)}} \frac{1}{2k\sqrt{(\rho\rho_0)}} \left\{ \frac{\hat{e}(-\Phi) - \hat{e}(\pi + \phi_0 - \phi - \Phi)}{\cos \frac{1}{2}(\phi - \phi_0)} + \frac{\hat{e}(\Phi) - \hat{e}(\pi - \phi_0 - \phi + \Phi)}{\cos \frac{1}{2}(\phi + \phi_0)} \right\} - \\ & - \sqrt{\frac{2}{\pi k R_1}} e^{-\frac{1}{2}i\pi} \left\{ \operatorname{sgn}(\pi + \phi_0 - \phi) \frac{\hat{e}(-\Phi) e^{ikR}}{\sqrt{\{k(R_1 + R)\}}} F[\sqrt{\{k(R_1 - R)\}}] + \right. \\ & \left. + \operatorname{sgn}(\pi - \phi_0 - \phi) \frac{\hat{e}(\Phi) e^{ikR'}}{\sqrt{\{k(R_1 + R')\}}} F[\sqrt{\{k(R_1 - R')\}}] \right\}. \quad (8.173) \end{aligned}$$

If, in addition, $k(R_1 - R)$, $k(R_1 - R') \gg 1$, asymptotic expansion of the Fresnel integrals gives

$$\tilde{\Pi}^d \sim - \frac{e^{i(kR_1 + \frac{1}{2}\pi)}}{\sqrt{(2\pi k R_1)}} \frac{1}{2k\sqrt{(\rho\rho_0)}} \left\{ \frac{\hat{e}(\pi + \phi_0 - \phi - \Phi)}{\cos \frac{1}{2}(\phi - \phi_0)} + \frac{\hat{e}(\pi - \phi_0 - \phi + \Phi)}{\cos \frac{1}{2}(\phi + \phi_0)} \right\}. \quad (8.174)$$

Bibliography

- BOWMAN, J. J. and T. B. A. SENIOR [1967], Diffraction of a Dipole Field by a Perfectly Conducting Half Plane, *Radio Science* **2**, 1339-1345.
- BRAUNBEK, W. and G. LAUKIEN [1952], Einzelheiten zur Halbebenen-Beugung, *Optik* **9**, 174-179.
- CARSLAW, H. S. [1899], Some Multiform Solutions of the Partial Differential Equations of Physical Mathematics and their Applications, *Proc. London Math. Soc.* **30**, 121-161.
- CLEMMOW, P. C. [1950], A Note on the Diffraction of a Cylindrical Wave by a Perfectly Conducting Half-Plane, *Quart. J. Mech. Appl. Math.* **3**, 377-384.
- CLEMMOW, P. C. [1951], A Method for the Exact Solution of a Class of Two-Dimensional Diffraction Problems, *Proc. Roy. Soc.* **A205**, 286-308.
- CLEMMOW, P. C. [1959], Rigorous Diffraction Theory, in: *Principles of Optics*, eds. M. Born and E. Wolf, Chapter 11, Pergamon Press, New York, N.Y.
- FEISEN, L. B. [1957], Alternative Field Representations in Regions Bounded by Spheres, Cones and Planes, *IRE Trans.* **AP-5**, 109-121. Note that in eq. (54) the components \mathcal{J}_θ and \mathcal{J}_ϕ must be evaluated at the source point.
- HARDEN, B. N. [1952], Diffraction of Electromagnetic Waves by a Half-Plane, *Proc. IRE* **99**, Pt. 3, 229-235.
- JONES, D. S. [1964], *The Theory of Electromagnetism*, The Macmillan Co., New York, N.Y. The scatter point source solutions on pp. 592 and 593 are in error by a factor k . This error carries over to the dipole solutions on p. 594. The "additional" terms in the expression for B are also in error by a factor 4π .
- MACDONALD, H. M. [1902], *Electric Waves*, Cambridge University Press, Cambridge, England.
- MACDONALD, H. M. [1915], A Class of Diffraction Problems, *Proc. London Math. Soc.* **14**, 410-427.

- MALYUZHINETS, G. D. and A. A. TUZHILIN [1963], The Electromagnetic Field excited by an Electric Dipole in a Wedge-Shaped Region, Soviet Phys. Doklady 7, 879-882 (English translation of Dokl. Akad. Nauk SSSR 146 (1962) 1039-1042). In eq. (8), replace -2ψ by 2ψ .
- MARCINKOWSKI, C. J. [1959], Diffraction by an Absorbing Half-Plane, Polytechnic Institute of Brooklyn Microwave Research Institute Report R-750-59, PIB-678.
- MOULLIN, E. B. [1949], *Radio Aerials*, Clarendon Press, Oxford, England. There is a factor 2 error in the formulas defining the surface and total current densities, but the graphs appear to have been computed from the correct formulas.
- MOULLIN, E. B. [1954], On the Current induced in a Conducting Ribbon by a Current Filament Parallel to It, Proc. IEE 101, Pt. IV, 7-17. The above comments apply and, in addition, some of the computed data appear to be of marginal accuracy.
- SAVORNIN, J. [1939], Étude de la diffraction éloignée, Ann. de Phys. 11, 129-255.
- SENIOR, T. B. A. [1953], The Diffraction of a Dipole Field by a Perfectly Conducting Half-Plane, Quart. J. Mech. Appl. Math. 6, 101-114.
- SOMMERFELD, A. [1896], Mathematische Theorie der Diffraction, Math. Ann. 47, 317-374.
- TAI, C. T. [1954], Radiation from Current Elements and Apertures in the Presence of a Perfectly Conducting Half-Plane Sheet, Stanford University Research Institute Technical Report No. 45.
- TAVENNER, M. S. [1960], Studies in Diffraction, University of Utah Research Report (AFOSR-TN-60-1487).
- TILSTON, W. V. [1952], Contributions to the Theory of Antennas, Technical Report, Antenna Laboratory, Dept. of Electrical Engineering, University of Toronto, Toronto, Ontario (October). Due to normalization errors in both the θ and ϕ integrations, a factor $2\pi/\phi_0$ is omitted and $I[(2m\pi/\phi_0) - 2n - 1]$ should be replaced by $[(2m\pi/\phi_0) - 2n - 1]$ throughout. Further, $mB \sin(m\pi\phi/\phi_0)$ should read $(m\pi B/\phi_0) \sin(m\pi\phi/\phi_0)$ whenever it appears (pp. 32, 33, 37). On the same pages replace C by $-C$ and on pp. 36, 37 replace A, B, C, by $-A$, $-B$, $-C$ respectively. In eq. (3.48) multiply the right hand side by -1 , and in eq. (3.59) divide the summand by $n![(m\pi/\phi_0) - n][(m\pi/\phi_0) - n - 1]$.
- TUZHILIN, A. A. [1963], New Representations of Diffraction Fields in Wedge-Shaped Regions with Ideal Boundaries, Soviet Phys. - Acoust. 9, 168-172 (English translation of Akust. Zh. 9 (1963) 209-214). In the expression for $s(x)$ on p. 168, \pm should be replaced by \mp , and in the table on p. 169, the right hand side of the eq. for I in the case of plane wave incidence should be multiplied by $-i$.
- TUZHILIN, A. A. [1964], Short-Wave Asymptotic Representation of Electromagnetic Diffraction Fields Produced by Arbitrarily Oriented Dipoles in a Wedge-Shaped Region with Ideally Conducting Sides, Annotation of Reports of the Third All-Union Symposium on Wave Diffraction, Acad. Sci. USSR, 93-95 (in Russian). In the line following eq. (8), replace ϕ by Φ . The integral in eq. (10) should be multiplied by $\text{sgn}(\beta - 4n\Phi)$. In eq. (14) replace ϕ_n by $4n$, and in the line following, the first Π_n^1 should read Π_n^2 .
- WILLIAMS, W. E. [1957], A Note on the Diffraction of a Dipole Field by a Half-Plane, Quart. J. Mech. Appl. Math. 10, 210-213.
- WOODS, B. J. [1957], The Diffraction of a Dipole Field by a Half-Plane, Quart. J. Mech. Appl. Math. 10, 90-100. The solutions given are correct if the scalar point sources are defined in terms of a Hertz potential $(kR)^{-1} \exp(-ikR)$, not $R^{-1} \exp(-ikR)$ as indicated.
- VANDAKUROV, Y. V. [1964], Diffraction of Electromagnetic Waves by an Arbitrarily-Oriented Electric or Magnetic Dipole on a Perfectly Conducting Half-Plane, Zh. Eksp. Teor. Fiz. 26, 3-18 (in Russian).

PART TWO

FINITE BODIES

PRECEDING PAGE BLANK

CHAPTER 9

GENERAL CONSIDERATIONS

The next five chapters are concerned with bodies which are finite in all dimensions and are, in consequence, physically achievable configurations. With one exception (the wire), the surface of each body is an entire coordinate surface in one of the coordinate systems in which the scalar wave equation separates; and even the wire, which is included because of its practical importance, can be regarded as the limiting case of a prolate spheroid as the minor axis tends to zero. But only in spherical coordinates, and hence for the sphere, is the vector wave equation separable.

In general three types of sources will be treated: plane waves with arbitrary incidence and polarization, point sources and electric and magnetic dipoles arbitrarily oriented. The wire, however, is again an exception inasmuch as we shall here confine ourselves to a perfectly conducting body with an incident plane wave whose electric vector is in the plane of incidence. In each case particular attention is paid to the far field scattering behavior, and the reader is referred to the definitions of the far field amplitude S and the scattering cross section σ in Sections I.2.4. and I.2.5, respectively.

In the three-dimensional problems considered in Part 2, the differential acoustic scattering cross section $\sigma(\theta, \phi)$ is defined by

$$\sigma(\theta, \phi) = \lim_{r \rightarrow \infty} 4\pi r^2 \frac{I_s^2}{I_i^2}; \quad (9.1)$$

it then follows from eqs. (I.27) and (9.1) that for an incident sound field of unit amplitude:

$$\sigma(\theta, \phi) = \frac{4\pi}{k^2} |S(\theta, \phi)|^2. \quad (9.2)$$

The total scattering cross section σ_T is still related to the bistatic cross section $\sigma(\theta, \phi)$ by eq. (I.52).

The emphasis put on far field results is justified not only by the practical importance of radar cross sections, but also by the fact that the near field is obtainable from the far field: the most important results presently available on this latter topic are outlined in the following. Let us firstly consider the scalar case. By using notation and results of Section I.2.13.3, the following asymptotic expansion is obtained (KELLER et al. [1956]):

$$V \sim \frac{e^{ikr}}{r} \sum_{n=0}^{\infty} (ik)^{-n} \sum_{l=0}^n a_{ln}(\theta, \phi) r^{-l}, \quad (9.3)$$

where

$$a_{ln} = \frac{1}{2l} [l(l-1) + B] a_{l-1, n-1}, \quad (l \geq 1, n \geq 1), \quad (9.4)$$

$$a_{0n} = r_0(\theta, \phi) v_n[r_0(\theta, \phi), \theta, \phi] - \sum_{l=1}^n a_{ln} r_0^{-l}, \quad (n \geq 1), \quad (9.5)$$

$$a_{00} = r_0(\theta, \phi) v_0[r_0(\theta, \phi), \theta, \phi], \quad (9.6)$$

and

$$B = \frac{1}{\sin \theta} \frac{\partial}{\partial \theta} \left(\sin \theta \frac{\partial}{\partial \theta} \right) + \frac{1}{\sin^2 \theta} \frac{\partial^2}{\partial \phi^2} \quad (9.7)$$

is Beltrami's operator. The quantities v_n are those appearing in eq. (I.113). The quantity a_{00} remains constant as r varies on the ray $\theta = \text{constant}$, $\phi = \text{constant}$, i.e.:

$$r_0(\theta, \phi) v_0[r_0(\theta, \phi), \theta, \phi] = r(\theta, \phi) v_0[r(\theta, \phi), \theta, \phi],$$

and $v_n(r_0, \theta, \phi)$ is the value of v_n at the point r_0 on the ray $\theta = \text{constant}$, $\phi = \text{constant}$. The result (9.3) is obtained by using $\Phi = s = r$ and $G(r) = r^{-2}$ in eq. (I.116) and by substituting the resulting v_n 's into eq. (I.113). If the expansion (I.113) is given on a surface $r = r_0(\theta, \phi)$, i.e. if all the $v_n(r_0, \theta, \phi)$ are known, then the asymptotic expansion (9.3) gives the field everywhere.

While expression (9.3) is only asymptotic, an exact result has been proven by WILCOX [1956b] for the region exterior to a sphere of given radius $r = r_1$ that encloses the scatterer. If V satisfies the scalar wave equation $(\nabla^2 + k^2)V = 0$ in $r \geq r_1$ and the radiation condition at infinity, then

$$V(r, \theta, \phi) = \frac{e^{ikr}}{r} \sum_{n=0}^{\infty} \frac{f_n(\theta, \phi)}{r^n}, \quad (9.8)$$

where the series converges absolutely and uniformly in r , θ and ϕ in any region $r \geq r_1 + \delta > r_1$. The series can be differentiated term by term with respect to r , θ and ϕ any number of times, and the resulting series are all absolutely and uniformly convergent. The quantities $f_n(\theta, \phi)$ with $n > 0$ are determined from the radiation pattern $f_0(\theta, \phi)$ by means of the formula:

$$f_n(\theta, \phi) = \frac{1}{2ikn} [n(n-1) + B] f_{n-1}(\theta, \phi), \quad (n \geq 1), \quad (9.9)$$

where B is given by eq. (9.7). Recursion relation (9.9) can be iterated to obtain f_n in terms of f_0 :

$$f_n(\theta, \phi) = [(2ik)^n n!]^{-1} \prod_{m=1}^n [m(m-1) + B] f_0(\theta, \phi). \quad (9.10)$$

WILCOX [1956a] has also studied the vector case. If $A(\mathbf{r})$ satisfies the vector wave

equation $(\nabla \wedge \nabla \wedge -k^2)A = 0$ in $r \geq r_1$ and the radiation condition (1.20) at infinity, then

$$A(r) = \frac{e^{ikr}}{r} \sum_{n=0}^{\infty} A_n(\theta, \phi) r^{-n}, \quad (9.11)$$

where the series converges absolutely and uniformly in r , θ and ϕ in any region $r \geq r_1 + \delta > r_1$. The series can be differentiated term by term with respect to r , θ and ϕ any number of times, and the resulting series are all absolutely and uniformly convergent. The radiation pattern $A_0(\theta, \phi)$ is tangent to the spheres $r = \text{constant}$; in general

$$A_n(\theta, \phi) = A_{nr}(\theta, \phi)\hat{r} + A_{n\theta}(\theta, \phi)\hat{\theta} + A_{n\phi}(\theta, \phi)\hat{\phi}, \quad (9.12)$$

where:

$$A_{0r} = 0, \quad (9.13)$$

$$ikA_{1r} = \frac{-1}{\sin \theta} \left[\frac{\partial}{\partial \theta} (\sin \theta A_{0\theta}) + \frac{\partial A_{0\phi}}{\partial \phi} \right] = -r \nabla \cdot A_0 \quad (9.14)$$

$$2iknA_{n+1,r} = [n(n-1) + B]A_{n,r}, \quad (n \geq 1), \quad (9.15)$$

$$2iknA_{n\theta} = [n(n-1) + B]A_{n-1,\theta} + D_\theta A_{n-1}, \quad (n \geq 1), \quad (9.16)$$

$$2iknA_{n\phi} = [n(n-1) + B]A_{n-1,\phi} + D_\phi A_{n-1}, \quad (n \geq 1). \quad (9.17)$$

B is given by eq. (9.7) and the operators D_θ and D_ϕ are defined by

$$D_\theta F = 2 \frac{\partial F_r}{\partial \theta} - \frac{F_\theta}{\sin^2 \theta} - \frac{2 \cos \theta}{\sin^2 \theta} \frac{\partial F_\phi}{\partial \phi}, \quad (9.18)$$

$$D_\phi F = \frac{2}{\sin \theta} \frac{\partial F_r}{\partial \phi} + \frac{2 \cos \theta}{\sin^2 \theta} \frac{\partial F_\theta}{\partial \phi} - \frac{F_\phi}{\sin^2 \theta}, \quad (9.19)$$

with $F = F_r\hat{r} + F_\theta\hat{\theta} + F_\phi\hat{\phi}$. If the vector $A(r)$ satisfies the wave equation and the radiation condition, so does the vector

$$B(r) = \nabla \wedge A(r); \quad (9.20)$$

furthermore, the radiation patterns A_0 of A and B_0 of B are related by

$$B_0(\theta, \phi) = ik\hat{r} \wedge A_0(\theta, \phi). \quad (9.21)$$

All the above scalar and vector results by Wilcox are valid for any wave number k such that $\text{Im } k \geq 0$. The original papers (WILCOX [1956a, 1956b]) also contain bibliographies of previous works on this subject, as well as uniqueness results and theorems connecting the scalar case to the vector case.

A result which is equivalent to expression (9.11) has been recently derived (WESTON et al. [1968]; WESTON and BOERNER [1969]) in connection with inverse electromagnetic scattering. Let us consider a vector field $A(r)$ satisfying the wave equation and the radiation condition and having a radiation pattern $A_0(\theta, \phi)$, as in eq. (9.11); $A(r)$

may represent a vector potential, or the electric field, or the magnetic field. If $\mathbf{r} = x\hat{x} + y\hat{y} + z\hat{z}$, and if the equivalent sources which produce the electromagnetic field represented by A are confined within the region $z_{\min} \leq z \leq z_{\max}$, then

$$A(\mathbf{r}) = \begin{cases} \frac{ik}{2\pi} \int_0^{\frac{1}{2}\pi - i\infty} \sin \alpha d\alpha \int_0^{2\pi} e^{ik'\cdot\mathbf{r}} A_0(\alpha, \beta) d\beta, & \text{for } z > z_{\max}, \\ -\frac{ik}{2\pi} \int_{\pi}^{\frac{1}{2}\pi + i\infty} \sin \alpha d\alpha \int_0^{2\pi} e^{ik'\cdot\mathbf{r}} A_0(\alpha, \beta) d\beta, & \text{for } z < z_{\min}, \end{cases} \quad (9.22)$$

where

$$\mathbf{k}' = k(\sin \alpha \cos \beta \hat{x} + \sin \alpha \sin \beta \hat{y} + \cos \alpha \hat{z}). \quad (9.23)$$

Thus, if the radiation pattern $A_0(\theta, \phi)$ is known for all $0 \leq \theta \leq \pi$ and all $0 \leq \phi \leq 2\pi$, the integrals (9.22) give the field everywhere outside the region $z_{\min} \leq z \leq z_{\max}$ which sandwiches the equivalent sources. By rotating the reference axes (x, y, z) , i.e. by choosing other paths of integration in the complex α -plane, the field may be obtained at all points in space outside the minimum convex surface which envelopes the equivalent sources. The analytic continuation of $A_0(\theta, \phi)$ in the complex θ -plane is given by WESTON et al. [1968].

Bibliography

- KELLER, J. B., R. M. LEWIS and B. D. SECKLER [1956], Asymptotic Solution of Some Diffraction Problems, *Comm. Pure Appl. Math.* **9**, 207-265.
- WESTON, V. H., J. J. BOWMAN and E. AR [1968], On the Electromagnetic Inverse Scattering Problem, *Arch. Rational Mech. Anal.* **31**, 199-213.
- WESTON, V. H. and W. M. BOERNER [1969], An Inverse Scattering Technique for Electromagnetic Bistatic Scattering, *Canad. J. Phys.* (to be published).
- WILCOX, C. H. [1956a], An Expansion Theorem for Electromagnetic Fields, *Comm. Pure Appl. Math.* **9**, 115-134.
- WILCOX, C. H. [1956b], A Generalization of Theorems of Rellich and Atkinson, *Proc. Amer. Math. Soc.* **7**, 271-276.

CHAPTER 10

THE SPHERE

D. L. SENGUPTA

The sphere is undoubtedly the most intensively studied body in diffraction theory. It is still one of the very few bodies for which an exact solution to the vector problem is available. Its solution has been used as a model for developing theories for bodies of more general shape. The scattering behavior of spheres has important applications in many fields.

10.1. Spherical geometry

The spherical polar coordinates (r, θ, ϕ) shown in Fig. 10.1 are related to the rectangular Cartesian coordinates (x, y, z) by the transformation

$$\begin{aligned}x &= r \sin \theta \cos \phi, \\y &= r \sin \theta \sin \phi, \\z &= r \cos \theta,\end{aligned}\tag{10.1}$$

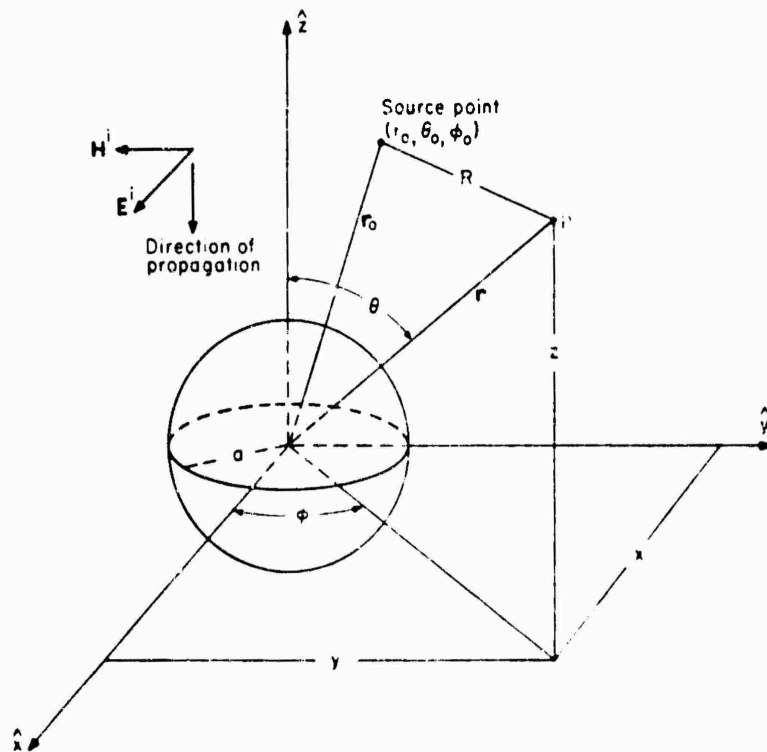


Fig. 10.1. Spherical geometry.

where $0 \leq r < \infty$, $0 \leq \theta \leq \pi$ and $0 \leq \phi < 2\pi$. The coordinate surfaces, $r = \text{constant}$, are concentric spheres intersected by meridian planes, $\phi = \text{constant}$, and a family of cones, $\theta = \text{constant}$. The z -axis is the polar axis. The unit vectors \hat{r} , $\hat{\theta}$ and $\hat{\phi}$ are drawn in the direction of increasing r , θ and ϕ such as to constitute a right-hand base system.

The scattering body is the sphere with surface $r = a$. The primary source is a point or dipole source located at (r_0, θ_0, ϕ_0) or a plane scalar wave or a plane electromagnetic wave (with polarization shown in Fig. 10.1).

Definitions, notation and bibliographical references to numerical tables for Bessel and Hankel functions, and for various functions which occur in the asymptotic developments, are given in the Introduction. The notation and definitions for the spherical vector wave functions and Legendre functions are those of STRATTON [1941]. In particular, the following symbols will appear frequently in the exact and approximate formulae:

$$\begin{aligned}
 m &= \left(\frac{1}{2}ka\right)^{\frac{1}{2}} \\
 \psi_n(x) &= xj_n(x) \\
 \zeta_n^{(1)}(x) &= xh_n^{(1)}(x) \\
 \psi_n'(x) &= \frac{d}{dx} [xj_n(x)] \\
 \zeta_n^{(1)'}(x) &= \frac{d}{dx} [xh_n^{(1)}(x)] \\
 a_n &= \frac{\psi_n(ka)}{\zeta_n^{(1)}(ka)} \\
 a_n' &= \frac{j_n'(ka)}{h_n^{(1)'}(ka)} \\
 b_n &= \frac{\psi_n'(ka)}{\zeta_n^{(1)'}(ka)}.
 \end{aligned} \tag{10.2}$$

10.2. Acoustically soft sphere

10.2.1. Point sources

10.2.1.1. EXACT SOLUTIONS

For a point source situated at $r_0 = (r_0, \theta_0, \phi_0)$, such that

$$V^i = \frac{e^{ikR}}{kR}, \tag{10.3}$$

the total field is

$$V^i + V^s = i \sum_{n=0}^{\infty} \sum_{l=1}^n (2n+1) [j_n(kr_<) - a_n h_n^{(1)}(kr_<)] h_n^{(1)}(kr_>) \\ \times \left\{ P_n(\cos \theta_0) P_n(\cos \theta) + 2 \frac{(n-1)!}{(n+1)!} P_n^l(\cos \theta_0) P_n^l(\cos \theta) \cos [l(\phi - \phi_0)] \right\}. \quad (10.4)$$

In particular, for a point source situated at $r_0 = (r_0, 0, 0)$, the total field is

$$V^i + V^s = i \sum_{n=0}^{\infty} (2n+1) P_n(\cos \theta) h_n^{(1)}(kr_>) [j_n(kr_<) - a_n h_n^{(1)}(kr_<)]. \quad (10.5)$$

If the source is situated on the surface ($r_0 = a$), the field $V^i + V^s \equiv 0$ everywhere.

On the surface $r = a$:

$$\frac{1}{k} \frac{\partial}{\partial r} (V^i + V^s) = \frac{i}{(ka)^2} \sum_{n=0}^{\infty} (2n+1) P_n(\cos \theta) \frac{h_n^{(1)}(kr_0)}{h_n^{(1)}(ka)}. \quad (10.6)$$

In the far zone ($r \rightarrow \infty$):

$$V^i + V^s = \frac{e^{ikr}}{kr} \sum_{n=0}^{\infty} (-i)^n (2n+1) P_n(\cos \theta) [j_n(kr_0) - a_n h_n^{(1)}(kr_0)]. \quad (10.7)$$

By using a Watson transformation, eq. (10.5) can be transformed into the following integral form (FRANZ [1954], LEVY and KELLER [1959]):

$$V^i + V^s = -\frac{1}{4} \int_D \frac{(2\mu+1) P_{\mu}(-\cos \theta)}{\sin \pi \mu} h_{\mu}^{(1)}(kr_>) \\ \times \left[h_{\mu}^{(2)}(kr_<) - \frac{h_{\mu}^{(2)}(ka)}{h_{\mu}^{(1)}(ka)} h_{\mu}^{(1)}(kr_<) \right] d\mu, \quad (10.8)$$

where D is a contour running from $-\infty + i\delta$ to $\infty + i\delta$ in the upper half of the complex μ -plane and parallel to the real axis with $\delta \rightarrow 0$. Similarly, on the surface $r = a$, eq. (10.6) can be written as

$$\frac{1}{k} \frac{\partial}{\partial r} (V^i + V^s) = \frac{i}{2(ka)^2} \int_D \frac{(2\mu+1) P_{\mu}(-\cos \theta)}{\sin \pi \mu} \frac{h_{\mu}^{(1)}(kr_0)}{h_{\mu}^{(1)}(ka)} d\mu. \quad (10.9)$$

Equations (10.8) and (10.9) are the basis for most high frequency approximations.

10.2.1.2. LOW FREQUENCY APPROXIMATIONS

No specific results are available; however, low frequency approximations for the various quantities can be derived from the exact results of the previous section.

10.2.1.3. HIGH FREQUENCY APPROXIMATIONS

At a point in the shadow region the field is given by (FRANZ [1954], LEVY and KELLER [1959]):

$$\begin{aligned}
 V^i + V^s &= \frac{m^{\frac{1}{2}}}{k^2} e^{-\frac{1}{2}i\pi(\pi r r_0 \sin \theta)^{-\frac{1}{2}}} \frac{\exp \{ik[(r^2 - a^2)^{\frac{1}{2}} + (r_0^2 - a^2)^{\frac{1}{2}}]\}}{(r^2 - a^2)^{\frac{1}{2}}(r_0^2 - a^2)^{\frac{1}{2}}} \\
 &\times \sum_{n=1}^{\infty} \frac{\exp \{i[v_n(2\pi - \theta) - \frac{1}{4}\pi]\} + \exp \{i[v_n\theta + \frac{1}{4}\pi]\}}{1 + \exp(2i\pi v_n)} \\
 &\times \frac{\exp[-iv_n\{\cos^{-1}(a/r) + \cos^{-1}(a/r_0)\}]}{[Ai'(-\alpha_n)]^2} [1 + O(m^{-2})], \quad (10.10)
 \end{aligned}$$

where

$$v_n = ka + e^{\frac{1}{2}i\pi} m \alpha_n - e^{-\frac{1}{2}i\pi} \frac{\alpha_n^2}{60m} + \frac{\alpha_n^3 - 10}{1400m^3} + O(m^{-5}), \quad (10.11)$$

with $n = 1, 2, 3, \dots$ and α_n are the zeros of the Airy functions, i.e. $Ai(-\alpha_n) = 0$. Equation (10.10) does not apply on the caustics $r = a$ and $\theta = \pi$.

For a point in the illuminated region the field is (LEVY and KELLER [1959], FRANZ [1954]):

$$\begin{aligned}
 V^s &= V_{\text{refl.}} - i \frac{m^{\frac{1}{2}}}{k^2} e^{-\frac{1}{2}i\pi(\pi r r_0 \sin \theta)^{-\frac{1}{2}}} \frac{\exp \{ik[(r^2 - a^2)^{\frac{1}{2}} + (r_0^2 - a^2)^{\frac{1}{2}}]\}}{(r^2 - a^2)^{\frac{1}{2}}(r_0^2 - a^2)^{\frac{1}{2}}} \\
 &\times \sum_{n=1}^{\infty} \frac{\exp[iv(2\pi + \theta) - \frac{1}{4}\pi] + \exp[iv(2\pi - \theta) + \frac{1}{4}\pi]}{1 + \exp(2iv_n\pi)} \\
 &\times \frac{\exp[-iv_n\{\cos^{-1}(a/r) + \cos^{-1}(a/r_0)\}]}{[Ai'(-\alpha_n)]^2} [1 + O(m^{-2})], \quad (10.12)
 \end{aligned}$$

where the summation over n represents the creeping wave contribution. $V_{\text{refl.}}$ is the reflected part of the field and is formally given by (FRANZ [1954]):

$$V_{\text{refl.}} = -V^i + \frac{1}{2}i \int_D (2\mu + 1) Q_{\mu}^{(2)}(\theta) h_{\mu}^{(1)}(kr_>) \left[h_{\mu}^{(2)}(kr_<) - \frac{h_{\mu}^{(2)}(ka)}{h_{\mu}^{(1)}(ka)} h_{\mu}^{(1)}(kr_<) \right] d\mu, \quad (10.13)$$

where the contour D is as defined in Section 10.2.1.1 and $Q_{\mu}^{(2)}(x) = i\pi Q_{\mu}(x - i0)$ with $Q_{\mu}(x - i0)$ as defined in the Introduction (see Section 1.3.5). An asymptotic expansion of eq. (10.13) in inverse powers of ka leads to the Luneburg-Kline series whose first term represents the reflected wave according to geometrical optics. The creeping wave contribution given in eq. (10.12) is not valid on the caustics $r = a$ and $\theta = 0$.

10.2.2. Plane wave incidence

10.2.2.1. EXACT SOLUTIONS

For a plane wave incident in the direction θ_0, ϕ_0 , such that

$$V^i = \exp \{ikr[\cos \theta_0 \cos \theta + \sin \theta_0 \sin \theta \cos(\phi - \phi_0)]\}, \quad (10.14)$$

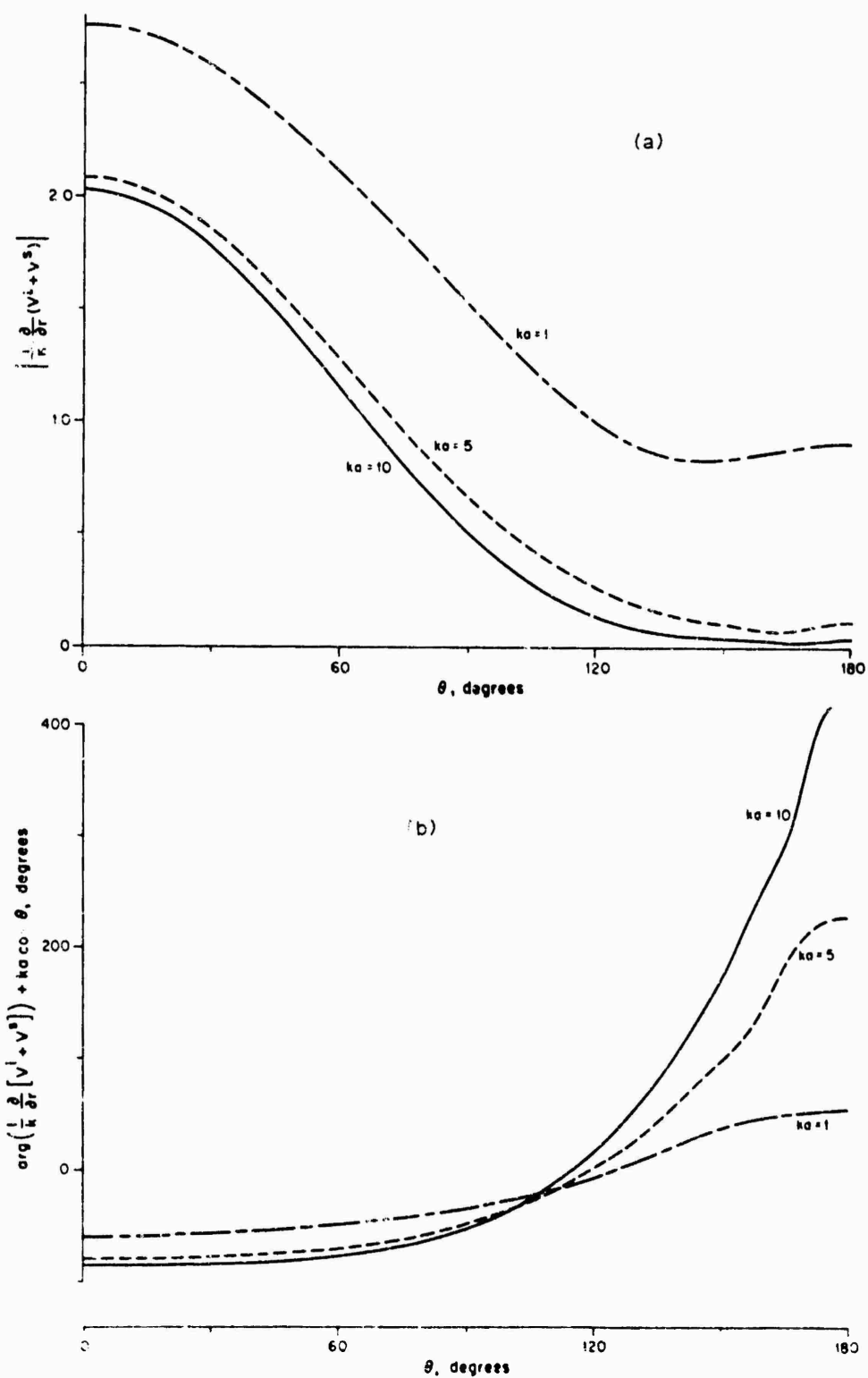


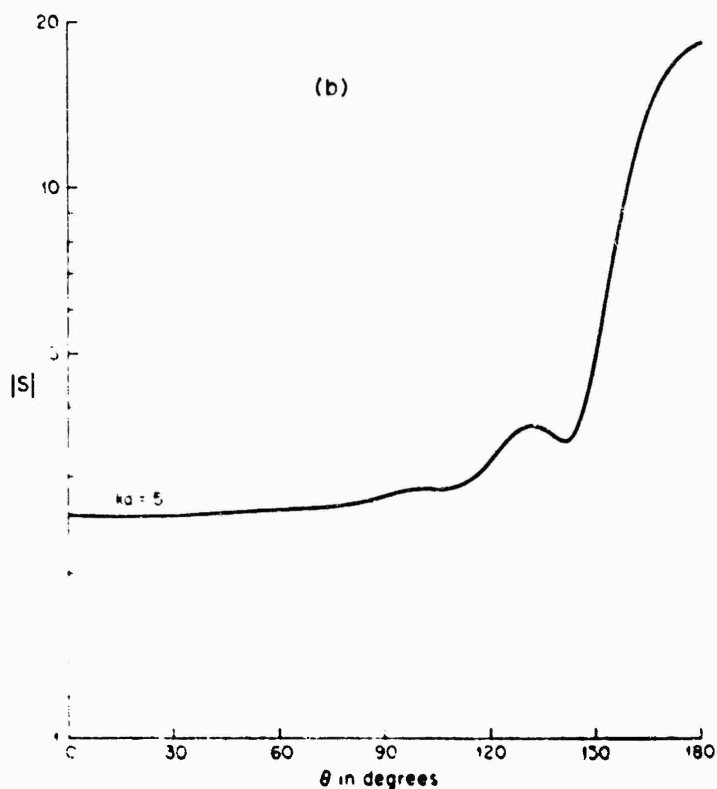
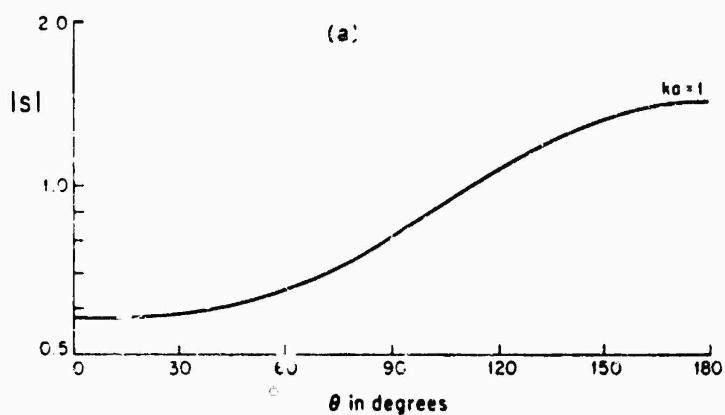
Fig. 10.2. Surface current as a function of θ for selected values of ka for a soft sphere.

the total field is

$$V^i + V^s = \sum_{n=0}^{\infty} i^n (2n+1) [j_n(kr) - a_n h_n^{(1)}(kr)] \left\{ P_n(\cos \theta_0) P_n(\cos \theta) + 2 \sum_{l=1}^n \frac{(n-l)!}{(n+l)!} P_n^l(\cos \theta_0) P_n^l(\cos \theta) \cos [l(\phi - \phi_0)] \right\}. \quad (10.15)$$

In particular for a plane wave incident in the direction of the negative z -axis the total field is

$$V^i + V^s = \sum_{n=0}^{\infty} (-i)^n (2n+1) [j_n(kr) - a_n h_n^{(1)}(kr)] P_n(\cos \theta). \quad (10.16)$$



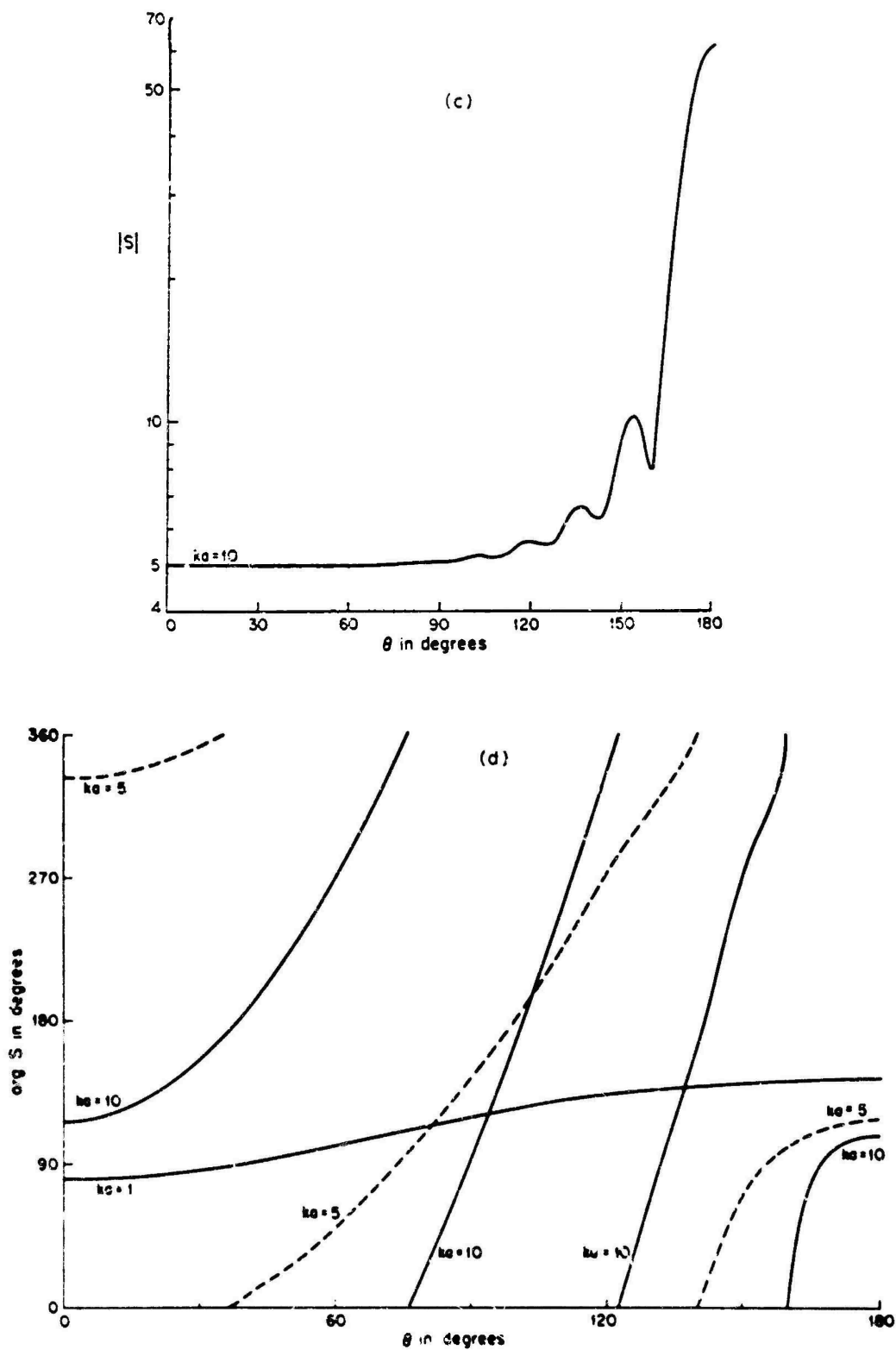


Fig. 10.3. The scattering function S as a function of θ for selected values of ka for a soft sphere.

On the surface $r = a$:

$$\frac{1}{k} \frac{\partial}{\partial r} (V^{(1)} + V^{(2)}) = - \frac{i}{(ka)^2} \sum_{n=0}^{\infty} (-i)^n (2n+1) \frac{P_n(\cos \theta)}{h_n^{(1)}(ka)}. \quad (10.17)$$

Computed values of the surface current S as a function of θ are shown in Fig. 10.2 for selected values of ka . In the far field ($r \rightarrow \infty$):

$$S = i \sum_{n=0}^{\infty} (-1)^n (2n+1) a_n P_n(\cos \theta). \quad (10.18)$$

Computed values of S as a function of θ are shown in Fig. 10.3 for selected values of ka .

The back scattering cross section is

$$\sigma = \frac{4\pi}{k^2} \left| \sum_{n=0}^{\infty} (-1)^n (2n+1) a_n \right|^2. \quad (10.19)$$

The normalized back scattering cross section $\sigma (\pi a^2)$ is shown as a function of ka in Fig. 10.4.

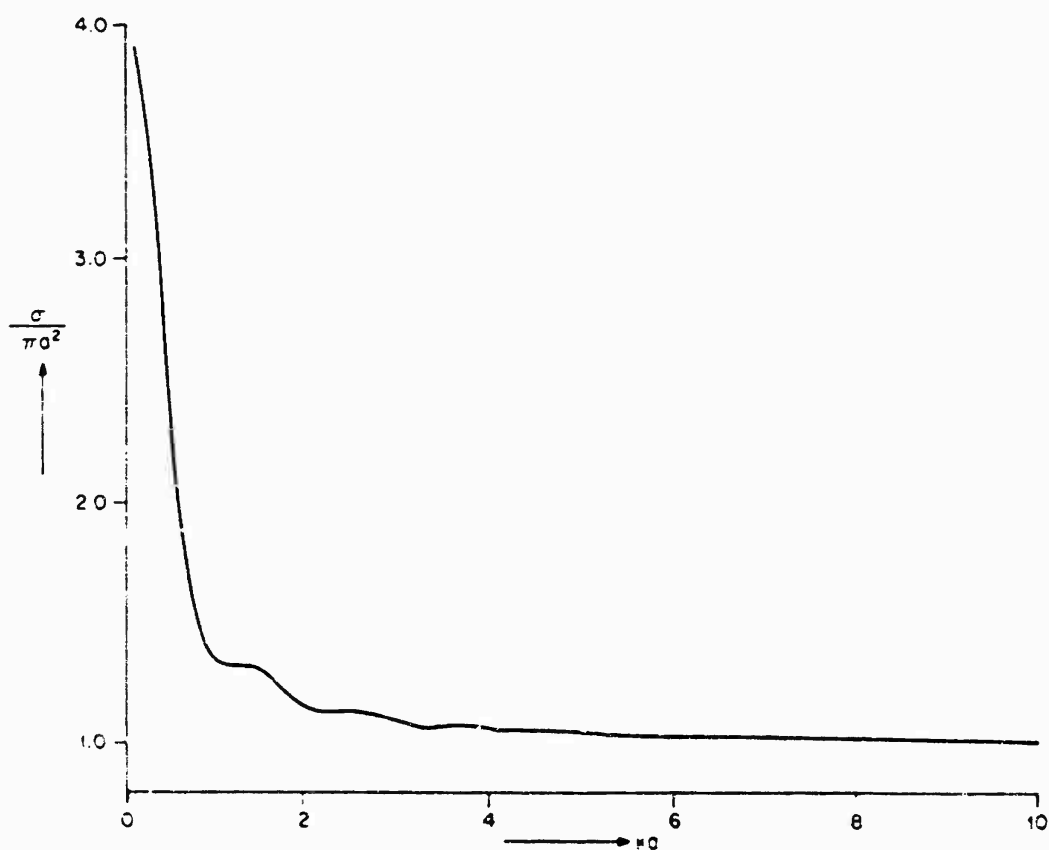


Fig. 10.4 Normalized back scattering cross section $\sigma (\pi a^2)$ as a function of ka for a soft sphere (SENIOK [1965]).

The total scattering cross section

$$\sigma_T = \frac{4\pi}{k^2} \sum_{n=0}^{\infty} (2n+1) |a_n|^2. \quad (10.20)$$

Figure 10.5 shows the normalized total scattering cross section $\sigma_T/(2\pi a^2)$ as a function of ka .

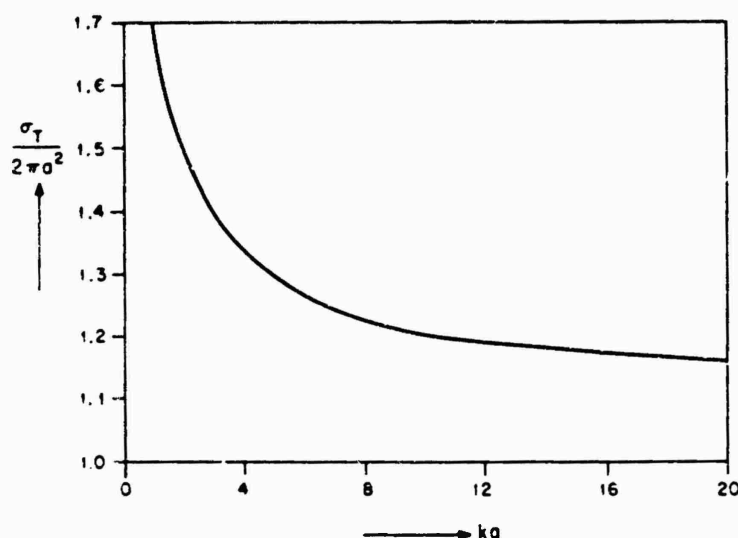


Fig. 10.5. Normalized total scattering cross section $\sigma_T/(2\pi a^2)$ as a function of ka for a soft sphere (KING and WU [1959]).

10.2.2.2. LOW FREQUENCY APPROXIMATIONS

For a plane wave incident in the direction of the negative z -axis, such that

$$V^i = e^{-ikz} \quad (10.21)$$

low frequency expansions may be obtained either directly or by power series developments of the Bessel and Hankel functions appearing in the exact solution (RAYLEIGH [1872], MORSE and FESHBACH [1953]). The first three coefficients appearing in eq. (10.18) are:

$$a_0 = ika \left\{ 1 - ika - \frac{1}{3}(ka)^2 + \frac{1}{3}i(ka)^3 + \frac{1}{15}(ka)^4 - \frac{2}{35}i(ka)^5 + O[(ka)^6] \right\}, \quad (10.22)$$

$$a_1 = \frac{1}{3}i(ka)^3 \left\{ 1 - \frac{1}{3}(ka)^2 - \frac{1}{3}i(ka)^3 + O[(ka)^6] \right\}, \quad (10.23)$$

$$a_2 = \frac{1}{4}i(ka)^5 \left\{ 1 - \frac{5}{4}(ka)^2 + O[(ka)^7] \right\}, \quad (10.24)$$

where $ka \ll 1$.

The scattering function in the direction $\theta = 0$ is (SENIOR [1965]):

$$S(0) = -ka \left\{ 1 - ika - \frac{1}{3}(ka)^2 - \frac{1}{3}i(ka)^3 - \frac{1}{4}(ka)^4 + \frac{1}{4}i(ka)^5 + O[(ka)^6] \right\}. \quad (10.25)$$

Similarly, in the forward direction $\theta = \pi$:

$$S(\pi) = -ka \left\{ 1 - ika - \frac{1}{3}(ka)^2 + \frac{1}{3}i(ka)^3 - \frac{1}{4}(ka)^4 - \frac{1}{4}i(ka)^5 + O[(ka)^6] \right\}. \quad (10.26)$$

The back scattering cross section is

$$\sigma \sim 4\pi a^2 \left[1 - \frac{7}{3}(ka)^2 + \frac{19}{5}(ka)^4 \right]. \quad (10.27)$$

The total scattering cross section is

$$\sigma_T \sim 4\pi a^2 \left[1 - \frac{1}{3}(ka)^2 + \frac{17}{45}(ka)^4 \right]. \quad (10.28)$$

10.2.2.3. HIGH FREQUENCY APPROXIMATIONS

For a plane wave incident in the direction of the negative z -axis, such that

$$V^i = e^{-ikz}, \quad (10.29)$$

the high frequency behavior of the field can be completely determined in both near and far zones by applying a modified Watson transformation based upon Poisson's summation formula to the exact expressions (NUSSENZVEIG [1965]). The various regions of space to be considered are shown in Fig. 10.6.

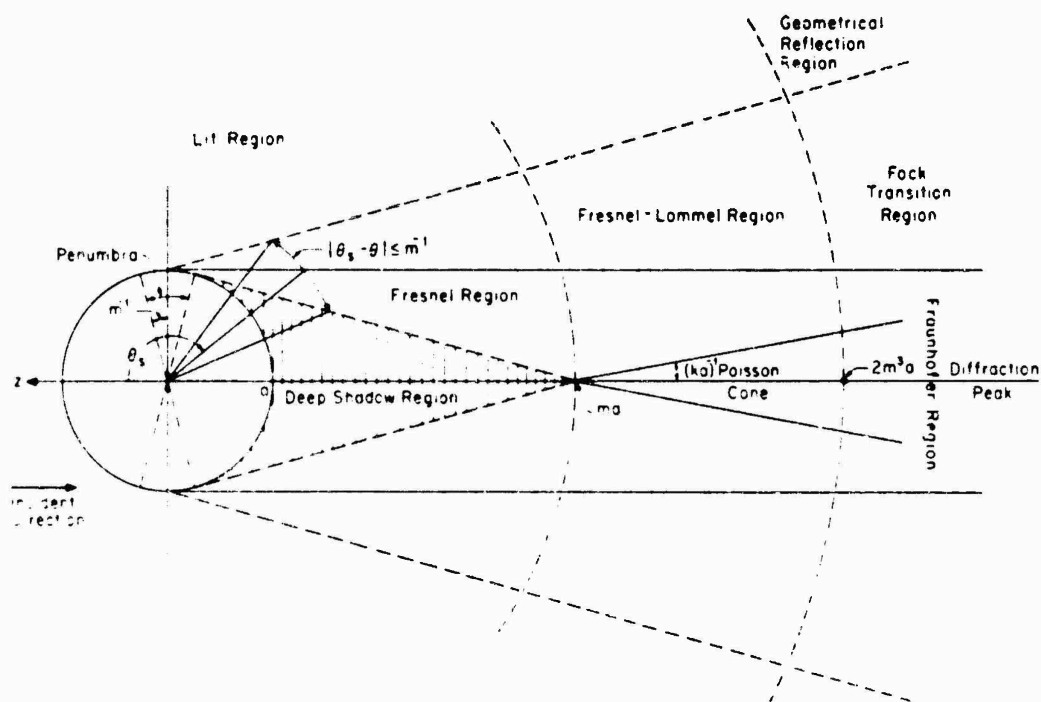


Fig. 10.6. Geometrical representation of the various regions in space (NUSSENZVEIG [1965]).

For points within the deep shadow region, not too close to the surface of the sphere (LIVY and KELLER [1959], NUSSENZVEIG [1965]),

$$V^i + V^s \sim \frac{e^{-ikr}}{(2\pi)^{1/2}} m \left(\frac{a^2}{r^2 - a^2} \right)^{1/2} \exp [ik(r^2 - a^2)^{1/2}] \times \sum_{n=-\infty}^{\infty} (-1)^n \sum_{l=0}^{\infty} \frac{\exp(i\nu_n \theta_l + \frac{1}{4}i\pi) + \exp(i\nu_n \phi_l - \frac{1}{4}i\pi)}{[\Delta_l'(-x_n)]^2}, \quad (10.30)$$

where

$$\begin{aligned}\gamma_l &= 2l\pi - \theta_s + \theta \\ \delta_l &= (l+1)2\pi - (\theta_s + \theta) \\ \pi - \theta_s &= \sin^{-1}(a/r) \quad (\text{Fig. 10.6}).\end{aligned}\quad (10.31)$$

Eq. (10.30) is valid under the following conditions:

$$\begin{aligned}\frac{1}{2}\pi &\leq \theta_s < \theta < \pi \\ (r-s) &\gg am^{-1} \\ (kr - |v_n|) &\gg |v_n|^{\frac{1}{2}} \\ (\pi - \theta) &\gg (ka)^{-1}\end{aligned}\quad (10.32)$$

with v_n and x_n defined in Section 10.2.1.3.

The physical interpretation of eq. (10.30) is that the incident rays at their points of tangency to the sphere launch a series of surface waves emanating from these points. These waves travel along the surface with phase velocity slightly smaller than that in free space. As they travel along the surface, they shed radiation along tangential directions. The angular damping factor due to radiation for the dominant surface waves ($l = 0$) is:

$$\begin{aligned}|\exp(iv_n\gamma_0)| &\sim \exp[-\frac{1}{2}\sqrt{3}x_nm(\theta_s - \theta)] \\ |\exp(iv_n\delta_0)| &\sim \exp[-\frac{1}{2}\sqrt{3}x_nm\{2\pi - (\theta_s + \theta)\}].\end{aligned}\quad (10.33)$$

If $0 \leq (\pi - \theta) \leq (ka)^{-1}$ (LEVY and KELLER [1959], NUSSENZVEIG [1965]):

$$\begin{aligned}V^i + V^s &\sim e^{-i\pi/2} m \left(\frac{a^2}{r^2 - a^2} \right)^{\frac{1}{2}} (a/r)^{\frac{1}{2}} \exp[ik(r^2 - a^2)^{\frac{1}{2}}] \\ &\times \sum_{l=0}^{\infty} (-1)^l \sum_{n=1}^{\infty} \frac{\exp[iv_n\{(2l+1)\pi - \theta_0\}]}{[Ai'(-x_n)]^2} J_0[v_n(\pi - \theta)].\end{aligned}\quad (10.34)$$

In the lit region, sufficiently far from the shadow boundary, the reflected portion of the scattered field in the region $0 \leq \theta \leq \theta_s - m^{-1}$ is (KELLER et al. [1956], NUSSENZVEIG [1965]):

$$\begin{aligned}V_{\text{refl.}}^s &= - \left[\frac{a^2 \sin^2 \zeta}{4s(s \sin^2 \zeta + a \cos^3 \zeta)} \right]^{\frac{1}{2}} \exp[ik(s - \frac{1}{2}a \sin \zeta)] \\ &\times \left\{ 1 + \frac{i}{2ka} \left[\frac{1}{\sin^3 \zeta} + \frac{1}{2^4 \sin^2 \zeta \cos^2 \zeta} (a/s) + \frac{3}{2^5} \left(\frac{2}{\sin \zeta} - 5 \sin \zeta \right) (a/s)^2 - \right. \right. \\ &\quad \left. \left. - \frac{15}{2^6} (\cos^2 \zeta)(a/s)^3 - \frac{1}{2^3 \sin \zeta \cos \zeta} \left(s \sin^2 \zeta + a \cos^3 \zeta \right) \right] \right\} + O[(ka)^{-2}],\end{aligned}\quad (10.35)$$

where

$$\begin{aligned}s &= r \cos \bar{w} - \frac{1}{2}a \sin \zeta \\ \zeta &= \frac{1}{2}(\pi - \theta - \bar{w}) \\ \sin \bar{w} &= \frac{a}{r} \cos \frac{1}{2}(\pi - \theta - \bar{w}).\end{aligned}\quad (10.36)$$

Eq. (10.35) is the Luneburg-Kline asymptotic expansion in inverse powers of (ka) ; its first term represents the reflected wave according to geometrical optics and the remainder represents the correction to geometrical optics (KELLER et al. [1956]). The physical interpretation of the geometrically reflected field term is shown in Fig. 10.7.

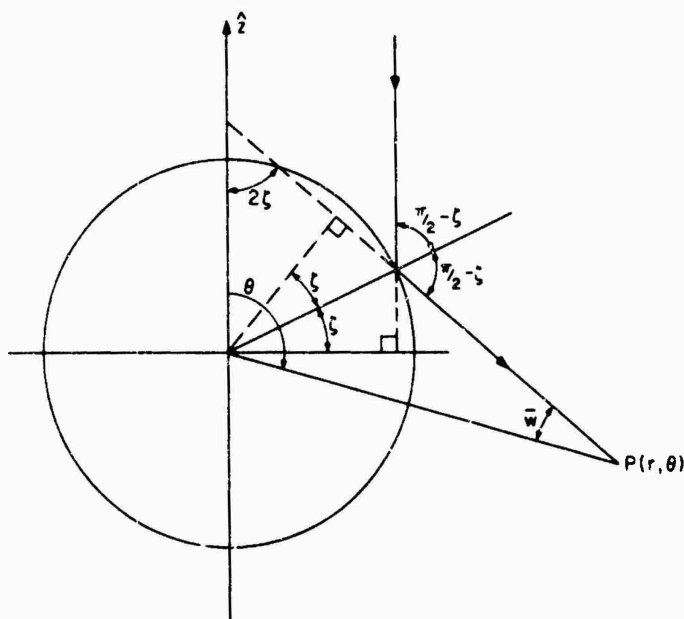


Fig. 10.7. Geometrical representation of the reflected field.

The creeping wave contribution to the scattered field at a point in the lit region sufficiently far from the shadow boundary, such that $m^{-1} \leq \theta \leq \theta_0 - m^{-1}$, is (LEVY and KELLER [1959], NUSSENZVEIG [1965]):

$$V_{\text{cr.w.}}^s \sim \frac{e^{-i\pi}}{(2\pi)^{\frac{1}{2}}} m \left(\frac{a^2}{r^2 - a^2} \right)^{\frac{1}{2}} \frac{\exp [ik(r^2 - a^2)^{\frac{1}{2}}]}{(kr \sin \theta)^{\frac{1}{2}}} \left\{ e^{-i\pi} \sum_{n=1}^{\infty} \frac{\exp (iv_n \delta_0)}{[Ai'(-x_n)]^2} + \right. \\ \left. + \sum_{l=1}^{\infty} (-1)^l \sum_{n=1}^{\infty} \frac{\exp (iv_n \gamma_l + \frac{1}{2} i \pi) + \exp (iv_n \delta_l - \frac{1}{2} i \pi)}{[Ai'(-x_n)]^2} \right\}. \quad (10.37)$$

In the range $0 \leq \theta \leq (ka)^{-1}$ (LEVY and KELLER [1959], NUSSENZVEIG [1965]):

$$V_{\text{cr.w.}}^s \sim e^{-i\pi} m (a/r)^{\frac{1}{2}} \left(\frac{a^2}{r^2 - a^2} \right)^{\frac{1}{2}} \exp [ik(r^2 - a^2)^{\frac{1}{2}}] \\ \times \sum_{l=0}^{\infty} (-1)^l \sum_{n=1}^{\infty} \frac{\exp [iv_n \{(l+1)2\pi - \theta\}]}{[Ai'(-x_n)]^2} J_0(v_n \theta). \quad (10.38)$$

On the surface of the sphere, outside the penumbra region $|\frac{1}{2}\pi - \theta| \leq m^{-1}$, an accurate approximation is provided by the Kirchhoff approximation (geometrical optics) and is:

$$\frac{1}{k} \frac{\partial}{\partial r} (V^s + V^i) = \begin{cases} 0 & \text{for } \theta > \frac{1}{2}\pi + m^{-1} \\ 1 - 2i \cos \theta \exp(-ika \cos \theta) & \text{for } \theta < \frac{1}{2}\pi - m^{-1}. \end{cases} \quad (10.39)$$

Within the penumbra region (NUSSENZVEIG [1965]):

$$\frac{1}{k} \frac{\partial}{\partial r} (V^i + V^s) \sim -\frac{1}{m \sin \theta} \exp \{ika(\theta - \frac{1}{2}\pi)\} f(\xi), \quad (10.40)$$

where $\xi = m(\theta - \frac{1}{2}\pi)$ and the modified Fock function $f(\xi)$ is defined in the Introduction. The Fock function $f(\xi)$ in eq. (10.40) interpolates smoothly the values in the lit and shadow regions on the surface of the sphere. However, it cannot be employed in the lit region too far beyond $(\frac{1}{2}\pi - \theta) \sim m^{-1}$.

Within the Fresnel region and near the boundary of the geometrical shadow such that $am^{-1} \lesssim z \lesssim am$ (RUBINOW and WU [1956]):

$$V^i + V^s \sim \frac{e^{\frac{1}{2}i\pi}}{\sqrt{2\pi}} e^{-ikz} \left[F(x\sqrt{\pi}) - M_0 \xi \frac{e^{\frac{1}{2}i\pi}}{\pi x} \right], \quad (10.41)$$

where

$$\xi = m(\theta_s - \theta), \quad x = (kz/\pi)^{\frac{1}{2}}(\theta - \theta_s), \quad (10.42)$$

$$M_0 = 1.2550743e^{\frac{1}{2}i\pi}$$

and $F(x\sqrt{\pi})$ is the Fresnel integral as defined in the Introduction.

In the Fresnel-Lommel region (Fig. 10.6) and within the geometrical shadow (NUSSENZVEIG [1965]):

$$V^i + V^s \sim \left(\frac{\pi - \theta}{\sin \theta} \right)^{\frac{1}{2}} f(s, t, u, v) \exp \left[ik \left(r + \frac{a^2}{2r} \right) \right], \quad (10.43)$$

where

$$f(s, t, u, v) = L(u, v) + i s F(s, t, v); \quad (10.44)$$

$L(u, v)$ represents Lommel's approximation (WATSON [1948]):

$$L(u, v) = V_0(u, v) + i V_1(u, v), \quad (10.45)$$

where $V_0(u, v)$, $V_1(u, v)$ are Lommel functions of order 0 and 1, and

$$F(s, t, v) = e^{\frac{1}{2}i\pi} \int_0^{\infty} \frac{\text{Ai}(xe^{\frac{1}{2}i\pi})}{\text{Ai}(xe^{-\frac{1}{2}i\pi})} e^{-isx} J_0(v - tx) dx +$$

$$+ e^{\frac{1}{2}i\pi} \int_0^{\infty} \frac{\text{Ai}(x)}{\text{Ai}(xe^{\frac{1}{2}i\pi})} e^{isx} J_0(v + tx) dx, \quad (10.46)$$

where

$$s = ma^2 r, \quad t = m(\pi - \theta) \quad (10.47)$$

$$u = ka^2 r, \quad v = ka(\pi - \theta) = tu s.$$

On the axis $\theta = \pi$:

$$V^i + V^s \sim f(s, 0, u, 0) \exp \left[ik \left(r + \frac{a^2}{2r} \right) \right], \quad (10.48)$$

where

$$f(s, 0, u, 0) = 1 + is \left[e^{\frac{1}{2}is} \int_0^\infty \frac{\text{Ai}(xe^{\frac{1}{2}is})}{\text{Ai}(xe^{-\frac{1}{2}is})} e^{-isx} dx + e^{\frac{1}{2}is} \int_0^\infty \frac{\text{Ai}(x)}{\text{Ai}(xe^{\frac{1}{2}is})} e^{isx} dx \right]. \quad (10.49)$$

If $r \ll ma$ (NUSSENZVEIG [1965]):

$$V^i + V^s \sim -e^{-\frac{1}{2}is} \frac{ma}{r} \exp \left[ik \left(r + \frac{a^2}{2r} \right) \right] \sum_{n=1}^{\infty} \frac{\exp [ie^{\frac{1}{2}is} \alpha_n ma/r]}{[\text{Ai}'(-\alpha_n)]^2}. \quad (10.50)$$

If $r \gg ma$ (RUBINOW and WU [1956]):

$$V^i + V^s \sim \left[1 + iM_0 \frac{ma}{r} - M_1 \frac{m^2 a^2}{r^2} + \dots \right] \exp \left[ik \left(r + \frac{a^2}{2r} \right) \right], \quad (10.51)$$

where

$$M_1 = 0.53225036 e^{\frac{1}{2}is}. \quad (10.52)$$

On comparing eq. (10.50) with eq. (10.49) it is found that a Poisson spot of intensity comparable to that of the incident wave is evident at a distance $r \sim ma$ from the sphere.

In a region away from the axis such that $r \gg ma$, $\theta \gg a/r$, the field is (NUSSENZVEIG [1965]):

$$\begin{aligned} V^i + V^s \sim & \left(\frac{\pi - \theta}{\sin \theta} \right)^{\frac{1}{2}} \exp \left[ik \left(r + \frac{a^2}{2r} \right) \right] \\ & \times \left\{ [1 + iM_0 ma/r - M_1 m^2 (a/r)^2 + \dots] J_0[ka(\pi - \theta)] - \right. \\ & \left. - i[1 + iM_1 m^2 (a/r)^2 + \dots] \frac{r(\pi - \theta)}{a} J_1[ka(\pi - \theta)] + \dots \right\}. \quad (10.53) \end{aligned}$$

In the neighborhood of the axis, for $r \gg ma$, the intensity according to eq. (10.53) behaves like $J_0^2[ka(\pi - \theta)]$ times the intensity of the incident wave, so that the Poisson spot actually corresponds to a Poisson cone of angular opening $(ka)^{-1}$ (Fig. 10.6).

In the far zone ($r \rightarrow \infty$)

$$S = S_{\text{refl.}} + S_{\text{cr.w.}}, \quad (10.54)$$

where $S_{\text{refl.}}$ is the contribution due to the reflected field and $S_{\text{cr.w.}}$ is that due to creeping waves.

For $0 \leq \theta \leq \pi - m^{-1}$,

$$S_{\text{refl.}} \sim -\frac{1}{2}ka \exp [-2ka \cos \frac{1}{2}\theta] \left(1 + \frac{i}{2ka \cos^3 \frac{1}{2}\theta} + \dots \right), \quad (10.55)$$

$$S_{\text{cr.w.}} \sim -e^{-\frac{1}{2}is} mka \left(\frac{\theta}{\sin \theta} \right)^{\frac{1}{2}} \sum_{l=0}^{\infty} (-1)^l \sum_{n=1}^{\infty} \frac{\exp \{i(2l+1)\pi v_n\}}{[\text{Ai}'(-\alpha_n)]^2} J_0(v_n \theta). \quad (10.56)$$

More refined expressions for $S_{\text{refl.}}$ and $S_{\text{cr.w.}}$ in the direction $\theta=0$ are (SENIOR [1965]):

$$S_{\text{refl.}} = -\frac{1}{2}ka e^{-2ika} \left\{ 1 + \frac{i}{2ka} + \frac{1}{2(ka)^2} - \frac{5i}{4(ka)^2} - \frac{5}{(ka)^4} + O[(ka)^{-5}] \right\}, \quad (10.57)$$

$$S_{\text{cr.w.}} = -e^{i\pi} mka \sum_{l=0}^{\infty} (-1)^l \sum_{n=l}^{\infty} \left\{ 1 + \frac{e^{i\pi} 8\alpha_n}{15m^2} - \frac{e^{-i\pi} 4\alpha_n^2}{175m^4} + O(m^{-6}) \right\} \\ \times \frac{1}{[Ai'(-\alpha_n)]^2} \exp \left[i(2l+1)\pi \left\{ ka + e^{i\pi} m\alpha_n - e^{-i\pi} \frac{\alpha_n^2}{60m} + \frac{\alpha_n^2 - 10}{1400m^3} + O(m^{-6}) \right\} \right]. \quad (10.58)$$

The first three terms in eq. (10.57) were previously obtained by KELLER et al. [1956] using Luneburg-Kline expansion techniques. The leading term in eq. (10.57) is the contribution due to geometrical optics. The second real term in eq. (10.57) produces a correction to the geometrical optics term exceeding 10 per cent if $ka < 2.23$ and the third real term in eq. (10.57) corrects the second by more than 10 per cent if $ka < 5$.

An accurate approximation to eq. (10.58) based on a single creeping wave alone and for $ka > 1$ is (SENIOR [1965]):

$$S_{\text{cr.w.}} = -e^{i\pi} mka \left\{ 1 + \frac{e^{i\pi} 8\alpha_1}{15m^2} + O(m^{-4}) \right\} \frac{1}{[Ai'(-\alpha_1)]^2} \\ \times \exp \left[i\pi ka - e^{-i\pi} \pi m\alpha_1 - e^{i\pi} \frac{\pi\alpha_1^2}{60m} + O(m^{-3}) \right], \quad (10.59)$$

where

$$\alpha_1 = 2.338\,107\,41 \dots,$$

$$Ai'(-\alpha_1) = 0.701\,210\,82 \dots$$

The normalized creeping wave contribution $2S_{\text{cr.w.}}/(ka)$ as computed from eq. (10.59) is shown as a function of ka in Fig. 10.8.

In the transition region $(\pi-\theta) \sim m^{-1}$ the scattering function is (NUSSENZVEIG [1965]):

$$S \sim \frac{1}{2}ik^2 a^2 \left(\frac{\pi-\theta}{\sin \theta} \right)^{\frac{1}{2}} \left\{ \frac{J_1[ka(\pi-\theta)]}{ka(\pi-\theta)} + \right. \\ + m^{-2} \left[\int_0^{\infty} \frac{Ai(x)}{Ai(xe^{-i\pi})} J_0[ka(\pi-\theta) - e^{-i\pi} m(\pi-\theta)x] dx + \right. \\ \left. + \int_0^{\infty} \frac{Ai(x)}{Ai(xe^{i\pi})} J_0[ka(\pi-\theta) + m(\pi-\theta)x] dx \right] + \dots \Big\} + \\ + e^{-i\pi} mka \left(\frac{\pi-\theta}{\sin \theta} \right)^{\frac{1}{2}} \sum_{l=1}^{\infty} (-1)^l \sum_{n=l}^{\infty} \frac{\exp[2il\pi v_n]}{[Ai'(-\alpha_n)]^2} J_0[v_n(\pi-\theta)]. \quad (10.60)$$

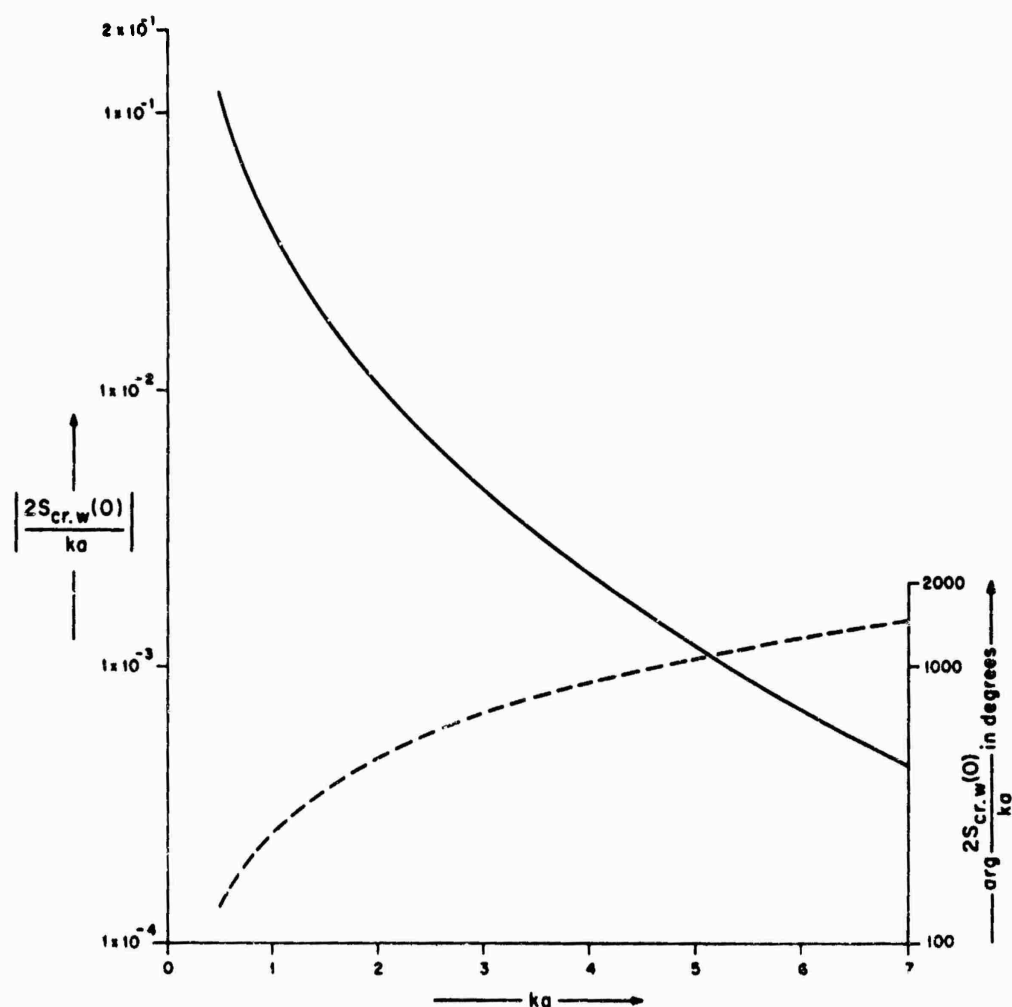


Fig. 10.8. Amplitude (—) and phase (---) of the normalized creeping wave contribution $2S_{cr.w.}/(ka)$ in the direction $\theta = 0$ as a function of ka for a soft sphere.

In the neighborhood of the forward direction $0 \leq \pi - \theta \lesssim m^{-1}$ (NUSSENZVEIG [1965]):

$$S_{refl.} \sim \frac{1}{2}i(ka)^2 \left(\frac{\pi - \theta}{\sin \theta} \right)^{\frac{1}{2}} \left\{ 2 \frac{J_1[ka(\pi - \theta)]}{ka(\pi - \theta)} + e^{i\pi} m^{-2} \{ 1.9923 J_0[ka(\pi - \theta)] + 0.5323 m(\pi - \theta) J_1[ka(\pi - \theta)] \} + \dots \right\}, \quad (10.61)$$

$$S_{cr.w.} \sim e^{-\frac{1}{2}i\pi} mka \left(\frac{\pi - \theta}{\sin \theta} \right)^{\frac{1}{2}} \sum_{l=1}^{\infty} (-1)^l \sum_{n=1}^{\infty} \frac{\exp[2il\pi v_n]}{[Ai'(-x_n)]^2} J_0[v_n(\pi - \theta)]. \quad (10.62)$$

In the forward direction $\theta = \pi$ the scattering function is (WU [1956]):

$$S(\pi) \sim \frac{1}{2}(ka)^2 \left[1 + M_0 \left(\frac{1}{2}ka \right)^{-4} + {}_1^8 M_1 \left(\frac{1}{2}ka \right)^{-4.3} + ({}_1^6 M_2 + {}_4^2 M_3) \left(\frac{1}{2}ka \right)^{-2} - \right. \\ \left. - ({}_0^6 M_3 + {}_1^2 M_0) \left(\frac{1}{2}ka \right)^{-8.3} + ({}_2^2 M_4 + {}_3^3 M_1) (ka)^{-10.3} + \dots \right], \quad (10.63)$$

where

$$\begin{aligned} M_0 &= 1.255\,074\,3e^{i\pi}, & M_1 &= 0.532\,250\,3e^{i\pi}, \\ M_2 &= 0.093\,521\,6, & M_3 &= 0.772\,793\,e^{i\pi}, \\ M_4 &= 1.099\,2e^{i\pi}. \end{aligned} \quad (10.64)$$

The total scattering cross section is (WU [1956], BECKMANN and FRANZ [1957]):

$$\begin{aligned} \frac{\sigma_T}{2\pi a^2} &\sim 1 + 0.996\,153\,19(ka)^{-\frac{1}{2}} - 0.357\,649\,83(ka)^{-\frac{3}{2}} + 0.227\,598\,2(ka)^{-2} - \\ &\quad - 0.007\,275\,3(ka)^{-\frac{5}{2}} - 0.007\,443(ka)^{-\frac{7}{2}} + \dots \end{aligned} \quad (10.65)$$

10.3. Acoustically hard sphere

10.3.1. Point sources

10.3.1.1. EXACT SOLUTIONS

For a point source at $\mathbf{r}_0 = (r_0, \theta_0, \phi_0)$ such that

$$V^i = \frac{e^{ikR}}{kR}, \quad (10.66)$$

the total field is

$$\begin{aligned} V^i + V^s &= i \sum_{n=0}^{\infty} \sum_{l=1}^n (2n+1) [j_n(kr_<) - a'_n h_n^{(1)}(kr_<)] h_n^{(1)}(kr_>) \\ &\quad \times \left\{ P_n(\cos \theta_0) P_n(\cos \theta) + 2 \frac{(n-l)!}{(n+l)!} P_n^l(\cos \theta_0) P_n^l(\cos \theta) \cos[l(\phi - \phi_0)] \right\}. \end{aligned} \quad (10.67)$$

In particular for a point source situated at $\mathbf{r}_0 = (r_0, 0, 0)$ the total field is

$$V^i + V^s = i \sum_{n=0}^{\infty} (2n+1) P_n(\cos \theta) h_n^{(1)}(kr_>) [j_n(kr_<) - a'_n h_n^{(1)}(kr_<)]. \quad (10.68)$$

On the surface $r = a$:

$$V^i + V^s = - \frac{1}{(ka)^2} \sum_{n=0}^{\infty} (2n+1) P_n(\cos \theta) \frac{h_n^{(1)}(kr_0)}{h_n^{(1)}(ka)}. \quad (10.69)$$

In the far zone ($r \rightarrow \infty$):

$$V^i + V^s = \frac{e^{ikr}}{kr} \sum_{n=0}^{\infty} (-i)^n (2n+1) P_n(\cos \theta) [j_n(kr_0) - a'_n h_n^{(1)}(kr_0)]. \quad (10.70)$$

By using a Watson transformation eq. (10.68) can be transformed into the following integral (FRANZ [1954], LEVY and KELLER [1959]):

$$V^i + V^s = - \frac{1}{4} \int_0^\pi \frac{(2\mu+1) P_\mu(-\cos \theta)}{\sin \pi \mu} h_\mu^{(1)}(kr_>) \left[h_\mu^{(2)}(kr_<) - \frac{h_\mu^{(2)}(ka)}{h_\mu^{(1)}(ka)} h_\mu^{(1)}(kr_<) \right] d\mu, \quad (10.71)$$

where D is a contour running from $-\infty + i\delta$ to $\infty + i\delta$ in the upper half of the complex μ -plane and parallel to the real axis with $\delta \rightarrow 0$.

Similarly, on the surface $r = a$, eq. (10.68) can be written as

$$V^i + V^s = -\frac{i}{2(ka)^2} \int_D \frac{(2\mu+1)P_\mu(-\cos\theta)}{\sin\pi\mu} \frac{h_\mu^{(1)}(kr_0)}{h_\mu^{(1)}(ka)} d\mu. \quad (10.72)$$

Equations (10.71) and (10.72) are the basis for most high frequency approximations.

10.3.1.2. LOW FREQUENCY APPROXIMATIONS

No specific results are available; however, low frequency approximations for different quantities can be derived from the exact results of the previous section.

10.3.1.3. HIGH FREQUENCY APPROXIMATIONS

At a point in the shadow region the field is given by (FRANZ [1954], LEVY and KELLER [1959]):

$$\begin{aligned} V^i + V^s = & \frac{m^{\frac{1}{2}}}{k^2} e^{-\frac{1}{2}i\pi} (\pi r r_0 \sin\theta)^{-\frac{1}{2}} \frac{\exp\{ik[(r^2 - a^2)^{\frac{1}{2}} + (r_0^2 - a^2)^{\frac{1}{2}}]\}}{(r^2 - a^2)^{\frac{1}{2}}(r_0^2 - a^2)^{\frac{1}{2}}} \\ & \times \sum_{n=1}^{\infty} \frac{\exp\{i[\bar{v}_n(2\pi - \theta) - \frac{1}{2}i\pi]\} + \exp\{i[\bar{v}_n\theta + \frac{1}{2}i\pi]\}}{1 + \exp(2i\bar{v}_n\pi)} \\ & \times \frac{\exp[-i\bar{v}_n\{\cos^{-1}(a/r) + \cos^{-1}(a/r_0)\}]}{\beta_n [Ai(-\beta_n)]^2} [1 + O(m^{-2})], \end{aligned} \quad (10.73)$$

where

$$\bar{v}_n = ka + e^{\frac{1}{2}i\pi} m\beta_n - \frac{e^{-\frac{1}{2}i\pi}}{60m\beta_n} (\beta_n^3 + 21) + \frac{1}{1400m^3\beta_n^3} (\beta_n^6 + 63\beta_n^3 + \frac{343}{4}) + O(m^{-5}), \quad (10.74)$$

where $n = 1, 2, 3, \dots$ and β_n are the zeros of the derivative of the Airy function, i.e. $Ai'(-\beta_n) = 0$. Eq. (10.73) does not apply on the caustics $r = a$ and $\theta = \pi$.

For a point in the illuminated region the field is (LEVY and KELLER [1959], FRANZ [1954]):

$$\begin{aligned} V^s = & V_{\text{refl.}} - i \frac{m^{\frac{1}{2}}}{k^2} e^{-\frac{1}{2}i\pi} (\pi r r_0 \sin\theta)^{-\frac{1}{2}} \frac{\exp\{ik[(r^2 - a^2)^{\frac{1}{2}} + (r_0^2 - a^2)^{\frac{1}{2}}]\}}{(r^2 - a^2)^{\frac{1}{2}}(r_0^2 - a^2)^{\frac{1}{2}}} \\ & \times \sum_{n=1}^{\infty} \frac{\exp[i\bar{v}_n(2\pi + \theta) - \frac{1}{2}i\pi] + \exp[i\bar{v}_n(2\pi - \theta) + \frac{1}{2}i\pi]}{1 + \exp(2i\bar{v}_n\pi)} \\ & \times \frac{\exp[-i\bar{v}_n\{\cos^{-1}(a/r) + \cos^{-1}(a/r_0)\}]}{\beta_n [Ai(-\beta_n)]^2} [1 + O(m^{-2})]. \end{aligned} \quad (10.75)$$

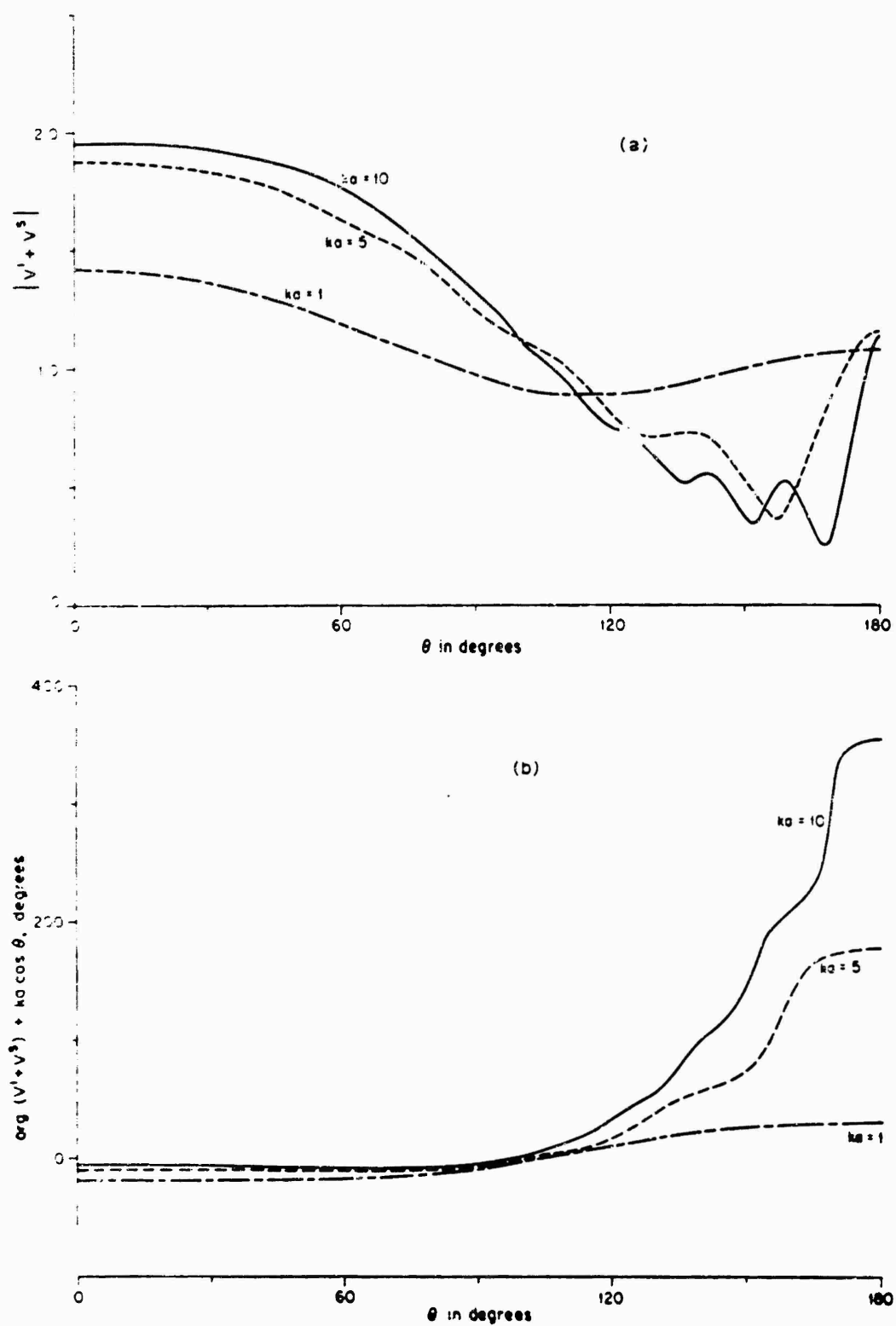
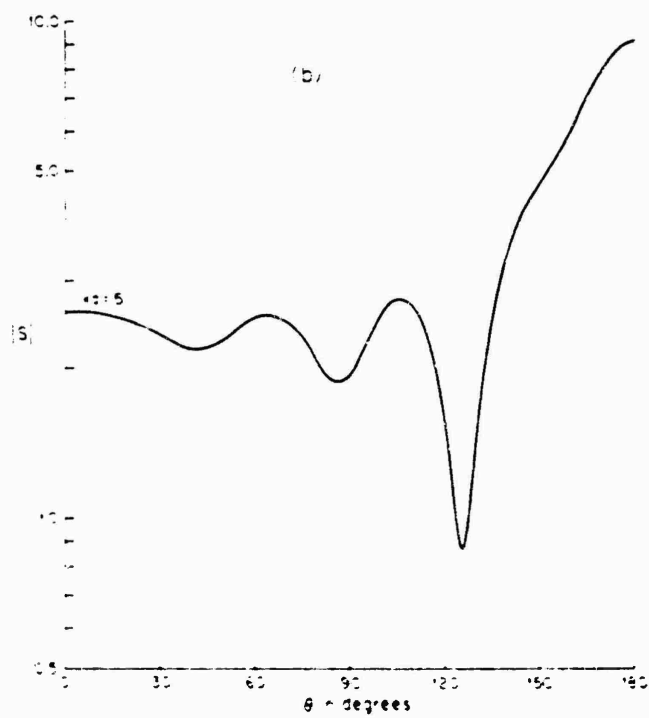
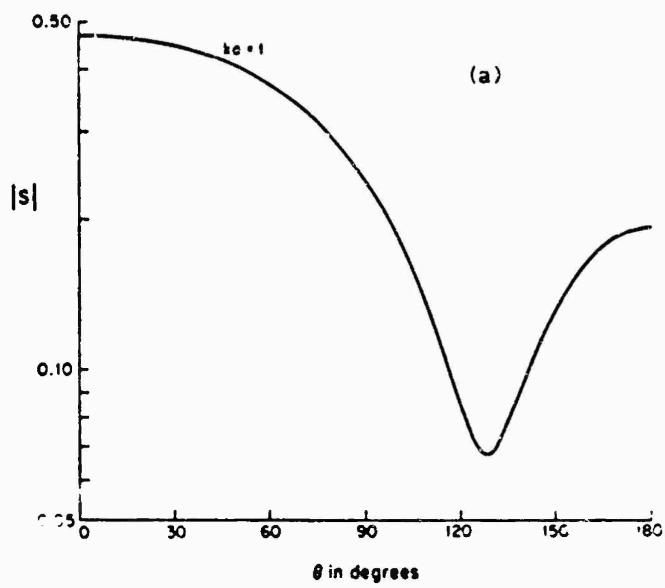


Fig. 10.9. Surface field as a function of θ for selected values of ka for a hard sphere.



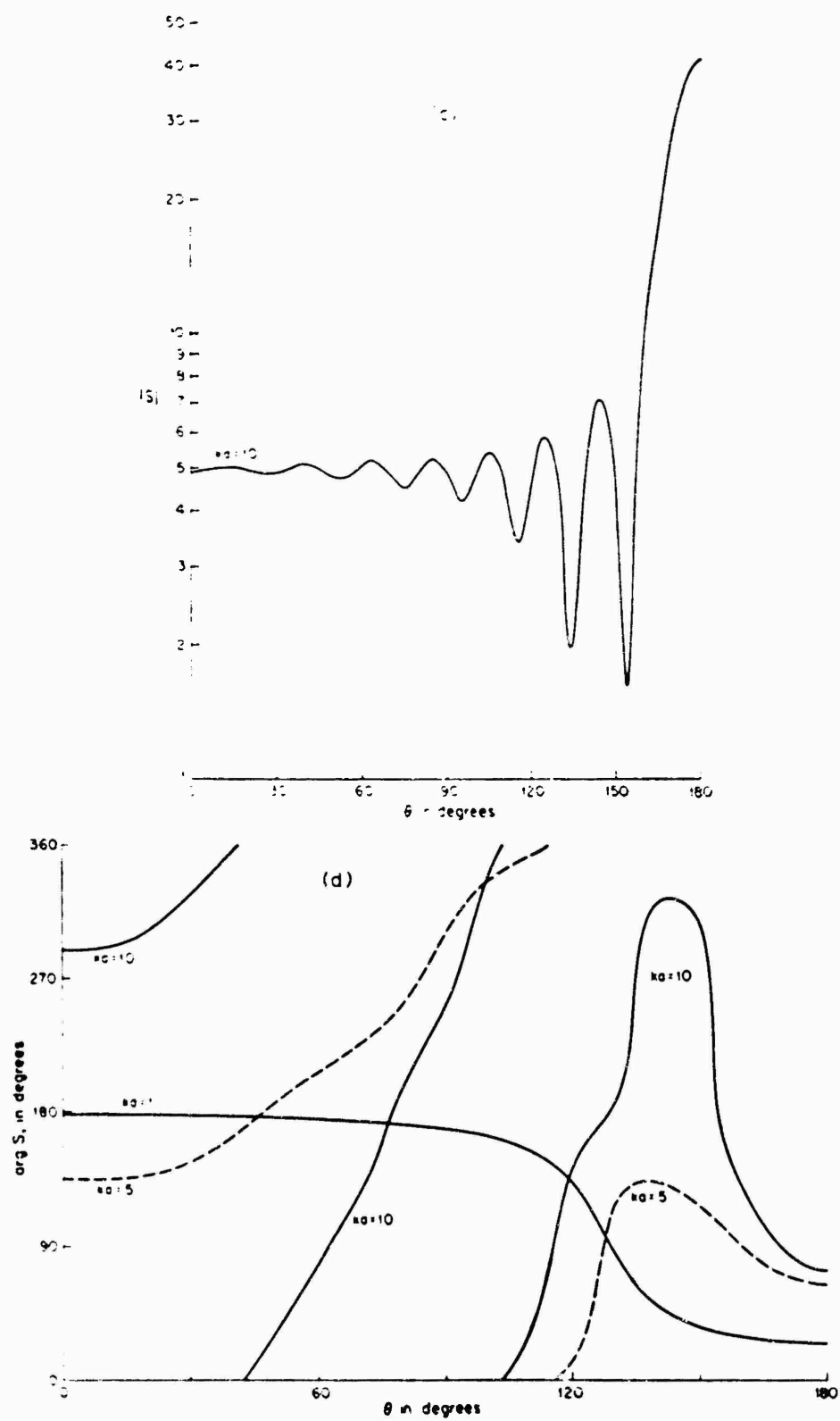


Fig. 10.10. The scattering function S as a function of θ for selected values of ka for a hard sphere

where the summation over n represents the creeping wave contribution and $V_{\text{refl.}}$ is the reflected part of the field formally given by (FRANZ [1954]):

$$V_{\text{refl.}} = -V^i + \frac{1}{2}i \int_D (2\mu+1) Q_\mu^{(2)}(\theta) h_\mu^{(1)}(kr_>) \left[h_\mu^{(2)}(kr_<) - \frac{h_\mu^{(2)'}(ka)}{h_\mu^{(1)'}(ka)} h_\mu^{(1)}(kr_<) \right] d\mu, \quad (10.76)$$

where the contour D and $Q_\mu^{(2)}(\theta)$ are as defined in Section 10.2.1.1. An asymptotic expansion of eq. (10.76) in inverse powers of ka leads to the Luneburg-Kline series whose first term represents the reflected wave according to geometrical optics. The creeping wave contribution given in eq. (10.75) is not valid on the caustics $r = a$ and $\theta = 0$.

10.3.2. Plane wave incidence

10.3.2.1. EXACT SOLUTIONS

For a plane wave incident in the direction θ_0, ϕ_0 , such that

$$V^i = \exp \{ikr[\cos \theta_0 \cos \theta + \sin \theta_0 \sin \theta \cos(\phi - \phi_0)]\}, \quad (10.77)$$

the total field is

$$V^i + V^s = \sum_{n=0}^{\infty} i^n (2n+1) [j_n(kr) - a'_n h_n^{(1)}(kr)] \left\{ P_n(\cos \theta_0) P_n(\cos \theta) + 2 \sum_{l=1}^n \frac{(n-l)!}{(n+l)!} P_n^l(\cos \theta_0) P_n^l(\cos \theta) \cos[l(\phi - \phi_0)] \right\}. \quad (10.78)$$

In particular for a plane wave incident in the direction of the negative z -axis the total field is

$$V^i + V^s = \sum_{n=0}^{\infty} (-i)^n (2n+1) [j_n(kr) - a'_n h_n^{(1)}(kr)] P_n(\cos \theta). \quad (10.79)$$

On the surface $r = a$:

$$V^i + V^s = \frac{i}{(ka)^2} \sum_{n=0}^{\infty} (-i)^n (2n+1) \frac{P_n(\cos \theta)}{h_n^{(1)}(ka)}. \quad (10.80)$$

Computed values of the surface field as a function of θ are shown in Fig. 10.9 for selected values of ka .

In the far field ($r \rightarrow \infty$):

$$S = i \sum_{n=0}^{\infty} (-1)^n (2n+1) a'_n P_n(\cos \theta). \quad (10.81)$$

Computed values of S as a function of θ are shown in Fig. 10.10 for selected values of ka .

The back scattering cross section is

$$\sigma = \frac{4\pi}{k^2} \left| \sum_{n=0}^{\infty} (-1)^n (2n+1) a'_n \right|^2. \quad (10.82)$$

The normalized back scattering cross section $\sigma/(\pi a^2)$ is shown as a function of ka in Fig. 10.11.

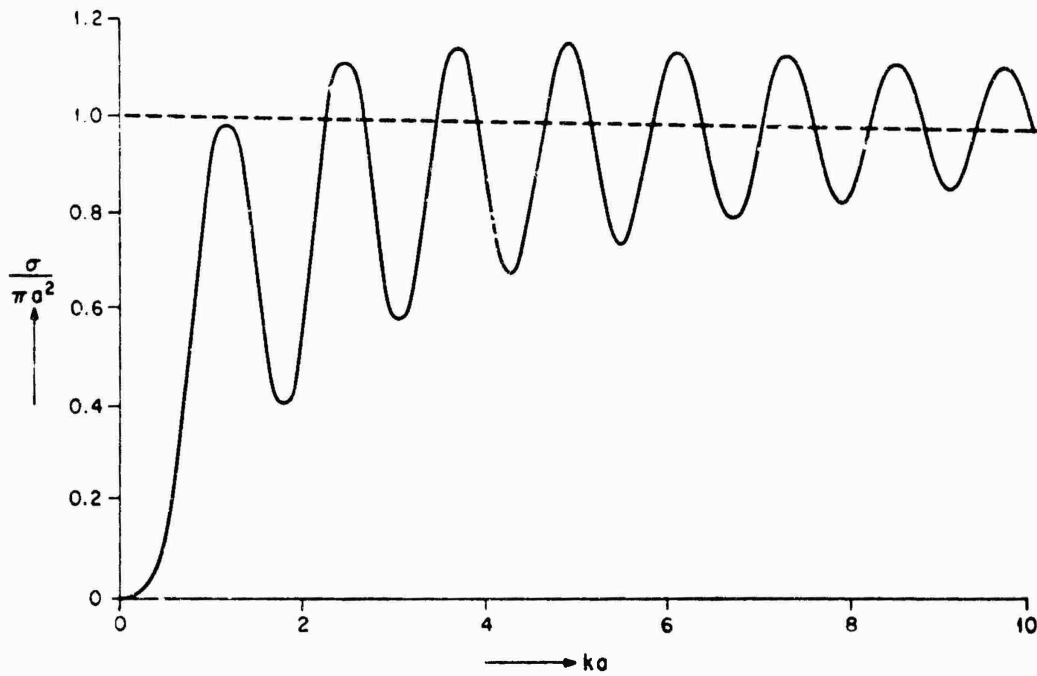


Fig. 10.11. Normalized back scattering cross section $\sigma/(\pi a^2)$ as a function of ka for a hard sphere (SENIOR [1965]).

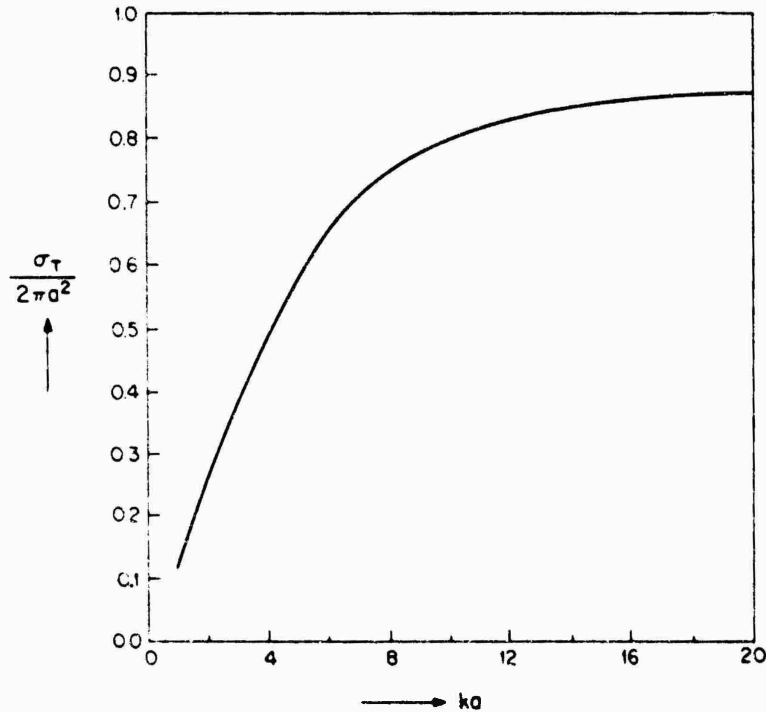


Fig. 10.12. Normalized total scattering cross section $\sigma_T/(2\pi a^2)$ as a function of ka for a hard sphere (KING and WU [1959]).

The total scattering cross section is

$$\sigma_T = \frac{4\pi}{k^2} \sum_{n=0}^{\infty} (2n+1) |a'_n|^2. \quad (10.83)$$

Fig. 10.12 shows the normalized total scattering cross section $\sigma_T/(2\pi a^2)$ as a function of ka .

10.3.2.2. LOW FREQUENCY APPROXIMATIONS

For a plane wave incident in the direction of the negative z -axis such that

$$V^i = e^{-ikz}, \quad (10.84)$$

low frequency expansions may be obtained either directly or by power series developments of the Bessel functions appearing in the exact solutions (RAYLEIGH [1872]). The first three coefficients appearing in eq. (10.81) are

$$a'_0 = \frac{1}{3}i(ka)^3 \left\{ 1 - \frac{3}{5}(ka)^2 - \frac{1}{3}i(ka)^3 + \frac{3}{7}(ka)^4 + O[(ka)^5] \right\}, \quad (10.85)$$

$$a'_1 = -\frac{1}{6}i(ka)^3 \left\{ 1 - \frac{3}{10}(ka)^2 + \frac{1}{6}i(ka)^3 + \frac{3}{8}(ka)^4 + O[(ka)^5] \right\}, \quad (10.86)$$

$$a'_2 = -\frac{1}{135}i(ka)^5 \left\{ 2 - \frac{25}{63}(ka)^2 + O[(ka)^3] \right\}, \quad (10.87)$$

where $ka \ll 1$.

The scattering function in the direction $\theta = 0$ is

$$S(0) = -\frac{5}{6}(ka)^3 \left\{ 1 - \frac{229}{450}(ka)^2 - \frac{1}{30}i(ka)^3 + O[(ka)^4] \right\}. \quad (10.88)$$

Similarly, in the forward direction $\theta = \pi$:

$$S(\pi) = \frac{1}{6}(ka)^3 \left\{ 1 + \frac{67}{90}(ka)^2 + \frac{7}{6}i(ka)^3 + O[(ka)^4] \right\}. \quad (10.89)$$

The back scattering cross section is

$$\sigma = \frac{25}{9}\pi a^2 (ka)^4 \left\{ 1 - \frac{229}{225}(ka)^2 + O[(ka)^4] \right\}. \quad (10.90)$$

The total scattering cross section is

$$\sigma_T \sim \frac{7}{9}\pi a^2 (ka)^4. \quad (10.91)$$

10.3.2.3. HIGH FREQUENCY APPROXIMATIONS

For a plane wave incident in the direction of the negative z -axis such that

$$V^i = e^{-ikz}, \quad (10.92)$$

the high frequency behavior of the field can be completely determined in both near and far zones by applying a modified Watson transformation based upon Poisson's summation formula to the exact expressions.

For points within the deep shadow region, not too close to the surface of the sphere (LEVY and KELLER [1959]),

$$V^i + V^s \sim \frac{e^{-\frac{1}{2}i\pi}}{(2\pi)^{\frac{1}{2}}} m \left(\frac{a^2}{r^2 - a^2} \right)^{\frac{1}{2}} \frac{\exp [ik(r^2 - a^2)^{\frac{1}{2}}]}{(kr \sin \theta)^{\frac{1}{2}}} \\ \times \sum_{l=0}^{\infty} (-1)^l \sum_{n=1}^{\infty} \frac{\exp(i\bar{v}_n \gamma_l + \frac{1}{2}i\pi) + \exp(i\bar{v}_n \delta_l - \frac{1}{2}i\pi)}{\beta_n [\text{Ai}(-\beta_n)]^2}, \quad (10.93)$$

where

$$\begin{aligned} \gamma_l &= 2l\pi - \theta_s + \theta \\ \delta_l &= (l+1)2\pi - (\theta_s + \theta) \\ \pi - \theta_s &= \sin^{-1}(a/r). \end{aligned} \quad (10.94)$$

Eq. (10.93) is valid under the following conditions:

$$\begin{aligned} \frac{1}{2}\pi &\leq \theta_s < \theta < \pi \\ (r-a) &\gg am^{-1} \\ (kr - |\bar{v}_n|) &\gg |\bar{v}_n|^{\frac{1}{2}} \\ (\pi - \theta) &\gg (ka)^{-1} \end{aligned} \quad (10.95)$$

with \bar{v}_n and β_n as defined in Section 10.3.1.3.

The physical interpretation of eq. (10.93) is that the incident rays at their points of tangency to the sphere launch a series of surface waves emanating from these points. These waves travel along the surface with phase velocity slightly smaller than that in free space. As they travel along the surface, they shed radiation along tangential directions. The angular damping factor due to the radiation, for the dominant surface wave ($l = 0$) is

$$\begin{aligned} |\exp(i\bar{v}_n \gamma_0)| &\sim \exp[-\frac{1}{2}\sqrt{3}\beta_n m(\theta_s - \theta)], \\ |\exp(i\bar{v}_n \delta_0)| &\sim \exp[-\frac{1}{2}\sqrt{3}\beta_n m\{2\pi - (\theta_s - \theta)\}]. \end{aligned} \quad (10.96)$$

If $0 \leq (\pi - \theta) \leq (ka)^{-1}$ (LEVY and KELLER [1959]):

$$V^i + V^s \sim e^{-\frac{1}{2}i\pi} m \left(\frac{a^2}{r^2 - a^2} \right)^{\frac{1}{2}} (a/r)^{\frac{1}{2}} \exp [ik(r^2 - a^2)^{\frac{1}{2}}] \\ \times \sum_{l=0}^{\infty} (-1)^l \sum_{n=1}^{\infty} \frac{\exp[i\bar{v}_n\{(2l+1)\pi - \theta_0\}]}{\beta_n [\text{Ai}(-\beta_n)]^2} J_0[\bar{v}_n(\pi - \theta)]. \quad (10.97)$$

In the lit region sufficiently far from the shadow boundary, the reflected portion of the scattered field in the region $0 \leq \theta < \theta_s - m^{-1}$ is (KELLER et al. [1956]):

$$V_{\text{refl}}^s = \left[\frac{a^2 \sin^2 \zeta}{4s(s \sin^2 \zeta + a \cos^3 \zeta)} \right]^{\frac{1}{2}} \exp [ik(s - \frac{1}{2}a \sin \zeta)] \left\{ 1 - \frac{i}{2ka} \left[\frac{1 + 2 \sin^2 \zeta}{\sin^3 \zeta} - \right. \right. \\ \left. \left. - \frac{1}{2^4 \sin^2 \zeta \cos^2 \zeta} (a/s) - \frac{3}{2^5} \left(\frac{2}{\sin \zeta} - 5 \sin \zeta \right) (a/s)^2 - \frac{15}{2^6} (\sin^2 \zeta - 1)(a/s)^3 - \right. \right. \\ \left. \left. - \frac{1}{2^4 (s \sin^2 \zeta + a \cos^3 \zeta)} \frac{a}{\sin \zeta \cos \zeta} \right] + O[(ka)^{-2}] \right\}, \quad (10.98)$$

where

$$\begin{aligned} s &= r \cos \bar{w} - \frac{1}{2} a \sin \zeta \\ \zeta &= \frac{1}{2}(\pi - \theta - \bar{w}) \\ \sin \bar{w} &= \frac{a}{r} \cos \frac{1}{2}(\pi - \theta - \bar{w}). \end{aligned} \quad (10.99)$$

Eq. (10.98) is the Luneburg-Kline asymptotic expansion in inverse powers of ka ; its first term represents the reflected wave according to geometrical optics and the remainder represents the correction to geometrical optics. The physical interpretation of the geometrically reflected field term is shown in Fig. 10.7.

The creeping wave contribution to the scattered field at a point in the lit region, sufficiently far from the shadow boundary, such that $m^{-1} \lesssim \theta \lesssim \theta_s - m^{-1}$, is (LEVY and KELLER [1959]):

$$\begin{aligned} U_{cr.w.}^s &\sim \frac{e^{-i\pi}}{(2\pi)^{\frac{1}{2}}} m \left(\frac{a^2}{r^2 - a^2} \right)^{\frac{1}{2}} \exp [ik(r^2 - a^2)^{\frac{1}{2}}] \left\{ e^{-i\pi} \sum_{n=1}^{\infty} \frac{\exp(i\bar{v}_n \delta_0)}{\beta_n [\text{Ai}(-\beta_n)]^2} + \right. \\ &\quad \left. + \sum_{l=1}^{\infty} (-1)^l \sum_{n=1}^{\infty} \frac{\exp(i\bar{v}_n \gamma_l + \frac{1}{4}i\pi) + \exp(i\bar{v}_n \delta_l - \frac{1}{4}i\pi)}{\beta_n [\text{Ai}(-\beta_n)]^2} \right\}. \end{aligned} \quad (10.100)$$

In the range $0 \leq \theta \leq (ka)^{-1}$ (LEVY and KELLER [1959]):

$$\begin{aligned} U_{cr.w.}^s &\sim e^{-i\pi} m(a/r)^{\frac{1}{2}} \left(\frac{a^2}{r^2 - a^2} \right)^{\frac{1}{2}} \exp [ik(r^2 - a^2)^{\frac{1}{2}}] \\ &\quad \times \sum_{l=0}^{\infty} (-1)^l \sum_{n=1}^{\infty} \frac{\exp [i\bar{v}_n \{(2l+2)\pi - \theta_0\}]}{\beta_n [\text{Ai}(-\beta_n)]^2} J_0(\bar{v}_n \theta). \end{aligned} \quad (10.101)$$

In the far zone ($r \rightarrow \infty$):

$$S = S_{\text{refl.}} + S_{\text{cr.w.}}, \quad (10.102)$$

where $S_{\text{refl.}}$ is the contribution due to the reflected field and $S_{\text{cr.w.}}$ is that due to creeping waves.

For $0 \leq \theta \lesssim \pi - m^{-1}$,

$$S_{\text{refl.}} \sim \frac{1}{2} ka \exp(-2ika \cos \frac{1}{2}\theta) \left\{ 1 - \frac{i}{2ka} \frac{1+2\cos^2 \frac{1}{2}\theta}{\cos^3 \frac{1}{2}\theta} + \dots \right\}, \quad (10.103)$$

$$S_{\text{cr.w.}} \sim -e^{i\pi} mka \left(\frac{\theta}{\sin \theta} \right)^{\frac{1}{2}} \sum_{l=0}^{\infty} (-1)^l \sum_{n=1}^{\infty} \frac{\exp [i(2l+1)\pi \bar{v}_n]}{\beta_n [\text{Ai}(-\beta_n)]^2} J_0(\bar{v}_n \theta). \quad (10.104)$$

More refined expressions for $S_{\text{refl.}}$ and $S_{\text{cr.w.}}$ in the direction $\theta=0$ are (SENIOR [1965]):

$$S_{\text{refl.}} = \frac{1}{2} ka e^{-2ika} \left\{ 1 - \frac{3i}{2ka} - \frac{5}{2(ka)^2} + \frac{25i}{4(ka)^3} + \frac{22}{(ka)^4} + O[(ka)^{-5}] \right\}, \quad (10.105)$$

$$\begin{aligned}
S_{\text{cr.w.}} = & -e^{i\pi} mka \sum_{l=0}^{\infty} (-1)^l \sum_{n=1}^{\infty} \left\{ 1 + \frac{e^{i\pi}}{60m^2\beta_n^2} (32\beta_n^3 - 21) - \right. \\
& - \frac{e^{-i\pi}}{m^4\beta_n^4} \left(\frac{4}{175}\beta_n^6 + \frac{147}{800} \right) + O(m^{-6}) \left. \right\} \frac{1}{\beta_n [\text{Ai}(-\beta_n)]^2} \\
& \times \exp \left[i(2l+1)\pi \left\{ ka + e^{i\pi} m\beta_n - \frac{e^{-i\pi}}{60m\beta_n} (\beta_n^3 + 21) + \right. \right. \\
& \left. \left. + \frac{1}{1400m^3\beta_n^3} (\beta_n^6 + 63\beta_n^3 + \frac{343}{4}) + O(m^{-5}) \right\} \right]. \quad (10.106)
\end{aligned}$$

The first three terms in eq. (10.105) were previously derived by KELLER et al. [1956] using the Luneburg-Kline expansion technique. The leading term in eq. (10.105) is the contribution due to geometrical optics. The 5-term expression for $S_{\text{refl.}}$ shown in eq. (10.105) is accurate for values of ka of order 10 or greater, and continues to be fairly accurate down to $ka \approx 5$. For $ka < 3$ a 3-term expression obtained by omitting the terms $(ka)^{-3}$ and $(ka)^{-4}$ in eq. (10.105) should be used.

An accurate approximation to eq. (10.106) based on a single creeping wave alone is (SENIOR [1965]):

$$\begin{aligned}
S_{\text{cr.w.}} = & -mka e^{i\pi} \left\{ 1 + \frac{e^{i\pi}}{60m^2\beta_1^2} (32\beta_1^3 - 21) + O(m^{-4}) \right\} \frac{1}{\beta_1 [\text{Ai}(-\beta_1)]^2} \\
& \times \exp \left\{ i\pi ka - e^{-i\pi} \pi m\beta_1 - e^{i\pi} \frac{\pi}{60m\beta_1} (\beta_1^3 + 21) + \right. \\
& \left. + \frac{i\pi}{1400m^3\beta_1^3} (\beta_1^6 + 63\beta_1^3 + \frac{343}{4}) + O(m^{-5}) \right\}, \quad (10.107)
\end{aligned}$$

where

$$\beta_1 = 1.01879297 \dots,$$

$$\text{Ai}(-\beta_1) = 0.53565666 \dots$$

In the forward direction $\theta = \pi$ the scattering function is (BECKMANN and FRANZ [1957]):

$$\begin{aligned}
S(\pi) \sim & i \left[\frac{1}{2}(ka)^2 + \frac{1}{24} + 2 \int_{ka}^{\infty} \frac{\Psi J_0(ka)}{\Psi H_0^{(1)}(ka)} v dv - \right. \\
& \left. - \int_{ka}^{ka + \pi e^{i\pi}} \frac{\Psi H_0^{(2)}(ka)}{\Psi H_0^{(1)}(ka)} v dv - 2\pi k \sum_n C_n \frac{e^{2i\pi v_n}}{1 + e^{2i\pi v_n}} \right], \quad (10.108)
\end{aligned}$$

where

$$\Psi \equiv \frac{\hat{c}}{\hat{c}(ka)} - \frac{1}{2ka}.$$

$$C_n = -\frac{m^4}{\pi} e^{-i\pi} \left\{ 1 + \frac{e^{i\pi}}{60m^2\beta_n^2} (32\beta_n^3 - 21) - \frac{e^{-i\pi}}{m^4\beta_n^4} \left(\frac{4}{175}\beta_n^6 + \frac{1}{8000} \right) + O(m^{-6}) \right\} \frac{1}{\beta_n [\text{Ai}(-\beta_n)]^2}. \quad (10.109)$$

The total scattering cross section is (BECKMANN and FRANZ [1957], WU [1955]):

$$\frac{\sigma_T}{2\pi a^2} = 1 - 0.8642(ka)^{-\frac{2}{3}} - 1.0052(ka)^{-4/3} + O[(ka)^{-2}]. \quad (10.110)$$

10.4. Perfectly conducting sphere

10.4.1. Electric dipole sources

10.4.1.1. EXACT SOLUTIONS

For an arbitrarily oriented electric dipole located at $\mathbf{r}_0 = (r_0, \theta_0, \phi_0)$ with moment $(4\pi\epsilon/k)\hat{\mathbf{e}}$, the total electric field is

$$\mathbf{E}^i(\mathbf{r}) + \mathbf{E}^s(\mathbf{r}) = 4\pi k \mathcal{G}_e(\mathbf{r}|\mathbf{r}_0) \cdot \hat{\mathbf{e}}, \quad (10.111)$$

where $\hat{\mathbf{e}}$ is an arbitrary unit vector and $\mathcal{G}_e(\mathbf{r}|\mathbf{r}_0)$ is the electric dyadic Green's function for the sphere (TAI [1959]):

$$\begin{aligned} \mathcal{G}_e(\mathbf{r}|\mathbf{r}_0) = & \frac{ik}{4\pi} \sum_{n=1}^{\infty} \sum_{m=0}^n \epsilon_m \frac{2n+1}{n(n+1)} \frac{(n-m)!}{(n+m)!} \{ \mathbf{M}_{emn}^{(3)}(\mathbf{r}) [\mathbf{M}_{emn}^{(1)}(\mathbf{r}_0) - a_n \mathbf{M}_{emn}^{(3)}(\mathbf{r}_0)] + \\ & + \mathbf{M}_{omn}^{(3)}(\mathbf{r}) [\mathbf{M}_{omn}^{(1)}(\mathbf{r}_0) - a_n \mathbf{M}_{omn}^{(3)}(\mathbf{r}_0)] + \mathbf{N}_{emn}^{(3)}(\mathbf{r}) [\mathbf{N}_{emn}^{(1)}(\mathbf{r}_0) - b_n \mathbf{N}_{emn}^{(3)}(\mathbf{r}_0)] + \\ & + \mathbf{N}_{omn}^{(3)}(\mathbf{r}) [\mathbf{N}_{omn}^{(1)}(\mathbf{r}_0) - b_n \mathbf{N}_{omn}^{(3)}(\mathbf{r}_0)] \}, \quad \text{for } r > r_0, \end{aligned} \quad (10.112)$$

$$\begin{aligned} \mathcal{G}_e(\mathbf{r}|\mathbf{r}_0) = & \frac{ik}{4\pi} \sum_{n=1}^{\infty} \sum_{m=0}^n \epsilon_m \frac{2n+1}{n(n+1)} \frac{(n-m)!}{(n+m)!} \{ [\mathbf{M}_{emn}^{(1)}(\mathbf{r}) - a_n \mathbf{M}_{emn}^{(3)}(\mathbf{r})] \mathbf{M}_{emn}^{(3)}(\mathbf{r}_0) + \\ & + [\mathbf{M}_{omn}^{(1)}(\mathbf{r}) - a_n \mathbf{M}_{omn}^{(3)}(\mathbf{r})] \mathbf{M}_{omn}^{(3)}(\mathbf{r}_0) + [\mathbf{N}_{emn}^{(1)}(\mathbf{r}) - b_n \mathbf{N}_{emn}^{(3)}(\mathbf{r})] \mathbf{N}_{emn}^{(3)}(\mathbf{r}_0) + \\ & + [\mathbf{N}_{omn}^{(1)}(\mathbf{r}) - b_n \mathbf{N}_{omn}^{(3)}(\mathbf{r})] \mathbf{N}_{omn}^{(3)}(\mathbf{r}_0) \}, \quad \text{for } r < r_0, \end{aligned} \quad (10.113)$$

where the vector wave functions are (STRATTON [1941]):

$$\mathbf{M}_{\epsilon mn}^{(j)}(\mathbf{r}) = \mp \frac{m}{\sin \theta} Z_n^{(j)}(kr) P_n^m(\cos \theta) \frac{\sin m\phi}{\cos \theta} \hat{\boldsymbol{\theta}} - Z_n^{(j)}(kr) \frac{\partial P_n^m}{\partial \theta} \frac{\cos m\phi}{\sin \theta} \hat{\boldsymbol{\phi}}, \quad (10.114)$$

$$\begin{aligned} \mathbf{N}_{\epsilon mn}^{(j)}(\mathbf{r}) = & \frac{n(n+1)}{kr} Z_n^{(j)}(kr) P_n^m(\cos \theta) \frac{\cos m\phi}{\sin \theta} \hat{\mathbf{r}} + \\ & + \frac{1}{kr} \frac{\partial}{\partial r} [r Z_n^{(j)}(kr)] \frac{\partial}{\partial \theta} P_n^m(\cos \theta) \frac{\cos m\phi}{\sin \theta} \hat{\boldsymbol{\theta}} \mp \\ & \mp \frac{m}{kr \sin \theta} \frac{\partial}{\partial r} [r Z_n^{(j)}(kr)] P_n^m(\cos \theta) \frac{\sin m\phi}{\cos \theta} \hat{\boldsymbol{\phi}}, \end{aligned} \quad (10.115)$$

$j = 1$ or 3 , and $Z_n^{(1)}(x) = j_n(x)$, $Z_n^{(3)}(x) = h_n^{(1)}(x)$.

In the particular case of a z -directed electric dipole at $\mathbf{r}_0 = (r_0, 0, 0)$ with moment $(4\pi\epsilon/k)\mathbf{z}$, the incident fields are

$$\begin{aligned} E_r^i &= \frac{e^{ikR}}{kR} \left[\frac{(r \cos \theta - r_0)(r - r_0 \cos \theta)}{R} \left(\frac{3}{R^3} - \frac{3ik}{R^3} - \frac{k^2}{R} \right) + \right. \\ &\quad \left. + \left(\frac{ik}{R} - \frac{1}{R^2} \right) \cos \theta + k^2 \cos \theta \right], \\ E_\theta^i &= \frac{e^{ikR}}{kR} \left[\frac{(r \cos \theta - r_0)r_0}{R} \left(\frac{3}{R^3} - \frac{3ik}{R^2} - \frac{k^2}{R} \right) - \frac{ik}{R} + \frac{1}{R^2} - k^2 \right] \sin \theta, \\ H_\phi^i &= -ikY \frac{e^{ikR}}{kR} \left[\left(\frac{1}{R^2} - \frac{ik}{R} \right) (r - r_0 \cos \theta) + r_0 \left(\frac{ik}{R} - \frac{1}{R^2} \right) \cos \theta \right] \sin \theta, \\ E_\phi^i &= H_r^i = H_\theta^i = 0. \end{aligned} \quad (10.116)$$

The total fields are (BELKINA and WEINSTEIN [1957], JONES [1964]):

$$\begin{aligned} E^i + E^s &= ik^2 \sum_{n=1}^{\infty} (2n+1) [\psi_n(kr_0) - b_n \zeta_n^{(1)}(kr_0)] \\ &\quad \times \left\{ \frac{n(n+1)}{(kr)^2} \zeta_n^{(1)}(kr) P_n(\cos \theta) \hat{\rho} + \frac{1}{kr} \zeta_n^{(1)'}(kr) \frac{\partial P_n(\cos \theta)}{\partial \theta} \hat{\theta} \right\}, \quad \text{for } r > r_0. \end{aligned} \quad (10.117)$$

$$\begin{aligned} H^i + H^s &= -k^2 Y \sum_{n=1}^{\infty} (2n+1) \frac{1}{(kr_0)^2} [\psi_n(kr_0) - b_n \zeta_n^{(1)}(kr_0)] \\ &\quad \times \frac{\zeta_n^{(1)}(kr)}{kr} \frac{\partial P_n(\cos \theta)}{\partial \theta} \hat{\phi}, \quad \text{for } r > r_0, \end{aligned} \quad (10.118)$$

$$\begin{aligned} E^i + E^s &= ik^2 \sum_{n=1}^{\infty} (2n+1) \frac{\zeta_n^{(1)}(kr_0)}{(kr_0)^2} \left[\frac{n(n+1)}{(kr)^2} \{\psi_n(kr) - b_n \zeta_n^{(1)}(kr)\} P_n(\cos \theta) \hat{\rho} + \right. \\ &\quad \left. + \frac{1}{kr} \{\psi_n'(kr) - b_n \zeta_n^{(1)'}(kr)\} \frac{\partial P_n(\cos \theta)}{\partial \theta} \hat{\theta} \right], \quad \text{for } a \leq r < r_0, \end{aligned} \quad (10.119)$$

$$\begin{aligned} H^i + H^s &= -k^2 Y \sum_{n=1}^{\infty} (2n+1) \frac{\zeta_n^{(1)}(kr_0)}{(kr_0)^2} \frac{1}{kr} [\psi_n(kr) - b_n \zeta_n^{(1)}(kr)] \frac{\partial P_n(\cos \theta)}{\partial \theta} \hat{\phi}, \\ &\quad \text{for } a \leq r < r_0. \end{aligned} \quad (10.120)$$

For a dipole on the surface ($r_0 = a$) the magnetic field on the surface is

$$H^i + H^s = -ik^2 Y \sum_{n=1}^{\infty} (2n+1) \frac{\zeta_n^{(1)}(ka)}{(ka)^3} \frac{\partial P_n(\cos \theta)}{\partial \theta} \frac{1}{\zeta_n^{(1)}(ka)} \hat{\phi} \quad (10.121)$$

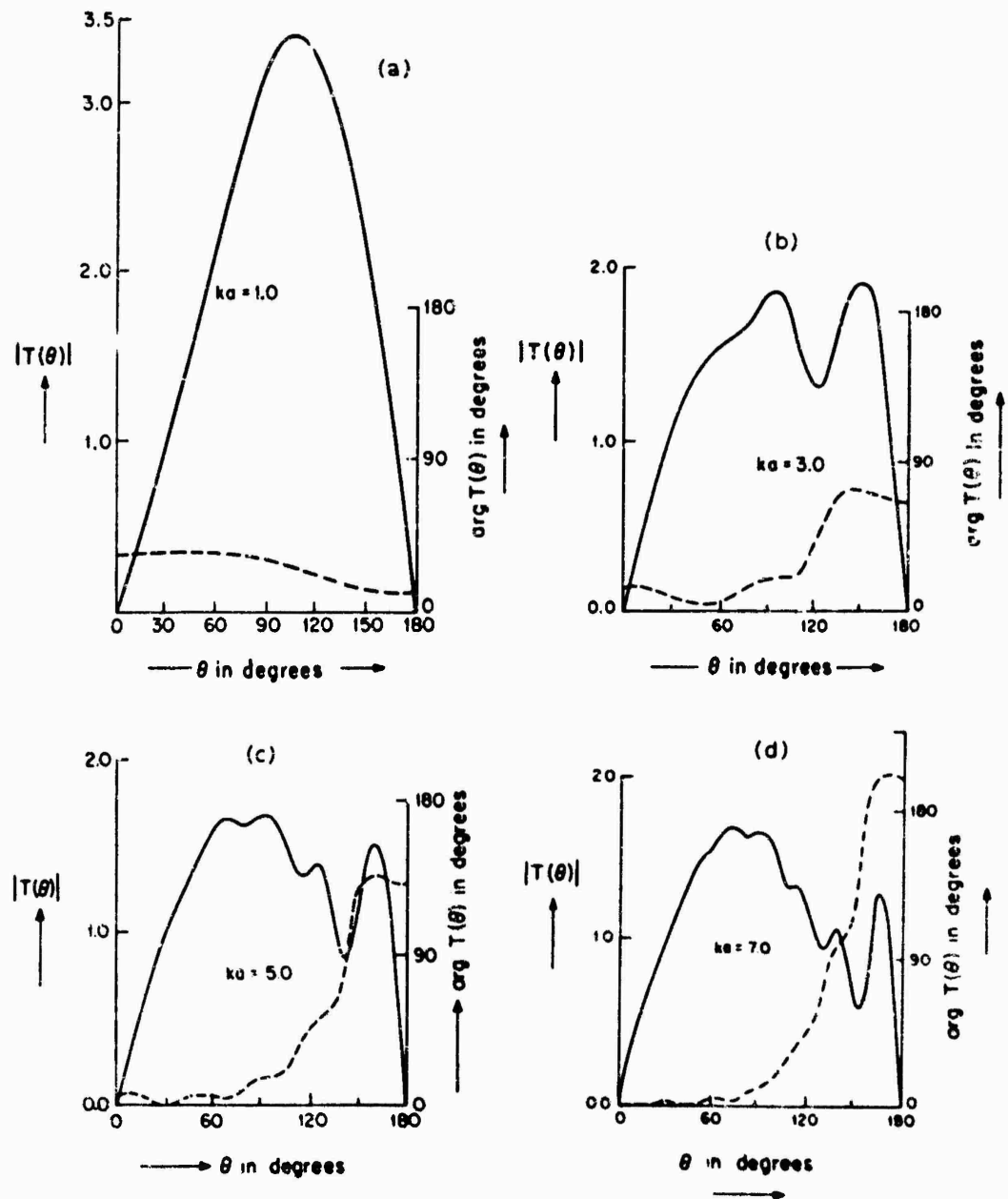
and the far field is (BELKINA and WEINSTEIN [1957], SOMMERFELD [1949]):

$$E_\theta = \frac{H_\phi}{Y} = -k^2 \frac{e^{ikR}}{kR} T(\theta), \quad (10.122)$$

where the pattern function $T(\theta)$ is

$$T(\theta) = \exp(ika \cos \theta) \frac{1}{(ka)^2} \sum_{n=1}^{\infty} (-i)^n (2n+1) \frac{1}{\zeta_n^{(1)'}(ka)} \frac{\partial P_n(\cos \theta)}{\partial \theta}. \quad (10.123)$$

$T(\theta)$ is shown as a function of θ for various values of ka in Fig. 10.13. The function $T(\theta)$ also gives the radiation pattern produced by an annular symmetric slot on the sphere, provided its radius is small in comparison with the wavelength and the radius of the sphere. Such a "magnetic ring" is equivalent to a radial electric dipole.



For an x -directed electric dipole of moment $(4\pi\epsilon k)\hat{x}$ located at $\mathbf{r}_0 = (r_0, 0, 0)$ the incident field is

$$\begin{aligned} E_r^i &= \frac{e^{ikR}}{kR} \left[\frac{r(r-r_0\cos\theta)}{R} \left(\frac{3}{R^3} - \frac{3ik}{R^2} - \frac{k^2}{R} \right) + \frac{ik}{R} - \frac{1}{R^2} + k^2 \right] \sin\theta \cos\phi, \\ E_\theta^i &= \frac{e^{ikR}}{kR} \left[\frac{rr_0\sin\theta}{R} \left(\frac{3}{R^3} - \frac{3ik}{R^2} - \frac{k^2}{R} \right) \sin\theta + \left(\frac{ik}{R} - \frac{1}{R^2} + k^2 \right) \cos\theta \right] \cos\phi, \\ E_\phi^i &= -\frac{e^{ikR}}{kR} \left[\frac{ik}{R} - \frac{1}{R^2} + k^2 \right] \sin\phi, \\ H_r^i &= ikY \frac{e^{ikR}}{kR} \left[\frac{ik}{R} - \frac{1}{R^2} \right] r_0 \sin\theta \sin\phi, \\ H_\theta^i &= -ikY \frac{e^{ikR}}{kR} \left(\frac{ik}{R} - \frac{1}{R^2} \right) (r \cos\theta - r_0) \sin\phi, \\ H_\phi^i &= -ikY \frac{e^{ikR}}{kR} \left(\frac{ik}{R} - \frac{1}{R^2} \right) (r \cos\theta - r_0) \cos\phi. \end{aligned} \quad (10.124)$$

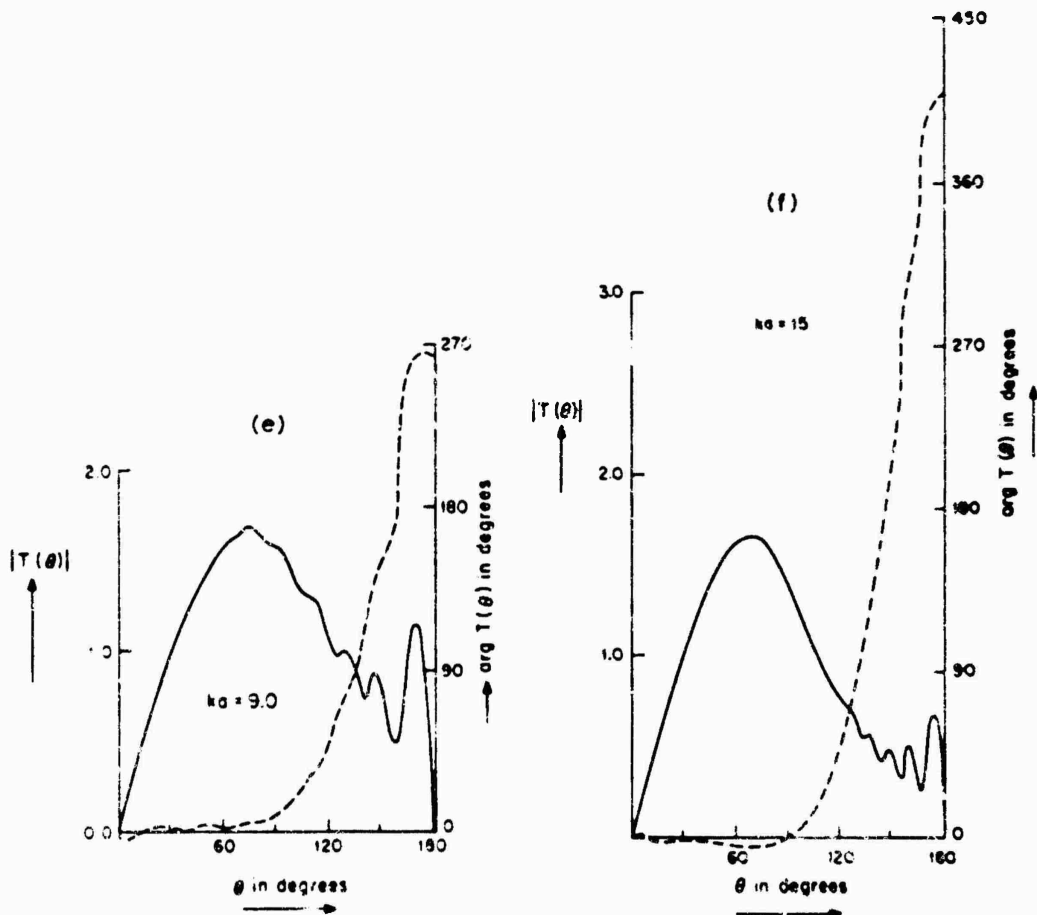


Fig. 10.13. Amplitude (—) and phase (---) of the far field component E_θ as functions of θ produced by a radial electric dipole located on the surface of a conducting sphere for different values of ka (BELKIN and WEINSTEIN [1957]).

and the total field is

$$E^i + E^s = ik^2 \sum_{n=1}^{\infty} \frac{2n+1}{n(n+1)} \frac{1}{kr_0} [\{\psi_n(kr_0) - a_n \zeta_n^{(1)}(kr_0)\} M_{01n}^{(3)}(r) + \{\psi'_n(kr_0) - b_n \zeta_n^{(1)'}(kr_0)\} N_{01n}^{(3)}(r)], \quad \text{for } r > r_0, \quad (10.125)$$

$$H^i + H^s = k^2 Y \sum_{n=1}^{\infty} \frac{2n+1}{n(n+1)} \frac{1}{kr_0} [\{\psi_n(kr_0) - a_n \zeta_n^{(1)}(kr_0)\} N_{01n}^{(3)}(r) + \{\psi'_n(kr_0) - b_n \zeta_n^{(1)'}(kr_0)\} M_{01n}^{(3)}(r)], \quad \text{for } r > r_0, \quad (10.126)$$

$$E^i + E^s = ik^2 \sum_{n=1}^{\infty} \frac{2n+1}{n(n+1)} \frac{1}{kr_0} [\{M_{01n}^{(1)}(r) - a_n M_{01n}^{(3)}(r)\} \zeta_n^{(1)}(kr_0) + \{N_{01n}^{(1)}(r) - b_n N_{01n}^{(3)}(r)\} \zeta_n^{(1)'}(kr_0)], \quad \text{for } r < r_0, \quad (10.127)$$

$$H^i + H^s = k^2 Y \sum_{n=1}^{\infty} \frac{2n+1}{n(n+1)} \frac{1}{kr_0} [\{N_{01n}^{(1)}(r) - a_n N_{01n}^{(3)}(r)\} \zeta_n^{(1)}(kr_0) + \{M_{01n}^{(1)}(r) - b_n M_{01n}^{(3)}(r)\} \zeta_n^{(1)'}(kr_0)], \quad \text{for } r < r_0. \quad (10.128)$$

In the far zone ($r \rightarrow \infty$) the components of the total field are:

$$E_\theta = ZH_\phi = k^2 \frac{e^{ikr}}{kr} \cos \phi \sum_{n=1}^{\infty} (-i)^n \frac{2n+1}{n(n+1)} \frac{1}{kr_0} \times \left[\{\psi_n(kr_0) - a_n \zeta_n^{(1)}(kr_0)\} \frac{P_n^1(\cos \theta)}{\sin \theta} + i \{\psi'_n(kr_0) - b_n \zeta_n^{(1)'}(kr_0)\} \frac{\partial P_n^1(\cos \theta)}{\partial \theta} \right]. \quad (10.129)$$

$$E_\phi = -ZH_\theta = -k^2 \frac{e^{ikr}}{kr} \sin \phi \sum_{n=1}^{\infty} (-i)^n \frac{2n+1}{n(n+1)} \frac{1}{kr_0} \times \left[\{\psi_n(kr_0) - a_n \zeta_n^{(1)}(kr_0)\} \frac{\partial P_n^1(\cos \theta)}{\partial \theta} + i \{\psi'_n(kr_0) - b_n \zeta_n^{(1)'}(kr_0)\} \frac{P_n^1(\cos \theta)}{\sin \theta} \right]. \quad (10.130)$$

For a y -directed electric dipole of moment $(4\pi\epsilon/k)\hat{y}$ situated at $\mathbf{r}_0 = (r_0, 0, 0)$ the incident field is

$$\begin{aligned} E_r^i &= \frac{e^{ikR}}{kR} \left[\frac{r(r-r_0 \cos \theta)}{R} \left(\frac{3}{R^3} - \frac{3ik}{R^2} - \frac{k^2}{R} \right) + \frac{ik}{R} - \frac{1}{R^2} + k^2 \right] \sin \theta \sin \phi, \\ E_\theta^i &= \frac{e^{ikR}}{kR} \left[\frac{rr_0 \sin \theta}{R} \left(\frac{3}{R^3} - \frac{3ik}{R^2} - \frac{k^2}{R} \right) \sin \theta + \left(\frac{ik}{R} - \frac{1}{R^2} + k^2 \right) \cos \theta \right] \sin \phi, \\ E_\phi^i &= \frac{e^{ikR}}{kR} \left[\frac{ik}{R} - \frac{1}{R^2} + k^2 \right] \cos \phi, \\ H_r^i &= -ikY \frac{e^{ikR}}{kR} \left(\frac{ik}{R} - \frac{1}{R^2} \right) r_0 \sin \theta \cos \phi, \end{aligned} \quad (10.131)$$

$$H_\theta^i = -ikY \frac{e^{ikR}}{kR} \left(\frac{1}{R^2} - \frac{ik}{R} \right) (r - r_0 \cos \theta) \cos \phi,$$

$$H_\phi^i = -ikY \frac{e^{ikR}}{kR} \left(\frac{ik}{R} - \frac{1}{R^2} \right) (r \cos \theta - r_0) \sin \phi,$$

and the total field is

$$E^i + E^s = -ik^2 \sum_{n=1}^{\infty} \frac{2n+1}{n(n+1)} \frac{1}{kr_0} [\{\psi_n(kr_0) - a_n \zeta_n^{(1)}(kr_0)\} M_{e1n}^{(3)}(r) - \{\psi'_n(kr_0) - b_n \zeta_n^{(1)'}(kr_0)\} N_{o1n}^{(3)}(r)], \quad \text{for } r > r_0, \quad (10.132)$$

$$H^i + H^s = k^2 Y \sum_{n=1}^{\infty} \frac{2n+1}{n(n+1)} \frac{1}{kr_0} [\{\psi_n(kr_0) - a_n \zeta_n^{(1)}(kr_0)\} N_{e1n}^{(3)}(r) - \{\psi'_n(kr_0) - b_n \zeta_n^{(1)'}(kr_0)\} M_{o1n}^{(3)}(r)], \quad \text{for } r > r_0, \quad (10.133)$$

$$E^i + E^s = -ik^2 \sum_{n=1}^{\infty} \frac{2n+1}{n(n+1)} \frac{1}{kr_0} [\{M_{e1n}^{(1)}(r) - a_n M_{e1n}^{(3)}(r)\} \zeta_n^{(1)'}(kr_0) - \{N_{o1n}^{(1)}(r) - b_n N_{o1n}^{(3)}(r)\} \zeta_n^{(1)}(kr_0)], \quad \text{for } r < r_0, \quad (10.134)$$

$$H^i + H^s = -k^2 Y \sum_{n=1}^{\infty} \frac{2n+1}{n(n+1)} \frac{1}{kr_0} [\{N_{e1n}^{(1)}(r) - a_n N_{e1n}^{(3)}(r)\} \zeta_n^{(1)'}(kr_0) - \{M_{o1n}^{(1)}(r) - b_n M_{o1n}^{(3)}(r)\} \zeta_n^{(1)}(kr_0)], \quad \text{for } r < r_0. \quad (10.135)$$

and in the far zone ($r \rightarrow \infty$):

$$E_\theta = ZH_\phi = k^2 \frac{e^{ikr}}{kr} \sin \phi \sum_{n=1}^{\infty} \frac{2n+1}{n(n+1)} (-i)^n \frac{1}{kr_0} \times \left[\{\psi_n(kr_0) - a_n \zeta_n^{(1)}(kr_0)\} \frac{P_n^1(\cos \theta)}{\sin \theta} + i \{\psi'_n(kr_0) - b_n \zeta_n^{(1)'}(kr_0)\} \frac{\partial P_n^1(\cos \theta)}{\partial \theta} \right], \quad (10.136)$$

$$E_\phi = -ZH_\theta = k^2 \frac{e^{ikr}}{kr} \cos \phi \sum_{n=1}^{\infty} \frac{2n+1}{n(n+1)} (-i)^n \frac{1}{kr_0} \times \left[\{\psi_n(kr_0) - a_n \zeta_n^{(1)}(kr_0)\} \frac{\partial P_n^1(\cos \theta)}{\partial \theta} + i \{\psi'_n(kr_0) - b_n \zeta_n^{(1)'}(kr_0)\} \frac{P_n^1(\cos \theta)}{\sin \theta} \right]. \quad (10.137)$$

10.4.1.2. LOW FREQUENCY APPROXIMATIONS

For a z -directed dipole situated at $(a, 0, 0)$ on the surface of the sphere (BELKINA and WEINSTEIN [1957]):

$$T(\theta) \sim 3 \sin \theta, \quad \text{as } ka \rightarrow 0. \quad (10.138)$$

Thus, to this approximation, the moment of the electric dipole is increased by a factor 3. No other specific results are available. However, low frequency expansions

may be obtained by using the small argument approximations of the Bessel functions in the exact expressions given in the preceding section.

10.4.1.3. HIGH FREQUENCY APPROXIMATIONS

For the z -directed electric dipole situated on the surface of the sphere, the far field pattern function $T(\theta)$ is (BELKINA and WEINSTEIN [1957]):

$$T(\theta) \sim \frac{e^{ika \cos \theta}}{\sqrt{\sin \theta}} [e^{ika(\theta - \frac{1}{2}\pi)} g(\xi) + ie^{ika(\frac{1}{2}\pi - \theta)} g(\xi_1)], \quad \text{for } \frac{1}{2}\pi < \theta \lesssim \pi - m^{-1}, \quad (10.139)$$

$$T(\theta) \sim 2\sqrt{\pi} m^{\frac{1}{2}} e^{\frac{1}{2}i(ka + \frac{1}{2}\pi)} e^{ika \cos \theta} \left(\frac{\pi - \theta}{\sin \theta}\right)^{\frac{1}{2}} \times J_1[\bar{v}_1(\pi - \theta)] g(\frac{1}{2}m\pi), \quad \text{for } \pi - m^{-1} \lesssim \theta \lesssim \pi, \quad (10.140)$$

where

$$\begin{aligned} \xi &= m(\theta - \tfrac{1}{2}\pi), \\ \xi_1 &= m(\tfrac{1}{2}\pi - \theta), \\ \bar{v}_1 &= ka + me^{i\pi}\beta_1 + O(m^{-1}), \end{aligned} \quad (10.141)$$

with β_1 and the modified Fock function $g(\xi)$ defined in the Introduction. In the range $m^{-1} \lesssim \theta \lesssim \frac{1}{2}\pi - m^{-1}$ (BELKINA and WEINSTEIN [1957]):

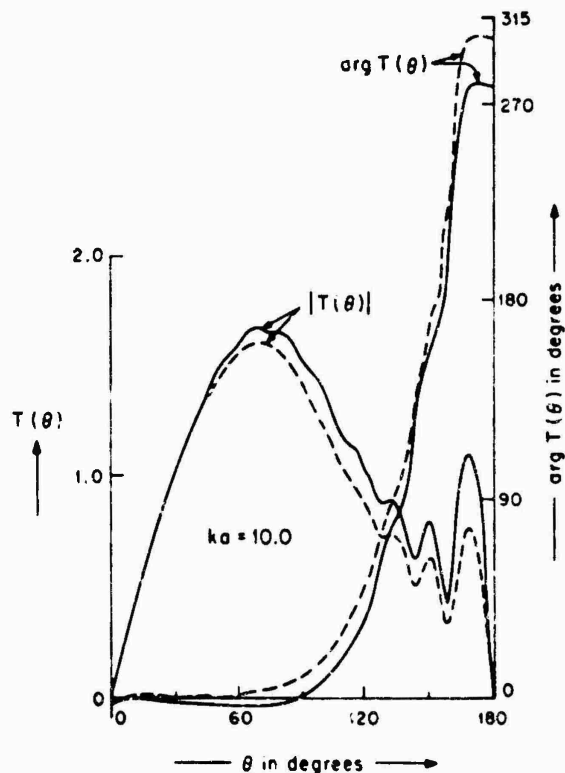


Fig. 10.14. Amplitude and phase of the far field component E_θ as functions of θ produced by a radial electric dipole located on the surface of a conducting sphere for $ka = 10$, (—) exact and (---) approximate (BELKINA and WEINSTEIN [1957]).

$$T(\theta) = \sin\theta e^{i(\xi')^3} g(\xi') + i \frac{\exp[ika(\cos\theta + \frac{1}{2}\pi - \theta)]}{\sqrt{\sin\theta}} g(\xi_1), \quad (10.142)$$

where

$$\xi' = -m \cos\theta.$$

In the range $0 \leq \theta \leq m^{-1}$, $T(\theta)$ is approximated by the first term in eq. (10.142). In the limit of geometrical optics:

$$T(\theta) \sim \begin{cases} 2 \sin\theta, & \text{for } 0 < \theta < \frac{1}{2}\pi, \\ 0, & \text{for } \frac{1}{2}\pi < \theta < \pi. \end{cases} \quad (10.143)$$

The approximation to $T(\theta)$ given by eqs. (10.139)–(10.143) is compared with the exact value given by eq. (10.123) in Fig. 10.14.

10.4.2. Magnetic dipole sources

10.4.2.1. EXACT SOLUTIONS

For an arbitrarily oriented magnetic dipole of moment $(4\pi/k)\hat{c}$ located at $\mathbf{r}_0 = (r_0, \theta_0, \phi_0)$, the total magnetic field is

$$\mathbf{H}^i(\mathbf{r}) + \mathbf{H}^s(\mathbf{r}) = 4\pi k \mathcal{G}_m(\mathbf{r}|\mathbf{r}_0) \cdot \hat{c}, \quad (10.144)$$

where \hat{c} is an arbitrary constant unit vector specifying the dipole orientation and $\mathcal{G}_m(\mathbf{r}|\mathbf{r}_0)$ is the magnetic dyadic Green's function for the sphere and is given by (TAI [1954]):

$$\begin{aligned} \mathcal{G}_m(\mathbf{r}|\mathbf{r}_0) = & \frac{ik}{4\pi} \sum_{n=1}^{\infty} \sum_{m=0}^n \varepsilon_m \frac{2n+1}{n(n+1)} \frac{(n-m)!}{(n+m)!} \{ N_{emn}^{(3)}(\mathbf{r}) [N_{emn}^{(1)}(\mathbf{r}_0) - a_n N_{emn}^{(3)}(\mathbf{r}_0)] + \\ & + N_{omn}^{(3)}(\mathbf{r}) [N_{omn}^{(1)}(\mathbf{r}_0) - a_n N_{omn}^{(3)}(\mathbf{r}_0)] + M_{emn}^{(3)}(\mathbf{r}) [M_{emn}^{(1)}(\mathbf{r}_0) - b_n M_{emn}^{(3)}(\mathbf{r}_0)] + \\ & + M_{omn}^{(3)}(\mathbf{r}) [M_{omn}^{(1)}(\mathbf{r}_0) - b_n M_{omn}^{(3)}(\mathbf{r}_0)] \}, \quad \text{for } r > r_0, \end{aligned} \quad (10.145)$$

$$\begin{aligned} \mathcal{G}_m(\mathbf{r}|\mathbf{r}_0) = & \frac{ik}{4\pi} \sum_{n=1}^{\infty} \sum_{m=0}^n \varepsilon_m \frac{2n+1}{n(n+1)} \frac{(n-m)!}{(n+m)!} \{ [N_{emn}^{(1)}(\mathbf{r}) - a_n N_{emn}^{(3)}(\mathbf{r})] N_{emn}^{(3)}(\mathbf{r}_0) + \\ & + [N_{omn}^{(1)}(\mathbf{r}) - a_n N_{omn}^{(3)}(\mathbf{r})] N_{omn}^{(3)}(\mathbf{r}_0) + [M_{emn}^{(1)}(\mathbf{r}) - b_n M_{emn}^{(3)}(\mathbf{r})] M_{emn}^{(3)}(\mathbf{r}_0) + \\ & + [M_{omn}^{(1)}(\mathbf{r}) - b_n M_{omn}^{(3)}(\mathbf{r})] M_{omn}^{(3)}(\mathbf{r}_0) \}, \quad \text{for } r < r_0. \end{aligned} \quad (10.146)$$

In the particular case of a z -directed magnetic dipole at $\mathbf{r}_0 = (r_0, 0, 0)$ with moment $(4\pi/k)\hat{z}$ the incident fields are

$$\begin{aligned} H_r^i = & \frac{e^{ikR}}{kR} \left[\frac{(r \cos\theta - r_0)(r - r_0 \cos\theta)}{R} \left(\frac{3}{R^3} - \frac{3ik}{R^2} - \frac{k^2}{R} \right) + \right. \\ & \left. + \left(\frac{ik}{R} - \frac{1}{R^2} \right) \cos\theta + k^2 \cos\theta \right], \end{aligned}$$

$$H_{\theta}^i = \frac{e^{ikR}}{kR} \left[\frac{(r \cos \theta - r_0)r_0}{R} \left(\frac{3}{R^3} - \frac{3ik}{R^2} - \frac{k^2}{R} \right) - \frac{ik}{R} + \frac{1}{R^2} - k^2 \right] \sin \theta, \quad (10.147)$$

$$E_{\phi}^i = ikZ \frac{e^{ikR}}{kR} \left[\left(\frac{1}{R^2} - \frac{ik}{R} \right) (r - r_0 \cos \theta) + \left(\frac{ik}{R} - \frac{1}{R^2} \right) r_0 \cos \theta \right] \sin \theta,$$

$$H_{\phi}^i = E_r^i = E_{\theta}^i = 0,$$

and the total fields are

$$\begin{aligned} H^i + H^s &= ik^2 \sum_{n=1}^{\infty} (2n+1) \frac{\zeta_n^{(1)}(kr_0)}{(kr_0)^2} \left[\frac{n(n+1)}{(kr)^2} \{ \psi_n(kr) - a_n \zeta_n^{(1)}(kr) \} P_n(\cos \theta) \hat{r} + \right. \\ &\quad \left. + \frac{1}{kr} \{ \psi_n'(kr) - a_n \zeta_n^{(1)'}(kr) \} \frac{\partial P_n(\cos \theta)}{\partial \theta} \hat{\theta} \right], \quad \text{for } a \leq r < r_0, \end{aligned} \quad (10.148)$$

$$\begin{aligned} E^i + E^s &= k^2 Z \sum_{n=1}^{\infty} (2n+1) \frac{\zeta_n^{(1)}(kr_0)}{(kr_0)^2} \frac{1}{kr} [\psi_n(kr) - a_n \zeta_n^{(1)}(kr)] \frac{\partial P_n(\cos \theta)}{\partial \theta} \hat{\phi}, \\ &\quad \text{for } a \leq r < r_0, \end{aligned} \quad (10.149)$$

$$\begin{aligned} H^i + H^s &= ik^2 \sum_{n=1}^{\infty} (2n+1) [\psi_n(kr_0) - a_n \zeta_n^{(1)}(kr_0)] \left[\frac{n(n+1)}{(kr)^2} \zeta_n^{(1)}(kr) P_n(\cos \theta) \hat{r} + \right. \\ &\quad \left. + \frac{1}{kr} \zeta_n^{(1)'}(kr) \frac{\partial P_n(\cos \theta)}{\partial \theta} \hat{\theta} \right], \quad \text{for } r > r_0, \end{aligned} \quad (10.150)$$

$$\begin{aligned} E^i + E^s &= k^2 Z \sum_{n=1}^{\infty} (2n+1) [\psi_n(kr_0) - a_n \zeta_n^{(1)}(kr_0)] \frac{\zeta_n^{(1)}(kr)}{kr} \frac{\partial P_n(\cos \theta)}{\partial \theta} \hat{\phi}, \\ &\quad \text{for } r > r_0. \end{aligned} \quad (10.151)$$

In the far zone ($r \rightarrow \infty$):

$$H_{\theta} = -Y E_{\phi} = ik^2 \frac{e^{ikR}}{kR} e^{ikr_0 \cos \theta} \sum_{n=1}^{\infty} (-i)^n [\psi_n(kr_0) - a_n \zeta_n^{(1)}(kr_0)] \frac{\partial P_n(\cos \theta)}{\partial \theta}. \quad (10.152)$$

For an x -directed magnetic dipole located at $r_0 = (r_0, 0, 0)$ with moment $(4\pi/k)\hat{x}$ the incident fields are

$$H_r^i = \frac{e^{ikR}}{kR} \left[\frac{r(r - r_0 \cos \theta)}{R} \left(\frac{3}{R^3} - \frac{3ik}{R^2} - \frac{k^2}{R} \right) + \frac{ik}{R} - \frac{1}{R^2} + k^2 \right] \sin \theta \cos \phi,$$

$$H_{\theta}^i = \frac{e^{ikR}}{kR} \left[\frac{rr_0 \sin \theta}{R} \left(\frac{3}{R^3} - \frac{3ik}{R^2} - \frac{k^2}{R} \right) \sin \theta + \left(\frac{ik}{R} - \frac{1}{R^2} + k^2 \right) \cos \theta \right] \cos \phi,$$

$$H_{\phi}^i = -\frac{e^{ikR}}{kR} \left[\frac{ik}{R} - \frac{1}{R^2} + k^2 \right] \sin \phi,$$

$$E_r^i = -ikZ \frac{e^{ikR}}{kR} \left(\frac{ik}{R} - \frac{1}{R^2} \right) r_0 \sin \theta \sin \phi, \quad (10.153)$$

$$E_\theta^i = ikZ \frac{e^{ikR}}{kR} \left(\frac{ik}{R} - \frac{1}{R^2} \right) (r - r_0 \cos \theta) \sin \phi,$$

$$E_\phi^i = ikZ \frac{e^{ikR}}{kR} \left(\frac{ik}{R} - \frac{1}{R^2} \right) (r \cos \theta - r_0) \cos \phi,$$

and the total fields are

$$\begin{aligned} H^i + H^s = ik^2 \sum_{n=1}^{\infty} \frac{2n+1}{n(n+1)} \left[\frac{\zeta_n^{(1)'}(kr_0)}{kr_0} \{N_{e1n}^{(1)}(r) - a_n N_{e1n}^{(3)}(r)\} + \right. \\ \left. + \frac{\zeta_n^{(1)}(kr_0)}{kr_0} \{M_{o1n}^{(1)}(r) - b_n M_{o1n}^{(3)}(r)\} \right], \quad \text{for } r < r_0, \end{aligned} \quad (10.154)$$

$$\begin{aligned} E^i + E^s = -k^2 Z \sum_{n=1}^{\infty} \frac{2n+1}{n(n+1)} \left[\frac{\zeta_n^{(1)'}(kr_0)}{kr_0} \{M_{e1n}^{(1)}(r) - a_n M_{e1n}^{(3)}(r)\} + \right. \\ \left. + \frac{\zeta_n^{(1)}(kr_0)}{kr_0} \{N_{o1n}^{(1)}(r) - b_n N_{o1n}^{(3)}(r)\} \right], \quad \text{for } r < r_0, \end{aligned} \quad (10.155)$$

whereas,

$$H_r^i + H_r^s = \frac{ik^2 \cos \phi}{kr_0} \sum_{n=1}^{\infty} (2n+1) A_n \frac{\zeta_n^{(1)'}(kr)}{(kr)^2} P_n^1(\cos \theta), \quad \text{for } r > r_0, \quad (10.156)$$

$$\begin{aligned} H_\theta^i + H_\theta^s = \frac{ik^2 \cos \phi}{kr_0} \sum_{n=1}^{\infty} \frac{2n+1}{n(n+1)} \left\{ A_n \frac{\zeta_n^{(1)'}(kr)}{kr} \frac{\partial P_n^1(\cos \theta)}{\partial \theta} + \right. \\ \left. + B_n \frac{\zeta_n^{(1)}(kr)}{kr} \frac{P_n^1(\cos \theta)}{\sin \theta} \right\}, \quad \text{for } r > r_0, \end{aligned} \quad (10.157)$$

$$\begin{aligned} H_\phi^i + H_\phi^s = -\frac{ik^2 \sin \phi}{kr_0} \sum_{n=1}^{\infty} \frac{2n+1}{n(n+1)} \left\{ A_n \frac{\zeta_n^{(1)'}(kr)}{kr} \frac{P_n^1(\cos \theta)}{\sin \theta} + \right. \\ \left. + B_n \frac{\zeta_n^{(1)}(kr)}{kr} \frac{\partial P_n^1(\cos \theta)}{\partial \theta} \right\}, \quad \text{for } r > r_0, \end{aligned} \quad (10.158)$$

$$E_r^i + E_r^s = -\frac{k^2 Z \sin \phi}{kr_0} \sum_{n=1}^{\infty} (2n+1) B_n \frac{\zeta_n^{(1)'}(kr)}{(kr)^2} P_n^1(\cos \theta), \quad \text{for } r > r_0, \quad (10.159)$$

$$\begin{aligned} E_\theta^i + E_\theta^s = \frac{k^2 Z \sin \phi}{kr_0} \sum_{n=1}^{\infty} \frac{2n+1}{n(n+1)} \left\{ A_n \frac{\zeta_n^{(1)'}(kr)}{kr} \frac{P_n^1(\cos \theta)}{\sin \theta} - \right. \\ \left. - B_n \frac{\zeta_n^{(1)}(kr)}{kr} \frac{\partial P_n^1(\cos \theta)}{\partial \theta} \right\}, \quad \text{for } r > r_0, \end{aligned} \quad (10.160)$$

$$E_{\phi}^i + E_{\phi}^s = \frac{k^2 Z \cos \phi}{kr_0} \sum_{n=1}^{\infty} \frac{2n+1}{n(n+1)} \left\{ A_n \frac{\zeta_n^{(1)}(kr)}{kr} \frac{\partial P_n^1(\cos \theta)}{\partial \theta} - B_n \frac{\zeta_n^{(1)'}(kr)}{kr} \frac{P_n^1(\cos \theta)}{\sin \theta} \right\}, \quad \text{for } r > r_0, \quad (10.161)$$

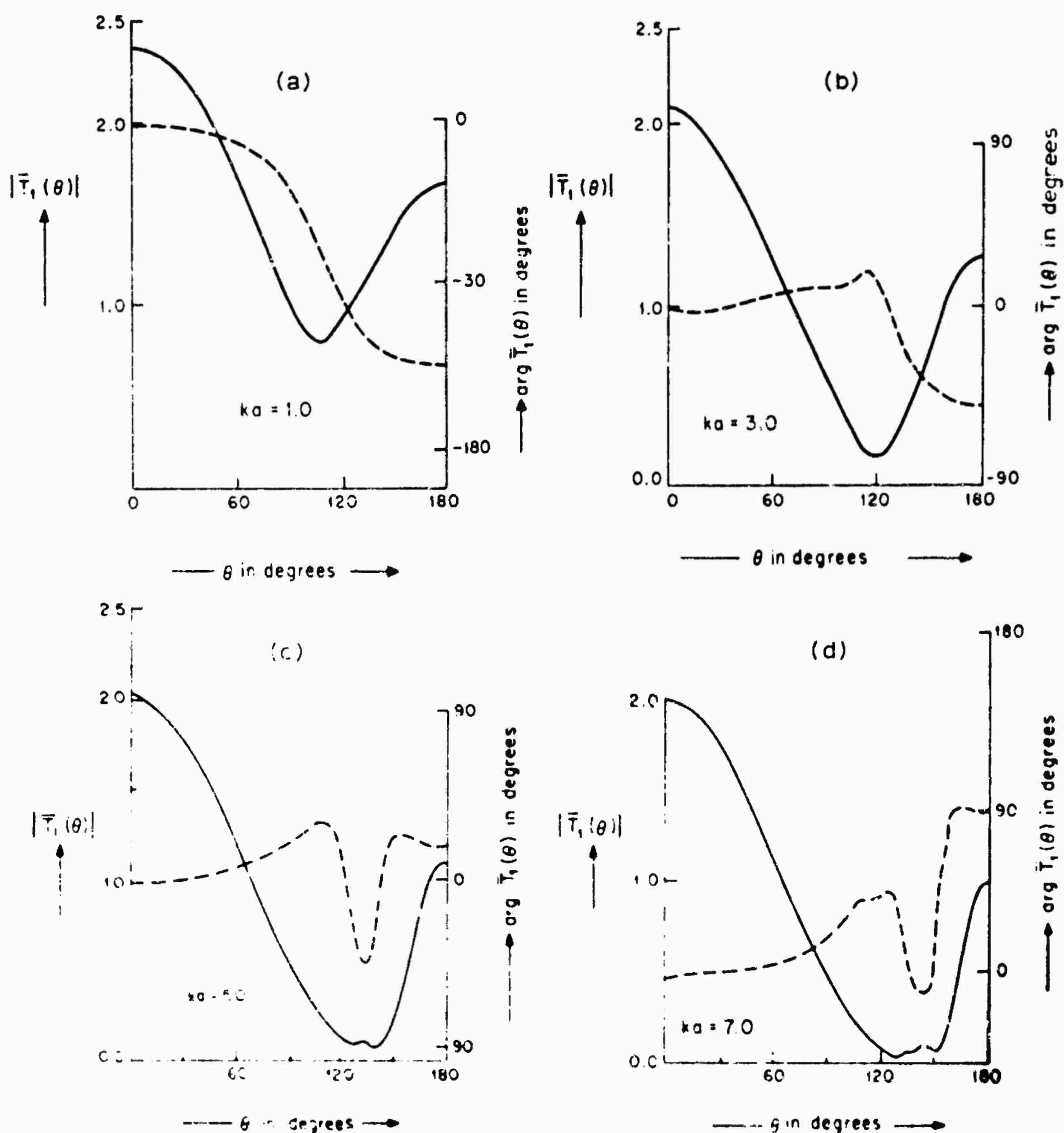
with

$$A_n = \psi_n'(kr_0) - a_n \zeta_n^{(1)'}(kr_0), \quad (10.162)$$

$$B_n = \psi_n(kr_0) - b_n \zeta_n^{(1)}(kr_0). \quad (10.163)$$

For a magnetic dipole located at $r_0 = (a, 0, 0)$ with moment $(4\pi/k)\hat{x}$ the field components in the far zone are (BELKINA and WEINSTEIN [1957]):

$$H_{\theta} = -YE_{\phi} = k^2 \frac{e^{ikR}}{kR} T_1(\theta) \cos \phi, \quad (10.164)$$



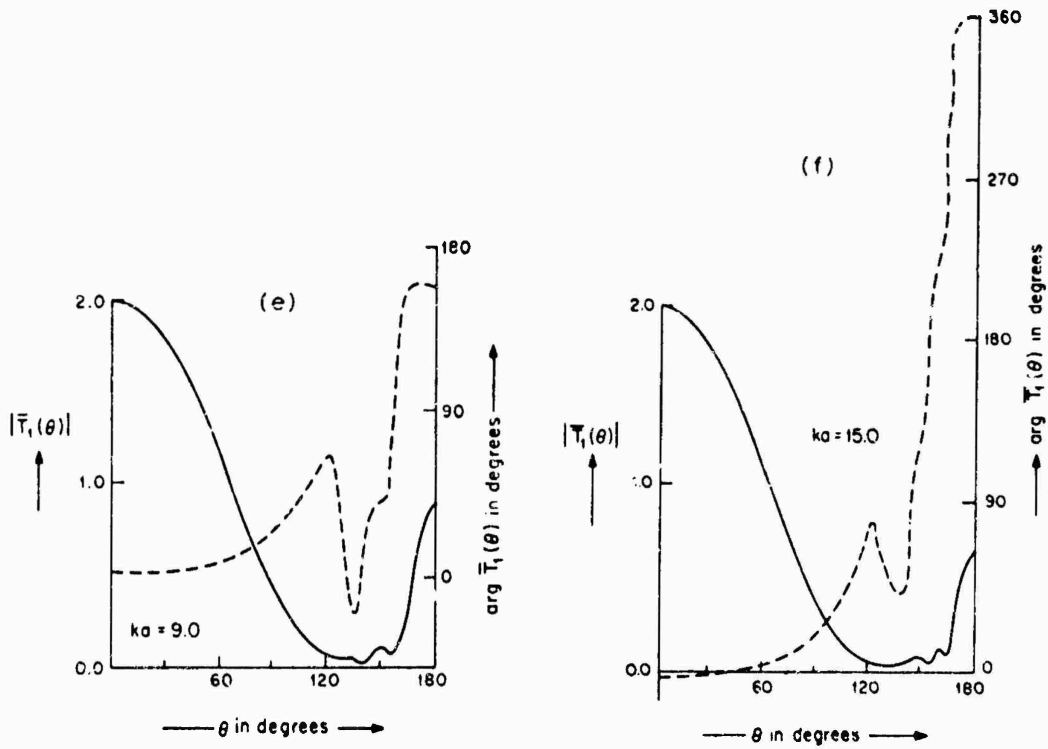


Fig. 10.15. Amplitude (—) and phase (---) of the far field component E_ϕ as functions of θ produced by an x -directed magnetic dipole located on the surface of a conducting sphere for different values of ka (BELKINA and WEINSTEIN [1957]).

$$H_\phi = YE_\theta = -k^2 \frac{e^{ikR}}{kR} T_2(\theta) \sin \phi, \quad (10.165)$$

where

$$\bar{T}_1(\theta) = i \frac{e^{iku \cos \theta}}{ka} \sum_{n=1}^{\infty} (-i)^n \frac{2n+1}{n(n+1)} \left[\frac{1}{\zeta_n^{(1)}(ka)} \frac{P_n^1(\cos \theta)}{\sin \theta} - \frac{i}{\zeta_n^{(1)}(ka)} \frac{\partial P_n^1(\cos \theta)}{\partial \theta} \right], \quad (10.166)$$

$$\bar{T}_2(\theta) = i \frac{e^{iku \cos \theta}}{ka} \sum_{n=1}^{\infty} (-i)^n \frac{2n+1}{n(n+1)} \left[\frac{1}{\zeta_n^{(1)}(ka)} \frac{\partial P_n^1(\cos \theta)}{\partial \theta} - \frac{i}{\zeta_n^{(1)}(ka)} \frac{P_n^1(\cos \theta)}{\sin \theta} \right]. \quad (10.167)$$

$\bar{T}_1(\theta)$ and $\bar{T}_2(\theta)$ as functions of ka are shown in Figs. 10.15 a. and 10.16. It should be noted that the functions $\bar{T}_1(\theta)$ and $\bar{T}_2(\theta)$ also give the radiation characteristics of an elementary (dumb-bell type) slot cut in the sphere because such a slot is equivalent to a magnetic dipole situated on the sphere (BELKINA and WEINSTEIN [1957]). The pattern functions $\bar{T}_1(\theta)$, $\bar{T}_2(\theta)$ in eqs. (10.166) and (10.167) are respectively proportional to the total magnetic fields $H_\theta(a, \theta, \frac{1}{2}\pi)$ and $H_\phi(a, \theta, 0)$ induced on the sphere by a plane electromagnetic wave incident in the negative z -direction and having its magnetic field vector polarized in the negative y -direction.

10.4.2.2. LOW FREQUENCY APPROXIMATIONS

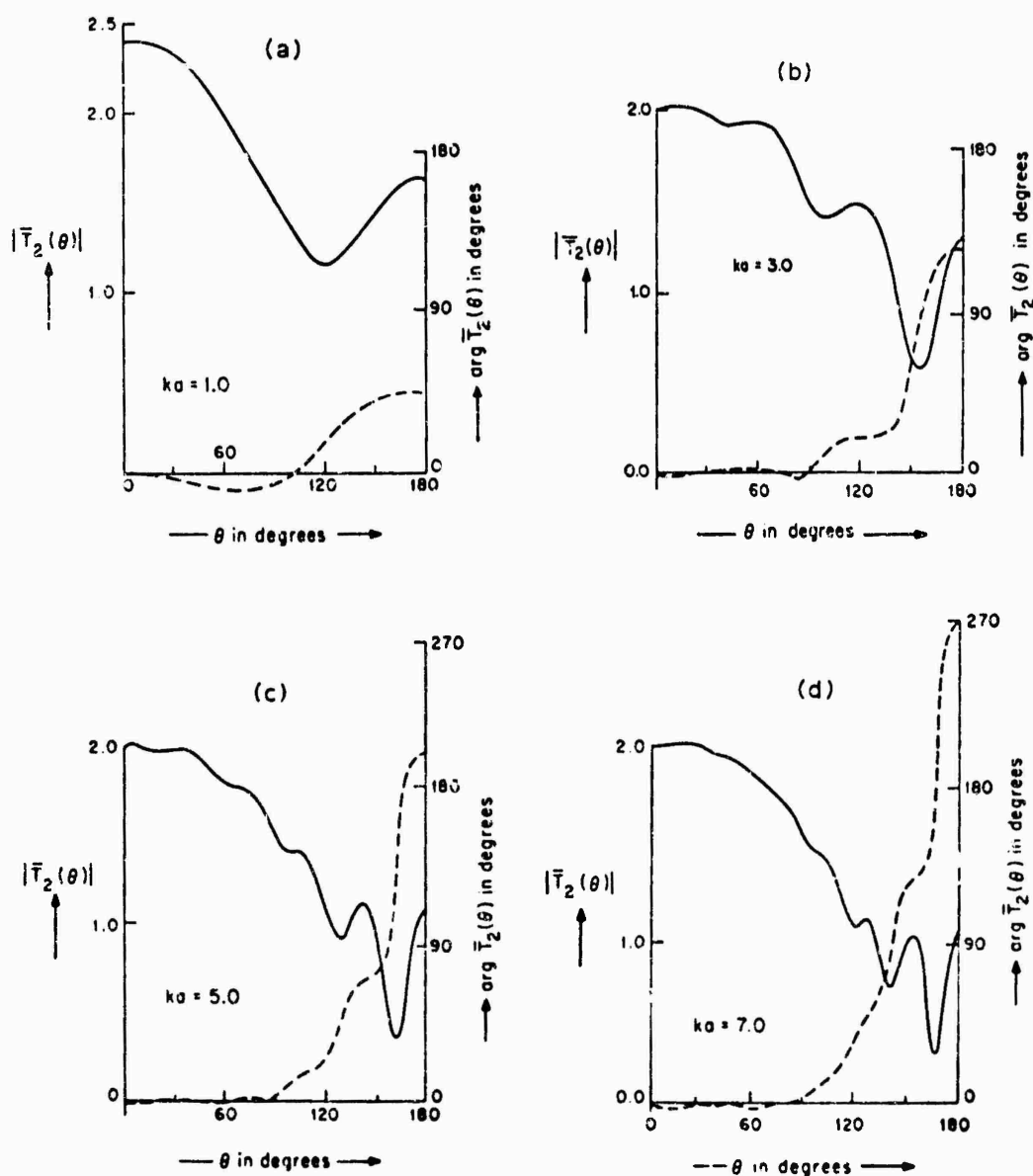
For an x -directed magnetic dipole situated on the sphere (BELKINA and WEINSTEIN [1957]):

$$\begin{aligned} T_1(\theta) &\sim \frac{1}{2} \cos \theta, \\ T_2(\theta) &\sim \frac{1}{2}, \text{ as } ka \rightarrow 0. \end{aligned} \quad (10.168)$$

Thus to this approximation the moment of the dipole increased by a factor of $\frac{1}{2}$. No other specific results are available.

10.4.2.3. HIGH FREQUENCY APPROXIMATIONS

For an x -directed magnetic dipole of moment $(4\pi/k)\hat{x}$ situated at $(a, 0, 0)$ on the surface of the sphere (BELKINA and WEINSTEIN [1957]):



$$\begin{aligned} \bar{T}_1(\theta) \sim & i \frac{e^{ika \cos \theta}}{m \sqrt{\sin \theta}} [e^{ika(\theta - \frac{1}{2}\pi)} f(\xi) - ie^{ika(\frac{1}{2}\pi - \theta)} f(\xi_1)] - \\ & - \frac{ie^{ika \cos \theta}}{ka \sin \theta \sqrt{\sin \theta}} [e^{ika(\theta - \frac{1}{2}\pi)} g(\xi) + ie^{ika(\frac{1}{2}\pi - \theta)} g(\xi_1)], \quad \text{for } \frac{1}{2}\pi < \theta \lesssim \pi - m^{-1}, \end{aligned} \quad (10.169)$$

$$\begin{aligned} \bar{T}_1(\theta) \sim & 2\pi^{\frac{1}{2}} m^{\frac{1}{2}} \exp \left[\frac{1}{2} i (ka + \frac{1}{2}) \pi \right] e^{ika \cos \theta} \left(\frac{\pi - \theta}{\sin \theta} \right)^{\frac{1}{2}} \\ & \times \left\{ \frac{1}{m} J'_1[v_1(\pi - \theta)] f(\frac{1}{2} m \pi) + i \frac{J_1[\bar{v}_1(\pi - \theta)]}{ka \sin \theta} g(\frac{1}{2} m \pi) \right\}, \quad \text{for } \pi - m^{-1} \lesssim \theta \leq \pi, \end{aligned} \quad (10.170)$$

where

$$\begin{aligned} \xi &= m(\theta - \frac{1}{2}\pi), \\ \xi_1 &= m(\frac{1}{2}\pi - \theta), \\ v_1 &= ka + me^{i\pi} \alpha_1 + O(m^{-1}), \\ \bar{v}_1 &= ka + me^{i\pi} \beta_1 + O(m^{-1}), \end{aligned} \quad (10.171)$$

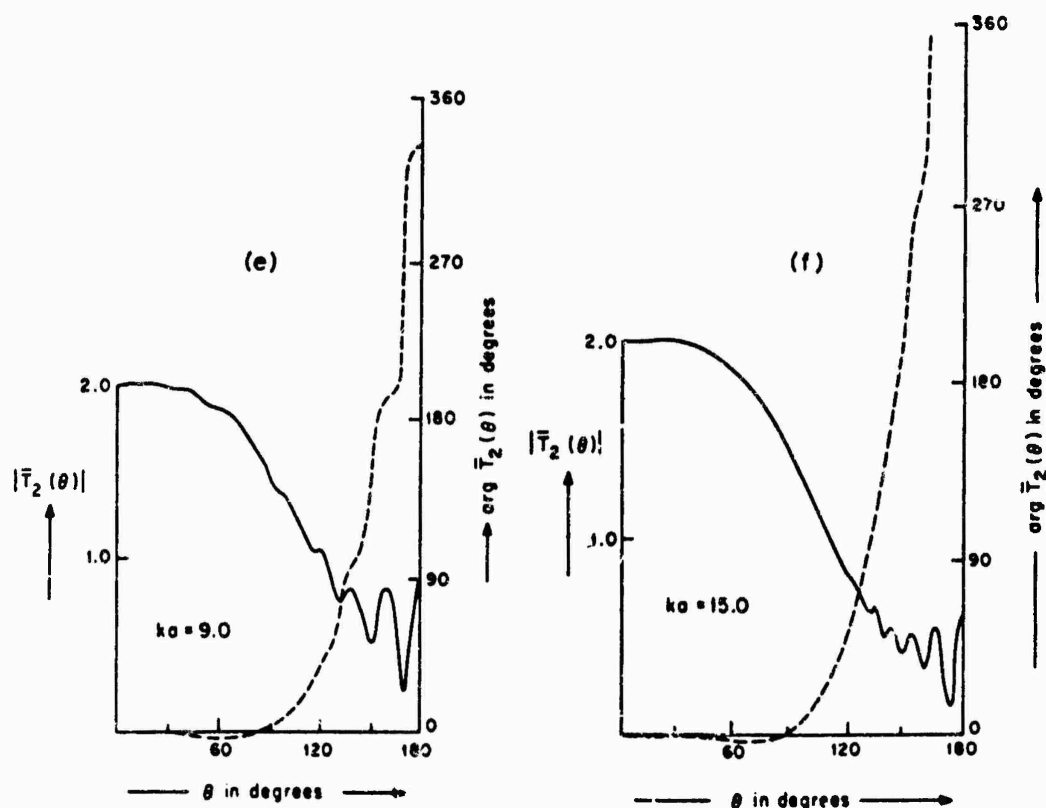


Fig. 10.16. Amplitude (—) and phase (---) of the far field component E_θ as functions of θ produced by an x -directed magnetic dipole located on the surface of a conducting sphere for different values of ka (BELKINA and WEINSTEIN [1957]).

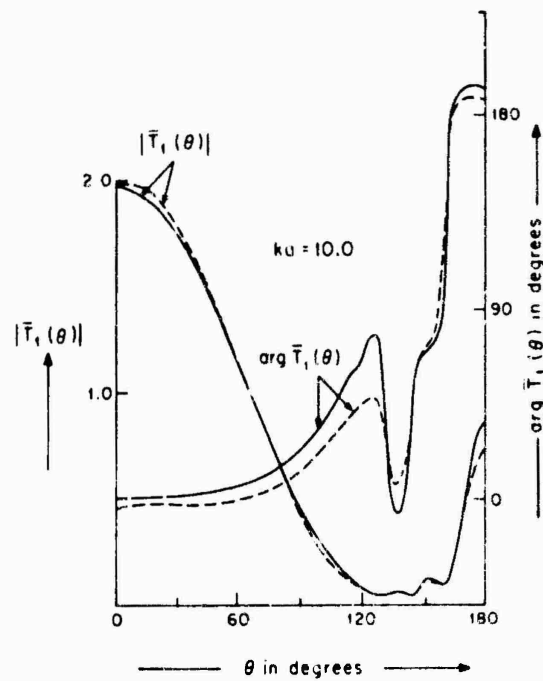


Fig. 10.17 Amplitude and phase of the far field component E_1 as functions of θ produced by an x -directed magnetic dipole located on the surface of a conducting sphere for $ka = 10$, (—) exact and (---) approximate (BELKINA and WEINSTEIN [1957]).

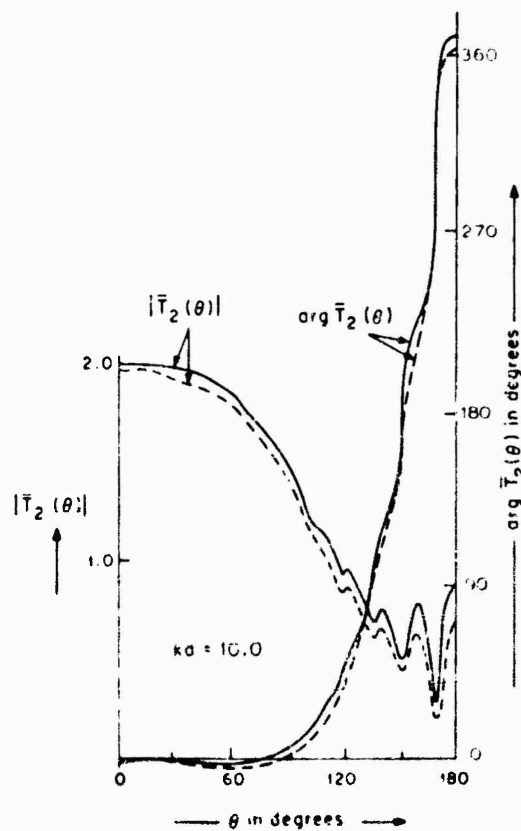


Fig. 10.18. Amplitude and phase of the far field component E_2 as functions of θ produced by an x -directed magnetic dipole located on the surface of a conducting sphere for $ka = 10$, (—) exact and (---) approximate (BELKINA and WEINSTEIN [1957]).

and the modified Fock functions $f(\xi)$ and $g(\xi)$ are defined in the Introduction;

$$\begin{aligned} \bar{T}_2(\theta) \sim & \frac{e^{ika \cos \theta}}{\sqrt{\sin \theta}} [e^{ika(\theta - \frac{1}{2}\pi)} g(\xi) - ie^{ika(\frac{1}{2}\pi - \theta)} g(\xi_1)] - \\ & - \frac{e^{ika \cos \theta}}{kam \sin \theta \sqrt{\sin \theta}} [e^{ika(\theta - \frac{1}{2}\pi)} f(\xi) + ie^{ika(\frac{1}{2}\pi - \theta)} f(\xi_1)], \quad \text{for } \pi \leq \theta \lesssim \pi - m^{-1}, \end{aligned} \quad (10.172)$$

$$\begin{aligned} \bar{T}_2(\theta) \sim & -2\pi^{\frac{1}{2}} m^{\frac{1}{2}} e^{\frac{1}{2}i(ka + \frac{1}{2})\pi} e^{ika \cos \theta} \left(\frac{\pi - \theta}{\sin \theta} \right)^{\frac{1}{2}} \\ & \times \left\{ \frac{J_1[\bar{v}_1(\pi - \theta)]}{mka \sin \theta} f(\tfrac{1}{2}m\pi) + iJ'_1[v_1(\pi - \theta)] g(\tfrac{1}{2}m\pi) \right\}, \quad \text{for } \pi - m^{-1} \lesssim \theta \leq \pi. \end{aligned} \quad (10.173)$$

For large positive values of ξ the function $f(\xi)$ tends towards zero much faster than the $g(\xi)$ function. This justifies the inclusion of the second term in eqs. (10.169) and (10.170). In the vicinity of $\theta \sim \pi$ the second terms become dominant. In contrast to this, the second term in eq. (10.172) and the first term in eq. (10.173) do not have any dominant role and are included only for symmetry.

At $\theta = \pi$:

$$\begin{aligned} \bar{T}_1(\pi) &= -\bar{T}_2(\pi) \\ &\sim \pi^{\frac{1}{2}} m^{\frac{1}{2}} \exp \{i[ka(\tfrac{1}{2}\pi - 1) + \tfrac{1}{4}\pi]\} \left[\frac{1}{m} f(\tfrac{1}{2}m\pi) + ig(\tfrac{1}{2}m\pi) \right]. \end{aligned} \quad (10.174)$$

In the range $m^{-1} \lesssim \theta \lesssim \tfrac{1}{2}\pi - m^{-1}$ (BELKINA and WEINSTEIN [1957]):

$$\bar{T}_1(\theta) \sim \frac{ie^{\frac{1}{2}i(\xi')^3}}{m} f(\xi') + \frac{\exp [ika(\cos \theta + \tfrac{1}{2}\pi - \theta)]}{m\sqrt{\sin \theta}} f(\xi_1), \quad (10.175)$$

$$\bar{T}_2(\theta) \sim e^{\frac{1}{2}i(\xi')^3} g(\xi') - i \frac{\exp [ika(\cos \theta + \tfrac{1}{2}\pi - \theta)]}{\sqrt{\sin \theta}} g(\xi_1), \quad (10.176)$$

where $\xi' = -m \cos \theta$.

In the range $0 \lesssim \theta \lesssim m^{-1}$, $\bar{T}_1(\theta)$ and $\bar{T}_2(\theta)$ can be approximated by the first terms of eqs. (10.175) and (10.176) respectively. Figs. 10.17 and 10.18 show the comparison between the approximate values of $\bar{T}_1(\theta)$ and $\bar{T}_2(\theta)$ given by eqs. (10.169)-(10.176) and the exact values given by eqs. (10.166) and (10.167).

10.4.3. Plane wave incidence

10.4.3.1. EXACT SOLUTIONS

The exact solution for the scattering of a plane electromagnetic wave by a sphere is usually referred to as the Mie series. Descriptions of the solution are available in the literature (STRATTON [1941], BORN and WOLF [1964], VAN DE HULST [1957]).

For a plane wave incident in the direction of the negative z -axis, such that

$$E^i = \hat{x}e^{-ikz}, \quad H^i = -\hat{y}Ye^{-ikz}, \quad (10.177)$$

the total field is

$$E_r^i + E_r^s = -\frac{\cos \phi}{(kr)^2} \sum_{n=1}^{\infty} (-i)^n (2n+1) [\psi_n(kr) - b_n \zeta_n^{(1)}(kr)] P_n^1(\cos \theta), \quad (10.178)$$

$$E_\theta^i + E_\theta^s = \frac{\cos \phi}{kr} \sum_{n=1}^{\infty} (-i)^n \frac{2n+1}{n(n+1)} \left[\{\psi_n(kr) - a_n \zeta_n^{(1)}(kr)\} \frac{P_n^1(\cos \theta)}{\sin \theta} + i\{\psi_n'(kr) - b_n \zeta_n^{(1)'}(kr)\} \frac{\partial P_n^1(\cos \theta)}{\partial \theta} \right], \quad (10.179)$$

$$E_\phi^i + E_\phi^s = -\frac{\sin \phi}{kr} \sum_{n=1}^{\infty} (-i)^n \frac{2n+1}{n(n+1)} \left[\{\psi_n(kr) - a_n \zeta_n^{(1)}(kr)\} \frac{\partial P_n^1(\cos \theta)}{\partial \theta} + i\{\psi_n'(kr) - b_n \zeta_n^{(1)'}(kr)\} \frac{P_n^1(\cos \theta)}{\sin \theta} \right], \quad (10.180)$$

$$H_r^i + H_r^s = -i \frac{Y \sin \phi}{(kr)^2} \sum_{n=1}^{\infty} (-i)^n (2n+1) [\psi_n(kr) - a_n \zeta_n^{(1)}(kr)] P_n^1(\cos \theta), \quad (10.181)$$

$$H_\theta^i + H_\theta^s = -\frac{Y \sin \phi}{kr} \sum_{n=1}^{\infty} (-i)^n \frac{2n+1}{n(n+1)} \left[\{\psi_n(kr) - b_n \zeta_n^{(1)}(kr)\} \frac{P_n^1(\cos \theta)}{\sin \theta} + i\{\psi_n'(kr) - a_n \zeta_n^{(1)'}(kr)\} \frac{\partial P_n^1(\cos \theta)}{\partial \theta} \right], \quad (10.182)$$

$$H_\phi^i + H_\phi^s = -\frac{Y \cos \phi}{kr} \sum_{n=1}^{\infty} (-i)^n \frac{2n+1}{n(n+1)} \left[\{\psi_n(kr) - b_n \zeta_n^{(1)}(kr)\} \frac{\partial P_n^1(\cos \theta)}{\partial \theta} + i\{\psi_n'(kr) - a_n \zeta_n^{(1)'}(kr)\} \frac{P_n^1(\cos \theta)}{\sin \theta} \right]. \quad (10.183)$$

The total electric field has been computed and measured by HUANG and KODIS [1951] in the plane perpendicular to the incident electric field vector at $kz = -4\pi$ and for small values of ka . Fig. 10.19 shows the total electric field in this plane for selected values of ka .

On the surface $r = a$:

$$E_r^i + E_r^s = -\frac{\cos \theta}{(ka)^2} \sum_{n=1}^{\infty} (-i)^n (2n+1) \frac{P_n^1(\cos \theta)}{\zeta_n^{(1)'}(ka)}, \quad (10.184)$$

$$H_\theta^i + H_\theta^s = YT_1(\theta) \sin \phi, \quad H_\phi^i + H_\phi^s = YT_2(\theta) \cos \phi, \quad (10.185)$$

where

$$T_1(\theta) = \frac{1}{ka} \sum_{n=1}^{\infty} (-i)^{n+1} \frac{2n+1}{n(n+1)} \left[\frac{1}{\zeta_n^{(1)'}(ka)} \frac{P_n^1(\cos \theta)}{\sin \theta} - \frac{i}{\zeta_n^{(1)}(ka)} \frac{\partial P_n^1(\cos \theta)}{\partial \theta} \right], \quad (10.186)$$

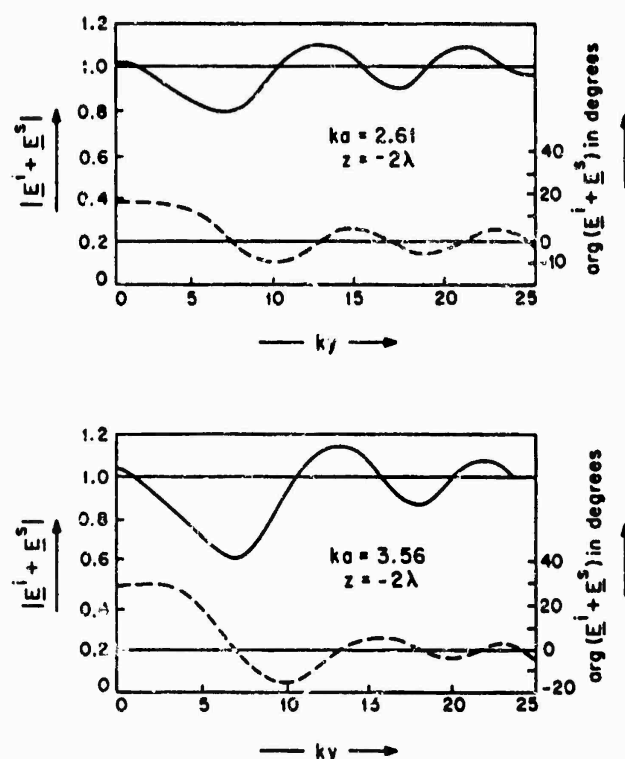


Fig. 10.19. Amplitude (—) and phase (---) of $E^i + E^s$ in the plane through the center of the sphere and perpendicular to E^i for two values of ka (HUANG and KODIS [1951]).

$$T_2(\theta) = \frac{1}{ka} \sum_{n=1}^{\infty} (-i)^{n+1} \frac{2n+1}{n(n+1)} \left[\frac{1}{\zeta_n^{(1)}(ka)} \frac{\partial P_n^1(\cos \theta)}{\partial \theta} - \frac{i}{\zeta_n^{(1)}(ka)} \frac{P_n^1(\cos \theta)}{\sin \theta} \right]. \quad (10.187)$$

DUCMANIS and LIEPA [1965] have computed $T_1(\theta)$ and $T_2(\theta)$ for $\theta = 0^\circ$ (5°) 180° and $ka = 0.1$ (0.1) 5.0 (0.2) 10.0 . Some typical results are shown in Fig. 10.20.

In the far field ($r \rightarrow \infty$):

$$E_\theta^s = ZH_\phi^s = \cos \phi \frac{e^{ikr}}{kr} S_1(\theta), \quad (10.188)$$

$$E_\phi^s = -ZH_\theta^s = \sin \phi \frac{e^{ikr}}{kr} S_2(\theta), \quad (10.189)$$

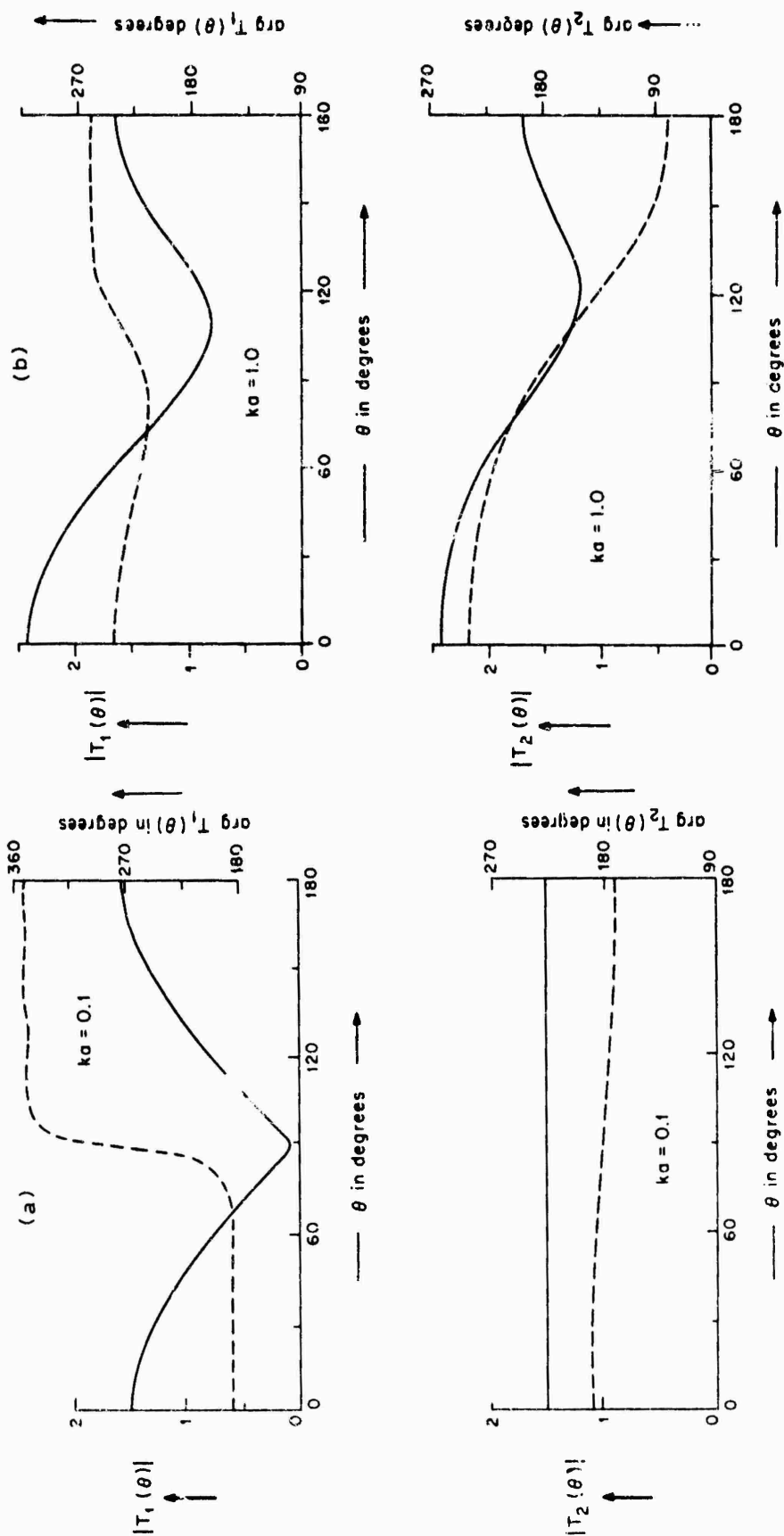
where

$$S_1(\theta) = -i \sum_{n=1}^{\infty} (-1)^n \frac{2n+1}{n(n+1)} \left[b_n \frac{\partial P_n^1(\cos \theta)}{\partial \theta} - a_n \frac{P_n^1(\cos \theta)}{\sin \theta} \right], \quad (10.190)$$

$$S_2(\theta) = i \sum_{n=1}^{\infty} (-1)^n \frac{2n+1}{n(n+1)} \left[b_n \frac{P_n^1(\cos \theta)}{\sin \theta} - a_n \frac{\partial P_n^1(\cos \theta)}{\partial \theta} \right]. \quad (10.191)$$

In the back scattering direction $\theta = 0$:

$$S_1(0) = -S_2(0) = -i \sum_{n=1}^{\infty} (-1)^n (n+1)(b_n - a_n); \quad (10.192)$$



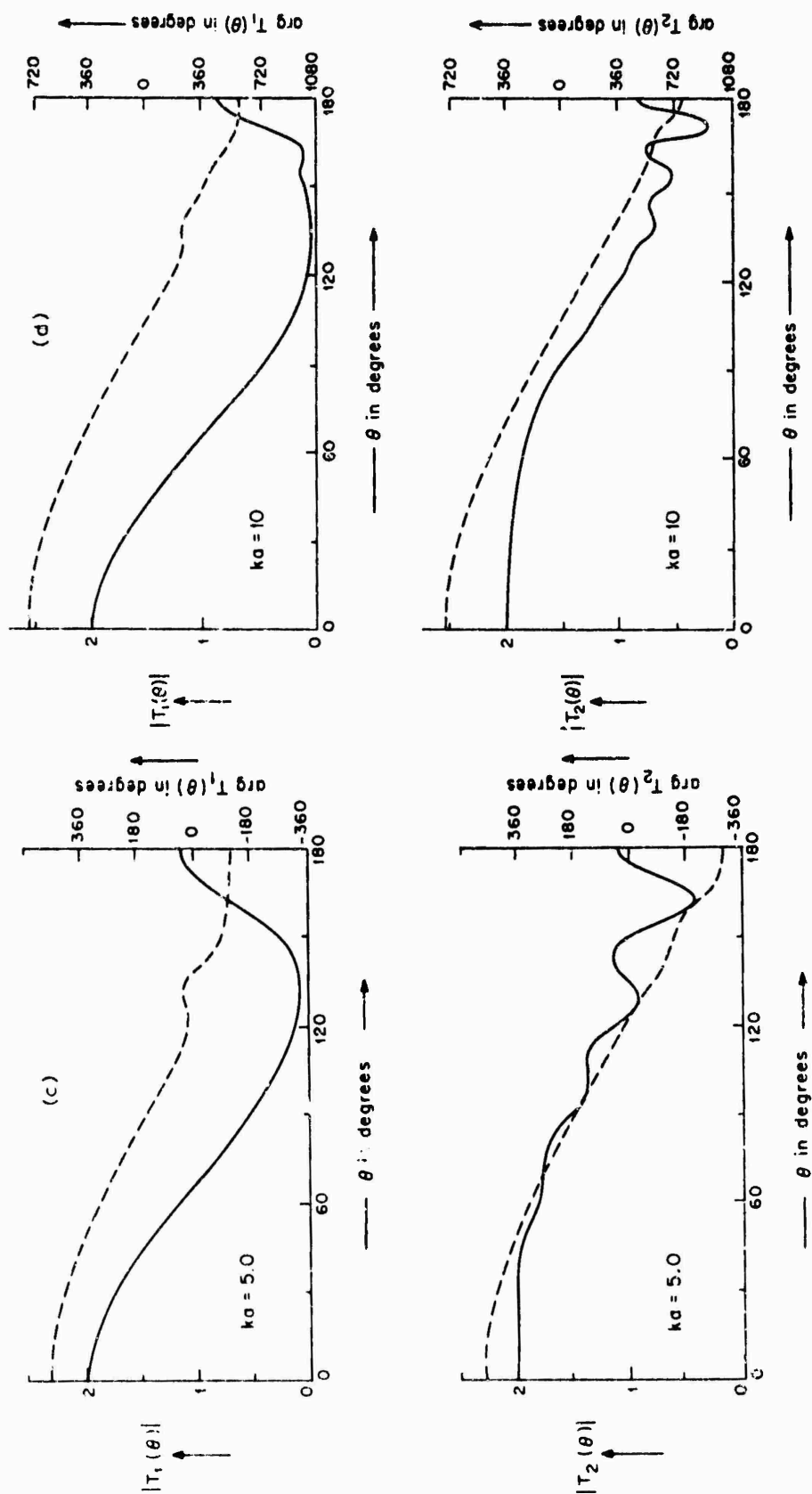


Fig. 10.20. Amplitude (—) and phase (---) of $T_1(\theta)$ and $T_2(\theta)$ as functions of θ for selected values of ka (DUCMANIS and LIEPA [1965]).

and in the forward scattering direction $\theta = \pi$:

$$S_1(\pi) = S_2(\pi) = -i \sum_{n=1}^{\infty} (n + \frac{1}{2})(b_n + a_n), \quad (10.193)$$

implying no depolarization in the back and forward directions. The quantity $G = 2S_1(0)/(ka)$ has been computed in amplitude and phase for $ka = 0$ (0.02) 50 by BECHTEL [1962]. RHEINSTEIN [1963] has computed $-iS_1(0)$ in amplitude and phase for $a/\lambda = 0.01$ (0.01) 19. Some typical results for selected values of ka are shown in Fig. 10.21. Additional data are given by HEY et al. [1956].

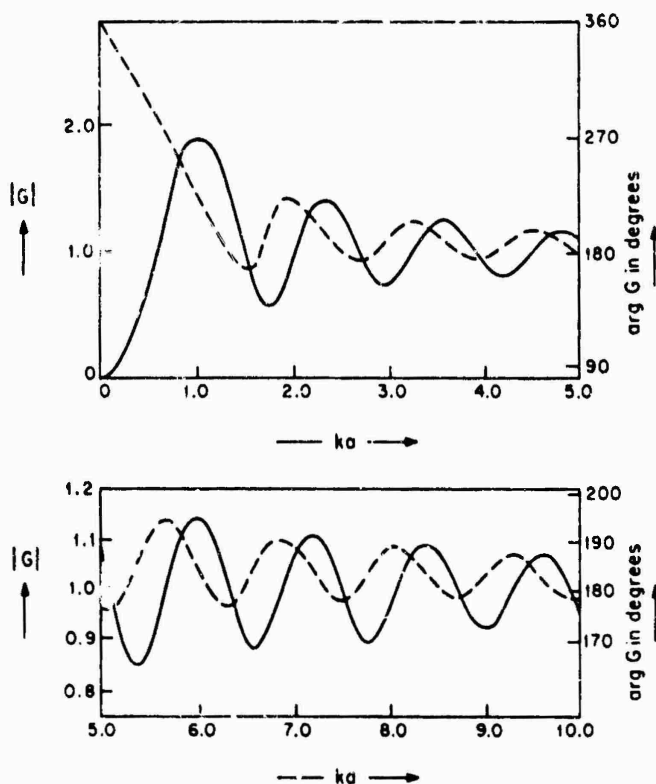


Fig. 10.21. Normalized amplitude (—) and phase (---) of the far back scattered field as functions of ka (BECHTEL [1962]).

The back scattering cross section is

$$\sigma = \frac{\pi}{k^2} \left| \sum_{n=1}^{\infty} (-1)^n (2n+1)(b_n - a_n) \right|^2. \quad (10.194)$$

σ/λ^2 has been computed for various values of ka (BECHTEL [1962], RHEINSTEIN [1963]). A typical normalized cross section $\sigma/(\pi a^2)$ is shown as a function of ka in Fig. 10.22.

The bistatic scattering cross section is

$$\sigma(\theta, \phi) = \frac{4\pi}{k^2} [|S_1(\theta)|^2 \cos^2 \phi + |S_2(\theta)|^2 \sin^2 \phi]; \quad (10.195)$$

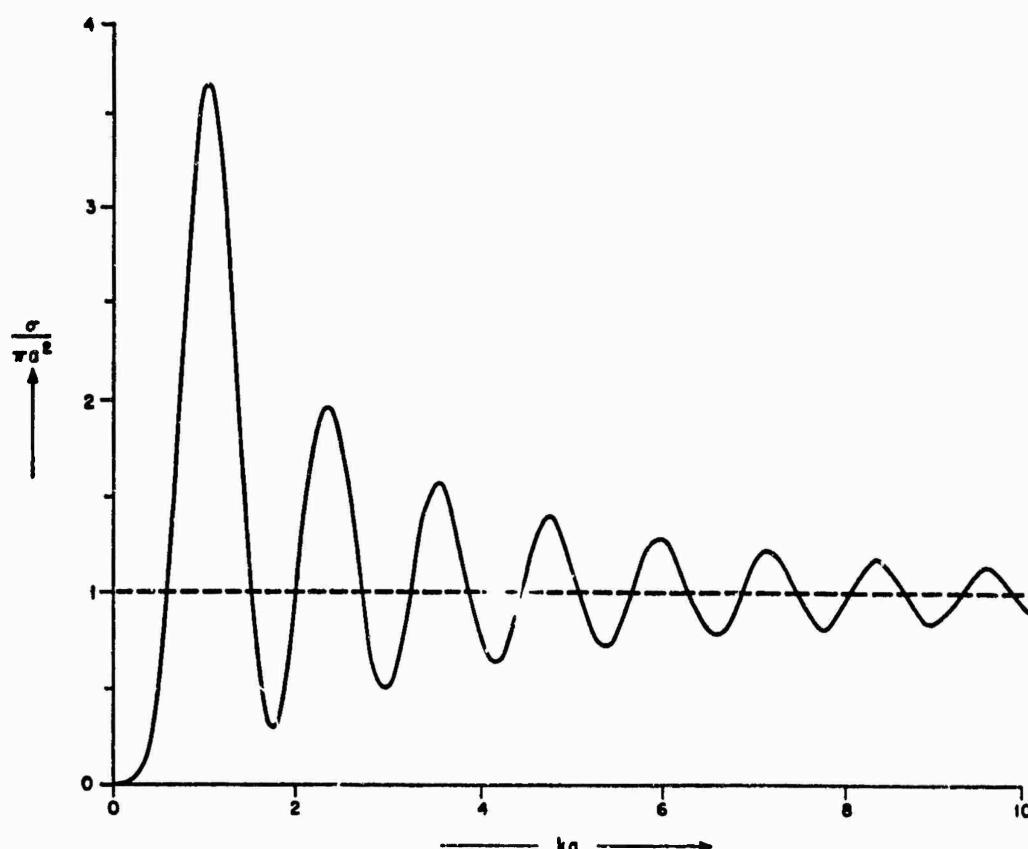


Fig. 10.22. Normalized back scattering cross section $\sigma/(\pi a^2)$ as a function of ka for a conducting sphere.

$\sigma(\theta, 0)$ and $\sigma(\theta, \frac{1}{2}\pi)$ are plotted as functions of θ for selected values of ka in Fig. 10.23.

The total scattering cross section is

$$\sigma_T = \frac{2\pi}{k^2} \sum_{n=1}^{\infty} (2n+1)(|a_n|^2 + |b_n|^2). \quad (10.196)$$

The normalized cross section $\sigma_T/(\pi a^2)$ is shown as a function of ka in Fig. 10.24.

10.4.3.2. LOW FREQUENCY APPROXIMATIONS

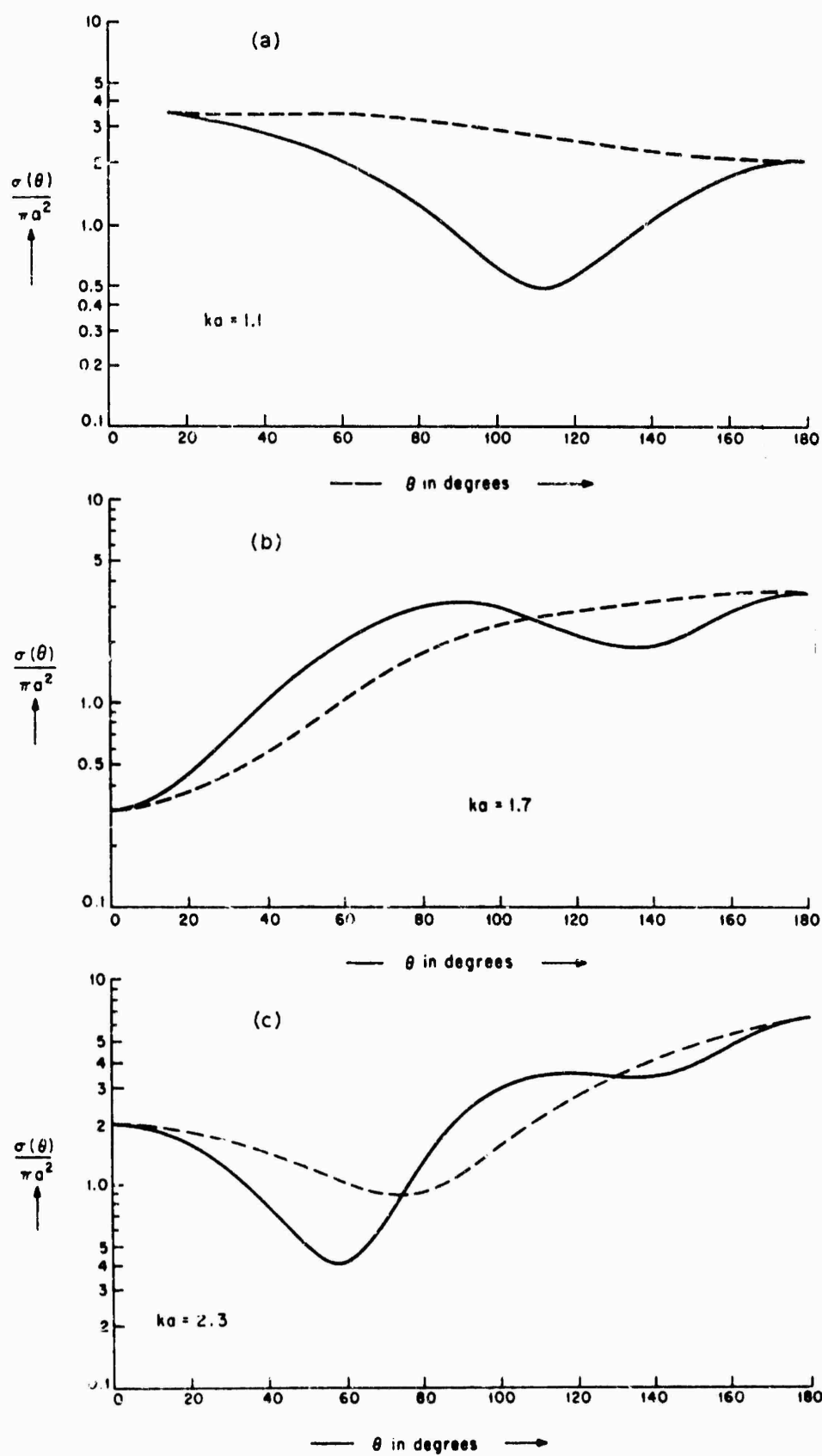
Low frequency expansions may be obtained by power series development of the Bessel functions appearing in the exact expansions (RAYLEIGH [1872]) or directly (KLEINMAN [1965]). The first few coefficients appearing in (10.190) and (10.191) are

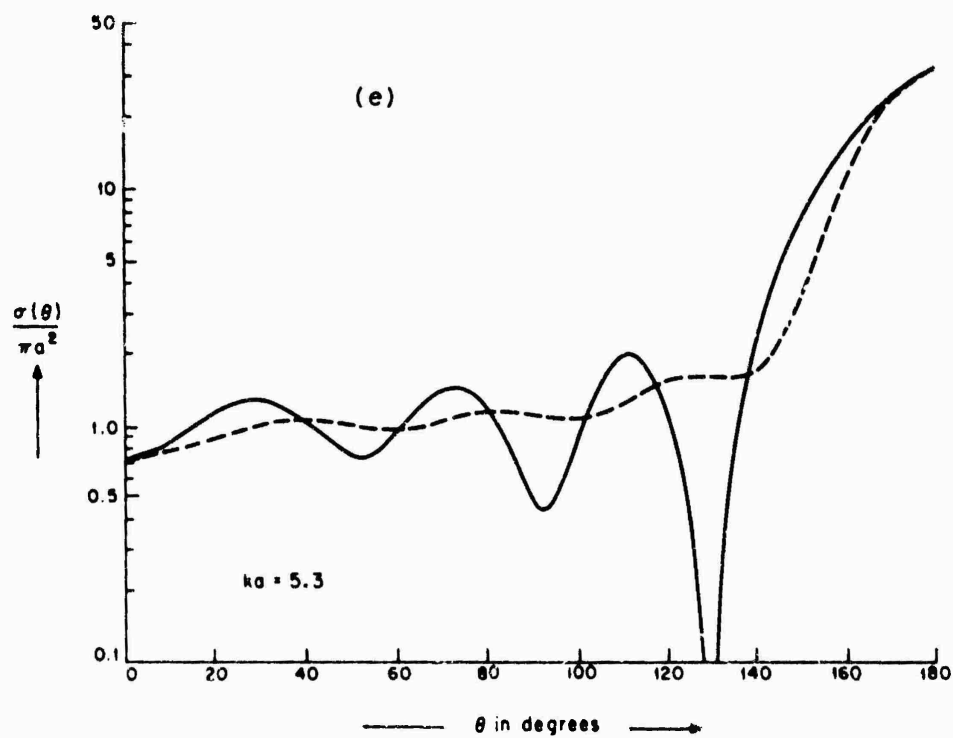
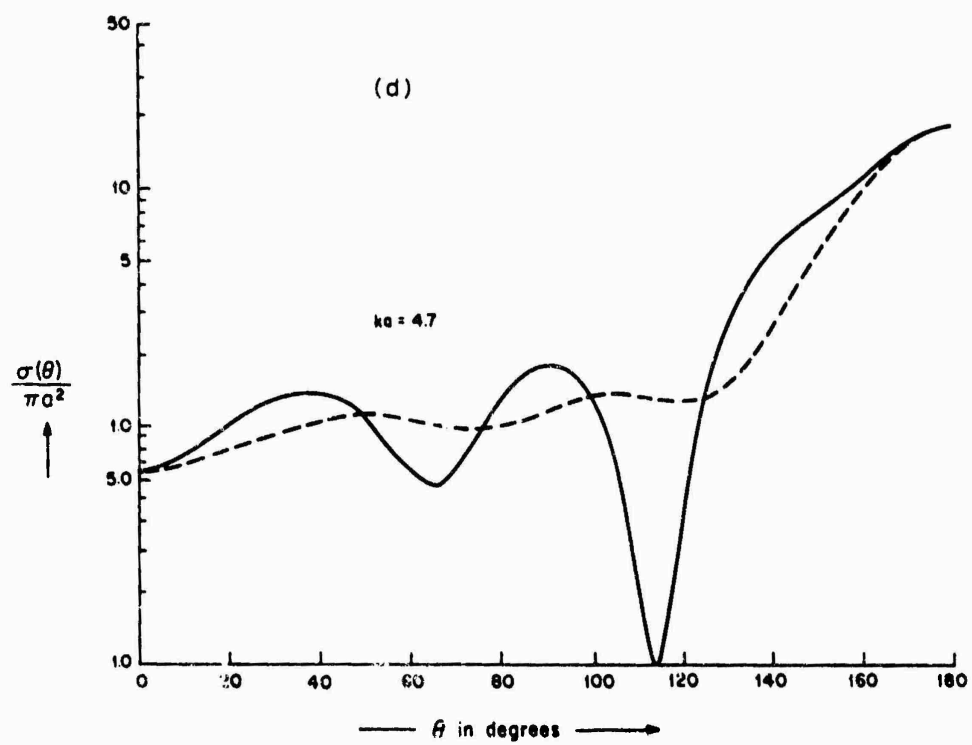
$$a_1 = \frac{1}{3}i(ka)^3 \left[1 - \frac{3}{3}(ka)^2 - \frac{1}{3}i(ka)^3 + \frac{3}{7}(ka)^4 + \frac{2}{5}i(ka)^5 - \frac{1}{27}(ka)^6 - \frac{7}{175}i(ka)^7 + \right. \\ \left. + \frac{6}{165}(ka)^8 + \frac{1}{2835}i(ka)^9 \right] + O[(ka)^{13}],$$

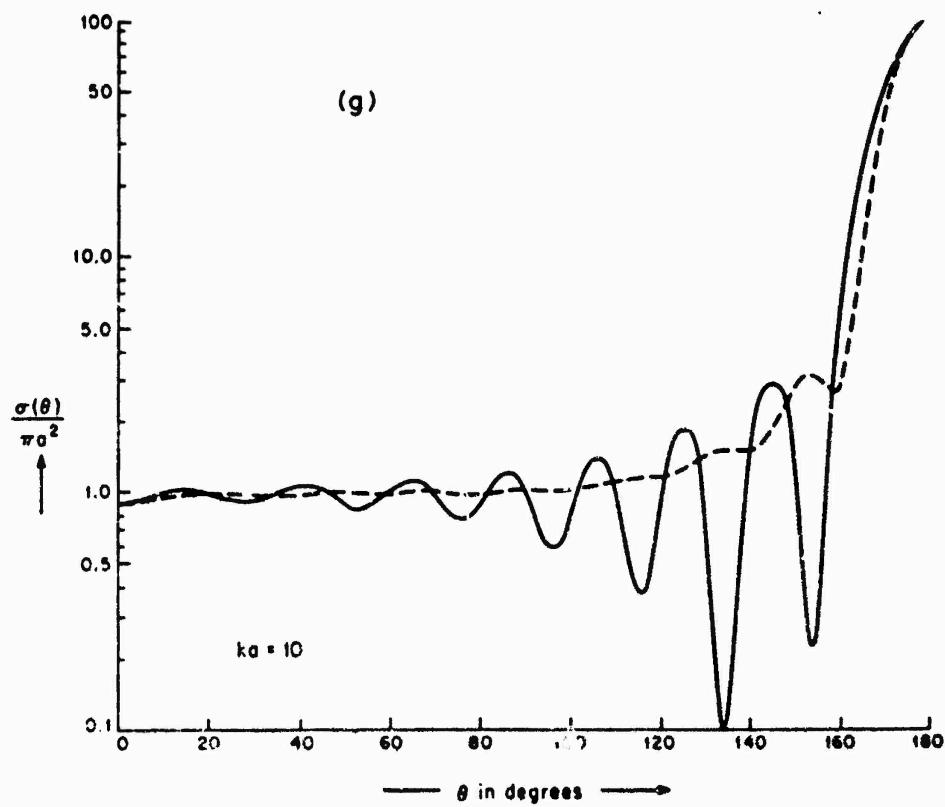
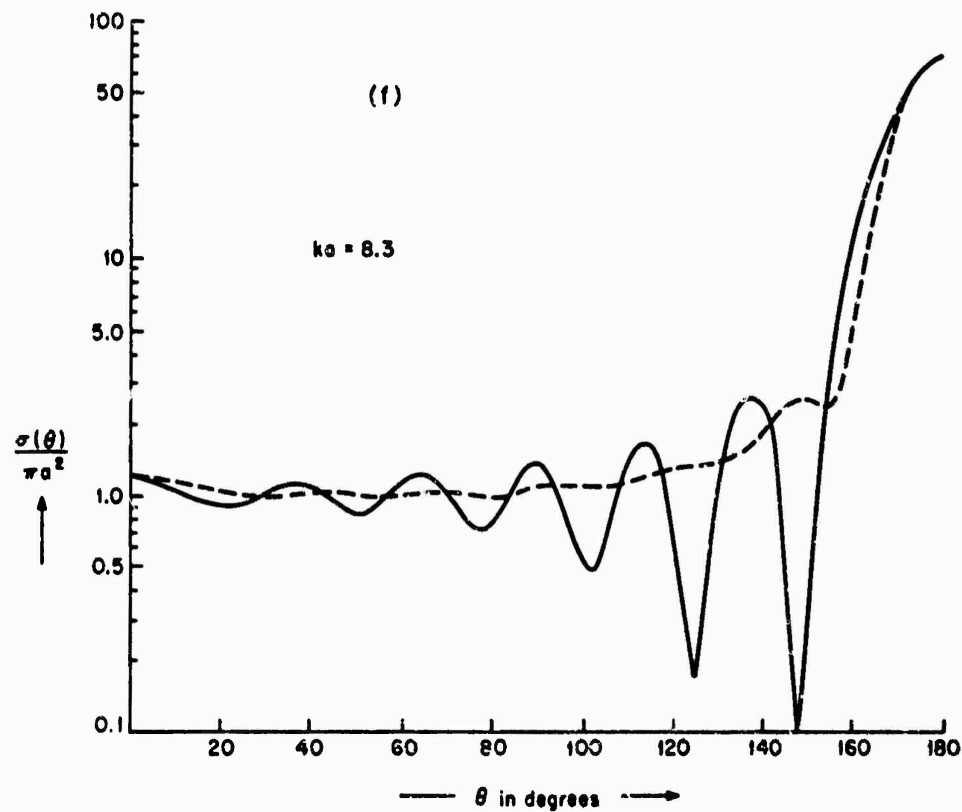
$$b_1 = -\frac{2}{3}i(ka)^3 \left[1 + \frac{3}{10}(ka)^2 + \frac{2}{3}i(ka)^3 - \frac{3}{4}(ka)^4 + \frac{2}{5}i(ka)^5 - \frac{1}{27}(ka)^6 - \frac{7}{350}i(ka)^7 - \right. \\ \left. - \frac{1}{330}(ka)^8 - \frac{1}{2835}i(ka)^9 \right] + O[(ka)^{13}],$$

$$a_2 = \frac{1}{45}i(ka)^5 \left[1 - \frac{5}{21}(ka)^2 - \frac{1}{45}i(ka)^3 + \frac{5}{9}(ka)^4 + \frac{2}{189}i(ka)^5 + \frac{1}{189}i(ka)^7 \right] + O[(ka)^{13}],$$

$$b_2 = -\frac{1}{30}i(ka)^5 \left[1 - \frac{5}{21}(ka)^2 + \frac{1}{108}(ka)^4 + \frac{1}{30}i(ka)^3 - \right. \\ \left. - \frac{5}{252}(ka)^6 - \frac{1}{252}i(ka)^7 \right] + O[(ka)^{13}],$$







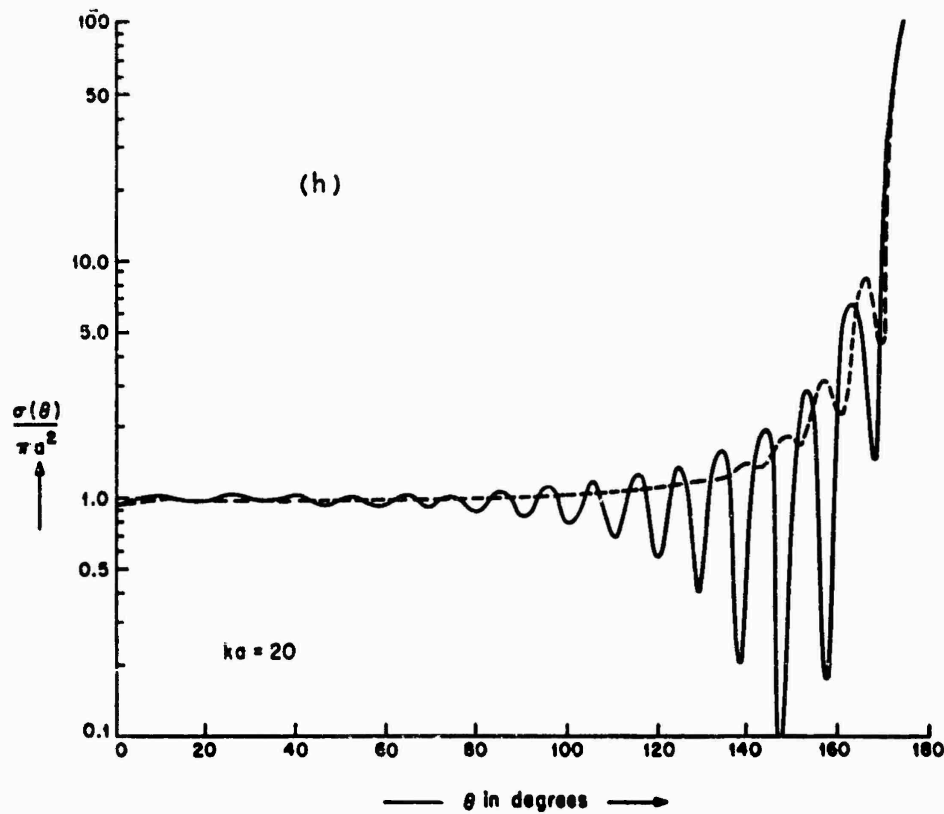


Fig. 10.23. Normalized bistatic cross sections $\sigma(\theta, 0)/(\pi a^2)$ (—) and $\sigma(\theta, \frac{1}{2}\pi)/(\pi a^2)$ (---) as functions of θ for selected values of ka (KING and WU [1959]).

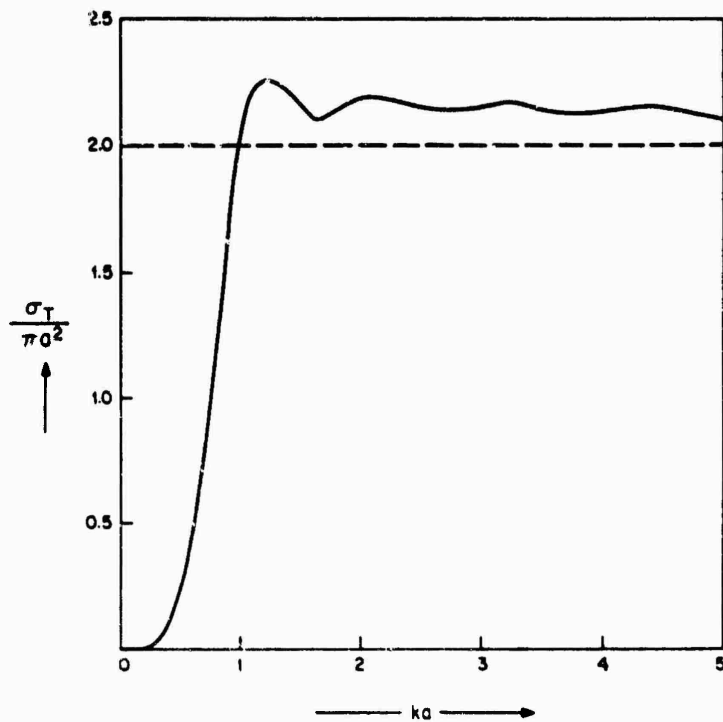


Fig. 10.24. Normalized total scattering cross section $\sigma_T/(\pi a^2)$ as a function of ka for a conducting sphere (VAN DE HULST [1957]).

$$\begin{aligned}
a_3 &= \frac{1}{1373} i(ka)^7 \left[1 - \frac{7}{43}(ka)^2 + \frac{7}{823}(ka)^4 \right] + O[(ka)^{13}], \\
b_3 &= -\frac{4}{723} i(ka)^7 \left[1 - \frac{7}{60}(ka)^2 + \frac{91}{900}(ka)^4 \right] + O[(ka)^{13}], \\
a_4 &= \frac{1}{9(105)^2} i(ka)^9 \left[1 - \frac{9}{77}(ka)^2 \right] + O[(ka)^{13}], \\
b_4 &= -\frac{1}{5(126)^2} i(ka)^9 \left[1 - \frac{153}{1340}(ka)^2 \right] + O[(ka)^{13}], \\
a_5 &= \frac{1}{11(945)^2} i(ka)^{11} + O[(ka)^{13}], \\
b_5 &= -\frac{2}{165(315)^2} i(ka)^{11} + O[(ka)^{13}].
\end{aligned} \tag{10.197}$$

From these, the far fields may be obtained. In particular, to the leading order in ka :

$$E^* \sim (ka)^3 \frac{e^{ikr}}{kr} \left[\left(\frac{1}{2} + \cos \theta \right) \cos \phi \hat{\theta} - \left(1 + \frac{1}{2} \cos \theta \right) \sin \phi \hat{\phi} \right]. \tag{10.198}$$

In the back and forward directions:

$$\begin{aligned}
S(0) &= \frac{3}{2}(ka)^3 \left\{ 1 - \frac{5}{34}(ka)^2 + \frac{1}{3}i(ka)^3 + \frac{17}{900}(ka)^4 + \frac{2}{5}i(ka)^5 - \frac{6651923}{7938000}(ka)^6 + \right. \\
&\quad \left. + \frac{1951}{6804}i(ka)^7 - \frac{249170261}{1875352500}(ka)^8 - \frac{5795}{20412}i(ka)^9 \right\} + O[(ka)^{13}],
\end{aligned} \tag{10.199}$$

$$\begin{aligned}
S(\pi) &= \frac{1}{2}(ka)^3 \left\{ 1 + \frac{113}{90}(ka)^2 + \frac{5}{3}i(ka)^3 - \frac{1783}{2100}(ka)^4 + \frac{2}{5}i(ka)^5 - \frac{670057}{7938000}(ka)^6 - \right. \\
&\quad \left. - \frac{2137}{5670}i(ka)^7 - \frac{249170261}{1875352500}(ka)^8 - \frac{56689}{34020}i(ka)^9 \right\} + O[(ka)^{13}].
\end{aligned} \tag{10.200}$$

The scattering cross sections may be obtained from the above expressions. In particular:

$$\frac{\sigma}{\pi a^2} \sim 9(ka)^4 \left[1 - \frac{5}{27}(ka)^2 + \frac{3379}{72900}(ka)^4 - \frac{18674419}{119070000}(ka)^6 \right], \tag{10.201}$$

$$\frac{\sigma_T}{\pi a^2} \sim \frac{10}{3}(ka)^4 \left[1 + \frac{6}{25}(ka)^2 - \frac{2137}{94500}(ka)^4 - \frac{56689}{567000}(ka)^6 \right]. \tag{10.202}$$

10.4.3.3. HIGH FREQUENCY APPROXIMATIONS

For a plane wave incident in the direction of the negative z -axis such that

$$E^i = \hat{x}e^{-ikz}, \quad H^i = -\hat{y}Ye^{-ikz}, \tag{10.203}$$

the high frequency behavior of the diffracted fields may be obtained by applying a Watson transform technique to the Mie series solutions.

In the shadow region $(\frac{1}{2}\pi + m^{-1}) \lesssim \theta < \pi$ and for $ka \sin \theta \gg 1$, the total field on the surface $r = a$ is

$$\begin{aligned}
H_\theta^i + H_\theta^s &\sim -i \frac{Y \sin \phi}{\sin \theta} \left[\frac{1}{\sin \theta} \sum_{l=0}^{\infty} (-1)^l \{ e^{ikan_l} f(m\eta_l) - ie^{ikan_l} f(m\bar{\eta}_l) \} - \right. \\
&\quad \left. - \frac{1}{2m^3} \frac{1}{\sin \theta} \sum_{l=0}^{\infty} (-1)^l \{ e^{ikan_l} g(m\eta_l) + ie^{ikan_l} g(m\bar{\eta}_l) \} \right],
\end{aligned} \tag{10.204}$$

$$H_{\phi}^i + H_{\phi}^s \sim - \frac{Y \cos \phi}{\sqrt{\sin \theta}} \left[\sum_{l=0}^{\infty} (-1)^l \{ e^{ika\eta_l} g(m\eta_l) - ie^{ika\bar{\eta}_l} g(m\bar{\eta}_l) \} - \frac{1}{2m^4} \frac{1}{\sin \theta} \sum_{l=0}^{\infty} (-1)^l \{ e^{ika\eta_l} f(m\eta_l) + ie^{ika\bar{\eta}_l} f(m\bar{\eta}_l) \} \right], \quad (10.205)$$

where

$$\begin{aligned} \eta_l &= (2l\pi + \theta - \tfrac{1}{2}\pi), \\ \bar{\eta}_l &= (2l\pi + \tfrac{3}{2}\pi - \theta), \end{aligned} \quad (10.206)$$

and the modified Fock functions $f(\xi)$ and $g(\xi)$ are defined in the Introduction.

In eqs. (10.204) and (10.205) the summation over l represents the contribution due to two groups of creeping waves which are launched at the shadow boundary on the surface of the sphere. These waves travel toward the point θ, ϕ along a geodesic. The dominant contribution is provided by the $l = 0$ terms which are the creeping waves that travel the distances $a(\theta - \frac{1}{2}\pi)$ and $a(\frac{3}{2}\pi - \theta)$ along the surface before reaching the point θ, ϕ . Higher order terms represent the contribution due to these waves after they have traveled l times around the sphere before reaching the point θ, ϕ . For computational purposes, the $l = 0$ terms are adequate in eqs. (10.204) and (10.205). For large positive values of ξ the function $f(\xi)$ tends towards zero much faster than the $g(\xi)$ function. This justifies the inclusion of the second summation in eq. (10.204). In contrast to this, the second summation in eq. (10.205) does not contribute appreciably to the field and is included only for symmetry. Eqs. (10.204) and (10.205) are not valid at $\theta = \pi$.

For $\theta \sim \pi$ the surface fields are:

$$\begin{aligned} H_{\theta}^i + H_{\theta}^s &\sim Y \sin \phi e^{-\frac{1}{2}i\pi} \sqrt{\pi m} \left(\frac{\pi - \theta}{\sin \theta} \right)^{\frac{1}{2}} \sum_{l=0}^{\infty} (-1)^l e^{ika(2l + \frac{1}{2})\pi} \\ &\times \left[\{ H_1^{(2)}[ka(\pi - \theta)] f(m\eta_l) + H_1^{(1)}[ka(\pi - \theta)] f(m\bar{\eta}_l) \} + \right. \\ &\left. + \frac{i}{2m^2 \sin \theta} \{ H_1^{(2)}[ka(\pi - \theta)] g(m\eta_l) + H_1^{(1)}[ka(\pi - \theta)] g(m\bar{\eta}_l) \} \right], \quad (10.207) \end{aligned}$$

$$\begin{aligned} H_{\phi}^i + H_{\phi}^s &\sim Y \cos \phi e^{\frac{1}{2}i\pi} \sqrt{\pi m} \left(\frac{\pi - \theta}{\sin \theta} \right)^{\frac{1}{2}} \sum_{l=0}^{\infty} (-1)^l e^{ika(2l + \frac{1}{2})\pi} \\ &\times \left[\{ H_1^{(2)}[ka(\pi - \theta)] g(m\eta_l) + H_1^{(1)}[ka(\pi - \theta)] g(m\bar{\eta}_l) \} - \right. \\ &\left. - \frac{i}{2m^4 \sin \theta} \{ H_1^{(2)}[ka(\pi - \theta)] f(m\eta_l) + H_1^{(1)}[ka(\pi - \theta)] f(m\bar{\eta}_l) \} \right]. \quad (10.208) \end{aligned}$$

For computational purposes it is sufficient to use the leading terms $l = 0$ in eqs. (10.207) and (10.208), namely (BELKINA and WEINSTEIN [1957]):

$$H_{\theta}^i + H_{\theta}^s \sim -Y \sin \phi \sqrt{\pi m^{\frac{1}{2}}} \left(\frac{\pi - \theta}{\sin \theta} \right)^{\frac{1}{2}} e^{\frac{1}{2}i(ka + \frac{1}{2})\pi} \\ \times \left[2f(\frac{1}{2}m\pi)J_1'[ka(\pi - \theta)] + \frac{i}{m^2 \sin \theta} g(\frac{1}{2}m\pi)J_1[ka(\pi - \theta)] \right], \quad (10.209)$$

$$H_{\phi}^i + H_{\phi}^s \sim iY \cos \phi \sqrt{\pi m^{\frac{1}{2}}} \left(\frac{\pi - \theta}{\sin \theta} \right)^{\frac{1}{2}} e^{\frac{1}{2}i(ka + \frac{1}{2})\pi} \\ \times \left[2g(\frac{1}{2}m\pi)J_1'[ka(\pi - \theta)] - \frac{i}{m^2 \sin \theta} f(\frac{1}{2}m\pi)J_1[ka(\pi - \theta)] \right]. \quad (10.210)$$

In the forward direction $\theta = \pi$:

$$H_{\theta}^i + H_{\theta}^s \sim -Y \sin \phi \pi^{\frac{1}{2}} m^{\frac{1}{2}} e^{\frac{1}{2}i(ka + \frac{1}{2})\pi} \left\{ \frac{1}{m} f(\frac{1}{2}m\pi) + ig(\frac{1}{2}m\pi) \right\}, \quad (10.211)$$

$$H_{\phi}^i + H_{\phi}^s \sim Y \cos \phi \pi^{\frac{1}{2}} m^{\frac{1}{2}} e^{\frac{1}{2}i(ka + \frac{1}{2})\pi} \left\{ \frac{1}{m} f(\frac{1}{2}m\pi) + ig(\frac{1}{2}m\pi) \right\}, \quad (10.212)$$

which imply that the magnetic field is polarized in the y -direction.

In the lit region ($0 \leq \theta \lesssim \frac{1}{2}\pi - m^{-1}$) the total field on the surface $r = a$ is

$$\mathbf{H} = \mathbf{H}_{\text{refl.}} + \mathbf{H}_{\text{cr.w.}} \quad (10.213)$$

The reflected field is

$$(H_{\theta}^i + H_{\theta}^s)_{\text{refl.}} \sim -2Y \cos \theta \sin \phi e^{-ika \cos \theta} \\ \times \left[1 + \frac{i \sin^2 \theta}{2ka \cos^3 \theta} + \frac{5 \sin^2 \theta - \sin^4 \theta}{2(ka)^2 \cos^5 \theta} + \dots \right], \quad (10.214)$$

$$(H_{\phi}^i + H_{\phi}^s)_{\text{refl.}} \sim -2Y \cos \phi e^{-ika \cos \theta} \left[1 - \frac{i \sin^2 \theta}{2ka \cos^3 \theta} - \frac{9 \sin^2 \theta - \sin^4 \theta}{2(ka)^2 \cos^5 \theta} + \dots \right], \quad (10.215)$$

and the leading terms in eqs. (10.214) and (10.215) represent the geometrical surface field.

The creeping wave contribution to the surface field for $m^{-1} \lesssim \theta \lesssim \frac{1}{2}\pi - m^{-1}$, and $ka \sin \theta \gg 1$ is:

$$(H_{\theta}^i + H_{\theta}^s)_{\text{cr.w.}} \sim i \frac{Y \sin \phi}{\sqrt{\sin \theta}} \\ \times \left[\frac{1}{m} \sum_{l=0}^{\infty} (-1)^l \{ \exp(ika\eta_{l+1}) f(m\eta_{l+1}) + i \exp(ika\bar{\eta}_l) f(m\bar{\eta}_l) \} - \right. \\ \left. - \frac{1}{2m^3 \sin \theta} \sum_{l=0}^{\infty} (-1)^l \{ \exp(ika\eta_{l+1}) g(m\eta_{l+1}) - i \exp(ika\bar{\eta}_l) g(m\bar{\eta}_l) \} \right], \quad (10.216)$$

$$(H_{\phi}^i + H_{\phi}^s)_{cr.w.} \sim \frac{Y \cos \phi}{\sqrt{\sin \theta}} \left[\sum_{l=0}^{\infty} (-1)^l \{ \exp(ika\eta_{l+1})g(m\eta_{l+1}) + i \exp(ika\bar{\eta}_l)g(m\bar{\eta}_l) \} - \right. \\ \left. - \frac{1}{2m^4 \sin \theta} \sum_{l=0}^{\infty} (-1)^l \{ \exp(ika\eta_{l+1})f(m\eta_{l+1}) - i \exp(ika\bar{\eta}_l)f(m\bar{\eta}_l) \} \right], \quad (10.217)$$

whereas for $0 \lesssim \theta \lesssim m^{-1}$,

$$(H_{\theta}^i + H_{\theta}^s)_{cr.w.} \sim Y\pi^{\frac{1}{2}}m^{\frac{3}{2}} \sin \phi \left(\frac{\theta}{\sin \theta} \right)^{\frac{1}{2}} e^{-\frac{1}{2}i\pi} \\ \times \left[\frac{i}{m} \sum_{l=0}^{\infty} (-1)^l e^{ika(2l\pi + \frac{1}{2}\pi)} \{ H_1^{(1)'}(ka\theta)f(m\eta_{l+1}) + H_1^{(2)'}(ka\theta)f(m\bar{\eta}_l) \} + \right. \\ \left. + \frac{1}{ka \sin \theta} \sum_{l=0}^{\infty} (-1)^l e^{ika(2l\pi + \frac{1}{2}\pi)} \{ H_1^{(1)}(ka\theta)g(m\eta_{l+1}) + H_1^{(2)}(ka\theta)g(m\bar{\eta}_l) \} \right], \quad (10.218)$$

$$(H_{\phi}^i + H_{\phi}^s)_{cr.w.} \sim Y\pi^{\frac{1}{2}}m^{\frac{3}{2}} \cos \phi \left(\frac{\theta}{\sin \theta} \right)^{\frac{1}{2}} e^{-\frac{1}{2}i\pi} \\ \times \left[\sum_{l=0}^{\infty} (-1)^l e^{ika(2l\pi + \frac{1}{2}\pi)} \{ H_1^{(1)'}(ka\theta)g(m\eta_{l+1}) + H_1^{(2)'}(ka\theta)g(m\bar{\eta}_l) \} + \right. \\ \left. + \frac{i}{mka \sin \theta} \sum_{l=0}^{\infty} (-1)^l e^{ika(2l\pi + \frac{1}{2}\pi)} \{ H_1^{(1)}(ka\theta)f(m\eta_{l+1}) + H_1^{(2)}(ka\theta)f(m\bar{\eta}_l) \} \right]. \quad (10.219)$$

For computational purposes it is sufficient to use the leading terms $l = 0$ in eqs. (10.218)–(10.219). For $0 \lesssim \theta \lesssim m^{-1}$ these leading terms are (BELKINA and WEINSTEIN [1957]):

$$(H_{\theta}^i + H_{\theta}^s)_{cr.w.} \sim 2Y\pi^{\frac{1}{2}}m^{\frac{3}{2}} e^{\frac{1}{2}i(ka - \frac{1}{2})\pi} \sin \phi \left(\frac{\theta}{\sin \theta} \right)^{\frac{1}{2}} \\ \times \left[\frac{J_1(ka\theta)}{ka\theta} g(\frac{1}{2}m\pi) + \frac{i}{m} J_1'(ka\theta)f(\frac{1}{2}m\pi) \right], \quad (10.220)$$

$$(H_{\phi}^i + H_{\phi}^s)_{cr.w.} \sim 2Y\pi^{\frac{1}{2}}m^{\frac{3}{2}} e^{\frac{1}{2}i(ka - \frac{1}{2})\pi} \cos \phi \left(\frac{\theta}{\sin \theta} \right)^{\frac{1}{2}} \\ \times \left[J_1'(ka\theta)g(\frac{1}{2}m\pi) + \frac{i}{m} \frac{J_1(ka\theta)}{ka\theta} f(\frac{1}{2}m\pi) \right]. \quad (10.221)$$

For $\theta \rightarrow 0$,

$$(H_{\theta}^i + H_{\theta}^s)_{cr.w.} \sim Y\pi^{\frac{1}{2}}m^{\frac{3}{2}} e^{\frac{1}{2}i(ka - \frac{1}{2})\pi} \sin \phi \left[g(\frac{1}{2}m\pi) + \frac{i}{m} f(\frac{1}{2}m\pi) \right], \quad (10.222)$$

$$(H_{\phi}^i + H_{\phi}^s)_{cr.w.} \sim Y\pi^{\frac{1}{2}}m^{\frac{3}{2}} e^{\frac{1}{2}i(ka - \frac{1}{2})\pi} \cos \phi \left[g(\frac{1}{2}m\pi) + \frac{i}{m} f(\frac{1}{2}m\pi) \right], \quad (10.223)$$

which implies that the magnetic field is polarized in the y -direction.

In the transition region $|\frac{1}{2}\pi - \theta| \lesssim m^{-1}$ the total field on the surface is

$$H_\theta^i + H_\theta^s \sim i \frac{Y \sin \phi}{m \sqrt{\sin \theta}} [\exp(-ika \cos \theta) f(-m \cos \theta) + \sum_{l=0}^{\infty} (-1)^l \{\exp(ika\eta_{l+1}) f(\eta_{l+1}) + i \exp(ika\bar{\eta}_l) f(\bar{\eta}_l)\}], \quad (10.224)$$

$$H_\phi^i + H_\phi^s \sim \frac{Y \cos \phi}{\sqrt{\sin \theta}} [\exp(-ika \cos \theta) f(-m \cos \theta) + \sum_{l=0}^{\infty} (-1)^l \{\exp(ika\eta_{l+1}) g(\eta_{l+1}) + i \exp(ika\bar{\eta}_l) g(\bar{\eta}_l)\}]. \quad (10.225)$$

In the back scattering direction ($\theta = 0$) an asymptotic expansion of the reflected portion of the scattered field, uniform in r , $a \leq r < \infty$, is (WESTON [1961]):

$$E^s \sim -\hat{x} \frac{a}{2r-a} e^{ik(r-2a)} \left[1 + \frac{a_1}{ka} + \frac{a_2}{(ka)^2} + \dots \right], \quad (10.226)$$

where

$$a_1 = -2i \frac{(r-a)^2}{(2r-a)^2},$$

$$a_2 = \frac{a(r-a)(2r^2 - 4ra + 3a^2)}{(2r-a)^4},$$

and, in particular, the near field back scattering cross section $\sigma = 4\pi(r-a)^2 |E^s|^2$ is

$$\sigma = 4\pi a^2 \left(\frac{r-a}{2r-a} \right)^2 \{1 + O[(ka)^{-2}]\}. \quad (10.227)$$

In the far field ($r \rightarrow \infty$) with $0 \leq \theta \lesssim \pi - m^{-1}$ the scattering coefficient is

$$S_1(\theta) = [S_1(\theta)]_{\text{refl.}} + [S_1(\theta)]_{\text{cr.w.}},$$

$$S_2(\theta) = [S_2(\theta)]_{\text{refl.}} + [S_2(\theta)]_{\text{cr.w.}} \quad (10.228)$$

The reflected portion is (LOGAN [1960]):

$$[S_1(\theta)]_{\text{refl.}} \sim -\frac{1}{2}ka e^{-2ika \cos \frac{1}{2}\theta} \left[1 - \frac{i}{2ka \cos^3 \frac{1}{2}\theta} - \frac{7 \sin^2 \frac{1}{2}\theta}{4(ka)^2 \cos^6 \frac{1}{2}\theta} + \frac{8 + 1076 \sin^2 \frac{1}{2}\theta + 1401 \sin^4 \frac{1}{2}\theta + 210 \sin^6 \frac{1}{2}\theta}{16(ka)^4 \cos^{12} \frac{1}{2}\theta} + \dots \right], \quad (10.229)$$

$$[S_2(\theta)]_{\text{refl.}} \sim \frac{1}{2}ka e^{-2ika \cos \frac{1}{2}\theta} \left[1 - i \frac{1 - 2 \sin^2 \frac{1}{2}\theta}{2ka \cos^3 \frac{1}{2}\theta} + \frac{7 \sin^2 \frac{1}{2}\theta - 2 \sin^4 \frac{1}{2}\theta}{4(ka)^2 \cos^6 \frac{1}{2}\theta} - i \frac{63 \sin^2 \frac{1}{2}\theta + 7 \sin^4 \frac{1}{2}\theta}{8(ka)^3 \cos^9 \frac{1}{2}\theta} + \frac{8 - 836 \sin^2 \frac{1}{2}\theta - 683 \sin^4 \frac{1}{2}\theta - 84 \sin^6 \frac{1}{2}\theta}{16(ka)^4 \cos^{12} \frac{1}{2}\theta} + \dots \right], \quad (10.230)$$

where the leading terms in eqs. (10.229) and (10.230) are the geometrical optics contribution.

The creeping wave contribution is

$$[S_1(\theta)]_{\text{cr.w.}} \sim -\frac{2m^{\frac{1}{2}}e^{\frac{1}{2}i\pi}}{\sqrt{\sin \theta}} \sum_{l=0}^{\infty} (-1)^l \{ \tilde{q}(m\tau_l) \exp(ika\tau_l) - i\tilde{q}(m\bar{\tau}_l) \exp(ika\bar{\tau}_l) \} + \\ + \frac{e^{\frac{1}{2}i\pi}}{m^{\frac{1}{2}}(\sin \theta)^{\frac{1}{2}}} \sum_{l=0}^{\infty} (-1)^l \{ i\tilde{p}(m\tau_l) \exp(ika\tau_l) - \tilde{p}(m\bar{\tau}_l) \exp(ika\bar{\tau}_l) \}, \quad (10.231)$$

$$[S_2(\theta)]_{\text{cr.w.}} \sim -\frac{2m^{\frac{1}{2}}e^{\frac{1}{2}i\pi}}{\sqrt{\sin \theta}} \sum_{l=0}^{\infty} (-1)^l \{ \tilde{p}(m\tau_l) \exp(ika\tau_l) - i\tilde{p}(m\bar{\tau}_l) \exp(ika\bar{\tau}_l) \} + \\ + \frac{e^{\frac{1}{2}i\pi}}{m^{\frac{1}{2}}(\sin \theta)^{\frac{1}{2}}} \sum_{l=0}^{\infty} (-1)^l \{ i\tilde{q}(m\tau_l) \exp(ika\tau_l) - \tilde{q}(m\bar{\tau}_l) \exp(ika\bar{\tau}_l) \}, \quad (10.232)$$

where

$$\tau_l = (2l+1)\pi - \theta, \quad (10.233) \\ \bar{\tau}_l = (2l+1)\pi + \theta,$$

and the functions \tilde{p} , \tilde{q} are defined in the Introduction (see eqs. (I.278) and (I.279)).

For computational purposes it is sufficient to retain the $l = 0$ terms in eqs. (10.231) and (10.232). However, it should be noted that the functions \tilde{p} decrease more rapidly than \tilde{q} with increase in the positive argument, and that for large positive arguments the last two terms in eq. (10.232) become comparable to the first two. In eq. (10.231) the second summation terms do not contribute appreciably to $[S_1(\theta)]_{\text{cr.w.}}$; they are retained for symmetry (FEDOROV [1957]).

For $0 \lesssim \theta \lesssim m^{-1}$ (FEDOROV [1957]):

$$[S_1(\theta)]_{\text{cr.w.}} \sim e^{i\pi(ka - \frac{1}{2})} 2m^{\frac{1}{2}}\pi^{\frac{1}{2}} \left(\frac{\theta}{\sin \theta} \right)^{\frac{1}{2}} \\ \times \left\{ \left[\frac{J_1(ka\theta)}{ka\theta} - J_2(ka\theta) \right] [\tilde{q}(m\tau_0) + \tilde{q}(m\bar{\tau}_0)] - \frac{J_1(ka\theta)}{ka \sin \theta} [\tilde{p}(m\tau_0) + \tilde{p}(m\bar{\tau}_0)] + \right. \\ \left. + i \left[\frac{J_2(ka\theta)}{ka\theta} - J_1(ka\theta) \right] [\tilde{q}(m\tau_0) - \tilde{q}(m\bar{\tau}_0)] + i \frac{J_2(ka\theta)}{ka \sin \theta} [\tilde{p}(m\tau_0) - \tilde{p}(m\bar{\tau}_0)] \right\}. \quad (10.234)$$

$$[S_2(\theta)]_{\text{cr.w.}} \sim e^{i\pi(ka - \frac{1}{2})} 2m^{\frac{1}{2}}\pi^{\frac{1}{2}} \left(\frac{\theta}{\sin \theta} \right)^{\frac{1}{2}} \\ \times \left\{ \left[\frac{J_1(ka\theta)}{ka\theta} - J_2(ka\theta) \right] [\tilde{p}(m\tau_0) + \tilde{p}(m\bar{\tau}_0)] - \frac{J_1(ka\theta)}{ka \sin \theta} [\tilde{q}(m\tau_0) + \tilde{q}(m\bar{\tau}_0)] + \right. \\ \left. + i \left[\frac{J_2(ka\theta)}{ka\theta} - J_1(ka\theta) \right] [\tilde{p}(m\tau_0) - \tilde{p}(m\bar{\tau}_0)] + i \frac{J_2(ka\theta)}{ka \sin \theta} [\tilde{q}(m\tau_0) - \tilde{q}(m\bar{\tau}_0)] \right\}; \quad (10.235)$$

more refined expressions are given by SENIOR and GOODRICH [1964].

In the back scattering direction $\theta = 0$ (SCOTT [1949], LOGAN [1960]):

$$[S_1(0)]_{\text{refl.}} = -[S_2(0)]_{\text{refl.}} = -\frac{1}{2}ka e^{-2ika} \left\{ 1 - \frac{i}{2ka} + \frac{1}{2(ka)^4} + O[(ka)^{-5}] \right\}, \quad (10.236)$$

and (SENIOR [1965], SCOTT [1949]):

$$\begin{aligned} [S_1(0)]_{\text{cr.w.}} = -[S_2(0)]_{\text{cr.w.}} = & m^4 e^{i\pi} \sum_{n=1}^{\infty} \left\{ 1 + \frac{e^{i\pi}}{60m^2 \beta_n^2} (32\beta_n^3 + 9) - \right. \\ & - \frac{e^{-i\pi}}{5600m^4 \beta_n^4} (128\beta_n^6 + 189) + O(m^{-6}) \left. \right\} \frac{1}{\beta_n \{ \text{Ai}(-\beta_n) \}^2} \\ & \times \sum_{l=0}^{\infty} (-1)^l \exp \left[i(2l+1)\pi \left\{ ka + e^{i\pi} m \beta_n - \frac{e^{-i\pi}}{60m \beta_n} (\beta_n^3 - 9) + \right. \right. \\ & + \left. \frac{1}{1400m^3 \beta_n^3} (\beta_n^6 - 7\beta_n^3 + \frac{6}{4}) + O(m^{-6}) \right\} \left. \right] - m^4 e^{i\pi} \sum_{n=1}^{\infty} \left\{ 1 + \frac{e^{i\pi} 8\alpha_n}{15m^2} - \right. \\ & - \frac{e^{-i\pi} 4\alpha_n^2}{175m^4} + O(m^{-6}) \left. \right\} \frac{1}{\{ \text{Ai}'(-\alpha_n) \}^2} \sum_{l=0}^{\infty} (-1)^l \exp \left[i(2l+1)\pi \left\{ ka + e^{i\pi} m \alpha_n - \right. \right. \\ & - \left. \frac{e^{-i\pi} \alpha_n^2}{60m} + \frac{\alpha_n^3 - 10}{1400m^3} + O(m^{-5}) \right\} \left. \right]. \quad (10.237) \end{aligned}$$

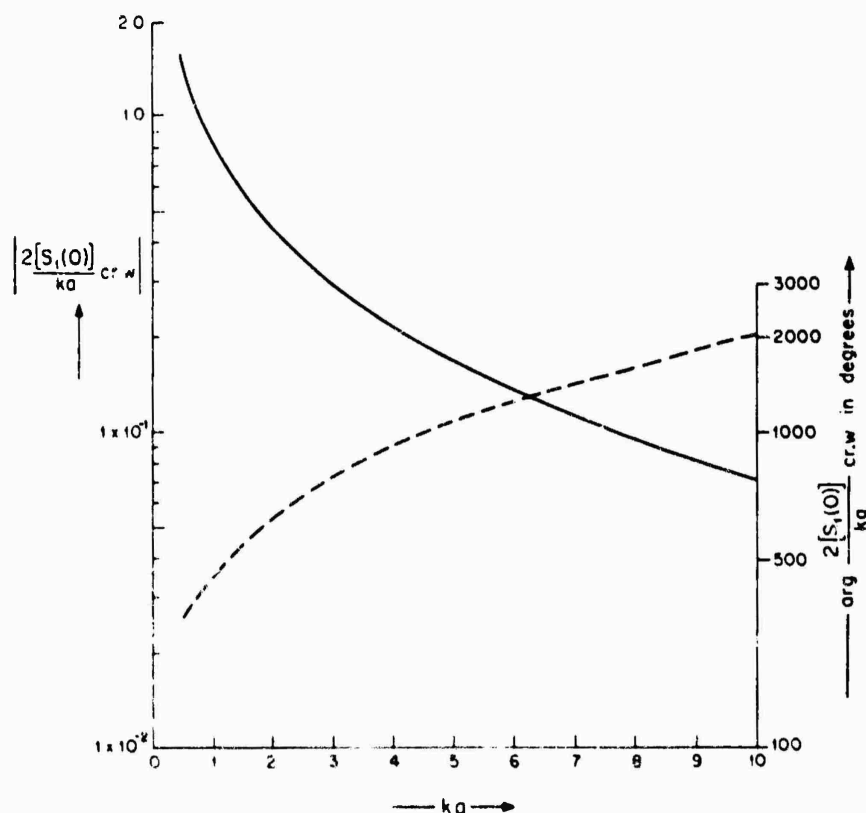


Fig. 10.25. Amplitude (—) and phase (---) of the normalized creeping wave contribution $2[S_1(0)]_{\text{cr.w.}}/(ka)$ as a function of ka for a conducting sphere (SENIOR [1965]).

The magnitude of various terms in eq. (10.237) has been discussed by SENIOR [1965] and for most computational purposes an adequate approximation is

$$[S_1(0)]_{cr.w.} = -[S_2(0)]_{cr.w.} = m^4 e^{i\pi} \left\{ 1 + \frac{e^{i\pi}}{60m^2 \beta_1^2} (32\beta_1^3 + 9) + O(m^{-4}) \right\} \\ \times \frac{1}{\beta_1 \{Ai(-\beta_1)\}^2} \exp \left\{ i\pi ka - e^{-i\pi} m\pi\beta_1 - \frac{e^{i\pi}}{60m\beta_1} (\beta_1^3 - 9) + O(m^{-6}) \right\}. \quad (10.238)$$

The normalized creeping wave contribution $2[S_1(0)]_{cr.w.}/(ka)$ as computed from eq. (10.238) is shown in Fig. 10.25 as a function of ka .

In the forward direction $\theta = \pi$ (SENIOR and GOODRICH [1964]):

$$S_1(\pi) = S_2(\pi) = -\frac{1}{2}i[(ka)^2 - \frac{1}{12}] + 2\sqrt{\pi}m^4 \left\{ p^{(0)} + q^{(0)} - \frac{1}{m^2} [\frac{1}{2}i(p^{(1)} + q^{(1)}) + \right. \\ \left. + \frac{1}{60}(r_0^{(2)} + 9s_0^{(0)} + is_0^{(3)})] - \frac{1}{m^4} [\frac{1}{140}(r_0^{(0)} - \frac{8}{90}ir_0^{(3)}) - \frac{1}{3600}r_1^{(4)} + \right. \\ \left. + \frac{1}{100}i(-\frac{1}{2}s_0^{(1)} + \frac{3}{504}is_0^{(4)}) + \frac{1}{400}(9s_1^{(0)} + 2is_1^{(3)} - \frac{1}{9}s_1^{(6)})] + O(m^{-6}) \right\} - \\ -im^4 e^{i\pi} \sum_{n=1}^{\infty} \frac{1}{\beta_n [Ai(-\beta_n)]^2} \left[1 + \frac{e^{i\pi}}{60m} \left(32\beta_n + \frac{9}{\beta_n^2} \right) + O(m^{-6}) \right] \\ \times \sum_{l=0}^{\infty} (-1)^l \exp \left\{ 2i\pi(l+1) \left[ka + m\beta_n e^{i\pi} + \frac{e^{i\pi}}{60m} \left(\beta_n^2 - \frac{9}{\beta_n} \right) \right] \right\} - \\ -im^4 e^{i\pi} \sum_{n=1}^{\infty} \frac{1}{[Ai(-\alpha_n)]^2} \left[1 + \frac{8\alpha_n}{15m^2} e^{i\pi} + O(m^{-4}) \right] \\ \times \sum_{l=0}^{\infty} (-1)^l \exp \left\{ 2i\pi(l+1) \left[ka + m\alpha_n e^{i\pi} + \frac{\alpha_n^2}{60m} e^{i\pi} \right] \right\}, \quad (10.239)$$

where

$$p^{(n)} = \left\{ \frac{1}{\sqrt{\pi}} \frac{\partial^n}{\partial t^n} \left[\int_0^x e^{ixt} \frac{v(x)}{w_1(x)} dx + \frac{1}{2}i \int_{-\infty}^0 e^{ixt} \frac{w_2(x)}{w_1(x)} dx \right] \right\}_{t=0}, \\ q^{(n)} = \left\{ \frac{1}{\sqrt{\pi}} \frac{\partial^n}{\partial t^n} \left[\int_0^x e^{ixt} \frac{v'(x)}{w_1'(x)} dx + \frac{1}{2}i \int_{-\infty}^0 e^{ixt} \frac{w_2'(x)}{w_1'(x)} dx \right] \right\}_{t=0}, \\ r_m^{(n)} = \left\{ \frac{1}{\sqrt{\pi}} \frac{\partial^n}{\partial t^n} \int_{-\infty}^x e^{ixt} \frac{1}{[w_1(x)]^2} \left[\frac{w_1'(x)}{w_1(x)} \right]^m dx \right\}_{t=0}, \\ s_m^{(n)} = \left\{ \frac{1}{\sqrt{\pi}} \frac{\partial^n}{\partial t^n} \int_{-\infty}^x e^{ixt} \frac{1}{[w_1'(x)]^2} \left[\frac{w_1(x)}{w_1'(x)} \right]^m dx \right\}_{t=0}.$$

are as defined in LOGAN [1959]. By neglecting the summations over l and n in eq. (10.239),

$$\begin{aligned}
 S_1(\pi) &= S_2(\pi) \\
 &= -i(2m^6 - \tfrac{1}{2}i) - im^4(0.082972 + 0.144019i) - im^2(0.385229 - 0.667169i) - \\
 &\quad - 0.069342i + O(m^{-2}).
 \end{aligned} \tag{10.240}$$

The total cross section is (BECKMANN and FRANZ [1957], WU [1956]):

$$\frac{\sigma_T}{2\pi a^2} = 1 + 0.0660(ka)^{-\frac{1}{2}} + 0.4853(ka)^{-\frac{3}{2}} + O[(ka)^{-2}]. \tag{10.241}$$

Bibliography

- BECHTEL, M. E. [1962], Scattering Coefficients for the Backscattering of Electromagnetic Waves from Perfectly Conducting Spheres, Cornell Aeronautical Laboratory Report No. AP/RIS-1, Buffalo, New York.
- BECKMANN, P. and W. FRANZ [1957], Berechnung der Streuquerschnitte von Kugel und Zylinder unter Anwendung einer modifizierten Watson-Transformation, *Z. Naturforsch.* **129**, 533-537.
- BILKINA, M. G. and L. A. WEINSTEIN [1957], Radiation Characteristics of Spherical Surface Antennas, in: *Symposium, Diffraction of Electromagnetic Waves on Certain Bodies of Revolution*, 57-125, Soviet Radio, Moscow.
- BORN, M. and E. WOLF [1964], *Principles of Optics*, 633-664, Pergamon Press, New York.
- DEGMANIS, J. A. and V. V. LIEPA [1965], Surface Field Components for a Perfectly Conducting Sphere, The University of Michigan Radiation Laboratory Report No. 5548-3-T, Ann Arbor, Michigan.
- FEDOROV, A. A. [1958], Asymptotic Solution of the Problem of Diffraction of Plane Electromagnetic Waves on Ideally Conducting Spheres, *Radio Eng. Electron. Phys.* **3**, 57-72.
- FRANZ, W. [1954], Über die Greenschen Funktionen des Zylinders und der Kugel, *Z. Naturforsch.* **9a**, 705-716.
- ILEY, J. S., G. S. STEWART, J. T. PINSON and P. E. V. PRINCE [1956], The Scattering of Electromagnetic Waves by Conducting Spheres and Discs, *Proc. Phys. Soc. (Great Britain)* **B 69**, 1038-1049. In the table, f (i.e. $S_1(0)$) should read $\frac{1}{2}f$.
- HUANG, C. and R. D. KODIS [1951], Diffraction by Spheres and Edges at 1.2 cm, Harvard University Cruft Laboratory Technical Report No. 138, Cambridge, Massachusetts.
- JONES, D. S. [1964], *The Theory of Electromagnetism*, The Macmillan Company, New York.
- KELLER, J. B., R. M. LEWIS and B. D. SECKLER [1956], Asymptotic Solution of Some Diffraction Problems, *Comm. Pure Appl. Math.* **9**, 207-255. In eqs. (219) and (221), the terms within the square brackets and containing powers of 2 should be multiplied by 2.
- KING, R. W. P. and T. T. WU [1959], *The Scattering and Diffraction of Waves*, Harvard University Press, Cambridge, Massachusetts.
- KLEINMAN, R. E. [1965], The Rayleigh Region, *Proc. IEEE* **53**, 848-856.
- LEVY, B. R. and J. B. KELLER [1959], Diffraction by a Smooth Object, *Comm. Pure Appl. Math.* **12**, 159-209.
- LOGAN, N. A. [1959], General Research in Diffraction Theory, Vols. 1 and 2, Lockheed Missiles and Space Division Technical Reports LMSD-288087 and LMSD 288088, Sunnyvale, California.
- LOGAN, N. A. [1960], Scattering Properties of Large Spheres, *Proc. IRE* **48**, 1782.
- MORSE, P. M. and H. FESHBACH [1953], *Methods of Theoretical Physics*, Vols. 1 and 2, McGraw-Hill Book Co., Inc., New York.
- NEUSCHNEIG, H. M. [1965], High Frequency Scattering by an Impenetrable Sphere, *Ann. Phys.* **34**, 23-95.
- ROBINSTEIN, J. [1963], Tables of the Amplitude and Phase of the Backscatter from a Conducting Sphere, MIT Lincoln Laboratory Report No. 226-16, Cambridge, Massachusetts.

- RUBINOW, S. I. and T. T. WU [1956], First Correction to the Geometrical-Optics Scattering Cross Section from Cylinders and Spheres, *J. Appl. Phys.* **27**, 1032-1039.
- SCOTT, J. M. C. [1949], An Asymptotic Series for the Radar Cross Section of a Spherical Target, Atomic Energy Research Establishment Technical Memorandum No. T/M-30, Harwell, Berks., England.
- SENIOR, T. B. A. and R. F. GOODRICH [1964], Scattering by a Sphere, *Proc. IEE (London)* **111**, 907-916. Equation (32) should have a negative sign in front. Equations (44), (45) and (54) are incorrect.
- SENIOR, T. B. A. [1965], Analytical and Numerical Studies of the Back Scattering Behavior of Spheres, The University of Michigan Radiation Laboratory Report No. 7030-1-T, Ann Arbor, Michigan. Equation (59) is incorrect: the factor $(2\beta_n^2 + 9)$ within the curly bracket should be replaced by $(32\beta_n^2 - 21)$.
- SOMMERFELD, A. [1949], *Partial Differential Equations in Physics*, Academic Press, Inc., New York.
- STRATTON, J. A. [1941], *Electromagnetic Theory*, McGraw-Hill Book Co., Inc., New York. Equations (35)-(38) on p. 571 are incorrect.
- STRUTT, J. W. (Lord Rayleigh) [1872], Investigation of the Disturbance Produced by a Spherical Obstacle on the Waves of Sound, *Proc. London Math. Soc.* **4**, 253-283.
- TAI, C. T. [1954], A Glossary of Dyadic Green's Functions, Stanford Research Institute Technical Report No. 46, Stanford, California.
- TAI, C. T. [1959], Some Electromagnetic Problems Involving a Sphere, in: *The McGill Symposium on Microwave Optics, Part II: Diffraction and Scattering*, ed. B. S. Karasik. Air Force Cambridge Research Laboratories Report No. TR-59-113-II, Bedford, Massachusetts.
- VAN DE HULST, H. C. [1957], *Light Scattering by Small Particles* John Wiley and Sons, Inc., New York.
- WATSON, G. N. [1948], *A Treatise on the Theory of Bessel Functions*, Cambridge University Press, Cambridge, England.
- WESTON, V. H. [1961], Near Zone Back Scattering from Large Spheres, *Appl. Sci. Res.* **B9**, 107-116.
- WU, T. T. [1956], High Frequency Scattering, *Phys. Rev.* **104**, 1201-1212. The third terms in the final expressions for σ_N and σ_E are incorrect (BECKMANN and FRANZ [1957], JONES [1964]).

CHAPTER 11

THE PROLATE SPHEROID

T. B. A. SENIOR and P. L. E. USLENGHI

The prolate spheroid, along with its companion shape, the oblate spheroid, is the most general finite shape for which a substantial number of exact and asymptotic scattering formulas is available. Even so, no exact solution of the vector scattering problem has yet been found.

Whereas the fat spheroid represents an obvious generalization of the sphere, the thin spheroid may be used as a model for the wire, which is of considerable importance in antenna theory. By bridging these two extremes, the prolate spheroid is a vehicle for studying the transition between the creeping and traveling wave concepts, and, more generally, constitutes a model for the development and testing of approximate methods of analyzing the scattering by still more complex shapes.

11.1. Prolate spheroidal geometry

The prolate spheroidal coordinates (ξ, η, ϕ) shown in Fig. 11.1 are related to the rectangular Cartesian coordinates (x, y, z) by the transformation

$$\begin{aligned} x &= \frac{1}{2}d\sqrt{(\xi^2-1)(1-\eta^2)} \cos \phi, \\ y &= \frac{1}{2}d\sqrt{(\xi^2-1)(1-\eta^2)} \sin \phi, \\ z &= \frac{1}{2}d\xi\eta, \end{aligned} \quad (11.1)$$

where $1 \leq \xi < \infty$, $-1 \leq \eta \leq 1$, and $0 \leq \phi < 2\pi$. The z -axis is the axis of symmetry, and the surfaces $\xi = \text{constant}$, $|\eta| = \text{constant}$ and $\phi = \text{constant}$ are respectively confocal prolate spheroids of interfocal distance d , major axis $d\xi$ and minor axis $d\sqrt{(\xi^2-1)}$; confocal hyperboloids of revolution of two sheets with interfocal distance d ; and semi-planes originating in the z -axis.

The scattering body is the prolate spheroid with surface $\xi = \xi_1$, and the primary source is either a plane wave whose direction of propagation forms the angle ζ with the positive z -axis, or a point or dipole source located at (ξ_0, η_0, ϕ_0) . The length-to-width ratio of the scatterer, i.e. the ratio between major and minor axes, is equal to $\xi_1/\sqrt{(\xi_1^2-1)}$. Values of ξ_1 corresponding to a few typical length-to-width ratios are tabulated in the following:

major axis minor axis	100 : 1	10 : 1	5 : 1	2 : 1
ξ_1	1.000 050 0	1.005 037 8	1.020 620 7	1.154 700 5

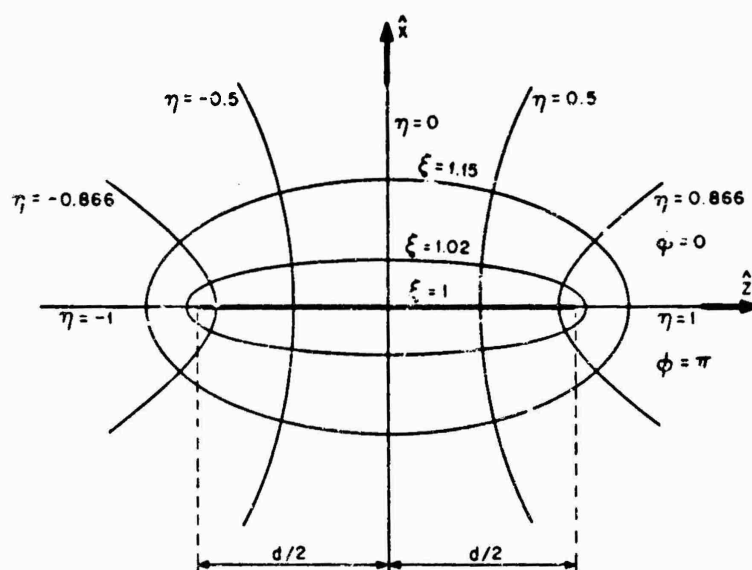


Fig. 11.1. Prolate spheroidal geometry.

The definitions and notation for the prolate spheroidal wave functions are those of FLAMMER [1957]. Thus the radial functions of the first, second and third kinds are indicated by $R_{mn}^{(j)}(c, \xi)$, where $j = 1, 2$ and 3 respectively, whereas the symbol $S_{mn}(c, \eta)$ is used for the angular functions; $m \geq 0$ and $n \geq m$ are integers. The quantities ρ_{mn} and N_{mn} which appear in the following sections are functions of m, n and c , and are defined by FLAMMER [1957]. The parameter c is the product of wave number and semi-focal distance: $c = \frac{1}{2}kd$. Numerical tables for prolate spheroidal wave functions and related quantities with the notation adopted in this chapter are given by FLAMMER [1957], LOWAN [1964], HUNTER et al. [1965a, b], and SLEPIAN and SONNENBLICK [1965]. Asymptotic expansions of prolate spheroidal wave functions can be found, for example, in FLAMMER [1957], MÜLLER [1962] and SLEPIAN [1965].

From the computations which were performed at the Radiation Laboratory of The University of Michigan, it would appear that the infinite eigenfunction series representing the exact solutions converge at least as rapidly as the corresponding eigenfunction series for a sphere of diameter $d\xi_1$.

11.2. Acoustically soft spheroid

11.2.1. Point sources

11.2.1.1. EXACT SOLUTIONS

For a point source at $r_0 = (\xi_0, \eta_0, \phi_0)$, such that

$$V^i = \frac{e^{ikR}}{kR}, \quad (11.2)$$

then (MORSE and FESHBACH [1953]):

$$\begin{aligned}
 V^i + V^s &= G(r, r_0) = 2i \sum_{m=0}^{\infty} \sum_{n=m}^{\infty} \frac{\varepsilon_m}{N_{mn}} \\
 &\times \left[R_{mn}^{(1)}(c, \xi_<) - \frac{R_{mn}^{(1)}(c, \xi_1)}{R_{mn}^{(3)}(c, \xi_1)} R_{mn}^{(3)}(c, \xi_<) \right] R_{mn}^{(3)}(c, \xi_>) \\
 &\times S_{mn}(c, \eta_0) S_{mn}(c, \eta) \cos m(\phi - \phi_0).
 \end{aligned} \tag{11.3}$$

On the surface $\xi = \xi_1$:

$$\begin{aligned}
 \frac{\partial}{\partial \xi} (V^i + V^s) &= \frac{2}{c(\xi_1^2 - 1)} \sum_{m=0}^{\infty} \sum_{n=m}^{\infty} \frac{\varepsilon_m}{N_{mn}} \frac{1}{R_{mn}^{(3)}(c, \xi_1)} \\
 &\times R_{mn}^{(3)}(c, \xi_0) S_{mn}(c, \eta_0) S_{mn}(c, \eta) \cos m(\phi - \phi_0).
 \end{aligned} \tag{11.4}$$

In the far field ($\xi \rightarrow \infty$):

$$\begin{aligned}
 V^i + V^s &= 2 \frac{e^{ic\xi}}{c\xi} \sum_{m=0}^{\infty} \sum_{n=m}^{\infty} \varepsilon_m \frac{(-i)^n}{N_{mn}} \left[R_{mn}^{(1)}(c, \xi_0) - \frac{R_{mn}^{(1)}(c, \xi_1)}{R_{mn}^{(3)}(c, \xi_1)} R_{mn}^{(3)}(c, \xi_0) \right] \\
 &\times S_{mn}(c, \eta_0) S_{mn}(c, \eta) \cos m(\phi - \phi_0).
 \end{aligned} \tag{11.5}$$

When the source is on the positive z -axis ($\eta_0 = 1$):

$$\begin{aligned}
 V^i + V^s &= 2i \sum_{n=0}^{\infty} \frac{1}{N_{on}} \left[R_{on}^{(1)}(c, \xi_<) - \frac{R_{on}^{(1)}(c, \xi_1)}{R_{on}^{(3)}(c, \xi_1)} R_{on}^{(3)}(c, \xi_<) \right] \\
 &\times R_{on}^{(3)}(c, \xi_>) S_{on}(c, 1) S_{on}(c, \eta).
 \end{aligned} \tag{11.6}$$

In particular, if the field point is on the surface $\xi = \xi_1$:

$$\frac{\partial}{\partial \xi} (V^i + V^s) = \frac{2}{c(\xi_1^2 - 1)} \sum_{n=0}^{\infty} \frac{1}{N_{on}} \frac{1}{R_{on}^{(3)}(c, \xi_1)} R_{on}^{(3)}(c, \xi_0) S_{on}(c, 1) S_{on}(c, \eta). \tag{11.7}$$

whereas in the far field ($\xi \rightarrow \infty$):

$$V^i + V^s = 2 \frac{e^{ic\xi}}{c\xi} \sum_{n=0}^{\infty} \frac{(-i)^n}{N_{on}} \left[R_{on}^{(1)}(c, \xi_0) - \frac{R_{on}^{(1)}(c, \xi_1)}{R_{on}^{(3)}(c, \xi_1)} R_{on}^{(3)}(c, \xi_0) \right] S_{on}(c, 1) S_{on}(c, \eta). \tag{11.8}$$

11.2.1.2. LOW FREQUENCY APPROXIMATIONS

General methods (e.g. KLEINMAN [1965a], NOBLE [1962], MORSE and FESHBACH [1953]) for the derivation of terms in the low frequency expansions are applicable to this case; however, no specific results are as yet available.

11.2.1.3. HIGH FREQUENCY APPROXIMATIONS

For a point source at $(\xi_0, \eta_0, 0)$, such that

$$V^i = \frac{e^{ikR}}{kR}, \tag{11.9}$$

the geometrical optics scattered field at a point $(\xi, \eta, \phi = 0 \text{ or } \pi)$ located in the illuminated region and in the plane containing the source and the z -axis is:

$$V_{g.o.}^s = - \frac{e^{i\phi(F_0+F)}}{cF_0} \left[\left(1 + \frac{F}{F_0} + \frac{2F^2}{(\xi_1^2 - \eta_1^2)G} \right) \left(1 + \frac{F}{F_0} + \frac{2\xi_1^2 G}{\xi_1^2 - \eta_1^2} \right) \right]^{-\frac{1}{2}}, \quad (11.10)$$

where

$$F = \{ [\sqrt{\{(\xi_1^2 - 1)(1 - \eta_1^2)\}} - (-1)^h \sqrt{\{(\xi^2 - 1)(1 - \eta^2)\}}]^2 + (\xi_1 \eta_1 - \xi \eta)^2 \}^{\frac{1}{2}}, \quad (11.11)$$

$$F_0 = \{ [\sqrt{\{(\xi_1^2 - 1)(1 - \eta_1^2)\}} - (-1)^h \sqrt{\{(\xi_0^2 - 1)(1 - \eta_0^2)\}}]^2 + (\xi_1 \eta_1 - \xi_0 \eta_0)^2 \}^{\frac{1}{2}}, \quad (11.12)$$

$$G = \frac{\xi}{\xi_1} \eta \eta_1 - 1 + (-1)^h \sqrt{\left\{ \frac{\xi^2 - 1}{\xi_1^2 - 1} (1 - \eta^2)(1 - \eta_1^2) \right\}}, \quad (11.13)$$

and

$$j = h = 0, \quad \text{if } \phi = 0;$$

$$j = 0, \quad h = 1, \quad \text{if } \phi = \pi \quad \text{and} \quad \sqrt{\{(\xi^2 - 1)(1 - \eta^2)\}} < \left| \frac{\xi \eta - \xi_1}{\xi_0 \eta_0 - \xi_1} \right| \\ \times \sqrt{\{(\xi_0^2 - 1)(1 - \eta_0^2)\}};$$

$$j = 1, \quad h = 0, \quad \text{if } \phi = \pi \quad \text{and} \quad \sqrt{\{(\xi^2 - 1)(1 - \eta^2)\}} > \left| \frac{\xi \eta - \xi_1}{\xi_0 \eta_0 - \xi_1} \right| \\ \times \sqrt{\{(\xi_0^2 - 1)(1 - \eta_0^2)\}}.$$

The parameter η_1 , $-1 \leq \eta_1 \leq 1$, is determined as a function of $\xi_0, \eta_0, \xi, \eta, \xi_1$ and ϕ by the relations:

$$\frac{\partial}{\partial \eta_1} (F_0 + F) = 0, \quad \frac{\partial^2}{\partial \eta_1^2} (F_0 + F) > 0. \quad (11.14)$$

In the geometrical shadow $V_{g.o.}^s = 0$. In particular, when the source is at $(\xi_0, 1)$ on the z -axis

$$F = \{ [\sqrt{\{(\xi_1^2 - 1)(1 - \eta_1^2)\}} - \sqrt{\{(\xi^2 - 1)(1 - \eta^2)\}}]^2 + (\xi_1 \eta_1 - \xi \eta)^2 \}^{\frac{1}{2}}, \quad (11.15)$$

$$F_0 = [(\xi_1^2 - 1)(1 - \eta_1^2) + (\xi_1 \eta_1 - \xi_0)^2]^{\frac{1}{2}}, \quad (11.16)$$

$$G = \frac{\xi}{\xi_1} \eta \eta_1 - 1 + \sqrt{\left\{ \frac{\xi^2 - 1}{\xi_1^2 - 1} (1 - \eta^2)(1 - \eta_1^2) \right\}}, \quad (11.17)$$

and η_1 is the positive root of the equation:

$$\frac{\sqrt{1 - \eta_1^2}(\eta_1 - \xi_1 \xi \eta) + \eta_1 \sqrt{\{(\xi_1^2 - 1)(\xi^2 - 1)(1 - \eta^2)\}}}{\{ [\sqrt{\{(\xi_1^2 - 1)(1 - \eta_1^2)\}} - \sqrt{\{(\xi^2 - 1)(1 - \eta^2)\}}]^2 + (\xi_1 \eta_1 - \xi \eta)^2 \}^{\frac{1}{2}}} + \\ + \frac{\sqrt{1 - \eta_1^2}(\eta_1 - \xi_1 \xi_0)}{[(\xi_1^2 - 1)(1 - \eta_1^2) + (\xi_1 \eta_1 - \xi_0)^2]^{\frac{1}{2}}} = 0. \quad (11.18)$$

If both source and observation points are on the z -axis ($\eta_0 = \eta = 1$),

$$V_{g.o.}^s = - \frac{\exp \{ic(\xi_0 + \xi - 2\xi_1)\}}{c[\xi_0 + \xi - 2\xi_1 + 2\xi_1(\xi_0 - \xi_1)(\xi - \xi_1)/(\xi_1^2 - 1)]} \quad (11.19)$$

in the illuminated region and zero in the shadow.

A more refined approximation, in which an asymptotic expression for the diffracted field is retained, is available only for the source on the z -axis. In this case

$$V^s \sim V_{g.o.}^s + V_d^s, \quad (11.20)$$

where $V_{g.o.}^s$ is given by eqs. (11.10, 15, 16, 17) and (LEVY and KELLER [1960]):

$$V_d^s = \frac{2^{\frac{1}{2}} \exp \{ \frac{1}{12} i\pi \} (\xi_1 \sqrt{(\xi_1^2 - 1)})^{\frac{1}{2}} \exp [(ic/\xi_0) \sqrt{(\xi_0^2 - 1)(\xi_0^2 - \xi_1^2)}]}{\pi^{\frac{1}{2}} (4c)^{\frac{1}{2}}} \frac{f_n(\eta_2) - i f_n'(\eta_3)}{[Ai'(-\alpha_n)]^2 [1 + \exp \{2X_n(1, -1)\}]}, \quad (11.21)$$

where

$$X_n(\alpha, \beta) = ic \int_{\beta}^{\alpha} \sqrt{\frac{\xi_1^2 - \eta^2}{1 - \eta^2}} d\eta + i(\frac{1}{2}c)^{\frac{1}{2}} e^{\frac{1}{2}i\pi} \alpha_n \{ \xi_1 \sqrt{(\xi_1^2 - 1)} \}^{\frac{1}{2}} \int_{\beta}^{\alpha} \sqrt{\frac{d\eta}{(\xi_1^2 - \eta^2)(1 - \eta^2)}}, \quad (11.22)$$

$$f_n(\eta_2) = (\xi_1^2 - \eta_2^2)^{\frac{1}{2}} T_2^{-\frac{1}{2}} \exp [- T_2 + X_n(\eta_1, \eta_2)], \quad (11.23)$$

$$f_n(\eta_3) = (\xi_1^2 - \eta_3^2)^{\frac{1}{2}} T_3^{-\frac{1}{2}} \exp [icT_3 + X_n^{\pm}], \quad (11.24)$$

$$X_n^+ = X_n(\eta_1, -1) + X_n(\eta_3, -1), \quad X_n^- = X_n(\eta_1, \eta_3), \quad (11.25)$$

X_n^+ is to be chosen if $\xi\eta + \xi_1 > 0$, and X_n^- if $\xi\eta + \xi_1 < 0$,

$$T_j = [(\xi\eta - \xi_1\eta_j)^2 + \{ \sqrt{(\xi^2 - 1)(1 - \eta^2)} \pm \sqrt{(\xi_1^2 - 1)(1 - \eta_j^2)} \}^2]^{\frac{1}{2}}, \quad (11.26)$$

$j = 2, 3$ and the ambiguity of sign in T is removed by choosing the minus sign if either $j = 2$, or $j = 3$ and $\xi\eta + \xi_1 > 0$, and the plus sign if $j = 3$ and $\xi\eta + \xi_1 < 0$. The coordinates η_1, η_2 and η_3 are indicated in Fig. 11.2. Eq. (11.21) is valid if the observation point is away from both the z -axis and the surface $\xi = \xi_1$, and if the

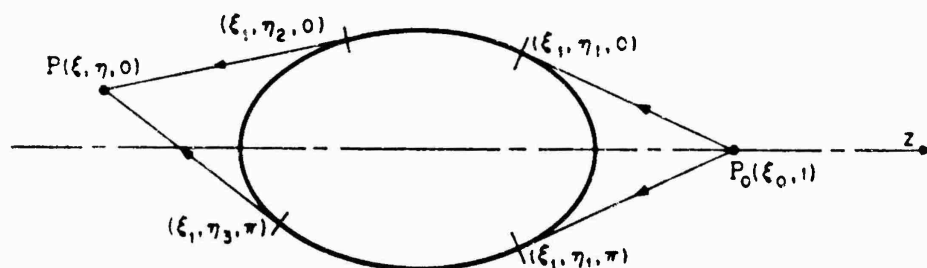


Fig. 11.2. Geometry for the diffracted field.

product of the wave number k and the radius of curvature of the surface $\xi = \xi_1$ at the end points $\eta = \pm 1$ is large compared to unity, i.e.

$$\frac{c(\xi_1^2 - 1)}{\xi_1} \gg 1. \quad (11.27)$$

The field on the surface: $\xi = \xi_1$ may be obtained by applying the appropriate caustic corrections to eq. (11.21) (LEVY and KELLER [1960]).

For a point source at $(\xi_0, 1)$ on the z -axis at a large distance from a long, thin spheroid, such that

$$\xi_0^2 \gg 1, \quad c\xi_1 \gg 1, \quad \frac{c(\xi_1^2 - 1)}{\xi_1} \ll 1, \quad (11.28)$$

the field at a point (ξ_1, η, ϕ) on the surface of the spheroid and near the tip in the shadow region ($c(1+\eta) \ll 1$) is given by the asymptotic expansion (GOODRICH and KAZARINOFF [1963]):

$$\frac{\partial}{\partial \xi} (V^i + V^s) \sim - \frac{e^{ic(1+\xi_0)}}{c\xi_0} \sqrt{\frac{2A \cos[c(1+\eta)]}{(1-\xi_1^{-2})_\lambda (1-\eta)}} \sum_{n=0}^N \sum_{m=0}^{\infty} \left(-\frac{i}{4c}\right)^n n! (-1)^m A_{mn}, \quad (11.29)$$

where N is the largest integer less than c , and

$$A = \frac{1}{\log[c(1-\xi_1^{-2})]}, \quad A_{mn} = \left[\frac{A e^{2ic(n!)^2}}{(4c)^{2n+1}} \right]^{2m}; \quad (11.30)$$

while in the shadow and near the shadow boundary ($c(1+\eta) \gg 1$):

$$\begin{aligned} \frac{\partial}{\partial \xi} (V^i + V^s) \sim & \frac{2A e^{ic(1+\xi_0)}}{c\xi_0 (1-\xi_1^{-2})_\lambda (1-\eta^2)} \\ & \times \sum_{n=0}^N \sum_{m=0}^{\infty} (-1)^m A_{mn} \left[(-1)^n \left(\frac{1+\eta}{1-\eta}\right)^{n+1} e^{-ic(1+\eta)} - \frac{i(n!)^2}{c(4c)^{2n}} A \left(\frac{1-\eta}{1+\eta}\right)^{n+1} e^{ic(1+\eta)} \right]. \end{aligned} \quad (11.31)$$

If only the first residue contribution ($n = 0$) to the surface field is considered, then (GOODRICH and KAZARINOFF [1963]):

$$\frac{\partial}{\partial \xi} (V^i + V^s) \sim - \frac{e^{ic\xi_0}}{c\xi_0 \sqrt{(1-\eta)}} \frac{A \sqrt{2}}{1-\xi_1^{-2}} \cos[c(1+\eta)] e^{ikL} \sum_{m=0}^{\infty} \left(\frac{iA}{4c}\right)^{2m} e^{2ikLm}, \quad (11.32)$$

for $c(1+\eta) \ll 1$ (near tip in shadow), and

$$\begin{aligned} \frac{\partial}{\partial \xi} (V^i + V^s) \sim & \frac{e^{ic\xi_0}}{c\xi_0 \sqrt{(1-\eta^2)}} \frac{2A}{1-\xi_1^{-2}} \\ & \times \sum_{m=0}^{\infty} \left[e^{ik(L_1 + 2Lm)} \right] \frac{1+\eta}{1-\eta} \left(\frac{iA}{4c}\right)^{2m} - 4e^{ik(L_2 + 2Lm)} \left[\frac{1-\eta}{1+\eta} \left(\frac{iA}{4c}\right)^{2m+1} \right], \end{aligned} \quad (11.33)$$

in the shadow and near the shadow boundary ($c(1+\eta) \gg i$), where

$$l_1 = -\frac{c}{k}\eta, \quad l_2 = \frac{c}{k}(2+\eta), \quad L = \frac{2c}{k}. \quad (11.34)$$

The parameter L is approximately equal to the length of a geodesic between the tips of the spheroid, whereas l_1 and l_2 can be approximately identified with the geodesic path lengths between the field point and those points of the shadow boundary which lie in the plane containing the field point and the z -axis, as shown in Fig. 11.3. Thus the various terms in series (11.32) and (11.33) are easily interpreted in terms of creeping waves (GOODRICH and KAZARINOFF [1963]).

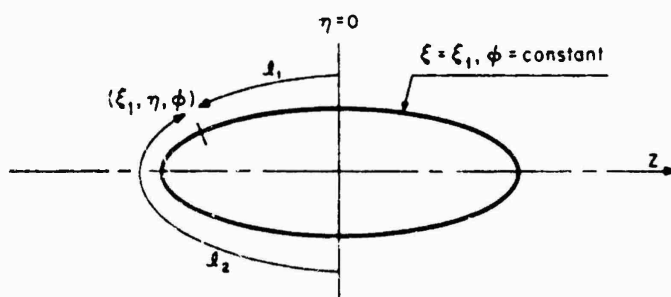


Fig. 11.3. Creeping wave interpretation.

11.2.2. Plane wave incidence

11.2.2.1. EXACT SOLUTIONS

For incidence at an angle ζ with respect to the positive z -axis, such that

$$V^i = \exp \{ik(x \sin \zeta + z \cos \zeta)\}, \quad (11.35)$$

then (SENIOR [1960]):

$$V^s = -2 \sum_{m=0}^{\infty} \sum_{n=m}^{\infty} \epsilon_m \frac{i^n}{N_{mn}} \frac{R_{mn}^{(1)}(c, \xi_1)}{R_{mn}^{(3)}(c, \xi_1)} R_{mn}^{(3)}(c, \xi) S_{mn}(c, \cos \zeta) S_{mn}(c, \eta) \cos m\phi. \quad (11.36)$$

On the surface $\xi = \xi_1$:

$$\frac{\partial}{\partial \xi} (V^i + V^s) = \frac{2}{c(\xi_1^2 - 1)} \sum_{m=0}^{\infty} \sum_{n=m}^{\infty} \epsilon_m \frac{i^{n-1}}{N_{mn}} \frac{1}{R_{mn}^{(3)}(c, \xi_1)} S_{mn}(c, \cos \zeta) S_{mn}(c, \eta) \cos m\phi. \quad (11.37)$$

In the far field ($\xi \rightarrow \infty$):

$$S = 2i \sum_{m=0}^{\infty} \sum_{n=m}^{\infty} \frac{\epsilon_m}{N_{mn}} \frac{R_{mn}^{(1)}(c, \xi_1)}{R_{mn}^{(3)}(c, \xi_1)} S_{mn}(c, \cos \zeta) S_{mn}(c, \eta) \cos m\phi. \quad (11.38)$$

The total scattering cross section is

$$\sigma_T = \frac{4\pi}{k^2} \sum_{m=0}^{\infty} \sum_{n=m}^{\infty} \frac{\epsilon_m^2}{N_{mn}^2} \left[\frac{R_{mn}^{(1)}(c, \xi_1)}{|R_{mn}^{(3)}(c, \xi_1)|} S_{mn}(c, \cos \zeta) \right]^2. \quad (11.39)$$

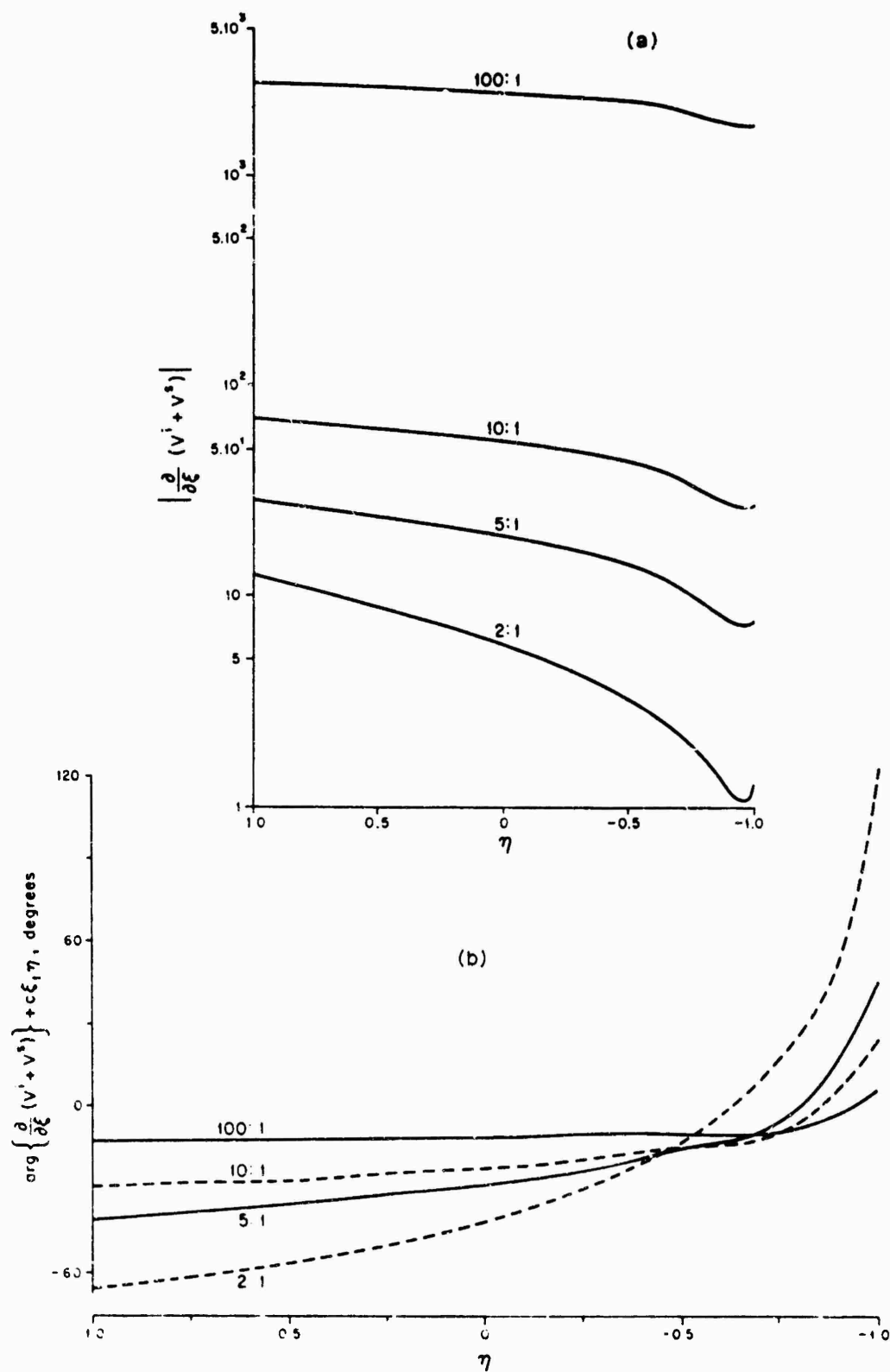
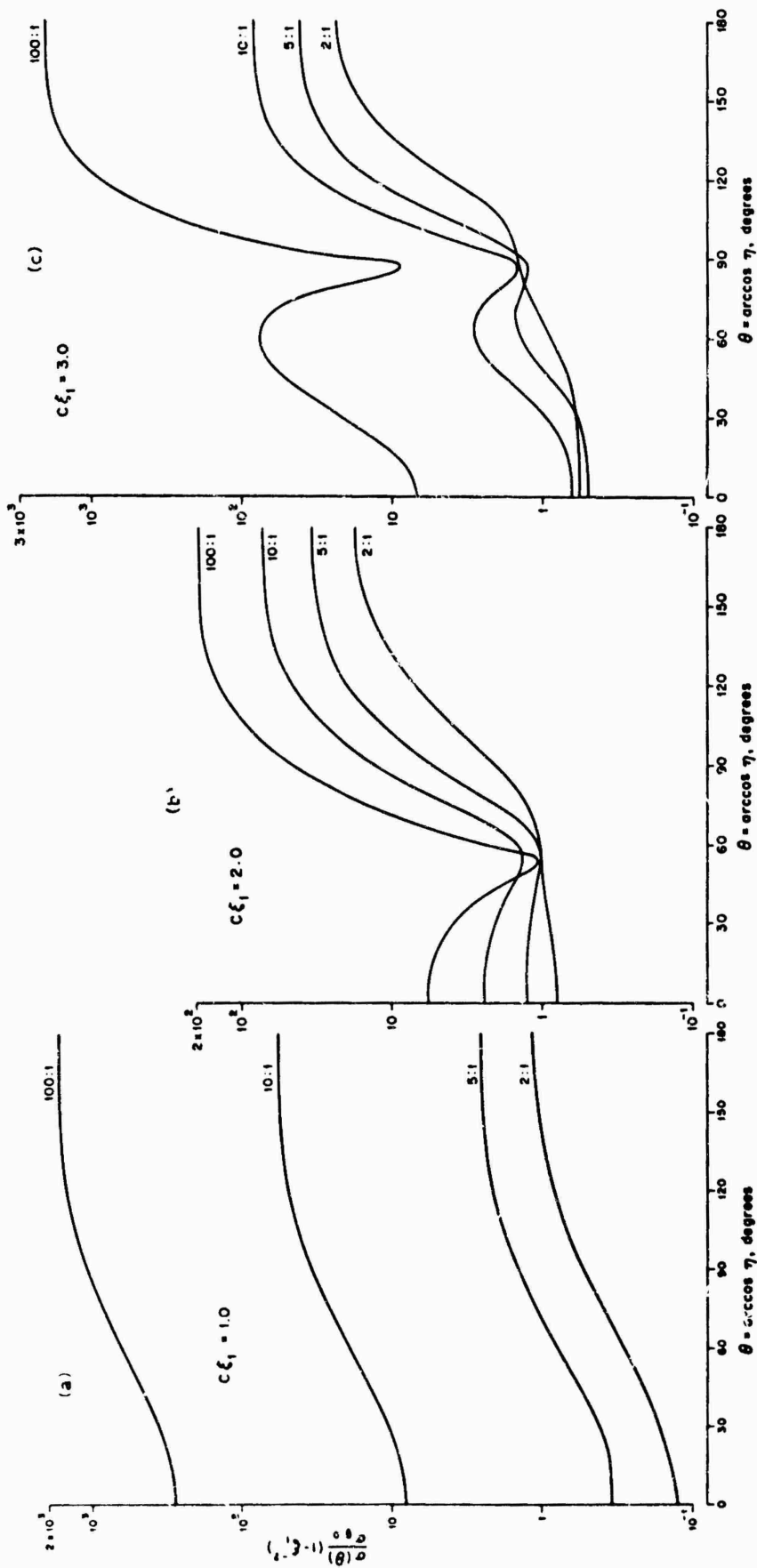


Fig. 11.4. Amplitude and phase of surface field for end-on incidence with $c = 5.0$ (SUNTOR [1969]).



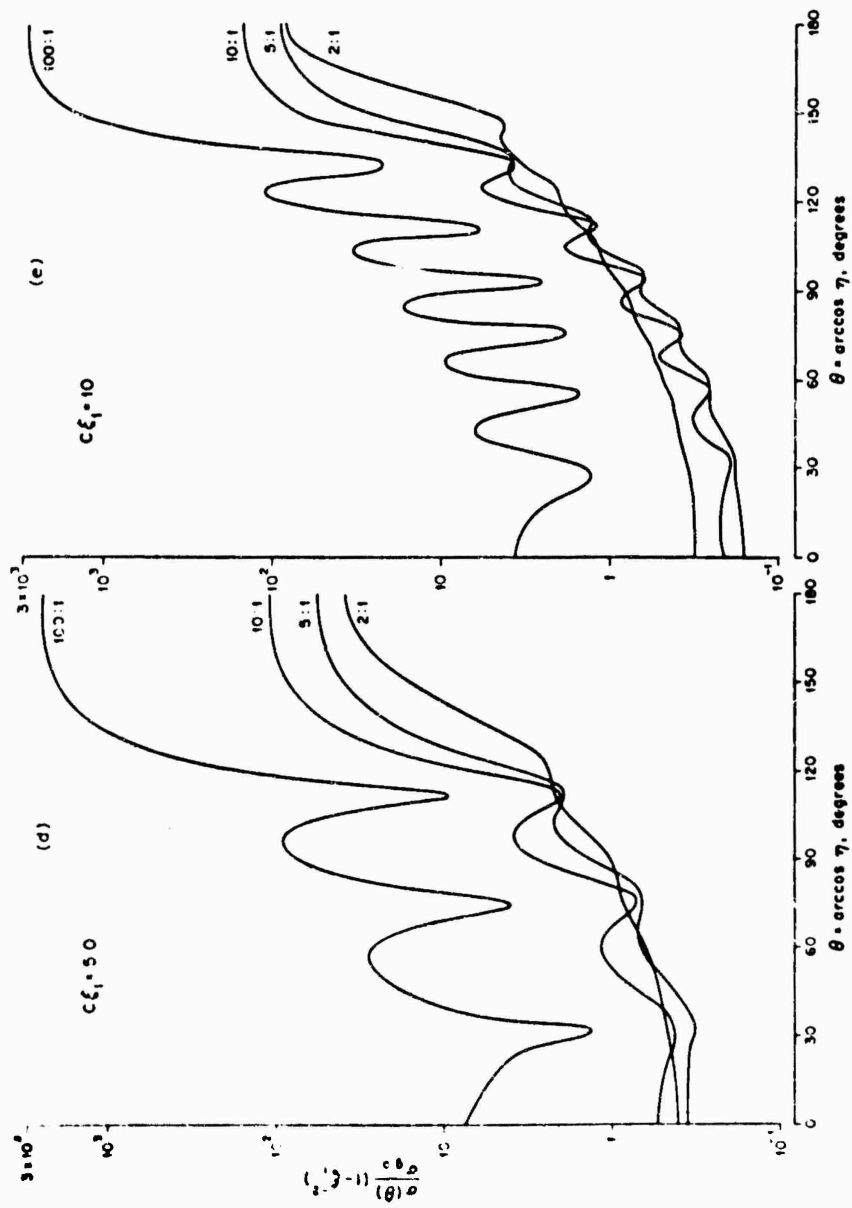


Fig. 11.5. Bistatic cross section normalized to $\sigma_{g.o.}$ as a function of $\theta = \arccos \eta$, for end-on incidence (SENIOR [1969]).

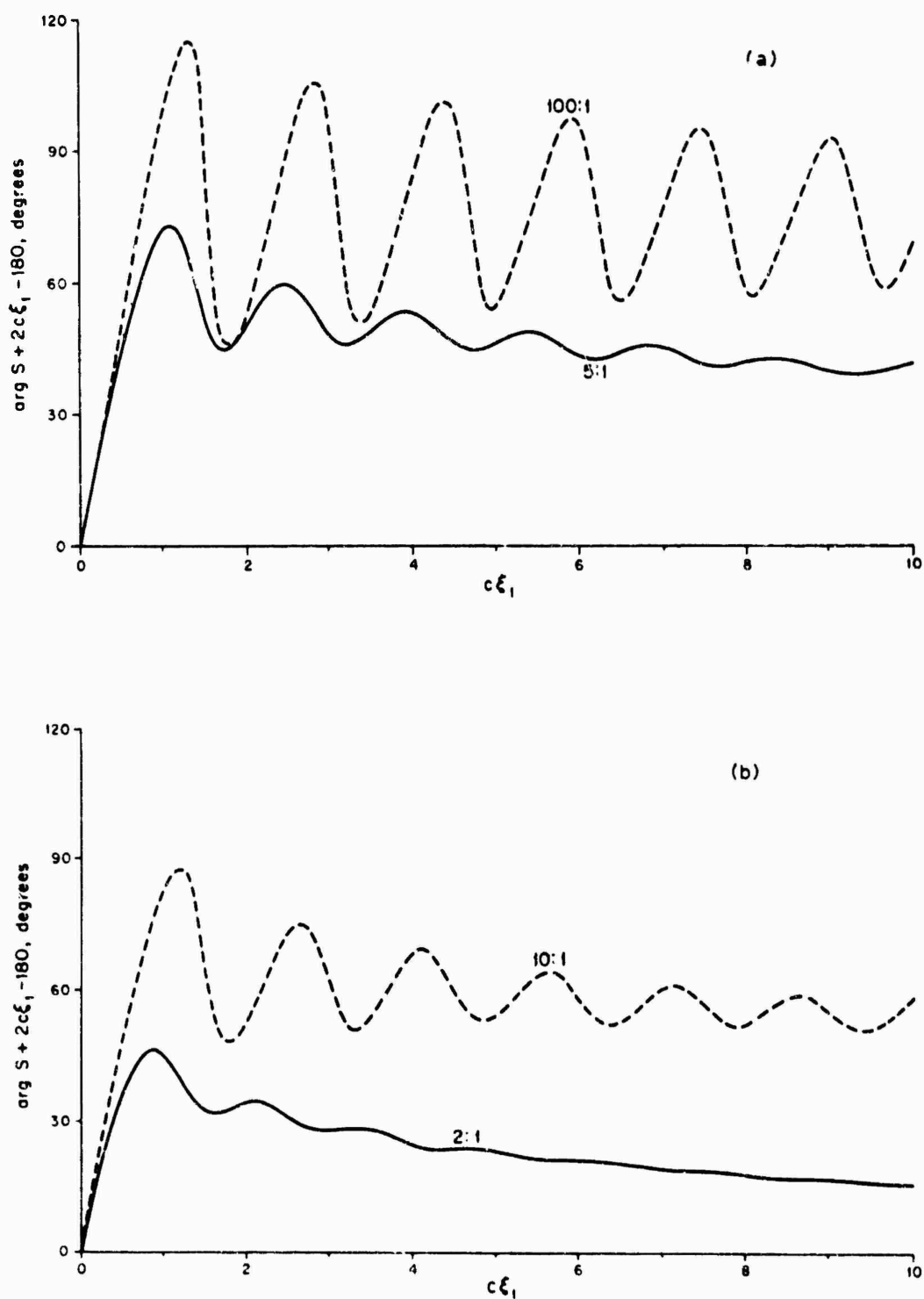


Fig. 11.6. Phase of back scattering coefficient S for end-on incidence (SENIOR [1969]).

For axial incidence ($\zeta = \pi$):

$$V^s = -2 \sum_{n=0}^{\infty} \frac{i^n}{N_{on}} \frac{R_{on}^{(1)}(c, \xi_1)}{R_{on}^{(3)}(c, \xi_1)} R_{on}^{(3)}(c, \xi) S_{on}(c, -1) S_{on}(c, \eta), \quad (11.40)$$

and on the surface $\xi = \xi_1$:

$$\frac{\partial}{\partial \xi} (V^i + V^s) = \frac{2}{c(\xi_1^2 - 1)} \sum_{n=0}^{\infty} \frac{i^{n-1}}{N_{on}} \frac{1}{R_{on}^{(3)}(c, \xi_1)} S_{on}(c, -1) S_{on}(c, \eta). \quad (11.41)$$

This last expression has been computed as a function of η for selected values of c and ξ_1 , and its amplitude and phase are shown in Fig. 11.4. In the far field ($\xi \rightarrow \infty$):

$$S = 2i \sum_{n=0}^{\infty} \frac{1}{N_{on}} \frac{R_{on}^{(1)}(c, \xi_1)}{R_{on}^{(3)}(c, \xi_1)} S_{on}(c, -1) S_{on}(c, \eta). \quad (11.42)$$

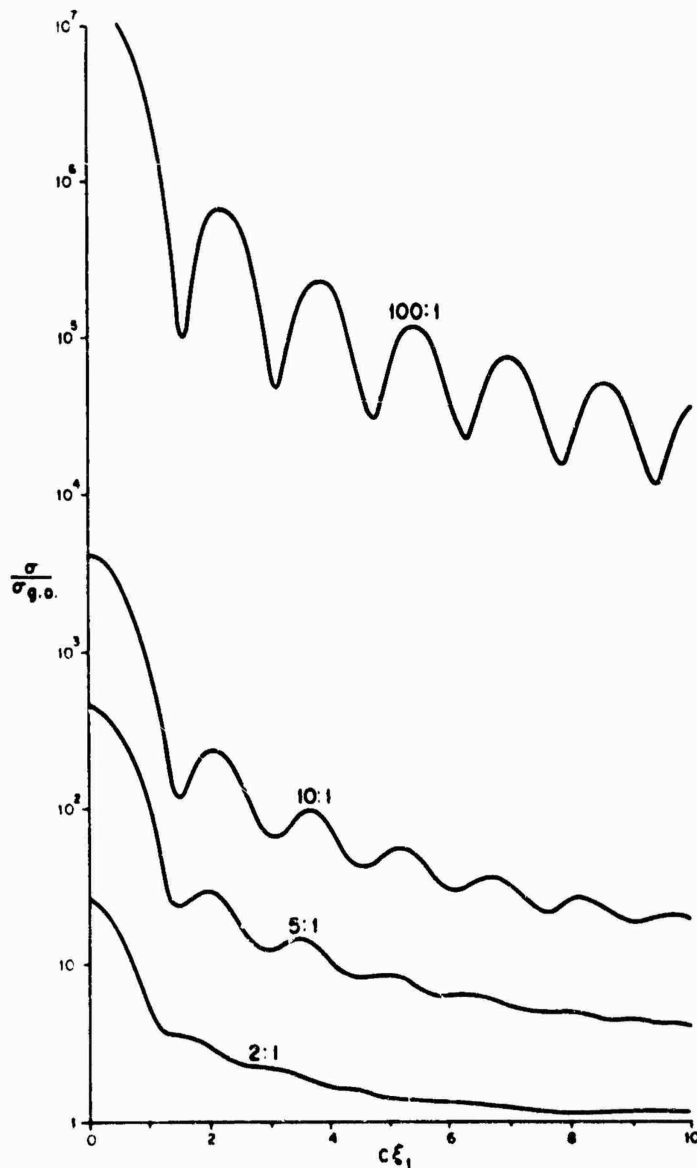


Fig. 11.7. Normalized back scattering cross section for end-on incidence (SENIOR [1966a]).

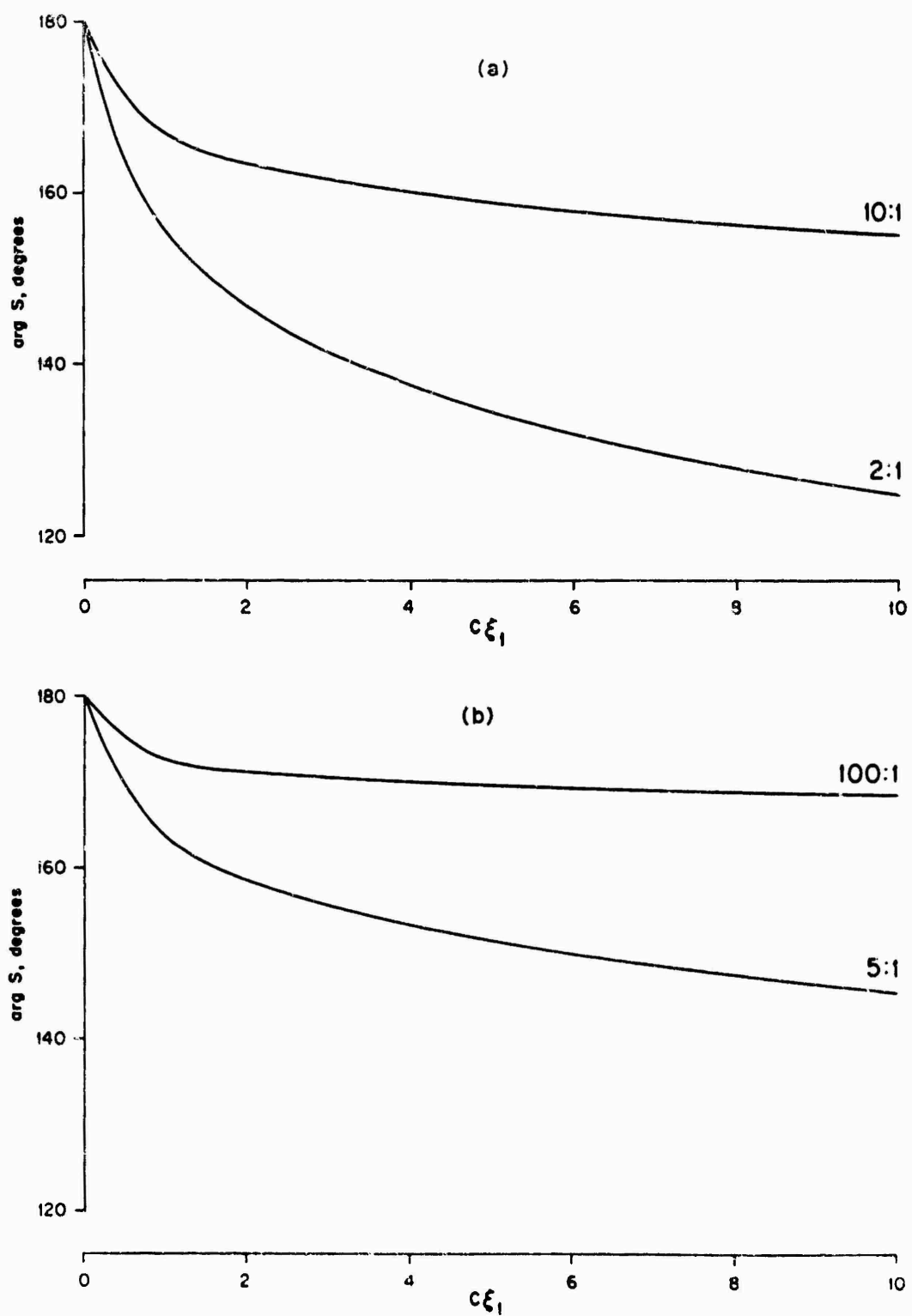


Fig. 11.8. Phase of forward scattering coefficient S for end-on incidence (SENIOR [1969]).

The bistatic cross section normalized to the geometrical optics back scattering cross section $\sigma_{g.o.}$ is shown as a function of $\theta = \arccos \eta$ in Fig. 11.5, for selected values of $c\xi_1$ and of the length-to-width ratio. For the particular case of back scattering ($\eta = 1$), $\arg S$ is plotted as a function of $c\xi_1$ for selected values of ξ_1 in Fig. 11.6. Corresponding values of the back scattering cross section, normalized to $\sigma_{g.o.}$, are shown in Fig. 11.7. For forward scattering ($\eta = -1$), $\arg S$ is plotted as a function of $c\xi_1$ for selected values of ξ_1 in Fig. 11.8. Corresponding values of the forward scattering cross section, normalized to

$$\frac{k^2}{\pi} A^2 = \pi \left[\frac{c^2}{k} (\xi_1^2 - 1) \right]^2 \quad (11.43)$$

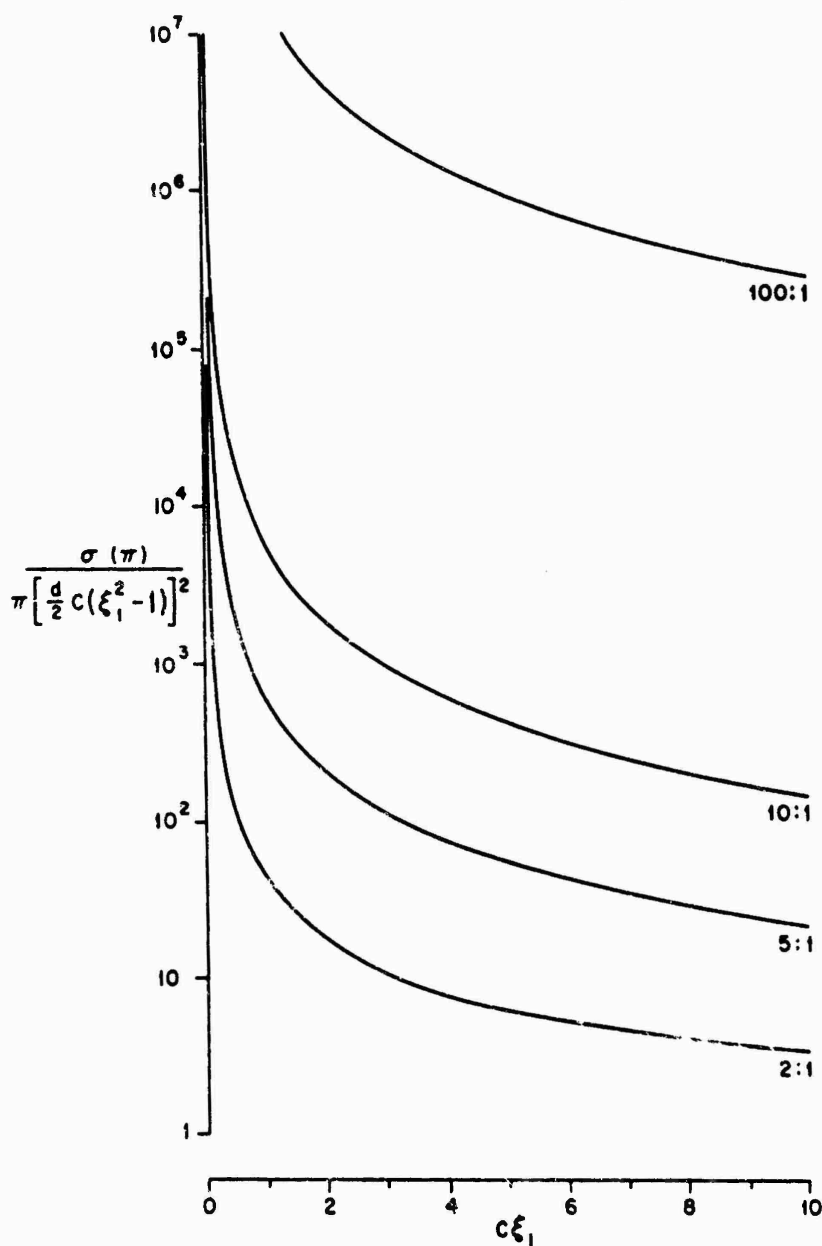


Fig. 11.9. Normalized forward scattering cross section for end-on incidence (SENIOR [1969]).

where A is the area of the geometrical shadow, are shown in Fig. 11.9. The total scattering cross section is:

$$\sigma_T = \frac{4\pi}{k^2} \sum_{n=0}^{\infty} \frac{1}{N_{on}} \left[\frac{R_{on}^{(1)}(c, \xi_1)}{R_{on}^{(3)}(c, \xi_1)} S_{on}(c, -1) \right]^2. \quad (11.44)$$

The total scattering cross section, normalized to $2A$ is shown in Fig. 11.10.

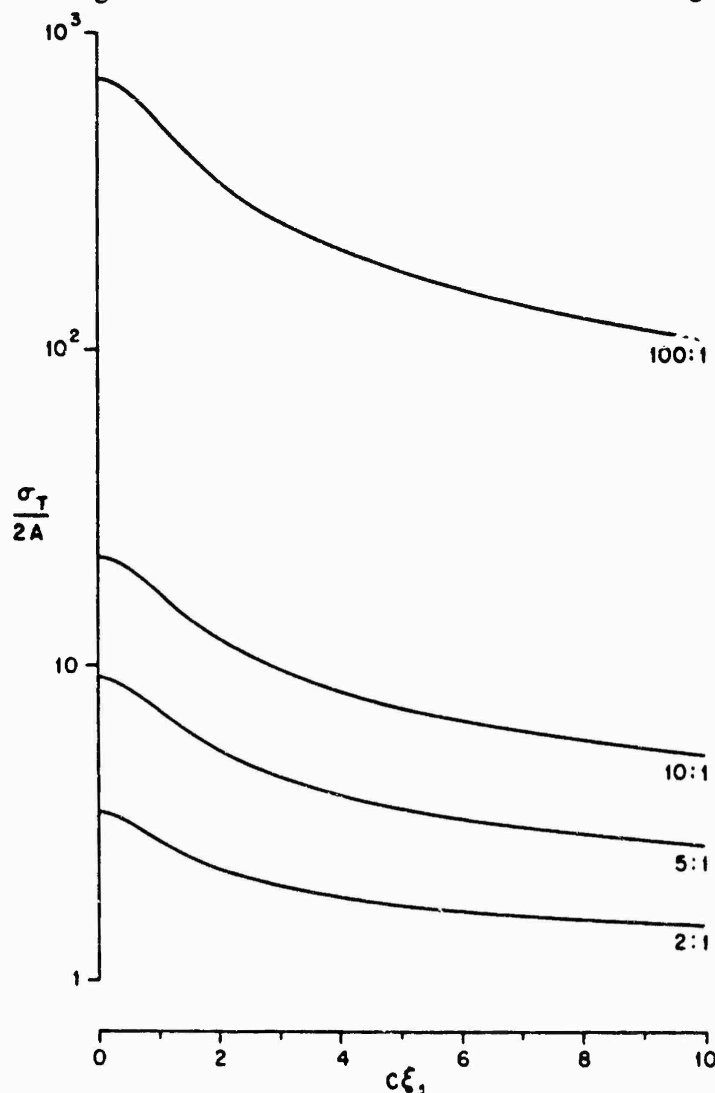


Fig. 11.10. Normalized total scattering cross section for end-on incidence (SENIOR [1969]).

11.2.2.2. LOW FREQUENCY APPROXIMATIONS

For incidence at an angle ζ with respect to the positive z -axis, such that

$$V^i = \exp \{ik(x \sin \zeta + z \cos \zeta)\}, \quad (11.45)$$

then (ASVESTAS and KLEINMAN [1967]):

$$V^s = e^{i\kappa z} \sum_{n=0}^{\infty} \sum_{m=0}^n \frac{(-ic)^n (\xi_1 - \eta)^{n-m}}{(n-m)!} \sum_{l=0}^m \sum_{h=0}^m \sum_{j=0}^m C_{l,h,j}^m Q_h^l(\xi) P_j^l(\eta) \cos l\phi, \quad (11.46)$$

where $C_{l,h,j}^m = C_{l,j,h}^m$ and $C_{l,h,j}^m$ is given by the recurrence relations:

$$C_{l,h,j}^{m+1} = \frac{2}{h(h+1)-j(j+1)} \left[\frac{h(h-1)}{2h-1} C_{l,h-1,j}^m - \frac{j(j-1)}{2j-1} C_{l,h,j-1}^m + \frac{(j+1)(j+1+1)}{2j+3} C_{l,h,j+1}^m - \frac{(h+1)(h+1+1)}{2h+3} C_{l,h+1,j}^m \right] \quad (11.47)$$

for $h \neq j$ and $m = 0, 1, 2, \dots$:

$$C_{l,j,j}^{m+1} = - \sum_{h=0}^{m+1} \frac{Q_h^l(\xi_1)}{Q_j^l(\xi_1)} C_{l,h,j}^{m+1} + A_{j,l}^{m+1} \quad (11.48)$$

for $m = 0, 1, 2, \dots$, where \sum' indicates that the term $h = j$ is omitted from the summation; and

$$C_{0,0,0}^0 = A_{0,0}^0, \quad (11.49)$$

$$A_{j,l}^m = \begin{cases} 0, & \text{for } m+j \text{ odd,} \\ -\epsilon_l \frac{\sqrt{\pi}}{2^{m+1}} (\xi_1 - \cos \zeta)^m (2j+1) \frac{(j-l)!}{(j+l)!} \frac{P_j^l\{(1-\xi_1 \cos \zeta)/(\xi_1 - \cos \zeta)\}}{\{\frac{1}{2}(m-j)\}!\{\frac{1}{2}(m+j+1)\}! Q_j^l(\xi_1)}, & \text{for } m+j \text{ even.} \end{cases} \quad (11.50)$$

In the far field ($\xi \rightarrow \infty$):

$$S = c \sum_{n=0}^{\infty} \sum_{m=0}^n (-ic)^n \frac{(\xi_1 - \eta)^{n-m}}{(n-m)!} \sum_{l=0}^m \sum_{j=0}^m C_{l,0,j}^m P_j^l(\eta) \cos l\phi. \quad (11.51)$$

Starting from the exact series solution, BURKE [1966a] has computed S through terms $O(k^6)$ for arbitrary angles of incidence and observation.

For axial incidence ($\zeta = \pi$):

$$S = e^{ic\xi} \sum_{n=0}^{\infty} \sum_{m=0}^n (-ic)^n \frac{(\xi_1 - \eta)^{n-m}}{(n-m)!} \sum_{h=0}^m \sum_{j=0}^m C_{0,h,j}^m Q_h(\xi) P_j(\eta), \quad (11.52)$$

and in the far field ($\xi \rightarrow \infty$):

$$S = -c \sum_{n=0}^{\infty} (-ic)^n u_n, \quad (11.53)$$

where

$$u_n = - \sum_{m=0}^n \frac{(\xi_1 - \eta)^{n-m}}{(n-m)!} \sum_{j=0}^m C_{0,0,j}^m P_j(\eta). \quad (11.54)$$

In particular (SINOR [1960]):

$$u_0 = \frac{P_0}{Q_0} P_0(\eta), \quad (11.55)$$

$$u_1 = \left(\frac{P_0}{Q_0}\right)^2 P_0(\eta), \quad (11.56)$$

$$u_2 = \frac{1}{9} \frac{P_0}{Q_0} P_2(\eta) + \frac{1}{3} \frac{P_1}{Q_1} P_1(\eta) + \frac{P_0}{Q_0} \left\{ \left(\frac{P_0}{Q_0}\right)^2 - \frac{1}{3} \frac{P_1}{Q_0} + \frac{2}{9} \right\} P_0(\eta), \quad (11.57)$$

$$u_3 = \frac{1}{9} \left(\frac{P_0}{Q_0}\right)^2 P_2(\eta) + \left(\frac{P_0}{Q_0}\right)^2 \left\{ \left(\frac{P_0}{Q_0}\right)^2 - \frac{2}{3} \frac{P_1}{Q_0} + \frac{1}{3} \right\} P_0(\eta), \quad (11.58)$$

$$\begin{aligned} u_4 = & \frac{1}{525} \frac{P_0}{Q_0} P_4(\eta) + \frac{1}{75} \frac{P_1}{Q_1} P_3(\eta) + \frac{1}{9} \left[\frac{4}{45} \frac{P_2}{Q_2} + \frac{P_0}{Q_0} \left\{ \left(\frac{P_0}{Q_0}\right)^2 - \frac{1}{3} \frac{P_1}{Q_0} + \frac{16}{63} \right\} \right] P_2(\eta) + \\ & + \frac{1}{3} \frac{P_1}{Q_1} \left\{ \frac{1}{25} \left(\frac{P_3}{P_1} - \frac{Q_3}{Q_1} \right) + \frac{1}{6} \frac{P_0}{Q_1} + \frac{4}{25} \right\} P_1(\eta) - \\ & - \frac{P_0}{Q_0} \left[\frac{1}{75} \frac{P_3}{Q_0} + \frac{P_1}{Q_0} \left\{ \left(\frac{P_0}{Q_0}\right)^2 - \frac{1}{27} \frac{Q_2}{Q_0} - \frac{1}{6} \frac{P_1}{Q_0} + \frac{91}{675} \right\} - \right. \\ & \left. - \left(\frac{P_0}{Q_0}\right)^4 - \frac{4}{9} \left(\frac{P_0}{Q_0}\right)^2 - \frac{2}{75} \right] P_0(\eta), \end{aligned} \quad (11.59)$$

$$\begin{aligned} u_5 = & \frac{1}{525} \left(\frac{P_0}{Q_0}\right)^2 P_4(\eta) + \frac{1}{9} \left(\frac{P_0}{Q_0}\right)^2 \left\{ \left(\frac{P_0}{Q_0}\right)^2 - \frac{2}{3} \frac{P_1}{Q_0} + \frac{23}{63} \right\} P_2(\eta) - \\ & - \frac{1}{27} \left(\frac{P_1}{Q_1}\right)^2 P_1(\eta) - \left(\frac{P_0}{Q_0}\right)^2 \left[\frac{2}{75} \frac{P_3}{Q_0} + \frac{4}{3} \frac{P_1}{Q_0} \left\{ \left(\frac{P_0}{Q_0}\right)^2 - \right. \right. \\ & \left. \left. - \frac{1}{18} \frac{Q_2}{Q_0} - \frac{1}{3} \frac{P_1}{Q_0} + \frac{58}{225} \right\} - \left(\frac{P_0}{Q_0}\right)^4 - \frac{5}{9} \left(\frac{P_0}{Q_0}\right)^2 - \frac{127}{2025} \right] P_0(\eta), \end{aligned} \quad (11.60)$$

where $P_j = P_j(\xi_1)$ and $Q_j = Q_j(\xi_1)$. The radius of convergence of eq. (11.53), regarded as a power series in $c\xi_1$, is indicated in Fig. 11.11.

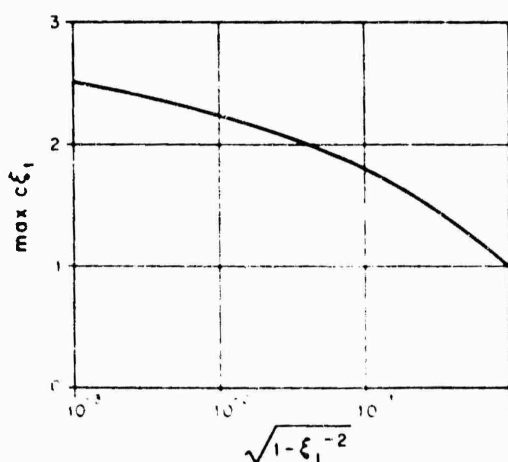


Fig. 11.11. Radius of convergence of low frequency expansion for end-on incidence (SENIOR [1961]).

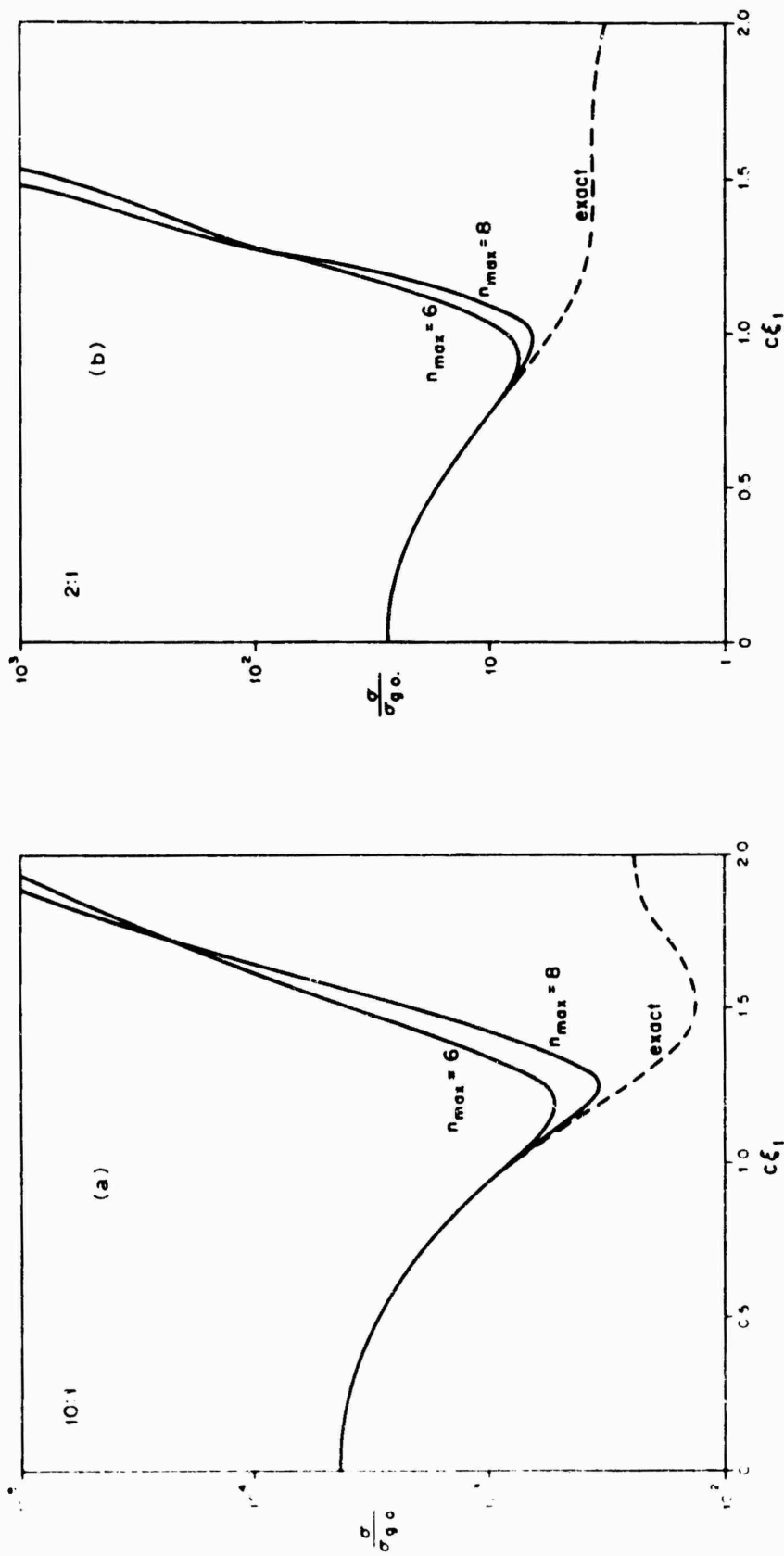


Fig. 11.12. Normalized back scattering cross section at end-on incidence for 10 : 1 and 2 : 1 spheroids (Asvestas and Kleinman [1967]).

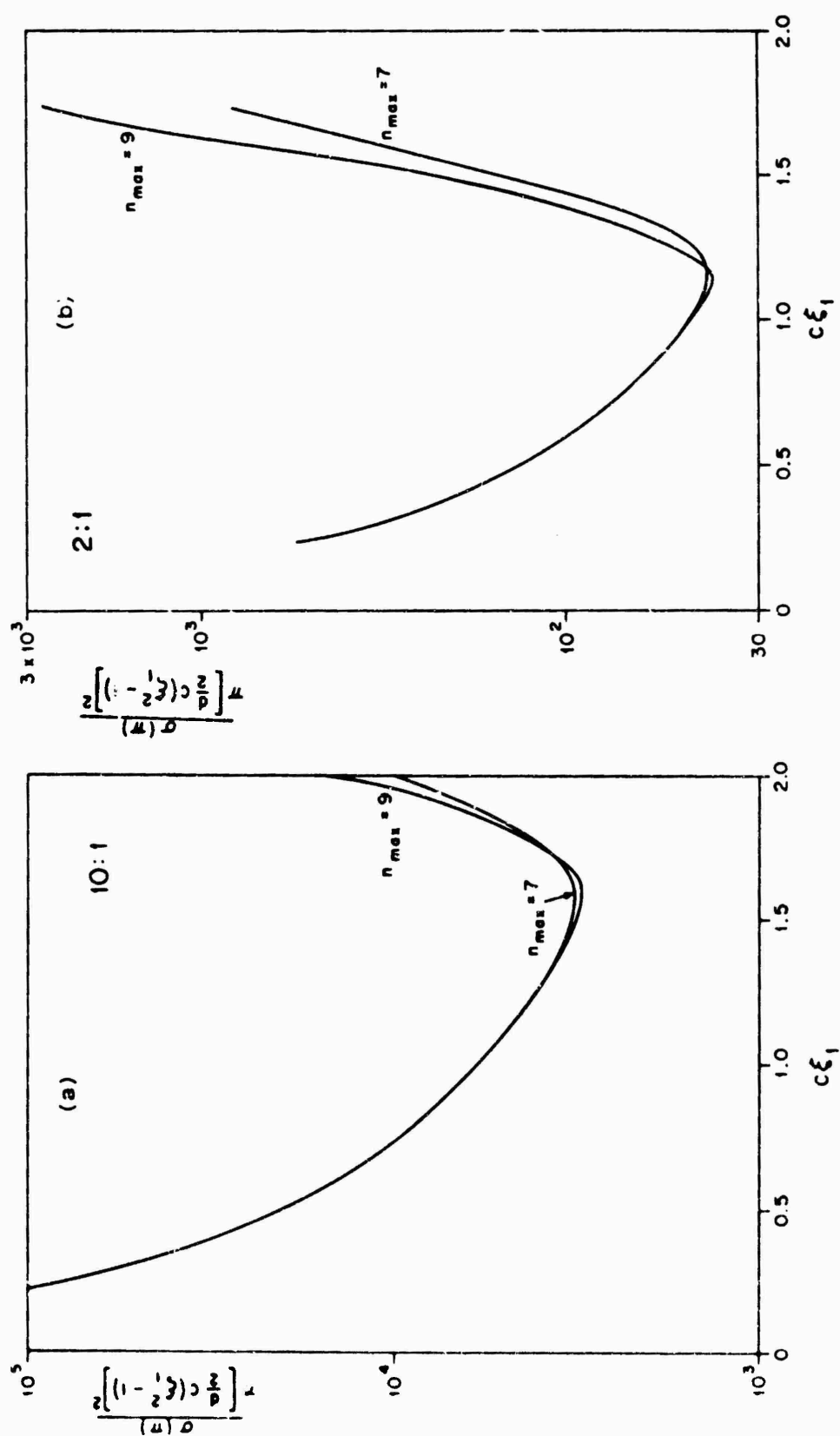


Fig. 11.13. Normalized forward scattering cross section at end-on incidence for 10 : 1 and 2 : 1 spheroids (ASVESTAS and KLEINMAN [1967]).

The back scattering cross section normalized to $\sigma_{g.o.}$ computed using seven and nine terms in the low frequency expansion (i.e. $n_{max} = 6$ and 8) is shown for two typical cases in Fig. 11.12, whereas the forward scattering cross section $\sigma(\pi)$ normalized to the quantity given in eq. (11.43), and computed using eight and ten terms in the low frequency expansion is shown for the same two typical cases in Fig. 11.13.

11.2.2.3. HIGH FREQUENCY APPROXIMATIONS

For the scattered field, no specific results are available for arbitrary incidence, but for axial incidence, such that

$$V^i = e^{-ikz}, \quad (11.61)$$

the geometrical optics scattered field at a point (ξ, η, ϕ) located in the illuminated region $\{(\xi^2 - 1)(1 - \eta^2) > (\xi_1^2 - 1) \text{ with } \eta < 0\}$ is:

$$V_{g.o.}^s = -\exp\{ic(F - \xi_1 \eta_1)\} \left[\left(1 + \frac{2F^2}{(\xi_1^2 - \eta_1^2)G}\right) \left(1 + \frac{2\xi_1^2 G}{\xi_1^2 - \eta_1^2}\right) \right]^{-\frac{1}{2}}, \quad (11.62)$$

where F and G are given by eqs. (11.15) and (11.17), and η_1 is the positive root of eq. (11.18) with $\xi_0 = \infty$. In the geometrical shadow $V_{g.o.}^s = 0$. In the far field ($\xi \rightarrow \infty$):

$$S_{g.o.} = \frac{c(\xi_1^2 - \eta_1^2)}{2\xi_1} \exp\{-ic[\xi_1 \eta_1(1 + \eta) + \sqrt{(\xi_1^2 - 1)(1 - \eta_1^2)(1 - \eta^2)}]\}. \quad (11.63)$$

In particular, if the observation point is on the z -axis ($\eta = 1$):

$$V_{g.o.}^s = -\frac{\xi_1^2 - 1}{2\xi\xi_1 - \xi_1^2 - 1} e^{ic(\xi - 2\xi_1)}, \quad (11.64)$$

and in the far field ($\xi \rightarrow \infty$):

$$S_{g.o.} = -\frac{c(\xi_1^2 - 1)}{2\xi_1} e^{-2ic\xi_1}, \quad (11.65)$$

so that the geometrical optics back scattering cross section is:

$$\sigma_{g.o.} = \frac{\pi c^2}{k^2} (\xi_1 - \xi_1^{-1})^2. \quad (11.66)$$

A more refined approximation, in which the dominant term in the asymptotic expression for the diffracted field is retained, is available only for the far back scattered field at end-on incidence (LIVY and KELLER [1960]). In this case ($\eta = 1, \xi \rightarrow \infty$):

$$S = -\frac{c(\xi_1^2 - 1)}{2\xi_1} e^{-2ic\xi_1} \left\{ 1 + \frac{2(\frac{1}{2}c)^{\frac{1}{2}} \xi_1^{\frac{1}{2}}}{(\xi_1^2 - 1)^{\frac{1}{2}} [Ai'(-x_1)]^2} \exp \left[\frac{1}{2}i\pi + 2ic\xi_1 + \right. \right. \\ \left. \left. + 2ic \int_0^1 \frac{\xi_1^2 - \eta^2}{1 - \eta^2} d\eta + \exp\left\{\frac{1}{2}i\pi\right\} c^{\frac{1}{2}} x_1 \{2\xi_1 \sqrt{(\xi_1^2 - 1)}\}^{\frac{1}{2}} \int_0^1 \frac{d\eta}{\sqrt{(\xi_1^2 - \eta^2)(1 - \eta^2)}} \right] \right\}. \quad (11.67)$$

where

$$\alpha_1 = 2.338\,10\dots, \quad \text{Ai}'(-\alpha_1) = 0.701\,21\dots \quad (11.68)$$

The total scattering cross section for end-on incidence ($\zeta = \pi$) is (JONES [1957]):

$$\sigma_T \sim \frac{2\pi c^2}{k^2} (\xi_1^2 - 1) \{1 + 0.9962[c(\xi_1 - \xi_1^{-1})]^{-4}\}; \quad (11.69)$$

this results in a good approximation if

$$c(\xi_1 - \xi_1^{-1}) \gg 1. \quad (11.70)$$

For broadside incidence ($\zeta = \frac{1}{2}\pi$), such that

$$V^i = e^{ikx}, \quad (11.71)$$

the total scattering cross section is (JONES [1957]):

$$\sigma_T \sim \frac{2\pi c^2}{k^2} \xi_1 \sqrt{\xi_1^2 - 1} [1 + 0.9962b(c\sqrt{(\xi_1^2 - 1)})^{-4}], \quad (11.72)$$

where b is the hypergeometric function:

$$b = {}_2F_1(-\frac{3}{2}, \frac{1}{2}; 1; \xi_1^{-2}). \quad (11.73)$$

The result (11.72) is a good approximation if

$$c\sqrt{(\xi_1^2 - 1)} \gg 1. \quad (11.74)$$

Values of b for a few length-to-width ratios are tabulated in the following:

major axis minor axis = 1 : 1	5 : 4	5 : 3	5 : 2	5 : 1
$b = 1$	0.874	0.761	0.673	0.608

11.2.2.4. SHAPE APPROXIMATION

For a spheroid whose surface $\xi = \xi_1$ is defined in terms of the spherical polar coordinates (r_1, θ_1, ϕ_1) by the equation

$$r_1 = a \left(\frac{\xi_1^2 - 1}{\xi_1^2 - \cos^2 \theta_1} \right)^{\frac{1}{2}}, \quad (11.75)$$

and is such that

$$\xi_1^2 - 1 \gg 1, \quad (11.76)$$

i.e. the spheroid departs only infinitesimally from the sphere $r_1 = a$, the scattered field may be expressed as a perturbation of the solution for this sphere.

For incidence at an angle ζ with respect to the positive z -axis, such that

$$V^i = \exp \{ik(x \sin \zeta + z \cos \zeta)\}, \quad (11.77)$$

then

$$V^s \sim - \sum_{m=0}^{\infty} \sum_{n=m}^{\infty} \varepsilon_m \frac{(n-m)!}{(n+m)!} \frac{i^n}{h_n^{(1)}(ka)} \left[(2n+1)j_n(ka) + \frac{i}{\xi_1^2-1} a_{mn}(\zeta) \right] h_n^{(1)}(kr) \\ \times P_n^m(\cos \zeta) P_n^m(\cos \theta) \cos m\phi + O[(\xi_1^2-1)^{-2}], \quad (11.78)$$

where

$$a_{mn}(\zeta) = \frac{1}{kah_n^{(1)}(ka)} \left[\frac{(2n+1)(n^2+n-1+m^2)}{(2n-1)(2n+3)} + \right. \\ \left. + \frac{(n+m-1)(n+m)}{2(2n-1)} \frac{h_n^{(1)}(ka)}{h_{n-2}^{(1)}(ka)} \frac{P_{n-2}^m(\cos \zeta)}{P_n^m(\cos \zeta)} + \right. \\ \left. + \frac{(n-m+1)(n-m+2)}{2(2n+3)} \frac{h_n^{(1)}(ka)}{h_{n+2}^{(1)}(ka)} \frac{P_{n+2}^m(\cos \zeta)}{P_n^m(\cos \zeta)} \right]. \quad (11.79)$$

In the far back scattered field ($r \rightarrow \infty$, $\theta = \pi - \zeta$, $\phi = \pi$):

$$S \sim \sum_{m=0}^{\infty} \sum_{n=m}^{\infty} \varepsilon_m \frac{(n-m)!}{(n+m)!} \frac{(-1)^n}{h_n^{(1)}(ka)} \left[i(2n+1)j_n(ka) - \frac{1}{\xi_1^2-1} a_{mn}(\zeta) \right] \\ \times [P_n^m(\cos \zeta)]^2 + O[(\xi_1^2-1)^{-2}]. \quad (11.80)$$

For axial incidence ($\zeta = \pi$):

$$V^s \sim - \sum_{n=0}^{\infty} \frac{(-i)^n}{h_n^{(1)}(ka)} \left[(2n+1)j_n(ka) + \frac{i}{\xi_1^2-1} a_{on}(\pi) \right] h_n^{(1)}(kr) P_n(\cos \theta) + O[(\xi_1^2-1)^{-2}], \quad (11.81)$$

where

$$a_{on}(\pi) = \frac{1}{kah_n^{(1)}(ka)} \left[\frac{(2n+1)(n^2+n+1)}{(2n-1)(2n+3)} + \frac{n(n-1)}{2(2n-1)} \frac{h_n^{(1)}(ka)}{h_{n-2}^{(1)}(ka)} + \right. \\ \left. + \frac{(n+1)(n+2)}{2(2n+3)} \frac{h_n^{(1)}(ka)}{h_{n+2}^{(1)}(ka)} \right], \quad (11.82)$$

and in the far back scattered field:

$$S \sim \sum_{n=0}^{\infty} \frac{(-1)^n}{h_n^{(1)}(ka)} \left[i(2n+1)j_n(ka) - \frac{1}{\xi_1^2-1} a_{on}(\pi) \right] + O[(\xi_1^2-1)^{-2}]. \quad (11.83)$$

11.3. Acoustically hard spheroid

11.3.1. Point sources

11.3.1.1. EXACT SOLUTIONS

For a point source at $\mathbf{r}_0 = (\xi_0, \eta_0, \phi_0)$, such that

$$V^i = \frac{e^{ikR}}{kR}, \quad (11.84)$$

then (MORSE and FESHBACH [1953]):

$$V^i + V^s = G(r, r_0) = 2i \sum_{n=0}^{\infty} \sum_{m=n}^{\infty} \frac{\varepsilon_m}{N_{mn}} \left[R_{mn}^{(1)}(c, \xi_<) - \frac{R_{mn}^{(1)'}(c, \xi_1)}{R_{mn}^{(3)'}(c, \xi_1)} R_{mn}^{(3)}(c, \xi_<) \right] \\ \times R_{mn}^{(3)}(c, \xi_>) S_{mn}(c, \eta_0) S_{mn}(c, \eta) \cos m(\phi - \phi_0). \quad (11.85)$$

On the surface $\xi = \xi_1$:

$$V^i + V^s = -\frac{2}{c(\xi_1^2 - 1)} \sum_{m=0}^{\infty} \sum_{n=m}^{\infty} \frac{\varepsilon_m}{N_{mn}} \frac{1}{R_{mn}^{(3)'}(c, \xi_1)} R_{mn}^{(3)}(c, \xi_0) \\ \times S_{mn}(c, \eta_0) S_{mn}(c, \eta) \cos m(\phi - \phi_0). \quad (11.86)$$

In the far field ($\xi \rightarrow \infty$):

$$V^i + V^s = 2 \frac{e^{ic\xi}}{c\xi} \sum_{m=0}^{\infty} \sum_{n=m}^{\infty} \varepsilon_m \frac{(-i)^n}{N_{mn}} \left[R_{mn}^{(1)}(c, \xi_0) - \frac{R_{mn}^{(1)'}(c, \xi_1)}{R_{mn}^{(3)'}(c, \xi_1)} R_{mn}^{(3)}(c, \xi_0) \right] \\ \times S_{mn}(c, \eta_0) S_{mn}(c, \eta) \cos m(\phi - \phi_0). \quad (11.87)$$

When the source is on the positive z -axis ($\eta_0 = 1$):

$$V^i + V^s = 2i \sum_{n=0}^{\infty} \frac{1}{N_{on}} \left[R_{on}^{(1)}(c, \xi_<) - \frac{R_{on}^{(1)'}(c, \xi_1)}{R_{on}^{(3)'}(c, \xi_1)} R_{on}^{(3)}(c, \xi_<) \right] \\ \times R_{on}^{(3)}(c, \xi_>) S_{on}(c, 1) S_{on}(c, \eta). \quad (11.88)$$

In particular, if the field point is on the surface $\xi = \xi_1$:

$$V^i + V^s = -\frac{2}{c(\xi_1^2 - 1)} \sum_{n=0}^{\infty} \frac{1}{N_{on}} \frac{1}{R_{on}^{(3)'}(c, \xi_1)} R_{on}^{(3)}(c, \xi_0) S_{on}(c, 1) S_{on}(c, \eta), \quad (11.89)$$

whereas in the far field ($\xi \rightarrow \infty$):

$$V^i + V^s = 2 \frac{e^{ic\xi}}{c\xi} \sum_{n=0}^{\infty} \frac{(-i)^n}{N_{on}} \left[R_{on}^{(1)}(c, \xi_0) - \frac{R_{on}^{(1)'}(c, \xi_1)}{R_{on}^{(3)'}(c, \xi_1)} R_{on}^{(3)}(c, \xi_0) \right] S_{on}(c, 1) S_{on}(c, \eta). \quad (11.90)$$

11.3.1.2. LOW FREQUENCY APPROXIMATIONS

General methods (e.g. AR and KLEINMAN [1966], NOBLE [1962], MORSE and FESHBACH [1953]) for the derivation of terms in the low frequency expansion are applicable to this case; however, no specific results are as yet available.

11.3.1.3. HIGH FREQUENCY APPROXIMATIONS

For a point source at $(\xi_0, \eta_0, 0)$, such that

$$V^i = \frac{e^{i\lambda R}}{kR}, \quad (11.91)$$

the geometrical optics scattered field at a point $(\xi, \eta, \phi = 0 \text{ or } \pi)$ located in the illuminated region and in the plane containing the source and the z -axis is:

$$V_{g.o.}^s = \frac{e^{ic(F_0+F)}}{cF_0} \left[\left(1 + \frac{F}{F_0} + \frac{2F^2}{(\xi_1^2 - \eta_1^2)G} \right) \left(1 + \frac{F}{F_0} + \frac{2\xi_1^2 G}{\xi_1^2 - \eta_1^2} \right) \right]^{-1}, \quad (11.92)$$

where F , F_0 , G and η_1 were defined in Section 11.2.1.3. In the geometrical shadow $V_{g.o.}^s = 0$. If both source and observation points are on the z -axis ($\eta_0 = \eta = 1$),

$$V_{g.o.}^s = \frac{\exp \{ic(\xi_0 + \xi - 2\xi_1)\}}{c[\xi_0 + \xi - 2\xi_1 + 2\xi_1(\xi_0 - \xi_1)(\xi - \xi_1)/(\xi_1^2 - 1)]} \quad (11.93)$$

in the illuminated region and zero in the shadow.

A more refined approximation, in which an asymptotic expression for the diffracted field is retained, is available only for the source on the z -axis. In this case

$$V^s = V_{g.o.}^s + V_d^s, \quad (11.94)$$

where $V_{g.o.}^s$ is given by eqs. (11.92, 15, 16, 17) and (LEVY and KELLER [1960]):

$$V_d^s = \frac{2^{\frac{1}{2}} \exp \{ \frac{1}{2} i \pi \} (\xi_1 \sqrt{(\xi_1^2 - 1)})^{\frac{1}{2}}}{\pi^{\frac{1}{2}} (4c)^{7/6}} \frac{\exp \{ (ic/\xi_0) \sqrt{(\xi_0^2 - 1)(\xi_0^2 - \xi_1^2)} \}}{[(\xi_0^2 - \xi_1^2)(\xi_0^2 - 1)(\xi^2 - 1)(1 - \eta^2)]^{\frac{1}{2}}} \\ \times \sum_{n=0}^{\infty} \frac{\tilde{f}_n(\eta_2) - i\tilde{f}_n(\eta_3)}{\beta_n [Ai(-\beta_n)]^2 [1 + \exp \{ 2\tilde{X}_n(1, -1) \}]}, \quad (11.95)$$

where

$$\tilde{X}_n(x, \beta) = ic \int_{\beta}^x \sqrt{\frac{\xi_1^2 - \eta^2}{1 - \eta^2}} d\eta + i(\frac{1}{2}c)^{\frac{1}{2}} e^{i\frac{1}{2}\pi} \beta_n \{ \xi_1 \sqrt{(\xi_1^2 - 1)} \}^{\frac{1}{2}} \int_{\beta}^x \frac{d\eta}{\sqrt{(\xi_1^2 - \eta^2)(1 - \eta^2)}}, \quad (11.96)$$

$$\tilde{f}_n(\eta_2) = (\xi_1^2 - \eta_2^2)^{\frac{1}{2}} T_2^{-\frac{1}{2}} \exp [icT_2 + \tilde{X}_n(\eta_1, \eta_2)], \quad (11.97)$$

$$\tilde{f}_n(\eta_3) = (\xi_1^2 - \eta_3^2)^{\frac{1}{2}} T_3^{-\frac{1}{2}} \exp [icT_3 + \tilde{X}_n^{\pm}], \quad (11.98)$$

$$\tilde{X}_n^{\pm} = \tilde{X}_n(\eta_1, -1) + \tilde{X}_n(\eta_3, -1), \quad \tilde{X}_n^{-} = \tilde{X}_n(\eta_1, \eta_3), \quad (11.99)$$

\tilde{X}_n^{\pm} is to be chosen if $\xi\eta + \xi_1 > 0$, and \tilde{X}_n^{-} if $\xi\eta + \xi_1 < 0$,

$$T_j = [(\xi\eta - \xi_1\eta_j)^2 + \{ \sqrt{(\xi^2 - 1)(1 - \eta^2)} \pm \sqrt{(\xi_1^2 - 1)(1 - \eta_j^2)} \}^2]^{\frac{1}{2}}, \quad (11.100)$$

$j = 2, 3$ and the ambiguity of sign in T is removed by choosing the minus sign if either $j = 2$, or $j = 3$ and $\xi\eta + \xi_1 > 0$, and the plus sign if $j = 3$ and $\xi\eta + \xi_1 < 0$. The coordinates η_1 , η_2 and η_3 are indicated in Fig. 11.2. Equation (11.95) is valid if the observation point is away from both the z -axis and the surface $\xi = \xi_1$, and if the product of the wave number k and the radius of curvature of the surface $\xi = \xi_1$ at the end points $\eta = \pm 1$ is large compared to unity, i.e.

$$\frac{c(\xi_1^2 - 1)}{\xi_1} \gg 1. \quad (11.101)$$

The field on the surface $\xi = \xi_1$ may be obtained by applying the appropriate caustic corrections to eq. (11.95) (LEVY and KELLER [1960]).

For a point source $(\xi_0, 1)$ on the z -axis at a large distance from a long, thin spheroid, such that

$$\xi_0^2 \gg 1, \quad c\xi_1 \gg 1, \quad \frac{c(\xi_1^2 - 1)}{\xi_1} \ll 1, \quad (11.102)$$

the field at a point (ξ_1, η, ϕ) on the surface of the spheroid and near the tip in the shadow region ($c(1+\eta) \ll 1$) is given by the asymptotic expansion (GOODRICH and KAZARINOFF [1953]):

$$V^i + V^s \sim \frac{e^{ic(1+\xi_0)}}{c\xi_0} \frac{\cos[c(1+\eta)]}{\sqrt{2(1-\eta)}} \sum_{n=0}^N \sum_{m=0}^{\infty} \left(-\frac{i}{4c}\right)^n n! B_{mn}, \quad (11.103)$$

where N is the largest integer less than c , and

$$B_{mn} = \left[\frac{e^{icn!}}{2(4c)^n} \sqrt{\frac{1}{2}(1-\xi_1^{-2})} \right]^{4m}; \quad (11.104)$$

while in the shadow and near the shadow boundary ($c(1+\eta) \gg 1$):

$$\begin{aligned} V^i + V^s \sim & -\frac{e^{ic(1+\xi_0)}}{c\xi_0\sqrt{(1-\eta^2)}} \sum_{n=0}^N \sum_{m=0}^{\infty} B_{mn} \left[(-1)^n \left(\frac{1+\eta}{1-\eta}\right)^{n+\frac{1}{2}} e^{-ic(1+\eta)} + \right. \\ & \left. + \frac{(n!)^2}{(4c)^{2n}} \frac{1-\xi_1^{-2}}{2} \left(\frac{1-\eta}{1+\eta}\right)^{n+\frac{1}{2}} e^{ic(1+\eta)} \right]. \end{aligned} \quad (11.105)$$

If only the first residue contribution ($n=0$) to the surface field is considered, then

$$V^i + V^s \sim \frac{e^{ic\xi_0}}{c\xi_0} \frac{\cos[c(1+\eta)]}{\sqrt{2(1-\eta)}} e^{ikL} \sum_{m=0}^{\infty} \left\{ \frac{1}{8}(1-\xi_1^{-2}) \right\}^{2m} e^{2ikLm}, \quad (11.106)$$

for $c(1+\eta) \ll 1$ (near tip in shadow), and

$$\begin{aligned} V^i + V^s \sim & -\frac{e^{ic\xi_0}}{c\xi_0\sqrt{(1-\eta^2)}} \sum_{m=0}^{\infty} \left\{ \frac{1}{8}(1-\xi_1^{-2}) \right\}^{2m} \left[\sqrt{\frac{1+\eta}{1-\eta}} e^{ik(l_1+2Lm)} + \right. \\ & \left. + \frac{1}{2}(1-\xi_1^{-2}) \sqrt{\frac{1-\eta}{1+\eta}} e^{ik(l_2+2Lm)} \right]. \end{aligned} \quad (11.107)$$

in the shadow and near the shadow boundary ($c(1+\eta) \gg 1$), where

$$l_1 = -\frac{c}{k}\eta, \quad l_2 = \frac{c}{k}(2+\eta), \quad L = \frac{2c}{k}. \quad (11.108)$$

The parameter L is approximately equal to the length of a geodesic between the tips of the spheroid, whereas l_1 and l_2 can be approximately identified with the geodesic path lengths between the field point and those points of the shadow boundary which lie in the plane containing the field and the z -axis, as shown in Fig. 11.3. Thus the various terms in series (11.106) and (11.107) are easily interpreted in terms of creeping waves.

11.3.2. Plane wave incidence

11.3.2.1. EXACT SOLUTIONS

For incidence at an angle ζ with respect to the positive z -axis, such that

$$V^i = \exp \{ik(x \sin \zeta + z \cos \zeta)\}, \quad (11.109)$$

then (SENIOR [1960]):

$$V^s = -2 \sum_{m=0}^{\infty} \sum_{n=m}^{\infty} \varepsilon_m \frac{i^n}{N_{mn}} \frac{R_{mn}^{(1)'}(c, \xi_1)}{R_{mn}^{(3)'}(c, \xi_1)} R_{mn}^{(3)}(c, \xi) S_{mn}(c, \cos \zeta) S_{mn}(c, \eta) \cos m\phi. \quad (11.110)$$

On the surface $\xi = \xi_1$:

$$V^i + V^s = \frac{2}{c(\xi_1^2 - 1)} \sum_{m=0}^{\infty} \sum_{n=m}^{\infty} \varepsilon_m \frac{i^{n+1}}{N_{mn}} \frac{1}{R_{mn}^{(3)'}(c, \xi_1)} S_{mn}(c, \cos \zeta) S_{mn}(c, \eta) \cos m\phi. \quad (11.111)$$

In the far field ($\xi \rightarrow \infty$):

$$S = 2i \sum_{m=0}^{\infty} \sum_{n=m}^{\infty} \frac{\varepsilon_m}{N_{mn}} \frac{R_{mn}^{(1)'}(c, \xi_1)}{R_{mn}^{(3)'}(c, \xi_1)} S_{mn}(c, \cos \zeta) S_{mn}(c, \eta) \cos m\phi. \quad (11.112)$$

SPENCE and GRANGER [1951] computed $|S|/(c\xi_1)$ as a function of $\theta = \arccos \eta$ for $\xi_1 = 1.005, 1.020, 1.044, 1.077$ with $\zeta = 0^\circ (30^\circ) 90^\circ$, $c = 1(1)3$.

The total scattering cross section is:

$$\sigma_T = \frac{4\pi}{k^2} \sum_{m=0}^{\infty} \sum_{n=m}^{\infty} \frac{\varepsilon_m^2}{N_{mn}} \left[\frac{R_{mn}^{(1)'}(c, \xi_1)}{R_{mn}^{(3)'}(c, \xi_1)} S_{mn}(c, \cos \zeta) \right]^2. \quad (11.113)$$

The total scattering cross section normalized to 2.4, where

$$A = \frac{1}{4} \pi d^2 \sqrt{\{(\xi_1^2 - 1)(\xi_1^2 - \cos^2 \zeta)\}} \quad (11.114)$$

is the area of the geometrical shadow, has been computed by SPENCE and GRANGER [1951] for selected values of ξ_1 and ζ , and is shown in Fig. 11.14.

For axial incidence ($\zeta = \pi$):

$$V^s = -2 \sum_{n=0}^{\infty} \frac{i^n}{N_{on}} \frac{R_{on}^{(1)'}(c, \xi_1)}{R_{on}^{(3)'}(c, \xi_1)} R_{on}^{(3)}(c, \xi) S_{on}(c, -1) S_{on}(c, \eta), \quad (11.115)$$

and on the surface $\xi = \xi_1$:

$$V^i + V^s = \frac{2}{c(\xi_1^2 - 1)} \sum_{n=0}^{\infty} \frac{i^{n+1}}{N_{on}} \frac{1}{R_{on}^{(3)'}(c, \xi_1)} S_{on}(c, -1) S_{on}(c, \eta). \quad (11.116)$$

Amplitude and phase of the surface field are shown for typical values of c and ξ_1 in Fig. 11.15. In the far field ($\xi \rightarrow \infty$):

$$S = 2i \sum_{n=0}^{\infty} \frac{1}{N_{on}} \frac{R_{on}^{(1)'}(c, \xi_1)}{R_{on}^{(3)'}(c, \xi_1)} S_{on}(c, -1) S_{on}(c, \eta). \quad (11.117)$$

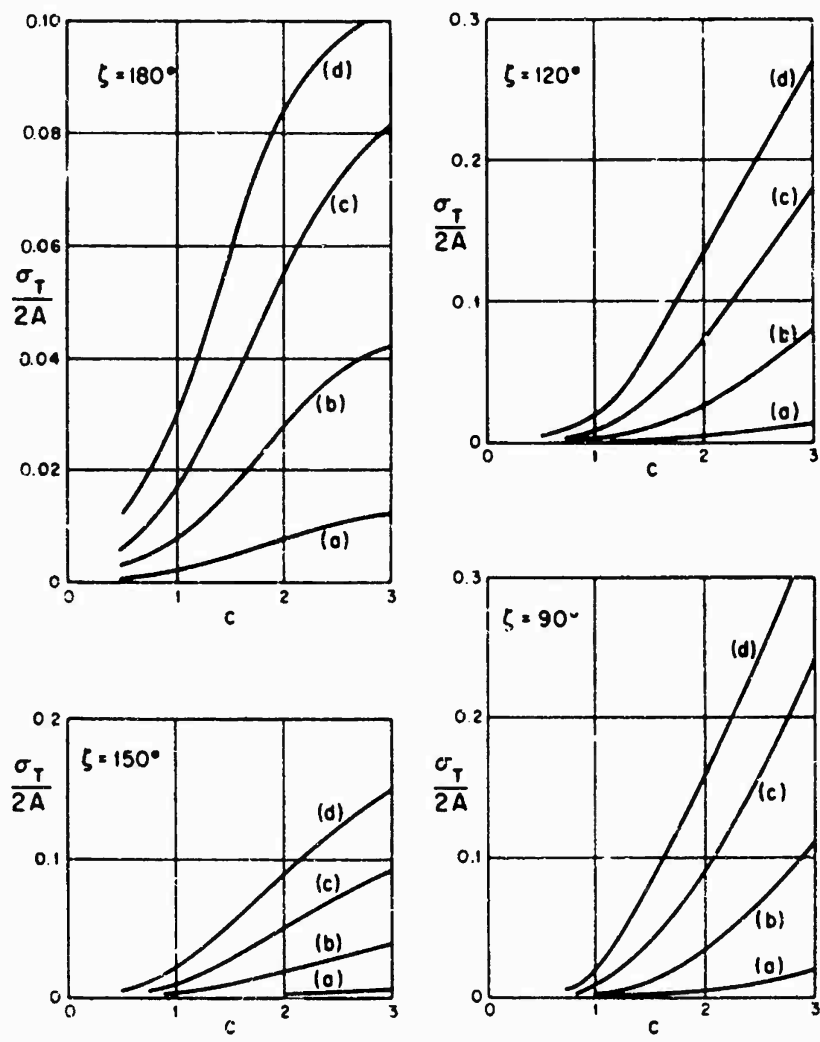


Fig. 11. 14. Normalized total scattering cross section $\frac{1}{2}\sigma_T/A$ for (a) $\xi_1 = 1.005$, (b) $\xi_1 = 1.020$, (c) $\xi_1 = 1.044$ and (d) $\xi_1 = 1.077$ (SPENCE and GRANGER [1951]).

The bistatic cross section normalized to the geometrical optics back scattering cross section $\sigma_{g.o.}$ is shown as a function of $\theta = \arccos \eta$ in Fig. 11.16, for selected values of $c\xi_1$ and of the length-to-width ratio. Computed results of $|S|/(c\xi_1)$ were given by SPENCE and GRANGER [1951], as previously mentioned. Using an integral equation approach for his numerical computations, BRUNDRIT [1965] has plotted $|S|$ as a function of $\theta = \arccos \eta$ for $c\xi_1 = 1, 2, 3$ and length-to-width ratios varying from 1:1 to 5:1. For the particular case of back scattering ($\eta = 1$), $\arg S$ is plotted as a function of $c\xi_1$ for selected values of ξ_1 in Fig. 11.17. Corresponding values of the back scattering cross section, normalized to $\sigma_{g.o.}$, are shown in Fig. 11.18. For forward scattering ($\eta = -1$), $\arg S$ is plotted as a function of $c\xi_1$ for selected values of ξ_1 in Fig. 11.19. Corresponding values of the forward scattering cross section, normalized to the quantity of eq. (11.43), are shown in Fig. 11.20.

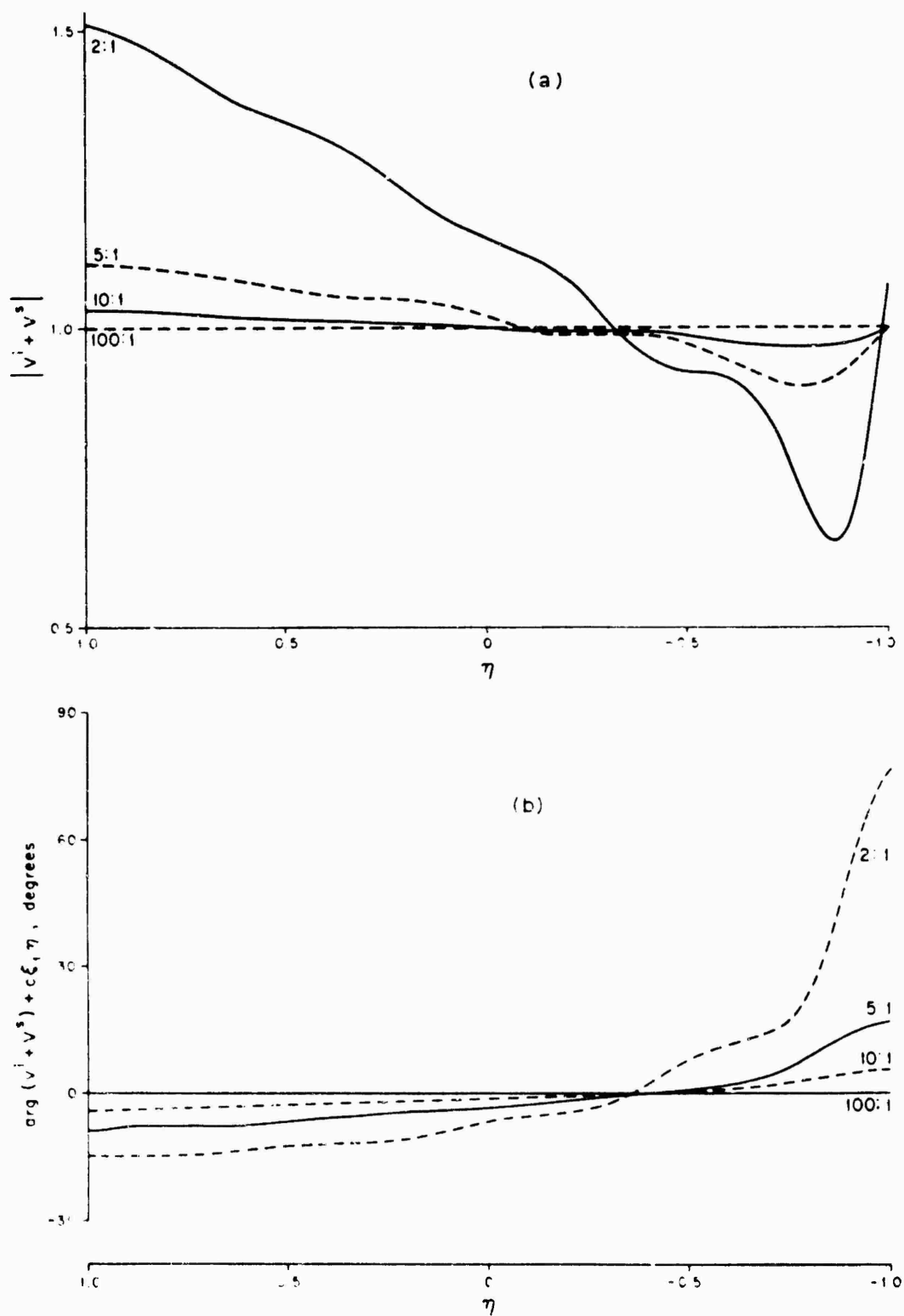
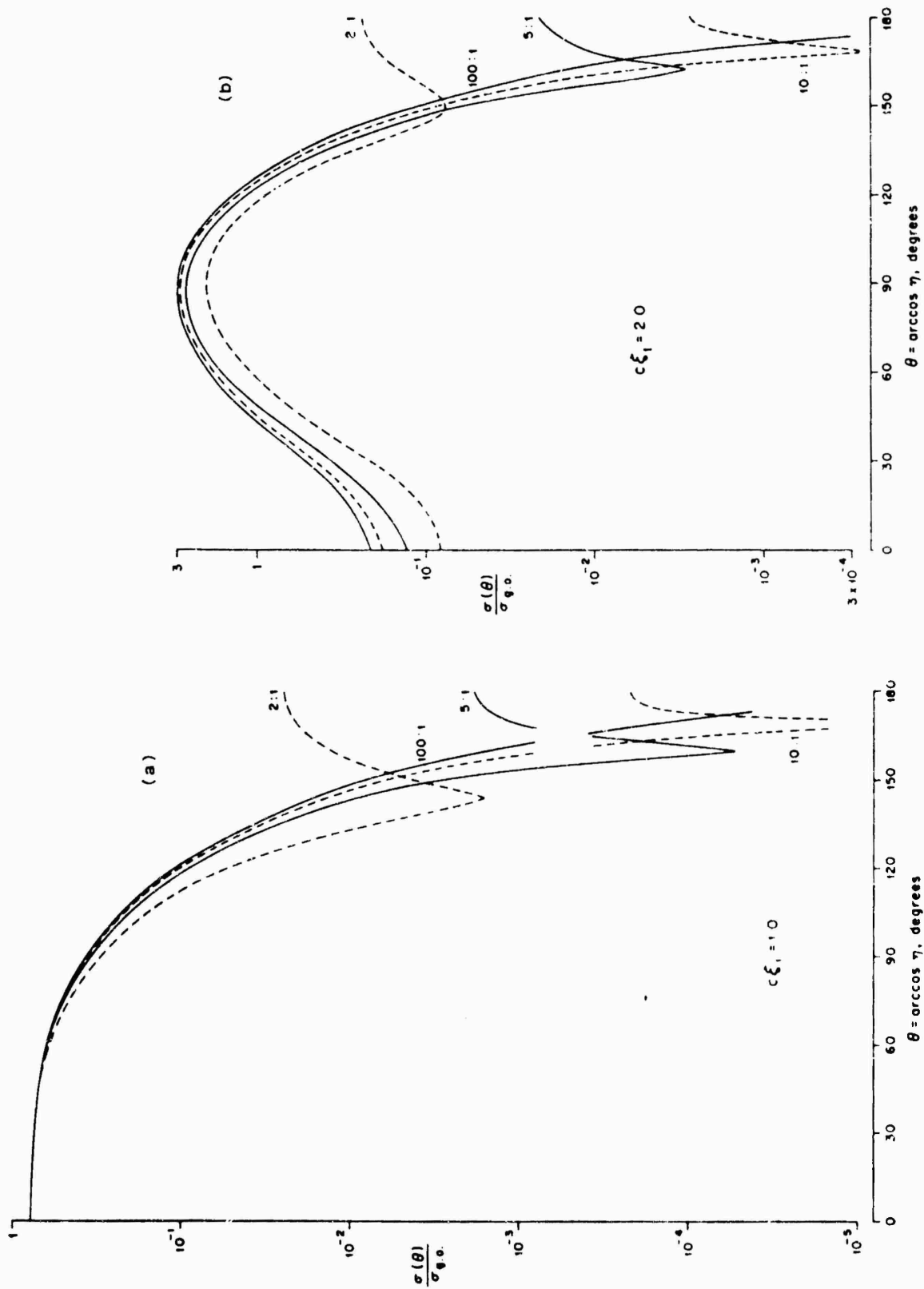
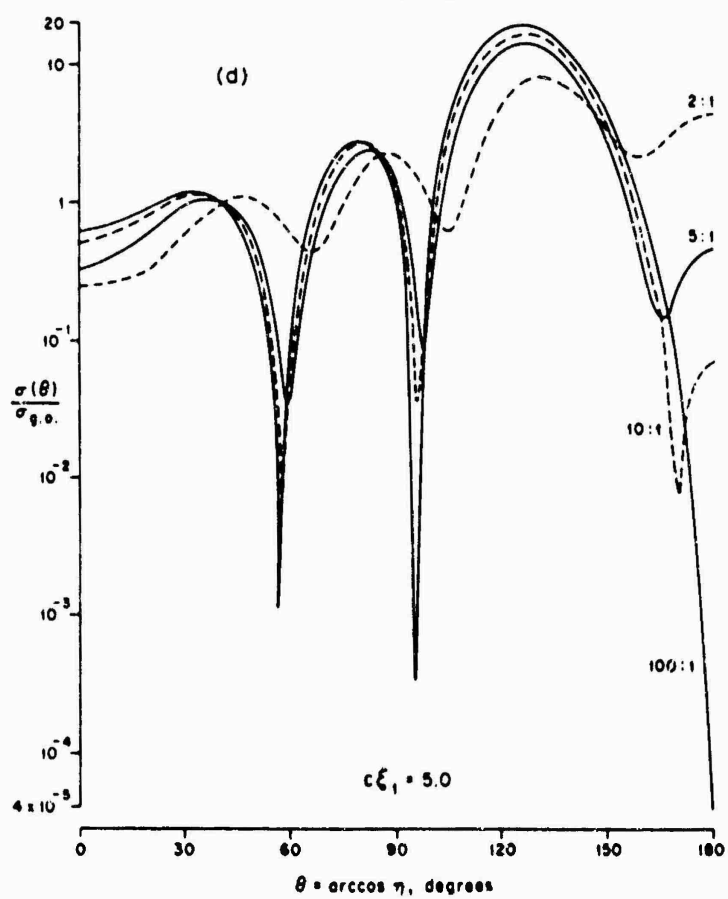
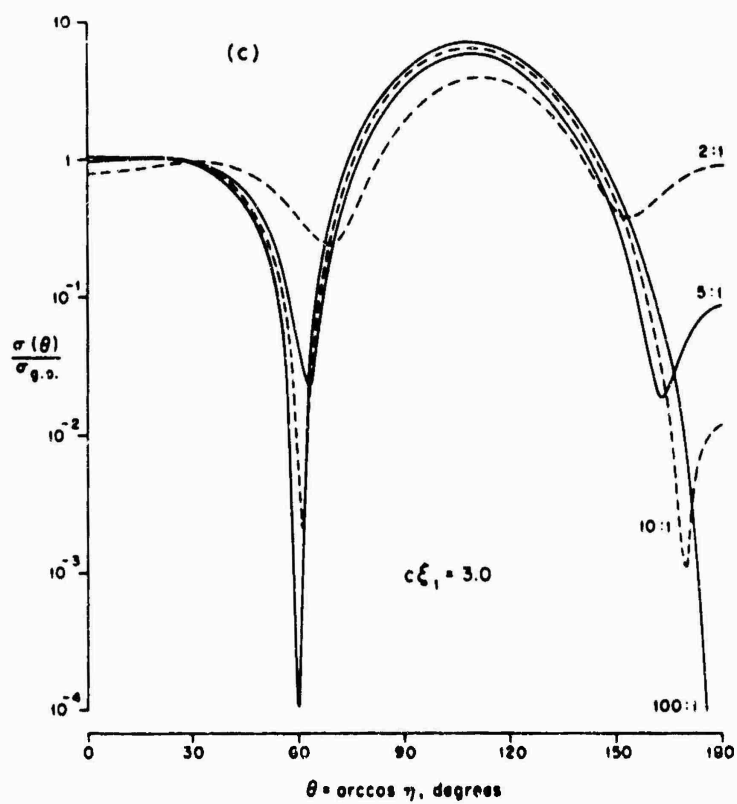


Fig. 11.15. Amplitude and phase of surface field for end-on incidence with $c = 5.0$ (SENIOR [1969]).





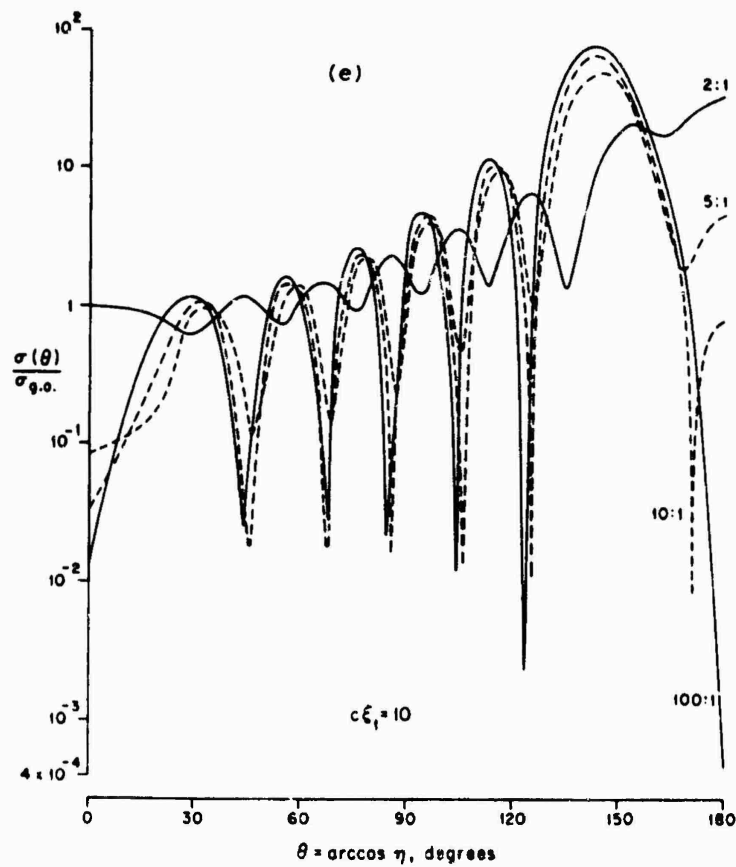


Fig. 11.16. Bistatic cross section normalized to $\sigma_{g.o.}$ as a function of $\theta = \arccos \eta$, for end-on incidence (SENIOR [1969]).

The total scattering cross section is

$$\sigma_T = \frac{4\pi}{k^2} \sum_{n=0}^{\infty} \frac{1}{N_{on}} \left[\frac{R_{on}^{(1)}(c, \xi_1)}{|R_{on}^{(3)}(c, \xi_1)|} S_{on}(c, -1) \right]^2. \quad (11.118)$$

The normalized cross section $\frac{1}{2}\sigma_T/A$ is shown for selected values of ξ_1 in Fig. 11.14 and for selected length-to-width ratios in Fig. 11.21. BRUNDRIT [1965] has plotted σ_T as a function of $c\xi_1$ ($c\xi_1 < 8$) for length-to-width ratios varying from 1:1 to 5:1.

11.3.2.2. LOW FREQUENCY APPROXIMATIONS

For incidence at an angle ζ with respect to the positive z -axis, such that

$$V^i = \exp \{ik(x \sin \zeta + z \cos \zeta)\}, \quad (11.119)$$

then (ASVESTAS and KLEINMAN [1967]):

$$V^s = e^{ic\xi} \sum_{n=0}^{\infty} \sum_{m=0}^n (-ic)^n \frac{(\xi_1 - \eta)^{n-m}}{(n-m)!} \sum_{l=0}^m \sum_{h=0}^m \sum_{j=0}^m C_{l,h,j}^m Q_h^l(\xi) P_j^l(\eta) \cos l\phi. \quad (11.120)$$

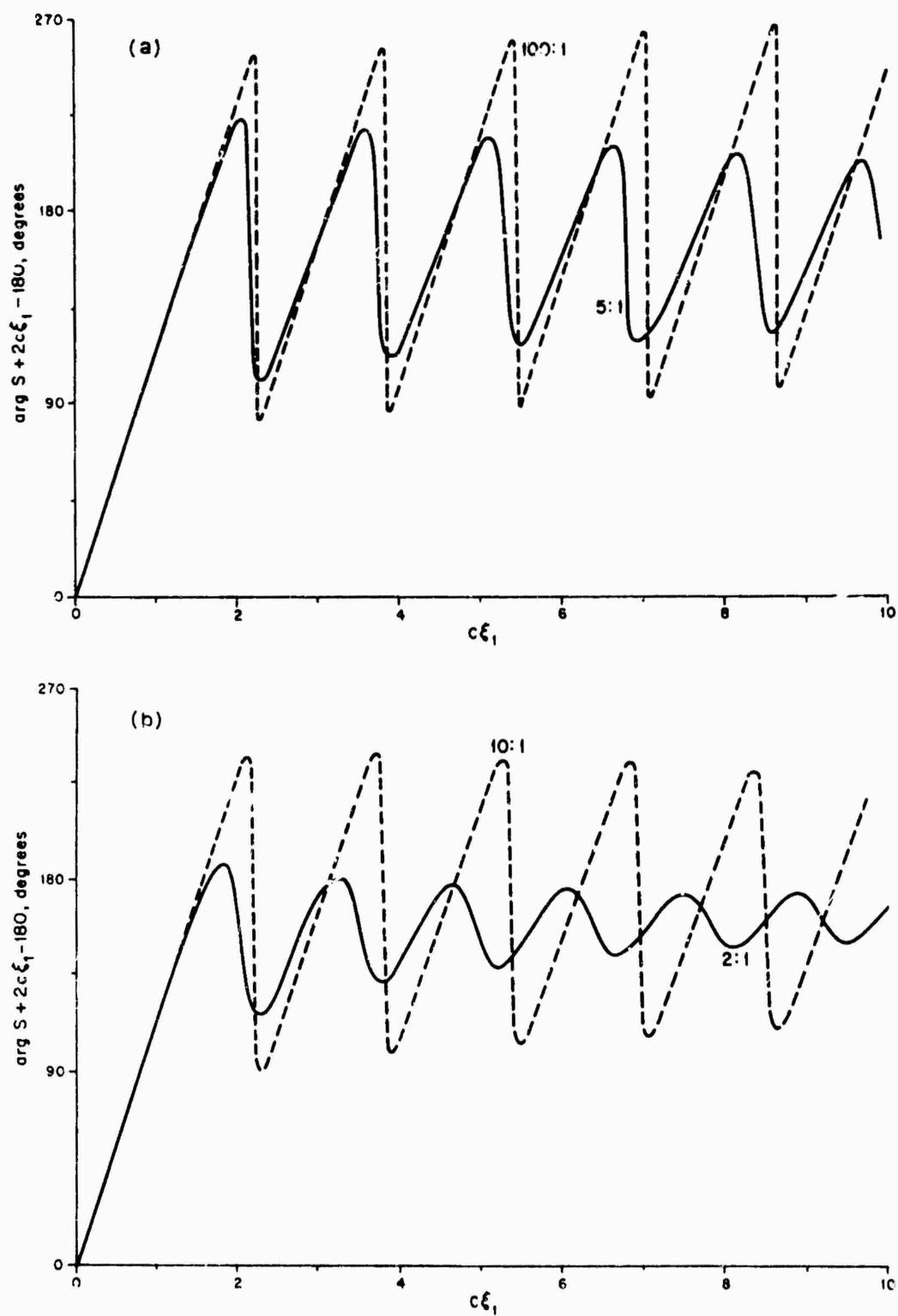
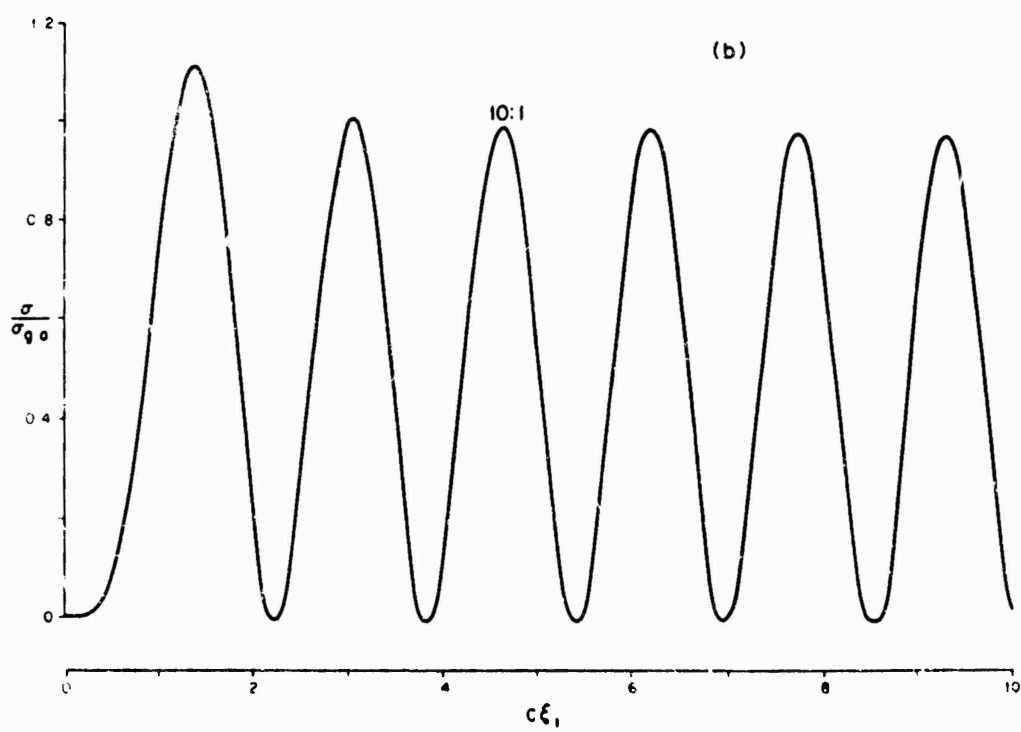
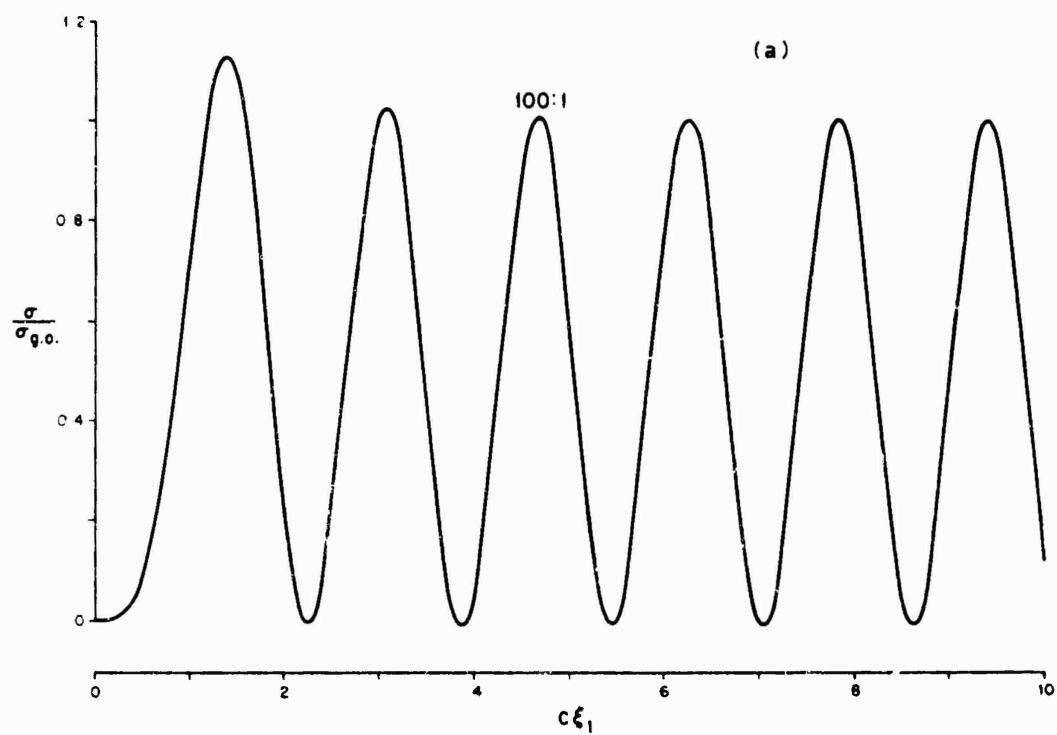


Fig. 11.17. Phase of back scattering coefficient S for end-on incidence (SENIOR [1969]).



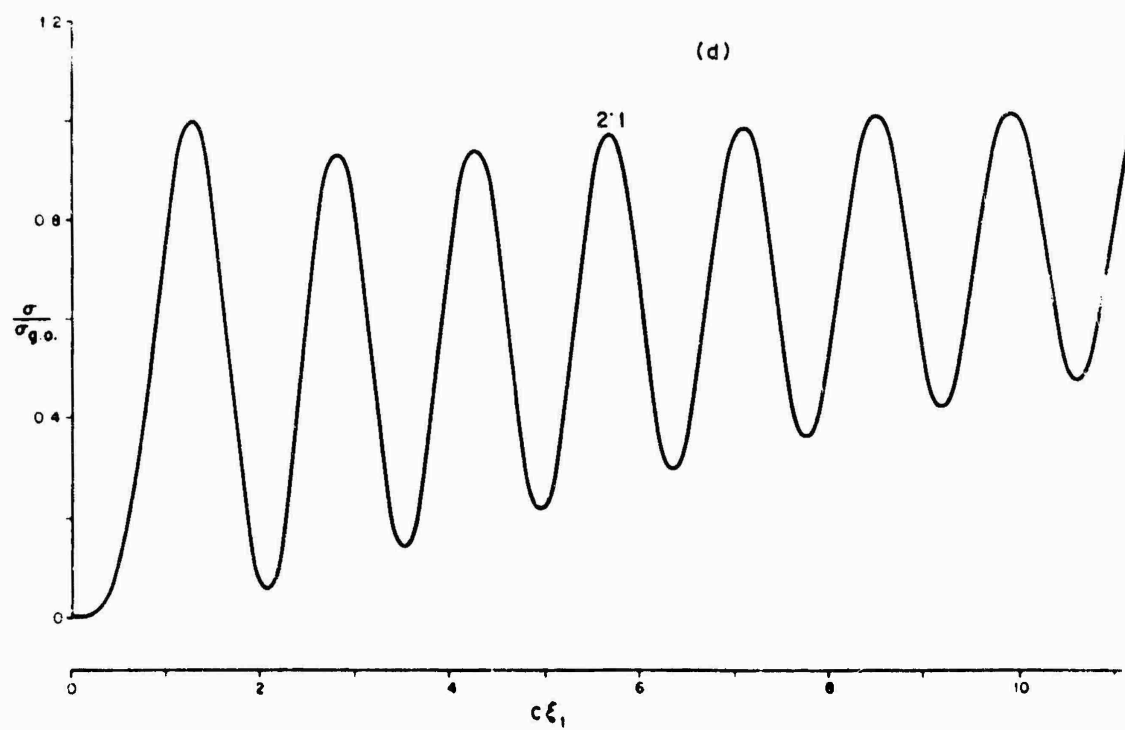
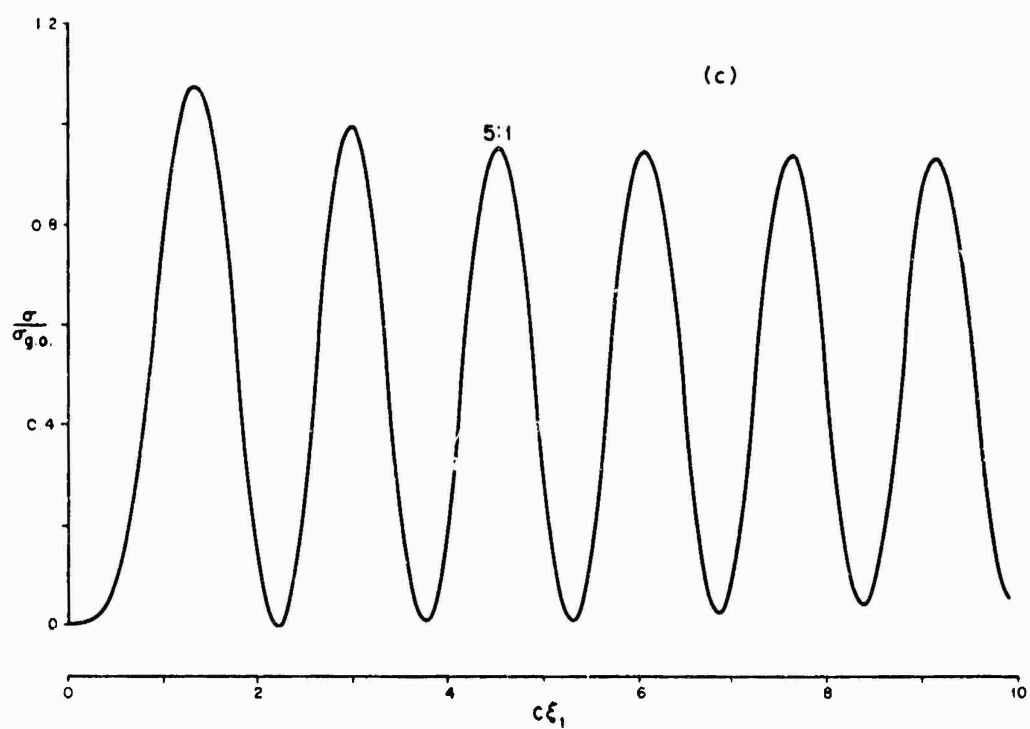


Fig. 11. 18. Normalized back scattering cross section for end-on incidence (SENIOR [1969]).

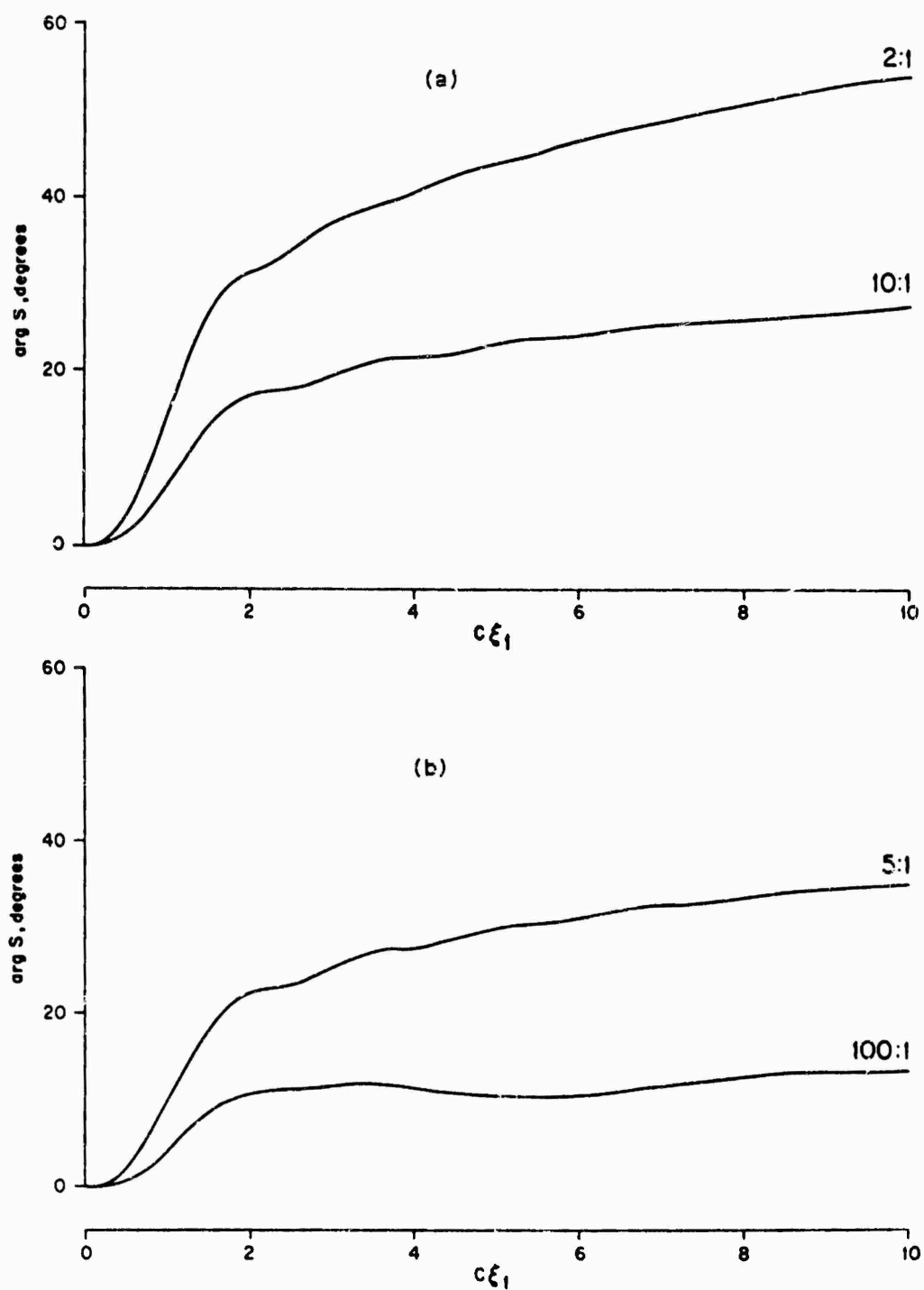


Fig. 11.19. Phase of forward scattering coefficient S for end-on incidence (SENIOR [1969]).

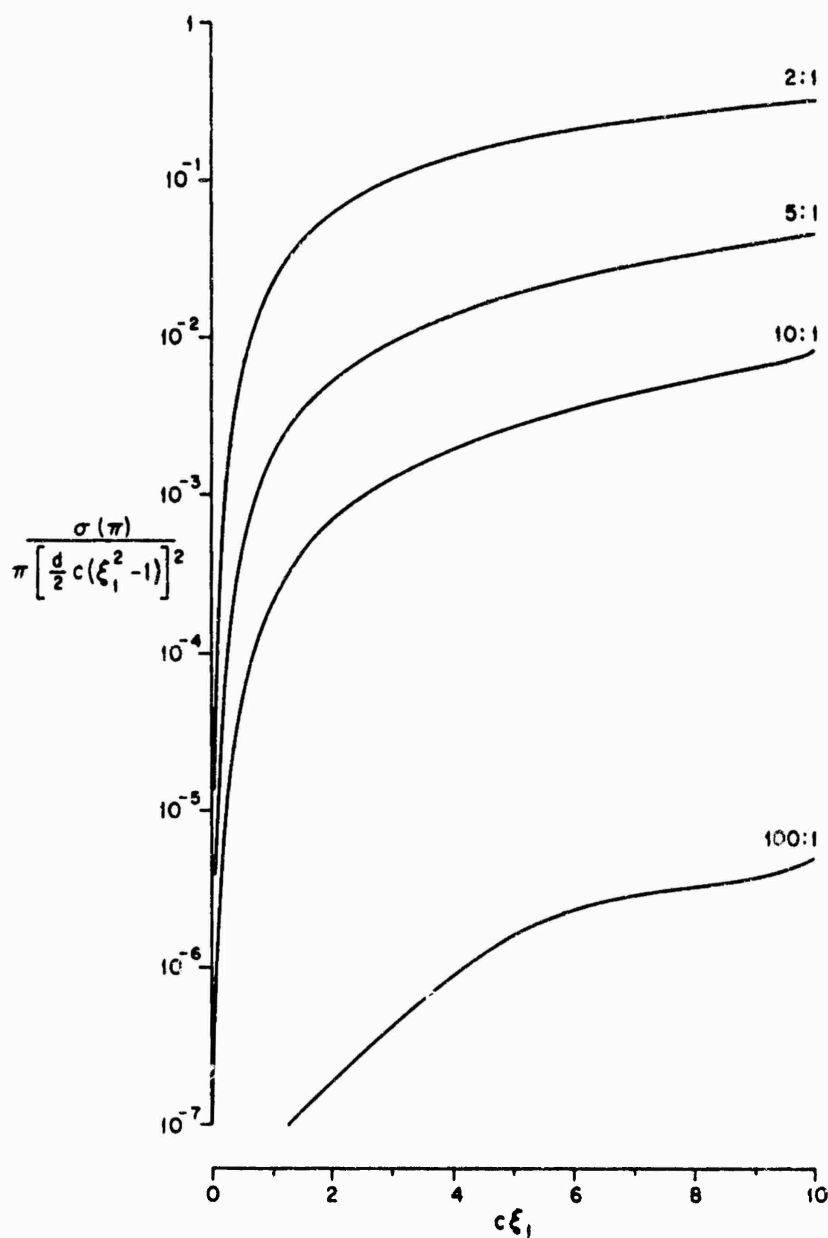


Fig. 11.20. Normalized forward scattering cross section for end-on incidence (SILVER [1966c]).

where $C_{l,h,j}^m = C_{l,j,h}^m$ and $C_{l,h,j}^m$ is given by the recurrence relations:

$$C_{l,h,j}^{m+1} = \frac{2}{h(h+1)-j(j+1)} \left[\frac{h(h-1)}{2h-1} C_{l,h-1,j}^m - \frac{j(j-1)}{2j-1} C_{l,h,j-1}^m + \right. \\ \left. + \frac{(j+1)(j+1+1)}{2j+3} C_{l,h,j+1}^m - \frac{(h+1)(h+1+1)}{2h+3} C_{l,h+1,j}^m \right], \quad (11.121)$$

for $h \neq j$ and $m = 0, 1, 2, \dots$;

$$C_{l,j,j}^{m+1} = - \sum_{h=1}^{m+1} \frac{Q_h^l(\xi_1)}{Q_j^l(\xi_1)} C_{l,h,j}^{m+1} + \sum_{h=0}^m \frac{Q_h^l(\xi_1)}{Q_j^l(\xi_1)} C_{l,h,j}^m + A_{j,l}^{m+1}, \quad (11.122)$$

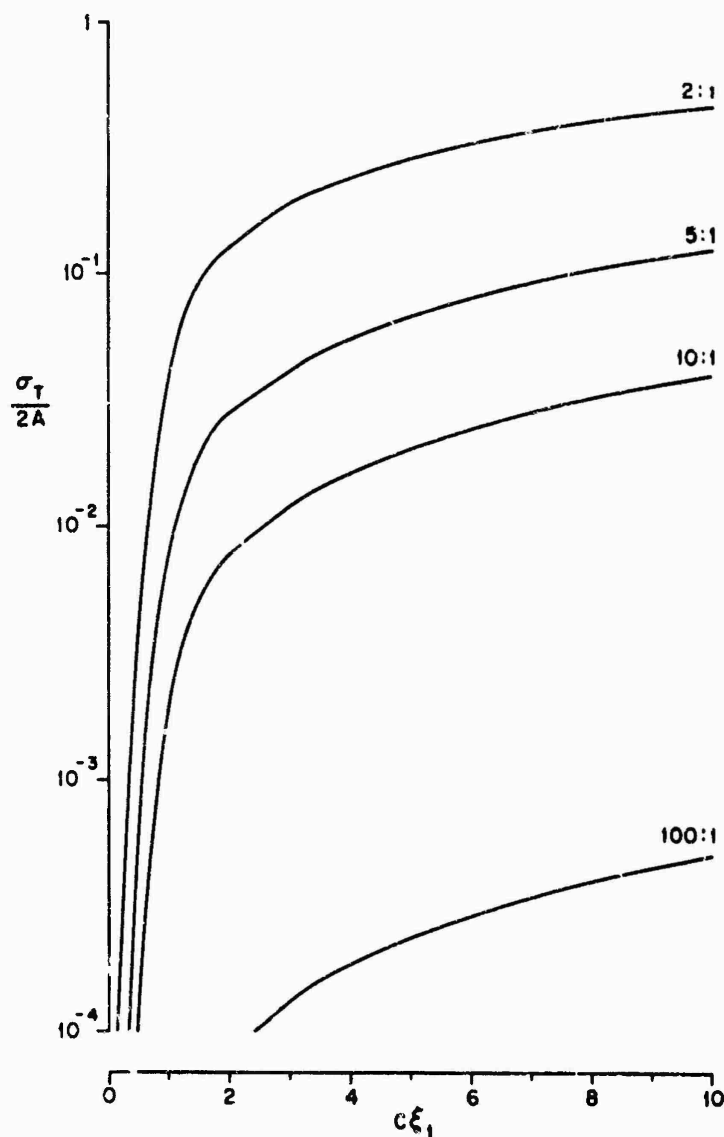


Fig. 11.21. Normalized total scattering cross section for end-on incidence (SENIOR [1969]).

for $m = 0, 1, 2, \dots$, where \sum' indicates that the term $h = j$ is omitted from the summation; and

$$C_{0,0,0}^0 = A_{0,0}^0 = 0, \quad (11.123)$$

$$A_{j,l}^m = 0, \quad \text{for } m+j \text{ odd,}$$

$$A_{j,l}^m = \frac{\sqrt{\pi}}{2^{m+1}} \frac{(\xi_1 - \cos \zeta)^{m-l}}{\{\frac{1}{2}(m-j)\}! \{\frac{1}{2}(m+j+1)\}!} Q_j^l(\xi_1) \frac{(j-l)!}{(j+l)!} \\ \times \left\{ c_l \cos \zeta \left[(m-j)(j-l+1) P_{j+1}^l \left(\frac{1-\xi_1 \cos \zeta}{\xi_1 - \cos \zeta} \right) + \right. \right. \\ \left. \left. + (j+l)(m+j+1) P_{j-1}^l \left(\frac{1-\xi_1 \cos \zeta}{\xi_1 - \cos \zeta} \right) \right] - \right.$$

$$\begin{aligned}
& - \frac{\xi_1 \sin \zeta}{\sqrt{(\xi_1^2 - 1)}} \left[(j+l)(m+j+1) \left\{ P_{j-1}^{l+1} \left(\frac{1 - \xi_1 \cos \zeta}{\xi_1 - \cos \zeta} \right) - \right. \right. \\
& \left. \left. -(j+l)(j+l-1) P_{j-1}^{l-1} \left(\frac{1 - \xi_1 \cos \zeta}{\xi_1 - \cos \zeta} \right) \right\} - \right. \\
& \left. -(m-j)(j-l+1) \left\{ P_{j+1}^{l+1} \left(\frac{1 - \xi_1 \cos \zeta}{\xi_1 - \cos \zeta} \right) - \right. \right. \\
& \left. \left. -(j-l+1)(j-l+2) P_{j+1}^{l-1} \left(\frac{1 - \xi_1 \cos \zeta}{\xi_1 - \cos \zeta} \right) \right\} \right] \Bigg\}, \quad \text{for } m+j \text{ even.}
\end{aligned} \tag{11.124}$$

In the far field ($\xi \rightarrow \infty$):

$$S = c \sum_{n=0}^{\infty} \sum_{m=0}^n (-ic)^n \frac{(\xi_1 - \eta)^{n-m}}{(n-m)!} \sum_{l=0}^m \sum_{j=0}^m C_{l,0,j}^m P_j^l(\eta) \cos l\phi. \tag{11.125}$$

Starting from the exact series solution, BUPKE [1966b] has computed S through terms $O(k^6)$ for arbitrary angles of incidence and observation.

For axial incidence ($\zeta = \pi$):

$$V^s = e^{ic\xi} \sum_{n=0}^{\infty} \sum_{m=0}^n (-ic)^n \frac{(\xi_1 - \eta)^{n-m}}{(n-m)!} \sum_{h=0}^m \sum_{j=0}^m C_{0,h,j}^m Q_h(\xi) P_j(\eta), \tag{11.126}$$

and in the far field ($\xi \rightarrow \infty$):

$$S = -c \sum_{n=0}^{\infty} (-ic)^n u_n, \tag{11.127}$$

where

$$u_n = - \sum_{m=0}^n \frac{(\xi_1 - \eta)^{n-m}}{(n-m)!} \sum_{j=0}^m C_{0,0,j}^m P_j(\eta). \tag{11.128}$$

In particular (SENIOR [1960]):

$$u_0 = u_1 = 0, \tag{11.129}$$

$$u_2 = \frac{1}{3} \frac{P_1'}{Q_1'} P_1(\eta) + \frac{1}{9} \frac{P_2'}{Q_0'} P_0(\eta), \tag{11.130}$$

$$u_3 = 0, \tag{11.131}$$

$$\begin{aligned}
u_4 = & \frac{1}{75} \frac{P_1'}{Q_1'} P_3(\eta) + \frac{1}{81} \left\{ \frac{4}{15} \frac{P_2'}{Q_2'} + \frac{P_2'}{Q_0'} \right\} P_2(\eta) + \frac{1}{75} \frac{P_1'}{Q_1'} \left\{ \frac{P_3'}{Q_1'} - \frac{Q_3'}{Q_1'} + 4 \right\} P_1(\eta) + \\
& + \frac{1}{3} \left[\frac{1}{175} \frac{P_4'}{Q_0'} - \frac{1}{27} \frac{P_2'}{Q_0'} \left\{ \frac{Q_2'}{Q_0'} + \frac{9}{2} \frac{P_1'}{Q_0'} - \frac{16}{7} \right\} \right] P_0(\eta),
\end{aligned} \tag{11.132}$$

$$u_5 = - \frac{1}{27} \left(\frac{P_1'}{Q_1'} \right)^2 P_1(\eta) + \frac{1}{81} \left(\frac{P_2'}{Q_0'} \right)^2 P_0(\eta), \tag{11.133}$$

where $P'_j = P'_j(\xi_1)$ and $Q'_j = Q'_j(\xi_1)$. The radius of convergence of eq. (11.127), regarded as a power series in $c\xi_1$, is indicated in Fig. 11.22. The back scattering cross section normalized to $\sigma_{\text{g.o.}}$, computed using seven and nine terms in the low frequency expansion (i.e. $n_{\text{max}} = 6$ and 8) is shown for two typical cases in Fig. 11.23,

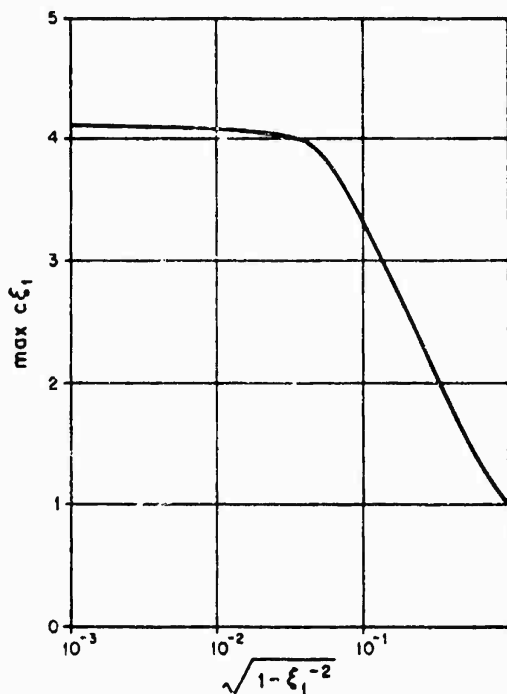


Fig 11.22. Radius of convergence of low frequency expansion for end-on incidence (SENIOR [1961]).

whereas the forward scattering cross section $\sigma(\pi)$ normalized to the quantity given in eq. (11.43), and computed using eight and ten terms in the low frequency expansion is shown for the same two typical cases in Fig. 11.24.

11.3.2.3. HIGH FREQUENCY APPROXIMATIONS

For the scattered field, no explicit results are available for arbitrary incidence, but for axial incidence, such that

$$V^1 = e^{-ikz}, \quad (11.134)$$

the geometrical optics scattered field at a point (ξ, η, ϕ) located in the illuminated region $\{(\xi^2 - 1)(1 - \eta^2) > (\xi_1^2 - 1) \text{ with } \eta < 0\}$ is:

$$V_{\text{g.o.}}^* = \exp \{ic(F - \xi_1 \eta_1)\} \left[\left(1 + \frac{2F^2}{(\xi_1^2 - \eta_1^2)G}\right) \left(i + \frac{2\xi_1^2 G}{\xi_1^2 - \eta_1^2}\right) \right]^{-1}, \quad (11.135)$$

where F and G are given by eqs. (11.15) and (11.17), and η_1 is the positive root of eq. (11.18) with $\xi_0 = \infty$. In the geometrical shadow $V_{\text{g.o.}}^* = 0$. In the far field ($\xi \rightarrow \infty$):

$$S_{\text{g.o.}} = \frac{c(\xi_1^2 - \eta_1^2)}{2\xi_1} \exp \{-ic[\xi_1 \eta_1(1 + \eta) + \sqrt{(\xi_1^2 - 1)(1 - \eta_1^2)(1 - \eta^2)}]\}. \quad (11.136)$$

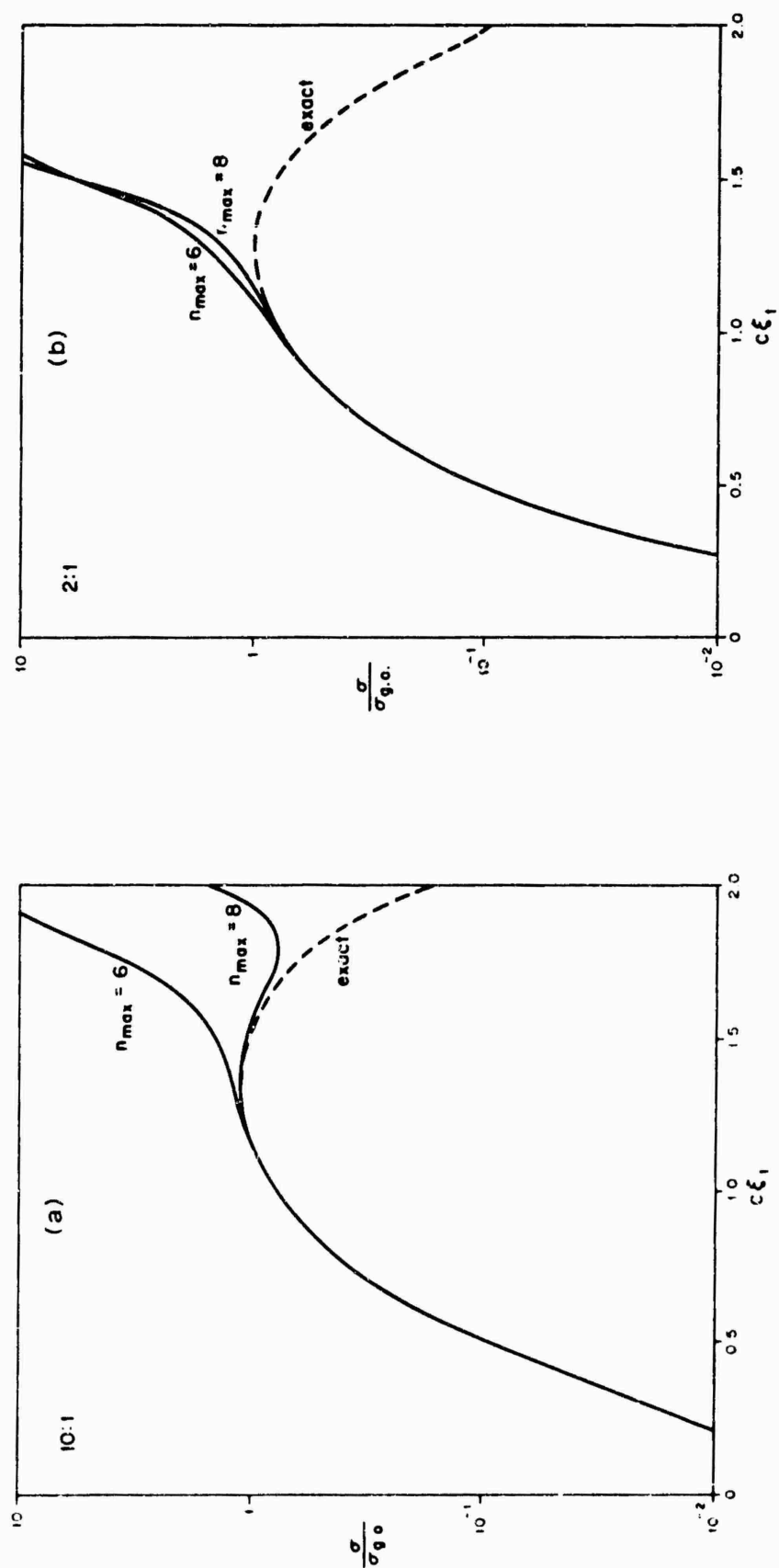


Fig. 11.23. Normalized back scattering cross section at end-on incidence for 10 : 1 and 2 : 1 spheroids (ASVESTAS and KLEINMAN [1967]).

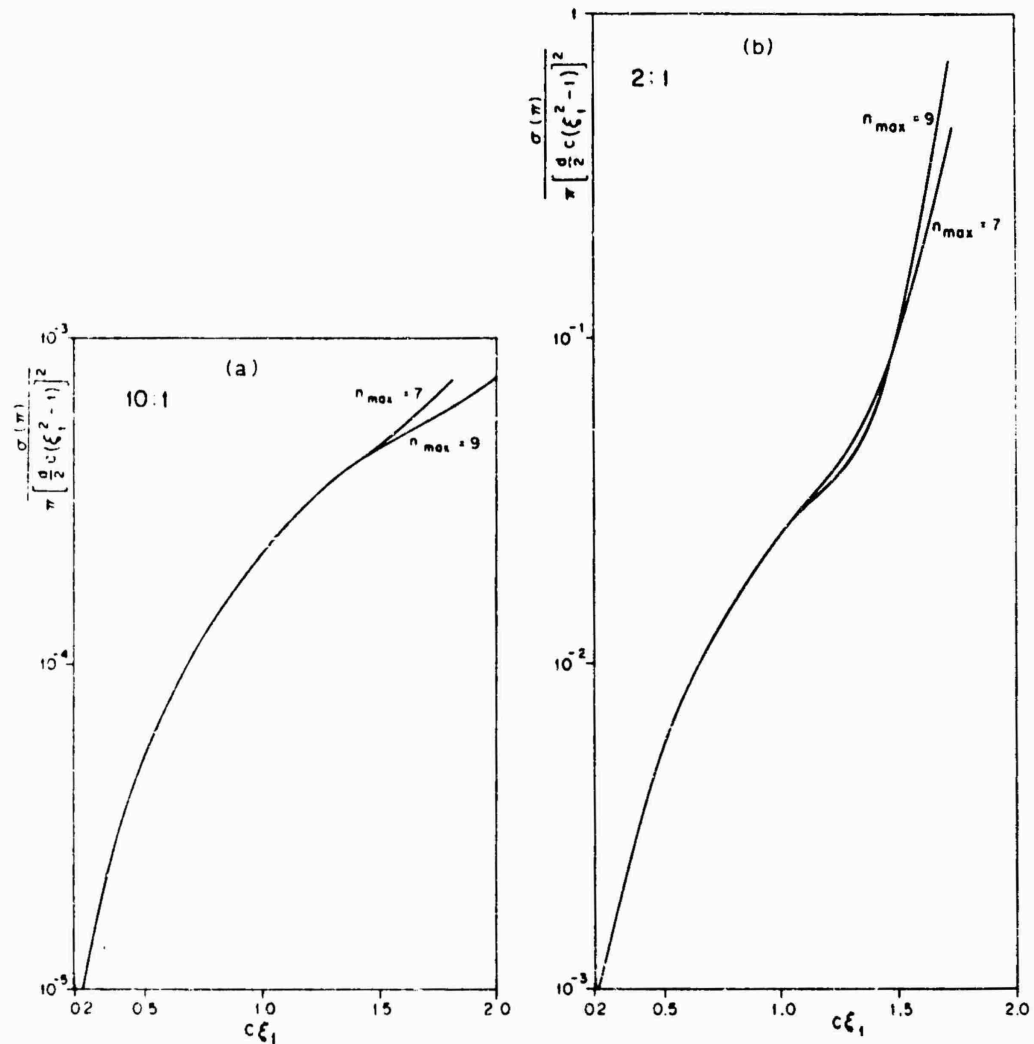


Fig. 11.24. Normalized forward scattering cross section at end-on incidence for 10 : 1 and 2 : 1 spheroids (ASVESTAS and KLEINMAN [1967]).

In particular, if the observation point is on the z -axis ($\eta = 1$):

$$V_{g.o.}^s = \frac{\xi_1^2 - 1}{2\xi\xi_1 - \xi_1^2 - 1} e^{ic(\xi - 2\xi_1)}, \quad (11.137)$$

and in the far field ($\xi \rightarrow \infty$):

$$S_{g.o.} = \frac{c(\xi_1^2 - 1)}{2\xi_1} e^{-2ic\xi_1}, \quad (11.138)$$

so that the geometrical optics back scattering cross section is still given by eq. (11.66).

A more refined approximation, in which an asymptotic expression for the diffracted field is retained, is available for the surface field and for the back scattered field. In both cases

$$V^s = V_{g.o.}^s + V_d^s. \quad (11.139)$$

On the surface $\xi = \xi_1$ (LEVY and KELLER [1960]):

$$V_d^s = \frac{\xi_1^{\frac{1}{2}}}{[(\xi_1^2 - \eta^2)(1 - \eta^2)]^{\frac{1}{2}}} \sum_{n=1}^{\infty} \frac{\exp \bar{X}_n(0, \eta) - i \exp [\bar{X}_n(\eta, -1) + \bar{X}_n(0, -1)]}{\beta_n \text{Ai}(-\beta_n) \{1 + \exp [2\bar{X}_n(1, -1)]\}}, \quad (11.140)$$

where $\bar{X}_n(x, \beta)$ is given by eq. (11.96). In the far back scattered field ($\eta = 1$, $\xi \rightarrow \infty$) (LEVY and KELLER [1960]):

$$S = \frac{c(\xi_1^2 - 1)}{2\xi_1} e^{-2ic\xi_1} \left\{ 1 - \frac{2(\frac{1}{2}c)^{\frac{1}{2}} \xi_1^{\frac{1}{2}}}{(\xi_1^2 - 1)^{\frac{3}{2}} \beta_1 [\text{Ai}(-\beta_1)]^2} \exp \left[\frac{1}{2}i\pi + 2ic\xi_1 + \right. \right. \\ \left. \left. + 2ic \int_0^1 \sqrt{\frac{\xi_1^2 - \eta^2}{1 - \eta^2}} d\eta + \exp \left\{ \frac{5}{6}i\pi \right\} c^{\frac{1}{2}} \beta_1 \{2\xi_1 \sqrt{(\xi_1^2 - 1)}\}^{\frac{1}{2}} \int_0^1 \frac{d\eta}{\sqrt{[(\xi_1^2 - \eta^2)(1 - \eta^2)]}} \right] \right\}, \quad (11.141)$$

where

$$\beta_1 = 1.01879 \dots, \quad \text{Ai}(-\beta_1) = 0.53565 \dots \quad (11.142)$$

If we require that the diffracted field contribution in eq. (11.141) be at most one fifth of the geometrical optics contribution, the following inequalities must be satisfied (CRISPIN et al. [1963]):

$\xi_1/\sqrt{(\xi_1^2 - 1)}$	10 : 1	8 : 1	5 : 1	2 : 1	4 : 3
$c\xi_1 \geq$	575	375	160	33	14
$c(\xi_1^2 - 1)/\xi_1 \geq$	5.75	5.86	6.40	8.25	10.05

The total scattering cross section for end-on incidence ($\zeta = \pi$) is (JONES [1957]):

$$\sigma_T \sim \frac{2\pi c^2}{k^2} (\xi_1^2 - 1) \{1 - 0.8640 [c(\xi_1 - \xi_1^{-1})]^{-\frac{1}{2}}\}; \quad (11.143)$$

this result is a good approximation if

$$c(\xi_1 - \xi_1^{-1}) \gg 1. \quad (11.144)$$

For broadside incidence ($\zeta = \frac{1}{2}\pi$), such that

$$V^i = e^{ikx}, \quad (11.145)$$

the total scattering cross section is (JONES [1957]):

$$\sigma_T \sim \frac{2\pi c^2}{k^2} \xi_1 \sqrt{\xi_1^2 - 1} [1 - 0.8640 b(c\sqrt{\xi_1^2 - 1})^{-\frac{1}{2}}], \quad (11.146)$$

where b is the hypergeometric function of eq. (11.73); the result (11.146) is a good approximation if

$$c\sqrt{(\xi_1^2 - 1)} \gg 1. \quad (11.147)$$

Values of b for a few length-to-width ratios are tabulated at the end of Section 11.2.2.3.

11.3.2.4. SHAPE APPROXIMATION

For a spheroid whose surface $\xi = \xi_1$ is defined in terms of the spherical polar coordinates (r_1, θ_1, ϕ_1) by the equation

$$r_1 = a \left(\frac{\xi_1^2 - 1}{\xi_1^2 - \cos^2 \theta_1} \right)^{\frac{1}{2}}, \quad (11.148)$$

and is such that

$$\xi_1^2 - 1 \gg 1, \quad (11.149)$$

i.e. the spheroid departs only infinitesimally from the sphere $r_1 = a$, the scattered field may be expressed as a perturbation of the solution for this sphere.

For incidence at an angle ζ with respect to the positive z -axis, such that

$$V^i = \exp \{ik(x \sin \zeta + z \cos \zeta)\}, \quad (11.150)$$

then

$$V^s \sim - \sum_{m=0}^{\infty} \sum_{n=m}^{\infty} \varepsilon_m \frac{(n-m)!}{(n+m)!} \frac{i^n}{h_n^{(1)'}(ka)} \left[(2n+1)j_n'(ka) + \frac{i}{\xi_1^2 - 1} h_{mn}(\zeta) \right] \\ \times h_n^{(1)}(kr) P_n^m(\cos \zeta) P_n^m(\cos \theta) \cos m\phi + O[(\xi_1^2 - 1)^{-2}], \quad (11.151)$$

where

$$b_{mn}(\zeta) = \frac{1}{(ka)^3 h_n^{(1)'}(ka)} \left\{ \frac{[(2n+1)[(ka)^2(n^2+n-1+m^2) - n^2(n+1)^2 - m^2(n^2+n-3)]}{(2n+3)(2n-1)} + \right. \\ \left. + \frac{(n+m-1)(n+m)(k^2a^2 - n^2 + n + 2)}{2(2n-1)} \frac{h_n^{(1)'}(ka)}{h_{n-2}^{(1)'}(ka)} \frac{P_{n-2}^m(\cos \zeta)}{P_n^m(\cos \zeta)} + \right. \\ \left. + \frac{(n-m+1)(n-m+2)(k^2a^2 - n^2 - 3n)}{2(2n+3)} \frac{h_n^{(1)'}(ka)}{h_{n+2}^{(1)'}(ka)} \frac{P_{n+2}^m(\cos \zeta)}{P_n^m(\cos \zeta)} \right\}. \quad (11.152)$$

In the far back scattered field ($r \rightarrow \infty$, $\theta = \pi - \zeta$, $\phi = \pi$):

$$S \sim \sum_{m=0}^{\infty} \sum_{n=m}^{\infty} \varepsilon_m \frac{(n-m)!}{(n+m)!} \frac{(-1)^n}{h_n^{(1)'}(ka)} \left[i(2n+1)j_n(ka) - \frac{1}{\xi_1^2 - 1} b_{mn}(\zeta) \right] \\ \times [P_n^m(\cos \zeta)]^2 + O[(\xi_1^2 - 1)^{-2}]. \quad (11.153)$$

For axial incidence ($\zeta = \pi$):

$$V^s \sim - \sum_{n=0}^{\infty} \frac{(-i)^n}{h_n^{(1)'}(ka)} \left[(2n+1)j_n'(ka) + \frac{i}{\xi_1^2 - 1} h_{0n}(\pi) \right] \\ \times h_n^{(1)}(kr) P_n(\cos \theta) + O[(\xi_1^2 - 1)^{-2}], \quad (11.154)$$

where

$$h_{0n}(\pi) = \frac{1}{(ka)^3 h_n^{(1)'}(ka)} \left\{ \frac{[(2n+1)[(ka)^2(n^2+n-1) - n^2(n+1)^2]}{(2n+3)(2n-1)} + \right. \\ \left. + \frac{n(n-1)(k^2a^2 - n^2 + n + 2)}{2(2n-1)} \frac{h_n^{(1)'}(ka)}{h_{n-2}^{(1)'}(ka)} + \frac{(n+1)(n+2)(k^2a^2 - n^2 - 3n)}{2(2n+3)} \frac{h_n^{(1)'}(ka)}{h_{n+2}^{(1)'}(ka)} \right\}, \quad (11.155)$$

and in the far back scattered field:

$$S \sim \sum_{n=0}^{\infty} \frac{(-1)^n}{h_n^{(1)'}(ka)} \left[i(2n+1)j_n'(ka) - \frac{1}{\xi_1^2 - 1} b_{on}(\pi) \right] + O[(\xi_1^2 - 1)^{-2}]. \quad (11.156)$$

11.4. Perfectly conducting spheroid

11.4.1. Dipole sources

11.4.1.1. EXACT SOLUTIONS

Results are available only in the case of a dipole on the z -axis and axially oriented. For an electric dipole at $(\xi_0, \eta_0 = 1)$ with moment $(4\pi\epsilon/k)\hat{z}$, corresponding to an incident electric Hertz vector $\hat{z}e^{ikR}/(kR)$, such that

$$\begin{aligned} H_\phi^i &= -k^2 c Y \frac{e^{ikR}}{kR} \left(1 - \frac{1}{ikR} \right) \frac{1}{kR} \sqrt{(\xi^2 - 1)(1 - \eta^2)}, \\ H_\xi^i &= H_\eta^i = E_\phi^i = 0, \end{aligned} \quad (11.157)$$

then (BELKINA [1957]):

$$\begin{aligned} H_\phi^i + H_\phi^s &= -\frac{2k^2 Y}{\sqrt{(\xi_0^2 - 1)}} \sum_{n=0}^{\infty} (-i)^{n-1} \frac{1}{\rho_{1n} N_{1n}} \left[R_{1n}^{(1)}(c, \xi_0) - \right. \\ &\quad \left. - \frac{(\partial/\partial \xi_1)\{R_{1n}^{(1)}(c, \xi_1)\sqrt{(\xi_1^2 - 1)}\}}{(\partial/\partial \xi_1)\{R_{1n}^{(3)}(c, \xi_1)\sqrt{(\xi_1^2 - 1)}\}} R_{1n}^{(3)}(c, \xi_0) \right] R_{1n}^{(3)}(c, \xi_0) S_{1n}(c, \eta). \end{aligned} \quad (11.158)$$

On the surface $\xi = \xi_1$:

$$\begin{aligned} H_\phi^i + H_\phi^s &= -\frac{2k^2 Y}{c \sqrt{(\xi_0^2 - 1)(\xi_1^2 - 1)}} \sum_{n=0}^{\infty} (-i)^n \frac{1}{\rho_{1n} N_{1n}} \frac{1}{(\partial/\partial \xi_1)\{R_{1n}^{(3)}(c, \xi_1)\sqrt{(\xi_1^2 - 1)}\}} \\ &\quad \times R_{1n}^{(3)}(c, \xi_0) S_{1n}(c, \eta). \end{aligned} \quad (11.159)$$

In the far field ($\xi \rightarrow \infty$):

$$\begin{aligned} H_\phi^i + H_\phi^s &= \frac{e^{ic\xi}}{c\xi} \frac{2k^2 Y}{\sqrt{(\xi_0^2 - 1)}} \sum_{n=0}^{\infty} (-1)^n \frac{1}{\rho_{1n} N_{1n}} \\ &\quad \times \left[R_{1n}^{(1)}(c, \xi_0) - \frac{(\partial/\partial \xi_1)\{R_{1n}^{(1)}(c, \xi_1)\sqrt{(\xi_1^2 - 1)}\}}{(\partial/\partial \xi_1)\{R_{1n}^{(3)}(c, \xi_1)\sqrt{(\xi_1^2 - 1)}\}} R_{1n}^{(3)}(c, \xi_0) \right] S_{1n}(c, \eta). \end{aligned} \quad (11.160)$$

If the dipole is on the surface ($\xi_0 = \xi_1$):

$$H_\phi^i + H_\phi^s = -\frac{2k^2 Y}{c(\xi_1^2 - 1)} \sum_{n=0}^{\infty} (-i)^n \frac{1}{\rho_{1n} N_{1n}} \frac{R_{1n}^{(3)}(c, \xi_1) S_{1n}(c, \eta)}{(\partial/\partial \xi_1)\{R_{1n}^{(3)}(c, \xi_1)\sqrt{(\xi_1^2 - 1)}\}}. \quad (11.161)$$

If also the observation point is on the surface ($\xi = \xi_1$):

$$H_\phi^i + H_\phi^s = -\frac{2k^2 Y}{c(\xi_1^2 - 1)} \sum_{n=0}^{\infty} (-i)^n \frac{1}{\rho_{1n} N_{1n}} \frac{R_{1n}^{(3)}(c, \xi_1) S_{1n}(c, \eta)}{(\partial/\partial \xi_1)\{R_{1n}^{(3)}(c, \xi_1)\sqrt{(\xi_1^2 - 1)}\}}. \quad (11.162)$$

whereas in the far field ($\xi \rightarrow \infty$):

$$H_{\phi}^i + H_{\phi}^s = \frac{e^{ic\xi}}{c\xi} - \frac{2ik^2Y}{c(\xi_1^2-1)} \sum_{n=0}^{\infty} (-1)^n \frac{1}{\rho_{1n} N_{1n}} \frac{S_{1n}(c, \eta)}{(\partial/\partial \xi_1)\{R_{1n}^{(3)}(c, \xi_1)\sqrt{(\xi_1^2-1)}\}}. \quad (11.163)$$

HATCHER and LEITNER [1954] have computed the quantity

$$\left| \frac{c}{2(\xi_1^2-1)} \sum_{n=0}^{\infty} (-1)^n \frac{1}{\rho_{1n} N_{1n}} \frac{S_{1n}(c, \eta)}{(\partial/\partial \xi_1)\{R_{1n}^{(3)}(c, \xi_1)\sqrt{(\xi_1^2-1)}\}} \right|^2 \quad (11.164)$$

for $c = 1, 2$ and 3 with $\xi_1 = 1.005, 1.020, 1.044$ and 1.077 . BELKINA [1957] has obtained the shape of the radiation pattern for $c = 0.9804, 3, 5$ and 7 with $\xi_1 = 1.000801, 1.005037, 1.02, 1.154700$ and 1.341641 .

For a magnetic dipole at $(\xi_0, \eta_0 = 1)$ with moment $(4\pi/k)\hat{z}$, corresponding to an incident magnetic Hertz vector $\hat{z}e^{ikR}/(kR)$, such that

$$\begin{aligned} E_{\phi}^i &= k^2 c Z \frac{e^{ikR}}{kR} \left(1 - \frac{1}{ikR}\right) \frac{1}{kR} \sqrt{(\xi^2-1)(1-\eta^2)}, \\ E_{\xi}^i &= E_{\eta}^i = H_{\phi}^i = 0, \end{aligned} \quad (11.165)$$

then

$$\begin{aligned} E_{\phi}^i + E_{\phi}^s &= -\frac{2k^2Z}{\sqrt{(\xi_0^2-1)}} \sum_{n=0}^{\infty} (-i)^{n-1} \frac{1}{\rho_{1n} N_{1n}} \\ &\times \left[R_{1n}^{(1)}(c, \xi_0) - \frac{R_{1n}^{(1)}(c, \xi_1)}{R_{1n}^{(3)}(c, \xi_1)} R_{1n}^{(3)}(c, \xi_0) \right] R_{1n}^{(3)}(c, \xi_1) S_{1n}(c, \eta). \end{aligned} \quad (11.166)$$

On the surface $\xi = \xi_1$:

$$H_{\eta}^i + H_{\eta}^s = \frac{2k^2}{c^2 \sqrt{(\xi_0^2-1)(\xi_1^2-1)(\xi_1^2-\eta^2)}} \sum_{n=0}^{\infty} (-i)^{n-1} \frac{1}{\rho_{1n} N_{1n}} \frac{R_{1n}^{(3)}(c, \xi_0)}{R_{1n}^{(3)}(c, \xi_1)} S_{1n}(c, \eta). \quad (11.167)$$

In the far field ($\xi \rightarrow \infty$):

$$\begin{aligned} E_{\phi}^i + E_{\phi}^s &= \frac{e^{ic\xi}}{c\xi} - \frac{2k^2Z}{c\xi \sqrt{(\xi_0^2-1)}} \sum_{n=0}^{\infty} (-1)^n \frac{1}{\rho_{1n} N_{1n}} \\ &\times \left[R_{1n}^{(1)}(c, \xi_0) - \frac{R_{1n}^{(1)}(c, \xi_1)}{R_{1n}^{(3)}(c, \xi_1)} R_{1n}^{(3)}(c, \xi_0) \right] S_{1n}(c, \eta). \end{aligned} \quad (11.168)$$

If the dipole is on the surface ($\xi_0 = \xi_1$), the electromagnetic field components are identically zero everywhere.

11.4.1.2. LOW FREQUENCY APPROXIMATIONS

A general procedure for the determination of successive terms in the low frequency expansion of the scattered field has been given by STEVENSON [1953a]; however, no specific results are available.

11.4.1.3. HIGH FREQUENCY APPROXIMATIONS

Although the geometrical and physical optics approximations to the scattered field are derivable by standard techniques, no specific results are available.

11.4.2. Plane wave incidence

11.4.2.1. EXACT SOLUTIONS

For arbitrary direction of incidence, the coefficients in the vector wave function expansion of the scattered field must be determined from an infinite set of infinite

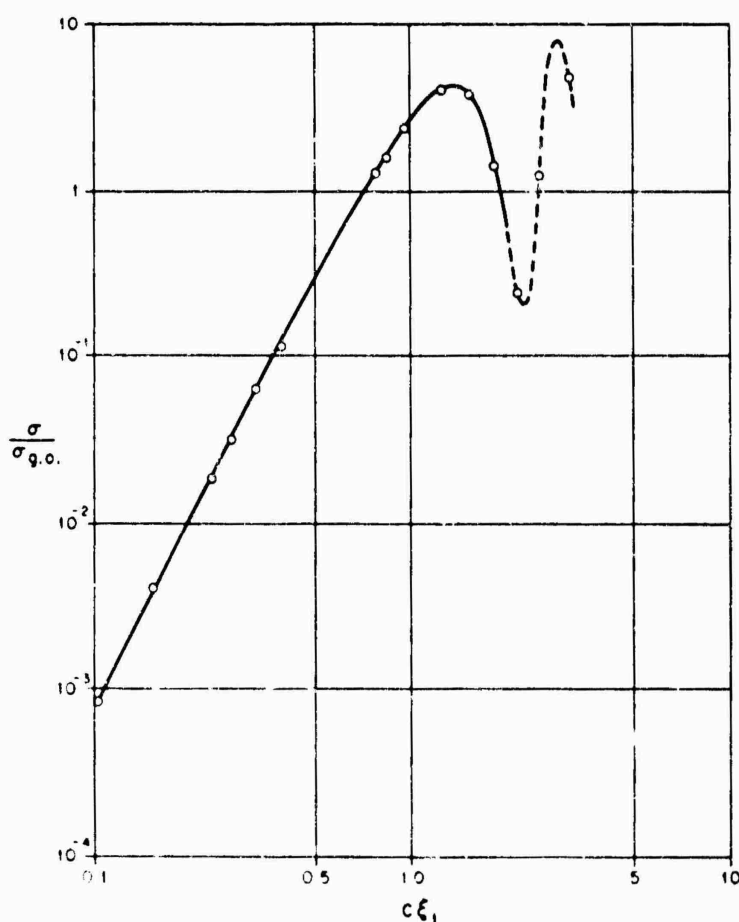


Fig. 11.25. Normalized back scattering cross section at end-on incidence for a 10 : 1 spheroid (SIEGEL et al. [1956]).

systems of equations (REITLINGER [1957]); no specific results have been found. In the particular case of end-on incidence ($\zeta = \pi$), the coefficients may be obtained by the inversion of a single infinite matrix (SCHULTZ [1950]); this method has been used to compute $\sigma/\sigma_{g.o.}$ for a 10:1 spheroid at selected values of $c\xi_1$ (SIEGEL et al. [1956]), as shown in Fig. 11.25.

Experimental data for back scattering and bistatic cross sections are available only for isolated values of the parameters involved (see SLEATOR [1964]). One of the more

complete sets is for end-on incidence on a 2:1 spheroid (MOFFATT and KENNAUGH [1956]), and is shown in Fig. 11.26. MOFFATT [1965] has measured the back scattering cross section as a function of ζ for a 2:1 spheroid with $c\xi_1 = 1.0(0.5)9.0$; his results for two values of $c\xi_1$ are shown in Fig. 11.27.

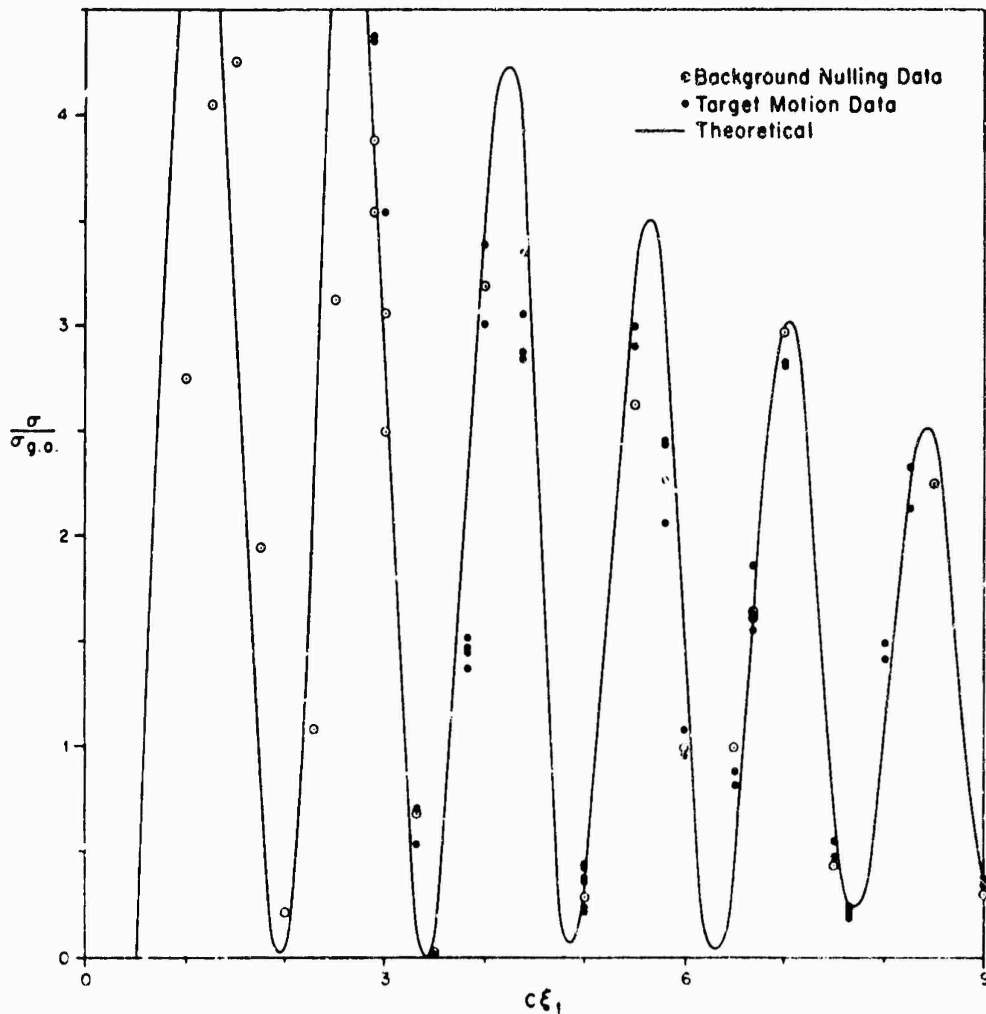


Fig. 11.26. Measured back scattering cross section for end-on incidence on a 2:1 spheroid (MOFFATT and KENNAUGH [1965]).

11.4.2.2. LOW FREQUENCY APPROXIMATIONS

Using the general procedure for the determination of the low frequency expansion given by STEVENSON [1953a], explicit results have been obtained for the far field corresponding to a plane wave incident in an arbitrary direction and with arbitrary polarization such that

$$\begin{aligned} E^i &= (l_1 \hat{x} + m_1 \hat{y} + n_1 \hat{z}) e^{ik(l_1 x + m_1 y + n_1 z)}, \\ H^i &= Y(l_2 \hat{x} + m_2 \hat{y} + n_2 \hat{z}) e^{ik(l_2 x + m_2 y + n_2 z)}, \end{aligned} \quad (11.169)$$

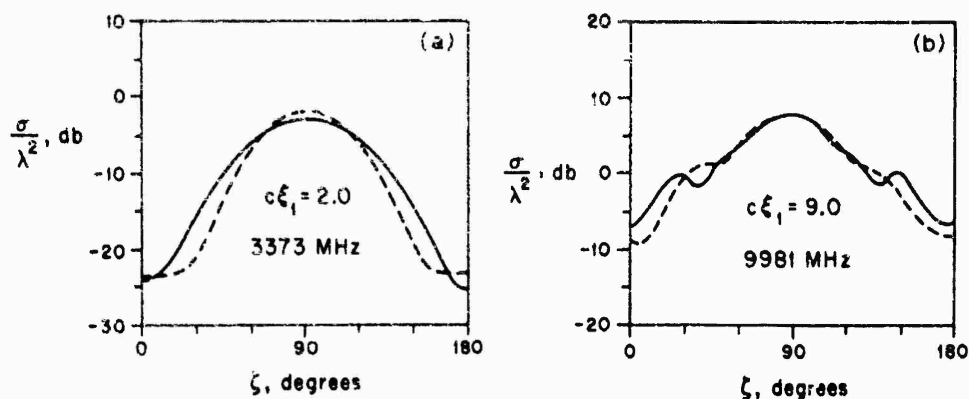


Fig. 11.27. Measured back scattering cross section normalized to the square of the wavelength (in db) as a function of the angle of incidence, for a 2 : 1 spheroid with either H^1 (—) or E^1 (---) parallel to the plane of incidence (MOFFATT [1965]).

where (l, m, n) , (l_1, m_1, n_1) and (l_2, m_2, n_2) are three sets of direction cosines satisfying the relations

$$\begin{aligned} l_1 \hat{x} + m_1 \hat{y} + n_1 \hat{z} &= (l_2 \hat{x} + m_2 \hat{y} + n_2 \hat{z}) \wedge (l \hat{x} + m \hat{y} + n \hat{z}), \\ l_2 \hat{x} + m_2 \hat{y} + n_2 \hat{z} &= (l \hat{x} + m \hat{y} + n \hat{z}) \wedge (l_1 \hat{x} + m_1 \hat{y} + n_1 \hat{z}) \end{aligned} \quad (11.170)$$

The scattered electric field in the far zone may be written as:

$$\begin{aligned} E_\theta^s = \frac{e^{ikr}}{kr} \sum_{m=0}^{\infty} \sum_{n=1}^{\infty} \left[\left(\alpha_{mn} \frac{\partial P_n^m(\cos \theta)}{\partial \theta} + m \beta_{mn} \frac{P_n^m(\cos \theta)}{\sin \theta} \right) \cos m\phi + \right. \\ \left. + \left(\beta_{mn} \frac{\partial P_n^m(\cos \theta)}{\partial \theta} - m \alpha_{mn} \frac{P_n^m(\cos \theta)}{\sin \theta} \right) \sin m\phi \right], \end{aligned} \quad (11.171)$$

$$\begin{aligned} E_\phi^s = -\frac{e^{ikr}}{kr} \sum_{m=0}^{\infty} \sum_{n=1}^{\infty} \left[\left(\bar{\alpha}_{mn} \frac{\partial P_n^m(\cos \theta)}{\partial \theta} - m \beta_{mn} \frac{P_n^m(\cos \theta)}{\sin \theta} \right) \cos m\phi + \right. \\ \left. + \left(\beta_{mn} \frac{\partial P_n^m(\cos \theta)}{\partial \theta} + m \alpha_{mn} \frac{P_n^m(\cos \theta)}{\sin \theta} \right) \sin m\phi \right], \end{aligned} \quad (11.172)$$

where (r, θ, ϕ) are the spherical polar coordinates of the observation point and the incident electric field has unit amplitude. Expressions have been worked out (STEVENS [1953b]) for the coefficients α_{mn} , β_{mn} , $\bar{\alpha}_{mn}$ and $\bar{\beta}_{mn}$ through terms $O(k^5)$. Explicitly,

$$\alpha_{01} = k^3 K_1 + k^5 L_3, \quad (11.173)$$

$$\alpha_{02} = -\frac{1}{3} k^5 (M_1 + M_2 - 2M_3), \quad (11.174)$$

$$\alpha_{03} = -\frac{1}{300} k^5 d^2 K_3, \quad (11.175)$$

$$\alpha_{11} = k^3 K_1 + k^5 L_1, \quad (11.176)$$

$$\alpha_{12} = \frac{1}{3} k^5 N_2, \quad (11.177)$$

$$\alpha_{13} = -\frac{1}{900}k^5d^2K_1, \quad (11.178)$$

$$\beta_{11} = k^3K_2 + k^5L_2, \quad (11.179)$$

$$\beta_{12} = \frac{1}{3}k^5N_1, \quad (11.180)$$

$$\beta_{13} = -\frac{1}{900}k^5d^2K_2, \quad (11.181)$$

$$\alpha_{22} = -\frac{1}{6}k^5(M_2 - M_1), \quad (11.182)$$

$$\beta_{22} = \frac{1}{6}k^5N_3, \quad (11.183)$$

with all other coefficients zero through $O(k^5)$. The corresponding "barred" quantities are obtained by "barring" the K_j , L_j , M_j and N_j , $j = 1, 2$ or 3 . The K_j , L_j , M_j and N_j and their "barred" analogues are complicated functions of the direction and polarization of the incident field, and of the spheroid parameters, and their expressions are given by (STEVENSON [1953b], SENIOR [1966b]):

$$K_1 = -\frac{1}{12}d^3l_1 \frac{P_1^1}{Q_1^1}, \quad (11.184)$$

$$K_2 = -\frac{1}{12}d^3m_1 \frac{P_1^1}{Q_1^1}, \quad (11.185)$$

$$K_3 = \frac{1}{24}d^3n_1 \frac{P_1^0}{Q_1^0}, \quad (11.186)$$

$$L_1 = \frac{1}{2400}d^5 \frac{P_1^1}{Q_1^1} \left\{ l_1 \left[22 - 5(l^2 + m^2) + \frac{4}{3} \left(\frac{P_3^1}{P_1^1} - \frac{Q_3^1}{Q_1^1} \right) - \frac{50}{3} \frac{Q_{-1}^1}{Q_1^1} \right] + 5mn_2 \right\}, \quad (11.187)$$

$$L_2 = \frac{1}{2400}d^5 \frac{P_1^1}{Q_1^1} \left\{ m_1 \left[22 - 5(m^2 + n^2) + \frac{4}{3} \left(\frac{P_3^1}{P_1^1} - \frac{Q_3^1}{Q_1^1} \right) - \frac{50}{3} \frac{Q_{-1}^1}{Q_1^1} \right] + 5nl_2 \right\}, \quad (11.188)$$

$$L_3 = \frac{1}{4800}d^5n_1 \frac{P_1^0}{Q_1^0} \left[14 + 5(l^2 + m^2) - 4 \left(\frac{P_3^0}{P_1^0} - \frac{Q_3^0}{Q_1^0} \right) + 7 \frac{P_0^0}{Q_1^0} \right], \quad (11.189)$$

$$M_1 = \frac{1}{8640}d^5 \left[6(l_1 - mm_1) \frac{P_2^2}{Q_2^2} - mn_1 \frac{P_2^0}{Q_2^0} \right], \quad (11.190)$$

$$M_2 = \frac{1}{8640}d^5 \left[6(nm_1 - ml_1) \frac{P_2^2}{Q_2^2} - ll_1 \frac{P_2^0}{Q_2^0} \right], \quad (11.191)$$

$$M_3 = \frac{1}{4320}d^5nm_1 \frac{P_2^0}{Q_2^0}, \quad (11.192)$$

$$N_1 = -\frac{1}{2880}d^5 \left[(mn_1 + ml_1) \frac{P_1^1}{Q_1^1} + 5l_2 \frac{P_1^1}{Q_1^1} \right], \quad (11.193)$$

$$N_2 = -\frac{1}{2880}d^5 \left[(nl_1 + ln_1) \frac{P_2^1}{Q_2^1} + 5m_2 \frac{P_1^{1'}}{Q_1^{1'}} \right], \quad (11.194)$$

$$N_3 = \frac{1}{720}d^5 (lm_1 + ml_1) \frac{P_2^2}{Q_2^2}, \quad (11.195)$$

where the argument of the Legendre functions is ξ_1 . The constants \bar{K}_j , \bar{L}_j , \bar{M}_j and \bar{N}_j are obtained from the corresponding unbarred quantities by making the substitutions

$$\begin{aligned} (l_1, m_1, n_1) &\rightarrow (l_2, m_2, n_2), \\ (i_2, m_2, n_2) &\rightarrow -(l_1, m_1, n_1), \end{aligned} \quad (11.196)$$

and by replacing the Legendre functions with their first derivatives and vice versa.

In the particular case of end-on incidence, such that

$$E^i = \hat{x}e^{-ikz}, \quad H^i = -\hat{y}e^{-ikz}, \quad (11.197)$$

eqs. (11.171) and (11.172) reduce to:

$$\begin{aligned} E^s = \frac{e^{ikr}}{kr} \sum_{n=1}^{\infty} \left[\left(\alpha_{1n} \frac{\partial P_n^1(\cos \theta)}{\partial \theta} + \beta_{1n} \frac{P_n^1(\cos \theta)}{\sin \theta} \right) \cos \phi \hat{\theta} - \right. \\ \left. - \left(\beta_{1n} \frac{\partial P_n^1(\cos \theta)}{\partial \theta} + \alpha_{1n} \frac{P_n^1(\cos \theta)}{\sin \theta} \right) \sin \phi \hat{\phi} \right], \quad (11.198) \end{aligned}$$

with

$$\alpha_{11} = -\frac{3}{2}c^3 \frac{P_1^1}{Q_1^1} \left[1 - \frac{1}{50}c^2 \left(22 - 10 \frac{Q_1^{1'}}{Q_1^1} \right) \right], \quad (11.199)$$

$$\alpha_{12} = \frac{1}{270}c^5 \left(\frac{P_2^1}{Q_2^1} - 5 \frac{P_1^{1'}}{Q_1^{1'}} \right), \quad (11.200)$$

$$\alpha_{13} = \frac{2}{675}c^5 \frac{P_1^1}{Q_1^1}, \quad (11.201)$$

$$\beta_{11} = \frac{3}{2}c^3 \frac{P_1^{1'}}{Q_1^{1'}} \left[1 - \frac{1}{50}c^2 \left(22 - 10 \frac{Q_1^{1'}}{Q_1^1} - 40 \frac{Q_0^1}{Q_1^{1'}} \right) \right], \quad (11.202)$$

$$\beta_{12} = -\frac{1}{270}c^5 \left(\frac{P_2^{1'}}{Q_2^{1'}} - 5 \frac{P_1^1}{Q_1^1} \right), \quad (11.203)$$

$$\beta_{13} = -\frac{2}{675}c^5 \frac{P_1^{1'}}{Q_1^{1'}}, \quad (11.204)$$

where the argument of the Legendre functions is ξ_1 , and all other coefficients are zero through $O(c^5)$.

By retaining only the dominant term $O(c^3)$ in eq. (11.198), and specializing to the case $\theta = 0$, we obtain the Rayleigh back scattering cross section (STRUTT [1897]):

$$\sigma \sim \frac{1}{36} \pi k^4 d^6 \left| \frac{P_1'(\xi_1)}{Q_1'(\xi_1)} - \frac{P_1^1(\xi_1)}{Q_1^1(\xi_1)} \right|^2. \quad (11.205)$$

A numerical approximation to eq. (11.205) has been proposed by SIEGEL [1959] in the form:

$$\sigma \sim \frac{4}{\pi} k^4 v^2 \left(1 + \frac{\exp \{ -\sqrt{(1-\xi_1^{-2})} \}}{\pi \sqrt{(1-\xi_1^{-2})}} \right)^2, \quad (11.206)$$

where $v = \frac{1}{6} \pi d^3 \xi_1 (\xi_1^2 - 1)$ is the volume of the spheroid.

The dominant term of the near-zone ($kr \ll 1$) field for both axial ($\zeta = \pi$) and broadside ($\zeta = \frac{1}{2}\pi$) incidence has been given by Lord Rayleigh (STRUTT [1897]).

11.4.2.3. HIGH FREQUENCY APPROXIMATIONS

For a wave of arbitrary polarization incident from the half-plane $\phi = 0$ at an angle ζ with the positive z -axis, the geometrical optics bistatic cross section in the direction ($\theta = \arccos \eta$, $\phi = 0$) is (CRISPIN et al. [1959]):

$$\sigma_{g.o.}(\theta) = \pi \left(\frac{1}{2} d \xi_1 \right)^2 \left[\frac{\xi_1^2 - 1}{\xi_1^2 - \cos^2(\frac{1}{2}(\zeta - \theta))} \right]^2. \quad (11.207)$$

For axial incidence ($\zeta = \pi$), the back scattering cross section is

$$\sigma_{g.o.} \equiv \sigma_{g.o.}(0) = \pi \left[\frac{d(\xi_1^2 - 1)}{2\xi_1} \right]^2, \quad (11.208)$$

whereas in a direction arbitrarily close to forward scattering ($\theta \rightarrow \pi$):

$$\sigma_{g.o.}(\pi) = \pi \left(\frac{1}{2} d \xi_1 \right)^2. \quad (11.209)$$

An expression for the physical optics bistatic cross section is available for a receiver in the plane containing the direction of incidence and the z -axis (SIEGEL et al. [1955]), viz.

$$\sigma_{p.o.}(\theta) = \sigma_{g.o.}(\theta) \left[1 - 2 \frac{\sin(2M)}{2M} + \frac{\sin^2 M}{M^2} \right], \quad (11.210)$$

where

$$M = c \sin(\frac{1}{2}(\zeta + \theta)) \sqrt{\xi_1^2 - \cos^2(\frac{1}{2}(\zeta - \theta))}; \quad (11.211)$$

this result is only valid if ζ and θ satisfy the condition:

$$\tan \frac{1}{2}(\zeta + \theta) = -2 \frac{\xi_1^2 - \cos^2(\frac{1}{2}(\zeta - \theta))}{\sin(\zeta - \theta)}. \quad (11.212)$$

A more refined approximation, in which an asymptotic expression for the diffracted field is retained, is available only for the far back scattered field with axial incidence ($\eta = 1$, $\zeta \rightarrow \infty$, $\zeta = \pi$). If this case, if

$$\mathbf{E}^i = \hat{x} e^{-ikz}, \quad \mathbf{H}^i = -\hat{y} e^{-ikz}, \quad (11.213)$$

then (LEVY and KELLER [1960]):

$$\begin{aligned}
 S = & -\frac{c(\xi_1^2-1)}{2\xi_1} e^{-2ic\xi_1} \left\{ 1 + 2\left(\frac{1}{2}c\right)^{\frac{1}{2}} \xi_1^{\frac{1}{2}} (\xi_1^2-1)^{-\frac{1}{2}} \right. \\
 & \times \exp\left(\frac{1}{2}i\pi + 2ic\xi_1 + 2ic \int_0^1 \sqrt{\frac{\xi_1^2-\eta^2}{1-\eta^2}} d\eta\right) \\
 & \times \left[(\text{Ai}'(-\alpha_1))^{-2} \exp\left(\exp\left\{\frac{5}{3}i\pi\right\} c^{\frac{1}{2}} \alpha_1 \{2\xi_1 \sqrt{(\xi_1^2-1)}\}^{\frac{1}{2}} \int_0^1 \frac{d\eta}{\sqrt{(\xi_1^2-\eta^2)(1-\eta^2)}}\right) - \right. \\
 & - \beta_1^{-1} (\text{Ai}(-\beta_1))^{-2} \exp\left(\exp\left\{\frac{5}{3}i\pi\right\} c^{\frac{1}{2}} \beta_1 \{2\xi_1 \sqrt{(\xi_1^2-1)}\}^{\frac{1}{2}} \right. \\
 & \left. \left. \times \int_0^1 \frac{d\eta}{\sqrt{(\xi_1^2-\eta^2)(1-\eta^2)}}\right) \right] \left. \right\}, \quad (11.214)
 \end{aligned}$$

where α_1 , β_1 , $\text{Ai}'(-\alpha_1)$ and $\text{Ai}(-\beta_1)$ are defined in eqs. (11.68) and (11.142).

The total scattering cross section for end-on incidence ($\zeta = \pi$) is (JONES [1957]):

$$\sigma_T \sim \frac{2\pi c^2}{k^2} (\xi_1^2-1) \{1 + 0.0661[c(\xi_1 - \xi_1^{-1})]^{-\frac{1}{2}}\}; \quad (11.215)$$

this result is a good approximation if

$$c(\xi_1 - \xi_1^{-1}) \gg 1. \quad (11.216)$$

For broadside incidence ($\zeta = \frac{1}{2}\pi$), the total scattering cross section is

$$\sigma_T \sim \frac{2\pi c^2}{k^2} \xi_1 \sqrt{\xi_1^2-1} \{1 + (c\sqrt{\xi_1^2-1})^{-\frac{1}{2}} [0.9301\bar{b} - 0.8640b]\} \quad (11.217)$$

if E^i is parallel to the z -axis, and

$$\sigma_T \sim \frac{2\pi c^2}{k^2} \xi_1 \sqrt{\xi_1^2-1} \{1 + (c\sqrt{\xi_1^2-1})^{-\frac{1}{2}} [0.9301\bar{b}(1 - \xi_1^{-2}) - 0.8640b]\} \quad (11.218)$$

if H^i is parallel to the z -axis (JONES [1957]); the quantity \bar{b} is the hypergeometric function

$$\bar{b} = {}_2F_1\left(\frac{1}{2}, \frac{3}{2}; 2; \xi_1^{-2}\right), \quad (11.219)$$

whereas b is given by eq. (11.73). In particular, one has the following numerical values:

major axis						
minor axis	$\infty:1$	$10:9$	$5:4$	$5:3$	$5:2$	$5:1$
$[0.9301\bar{b} - 0.8640b]^{-1}$	∞	0.136	0.204	0.336	0.442	0.535
$[0.9301\bar{b}(1 - \xi_1^{-2}) - 0.8640b]^{-1}$	∞	0.0139	-0.0932	-0.242	-0.361	-0.458

The results (11.217) and (11.218) are good approximations if

$$c\sqrt{(\xi_1^2-1)} \gg 1. \quad (11.220)$$

11.4.2.4. SHAPE APPROXIMATION

For a spheroid whose surface $\xi = \xi_1$, defined in terms of the spherical polar coordinates (r_1, θ_1, ϕ_1) by the equation

$$r_1 = a \left(\frac{\xi_1^2 - 1}{\xi_1^2 - \cos^2 \theta_1} \right)^{\frac{1}{2}}, \quad (11.221)$$

and is such that

$$\xi_1^2 - 1 \gg 1, \quad (11.222)$$

i.e. the spheroid departs only infinitesimally from the sphere $r_1 = a$, the scattered field may be expressed as a perturbation of the solution for this sphere.

The scattered field corresponding to an incident wave with arbitrary polarization and whose direction of propagation forms an angle ζ with the positive z -axis has been derived by MUSHIAKE [1956]. For the particular case of back scattering, the cross sections σ_{\parallel} and σ_{\perp} corresponding to an incident electric field respectively parallel and perpendicular to the plane of the direction of propagation and the z -axis are:

$$\sigma_{\parallel, \perp} = \pi a^2 \left| (ka)^{-2} \sum_{n=1}^{\infty} \frac{(-1)^n (2n+1)}{h_n^{(1)}(ka) \zeta'_n} - \frac{1}{\xi_1^2 - 1} A_{\parallel, \perp} \right|^2 + O[(\xi_1^2 - 1)^{-2}], \quad (11.223)$$

where

$$\zeta_n = ka h_n^{(1)}(ka), \quad (11.224)$$

the prime indicates the derivative with respect to ka , and (MUSHIAKE [1956]):

$$\begin{aligned} A_{\parallel} = & \sum_{m=0}^{\infty} \sum_{n=m}^{\infty} \left\{ \frac{i^n}{\zeta_n} \frac{m P_n^m(\cos \zeta)}{\sin \zeta} \sum_{l=m}^{\infty} \frac{1}{2} i^l m \left[\frac{1}{\zeta'_l} \frac{\partial P_l^m(\cos \zeta)}{\partial \zeta} I_{nl}^{2m} - \right. \right. \\ & \left. \left. - \frac{1}{\zeta_l} \frac{P_l^m(\cos \zeta)}{\sin \zeta} I_{nl}^{1m} \right] + \frac{i^n}{\zeta_n} \frac{\partial P_n^m(\cos \zeta)}{\partial \zeta} \sum_{l=m}^{\infty} \frac{1}{2} i^l \left[\frac{1}{\zeta'_l} \left[\frac{l(l+1)}{(ka)^2} - 1 \right] I_{nl}^{1m} + \right. \right. \\ & \left. \left. + \frac{l(l+1)}{(ka)^2} I_{nl}^{4m} \right] \frac{\partial P_l^m(\cos \zeta)}{\partial \zeta} - \frac{i}{\zeta_l} \frac{m^2 P_l^m(\cos \zeta)}{\sin \zeta} I_{nl}^{2m} \right\}. \end{aligned} \quad (11.225)$$

A_{\perp} is obtained from A_{\parallel} by interchanging $m P_j^m(\cos \zeta)/\sin \zeta$ and $-\partial P_j^m(\cos \zeta)/\partial \zeta$ with $j = n$ or l in eq. (11.225),

$$I_{nl}^{1m} = M \int_0^{\pi} \left(\frac{\partial P_n^m}{\partial \theta} \frac{\partial P_l^m}{\partial \theta} + m^2 \frac{P_n^m P_l^m}{\sin^2 \theta} \right) \sin^3 \theta \, d\theta, \quad (11.226)$$

$$I_{nl}^{2m} = M \int_0^{\pi} \left(\frac{\partial P_n^m}{\partial \theta} P_l^m + \frac{\partial P_l^m}{\partial \theta} P_n^m \right) \sin^2 \theta \, d\theta, \quad (11.227)$$

$$I_{nl}^{4m} = M \int_0^{\pi} \frac{\partial P_n^m}{\partial \theta} P_l^m \sin 2\theta \sin \theta \, d\theta, \quad (11.228)$$

and

$$M = \varepsilon_m \frac{(2n+1)(n-m)!(2l+1)(l-m)!}{n(n+1)(n+m)!l(l+1)(l+m)!}. \quad (11.229)$$

The normalized back scattering cross section at end-on incidence is shown for a 5:4 spheroid in Fig. 11.28.

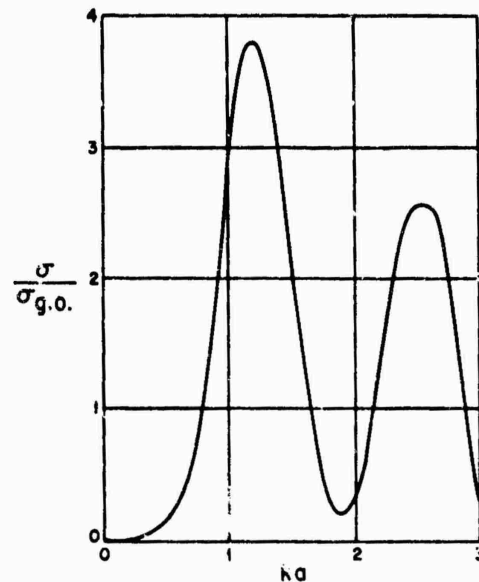


Fig. 11.28. Normalized back scattering cross section for a 5 : 4 spheroid at end-on incidence (MUSHIAKE [1956]).

Bibliography

- AR, E. and R. E. KLEINMAN [1966], The Exterior Neumann Problem for the Three-Dimensional Helmholtz Equation, *Arch. Rational Mech. Anal.* **23**, 218-236.
- ASVESTAS, J. S. and R. E. KLEINMAN [1967], Low Frequency Scattering by Spheroids and Discs, The University of Michigan Radiation Laboratory Report No. 7133-5-T, Ann Arbor, Michigan.
- BEUKINA, M. G. [1957], Radiation Characteristics of an Elongated Rotary Ellipsoid, in: *Diffraction of Electromagnetic Waves by Some Bodies of Revolution*, Soviet Radio, Moscow.
- BRUNDRELL, G. B. [1965], A Solution to the Problem of Scalar Scattering from a Smooth, Bounded Obstacle Using Integral Equations, *Quart. J. Mech. Appl. Math.* **19**, 473-489. It is not clear what normalization has been used in plotting 'S'; furthermore, the shapes of the curves representing 'S' are incorrect. It is suggested that no diagram of this paper be used without a numerical verification.
- BURKE, J. E. [1966a], Low-Frequency Scattering by Soft Spheroids, *J. Acoust. Soc. Am.* **39**, 826-831.
- BURKE, J. E. [1966b], Long-Wavelength Scattering by Hard Spheroids, *J. Acoust. Soc. Am.* **40**, 323-330.
- CRISPIN JR., J. W., R. F. GOODRICH and K. M. SIEGEL [1959], A Theoretical Method for the Calculation of the Radar Cross Sections of Aircraft and Missiles, The University of Michigan Radiation Laboratory Report No. 2591-1-H, Ann Arbor, Michigan.
- CRISPIN JR., J. W., K. M. SIEGEL and F. B. SLEATOR [1963], The Resonance Region, in: *Radio Waves and Circuits*, ed. S. Silver, 11-37, Elsevier Publishing Co., Amsterdam.

- FLAMMER, C. [1957], *Spheroidal Wave Functions*, Stanford University Press, Stanford, California.
- GOODRICH, R. F. and N. D. KAZARINOFF [1963], Scalar Diffraction by Prolate Spheroids whose Eccentricities are almost One, *Proc. Cambridge Phil. Soc.* **59**, 167-183. The formulas of sections 6 and 7 have several errors.
- HATCHER, E. C. and A. LEITNER [1954], Radiation from a Point Dipole Located at the Tip of a Prolate Spheroid, *J. Appl. Phys.* **25**, 1250-1253.
- HUNTER, H. E., D. B. KIRK, T. B. A. SENIOR and E. R. WITTENBERG [1965a], Tables of Prolate Spheroidal Functions for $m = 0$; Volume I, The University of Michigan Radiation Laboratory Report No. 7133-1-T (AD-619979), Ann Arbor, Michigan. The normalization constants $N_{on}(c)$ are tabulated for $c = 0.1(0.1)10.0$ and n ranging from zero up to a maximum of 20. The radial functions $R_{on}^{(1)}(c, \xi)$ and $R_{on}^{(2)}(c, \xi)$, and their first derivatives, are given for the same c and n and for $\xi = 1.000\,050\,0, 1.005\,037\,8, 1.020\,620\,7$ and $1.154\,700\,5$.
- HUNTER, H. E., D. B. KIRK, T. B. A. SENIOR and E. R. WITTENBERG [1965b], Tables of Prolate Spheroidal Functions for $m = 0$; Volume II, The University of Michigan Radiation Laboratory Report No. 7133-2-T (AD-619980), Ann Arbor, Michigan. The angular functions $S_{on}(c, \eta)$ and $S'_{on}(c, \eta)$ are tabulated for $c = 0.1(0.1)10.0$, n ranging from zero up to a maximum of 20, and $\eta = 0(0.05)1$.
- JONES, D. S. [1957], High-Frequency Scattering of Electromagnetic Waves, *Proc. Roy. Soc.* **A240**, 206-213.
- KLEINMAN, R. E. [1965a], The Dirichlet Problem for the Helmholtz Equation, *Arch. Rational Mech. Anal.* **18**, 205-229.
- KLEINMAN, R. E. [1965b], Low Frequency Solution of Electromagnetic Scattering Problems, presented at the URSI Symposium on Electromagnetic Wave Theory, Delft, the Netherlands; reprinted in: *Electromagnetic Wave Theory*, ed. J. Brown, 891-905, Pergamon Press, London (1967).
- LEVY, B. R. and J. B. KELLER [1960], Diffraction by a Spheroid, *Can. J. Phys.* **38**, 128-144. Formulas (11), (14) and (15) of section 2 and formula (2) of section 4 have some errors which have been corrected by CRISPIN et al. [1963].
- LOWAN, A. N. [1964], Spheroidal Wave Functions, in: *Handbook of Mathematical Functions with Formulas, Graphs, and Mathematical Tables*, eds. M. Abramowitz and I. A. Stegun, 751-769, N.B.S. Applied Mathematics Series No. 55, U.S. Government Printing Office, Washington, D.C.
- MOFFATT, D. L. [1965], Electromagnetic Scattering by a Perfectly Conducting Prolate Spheroid, The Ohio State University Antenna Laboratory Report No. 1774-11, Columbus, Ohio.
- MOFFATT, D. L. and E. M. KENNAUGH [1965], The Axial Echo Area of a Perfectly Conducting Prolate Spheroid, *IEEE Trans.* **AP-13**, 401-409.
- MORSE, P. M. and H. FESHBACH [1953], *Methods of Theoretical Physics*, Vols. 1 and 2, McGraw-Hill Book Co., New York.
- MÜLLER, H. J. W. [1952], Asymptotic Expansions of Prolate Spheroidal Wave Functions and their Characteristic Numbers, *J. Reine Angew. Mat.* **212**, 26-48.
- MUSHIAKE, Y. [1956], Backscattering for Arbitrary Angles of Incidence of a Plane Electromagnetic Wave on a Perfectly Conducting Spheroid with Small Eccentricity, *J. Appl. Phys.* **27**, 1549-1556.
- NORLL, B. [1962], Integral Equation Perturbation Methods in Low-frequency Diffraction, in: *Electromagnetic Waves*, ed. R. F. Langer, 323-360, The University of Wisconsin Press, Madison, Wisconsin.
- REITHINGER, N. [1957], Scattering of a Plane Wave Incident on a Prolate Spheroid at an Arbitrary Angle, The University of Michigan Radiation Laboratory Memorandum No. 2686-506 M, Ann Arbor, Michigan.
- SCHULTZ, F. V. [1950], Scattering by a Prolate Spheroid, The University of Michigan Willow Run Research Center Report No. UMM-42, Ann Arbor, Michigan.
- SENIOR, T. B. A. [1960], Scalar Diffraction by a Prolate Spheroid at Low Frequencies, *Can. J. Phys.* **38**, 1632-1641. The coefficients u_i and v_i have a sign error.

- SENIOR, T. B. A. [1961], The Convergence of Low Frequency Expansions in Scalar Scattering by Spheroids, The University of Michigan Radiation Laboratory Report No. 3648-4-T, Ann Arbor, Michigan.
- SENIOR, T. B. A. [1966a], The Scattering from Acoustically Hard and Soft Prolate Spheroids for Axial Incidence, *Can. J. Phys.* **44**, 655-667.
- SENIOR, T. B. A. [1966b], The Scattering of an Electromagnetic Wave by a Spheroid, *Can. J. Phys.* **44**, 1353-1359.
- SENIOR, T. B. A. [1969], to be published.
- SIEGEL, K. M., H. A. ALPERIN, R. R. BONKOWSKI, J. W. CRISPIN, A. L. MAFFETT, C. E. SCHENSTED and I. V. SCHENSTED [1955], Bistatic Radar Cross Sections of Surfaces of Revolution, *J. Appl. Phys.* **26**, 297-305.
- SIEGEL, K. M., F. V. SCHULTZ, B. H. GERE and F. B. SLEATOR [1956], The Theoretical and Numerical Determination of the Radar Cross Section of a Prolate Spheroid, *IRE Trans. AP-4*, 266-275.
- SIEGEL, K. M. [1959], Far Field Scattering from Bodies of Revolution, *Appl. Sci. Res.* **7B**, 293-328. See also *Appl. Sci. Res.* **8B**, 8-12.
- SLEATOR, F. B. [1964], Studies in Radar Cross Sections XLIX-Diffraction and Scattering by Regular Bodies III: The Prolate Spheroid, The University of Michigan Radiation Laboratory Report No. 3648-6-T, Ann Arbor, Michigan.
- SLEPIAN, D. [1965], Some Asymptotic Expansions for Prolate Spheroidal Wave Functions, *J. Math. Phys.* **44**, 99-140.
- SLEPIAN, D. and E. SONNENBLICK [1965], Eigenvalues Associated with Prolate Spheroidal Wave Functions of Zero Order, *Bell System Tech. J.* **44**, 1745-1759. The eigenvalues $\chi_n = \lambda_{on}$ of the differential equation satisfied by $S_{on}(c, \eta)$, and the eigenvalues of the corresponding integral equation, are tabulated to eight figures and plotted for $n = 0$ (1) 20, 25 (5) 40 and $c = 1$ (1) 20, 25 (5) 40.
- SPENCE, R. D. and S. GRANGER [1951], The Scattering of Sound from a Prolate Spheroid, *J. Acoust. Soc. Am.* **23**, 701-706.
- STEVENSON, A. F. [1953a], Solution of Electromagnetic Scattering Problems as Power Series in the Ratio (Dimension of Scatterer)/Wavelength, *J. Appl. Phys.* **24**, 1134-1142. See also KLEINMAN [1965b].
- STEVENSON, A. F. [1953b], Electromagnetic Scattering by an Ellipsoid in the Third Approximation, *J. Appl. Phys.* **24**, 1143-1151.
- STROUT, J. W. (Lord Rayleigh) [1897], On the Incidence of Aerial and Electric Waves upon Small Obstacles in the Form of Ellipsoids or Elliptic Cylinders, and on the Passage of Electric Waves through a Circular Aperture in a Conducting Screen, *Phil. Mag.* **44**, 28-52.

CHAPTER 12

THE WIRE

O. EINARSSON

The geometrical shape corresponding to a thin wire is a finite circular cylinder whose cross section is small compared to its length and to the wavelength. The contribution to the scattered field from the end surfaces of the cylinder is assumed to be negligible. The wire may, for example, be either a thin-walled tube or a solid cylinder with plane end-caps.

The thin wire concept is meaningful only for acoustically soft or perfectly conducting cylinders. The acoustically soft wire may be treated by the same methods as the perfectly conducting wire (WILLIAMS [1956]); however, no specific results are available. Furthermore, the existing formulae for the perfectly conducting wire are limited to plane wave incidence.

Thin wire formulae can be considered as combinations of low frequency and resonance region expansions (sometimes extending up into the high frequency region). The oldest approach, which we will call "the integral equation method", is to obtain solutions by iterations applied to the linearized integral equation of HALLÉN [1938]. We give only a few formulae related to this method, and for a more complete account the reader is referred to the book by KING [1956].

The scattering cross section may be expressed as a functional which is stationary with respect to small changes in the current distribution on the wire. This approach was introduced by TAI [1951], and will be called "the variational method".

For the case of a finite thin-walled tube, there exists an exact solution of the scattering problem expressible as an infinite sum of traveling waves (HALLÉN [1961], EINARSSON [1963]). In the thin wire case, each term in the sum can be expanded asymptotically and the resulting sum can be expressed in closed form (EINARSSON [1969]). We designate this and related methods "the direct method".

12.1. Thin wire geometry

The geometry of the wire and the orientation of the incident plane electromagnetic wave are shown in Fig. 12.1.

The incident wave is linearly polarized with the electric field vector in the plane of the direction of propagation and the wire axis; this is no limitation since only the component of the electric field parallel to the wire contributes to the far field scattering.

Although the results are derived for wires of circular cross section, they are also valid for non-circular cross sections provided that the cylinder radius a is replaced by an equivalent radius (HALLÉN [1938], FLAMMER [1950]). This equivalent radius is

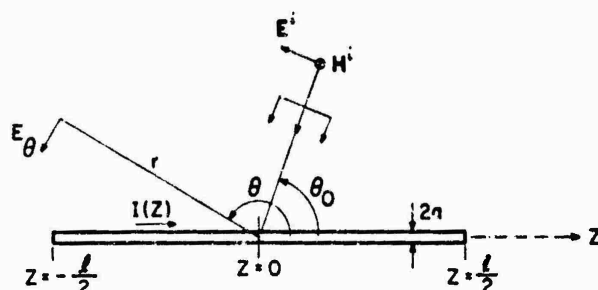


Fig. 12.1. Thin wire geometry.

equal to the radius of an infinite circular cylinder that in conjunction with a distant concentric conductor has the same capacitance per unit length as an infinite cylinder of the given cross section; values for some simple geometries are given in Fig. 12.2.

CROSS SECTION				
EQUIVALENT RADII	$(d + b) / 2$	$d / 4$	$0.42 d$	$0.59 d$

Fig. 12.2. Equivalent wire radii.

SU and GERMAN [1966] have computed the equivalent radii for a number of more complicated shapes employing an approximate formula given by UDA and MUSHIAKE [1954].

The following notation will be used throughout the chapter:

$$\begin{aligned}
 L &= \frac{1}{2}kl = \pi l / \lambda, \\
 \gamma &= 0.577\,215\,664\,9 \dots \quad (\text{Euler's constant}), \\
 \zeta(3) &= \sum_{n=1}^{\infty} \frac{1}{n^3} = 1.202\,056\,903 \dots
 \end{aligned}
 \tag{12.1}$$

Various special functions are defined and discussed in Section 12.6. For a plane incident wave of unit amplitude

$$E_{\theta}^i = \exp \{ -ikr(\sin \theta \sin \theta_0 + \cos \theta \cos \theta_0) \}, \tag{12.2}$$

the scattered far field is written as

$$E_{\theta}^s(r, \theta, \theta_0) = \frac{e^{ikr}}{kr} S(\theta, \theta_0). \tag{12.3}$$

12.2. The average back scattering cross section

The average back scattered return for arbitrary angle of incidence and polarization is defined as

$$\bar{\sigma} = \frac{3}{8} \int_0^{2\pi} \sigma(\theta) \sin \theta d\theta, \quad (12.4)$$

where $\sigma(\theta)$ is the back scattering cross section related to the polarization of the incident wave shown in Fig. 12.1, and is defined by eq. (12.21). Whereas the cross section of eq. (12.4) is specified by the component of the scattered field parallel to the incident field, the corresponding cross section specified by the perpendicular component is $\frac{1}{2}\bar{\sigma}$.

The average cross section has been calculated by Chu (see VAN VLECK et al. [1947]) by assuming a simple current distribution along the wire and determining its magnitude by equating the real power calculated at the wire surface to that in the far field (EMF method). For resonant wires ($l = \frac{1}{2}n\lambda$; $n = 1, 2, 3, \dots$), the result is

$$\frac{\bar{\sigma}}{\lambda^2} = \frac{3}{16\pi} \frac{2\pi L - \frac{1}{2} + 3 \log 4L + 3\gamma - \log 2}{(\gamma + \log 4L)^2}. \quad (12.5)$$

For long wires, Chu gives a non-resonant formula (VAN VLECK et al. [1947]):

$$\frac{\bar{\sigma}}{\lambda^2} = \frac{3}{16\pi} \frac{2\pi L - 1}{\pi^2 + 4(\gamma + \log \frac{1}{2}ka)^2}, \quad (12.6)$$

which does not predict any oscillations in the cross section as a function of wire length.

The result

$$\frac{\bar{\sigma}}{\lambda^2} = \frac{L^6}{45\pi \{\log(2l/a) - 1\}^2}, \quad (12.7)$$

which is valid for short wires ($L \lesssim 0.3$), has been obtained by VAN VLECK et al. [1947] by means of the integral equation method.

For longer wires ($L \gtrsim \frac{1}{2}\pi$), VAN VLECK et al. [1947] give:

$$\begin{aligned} \frac{\bar{\sigma}}{\lambda^2} = \frac{3}{16\pi} \{ & (F'^2 + F''^2)(2\pi L - 1) + (G'^2 + G''^2)[2\pi L - 1 + \gamma + \log 4L + \\ & + (\pi + 4L \log 2) \sin 2L + (\frac{1}{2} - 2\gamma - 2 \log 4L) \cos 2L - (\log 2) \cos 4L] + \\ & + (H'^2 + H''^2)[2\pi L - 1 + \gamma + \log 4L - (\pi + 4L \log 2) \sin 2L + \\ & + (2 \log 4L + 2\gamma - \frac{1}{2}) \cos 2L - (\log 2) \cos 4L] + \\ & + (G'H' + G''H'')[8L(\log 2) \cos 2L - \sin 2L] + \\ & + (F'G' + F''G'')[7\pi \sin L - 2(\gamma + \log 4L) \cos L - 2(\log 2) \cos 3L] + \\ & + (F'H' + F''H'')[\pi \cos L - 2(\gamma + \log 4L) \sin L + 2(\log 2) \sin 3L] \}, \end{aligned} \quad (12.8)$$

where

$$F' = \frac{\Omega}{\pi^2 + \Omega^2}, \quad (12.9)$$

$$F'' = \frac{\pi}{\pi^2 + \Omega^2}, \quad (12.10)$$

$$\Omega = -2\gamma - 2 \log(\tfrac{1}{2}ka), \quad (12.11)$$

$$G' = \frac{\tfrac{1}{2}\Psi(L)}{\Psi^2(L) + \Xi^2(L)} - \frac{\pi}{2\Omega} G'', \quad (12.12)$$

$$G'' = \frac{\tfrac{1}{2}\Xi(L)}{\Psi^2(L) + \Xi^2(L)}, \quad (12.13)$$

$$H' = \frac{\tfrac{1}{2}\Psi(L - \tfrac{1}{2}\pi)}{\Psi^2(L - \tfrac{1}{2}\pi) + \Xi^2(L - \tfrac{1}{2}\pi)} - \frac{\pi}{2\Omega} H'', \quad (12.14)$$

$$H'' = \frac{\tfrac{1}{2}\Xi(L - \tfrac{1}{2}\pi)}{\Psi^2(L - \tfrac{1}{2}\pi) + \Xi^2(L - \tfrac{1}{2}\pi)}, \quad (12.15)$$

$$\Psi(x) = \tfrac{1}{4}\pi \sin x + (1 - \tfrac{1}{2}\gamma - \tfrac{1}{2} \log L - \Omega) \cos x, \quad (12.16)$$

$$\Xi(x) = \tfrac{1}{2}(\gamma + \log 4L) \sin x - \tfrac{1}{4}\pi \cos x. \quad (12.17)$$

Computed values based on eqs. (12.5), (12.6) and (12.8) are shown in Fig. 12.3.

12.3. The back scattering cross section

The back scattering cross section has been derived by VAN VLECK et al. [1947] using the integral equation method, and results for normal incidence are given by DIKE and KING [1952]. Higher order terms are given by LINDROTH [1955], and one of Lindroth's graphs is shown in Fig. 12.6. The curves by VAN VLECK et al. [1947] and by DIKE and KING [1952] are reproduced in KING [1956]. No formulae related to the integral equation method will be given here because the results obtained by the variational and direct methods are no more complex and seem to be at least as reliable.

The functional for the far field,

$$\frac{1}{S(\theta, \theta)} = - \frac{\int_{-1/2}^{1/2} \int_{-1/2}^{1/2} I(z) I(z') K(z - z') dz dz'}{\left[k \sin \theta \int_{-1/2}^{1/2} I(z) e^{-ikz \cos \theta} dz \right]^2}, \quad (12.18)$$

where

$$K(z - z') = \left(k^2 + \frac{\partial^2}{\partial z^2} \right) \frac{e^{ikR}}{kR} \quad (12.19)$$

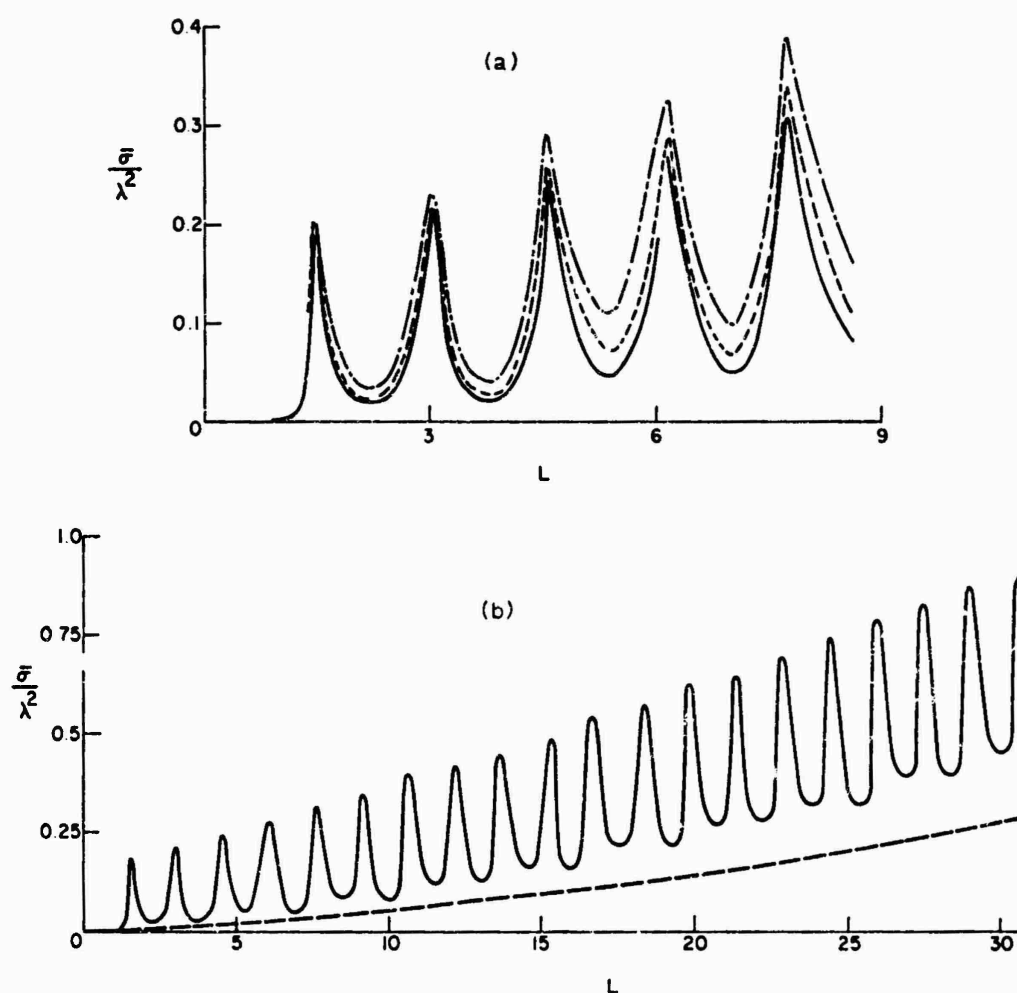


Fig. 12.3. Average back scattering cross section: (a) integral equation method (VAN VLECK et al. [1947]) for $l/a = 900$ (—), $l/a = 450$ (---) and $l/a = 225$ (- - -); (b) integral equation method (VAN VLECK et al. [1947]) for $l/a = 900$ (- - -), Chu non-resonant formula (---).

$$R = \sqrt{\{(z - z')^2 + a^2\}}, \quad (12.20)$$

and

$$\frac{\sigma(\theta)}{\lambda^2} = \frac{1}{\pi} |S(\theta, \theta)|^2, \quad (12.21)$$

is used by TAI [1951] to calculate a first order approximation to the cross section; although the integral equation related to eq. (12.18) does not possess an exact solution, the validity of the numerical results is not affected. The trial function for the current distribution is (TAI [1951]):

$$I(z) = I_0 \{ \cos kz \cos (L \cos \theta) - \cos L \cos (kz \cos \theta) + A [\sin kz \sin (L \cos \theta) - \sin L \sin (kz \cos \theta)] \}, \quad (12.22)$$

where the arbitrary constant I_0 does not affect the value of the cross section, and the constant A is determined by the condition $\partial S / \partial A = 0$. When eq. (12.22) is substituted

into eq. (12.18) and approximations valid for small ka are made, one finds:

$$S(\theta, \theta) \approx i \left(\frac{g_c^2}{\gamma_c} + \frac{g_s^2}{\gamma_s} \right), \quad (12.23)$$

where

$$g_c = \frac{1}{\sin 2\theta} [4 \cos \theta \cos^2 (L \cos \theta) \sin L - (1 + \cos^2 \theta) \sin (2L \cos \theta) \cos L - 2L \cos \theta \sin^2 \theta \cos L], \quad (12.24)$$

$$g_s = \frac{i}{\sin 2\theta} [4 \cos \theta \sin^2 (L \cos \theta) \cos L - (1 + \cos^2 \theta) \sin (2L \cos \theta) \sin L + 2L \cos \theta \sin^2 \theta \sin L], \quad (12.25)$$

$$\begin{aligned} \gamma_c = & \cos^2 L \{ -1 + \cos 2L \cos (2L \cos \theta) + \cos \theta \sin 2L \sin (2L \cos \theta) + \\ & + i[\sin 2L \cos (2L \cos \theta) - \cos \theta \cos 2L \sin (2L \cos \theta)] \} - \\ & - \frac{1}{2} \left[\frac{1 + \cos^2 \theta}{\cos^2 \theta} \cos^2 L \cos (2L \cos \theta) + \sin 2L \sin (2L \cos \theta) \right] \\ & \times [A(2L + 2L \cos \theta) - A(2L - 2L \cos \theta)] + \\ & + \cos^2 (L \cos \theta) A(4L) - i[2 \log (2l/a) - A(2L + 2L \cos \theta) - A(2L - 2L \cos \theta)] \\ & \times \left\{ \left[L \sin^2 \theta + \frac{1 + \cos^2 \theta}{\cos^2 \theta} \sin (2L \cos \theta) \right] \cos^2 L - \sin 2L \cos^2 (L \cos \theta) \right\}, \end{aligned} \quad (12.26)$$

$$\begin{aligned} \gamma_s = & \sin^2 L \{ -1 + \cos 2L \cos (2L \cos \theta) + \cos \theta \sin 2L \sin (2L \cos \theta) + \\ & + i[\sin 2L \cos (2L \cos \theta) - \cos \theta \cos 2L \sin (2L \cos \theta)] \} + \\ & + \frac{1}{2} \left[\frac{1 + \cos^2 \theta}{\cos^2 \theta} \sin^2 L \cos (2L \cos \theta) - \sin 2L \sin (2L \cos \theta) \right] \\ & \times [A(2L + 2L \cos \theta) - A(2L - 2L \cos \theta)] + \sin^2 (L \cos \theta) A(4L) - \\ & - i[2 \log (2l/a) - A(2L + 2L \cos \theta) - A(2L - 2L \cos \theta)] \\ & \times \left\{ \left[L \sin^2 \theta - \frac{1 + \cos^2 \theta}{\cos^2 \theta} \sin (2L \cos \theta) \right] \sin^2 L + \sin 2L \sin^2 (L \cos \theta) \right\}, \end{aligned} \quad (12.27)$$

with

$$A(x) = \text{Cin}(x) - i \text{Si}(x), \quad (12.28)$$

and $\text{Cin}(x)$ and $\text{Si}(x)$ are defined by eqs. (12.68) and (12.66). Computations based on eqs. (12.23) to (12.27) are shown in Figs. 12.4 and 12.5, and are compared with the results of the direct method (see Section 12.4). Comparisons between the direct method and experimental data are given in Fig. 12.6, from which it would appear that the discrepancies evident in Figs. 12.4 and 12.5 are due to failures of the variational method.

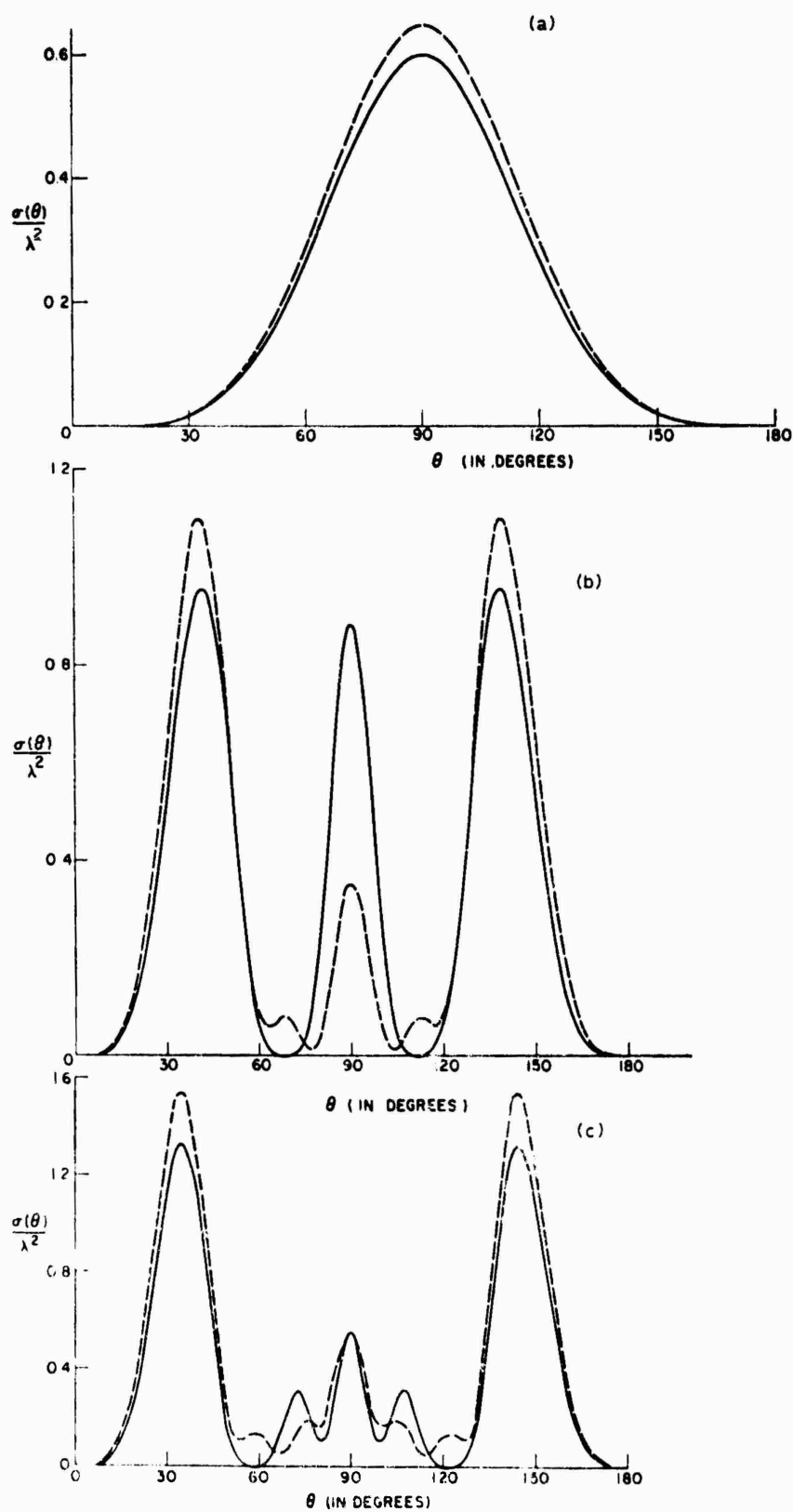


Fig. 12.4. Angular distribution of the back scattering cross section for wires with $l/a = 900$ and (a) $l/\lambda = 0.5$, (b) $l/\lambda = 1.5$, (c) $l/\lambda = 2.0$; (—) direct method (EINARSSON [1969]), (---) variational method (TAI [1951]).

In the particular case of broadside incidence, a first order approximation has been obtained by HU [1958] using a trial function for the current distribution different from and apparently more accurate than that of TAI [1951]. The assumed current is:

$$I(z) = I_0 \left\{ \frac{\cos kz - \cos L}{1 - \cos L} + A[\sin(L - k|z|) + \sin k|z| - \sin L] \right\}. \quad (12.29)$$

The corresponding far field coefficient is:

$$S(\frac{1}{2}\pi, \frac{1}{2}\pi) = \frac{1}{E - iF} \left\{ -H^2 + \frac{[G(E - iF) - H(C - iD)]^2}{(C - iE)^2 - (A - iB)(E - iF)} \right\}, \quad (12.30)$$

where

$$A = \frac{1}{(1 - \cos L)^2} \left\{ \text{Si}(4L) + 4(L \cos L - \sin L) \cos L [\log(2l/a) - \text{Cin}(2L)] - \frac{8ka}{\pi} \sin^2 L - 2 \cos^2 L \sin 2L \right\}, \quad (12.31)$$

$$B = \frac{1}{(1 - \cos L)^2} \{ -\text{Cin}(4L) - (4L \cos^2 L - 2 \sin 2L) \text{Si}(2L) + \sin^2 2L \}, \quad (12.32)$$

$$C = \frac{1}{1 - \cos L} \left\{ \text{Si}(4L) \sin L + (1 - \cos L) \text{Cin}(4L) + 4(1 - \cos L - L \sin L) \text{Cin}(2L) \cos L + 4(1 - \cos L) \text{Cin}(L) \cos L + 4(L \cos L - \sin L) \log(2l/a) \sin L + 4(1 - \cos L)^2 \log(l/a) - \frac{8ka}{\pi} (1 - \cos L) \sin L - \sin^2 2L \right\}, \quad (12.33)$$

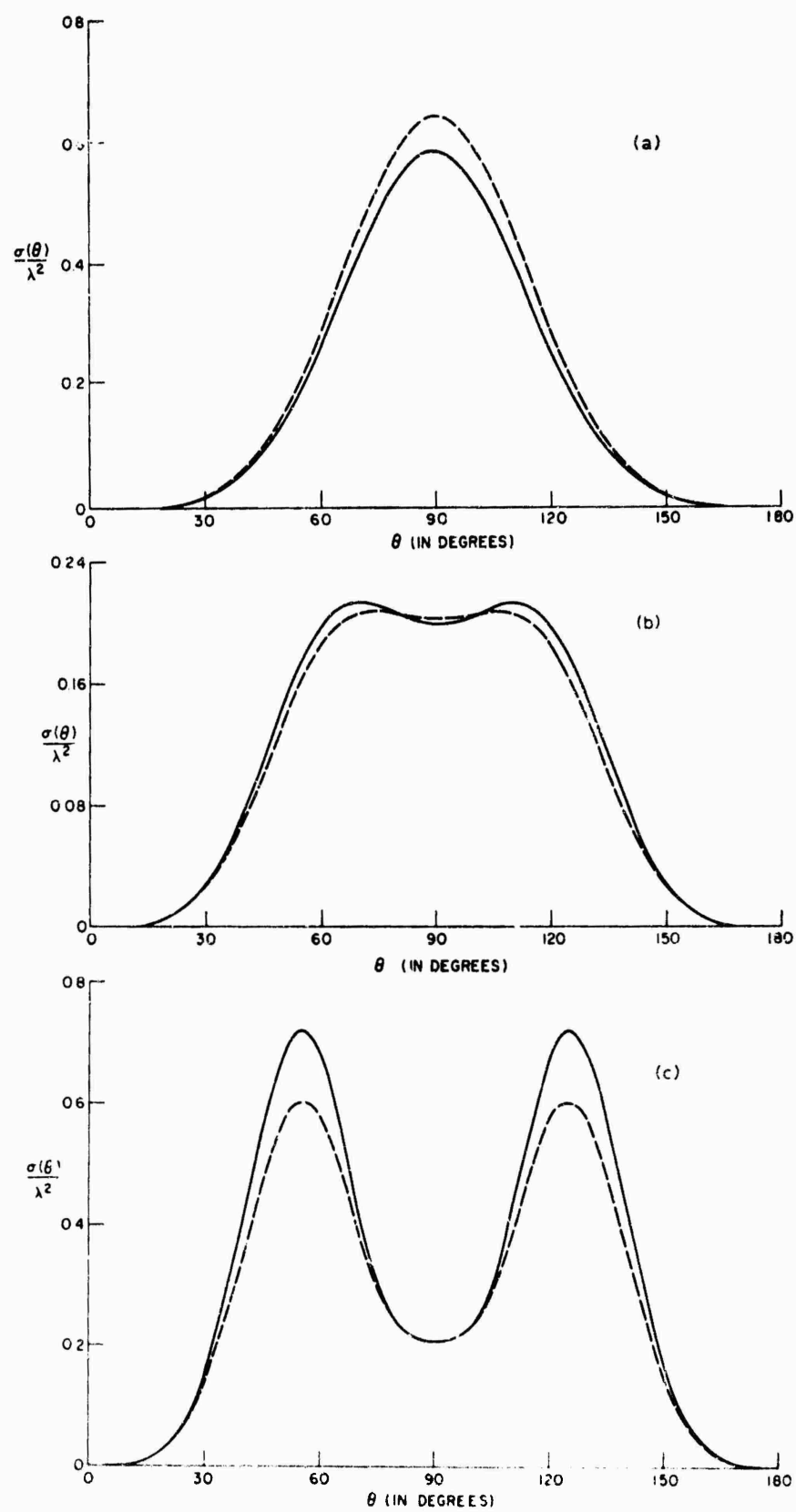
$$D = \frac{1}{1 - \cos L} \{ (1 - \cos L) \text{Si}(4L) - \text{Cin}(4L) \sin L + 4(1 - \cos L - L \sin L) \text{Si}(2L) \cos L + 4(1 - \cos L) \text{Si}(L) \cos L + 2 \sin^2 L \sin 2L \}, \quad (12.34)$$

$$E = 2(1 - \cos L) \text{Si}(4L) \cos L + 2(1 - \cos L) \text{Cin}(4L) \sin L + 4(1 - \cos L)^2 \text{Si}(2L) - 4L \text{Cin}(2L) \sin^2 L + 8(1 - \cos L) \text{Cin}(L) \sin L + 4 \sin L [L \sin L - 2(1 - \cos L)] \log(2l/a) - \frac{24ka}{\pi} (1 - \cos L)^2 - 2 \sin^2 L \sin 2L, \quad (12.35)$$

$$F = 2(1 - \cos L) \text{Si}(4L) \sin L - 2(1 - \cos L) \text{Cin}(4L) \cos L - 4L \text{Si}(2L) \sin^2 L - 4(1 - \cos L)^2 \text{Cin}(2L) + 8(1 - \cos L) \text{Si}(L) \sin L + 4 \sin^4 L, \quad (12.36)$$

$$G = \frac{2}{1 - \cos L} (\sin L - L \cos L), \quad (12.37)$$

$$H = 4(1 - \cos L) - 2L \sin L. \quad (12.38)$$



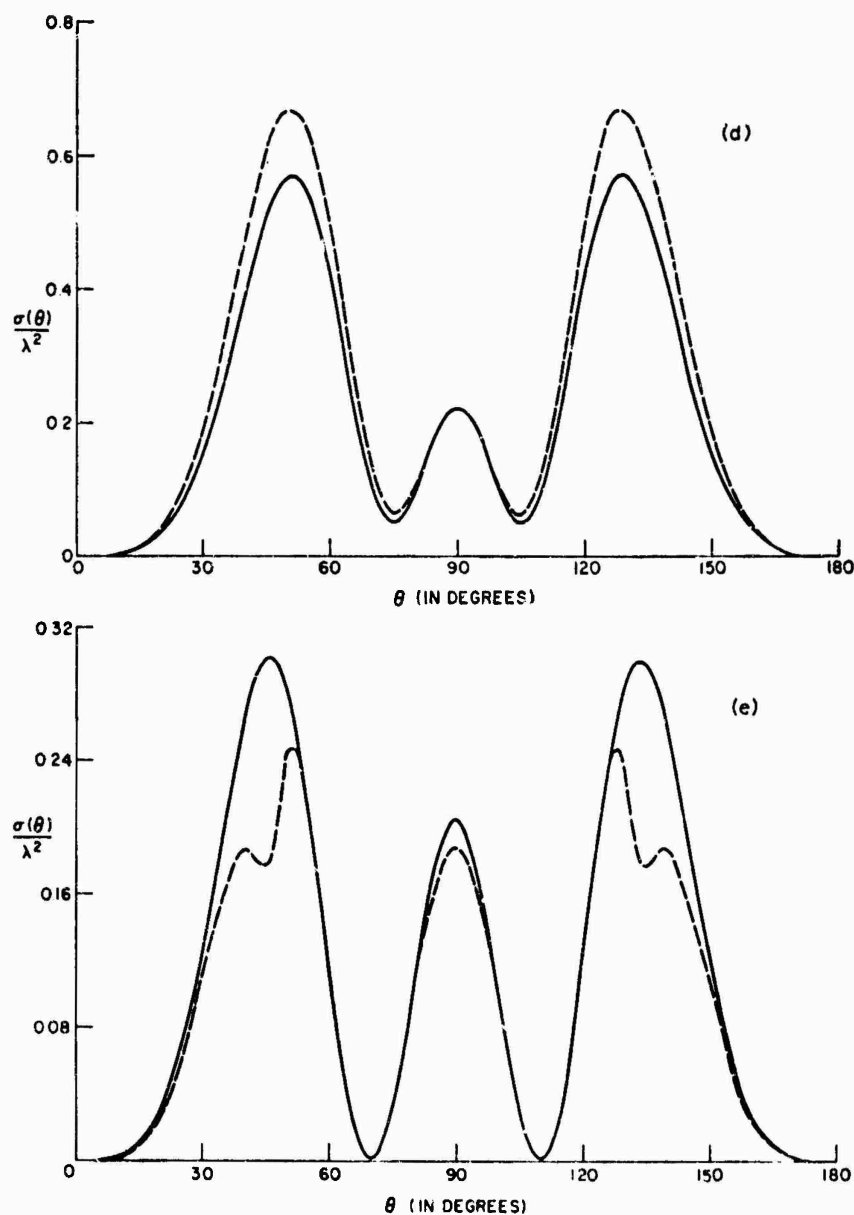


Fig. 12.5. Angular distribution of the back scattering cross section for wires with $l/a = 150$ and (a) $l/\lambda = 0.5$, (b) $l/\lambda = 0.8$, (c) $l/\lambda = 0.9$, (d) $l/\lambda = 1.0$, (e) $l/\lambda = 1.25$; (—) direct method (EINARSSON [1969]), (---) variational method (DE BETTENCOURT [1961]).

The functions $\text{Cin}(x)$ and $\text{Si}(x)$ are defined by eqs. (12.68) and (12.66).

In contrast to the integral equation and variational methods, which are limited to wires one or at most two wavelengths in length, the direct method gives results which are more accurate the longer the wire. The back scattering cross section is obtained by putting $\theta = \theta_0$ in the bistatic scattering formulae (12.46) through (12.49) of the direct method. At broadside incidence, the first order formula (12.50) simplifies to (UFIMTSEV [1962]):

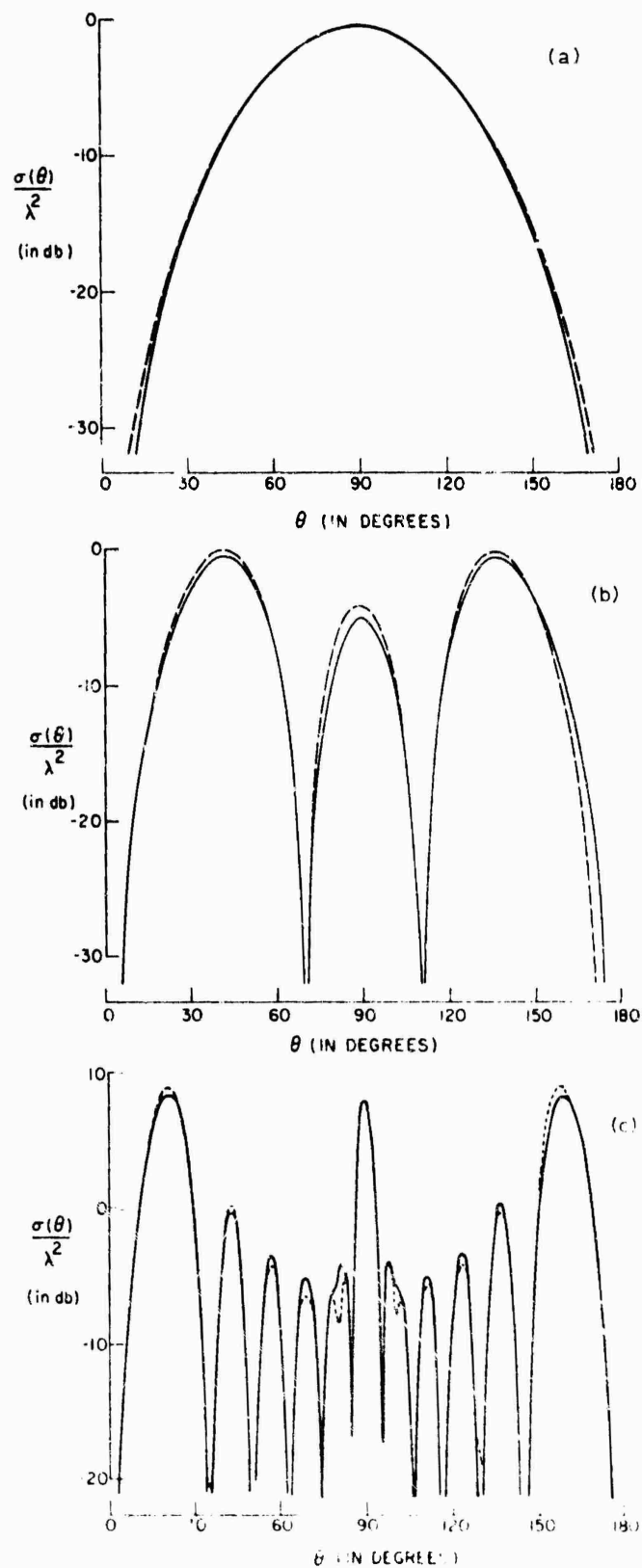


Fig. 12.6. Angular distribution of the back scattering cross section for wires with $ka = 0.9394$ and (a) $l/\lambda = 0.452$, (b) $l/\lambda = 1.381$, (c) $l/\lambda = 5.422$; (—) direct method (EINARSSON [1969]), (---) experimental (CHANG and LILPA [1967]).

$$S(\tfrac{1}{2}\pi, \tfrac{1}{2}\pi) = \frac{2i}{(\Omega_0 + 2 \log 2)^2} \left\{ -1 + (\Omega_0 + \log 2)(1 + iL) - 2e^{2iL}(\Omega_0 + \log 2)^2 g(2L, \tfrac{1}{2}\pi) \right. \\ \left. \times \left[1 - g(2L, \tfrac{1}{2}\pi) \{ \tfrac{1}{2} + iLT(2L) \} - \frac{e^{2iL} \Omega_0 g(2L, \tfrac{1}{2}\pi)}{1 + e^{2iL} \Omega_0 g(2L, 0)} \right] \right\}, \quad (12.39)$$

where Ω_0 , g and T are defined in eqs. (12.54), (12.55) and (12.65). The results of computations based on eqs. (12.30) and (12.39) are compared in Fig. 12.7.

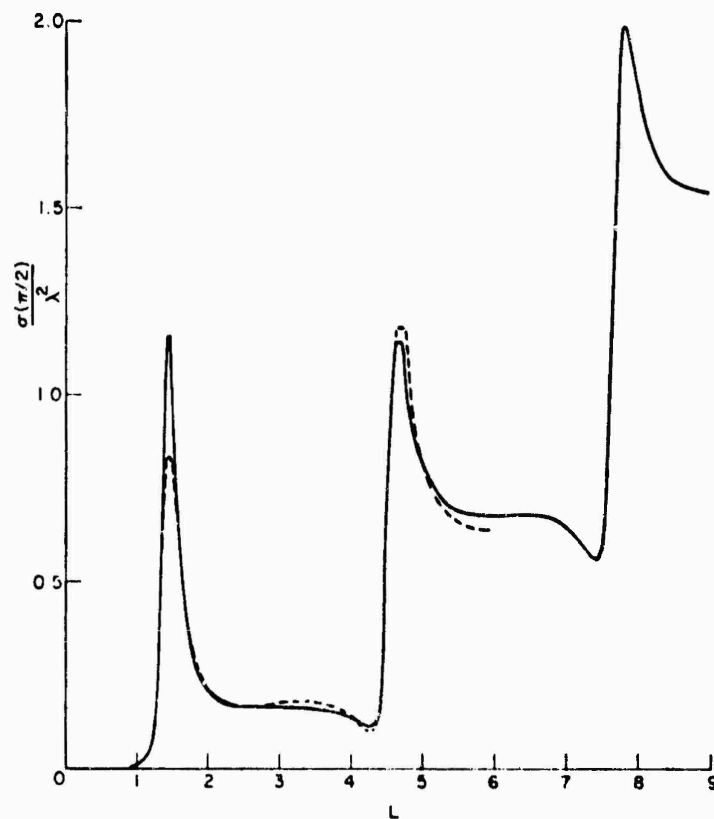
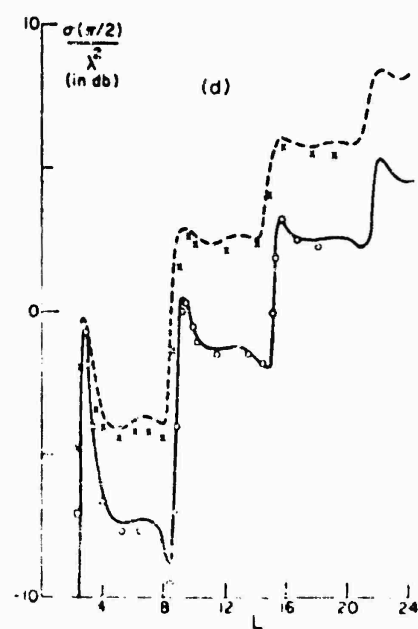
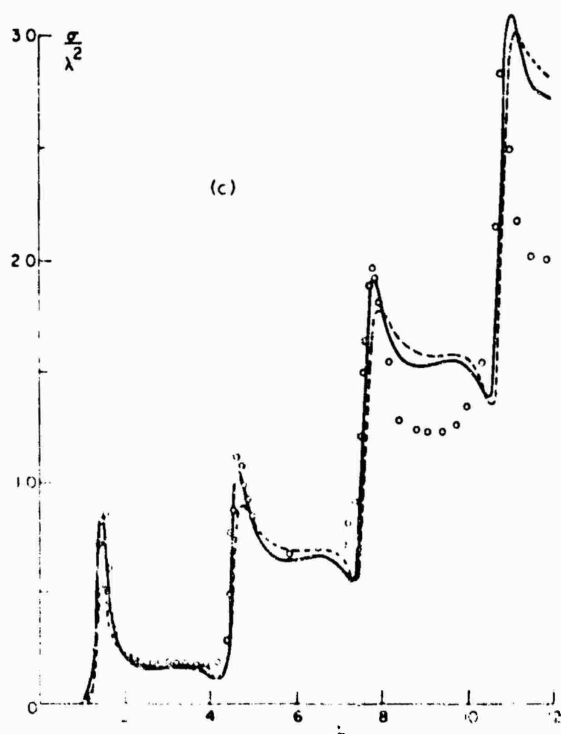
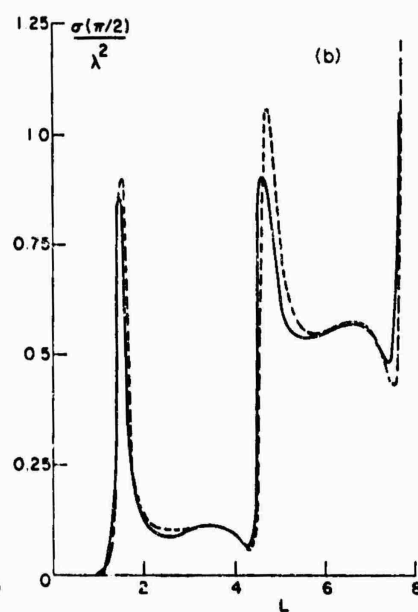
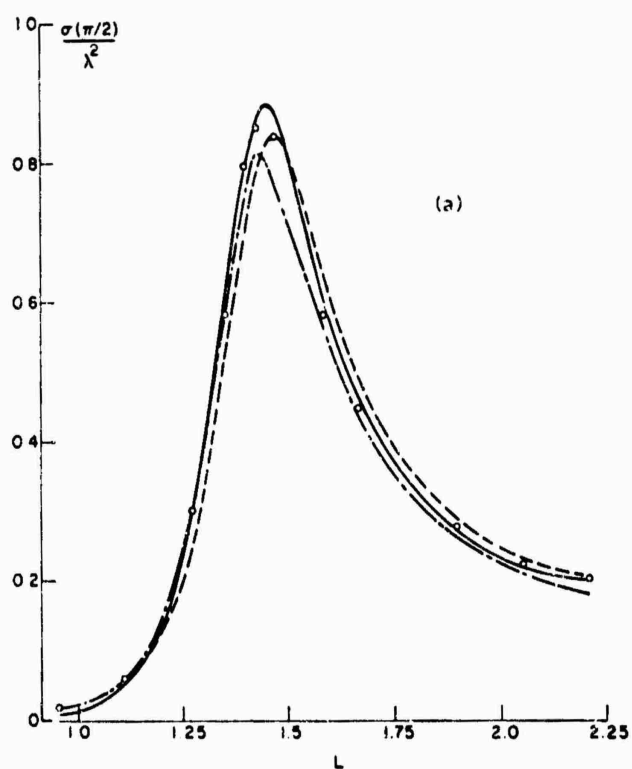


Fig. 12.7. Back scattering cross section for wires with $ka = 0.022$ at broadside incidence: (—) direct method (Ufimtsev [1962]), (---) variational method (Hu [1958]).

At broadside incidence, the second order formula (12.52) becomes (Einarsson [1969]):

$$S(\tfrac{1}{2}\pi, \tfrac{1}{2}\pi) = \frac{2i}{\Omega_0 + 2 \log 2} \left\{ 1 + iL - \frac{\Phi'(0)}{\Phi(0)} - 2 \frac{e^{2iL}}{\Phi^2(1)} \right. \\ \times [f(\tfrac{1}{2}\pi) + 2iLg^3(2L, \tfrac{1}{2}\pi) \{ T_{01}(2L) - T^2(2L) \} - g^2(2L, \tfrac{1}{2}\pi) \{ \tfrac{1}{2} + iLT(2L) \}] + \\ \left. + 2 \frac{e^{4iL}}{\Phi^4(1)} f^2(\tfrac{1}{2}\pi) [1 + \Omega_0^{-2} \{ T(2L) + iLT^2(2L) - T(4L) \}] - \frac{2e^{6iL} f(0) h^2(\tfrac{1}{2}\pi)}{\Phi^4(1) [\Phi^2(1) + e^{2iL} h(0)]} \right\} \quad (12.40)$$



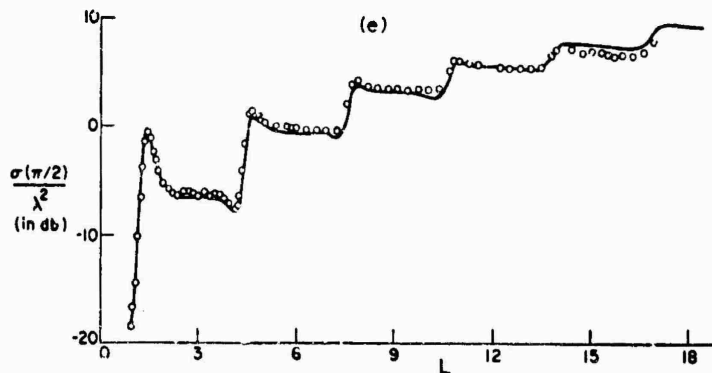


Fig. 12.8. Back scattering cross section at broadside incidence: (a) $ka = 0.0314$, (—) direct method (EINARSSON [1969]), (---) variational method (TAI [1951]), (OOO) numerical solution of integral equation (RICHMOND [1965]), (---) experimental (KOUYOUMJIAN [1953]); (b) $l/a = 900$, (—) direct method (EINARSSON [1969]), (---) integral equation method (LINDROTH [1955]); (c) $ka = 0.022$, (—) direct method (EINARSSON [1969]), (---) first order direct method (WU [1961]), (OOO) experimental (SEVICK [1952]); (d) $ka = 0.026$ (—), $ka = 0.132$ (---) direct method (EINARSSON [1969]), (OOO, XXX) experimental (ÅS and SCHMITT [1958]); (e) $ka = 0.0394$, (—) direct method (EINARSSON [1969]), (OOO) experimental (CHANG and LIEPA [1967]).

where Ω_0 , f , g , h , T , l_{01} and Φ are defined in eqs. (12.54), (12.56), (12.55), (12.57), (12.65), (12.70) and (12.93), respectively.

In Fig. 12.8, computations of the back scattering cross section based on eq. (12.40) are compared with a numerical solution of the integral equation for the wire current, with experimental data, and with the results of a first order direct method formula derived by WU [1961] using the approximation that the vector potential is vanishing on the z -axis outside the wire.

12.4. The bistatic cross section

The functional corresponding to eq. (12.18) for the bistatic scattering cross section is:

$$\begin{aligned}
 \frac{1}{S(\theta, \theta_0)} &= \\
 &= \frac{- \int_{-l}^{+l} \int_{-l}^{+l} I(z, \theta) I(z', \theta_0) K(z - z') dz dz'}{k^2 \sin \theta \sin \theta_0 \int_{-l}^{+l} I(z, \theta_0) \exp(-ikz \cos \theta) dz \int_{-l}^{+l} I(z, \theta) \exp(-ikz \cos \theta_0) dz}
 \end{aligned}
 \quad (12.41)$$

where $K(z - z')$ is given by eq. (12.19), and $I(z, \theta_0)$ and $I(z, \theta)$ are the current distributions for incidence at angles θ_0 and θ , respectively. The bistatic cross section is

$$\frac{\sigma(\theta, \theta_0)}{\lambda^2} = \frac{1}{\pi} |S(\theta, \theta_0)|^2. \quad (12.42)$$

No specific results based on eq. (12.41) are available. However, the first order current distribution of eq. (12.22), from which the back scattering cross section was derived, has been employed by DE BETTENCOURT [1961] to calculate the bistatic cross section. The result is:

$$S(\theta, \theta_0) \approx i \left[\frac{g_e(\theta_0)}{\gamma_e(\theta_0)} G_e(\theta_0, \theta) + \frac{g_s(\theta_0)}{\gamma_s(\theta_0)} G_s(\theta_0, \theta) \right], \quad (12.43)$$

where g_e , g_s , γ_e and γ_s are given by eqs. (12.24) through (12.27) with $\theta = \theta_0$, and

$$\begin{aligned} G_e(\theta_0, \theta) = & \frac{2 \cos(L \cos \theta_0)}{\sin \theta} [\sin L \cos(L \cos \theta) - \cos \theta \cos L \sin(L \cos \theta)] - \\ & - \frac{2 \sin \theta \cos L}{\cos^2 \theta_0 - \cos^2 \theta} [\cos \theta_0 \sin(L \cos \theta_0) \cos(L \cos \theta) - \\ & - \cos \theta \cos(L \cos \theta_0) \sin(L \cos \theta)], \end{aligned} \quad (12.44)$$

$$\begin{aligned} G_s(\theta_0, \theta) = & \frac{2 \sin(L \cos \theta_0)}{i \sin \theta} [\cos \theta \sin L \cos(L \cos \theta) - \cos L \sin(L \cos \theta)] + \\ & + \frac{2i \sin \theta \sin L}{\cos^2 \theta_0 - \cos^2 \theta} [\cos \theta \sin(L \cos \theta_0) \cos(L \cos \theta) - \\ & - \cos \theta_0 \cos(L \cos \theta_0) \sin(L \cos \theta)]. \end{aligned} \quad (12.45)$$

As in the back scattering case, the result of eq. (12.43) does not seem reliable for $L > \pi$.

For $\theta \neq \pi - \theta_0$, the far field amplitude coefficient obtained by the direct method is:

$$S(\theta, \theta_0) = \frac{2i[F(\theta, \theta_0) + F(\pi - \theta, \pi - \theta_0)]}{[\Omega_0 - 2 \log(\frac{1}{2} \sin \theta)][\Omega_0 - 2 \log(\frac{1}{2} \sin \theta_0)] \sin \theta \sin \theta_0}. \quad (12.46)$$

It should be noted that, in contrast to eq. (12.43), the result (12.46) satisfies the reciprocity relation

$$S(\theta, \theta_0) = S(\theta_0, \theta). \quad (12.47)$$

A first order expression for $F(\theta, \theta_0)$ is (UFIMTSEV [1962], FIALKOVSKII [1967]):

$$\begin{aligned} F(\theta, \theta_0) = & \frac{2 \cos^2 \frac{1}{2} \theta \cos^2 \frac{1}{2} \theta_0}{\cos \theta + \cos \theta_0} [\Omega_0 - 2 \log(\cos \frac{1}{2} \theta \cos \frac{1}{2} \theta_0)] e^{iL(\cos \theta + \cos \theta_0)} + \\ & + \frac{2}{\cos \theta + \cos \theta_0} [g(2L, \theta) \sin^2 \frac{1}{2} \theta \sin^2 \frac{1}{2} \theta_0 - g(2L, \pi - \theta_0) \cos^2 \frac{1}{2} \theta \cos^2 \frac{1}{2} \theta_0] \\ & \times (\Omega_0 - 2 \log \cos \frac{1}{2} \theta)(\Omega_0 - 2 \log \sin \frac{1}{2} \theta_0) e^{iL(\cos \theta - \cos \theta_0 + 2)} + \\ & + \frac{\Omega_0(\Omega_0 - 2 \log \cos \frac{1}{2} \theta)g(2L, \theta)}{1 - [\Omega_0 g(2L, 0)e^{2iL}]^2} e^{iL(\cos \theta + 4)} \\ & \times [(\Omega_0 - 2 \log \cos \frac{1}{2} \theta_0)g(2L, \theta_0)e^{iL \cos \theta_0} - \\ & - \Omega_0(\Omega_0 - 2 \log \sin \frac{1}{2} \theta_0)g(2L, 0)g(2L, \pi - \theta_0)e^{iL(2 - \cos \theta_0)}], \end{aligned} \quad (12.48)$$

where Ω_0 and g are defined by eqs. (12.54) and (12.55). The corresponding second order formula is (EINARSSON [1969]):

$$\begin{aligned}
 F(\theta, \theta_0) = & \frac{2 \cos^2 \frac{1}{2}\theta \cos^2 \frac{1}{2}\theta_0 e^{iL(\cos \theta + \cos \theta_0)}}{(\cos \theta + \cos \theta_0) \Phi(\cos \theta) \Phi(\cos \theta_0)} + \\
 & + \frac{2[f(\theta) \sin^2 \frac{1}{2}\theta \sin^2 \frac{1}{2}\theta_0 - (\pi - \theta_0) \cos^2 \frac{1}{2}\theta \cos^2 \frac{1}{2}\theta_0] e^{iL(\cos \theta - \cos \theta_0 + 2)}}{(\cos \theta + \cos \theta_0) \Phi^2(1) \Phi(\cos \theta) \Phi(-\cos \theta_0)} + \\
 & + \frac{f(\theta) f(\theta_0) e^{iL(\cos \theta + \cos \theta_0 - 4)}}{\Phi^4(1) \Phi(\cos \theta) \Phi(\cos \theta_0)} \left\{ 1 + \frac{(1 + \cos \theta)(1 + \cos \theta_0)}{2(\cos \theta + \cos \theta_0) \Omega_0^2} \right. \\
 & \times [I_2(4L, 4L \cos^2 \frac{1}{2}\theta) + I_2(4L, 4L \cos^2 \frac{1}{2}\theta_0) - T(4L \cos^2 \frac{1}{2}\theta) T(4L \cos^2 \frac{1}{2}\theta_0)] \Big\} + \\
 & + \frac{f(0) h(\theta) e^{iL(\cos \theta + 6)}}{\Phi^2(1) [\Phi^4(1) - h^2(0) e^{4iL}]} \left[\frac{h(0) h(\theta_0) e^{iL(\cos \theta_0 + 2)}}{\Phi^2(1) \Phi(\cos \theta) \Phi(\cos \theta_0)} - \frac{h(\pi - \theta_0) e^{-iL \cos \theta_0}}{\Phi(\cos \theta) \Phi(-\cos \theta_0)} \right].
 \end{aligned} \quad (12.49)$$

where Ω_0 , f , h , T , I_2 and Φ are defined in eqs. (12.54), (12.56), (12.57), (12.65), (12.69) and (12.93), respectively.

For $\theta = \pi - \theta_0$, and to the first order (UFIMTSEV [1962]):

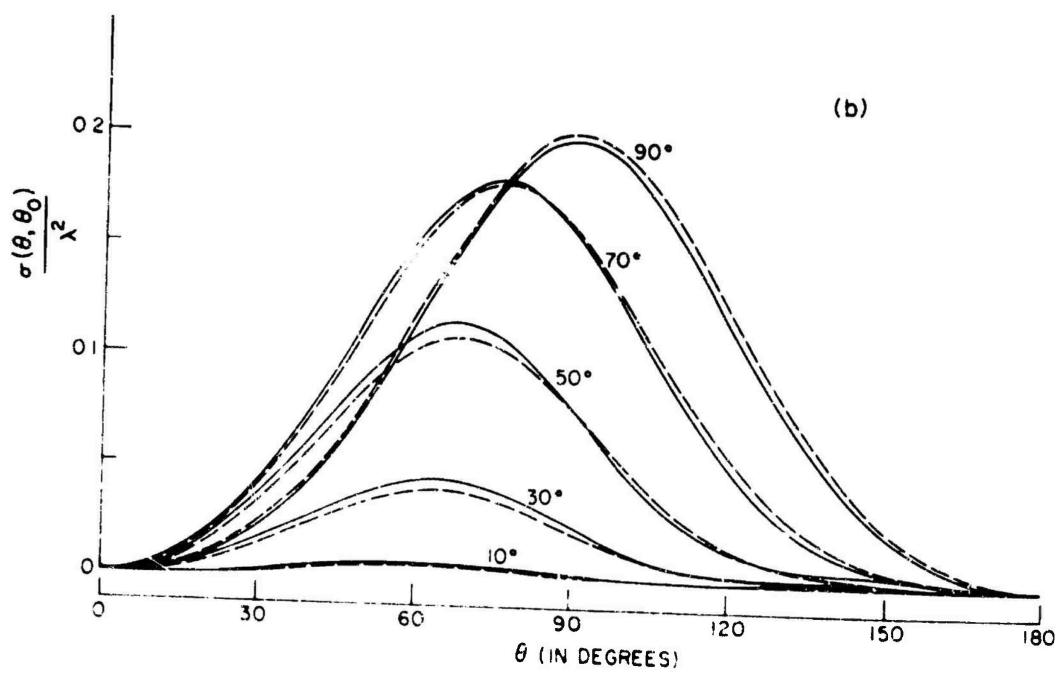
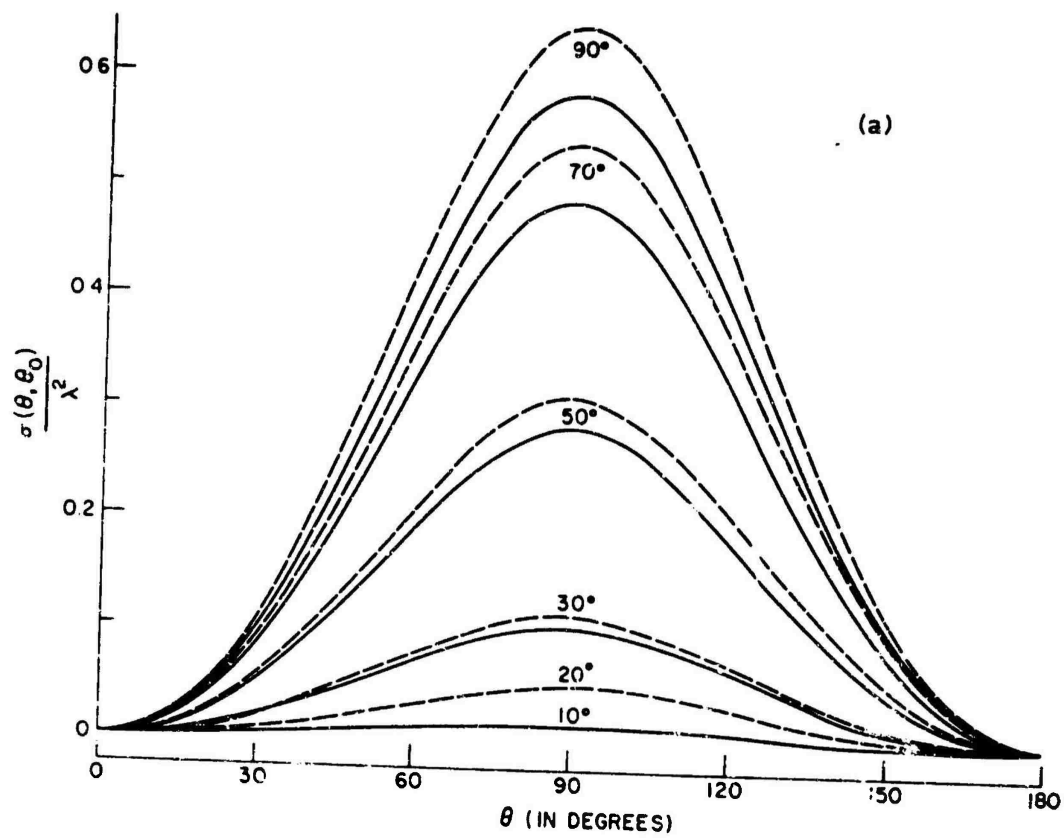
$$\begin{aligned}
 S(\theta, \pi - \theta) = & \frac{2i}{\{\Omega_0 - 2 \log(\frac{1}{2} \sin \theta)\}^2 \sin^2 \theta} \left[-1 + \right. \\
 & \left. + \{\Omega_0 - 2 \log(\frac{1}{2} \sin \theta)\} (1 + iL \sin^2 \theta) + G(\theta) + G(\pi - \theta) \right],
 \end{aligned} \quad (12.50)$$

where

$$\begin{aligned}
 G(\theta) = & -(\Omega_0 - 2 \log \sin \frac{1}{2}\theta)^2 g(2L, \pi - \theta) e^{2iL(1 - \cos \theta)} \\
 & \times \{1 - [\cos^2 \frac{1}{2}\theta + iL \sin^2 \theta T(4L \sin^2 \frac{1}{2}\theta)] g(2L, \pi - \theta)\} + \\
 & + \frac{\Omega_0(\Omega_0 - 2 \log \cos \frac{1}{2}\theta) g(2L, \theta)}{1 - [\Omega_0 g(2L, 0) e^{2iL}]^2} e^{iL(\cos \theta + 4)} \\
 & \times [(\Omega_0 - 2 \log \sin \frac{1}{2}\theta) g(2L, \pi - \theta) e^{-iL \cos \theta} - \\
 & - \Omega_0(\Omega_0 - 2 \log \cos \frac{1}{2}\theta) g(2L, 0) g(2L, \theta) e^{iL(\cos \theta + 2)}],
 \end{aligned} \quad (12.51)$$

and Ω_0 , g and T are given by eqs. (12.54), (12.55) and (12.65). The corresponding second order result is (EINARSSON [1969]):

$$\begin{aligned}
 S(\theta, \pi - \theta) = & \frac{2i}{\{\Omega_0 - 2 \log(\frac{1}{2} \sin \theta)\}^2 \sin^2 \theta} \left\{ -\cos \theta + \{\Omega_0 - 2 \log(\frac{1}{2} \sin \theta)\} \right. \\
 & \times \left[1 + iL \sin^2 \theta - \sin^2 \theta \frac{\Phi'(\cos \theta)}{\Phi(\cos \theta)} \right] + G(\theta) + G(\pi - \theta) \Big\},
 \end{aligned} \quad (12.52)$$



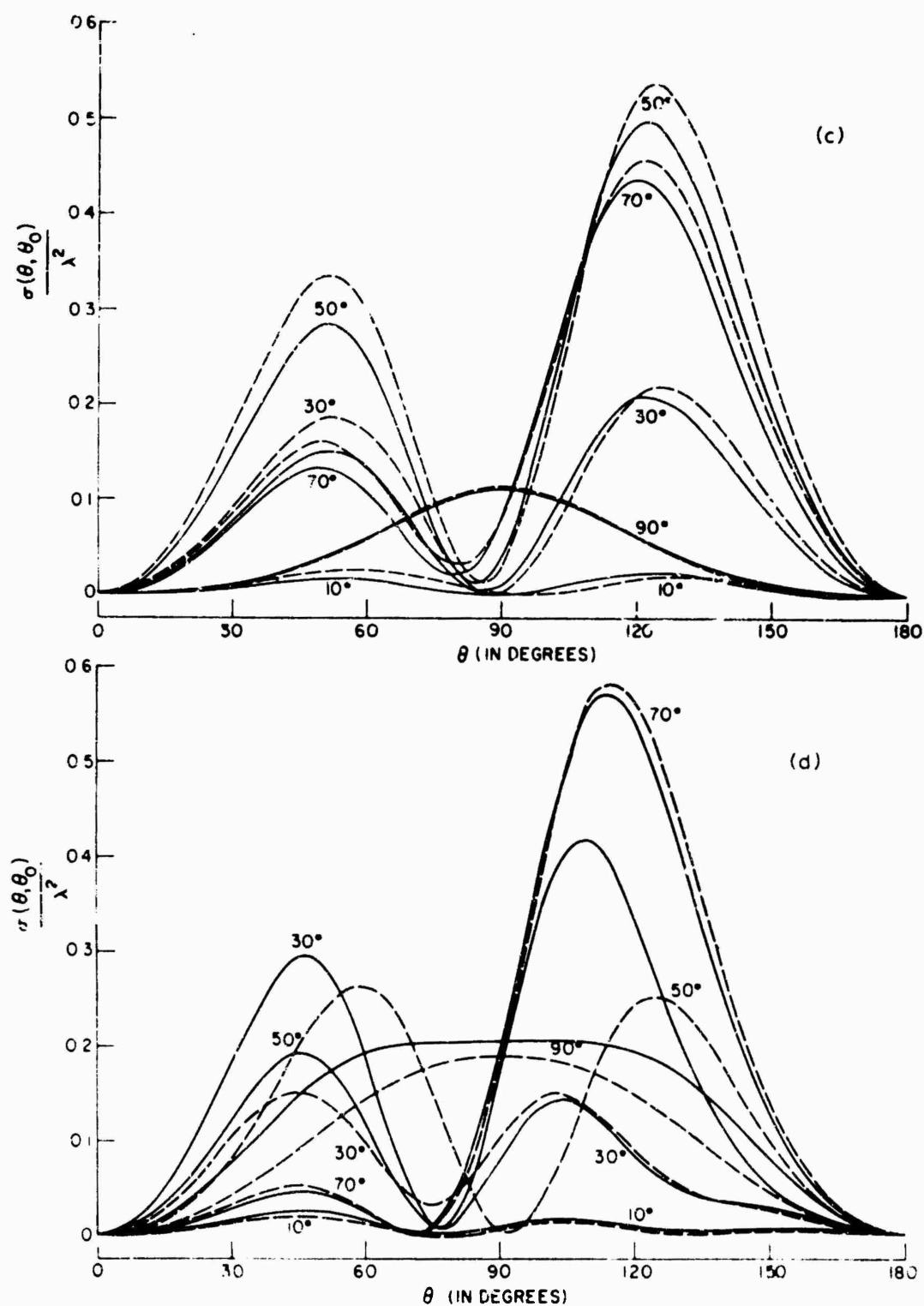


Fig. 12.9. Angular distribution of the bistatic scattering cross section for $\theta_0 = 10$ (20 30 50 70 90 120 150) and (a) $l/\lambda = 0.5$, (b) $l/\lambda = 0.75$, (c) $l/\lambda = 1.0$, (d) $l/\lambda = 1.25$: (—) direct method (FINARSSON [1969]), (---) variational method (DE BETENCOURT [1961]).

where

$$\begin{aligned}
 G(\theta) = & -\frac{e^{2iL(1-\cos\theta)}}{\Phi^2(1)\Phi^2(-\cos\theta)} \{f(\pi-\theta) + \\
 & + 2iL \sin^2 \theta g^3(2L, \pi-\theta)[l_{01}(4L \sin^2 \frac{1}{2}\theta) - T^2(4L \sin^2 \frac{1}{2}\theta)] - \\
 & - g^2(2L, \pi-\theta)[\cos^2 \frac{1}{2}\theta + iL \sin^2 \theta T(4L \sin^2 \frac{1}{2}\theta)]\} + \\
 & + \frac{e^{4iL}}{\Phi^4(1)} [\Omega_0 - 2 \log(\frac{1}{2} \sin \theta)] f(\theta) f(\pi-\theta) \{1 + \\
 & + \Omega_0^{-2} [\sin^2 \frac{1}{2}\theta T(4L \sin^2 \frac{1}{2}\theta) + \cos^2 \frac{1}{2}\theta T(4L \cos^2 \frac{1}{2}\theta) + \\
 & + iL \sin^2 \theta T(4L \sin^2 \frac{1}{2}\theta) T(4L \cos^2 \frac{1}{2}\theta) - T(4L)]\} - \\
 & - \frac{f(0)h(\pi-\theta)e^{6iL}}{\Phi^2(1)[\Phi^4(1) - h^2(0)e^{4iL}]} \left\{ \frac{h(\pi-\theta)}{\Phi^2(-\cos\theta)} e^{-2iL \cos\theta} - \right. \\
 & \left. - \frac{h(0)h(\theta)}{\Phi^2(1)} e^{2iL} [\Omega_0 - 2 \log(\frac{1}{2} \sin \theta)] \right\}, \quad (12.53)
 \end{aligned}$$

with

$$\Omega_0 = -2 \log ka - 2\gamma + i\pi, \quad (12.54)$$

$$g(x, \theta) = [\Omega_0 + l_0(2x) + T(2x \cos^2 \frac{1}{2}\theta)]^{-1}, \quad (12.55)$$

$$f(\theta) = \left\{ \Omega_0 + \frac{l_0(4L) + T(4L \cos^2 \frac{1}{2}\theta)}{1 + \frac{2l_{01}(4L \cos^2 \frac{1}{2}\theta) - T^2(4L \cos^2 \frac{1}{2}\theta) - \frac{1}{6}\pi^2}{\Omega_0[l_0(4L) + T(4L \cos^2 \frac{1}{2}\theta)]}} \right\}^{-1}, \quad (12.56)$$

$$h(\theta) = \left\{ \Omega_0 + \frac{l_0(4L) + T(4L \cos^2 \frac{1}{2}\theta)}{1 + \frac{2l_{01}(4L \cos^2 \frac{1}{2}\theta) + l_{01}(4L) + l_2(4L, 4L \cos^2 \frac{1}{2}\theta) - T^2(4L \cos^2 \frac{1}{2}\theta) - T(4L)T(4L \cos^2 \frac{1}{2}\theta) - \frac{1}{6}\pi^2}{\Omega_0[l_0(4L) + T(4L \cos^2 \frac{1}{2}\theta)]}} \right\}^{-1}, \quad (12.57)$$

and in particular

$$h(0) = \left\{ \Omega_0 + \frac{l_0(4L) + T(4L)}{1 + \frac{4l_{01}(4L) - 2T^2(4L) - \frac{1}{6}\pi^2}{\Omega_0[l_0(4L) + T(4L)]}} \right\}^{-1}; \quad (12.58)$$

the quantities l_0 , T , l_{01} and l_2 are the amplitude functions of the iterated sine and cosine integrals and are defined in eqs. (12.64), (12.65), (12.70) and (12.69), whereas $\Phi(x)$ is the linearized split function related to the Wiener-Hopf technique and is given by eq. (12.93).

The normalized bistatic cross sections computed from eq. (12.43) and from eqs. (12.46) and (12.49) are shown in Fig. 12.9 as functions of θ for various values of ka , L and θ_0 .

12.5. The current distribution

The current distribution of eq. (12.22) which is assumed in the derivation of the back scattering and bistatic cross sections by the variational method is (TAI [1951], DE BETTENCOURT [1961]):

$$I(z) = -\frac{4\pi Y}{k} \left[\frac{\gamma_c}{\gamma_c} f_c(z) + \frac{g_s}{\gamma_s} f_s(z) \right], \quad (12.59)$$

where

$$f_c(z) = \cos(L \cos \theta) \cos kz - \cos(kz \cos \theta) \cos L, \quad (12.60)$$

$$f_s(z) = \sin(L \cos \theta) \sin kz - \sin(kz \cos \theta) \sin L, \quad (12.61)$$

and g_c , g_s , γ_c and γ_s are given by eqs. (12.24) through (12.27).

The current distribution associated with the direct method is obtained by taking the Fourier transform of the far field of eq. (12.46) and by expanding the resulting expressions asymptotically. The result is (EINARSSON [1969]):

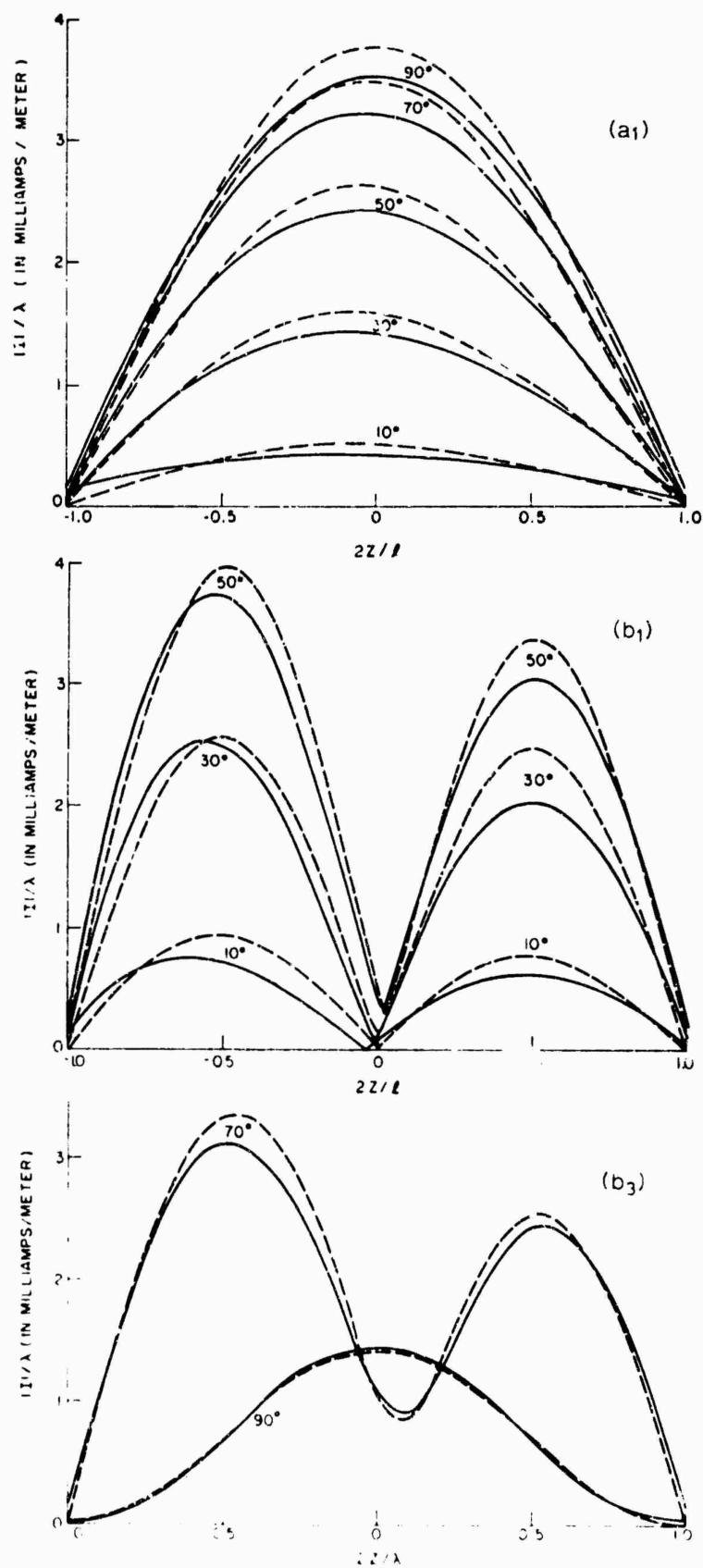
$$I(z, \theta_0) = \frac{4\pi Y}{ik \sin \theta_0 \{\Omega_0 - 2 \log(\frac{1}{2} \sin \theta_0)\}} [e^{-ikz \cos \theta_0} + \psi(L + kz, \theta_0) + \psi(L - kz, \pi - \theta_0)], \quad (12.62)$$

where

$$\begin{aligned} \psi(x, \theta_0) = & -\frac{\exp(ix + iL \cos \theta_0)}{\Phi(1)\Phi(\cos \theta_0)} \{g(x, \theta_0) + g^3(x, \theta_0)[l_{11}(2x) + \\ & + 2l_{01}(2x \cos^2 \frac{1}{2}\theta_0) - T^2(2x \cos^2 \frac{1}{2}\theta_0) - l_2(2x \cos^2 \frac{1}{2}\theta_0, 2x) - \frac{1}{8}\pi^2]\} + \\ & + \frac{f(\pi - \theta_0) \exp\{ix + iL(2 - \cos \theta_0)\}}{\Phi^3(1)\Phi(-\cos \theta_0)} \{g(x, 0) + g^3(x, 0)[l_{11}(2x) + \\ & + l_{01}(2x) - T^2(2x) + T(4L \sin^2 \frac{1}{2}\theta_0)(T(2x \cos^2 \frac{1}{2}\theta_0) - T(2x)) + \\ & + l_2(2x, 4L) - l_2(4L \sin^2 \frac{1}{2}\theta_0 + 2x \cos^2 \frac{1}{2}\theta_0, 2x \cos^2 \frac{1}{2}\theta_0) - \\ & - l_2(4L \sin^2 \frac{1}{2}\theta_0 + 2x \cos^2 \frac{1}{2}\theta_0, 4L) + l_2(4L \sin^2 \frac{1}{2}\theta_0 + 2x \cos^2 \frac{1}{2}\theta_0, 2x) - \frac{1}{8}\pi^2]\} - \\ & - \frac{f(0)e^{ix + 4iL}}{\Phi(1)[\Phi^4(1) - h^2(0)e^{4iL}]} \left[\frac{h(\theta_0)}{\Phi(\cos \theta_0)} e^{iL \cos \theta_0} - \frac{h(0)h(\pi - \theta_0)}{\Phi^2(1)\Phi(-\cos \theta_0)} e^{iL(2 - \cos \theta_0)} \right] \\ & \times \{g(x, 0) + g^3(x, 0)[l_{11}(2x) + l_{01}(2x) - T^2(2x) + l_2(4L, 2x) + l_2(2x, 4L) - \\ & - T(4L)T(2x) - \frac{1}{8}\pi^2]\}, \end{aligned} \quad (12.63)$$

and the functions g , f and h are given by eqs. (12.55) through (12.58), whereas the quantities T , l_2 , l_{01} , l_{11} and Φ are defined in eqs. (12.65), (12.69), (12.70), (12.71) and (12.93).

Numerical values calculated from a version of eq. (12.63), in which the second order quantities only are retained in the last term, are compared to computations of the variational expression of eq. (12.59) in Fig. 12.10, and to a numerical solution of the integral equation for the current in Fig. 12.11.



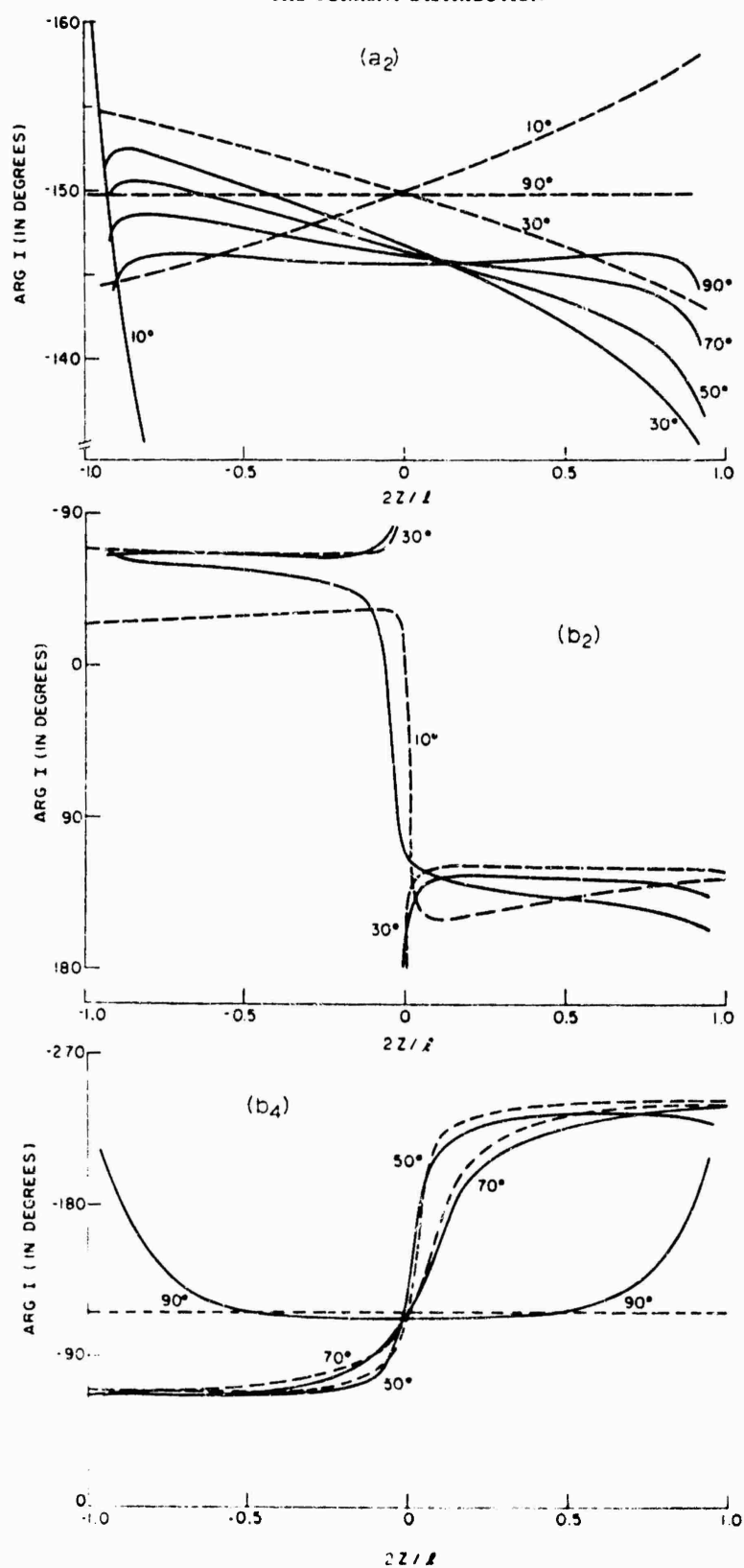


Fig. 12.10. Amplitude and phase of current distribution for $\theta_0 = 10^\circ (20^\circ) 90^\circ$, $l/a = 150$ and (a) $l/\lambda = 0.5$, (b) $l/\lambda = 1.0$; (—) direct method (EINARSSON [1969]), (---) variational method (DE BELLEN-COURT [1961]).

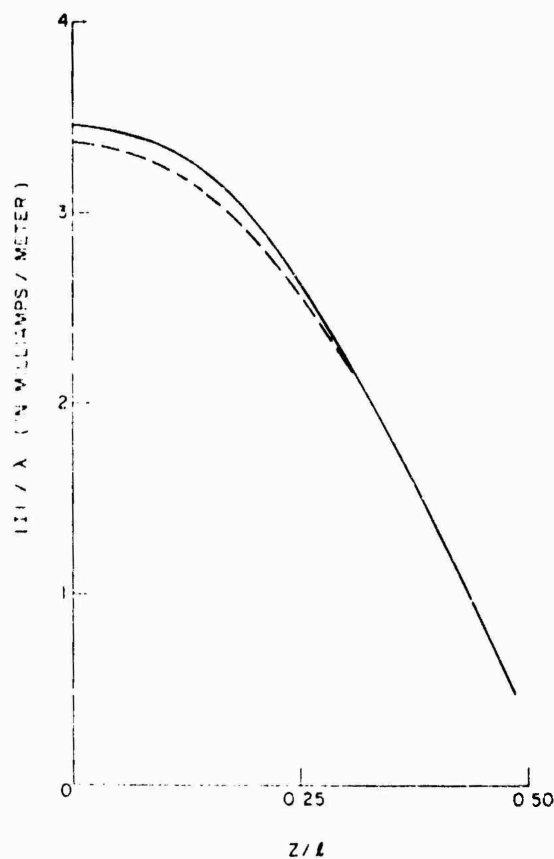


Fig. 12.11. Current distribution for broadside incidence on a half-wavelength wire ($L = 1.57$, $ka = 0.0314$): (—) direct method (EINARSSON [1969]), (---) numerical solution of integral equation (RICHMOND [1965]).

12.6. Special functions

The functions $I_0(x)$ and $T(x)$ are defined as:

$$I_0(x) = \gamma + \log x - \frac{1}{2}i\pi, \quad (12.64)$$

$$\begin{aligned} T(x) &= c(x) - is(x) \\ &= \int_x^\infty \frac{e^{i(\xi-x)}}{\xi} d\xi = \int_0^\infty \frac{e^{i u}}{1+u} du \\ &= -e^{-ix} [\text{Ci}(x) + i \text{Si}(x) - \frac{1}{2}i\pi], \end{aligned} \quad (12.65)$$

where

$$\text{Ci}(x) = -\int_x^\infty \frac{\cos \xi}{\xi} d\xi, \quad \text{Si}(x) = \int_0^x \frac{\sin \xi}{\xi} d\xi; \quad (12.66)$$

the cosine integral can be rewritten in the form

$$\text{Ci}(x) = \gamma + \log x - \text{Cin}(x), \quad (12.67)$$

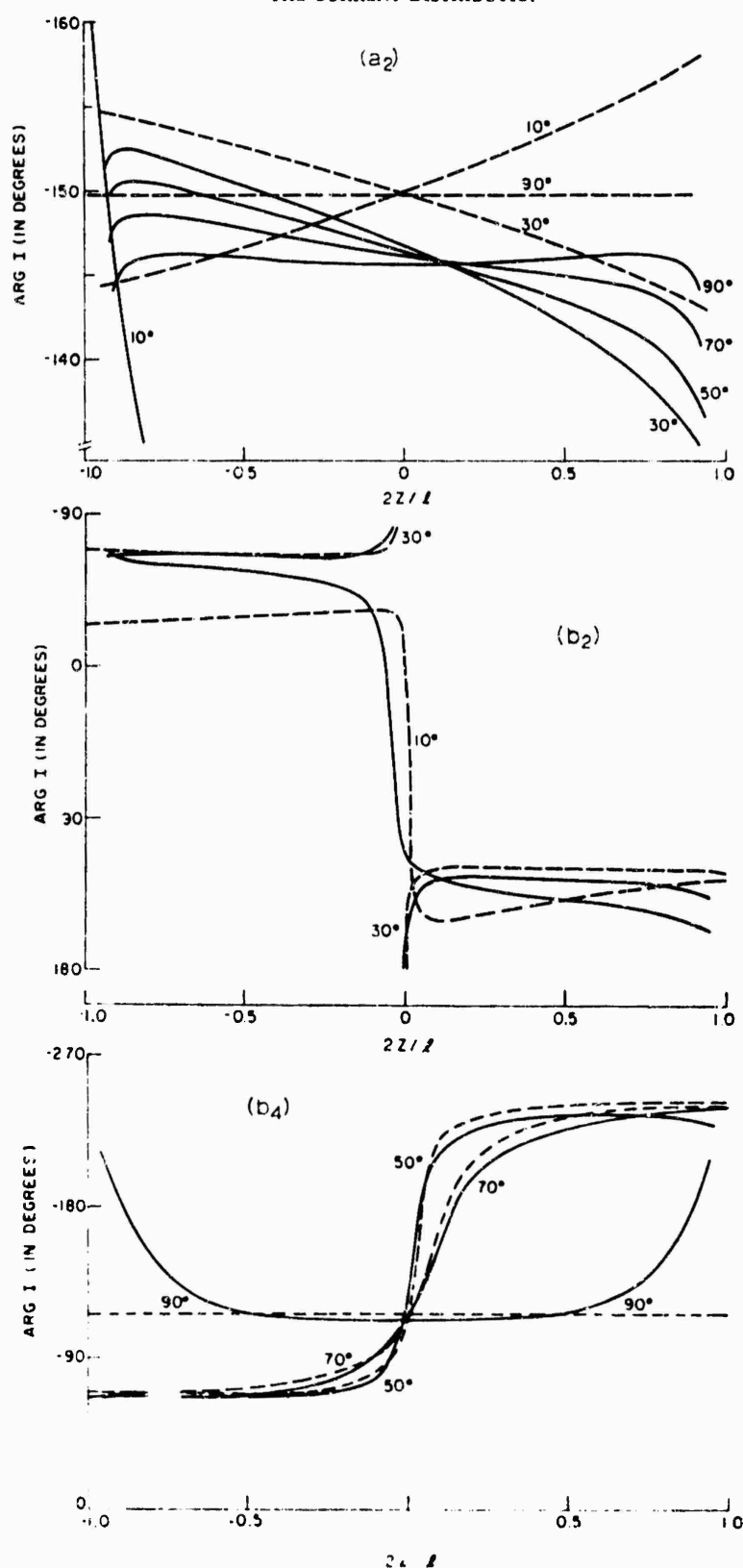


Fig. 12.10. Amplitude and phase of current distribution for $\theta_0 = 10^\circ (20^\circ) 90^\circ$, $l/a = 150$ and (a) $l/2 = 0.5$, (b) $l/2 = 1.0$; (—) direct method (BINARSSON [1969]), (---) variational method (DE BETTENHOURT [1961]).

with

$$\text{Cin}(x) = \int_0^x \frac{1 - \cos \xi}{\xi} d\xi. \quad (12.68)$$

The general iterated amplitude function $l_2(x, y)$ is:

$$\begin{aligned} l_2(x, y) &= c_2(x, y) - is_2(x, y) \\ &= \int_0^\infty \frac{T(y + \tau y)}{1 + \tau} e^{ix\tau} d\tau \\ &= \int_0^\infty \frac{\log(1 + xu/y)}{1 + u} e^{ixu} du, \end{aligned} \quad (12.69)$$

with the special cases

$$\begin{aligned} l_{01}(x) = l_2(x, x) = c_{01}(x) - is_{01}(x) &= \int_x^\infty \frac{T(\xi)}{\xi} e^{i(\xi-x)} d\xi \\ &= \int_0^\infty \frac{\log(1+u)}{1+u} e^{ixu} du, \end{aligned} \quad (12.70)$$

$$\begin{aligned} l_{11}(x) = l_2(0, x) = c_{11}(x) - is_{11}(x) &= \int_x^\infty \frac{T(\xi)}{\xi} d\xi \\ &= \int_0^\infty \frac{\log(1+u)}{u} e^{ixu} du. \end{aligned} \quad (12.71)$$

Tables of functions which are the complex conjugates of T , l_{01} and l_{11} are given in HALLÉN [1955] and in BRUNDELL [1957], whereas the function l_2 is tabulated in STRÖMGREN [1962]. Some amplitude functions of the iterated sine and cosine integrals are shown in Fig. 12.12.

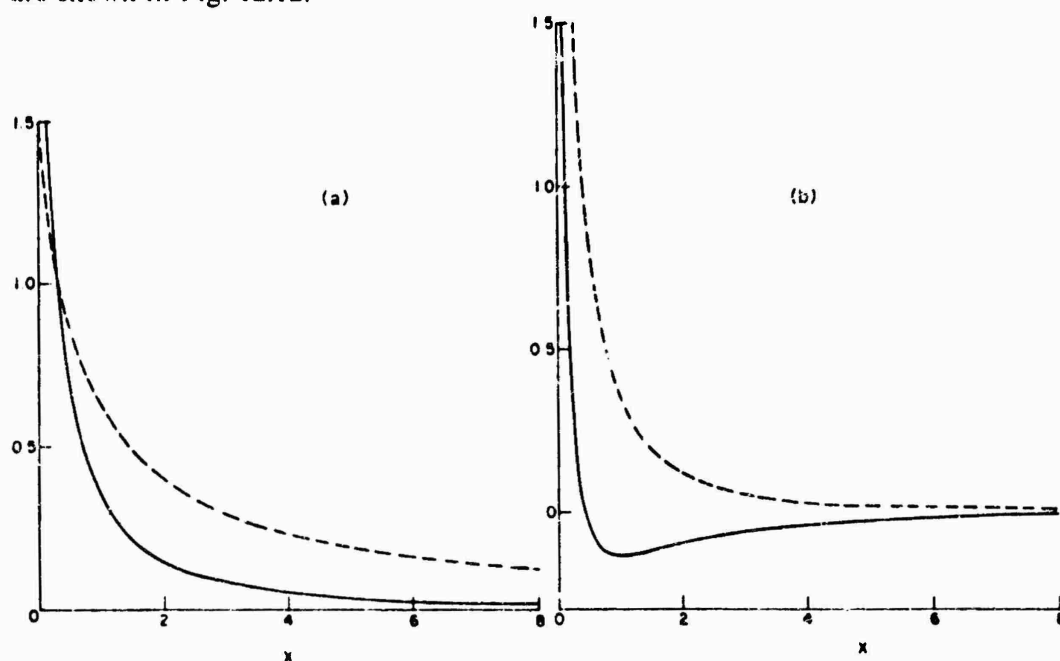


Fig. 12.12. Amplitude functions of iterated sine and cosine integrals: (a) (—) $c(x)$, (---) $s(x)$; (b) (—) $c_{01}(x)$, (---) $s_{01}(x)$.

For $1 \leq x < \infty$, the real functions $c(x)$ and $s(x)$ have the rational approximations (HASTINGS [1955]):

$$c(x) = x^{-2} \left[\frac{21.821899 + 352.018498x^2 + 302.757865x^4 + 42.242855x^6 + x^8}{449.690326 + 1114.978885x^2 + 482.485984x^4 + 48.196927x^6 + x^8} \right] + \varepsilon(x),$$

$$|\varepsilon(x)| < 3 \times 10^{-7}, \quad (12.72)$$

$$s(x) = -x^{-1} \left[\frac{38.102495 + 335.677320x^2 + 265.187033x^4 + 38.027264x^6 + x^8}{157.105423 + 570.236280x^2 + 322.624911x^4 + 40.021433x^6 + x^8} \right] + \varepsilon(x),$$

$$|\varepsilon(x)| < 5 \times 10^{-7}. \quad (12.73)$$

Approximations which are useful for digital computers are listed in the following (EINARSSON [1969]):

for $0 < x \leq 1$:

$$c(x) = f(x) \cos x - g(x) \sin x + \varepsilon_1(x), \quad |\varepsilon_1(x)| < 3 \times 10^{-9}, \quad (12.74)$$

$$s(x) = g(x) \cos x + f(x) \sin x + \varepsilon_2(x), \quad |\varepsilon_2(x)| < 2 \times 10^{-9}, \quad (12.75)$$

where

$$f(x) = -\gamma - \log x + 0.25x^2 - 0.010416660x^4 + 0.000231447x^6 - 0.000003046x^8, \quad (12.76)$$

$$g(x) = -\frac{1}{2}\pi + 0.999999998x - 0.055555480x^3 + 0.001666289x^5 - 0.000027739x^7; \quad (12.77)$$

for $0 < x \leq 2$:

$$c_{01}(x) = f(x) \cos x + g(x) \sin x + \varepsilon_1(x), \quad |\varepsilon_1(x)| < 8 \times 10^{-10}, \quad (12.78)$$

$$s_{01}(x) = f(x) \sin x - g(x) \cos x + \varepsilon_2(x), \quad |\varepsilon_2(x)| < 6 \times 10^{-10}, \quad (12.79)$$

where

$$f(x) = \frac{1}{2}(\gamma + \log x)^2 - \frac{1}{24}\pi^2 - x^2(0.125 - 2.60416632 \times 10^{-3}x^2 + 3.857955 \times 10^{-5}x^4 - 3.87035 \times 10^{-7}x^6 + 2.61455 \times 10^{-9}x^8), \quad (12.80)$$

$$g(x) = -\frac{1}{2}\pi(\gamma + \log x) - x(0.999999992 - 0.0185185136x^2 + 3.3332344 \times 10^{-4}x^4 - 4.0422785 \times 10^{-6}x^6 + 3.201246 \times 10^{-8}x^8); \quad (12.81)$$

for $2 < x < \infty$:

$$c_{01}(x) = -x^{-2} \times \left(\frac{0.005415749186x^8 + 0.4371420242x^6 + 7.150169966x^4 + 20.96173922x^2 - 3.85642854}{0.005415884237x^8 + 0.4965990580x^6 + 11.16783932x^4 + 70.34218899x^2 + 1} \right) + \varepsilon_1(x), \quad |\varepsilon_1(x)| < 9 \times 10^{-9}, \quad (12.82)$$

$$s_{01}(x) = -x^{-3}$$

$$\times \left(\frac{0.009942860283x^8 + 0.8460999768x^6 + 14.246573437x^4 + 43.88413692x^2 + 0.5423489064}{0.003314700857x^8 + 0.3369899234x^6 + 8.503549177x^4 + 60.93657000x^2 + 1} \right) + \varepsilon_2(x), \quad |\varepsilon_2(x)| < 6 \times 10^{-9}; \quad (12.83)$$

for $2 \leq x < \infty$ and $1 \leq y \leq x$:

$$c_2(x, y) = f(x, y) + \varepsilon_1(x, y), \quad (12.84)$$

$$s_2(x, y) = g(x, y) + \varepsilon_2(x, y), \quad (12.85)$$

with

$$|\varepsilon_1(x, y)| \leq |\varepsilon_2(x, y)| < 2 \times 10^{-5}, \quad (12.86)$$

whereas for $2 \leq x < \infty$ and $0 \leq y < 1$:

$$c_2(x, y) = c(y)c(x-y) - s(y)s(x-y) - f(x, x-y) - \varepsilon_1(x, x-y), \quad (12.87)$$

$$s_2(x, y) = c(y)s(x-y) + s(y)c(x-y) - g(x, x-y) - \varepsilon_2(x, x-y); \quad (12.88)$$

in eqs. (12.84) through (12.88):

$$f(x, y) = \frac{1}{2}[c^2(\frac{1}{2}x) - s^2(\frac{1}{2}x)] - c(x) \log \frac{2y}{x} + \frac{A_0}{x^2} \left(2 - \frac{x}{y} + \log \frac{2y}{x} \right) + \sum_{n=1}^3 \frac{A_n}{x^2 + a_n} \left[\frac{1}{2} \log \frac{y^2 + a_n}{\frac{1}{4}x^2 + a_n} + \frac{x}{\sqrt{a_n}} \arctan \frac{(2y-x)\sqrt{a_n}}{xy + 2a_n} \right], \quad (12.89)$$

with

$$\begin{aligned} A_0 &= 0.066349174, & a_1 &= 21.8504560, \\ A_1 &= 0.163725227, & a_2 &= 0.770345382, \\ A_2 &= 0.341159970, & a_3 &= 4.55715659, \\ A_3 &= 0.428765629; \end{aligned} \quad (12.90)$$

$$g(x, y) = c(\frac{1}{2}x)s(\frac{1}{2}x) - s(x) \log \frac{2y}{x} - \frac{B_0}{x} \log \frac{2y}{x} - \sum_{n=1}^3 \frac{B_n}{x^2 + b_n} \left[\frac{1}{2}x \log \frac{y^2 + b_n}{\frac{1}{4}x^2 + b_n} - \sqrt{b_n} \arctan \frac{(2y-x)\sqrt{b_n}}{xy + 2b_n} \right], \quad (12.91)$$

with

$$\begin{aligned} B_0 &= 0.262750417, & b_1 &= 17.420076, \\ B_1 &= 0.052999360, & b_2 &= 0.501312744, \\ B_2 &= 0.422384803, & b_3 &= 3.43966581, \\ B_3 &= 0.241865419 \end{aligned} \quad (12.92)$$

The function $\Phi(x)$ is the linearized split function:

$$\Phi(x) = \exp \left\{ \frac{i}{2\pi} \int_{-\infty}^x \frac{dz}{\tau - \alpha} \log \left[\Omega_0 + \log \frac{4}{1 - \tau^2} \right] \right\}, \quad (12.93)$$

where Ω_0 is given by eq. (12.54) and where the path of integration passes above the point -1 and below x and $+1$. In the interval $0 \leq \theta < \frac{1}{2}\pi$ (HALLÉN [1961]):

$$\begin{aligned} \frac{1}{\Phi(\cos \theta)} &\approx \frac{1}{\Phi(1)} \{ 1 - \Omega_0^{-1} \log(\cos^2 \frac{1}{2}\theta) + \Omega_0^{-2} \text{Li}_2(\sin^2 \frac{1}{2}\theta) + \\ &+ \Omega_0^{-3} [\log(\cos^2 \frac{1}{2}\theta) (\text{Li}_2(\cos^2 \frac{1}{2}\theta) - \frac{1}{6}\pi^2) + 2 \text{Li}_3(\sin^2 \frac{1}{2}\theta) - 2 \text{Li}_3(\cos^2 \frac{1}{2}\theta) + 2\zeta(3)] \}, \end{aligned} \quad (12.94)$$

with $\zeta(3)$ given in eq. (12.1); by differentiating with respect to $\cos \theta$ ($0 \leq \theta \leq \frac{1}{2}\pi$):

$$\begin{aligned} \frac{\Phi'(\cos \theta)}{\Phi(\cos \theta)} &\approx \Omega_0^{-1} \left\{ \frac{1 + \pi^2/(3\Omega_0^2)}{1 + \cos \theta} - \frac{4 \cos \theta}{\sin^2 \theta} [\Omega_0^{-1} \log \cos \frac{1}{2}\theta - \right. \\ &\left. - \Omega_0^{-2} \{ \text{Li}_2(\sin^2 \frac{1}{2}\theta) - 2(\log \cos \frac{1}{2}\theta)^2 \} \right\}; \end{aligned} \quad (12.95)$$

the dilogarithm Li_2 and the trilogarithm Li_3 are defined by:

$$\text{Li}_2(x) = - \int_0^x \frac{\log(1-\tau)}{\tau} d\tau = \sum_{n=1}^{\infty} \frac{x^n}{n^2}, \quad \text{when } |x| \leq 1, \quad (12.96)$$

$$\text{Li}_3(x) = \int_0^x \frac{\text{Li}_2(\tau)}{\tau} d\tau = \sum_{n=1}^{\infty} \frac{x^n}{n^3}, \quad \text{when } |x| \leq 1. \quad (12.97)$$

The approximations (12.94) and (12.95) can be extended to the interval $\frac{1}{2}\pi \leq \theta < \pi$ by means of the relations:

$$\frac{1}{\Phi(\cos \theta)} = \Phi(-\cos \theta) \{ \Omega_0 - 2 \log(\frac{1}{2} \sin \theta) \}, \quad (12.98)$$

$$\frac{1}{\Phi(0)} = \sqrt{(\Omega_0 + 2 \log 2)}. \quad (12.99)$$

$$\frac{\Phi'(\cos \theta)}{\Phi(\cos \theta)} = \frac{\Phi'(-\cos \theta)}{\Phi(-\cos \theta)} - \frac{2 \cos \theta}{\sin^2 \theta \{ \Omega_0 - 2 \log(\frac{1}{2} \sin \theta) \}}. \quad (12.100)$$

For small values of ka (HALLÉN [1956]):

$$\frac{1}{\Phi^2(1)} \approx \Omega_0 - \frac{1}{6}\pi^2 \Omega_0^{-1} - 4\zeta(3) \Omega_0^{-2}. \quad (12.101)$$

The dilogarithm and the trilogarithm are shown in Fig. 12.13, and the real and imaginary parts of the linearized split function $[\Phi(1)]^{-2}$ in Fig. 12.14. Numerical values of $[\Phi(1)]^{-2}$ and of an auxiliary function useful for interpolation are given in Table 12.1. Polynomial approximations for Li_2 and Li_3 are (EINARSSON [1969]):

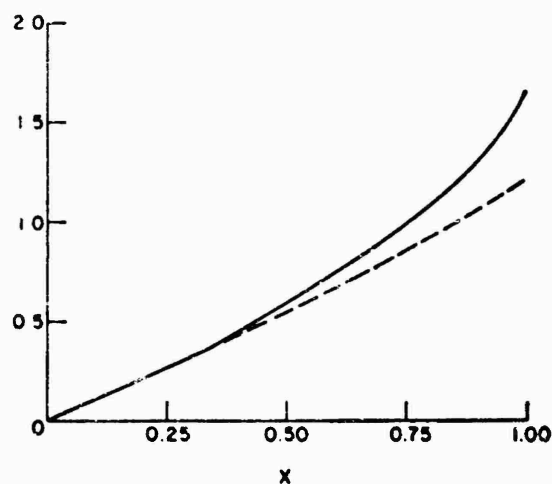
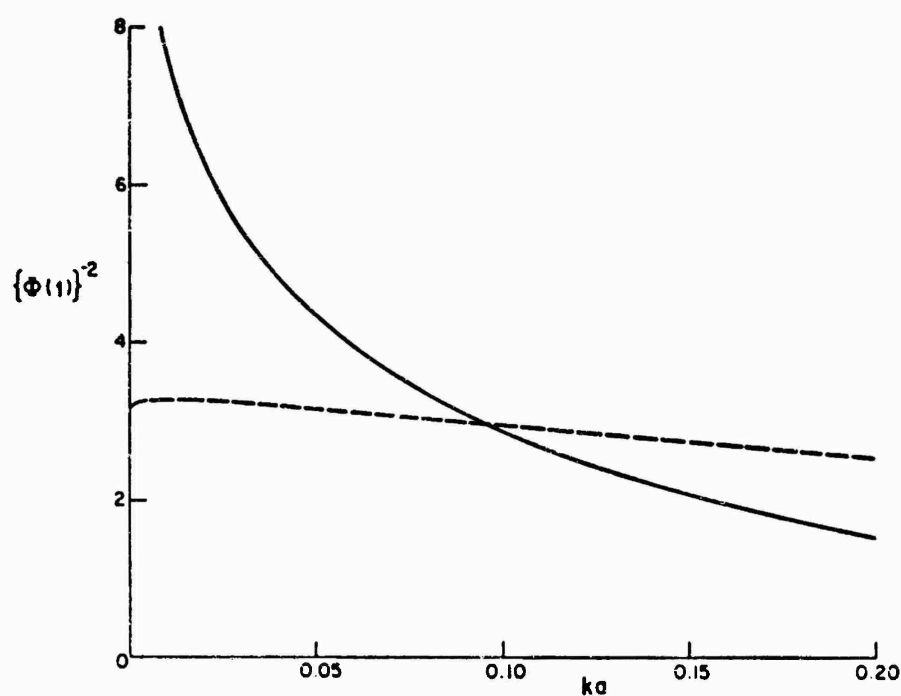


Fig. 12.13. The dilogarithm (—) and trilogarithm (---).

Fig. 12.14. Real (—) and imaginary (---) parts (in radians) of the linearized split function $\{\Phi(1)\}^{-2}$.

$$\text{Li}_2(x) = f_2(x) + \varepsilon(x), \quad \text{for } 0 \leq x \leq 0.5, \quad (12.102)$$

$$\text{Li}_2(x) = \frac{1}{6}\pi^2 - f_2(1-x) - \log x \log(1-x) - \varepsilon(1-x), \quad \text{for } 0.5 < x \leq 1, \quad (12.103)$$

where

$$|\varepsilon(x)| < 5 \times 10^{-7}, \quad (12.104)$$

$$\begin{aligned} f_2(x) = & 0.999999268x + 0.250101283x^2 + 0.103876764x^3 + \\ & + 0.080075448x^4 - 0.019452752x^5 + 0.109355762x^6; \end{aligned} \quad (12.105)$$

Table 12.1

The linearized split function

ka	$\text{Re}\{1/\Phi^2(1)\}$	$\text{Im}\{1/\Phi^2(1)\}$	$\text{Re}\{\Omega_0^{-1}/\Phi^2(1)\}$	$\text{Im}\{\Omega_0^{-1}/\Phi^2(1)\}$
0.005	9.18195	3.24373	0.978425	0.017995
0.010	7.73618	3.25549	0.970336	0.025706
0.015	6.88188	3.25435	0.963496	0.031392
0.020	6.27173	3.24673	0.957253	0.035899
0.025	5.79634	3.23514	0.951371	0.039581
0.030	5.40680	3.22089	0.945732	0.042636
0.035	5.07690	3.20475	0.940269	0.045187
0.040	4.79093	3.18721	0.934941	0.047320
0.045	4.53874	3.16862	0.929717	0.049097
0.050	4.31336	3.14925	0.924579	0.050568
0.055	4.10979	3.12927	0.919511	0.051768
0.060	3.92435	3.10883	0.914502	0.052731
0.065	3.75421	3.08804	0.909543	0.053480
0.070	3.59718	3.06599	0.904627	0.054039
0.075	3.45150	3.04376	0.899749	0.054425
0.080	3.31576	3.02441	0.894903	0.054655
0.085	3.18879	3.00298	0.890087	0.054742
0.090	3.06963	2.98153	0.885297	0.054701
0.095	2.95747	2.96007	0.880531	0.054541
0.100	2.85161	2.93865	0.875787	0.054273
0.105	2.75146	2.91728	0.871062	0.053907
0.110	2.65651	2.89599	0.866356	0.053450
0.115	2.56631	2.87480	0.861668	0.052910
0.120	2.48048	2.85372	0.856996	0.052295
0.125	2.39867	2.83277	0.852340	0.051611
0.130	2.32058	2.81195	0.847699	0.050864
0.135	2.24594	2.79128	0.843072	0.050059
0.140	2.17450	2.77077	0.838460	0.049201
0.145	2.10605	2.75042	0.833861	0.048296
0.150	2.04039	2.73024	0.829277	0.047348
0.155	1.97734	2.71023	0.824706	0.046360
0.160	1.91674	2.69041	0.820149	0.045338
0.165	1.85845	2.67076	0.815606	0.044284
0.170	1.80233	2.65131	0.811077	0.043202
0.175	1.74826	2.63204	0.806562	0.042096
0.180	1.69612	2.61296	0.802062	0.040967
0.185	1.64581	2.59407	0.797576	0.039820
0.190	1.59724	2.57538	0.793105	0.038657
0.195	1.55031	2.55689	0.788650	0.037479
0.200	1.50495	2.53859	0.784210	0.036291

$$Li_3(x) = f_3(x) + \varepsilon(x), \quad \text{for } 0 \leq x \leq 0.62, \quad (12.106)$$

$$Li_3(x) = \zeta(3) + \frac{1}{6}\pi^2 \log x - \frac{1}{2}(\log x)^2 \log(1-x) + \frac{1}{6}(\log x)^3 - f_3(1-x) + \\ + f_3\left(\frac{1-x}{x}\right) - \frac{1}{2}f_3\left(\frac{(1-x)^2}{x^2}\right) + \varepsilon_1(x), \quad \text{for } 0.62 < x \leq 1, \quad (12.107)$$

where

$$|\varepsilon(x)| \leq |\varepsilon_1(x)| < 5 \times 10^{-7}, \quad (12.108)$$

$$f_3(x) = 0.999\,999\,526x + 0.125\,052\,531x^2 + 0.036\,110\,095x^3 + \\ + 0.021\,439\,379x^4 - 0.007\,595\,118x^5 + 0.021\,356\,189x^6. \quad (12.109)$$

Bibliography

- AS, B. O. and H. J. SCHMITT [1958], Backscattering Cross Section of Reactively Loaded Cylindrical Antennas. Cruft Laboratory Scientific Report No. 18, Harvard University, Cambridge, Massachusetts (AFCRC-TN-58-365, ASTIA Document No. AD 160 809).
- BRUNDELL, P. O. [1957], A New Table of the Amplitude Functions of the Iterated Sine- and Cosine-Integrals and Some Comments on the Aperiodic Functions in Hallén's Antenna Theory, Trans. Roy. Inst. Technol. Stockholm, No. 108.
- CHANG, S. and V. V. LIEPA [1967], Measured Backscattering Cross Section of Thin Wires, The University of Michigan Radiation Laboratory Report No. 8077-4-T, Ann Arbor, Michigan.
- DE BETTENCOURT, J. T. [1961], Bistatic Cross Sections of Cylindrical Wires, Scientific Report No. 1, Pickard and Burns, Inc., Needham, Massachusetts, (RADC-TDR-61-285).
- DIKE, S. H. and D. D. KING [1952], The Absorption Gain and Backscattering Cross Section of the Cylindrical Antenna, Proc. IRE 40, 853-860; discussion in Proc. IRE 41, 926-934.
- EINARSSON, O. [1963], The Current Distribution on Cylindrical Antennas of Arbitrary Length, Trans. Roy. Inst. Technol. Stockholm, No. 216.
- EINARSSON, O. [1969], Electromagnetic Scattering by a Thin Finite Wire, Acta Polytech. Scand., Elec. Eng. Ser.
- FIALKOVSKII, A. T. [1967], Scattering of Plane Electromagnetic Waves by a Thin Cylindrical Conductor of Finite Length, Soviet Phys. - Techn. Phys. 11, 1300-1304 (Engl. transl. of Zh. Tekhn. Fiz. 36).
- FLAMMER, C. [1950], Equivalent Radii of Thin Cylindrical Antennas with Arbitrary Cross Sections, Stanford Research Institute Technical Report No. 4, Stanford, California.
- HALLÉN, E. [1938], Theoretical Investigations into the Transmitting and Receiving Qualities of Antennae, Nova Acta Regiae Societatis Scientiarum Upsaliensis, Ser. IV, 11, No. 4.
- HALLÉN, E. [1955], Further Investigations into Iterated Sine- and Cosine-Integrals and their Amplitude Functions with Reference to Antenna Theory, Trans. Roy. Inst. Technol. Stockholm, No. 89.
- HALLÉN, E. [1956], Exact Treatment of Antenna Current Wave Reflection at the End of a Tube-Shaped Cylindrical Antenna, IRE Trans. AP-4, 479-491.
- HALLÉN, E. [1961], Exact Solution of the Antenna Equation, Trans. Roy. Inst. Technol. Stockholm, No. 183.
- HALLÉN, E. [1962], *Electromagnetic Theory*, John Wiley and Sons, Inc., New York.
- HASTINGS, C. [1955], *Approximations for Digital Computers*, Princeton University Press, Princeton, New Jersey.
- HU, Y. Y. [1958], Backscattering Cross Section of a Center-Loaded Cylindrical Antenna, IRE Trans. AP-6, 140-148.
- KING, R. W. P. [1956], *The Theory of Linear Antennas*, Harvard University Press, Cambridge, Massachusetts.

- KOUYOUMJIAN, R. G. [1953], The Calculation of the Echo Areas of Perfectly Conducting Objects by the Variationed Method, Ph. D. Dissertation, Department of Electrical Engineering, The Ohio State University, Columbus, Ohio.
- LINDROTH, K. [1955], Reflection of Electromagnetic Waves from Thin Metal Strips, Trans. Roy. Inst. Technol. Stockholm, No. 91.
- RICHMOND, J. H. [1965], Digital Computer Solutions of the Rigorous Equations for Scattering Problems, Proc. IEEE 53, 796-804.
- SEVICK, J. [1952], Experimental and Theoretical Results on the Backscattering Cross Section of Coupled Antennas, Cruft Laboratory Technical Report No. 150, Harvard University, Cambridge, Massachusetts.
- STRÖMGREN, L. [1962], Table of the Amplitude Functions of the Iterated Sine and Cosine Integrals of Two Variables, Trans. Roy. Inst. Technol. Stockholm, No. 193.
- SU, C. W. H. and J. P. GERMAN [1966], The Equivalent Radius of Noncircular Antennas, Microwave J. 9, 64-67.
- TAI, C. T. [1951], Radar Response from Thin Wires, Stanford Research Institute Technical Report No. 18, Stanford, California. (Corrections to Equations 3, 6, 7 of the Appendix are given by DE BETTENCOURT [1961].)
- UDA, S. and Y. MUSHIAKE (1954), *Yagi-Uda Antenna*, Sasaki Printing and Publishing Co. Ltd., Sendai, Japan.
- UFIMTSEV, P. Ya. [1962], Diffraction of Plane Electromagnetic Waves by a Thin Cylindrical Conductor, Radio Eng. Electron. 7, 241-249 (English transl. of Radiotekhn. i Elektron. 7).
- VAN VLECK, J. H., F. BLOCK and M. HAMERMESH [1947], Theory of Radar Reflections from Wires and Thin Metallic Strips, J. Appl. Phys. 18, 274-294.
- WILLIAMS, W. E. [1956], Diffraction by a Cylinder of Finite Length, Proc. Cambridge Phil. Soc. 52, 322-335.
- WU, T. T. [1961], Theory of the Dipole Antenna and the Two - Wire Transmission Line, J. Math. Phys. 2, 550-574.

THE OBLATE SPHEROID

T. B. A. SENIOR and P. L. E. USLENGHI

Although many exact scattering formulae are available for the oblate spheroid, numerical results are almost non-existent. Furthermore, only a few asymptotic formulae have been derived, and no exact solution of the vector scattering problem has yet been found.

The fat spheroid represents an obvious generalization of the sphere, and the thin spheroid becomes a disc in the limiting case of an eccentricity equal to unity.

13.1. Oblate spheroidal geometry

The oblate spheroidal coordinates (ξ, η, ϕ) shown in Fig. 13.1 are related to the rectangular Cartesian coordinates (x, y, z) by the transformation

$$\begin{aligned} x &= \frac{1}{2}d\sqrt{(\xi^2+1)(1-\eta^2)}\cos\phi, \\ y &= \frac{1}{2}d\sqrt{(\xi^2+1)(1-\eta^2)}\sin\phi, \\ z &= \frac{1}{2}d\xi\eta, \end{aligned} \quad (13.1)$$

where $0 \leq \xi < \infty$, $-1 \leq \eta \leq 1$ and $0 \leq \phi < 2\pi$. The z -axis is the axis of symmetry,

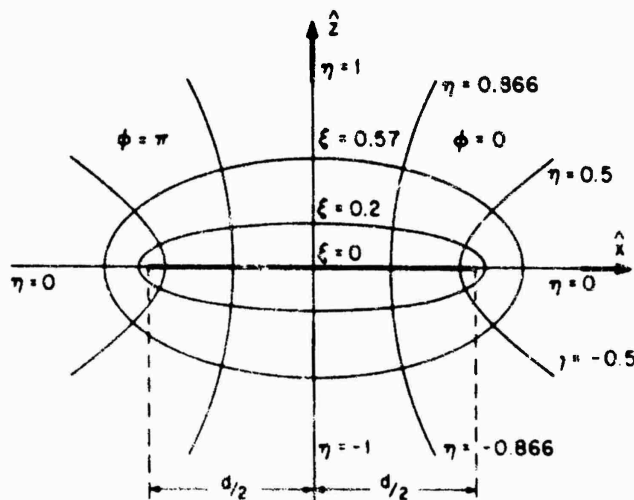


Fig. 13.1. Oblate spheroidal geometry.

and the surfaces $\xi = \text{constant}$, $\eta = \text{constant}$ and $\phi = \text{constant}$ are respectively confocal oblate spheroids of interfocal distance d , minor axis $d\xi$ and major axis $d\sqrt{(\xi^2 + 1)}$; confocal semi-hyperboloids of revolution of one sheet with interfocal distance d ; and semi-planes originating in the z -axis.

The scattering body is the oblate spheroid with surface $\xi = \xi_1$, and the primary source is either a plane wave whose direction of propagation forms the angle ζ with the positive z -axis, or a point or dipole source located at (ξ_0, η_0, ϕ_0) . The length-to-width ratio of the scatterer, i.e. the ratio between the minor and major axes, is $\xi_1/\sqrt{(\xi_1^2 + 1)}$.

The definitions and notation for the oblate spheroidal wave functions are those of FLAMMER [1957]. Thus the radial functions of first, second and third kind are indicated by $R_{mn}^{(j)}(-ic, i\xi)$, where $j = 1, 2$ and 3 respectively, whereas the symbol $S_{mn}(-ic, \eta)$ is used for the angular functions; $m \geq 0$ and $n \geq m$ are integers. The parameter c is the product of wave number and semi-focal distance: $c = \frac{1}{2}kd$. The quantities $\tilde{\rho}_{mn}$ and \tilde{N}_{mn} which appear in the following sections are functions of m , n and c , and are obtained from the quantities $\rho_{mn} = \rho_{mn}(c)$ and $N_{mn} = N_{mn}(c)$ introduced in Chapter 11 and defined by FLAMMER [1957] through the relations:

$$\tilde{\rho}_{mn} = \rho_{mn}(-ic), \quad \tilde{N}_{mn} = N_{mn}(-ic). \quad (13.2)$$

Numerical tables for oblate spheroidal wave functions and related quantities with the notation adopted in this chapter are given by FLAMMER [1957] and LOWAN [1964]. Asymptotic expansions of oblate spheroidal wave functions are found, for example, in FLAMMER [1957] and MÜLLER [1962].

Owing to the scarceness of computed data, no reliable statement can be made on the rapidity of convergence of the infinite series of eigenfunctions representing the exact solutions.

13.2. Acoustically soft spheroid

13.2.1. Point sources

13.2.1.1. EXACT SOLUTIONS

For a point source at $\mathbf{r}_0 = (\xi_0, \eta_0, \phi_0)$, such that

$$V^i = \frac{e^{ikR}}{kR}, \quad (13.3)$$

then

$$\begin{aligned} V^i + V^s = G(\mathbf{r}, \mathbf{r}_0) &= 2i \sum_{m=0}^{\infty} \sum_{n=m}^{\infty} \frac{\varepsilon_m}{\tilde{N}_{mn}} \\ &\times \left[R_{mn}^{(1)}(-ic, i\xi) - \frac{R_{mn}^{(1)}(-ic, i\xi_1)}{R_{mn}^{(3)}(-ic, i\xi_1)} R_{mn}^{(3)}(-ic, i\xi) \right] R_{mn}^{(3)}(-ic, i\xi_0) \\ &\times S_{mn}(-ic, \eta_0) S_{mn}(-ic, \eta) \cos m(\phi - \phi_0). \end{aligned} \quad (13.4)$$

On the surface $\xi = \xi_1$:

$$\frac{\partial}{\partial \xi} (V^i + V^s) = \frac{-2i}{c(\xi_1^2 + 1)} \sum_{m=0}^{\infty} \sum_{n=m}^{\infty} \frac{\varepsilon_m}{\tilde{N}_{mn}} \frac{1}{R_{mn}^{(3)}(-ic, i\xi_1)} \times R_{mn}^{(3)}(-ic, i\xi_0) S_{mn}(-ic, \eta_0) S_{mn}(-ic, \eta) \cos m(\phi - \phi_0). \quad (13.5)$$

In the far field ($\xi \rightarrow \infty$):

$$V^i + V^s = 2 \frac{e^{ic\xi}}{c\xi} \sum_{m=0}^{\infty} \sum_{n=m}^{\infty} \frac{\varepsilon_m}{\tilde{N}_{mn}} \frac{(-i)^n}{\tilde{N}_{mn}} \left[R_{mn}^{(1)}(-ic, i\xi_0) - \frac{R_{mn}^{(1)}(-ic, i\xi_1)}{R_{mn}^{(3)}(-ic, i\xi_1)} R_{mn}^{(3)}(-ic, i\xi_0) \right] \times S_{mn}(-ic, \eta_0) S_{mn}(-ic, \eta) \cos m(\phi - \phi_0). \quad (13.6)$$

When the source is on the positive z -axis ($\eta_0 = 1$):

$$V^i + V^s = 2i \sum_{n=0}^{\infty} \frac{1}{\tilde{N}_{0n}} \left[R_{0n}^{(1)}(-ic, i\xi_0) - \frac{R_{0n}^{(1)}(-ic, i\xi_1)}{R_{0n}^{(3)}(-ic, i\xi_1)} R_{0n}^{(3)}(-ic, i\xi_0) \right] \times R_{0n}^{(3)}(-ic, i\xi_1) S_{0n}(-ic, 1) S_{0n}(-ic, \eta). \quad (13.7)$$

In particular, if the field point is on the surface $\xi = \xi_1$:

$$\frac{\partial}{\partial \xi} (V^i + V^s) = \frac{-2i}{c(\xi_1^2 + 1)} \sum_{n=0}^{\infty} \frac{1}{\tilde{N}_{0n}} \frac{1}{R_{0n}^{(3)}(-ic, i\xi_1)} R_{0n}^{(3)}(-ic, i\xi_0) S_{0n}(-ic, 1) S_{0n}(-ic, \eta), \quad (13.8)$$

whereas in the far field ($\xi \rightarrow \infty$):

$$V^i + V^s = 2 \frac{e^{ic\xi}}{c\xi} \sum_{n=0}^{\infty} \frac{(-i)^n}{\tilde{N}_{0n}} \left[R_{0n}^{(1)}(-ic, i\xi_0) - \frac{R_{0n}^{(1)}(-ic, i\xi_1)}{R_{0n}^{(3)}(-ic, i\xi_1)} R_{0n}^{(3)}(-ic, i\xi_0) \right] \times S_{0n}(-ic, 1) S_{0n}(-ic, \eta). \quad (13.9)$$

13.2.1.2. LOW FREQUENCY APPROXIMATIONS

General methods (e.g. MORSE and FESHBACH [1953], NOBLE [1962], KLEINMAN [1965a]) for the derivation of terms in the low frequency expansion are applicable to this case; however, no specific results are as yet available.

13.2.1.3. HIGH FREQUENCY APPROXIMATIONS

For a point source at $(\xi_0, \eta_0, 0)$, such that

$$V^i = \frac{e^{ikR}}{kR}, \quad (13.10)$$

the geometrical optics scattered field at a point $(\xi, \eta, \phi = 0 \text{ or } \pi)$ located in the illuminated region and in the plane containing the source and the z -axis is:

$$V_{s.o.}^s = -\frac{e^{ic(F_0+F)}}{cF_0} \left[\left(1 + \frac{F}{F_0} + \frac{2F^2}{(\xi_1^2 + \eta_1^2)G} \right) \left(1 + \frac{F}{F_0} + \frac{2\xi_1^2 G}{\xi_1^2 + \eta_1^2} \right) \right]^{-\frac{1}{2}}, \quad (13.11)$$

where

$$F = \{ [\sqrt{\{(\xi_1^2 + 1)(1 - \eta_1^2)\}} - (-1)^h \sqrt{\{(\xi^2 + 1)(1 - \eta^2)\}}]^2 + (\xi_1 \eta_1 - \xi \eta)^2 \}^{\frac{1}{2}}, \quad (13.12)$$

$$F_0 = \{ [\sqrt{\{(\xi_1^2 + 1)(1 - \eta_1^2)\}} - (-1)^j \sqrt{\{(\xi_0^2 + 1)(1 - \eta_0^2)\}}]^2 + (\xi_1 \eta_1 - \xi_0 \eta_0)^2 \}^{\frac{1}{2}}, \quad (13.13)$$

$$G = \frac{\xi}{\xi_1} \eta \eta_1 - 1 + (-1)^h \sqrt{\frac{\xi^2 + 1}{\xi_1^2 + 1} (1 - \eta^2)(1 - \eta_1^2)}, \quad (13.14)$$

and

$$j = h = 0, \quad \text{if } \phi = 0;$$

$$j = 0, h = 1, \quad \text{if } \phi = \pi \text{ and } \sqrt{\{(\xi^2 + 1)(1 - \eta^2)\}} < |(\xi \eta - \xi_1)/(\xi_0 \eta_0 - \xi_1)| \sqrt{\{(\xi_0^2 + 1)(1 - \eta_0^2)\}};$$

$$j = 1, h = 0, \quad \text{if } \phi = \pi \text{ and } \sqrt{\{(\xi^2 + 1)(1 - \eta^2)\}} > |(\xi \eta - \xi_1)/(\xi_0 \eta_0 - \xi_1)| \sqrt{\{(\xi_0^2 + 1)(1 - \eta_0^2)\}}.$$

The parameter η_1 , $-1 \leq \eta_1 \leq 1$, is determined as a function of ξ_0 , η_0 , ξ , η , ξ_1 and ϕ by the relations:

$$\frac{\partial}{\partial \eta_1} (F_0 + F) = 0, \quad \frac{\partial^2}{\partial \eta_1^2} (F_0 + F) > 0. \quad (13.15)$$

In the geometrical shadow $V_{s.o.}^s = 0$. In particular, when the source is at $(\xi_0, 1)$ on the z -axis

$$F = \{ [\sqrt{\{(\xi_1^2 + 1)(1 - \eta_1^2)\}} - \sqrt{\{(\xi^2 + 1)(1 - \eta^2)\}}]^2 + (\xi_1 \eta_1 - \xi \eta)^2 \}^{\frac{1}{2}}, \quad (13.16)$$

$$F_0 = [(\xi_1^2 + 1)(1 - \eta_1^2) + (\xi_1 \eta_1 - \xi_0)^2]^{\frac{1}{2}}, \quad (13.17)$$

$$G = \frac{\xi}{\xi_1} \eta \eta_1 - 1 + \sqrt{\frac{\xi^2 + 1}{\xi_1^2 + 1} (1 - \eta^2)(1 - \eta_1^2)}, \quad (13.18)$$

and η_1 is the positive root of the equation:

$$\begin{aligned} & \frac{\sqrt{1 - \eta_1^2}(\eta_1 + \xi_1 \xi \eta) + \eta_1 \sqrt{\{(\xi_1^2 + 1)(\xi^2 + 1)(1 - \eta^2)\}}}{\{ [\sqrt{\{(\xi_1^2 + 1)(1 - \eta_1^2)\}} - \sqrt{\{(\xi^2 + 1)(1 - \eta^2)\}}]^2 + (\xi_1 \eta_1 - \xi \eta)^2 \}^{\frac{1}{2}}} + \\ & + \frac{\sqrt{1 - \eta_1^2}(\eta_1 + \xi_1 \xi_0)}{[(\xi_1^2 + 1)(1 - \eta_1^2) + (\xi_1 \eta_1 - \xi_0)^2]^{\frac{1}{2}}} = 0. \end{aligned} \quad (13.19)$$

If both source and observation points are on the z -axis ($\eta_0 = \eta = 1$),

$$V_{s.o.}^s = -\frac{\exp \{ic(\xi_0 + \xi - 2\xi_1)\}}{c[\xi_0 + \xi - 2\xi_1 + 2\xi_1(\xi_0 - \xi_1)(\xi - \xi_1)(\xi_1^2 + 1)]} \quad (13.20)$$

in the illuminated region and zero in the shadow.

A more refined approximation, in which an asymptotic expression for the diffracted field is retained, can be derived by means of Keller's theory of diffraction; however, no specific results are available.

For a point source $(\xi_0, 1)$ on the z -axis at a large distance from a flat spheroid (almost a disc), such that

$$\xi_0^2 \gg 1, \quad c \gg 1, \quad c^{\frac{1}{2}} \xi_1 \ll 1, \quad (13.21)$$

the field at a point (ξ_1, η, ϕ) on the shadowed portion of the surface of the spheroid is given by the asymptotic expansions (GOODRICH, KAZARINOFF and WESTON [1963]):

$$\frac{\partial}{\partial \xi} (V^i + V^s) \sim \frac{e^{ic\xi_0}}{c\xi_0} (1 - \eta^2)^{-\frac{1}{2}} \sum_{n=0}^N \frac{T_{n,0}}{1 + R_n e^{2ic}} \quad (13.22)$$

for $|c^{\frac{1}{2}}\eta| \ll 1$ and $\eta < 0$,

$$\begin{aligned} \frac{\partial}{\partial \xi} (V^i + V^s) &\sim \frac{e^{ic\xi_0}}{c\xi_0} (-\eta)^{-1} (1 - \eta^2)^{-\frac{1}{2}} \sum_{n=0}^N \frac{T_n}{1 + R_n e^{2ic}} \\ &\times \{ \exp \{ ic(1 - \sqrt{1 - \eta^2}) \} [f(\eta)]^{n+\frac{1}{2}} + i \exp \{ ic(1 + \sqrt{1 - \eta^2}) \} [f(\eta)]^{-n-\frac{1}{2}} \} \end{aligned} \quad (13.23)$$

for $c\sqrt{1 - \eta^2} \gg 1$ and $-1 < \eta \leq -\delta < 0$ with δ arbitrarily small, and

$$\frac{\partial}{\partial \xi} (V^i + V^s) \sim \frac{e^{ic(1+\xi_0)}}{c\xi_0} \sqrt{\frac{2\pi i}{\eta}} \sum_{n=0}^N \frac{T_n}{1 + R_n e^{2ic}} \quad (13.24)$$

for $c\sqrt{1 - \eta^2} \ll 1$ and $\eta < 0$. In the preceding expansions,

$$R_n = \frac{(-1)^n (2n+1)! e^{\frac{1}{2}i\pi}}{2^{6n+4} \pi^{\frac{1}{2}} c^{2n+\frac{1}{2}}}, \quad (13.25)$$

$$f(\eta) = \frac{1 + \sqrt{1 - \eta^2}}{1 - \sqrt{1 - \eta^2}}, \quad (13.26)$$

$$T_{n,0} = \frac{(-1)^n (2n+1)! c^{\frac{1}{2}} e^{\frac{1}{2}i\pi}}{2^n n! \Gamma(n + \frac{1}{2})}, \quad (13.27)$$

$$T_n = \frac{i^{n+\frac{1}{2}} (2n+1)!}{2^{4n+\frac{1}{2}} n! \pi^{\frac{1}{2}} c^n}, \quad (13.28)$$

and N is a positive integer; how large N may be once c is chosen is not known. The preceding residue series may be physically interpreted in terms of traveling waves, as has been done for the thin prolate spheroid; for details, see GOODRICH, KAZARINOFF and WESTON [1963].

13.2.2. Plane wave incidence

13.2.2.1. EXACT SOLUTIONS

For incidence at an angle ζ with respect to the positive z -axis, such that

$$V^i = \exp \{ ik(x \sin \zeta + z \cos \zeta) \}, \quad (13.29)$$

then

$$V^s = -2 \sum_{m=0}^{\infty} \sum_{n=m}^{\infty} \varepsilon_m \frac{i^n}{\tilde{N}_{mn}} \frac{R_{mn}^{(1)}(-ic, i\xi_1)}{R_{mn}^{(3)}(-ic, i\xi_1)} R_{mn}^{(3)}(-ic, i\xi) \\ \times S_{mn}(-ic, \cos \zeta) S_{mn}(-ic, \eta) \cos m\phi. \quad (13.30)$$

On the surface $\xi = \xi_1$:

$$\frac{\partial}{\partial \xi} (V^i + V^s) = \frac{-2}{c(\xi_1^2 + 1)} \sum_{m=0}^{\infty} \sum_{n=m}^{\infty} \varepsilon_m \frac{i^n}{\tilde{N}_{mn}} \frac{1}{R_{mn}^{(3)}(-ic, i\xi_1)} \\ \times S_{mn}(-ic, \cos \zeta) S_{mn}(-ic, \eta) \cos m\phi. \quad (13.31)$$

In the far field ($\xi \rightarrow \infty$):

$$S = 2i \sum_{m=0}^{\infty} \sum_{n=m}^{\infty} \frac{\varepsilon_m}{\tilde{N}_{mn}} \frac{R_{mn}^{(1)}(-ic, i\xi_1)}{R_{mn}^{(3)}(-ic, i\xi_1)} S_{mn}(-ic, \cos \zeta) S_{mn}(-ic, \eta) \cos m\phi. \quad (13.32)$$

The total scattering cross section is

$$\sigma_T = \frac{4\pi}{k^2} \sum_{m=0}^{\infty} \sum_{n=m}^{\infty} \frac{\varepsilon_m^2}{\tilde{N}_{mn}} \left[\frac{R_{mn}^{(1)}(-ic, i\xi_1)}{|R_{mn}^{(3)}(-ic, i\xi_1)|} S_{mn}(-ic, \cos \zeta) \right]^2. \quad (13.33)$$

For axial incidence ($\zeta = \pi$):

$$V^s = -2 \sum_{n=0}^{\infty} \frac{i^n}{\tilde{N}_{0n}} \frac{R_{0n}^{(1)}(-ic, i\xi_1)}{R_{0n}^{(3)}(-ic, i\xi_1)} R_{0n}^{(3)}(-ic, i\xi) S_{0n}(-ic, -1) S_{0n}(-ic, \eta). \quad (13.34)$$

and on the surface $\xi = \xi_1$:

$$\frac{\partial}{\partial \xi} (V^i + V^s) = \frac{-2}{c(\xi_1^2 + 1)} \sum_{n=0}^{\infty} \frac{i^n}{\tilde{N}_{0n}} \frac{1}{R_{0n}^{(3)}(-ic, i\xi_1)} S_{0n}(-ic, -1) S_{0n}(-ic, \eta). \quad (13.35)$$

In the far field ($\xi \rightarrow \infty$):

$$S = 2i \sum_{n=0}^{\infty} \frac{1}{\tilde{N}_{0n}} \frac{R_{0n}^{(1)}(-ic, i\xi_1)}{R_{0n}^{(3)}(-ic, i\xi_1)} S_{0n}(-ic, -1) S_{0n}(-ic, \eta). \quad (13.36)$$

The total scattering cross section is:

$$\sigma_T = \frac{4\pi}{k^2} \sum_{n=0}^{\infty} \frac{1}{\tilde{N}_{0n}} \left[\frac{R_{0n}^{(1)}(-ic, i\xi_1)}{|R_{0n}^{(3)}(-ic, i\xi_1)|} S_{0n}(-ic, -1) \right]^2. \quad (13.37)$$

13.2.2.2. LOW FREQUENCY APPROXIMATIONS

For incidence at an angle ζ with respect to the positive z -axis, such that

$$V^i = \exp \{ik(x \sin \zeta + z \cos \zeta)\}, \quad (13.38)$$

then (ASVESTAS and KLEINMAN [1967]):

$$V^s = e^{i\alpha} \sum_{n=0}^{\infty} \sum_{m=0}^n (-c)^n \frac{(i\xi_1 - \eta)^{n-m}}{(n-m)!} \sum_{l=0}^m \sum_{h=0}^m \sum_{j=0}^m C_{l,h,j}^m Q_h^l(i\xi) P_j^l(\eta) \cos l\phi, \quad (13.39)$$

where $C_{l,h,j}^m = C_{l,j,h}^m$, and $C_{l,h,j}^m$ is given by the recurrence relations:

$$C_{l,h,j}^{m+1} = \frac{2}{h(h+1)-j(j+1)} \left[\frac{h(h-1)}{2h-1} C_{l,h-1,j}^m - \frac{j(j-1)}{2j-1} C_{l,h,j-1}^m + \right. \\ \left. + \frac{(j+1)(j+1+1)}{2j+3} C_{l,h,j+1}^m - \frac{(h+1)(h+1+1)}{2h+3} C_{l,h+1,j}^m \right] \quad (13.40)$$

for $h \neq j$ and $m = 0, 1, 2, \dots$;

$$C_{l,j,j}^{m+1} = - \sum_{h=0}^{m+1} \frac{Q_h^l(i\xi_1)}{Q_j^l(i\xi_1)} C_{l,h,j}^{m+1} + A_{j,l}^{m+1} \quad (13.41)$$

for $m = 0, 1, 2, \dots$ where \sum' indicates that the term $h = j$ is omitted from the summation; and

$$C_{0,0,0}^0 = A_{0,0}^0, \quad (13.42)$$

$$A_{j,l}^m = \begin{cases} 0, & \text{for } m+j \text{ odd,} \\ -e_l \frac{\sqrt{\pi}}{2^{m+1}} (i\xi_1 - \cos \zeta)^m (2j+1) \frac{(j-l)!}{(j+l)!} \frac{P_j^l((1-i\xi_1 \cos \zeta)/(i\xi_1 - \cos \zeta))}{\{\frac{1}{2}(m-j)\}! \{\frac{1}{2}(m+j+1)\}! Q_j^l(i\xi_1)}, & \text{for } m+j \text{ even.} \end{cases} \quad (13.43)$$

In the far field ($\xi \rightarrow \infty$):

$$S = -ic \sum_{n=0}^{\infty} \sum_{m=0}^n (-c)^n \frac{(i\xi_1 - \eta)^{n-m}}{(n-m)!} \sum_{l=0}^m \sum_{j=0}^m C_{l,0,j}^m P_j^l(\eta) \cos l\phi. \quad (13.44)$$

Starting from the exact series solution, BURKE [1966a] has computed S through terms $O(k^6)$ for arbitrary angles of incidence and observation.

For axial incidence ($\zeta = \pi$):

$$V^s = e^{ic\xi} \sum_{n=0}^{\infty} \sum_{m=0}^n (-c)^n \frac{(i\xi_1 - \eta)^{n-m}}{(n-m)!} \sum_{h=0}^m \sum_{j=0}^m C_{h,h,j}^m Q_h(i\xi) P_j(\eta), \quad (13.45)$$

and in the far field ($\xi \rightarrow \infty$):

$$S = -ic \sum_{n=0}^{\infty} \sum_{m=0}^n (-c)^n \frac{(i\xi_1 - \eta)^{n-m}}{(n-m)!} \sum_{j=0}^m C_{0,0,j}^m P_j(\eta). \quad (13.46)$$

13.2.2.3. HIGH FREQUENCY APPROXIMATIONS

No specific results are available for arbitrary incidence, but for axial incidence, such that

$$V^i = e^{-ikz}, \quad (13.47)$$

the geometrical optics scattered field at a point (ξ, η, ϕ) located in the illuminated region $\{(\xi^2 + 1)(1 - \eta^2) > (\xi_1^2 + 1) \text{ when } \eta < 0\}$ is:

$$V_{g.o.}^s = -\exp \{ic(F - \xi_1 \eta_1)\} \left[\left(1 + \frac{2F^2}{(\xi_1^2 + \eta_1^2)G} \right) \left(1 + \frac{2\xi_1^2 G}{\xi_1^2 + \eta_1^2} \right) \right]^{-1} \quad (13.48)$$

where F and G are given by eqs. (13.16) and (13.18), and η_1 is the positive root of eq. (13.19) with $\xi_0 = \infty$. In the geometrical shadow $V_{g.o.}^s = 0$. In the far field ($\xi \rightarrow \infty$):

$$S_{g.o.} = -\frac{c(\xi_1^2 + \eta_1^2)}{2\xi_1} \exp \{ -ic[\xi_1 \eta_1(1 + \eta) + \sqrt{(\xi_1^2 + 1)(1 - \eta_1^2)(1 - \eta^2)}] \}. \quad (13.49)$$

In particular, if the observation point is on the z -axis ($\eta = 1$):

$$V_{g.o.}^s = -\frac{\xi_1^2 + 1}{2\xi\xi_1 - \xi_1^2 + 1} e^{ic(\xi - 2\xi_1)}, \quad (13.50)$$

and in the far field ($\xi \rightarrow \infty$):

$$S_{g.o.} = -\frac{c(\xi_1^2 + 1)}{2\xi_1} e^{-2ic\xi_1}, \quad (13.51)$$

so that the geometrical optics back scattering cross section is:

$$\sigma_{g.o.} = \frac{\pi c^2}{k^2} (\xi_1 + \xi_1^{-1})^2. \quad (13.52)$$

A more refined approximation, in which an asymptotic expression for the diffracted field is retained, can be derived by means of Keller's geometrical theory of diffraction; however, no specific results are available.

The total scattering cross section for axial incidence ($\zeta = \pi$) is (JONES [1957]):

$$\sigma_T \sim \frac{2\pi c^2}{k^2} (\xi_1^2 + 1) \{1 + 0.9962[c(\xi_1 + \xi_1^{-1})]^{-\frac{1}{2}}\}; \quad (13.53)$$

this results in a good approximation if

$$c(\xi_1 + \xi_1^{-1}) \gg 1. \quad (13.54)$$

13.2.2.4. SHAPE APPROXIMATION

For a spheroid whose surface $\xi = \xi_1$ is defined in terms of the spherical polar coordinates (r_1, θ_1, ϕ_1) by the equation

$$r_1 = a \left(\frac{\xi_1^2 + 1}{\xi_1^2 + \cos^2 \theta_1} \right)^{\frac{1}{2}}, \quad (13.55)$$

and is such that

$$\xi_1^2 + 1 \gg 1, \quad (13.56)$$

i.e. the spheroid departs only infinitesimally from the sphere $r_1 = a$, the scattered field may be expressed as a perturbation of the solution for this sphere.

For incidence at an angle ζ with respect to the positive z -axis, such that

$$V^i = \exp \{ ik(x \sin \zeta + z \cos \zeta) \}, \quad (13.57)$$

then

$$V^s \sim - \sum_{m=0}^{\infty} \sum_{n=m}^{\infty} \varepsilon_m \frac{(n-m)!}{(n+m)!} \frac{i^n}{h_n^{(1)}(ka)} \left[(2n+1)j_n(ka) - \frac{i}{\xi_1^2+1} a_{mn}(\zeta) \right] \\ \times h_n^{(1)}(kr) P_n^m(\cos \zeta) P_n^m(\cos \theta) \cos m\phi + O[(\xi_1^2+1)^{-2}], \quad (13.58)$$

where

$$a_{mn}(\zeta) = \frac{1}{ka h_n^{(1)}(ka)} \left[\frac{(2n+1)(n^2+n-i+m^2)}{(2n-1)(2n+3)} + \frac{(n+m-1)(n+m)}{2(2n-1)} \right. \\ \left. \times \frac{h_n^{(1)}(ka)}{h_{n-2}^{(1)}(ka)} \frac{P_{n-2}^m(\cos \zeta)}{P_n^m(\cos \zeta)} + \frac{(n-m+1)(n-m+2)}{2(2n+3)} \frac{h_n^{(1)}(ka)}{h_{n+2}^{(1)}(ka)} \frac{P_{n+2}^m(\cos \zeta)}{P_n^m(\cos \zeta)} \right]. \quad (13.59)$$

In the far back scattered field ($r \rightarrow \infty$, $\theta = \pi - \zeta$, $\phi = \pi$):

$$S \sim \sum_{m=0}^{\infty} \sum_{n=m}^{\infty} \varepsilon_m \frac{(n-m)!}{(n+m)!} \frac{(-1)^n}{h_n^{(1)}(ka)} \left[i(2n+1)j_n(ka) + \frac{1}{\xi_1^2+1} a_{mn}(\zeta) \right] \\ \times [P_n^m(\cos \zeta)]^2 + O[(\xi_1^2+1)^{-2}]. \quad (13.60)$$

For axial incidence ($\zeta = \pi$):

$$V^s \sim - \sum_{n=0}^{\infty} \frac{(-i)^n}{h_n^{(1)}(ka)} \left[(2n+1)j_n(ka) - \frac{i}{\xi_1^2+1} a_{0n}(\pi) \right] h_n^{(1)}(kr) P_n(\cos \theta) + \\ + O[(\xi_1^2+1)^{-2}], \quad (13.61)$$

where

$$a_{0n}(\pi) = \frac{1}{ka h_n^{(1)}(ka)} \left[\frac{(2n+1)(n^2+n+1)}{(2n-1)(2n+3)} + \frac{n(n-1)}{2(2n-1)} \frac{h_n^{(1)}(ka)}{h_{n-2}^{(1)}(ka)} + \right. \\ \left. + \frac{(n+1)(n+2)}{2(2n+3)} \frac{h_n^{(1)}(ka)}{h_{n+2}^{(1)}(ka)} \right], \quad (13.62)$$

and in the far back scattered field:

$$S \sim \sum_{n=0}^{\infty} \frac{(-1)^n}{h_n^{(1)}(ka)} \left[i(2n+1)j_n(ka) + \frac{1}{\xi_1^2+1} a_{0n}(\pi) \right] + O[(\xi_1^2+1)^{-2}]. \quad (13.63)$$

13.3. Acoustically hard spheroid

13.3.1. Point sources

13.3.1.1. EXACT SOLUTIONS

For a point source at $r_0 = (\xi_0, \eta_0, \phi_0)$, such that

$$V^i = \frac{e^{ikR}}{kR}, \quad (13.64)$$

then

$$\begin{aligned}
 V^i + V^s &= G(\mathbf{r}, \mathbf{r}_0) = \\
 &= 2i \sum_{m=0}^{\infty} \sum_{n=m}^{\infty} \frac{\epsilon_m}{\tilde{N}_{mn}} \left[R_{mn}^{(1)}(-ic, i\xi_0) - \frac{R_{mn}^{(1)'}(-ic, i\xi_1)}{R_{mn}^{(3)'}(-ic, i\xi_1)} R_{mn}^{(2)}(-ic, i\xi_0) \right] \\
 &\quad \times R_{mn}^{(3)}(-ic, i\xi_0) S_{mn}(-ic, \eta_0) S_{mn}(-ic, \eta) \cos m(\phi - \phi_0). \quad (13.65)
 \end{aligned}$$

On the surface $\xi = \xi_1$:

$$\begin{aligned}
 V^i + V^s &= \frac{2i}{c(\xi_1^2 + 1)} \sum_{m=0}^{\infty} \sum_{n=m}^{\infty} \frac{\epsilon_m}{\tilde{N}_{mn}} \frac{1}{R_{mn}^{(3)'}(-ic, i\xi_1)} R_{mn}^{(3)}(-ic, i\xi_0) \\
 &\quad \times S_{mn}(-ic, \eta_0) S_{mn}(-ic, \eta) \cos m(\phi - \phi_0). \quad (13.66)
 \end{aligned}$$

In the far field ($\xi \rightarrow \infty$):

$$\begin{aligned}
 V^i + V^s &= 2 \frac{e^{ic\xi}}{c\xi} \sum_{m=0}^{\infty} \sum_{n=m}^{\infty} \frac{(-i)^n}{\tilde{N}_{mn}} \left[R_{mn}^{(1)}(-ic, i\xi_0) - \frac{R_{mn}^{(1)'}(-ic, i\xi_1)}{R_{mn}^{(3)'}(-ic, i\xi_1)} R_{mn}^{(3)}(-ic, i\xi_0) \right] \\
 &\quad \times S_{mn}(-ic, \eta_0) S_{mn}(-ic, \eta) \cos m(\phi - \phi_0). \quad (13.67)
 \end{aligned}$$

When the source is on the positive z -axis ($\eta_0 = 1$):

$$\begin{aligned}
 V^i + V^s &= 2i \sum_{n=0}^{\infty} \frac{1}{\tilde{N}_{0n}} \left[R_{0n}^{(1)}(-ic, i\xi_0) - \frac{R_{0n}^{(1)'}(-ic, i\xi_1)}{R_{0n}^{(3)'}(-ic, i\xi_1)} R_{0n}^{(2)}(-ic, i\xi_0) \right] \\
 &\quad \times R_{0n}^{(3)}(-ic, i\xi_0) S_{0n}(-ic, 1) S_{0n}(-ic, \eta). \quad (13.68)
 \end{aligned}$$

In particular, if the field point is on the surface $\xi = \xi_1$:

$$\begin{aligned}
 V^i + V^s &= \frac{2i}{c(\xi_1^2 + 1)} \sum_{n=0}^{\infty} \frac{1}{\tilde{N}_{0n}} \frac{1}{R_{0n}^{(3)'}(-ic, i\xi_1)} R_{0n}^{(3)}(-ic, i\xi_0) S_{0n}(-ic, 1) S_{0n}(-ic, \eta), \quad (13.69)
 \end{aligned}$$

whereas in the far field ($\xi \rightarrow \infty$):

$$\begin{aligned}
 V^i + V^s &= 2 \frac{e^{ic\xi}}{c\xi} \sum_{n=0}^{\infty} \frac{(-i)^n}{\tilde{N}_{0n}} \left[R_{0n}^{(1)}(-ic, i\xi_0) - \frac{R_{0n}^{(1)'}(-ic, i\xi_1)}{R_{0n}^{(3)'}(-ic, i\xi_1)} R_{0n}^{(3)}(-ic, i\xi_0) \right] \\
 &\quad \times S_{0n}(-ic, 1) S_{0n}(-ic, \eta). \quad (13.70)
 \end{aligned}$$

13.3.1.2. LOW FREQUENCY APPROXIMATIONS

General methods (e.g. MORSE and FESHBACH [1953], NOBLE [1962], AR and KLEINMAN [1966]) for the derivation of terms in the low frequency expansion are applicable to this case; however, no specific results are as yet available.

13.3.1.3. HIGH FREQUENCY APPROXIMATIONS

For a point source at $(\xi_0, \eta_0, 0)$, such that

$$V^i = \frac{e^{ikR}}{kR}, \quad (13.71)$$

the geometrical optics scattered field at a point $(\xi, \eta, \phi = 0 \text{ or } \pi)$ located in the illuminated region and in the plane containing the source and the z -axis is:

$$V_{g.o.}^s = \frac{e^{ic(F_0 + i)}}{cF_0} \left[\left(1 + \frac{F}{F_0} + \frac{2F^2}{(\xi_1^2 + \eta_1^2)G} \right) \left(1 + \frac{F}{F_0} + \frac{2\xi_1^2 G}{\xi_1^2 + \eta_1^2} \right) \right]^{-\frac{1}{2}}, \quad (13.72)$$

where F, F_0, G and η_1 were defined in Section 13.2.1.3. In the geometrical shadow $V_{g.o.}^s = 0$. If both source and observation points are on the z -axis ($\eta_0 = \eta = 1$),

$$V_{g.o.}^s = \frac{\exp \{ic(\xi_0 + \xi - 2\xi_1)\}}{c[\xi_0 + \xi - 2\xi_1 + 2\xi_1(\xi_0 - \xi_1)(\xi - \xi_1)/(\xi_1^2 + 1)]} \quad (13.73)$$

in the illuminated region and zero in the shadow.

A more refined approximation, in which an asymptotic expression for the diffracted field is retained, can be derived by means of Keller's geometrical theory of diffraction; however, no specific results are available.

For a point source $(\xi_0, 1)$ on the z -axis at a large distance from a flat spheroid (almost a disc), such that

$$\xi_0^2 \gg 1, \quad c \gg 1, \quad c^{\frac{1}{2}}\xi_1 \ll 1, \quad (13.74)$$

the field at a point (ξ_1, η, ϕ) on the shadowed portion of the surface of the spheroid is given by the asymptotic expansions (GOODRICH, KAZARINOFF and WESTON [1963]):

$$V^i + V^s \sim \frac{e^{ic\xi_0}}{c\xi_0} (1 - \eta^2)^{-\frac{1}{2}} \sum_{n=0}^N \frac{T_{n,0}}{1 + \bar{R}_n e^{2ic}} \quad (13.75)$$

for $|c^{\frac{1}{2}}\eta| \gg 1$ and $\eta < 0$.

$$V^i + V^s \sim \frac{e^{ic\xi_0}}{c\xi_0} (-\eta)^{-\frac{1}{2}} (1 - \eta^2)^{-\frac{1}{2}} \sum_{n=0}^N \frac{T_n}{1 + \bar{R}_n e^{2ic}} \left\{ ic(1 - \sqrt{(1 - \eta^2)}) [f(\eta)]^{n+\frac{1}{2}} + i \exp \{ic(1 + \sqrt{(1 - \eta^2)})\} [f(\eta)]^{-n-\frac{1}{2}} \right\} \quad (13.76)$$

for $c\sqrt{(1 - \eta^2)} \gg 1$ and $-1 < \eta \leq -\delta < 0$ with δ arbitrarily small, and

$$V^i + V^s \sim \frac{e^{ic(1 + \xi_0)}}{c\xi_0} \sqrt{\frac{2\pi ic}{\eta}} \sum_{n=0}^N \frac{T_n}{1 + \bar{R}_n e^{2ic}} \quad (13.77)$$

for $c\sqrt{(1 - \eta^2)} \ll 1$ and $\eta < 0$. In the preceding expansions,

$$\bar{R}_n = \frac{(-1)^n (2n)! e^{i\pi}}{2^{2n+1} \pi^{\frac{1}{2}} c^{2n+\frac{1}{2}}}, \quad (13.78)$$

$$f(\eta) = \frac{1 + \sqrt{(1 - \eta^2)}}{1 - \sqrt{(1 - \eta^2)}}, \quad (13.79)$$

$$T_{n,0} = \frac{i(-1)^n (2n)!}{2^{2n} (n!)^2}, \quad (13.80)$$

$$T_n = \frac{(-i)^n (2n)! e^{\frac{1}{2}i\pi}}{2^{4n+\frac{1}{2}} n! \pi^{\frac{1}{2}} c^{n+\frac{1}{2}}}, \quad (13.81)$$

and N is a positive integer; how large N may be once c is chosen is not known. The preceding residue series may be physically interpreted in terms of traveling waves, as has been done for the thin prolate spheroid; for details, see GOODRICH, KAZARI NOFF and WESTON [1963].

13.3.2. Plane wave incidence

13.3.2.1. EXACT SOLUTIONS

For incidence at an angle ζ with respect to the positive z -axis, such that

$$V^i = \exp \{ik(x \sin \zeta + z \cos \zeta)\}, \quad (13.82)$$

then

$$\begin{aligned} V^s = & -2 \sum_{m=0}^{\infty} \sum_{n=m}^{\infty} \varepsilon_m \frac{i^n}{\tilde{N}_{mn}} \frac{R_{mn}^{(1)'}(-ic, i\xi_1)}{R_{mn}^{(3)'}(-ic, i\xi_1)} R_{mn}^{(3)}(-ic, i\xi) \\ & \times S_{mn}(-ic, \cos \zeta) S_{mn}(-ic, \eta) \cos m\phi. \end{aligned} \quad (13.83)$$

On the surface $\xi = \xi_1$:

$$\begin{aligned} V^i + V^s = & \frac{2}{c(\xi_1^2 + 1)} \sum_{m=0}^{\infty} \sum_{n=m}^{\infty} \varepsilon_m \frac{i^n}{\tilde{N}_{mn}} \frac{1}{R_{mn}^{(3)'}(-ic, i\xi_1)} \\ & \times S_{mn}(-ic, \cos \zeta) S_{mn}(-ic, \eta) \cos m\phi. \end{aligned} \quad (13.84)$$

In the far field ($\xi \rightarrow \infty$):

$$S = 2i \sum_{m=0}^{\infty} \sum_{n=m}^{\infty} \frac{\varepsilon_m}{\tilde{N}_{mn}} \frac{R_{mn}^{(1)'}(-ic, i\xi_1)}{R_{mn}^{(3)'}(-ic, i\xi_1)} S_{mn}(-ic, \cos \zeta) S_{mn}(-ic, \eta) \cos m\phi, \quad (13.85)$$

and the total scattering cross section is:

$$\sigma_T = \frac{4\pi}{k^2} \sum_{m=0}^{\infty} \sum_{n=m}^{\infty} \frac{\varepsilon_m^2}{\tilde{N}_{mn}^2} \left[\frac{R_{mn}^{(1)'}(-ic, i\xi_1)}{R_{mn}^{(3)'}(-ic, i\xi_1)} S_{mn}(-ic, \cos \zeta) \right]^2. \quad (13.86)$$

For axial incidence ($\zeta = \pi$):

$$V^s = -2 \sum_{n=0}^{\infty} \frac{i^n}{\tilde{N}_{0n}} \frac{R_{0n}^{(1)'}(-ic, i\xi_1)}{R_{0n}^{(3)'}(-ic, i\xi_1)} R_{0n}^{(3)}(-ic, i\xi_1) S_{0n}(-ic, -1) S_{0n}(-ic, \eta), \quad (13.87)$$

and on the surface $\xi = \xi_1$:

$$V^i + V^s = \frac{2}{c(\xi_1^2 + 1)} \sum_{n=0}^{\infty} \frac{i^n}{\tilde{N}_{0n}} \frac{1}{R_{0n}^{(3)'}(-ic, i\xi_1)} S_{0n}(-ic, -1) S_{0n}(-ic, \eta). \quad (13.88)$$

In the far field ($\xi \rightarrow \infty$):

$$S = 2i \sum_{n=0}^{\infty} \frac{1}{\tilde{N}_{0n}} \frac{R_{0n}^{(1)'}(-ic, i\xi_1)}{R_{0n}^{(3)'}(-ic, i\xi_1)} S_{0n}(-ic, -1) S_{0n}(-ic, \eta), \quad (13.89)$$

and the total scattering cross section is:

$$\sigma_T = \frac{4\pi}{k^2} \sum_{n=0}^{\infty} \frac{1}{N_{0n}} \left[\frac{R_{0n}^{(1)'}(-ic, i\xi_1)}{|R_{0n}^{(3)'}(-ic, i\xi_1)|} S_{0n}(-ic, -1) \right]^2. \quad (13.90)$$

Using an integral equation approach for his numerical computations, BRUNDRIT [1965] has plotted the amplitude $|S|$ of the far field coefficient of eq. (13.89) as a function of η for $c\sqrt{(\xi_1^2 + 1)} = 1, 2, 4$ and length-to-width ratios varying from 1:1 to 1:5, and the total scattering cross section σ_T of eq. (13.90) as a function of $c\sqrt{(\xi_1^2 + 1)}$, ($c\sqrt{(\xi_1^2 + 1)} \leq 8$), for 1:1, 9:10, 4:5, 3:5, 2:5 and 1:5 spheroids.

13.3.2.2. LOW FREQUENCY APPROXIMATIONS

For incidence at an angle ζ with respect to the positive z -axis, such that

$$V^i = \exp \{ik(x \sin \zeta + z \cos \zeta)\}, \quad (13.91)$$

then (ASVESTAS and KLEINMAN [1967]):

$$V^s = e^{ic\xi} \sum_{n=0}^{\infty} \sum_{m=0}^n (-c)^n \frac{(i\xi_1 - \eta)^{n-m}}{(n-m)!} \sum_{l=0}^m \sum_{h=0}^m \sum_{j=0}^m C_{l,h,j}^m Q_h^l(i\xi) P_j^l(\eta) \cos l\phi, \quad (13.92)$$

where $C_{l,h,j}^m = C_{l,j,h}^m$, and $C_{l,h,j}^m$ is given by the recurrence relations:

$$C_{l,h,j}^{m+1} = \frac{2}{h(h+1) - j(j+1)} \left[\frac{h(h-l)}{2h-1} C_{l,h-1,j}^m - \frac{j(j-l)}{2j-1} C_{l,h,j-1}^m + \frac{(j+1)(j+l+1)}{2j+3} C_{l,h,j+1}^m - \frac{(h+1)(h+l+1)}{2h+3} C_{l,h+1,j}^m \right] \quad (13.93)$$

for $h \neq j$ and $m = 0, 1, 2, \dots$;

$$C_{l,j,j}^{m+1} = - \sum_{h=1}^{m+1} \frac{Q_h^l(i\xi_1)}{Q_j^l(i\xi_1)} C_{l,h,j}^{m+1} + \sum_{h=0}^m \frac{Q_h^l(i\xi_1)}{Q_j^l(i\xi_1)} C_{l,h,j}^m + A_{j,l}^{m+1} \quad (13.94)$$

for $m = 0, 1, 2, \dots$, where \sum' indicates that the term $h = j$ is omitted from the summation; and

$$C_{0,0,0}^0 = A_{0,0}^0 = 0, \quad (13.95)$$

$A_{j,l}^m = 0$, for $m+j$ odd;

$$\begin{aligned} &= \frac{\sqrt{\pi}}{2^{m+1}} \frac{(i\xi_1 - \cos \zeta)^{m-1}}{\{\frac{1}{2}(m-j)\}! \{\frac{1}{2}(m+j+1)\}! Q_j^l(i\xi_1)} \frac{(j-l)!}{(j+l)!} \\ &\times \left\{ \varepsilon_l \cos \zeta \left[(m-j)(j-l+1) P_{j+1}^l \left(\frac{1-i\xi_1 \cos \zeta}{i\xi_1 - \cos \zeta} \right) + \right. \right. \\ &\left. \left. + (j+l)(m+j+1) P_{j-1}^l \left(\frac{1-i\xi_1 \cos \zeta}{i\xi_1 - \cos \zeta} \right) \right] - \frac{\xi_1 \sin \zeta}{\sqrt{(\xi_1^2 + 1)}} \right. \\ &\times \left[(j+l)(m+j+1) \left\{ P_{j-1}^{l+1} \left(\frac{1-i\xi_1 \cos \zeta}{i\xi_1 - \cos \zeta} \right) - (j+l)(j+l-1) P_{j-1}^{l-1} \left(\frac{1-i\xi_1 \cos \zeta}{i\xi_1 - \cos \zeta} \right) \right\} - \right. \end{aligned}$$

$$-(m-j)(j-l+1) \left\{ P_{j+1}^{l+1} \left(\frac{1-i\xi_1 \cos \zeta}{i\xi_1 - \cos \zeta} \right) - (j-l+1)(j-l+2) P_{j+1}^{l+2} \left(\frac{1-i\xi_1 \cos \zeta}{i\xi_1 - \cos \zeta} \right) \right\} \Big| \Big|, \\ \text{for } m+j \text{ even.} \quad (13.96)$$

In the far field ($\xi \rightarrow \infty$):

$$S = -ic \sum_{n=0}^{\infty} \sum_{m=0}^n (-c)^n \frac{(i\xi_1 - \eta)^{n-m}}{(n-m)!} \sum_{l=0}^m \sum_{j=0}^m C_{l,c,j}^m P_j^l(\eta) \cos l\phi. \quad (13.97)$$

Starting from the exact series solution, BURKE [1966b] has computed S through terms $O(k^6)$ for arbitrary angles of incidence and observation.

For axial incidence ($\zeta = \pi$):

$$V^s = e^{ic\xi} \sum_{n=0}^{\infty} \sum_{m=0}^n (-c)^n \frac{(i\xi_1 - \eta)^{n-m}}{(n-m)!} \sum_{h=0}^m \sum_{j=0}^m C_{0,h,j}^m Q_h(i\xi) P_j(\eta), \quad (13.98)$$

and in the far field ($\xi \rightarrow \infty$):

$$S = -ic \sum_{n=0}^{\infty} \sum_{m=0}^n (-c)^n \frac{(i\xi_1 - \eta)^{n-m}}{(n-m)!} \sum_{j=0}^m C_{0,0,j}^m P_j(\eta). \quad (13.99)$$

13.3.2.3. HIGH FREQUENCY APPROXIMATIONS

No specific results are available for arbitrary incidence, but for axial incidence, such that

$$V^i = e^{-ikz}, \quad (13.100)$$

the geometrical optics scattered field at a point (ξ, η, ϕ) located in the illuminated region $\{(\xi^2 + 1)(1 - \eta^2) > (\xi_1^2 + 1) \text{ when } \eta < 0\}$ is:

$$V_{g.o.}^s = \exp \{ic(F - \xi_1 \eta_1)\} \left[\left(1 + \frac{2F^2}{(\xi_1^2 + \eta_1^2)G} \right) \left(1 + \frac{2\xi_1^2 G}{\xi_1^2 + \eta_1^2} \right) \right]^{-\frac{1}{2}}, \quad (13.101)$$

where F and G are given by eqs. (13.16) and (13.18), and η_1 is the positive root of eq. (13.19) with $\xi_0 = \infty$. In the geometrical shadow $V_{g.o.}^s = 0$. In the far field ($\xi \rightarrow \infty$):

$$S_{g.o.} = \frac{c(\xi_1^2 + \eta_1^2)}{2\xi_1} \exp \{ -ic[\xi_1 \eta_1(1 + \eta) + \sqrt{(\xi_1^2 + 1)(1 - \eta_1^2)(1 - \eta^2)}] \}. \quad (13.102)$$

In particular, if the observation point is on the z -axis ($\eta = 1$):

$$V_{g.o.}^s = \frac{\xi_1^2 + 1}{2\xi\xi_1 - \xi_1^2 + 1} e^{ic(\xi - 2\xi_1)}, \quad (13.103)$$

and in the far field ($\xi \rightarrow \infty$):

$$S_{g.o.} = \frac{c(\xi_1^2 + 1)}{2\xi_1} e^{-2ic\xi_1}, \quad (13.104)$$

so that the geometrical optics back scattering cross section is:

$$\sigma_{g.o.} = \frac{\pi c^2}{k^2} (\xi_1 + \xi_1^{-1})^2. \quad (13.105)$$

A more refined approximation, in which an asymptotic expression for the diffracted field is retained, can be derived by means of Keller's geometrical theory of diffraction; however, no specific results are available.

The total scattering cross section for axial incidence ($\zeta = \pi$) is (JONES [1957]):

$$\sigma_T \sim \frac{2\pi c^2}{k^2} (\xi_1^2 + 1) \{1 - 0.8640 [c(\xi_1 + \xi_1^{-1})]^{-1}\}; \quad (13.106)$$

this result is a good approximation if:

$$c(\xi_1 + \xi_1^{-1}) \gg 1. \quad (13.107)$$

13.3.2.4. SHAPE APPROXIMATION

For a spheroid whose surface $\xi = \xi_1$ is defined in terms of the spherical polar coordinates (r_1, θ_1, ϕ_1) by the equation

$$r_1 = a \left(\frac{\xi_1^2 + 1}{\xi_1^2 + \cos^2 \theta_1} \right)^{1/2}, \quad (13.108)$$

and is such that

$$\xi_1^2 + 1 \gg 1, \quad (13.109)$$

i.e. the spheroid departs only infinitesimally from the sphere $r_1 = a$, the scattered field may be expressed as a perturbation of the solution for this sphere.

For incidence at an angle ζ with respect to the positive z -axis, such that

$$V^i = \exp \{ik(x \sin \zeta + z \cos \zeta)\}, \quad (13.110)$$

then

$$V^s \sim - \sum_{m=0}^{\infty} \sum_{n=m}^{\infty} \epsilon_m \frac{(n-m)!}{(n+m)!} \frac{i^n}{h_n^{(1)'}(ka)} \left[(2n+1)j_n'(ka) - \frac{i}{\xi_1^2 + 1} b_{mn}(\zeta) \right] \\ \times h_n^{(1)}(kr) P_n^m(\cos \zeta) P_n^m(\cos \theta) \cos m\phi + O[(\xi_1^2 + 1)^{-2}], \quad (13.111)$$

where

$$b_{mn}(\zeta) = \frac{1}{(ka)^3 h_n^{(1)'}(ka)} \left\{ \frac{[(2n+1)[(ka)^2(n^2 + n - 1 + m^2) - n^2(n+1)^2 - m^2(n^2 + n - 3)]}{(2n+3)(2n-1)} + \right. \\ + \frac{(n+m-1)(n+m)(k^2 a^2 - n^2 + n + 2)}{2(2n-1)} \frac{h_n^{(1)'}(ka)}{h_{n-2}^{(1)'}(ka)} \frac{P_{n-2}^m(\cos \zeta)}{P_n^m(\cos \zeta)} + \\ \left. + \frac{(n-m+1)(n-m+2)(k^2 a^2 - n^2 - 3n)}{2(2n+3)} \frac{h_n^{(1)'}(ka)}{h_{n+2}^{(1)'}(ka)} \frac{P_{n+2}^m(\cos \zeta)}{P_n^m(\cos \zeta)} \right\}. \quad (13.112)$$

In the far back scattered field ($r \rightarrow \infty$, $\theta = \pi - \zeta$, $\phi = \pi$):

$$S \sim \sum_{m=0}^{\infty} \sum_{n=m}^{\infty} \varepsilon_m \frac{(n-m)!}{(n+m)!} \frac{(-1)^n}{h_n^{(1)'}(ka)} \left[i(2n+1)j_n'(ka) + \frac{1}{\xi_1^2 + 1} b_{mn}(\zeta) \right] \times [P_n^m(\cos \zeta)]^2 + O[(\xi_1^2 + 1)^{-2}]. \quad (13.113)$$

For axial incidence ($\zeta = \pi$):

$$V^s \sim - \sum_{n=0}^{\infty} \frac{(-i)^n}{h_n^{(1)'}(ka)} \left[(2n+1)j_n'(ka) - \frac{i}{\xi_1^2 + 1} b_{0n}(\pi) \right] h_n^{(1)}(kr) P_n(\cos \theta) + O[(\xi_1^2 + 1)^{-2}], \quad (13.114)$$

where

$$b_{0n}(\pi) = \frac{1}{(ka)^3 h_n^{(1)'}(ka)} \left\{ \frac{[(2n+1)(ka)^2(n^2+n-1) - n^2(n+1)^2]}{(2n+3)(2n-1)} + \frac{n(n-1)(k^2 a^2 - n^2 + n + 2)}{2(2n-1)} \frac{h_n^{(1)'}(ka)}{h_{n-2}^{(1)'}(ka)} + \frac{(n+1)(n+2)(k^2 a^2 - n^2 - 3n)}{2(2n+3)} \frac{h_n^{(1)'}(ka)}{h_{n+2}^{(1)'}(ka)} \right\}, \quad (13.115)$$

and in the far back scattered field:

$$S \sim \sum_{n=0}^{\infty} \frac{(-1)^n}{h_n^{(1)'}(ka)} \left[i(2n+1)j_n'(ka) + \frac{1}{\xi_1^2 + 1} b_{0n}(\pi) \right] + O[(\xi_1^2 + 1)^{-2}]. \quad (13.116)$$

13.4. Perfectly conducting spheroid

13.4.1. Dipole sources

13.4.1.1. EXACT SOLUTIONS

Results are available only in the case of a dipole on the z -axis and axially oriented. For an electric dipole at $(\xi_0, \eta_0 = 1)$ with moment $(4\pi\epsilon/k)\hat{z}$, corresponding to an incident electric Hertz vector $\hat{z}e^{ikR}/(kR)$, such that

$$H_{\phi}^i = -k^2 c Y \frac{e^{ikR}}{kR} \left(1 + \frac{i}{kR} \right) \frac{1}{kR} \sqrt{(\xi^2 + 1)(1 - \eta^2)}, \quad (13.117)$$

$$H_{\xi}^i = H_{\eta}^i = E_{\phi}^i = 0,$$

then

$$H_{\phi}^i + H_{\phi}^s = \frac{2k^2 Y}{\sqrt{(\xi_0^2 + 1)}} \sum_{n=0}^{\infty} (-i)^n \frac{1}{\tilde{\rho}_{1n} \tilde{N}_{1n}} \left[R_{1n}^{(1)}(-ic, i\xi_0) - \frac{\partial}{\partial \xi_1} \left\{ \sqrt{\xi_1^2 + 1} R_{1n}^{(1)}(-ic, i\xi_1) \right\} \right. \\ \left. \times R_{1n}^{(3)}(-ic, i\xi_0) \right] R_{1n}^{(3)}(-ic, i\xi_0) S_{1n}(-ic, \eta). \quad (13.118)$$

On the surface $\xi = \xi_1$:

$$H_\phi^i + H_\phi^s = \frac{2k^2 Y}{c\sqrt{(\xi_0^2+1)(\xi_1^2+1)}} \sum_{n=0}^{\infty} (-i)^{n+1} \frac{1}{\tilde{\rho}_{1n} \tilde{N}_{1n}} \left[\frac{\partial}{\partial \xi_1} \{ \sqrt{\xi_1^2+1} R_{1n}^{(3)}(-ic, i\xi_1) \} \right]^{-1} \times R_{1n}^{(3)}(-ic, i\xi_0) S_{1n}(-ic, \eta). \quad (13.119)$$

In the far field ($\xi \rightarrow \infty$):

$$H_\phi^i + H_\phi^s = \frac{e^{ic\xi}}{c\xi} \frac{2ik^2 Y}{\sqrt{(\xi_0^2+1)}} \sum_{n=0}^{\infty} (-1)^{n-1} \frac{1}{\tilde{\rho}_{1n} \tilde{N}_{1n}} \left[R_{1n}^{(1)}(-ic, i\xi_0) - \frac{\frac{\partial}{\partial \xi_1} \{ \sqrt{\xi_1^2+1} R_{1n}^{(1)}(-ic, i\xi_1) \}}{\frac{\partial}{\partial \xi_1} \{ \sqrt{\xi_1^2+1} R_{1n}^{(3)}(-ic, i\xi_1) \}} R_{1n}^{(3)}(-ic, i\xi_0) \right] S_{1n}(-ic, \eta). \quad (13.120)$$

If the dipole is on the surface ($\xi_0 = \xi_1$):

$$H_\phi^i + H_\phi^s = \frac{2k^2 Y}{c(\xi_1^2+1)} \sum_{n=0}^{\infty} (-i)^{n-1} \frac{1}{\tilde{\rho}_{1n} \tilde{N}_{1n}} \left[\frac{\partial}{\partial \xi_1} \{ \sqrt{\xi_1^2+1} R_{1n}^{(3)}(-ic, i\xi_1) \} \right]^{-1} \times R_{1n}^{(3)}(-ic, i\xi) S_{1n}(-ic, \eta). \quad (13.121)$$

If also the observation point is on the surface ($\xi = \xi_1$):

$$H_\phi^i + H_\phi^s = \frac{2k^2 Y}{c(\xi_1^2+1)} \sum_{n=0}^{\infty} (-i)^{n-1} \frac{1}{\tilde{\rho}_{1n} \tilde{N}_{1n}} \left[\frac{\partial}{\partial \xi_1} \{ \sqrt{\xi_1^2+1} R_{1n}^{(3)}(-ic, i\xi_1) \} \right]^{-1} \times R_{1n}^{(3)}(-ic, i\xi_1) S_{1n}(-ic, \eta), \quad (13.122)$$

whereas in the far field ($\xi \rightarrow \infty$):

$$H_\phi^i + H_\phi^s = \frac{e^{ic\xi}}{c\xi} \frac{2k^2 Y}{c(\xi_1^2+1)} \sum_{n=0}^{\infty} (-i)^n \frac{1}{\tilde{\rho}_{1n} \tilde{N}_{1n}} \left[\frac{\partial}{\partial \xi_1} \{ \sqrt{\xi_1^2+1} R_{1n}^{(3)}(-ic, i\xi_1) \} \right]^{-1} \times S_{1n}(-ic, \eta). \quad (13.123)$$

For a magnetic dipole at $(\xi_0, \eta_0 = 1)$ with moment $(4\pi/k)\hat{z}$, corresponding to an incident magnetic Hertz vector $\hat{z}e^{ikR}/(kR)$, such that

$$E_\phi^i = k^2 c Z \frac{e^{ikR}}{kR} \left(1 + \frac{i}{kR} \right) \frac{1}{kR} \sqrt{(\xi^2+1)(1-\eta^2)}, \quad (13.124)$$

$$E_\xi^i = E_\eta^i = H_\phi^i = 0,$$

then

$$E_{\phi}^i + E_{\phi}^s = - \frac{2k^2 Z}{\sqrt{(\xi_0^2 + 1)}} \sum_{n=0}^{\infty} (-i)^n \frac{1}{\tilde{\rho}_{1n} \tilde{N}_{1n}} \left[R_{1n}^{(1)}(-ic, i\xi_0) - \frac{R_{1n}^{(1)}(-ic, i\xi_1)}{R_{1n}^{(3)}(-ic, i\xi_1)} R_{1n}^{(3)}(-ic, i\xi_0) \right] R_{1n}^{(3)}(-ic, i\xi_1) S_{1n}(-ic, \eta). \quad (13.125)$$

On the surface $\xi = \xi_1$:

$$H_{\eta}^i + H_{\eta}^s = \frac{2k^2}{c^2 \sqrt{(\xi_0^2 + 1)(\xi_1^2 + 1)(\xi_1^2 + \eta^2)}} \sum_{n=0}^{\infty} (-i)^n \frac{1}{\tilde{\rho}_{1n} \tilde{N}_{1n}} \frac{R_{1n}^{(3)}(-ic, i\xi_0)}{R_{1n}^{(3)}(-ic, i\xi_1)} S_{1n}(-ic, \eta). \quad (13.126)$$

In the far field ($\xi \rightarrow \infty$):

$$E_{\phi}^i + E_{\phi}^s = \frac{e^{ic\xi}}{c\xi} \frac{2ik^2 Z}{\sqrt{(\xi_0^2 + 1)}} \sum_{n=0}^{\infty} (-1)^n \frac{1}{\tilde{\rho}_{1n} \tilde{N}_{1n}} \times \left[R_{1n}^{(1)}(-ic, i\xi_0) - \frac{R_{1n}^{(1)}(-ic, i\xi_1)}{R_{1n}^{(3)}(-ic, i\xi_1)} R_{1n}^{(3)}(-ic, i\xi_0) \right] S_{1n}(-ic, \eta). \quad (13.127)$$

If the dipole is on the surface ($\xi_0 = \xi_1$), the electromagnetic field components are identically zero everywhere.

13.4.1.2. LOW FREQUENCY APPROXIMATIONS

A general procedure for the determination of successive terms in the low frequency expansion of the scattered field has been given by STEVENSON [1953a]; however, no specific results are available.

13.4.1.3. HIGH FREQUENCY APPROXIMATIONS

Although the geometrical and physical optics approximations to the scattered field are derivable by standard techniques, no specific results are available.

13.4.2. Plane wave incidence

13.4.2.1. EXACT SOLUTIONS

For arbitrary direction of incidence, the coefficients in the vector wave function expansion of the scattered field must be determined from an infinite set of infinite systems of equations; no specific results have been found. In the particular case of axial incidence ($\zeta = \pi$), the coefficients may be obtained by the inversion of a single infinite matrix.

13.4.2.2. LOW FREQUENCY APPROXIMATIONS

Using the general procedure for the determination of the low frequency expansion given by STEVENSON [1953a], explicit results have been obtained for the far field corresponding to a plane wave incident in an arbitrary direction and with arbitrary polarization, such that

$$\begin{aligned} E^i &= (l_1 \hat{x} + m_1 \hat{y} + n_1 \hat{z}) e^{ik(lx + my + nz)}, \\ H^i &= Y(l_2 \hat{x} + m_2 \hat{y} + n_2 \hat{z}) e^{ik(lx + my + nz)}, \end{aligned} \quad (13.128)$$

where (l, m, n) , (l_1, m_1, n_1) and (l_2, m_2, n_2) are three sets of direction cosines satisfying the relations

$$\begin{aligned} l_1 \hat{x} + m_1 \hat{y} + n_1 \hat{z} &= (l_2 \hat{x} + m_2 \hat{y} + n_2 \hat{z}) \wedge (l \hat{x} + m \hat{y} + n \hat{z}), \\ l_2 \hat{x} + m_2 \hat{y} + n_2 \hat{z} &= (l \hat{x} + m \hat{y} + n \hat{z}) \wedge (l_1 \hat{x} + m_1 \hat{y} + n_1 \hat{z}). \end{aligned} \quad (13.129)$$

The scattered electric field in the far zone may be written as:

$$\begin{aligned} E_\theta^s &= \frac{e^{ikr}}{kr} \sum_{m=0}^{\infty} \sum_{n=1}^{\infty} \left[\left(\alpha_{mn} \frac{\partial P_n^m(\cos \theta)}{\partial \theta} + m \beta_{mn} \frac{P_n^m(\cos \theta)}{\sin \theta} \right) \cos m\phi + \right. \\ &\quad \left. + \left(\bar{\beta}_{mn} \frac{\partial P_n^m(\cos \theta)}{\partial \theta} - m \bar{\alpha}_{mn} \frac{P_n^m(\cos \theta)}{\sin \theta} \right) \sin m\phi \right], \end{aligned} \quad (13.130)$$

$$\begin{aligned} E_\phi^s &= -\frac{e^{ikr}}{kr} \sum_{m=0}^{\infty} \sum_{n=1}^{\infty} \left[\left(\bar{\alpha}_{mn} \frac{\partial P_n^m(\cos \theta)}{\partial \theta} - m \beta_{mn} \frac{P_n^m(\cos \theta)}{\sin \theta} \right) \cos m\phi + \right. \\ &\quad \left. + \left(\beta_{mn} \frac{\partial P_n^m(\cos \theta)}{\partial \theta} + m \alpha_{mn} \frac{P_n^m(\cos \theta)}{\sin \theta} \right) \sin m\phi \right], \end{aligned} \quad (13.131)$$

where (r, θ, ϕ) are the spherical polar coordinates of the observation point and the incident electric field has unit amplitude. Expressions have been worked out (STEVENSON [1953b]) for the coefficients α_{mn} , β_{mn} , $\bar{\alpha}_{mn}$ and $\bar{\beta}_{mn}$ through terms $O(k^5)$. Explicitly,

$$\alpha_{01} = k^3 K_3 + k^5 L_3, \quad (13.132)$$

$$\alpha_{02} = -\frac{1}{3} k^5 (M_1 + M_2 - 2M_3), \quad (13.133)$$

$$\alpha_{03} = \frac{1}{300} k^5 d^2 K_3, \quad (13.134)$$

$$\alpha_{11} = k^3 K_1 + k^5 L_1, \quad (13.135)$$

$$\alpha_{12} = \frac{1}{3} k^5 N_2, \quad (13.136)$$

$$\alpha_{13} = \frac{1}{900} k^5 d^2 K_1, \quad (13.137)$$

$$\beta_{11} = k^3 K_2 + k^5 L_2, \quad (13.138)$$

$$\beta_{12} = \frac{1}{3} k^5 N_1, \quad (13.139)$$

$$\beta_{13} = \frac{1}{900} k^5 d^2 K_2, \quad (13.140)$$

$$\alpha_{22} = \frac{1}{6} k^5 (M_1 - M_2), \quad (13.141)$$

$$\beta_{22} = \frac{1}{6} k^5 N_3, \quad (13.142)$$

with all other coefficients zero through $O(k^5)$. The corresponding "barred" quantities are obtained by "barring" the K_j , L_j , M_j and N_j , $j = 1, 2$ or 3 . The K_j , L_j , M_j and N_j and their "barred" analogues are complicated functions of the direction and polarization of the incident field, and of the spheroid parameters, and their expressions are given by (STEVENSON [1953b], SENIOR [1966]):

where (l, m, n) , (l_1, m_1, n_1) and (l_2, m_2, n_2) are three sets of direction cosines satisfying the relations

$$\begin{aligned} l_1 \hat{x} + m_1 \hat{y} + n_1 \hat{z} &= (l_2 \hat{x} + m_2 \hat{y} + n_2 \hat{z}) \wedge (l \hat{x} + m \hat{y} + n \hat{z}), \\ l_2 \hat{x} + m_2 \hat{y} + n_2 \hat{z} &= (l \hat{x} + m \hat{y} + n \hat{z}) \wedge (l_1 \hat{x} + m_1 \hat{y} + n_1 \hat{z}). \end{aligned} \quad (13.129)$$

The scattered electric field in the far zone may be written as:

$$\begin{aligned} E_\theta^s &= \frac{e^{ikr}}{kr} \sum_{m=0}^{\infty} \sum_{n=1}^{\infty} \left[\left(\alpha_{mn} \frac{\partial P_n^m(\cos \theta)}{\partial \theta} + m \bar{\beta}_{mn} \frac{P_n^m(\cos \theta)}{\sin \theta} \right) \cos m\phi + \right. \\ &\quad \left. + \left(\beta_{mn} \frac{\partial P_n^m(\cos \theta)}{\partial \theta} - m \bar{\alpha}_{mn} \frac{P_n^m(\cos \theta)}{\sin \theta} \right) \sin m\phi \right], \end{aligned} \quad (13.130)$$

$$\begin{aligned} E_\phi^s &= -\frac{e^{ikr}}{kr} \sum_{m=0}^{\infty} \sum_{n=1}^{\infty} \left[\left(\bar{\alpha}_{mn} \frac{\partial P_n^m(\cos \theta)}{\partial \theta} - m \beta_{mn} \frac{P_n^m(\cos \theta)}{\sin \theta} \right) \cos m\phi + \right. \\ &\quad \left. + \left(\bar{\beta}_{mn} \frac{\partial P_n^m(\cos \theta)}{\partial \theta} + m \alpha_{mn} \frac{P_n^m(\cos \theta)}{\sin \theta} \right) \sin m\phi \right]. \end{aligned} \quad (13.131)$$

where (r, θ, ϕ) are the spherical polar coordinates of the observation point and the incident electric field has unit amplitude. Expressions have been worked out (STEVENSON [1953b]) for the coefficients α_{mn} , β_{mn} , $\bar{\alpha}_{mn}$ and $\bar{\beta}_{mn}$ through terms $O(k^5)$. Explicitly,

$$\alpha_{01} = k^3 K_3 + k^5 L_3, \quad (13.132)$$

$$\alpha_{02} = -\frac{1}{3}k^5(M_1 + M_2 - 2M_3), \quad (13.133)$$

$$\alpha_{03} = \frac{1}{300}k^5 d^2 K_3, \quad (13.134)$$

$$\alpha_{11} = k^3 K_1 + k^5 L_1, \quad (13.135)$$

$$\alpha_{12} = \frac{1}{3}k^5 N_2, \quad (13.136)$$

$$\alpha_{13} = \frac{1}{900}k^5 d^2 K_1, \quad (13.137)$$

$$\beta_{11} = k^3 K_2 + k^5 L_2, \quad (13.138)$$

$$\beta_{12} = \frac{1}{3}k^5 N_1, \quad (13.139)$$

$$\beta_{13} = \frac{1}{900}k^5 d^2 K_2, \quad (13.140)$$

$$\alpha_{22} = \frac{1}{6}k^5(M_1 - M_2), \quad (13.141)$$

$$\beta_{22} = \frac{1}{6}k^5 N_3, \quad (13.142)$$

with all other coefficients zero through $O(k^5)$. The corresponding "barred" quantities are obtained by "barring" the K_j , L_j , M_j and N_j , $j = 1, 2$ or 3 . The K_j , L_j , M_j and N_j and their "barred" analogues are complicated functions of the direction and polarization of the incident field, and of the spheroid parameters, and their expressions are given by (STEVENSON [1953b], SENIOR [1966]):

$$K_1 = -\frac{1}{12}id^3l_1 \frac{P_1^1}{Q_1^1}, \quad (13.143)$$

$$K_2 = -\frac{1}{12}id^3m_1 \frac{P_1^1}{Q_1^1}, \quad (13.144)$$

$$K_3 = \frac{1}{24}id^3n_1 \frac{P_1^0}{Q_1^0}, \quad (13.145)$$

$$L_1 = \frac{-id^5}{2400} \frac{P_1^1}{Q_1^1} \left\{ l_1 \left[22 - 5(l^2 + m^2) + \frac{4}{3} \left(\frac{P_3^1}{P_1^1} - \frac{Q_3^1}{Q_1^1} \right) - \frac{50}{3} \frac{Q_{-1}^1}{Q_1^1} \right] + 5mn_2 \right\}, \quad (13.146)$$

$$L_2 = \frac{-id^5}{2400} \frac{P_1^1}{Q_1^1} \left\{ m_1 \left[22 - 5(m^2 + n^2) + \frac{4}{3} \left(\frac{P_3^1}{P_1^1} - \frac{Q_3^1}{Q_1^1} \right) - \frac{50}{3} \frac{Q_{-1}^1}{Q_1^1} \right] + 5nl_2 \right\}, \quad (13.147)$$

$$L_3 = \frac{-id^5}{4800} n_1 \frac{P_1^0}{Q_1^0} \left[14 + 5(l^2 + m^2) - 4 \left(\frac{P_3^0}{P_1^0} - \frac{Q_3^0}{Q_1^0} \right) + 7 \frac{P_0^0}{Q_1^0} \right], \quad (13.148)$$

$$M_1 = \frac{-id^5}{8640} \left[6(ll_1 - mm_1) \frac{P_2^2}{Q_2^2} - nn_1 \frac{P_2^0}{Q_2^0} \right], \quad (13.149)$$

$$M_2 = \frac{-id^5}{8640} \left[6(rn_1 - nn_1) \frac{P_2^2}{Q_2^2} - ll_1 \frac{P_2^0}{Q_2^0} \right], \quad (13.150)$$

$$M_3 = \frac{-id^5}{4320} nn_1 \frac{P_2^0}{Q_2^0}, \quad (13.151)$$

$$N_1 = \frac{id^5}{2880} \left[(nn_1 + nm_1) \frac{P_2^1}{Q_2^1} + 5l_2 \frac{P_1^{1'}}{Q_1^{1'}} \right], \quad (13.152)$$

$$N_2 = \frac{id^5}{2880} \left[(nl_1 + ln_1) \frac{P_2^1}{Q_2^1} + 5m_2 \frac{P_1^{1'}}{Q_1^{1'}} \right], \quad (13.153)$$

$$N_3 = \frac{-id^5}{720} (lm_1 + ml_1) \frac{P_2^2}{Q_2^2}, \quad (13.154)$$

where the argument of the Legendre functions is $(i\xi_1)$. The constants K_j , L_j , M_j and N_j are obtained from the corresponding unbarred quantities by making the substitutions

$$\begin{aligned} (l_1, m_1, n_1) &\rightarrow (l_2, m_2, n_2) \\ (l_2, m_2, n_2) &\rightarrow -(l_1, m_1, n_1), \end{aligned} \quad (13.155)$$

and by replacing the Legendre functions with their first derivatives and vice versa.

In the particular case of axial incidence, such that

$$E^i = \mathbf{x}e^{-ikz}, \quad H^i = -\mathbf{y}Ye^{-ikz}, \quad (13.156)$$

eqs. (13.130) and (13.131) reduce to:

$$E^s = \frac{e^{ikr}}{kr} \sum_{n=1}^{\infty} \left[\left(\alpha_{1n} \frac{\partial P_n^1(\cos \theta)}{\partial \theta} + \beta_{1n} \frac{P_n^1(\cos \theta)}{\sin \theta} \right) \cos \phi \hat{\theta} - \left(\beta_{1n} \frac{\partial P_n^1(\cos \theta)}{\partial \theta} + \alpha_{1n} \frac{P_n^1(\cos \theta)}{\sin \theta} \right) \sin \phi \hat{\phi} \right], \quad (13.157)$$

with

$$\alpha_{11} = -\frac{2}{3}ic^3 \frac{P_1^1}{Q_1^1} \left[1 + \frac{1}{5}c^2 \left(22 - 10 \frac{Q_{-1}^1}{Q_1^1} \right) \right], \quad (13.158)$$

$$\alpha_{12} = -\frac{1}{27}ic^5 \left(\frac{P_2^1}{Q_2^1} - 5 \frac{P_1^{1'}}{Q_1^{1'}} \right), \quad (13.159)$$

$$\alpha_{13} = -\frac{2}{675}ic^5 \frac{P_1^1}{Q_1^1}, \quad (13.160)$$

$$\beta_{11} = \frac{2}{3}ic^3 \frac{P_1^{1'}}{Q_1^{1'}} \left[1 + \frac{1}{5}c^2 \left(22 - 10 \frac{Q_{-1}^{1'}}{Q_1^{1'}} - 40 \frac{Q_0^1}{Q_1^{1'}} \right) \right], \quad (13.161)$$

$$\beta_{12} = \frac{1}{27}ic^5 \left(\frac{P_2^{1'}}{Q_2^{1'}} - 5 \frac{P_1^1}{Q_1^1} \right), \quad (13.162)$$

$$\beta_{13} = \frac{2}{675}ic^5 \frac{P_1^{1'}}{Q_1^{1'}}, \quad (13.163)$$

where the argument of the Legendre functions is $(i\xi_1)$, and all other coefficients are zero through $O(c^5)$.

By retaining only the dominant term $O(c^3)$ in eq. (13.157), and specializing to the case $\theta = 0$, we obtain the Rayleigh back scattering cross section (STRUTT [1897]):

$$\sigma \sim \frac{\pi}{36} k^4 d^6 \left| \frac{P_1^{1'}(i\xi_1)}{Q_1^{1'}(i\xi_1)} - \frac{P_1^1(i\xi_1)}{Q_1^1(i\xi_1)} \right|^2. \quad (13.164)$$

A numerical approximation to eq. (13.164) has been proposed by SIEGEL [1959] in the form

$$\sigma \sim \frac{4}{\pi} k^4 v^2 \left(1 + \frac{\exp \left\{ -\sqrt{(1+\xi_1^{-2})} \right\}}{\pi \sqrt{(1+\xi_1^{-2})}} \right)^2, \quad (13.165)$$

where $v = \frac{1}{6}\pi d^3 \xi_1 (\xi_1^2 + 1)$ is the volume of the spheroid.

The near-zone ($kr \ll 1$) scattered fields have been derived by TAI [1952a, b] for the case of axial incidence ($\zeta = \pi$) and through terms $O[(kr)^2]$. The dominant terms in the surface field expressions for the case of broadside incidence ($\zeta = \frac{1}{2}\pi$) have been given by BOLLJAHN [1950].

13.4.2.3. HIGH FREQUENCY APPROXIMATIONS

For a wave of arbitrary polarization incident from the half-plane $\phi = 0$ at an angle ζ with the positive z -axis, the geometrical optics bistatic cross section in the direction ($\theta = \arccos \eta$, $\phi = 0$) is (CRISPIN et al. [1959]):

$$\sigma_{g.o.}(\theta) = \pi(\frac{1}{2}d\xi_1)^2 \left[\frac{\xi_1^2 + 1}{\xi_1^2 + \cos^2 \{\frac{1}{2}(\zeta - \theta)\}} \right]^2. \quad (13.166)$$

For axial incidence ($\zeta = \pi$), the back scattering cross section is

$$\sigma_{g.o.} \equiv \sigma_{g.o.}(0) = \pi \left[\frac{d(\xi_1^2 + 1)}{2\xi_1} \right]^2, \quad (13.167)$$

whereas in a direction arbitrarily close to forward scattering ($\theta \rightarrow \pi$):

$$\sigma_{g.o.}(\pi) = \pi(\frac{1}{2}d\xi_1)^2. \quad (13.168)$$

An expression for the physical optics bistatic cross section is available for a receiver in the plane containing the direction of incidence and the z -axis (SIEGEL et al. [1955]), viz.

$$\sigma_{p.o.}(\theta) = \sigma_{g.o.}(\theta) \left[1 - 2 \frac{\sin(2M)}{2M} + \frac{\sin^2 M}{M^2} \right], \quad (13.169)$$

where

$$M = c[\sin \frac{1}{2}(\zeta + \theta)] \sqrt{\{\xi_1^2 + \cos^2 [\frac{1}{2}(\zeta - \theta)]\}}; \quad (13.170)$$

this result is only valid if ζ and θ satisfy the condition:

$$\tan \frac{1}{2}(\zeta + \theta) = 2 \frac{\xi_1^2 + \cos^2 [\frac{1}{2}(\zeta - \theta)]}{\sin(\zeta - \theta)}. \quad (13.171)$$

A more refined approximation, in which an asymptotic expression for the diffracted field is retained, can be derived for the back scattered field with axial incidence by means of Keller's geometrical theory of diffraction; however, no specific results are available.

The total scattering cross section for axial incidence ($\zeta = \pi$) is (JONES [1957]):

$$\sigma_T \sim \frac{2\pi c^2}{k^2} (\xi_1^2 + 1) \{1 + 0.0661 [c(\xi_1 + \xi_1^{-1})]^{-\frac{1}{2}}\}; \quad (13.172)$$

this result is a good approximation if:

$$c(\xi_1 + \xi_1^{-1}) \gg 1. \quad (13.173)$$

13.4.2.4. SHAPE APPROXIMATION

For a spheroid whose surface $\xi = \xi_1$ is defined in terms of the spherical polar coordinates (r_1 , θ_1 , ϕ_1) by the equation

$$r_1 = a \left(\frac{\xi_1^2 + 1}{\xi_1^2 + \cos^2 \theta_1} \right)^{\frac{1}{2}}, \quad (13.174)$$

and is such that

$$\xi_1^2 + 1 \gg 1, \quad (13.175)$$

i.e. the spheroid departs only infinitesimally from the sphere $r_1 = a$, the scattered field may be expressed as a perturbation of the solution for this sphere.

The scattered field corresponding to an incident wave with arbitrary polarization and whose direction of propagation forms an angle ζ with the positive z -axis has been derived by MUSHIAKE [1956]. For the particular case of backscattering, the cross sections σ_{\parallel} and σ_{\perp} corresponding to an incident electric field respectively parallel and perpendicular to the plane of the direction of propagation and the z -axis are:

$$\sigma_{\parallel, \perp} \sim \pi a^2 \left| (ka)^{-2} \sum_{n=1}^{\infty} \frac{(-1)^n (2n+1)}{h_n^{(1)}(ka) \zeta'_n} + \frac{1}{\xi_1^2 + 1} A_{\parallel, \perp} \right|^2 + O[(\xi_1^2 + 1)^{-2}], \quad (13.176)$$

where

$$\zeta_n = kah_n^{(1)}(ka), \quad (13.177)$$

the prime indicates the derivative with respect to ka , and (MUSHIAKE [1956]):

$$\begin{aligned} A_{\parallel} = & \sum_{m=0}^{\infty} \sum_{n=m}^{\infty} \left\{ \frac{i^n}{\zeta_n} \frac{m P_n^m(\cos \zeta)}{\sin \zeta} \sum_{l=m}^{\infty} \frac{1}{2} l! m \left[\frac{i}{\zeta'_l} \frac{\partial P_l^m(\cos \zeta)}{\partial \zeta} I_{nl}^{2m} - \frac{1}{\zeta_l} \frac{P_l^m(\cos \zeta)}{\sin \zeta} I_{nl}^{1m} \right] + \right. \\ & + \frac{i^n}{\zeta'_n} \frac{\partial P_n^m(\cos \zeta)}{\partial \zeta} \sum_{l=m}^{\infty} \frac{1}{2} l! \left[\frac{1}{\zeta'_l} \left(\left[\frac{l(l+1)}{(ka)^2} - 1 \right] I_{nl}^{1m} + \frac{l(l+1)}{(ka)^2} I_{nl}^{4m} \right) \frac{\partial P_l^m(\cos \zeta)}{\partial \zeta} - \right. \\ & \left. \left. - \frac{i}{\zeta_l} \frac{m^2 P_l^m(\cos \zeta)}{\sin \zeta} I_{nl}^{2m} \right] \right\}; \quad (13.178) \end{aligned}$$

A_{\perp} is obtained from A_{\parallel} by interchanging $[m P_l^m(\cos \zeta)/\sin \zeta]$ and $[-\partial P_l^m(\cos \zeta)/\partial \zeta]$ with $j = n$ or l in eq. (13.178),

$$I_{nl}^{1m} = M \int_0^{\pi} \left(\frac{\partial P_n^m}{\partial \theta} \frac{\partial P_l^m}{\partial \theta} + m^2 \frac{P_n^m P_l^m}{\sin^2 \theta} \right) \sin^3 \theta d\theta, \quad (13.179)$$

$$I_{nl}^{2m} = M \int_0^{\pi} \left(\frac{\partial P_n^m}{\partial \theta} P_l^m + \frac{\partial P_l^m}{\partial \theta} P_n^m \right) \sin^2 \theta d\theta, \quad (13.180)$$

$$I_{nl}^{4m} = M \int_0^{\pi} \frac{\partial P_n^m}{\partial \theta} P_l^m \sin 2\theta \sin \theta d\theta, \quad (13.181)$$

and

$$M = c_m \frac{(2n+1)(n-m)!(2l+1)(l-m)!}{n(n+1)(n+m)!l(l+1)(l+m)!}. \quad (13.182)$$

Bibliography

- AR, E. and R. E. KLEINMAN [1966], The Exterior Neumann Problem for the Three-Dimensional Helmholtz Equation, *Arch. Rational Mech. Anal.* **23**, 218-236.
- ASVESTAS, J. S. and R. E. KLEINMAN [1967], Low Frequency Scattering by Spheroids and Disks, The University of Michigan Radiation Laboratory Report No. 7133-5-T, Ann Arbor, Michigan.
- BOLLJAHN, J. T. [1950], Small Dipole-Type Antennas, Stanford Research Institute Technical Report No. 14, Stanford, California.
- BRUNDRIT, G. B. [1965], A Solution to the Problem of Scalar Scattering from a Smooth, Bounded Obstacle using Integral Equations, *Quart. J. Mech. Appl. Math.* **18**, 473-489. It is unclear what normalization has been used in plotting $|S|$; see, also, comment in Chapter 11.
- BURKE, J. E. [1966a], Low-Frequency Scattering by Soft Spheroids, *J. Acoust. Soc. Am.* **39**, 826-831.
- BURKE, J. E. [1966b], Long-Wavelength Scattering by Hard Spheroids, *J. Acoust. Soc. Am.* **40**, 325-330.
- CRISPIN JR., J. W., R. F. GOODRICH and K. M. SIEGEL [1959], A Theoretical Method for the Calculation of the Radar Cross Sections of Aircraft and Missiles, The University of Michigan Radiation Laboratory Report No. 2591-1-H, Ann Arbor, Michigan.
- FLAMMER, C. [1957], *Spheroidal Wave Functions*, Stanford University Press, Stanford, California.
- GOODRICH, R. F., N. D. KAZARINOFF and V. H. WESTON [1963], Scalar Diffraction by a Thin, Oblate Spheroid, in: *Electromagnetic Theory and Antennas*, ed. E. C. Jordan, 27-38, Pergamon Press, Oxford. For a criticism of this paper see KELLER and HANSEN [1965].
- JONES, D. S. [1957], High-Frequency Scattering of Electromagnetic Waves, *Proc. Roy. Soc. A* **240**, 206-213.
- KELLER, J. B. and E. B. HANSEN [1965], Survey of the Theory of Diffraction of Short Waves by Edges, *Acta Phys. Polon.* **27**, 217-234.
- KLEINMAN, R. E. [1965a], The Dirichlet Problem for the Helmholtz Equation, *Arch. Rational Mech. Anal.* **18**, 205-229.
- KLEINMAN, R. E. [1965b], Low Frequency Solution of Electromagnetic Scattering Problems, presented at the URSI Symposium on Electromagnetic Wave Theory, Delft, The Netherlands; reprinted in: *Electromagnetic Wave Theory*, ed. J. Brown, 891-905, Pergamon Press, London (1967).
- LOWAN, A. N. [1964], Spheroidal Wave Functions, in: *Handbook of Mathematical Functions with Formulas, Graphs, and Mathematical Tables*, eds. M. Abramowitz and I. A. Stegun, 751-769, N.B.S. Applied Mathematics Series No. 55, U.S. Government Printing Office, Washington, D.C.
- MORSE, P. M. and H. FESHBACH [1953], *Methods of Theoretical Physics*, McGraw-Hill Book Co., New York.
- MULLER, H. J. W. [1962], Asymptotic Expansions of Oblate Spheroidal Wave Functions and their Characteristic Numbers, *J. Reine Angew. Math.* **211**, 33-47.
- MUSHAKE, Y. [1956], Backscattering for Arbitrary Angles of Incidence of a Plane Electromagnetic Wave on a Perfectly Conducting Spheroid with Small Eccentricity, *J. Appl. Phys.* **27**, 1549-1556.
- NOBLE, B. [1962], Integral Equation Perturbation Methods in Low-Frequency Diffraction, in: *Electromagnetic Waves*, ed. R. E. Langer, 139-180, The University of Wisconsin Press, Madison, Wisconsin.
- SENIOR, T. B. A. [1966], The Scattering of an Electromagnetic Wave by a Spheroid, *Can. J. Phys.* **44**, 1353-1359.
- SIEGEL, K. M., H. A. ALPERIN, R. R. BONKOWSKI, J. W. CRISPIN, A. L. MAZZILLI, C. F. SCHENSLIED and I. V. SCHENSLIED [1955], Bistatic Radar Cross Sections of Surfaces of Revolution, *J. Appl. Phys.* **26**, 297-305.
- SIEGEL, K. M. [1959], Far Field Scattering from Bodies of Revolution, *Appl. Sci. Res.* **7B**, 293-328.
- STEVENS, A. F. [1953a], Solution of Electromagnetic Scattering Problems as Power Series in the Ratio (Dimension of Scatterer)/Wavelength, *J. Appl. Phys.* **24**, 1134-1142. See, also, KLEINMAN [1965b].

- STEVENSON, A. F. [1953b], Electromagnetic Scattering by an Ellipsoid in the Third Approximation, *J. Appl. Phys.* **24**, 1143-1151.
- STRUTT, J. W. (Lord Rayleigh)[1897], On the Incidence of Aerial and Electric Waves upon Small Obstacles in the Form of Ellipsoids or Elliptic Cylinders, and on the Passage of Electric Waves Through a Circular Aperture in a Conducting Screen, *Phil. Mag.* **44**, 28-52.
- TAI, C. T. [1952a], Quasi-Static Solution for Diffraction of a Plane Electromagnetic Wave by a Small Oblate Spheroid, *IRE Trans.* **AP-1**, 13-36. This article contains several misprints, which have been corrected in TAI [1952b].
- TAI, C. T. [1952b], Quasi-Static Solution for Diffraction of a Plane Electromagnetic Wave by a Small Oblate Spheroid, Stanford Research Institute Technical Report No. 24, Stanford, California.

CHAPTER 14

THE DISC

F. B. SLFATOR

By virtue of its geometric simplicity, its status as a separable surface and limiting case of the oblate spheroid, and its complementarity to the aperture problem, the circular disc is amenable to a wide variety of analytical treatments. Since Babinet's principle (see Introduction) permits the trivial conversion of results for the aperture into corresponding ones for the disc, nearly all the literature on the former problem is pertinent here, and many of the formulas and curves included hereafter were originally derived for the aperture and converted via the above-mentioned principle to forms appropriate to the disc. Furthermore, since the transformation which takes the oblate spheroid into the disc is continuous, the exact results for the former body are easily modified to apply to the disc.

14.1. Disc geometry

The separable coordinate system which contains the disc as a coordinate surface is the oblate spheroidal system (ξ, η, ϕ) described in the preceding chapter (see Fig. 13.1). The disc itself is specified by the extreme value $\xi_1 = 0$ and its radius is $a = \frac{1}{2}d$, so that c , the product of wave number and semi-focal distance, is now ka . Aside from these modifications, the geometry of the system is identical to that of the oblate spheroid, and the eigenfunctions employed in the exact solutions are again the oblate spheroidal functions. Explicit forms for the limiting values of the radial functions, $R_{mn}^{(1),(3)}(-ic, i0)$, and of their first derivatives, are given by FLAMMER [1957].

In some instances a cylindrical coordinate system (ρ, ϕ, z) is preferable to the spheroidal system, and the disc is then located in the plane $z = 0$ with center at the origin.

As in Chapter 13, the primary source is either a plane wave whose direction of propagation forms the angle ζ with the positive z -axis, or a point or dipole source located at (ξ_0, η_0, ϕ_0) . In particular, for normal or axial incidence, either $\zeta = \pi$ or $\eta_0 = 1$.

14.2. Acoustically soft disc

14.2.1. Point sources

14.2.1.1. EXACT SOLUTIONS

For a point source at $r_0 = (\xi_0, \eta_0, \phi_0)$, such that

$$V^i = \frac{e^{ikR}}{kR}, \quad (14.1)$$

the total field is

$$V^i + V^s = 2i \sum_{m=0}^{\infty} \sum_{n=m}^{\infty} \frac{\varepsilon_m}{\tilde{N}_{mn}} \left[R_{mn}^{(1)}(-ic, i\xi_<) - \frac{R_{mn}^{(1)}(-ic, i0)}{R_{mn}^{(3)}(-ic, i0)} R_{mn}^{(3)}(-ic, i\xi_<) \right] \\ \times R_{mn}^{(3)}(-ic, i\xi_>) S_{mn}(-ic, \eta_0) S_{mn}(-ic, \eta) \cos m(\phi - \phi_0). \quad (14.2)$$

On the surface $\xi = 0$:

$$\frac{\partial}{\partial \xi} (V^i + V^s) = \frac{-2i}{c} \sum_{m=0}^{\infty} \sum_{n=m}^{\infty} \frac{\varepsilon_m}{\tilde{N}_{mn}} \frac{R_{mn}^{(3)}(-ic, i\xi_0)}{R_{mn}^{(3)}(-ic, i0)} \\ \times S_{mn}(-ic, \eta_0) S_{mn}(-ic, \eta) \cos m(\phi - \phi_0). \quad (14.3)$$

In the far field ($\xi \rightarrow \infty$):

$$V^i + V^s = \frac{e^{ic\xi}}{c\xi} 2 \sum_{m=0}^{\infty} \sum_{n=m}^{\infty} \frac{\varepsilon_m (-i)^n}{\tilde{N}_{mn}} \left[R_{mn}^{(1)}(-ic, i\xi_0) - \frac{R_{mn}^{(1)}(-ic, i0)}{R_{mn}^{(3)}(-ic, i0)} R_{mn}^{(3)}(-ic, i\xi_0) \right] \\ S_{mn}(-ic, \eta_0) S_{mn}(-ic, \eta) \cos m(\phi - \phi_0). \quad (14.4)$$

If the source is on the positive z -axis ($\eta_0 = 1$):

$$V^i + V^s = 2i \sum_{n=0}^{\infty} \frac{1}{\tilde{N}_{0n}} \left[R_{0n}^{(1)}(-ic, i\xi_<) - \frac{R_{0n}^{(1)}(-ic, i0)}{R_{0n}^{(3)}(-ic, i0)} R_{0n}^{(3)}(-ic, i\xi_<) \right] \\ \times R_{0n}^{(3)}(-ic, i\xi_>) S_{0n}(-ic, 1) S_{0n}(-ic, \eta), \quad (14.5)$$

and, in particular, when the observation point is on the surface $\xi = 0$:

$$\frac{\partial}{\partial \xi} (V^i + V^s) = \frac{-2i}{c} \sum_{n=0}^{\infty} \frac{1}{\tilde{N}_{0n}} \frac{R_{0n}^{(3)}(-ic, i\xi_0)}{R_{0n}^{(3)}(-ic, i0)} S_{0n}(-ic, 1) S_{0n}(-ic, \eta), \quad (14.6)$$

whereas in the far field ($\xi \rightarrow \infty$):

$$V^i + V^s = \frac{e^{ic\xi}}{c\xi} 2 \sum_{n=0}^{\infty} \frac{(-i)^n}{\tilde{N}_{0n}} \left[R_{0n}^{(1)}(-ic, i\xi_0) - \frac{R_{0n}^{(1)}(-ic, i0)}{R_{0n}^{(3)}(-ic, i0)} R_{0n}^{(3)}(-ic, i\xi_0) \right] \\ \times S_{0n}(-ic, 1) S_{0n}(-ic, \eta). \quad (14.7)$$

14.2.1.2. LOW FREQUENCY APPROXIMATIONS

No explicit results are available. Various authors (see, for example, BAZER and BROWN [1959]) have considered general low frequency methods in relation to this problem, but final results are given only for the special case of plane wave excitation.

14.2.1.3. HIGH FREQUENCY APPROXIMATIONS

In addition to results obtained by rigorous asymptotic theory, a variety of results

based on Kirchhoff's formula (see, e.g., BOUWKAMP [1954]) are available. The latter are here included primarily for historical reasons, and though they have found considerable application, their accuracy is difficult to predict.

The scattered field is:

$$V^s = \frac{1}{4\pi} \iint \left[V \frac{\partial}{\partial n} \left(\frac{e^{ikr}}{r} \right) - \frac{e^{ikr}}{r} \frac{\partial V}{\partial n} \right] dS, \quad (14.8)$$

where r is the distance from integration point to observation point, the normal \hat{n} is directed from the disc into free space, and the integral is over both faces of the disc. Kirchhoff's approximation is to assume that the values of the total field and its derivative are those of the incident field on the geometrically illuminated face, and are zero on the shadowed face of the disc. This approximation is valid for the "black" disc; however, it has been applied to both soft and hard discs. The resulting normalized scattered field amplitude was computed by LOMMEL [1884] for a point source on the axis and the observation point on the opposite side of the disc; selected results are shown in Fig. 14.1.

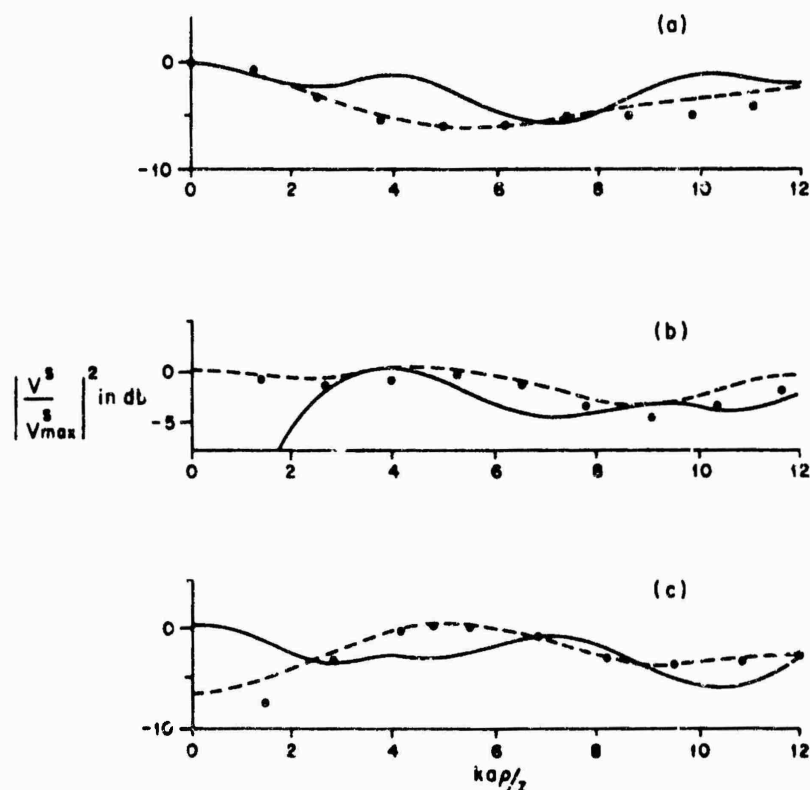


Fig. 14.1. Normalized scattered near field intensity behind the disc for point source on axis with $Az_0 = 710$, $c = 29.8$ and (a) $kz = 50.5$, (b) $kz = 42.9$, (c) $kz = 37.3$; — Kirchhoff approximation, ●●● Kirchhoff double layer, --- experimental (BEKEFI [1953a]).

Approximations based on Rayleigh's formulas (see, e.g., BOUWKAMP [1954]) lead to the Kirchhoff double and single layer results, i.e. respectively:

$$V_1 = V^i \pm \frac{1}{2\pi} \iint V^i \frac{\partial}{\partial n} \left(\frac{e^{ikr}}{r} \right) dS, \quad (14.9)$$

$$V_2 = V^i \pm \frac{1}{2\pi} \iint \frac{\partial V^i}{\partial n} \frac{e^{ikr}}{r} dS, \quad (14.10)$$

where the integration is over one face of the disc, the normal is directed into the illuminated region and the upper (lower) sign obtains according as the observation point is on the same (opposite) side as the source. The validity of the approximations (14.9) and (14.10) has been discussed by BOUWKAMP [1954] and BEKEFI [1957].

For a point source on the z -axis at $(\rho = 0, z = z_0)$, such that

$$V^i = \frac{e^{ikR}}{kR}, \quad (14.11)$$

an approximate expression for the scattered field at (ρ, z) with $0 > z > -z_0$ and $kz_0 \gg 1$ based on eq. (14.9) is (BEKEFI [1953]):

$$\begin{aligned} V_1^s \sim & \frac{1}{k} (z_0^2 + \rho^2)^{-1/2} \exp[-ik(z - \sqrt{z_0^2 + a^2})] + \frac{z}{k} [(z^2 + a^2)(z_0^2 + a^2)]^{-1/2} \\ & \times \exp \left[ik \left(\sqrt{z_0^2 + a^2} + \sqrt{z^2 + a^2} + \frac{\rho^2}{2\sqrt{z^2 + a^2}} \right) \right] \\ & \times \left[J_0 \left(\frac{c\rho}{\sqrt{z^2 + a^2}} \right) - i \frac{\rho}{a} J_1 \left(\frac{c\rho}{\sqrt{z^2 + a^2}} \right) + O \left(\frac{\rho^2}{a^2} \right) \right], \end{aligned} \quad (14.12)$$

which is valid provided that

$$|V_1^s| \sim \frac{\rho z}{z_0^2 + a^2} \sinh^{-1} \left(\frac{a}{z} \right). \quad (14.13)$$

Results of approximations based on eq. (14.12) are shown in Fig. 14.1. If the observation point is also on the axis, an approximate evaluation of the double layer formula yields (SEVERIN and STARKE [1952]):

$$\begin{aligned} \frac{V_1^s}{V^i} \sim & - \left(1 - \frac{z}{z_0} - \frac{z^2}{z_0^2} + \frac{i|z|}{kz_0^2} \right) e^{ik|z|} + \left(1 - \frac{\sqrt{z^2 + a^2}}{|z_0|} + \frac{z^2 + a^2}{z_0^2} - \frac{c^2 a^2}{8z_0^2} + \right. \\ & \left. + i \left[\frac{ca}{2|z_0|} \left(1 - \frac{\sqrt{z^2 + a^2}}{|z_0|} \right) + \frac{\sqrt{z^2 + a^2}}{kz_0^2} \right] \right) \frac{z}{z_0} \exp \{ ik \sqrt{z^2 + a^2} \}, \end{aligned} \quad (14.14)$$

whereas the corresponding result for the single layer formula is:

$$\begin{aligned}
\frac{V_2^s}{V^i} \sim & - \left[1 - \left| \frac{z}{z_0} \right| + \frac{z^2}{z_0^2} - \frac{3}{k^2 z_0^2} - \frac{i}{k|z_0|} \left(1 - 3 \left| \frac{z}{z_0} \right| \right) \right] e^{ik|z|} + \\
& + \left\{ 1 - \frac{\sqrt{(z^2 + a^2)}}{|z_0|} + \frac{z^2 + a^2}{z_0^2} + \frac{a^2}{2z_0^2} - \frac{c^2 a^2}{8z_0^2} - \frac{3}{k^2 z_0^2} + \right. \\
& \left. + i \left[\frac{ca}{2|z_0|} \left(1 - \frac{\sqrt{(z^2 + a^2)}}{|z_0|} \right) - \frac{1}{k|z_0|} \left(1 - 3 \frac{\sqrt{(z^2 + a^2)}}{|z_0|} \right) \right] \right\} \exp \{ ik\sqrt{(z^2 + a^2)} \}.
\end{aligned}
\tag{14.15}$$

SEVERIN and STARKE [1952] have compared values computed from eqs. (14.14) and (14.15) with experiment; typical results are shown in Fig. 14.2.

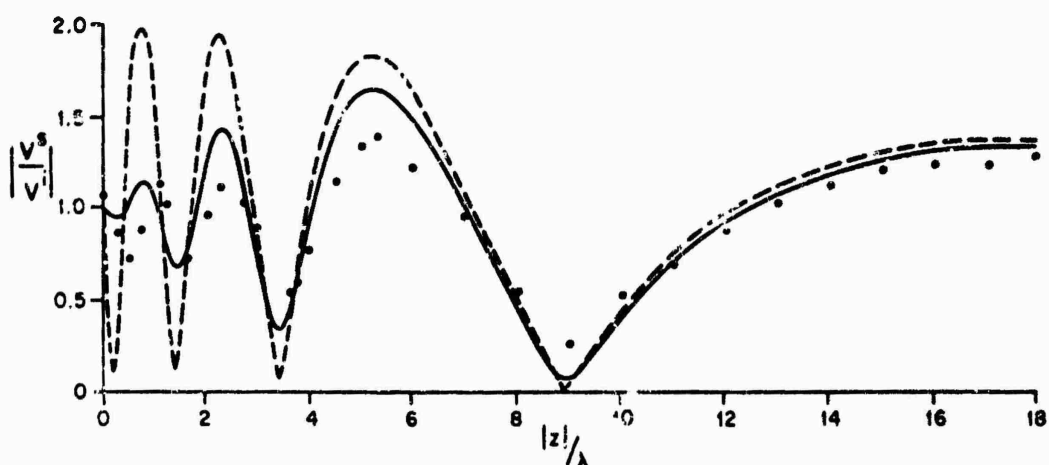


Fig. 14.2. Normalized scattered near field intensity on axis behind the disc for point source on axis with $kz_0 = 396$ and $c = 8\pi$: — Kirchhoff double layer, --- Kirchhoff single layer, ●●● experimental (SEVERIN and STARKE [1952]).

Rigorous asymptotic results are available only for a source on the axis of symmetry. Using an asymptotic development of an exact solution of the Sommerfeld type, the total field in the region of geometrical shadow resulting from the source of eq. (14.11) located at $(\xi_0, \eta_0 = 1)$ is (HANSEN [1962]):

$$\begin{aligned}
V \sim & - \frac{1}{2c} \exp [ic\{\sqrt{(1+\xi^2)} + \sqrt{(1+\xi_0^2)}\}] \left[\frac{-(1+\xi^2)^{-1/2}}{1 - (1+\xi_0^2)^{-1/2}} \right]^{1/2} \\
& \times \left\{ \frac{(1+\sqrt{(1-\eta^2)})^{1/2} [J_0(c\sqrt{(1-\eta^2)}) - iJ_1(c\sqrt{(1-\eta^2)})]}{\sqrt{(1+\xi^2) + \sqrt{(1+\xi_0^2)} - \sqrt{(1-\eta^2)} - \sqrt{\{(1+\xi^2)(1+\xi_0^2)(1-\eta^2)\}}}} + \right. \\
& \left. + \frac{(1-\sqrt{(1-\eta^2)})^{1/2} [J_0(c\sqrt{(1-\eta^2)}) + iJ_1(c\sqrt{(1-\eta^2)})]}{\sqrt{(1+\xi^2) - \sqrt{(1+\xi_0^2)} + \sqrt{(1-\eta^2)} + \sqrt{\{(1+\xi^2)(1+\xi_0^2)(1-\eta^2)\}}}} \right\}.
\end{aligned}
\tag{14.16}$$

In particular, if the observation point is not too near the axis, i.e. $k\rho = O(c)$ (HANSEN [1962, 1964]):

$$V \sim \frac{\exp(ikr_0 + \frac{1}{2}i\pi)}{2kr_0\sqrt{2\pi}} \left\{ \frac{\sec \frac{1}{2}(\theta_1 + \beta) + \operatorname{cosec} \frac{1}{2}(\theta_1 - \beta)}{\sqrt{\{kr_1(1 + (r_1/a) \sin \theta_1)\}}} e^{ikr_1} - \frac{\sec \frac{1}{2}(\theta_2 + \beta) + \operatorname{cosec} \frac{1}{2}(\theta_2 - \beta)}{\sqrt{\{kr_2(1 + (r_2/a) \sin \theta_2)\}}} e^{ikr_2} \right\}, \quad (14.17)$$

whereas if the point is near the axis, i.e. $k\rho = O(1)$ (HANSEN [1964]):

$$V \sim - \frac{\exp\{ik(r_0 + \sqrt{(z^2 + a^2)})\}}{k(r_0 + \sqrt{(z^2 + a^2)})} \sqrt{2 \left(1 - \frac{a}{r_0}\right)} (\sin \frac{1}{2}\delta) J_0(k\rho \cos \delta), \quad (14.18)$$

where the geometrical quantities are defined in Fig. 14.3. The above forms take account only of singly diffracted rays. A partial asymptotic expansion can be constructed

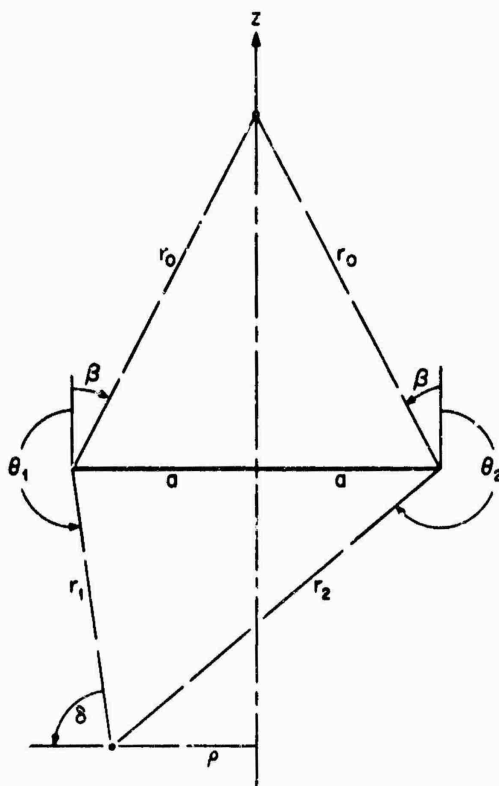


Fig. 14.3. Geometry and notation for asymptotic theory.

by taking into account rays diffracted p times at diametrically opposite points on the edge of the disc. For points within the geometrical shadow and not too near the axis ($k\rho = O(c)$), the contribution of the ray diffracted p times ($p = 2, 3, \dots$) is (HANSEN [1964]):

$$V_p \sim - \sqrt{\frac{2}{\pi}} \frac{e^{ikr_0 + \frac{1}{2}i\pi}}{kr_0} \left[\frac{e^{2ic + \frac{1}{2}i\pi}}{16c\sqrt{\pi e}} \right]^{p-1} \frac{\cos \frac{1}{2}\beta - \sin \frac{1}{2}\beta}{1 + \sin \beta} \times \left\{ \frac{\sin \frac{1}{2}\theta_1 + \cos \frac{1}{2}\theta_1}{1 - \sin \theta_1} \frac{e^{ikr_1}}{\sqrt{\{kr_1(1 + (r_1/a) \sin \theta_1)\}}} - \frac{\sin \frac{1}{2}\theta_2 + \cos \frac{1}{2}\theta_2}{1 - \sin \theta_2} \frac{e^{ikr_2}}{\sqrt{\{kr_2(1 + (r_2/a) \sin \theta_2)\}}} \right\}. \quad (14.19)$$

14.2.2. Plane wave incidence

14.2.2.1. EXACT SOLUTIONS

For an incident wave whose direction of propagation makes an angle ζ with the positive z -axis, such that

$$V^i = \exp \{ik(x \sin \zeta + z \cos \zeta)\}, \quad (14.20)$$

then

$$\begin{aligned} V^s = & -2 \sum_{m=0}^{\infty} \sum_{n=m}^{\infty} \frac{\varepsilon_m i^n}{\tilde{N}_{mn}} \frac{R_{mn}^{(1)}(-ic, i0)}{R_{mn}^{(3)}(-ic, i0)} R_{mn}^{(3)}(-ic, i\xi) \\ & \times S_{mn}(-ic, \cos \zeta) S_{mn}(-ic, \eta) \cos m\phi. \end{aligned} \quad (14.21)$$

On the surface $\xi = 0$:

$$\begin{aligned} \frac{\partial}{\partial \xi} (V^i + V^s) = & -\frac{2}{c} \sum_{m=0}^{\infty} \sum_{n=m}^{\infty} \frac{\varepsilon_m i^n}{\tilde{N}_{mn}} \frac{1}{R_{mn}^{(3)}(-ic, i0)} \\ & \times S_{mn}(-ic, \cos \zeta) S_{mn}(-ic, \eta) \cos m\phi, \end{aligned} \quad (14.22)$$

and in the far field ($\xi \rightarrow \infty$):

$$S = 2i \sum_{m=0}^{\infty} \sum_{n=m}^{\infty} \frac{\varepsilon_m}{\tilde{N}_{mn}} \frac{R_{mn}^{(1)}(-ic, i0)}{R_{mn}^{(3)}(-ic, i0)} S_{mn}(-ic, \cos \zeta) S_{mn}(-ic, \eta) \cos m\phi. \quad (14.23)$$

The total scattering cross section is

$$\sigma_T = \frac{4\pi}{k^2} \sum_{m=0}^{\infty} \sum_{n=m}^{\infty} \frac{\varepsilon_m^2}{\tilde{N}_{mn}} \left[\frac{R_{mn}^{(1)}(-ic, i0)}{|R_{mn}^{(3)}(-ic, i0)|} S_{mn}(-ic, \cos \zeta) \right]^2. \quad (14.24)$$

For normal incidence ($\zeta = \pi$):

$$V^s = -2 \sum_{n=0}^{\infty} \frac{i^n}{\tilde{N}_{0n}} \frac{R_{0n}^{(1)}(-ic, i0)}{R_{0n}^{(3)}(-ic, i0)} R_{0n}^{(3)}(-ic, i\xi) S_{0n}(-ic, -1) S_{0n}(-ic, \eta), \quad (14.25)$$

and on the surface $\xi = 0$:

$$\frac{\partial}{\partial \xi} (V^i + V^s) = -\frac{2}{c} \sum_{n=0}^{\infty} \frac{i^n}{\tilde{N}_{0n}} \frac{1}{R_{0n}^{(3)}(-ic, i0)} S_{0n}(-ic, -1) S_{0n}(-ic, \eta), \quad (14.26)$$

whereas in the far field ($\xi \rightarrow \infty$):

$$S = 2i \sum_{n=0}^{\infty} \frac{1}{\tilde{N}_{0n}} \frac{R_{0n}^{(1)}(-ic, i0)}{R_{0n}^{(3)}(-ic, i0)} S_{0n}(-ic, -1) S_{0n}(-ic, \eta). \quad (14.27)$$

Computed values of $|S|$ are shown in Fig. 14.4.

The total scattering cross section is:

$$\sigma_T = \frac{4\pi}{k^2} \sum_{n=0}^{\infty} \frac{1}{\tilde{N}_{0n}} \left[\frac{R_{0n}^{(1)}(-ic, i0)}{|R_{0n}^{(3)}(-ic, i0)|} S_{0n}(-ic, -1) \right]^2, \quad (14.28)$$

and its normalized form is plotted as a function of c in Fig. 14.5.

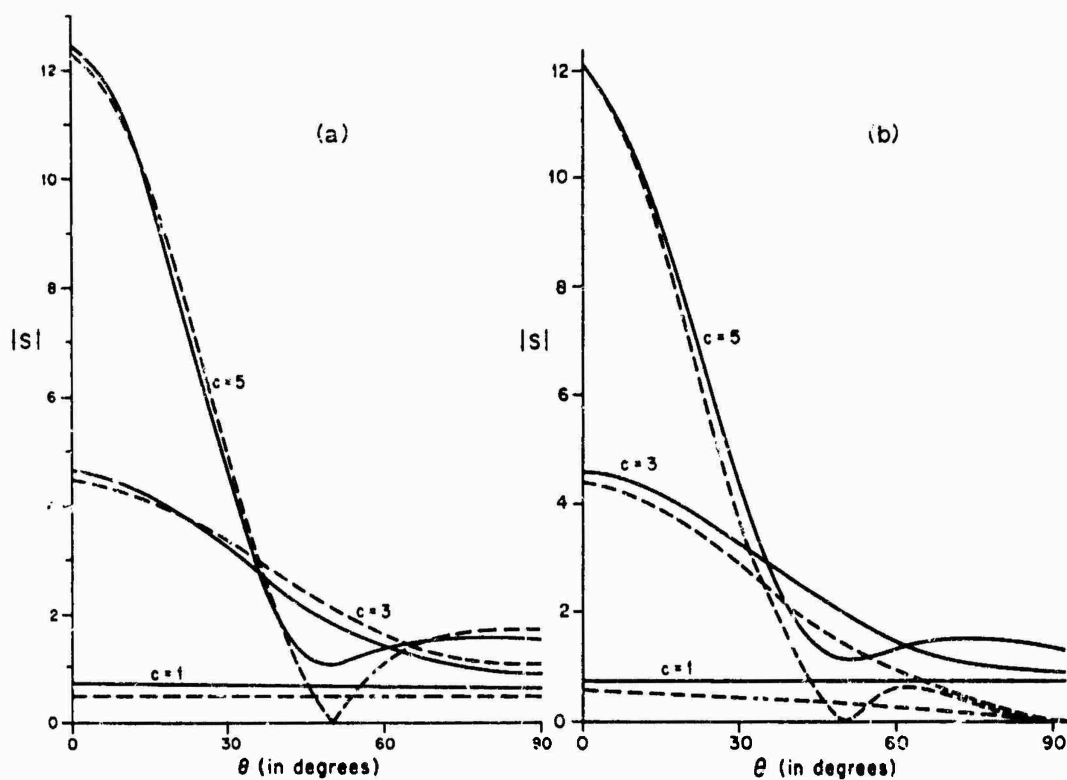


Fig. 14.4. Amplitude of far field coefficient for three disc sizes: — exact, (a) --- Kirchhoff double layer (SPENCE [1949]), (b) --- Kirchhoff single layer (SEVERIN [1952]).

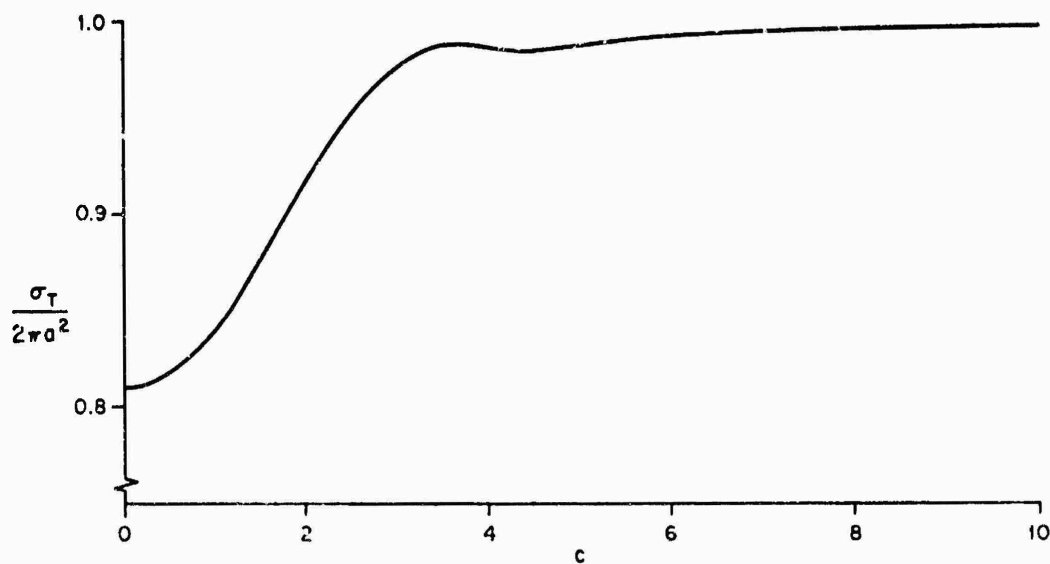


Fig. 14.5. Normalized total scattering cross section (BOUWKAMP [1954]).

14.2.2.2. LOW FREQUENCY APPROXIMATIONS

For an incident wave whose direction of propagation makes an angle ζ with the positive z -axis, such that

$$V^i = \exp \{ik(x \sin \zeta + z \cos \zeta)\}, \quad (14.29)$$

a complete low frequency expansion of the scattered field at the point (ξ, η, ϕ) is (ASVESTAS and KLEINMAN [1967]):

$$V^s = e^{ic\xi} \sum_{n=0}^{\infty} (-c)^n \sum_{m=0}^{\infty} \frac{\eta^{n-m}}{(n-m)!} \sum_{t=0}^m \sum_{r=0}^m \sum_{s=0}^t D_{r,t}^{m,s} Q_r^s(i\xi) P_t^s(\eta) \cos s\phi, \quad (14.30)$$

where the coefficients $D_{r,t}^{m,s}$ are determined from the recurrence relations:

$$D_{r,t}^{m+1,s} = \frac{2}{r(r+1)-t(t+1)} \left[\frac{r(r-s)}{2r-1} D_{r-1,t}^{m,s} + \frac{t(t-s)}{2t-1} D_{r,t-1}^{m,s} - \frac{(t+1)(t+s+1)}{2t+3} D_{r,t+1}^{m,s} - \frac{(r+1)(r+s+1)}{2r+3} D_{r+1,t}^{m,s} \right], \quad r \neq t; m = 0, 1, 2, \dots, \quad (14.31)$$

$$D_{t,t}^{m+1,s} = - \sum_{r=0}^{m+1} \frac{Q_r^s(i0)}{Q_t^s(i0)} D_{r,t}^{m+1,s} + A_t^{m+1,s}, \quad m = 0, 1, 2, \dots, \quad (14.32)$$

$$D_{0,0}^{0,0} = A_{0,0}^{0,0}, \quad (14.33)$$

$$A_t^{m,s} = \begin{cases} \frac{-e_s(-1)^t \sqrt{\pi}(2t+1)(t-s)! P_t^s(\sec \zeta) \cos^m \zeta}{2^{m+1}(t+s)! \{\frac{1}{2}(m-t)\}! \{\frac{1}{2}(m+t+1)\}! Q_t^s(i0)}, & \text{for } m+t \text{ even,} \\ 0, & \text{for } m+t \text{ odd,} \end{cases} \quad (14.34)$$

and the prime in eq. (14.32) indicates that the term with $r = s$ is to be omitted from the summation.

In the far field ($\xi \rightarrow \infty$):

$$S = -i \sum_{n=0}^{\infty} (-c)^{n+1} \sum_{m=0}^n \frac{\eta^{n-m}}{(n-m)!} \sum_{t=0}^n \sum_{s=0}^t (-1)^s s! D_{0,t}^{m,s} P_t^s(\eta) \cos s\phi, \quad (14.35)$$

and the bistatic scattering cross section is:

$$\sigma(\eta, \phi) = 4\pi a^2 \sum_{n=0}^{\infty} (-c)^n \sum_{m=0}^n V_{n-m} V_m^*, \quad (14.36)$$

where

$$V_n = \sum_{m=0}^n \frac{\eta^{n-m}}{(n-m)!} \sum_{t=0}^m \sum_{s=0}^t (-1)^s s! D_{0,t}^{m,s} P_t^s(\eta) \cos s\phi, \quad (14.37)$$

and the asterisk indicates the complex conjugate.

For normal incidence ($\zeta = \pi$), the coefficients $A_t^{m,s}$, $D_{0,t}^{m,s}$ vanish for $s \neq 0$, thus eliminating the summations over s .

In the far field ($\xi \rightarrow \infty$):

$$S = -i \sum_{n=0}^{\infty} (-c)^{n+1} \sum_{m=0}^n \frac{\eta^{n-m}}{(n-m)!} \sum_{t=0}^m D_{0,t}^{m,0} P_t(\eta), \quad (14.38)$$

where the coefficients $D_{0,i}^{m,0}$ are given by eqs. (14.31) through (14.34) with $\zeta = \pi$. The bistatic scattering cross section is still given by eq. (14.36), but with

$$V_n = \sum_{m=0}^n \frac{\eta^{n-m}}{(n-m)!} \sum_{i=0}^m D_{0,i}^{m,0} P_i(\eta). \quad (14.39)$$

Explicitly, the far field coefficient is:

$$\begin{aligned} S = & -\frac{2c}{\pi} \left\{ P_0 - \frac{2ic}{\pi} P_1 + c^2 \left[\frac{1}{9} P_2 + \left(\frac{2}{9} - \frac{4}{\pi^2} \right) P_0 \right] - \frac{2ic^3}{\pi} \left[\frac{1}{9} P_2 + \left(\frac{1}{3} - \frac{4}{\pi^2} \right) P_0 \right] + \right. \\ & + c^4 \left[\frac{1}{525} P_4 + \left(\frac{4}{105} - \frac{4}{9\pi^2} \right) P_2 + \left(\frac{2}{75} - \frac{16}{9\pi^2} + \frac{16}{\pi^4} \right) P_0 \right] - \\ & \left. - \frac{2ic^5}{\pi} \left[\frac{1}{525} P_4 + \left(\frac{23}{567} - \frac{4}{9\pi^2} \right) P_2 + \left(\frac{127}{2025} - \frac{20}{9\pi^2} + \frac{16}{\pi^4} \right) P_0 \right] + O(c^6) \right\}. \end{aligned} \quad (14.40)$$

An alternative formulation, in which the incident and scattered fields are expanded in Fourier series in the azimuthal angle ϕ , has been developed by several authors (see, for example, WILLIAMS [1962] and BOERSMA [1964]). For arbitrary incidence and in the far field ($\xi \rightarrow \infty$):

$$S = \sum_{m=0}^{\infty} S_m \cos m\phi, \quad (14.41)$$

where

$$\begin{aligned} S_m = & \frac{\epsilon_m 4^{m+1} m! (m+1)! c^{2m+1} (\sqrt{1-\epsilon^2} \sin \zeta)^m}{\pi (2m)! (2m+2)!} \\ & \times \left[1 - \frac{2m+1+(2m-1)(\sin^2 \zeta - \eta^2)}{2(2m-1)(2m+3)} c^2 - \frac{4i}{9\pi} \delta_{m,1} c^3 + O(c^4) \right], \end{aligned} \quad (14.42)$$

and $\delta_{m,1}$ is the Kronecker delta ($\delta_{1,1} = 1$, $\delta_{m,1} = 0$ for $m \neq 1$). The normalized total scattering cross section is:

$$\begin{aligned} \frac{\sigma_T}{2\pi a^2} = & \pi^{-2} \sum_{m=0}^{\infty} \epsilon_m (c^2 \sin \zeta)^{2m} (2m)! \left[\frac{4^{m+1} m! (m+1)!}{(2m)! (2m+2)!} \right]^3 \\ & \times \left\{ 1 - c^2 \left[\frac{2(2m^2+3m+2)}{(2m-1)(2m+3)^2} + \frac{\sin^2 \zeta}{2m+3} \right] + \right. \\ & + c^4 \left[\frac{32m^6+144m^5+136m^4-364m^3-960m^2-758m-213}{(2m-3)(2m-1)^2(2m+3)^3(2m+5)^2} + \right. \\ & \left. \left. + \frac{8m^3+32m^2+40m+19}{(2m-1)(2m+3)^3(2m+5)} \sin^2 \zeta + \frac{m+2}{(2m+3)^2(2m+5)} \sin^4 \zeta \right] + O(c^6) \right\}. \end{aligned} \quad (14.43)$$

BAZER and HOCHSTADT [1962] have given explicitly the first two Fourier components ($m = 0$ and 1). HEINS and MACCAMY [1960] have obtained similar results for the surface field.

For normal incidence ($\zeta = \pi$) and on the illuminated face (BAZER and BROWN [1959]):

$$\frac{\partial}{\partial \xi} (V^i + V^s)|_{z=0^+} = -ic\eta + \frac{2}{\pi} \sum_{n=0}^{\infty} A_n \eta^{2n}, \quad (14.44)$$

in which the first few coefficients are:

$$\begin{aligned} A_0 = & 1 - \frac{2ic}{\pi} + \left(\frac{1}{2} - \frac{4}{\pi^2}\right) c^2 - \frac{i}{\pi} \left(\frac{7}{9} - \frac{8}{\pi^2}\right) c^3 + \\ & + \left(\frac{1}{24} - \frac{2}{\pi^2} + \frac{16}{\pi^4}\right) c^4 - \frac{i}{\pi} \left(\frac{143}{900} - \frac{44}{9\pi^2} + \frac{32}{\pi^4}\right) c^5 + \\ & + \left(\frac{1}{720} - \frac{2171}{4050\pi^2} + \frac{104}{9\pi^4} - \frac{64}{\pi^6}\right) c^6 + O(c^7), \end{aligned} \quad (14.45)$$

$$\begin{aligned} A_1 = & -\frac{1}{2} c^2 - \frac{i}{3\pi} c^3 + \left(\frac{1}{12} - \frac{2}{3\pi^2}\right) c^4 - \frac{i}{\pi} \left(\frac{13}{90} - \frac{4}{3\pi^2}\right) c^5 + \\ & + \left(\frac{1}{80} - \frac{49}{135\pi^2} + \frac{8}{3\pi^4}\right) c^6 + O(c^7), \end{aligned} \quad (14.46)$$

$$A_2 = -\frac{1}{72} c^4 - \frac{i}{60\pi} c^5 + \left(\frac{1}{240} - \frac{1}{30\pi^2}\right) c^6 + O(c^7), \quad (14.47)$$

$$A_3 = -\frac{1}{5600} c^6 + O(c^7), \quad (14.48)$$

and the remaining coefficients are $O(c^8)$.

In the far field ($\xi \rightarrow \infty$):

$$\begin{aligned} S = & -\frac{2c}{\pi} \left\{ 1 - \frac{2i}{\pi} c + \left(\frac{1}{3} - \frac{4}{\pi^2} - \frac{1}{6} \sin^2 \theta\right) c^2 - \frac{2i}{\pi} \left(\frac{4}{9} - \frac{4}{\pi^2} - \frac{1}{6} \sin^2 \theta\right) c^3 + \right. \\ & + \left[\frac{16}{\pi^4} - \frac{20}{9\pi^2} + \frac{1}{15} + \left(\frac{2}{3\pi^2} - \frac{1}{15}\right) \sin^2 \theta + \frac{1}{120} \sin^4 \theta \right] c^4 - \\ & - \frac{2i}{\pi} \left[\frac{16}{\pi^4} - \frac{8}{3\pi^2} + \frac{71}{675} + \left(\frac{2}{3\pi^2} - \frac{19}{270}\right) \sin^2 \theta + \frac{1}{120} \sin^4 \theta \right] c^5 + \\ & + \left[\frac{112}{9\pi^4} + \frac{2}{315} - \frac{64}{\pi^6} - \frac{448}{675\pi^2} + \left(\frac{16}{45\pi^2} - \frac{8}{3\pi^4} - \frac{1}{105}\right) \sin^2 \theta + \right. \\ & \left. \left. + \left(\frac{1}{270} - \frac{1}{30\pi^2}\right) \sin^4 \theta - \frac{1}{5040} \sin^6 \theta \right] c^6 + O(c^7) \right\}, \end{aligned} \quad (14.49)$$

where $\theta = \pi - \cos \eta$.

The normalized total scattering cross section is (HURD [1961]):

$$\frac{\sigma_T}{2\pi a^2} = \frac{8}{\pi^2} [1 + 0.039\,160\,c^2 - 0.000\,748\,9\,c^4 - 0.000\,260\,2\,c^6 + \\ + 0.000\,009\,206\,c^8 + 0.000\,001\,846\,c^{10} + O(c^{12})]; \quad (14.50)$$

numerical values computed from this series agree with the exact results of BOUWKAMP [1954] to within one percent for $c \lesssim 2.5$.

14.2.2.3. HIGH FREQUENCY APPROXIMATIONS

No explicit results are available for arbitrary incidence. For normal incidence, results have been obtained by Kirchhoff theory, geometrical theory of diffraction (KEILER [1957]), rigorous asymptotic methods (JONES [1965a], HANSEN [1964]) and variational techniques (LEVINE and WU [1957]).

The amplitude of the far field coefficient computed from Kirchhoff's single and double layer formulas is compared with the exact result in Fig. 14.4. The normalized scattered field amplitude is shown as a function of the distance along the axis behind the disc in Fig. 14.6, and as a function of the radial distance in the plane $z = 0 +$ in Fig. 14.7.

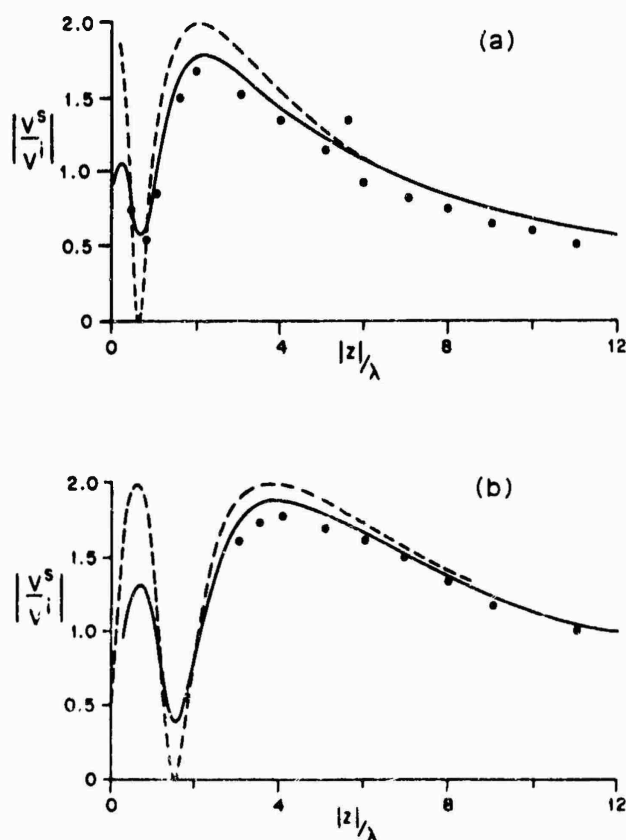


Fig. 14.6. Normalized scattered amplitude on axis behind disc with (a) $c = 3\pi$ and (b) $c = 4\pi$: — — — Kirchhoff double layer, — · — · — Kirchhoff single layer, ●●● experimental (SEVERIN [1952]).

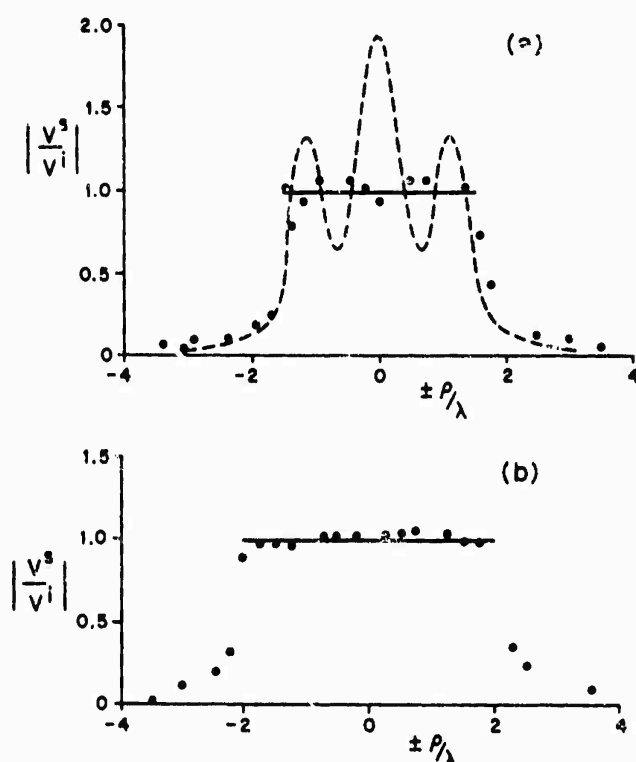


Fig. 14.7. Normalized scattered amplitude on $z = 0+$ with (a) $c = 3\pi$ and (b) $c = 4\pi$: ——— Kirchhoff double layer, --- Kirchhoff single layer, ●●● experimental (SEVERIN [1952]).

For a plane wave at axial incidence ($\zeta = \pi$), such that

$$V^i = e^{-ikz}, \quad (14.51)$$

an approximation for the far field coefficient based on an integral equation formulation is (CASE [1964]):

$$S \sim \frac{1}{2}ic \left[\frac{J_1(c \sin \theta)}{\sin \frac{1}{2}\theta} + i \frac{J_0(c \sin \theta)}{\sin \frac{1}{2}\theta} \right], \quad (14.52)$$

where θ is the spherical polar angle; eq. (14.52) is valid for $\theta < \frac{1}{2}\pi$, and for $\theta > \frac{1}{2}\pi$ the symmetry relation $S(\pi - \theta) = S(\theta)$ may be used. In the far field and in the back scattering direction (HANSEN [1964]):

$$S \sim \frac{1}{2}ic^2 \left[1 - \frac{i}{c} - \frac{1}{4c^2} + \frac{e^{2ic - \frac{1}{2}\pi}}{4c^2 \sqrt{\pi c}} + O(c^{-3}) \right]. \quad (14.53)$$

The normalized total scattering cross section is (JONES [1965a]):

$$\begin{aligned} \frac{\sigma_1}{2\pi a^2} \sim & 1 - \frac{1}{4c^2} + \frac{\cos(2c - \frac{1}{2}\pi)}{4c^2 \sqrt{\pi c}} + \frac{7 \sin(2c - \frac{1}{2}\pi)}{64c^3 \sqrt{\pi c}} + \\ & + \frac{1}{16c^4} - \frac{\sin(4c - \frac{1}{2}\pi)}{64\pi c^4} + O(c^{-5}). \end{aligned} \quad (14.54)$$

The first three terms of this expression have also been derived via a variational formulation (LEVINE and WU [1957]) and via the geometrical theory of diffraction (KARP and KELLER [1961]). Numerical values computed from the first three terms of eq. (14.54) agree with Bouwkamp's exact values out to three decimal places for $c \geq 4.0$ (LEVINE and WU [1957]).

Rigorous asymptotic results are available only for a plane wave at axial incidence. Using an asymptotic development of an exact solution of the Sommerfeld type, the total field in the region of geometrical shadow and away from the axis resulting from the incident field of eq. (14.51) is (HANSEN [1964]):

$$V \sim \frac{1}{\sqrt{2\pi}} \left\{ \frac{e^{ikr_1 + \frac{1}{2}i\pi}}{\sqrt{\{kr_1(1+(r_1/a)\sin\theta_1)\}}} \frac{\sin \frac{1}{2}\theta_1 + \cos \frac{1}{2}\theta_1}{\sin \theta_1} [1+f_1(r_1, \theta_1)] + \frac{e^{ikr_2 + \frac{1}{2}i\pi}}{\sqrt{\{kr_2(1+(r_2/a)\sin\theta_2)\}}} \frac{\sin \frac{1}{2}\theta_2 + \cos \frac{1}{2}\theta_2}{\sin \theta_2} [1+f_1(r_2, \theta_2)] \right\}, \quad (14.55)$$

where the geometrical quantities r_1 , r_2 , θ_1 and θ_2 are shown in Fig. 14.3, and

$$f_1(r, \theta) = \frac{1}{c \sin^2 \theta} \left[(2 - \sin \theta) \left(\frac{2a}{r} + \sin \theta \right) - \frac{\sin^2 \theta}{2(a/r + \sin \theta)} \right] \quad (14.56)$$

represents the second order term in the contribution of the singly diffracted rays. A partial asymptotic expansion can be constructed by summing the contributions due to rays diffracted p times at diametrically opposite points on the edge of the disc. For points within the geometrical shadow and not too near the axis, the contribution of the ray diffracted p times ($p = 2, 3, \dots$) is (HANSEN [1964]):

$$V_p \sim - \sqrt{\frac{2}{\pi}} \left[\frac{e^{2ic + \frac{1}{2}i\pi}}{16c\sqrt{\pi c}} \right]^{p-1} \times \left\{ \frac{e^{ikr_1 + \frac{1}{2}i\pi}}{\sqrt{\{kr_1(1+(r_1/a)\sin\theta_1)\}}} \frac{\sin \frac{1}{2}\theta_1 + \cos \frac{1}{2}\theta_1}{1 - \sin \theta_1} [1+f_p(r_1, \theta_1)] - \frac{e^{ikr_2 + \frac{1}{2}i\pi}}{\sqrt{\{kr_2(1+(r_2/a)\sin\theta_2)\}}} \frac{\sin \frac{1}{2}\theta_2 + \cos \frac{1}{2}\theta_2}{1 - \sin \theta_2} [1+f_p(r_2, \theta_2)] \right\}, \quad (14.57)$$

where

$$f_p(r, \theta) = \frac{i\pi}{c} \left[\frac{6a/r + 3}{1 - \sin \theta} - \frac{31 - 19p}{4} - \frac{1}{2} \left(\frac{a}{r} + \sin \theta \right)^{-1} \right] \quad (14.58)$$

represents the second order term in the contribution of the ray diffracted p times. In the region near and including the axis, a caustic correction must be made. The result, for the first two terms of the singly diffracted field, is (HANSEN [1964], BUCHAL and KELLER [1960]):

$$V \sim \frac{1}{2} e^{ikr_1} (\sin \frac{1}{2}\theta_1 + \cos \frac{1}{2}\theta_1) (R_0^{(1)} + c^{-1} R_1^{(1)}) + \frac{1}{2} e^{ikr_2} (\sin \frac{1}{2}\theta_2 + \cos \frac{1}{2}\theta_2) (R_0^{(2)} + c^{-1} R_1^{(2)}), \quad (14.59)$$

where

$$R_0^{(1)} = H_0^{(2)}(-T_1)e^{-iT_1}, \quad (14.60)$$

$$R_0^{(2)} = H_0^{(1)}(T_2)e^{-iT_2}, \quad (14.61)$$

$$R_1^{(1)} = -e^{-iT_1} \left\{ \left[\frac{i \cos^2 \theta_1}{\sin \theta_1} T_1^2 + \frac{1}{2}(\sin \theta_1 - 1)T_1 - \frac{1}{8}i \sin \theta_1 \right] H_0^{(2)}(-T_1) - \left[\frac{\cos^2 \theta_1}{\sin \theta_1} T_1^2 - i \frac{2 - \sin \theta_1}{2 \sin \theta_1} T_1 \right] H_1^{(2)}(-T_1) \right\}, \quad (14.62)$$

$$R_1^{(2)} = -e^{-iT_2} \left\{ \left[\frac{i \cos^2 \theta_2}{\sin \theta_2} T_2^2 + \frac{1}{2}(\sin \theta_2 - 1)T_2 - \frac{1}{8}i \sin \theta_2 \right] H_0^{(1)}(T_2) + \left[\frac{\cos^2 \theta_2}{\sin \theta_2} T_2^2 - i \frac{2 - \sin \theta_2}{2 \sin \theta_2} T_2 \right] H_1^{(1)}(T_2) \right\}, \quad (14.63)$$

$$T_n = \left(kr_n + \frac{c}{\sin \theta_n} \right) \sin^2 \theta_n, \quad (n = 1 \text{ or } 2). \quad (14.64)$$

For the field of the doubly diffracted rays near the axis, only terms of order c^0 are given. The result is:

$$V_2 \sim \frac{e^{2ic - 4i\pi}}{16c\sqrt{\pi c}} \left[\frac{\sin \theta_1}{1 - \sin \theta_1} (\sin \frac{1}{2}\theta_1 + \cos \frac{1}{2}\theta_1) e^{ikr_1} R_0^{(1)} + \frac{\sin \theta_2}{1 - \sin \theta_2} (\sin \frac{1}{2}\theta_2 + \cos \frac{1}{2}\theta_2) e^{ikr_2} R_0^{(2)} \right]. \quad (14.65)$$

The above forms based on asymptotic treatment of the exact solution agree with results derived from variational methods or the geometric theory of diffraction whenever comparison is possible.

14.3. Acoustically hard disc

14.3.1. Point sources

14.3.1.1. EXACT SOLUTIONS

For a point source at $r_0 = (\xi_0, \eta_0, \phi_0)$, such that

$$V^i = \frac{e^{ikR}}{kR}, \quad (14.66)$$

the total field is

$$V^i + V^s = 2i \sum_{m=0}^{\infty} \sum_{n=0}^{\infty} \frac{c_m}{N_{mn}} \left[R_{mn}^{(1)}(-ic, i\xi_0) - \frac{R_{mn}^{(1)}(-ic, i0)}{R_{mn}^{(3)}(-ic, i0)} R_{mn}^{(3)}(-ic, i\xi_0) \right] \times R_{mn}^{(3)}(-ic, i\xi_0) S_{mn}(-ic, \eta_0) S_{mn}(-ic, \eta) \cos m(\phi - \phi_0). \quad (14.67)$$

On the surface $\xi = 0$:

$$V^i + V^s = \frac{2i}{c} \sum_{m=0}^{\infty} \sum_{n=m}^{\infty} \frac{\varepsilon_m}{\tilde{N}_{mn}} \frac{R_{mn}^{(3)}(-ic, i\xi_0)}{R_{mn}^{(3)'}(-ic, i0)} S_{mn}(-ic, \eta_0) S_{mn}(-ic, \eta) \cos m(\phi - \phi_0). \quad (14.68)$$

In the far field ($\xi \rightarrow \infty$):

$$V^i + V^s = \frac{e^{ic\xi}}{c\xi} 2 \sum_{m=0}^{\infty} \sum_{n=m}^{\infty} \varepsilon_m \frac{(-i)^n}{\tilde{N}_{mn}} \left[R_{mn}^{(1)}(-ic, i\xi_0) - \frac{R_{mn}^{(1)'}(-ic, i0)}{R_{mn}^{(3)'}(-ic, i0)} R_{mn}^{(3)}(-ic, i\xi_0) \right] S_{mn}(-ic, \eta_0) S_{mn}(-ic, \eta) \cos m(\phi - \phi_0). \quad (14.69)$$

If the source is on the positive z -axis ($\eta_0 = 1$):

$$V^i + V^s = 2i \sum_{n=0}^{\infty} \frac{1}{\tilde{N}_{0n}} \left[R_{0n}^{(1)}(-ic, i\xi_0) - \frac{R_{0n}^{(1)'}(-ic, i0)}{R_{0n}^{(3)'}(-ic, i0)} R_{0n}^{(3)}(-ic, i\xi_0) \right] \times R_{0n}^{(3)}(-ic, i\xi_0) S_{0n}(-ic, 1) S_{0n}(-ic, \eta), \quad (14.70)$$

and, in particular, when the observation point is on the surface $\xi = 0$:

$$V^i + V^s = \frac{2i}{c} \sum_{n=0}^{\infty} \frac{1}{\tilde{N}_{0n}} \frac{R_{0n}^{(3)}(-ic, i\xi_0)}{R_{0n}^{(3)'}(-ic, i0)} S_{0n}(-ic, 1) S_{0n}(-ic, \eta), \quad (14.71)$$

whereas in the far field ($\xi \rightarrow \infty$):

$$V^i + V^s = \frac{e^{ic\xi}}{c\xi} 2 \sum_{n=0}^{\infty} \frac{(-i)^n}{\tilde{N}_{0n}} \left[R_{0n}^{(1)}(-ic, i\xi_0) - \frac{R_{0n}^{(1)'}(-ic, i0)}{R_{0n}^{(3)'}(-ic, i0)} R_{0n}^{(3)}(-ic, i\xi_0) \right] \times S_{0n}(-ic, 1) S_{0n}(-ic, \eta). \quad (14.72)$$

14.3.1.2. LOW FREQUENCY APPROXIMATIONS

For a point source on the z -axis at $(\xi_0, \eta_0 = 1)$, the normalized total scattering cross section can be formally written as (JONES [1956]):

$$\frac{\sigma_T}{2\pi a^2} = -\operatorname{Re} \sum_{n=0}^{\infty} \frac{A_n c^{2n}}{(2n+1)!(2n+3)} - \xi_0^{-2} \operatorname{Im} \sum_{n=0}^{\infty} \frac{c^{2n}}{(2n+1)!(2n+3)} \times \left\{ iC_n + \left(1 + \frac{c^2}{2n+5} \right) \frac{B_n}{c} + i \left[\frac{3}{4} - \frac{c^2 + 3(2n+7)}{(2n+5)(2n+7)} \right] A_n \right\} + O(\xi_0^{-4}), \quad (14.73)$$

which is valid if

$$\xi_0 \gg 1, \quad \xi_0 \gg \frac{1}{2}c; \quad (14.74)$$

only the first inequality is significant at low frequencies. The first summation in eq. (14.73) corresponds to plane wave excitation, whereas the second summation is a correction due to the finite distance of the source. The coefficients A_n , B_n and C_n

are specified by an infinite system of linear equations; if the system is truncated at $n = 1$, i.e. A_n , B_n and C_n are set equal to zero for $n \geq 2$, then:

$$\frac{\sigma_T}{2\pi a^2} \sim \frac{\xi c^4}{27\pi^2} \left[1 + \frac{8}{25} c^2 + (c\xi_0)^{-2} \left(1 + \frac{27\pi^2}{100} c^2 \right) \right]. \quad (14.75)$$

14.3.1.3. HIGH FREQUENCY APPROXIMATIONS

No results are available for an arbitrary location of the source. For a point source located on the axis of symmetry at $(\xi_0, \eta_0 = 1)$, such that

$$V^1 = \frac{e^{ikR}}{kR}, \quad (14.76)$$

the total field in the region of geometrical shadow is (HANSEN [1962, 1964]):

$$\begin{aligned} V \sim & -\frac{1}{2c} \exp [ic(\sqrt{(1+\xi^2)} + \sqrt{(1+\xi_0^2)})] \left[\frac{1+(1+\xi^2)^{-1/2}}{1+(1+\xi_0^2)^{-1/2}} \right]^{\frac{1}{2}} \\ & \times \left\{ \frac{(1-\sqrt{(1-\eta^2)})^{\frac{1}{2}} [J_0(c\sqrt{(1-\eta^2)}) - iJ_1(c\sqrt{(1-\eta^2)})]}{\sqrt{(1+\xi^2)} + \sqrt{(1+\xi_0^2)} - \sqrt{(1-\eta^2)} - \sqrt{\{(1+\xi^2)(1+\xi_0^2)(1-\eta^2)\}}} + \right. \\ & \left. + \frac{(1+\sqrt{(1-\eta^2)})^{\frac{1}{2}} [J_0(c\sqrt{(1-\eta^2)}) + iJ_1(c\sqrt{(1-\eta^2)})]}{\sqrt{(1+\xi^2)} + \sqrt{(1+\xi_0^2)} + \sqrt{(1-\eta^2)} + \sqrt{\{(1+\xi^2)(1+\xi_0^2)(1-\eta^2)\}}} \right\}. \quad (14.77) \end{aligned}$$

In particular, if the observation point is not too near the axis, i.e. $k\rho = O(c)$:

$$\begin{aligned} V \sim & \frac{e^{ikr_0 + \frac{1}{2}i\pi}}{2kr_0\sqrt{2\pi}} \left\{ \frac{\sec \frac{1}{2}(\theta_1 + \beta) - \operatorname{cosec} \frac{1}{2}(\theta_1 - \beta)}{\sqrt{\{kr_1(1+(r_1/a)\sin \theta_1)\}}} e^{ikr_1} - \right. \\ & \left. - \frac{\sec \frac{1}{2}(\theta_2 + \beta) - \operatorname{cosec} \frac{1}{2}(\theta_2 - \beta)}{\sqrt{\{kr_2(1+(r_2/a)\sin \theta_2)\}}} e^{ikr_2} \right\}, \quad (14.78) \end{aligned}$$

whereas if the point is near the axis, i.e. $k\rho = O(1)$:

$$V \sim \frac{\exp \{ik(r_0 + \sqrt{(z^2 + a^2)})\}}{k(r_0 + \sqrt{(z^2 + a^2)})} \sqrt{2 \left(1 + \frac{a}{r_0} \right)} (\cos \frac{1}{2}\delta) J_0(k\rho \cos \delta), \quad (14.79)$$

where the geometrical quantities are defined in Fig. 14.3. The above forms take account only of singly diffracted rays. A partial asymptotic expansion can be constructed by taking into account rays diffracted p times at diametrically opposite points on the edge of the disc. For points within the geometrical shadow and not too near the axis ($k\rho = O(c)$), the contribution of the ray diffracted p times ($p = 2, 3, \dots$) is (HANSEN [1964]):

$$\begin{aligned} V_p \sim & \sqrt{\frac{2}{\pi}} \frac{e^{ikr_0 + \frac{1}{2}i\pi}}{kr_0} \left[\frac{e^{i\pi/4}}{2\sqrt{\pi c}} \right]^{p-1} (\cos \frac{1}{2}\beta + \sin \frac{1}{2}\beta)^{-1} \\ & \times \left\{ \frac{e^{ikr_1}}{\sqrt{\{kr_1(1+(r_1/a)\sin \theta_1)\}}} (\cos \frac{1}{2}\theta_1 - \sin \frac{1}{2}\theta_1)^{-1} + \right. \\ & \left. + \frac{e^{ikr_2}}{\sqrt{\{kr_2(1+(r_2/a)\sin \theta_2)\}}} (\cos \frac{1}{2}\theta_2 - \sin \frac{1}{2}\theta_2)^{-1} \right\}. \quad (14.80) \end{aligned}$$

If the point source is located at the center ($\rho = 0, z = 0+$) of the disc, the total field obtained by the geometrical theory of diffraction is (KELLER [1963]):

$$V \sim \frac{e^{ikr+ic}}{kr} (2\pi c \sin \theta)^{-\frac{1}{2}} \left[\pm \frac{e^{ic \sin \theta - \frac{1}{2}i\pi}}{\cos(\frac{1}{2}\pi - \frac{1}{2}\theta)} - \frac{e^{-ic \sin \theta + \frac{1}{2}i\pi}}{\sin(\frac{1}{2}\pi - \frac{1}{2}\theta)} \right], \quad (14.81)$$

where r and $\theta = \arccos \eta$ are the spherical polar coordinates of the observation point with origin at the center of the disc, the upper sign applies in the shadow region $\frac{1}{2}\pi < \theta \leq \pi$ and the lower sign in the illuminated region $0 \leq \theta < \frac{1}{2}\pi$.

14.3.2. Plane wave incidence

14.3.2.1. EXACT SOLUTIONS

For a plane wave incident at an angle ζ with the positive z -axis, such that

$$V^i = \exp \{ik(x \sin \zeta + z \cos \zeta)\}, \quad (14.82)$$

the scattered field is

$$V^s = -2 \sum_{m=0}^{\infty} \sum_{n=m}^{\infty} \frac{\epsilon_m}{N_{mn}} \frac{i^n}{R_{mn}^{(3)'}(-ic, i0)} \frac{R_{mn}^{(1)'}(-ic, i0)}{R_{mn}^{(3)'}(-ic, i0)} R_{mn}^{(3)}(-ic, i\xi) \\ \times S_{mn}(-ic, \cos \zeta) S_{mn}(-ic, \eta) \cos m\phi. \quad (14.83)$$

On the surface $\xi = 0$:

$$V^i + V^s = \frac{2}{c} \sum_{m=0}^{\infty} \sum_{n=m}^{\infty} \frac{\epsilon_m}{N_{mn}} \frac{i^n}{R_{mn}^{(3)'}(-ic, i0)} \frac{1}{R_{mn}^{(3)'}(-ic, i0)} S_{mn}(-ic, \cos \zeta) S_{mn}(-ic, \eta) \cos m\phi. \quad (14.84)$$

In the far field ($\xi \rightarrow \infty$):

$$S = 2i \sum_{m=0}^{\infty} \sum_{n=m}^{\infty} \frac{\epsilon_m}{N_{mn}} \frac{R_{mn}^{(1)'}(-ic, i0)}{R_{mn}^{(3)'}(-ic, i0)} S_{mn}(-ic, \cos \zeta) S_{mn}(-ic, \eta) \cos m\phi. \quad (14.85)$$

The total scattering cross section is:

$$\sigma_T = \frac{4\pi}{k^2} \sum_{m=0}^{\infty} \sum_{n=m}^{\infty} \frac{\epsilon_m^2}{N_{mn}} \left[\frac{R_{mn}^{(1)'}(-ic, i0)}{|R_{mn}^{(3)'}(-ic, i0)|} S_{mn}(-ic, \cos \zeta) \right]^2. \quad (14.36)$$

For axial incidence ($\zeta = \pi$), the scattered field is:

$$V^s = -2 \sum_{n=0}^{\infty} \frac{i^n}{N_{0n}} \frac{R_{0n}^{(1)'}(-ic, i0)}{R_{0n}^{(3)'}(-ic, i0)} R_{0n}^{(3)}(-ic, i0) S_{0n}(-ic, -1) S_{0n}(-ic, \eta), \quad (14.87)$$

and on the surface $\xi = 0$:

$$V^i + V^s = \frac{2}{c} \sum_{n=0}^{\infty} \frac{i^n}{N_{0n}} \frac{1}{R_{0n}^{(3)'}(-ic, i0)} S_{0n}(-ic, -1) S_{0n}(-ic, \eta), \quad (14.88)$$

whereas in the far field ($\zeta \rightarrow \infty$):

$$S = 2i \sum_{n=0}^{\infty} \frac{1}{\tilde{N}_{0n}} \frac{R_{0n}^{(1)'}(-ic, i0)}{R_{0n}^{(3)'}(-ic, i0)} S_{0n}(-ic, -1) S_{0n}(-ic, \eta). \quad (14.89)$$

The total scattering cross section is:

$$\sigma_T = \frac{4\pi}{k^2} \sum_{n=0}^{\infty} \frac{1}{\tilde{N}_{0n}} \left[\frac{R_{0n}^{(1)'}(-ic, i0)}{R_{0n}^{(3)'}(-ic, i0)} S_{0n}(-ic, -1) \right]^2. \quad (14.90)$$

A variety of results for the field on the disc surface and along the axis have been computed by LEITNER [1949], MEIXNER and FRITZE [1949], BRAUNBEK [1950] and SEVERIN [1952]. Selected results are shown in Figs. 14.8 through 14.11, together with high-frequency Kirchhoff approximations.

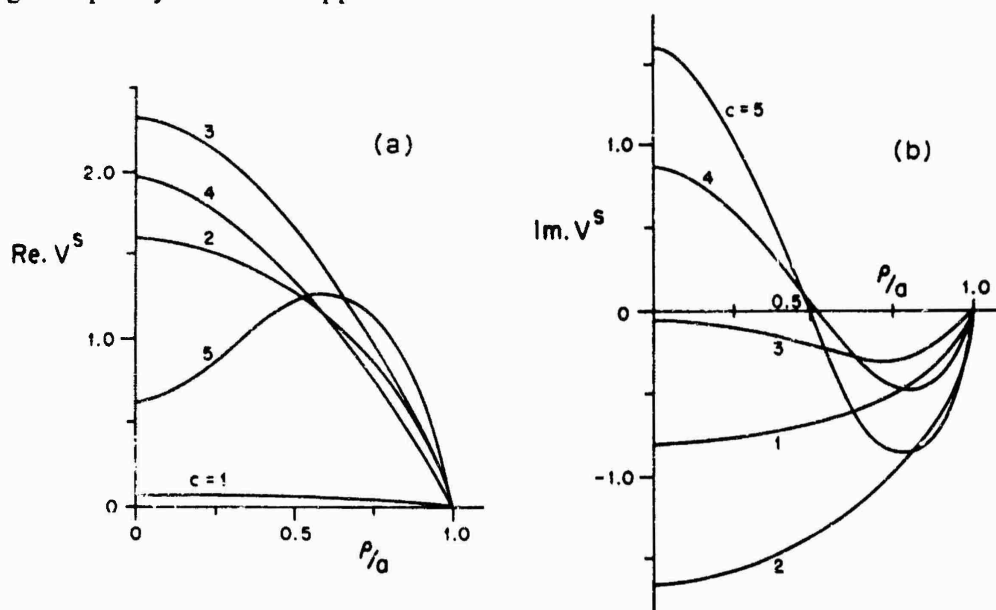


Fig. 14.8. Real and imaginary parts of scattered field on upper surface ($z = 0+$) for five different disc sizes (LEITNER [1949]).

The amplitude $|S|$ of the far field coefficient is shown in Fig. 14.12 for various values of c , and the normalized total scattering cross section is plotted in Fig. 14.13.

14.3.2.2. LOW FREQUENCY APPROXIMATIONS

For an incident wave whose direction of propagation makes an angle ζ with the positive z -axis, such that

$$V^i = \exp \{ik(x \sin \zeta + z \cos \zeta)\}, \quad (14.91)$$

a complete low frequency expansion of the scattered field at the point (ξ, η, ϕ) is (ASVESTAS and KLEINMAN [1967]):

$$V^s = e^{ic\xi} \sum_{n=0}^{\infty} (-c)^n \sum_{m=0}^{\infty} \frac{\eta^{n-m}}{(n-m)!} \sum_{l=0}^m \sum_{r=0}^m \sum_{s=0}^l D_{r,l}^{m,s} Q_r^s(i\xi) P_l^s(\eta) \cos s\phi. \quad (14.92)$$

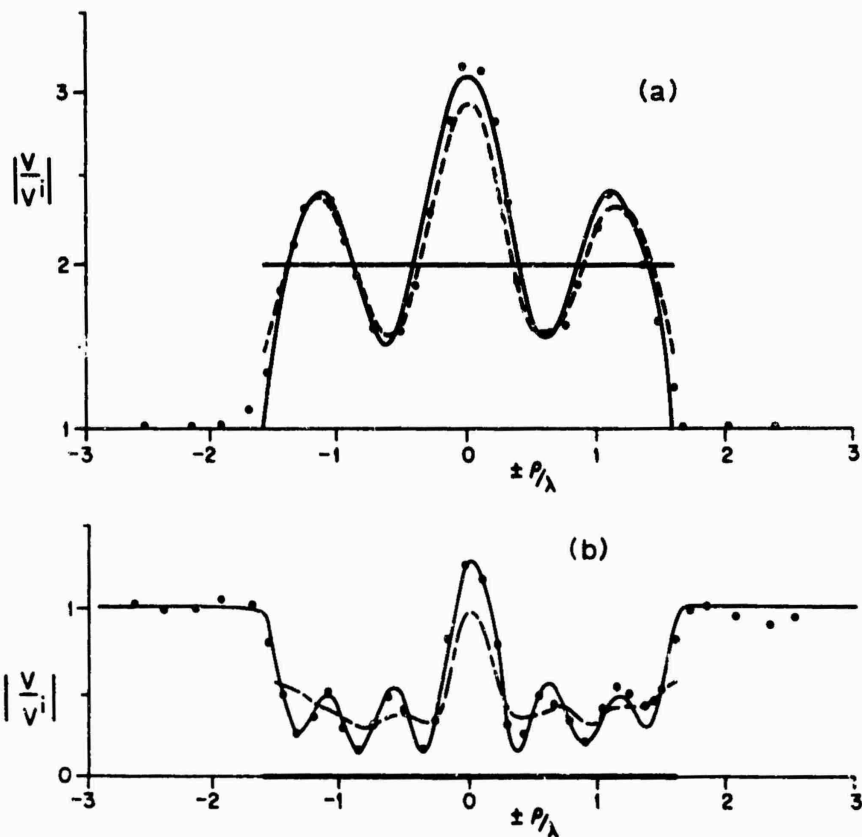


Fig. 14.9. Normalized total field on surfaces (a) $z = 0+$ and (b) $z = 0-$ for $c = 10$: — exact, --- Kirchhoff double layer, -.- Kirchhoff single layer, ●●● experimental (SEVERIN [1952]).

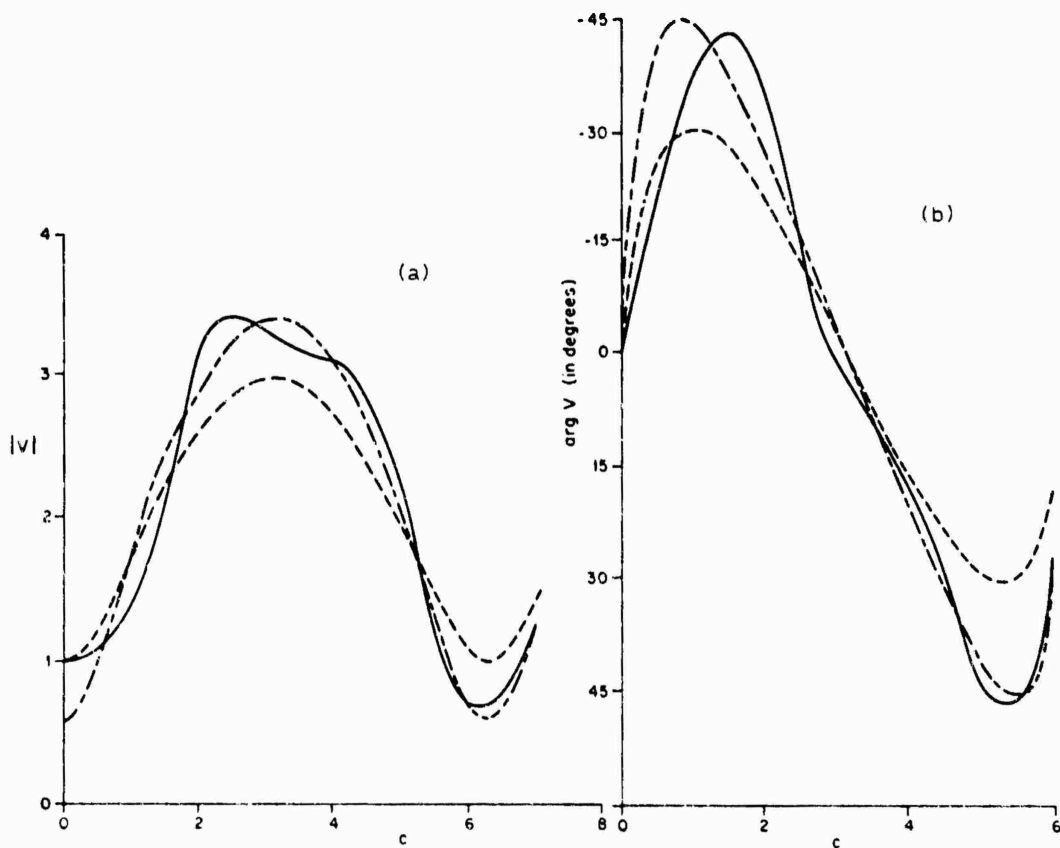


Fig. 14.10. Amplitude and phase of total field at center $\rho = 0$ of illuminated face ($z = 0+$): — exact, --- Kirchhoff single layer, -.- edge-current theory (BRAUNBEK [1950]).

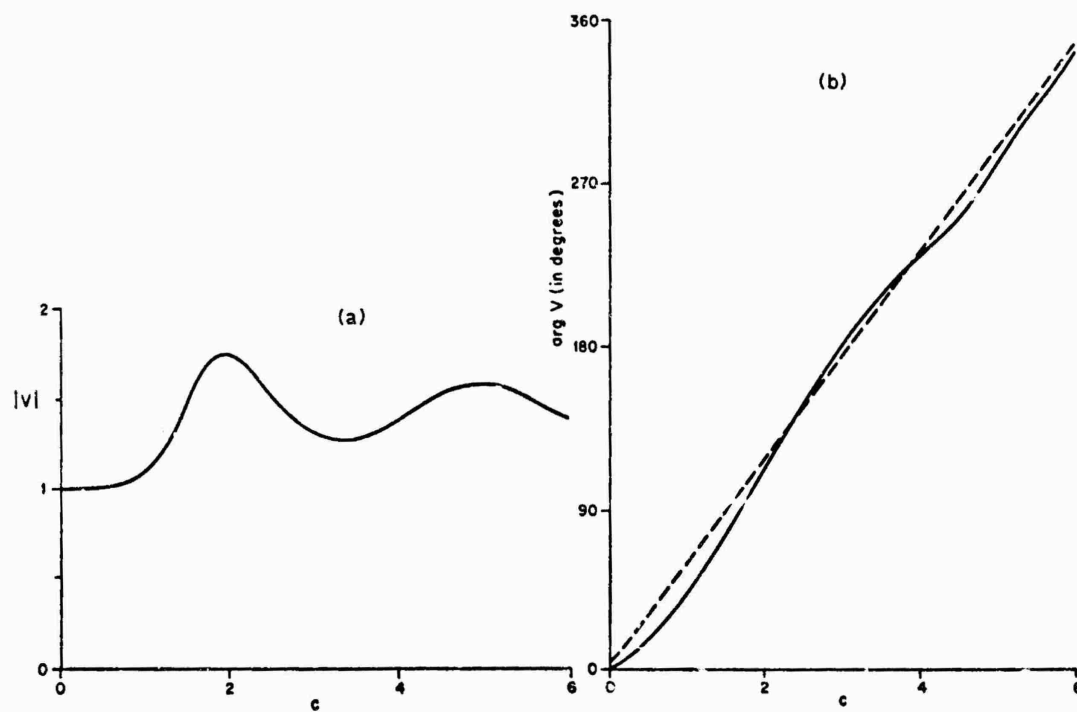


Fig. 14.11. Amplitude and phase of total field at center $\rho = 0$ of illuminated face ($z = 0+$):
 — exact, --- Kirchhoff single layer (MEIXNER and FRITZE [1949]).

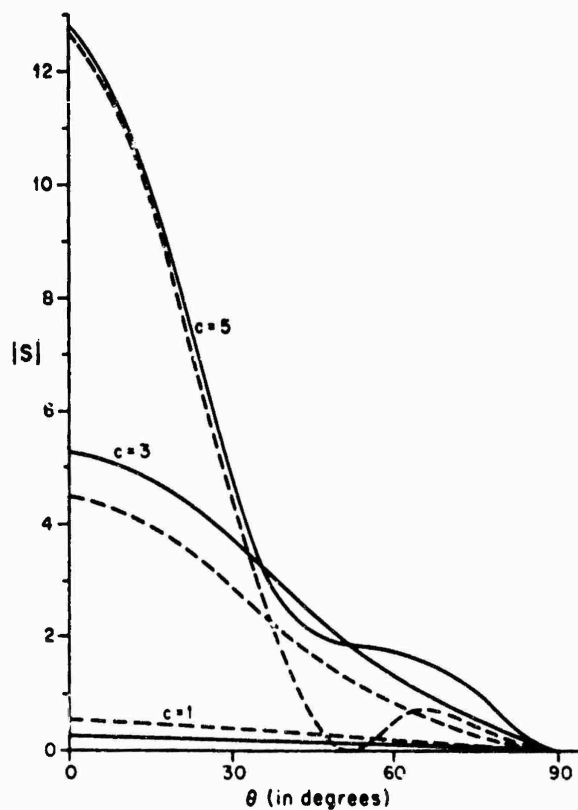


Fig. 14.12. Amplitude of far field coefficient for three disc sizes: — exact, --- Kirchhoff single layer (SEVERIN [1952]).

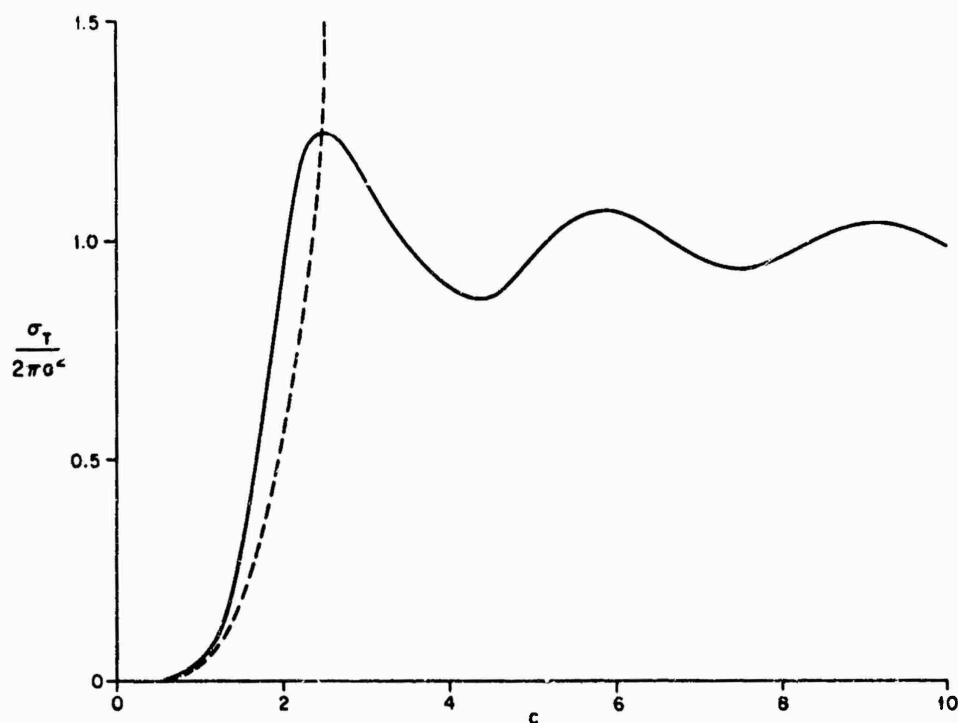


Fig. 14.13. Normalized total scattering cross section: — exact (BOUWKAMP [1954]), --- Rayleigh (see eq. (14.104)).

where the coefficients $D_{r,t}^{m,s}$ are determined from the recurrence relations:

$$D_{r,t}^{m+1,s} = \frac{2}{r(r+1)-t(t+1)} \left[\frac{r(r-s)}{2r-1} D_{r-1,t}^{m,s} + \frac{t(t-s)}{2t-1} D_{r,t-1}^{m,s} - \frac{(t+1)(t+s+1)}{2t+3} D_{r,t+1}^{m,s} - \frac{(r+1)(r+s+1)}{2r+3} D_{r+1,t}^{m,s} \right],$$

$$r \neq t, \quad m = 0, 1, 2, \dots, \quad (14.93)$$

$$D_{t,t}^{m+1,s} = - \sum_{r=0}^{m+1} \frac{Q_r^{s'}(i0)}{Q_t^s(i0)} D_{r,t}^{m+1,s} + \sum_{r=0}^m \frac{Q_r^s(i0)}{Q_t^{s'}(i0)} D_{r,t}^{m,s} + A_t^{m+1,s}, \quad m = 0, 1, 2, \dots, \quad (14.94)$$

$$D_{0,0}^{0,0} = 0, \quad (14.95)$$

$$A_t^{m,s} = \frac{(-1)^m \varepsilon_s \sqrt{\pi} \cos^m \zeta}{2^{m+1} \{\frac{1}{2}(m-t)\}! \{\frac{1}{2}(m+t+1)\}! Q_t^{s'}(i0)} \frac{(t-s)!}{(t+s)!} \times [(m-t)(t-s-1) P_{t+1}^s(\sec \zeta) + (m+t+1)(t+s) P_{t-1}^s(\sec \zeta)], \quad \text{for } m+t \text{ even,}$$

$$= 0, \quad \text{for } m+t \text{ odd,} \quad (14.96)$$

where \sum' in eq. (14.94) indicates that the term with $r = s$ is to be omitted from the summation.

In the far field ($\xi \rightarrow \infty$):

$$S = -i \sum_{n=0}^{\infty} (-c)^{n+1} \sum_{m=0}^n \frac{\eta^{n-m}}{(n-m)!} \sum_{t=0}^m \sum_{s=0}^t (-1)^s s! D_{0,t}^{m,s} P_t^s(\eta) \cos s\phi, \quad (14.97)$$

and the bistatic scattering cross section is:

$$\sigma(\eta, \phi) = 4\pi a^2 \sum_{n=0}^{\infty} (-c)^n \sum_{m=0}^n V_{n-m} V_m^*, \quad (14.98)$$

where

$$V_n = \sum_{m=0}^n \frac{\eta^{n-m}}{(n-m)!} \sum_{t=0}^m \sum_{s=0}^t (-1)^s s! D_{0,t}^{m,s} P_t^s(\eta) \cos s\phi, \quad (14.99)$$

and the asterisk indicates the complex conjugate.

For normal incidence ($\zeta = \pi$), the coefficients $A_t^{m,s}$, $D_{r,t}^{m,s}$ vanish for $s \neq 0$, thus eliminating the summations over s . Explicitly, the far field coefficient is:

$$S = -\frac{2c^3}{3\pi} \left\{ P_1(\eta) + \frac{1}{25} c^2 [P_3(\eta) + 4P_1(\eta)] + \frac{2i}{9\pi} c^3 P_1(\eta) + O(c^4) \right\}. \quad (14.100)$$

An alternative formulation, in which the incident and scattered fields are expanded in Fourier series in the azimuthal angle ϕ , has been developed by several authors (see, for example, WILLIAMS [1962] and BOERSMA [1964]). For arbitrary incidence and in the far field ($\xi \rightarrow \infty$):

$$S = \sum_{m=0}^{\infty} S_m \cos m\phi, \quad (14.101)$$

where

$$S_m = -\frac{\epsilon_m 4^{m+1} m! (m+1)! c^{2m+3} \eta (\sqrt{1-\eta^2} \sin \zeta)^m \cos \zeta}{\pi (2m+1)! (2m+3)!} \times \left[1 - \frac{2m-1+(2m+1)(\sin^2 \zeta - \eta^2)}{2(2m+1)(2m+5)} c^2 + \frac{2i}{9\pi} \delta_{m,0} c^3 + O(c^4) \right], \quad (14.102)$$

and $\delta_{m,0}$ is the Kronecker delta ($\delta_{0,0} = 1$, $\delta_{m,0} = 0$ for $m \neq 0$). The normalized total scattering cross section is:

$$\begin{aligned} \frac{\sigma_1}{2\pi a^2} &= \pi^{-2} \sum_{m=0}^{\infty} \epsilon_m c^{4m+4} \cos^2 \zeta \sin^{2m} \zeta (2m+1)! \left[\frac{4^{m+1} m! (m+1)!}{(2m+1)! (2m+3)!} \right]^2 \\ &\times \left[1 - c^2 \left(\frac{4m^2 + 2m - 8}{(2m+1)(2m+5)^2} + \frac{\sin^2 \zeta}{2m+5} \right) + \right. \\ &+ c^4 \left(\frac{32m^6 + 144m^5 + 24m^4 - 156m^3 + 1236m^2 + 1758m - 311}{(2m-1)(2m+1)^2(2m+5)^3(2m+7)^2} + \right. \\ &+ \left. \frac{8m^3 + 32m^2 + 4m - 53}{(2m+1)(2m+5)^3(2m+7)} \sin^2 \zeta + \frac{m+3}{(2m+5)^2(2m+7)} \sin^4 \zeta \right) + O(c^6) \Big]. \end{aligned} \quad (14.103)$$

Explicitly, for normal incidence (BOUWKAMP [1954], BAZER and BROWN [1959]):

$$\frac{\sigma_T}{2\pi a^2} = \frac{8c^4}{27\pi^2} \left[1 + \frac{8}{25}c^2 + \frac{311}{6125}c^4 + \left(\frac{2612}{496125} - \frac{4}{81\pi^2} \right) c^6 + O(c^8) \right]. \quad (14.104)$$

Results of computations based on eq. (14.104) are shown in Fig. 14.5. Formulas based on Fourier series expansions are also available for the surface field.

For normal incidence ($\zeta = \pi$) and on the illuminated face (BAZER and BROWN [1959]):

$$(V^i + V^s)_{z=0+} = 1 + \frac{4ic}{\pi} \sum_{n=0}^{\infty} B_n \eta^{2n+1}, \quad (14.105)$$

in which the first few coefficients are:

$$\begin{aligned} B_0 = & 1 + \frac{1}{6}c^2 + \frac{2i}{9\pi}c^3 + \frac{1}{120}c^4 + \frac{13i}{225\pi}c^5 + \left(\frac{1}{5040} - \frac{4}{81\pi^2} \right) c^6 + \\ & + \frac{323i}{44100\pi}c^7 + \left(\frac{1}{362880} - \frac{38}{2025\pi^2} \right) c^8 + \\ & + \left(\frac{269i}{5715360\pi} - \frac{4i}{729\pi^3} \right) c^9 + O(c^{10}), \end{aligned} \quad (14.106)$$

$$\begin{aligned} B_1 = & \frac{1}{6}c^2 + \frac{1}{20}c^4 + \frac{i}{15\pi}c^5 + \frac{1}{336}c^6 + \frac{19i}{1050\pi}c^7 + \\ & + \left(\frac{1}{12960} - \frac{2}{135\pi^2} \right) c^8 + \frac{631}{2381400}c^9 + O(c^{10}), \end{aligned} \quad (14.107)$$

$$B_2 = \frac{c^4}{600} \left[1 + \frac{5}{14}c^2 + \frac{10i}{21\pi}c^3 + \frac{5}{216}c^4 + \frac{76i}{567\pi}c^5 \right] + O(c^{10}), \quad (14.108)$$

$$B_3 = \frac{c^6}{35280} \left[1 + \frac{7}{18}c^2 + \frac{58i}{81\pi}c^3 \right] + O(c^{10}), \quad (14.109)$$

$$B_4 = \frac{c^8}{3265920} + O(c^{10}), \quad (14.110)$$

and the remaining coefficients are $O(c^{10})$. An alternative formulation for the surface field in terms of an infinite series of Legendre polynomials has been given by DEHOOP [1954].

In the far field ($\xi \rightarrow \infty$):

$$\begin{aligned} S = & -\frac{2\eta}{3\pi}c^3 \left\{ 1 + \frac{1+\eta^2}{10}c^2 + \frac{2i}{9\pi}c^3 + \left(\frac{1+\eta^4}{280} + \frac{\eta^2}{84} \right) c^4 + \right. \\ & \left. + \frac{i}{45\pi} \left(\frac{11}{5} + \eta^2 \right) c^5 + \frac{1}{27} \left(\frac{1+\eta^6}{560} + \frac{\eta^2+\eta^4}{80} - \frac{4}{3\pi^2} \right) c^6 + \right. \end{aligned}$$

$$+ \frac{i}{10\pi} \left(\frac{131}{2450} + \frac{9}{175} \eta^2 + \frac{\eta^4}{126} \right) c^7 - \frac{1}{90} \left(\frac{68}{45\pi^2} + \frac{4}{9\pi^2} \eta^2 - \frac{3\eta^4}{1760} - \frac{\eta^2 + \eta^6 + \frac{1}{12}(1 + \eta^8)}{1232} \right) c^8 + O(c^9) \}. \quad (14.111)$$

14.3.2.3. HIGH FREQUENCY APPROXIMATIONS

For an incident wave whose direction of propagation makes an angle ζ with the positive z -axis, the only results available are the following expressions for the normalized forward scattering cross section (LEVINE and WU [1957]). For the angular region away from the axis ($\sin \zeta$ bounded away from zero):

$$\frac{\sigma_T}{2\pi a^2 |\cos \zeta|} \sim 1 - \frac{1}{4c^2 |\cos^3 \zeta|} - \frac{1}{\pi c^2 |\cos \zeta| \sqrt{\sin \zeta}} \left\{ (1 - \sin \zeta)^{-\frac{1}{2}} \times \sin [2c(1 - \sin \zeta)] - (1 + \sin \zeta)^{-\frac{1}{2}} \cos [2c(1 + \sin \zeta)] \right\}, \quad (14.112)$$

whereas for near-axial incidence ($\sin \zeta \approx 0$):

$$\frac{\sigma_T}{2\pi a^2 |\cos \zeta|} \sim 1 - \frac{2 \sin(2c - \frac{1}{2}\pi)}{c \sqrt{\pi c}} J_0(2c \sin \zeta) - \frac{1}{4c^2} - \frac{1}{\pi c^2} \cos [2c(2 + \sin^2 \zeta)] J_0(c \sin^2 \zeta). \quad (14.113)$$

For axial incidence, a variety of results have been obtained using the Kirchhoff approximation or its various modifications. However, these have in large measure been superseded by the more accurate results obtained from an integral equation formulation by WESTFAHL and WITTE [1967].

In the far field and near the axis ($c \sin \theta \lesssim 1$):

$$S \sim - \frac{ic}{\sin \theta} J_1(c \sin \theta) - c \sum_{n=0}^5 c^{-1n} S_n + O(c^{-2}), \quad (14.114)$$

where θ is the spherical polar angle ($\eta = \cos \theta$), the Kirchhoff approximation is represented by the term outside the summation, and

$$S_0 = \frac{1}{2} J_0(c \sin \theta), \quad (14.115)$$

$$S_1 = \pi^{-\frac{1}{2}} e^{2ic} + \frac{1}{4} i \pi J_0(c \sin \theta), \quad (14.116)$$

$$S_2 = -\frac{1}{2} i \left(\frac{1}{4} + \pi^{-1} e^{4ic} \right) J_0(c \sin \theta) - \frac{1}{8} ic \sin \theta J_1(c \sin \theta), \quad (14.117)$$

$$S_3 = \frac{e^{4ic}}{2\sqrt{\pi}} \left[\left(\frac{e^{6ic}}{2\pi} + \frac{3}{8} e^{2ic} \right) J_0(c \sin \theta) + c \sin \theta e^{2ic} J_1(c \sin \theta) \right], \quad (14.118)$$

$$S_4 = -\frac{1}{8} \left(\pi^{-2} e^{8ic} + \frac{5}{2\pi} e^{4ic} + \frac{19 + 45i}{256} \right) J_0(c \sin \theta) + \frac{1}{4} c \sin \theta (\pi^{-1} e^{4ic} - \frac{1}{4}) J_1(c \sin \theta) + \frac{1}{16} c^2 \sin^2 \theta J_2(c \sin \theta), \quad (14.119)$$

$$S_5 = \frac{e^{-\frac{1}{2}i\pi}}{32\sqrt{\pi}} \left\{ \left[\pi^{-2} e^{10ic} + \frac{17}{2\pi} e^{6ic} + \frac{11+63i}{32} e^{2ic} \right] J_0(c \sin \theta) + \right. \\ \left. + 4c \sin \theta (\pi^{-1} e^{6ic} - \frac{9}{4} e^{2ic}) J_1(c \sin \theta) + 12c^2 \sin^2 \theta e^{2ic} J_2(c \sin \theta) \right\}. \quad (14.120)$$

In the far field and away from the axis ($c \sin \theta \gg 1$):

$$S \sim - \sqrt{\frac{c}{2\pi \sin \theta}} \sum_{n=0}^5 c^{-\frac{1}{2}n} [\bar{S}_n(\theta) e^{-ic \sin \theta + \frac{1}{2}i\pi} + \bar{S}_n(-\theta) e^{ic \sin \theta - \frac{1}{2}i\pi}] + O(c^{-\frac{1}{2}}), \quad (14.121)$$

where

$$\bar{S}_0(\theta) = \frac{-\sqrt{(1-\sin \theta)}}{\sin \theta}, \quad (14.122)$$

$$\bar{S}_1(\theta) = \frac{e^{2ic + \frac{1}{2}i\pi}}{\sqrt{\{\pi(1-\sin \theta)\}}}, \quad (14.123)$$

$$\bar{S}_2(\theta) = \frac{-ie^{4ic}}{2\pi\sqrt{(1-\sin \theta)}} + \frac{i\sqrt{(1-\sin \theta)}}{4 \sin \theta} \left(1 + \frac{3}{2 \sin \theta} \right), \quad (14.124)$$

$$\bar{S}_3(\theta) = \frac{e^{4i\pi}}{4\sqrt{\{\pi(1-\sin \theta)\}}} \left[\frac{e^{6ic}}{\pi} + \frac{1}{2} e^{2ic} \left(\frac{3}{2} - \frac{1}{\sin \theta} + \frac{2}{1-\sin \theta} \right) \right], \quad (14.125)$$

$$\bar{S}_4(\theta) = \frac{1}{8\pi\sqrt{(1-\sin \theta)}} \left[-\frac{e^{8ic}}{\pi} + \frac{1}{2} e^{4ic} \left(5 - \frac{i}{\sin \theta} + \frac{2}{1-\sin \theta} \right) \right] - \\ - \frac{\sqrt{(1-\sin \theta)}}{128 \sin \theta} \left(\frac{59-27i}{8} + \frac{33-9i}{2 \sin \theta} + \frac{24-9i}{\sin^2 \theta} \right) + \frac{39-9i}{128 \sin^3 \theta}, \quad (14.126)$$

$$\bar{S}_5(\theta) = \frac{e^{-\frac{1}{2}i\pi}}{16\sqrt{\{\pi(1-\sin \theta)\}}} \left\{ \pi^{-2} e^{10ic} + \frac{e^{6ic}}{4\pi} \left(17 - \frac{2}{\sin \theta} + \frac{4}{1-\sin \theta} \right) - e^{2ic} \left[\frac{53-63i}{64} + \right. \right. \\ \left. \left. + \frac{3}{8 \sin \theta} - \frac{9}{8 \sin^2 \theta} - \frac{13}{4(1-\sin \theta)} - 3(1-\sin \theta)^{-2} + \frac{3}{2 \sin \theta(1-\sin \theta)} \right] \right\}. \quad (14.127)$$

The first term of expansion (14.121) was derived earlier by BRAUNBEK [1950] using the Kirchhoff formula with a more refined approximation for the field near the edge. Other expansions have been obtained via the geometrical theory of diffraction by KELLER [1957] and via an asymptotic solution of the exact boundary value problem by HANSEN [1964]. The latter's results are analogous to those presented for the soft disc in Section 14.2.2.3, but their regions of validity are somewhat in doubt.

The normalized total scattering cross section is (WESTPFAHL and WITTE [1967]):

$$\begin{aligned}
\frac{\sigma_T}{2\pi a^2} \sim & 1 - \frac{2}{c\sqrt{\pi c}} \sin(2c - \tfrac{1}{4}\pi) - c^{-2} \left(\frac{1}{4} + \frac{1}{\pi} \cos 4c \right) + \\
& + \frac{1}{c^2\sqrt{\pi c}} \left[\frac{3}{8} \cos(2c - \tfrac{1}{4}\pi) + \frac{1}{2\pi} \cos(6c - \tfrac{1}{4}\pi) \right] - \\
& - c^{-3} \left[\frac{45}{1024} + \frac{\sin 8c}{4\pi^2} + \frac{5}{8\pi} \sin 4c \right] + \frac{1}{c^3\sqrt{\pi c}} \left[\frac{\sin(10c - \tfrac{1}{4}\pi)}{16\pi^2} + \right. \\
& \left. + \frac{17}{32\pi} \sin(6c - \tfrac{1}{4}\pi) + \frac{11}{2048} \sin(2c - \tfrac{1}{4}\pi) + \frac{63}{2048} \cos(2c - \tfrac{1}{4}\pi) \right]. \quad (14.128)
\end{aligned}$$

The first four terms of this series have been determined also by LEVINE and WU [1957], HANSEN [1964] and JONES [1965c]. The form given by Levine and Wu contains a value $\frac{1}{4}$ replacing the coefficient $\frac{3}{8}$ in the term $O(c^{-2})$ of eq. (14.128). The results of Hansen and Jones, however, corroborate the value given here.

14.4. Perfectly conducting disc

14.4.1. Dipole sources

14.4.1.1. EXACT SOLUTIONS

For an arbitrarily oriented electric dipole located at the point (ξ_0, η_0, ϕ_0) in the oblate spheroidal coordinate system and with a moment $(4\pi\epsilon/k)\hat{\mathbf{e}}$, corresponding to an incident electric Hertz vector

$$\begin{aligned}
\Pi_{\mathbf{e}}^i = \frac{e^{ikR}}{kR} \hat{\mathbf{e}} = 2i\hat{\mathbf{e}} \sum_{m=0}^{\infty} \sum_{n=m}^{\infty} \frac{\epsilon_m}{N_{mn}} K_{mn}^{(1)}(-ic, i\xi_0) R_{mn}^{(3)}(-ic, i\xi_0) \\
\times S_{mn}(-ic, \eta) S_{mn}(-ic, \eta_0) \cos m(\phi - \phi_0), \quad (14.129)
\end{aligned}$$

the electric Hertz vector $\Pi_{\mathbf{e}}^s$ of the scattered field can be split into two parts,

$$\Pi_{\mathbf{e}}^s = \Pi^1 + \Pi^2, \quad (14.130)$$

whose rectangular Cartesian components are (MEIXNER [1953]):

$$\begin{aligned}
\Pi_x^1 \pm i\Pi_y^1 &= -i(c_x \pm ic_y) \sum_{m=0}^{\infty} \epsilon_m L_m \cos m(\phi - \phi_0), \\
\Pi_z^1 &= -ic_z \sum_{m=0}^{\infty} \epsilon_m M_m \cos m(\phi - \phi_0), \\
\Pi_x^2 \pm i\Pi_y^2 &= e^{\pm i\phi} \sum_{m=-\infty}^{\infty} U_m N_{m\pm 1} e^{-im(\phi - \phi_0)} \\
\Pi_z^2 &= 0,
\end{aligned} \quad (14.131)$$

where

$$\begin{aligned}
L_m = \sum_{(n-m) \text{ even}} \frac{1}{N_{mn}} \frac{R_{mn}^{(1)}(-ic, i0)}{R_{mn}^{(3)}(-ic, i0)} R_{mn}^{(3)}(-ic, i\xi) R_{mn}^{(3)}(-ic, i\xi_0) \\
\times S_{mn}(-ic, \eta) S_{mn}(-ic, \eta_0), \quad (14.132)
\end{aligned}$$

$$M_m = \sum_{(n-m) \text{ odd}} \frac{1}{\tilde{N}_{mn}} \frac{R_{mn}^{(1)'(-ic, i0)}}{R_{mn}^{(3)'(-ic, i0)}} R_{mn}^{(3)}(-ic, i\xi) R_{mn}^{(3)}(-ic, i\xi_0) \times S_{mn}(-ic, i, j) \tilde{S}_{mn}(-ic, \eta_0), \quad (14.133)$$

$$N_m = \sum_{(n-m) \text{ even}} \frac{(-i)^n}{\tilde{N}_{mn}} \frac{R_{mn}^{(1)}(-ic, i0)}{R_{mn}^{(3)}(-ic, i0)} R_{mn}^{(3)}(-ic, i\xi) S_{mn}(-ic, \eta) S_{mn}(-ic, 0), \quad (14.134)$$

$$U_m = [\bar{N}_{m-1} + \bar{N}_{m+1}]^{-1} [2c_x \bar{M}_m + ie^{-i\phi_0}(c_x + ic_y) \bar{L}_{m-1} + ie^{i\phi_0}(c_x - ic_y) \bar{L}_{m+1}], \quad (14.135)$$

$$L_m = -ic \left. \frac{\partial L_m}{\partial \xi} \right|_{\xi=\eta=0} = \sum_{(n-m) \text{ even}} \frac{1}{\tilde{N}_{mn}} \frac{R_{mn}^{(3)}(-ic, i\xi_0)}{R_{mn}^{(3)}(-ic, i0)} S_{mn}(-ic, 0) S_{mn}(-ic, \eta_0), \quad (14.136)$$

$$\bar{M}_m = c \left. \frac{\partial M_m}{\partial \eta} \right|_{\xi=\eta=0} = - \sum_{(n-m) \text{ odd}} \frac{1}{\tilde{N}_{mn}} \frac{R_{mn}^{(3)}(-ic, i\xi_0)}{R_{mn}^{(3)'(-ic, i0)}} S_{mn}'(-ic, 0) S_{mn}(-ic, \eta_0), \quad (14.137)$$

$$\bar{N}_m = -ic \left. \frac{\partial N_m}{\partial \xi} \right|_{\xi=\eta=0} = \sum_{(n-m) \text{ even}} \frac{(-i)^n}{\tilde{N}_{mn}} \frac{[S_{mn}(-ic, 0)]^2}{R_{mn}^{(3)}(-ic, i0)}. \quad (14.138)$$

For the notation on the spheroidal wave functions, see Chapters 11 and 13. Here the summations are over values of $n \geq |m|$ such that $n-m$ is even or odd as noted and the functions L_m , \bar{M}_m and \bar{N}_m are even in m . When the dipole is located on the axis ($\eta_0 = 1$), these forms simplify to the extent that

$$L_m = L_m = M_m = \bar{M}_m = 0, \quad \text{for } m > 0, \quad (14.139)$$

implying that the only non-zero U 's are:

$$U_0 = \frac{\bar{M}_0}{\bar{N}_1} c_z, \quad (14.140)$$

$$U_1 = \frac{iL_0}{\bar{N}_0 + \bar{N}_2} e^{-i\phi_0}(c_x + ic_y), \quad (14.141)$$

$$U_{-1} = \frac{iL_0}{\bar{N}_0 + \bar{N}_2} e^{i\phi_0}(c_x - ic_y). \quad (14.142)$$

If the electric dipole is on the axis at $(\xi_0, 1)$ and is axially oriented, the only non-vanishing component of the total magnetic field is:

$$H_\phi + H_\phi^* = \frac{2k^2 Y}{(\xi^2 + 1)^{n+1}} \sum_{n=0}^{\infty} \frac{(-i)^n}{\tilde{\rho}_{1n} \tilde{N}_{1n}} \left[R_{1n}^{(1)}(-ic, i\xi_0) - \frac{R_{1n}^{(1)'(-ic, i0)}}{R_{1n}^{(3)'(-ic, i0)}} \right. \\ \left. \times R_{1n}^{(3)}(-ic, i\xi_0) \right] R_{1n}^{(3)}(-ic, i\xi_0) S_{1n}(-ic, \eta). \quad (14.143)$$

If the observation point is on the surface of the disc ($\xi = 0$):

$$H_{\phi}^i + H_{\phi}^s = \frac{2k^2 Y}{c \sqrt{(\xi_0^2 + 1)}} \sum_{n=0}^{\infty} \frac{(-i)^{n+1}}{\tilde{\rho}_{1n} \tilde{N}_{1n}} \frac{R_{1n}^{(3)}(-ic, i\xi_0)}{(\partial/\partial \xi) R_{1n}^{(3)}(-ic, i\xi)|_{\xi=0}} S_{1n}(-ic, \eta), \quad (14.144)$$

whereas in the far field ($\xi \rightarrow \infty$):

$$H_{\phi}^i + H_{\phi}^s = \frac{e^{ic\xi}}{c\xi} \frac{2ik^2 Y}{\sqrt{(\xi_0^2 + 1)}} \sum_{n=0}^{\infty} \frac{(-1)^{n-1}}{\tilde{\rho}_{1n} \tilde{N}_{1n}} \left[R_{1n}^{(1)}(-ic, i\xi_0) - \frac{R_{1n}^{(1)}(-ic, i0)}{R_{1n}^{(3)}(-ic, i0)} \right. \\ \left. \times R_{1n}^{(3)}(-ic, i\xi_0) \right] S_{1n}(-ic, \eta). \quad (14.145)$$

If the dipole is on the surface of the disc ($\xi_0 = 0$), the field at an arbitrary point is

$$H_{\phi}^i + H_{\phi}^s = \frac{2k^2 Y}{c} \sum_{n=0}^{\infty} \frac{(-i)^{n-1}}{\tilde{\rho}_{1n} \tilde{N}_{1n}} \frac{R_{1n}^{(3)}(-ic, i\xi)}{(\partial/\partial \xi) R_{1n}^{(3)}(-ic, i\xi)|_{\xi=0}} S_{1n}(-ic, \eta). \quad (14.146)$$

On the surface ($\xi = 0$):

$$H_{\phi}^i + H_{\phi}^s = \frac{2k^2 Y}{c} \sum_{n=0}^{\infty} \frac{(-i)^{n-1}}{\tilde{\rho}_{1n} \tilde{N}_{1n}} \frac{R_{1n}^{(3)}(-ic, i0)}{(\partial/\partial \xi) R_{1n}^{(3)}(-ic, i\xi)|_{\xi=0}} S_{1n}(-ic, \eta), \quad (14.147)$$

whereas in the far field ($\xi \rightarrow \infty$):

$$H_{\phi}^i + H_{\phi}^s = \frac{e^{ic\xi}}{c\xi} \frac{2k^2 Y}{c} \sum_{n=0}^{\infty} \frac{(-i)^n}{\tilde{\rho}_{1n} \tilde{N}_{1n}} \frac{S_{1n}(-ic, \eta)}{(\partial/\partial \xi) R_{1n}^{(3)}(-ic, i\xi)|_{\xi=0}}. \quad (14.148)$$

For an axial magnetic dipole at ($\xi_0, \eta_0 = 1$) with moment $(4\pi/k)\hat{z}$, corresponding to an incident magnetic Hertz vector $\hat{z}e^{ikR}/(kR)$, so that

$$E_{\phi}^i = k^2 c Z \frac{e^{ikR}}{kR} \left(1 + \frac{i}{kR} \right) \sqrt{(\xi^2 + 1)(1 - \eta^2)}, \quad (14.149)$$

$$E_{\xi}^i = E_{\eta}^i = H_{\phi}^i = 0,$$

the total electric field is

$$E_{\phi}^i + E_{\phi}^s = \frac{-2k^2 Z}{\sqrt{(\xi_0^2 + 1)}} \sum_{n=0}^{\infty} \frac{(-i)^n}{\tilde{\rho}_{1n} \tilde{N}_{1n}} \left[R_{1n}^{(1)}(-ic, i\xi_0) - \frac{R_{1n}^{(1)}(-ic, i0)}{R_{1n}^{(3)}(-ic, i0)} \right. \\ \left. \times R_{1n}^{(3)}(-ic, i\xi_0) \right] R_{1n}^{(3)}(-ic, i\xi_0) S_{1n}(-ic, \eta). \quad (14.150)$$

On the surface of the disc ($\xi = 0$):

$$H_{\eta}^i + H_{\eta}^s = \frac{2k^2}{c^2 \eta \sqrt{(\xi_0^2 + 1)}} \sum_{n=0}^{\infty} \frac{(-i)^n}{\tilde{\rho}_{1n} \tilde{N}_{1n}} \frac{R_{1n}^{(3)}(-ic, i\xi_0)}{R_{1n}^{(3)}(-ic, i0)} S_{1n}(-ic, \eta), \quad (14.151)$$

and in the far field ($\xi \rightarrow \infty$):

$$E_{\phi}^i + E_{\phi}^s = \frac{e^{ic\xi}}{c\xi} \frac{2ik^2Z}{\sqrt{(\xi_0^2+1)}} \sum_{n=0}^{\infty} \frac{(-1)^n}{\tilde{\rho}_{1n}\tilde{N}_{1n}} \times \left[R_{1n}^{(1)}(-ic, i\xi_0) - \frac{R_{1n}^{(1)}(-ic, i0)}{R_{1n}^{(3)}(-ic, i0)} R_{1n}^{(3)}(-ic, i\xi_0) \right] S_{1n}(-ic, \eta). \quad (14.152)$$

If the dipole is on the surface ($\xi_0 = 0$), the field is identically zero everywhere.

For the case of an electric dipole at an arbitrary location but oriented parallel to the plane of the disc, a solution has been derived without the aid of spheroidal functions by INAWASHIRO [1963], using a technique developed by NOMURA and KATSURA [1955]. If the dipole is located at $(x_0, y_0, z_0) = (\rho_0, \phi_0, z_0)$ and is oriented in the x direction, so that the incident electric Hertz vector is

$$\Pi_e^i = \frac{e^{ikR}}{kR} \hat{x}, \quad (14.153)$$

the Hertz vector of the scattered field is

$$\Pi_e^s = \Pi_1 + \Pi_2, \quad (14.154)$$

with

$$\Pi_1 = (\Pi_{1x}, 0, 0), \quad \Pi_2 = (\Pi_{2x}, \Pi_{2y}, 0), \quad (14.155)$$

where

$$\Pi_{1x} = -c^{-1} \sum_{m=0}^{\infty} \sum_{n=0}^{\infty} 4_n^m S_n^m(\rho, z) \cos m(\phi - \phi_0), \quad (14.156)$$

$$\Pi_{2x} = \frac{k}{2c} \sum_{m=0}^{\infty} \sum_{n=0}^{\infty} \left\{ (U_{m+1}^{(1)} \mp U_{m-1}^{(1)}) \frac{\sin m\phi}{\cos} \pm (U_{m+1}^{(2)} \mp U_{m-1}^{(2)}) \frac{\cos m\phi}{\sin} \right\} B_n^m S_n^m(\rho, z), \quad (14.157)$$

and

$$S_n^m(\rho, z) = \int_0^{\infty} \frac{\xi J_m(\rho\xi/a) J_{m+2n+1}(\xi)}{\sqrt{(\xi^2 - c^2)}} \exp \left[-\sqrt{\xi^2 - c^2} \frac{|z|}{a} \right] d\xi, \quad (14.158)$$

$$A_n^m = -\varepsilon_m \sum_{s=0}^{\infty} X_{ns}^m a_s^m, \quad (\varepsilon_0 = 1; \varepsilon_m = 2, \text{ for } m \geq 1), \quad (14.159)$$

$$B_n^m = -\sum_{s=0}^{\infty} X_{ns}^m b_s^m, \quad (14.160)$$

$$a_n^m = (2m + 4n + 1) S_n^m(\rho_0, z_0), \quad (14.161)$$

$$b_n^m = (2m + 4n + 1)(-1)^m \sqrt{\frac{2}{\pi}} j_{m+2n}(c), \quad (14.162)$$

$$U_m^{(1)} = \frac{\sum_{n=0}^{\infty} (-1)^n [A_n^{m-1} \sin(m-1)\phi_0 + A_n^{m+1} \sin(m+1)\phi_0]}{\sum_{n=0}^{\infty} (-1)^n (B_n^{m-1} - B_n^{m+1})}, \quad (m \geq 2), \quad (14.163)$$

$$U_m^{(2)} = \frac{\sum_{n=0}^{\infty} (-1)^n [A_n^{m-1} \cos(m-1)\phi_0 + A_n^{m+1} \cos(m+1)\phi_0]}{\sum_{n=0}^{\infty} (-1)^n (B_n^{m-1} - B_n^{m+1})}, \quad (m \geq 2). \quad (14.164)$$

$$U_1^{(1)} = \frac{\sum_{n=0}^{\infty} (-1)^n A_n^2 \sin 2\phi_0}{\sum_{n=0}^{\infty} (-1)^n (B_n^0 - B_n^2)}, \quad (14.165)$$

$$U_1^{(2)} = \frac{\sum_{n=0}^{\infty} (-1)^n (2A_n^0 + A_n^2 \cos 2\phi_0)}{\sum_{n=0}^{\infty} (-1)^n (B_n^0 - B_n^2)}, \quad (14.166)$$

$$U_0^{(2)} = - \frac{\sum_{n=0}^{\infty} (-1)^n A_n^1 \cos \phi_0}{\sum_{n=0}^{\infty} (-1)^n B_n^1}. \quad (14.167)$$

The X_{ns}^m are elements of the inverse of the matrix $[G_{ns}^m]$, whose elements are defined by the expressions (NOMURA and KATSURA [1955]):

$$G_{ns}^m = (2m+4s+1)(g_1 - ig_2), \quad (14.168)$$

$$g_1 = \int_c^{\infty} \frac{J_{m+2n+\frac{1}{2}}(\xi) J_{m+2s+\frac{1}{2}}(\xi) d\xi}{\sqrt{(\xi^2 - c^2)}}, \quad (14.169)$$

$$g_2 = \int_0^c \frac{J_{m+2n+\frac{1}{2}}(\xi) J_{m+2s+\frac{1}{2}}(\xi) d\xi}{\sqrt{(c^2 - \xi^2)}}; \quad (14.170)$$

that is, the X_{ns}^m are solutions of the infinite systems of equations:

$$\sum_{n=0}^{\infty} G_{nv}^m X_{ns}^m = \delta_{s,v}, \quad (s, v = 0, 1, 2, \dots, \infty; \\ \delta_{s,s} = 1, \quad \delta_{s,v} = 0 \quad \text{for } s \neq v), \quad (14.171)$$

for $m = 0, 1, 2, \dots$. Explicitly:

$$X_{00}^0 = 1 - \frac{2i}{\pi} c - \left(\frac{4}{\pi^2} - \frac{1}{3} \right) c^2 - i0.0249298 c^3 + 0.0057643 c^4 + \\ + i0.0004768 c^5 + 0.0002861 c^6 + i0.0001657 c^7 + \dots$$

$$X_{10}^0 = -\frac{1}{6} c^2 - \frac{i}{9\pi} c^3 + 0.0251032 c^4 - i0.0025078 c^5 + \\ + 0.0011928 c^6 + i0.0002944 c^7 + \dots$$

$$\begin{aligned}
X_{20}^0 &= -\frac{1}{840}c^4 - i0.0004547c^5 + 0.0000352c^6 - i0.0000362c^7 + \dots \\
X_{30}^0 &= -0.0001685c^6 + i0.0001007c^7 + \dots \\
X_{01}^0 &= -\frac{1}{30}c^2 - \frac{i}{45\pi}c^3 + 0.0002587c^4 - i0.0005016c^5 + \dots \\
X_{11}^0 &= 1 - \frac{1}{21}c^2 - \frac{1}{252}c^4 - i0.0016505c^5 + \dots \\
X_{21}^0 &= -\frac{1}{70}c^2 - \frac{1}{231}c^4 + \dots \\
X_{11}^0 &= -0.0000361c^4 + \dots \\
X_{02}^0 &= -0.0001323c^4 - i0.0000505c^5 + \dots \\
X_{12}^0 &= -0.0093650c^2 - 0.0002405c^4 + \dots \\
X_{22}^0 &= 1 - \frac{1}{7}c^2 + \dots \\
X_{32}^0 &= \frac{1}{148}c^2 + \dots \\
X_{03}^0 &= 0.0001685c^6 + i0.0001007c^7 + \dots \\
X_{00}^2 &= 1 - \frac{1}{21}c^2 - \frac{1}{105}c^4 - i0.0075450c^5 + \dots \\
X_{10}^2 &= -\frac{1}{70}c^2 - \frac{1}{231}c^4 + \dots \\
X_{20}^0 &= -0.0000361c^4 + \dots
\end{aligned} \tag{14.172}$$

When the dipole is located on the axis ($\rho_0 = 0$) and oriented in the x direction, the coefficients a_n^m vanish for $m > 0$; the non-vanishing coefficients are:

$$a_n^0 = \frac{c}{\sqrt{2}} (-1)^n (4n+1) \sum_{p=0}^{\infty} \frac{(n+p)!}{p!(2n+p+\frac{1}{2})!} \left(\frac{ca}{2|z_0|} \right)^{n+p} h_{n+p}^{(1)}(k|z_0|). \tag{14.173}$$

The imaginary part of series (14.173) converges for all $|z_0|$, but the real part only for $|z_0| \geq a$. For $|z_0| < a$, the real part may be written as

$$\begin{aligned}
\operatorname{Re}(a_n^0) &= (-1)^n (4n+1) \sqrt{\frac{1}{2}\pi} \frac{\Gamma(n+1)}{\Gamma(2n+\frac{3}{2})} \sum_{q=0}^{\infty} \frac{(-1)^q (\frac{1}{2}c)^{2q} (1+h^2)^{q-n-\frac{1}{2}}}{\Gamma(q+1)\Gamma(\frac{1}{2}-n+q)} \\
&\quad \times F\left(n-q+\frac{1}{2}, n+\frac{1}{2}; 2n+\frac{3}{2}; \frac{1}{1+h^2}\right), \tag{14.174}
\end{aligned}$$

where $h = |z_0|/a$.

The surface current components for $\rho_0 = 0$ are:

$$H_{\rho}|_{z=\pm 0} = \pm \frac{iY}{c} k^2 [A(\rho) + B(\rho) \pm C(\rho)] \sin \phi, \tag{14.175}$$

$$H_{\phi}|_{z=\pm 0} = \pm \frac{iY}{c} k^2 [A(\rho) - B(\rho) \pm C(\rho)] \cos \phi, \tag{14.176}$$

where the upper (lower) signs correspond to the illuminated (shadow) side, and

$$A(\rho) = c^{-1} \left[\frac{2}{\pi(1-\rho^2/a^2)} \right]^{\frac{1}{2}} \sum_{n=0}^{\infty} (-1)^n [A_n^0 - \frac{1}{2}B_n^0 U_1^{(2)}] F(-n, n+\frac{1}{2}; \frac{1}{2}; 1-\rho^2/a^2), \tag{14.177}$$

$$B(\rho) = -\frac{\rho^2}{2ca^2} \left[\frac{2}{\pi(1-\rho^2/a^2)} \right]^{\frac{1}{2}} \sum_{n=0}^{\infty} (-1)^n B_n^2 U_1^{(2)} F(-n, n+\frac{1}{2}; \frac{1}{2}; 1-\rho^2/a^2), \quad (14.178)$$

$$C(\rho) = -\frac{ia|z_0|}{R^2} \left(1 + \frac{i}{kR} \right) e^{ikR}. \quad (14.179)$$

From eqs. (14.175) and (14.176) it follows that the surface field is parallel to the dipole moment for $\phi = 0, \frac{1}{2}\pi, \pi, \frac{3}{2}\pi$. INAWASHIRO [1963] has computed the normalized surface field intensity along these radii for $c = 1, 3$ and 5 for various $|z_0|/a$; typical results are shown in Fig. 14.14.

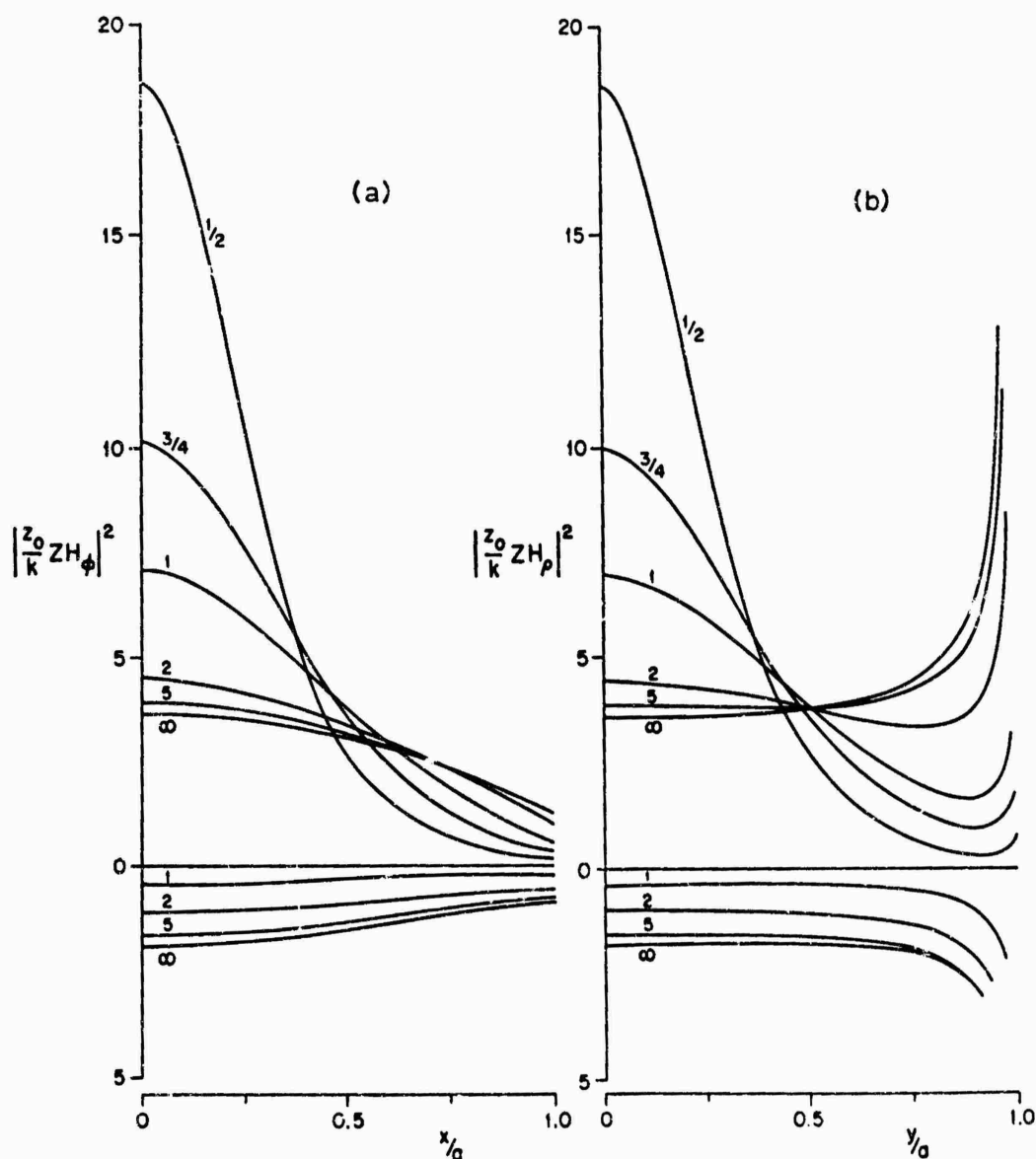


Fig. 14.14. Normalized surface field components on a disc with $c = 1.0$ for an electric dipole on the axis with moment in the x direction for various $|z_0|/a$; upper curves are for $z = 0+$, lower curves for $z = 0-$: (a) along x -axis, (b) along y -axis (INAWASHIRO [1963]).

The normalized total scattering cross section with the source on the axis is

$$\begin{aligned} \frac{\sigma_T}{2\pi a^2} = & -\frac{4}{c^3 \Omega} \operatorname{Im} \left\{ \sum_{n=0}^{\infty} \frac{c^2}{4n+1} a_n^0 [A_n^0 - \frac{1}{2} B_n^0 U_1^{(2)}]^* + \right. \\ & + \sum_{m=0}^{\infty} \sum_{n=m+1}^{\infty} (-1)^{m+n} (n-m) [(n+m+\frac{1}{2}) a_n^0 (A_n^0 - \frac{1}{2} B_n^0 U_1^{(2)})^* - \\ & \left. - \frac{1}{2} (n+m+\frac{1}{2}) a_{n+1}^0 (B_{n+1}^0 U_1^{(2)})^*] \right\}, \end{aligned} \quad (14.180)$$

where

$$\Omega = \frac{4}{3} - \frac{|z_0|}{\sqrt{(a^2 + z_0^2)}} - \frac{1}{3} \left[\frac{|z_0|}{\sqrt{(a^2 + z_0^2)}} \right]^3, \quad (14.181)$$

and the asterisk indicates the complex conjugate; computed values are shown in Fig. 14.15.

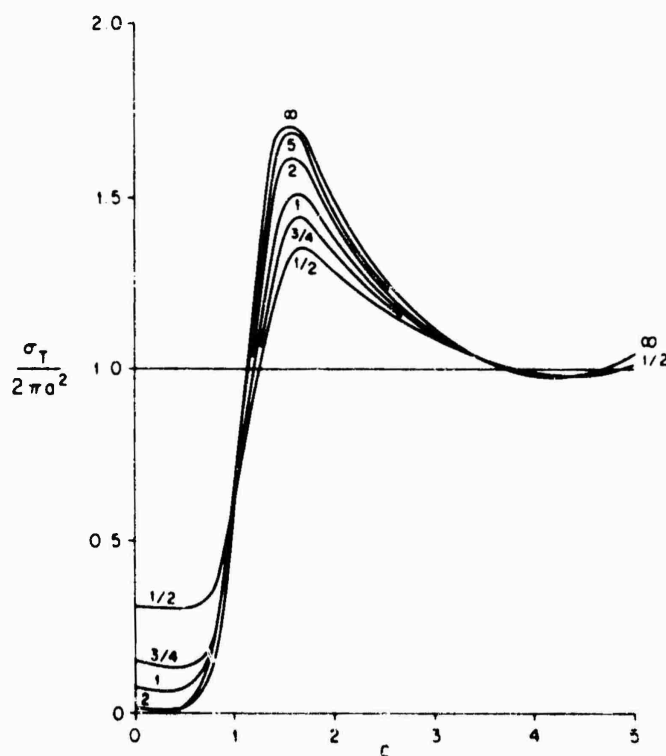


Fig. 14.15. Normalized total scattering cross section for an electric dipole on the axis with moment in the x direction, for various z_0/a (INAWASHIRO [1963]).

14.4.1.2. LOW FREQUENCY APPROXIMATIONS

For an arbitrary incident field, the first few terms in the low-frequency expansions for the far field components can be written as (EGGMANN [1961]):

$$\begin{aligned}
 H_\theta^s = -YE_\phi^s \approx & \frac{e^{ikR}}{kR} \frac{c^2}{\pi} \left\{ \frac{\omega}{4a^2} (P_x \sin \phi - P_y \cos \phi) - c \frac{M_z \sin \theta}{4a^3} - \right. \\
 & - \frac{1}{15} c^3 \left[\frac{4}{3} H_z^i \sin \theta + \frac{8iY \sin \theta}{3k} \left(-\frac{\partial E_x^i}{\partial y} \cos^2 \phi + \frac{\partial E_y^i}{\partial x} \sin^2 \phi + \right. \right. \\
 & + \left. \left. \left(\frac{\partial E_x^i}{\partial x} - \frac{\partial E_y^i}{\partial y} \right) \sin \phi \cos \phi \right) - \frac{2}{3} \sin^2 \theta \left(\left[5YE_y^i - \frac{2i}{k} \frac{\partial H_z^i}{\partial x} \right] \cos \phi - \right. \right. \\
 & \left. \left. - \left[5YE_x^i + \frac{2i}{k} \frac{\partial H_z^i}{\partial y} \right] \sin \phi \right) + H_z^i \sin^3 \theta \right] \Big\}_{x=y=z=0}, \quad (14.182)
 \end{aligned}$$

$$\begin{aligned}
 H_\phi^s = YE_\theta^s \approx & \frac{e^{ikR}}{kR} \frac{c^2}{\pi} \cos \theta \left\{ \frac{\omega}{4a^2} (P_x \cos \phi + P_y \sin \phi) + \right. \\
 & + \frac{2}{45} c^3 \left[\frac{iY \sin \theta}{k} \left(3 \frac{\partial E_z^i}{\partial z} + 4 \frac{\partial E_y^i}{\partial y} \cos^2 \phi + 4 \frac{\partial E_x^i}{\partial x} \sin^2 \phi - \right. \right. \\
 & \left. \left. - 4 \left(\frac{\partial E_x^i}{\partial y} + \frac{\partial E_y^i}{\partial x} \right) \sin \phi \cos \phi \right) - 3Y \sin^2 \theta (E_x^i \cos \phi + E_y^i \sin \phi) \right] \Big\}_{x=y=z=0}, \quad (14.183)
 \end{aligned}$$

$$E_r^s = H_r^s = 0, \quad (14.184)$$

where $\omega = k \sqrt{\epsilon \mu}$ is the angular frequency. Here the quantities P_x, P_y, M_z are the only non-vanishing components of the induced electric and magnetic dipole moments, which are expressible in terms of the incident field as:

$$P_x = \frac{16}{3} a^3 \epsilon \left[E_x^i + \frac{1}{30} c^2 \left(13E_x^i - \frac{3}{k^2} \frac{\partial^2 E_x^i}{\partial z^2} - \frac{2iZ}{k} \frac{\partial H_z^i}{\partial y} \right) + \frac{8i}{9\pi} c^3 E_x^i \right]_{x=y=z=0}, \quad (14.185)$$

$$P_y = \frac{16}{3} a^3 \epsilon \left[E_y^i + \frac{1}{30} c^2 \left(13E_y^i - \frac{3}{k^2} \frac{\partial^2 E_y^i}{\partial z^2} + \frac{2iZ}{k} \frac{\partial H_z^i}{\partial x} \right) + \frac{8i}{9\pi} c^3 E_y^i \right]_{x=y=z=0}, \quad (14.186)$$

$$M_z = \frac{-8a^3}{3} \left[H_z^i - \frac{1}{10} c^2 \left(3H_z^i + \frac{1}{k^2} \frac{\partial^2 H_z^i}{\partial z^2} \right) - \frac{4i}{9\pi} c^3 H_z^i \right]_{x=y=z=0}. \quad (14.187)$$

In the special case where an electric dipole of moment $(4\pi\epsilon/k)\hat{y}$ is located in the plane of the disc at $(x_0, y_0, 0)$ and oriented parallel to the y -axis, the induced electric dipole moment becomes:

$$\begin{aligned}
 P_y = & \frac{16}{3} \epsilon \frac{a^3}{R^2} \frac{e^{ikR}}{kR} \left\{ 2(1 - ikR) - \left(\frac{3}{(kR)^2} - \frac{3i}{kR} - 1 \right) (kx_0)^2 + \right. \\
 & + \frac{1}{30} c^2 \left[12 \left(\frac{3}{(kR)^2} - \frac{3i}{kR} + 1 - 2ikR \right) - \right. \\
 & \left. - \left(\frac{45}{(kR)^4} - \frac{45i}{(kR)^3} + \frac{15}{(kR)^2} - \frac{30i}{kR} - 11 \right) (kx_0)^2 \right] + \\
 & \left. + \frac{8i}{9\pi} c^3 \left[2(1 - ikR) - \left(\frac{3}{(kR)^2} - \frac{3i}{kR} - 1 \right) (kx_0)^2 \right] \right\}. \quad (14.188)
 \end{aligned}$$

whereas the induced magnetic dipole moment is:

$$M_z = \frac{8iY}{3} \frac{a^3}{R^2} kx_0 \frac{e^{ikR}}{kR} \left\{ (1-ikR) + \frac{1}{10} c^2 \left(\frac{3}{(kR)^2} - \frac{3i}{kR} - 4 + 3ikR \right) - \frac{4i}{9\pi} c^3 (1-ikR) \right\}, \quad (14.189)$$

where

$$R = \sqrt{(x_0^2 + y_0^2)}. \quad (14.190)$$

In the case of a magnetic dipole of moment $(4\pi/k)\hat{z}$, located in the plane of the disc at $(x_0, y_0, 0)$ and oriented parallel to the z -axis, the far field is still given by eqs. (14.182) to (14.184), where now:

$$P_x = \frac{16ia^3}{3\omega R^3} ky_0 e^{ikR} \left\{ (1-ikR) + \frac{1}{30} c^2 \left(\frac{15}{(kR)^2} - \frac{15}{kR} + 6 - 11ikR \right) - \frac{8i}{9\pi} c^3 (1-ikR) \right\}, \quad (14.191)$$

$$P_y = -\frac{x_0}{y_0} P_x, \quad (14.192)$$

$$M_z = \frac{8a^3}{3R^2} \frac{e^{ikR}}{kR} \left\{ (1-ikR - (kR)^2) - \frac{1}{10} c^2 \left(-\frac{7}{(kR)^2} + \frac{7i}{kR} + 5 - 4ikR - 3(kR)^2 \right) - \frac{4i}{9\pi} c^3 (1-ikR - (kR)^2) \right\}, \quad (14.193)$$

and R is given by eq. (14.190).

For an electric dipole with moment $(4\pi\epsilon/k)\hat{x}$ located on the axis of symmetry at $(0, 0, z_0)$ and oriented parallel to the x -axis, the total surface current density when both z_0 and a are small compared to the wavelength is (GRINBERG and PIMENOV [1957]):

$$J_x \approx \frac{iYz_0}{\pi^2 R^2} \left\{ \frac{1}{R} \tan^{-1} \left(\frac{\sqrt{(a^2 - \rho^2)}}{R} \right) + \frac{\sqrt{(a^2 - \rho^2)}}{z_0^2 + a^2} \right\}, \quad (14.194)$$

$$J_y \approx 0. \quad (14.195)$$

Similarly, if the dipole is oriented along the z -axis, the only non-vanishing component of the total surface current density is:

$$J_r \approx \frac{iY\rho}{\pi^2 R^2} \left\{ \frac{\sqrt{(a^2 - \rho^2)}}{z_0^2 + a^2} + \frac{1}{R} \tan^{-1} \left(\frac{\sqrt{(a^2 - \rho^2)}}{R} \right) \right\}, \quad (14.196)$$

where if the dipole is magnetic with moment $(4\pi/k)\hat{z}$:

$$J_\theta \approx \frac{z_0 \rho Y}{\pi^2 k R^2} \left\{ \frac{\sqrt{(a^2 - \rho^2)}}{z_0^2 + a^2} + \frac{3}{R} \tan^{-1} \left(\frac{\sqrt{(a^2 - \rho^2)}}{R} \right) + \frac{2}{\sqrt{(a^2 - \rho^2)}} \right\}. \quad (14.197)$$

Finally, observe that the results (14.172) represent low-frequency expansions of the solution given by INAWASHIRO [1963].

14.4.1.3. HIGH FREQUENCY APPROXIMATIONS

The only explicit high-frequency result available is for an electric dipole at the center of the disc and oriented normal to it. This case has been treated via the Wiener-Hopf technique (TANG [1962]) and by means of the geometrical theory of diffraction (KELLER [1963]). For an electric dipole with moment $(4\pi\epsilon/k)\mathbf{d}$, the singly diffracted magnetic far field at a point (r, θ) off the z -axis is (KELLER [1963]):

$$H_{\phi}^1 = \frac{ike^{ik(r+a)}}{4\pi r \sqrt{(2\pi ka \sin \theta)}} \left\{ \cos(ka \sin \theta - \tfrac{1}{2}\pi) [\pm \sec(\tfrac{1}{2}\pi - \tfrac{1}{2}\theta) - \operatorname{cosec}(\tfrac{1}{2}\pi - \tfrac{1}{2}\theta)] + \right. \\ \left. \pm i \sin(ka \sin \theta - \tfrac{1}{2}\pi) [\pm \sec(\tfrac{1}{2}\pi - \tfrac{1}{2}\theta) + \operatorname{cosec}(\tfrac{1}{2}\pi - \tfrac{1}{2}\theta)] \right\}, \quad (14.198)$$

where the upper (lower) sign applies when $0 \leq \theta < \frac{1}{2}\pi$ ($\frac{1}{2}\pi < \theta \leq \pi$). If the observation point is on or near the axis, a caustic correction must be applied and the result simplifies to

$$H_{\phi}^1 = -\frac{ke^{ik(r+a)}}{2\sqrt{2}} J_1(ka \sin \theta). \quad (14.199)$$

The scattered field, including the diffracted rays of all orders, is the sum of a geometric series and has the form

$$H_{\phi}^s \sim \left[1 + \frac{e^{i(2ka - \frac{1}{2}\pi)}}{2\sqrt{\pi ka}} \right]^{-1} H_{\phi}^1. \quad (14.200)$$

14.4.2. Plane wave incidence

14.4.2.1. EXACT SOLUTIONS

14.4.2.1.1. Arbitrary incident direction

The solution for this case is again most conveniently expressed in terms of Hertz vectors (see Section 14.4.1.1). If the incident direction is in the (x, z) plane and makes an angle ζ with the positive z -axis, then the incident field vectors for the two standard polarizations can be written in terms of spheroidal functions as:

$$\begin{aligned} \mathbf{E}_{\perp}^i &= (0, 1, 0)V^i, & \mathbf{H}_{\perp}^i &= -Y(\cos \zeta, 0, -\sin \zeta)V^i, \\ \mathbf{E}_{\parallel}^i &= (-\cos \zeta, 0, \sin \zeta)V^i, & \mathbf{H}_{\parallel}^i &= -Y(0, 1, 0)V^i, \end{aligned} \quad (14.201)$$

where

$$\begin{aligned} V^i &= \exp \{ik(x \sin \zeta + z \cos \zeta)\} \\ &= 2 \sum_{m=0}^{\infty} \sum_n \frac{e_m(-i)^n}{N_{mn}} R_{mn}^{(1)}(-ic, i\xi) S_{mn}(-ic, \cos \zeta) S_{mn}(-ic, \eta) \cos n\phi. \end{aligned} \quad (14.202)$$

The scattered electric Hertz vector is:

$$\Pi_{\epsilon}^s = \Pi^1 + \Pi^2, \quad (14.203)$$

where (MEIXNER and ANDREJWSKI [1950]):

$$\Pi_{x\perp}^1 = 0, \quad (14.204)$$

$$\Pi_{y\perp}^1 = -\frac{1}{k^2} \sum_{m=-\infty}^{\infty} V_m(\xi, \eta; c; \zeta) e^{im\phi}, \quad (14.205)$$

$$\Pi_{x\parallel}^1 = \frac{1}{k^2 \cos \zeta} \sum_{m=-\infty}^{\infty} V_m(\xi, \eta; c; \zeta) e^{im\phi}, \quad (14.206)$$

$$\Pi_{y\parallel}^1 = 0, \quad (14.207)$$

$$\Pi_x^2 = -\frac{1}{2}k \sum_{m=-\infty}^{\infty} (U_{m+1} - U_{m-1}) i^{-m} \Phi_m(\xi, \eta; c) e^{im\phi}, \quad (14.208)$$

$$\Pi_y^2 = -\frac{1}{2}ik \sum_{m=-\infty}^{\infty} (U_{m+1} + U_{m-1}) i^{-m} \Phi_m(\xi, \eta; c) e^{im\phi}, \quad (14.209)$$

with

$$U_{m\perp} = \frac{-i^m}{k^3} \left[\frac{W_{m+1} - W_{m-1}}{\Psi_{m+1} + \Psi_{m-1}} \right], \quad (14.210)$$

$$U_{m\parallel} = \frac{-i^{m+1}}{k^3 \cos \zeta} \left[\frac{W_{m+1} + W_{m-1}}{\Psi_{m+1} + \Psi_{m-1}} \right], \quad (13.211)$$

$$U_{m\perp} = (-1)^{m+1} U_{-m\perp}, \quad U_{m\parallel} = (-1)^m U_{-m\parallel}, \quad (14.212)$$

$$\begin{aligned} V_m(\xi, \eta; c; \zeta) &= V_{-m}(\xi, \eta; c; \zeta) \\ &= (-1)^m \sum_{n=|m|}^{\infty} \frac{(-i)^n}{\tilde{N}_{mn}} \frac{R_{mn}^{(1)}(-ic, i0)}{R_{mn}^{(3)}(-ic, i0)} R_{mn}^{(3)}(-ic, i\xi) S_{mn}(-ic, \eta) S_{-mn}(-ic, \cos \zeta), \end{aligned} \quad (14.213)$$

$$\begin{aligned} W_m(c; \zeta) &= W_{-m}(c; \zeta) = -ic \left. \frac{\partial V_m(\xi, \eta; c; 0)}{\partial \xi} \right|_{\xi=\eta=0} \\ &= (-1)^{m+1} \sum_{n=|m|}^{\infty} \frac{(-i)^n}{\tilde{N}_{mn}} \frac{S_{mn}(-ic, 0) S_{-mn}(-ic, \cos \zeta)}{R_{mn}^{(3)}(-ic, i0)} \end{aligned} \quad (14.214)$$

$$\begin{aligned} \Phi_m(\xi, \eta; c) &= \Phi_{-m}(\xi, \eta; c) = (-1)^m \sum_{n=|m|}^{\infty} \frac{(-i)^n}{\tilde{N}_{mn}} \frac{R_{mn}^{(1)}(-ic, i0)}{R_{mn}^{(3)}(-ic, i0)} \\ &\quad \times R_{mn}^{(3)}(-ic, i\xi) S_{mn}(-ic, \eta) S_{-mn}(-ic, 0), \end{aligned} \quad (14.215)$$

$$\begin{aligned} \Psi_m(c) &= \Psi_{-m}(c) = -ic \left. \frac{\partial \Phi_m(\xi, \eta; c)}{\partial \xi} \right|_{\xi=\eta=0} \\ &= (-1)^m \sum_{n=|m|}^{\infty} \frac{(-i)^n}{\tilde{N}_{mn}} \frac{S_{mn}(-ic, 0) S_{-mn}(-ic, 0)}{R_{mn}^{(3)}(-ic, i0)}. \end{aligned} \quad (14.216)$$

Another spheroidal wave-function solution has been derived without the use of Hertz vectors by FLAMMER [1953]. The problem has also been solved for arbitrary incident direction by LUR'E [1960] using sets of paired integral equations. The

formulas given are not sufficiently explicit to make their use for computation practical, though certain numerical results are included in the article.

Still another exact solution for arbitrary directions of incidence and polarization is provided by NOMURA and KATSURA [1955], who employed hypergeometric polynomials rather than spheroidal functions. If the incident field in rectangular Cartesian coordinates is:

$$\begin{aligned} E^i &= (-E_2 \cos \zeta, E_1, E_2 \sin \zeta) \exp \{ik(z \cos \zeta + x \sin \zeta)\}, \\ H^i &= -Y(E_1 \cos \zeta, E_2, E_1 \sin \zeta) \exp \{ik(z \cos \zeta + x \sin \zeta)\}, \end{aligned} \quad (14.217)$$

where ζ is the angle between the direction of propagation and the z -axis and $E_1(E_2)$ is the component of the incident electric vector perpendicular (parallel) to the plane (x, z) of incidence, then the incident electric Hertz vector is:

$$\Pi_e^i = \frac{1}{k^2} \left(\frac{E_2}{\cos \zeta}, E_1, 0 \right) \exp \{ik(z \cos \zeta + x \sin \zeta)\}. \quad (14.218)$$

The electric Hertz vector of the scattered field is again written in the form of eq. (14.154), and its non-vanishing rectangular components are:

$$\Pi_{1x} = \frac{E_2}{k^2 \cos \zeta} \sum_{m=0}^{\infty} \sum_{n=0}^{\infty} A_n^m S_{n-}^m(\rho, z) \cos m\phi, \quad (14.219)$$

$$\Pi_{1y} = E_1 k^{-2} \sum_{m=0}^{\infty} \sum_{n=0}^{\infty} A_n^m S_{n+}^m(\rho, z) \cos m\phi, \quad (14.220)$$

$$\begin{aligned} \left. \begin{aligned} \Pi_{2x} \\ \Pi_{2y} \end{aligned} \right\} &= ik \sum_{m=0}^{\infty} \sum_{n=0}^{\infty} \left[(U_{m+1}^{(1)} \mp U_{m-1}^{(1)}) \frac{\sin m\phi}{\cos m\phi} \pm (U_{m+1}^{(2)} \mp U_{m-1}^{(2)}) \frac{\cos m\phi}{\sin m\phi} \right] \\ &\quad \times B_n^m S_{n\mp}^m(\rho, z), \end{aligned} \quad (14.221)$$

where

$$S_{n\mp}^m(\rho, z) = \int_0^{\pi} \frac{\sqrt{\xi} J_m(\rho\xi/a) J_{m+2n+1}(\xi)}{\sqrt{(\xi^2 - c^2)}} \exp \left(\mp \sqrt{\xi^2 - c^2} \frac{z}{a} \right) d\xi, \quad (14.222)$$

$$\left. \begin{aligned} A_n^m \\ B_n^m \end{aligned} \right\} = \sum_{s=0}^{\infty} \frac{a_s^m}{b_s^m} X_{ns}^m, \quad (14.223)$$

$$a_n^m = - \sqrt{\frac{2}{\pi}} 2i^m (2m+4n+1) j_{m+2n}(c \sin \zeta), \quad (14.224)$$

$$b_n^m = \sqrt{\frac{2}{\pi}} (2m+4n+1) j_{m+2n}(c), \quad (14.225)$$

and the X_{ns}^m are defined in eqs. (14.171) and (14.172). Further,

$$U_m^{(1)} = -E_1 k^{-2} \frac{A_n^{m-1} - A_n^{m+1}}{B_n^{m-1} - B_n^{m+1}}, \quad (m = 2, 3, 4, \dots), \quad (14.226)$$

$$U_m^{(2)} = \frac{E_2}{k^3 \cos \zeta} \frac{A_n^{m-1} + A_n^{m+1}}{B_n^{m-1} - B_n^{m+1}}, \quad (m = 2, 3, 4, \dots), \quad (14.227)$$

$$U_1^{(1)} = -E_1 k^{-3} \frac{2A_n^0 - A_n^2}{B_n^0 - B_n^2}, \quad (14.228)$$

$$U_1^{(2)} = \frac{E_2}{k^3 \cos \zeta} \frac{2A_n^0 - A_n^2}{B_n^0 - B_n^2}, \quad (14.229)$$

$$U_0^{(2)} = -\frac{E_2}{k^3 \cos \zeta} \frac{A_n^1}{B_n^1}. \quad (14.230)$$

In the far field:

$$(\Pi_\epsilon^s)_x = \sqrt{\frac{2}{\pi}} c \frac{e^{ikr}}{kr} \sum_{m=0}^{\infty} (-i)^m \sum_{n=0}^{\infty} [{}^2C_n^m \cos m\phi + {}^1C_n^m \sin m\phi] j_{m+1/2}(c \sin \theta), \quad (14.231)$$

$$(\Pi_\epsilon^s)_y = \sqrt{\frac{2}{\pi}} c \frac{e^{ikr}}{kr} \sum_{m=0}^{\infty} (-i)^m \sum_{n=0}^{\infty} [{}^1D_n^m \cos m\phi + {}^2D_n^m \sin m\phi] j_{m+2/2}(c \sin \theta), \quad (14.232)$$

where:

$${}^2C_n^m = \frac{1}{2}k(U_{m+1}^{(2)} - U_{m-1}^{(2)})B_n^m - \frac{E_2}{k^2 \cos \zeta} A_n^m, \quad (14.233)$$

$${}^1C_n^m = \frac{1}{2}k(U_{m+1}^{(1)} - U_{m-1}^{(1)})B_n^m, \quad (14.234)$$

$${}^1D_n^m = \frac{1}{2}k(U_{m+1}^{(1)} + U_{m-1}^{(1)})B_n^m + \frac{E_1}{k^2} A_n^m, \quad (14.235)$$

$${}^2D_n^m = -\frac{1}{2}k(U_{m+1}^{(2)} + U_{m-1}^{(2)})B_n^m. \quad (14.236)$$

On the surface of the disc ($\zeta = 0$), the scattered field components are:

$$E_z^s = \pm \left\{ \frac{\partial}{\partial z} \left[\frac{\partial}{\partial x} (\Pi_\epsilon^s)_x + \frac{\partial}{\partial y} (\Pi_\epsilon^s)_y \right] \right\}_{z=0+}, \quad (14.237)$$

$$H_x^s = \pm ikY \left\{ \frac{\partial}{\partial z} (\Pi_\epsilon^s)_y \right\}_{z=0+}, \quad (14.238)$$

$$H_y^s = \mp ikY \left\{ \frac{\partial}{\partial z} (\Pi_\epsilon^s)_x \right\}_{z=0+}, \quad (14.239)$$

where the upper (lower) signs pertain to the illuminated (shadow) side, and

$$\left\{ \frac{\partial}{\partial z} (\Pi_\epsilon^s)_x \right\}_{z=0+} = \sum_{m=0}^{\infty} \sum_{n=0}^{\infty} ({}^2C_n^m \cos m\phi + {}^1C_n^m \sin m\phi) \frac{\partial S_n^m(\rho, +0)}{\partial z}, \quad (14.240)$$

$$\left\{ \frac{\partial}{\partial z} (\Pi_\epsilon^s)_y \right\}_{z=0+} = \sum_{m=0}^{\infty} \sum_{n=0}^{\infty} ({}^1D_n^m \cos m\phi + {}^2D_n^m \sin m\phi) \frac{\partial S_n^m(\rho, +0)}{\partial z}, \quad (14.241)$$

with

$$\frac{\partial S_n^m(\rho, +0)}{\partial z} = \sqrt{\frac{2}{\pi}} (-1)^n (\rho/a)^m (a^2 - \rho^2)^{-\frac{1}{2}} F(m+n+\frac{1}{2}, -n; \frac{1}{2}; 1 - \rho^2/a^2). \quad (14.242)$$

The normalized total scattering cross section is:

$$\frac{\sigma_T}{2\pi a^2} = 2 \sqrt{\frac{2}{\pi}} \frac{c}{a^2} \operatorname{Im} \left\{ \sum_{m=0}^{\infty} i^m \sum_{n=0}^{\infty} {}^1D_n^m j_{m+2n}(c \sin \zeta) \right\}. \quad (14.243)$$

No results computed from the above formula are available; there is, however, a wealth of experimental data for the back scattering cross sections of electrically-thin discs, particularly for incidence normal to the disc and for glancing incidence with the electric vector parallel to the plane of the disc. Typical results for the latter case are shown in Fig. 14.16, and RYAN and PETERS [1968] have proposed an empirical formula to fit such data.

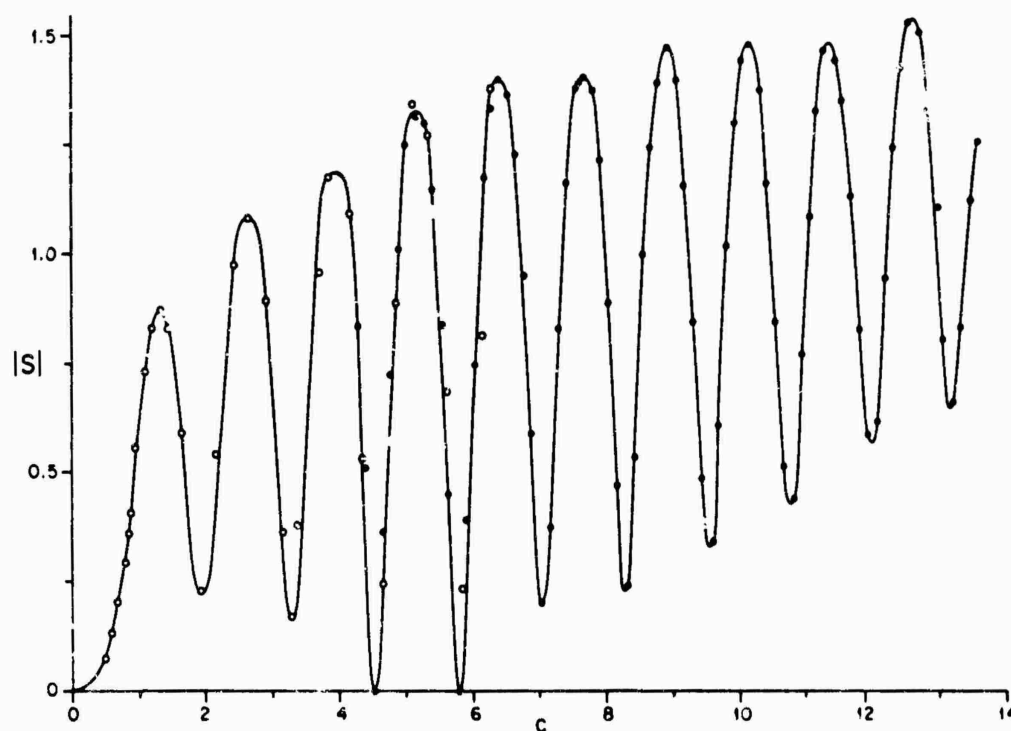


Fig. 14.16. Measured amplitude of back scattered far field coefficient for glancing incidence ($\zeta = \frac{1}{2}\pi$) with electric vector in the plane of the disc: disc thickness $t = 0.00355\lambda$, ooo (HEY et al. [1956]); $t = 0.00272\lambda$, ●●● (Radiation Laboratory; unpublished). The curve is only to guide the eye.

14.4.2.1.2. Normal incidence

For an incident plane wave propagating in the direction of the negative z -axis such that

$$E^i = \hat{x} e^{-ikz}, \quad H^i = -Y \hat{y} e^{-ikz}. \quad (14.244)$$

the Hertz vector of the scattered far field in eqs. (14.204) to (14.209) reduces to the components (MEIXNER and ANDREJEWSKI [1950]):

$$\Pi_x^s = -k^{-2} V_0(\xi, \eta; c; \pi) + k U_1(c) [\Phi_0(\xi, \eta; c) + \Phi_2(\xi, \eta; c) \cos 2\phi], \quad (14.245)$$

$$\Pi_y^s = k U_1(c) \Phi_2(\xi, \eta; c) \sin 2\phi, \quad (14.246)$$

with

$$U_1(c) = -k^{-3} \frac{W_0(c; 0)}{\Psi_0(c) + \Psi_2(c)}. \quad (14.247)$$

Formulas for the back scattered field and the back scattering cross section have been given by SCHMITT [1957]. Experimental data for the back scattering cross section as a function of c are shown in Fig. 14.17.

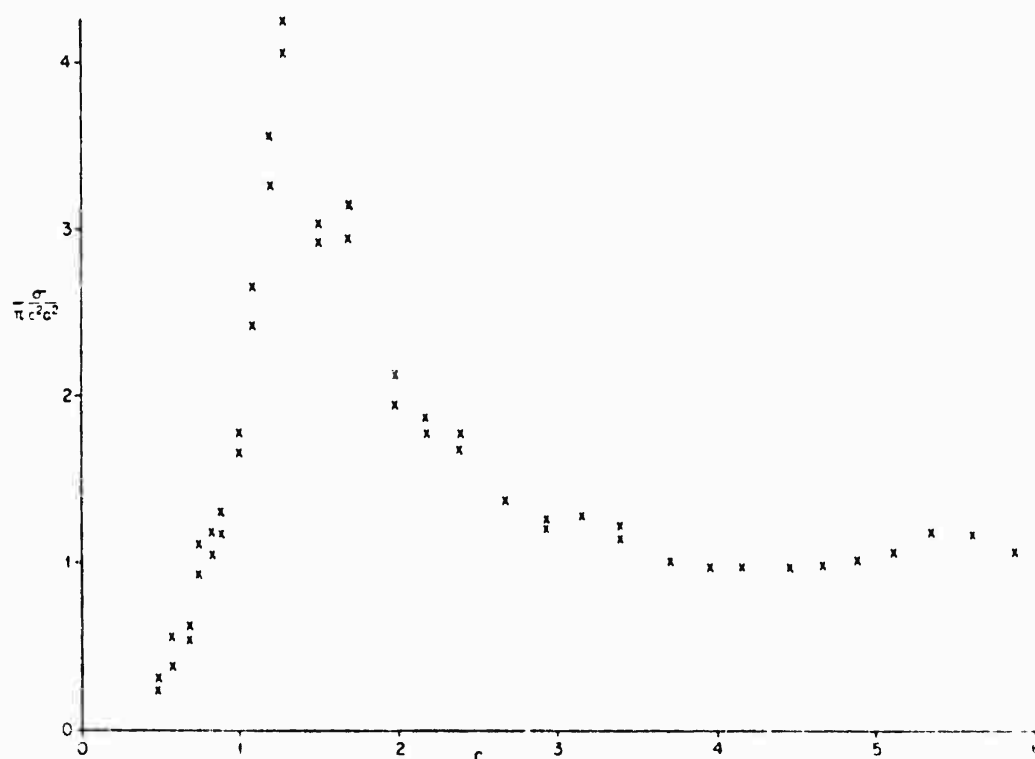


Fig. 14.17. Measured values of normalized back scattering cross section for a disc of thickness $t = 0.00355\lambda$ (HEY et al. [1956]).

ANDREJEWSKI [1953] has computed the surface field on both the illuminated and shadow sides and the far field for $c = 10$, and the field at the center of the disc as a function of c (see Fig. 14.18).

The solution involving the hypergeometric functions gives the following results in the case of normal incidence ($\zeta = \pi$, $E_z = 0$; see eq. (14.217)) (NOMURA and KATSURA

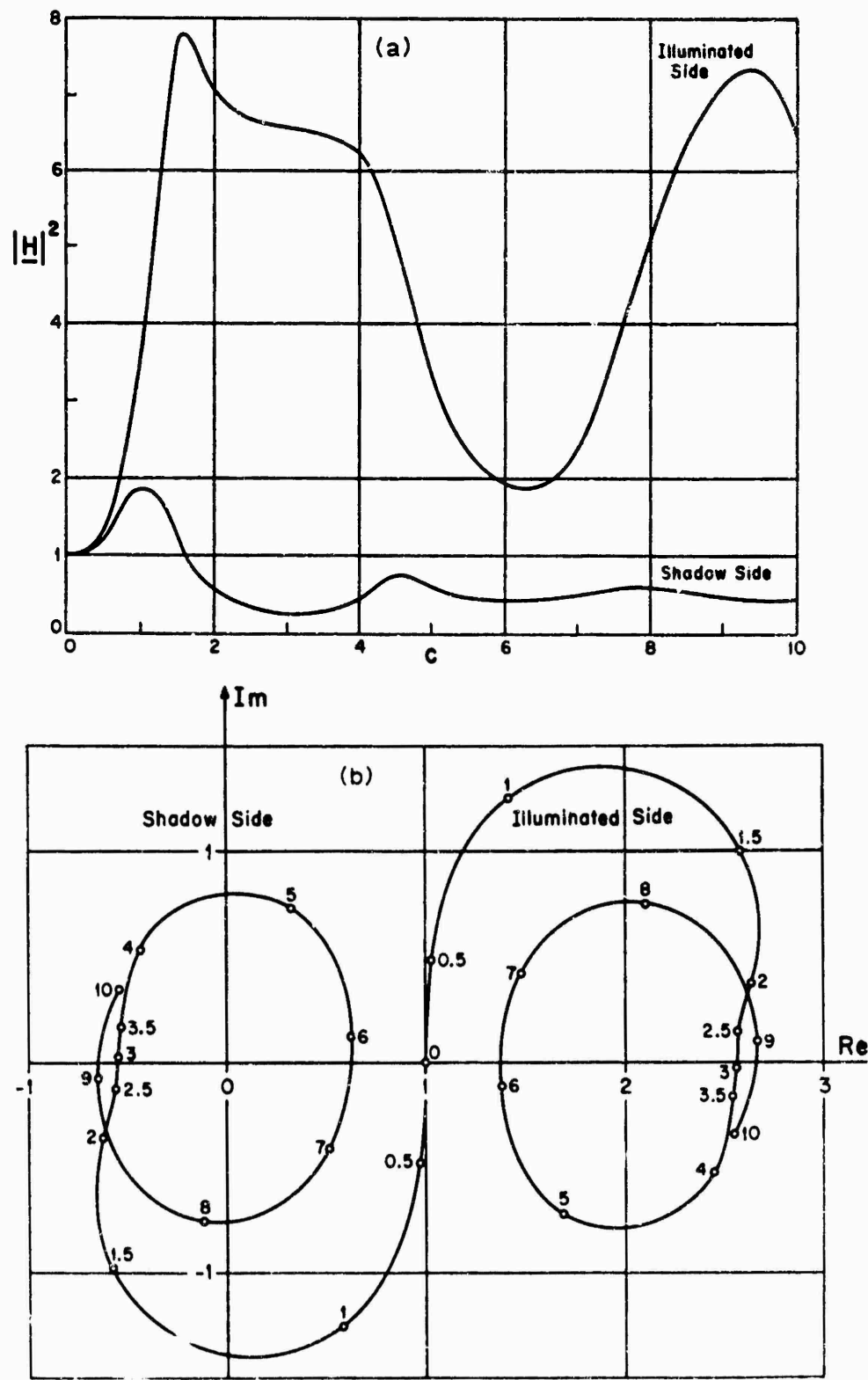


Fig. 14.18. Intensity and phase of magnetic field at the center ($\rho = 0$) of the disc (ANDREJEWSKI [1953]).

[1955]). The electric Hertz vector of the scattered far field has the spherical components

$$\Pi_{\theta}^s = \int \frac{2}{\pi} \frac{e^{ikr}}{kr} c \cos \theta \sin \phi \sum_{n=0}^{\infty} \{ {}^1D_n^0 j_{2n}(c \sin \theta) + {}^1D_n^2 j_{2n+2}(c \sin \theta) \}, \quad (14.248)$$

$$\Pi_{\phi}^s = \int \frac{2}{\pi} \frac{e^{ikr}}{kr} c \cos \phi \sum_{n=0}^{\infty} \{ {}^1D_n^0 j_{2n}(c \sin \theta) - {}^1D_n^2 j_{2n+2}(c \sin \theta) \}, \quad (14.249)$$

where the D 's are defined in eqs. (14.235) and (14.236). The normalized electric field intensity in the plane perpendicular to the incident electric vector is

$$I_1(k, \theta) = \frac{1}{2} \pi \frac{k^4}{E_1^2} \cos^2 \theta \left| \sum_{n=0}^{\infty} \{ {}^1D_n^0 j_{2n}(c \sin \theta) + {}^1D_n^2 j_{2n+2}(c \sin \theta) \} \right|^2, \quad (14.250)$$

whereas in the plane parallel to the incident electric vector:

$$I_2(k, \theta) = \frac{1}{2} \pi \frac{k^4}{E_1^2} \left| \sum_{n=0}^{\infty} \{ {}^1D_n^0 j_{2n}(c \sin \theta) - {}^1D_n^2 j_{2n+2}(c \sin \theta) \} \right|^2. \quad (14.251)$$

Graphs of these quantities for various values of c are shown in Fig. 14.19.

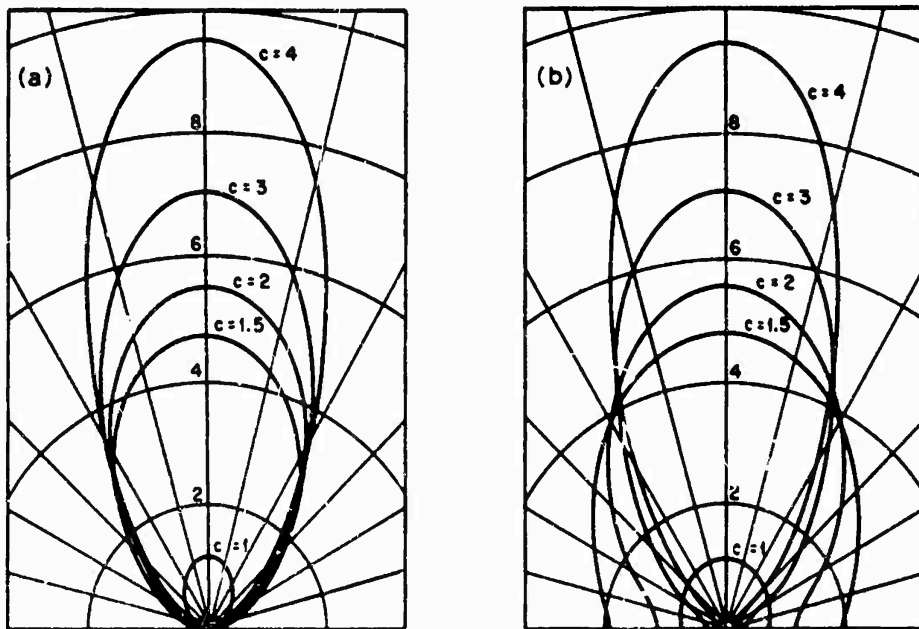


Fig. 14.19. Scattered electric field intensity in plane (a) perpendicular and (b) parallel to the incident electric vector (NOMURA and KATSURA [1955]).

The normalized total scattering cross section is

$$\frac{\sigma_T}{2\pi a^2} = 2 \int \frac{2}{\pi} \frac{c}{a^2} \operatorname{Im} {}^1D_0^0. \quad (14.252)$$

and is shown as a function of c in Fig. 14.20, along with variational approximations (LEVINE and SCHWINGER [1950]).

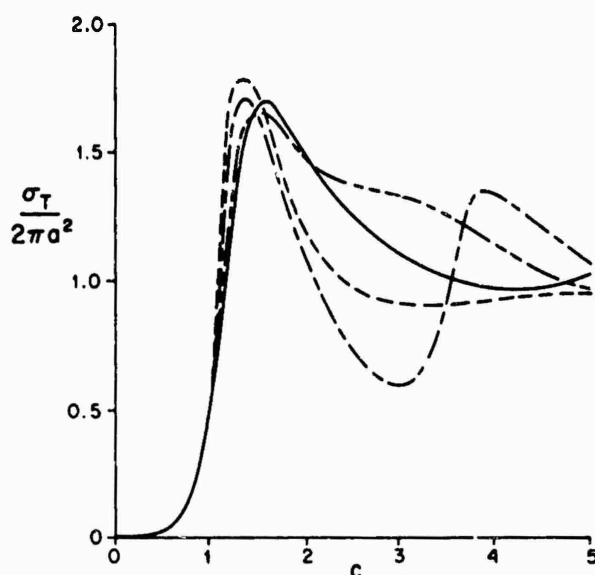


Fig. 14.20. Normalized total scattering cross section: — low frequency: ---, — — —, - - - - - Levine and Schwinger variational approximations (NOMURA and KATSURA [1955]).

The normalized total surface current density on the radii parallel and perpendicular to the incident electric vector ($\phi = 0$ and $\frac{1}{2}\pi$, respectively) is:

$$\left| \frac{J}{YE_1} \right|^2 = \begin{cases} [\text{Im} \{\alpha(x) + \beta(x) \pm i\}]^2 + [\text{Re} \{\alpha(x) + \beta(x)\}]^2, & \text{for } \phi = 0, \\ [\text{Im} \{\alpha(x) - \beta(x) \pm i\}]^2 + [\text{Re} \{\alpha(x) - \beta(x)\}]^2, & \text{for } \phi = \frac{1}{2}\pi, \end{cases} \quad (14.253)$$

where

$$\alpha(x) = \sqrt{\frac{2}{\pi}} \frac{c}{a^2 E_1} (1-x)^{-\frac{1}{2}} \sum_{n=0}^{\infty} (-1)^n {}^1D_n^0 F(-n, n + \frac{1}{2}; \frac{1}{2}; 1-x), \quad (14.254)$$

$$\beta(x) = \sqrt{\frac{2}{\pi}} \frac{c}{a^2 E_1} x(1-x)^{-\frac{1}{2}} \sum_{n=0}^{\infty} (-1)^n {}^1D_n^2 F(-n, n + \frac{1}{2}; \frac{1}{2}; 1-x), \quad (14.255)$$

with

$$x = \rho^2/a^2, \quad (14.256)$$

the current being parallel to the incident field on both radii, and the upper (lower) sign pertaining to the illuminated (shadow) side. Computed values based on eq. (14.253) are shown in Fig. 14.21.

Several variational solutions have been developed for the electromagnetic disc problem with normally incident plane wave. Most of these are useful only in the extremes of the frequency range. One which might be termed exact, since it gives

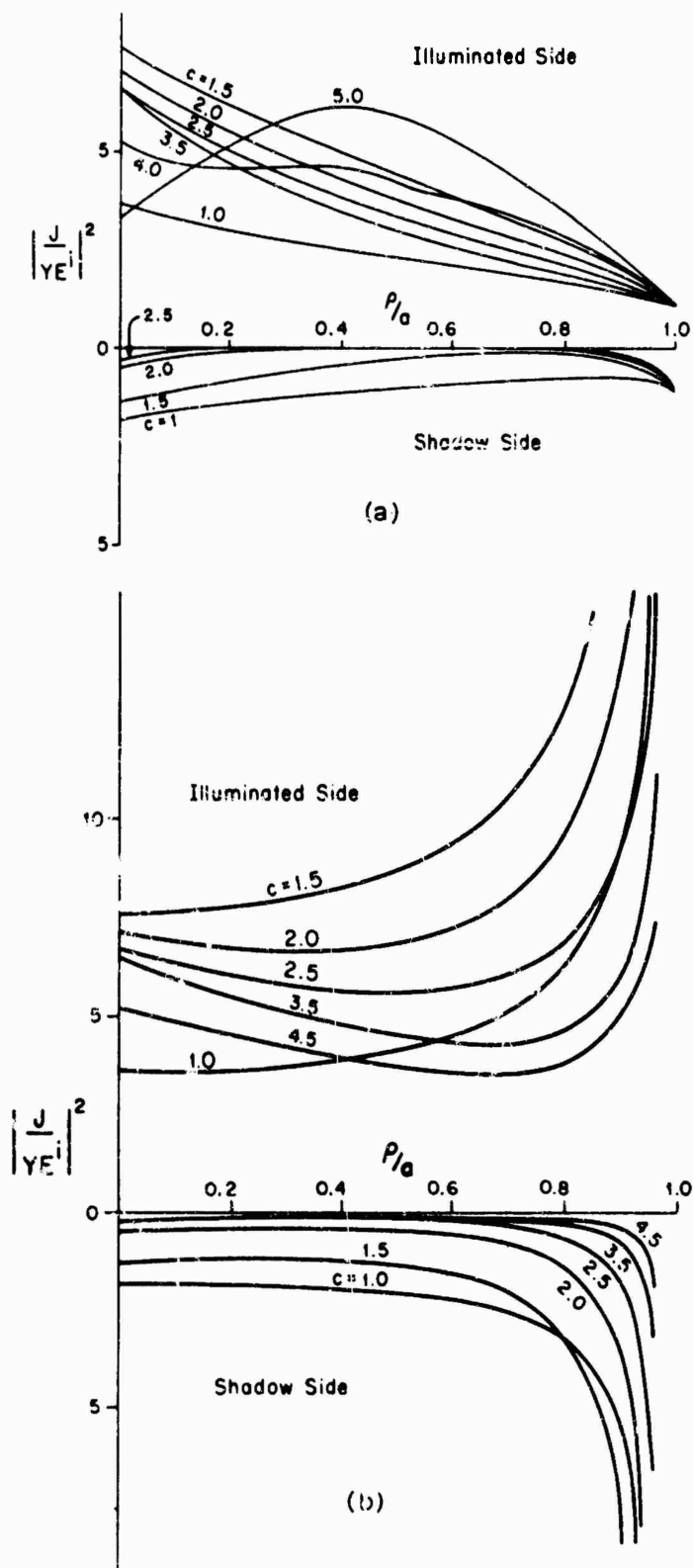


Fig. 14.21. Normalized total surface current density on (a) radius $\phi = 0$ parallel and (b) radius $\phi = a/2$ perpendicular to the incident electric vector (NOMURA and KATSURA [1955]).

reasonable accuracy over the entire range, is the expression for the normalized total scattering cross section (HUANG et al. [1955]):

$$\frac{\sigma_T}{2\pi a^2} \approx \frac{64c}{9\pi} \operatorname{Im} \left(\frac{4P - 2Q + R}{Q^2 - 4PR} \right), \quad (14.257)$$

where

$$\begin{aligned} P = & \left[\left(2 - \frac{11}{8} c^{-2} \right) J_0(2c) - \frac{11}{4c} J_1(2c) + \left(\frac{1}{2} c - \frac{1}{4c} + \frac{11}{16} c^{-3} \right) \int_0^{2c} J_0(t) dt \right] + \\ & + i \left[-\frac{3}{2\pi} c + \frac{11}{4\pi c} + \left(2 - \frac{11}{8} c^{-2} \right) S_0(2c) - \frac{11}{4c} S_1(2c) + \right. \\ & \left. + \left(\frac{1}{2} c - \frac{1}{4c} + \frac{11}{16} c^{-3} \right) \int_0^{2c} S_0(t) dt \right], \end{aligned} \quad (14.258)$$

$$\begin{aligned} Q = & \left[\left(3 - c^{-2} \right) J_0(2c) - \frac{2}{c} J_1(2c) + \left(c - \frac{3}{2c} + \frac{1}{2} c^{-3} \right) \int_0^{2c} J_0(t) dt \right] + \\ & + i \left[-\frac{2}{\pi} c + \frac{2}{\pi c} + \left(3 - c^{-2} \right) S_0(2c) - \frac{2}{c} S_1(2c) + \left(c - \frac{3}{2c} + \frac{1}{2} c^{-3} \right) \int_0^{2c} S_0(t) dt \right], \end{aligned} \quad (14.259)$$

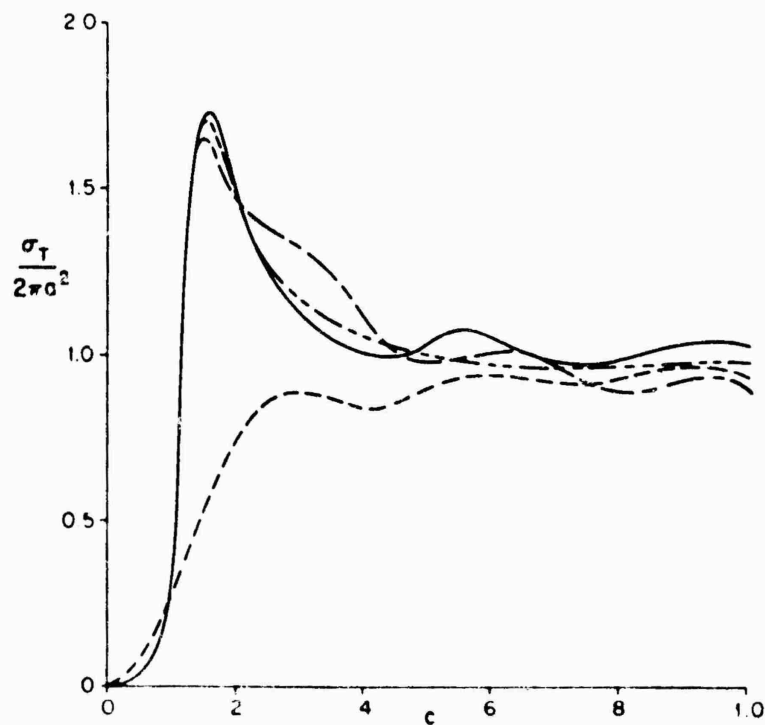


Fig. 14.22. Normalized total scattering cross section: — exact, --- eq. (14.257), - - - - - Levine and Schwinger zeroth-order variational approximation, - - - Kirchhoff approximation (HUANG et al. [1955]).

$$\begin{aligned}
R = & \left[\left(1 + \frac{1}{8}c^{-2}\right)J_0(2c) + \frac{1}{4c}J_1(2c) + \left(\frac{1}{2}c - \frac{5}{4c} - \frac{1}{16}c^{-3}\right) \int_0^{2c} J_0(t)dt \right] + \\
& + i \left[\frac{1}{2\pi}c - \frac{1}{4\pi c} + \left(1 + \frac{1}{8}c^{-2}\right)S_0(2c) + \frac{1}{4c}S_1(2c) + \right. \\
& \left. + \left(\frac{1}{2}c - \frac{5}{4c} - \frac{1}{16}c^{-3}\right) \int_0^{2c} S_0(t)dt \right], \quad (14.260)
\end{aligned}$$

and J_0 and S_1 are Struve functions (see, for example, WATSON [1958]). A graph of this result, along with the exact solution of Andrejewski and several other approximations, is shown in Fig. 14.22.

14.4.2.2. LOW FREQUENCY APPROXIMATIONS

14.4.2.2.1. Arbitrary incidence

For an incident plane wave whose direction of propagation makes an angle ζ with the positive z -axis and whose electric vector has unit amplitude and makes an angle ϕ^i with the plane of incidence (z, x), the spherical components of the scattered far field are (EGGIMANN [1961]):

$$\begin{aligned}
E_\phi^s = -ZH_\theta^s \approx & -\frac{e^{ikr}}{\pi kr} c^3 \left\{ \frac{2}{3} \sin \phi^i \sin \zeta \sin \theta + \frac{4}{3} \cos \phi^i \cos \zeta \sin \phi - \right. \\
& - \frac{4}{3} \sin \phi^i \cos \phi + \frac{1}{4} c^2 [(32 - 6 \sin^2 \zeta) \cos \phi^i \cos \zeta \sin \phi - (32 - 10 \sin^2 \zeta) \\
& \times \sin \phi^i \cos \phi + \sin \theta (2 \cos \phi^i \sin 2\zeta \sin 2\phi - (2 + 3 \sin^2 \zeta + 8 \cos^2 \phi) \sin \phi^i \sin \zeta) + \\
& \left. + \sin^2 \theta (-10 \cos \phi^i \cos \zeta \sin \phi + (10 + 4 \sin^2 \zeta) \sin \phi^i \cos \phi) - 3 \sin^3 \theta \sin \phi^i \sin \zeta \right\}, \quad (14.261)
\end{aligned}$$

$$\begin{aligned}
E_\theta^s = ZH_\phi^s \approx & \frac{e^{ikr}}{\pi kr} c^3 \cos \theta \left\{ \frac{4}{3} (\cos \phi^i \cos \zeta \cos \phi + \sin \phi^i \sin \phi) + \right. \\
& + \frac{1}{4} c^2 [(32 - 6 \sin^2 \zeta) \cos \phi^i \cos \zeta \cos \phi + (32 - 10 \sin^2 \zeta) \sin \phi^i \sin \phi + \\
& + \sin \theta \sin \zeta ((6 - 8 \sin^2 \phi) \cos \phi^i \cos \zeta + 4 \sin \phi^i \sin 2\phi) - \\
& \left. - 6 \sin^2 \theta (\cos \phi^i \cos \zeta \cos \phi + \sin \phi^i \sin \phi) \right\}. \quad (14.262)
\end{aligned}$$

The components of the induced surface current density for $\phi^i = 0$ are (LUR'E [1960]):

$$J_\rho \approx -\frac{16iYc}{3\pi} \left(1 - \frac{\rho^2}{a^2}\right)^{\frac{1}{2}} \left(\cos \zeta \cos \phi + \frac{ic\rho}{4a} \sin 2\zeta\right), \quad (14.263)$$

$$J_\phi \approx -\frac{8iYc}{3\pi} \left(1 - \frac{\rho^2}{a^2}\right)^{\frac{1}{2}} \left[\left(2 - \frac{\rho^2}{a^2}\right) \cos \zeta \sin \phi + \frac{ic\rho}{10a} \left(3 - 2 \frac{\rho^2}{a^2}\right) \sin 2\zeta \sin 2\phi\right], \quad (14.264)$$

and for $\phi^i = \frac{1}{2}\pi$:

$$J_\rho \approx -\frac{8iYc}{3\pi} \left(1 - \frac{\rho^2}{a^2}\right)^{\frac{1}{2}} \left[(2 - \sin^2 \zeta) \sin \phi + \frac{ic\rho}{5a} (3 - 2 \sin^2 \zeta) \sin \zeta \sin 2\phi\right], \quad (14.265)$$

$$J_{\phi} \approx -\frac{4}{\pi} Y \left(1 - \frac{\rho^2}{a^2}\right)^{-\frac{1}{2}} \left[\frac{\rho}{a} \sin \zeta + \frac{2}{3} i c \left(2 - \sin^2 \zeta - \frac{\rho^2}{a^2} (1 - 2 \sin^2 \zeta)\right) \cos \phi \right]. \quad (14.266)$$

The induced dipole moments of the disc (see Section 14.4.1.2) are given in terms of the incident field components at the center by (EGGIMANN [1961]):

$$P_x = \frac{16}{3} \epsilon a^3 \left[1 + \left(\frac{8}{15} - \frac{1}{10} \sin^2 \zeta \right) c^2 + \frac{8i}{9\pi} c^3 \right] E_x^i(0, 0, 0), \quad (14.267)$$

$$P_y = \frac{16}{3} \epsilon a^3 \left[1 + \left(\frac{8}{15} - \frac{1}{6} \sin^2 \zeta \right) c^2 + \frac{8i}{9\pi} c^3 \right] E_y^i(0, 0, 0), \quad (14.268)$$

for the electric dipole moment, and

$$M_z = -\frac{8}{3} a^3 \left[1 - \frac{1}{10} (2 + \sin^2 \zeta) c^2 - \frac{4i}{9\pi} c^3 \right] H_z^i(0, 0, 0), \quad (14.269)$$

for the magnetic dipole moment.

The normalized total scattering cross section is:

$$\frac{\sigma_T}{2\pi a^2} = \frac{128c^4}{27\pi^2 |\cos \zeta|} \left\{ 1 + \left(\frac{5}{4} \sin^2 \phi^i - 1 \right) \sin^2 \zeta + \frac{1}{2} c^2 [(22 - 5 \sin^2 \zeta) \times \cos^2 \zeta \cos^2 \phi^i + \frac{1}{4} (88 - 54 \sin^2 \zeta - 5 \sin^4 \zeta) \sin^2 \phi^i] \right\}. \quad (14.270)$$

14.4.2.2.2. Normal incidence

For a plane incident wave

$$E^i = \hat{x} e^{-ikz}, \quad H^i = -Y \hat{y} e^{-ikz}, \quad (14.271)$$

the spherical components of the scattered far field are (BOERSMA [1964]):

$$\begin{aligned} E_{\theta} = Z H_{\phi}^s \approx & -\frac{4c^3}{3\pi} \cos \theta \cos \phi \frac{e^{ikr}}{kr} \left\{ 1 + \frac{8}{15} \left(1 - \frac{3}{16} \sin^2 \theta \right) c^2 + \right. \\ & + \frac{16}{105} \left(1 - \frac{11}{32} \sin^2 \theta + \frac{3}{128} \sin^4 \theta \right) c^4 + \frac{128}{4725} \left[\left(1 - \frac{175}{6\pi^2} \right) - \frac{69}{128} \sin^2 \theta + \right. \\ & + \frac{35}{512} \sin^4 \theta - \frac{5}{2048} \sin^6 \theta \left. \right] c^6 + \frac{512}{155925} \left[\left(1 - \frac{9317}{32\pi^2} \right) - \left(\frac{783}{1024} - \frac{385}{16\pi^2} \right) \sin^2 \theta + \right. \\ & + \frac{635}{4096} \sin^4 \theta - \frac{85}{8192} \sin^6 \theta + \frac{15}{65536} \sin^8 \theta \left. \right] c^8 + \frac{8i}{9\pi} c^3 \left[1 + \frac{22}{25} \left(1 - \frac{5}{44} \sin^2 \theta \right) c^2 + \right. \\ & + \frac{7312}{18375} \left(1 - \frac{399}{1828} \sin^2 \theta + \frac{525}{58496} \sin^4 \theta \right) c^4 \left. \right] + O(c^9) \left. \right\}. \quad (14.272) \end{aligned}$$

$$\begin{aligned}
E_{\phi}^s = -ZH_{\theta}^s \approx & \frac{4c^3}{3\pi} \sin \phi \frac{e^{ikr}}{kr} \left\{ 1 + \frac{8}{15} \left(1 - \frac{5 \sin^2 \theta}{16} \right) c^2 + \right. \\
& + \frac{16}{105} \left(1 - \frac{21 \sin^2 \theta}{32} + \frac{7 \sin^4 \theta}{128} \right) c^4 + \frac{128}{4725} \left[1 - \frac{175}{6\pi^2} - \frac{123 \sin^2 \theta}{128} + \right. \\
& + \frac{99 \sin^4 \theta}{512} - \frac{15 \sin^6 \theta}{2048} \left. \right] c^6 + \frac{512}{155925} \left[1 - \frac{9317}{32\pi^2} - \left(\frac{1265}{1024} - \frac{385}{8\pi^2} \right) \sin^2 \theta + \right. \\
& + \frac{1639 \sin^4 \theta}{4096} - \frac{319 \sin^6 \theta}{8192} + \frac{55 \sin^8 \theta}{65536} \left. \right] c^8 + \frac{8i}{9\pi} c^3 \left[1 + \frac{22}{25} \left(1 - \frac{5 \sin^2 \theta}{22} \right) c^2 + \right. \\
& + \frac{7312}{18375} \left(1 - \frac{385 \sin^2 \theta}{914} + \frac{1575 \sin^4 \theta}{58496} \right) c^4 \left. \right] + O(c^9) \left. \right\}. \quad (14.273)
\end{aligned}$$

The polar components of the total induced surface current density are (BOUWKAMP [1950]):

$$\begin{aligned}
J_{\rho} \approx & -\frac{16iYc}{3\pi} \cos \phi \sqrt{1 - \frac{\rho^2}{a^2}} \left\{ 1 + \frac{1}{15} \left(7 - \frac{\rho^2}{a^2} \right) c^2 + \frac{1}{4200} \left(664 - 188 \frac{\rho^2}{a^2} + 9 \frac{\rho^4}{a^4} \right) c^4 + \right. \\
& + \frac{2i}{3\pi} c^3 \left[1 + \frac{1}{150} \left(148 - 15 \frac{\rho^2}{a^2} \right) c^2 \right] \left. \right\} + O(c^7), \quad (14.274)
\end{aligned}$$

$$\begin{aligned}
J_{\phi} \approx & \frac{16iYc}{3\pi} \frac{\sin \phi}{\sqrt{1 - (\rho^2/a^2)}} \left\{ 1 - \frac{\rho^2}{2a^2} + \frac{1}{15} \left(7 - 2 \frac{\rho^2}{a^2} + \frac{\rho^4}{4a^4} \right) c^2 + \right. \\
& + \frac{1}{4200} \left(664 - 352 \frac{\rho^2}{a^2} + 27 \frac{\rho^4}{a^4} - \frac{3 \rho^6}{2a^6} \right) c^4 + \\
& + \frac{2i}{3\pi} c^3 \left[1 + \frac{1}{150} \left(148 - 29 \frac{\rho^2}{a^2} \right) c^2 \right] \left. \right\} + O(c^7). \quad (14.275)
\end{aligned}$$

The induced electric dipole moment of the disc is (EGGIMANN [1961]):

$$\mathbf{P} = \frac{16}{3} a^3 \epsilon \left[1 + \frac{8}{15} c^2 + \frac{8i}{9\pi} c^3 + \frac{16}{105} c^4 + \frac{176i}{225\pi} c^5 \right] \mathbf{E}^i(0, 0, 0). \quad (14.276)$$

The magnetic dipole moment is identically zero.

The normalized total scattering cross section is (BOERSMA [1964]):

$$\begin{aligned}
\frac{\sigma_T}{2\pi a^2} \approx & \frac{128}{27\pi^2} c^4 \left[1 + \frac{22}{25} c^2 + \frac{7312}{18375} c^4 + \left(\frac{60224}{496125} - \frac{64}{81\pi^2} \right) c^6 + \right. \\
& + \left. \left(\frac{35048192}{1260653625} - \frac{2464}{2025\pi^2} \right) c^8 + O(c^{10}) \right]. \quad (14.277)
\end{aligned}$$

14.4.2.3. HIGH FREQUENCY APPROXIMATIONS

14.4.2.3.1 Arbitrary incidence

For an incident wave propagating in a direction parallel to the (y, z) plane

and making an angle ζ ($< \frac{1}{2}\pi$) with the positive z -axis, and an angle $\frac{1}{2}\pi - \zeta$ with the positive y -axis, such that

$$E^i = \hat{x} \exp \{ik(y \sin \zeta + z \cos \zeta)\}, \quad (E \text{ polarization}), \quad (14.278)$$

the non-vanishing components of the scattered far field in the half-plane ($x = 0$, $z > 0$) are (UFIMTSEV [1958a, b]):

$$E_\phi^s = -ZH_\theta^s = \frac{1}{2}ic \frac{e^{ikr}}{kr} \{ [F^-(\theta)F^+(\delta)f^{--}(\delta) - F^+(\theta)F^-(\delta)f^{+-}(\delta)]J_1(\gamma) + \\ + i[F^-(\theta)F^+(\delta)f^{--}(\delta) + F^+(\theta)F^-(\delta)f^{+-}(\delta)]J_2(\gamma) \}, \quad (14.279)$$

whereas for an incident wave such that

$$H^i = Y\hat{x} \exp \{ik(y \sin \zeta + z \cos \zeta)\}, \quad (H \text{ polarization}), \quad (14.280)$$

then:

$$E_\theta^s = ZH_\phi^s = \frac{1}{2}ic \frac{e^{ikr}}{kr} \{ [G^-(\theta)G^+(\delta)f^{--}(\delta) - G^+(\theta)G^-(\delta)f^{++}(\delta)]J_1(\gamma) + \\ + i[G^-(\theta)G^+(\delta)f^{--}(\delta) + G^+(\theta)G^-(\delta)f^{++}(\delta)]J_2(\gamma) \}, \quad (14.281)$$

where:

$$\delta = \begin{cases} \zeta, & \text{for } \phi = \frac{1}{2}\pi, \\ -\zeta, & \text{for } \phi = -\frac{1}{2}\pi, \end{cases} \quad (14.282)$$

$$\gamma = c(\sin \theta - \sin \delta), \quad (14.283)$$

$$F^\pm(\theta) = G^\pm(\theta) + \frac{\pi^{-\frac{1}{2}}}{A^\pm} \exp [2ic(1 \pm \sin \theta) + \frac{1}{2}i\pi], \quad (14.284)$$

$$G^\pm(\theta) = 2\pi^{-\frac{1}{2}}e^{-\frac{1}{2}i\pi} \int_0^{A^\pm} e^{ig^2} dg, \quad (14.285)$$

$$A^\pm = \sqrt{2c}(\cos \frac{1}{2}\theta \pm \sin \frac{1}{2}\theta), \quad (14.286)$$

$$f^{\pm\pm}(\delta) = \frac{\pm \cos \frac{1}{2}(\delta + \theta) \pm \sin \frac{1}{2}(\delta - \theta)}{\sin \delta - \sin \theta}. \quad (14.287)$$

Results (14.279) and (14.281) include effects of multiple diffraction and are valid for all ζ and θ less than $\frac{1}{2}\pi$ and bounded away from zero, provided that $|\gamma| \gg 1$. If both ζ and θ are small, then

$$E_\phi^s = -ZH_\theta^s = \frac{1}{2}ic \frac{e^{ikr}}{kr} \{ [f^{--}(\delta) - f^{+-}(\delta)]J_1(\gamma) + i[f^{--}(\delta) + f^{+-}(\delta)]J_2(\gamma) \} \quad (14.288)$$

for E polarization, and

$$ZH_\phi^s = E_\theta^s = \frac{1}{2}ic \frac{e^{ikr}}{kr} \{ [f^{--}(\delta) - f^{++}(\delta)]J_1(\gamma) + i[f^{--}(\delta) + f^{++}(\delta)]J_2(\gamma) \} \quad (14.289)$$

for H polarization.

For the fields in the half-plane ($x = 0, z < 0$), the functions f^{--} and f^{-+} should be respectively replaced by f^{++} and f^{+-} , and the right hand sides of eqs. (14.279) and (14.281) should have the opposite sign. For forward scattering ($\zeta = \theta$) with incidence not too near normal (ζ bounded away from zero), eqs. (14.279) and (14.281) reduce respectively to:

$$E_{\phi}^s = -ZH_{\theta}^s = \frac{1}{2}ic^2 \frac{e^{ikr}}{kr} F^-(\zeta)F^+(\zeta) \cos \zeta, \quad (14.290)$$

$$E_{\theta}^s = ZH_{\phi}^s = \frac{1}{2}ic^2 \frac{e^{ikr}}{kr} G^-(\zeta)G^+(\zeta) \cos \zeta. \quad (14.291)$$

For back scattering with ζ bounded away from zero:

$$E_{\phi}^s = -ZH_{\theta}^s = \frac{ic}{4 \sin \zeta} \frac{e^{ikr}}{kr} \{([F^+(-\zeta)]^2(1 - \sin \zeta) + [F^-(-\zeta)]^2(1 + \sin \zeta))J_1(\gamma) + \\ + i([F^+(-\zeta)]^2(1 - \sin \zeta) - [F^-(-\zeta)]^2(1 + \sin \zeta))J_2(\gamma)\} \quad (14.292)$$

for E polarization, and

$$E_{\theta}^s = ZH_{\phi}^s = \frac{ic}{4 \sin \zeta} \frac{e^{ikr}}{kr} \{(-[G^+(-\zeta)]^2(1 + \sin \zeta) - [G^-(-\zeta)]^2(1 - \sin \zeta))J_1(\gamma) + \\ + i(-[G^+(-\zeta)]^2(1 + \sin \zeta) + [G^-(-\zeta)]^2(1 - \sin \zeta))J_2(\gamma)\} \quad (14.293)$$

for H polarization, whereas if ζ is near zero:

$$E_{\phi}^s = -ZH_{\theta}^s = \frac{1}{2}ic \frac{e^{ikr}}{kr} \left[\frac{1}{\sin \zeta} J_1(2c \sin \zeta) - iJ_2(2c \sin \zeta) \right] \quad (14.294)$$

for E polarization, and

$$E_{\theta}^s = ZH_{\phi}^s = -\frac{1}{2}ic \frac{e^{ikr}}{kr} \left[\frac{1}{\sin \zeta} J_1(2c \sin \zeta) + iJ_2(2c \sin \zeta) \right] \quad (14.295)$$

for H polarization. The results of some computations based on eqs. (14.292) through (14.295) are shown in Fig. 14.23.

The scattered far field for normal incidence and for all values of ϕ has been derived by UFIMTSEV [1958b].

The geometrical theory of diffraction yields the following expression for the normalized back scattering cross section (BECHTEL [1965]):

$$\frac{\sigma}{\lambda^2} = \frac{c}{16\pi^2 \sin \zeta} \left| \left(1 \pm \frac{1}{\sin \zeta} \right) e^{-2ic \sin \zeta + \frac{1}{2}i\pi} + \left(1 \mp \frac{1}{\sin \zeta} \right) e^{2ic \sin \zeta - \frac{1}{2}i\pi} \right|^2, \quad (14.296)$$

where the upper (lower) sign corresponds to $H(E)$ polarization. A comparison of values computed from eq. (14.296) with experimental data is shown in Fig. 14.24.

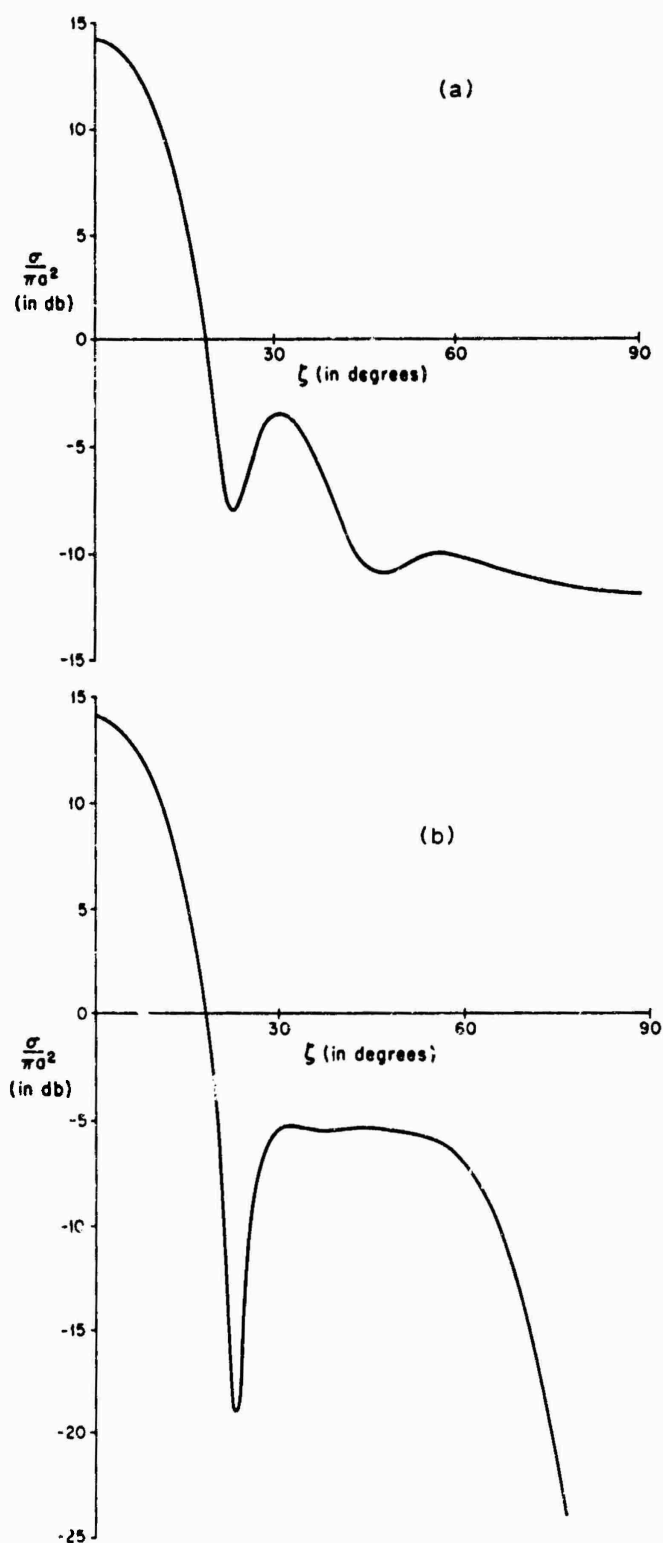


Fig. 14.23. Normalized backscattering cross section in the plane $x = 0$ for a disc with $c = 5.0$ and (a) E polarization, (b) H polarization (UFIMTSEV [1958a]).

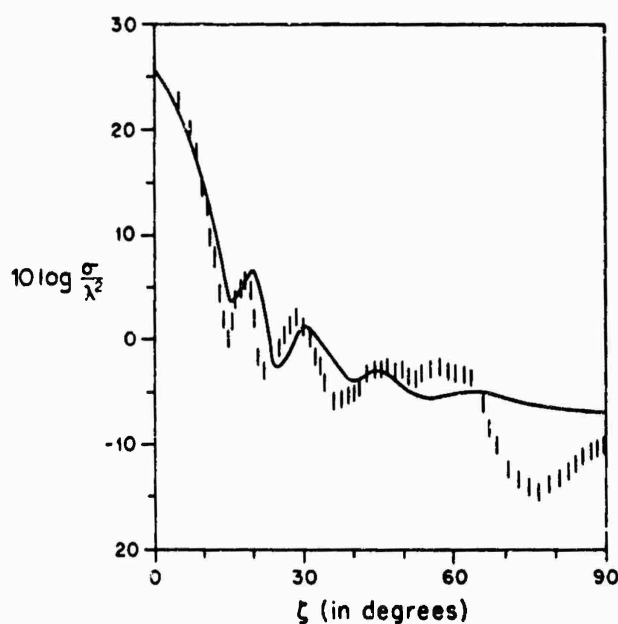


Fig. 14.24. Normalized back scattering cross section of a disc with $c = 8.28$ and E polarisation: — geometrical theory of diffraction, ||| bounds on measured values (BECHTEL [1965])

14.4.2.3.2. Normal incidence

For the incident plane wave

$$\mathbf{E}^i = \hat{x} e^{-ikz}, \quad \mathbf{H}^i = -Y \hat{y} e^{-ikz}, \quad (14.297)$$

approximations analogous to those of the Kirchhoff double and single layer results (see eqs. (14.9) and (14.10)) yield the following expressions for the normalized bistatic scattering cross section (FRAHN [1959a]):

$$\frac{\sigma_1(\theta, \phi)}{\pi a^2} = \frac{4}{\pi c} (1 - \sin^2 \theta \cos^2 \phi) \{1 - \sin(2c \sin \theta)\}, \quad (14.298)$$

$$\frac{\sigma_2(\theta, \phi)}{\pi a^2} = \frac{4}{\pi c} (\cos^2 \theta - \sin^2 \theta \cos^2 \phi) \{1 - \sin(2c \sin \theta)\}, \quad (14.299)$$

where (θ, ϕ) are the spherical polar angles. If the surface field is approximated using half-plane (i.e. edge) currents, the double and single layer results both give (FRAHN [1959a]):

$$\frac{\sigma(\theta, \phi)}{\pi a^2} = \frac{4}{\pi c} \{1 - \cos \theta \sin(2c \sin \theta)\}, \quad (14.300)$$

which is independent of ϕ and valid only at points not too near the axis ($c \sin \theta \geq 1$). At points on or near the axis in the far field and lying in the yz plane (NEUGEBAUER [1952]):

$$\mathbf{E}^s \sim -\hat{x} \exp \{ik\sqrt{(z^2 + a^2)}\} \left\{ J_0 \left(\frac{c\rho}{\sqrt{(z^2 + a^2)}} \right) - \frac{a}{k\rho\sqrt{(z^2 + a^2)}} J_1 \left(\frac{c\rho}{\sqrt{(z^2 + a^2)}} \right) \right\}, \quad (14.301)$$

whereas in the xz plane (NEUGEBAUER [1952]):

$$E^* \sim -\hat{x} \exp \{ik\sqrt{z^2 + a^2}\} \\ \times \left\{ \frac{z^2}{z^2 + a^2} J_0 \left(\frac{c\rho}{\sqrt{z^2 + a^2}} \right) + \frac{a}{k\rho\sqrt{z^2 + a^2}} J_1 \left(\frac{c\rho}{\sqrt{z^2 + a^2}} \right) \right\}. \quad (14.302)$$

Expressions similar to those of eqs. (14.301) and (14.302) have been derived by BEKEFI and WOONTON [1952].

The physical optics approximation to the scattered far field is (BELKINA [1957]):

$$E_{\phi}^{p.o.} = \frac{e^{ikr}}{kr} \frac{icJ_1(c \sin \theta)}{\sin \theta} \cos \phi, \quad (14.303)$$

$$E_{\theta}^{p.o.} = -\frac{e^{ikr}}{kr} \frac{icJ_1(c \sin \theta)}{\sin \theta} \cos \theta \sin \phi, \quad (14.304)$$

implying

$$E_x^{p.o.} = \frac{e^{ikr}}{kr} icJ_1(c \sin \theta) \cot \theta, \quad (14.305)$$

$$\bar{E}_y^{p.o.} = 0. \quad (14.306)$$

BELKINA [1957] has compared the physical optics and exact values for the far field amplitudes in the planes $\phi = 0$ and $\frac{1}{2}\pi$. Correction of the physical optics surface field by the introduction of an approximation to the edge behavior modifies the above forms as follows (UFIMTSEV [1958b]): for $0 \leq \theta \leq \frac{1}{2}\pi$

$$E_{\phi}^* \sim \frac{e^{ikr}}{kr} \frac{1}{2} ic \left\{ \frac{J_1(c \sin \theta)}{\sin \frac{1}{2}\theta} - i \frac{J_2(c \sin \theta)}{\cos \frac{1}{2}\theta} \right\} \cos \phi, \quad (14.307)$$

$$E_{\theta}^* \sim -\frac{e^{ikr}}{kr} \frac{1}{2} ic \left\{ \frac{J_1(c \sin \theta)}{\sin \frac{1}{2}\theta} + i \frac{J_2(c \sin \theta)}{\cos \frac{1}{2}\theta} \right\} \sin \phi; \quad (14.308)$$

and for $\frac{1}{2}\pi \leq \theta \leq \pi$

$$E_{\phi}^* \sim \frac{e^{ikr}}{kr} \frac{1}{2} ic \left\{ \frac{J_1(c \sin \theta)}{\cos \frac{1}{2}\theta} - i \frac{J_2(c \sin \theta)}{\sin \frac{1}{2}\theta} \right\} \cos \phi, \quad (14.309)$$

$$E_{\theta}^* \sim -\frac{e^{ikr}}{kr} \frac{1}{2} ic \left\{ \frac{J_1(c \sin \theta)}{\cos \frac{1}{2}\theta} + i \frac{J_2(c \sin \theta)}{\sin \frac{1}{2}\theta} \right\} \sin \phi. \quad (14.310)$$

UFIMTSEV [1958b] has computed these (and other) approximations to the scattered far field as functions of θ for selected c and ϕ and has compared them to the exact results.

On the axis behind the disc ($\rho = 0, z < 0$), the Kirchhoff approximation provides a closed form expression for the scattered field at all distances (ANDREWS [1947]).

For the incident field of eq. (14.297),

$$E_x^s = i \exp \{ik(z + \sqrt{(z^2 + a^2)})\} \left\{ 1 - \exp \{-ik(z + \sqrt{(z^2 + a^2)})\} + \frac{z}{\sqrt{(z^2 + a^2)}} \right\}, \quad (14.311)$$

the amplitude and phase of which have been computed by ANDREWS [1947] at fixed points on the axis as functions of a . The analogous expression obtained from the Kirchhoff double layer result (see eq. (14.9)) is (FRAHN [1959b]):

$$E_x^s = -ZH_y^s = \frac{z}{\sqrt{(z^2 + a^2)}} \exp \{ik\sqrt{(z^2 + a^2)}\}, \quad (14.312)$$

whilst the single layer result (see eq. (14.10)) is (FRAHN [1959b]):

$$E_x^s = -ZH_y^s = \exp \{ik\sqrt{(z^2 + a^2)}\} \left\{ 1 - \frac{a^2}{2(z^2 + a^2)} + i \frac{a^2}{2k(z^2 + a^2)^{\frac{3}{2}}} \right\}. \quad (14.313)$$

Alternatively, by assuming that the surface field near to the edge is locally that of a half-plane, both the double and single layer results give (FRAHN [1959b]):

$$E_x^s = -ZH_y^s = \exp \{ik\sqrt{(z^2 + a^2)}\} \left(1 - \frac{a}{2\sqrt{(z^2 + a^2)}} \right) \left(1 + \frac{a}{\sqrt{(z^2 + a^2)}} \right)^{\frac{1}{2}}, \quad (14.314)$$

compared with which MILLAR [1956] gives

$$E_x^s = -e^{-ikz} + \frac{1}{2} \exp \{ik\sqrt{(z^2 + a^2)}\} \left\{ \left(1 - \frac{a}{\sqrt{(z^2 + a^2)}} \right)^{\frac{1}{2}} - \frac{z}{\sqrt{(z^2 + a^2)}} \left(1 + \frac{a}{\sqrt{(z^2 + a^2)}} \right)^{\frac{1}{2}} \right\}, \quad (14.315)$$

$$ZH_y^s = e^{-ikz} - \frac{1}{2} \exp \{ik\sqrt{(z^2 + a^2)}\} \left\{ \left(1 + \frac{a}{\sqrt{(z^2 + a^2)}} \right)^{\frac{1}{2}} - \frac{z}{\sqrt{(z^2 + a^2)}} \left(1 - \frac{a}{\sqrt{(z^2 + a^2)}} \right)^{\frac{1}{2}} \right\}, \quad (14.316)$$

and

$$E_y^s = E_z^s = H_x^s = H_z^s = 0. \quad (14.317)$$

The normalized total scattering cross section is (JONES [1965b]):

$$\begin{aligned} \frac{\sigma_T}{2\pi a^2} = & 1 - \frac{1}{c\sqrt{\pi c}} \sin(2c - \frac{1}{4}\pi) + \frac{1}{c^2} \left(\frac{3}{4} - \frac{1}{2\pi} \cos 4c \right) - \\ & - \frac{1}{4c^2\sqrt{\pi c}} \left\{ \frac{1}{\pi} \sin(6c - \frac{3}{4}\pi) + \frac{27}{4} \cos(2c - \frac{1}{4}\pi) \right\} + O(c^{-3}). \end{aligned} \quad (14.318)$$

SESHADRI and WU [1960] have given an expression which differs from the above in having $\frac{7}{4}$ (instead of $\frac{27}{4}$) for the coefficient of the final cosine term. Which form is strictly correct has not yet been determined. CHANG [1955] compared the various expressions then available, and the quantitative significance of each term in eq. (14.318) has been examined by SESHADRI and WU [1960].

On the lower surface ($z = 0 -$) of the disc (BEKEFI [1953b]):

$$ZH_x^s = \frac{1}{2} \sin 2\phi \sum_{m=0}^{\infty} t_m(k\rho)^m J_{m-2}(k\rho), \quad (14.319)$$

$$ZH_y^s = 1 - \sum_{m=0}^{\infty} t_m(k\rho)^m \left\{ J_m(k\rho) + \frac{1}{k\rho} J_{m-1}(k\rho) + J_{m-2}(k\rho) \cos^2 \phi \right\}, \quad (14.320)$$

where

$$t_m = \frac{\Gamma(m + \frac{1}{2})}{\Gamma(\frac{1}{2})} \frac{h_{m-1}^{(1)}(c)}{c^{m-1} m!}. \quad (14.321)$$

On the upper surface ($z = 0 +$), the field is the negative of the above. Eqs. (14.319) and (14.320) imply

$$ZH_x^s = \frac{1}{2} e^{ic} \sin 2\phi \{J_2(k\rho) + O(c^{-1})\}, \quad (14.322)$$

$$ZH_y^s = 1 - \frac{1}{2} e^{ic} \{J_0(k\rho) + J_2(k\rho) \cos 2\phi + O(c^{-1})\}, \quad (14.323)$$

and FRAHN [1959a] has given results which differ from these in having factors $2^{-\frac{1}{2}}$ in place of $\frac{1}{2}$. Computations based (essentially) on the first few terms of eqs. (14.319) and (14.320) have been made by DUNHAM [1964]. Alternatively, using edge-current theory with $\rho \ll a$ (MILLAR [1956]):

$$ZH_x^s = \frac{\sin 2\phi}{2\sqrt{2}} \left\{ e^{ic} \left[J_0(k\rho) - J_2(k\rho) - \frac{i\rho}{2a} \{3J_1(k\rho) - J_3(k\rho)\} \right] - \frac{2}{k\rho} \exp \{ik\sqrt{(\rho^2 + a^2)}\} J_1 \left(\frac{c\rho}{\sqrt{(\rho^2 + a^2)}} \right) \right\} + O(c^{-1}), \quad (14.324)$$

$$ZH_y^s = 1 - \frac{1}{\sqrt{2}} \left\{ e^{ic} \cos^2 \phi \left[J_0(k\rho) - J_2(k\rho) - \frac{i\rho}{2a} \{3J_1(k\rho) - J_3(k\rho)\} \right] + \frac{2}{k\rho} \exp \{ik\sqrt{(\rho^2 + a^2)}\} \sin^2 \phi J_1 \left(\frac{c\rho}{\sqrt{(\rho^2 + a^2)}} \right) \right\} + O(c^{-1}), \quad (14.325)$$

and if, in addition, $k\rho \gg 1$ (MILLAR [1957]):

$$ZH_x^s = \frac{1}{2} \sqrt{\frac{a}{\pi k\rho}} \sin 2\phi \left\{ \frac{e^{ik(a-\rho) + \frac{1}{2}i\pi}}{(a-\rho)^{\frac{1}{2}}} + \frac{e^{ik(a+\rho) - \frac{1}{2}i\pi}}{(a+\rho)^{\frac{1}{2}}} + \frac{1}{2\rho c} \left[\frac{e^{ik(a-\rho) - \frac{1}{2}i\pi}}{(a-\rho)^{\frac{1}{2}}} - (4a^2 - 2\rho a - 2\rho^2) + \frac{e^{ik(a+\rho) + \frac{1}{2}i\pi}}{(a+\rho)^{\frac{1}{2}}} (4a^2 + 3\rho a + 2\rho^2) \right] \right\} + O(c^{-\frac{1}{2}}), \quad (14.326)$$

$$\begin{aligned}
ZH_y^s = 1 - \sqrt{\frac{a}{\pi k \rho}} \cos^2 \phi \left\{ \frac{e^{ik(a-\rho)+\frac{1}{2}i\pi}}{(a-\rho)^{\frac{1}{2}}} + \frac{e^{ik(a+\rho)-\frac{1}{2}i\pi}}{(a+\rho)^{\frac{1}{2}}} \right\} - \\
- \frac{1}{2k\rho} \sqrt{\frac{a}{\pi k \rho}} \cos 2\phi \left\{ \frac{e^{ik(a-\rho)-\frac{1}{2}i\pi}}{(a-\rho)^{\frac{1}{2}}} \left(\frac{a-\rho}{a} + \frac{a}{a-\rho} \right) + \right. \\
+ \left. \frac{e^{ik(a+\rho)+\frac{1}{2}i\pi}}{(a+\rho)^{\frac{1}{2}}} \left(\frac{a+\rho}{a} + \frac{a}{a+\rho} \right) \right\} - \frac{1}{2k} \sqrt{\frac{a}{\pi k \rho}} \left(\frac{\rho}{a} + \cos^2 \phi \right) \left\{ \frac{e^{ik(a-\rho)-\frac{1}{2}i\pi}}{(a-\rho)^{\frac{1}{2}}} + \right. \\
+ \left. \frac{e^{ik(a+\rho)+\frac{1}{2}i\pi}}{(a+\rho)^{\frac{1}{2}}} \right\} + O(c^{-\frac{1}{2}}). \quad (14.327)
\end{aligned}$$

More generally, for $0 < \rho < a$ (MILLAR [1957]):

$$\begin{aligned}
ZH_x^s \sim \frac{\sin 2\phi}{2\sqrt{\pi}} \left\{ \frac{e^{ik(a-\rho)+\frac{1}{2}i\pi}}{\sqrt{\{k(a-\rho)\}}} + \left(\frac{a}{\rho} \right)^{\frac{1}{2}} \frac{e^{ik(a+\rho)-\frac{1}{2}i\pi}}{\sqrt{\{k(a+\rho)\}}} + \right. \\
+ \left. \frac{i}{\sqrt{2\pi c}} e^{ik(a+\rho)} F[\sqrt{\{2k(a-\rho)\}}] \right\}, \quad (14.328)
\end{aligned}$$

$$\begin{aligned}
ZH_y^s \sim 1 - \frac{2}{\sqrt{\pi}} \left\{ e^{-\frac{1}{2}i\pi} F[\sqrt{\{k(a-\rho)\}}] + \frac{1}{2} \sin^2 \phi \frac{e^{ik(a-\rho)+\frac{1}{2}i\pi}}{\sqrt{\{k(a-\rho)\}}} - \right. \\
- \frac{1}{2} \cos^2 \phi \sqrt{\frac{a}{\rho}} \frac{e^{ik(a+\rho)-\frac{1}{2}i\pi}}{\sqrt{\{k(a+\rho)\}}} - \left. \frac{i}{\sqrt{2\pi c}} \cos^2 \phi e^{ik(a+\rho)} F[\sqrt{\{2k(a-\rho)\}}] \right\}, \quad (14.329)
\end{aligned}$$

where

$$F(\tau) = \int_{\tau}^{\infty} e^{i\mu^2} d\mu \quad (14.330)$$

is the Fresnel integral. Results of some computations based on eqs. (14.328) and (14.329) are shown in Fig. 14.25.

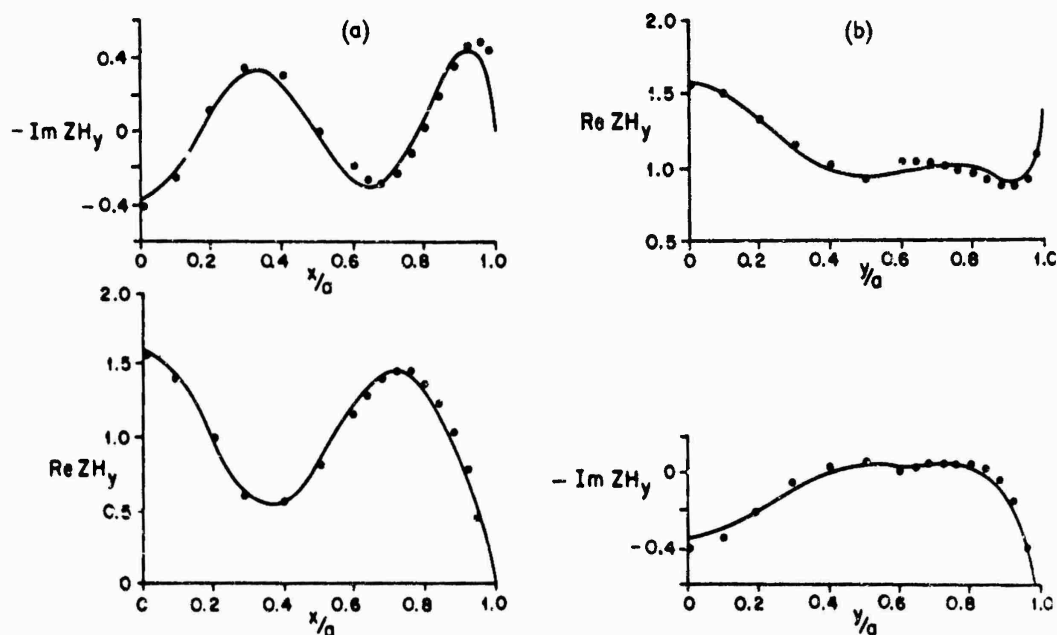


Fig. 14.25 Scattered magnetic field component H^s on the surface $z = 0+$ of the disc for (a) $\phi = 0$ (b) $\phi = \frac{1}{2}\pi$: — exact, ... high frequency approximation (MILLAR [1957]).

Bibliography

- ANDREJEWSKI, W. [1953], Die Beugung elektromagnetischer Wellen an der leitenden Kreisscheibe und an der kreisförmigen Öffnung im leitenden ebenen Schirm, *Z. Angew. Phys.* **5**, 178-186.
- ANDREWS, C. L. [1947], Diffraction Pattern of a Circular Aperture at Short Distances, *Phys. Rev.* **71**, 777-786.
- ASVESTAS, J. S. and R. E. KLEINMAN [1967], Low Frequency Scattering by Spheroids and Discs, The University of Michigan Radiation Laboratory Report No. 7133-5-T, Ann Arbor, Michigan.
- BAZER, J. and A. BROWN [1959], Diffraction of Scalar Waves by a Circular Aperture, *IRE Trans. AP-7*, S12-S20.
- BAZER, J. and H. HOCHSTADT [1962], Diffraction of Scalar Waves by a Circular Aperture - II, *Comm. Pure Appl. Math.* **15**, 1-33.
- BECHTEL, M. E. [1965], Application of Geometric Diffraction Theory to Scattering from Cones and Disks, *Proc. IEEE* **53**, 877-881. [This article contains a typographical error below eq. (1), where the expression $n = \frac{1}{2} + \frac{1}{2}\gamma$ should read $n = \frac{1}{2} + \gamma/\pi$.]
- BEKEFI, G. [1953a], Diffraction of Sound Waves by a Circular Aperture, *J. Acoust. Soc. Am.* **25**, 205-211.
- BEKEFI, G. [1953b], Diffraction of Electromagnetic Waves by an Aperture in a Large Screen, *J. Appl. Phys.* **24**, 1123-1130.
- BEKEFI, G. [1957], Studies in Microwave Optics, Eaton Electronics Research Laboratory Technical Report No. 38, McGill University, Montreal, Canada.
- BEKEFI, G. and G. A. WOONTON [1952], Microwave Diffraction Measurements on Circular Apertures, Eaton Electronics Research Laboratory Technical Report No. TR-24, McGill University, Montreal, Canada.
- BELKINA, M. G. [1957], Diffraction of Electromagnetic Waves by a Disk, Monograph, eds. Fok, Belkina and Vaynshteyn.
- BOERSMA, J. [1964], Boundary Value Problems in Diffraction Theory and Lifting Surface Theory, Thesis, Groningen, Holland.
- BOUWKAMP, C. J. [1950], On the Diffraction of Electromagnetic Waves by Small Circular Disks and Holes, *Philips Res. Rep.* **5**, 401-522.
- BOUWKAMP, C. J. [1954], Diffraction Theory, *Rep. Progr. Phys.* **17**, 35-100.
- BRAUNBEK, W. [1950], Zur Beugung an der Kreisscheibe, *Z. Physik* **127**, 405-415.
- BUCHAL, R. N. and J. B. KELLER [1960], Boundary Layer Problems in Diffraction Theory, *Comm. Pure Appl. Math.* **13**, 85-114.
- CASE, K. M. [1964], An Approximation Method for Diffraction Problems, *Rev. Modern Phys.* **36**, 669-679.
- CHANG, H. H. C. [1955], On the Diffraction of Electromagnetic Waves by a Circular Aperture, Harvard University Scientific Report No. 2, Cambridge, Mass.
- DE HOOP, A. T. [1954], On the Scalar Diffraction by a Circular Aperture in an Infinite Plane Screen, *Appl. Sci. Res.* **B4**, 151-160.
- DUNHAM, R. W. [1964], Diffraction by a Circular Aperture, *J. Opt. Soc. Am.* **54**, 1102-1105.
- EGGMANN, W. H. [1961], Higher-Order Evaluation of Electromagnetic Diffraction by Circular Disks, *IRE Trans. MTT-9*, 408-418.
- FLAMMER, C. [1953], The Vector Wave Function Solution of the Diffraction of Electromagnetic Waves by Circular Disks and Apertures-II: The Diffraction Problems, *J. Appl. Phys.* **24**, 1224-1231.
- FLAMMER, C. [1957], *Spheroidal Wave Functions*, Stanford University Press, Stanford, California.
- FRANZ, W. F. [1959a], Beugung elektromagnetischer Wellen in Braunbekscher Näherung-I, *Z. Physik* **156**, 78-98.
- FRANZ, W. F. [1959b], Beugung elektromagnetischer Wellen in Braunbekscher Näherung-II, *Z. Physik* **156**, 99-116.
- GRINBERG, G. A. and Ju. V. PIMENOV [1957], On the Question of Diffraction of Electromagnetic

- Waves from Infinitesimally Thin Ideally Conducting Plane Screens, *Soviet Phys.* **2**, 2160-2175.
- HANSEN, E. B. [1962], Scalar Diffraction by an Infinite Strip and a Circular Disc, *J. Math. and Phys.* **41**, 229-245.
- HANSEN, E. B. [1964], Higher Order Diffraction by a Circular Disk, *Acta Polytech. Scandinav. Series* **33**, UDC 534, 26 (47pp).
- HEINS, A. and R. C. MACCAMY [1960], On the Scattering of Waves by a Disk, *Z. Angew. Math. Phys.* **11**, 249-264.
- HEY, J. S., G. S. STEWART, J. T. PINSON and P. E. V. PRINCE [1956], The Scattering of Electromagnetic Waves by Conducting Spheres and Discs, *Proc. Phys. Soc. (London)* **69**, 1038-1049.
- HUANG, C., R. D. KODIS and H. LEVINE [1955], Diffraction by Apertures, *J. Appl. Phys.* **26**, 151-165.
- HURD, R. A. [1961], A Note on the Diffraction of a Scalar Wave by a Small Circular Aperture, *Can. J. Phys.* **39**, 1065-1070.
- INAWASHIRO, S. [1963], Diffraction of Electromagnetic Waves from an Electric Dipole by a Conducting Circular Disc, *J. Phys. Soc. Japan* **18**, 273-287.
- JONES, D. S. [1956], A New Method for Calculating Scattering, with Particular Reference to the Circular Disc, *Comm. Pure Appl. Math.* **9**, 713-746.
- JONES, D. S. [1965a], Diffraction at High Frequencies by a Circular Disc, *Proc. Cambridge Phil. Soc.* **61**, 223-245.
- JONES, D. S. [1965b], Diffraction of a High-Frequency Plane Electromagnetic Wave by a Perfectly Conducting Circular Disc, *Proc. Cambridge Phil. Soc.* **61**, 247-270.
- JONES, D. S. [1965c], Diffraction of Short Wavelengths by a Rigid Circular Disk, *Quart. J. Mech. Appl. Math.* **18**, 191-208.
- KARP, S. N. and J. B. KELLER [1961], Multiple Diffraction by an Aperture in a Hard Screen, *European J. Opt.* **8**, 61-72.
- KELLER, J. B. [1957], Diffraction by an Aperture, *J. Appl. Phys.* **28**, 426-444.
- KELLER, J. B. [1963], The Field of an Antenna Near the Center of a Large Circular Disk, *J. Soc. Indust. Appl. Math.* **11**, 1110-1112.
- LEHNER, A. [1949], Diffraction of Sound by a Circular Disk, *J. Acoust. Soc. Am.* **21**, 331-334.
- LEVINE, H. and J. SCHWINGER [1950], On the Theory of Electromagnetic Wave Diffraction by an Aperture in an Infinite Plane Conducting Screen, *Comm. Pure Appl. Math.* **3**, 355-391.
- LEVINE, H. and T. F. WU [1957], Diffraction by an Aperture at High Frequencies, Stanford University Applied Mathematics and Statistics Laboratory Technical Report No. 71, Stanford, California.
- LOMEL, E. [1884], *Bayerisch. Akad. d. Wiss.* **15**, 233. English transl. by G. Bekeli and G. A. Wootton, *Eaton Electronics Research Laboratory Technical Report No. 4*, McGill University, Montreal, Canada (1951).
- LUTT, K. A. [1960], Diffraction of a Plane Electromagnetic Wave on an Ideally Conducting Circular Disc, *Soviet Phys.* **4**, 1313-1325.
- MEIXNER, J. [1953], Theorie der Beugung elektromagnetischer Wellen an der vollkommen leitenden Kreisscheibe und verwandte Probleme, *Ann. Physik* **12**, 227-236.
- MEIXNER, J. and W. ANDRZEJSKI [1950], Strenge Theorie der Beugung ebener elektromagnetischer Wellen an der vollkommen leitenden Kreisscheibe und an der kreisförmigen Öffnung im vollkommen leitenden ebenen Schirm, *Ann. Physik* **7**, 157-168.
- MEIXNER, J. and U. FRETZ [1949], Das Schallfeld in der Nähe der freischwingenden Kolbenmembran, *Z. Angew. Phys.* **1**, 535-542.
- MUTAR, R. E. [1956], An Approximate Theory of the Diffraction of an Electromagnetic Wave by an Aperture in a Plane Screen, *Proc. IEE* **103C**, 177-185.
- MUTAR, R. E. [1957], The Diffraction of an Electromagnetic Wave by a Circular Aperture, *Proc. IEE* **104C**, 87-95.

- NEUGEBAUER, H. E. J. [1952], A Method of Solving Diffraction Problems by Approximation, Eaton Electronics Research Laboratory Technical Report No. 23, McGill University, Montreal, Canada.
- NOMURA, Y. and S. Katsura [1955], Diffraction of Electromagnetic Waves by Circular Plate and Circular Hole, J. Phys. Soc. Japan **10**, 285-304.
- RAYLEIGH, Lord [1897], On the Incidence of Aerial and Electric Waves Upon Small Obstacles in the Form of Ellipsoids or Elliptic Cylinders, and on the Passage of Electric Waves through a Circular Aperture in a Conducting Screen, Phil. Mag. **44**, 28-52.
- RYAN, C. E. and L. PETERS [1968], A Creeping-Wave Analysis of the Edge-on Echo Area of Disks, IEEE Trans. **AP-16**, 274-275.
- SCHMITT, H. J. [1957], Experimental Radar Cross Section of Metallic Disks at 1 and 3 cm, Cruft Laboratory Report No. 14, Harvard University, Cambridge, Massachusetts.
- SESHADRI, S. R. and T. T. WU [1960], High-Frequency Diffraction of Electromagnetic Waves by a Circular Aperture in an Infinite Plane Conducting Screen, IRE Trans. **AP-8**, 27-36.
- SEVERIN, H. [1952], Methods of Light Optics for the Calculation of the Diffraction Phenomena within the Range of Centimeter Waves, Suppl. Nuovo Cimento **9**, 381-400.
- SEVERIN, H. and C. STARKE [1952], Beugung von Schallwellen an der kreisförmigen Öffnung im schallharten Schirm, Akust. Beihefte **AB2**, 59-66.
- SPENCE, R. D. [1949], A Note on the Kirchhoff Approximation in Diffraction Theory, J. Acoust. Soc. Am. **21**, 98-100.
- TANG, C. L. [1962], On the Radiation Pattern of a Base-Driven Antenna over a Circular Conducting Screen, J. Soc. Indust. Appl. Math. **10**, 695-708.
- UFIMTSEV, P. Ia. [1958a], Secondary Diffraction of Electromagnetic Waves by a Disk, Soviet Phys. **3**, 549-556.
- UFIMTSEV, P. Ia. [1958b], Approximate Calculation of the Diffraction of Plane Electromagnetic Waves by Certain Metal Objects, Soviet Phys. **3**, 2386-2396.
- WATSON, G. N. [1958], *A Treatise on the Theory of Bessel Functions*, Cambridge University Press, London.
- WESTPFAHL, K. and H. H. WITTE [1967], Beugung skalarer hochfrequenter Wellen an einer Kreisblende, Ann. Physik **20**, 14-28.
- WILLIAMS, W. E. [1962], Diffraction by a Disk, Proc. Roy. Soc. **A267**, 77-87.

PART THREE

SEMI-INFINITE BODIES

GENERAL CONSIDERATIONS

The three semi-infinite bodies considered in this part, namely the paraboloid and hyperboloid of revolution and the circular cone, are shapes for which an exact solution to the scalar (and, for particular cases, to the vector) scattering problem may be obtained by the standard procedure of separation of variables. However, exact solutions are also known for other semi-infinite scatterers, such as the quarter plane (RADLOW [1961, 1965]), the elliptic cone (KRAUS and LEVINE [1961]) and the half-cylinder (EINARSSON et al. [1966]), which are not presented in this book. Furthermore, a general method exists for deriving the solutions of scattering problems from the solutions of potential problems if the primary sources are dipoles or multipoles located at the common vertex of arbitrary conical surfaces which are the boundaries of scatterers that are either perfect conductors or lossless dielectrics (POTEKHIN [1958], POTEKHIN and TARTAKOVSKII [1958]).

The circular cone is important because it is the shape of the nose of many airplanes and missiles; parabolic reflectors find widespread application to antennas and radiotelescopes, and both parabolic and hyperbolic reflectors are used in Cassegrainian antennas. The cases considered are those in which the primary sources are either on the convex or the concave side of the scattering surface; the former case is of special importance for the cone, and the latter for the paraboloid.

It has often been conjectured that for a plane electromagnetic wave axially incident on a convex semi-infinite body of revolution whose entire surface is illuminated, the back scattered physical optics field should yield the exact solution. This has only been proven for the paraboloid (SCHENSTED [1955]), but there are indications that it may also be true for the cone (see, for example, SIEGEL et al. [1955] and Chapter 18).

The concept of radar cross section needs clarification for a semi-infinite body, because both the distance of the observation point from the scatterer and a characteristic dimension of the scatterer tend to infinity; this topic has been discussed by BRYSK [1960], among others. The reader is referred to Chapter 9 for the definition of acoustic cross section.

Bibliography

- BRYSK, H. [1960], The Radar Cross Section of a Semi-Infinite Body, *Can. J. Phys.* **38**, 48-56.
 EINARSSON, O., R. E. KEELMAN, P. LAURIN and P. L. E. USTENGHI [1966], *Studies in Radar Cross Sections I-Diffraction and Scattering by Regular Bodies IV: The Circular Cylinder*, University

- of Michigan Radiation Laboratory Report No. 7133-3-T, Ann Arbor, Michigan.
- KRAUS, L. and L. M. LEVINE [1961], Diffraction by an Elliptic Cone, *Comm. Pure Appl. Math.* **24**, 49-68.
- POTEKHIN, A. I. [1958], Solution of Electrodynanic Problems from Known Solutions of Corresponding Electrostatic and Magnetostatic Problems, *Radio Eng. Electron.* **3**, 1-7 (translated from *Radiotekhn. i Elektron.*).
- POTEKHIN, A. I. and L. B. TARTAKOVSKII [1958], Radiation of a Hertzian Dipole on the Edge of an Ideally Conducting Wedge, *Radio Eng. Electron.* **3**, 8-22 (translated from *Radiotekhn. i Elektron.*).
- RADLOW, J. [1961], Diffraction by a Quarter-Plane, *Arch. Rational Mech. Anal.* **8**, 139-158.
- RADLOW, J. [1965], Note on the Diffraction at a Corner, *Arch. Rational Mech. Anal.* **19**, 62-70.
- SCHENSTED, C. E. [1955], Electromagnetic and Acoustical Scattering by a Semi-Infinite Body of Revolution, *J. Appl. Phys.* **26**, 306-308.
- SIEGEL, K. M., H. A. ALPERIN, R. R. BONKOWSKI, J. W. CRISPIN, A. L. MAFFETT, C. E. SCHENSTED and I. V. SCHENSTED [1955], Bistatic Radar Cross Sections of Surfaces of Revolution, *J. Appl. Phys.* **26**, 297-305.

THE PARABOLOID

P. L. E. USLENGHI

The convex infinite paraboloid of revolution is especially interesting in diffraction theory because it is the only known body with variable curvature for which the exact scattered field produced by a plane electromagnetic wave at axial incidence is equal to the geometrical and physical optics approximations.

Both convex and concave paraboloids are important in scattering and antenna applications. Although only the convex paraboloid is here considered in detail, an outline of the available literature on the concave paraboloid is given in Section 16.5. It should be noted that a time-dependent study for the acoustical case has been performed by FRIEDLANDER [1943].

16.1. Geometry and eigenfunctions for paraboloid of revolution

The parabolic coordinates (ξ, η, ϕ) shown in Fig. 16.1 are related to the rectangular Cartesian coordinates (x, y, z) by the transformation

$$\begin{aligned} x &= 2\sqrt{\xi\eta} \cos \phi, \\ y &= 2\sqrt{\xi\eta} \sin \phi, \\ z &= \xi - \eta, \end{aligned} \tag{16.1}$$

where $0 \leq \xi < \infty$, $0 \leq \eta < \infty$, and $0 \leq \phi < 2\pi$. The z -axis is the axis of symmetry

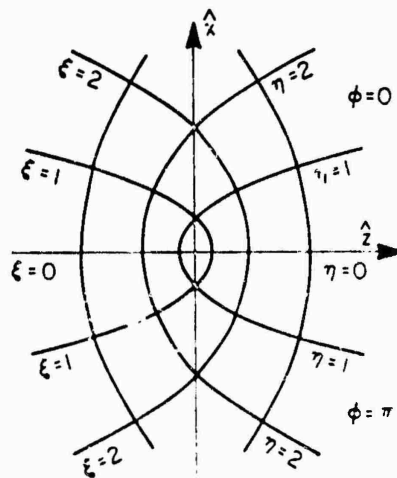


Fig. 16.1. Parabolic geometry

and the surfaces $\xi = \text{constant}$ and $\eta = \text{constant}$ are paraboloids of revolution with foci at the origin $O \equiv (x = 0, y = 0, z = 0)$, whereas the surfaces $\phi = \text{constant}$ are semiplanes originating in the z -axis. The metric coefficients, as defined in Appendix C, are

$$h_\xi = \sqrt{1 + \eta/\xi}, \quad h_\eta = \sqrt{1 + \xi/\eta}, \quad h_\phi = 2\sqrt{\xi\eta}. \quad (16.2)$$

It is also useful to introduce the spherical polar coordinates (r, θ, ϕ) , for which

$$r = \xi + \eta, \quad \theta = \arccos \frac{\xi - \eta}{\xi + \eta}. \quad (16.3)$$

The scattering body is the convex paraboloid with surface $\eta = \eta_1$. The principal radius of curvature of the surface in the plane $\phi = \text{constant}$ and at the point (ξ, η_1, ϕ) is

$$\rho_1 = \rho_1(\xi) = 2\eta_1^{-1/2}(\xi + \eta_1)^{3/2}, \quad (16.4)$$

while the other principal radius at the same point is:

$$\rho_2 = \rho_2(\xi) = 2\eta_1^{1/2}(\xi + \eta_1)^{3/2}. \quad (16.5)$$

The Gaussian curvature therefore is

$$\sqrt{\rho_1 \rho_2} = 2(\xi + \eta_1).$$

In particular, at the nose ($\xi = 0, \eta = \eta_1$):

$$\rho_1 = \rho_2 = 2\eta_1.$$

The primary source is located on the convex side of the scatterer, and is either a plane wave whose direction of propagation forms the angle α with the positive z -axis, or a point or dipole source located at (ξ_0, η_0, ϕ_0) . If the product $k\eta_1$ of the free-space wave number k and the focal length η_1 of the scatterer is very small (very large) compared with unity, one speaks of low (high) frequencies; alternatively, the terminology "thin" ("fat") paraboloid also appears in the literature. No detailed low-frequency results are presently available for the convex paraboloid.

No generally accepted definitions exist for the eigenfunctions which occur in the solution of the wave equation by separation of variables in parabolic coordinates. The more widely used symbols are those of BUCHHOLZ [1953], PINNEY [1946] and FOCK [1957; 1965, Chapter 3]. In this chapter the notation of BUCHHOLZ [1953] is adopted, except in a few formulas where Pinney's notation is retained because of existing numerical tables. The eigenfunctions $m_r^{(\mu)}(z)$ and $w_r^{(\mu)}(z)$ of BUCHHOLZ [1953] are related to the Whittaker functions $M_{r, \frac{1}{2}\mu}(z)$ and $W_{r, \frac{1}{2}\mu}(z)$ by:

$$\begin{aligned} m_r^{(\mu)}(z) &= \frac{M_{r, \frac{1}{2}\mu}(z)}{z^{\frac{1}{2}}\Gamma(1+\mu)}, \\ w_r^{(\mu)}(z) &= z^{-\frac{1}{2}}W_{r, \frac{1}{2}\mu}(z). \end{aligned} \quad (16.6)$$

where τ , μ and z are any complex quantities; their Wronskian is

$$w_{\tau}^{(\mu)}(z) \frac{d}{dz} m_{\tau}^{(\mu)}(z) - m_{\tau}^{(\mu)}(z) \frac{d}{dz} w_{\tau}^{(\mu)}(z) = \{z\Gamma(\tfrac{1}{2}(1+\mu) - \tau)\}^{-1}. \quad (16.7)$$

It should be noted that BUCHHOLZ [1943a, b; 1947] uses the same symbols of eqs. (16.6) for different functions; thus:

$$\begin{aligned} \{m_{\tau}^{(\mu)}(z)\}_{1943a, b; 1947} &= \left(\frac{\pi}{2z}\right)^{\frac{1}{2}} M_{\tau, \frac{1}{2}\mu}(z) = \sqrt{\tfrac{1}{2}\pi} \Gamma(1+\mu) m_{\tau}^{(\mu)}(z), \\ \{w_{\tau}^{(\mu)}(z)\}_{1943a, b; 1947} &= \left(\frac{\pi}{2z}\right)^{\frac{1}{2}} W_{\tau, \frac{1}{2}\mu}(z) = \sqrt{\tfrac{1}{2}\pi} w_{\tau}^{(\mu)}(z). \end{aligned} \quad (16.6a)$$

Detailed studies of $m_{\tau}^{(\mu)}(z)$ and $w_{\tau}^{(\mu)}(z)$ are found in BUCHHOLZ [1953; see also 1943b, 1947]; the book by BUCHHOLZ [1953] also contains an extensive bibliography. Asymptotic formulas are also found in ERDÉLYI and SWANSON [1957], and addition theorems have been developed by HOCHSTADT [1956b].

The eigenfunctions $S_v^{\mu}(z)$ and $V_v^{\mu}(z)$ introduced by PINNEY [1946] are related to the functions (16.6) by:

$$\begin{aligned} S_v^{\mu}(z) &= z^{\frac{1}{2}\mu} e^{-\frac{1}{2}z} L_v^{\mu}(z) = \frac{\Gamma(\mu+v+1)}{\Gamma(v+1)} m_{v+\frac{1}{2}(1+\mu)}^{(\mu)}(z), \\ V_v^{\mu}(z) &= z^{\frac{1}{2}\mu} e^{-\frac{1}{2}z} U_v^{\mu}(z) = \pi^{-1} e^{\mp \frac{1}{2}i\pi\mu} \Gamma(\mu+v+1) w_{-v-\frac{1}{2}(1+\mu)}^{(\mu)}(ze^{\mp i\pi}), \quad (\text{Im } z \geq 0), \end{aligned} \quad (16.8)$$

where μ , v and z are any complex quantities; their Wronskian is

$$S_v^{\mu}(z) \frac{d}{dz} V_v^{\mu}(z) - V_v^{\mu}(z) \frac{d}{dz} S_v^{\mu}(z) = \pm \frac{i}{\pi z} \frac{\Gamma(\mu+v+1)}{\Gamma(v+1)}, \quad (\text{Im } z \geq 0). \quad (16.9)$$

The properties of $S_v^{\mu}(z)$ and $V_v^{\mu}(z)$ have been studied in detail by PINNEY [1946]; see also MIRIMANOV [1948a, b]. HORTON [1952] has published numerical tables of $L_n^m(iy)$, $U_n^m(iy)$, $S_n^m(iy)$ and $V_n^m(iy)$ to seven decimals for $y = 0$ (0.1) 1.0 with either $m = 0$ and $n = 0, 1, 2, 3$, or $m = 1$ and $n = 0, 1, 2$. HORTON [1953] has given eight-decimal tables of $U_n^0(iy)$ with $n = 0, 1, 2, 3$; $U_n^1(iy)$ with $n = 0, 1, 2$; $U_n^2(iy)$ and $U_n^3(iy)$ with $n = 0, 1$, for $y = 0$ (0.1) 2.0.

The eigenfunctions ξ , ζ_1 and ψ of FOCK [1957; 1965, Chapter 3] are related to the functions (16.6) by:

$$\begin{aligned} \xi(u, s, t) &= e^{-\frac{1}{2}i\pi s} m_{\frac{1}{2}(s+1)}^{(s)}(iu), \\ \zeta_1(u, s, t) &= \exp\left\{-\frac{1}{2}i\pi(1+\tfrac{1}{2}s) - \tfrac{1}{2}\pi t\right\} w_{\frac{1}{2}(s+1)}^{(s)}(-iu), \\ \psi(u, s, t) &= \Gamma(\tfrac{1}{2}(s+1+it)) \xi(u, s, t). \end{aligned} \quad (16.10)$$

16.2. Acoustically soft convex paraboloid

16.2.1. Point sources

16.2.1.1. EXACT SOLUTIONS

The Green function for a point source located between two coaxial and confocal paraboloids has been given by BUCHHOLZ [1953; Section 18.2].

For a point source at $(\xi_0, \eta_0 \geq \eta_1, \phi_0)$, such that

$$V^i = \frac{e^{ikR}}{kR}, \quad (16.11)$$

then

$$\begin{aligned} V^i + V^s = & -\frac{1}{\pi} \sum_{n=-\infty}^{\infty} e^{in(\phi-\phi_0)} \int_{-\gamma_n-i\infty}^{-\gamma_n+i\infty} d\tau \Gamma\left(\frac{1}{2}(1+n)+\tau\right) \Gamma\left(\frac{1}{2}(1+n)-\tau\right) \\ & \times m_{\tau}^{(n)}(-2ik\xi_<) w_{\tau}^{(n)}(-2ik\xi_>) \\ & \times \left[m_{\tau}^{(n)}(-2ik\eta_<) - \frac{m_{\tau}^{(n)}(-2ik\eta_1)}{w_{\tau}^{(n)}(-2ik\eta_1)} w_{\tau}^{(n)}(-2ik\eta_<) \right] w_{\tau}^{(n)}(-2ik\eta_>), \end{aligned} \quad (16.12)$$

where

$$|\gamma_n| < \frac{1}{2}(1+|n|). \quad (16.13)$$

On the surface $(\eta = \eta_1)$:

$$\begin{aligned} \frac{\partial}{\partial \eta} (V^i + V^s) \Big|_{\eta=\eta_1} = & -\frac{1}{\pi \eta_1} \sum_{n=-\infty}^{\infty} e^{in(\phi-\phi_0)} \int_{-\gamma_n-i\infty}^{-\gamma_n+i\infty} d\tau \Gamma\left(\frac{1}{2}(1+n)-\tau\right) \\ & \times m_{\tau}^{(n)}(-2ik\xi_<) w_{\tau}^{(n)}(-2ik\xi_>) \frac{w_{\tau}^{(n)}(-2ik\eta_0)}{w_{\tau}^{(n)}(-2ik\eta_1)}. \end{aligned} \quad (16.14)$$

In particular, if the source is on the z -axis $(\xi_0 = 0)$:

$$\begin{aligned} V^i + V^s = & -\int_{-\gamma_0-i\infty}^{-\gamma_0+i\infty} w_{\tau}^{(0)}(-2ik\xi) \left[m_{\tau}^{(0)}(-2ik\eta_<) - \right. \\ & \left. - \frac{m_{\tau}^{(0)}(-2ik\eta_1)}{w_{\tau}^{(0)}(-2ik\eta_1)} w_{\tau}^{(0)}(-2ik\eta_<) \right] w_{\tau}^{(0)}(-2ik\eta_>) \frac{d\tau}{\cos(\pi\tau)}, \end{aligned} \quad (16.15)$$

with

$$|\gamma_0| < \frac{1}{2}, \quad (16.16)$$

and on the surface $(\eta = \eta_1)$:

$$\frac{\partial}{\partial \eta} (V^i + V^s) \Big|_{\eta=\eta_1} = -\frac{1}{\pi \eta_1} \int_{-\gamma_0-i\infty}^{-\gamma_0+i\infty} d\tau \Gamma\left(\frac{1}{2}-\tau\right) w_{\tau}^{(0)}(-2ik\xi) \frac{w_{\tau}^{(0)}(-2ik\eta_0)}{w_{\tau}^{(0)}(-2ik\eta_1)}. \quad (16.17)$$

16.2.1.2. HIGH FREQUENCY APPROXIMATIONS

For a point source at $P_0 \equiv (\xi_0, \eta_0 \geq \eta_1, \phi_0 = 0)$, such that

$$V^i = \frac{e^{ikR}}{kR}, \quad (16.18)$$

the geometrical optics scattered field at a point P located in the illuminated region of the $y = 0$ plane is

$$V_{g.o.}^s = - \frac{\exp \{ik[(P_0 P_1) + (P_1 P)]\}}{k(P_0 P_1)} \left[\left(1 + \frac{(P_1 P)}{(P_0 P_1)} + \frac{2(P_1 P)}{\rho_1 \cos \psi} \right) \times \left(1 + \frac{(P_1 P)}{(P_0 P_1)} + \frac{2(P_1 P) \cos \psi}{\rho_2} \right) \right]^{-\frac{1}{2}}, \quad (16.19)$$

where $(P_0 P_1)$ and $(P_1 P)$ are respectively the distances between the source P_0 and the reflection point $P_1 \equiv (x_1, 0, z_1) \equiv (\xi_1, \eta_1, \phi_1 = 0 \text{ or } \pi)$, and between P_1 and

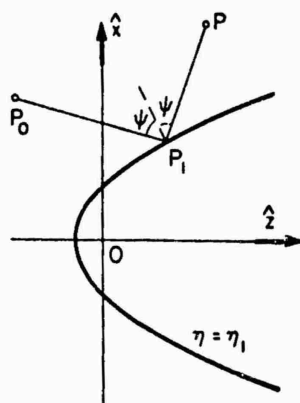


Fig. 16.2. Geometry for reflected field.

the observation point $P \equiv (x, 0, z) = (\xi, \eta, \phi = 0 \text{ or } \pi)$ (see Fig. 16.2); the principal radii of curvature ρ_1 and ρ_2 are given by eqs. (16.4) and (16.5), the reflection angle ψ is given by

$$\psi = \arccos \{ (\xi_1 + \eta_1)^{-\frac{1}{2}} [4(\sqrt{\xi_0 \eta_0} - \sqrt{\xi_1 \eta_1})^2 + (\xi_0 - \eta_0 - \xi_1 + \eta_1)^2]^{-\frac{1}{2}} \times [2\sqrt{\xi_1 \xi_0 \eta_0} - \sqrt{\eta_1}(\xi_0 - \eta_0 + \xi_1 + \eta_1)] \}, \quad (16.20)$$

and ξ_1 is a root of:

$$[2\sqrt{\xi_1 \xi_0 \eta_0} - \sqrt{\eta_1}(\xi_0 - \eta_0 + \xi_1 + \eta_1)][4(\sqrt{\xi_0 \eta_0} - \sqrt{\xi_1 \eta_1})^2 + (\xi_0 - \eta_0 - \xi_1 + \eta_1)^2]^{-\frac{1}{2}} = [2\sqrt{\xi_1 \xi \eta} - \sqrt{\eta_1}(\xi - \eta + \xi_1 + \eta_1)][4(\sqrt{\xi \eta} - \sqrt{\xi_1 \eta_1})^2 + (\xi - \eta - \xi_1 + \eta_1)^2]^{-\frac{1}{2}}. \quad (16.21)$$

Formula (16.19) is applicable if $k\rho_{1,2} \gg 1$. In the shadow region, $V_{g.o.} = 0$.

For a point source on the axis of symmetry, an asymptotic analysis of the exact results of eqs. (16.15) and (16.17) has been performed by KLANTÉ [1959] and by IVANOV [1962].

For a point source of strength given by eq. (16.18) and located on the z -axis ($\xi_0 = 0$), and for an observation point $P \equiv (\xi, \eta_1, \phi)$ located in the illuminated region ($\xi < \eta_0 - \eta_1$) of the surface $\eta = \eta_1$,

$$\left\{ \frac{\partial}{\partial \eta} (V^i + V^s) \right\}_{\eta=\eta_1, g.o.} = -2ik \sqrt{\frac{\xi}{\eta_1} + 1} \frac{\exp \{ik(P_0 P)\}}{k(P_0 P)} \cos \psi, \quad (16.22)$$

where

$$\psi = \arccos \left\{ \left(\frac{\eta_1}{\xi + \eta_1} \right)^{\frac{1}{2}} (\eta_0 - \eta_1 - \xi) [4\xi\eta_1 + (\eta_0 - \eta_1 - \xi)^2]^{-\frac{1}{2}} \right\}. \quad (16.23)$$

Result (16.22) is the leading term in the high frequency expansion of (16.17), provided that P is not too close to the shadow boundary, i.e. that (IVANOV [1962]):

$$\cos \psi \gg (k\rho_1)^{-\frac{1}{2}} = [2k\eta_1^{-\frac{1}{2}}(\xi + \eta_1)^{\frac{1}{2}}]^{-\frac{1}{2}}, \quad (16.24)$$

where ρ_1 is the principal radius of curvature given by eq. (16.4).

On the surface $\eta = \eta_1$, in the shadow region, and for a source located at a sufficiently large distance from the nose of the paraboloid, such that

$$k(\eta_0 - \eta_1) \gg (k\eta_1)^{\frac{1}{2}}, \quad (16.25)$$

then (IVANOV [1962]):

$$\frac{\partial}{\partial \eta} (V^i + V^s) \Big|_{\eta=\eta_1} \sim \frac{1}{2} (k\eta_1)^{-\frac{1}{2}} [\xi(\xi + \eta_1)\eta_0(\eta_0 - \eta_1)]^{-\frac{1}{2}} f(D) e^{ikL}, \quad (16.26)$$

where

$$L = \sqrt{\xi(\xi + \eta_1)} + \sqrt{\eta_0(\eta_0 - \eta_1)} + \eta_1 \log \frac{\sqrt{\xi} + \sqrt{\xi + \eta_1}}{\sqrt{\eta_0} + \sqrt{\eta_0 - \eta_1}}, \quad (16.27)$$

$$D = (\frac{1}{2}k)^{\frac{1}{2}} \int_{\xi_1}^{\xi} [\rho_1(\cdot)]^{-\frac{1}{2}} \left(1 + \frac{\tau}{\eta_1}\right)^{\frac{1}{2}} d\tau = (k\eta_1)^{\frac{1}{2}} \log \frac{\sqrt{\xi} + \sqrt{\xi + \eta_1}}{\sqrt{\eta_0} + \sqrt{\eta_0 - \eta_1}}, \quad (16.28)$$

$\rho_1(\xi)$ is given by eq. (16.4) and $f(D)$ is the Fock function defined in the Introduction (see eq. (1.267)). The distance L is the length of the optical ray path from P_0 to P (see Fig. 16.3):

$$L = (P_0 P_1) + \widehat{P_1 P}, \quad (16.29)$$

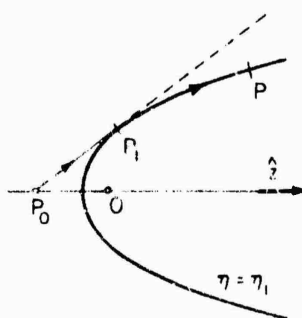


Fig. 16.3. Geometry for surface field in the shadow, with point source on the axis of symmetry.

where $(P_0 P_1)$ is the distance between the source at $P_0 \equiv (\xi_0 = 0, \eta_0)$ and the point $P_1 \equiv (\xi_1 = \eta_0 - \eta_1, \eta_1, \phi)$ on the shadow boundary, and $\widehat{P_1 P}$ is the length of the arc of the parabola between P_1 and the observation point $P \equiv (\xi, \eta_1, \phi)$.

On the surface $\eta = \eta_1$, in the shadow region, and for a source located near the nose of the paraboloid, such that

$$k(\eta_0 - \eta_1) \lesssim (k\eta_1)^{\frac{1}{2}}, \quad (16.30)$$

then (IVANOV [1962]):

$$\begin{aligned} \frac{\partial}{\partial \eta} (V^I + V^S) \Big|_{\eta=\eta_1} &\sim \frac{1}{2} (k\eta_1)^{-\frac{1}{2}} [\xi(\xi + \eta_1)\eta_1^2]^{-\frac{1}{2}} \{ \exp(ikL_1 - \frac{1}{4}i\pi) \} \\ &\times \frac{1}{\sqrt{\pi}} \int_{-\infty}^{\infty} \frac{w_1(t-y_0)}{w_1(t)} e^{iD_1 t} dt, \end{aligned} \quad (16.31)$$

where

$$L_1 = \sqrt{\xi(\xi + \eta_1)} + \eta_1 \log \frac{\sqrt{\xi} + \sqrt{(\xi + \eta_1)}}{\sqrt{\eta_1}}, \quad (16.32)$$

$$D_1 = (k\eta_1)^{\frac{1}{2}} \log \frac{\sqrt{\xi} + \sqrt{(\xi + \eta_1)}}{\sqrt{\eta_1}}, \quad (16.33)$$

$$y_0 = \frac{\eta_0 - \eta_1}{\eta_1} (k\eta_1)^{\frac{1}{2}}, \quad (16.34)$$

$w_1(t)$ is the Airy function in Fock's notation defined in the Introduction (see eqs. (1.265)), and the geometry of the problem is shown in Fig. 16.3.

The total field in the shadow region at points near the surface $\eta = \eta_1$, such that

$$k(\eta - \eta_1) \lesssim (k\eta_1)^{\frac{1}{2}}, \quad (16.35)$$

is given by (IVANOV [1962]):

$$\begin{aligned} V^I + V^S &\sim \frac{1}{4\sqrt{\pi}k} [\xi(\xi + \eta_1)\eta_0(\eta_0 - \eta_1)]^{-\frac{1}{2}} e^{ikL} \\ &\times \int_{-\infty}^{\infty} \left[w_2(t-y) - \frac{w_2(t)}{w_1(t)} w_1(t-y) \right] e^{iD_1 t} dt, \end{aligned} \quad (16.36)$$

when inequality (16.25) holds, whereas

$$\begin{aligned} V^I + V^S &\sim \frac{1}{4\sqrt{\pi}k} (k\eta_1)^{\frac{1}{2}} [\xi(\xi + \eta_1)\eta_1^2]^{-\frac{1}{2}} \{ \exp(ikL_1 - \frac{1}{4}i\pi) \} \\ &\times \int_{-\infty}^{\infty} w_1(t-y_0) \left[w_2(t-y) - \frac{w_2(t)}{w_1(t)} w_1(t-y) \right] e^{iD_1 t} dt, \end{aligned} \quad (16.37)$$

when relation (16.30) is satisfied. The quantities L , D , L_1 , D_1 and y_0 are respectively given by eqs. (16.27), (16.28), (16.32), (16.33) and (16.34),

$$y = \frac{\eta - \eta_1}{\eta_1} (k\eta_1)^{\frac{1}{2}}, \quad (16.38)$$

w_1 and w_2 are the Airy functions in Fock's notation defined in the Introduction (see eqs. (I.265)), and the geometry of the problem is illustrated in Fig. 16.4.

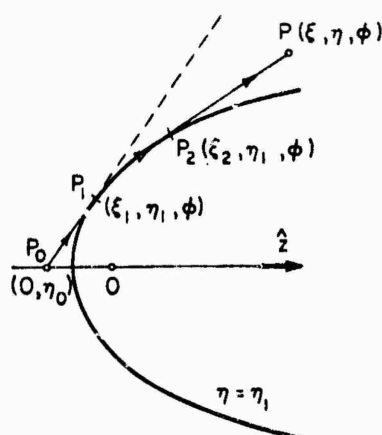


Fig. 16.4. Geometry for observation point in the shadow region, with point source on the axis of symmetry.

An expression for the total field at all points in the deep shadow region that is particularly useful for numerical purposes is the residue series (IVANOV [1962]):

$$V^i + V^s \sim A e^{ikL_2} \sum_{n=1}^{\infty} \frac{w_2(t_n)}{w_1'(t_n)} e^{iD_2 t_n}, \quad (16.39)$$

where

$$A = \frac{1}{2} \sqrt{\pi} e^{i\pi} k^{-\frac{1}{2}} (k\eta_1)^{\frac{1}{2}} [\xi(\xi + \eta_1)\eta(\eta - \eta_1)\eta_0(\eta_0 - \eta_1)]^{-\frac{1}{2}}, \quad (16.40)$$

$$L_2 = \sqrt{\{\xi(\xi + \eta_1)\}} + \sqrt{\{\eta(\eta - \eta_1)\}} + \sqrt{\{\eta_0(\eta_0 - \eta_1)\}} + \eta_1 \log \frac{\sqrt{\eta_1}(\sqrt{\xi} + \sqrt{(\xi + \eta_1)})}{(\sqrt{\eta} + \sqrt{(\eta - \eta_1)})(\sqrt{\eta_0} + \sqrt{(\eta_0 - \eta_1)})}, \quad (16.41)$$

$$\begin{aligned} D_2 &= \left(\frac{1}{2}k\right)^{\frac{1}{2}} \int_{\xi_1}^{\xi_2} [\rho_1(\tau)]^{-\frac{1}{2}} \left(1 + \frac{\tau}{\eta_1}\right)^{\frac{1}{2}} d\tau \\ &= (k\eta_1)^{\frac{1}{2}} \log \frac{\sqrt{\eta_1}(\sqrt{\xi} + \sqrt{(\xi + \eta_1)})}{(\sqrt{\eta} + \sqrt{(\eta - \eta_1)})(\sqrt{\eta_0} + \sqrt{(\eta_0 - \eta_1)})} \\ &= (k\eta_1)^{\frac{1}{2}} \log \frac{\sqrt{\xi_2} + \sqrt{(\xi_2 + \eta_1)}}{\sqrt{\xi_1} + \sqrt{(\xi_1 + \eta_1)}}, \end{aligned} \quad (16.42)$$

and t_n is the n -th root of the equation $w_1(t_n) = 0$ that has a positive imaginary part. The distance L_2 is the length of the optical ray path from P_0 to P (see Fig. 16.4):

$$L_2 = (P_0 P_1) + \widehat{P_1 P_2} + (P_2 P) \quad (16.43)$$

The coordinates of P_0 , P_1 , P_2 and P are shown in Fig. 16.4.

The result (16.39) may be rewritten as (IVANOV [1962]):

$$V^I + V^S \sim - \frac{e^{ik(P_0 P_1)}}{k(P_0 P_1)} \sqrt{\frac{2}{k(P_2 P)}} [\frac{1}{2} k^2 \rho_1(\xi_1) \rho_1(\xi_2)]^{\frac{1}{2}} \times \left(\frac{d_1}{d_2}\right)^{\frac{1}{2}} \tilde{p}(D_2) \exp \{ik[\widehat{P_1 P_2} + (P_2 P)] + \frac{1}{2} i\pi\}, \quad (16.44)$$

where d_1 and d_2 are the distances of P_1 and P_2 from the z -axis (see Fig. 16.4):

$$d_1 = 2\sqrt{\xi_1 \eta_1}, \quad d_2 = 2\sqrt{\xi_2 \eta_1}, \quad (16.45)$$

$\rho_1(\xi_1)$ and $\rho_1(\xi_2)$ are given by eq. (16.4), D_2 is given by eq. (16.42), and \tilde{p} is the reflection coefficient function defined in the Introduction (see eq. (I.278)).

16.2.2. Plane wave incidence

16.2.2.1. EXACT SOLUTIONS

For a plane wave whose direction of propagation is parallel to the $y = 0$ plane and forms the angle α with the positive z -axis, such that

$$V^I = \exp \{ik(z \cos \alpha + x \sin \alpha)\}, \quad (16.46)$$

then (BUCHHOLZ [1953]):

$$V^S = \frac{i}{\pi \sin \alpha} \sum_{n=-\infty}^{\infty} (-1)^n e^{in\phi} \int_{-\gamma_n - i\infty}^{-\gamma_n + i\infty} d\tau \Gamma(\frac{1}{2}(1+n) + \tau) \Gamma(\frac{1}{2}(1+n) - \tau) \times (\tan \frac{1}{2}\alpha)^{2\tau} \frac{m_{-\tau}^{(n)}(-2ik\eta_1)}{w_{-\tau}^{(n)}(-2ik\eta_1)} m_{\tau}^{(n)}(-2ik\xi) w_{\tau}^{(n)}(-2ik\eta), \quad (16.47)$$

where

$$|\gamma_n| < \frac{1}{2}(1 + |n|). \quad (16.48)$$

On the surface ($r = \eta_1$):

$$\frac{\partial}{\partial \eta} (V^I + V^S) \Big|_{\eta=\eta_1} = - \frac{i}{\pi \eta_1 \sin \alpha} \sum_{n=-\infty}^{\infty} (-1)^n e^{in\phi} \int_{-\gamma_n - i\infty}^{-\gamma_n + i\infty} d\tau \Gamma(\frac{1}{2}(1+n) - \tau) \times (\tan \frac{1}{2}\alpha)^{2\tau} \frac{m_{\tau}^{(n)}(-2ik\xi)}{w_{-\tau}^{(n)}(-2ik\eta_1)}. \quad (16.49)$$

Under the restriction

$$\alpha < \frac{1}{2}\pi, \quad (16.50)$$

the result of eq. (16.47) may be rewritten either as (BUCHHOLZ [1943b]):

$$V^S = -(\cos \frac{1}{2}\alpha)^{-\frac{1}{2}} \sum_{l=0}^{\infty} \sum_{n=0}^{\infty} \frac{(l+n)!}{n!} (-1)^n \varepsilon_l i^l (\tan \frac{1}{2}\alpha)^{2n+l} \times \frac{m_{n+\frac{1}{2}(1+l)}^{(l)}(2ik\eta_1)}{w_{-n-\frac{1}{2}(1+l)}^{(l)}(-2ik\eta_1)} w_{-n-\frac{1}{2}(1+l)}^{(l)}(-2ik\eta) \cos(l\phi), \quad (16.51)$$

or in the alternate form (HORTON and KARAL [1950]):

$$V^s = -(\cos \tfrac{1}{2}\alpha)^{-2} \sum_{l=0}^{\infty} \sum_{n=0}^{\infty} \frac{(-1)^n n!}{(l+n)!} e_l i^l (\tan \tfrac{1}{2}\alpha)^{2n+l} \\ \times \frac{S_n^l(2ik\eta_1)}{V_n^l(2ik\eta_1)} S_n^l(-2ik\xi) V_n^l(2ik\eta) \cos(l\phi). \quad (16.52)$$

On the surface ($\eta = \eta_1$) and for $\alpha < \frac{1}{2}\pi$:

$$\left. \frac{\partial}{\partial \eta} (V^l + V^s) \right|_{\eta=\eta_1} = -\frac{i}{\pi\eta_1} (\cos \tfrac{1}{2}\alpha)^{-2} \sum_{l=0}^{\infty} \sum_{n=0}^{\infty} (-1)^n e_l i^l (\tan \tfrac{1}{2}\alpha)^{2n+l} \\ \times \frac{S_n^l(-2ik\xi)}{V_n^l(2ik\eta_1)} \cos(l\phi). \quad (16.53)$$

In particular, for axial incidence ($\alpha = 0$), such that

$$V^l = e^{ikz}, \quad (16.54)$$

then:

$$V^s = -\frac{S_0^0(2ik\eta_1)}{V_0^0(2ik\eta_1)} S_0^0(-2ik\xi) V_0^0(2ik\eta), \quad (16.55)$$

which may be rewritten as:

$$V^s = -\frac{\frac{1}{2}\pi - \text{Si}(2k\eta) + i \text{Ci}(2k\eta)}{\frac{1}{2}\pi - \text{Si}(2k\eta_1) + i \text{Ci}(2k\eta_1)} e^{ik(\xi-\eta)}, \quad (16.56)$$

where Si and Ci are the sine and cosine integrals,

$$\text{Si}(x) = \int_0^x \frac{\sin t}{t} dt, \quad \text{Ci}(x) = -\int_x^\infty \frac{\cos t}{t} dt. \quad (16.57)$$

On the surface ($\eta = \eta_1$):

$$\left. \frac{\partial}{\partial \eta} (V^l + V^s) \right|_{\eta=\eta_1} = -\frac{i}{\pi\eta_1} \frac{S_0^0(-2ik\xi)}{V_0^0(2ik\eta_1)} \\ = \frac{\exp[ik(\xi + \eta_1) - \frac{1}{2}i\pi]}{\eta_1 [\frac{1}{2}\pi - \text{Si}(2k\eta_1) + i \text{Ci}(2k\eta_1)]}. \quad (16.58)$$

In the far field ($\xi + \eta \rightarrow \infty$) and for axial incidence (LAMB [1906], KELLER et al. [1956]):

$$V^s = -A \frac{\eta_1}{\eta} \exp\{ik(\xi + \eta - 2\eta_1)\}, \quad (16.59)$$

where

$$A = \left[-4ik\eta_1 e^{-2ik\eta_1} \int_{\sqrt{2k\eta_1}}^\infty \frac{e^{i\tau^2}}{\tau} d\tau \right]^{-1}. \quad (16.60)$$

The coefficient A is the ratio between the exact field V^s and its geometrical optics approximation $V_{g.o.}^s$:

$$A = V^s / V_{g.o.}^s. \quad (16.61)$$

The amplitude and phase of A are shown as functions of $k\eta_1$ in Fig. 16.5.

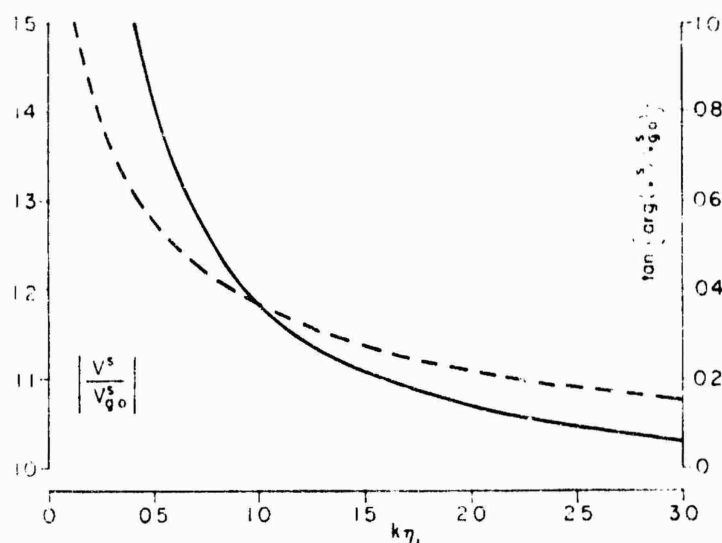


Fig. 16.5. Amplitude (—) and phase (---) of the normalized far field, for axial incidence (KELLER et al. [1956]).

16.2.2.2. HIGH FREQUENCY APPROXIMATIONS

For a plane wave whose direction of propagation is parallel to the $y = 0$ plane and forms the angle α with the positive z -axis, such that

$$V^i = \exp \{ik(z \cos \alpha + x \sin \alpha)\}, \quad (16.62)$$

the geometrical optics scattered field at a point P located in the illuminated region of the $y = 0$ plane is:

$$V_{g.o.}^s = - \left[\left(1 + \frac{2(P_1 P)}{\rho_1 \cos \psi} \right) \left(1 + \frac{2(P_1 P) \cos \psi}{\rho_2} \right) \right]^{-1} \times \exp \{ik[(P_1 P) + z_1 \cos \alpha + x_1 \sin \alpha]\}, \quad (16.63)$$

where $(P_1 P)$ is the distance between the reflection point $P_1 \equiv (x_1, 0, z_1) = (\xi_1, \eta_1, \phi_1 = 0 \text{ or } \pi)$ and the observation point $P \equiv (x, 0, z) = (\xi, \eta, \phi = 0 \text{ or } \pi)$,

$$(P_1 P) = [(x - x_1)^2 + (z - z_1)^2]^{1/2}, \quad (16.64)$$

the principal radii of curvature ρ_1 and ρ_2 at P_1 are given by eqs. (16.4) and (16.5), the reflection angle ψ is given by

$$\psi = \arccos \left\{ \frac{\sin \alpha}{\sqrt{(1 + \eta_1/\xi_1)}} + \frac{\cos \alpha}{\sqrt{(1 + \xi_1/\eta_1)}} \right\}, \quad (16.65)$$

and ξ_1 is a root of:

$$\begin{aligned} \sqrt{\xi_1} \sin \alpha + \sqrt{\eta_1} \cos \alpha = [2\sqrt{\xi_1 \xi \eta} - \sqrt{\eta_1}(\xi - \eta + \xi_1 + \eta_1)] \\ \times [4(\sqrt{\xi \eta} - \sqrt{\xi_1 \eta_1})^2 + (\xi - \eta - \xi_1 + \eta_1)^2]^{-\frac{1}{2}}. \end{aligned} \quad (16.66)$$

Formula (16.63) is applicable if $k\rho_1 \gg 1$ and $k\rho_2 \gg 1$. In the shadow region, $V_{g.o.} = 0$. In particular, for back scattering ($\psi = 0$):

$$V_{g.o.}^{b.s.} = - \sqrt{\frac{\rho_1 \rho_2}{[\rho_1 + 2(P_1 P)][\rho_2 + 2(P_1 P)]}} \exp \{ik[(P_1 P) + z_1 \cos \alpha + x_1 \sin \alpha]\}. \quad (16.67)$$

The geometrical optics back scattering cross section is:

$$\sigma_{g.o.} = 4\pi(\xi_1 + \eta_1)^2. \quad (16.68)$$

For a plane wave at axial incidence ($\alpha = 0$), such that

$$V^i = e^{ikz}, \quad (16.69)$$

the scattered field is given by the Luneburg-Kline expansion (KELLER et al. [1956]):

$$V^s \sim \exp \{ik[(OP) - 2\eta_1]\} \sum_{n=0}^{\infty} (ik\eta_1)^{-n} \sum_{j=0}^{\infty} a_{jn} \left[\frac{2\eta_1}{(OP)(1 - \cos \theta)} \right]^{j+1}, \quad (16.70)$$

where (OP) is the distance between the focus O and the observation point P (see Fig. 16.6),

$$(OP) = (OP_1) + (P_1 P) = \xi_1 + \eta_1 + (P_1 P) = \frac{2\eta_1}{1 - \cos \theta} + (P_1 P) = \xi + \eta, \quad (16.71)$$

θ is the angle that the reflected ray $P_1 P$ forms with the positive z -axis, and

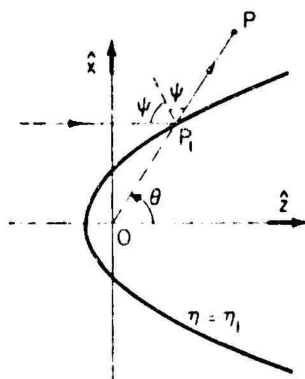


Fig. 16.6. Geometry for reflected field at axial incidence.

$$a_{jn} = \frac{1}{2} j a_{j-1, n-1}, \quad (j \geq 1, n \geq 1), \quad (16.72)$$

$$a_{0n} = - \sum_{j=1}^n a_{jn}, \quad (n \geq 1), \quad (16.73)$$

$$a_{00} = -1. \quad (16.74)$$

The first few terms of the expansion (16.70) are:

$$V^s \sim - \frac{2\eta_1}{(OP)(1-\cos\theta)} \exp\{ik[(OP)-2\eta_1]\} \left\{ 1 + \frac{i}{2k\eta_1} \left[1 - \frac{2\eta_1}{(OP)(1-\cos\theta)} \right] + \dots \right\}. \quad (16.75)$$

For $\alpha = 0$, result (16.63) is equal to the leading term of eq. (16.75). The amplitude and phase of a normalized quantity obtained by retaining the first three terms (through $n = 2$) in the infinite series (16.70) are shown in Fig. 16.7, when the observation point is in the far field ($(OP) \rightarrow \infty$).

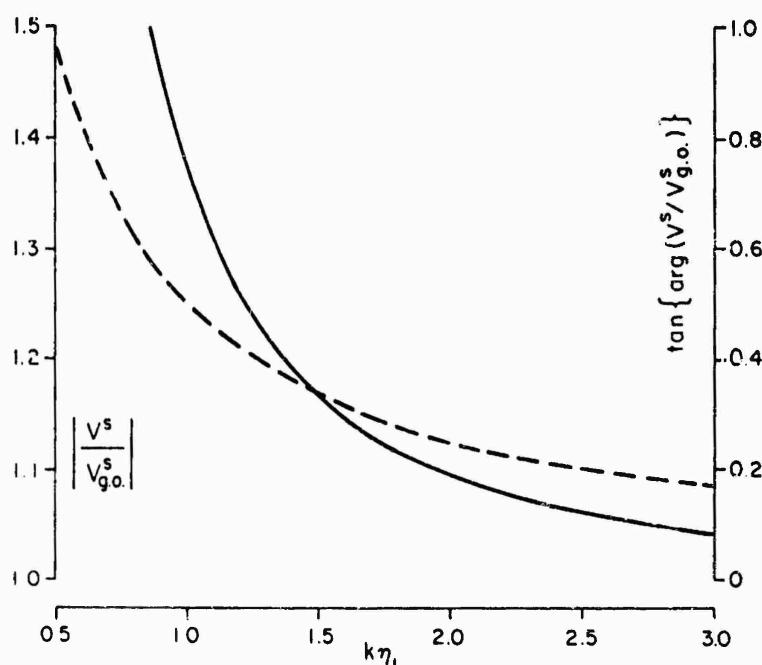


Fig. 16.7. Amplitude (—) and phase (---) of the normalized far field, through $O[(k\eta_1)^{-2}]$ (KELLER et al. [1956]).

16.3. Acoustically hard convex paraboloid

16.3.1. Point sources

16.3.1.1. EXACT SOLUTIONS

The Green function for a point source located between two coaxial and confocal paraboloids has been given by BUCHHOLZ [1953; Section 18.2].

For a point source at $(\xi_0, \eta_0 \geq \eta_1, \phi_0)$, such that

$$V^i = \frac{e^{ikR}}{kR}, \quad (16.76)$$

then

$$\begin{aligned}
 V^i + V^s = & -\frac{1}{\pi} \sum_{n=-\infty}^{\infty} e^{in(\phi-\phi_0)} \int_{-\gamma_n-i\infty}^{-\gamma_n+i\infty} d\tau \Gamma\left(\frac{1}{2}(1+n)+\tau\right) \Gamma\left(\frac{1}{2}(1+n)-\tau\right) \\
 & \times m_{\tau}^{(n)}(-2ik\xi_<) w_{\tau}^{(n)}(-2ik\xi_>) \\
 & \times \left[m_{-\tau}^{(n)}(-2ik\eta_<) - \frac{m_{-\tau}^{(n)'}(-2ik\eta_1)}{w_{-\tau}^{(n)'}(-2ik\eta_1)} w_{-\tau}^{(n)}(-2ik\eta_<) \right] w_{-\tau}^{(n)}(-2ik\eta_>), \quad (16.77)
 \end{aligned}$$

where

$$|\gamma_n| < \frac{1}{2}(1+|n|). \quad (16.78)$$

On the surface ($\eta = \eta_1$):

$$\begin{aligned}
 (V^i + V^s)_{\eta=\eta_1} = & \frac{1}{\pi\eta_1} \sum_{n=-\infty}^{\infty} e^{in(\phi-\phi_0)} \int_{-\gamma_n-i\infty}^{-\gamma_n+i\infty} d\tau \Gamma\left(\frac{1}{2}(1+n)-\tau\right) \\
 & \times m_{\tau}^{(n)}(-2ik\xi_<) w_{\tau}^{(n)}(-2ik\xi_>) \frac{w_{-\tau}^{(n)}(-2ik\eta_0)}{(\partial/\partial\eta_1)w_{-\tau}^{(n)}(-2ik\eta_1)}. \quad (16.79)
 \end{aligned}$$

In particular, if the source is on the z -axis ($\xi_0 = 0$):

$$\begin{aligned}
 V^i + V^s = & -\int_{-\gamma_0-i\infty}^{-\gamma_0+i\infty} w_{\tau}^{(0)}(-2ik\xi) \left[m_{-\tau}^{(0)}(-2ik\eta_<) - \right. \\
 & \left. - \frac{m_{-\tau}^{(0)'}(-2ik\eta_1)}{w_{-\tau}^{(0)'}(-2ik\eta_1)} w_{-\tau}^{(0)}(-2ik\eta_<) \right] w_{-\tau}^{(0)}(-2ik\eta_>) \frac{d\tau}{\cos(\pi\tau)}, \quad (16.80)
 \end{aligned}$$

with

$$|\gamma_0| < \frac{1}{2}, \quad (16.81)$$

and on the surface ($\eta = \eta_1$):

$$(V^i + V^s)_{\eta=\eta_1} = \frac{1}{\pi\eta_1} \int_{-\gamma_0-i\infty}^{-\gamma_0+i\infty} d\tau \Gamma\left(\frac{1}{2}-\tau\right) w_{\tau}^{(0)}(-2ik\xi) \frac{w_{-\tau}^{(0)}(-2ik\eta_0)}{(\partial/\partial\eta_1)w_{-\tau}^{(0)}(-2ik\eta_1)}. \quad (16.82)$$

16.3.1.2. HIGH FREQUENCY APPROXIMATIONS

For a point source at $P_0 \equiv (\xi_0, \eta_0 \geq \eta_1, \phi_0 = 0)$, such that

$$V^i = \frac{e^{ikR}}{kR}, \quad (16.83)$$

the geometrical optics scattered field at a point P located in the illuminated region of the $y = 0$ plane is:

$$\begin{aligned}
 V_{\text{g.o.}}^s = & \frac{\exp\{ik[(P_0 P_1) + (P_1 P)]\}}{k(P_0 P_1)} \left[\left(1 + \frac{(P_1 P)}{(P_0 P_1)} + \frac{2(P_1 P)}{\rho_1 \cos \psi} \right) \right. \\
 & \left. \times \left(1 + \frac{(P_1 P)}{(P_0 P_1)} + \frac{2(P_1 P) \cos \psi}{\rho_2} \right) \right]^{-1}, \quad (16.84)
 \end{aligned}$$

where $(P_0 P_1)$ and $(P_1 P)$ are respectively the distances between the source P_0 and the reflection point $P_1 \equiv (x_1, 0, z_1) = (\xi_1, \eta_1, \phi_1 = 0 \text{ or } \pi)$, and between P_1 and the observation point $P \equiv (x, 0, z) = (\xi, \eta, \phi = 0 \text{ or } \pi)$ (see Fig. 16.2); the principal radii of curvature ρ_1 and ρ_2 , the reflection angle ψ and the coordinate ξ_1 are given by eqs. (16.4), (16.5), (16.20) and (16.21), respectively. Formula (16.84) is applicable if $k\rho_{1,2} \gg 1$. In the shadow region, $V_{\text{g.o.}} = 0$.

For a point source on the axis of symmetry, an asymptotic analysis of the exact results of eqs. (16.80) and (16.82) has been performed by KLANTE [1959] and by IVANOV [1962].

For a point source of strength given by eq. (16.83) and located on the z -axis ($\xi_0 = 0$), and for an observation point $P \equiv (\xi, \eta_1, \phi)$ located in the illuminated region ($\xi < \eta_0 - \eta_1$) of the surface $\eta = \eta_1$,

$$\{(V^i + V^s)_{\eta=\eta_1}\}_{\text{g.o.}} = 2 \frac{\exp\{ik(P_0 P_1)\}}{k(P_0 P_1)}; \quad (16.85)$$

this result is the leading term in the high frequency expansion of (16.82), provided that P is not too close to the shadow boundary, i.e. that (IVANOV [1962]):

$$\cos \psi \gg (k\rho_1)^{-\frac{1}{2}} = [2k\eta_1^{-\frac{1}{2}}(\xi + \eta_1)^{\frac{1}{2}}]^{-\frac{1}{2}}, \quad (16.86)$$

where the angle of incidence ψ is given by eq. (16.23), and ρ_1 is the principal radius of curvature given by eq. (16.4).

On the surface $\eta = \eta_1$, in the shadow region, and for a source located at a sufficiently large distance from the nose of the paraboloid, such that

$$k(\eta_0 - \eta_1) \gg (k\eta_1)^{\frac{1}{2}}, \quad (16.87)$$

then (IVANOV [1962]):

$$(V^i + V^s)_{\eta=\eta_1} \sim \frac{1}{2} k^{-\frac{1}{2}} [\xi(\xi + \eta_1)\eta_0(\eta_0 - \eta_1)]^{-\frac{1}{2}} g(D) e^{ikL}, \quad (16.88)$$

where L and D are given by eqs. (16.27) and (16.28), and $g(D)$ is the Fock function defined in the Introduction (see eq. (I.268)). The geometrical interpretation of L is given in eq. (16.29) (see also Fig. 16.3).

On the surface $\eta = \eta_1$, in the shadow region, and for a source located near the nose of the paraboloid, such that

$$k(\eta_0 - \eta_1) \lesssim (k\eta_1)^{\frac{1}{2}}, \quad (16.89)$$

then (IVANOV [1962]):

$$(V^i + V^s)_{\eta=\eta_1} \sim \frac{1}{2} k^{-\frac{1}{2}} (k\eta_1)^{\frac{1}{2}} [\xi(\xi + \eta_1)\eta_1^2]^{-\frac{1}{2}} \{\exp(ikL_1 - \frac{1}{2}i\pi)\} \\ \times \frac{1}{\sqrt{\pi}} \int_{-\infty}^{\infty} \frac{w_1(t - y_0)}{w_1'(t)} e^{iD_1 t} dt, \quad (16.90)$$

where L_1 , D_1 and y_0 are given by eqs. (16.32) through (16.34), $w_1(t)$ is the Airy function in Fock's notation defined in the Introduction (see eqs. (I.26.6)), and the geometry of the problem is shown in Fig. 16.3.

The total field in the shadow region at points near the surface $\eta = \eta_1$, such that

$$k(\eta - \eta_1) \lesssim (k\eta_1)^{\frac{1}{2}}, \quad (16.91)$$

is given by (IVANOV [1962]):

$$V^i + V^s \sim \frac{i}{4\sqrt{\pi k}} [\xi(\xi + \eta_1)\eta_0(\eta_0 - \eta_1)]^{-\frac{1}{2}} e^{ikL} \\ \times \int_{-\infty}^{\infty} \left[w_2(t-y) - \frac{w'_2(t)}{w'_1(t)} w_1(t-y) \right] e^{iD_1 t} dt, \quad (16.92)$$

when

$$k(\eta_0 - \eta_1) \gg (k\eta_1)^{\frac{1}{2}}, \quad (16.93)$$

whereas

$$V^i + V^s \sim \frac{i}{4\sqrt{\pi k}} (k\eta_1)^{\frac{1}{2}} [\xi(\xi + \eta_1)\eta_1^2]^{-\frac{1}{2}} \{ \exp(ikL_1 - \frac{1}{4}i\pi) \\ \times \int_{-\infty}^{\infty} w_1(t-y_0) \left[w_2(t-y) - \frac{w'_2(t)}{w'_1(t)} w_1(t-y) \right] e^{iD_1 t} dt, \quad (16.94)$$

when

$$k(\eta_0 - \eta_1) \lesssim (k\eta_1)^{\frac{1}{2}}. \quad (16.95)$$

The quantities L , D , L_1 , D_1 , y_0 and y are respectively given by eqs. (16.27), (16.28), (16.32), (16.33), (16.34) and (16.38); w_1 and w_2 are the Airy functions in Fock's notation defined in the Introduction (see eqs. (I.265)), and the geometry of the problem is illustrated in Fig. 16.4.

An expression for the total field at all points in the deep shadow region that is particularly useful for numerical purposes is the residue series (IVANOV [1962]):

$$V^i + V^s \sim A e^{ikL_2} \sum_{n=1}^{\infty} \frac{w'_2(\bar{i}_n)}{\bar{i}_n w_1(\bar{i}_n)} e^{iD_2 \bar{i}_n}, \quad (16.96)$$

where A , L_2 and D_2 are given by eqs. (16.40) through (16.42), and \bar{i}_n is the n -th root of the equation $w'_1(\bar{i}_n) = 0$ that has a positive imaginary part. The geometrical interpretation of L_2 is given by eq. (16.43) (see also Fig. 16.4).

The result (16.96) may be rewritten as (IVANOV [1962]):

$$V^i + V^s \sim - \frac{\exp\{ik(P_0 P_1)\}}{k(P_0 P_1)} \sqrt{\frac{2}{k(P_2 P)}} [k^2 \rho_1(\xi_1) \rho_1(\xi_2)]^{\frac{1}{2}} \\ \times \left(\frac{d_1}{d_2} \right)^{\frac{1}{2}} \tilde{q}(D_2) \exp\{ik[\widehat{P_1 P_2} + (P_2 P)] + \frac{1}{4}i\pi\}, \quad (16.97)$$

where $\rho_1(\xi_1)$ and $\rho_1(\xi_2)$ are given by eq. (16.4), d_1 and d_2 by eqs. (16.45), D_2 by eq. (16.42), \tilde{q} is the reflection coefficient function defined in the Introduction (see eq. (I.279)), and the geometry of the problem is shown in Fig. 16.4.

16.3.2. Plane wave incidence

16.3.2.1. EXACT SOLUTIONS

For a plane wave whose direction of propagation is parallel to the $y = 0$ plane and forms the angle α with the positive z -axis, such that

$$V^i = \exp \{ik(z \cos \alpha + x \sin \alpha)\}, \quad (16.98)$$

then (BUCHHOLZ [1953]):

$$V^s = \frac{i}{\pi \sin \alpha} \sum_{n=-\infty}^{\infty} (-1)^n e^{in\phi} \int_{-\gamma_n-1\infty}^{-\gamma_n+1\infty} d\tau \Gamma(\tfrac{1}{2}(1+n)+\tau) \Gamma(\tfrac{1}{2}(1+n)-\tau) \\ \times (\tan \tfrac{1}{2}\alpha)^{2\tau} \frac{m_{-\tau}^{(n)}(-2ik\eta_1)}{w_{-\tau}^{(n)}(-2ik\eta_1)} m_{\tau}^{(n)}(-2ik\xi) w_{\tau}^{(n)}(-2ik\eta), \quad (16.99)$$

where

$$|\gamma_n| = \tfrac{1}{2}(1+|n|). \quad (16.100)$$

On the surface ($\eta = \eta_1$):

$$(V^i + V^s)_{\eta=\eta_1} = \frac{i}{\pi \eta_1 \sin \alpha} \sum_{n=-\infty}^{\infty} (-1)^n e^{in\phi} \int_{-\gamma_n-1\infty}^{-\gamma_n+1\infty} d\tau \Gamma(\tfrac{1}{2}(1+n)-\tau) \\ \times (\tan \tfrac{1}{2}\alpha)^{2\tau} \frac{m_{\tau}^{(n)}(-2ik\xi)}{(\partial/\partial\eta_1)w_{\tau}^{(n)}(-2ik\eta_1)}. \quad (16.101)$$

Under the restriction

$$\alpha < \tfrac{1}{2}\pi, \quad (16.102)$$

the result of eq. (16.99) may be rewritten either as (BUCHHOLZ [1943b]):

$$V^s = (\cos \tfrac{1}{2}\alpha)^{-2} \sum_{l=0}^{\infty} \sum_{n=0}^{\infty} \frac{(l+n)!}{n!} (-1)^n \varepsilon_l i^l (\tan \tfrac{1}{2}\alpha)^{2n+l} \\ \times \frac{m_{n+\frac{1}{2}(1+l)}^{(l)}(2ik\eta_1)}{w_{-n-\frac{1}{2}(1+l)}^{(l)}(-2ik\eta_1)} w_{-n-\frac{1}{2}(1+l)}^{(l)}(-2ik\eta) \cos(l\phi), \quad (16.103)$$

or in the alternate form (HORTON and KARAL [1950]):

$$V^s = -(\cos \tfrac{1}{2}\alpha)^{-2} \sum_{l=0}^{\infty} \sum_{n=0}^{\infty} \frac{(-1)^n n!}{(l+n)!} \varepsilon_l i^l (\tan \tfrac{1}{2}\alpha)^{2n+l} \\ \times \frac{S_n^{(l)}(2ik\eta_1)}{V_n^{(l)}(2ik\eta_1)} S_n^{(l)}(-2ik\xi) V_n^{(l)}(2ik\eta) \cos(l\phi). \quad (16.104)$$

On the surface ($\eta = \eta_1$) and for $\alpha < \tfrac{1}{2}\pi$:

$$(V^i + V^s)_{\eta=\eta_1} = \frac{i}{\pi \eta_1} (\cos \tfrac{1}{2}\alpha)^{-2} \sum_{l=0}^{\infty} \sum_{n=0}^{\infty} (-1)^n \varepsilon_l i^l (\tan \tfrac{1}{2}\alpha)^{2n+l} \frac{S_n^{(l)}(-2ik\xi)}{(\partial/\partial\eta_1)V_n^{(l)}(2ik\eta_1)} \cos(l\phi). \quad (16.105)$$

For $k\eta_1 = 0.25$ and $\alpha = 36.9^\circ$, HORTON [1953] has plotted the amplitude and phase of expression (16.105) as a function of $k\xi$ for $0 \leq k\xi \leq 1$ and $\phi = 0, \frac{1}{2}\pi, \pi, \frac{3}{2}\pi$. Starting from eq. (16.104), HORTON [1953] has developed some considerations on the far field; in particular, he has proved that as $\eta \rightarrow \infty$, the scattered field on the z -axis ($\xi = 0$) depends only on the mode $l = n = 0$.

In particular, for axial incidence ($\alpha = 0$), such that

$$V^i = e^{ikz}, \quad (16.106)$$

then

$$V^s = - \frac{S_0^0(2ik\eta_1)}{V_0^0(2ik\eta_1)} S_0^0(-2ik\xi) V_0^0(2ik\eta), \quad (16.107)$$

which may be rewritten either as:

$$V^s = \frac{\frac{1}{2}\pi - \text{Si}(2k\eta) + i \text{Ci}(2k\eta)}{\exp(2ik\eta_1)/k\eta_1 - [\frac{1}{2}\pi - \text{Si}(2k\eta_1) + i \text{Ci}(2k\eta_1)]} e^{ik(\xi - \eta)}, \quad (16.108)$$

or in the form (SCHLESSTED [1955]):

$$V^s = \frac{\frac{1}{2}\pi - \text{Si}(kQ) + i \text{Ci}(kQ)}{\exp(2ik\eta_1)/k\eta_1 - [\frac{1}{2}\pi - \text{Si}(2k\eta_1) + i \text{Ci}(2k\eta_1)]} e^{ik(\xi + \eta - Q)}, \quad (16.109)$$

where

$$Q = 2\eta_1 \frac{\xi + \eta}{\xi_1 + \eta_1}, \quad (16.110)$$

Si and Ci are the sine and cosine integrals of eqs. (16.57), and ξ_1 is the coordinate of the point $P_1 \equiv (\xi_1, \eta_1, \phi_1 = \phi)$ at which the straight line from the focus to the observation point intersects the paraboloid (see Fig. 16.6), and is a root of:

$$2 \left(\frac{\xi_1 \xi \eta}{\eta_1} \right)^{\frac{1}{2}} - \xi + \eta - \xi_1 - \eta_1 = [4(\sqrt{\xi \eta} - \sqrt{\xi_1 \eta_1})^2 + (\xi - \eta - \xi_1 + \eta_1)^2]^{\frac{1}{2}}. \quad (16.111)$$

On the surface ($\eta = \eta_1$):

$$\begin{aligned} (V^i + V^s)_{\eta = \eta_1} &= \frac{i}{\pi \eta_1} \frac{S_0^0(-2ik\xi)}{(\partial/\partial \eta_1) V_0^0(2ik\eta_1)} \\ &= \frac{\exp\{ik(\xi + \eta_1)\}}{\exp\{2ik\eta_1\} - k\eta_1 [\frac{1}{2}\pi - \text{Si}(2k\eta_1) + i \text{Ci}(2k\eta_1)]} \end{aligned} \quad (16.112)$$

and, in particular, at the nose of the scatterer:

$$|V^i + V^s|_{\xi=0, \eta=\eta_1} = \frac{1}{\pi \eta_1} \frac{\partial}{\partial \eta_1} V_0^0(2ik\eta_1)^{-1}. \quad (16.113)$$

The quantity (16.113) is plotted as a function of $k\eta_1$ for $0 \leq k\eta_1 \leq 4$ in Fig. 16.8, and

is compared with the corresponding quantity for a hard sphere of radius $2\eta_1$, equal to the radius of curvature of the paraboloid at the nose.

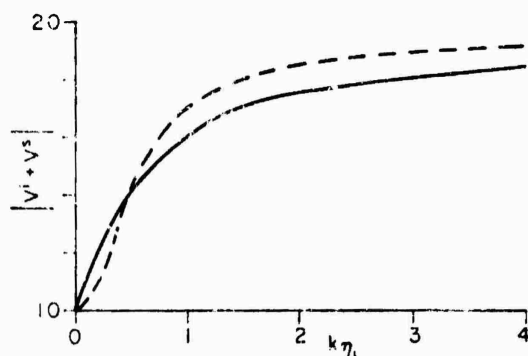


Fig. 16.8. Amplitude of surface field at the nose ($\xi = 0$, $\eta = \eta_1$) for the paraboloid (—), and for the tangent sphere of radius $2\eta_1$ (---) (HORTON and KARAL [1950]).

In the far field ($\xi + \eta \rightarrow \infty$) and for axial incidence (LAMB [1906]; KELLER et al. [1956]):

$$V^s = B \frac{\eta_1}{\eta} \exp \{ik(\xi + \eta - 2\eta_1)\}, \quad (16.114)$$

where

$$B = \left[2 + 4ik\eta_1 e^{-2ik\eta_1} \int_{\sqrt{2k\eta_1}}^{\infty} \frac{e^{i\tau^2}}{\tau} d\tau \right]^{-1}. \quad (16.115)$$

The coefficient B is the ratio between the exact field V^s and its geometrical optics approximation $V_{g.o.}^s$:

$$B = V^s / V_{g.o.}^s. \quad (16.116)$$

The amplitude and phase of B are shown as functions of $k\eta_1$ in Fig. 16.9.

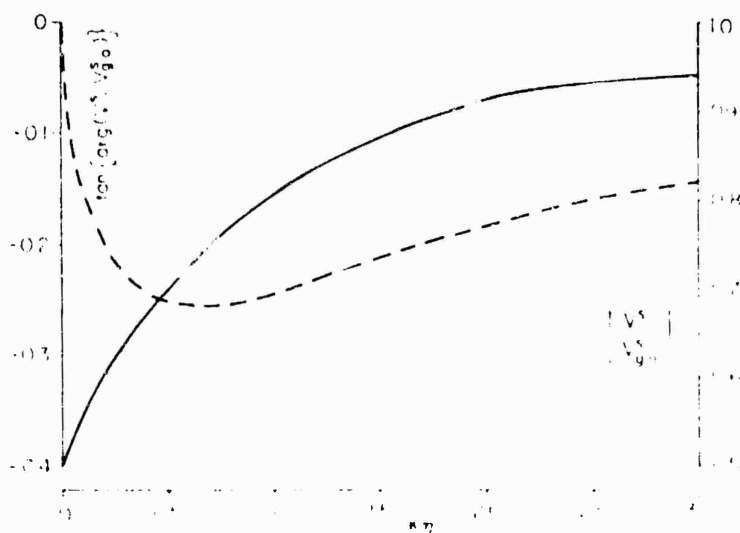


Fig. 16.9. Amplitude (—) and phase (---) of the normalized far field for axial incidence (KELLER et al. [1956]).

For axial incidence, the bistatic scattering cross section as derived from eq. (16.109) is (SCHENSTED [1955]):

$$\begin{aligned}\sigma(\theta) &= 4\pi(\xi_1 + \eta_1)^2 C \\ &= 4\pi\eta_1^2 (\sin \frac{1}{2}\theta)^{-4} C,\end{aligned}\quad (16.117)$$

where:

$$\begin{aligned}C &= \frac{1}{4}\{1 + (k\eta_1)^2 [\{\text{Si}(2k\eta_1) - \frac{1}{2}\pi\}^2 + \{\text{Ci}(2k\eta_1)\}^2] + \\ &\quad + 2k\eta_1 [\{\text{Si}(2k\eta_1) - \frac{1}{2}\pi\} \cos(2k\eta_1) - \text{Ci}(2k\eta_1) \sin(2k\eta_1)]\}^{-1},\end{aligned}\quad (16.118)$$

and

$$\theta = \arccos \frac{\xi - \eta}{\xi + \eta} \quad (16.119)$$

is the angle that the line from the focus to the observation point forms with the positive z -axis. In particular, the back scattering cross section ($\theta = \pi$) is:

$$\sigma = 4\pi\eta_1^2 C. \quad (16.120)$$

The quantity C is the ratio between the back scattering cross section and its geometrical optics approximation; it varies monotonically from 0.25 for $k\eta_1 = 0.5$ to unity for $k\eta_1 = \infty$.

16.3.2.2. HIGH FREQUENCY APPROXIMATIONS

For a plane wave whose direction of propagation is parallel to the $y = 0$ plane and forms the angle α with the positive z -axis such that

$$V^i = \exp \{ik(z \cos \alpha + x \sin \alpha)\}, \quad (16.121)$$

the geometrical optics scattered field at a point P located in the illuminated region of the $y = 0$ plane is:

$$V_{g.o.}^s = \left[\left(1 + \frac{2(P_1 P)}{\rho_1 \cos \psi} \right) \left(1 + \frac{2(P_1 P) \cos \psi}{\rho_2} \right) \right]^{-\frac{1}{2}} \exp \{ik[(P_1 P) + z \cos \alpha + x \sin \alpha]\}, \quad (16.122)$$

where the distance $(P_1 P)$ between the reflection point $P_1 \equiv (x_1, 0, z_1) = (\xi_1, \eta_1, \phi_1 = 0 \text{ or } \pi)$ and the observation point $P \equiv (x, 0, z) = (\xi, \eta, \phi = 0 \text{ or } \pi)$, the principal radii of curvature ρ_1 and ρ_2 at P_1 , the reflection angle ψ and the coordinate ξ_1 are given by eqs. (16.64) through (16.67), and by eqs. (16.4) and (16.5) with $\xi = \xi_1$. Formula (16.122) is applicable if $k\rho_1 \gg 1$ and $k\rho_2 \gg 1$. In the shadow region, $V_{g.o.}^s = 0$. In particular, for back scattering ($\psi = 0$):

$$V_{g.o.}^{b.s.} = \sqrt{\frac{\rho_1 \rho_2}{[\rho_1 + 2(P_1 P)][\rho_2 + 2(P_1 P)]}} \exp \{ik[(P_1 P) + z \cos \alpha + x \sin \alpha]\}. \quad (16.123)$$

The geometrical optics back scattering cross section is:

$$\sigma_{g.o.} = 4\pi(\xi_1 + \eta_1)^2. \quad (16.124)$$

For a plane wave at axial incidence ($\alpha = 0$), such that

$$V^i = e^{ikz}, \quad (16.125)$$

the scattered field is given by the Luneburg-Kline expansion (KELLER et al. [1956]):

$$V^s \sim \exp \{ ik[(OP) - 2\eta_1] \} \sum_{n=0}^{\infty} (ik\eta_1)^{-n} \sum_{j=0}^n a_{jn} \left[\frac{2\eta_1}{(OP)(1 - \cos \theta)} \right]^{j+1}, \quad (16.126)$$

where the distance (OP) between the focus O and the observation point P is given by eq. (16.71), the angle θ that the reflected ray P_1P forms with the positive z -axis is shown in Fig. 16.6, and

$$a_{jn} = \frac{1}{2} j a_{j-1, n-1}, \quad (j \geq 1, n \geq 1), \quad (16.127)$$

$$a_{0n} = \sum_{j=1}^n a_{jn}, \quad (n \geq 1), \quad (16.128)$$

$$a_{00} = 1. \quad (16.129)$$

The first few terms of the expansion (16.126) are:

$$V^s \sim \frac{2\eta_1}{(OP)(1 - \cos \theta)} \exp \{ ik[(OP) - 2\eta_1] \} \left\{ 1 - \frac{i}{2k\eta_1} \left[1 + \frac{2\eta_1}{(OP)(1 - \cos \theta)} \right] + \dots \right\}. \quad (16.130)$$

For $\alpha = 0$, result (16.122) is equal to the leading term of eq. (16.130). The amplitude and phase of a normalized quantity obtained by retaining the first three terms (through $n = 2$) in the infinite series (16.126) are shown in Fig. 16.10, when the observation point is in the far field ((OP) $\rightarrow \infty$).

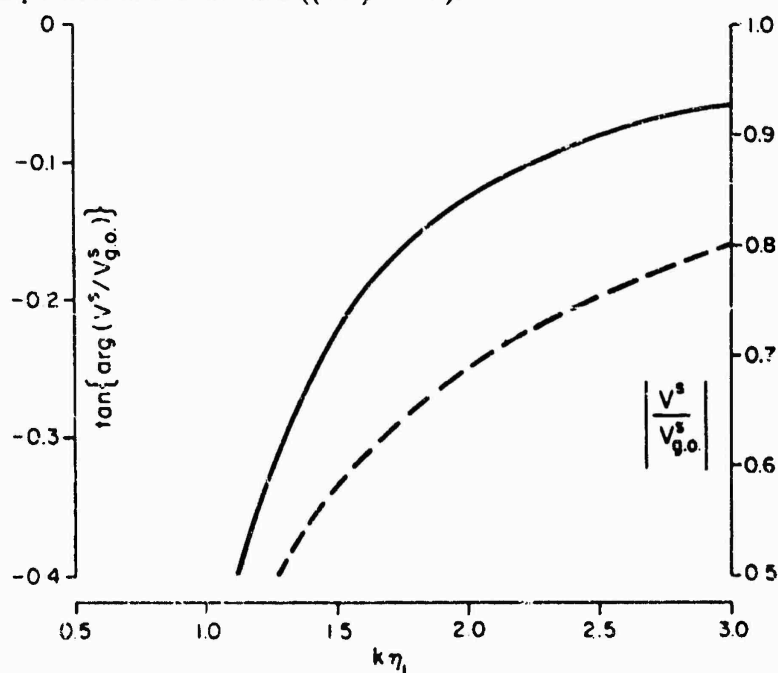


Fig. 16.10. Amplitude (—) and phase (---) of the normalized far field, through O[($k\eta_1$) $^{-1}$] (KELLER et al. [1956]).

16.4. Perfectly conducting convex paraboloid

16.4.1. Dipole sources

Results are available only in the case of an electric dipole located on the z -axis. For an electric dipole at $(\xi_0 = 0, \eta_0 \geq \eta_1)$ with moment $(4\pi\epsilon/k)\hat{z}$, corresponding to an incident electric Hertz vector $\{\exp(ikR)/kR\}\hat{z}$, the components of the total field are (BUCHHOLZ [1948]):

$$E_z = \frac{iZ}{k} \sqrt{\frac{\eta}{\xi + \eta}} \left(\frac{1}{2\eta} + \frac{\partial}{\partial \eta} \right) H_\phi, \quad (16.131)$$

$$E_\eta = -\frac{iZ}{k} \sqrt{\frac{\xi}{\xi + \eta}} \left(\frac{1}{2\xi} + \frac{\partial}{\partial \xi} \right) H_\phi, \quad (16.132)$$

$$E_\phi = H_z = H_\eta = 0, \quad (16.133)$$

$$H_\phi = \frac{Y}{2\eta_0 \sqrt{\xi \eta_1}} \int_{-\gamma - ix}^{-\gamma + ix} d\tau \frac{\tau}{\sin(\pi\tau)} \left[M_{\tau, \frac{1}{2}}(-2ik\eta_-) - \frac{M'_{\tau, \frac{1}{2}}(-2ik\eta_1)}{W'_{\tau, \frac{1}{2}}(-2ik\eta_1)} W_{\tau, \frac{1}{2}}(-2ik\eta_-) \right] W_{-\tau, \frac{1}{2}}(-2ik\xi) W_{\tau, \frac{1}{2}}(-2ik\eta_+), \quad (16.134)$$

where

$$|\gamma| < 1. \quad (16.135)$$

On the surface $(\eta = \eta_1)$:

$$H_\phi = \frac{ikY}{2\eta_0 \sqrt{\xi \eta_1}} \int_{-\gamma - ix}^{-\gamma + ix} d\tau \frac{\tau}{\Gamma(1-\tau) \sin(\pi\tau)} W_{-\tau, \frac{1}{2}}(-2ik\xi) \frac{W_{\tau, \frac{1}{2}}(-2ik\eta_0)}{(\partial/\partial \eta_1) W_{\tau, \frac{1}{2}}(-2ik\eta_1)}. \quad (16.136)$$

The surface field produced by an electric dipole located on the z -axis and parallel to the x -axis has been derived by KORBANSKIY [1968].

16.4.2. Plane wave incidence

16.4.2.1. EXACT SOLUTIONS

For a plane wave whose direction of propagation is parallel to the $y = 0$ plane and forms the angle α with the positive z -axis, and whose magnetic field vector is parallel to the x -axis, such that

$$\begin{aligned} E^i &= (\hat{x} \cos \alpha - \hat{z} \sin \alpha) \exp \{ik(z \cos \alpha + x \sin \alpha)\}, \\ H^i &= Y \hat{y} \exp \{ik(z \cos \alpha + x \sin \alpha)\}, \end{aligned} \quad (16.137)$$

the components of the incident, scattered and total fields may be expanded in Fourier series (FOCK [1957]; FOCK and FEDOROV [1958]; see also FOCK [1965], chapters 3 and 4); thus, for the total field:

$$\begin{aligned}
E_{\xi} &= \frac{1}{2}E_{\xi}^{(0)} + \sum_{n=1}^{\infty} E_{\xi}^{(n)} \cos(n\phi), \\
E_{\eta} &= \frac{1}{2}E_{\eta}^{(0)} + \sum_{n=1}^{\infty} E_{\eta}^{(n)} \cos(n\phi), \\
E_{\phi} &= \sum_{n=1}^{\infty} E_{\phi}^{(n)} \sin(n\phi), \\
H_{\xi} &= \sum_{n=1}^{\infty} H_{\xi}^{(n)} \sin(n\phi), \\
H_{\eta} &= \sum_{n=1}^{\infty} H_{\eta}^{(n)} \sin(n\phi), \\
H_{\phi} &= \frac{1}{2}H_{\phi}^{(0)} + \sum_{n=1}^{\infty} H_{\phi}^{(n)} \cos(n\phi),
\end{aligned} \tag{16.138}$$

where

$$E_{\xi}^{(n)} = \frac{(4k^2\xi\eta)^{\frac{1}{2}n}}{2\sqrt{\{\xi(\xi+\eta)\}}} \left[\frac{1}{k} \frac{\partial C_{n-1}}{\partial r} - nF_n \right], \tag{16.139}$$

$$E_{\eta}^{(n)} = \frac{-(4k^2\xi\eta)^{\frac{1}{2}n}}{2\sqrt{\{\eta(\xi+\eta)\}}} \left[\frac{1}{k} \frac{\partial C_{n-1}}{\partial \xi} + nF_n \right], \tag{16.140}$$

$$E_{\phi}^{(n)} = \frac{(4k^2\xi\eta)^{\frac{1}{2}n}}{2\sqrt{\xi\eta}} (D_{n-1} - nF_n), \tag{16.141}$$

$$H_{\xi}^{(n)} = Y \frac{(4k^2\xi\eta)^{\frac{1}{2}n}}{2i\sqrt{\{\xi(\xi+\eta)\}}} \left[\frac{1}{k} \frac{\partial D_{n-1}}{\partial \eta} - nG_n \right], \tag{16.142}$$

$$H_{\eta}^{(n)} = -Y \frac{(4k^2\xi\eta)^{\frac{1}{2}n}}{2i\sqrt{\{\eta(\xi+\eta)\}}} \left[\frac{1}{k} \frac{\partial D_{n-1}}{\partial \xi} + nG_n \right], \tag{16.143}$$

$$H_{\phi}^{(n)} = Y \frac{(4k^2\xi\eta)^{\frac{1}{2}n}}{2i\sqrt{\xi\eta}} (C_{n-1} + nG_n), \tag{16.144}$$

with

$$C_{n-1} = \tilde{P}_{n-1} - \frac{1}{2}nQ_{n-1}, \tag{16.145}$$

$$D_{n-1} = \tilde{Q}_{n-1} + \frac{1}{2}nP_{n-1}, \tag{16.146}$$

$$F_n = \frac{1}{4} \left(1 + k^{-2} \frac{\partial^2}{\partial \xi \partial \eta} \right) P_{n-1} + \frac{1}{4k} \left(\frac{\partial}{\partial \xi} - \frac{\partial}{\partial \eta} \right) Q_{n-1}, \tag{16.147}$$

$$G_n = \frac{1}{4} \left(1 + k^{-2} \frac{\partial^2}{\partial \xi \partial \eta} \right) Q_{n-1} - \frac{1}{4k} \left(\frac{\partial}{\partial \xi} - \frac{\partial}{\partial \eta} \right) P_{n-1}, \tag{16.148}$$

$$\tilde{P}_{n-1} = \frac{1}{2} \left\{ k \frac{\partial^2}{\partial \xi^2} + \frac{n}{k} \frac{\partial}{\partial \xi} + k\xi \right\} P_{n-1} = -\frac{1}{2} \left\{ \eta \frac{\partial^2}{\partial \eta^2} + \frac{n}{k} \frac{\partial}{\partial \eta} + k\eta \right\} P_{n-1}, \tag{16.149}$$

and \tilde{Q}_{n-1} is given by eq. (16.149) with Q_{n-1} replacing P_{n-1} . The potentials P_{n-1} and Q_{n-1} are given by:

$$P_{n-1} = P_{n-1}^i + P_{n-1}^s, \quad Q_{n-1} = Q_{n-1}^i + Q_{n-1}^s, \quad (16.150)$$

where

$$P_{n-1}^i = \frac{-2i}{\pi k \sin \alpha} (4k^2 \xi \eta)^{\frac{1}{2}(1-n)} \int_{-\infty}^{\infty} \tau \rho_n^i(\tau) d\tau, \quad (16.151)$$

$$Q_{n-1}^i = \frac{-2i}{\pi k \sin \alpha} (4k^2 \xi \eta)^{\frac{1}{2}(1-n)} \int_{-\infty}^{\infty} n \rho_n^i(\tau) d\tau, \quad (16.152)$$

$$P_{n-1}^s = \frac{2}{\pi k \sin \alpha} (4k^2 \xi \eta)^{\frac{1}{2}(1-n)} \int_{-\infty}^{\infty} \tau \rho_n^s(\tau) d\tau, \quad (16.153)$$

$$Q_{n-1}^s = \frac{2}{\pi k \sin \alpha} (4k^2 \xi \eta)^{\frac{1}{2}(1-n)} \int_{-\infty}^{\infty} n q_n^s(\tau) d\tau, \quad (16.154)$$

with

$$\rho_n^i(\tau) = (n^2 + \tau^2)^{-1} (\tan \frac{1}{2}\alpha)^{i\tau} \Gamma(\frac{1}{2}(n+i\tau)) \Gamma(\frac{1}{2}(n-i\tau)) m_{-\frac{1}{2}i\tau}^{(n-1)}(2ik\xi) m_{\frac{1}{2}i\tau}^{(n-1)}(2ik\eta), \quad (16.155)$$

$$\rho_n^s(\tau) = (n^2 + \tau^2)^{-1} e^{\frac{1}{2}\pi\tau} (\tan \frac{1}{2}\alpha)^{i\tau} \Gamma(\frac{1}{2}(n+i\tau)) m_{-\frac{1}{2}i\tau}^{(n-1)}(2ik\xi) w_{-\frac{1}{2}i\tau}^{(n-1)}(-2ik\eta), \quad (16.156)$$

$$p_n^s(\tau) = q_n^s(\tau) + \frac{n^2 + \tau^2}{2\tau} e^{\frac{1}{2}\pi(\tau-i)} \frac{\Gamma(\frac{1}{2}(n-i\tau))}{\Gamma(1 + \frac{1}{2}(n+i\tau))}, \quad (16.157)$$

$$q_n^s(\tau) = e^{-\frac{1}{2}\pi\tau} \Gamma(1 + \frac{1}{2}(n-i\tau)) d_n(\tau, \eta) \{ m_{\frac{1}{2}(1-i\tau)}^{(n)}(2ik\eta) w_{\frac{1}{2}(1-i\tau)}^{(n)}(-2ik\eta) - \\ - \frac{1}{2}(n+i\tau) m_{\frac{1}{2}(1+i\tau)}^{(n)}(2ik\eta) w_{-\frac{1}{2}(1+i\tau)}^{(n)}(-2ik\eta) \}, \quad (16.158)$$

and

$$d_n(\tau, \eta) = \{ [w_{\frac{1}{2}(1-i\tau)}^{(n)}(-2ik\eta)]^2 + \frac{1}{4}(n^2 + \tau^2) [w_{-\frac{1}{2}(1+i\tau)}^{(n)}(-2ik\eta)]^2 \}^{-1}. \quad (16.159)$$

If P_{n-1}^i , Q_{n-1}^i or P_{n-1}^s , Q_{n-1}^s are used in the previous formulas in place of P_{n-1} , Q_{n-1} , then eqs. (16.138) give the incident or scattered field components, respectively.

In particular, the total magnetic field components on the surface ($\eta = \eta_1$) are:

$$H_\xi = \frac{-iY}{4\pi \sin \alpha} \sqrt{\frac{\eta_1}{\xi + \eta_1}} \int_{-\infty}^{\infty} (\tan \frac{1}{2}\alpha)^{i\tau} \{ T(\tau, \phi) - T(\tau, -\phi) \} d\tau, \quad (16.160)$$

$$H_\phi = \frac{Y}{4\pi \sin \alpha} \int_{-\infty}^{\infty} (\tan \frac{1}{2}\alpha)^{i\tau} \{ T(\tau, \phi) + T(\tau, -\phi) \} d\tau, \quad (16.161)$$

where

$$T(\tau, \phi) = t_0(\tau) + \sum_{n=1}^{\infty} (-1)^n [t_n^{(1)}(\tau) e^{in\phi} + t_n^{(2)}(\tau) e^{-in\phi}], \quad (16.162)$$

$$t_n^{(1)}(\tau) = 2(-i)^{n+1} \Gamma(\frac{1}{2}(n-i\tau)) d_n(\tau, \eta_1) m_{-\frac{1}{2}i\tau}^{(n-1)}(2ik\xi) w_{-\frac{1}{2}i\tau}^{(n-1)}(-2ik\eta_1), \quad (16.163)$$

$$t_n^{(2)}(\tau) = -(-i)^{n+1}(n-i\tau)\Gamma(\frac{1}{2}(n-i\tau))d_n(\tau, \eta_1)m_{-\frac{1}{2}i\tau}^{(n+1)}(2ik\xi)w_{-\frac{1}{2}i\tau}^{(n-1)}(-2ik\eta_1), \quad (16.164)$$

$$t_0(\tau) = t_0^{(1)}(\tau) = t_0^{(2)}(\tau), \quad (16.165)$$

and $d_n(\tau, \eta_1)$ is given by eq. (16.159) in which $\eta = \eta_1$.

For a plane wave whose direction of propagation is parallel to the $y = 0$ plane and forms the angle α with the positive z -axis, and whose electric field vector is parallel to the y -axis, such that

$$E^i = \hat{y} \exp \{ik(z \cos \alpha + x \sin \alpha)\}, \quad (16.166)$$

$$H^i = Y(\hat{z} \sin \alpha - \hat{x} \cos \alpha) \exp \{ik(z \cos \alpha + x \sin \alpha)\},$$

the components of the incident, scattered and total fields may be expanded in Fourier series (FOCK and FEDOROV [1958]; see also FOCK [1965], chapter 4); thus, for the total field:

$$\begin{aligned} E_z &= \sum_{n=1}^{\infty} E_z^{(n)} \sin(n\phi), \\ E_\eta &= \sum_{n=1}^{\infty} E_\eta^{(n)} \sin(n\phi), \\ E_\phi &= \frac{1}{2}E_\phi^{(0)} + \sum_{n=1}^{\infty} E_\phi^{(n)} \cos(n\phi), \\ H_z &= \frac{1}{2}H_z^{(0)} + \sum_{n=1}^{\infty} H_z^{(n)} \cos(n\phi), \\ H_\eta &= \frac{1}{2}H_\eta^{(0)} + \sum_{n=1}^{\infty} H_\eta^{(n)} \cos(n\phi), \\ H_\phi &= \sum_{n=1}^{\infty} H_\phi^{(n)} \sin(n\phi), \end{aligned} \quad (16.167)$$

where

$$E_z^{(n)} = \frac{(4k^2\xi\eta)^{\frac{1}{2}n}}{2i\sqrt{\{\xi(\xi+\eta)\}}} \left[\frac{1}{k} \frac{\partial D_{n-1}}{\partial \eta} - nG_n \right], \quad (16.168)$$

$$E_\eta^{(n)} = -\frac{(4k^2\xi\eta)^{\frac{1}{2}n}}{2i\sqrt{\{\eta(\xi+\eta)\}}} \left[\frac{1}{k} \frac{\partial D_{n-1}}{\partial \xi} + nG_n \right], \quad (16.169)$$

$$E_\phi^{(n)} = \frac{(4k^2\xi\eta)^{\frac{1}{2}n}}{2i\sqrt{\xi\eta}} (C_{n-1} + nG_n), \quad (16.170)$$

$$H_z^{(n)} = -Y \frac{(4k^2\xi\eta)^{\frac{1}{2}n}}{2\sqrt{\{\xi(\xi+\eta)\}}} \left[\frac{1}{k} \frac{\partial C_{n-1}}{\partial \eta} - nF_n \right], \quad (16.171)$$

$$H_\eta^{(n)} = Y \frac{(4k^2\xi\eta)^{\frac{1}{2}n}}{2\sqrt{\{\eta(\xi+\eta)\}}} \left[\frac{1}{k} \frac{\partial C_{n-1}}{\partial \xi} + nF_n \right], \quad (16.172)$$

$$H_\phi^{(n)} = -Y \frac{(4k^2\xi\eta)^{\frac{1}{2}n}}{2\sqrt{\xi\eta}} (D_{n-1} - nF_n). \quad (16.173)$$

The auxiliary functions C_{n-1} , D_{n-1} , F_n and G_n are still given by eqs. (16.145) through (16.159), with the exception of eq. (16.157) which is now replaced by:

$$p_n^*(\tau) = q_n^*(\tau) - \frac{n^2 + \tau}{2\tau} e^{\frac{1}{2}\pi(\tau-1)} \frac{\Gamma(\frac{1}{2}(n-i\tau))}{\Gamma(1+\frac{1}{2}(n+i\tau))}. \quad (16.174)$$

For axial incidence ($\alpha = 0$), such that

$$E^i = \hat{x} e^{ikz}, \quad (16.175)$$

then (SCHENSTED [1955]):

$$E^s = \frac{\exp \{ik[(OP) - 2\eta_1]\}}{(OP)} \{[-\eta_1 + \xi_1 \cos(2\phi)]\hat{x} + \xi_1 \sin(2\phi)\hat{y} - 2\sqrt{\xi_1 \eta_1} \cos \phi \hat{z}\}, \quad (16.176)$$

where (OP) is the distance between the focus O and the observation point P (see Fig. 16.6), and the coordinate ξ_1 of the reflection point $P_1 \equiv (\xi_1, \eta_1, \phi_1 = \phi)$ is a root of:

$$2 \left(\frac{\xi_1 \eta_1}{\eta_1} \right)^{\frac{1}{2}} - \xi + \eta - \xi_1 - \eta_1 = [4(\sqrt{\xi \eta} - \sqrt{\xi_1 \eta_1})^2 + (\xi - \eta - \xi_1 + \eta_1)^2]^{\frac{1}{2}}; \quad (16.177)$$

in terms of the observation angle θ ,

$$\xi_1 = \eta_1 \frac{1 + \cos \theta}{1 - \cos \theta}. \quad (16.178)$$

The exact result (16.176) is identical with the geometrical optics scattered field. The bistatic scattering cross section is (SCHENSTED [1955]):

$$\sigma(\theta) = 4\pi(\xi_1 + \eta_1)^2 = 4\pi\eta_1^2(\sin \frac{1}{2}\theta)^{-4}, \quad (16.179)$$

and in particular, the back scattering cross section ($\theta = \pi$) is:

$$\sigma = 4\pi\eta_1^2. \quad (16.180)$$

A result equivalent to eq. (16.176), but expressed in a much more complicated form, that is as an infinite series involving the functions S_n^1 and V_n^1 , had been previously obtained by HORTON and KARAL [1951].

16.4.2.2. HIGH FREQUENCY APPROXIMATIONS

For a plane wave whose direction of propagation is parallel to the $y = 0$ plane and forms the angle α with the positive z -axis, and whose magnetic field vector is parallel to the y -axis, such that

$$\begin{aligned} E^i &= (\hat{x} \cos \alpha - \hat{z} \sin \alpha) \exp \{ik(z \cos \alpha + x \sin \alpha)\}, \\ H^i &= Y \hat{y} \exp \{ik(z \cos \alpha + x \sin \alpha)\}, \end{aligned} \quad (16.181)$$

the total magnetic field on the surface ($\eta = \eta_1$) is (FOCK [1946]; FOCK and FIDOROV

[1958]; see also FOCK [1965], chapters 2 and 4):

$$H_z \sim Y \sqrt{\frac{\eta_1}{\xi + \eta_1}} G(u) \sin \phi \exp \{ik(z \cos \alpha + x \sin \alpha)\}, \quad (16.182)$$

$$H_\phi \sim Y G(u) \cos \phi \exp \{ik(z \cos \alpha + x \sin \alpha)\}, \quad (16.183)$$

where $G(u)$ is defined in the Introduction (see the second of eqs. (I.275)), and

$$u = k(\sqrt{\xi \eta_1} \sin \alpha \cos \phi - \eta_1 \cos \alpha) \{k^2 \eta_1 (\xi + \eta_1) \sin^2 \alpha\}^{-\frac{1}{2}}. \quad (16.184)$$

Results (16.182) and (16.183) are valid in the illuminated, penumbra and deep shadow regions, provided that $(k\eta_1)^{\frac{1}{2}} \gg 1$. In particular, in the illuminated region and far from the shadow line $\xi_1 = \xi_1(\phi)$ given by the equation

$$\sqrt{\xi_1} \cos \phi = \sqrt{\eta_1} \cot \alpha, \quad (16.185)$$

such that

$$k(\eta_1 \cos \alpha - \sqrt{\xi \eta_1} \sin \alpha \cos \phi) \gg 1, \quad (16.186)$$

expressions (16.182) and (16.183) become:

$$H_z \sim 2Y \sqrt{\frac{\eta_1}{\xi + \eta_1}} \sin \phi \exp \{ik(z \cos \alpha + x \sin \alpha)\}, \quad (16.187)$$

$$H_\phi \sim 2Y \cos \phi \exp \{ik(z \cos \alpha + x \sin \alpha)\}, \quad (16.188)$$

which coincide with the geometrical optics approximation.

For a plane wave whose direction of propagation is parallel to the $y = 0$ plane and forms the angle α with the positive z -axis, and whose electric field vector is parallel to the y -axis, such that

$$\begin{aligned} E^i &= \hat{y} \exp \{ik(z \cos \alpha + x \sin \alpha)\}, \\ H^i &= Y(\hat{z} \sin \alpha - \hat{x} \cos \alpha) \exp \{ik(z \cos \alpha + x \sin \alpha)\}, \end{aligned} \quad (16.189)$$

the total magnetic field on the surface ($\eta = \eta_1$) is (FOCK and FEDOROV [1958]; see also FOCK [1965], chapter 4):

$$\begin{aligned} H_z \sim Y \sqrt{\frac{\eta_1}{\xi + \eta_1}} \exp \{ik(z \cos \alpha + x \sin \alpha)\} \left\{ \sqrt{\frac{\xi}{\eta_1}} G(u) \sin \alpha \sin^2 \phi - \right. \\ \left. - iF(u)(k\eta_1)^{-1} [k^2 \eta_1 (\xi + \eta_1) \sin^2 \alpha]^{\frac{1}{2}} \cos \phi \right\}, \end{aligned} \quad (16.190)$$

$$\begin{aligned} H_\phi \sim Y \exp \{ik(z \cos \alpha + x \sin \alpha)\} \left\{ \sqrt{\frac{\xi}{\eta_1}} G(u) \sin \alpha \sin \phi \cos \phi + \right. \\ \left. + iF(u)(k\eta_1)^{-1} [k^2 \eta_1 (\xi + \eta_1) \sin^2 \alpha]^{\frac{1}{2}} \sin \phi \right\}, \end{aligned} \quad (16.191)$$

where $F(u)$ and $G(u)$ are defined in the Introduction (see eqs. (I.275)), and u is given by eq. (16.184). Results (16.190) and (16.191) are valid in the illuminated, penumbra

and deep shadow regions, provided that $(k\eta_1)^{\frac{1}{2}} \gg 1$. In particular, in the illuminated region and far from the shadow line so that inequality (16.186) is satisfied, eqs. (16.190) and (16.191) become:

$$H_z \sim \frac{2Y}{\sqrt{(\xi + \eta_1)}} \exp \{ik(z \cos \alpha + x \sin \alpha)\} (\sqrt{\xi} \sin \alpha - \sqrt{\eta_1} \cos \alpha \cos \phi), \quad (16.192)$$

$$H_\phi \sim 2Y \exp \{ik(z \cos \alpha + x \sin \alpha)\} \cos \alpha \sin \phi, \quad (16.193)$$

which coincide with the geometrical optics approximation.

For axial incidence ($\alpha = 0$), the geometrical optics scattered field is identical to the exact result of eq. (16.176).

16.5. Survey of concave paraboloid

The field produced by a point source located anywhere on the concave side of an acoustically soft or hard paraboloid has been studied by BUCHHOLZ [1953], from whose results the exact solution can be extracted in the form of an integral representation or of an infinite series. In a previous work, BUCHHOLZ [1943a] had examined the case of a point source at the focus.

Low frequency results, corresponding to the case $k\eta_1 \ll 1$, have been obtained by STONE [1967] for both soft and hard bodies, when the point source is on the axis of symmetry, and for source and observation points either both in the near field, or one in the near field and the other in the far field.

High frequency results, corresponding to the case $k\eta_1 \gg 1$, have been obtained by STONE [1967], who has given the total surface field at points far from the nose of a hard paraboloid, as produced by a point source located on the axis and far from the focus; Stone has interpreted his asymptotic results in terms of geometrical optics. A Luneburg-Kline expansion for the field produced by a point source at the focus of a soft or hard paraboloid has been derived by KELLER et al. [1956]. HOCHSTADT [1956a] has considered a point source on the axis of symmetry, and has devoted special attention to the behavior of the field at or near a caustic.

For the case in which the primary field is a scalar plane wave, an exact integral representation of the solution has been given by BUCHHOLZ [1953], and high frequency expansions have been obtained by HOCHSTADT [1956a].

The exact electromagnetic field produced by an electric dipole located on the axis of symmetry of a perfectly conducting concave paraboloid has been derived by BUCHHOLZ [1948]. The cases of an electric dipole at the focus and oriented (i) parallel to the symmetry axis, or (ii) perpendicular to the axis, or (iii) perpendicular to the axis and backed by a dummy reflector have been considered by PINNEY [1947], who has given the exact solutions as infinite series of eigenfunctions. The field produced by an electric dipole at the focus and perpendicular to the symmetry axis has also been studied by SKALSKAYA [1955], who has obtained an integral representation for the exact solution as well as high frequency results, and by FOCK [1957; 1965, chap-

ter 3], who has expressed the exact solution both as an integral and as an infinite series, and has derived high frequency expansions.

If the primary field is a plane electromagnetic wave, an integral representation of the exact solution may be obtained from BUCHHOLZ [1953].

Bibliography

- BUCHHOLZ, H. [1943a], Die Ausbreitung der Schallwellen in einem Horn von der Gestalt eines Rotationsparaboloides bei Anregung durch eine im Brennpunkt befindliche punktförmige Schallquelle, *Ann. Physik* (5. Folge) **42**, 423-460.
- BUCHHOLZ, H. [1943b], Die konfluente hypergeometrische Funktion mit besonderer Berücksichtigung ihrer Bedeutung für die Integration der Wellengleichung in den Koordinaten eines Rotationsparaboloides, *Z. Angew. Math. Mech.* **23**, 47-58; 101-118.
- BUCHHOLZ, H. [1947], Integral- und Reihendarstellungen für die verschiedenen Wellentypen der mathematischen Physik in den Koordinaten des Rotationsparaboloides, *Z. Physik* **124**, 196-218.
- BUCHHOLZ, H. [1948], Die axialsymmetrische elektromagnetische Strahlung zwischen konfokalen Drehparabolen bei verschiedenen Anregungsarten, *Ann. Physik* (6. Folge) **2**, 185-210.
- BUCHHOLZ, H. [1953], *Die konfluente hypergeometrische Funktion*, Springer, Berlin.
- ERDÉLYI, A. and C. A. SWANSON [1957], Asymptotic Forms of Whittaker's Confluent Hypergeometric Functions, *Mem. Am. Math. Soc.* No. 25.
- FOCK, V. A. [1946], The Distribution of Currents Induced by a Plane Wave on the Surface of a Conductor, *J. Phys. USSR* **10**, 130-136.
- FOCK, V. A. [1957], The Theory of Diffraction of a Paraboloid of Revolution, in: *Diffraction of Electromagnetic Waves on Certain Bodies of Revolution*, Sovetskoe Radio, Moscow (in Russian).
- FOCK, V. A. [1965], *Electromagnetic Diffraction and Propagation Problems*, Pergamon Press, London. A factor 2 is missing in the right-hand sides of formulas (1.09) on p. 25.
- FOCK, V. A. and A. A. FEDOROV [1958], Diffraction of a Plane Electromagnetic Wave by a Perfectly Conducting Paraboloid of Revolution, *Zh. Tekhn. Fiz.* **28**, 2548 (in Russian).
- FRIEDLANDER, F. G. [1943], On the Reflection of a Spherical Sound Pulse by a Parabolic Mirror, *Proc. Cambridge Phil. Soc.* **38**, 383-393.
- HOCHSTADT, H. [1956a], Asymptotic Formulas for Diffraction by Parabolic Surfaces, Research Report No. EM-89, Institute of Mathematical Sciences, New York University, New York.
- HOCHSTADT, H. [1956b], Addition Theorems for the Functions of the Paraboloid of Revolution, Research Report No. BR-18, Institute of Mathematical Sciences, New York University, New York (ASTIA Document No. AD 83063).
- HORTON, C. W. [1952], Some Numerical Tables of Functions Required in Treating the Wave Equation in Rotational Paraboloidal Coordinates, Report No. CM626, DRL-254, Defense Research Laboratory, Canada (errata issued August 12, 1952).
- HORTON, C. W. [1953], On the Diffraction of a Plane Sound Wave by a Paraboloid of Revolution. II, *J. Acoust. Soc. Am.* **25**, 632-637.
- HORTON, C. W. and F. C. KARAL Jr. [1950], On the Diffraction of a Plane Sound Wave by a Paraboloid of Revolution, *J. Acoust. Soc. Am.* **22**, 855-856. The formulas contain a factor $(-1)^n$ which does not appear in BUCHHOLZ [1943b].
- HORTON, C. W. and F. C. KARAL Jr. [1951], On the Diffraction of a Plane Electromagnetic Wave by a Paraboloid of Revolution, *J. Appl. Phys.* **22**, 575-581.
- IVANOV, V. I. [1962], The Asymptotic Expansion of Green's Function for the Diffraction of Short Waves by a Paraboloid of Revolution (Axisymmetric Case), *USSR Comput. Math. and Math. Phys.* **1**, 97-113. (Translation from *Zh. Vychisl. Mat. i. Mat. Fiz.*, 1961.)
- KIANE, K. [1959], Zur Beugung skalarer Wellen am Rotations-Paraboloid, *Ann. Physik* (7. Folge) **3**, 171-182. An error has been corrected by IVANOV [1962].

- KELLER, J. B., R. M. LEWIS and B. D. SECKLER [1956], Asymptotic Solution of Some Diffraction Problems, *Comm. Pure Appl. Math.* **9**, 207-265.
- KORBANSKIY, I. N. [1968], Electric Field of a Hertz Dipole on the Axis of an Ideally Conducting Paraboloid of Revolution, *Radio Eng. Electron.* **13**, 1460-1463 (translation of *Radiotekhn. i Elektron.*).
- LAMB, H. [1906], On Sommerfeld's Diffraction Problem; and on Reflection by a Parabolic Mirror, *Proc. London Math. Soc.* (2) **4**, 190-203.
- MIRIMANOV, R. G. [1948a], Solution of the Problem of the Diffraction of a Plane Wave from a Paraboloid of Revolution of Infinite Size with the Aid of the Laguerre Function, *Dokl. Akad. Nauk. SSSR* **60**, 203-206 (in Russian).
- MIRIMANOV, R. G. [1948b], Solution of the Problem of Diffraction of Spherical Electromagnetic Waves from a Paraboloid of Revolution of Infinite Size, *Dokl. Akad. Nauk. SSSR* **60**, 357-360 (in Russian).
- PINNEY, E. [1946], Laguerre Functions in the Mathematical Foundations of the Electromagnetic Theory of the Paraboloidal Reflector, *J. Math. and Phys.* **25**, 49-79.
- PINNEY, E. [1947], Electromagnetic Fields in a Paraboloidal Reflector, *J. Math. Phys.* and **26**, 42-55.
- SCHENSTED, C. E. [1955], Electromagnetic and Acoustic Scattering by a Semi-Infinite Body of Revolution, *J. Appl. Phys.* **26**, 306-308.
- SKALSKAYA, I. P. [1955], The Electromagnetic Field of a Dipole Located in the Interior of a Parabolic Reflector, *Zh. Tekhn. Fiz.* **25**, 2371-2380 (in Russian; translated into English in New York University Report No. EM-103).
- STONE, S. E. [1967], Diffraction by the Concave Surface of the Paraboloid of Revolution, The University of Michigan Radiation Laboratory Report No. 8525-3-T, Ann Arbor, Michigan (ASTIA Document No. AD 818382).

CHAPTER 17

THE HYPERBOLOID

P. L. E. USLENGHI

The hyperboloid is the only separable shape among those considered in this book for which no exact solution is presently available. However, in the acoustical case it would be possible to apply a technique similar to that used by BLOOM [1964] for the hard hyperbolic cylinder. The hyperboloid degenerates into a cone when the interfocal distance becomes zero.

17.1. Hyperboloidal geometry

The coordinates appropriate to this shape are the prolate spheroidal coordinates (ξ, η, ϕ) shown in Fig. 17.1 and related to the rectangular Cartesian coordinates (x, y, z) by the transformation

$$\begin{aligned} x &= \frac{1}{2}d\sqrt{(\xi^2-1)(1-\eta^2)} \cos \phi, \\ y &= \frac{1}{2}d\sqrt{(\xi^2-1)(1-\eta^2)} \sin \phi, \\ z &= \frac{1}{2}d\xi\eta, \end{aligned} \quad (17.1)$$

where $1 \leq \xi < \infty$, $-1 \leq \eta \leq 1$ and $0 \leq \phi < 2\pi$. The z -axis is the axis of symmetry, and the surfaces $\xi = \text{constant}$, $|\eta| = \text{constant}$ and $\phi = \text{constant}$ are respectively

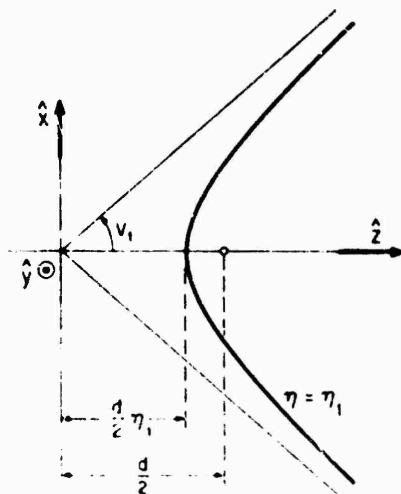


Fig. 17.1. Geometry for the hyperboloid of revolution

confocal prolate spheroids of interfocal distance d , major axis $d\xi$, and minor axis $d\sqrt{(\xi^2 - 1)}$; confocal hyperboloids of revolution of two sheets with interfocal distance d ; and semi-planes originating in the z -axis.

The scattering body is the hyperboloid of revolution with surface $\eta = \eta_1 = \cos v_1 > 0$ (see Fig. 17.1), and the primary source is either a plane wave whose direction of propagation is parallel to the (x, z) plane and forms the angle $\zeta > v_1$ with the negative z -axis, or a point or dipole source located either at $(\xi_0, \eta_0, \phi_0 = 0)$ on the convex side or at the focus ($x_0 = y_0 = 0, z_0 = \frac{1}{2}d$) on the concave side of the hyperboloid. The constant c is given by: $c = \frac{1}{2}kd$.

17.2. Acoustically soft hyperboloid

17.2.1. Point sources

For a point source at $P_0 = (\xi_0, \eta_0, \phi_0 = 0)$, such that

$$V^i = \frac{e^{ikR}}{kR}, \quad (17.2)$$

the geometric optics scattered field at a point $P = (\xi, \eta, \phi = 0 \text{ or } \pi)$ located in the illuminated region is:

$$V_{g.o.}^s = - \frac{\exp \{ik[(P_0 P_1) + (P_1 P)]\}}{k(P_0 P_1)} \times \left\{ \left[1 + \frac{(P_1 P)}{(P_0 P_1)} + \frac{2(P_1 P)}{a_1 \cos \psi_1} \right] \left[1 + \frac{(P_1 P)}{(P_0 P_1)} + \frac{2(P_1 P) \cos \psi_1}{b_1} \right] \right\}^{-\frac{1}{2}}, \quad (17.3)$$

where $(P_0 P_1)$ and $(P_1 P)$ are, respectively, the distances between the source P_0 and the reflection point P_1 , and between P_1 and the observation point P (see Fig. 17.2),

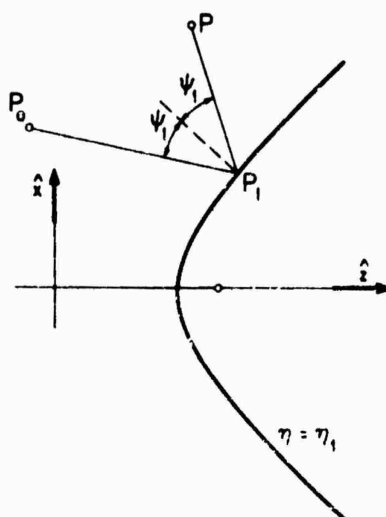


Fig. 17.2. Geometry for the reflected field with point source incidence.

$$\cos \psi_1 = \frac{d}{2(P_1 P) \sqrt{(\xi_1^2 - \eta_1^2)}} \left[\sqrt{1 - \eta_1^2} (\eta_1 - \xi_1 \xi \eta) \pm \eta_1 \sqrt{\{(\xi_1^2 - 1)(\xi^2 - 1)(1 - \eta^2)\}} \right],$$

(+ if x_1 and x have the same sign; - if x_1 and x have opposite signs), (17.4)

a_1 is the radius of curvature of the scatterer's surface in the (x, z) plane, evaluated at P_1 :

$$a_1 = \frac{1}{2} d \frac{(\xi_1^2 - \eta_1^2)^{3/2}}{\eta_1 \sqrt{(1 - \eta_1^2)}}, \quad (17.5)$$

b_1 is the other principal radius of curvature at P_1 :

$$b_1 = \frac{d}{2\eta_1} \sqrt{\{(\xi_1^2 - \eta_1^2)(1 - \eta_1^2)\}}, \quad (17.6)$$

and the coordinate ξ_1 is determined as a function of $\xi_0, \eta_0, \xi, \eta, \eta_1$ and ϕ by the relation

$$\frac{\partial}{\partial \xi_1} [(P_0 P_1) + (P_1 P)] = 0. \quad (17.7)$$

The result (17.3) is applicable if $kb_1 \gg 1$, and this is always the case if

$$\frac{c}{\eta_1} (1 - \eta_1^2) \gg 1. \quad (17.8)$$

In the shadowed region, $V_{g.o.}^s = 0$.

In particular, when both source and observation points are on the z -axis:

$$V_{g.o.}^s = - \frac{(1 - \eta_1^2) \exp \{ic(2\eta_1 - \xi_0 \eta_0 - \xi \eta)\}}{c[2\eta_1(1 + \xi \eta \xi_0 \eta_0) - (1 + \eta_1^2)(\xi_0 \eta_0 + \xi \eta)]}, \quad (17.9)$$

where either $\xi_0 = 1$ if $z_0 > -\frac{1}{2}d$ or $\eta_0 = -1$ if $z_0 < -\frac{1}{2}d$, and either $\xi = 1$ if $z > -\frac{1}{2}d$ or $\eta = -1$ if $z < -\frac{1}{2}d$; in the far field ($\eta = -1, \xi \rightarrow \infty$):

$$V_{g.o.}^s = - \frac{1 - \eta_1^2}{1 + \eta_1^2 - 2\eta_1 \xi_0 \eta_0} \frac{\exp \{ic(\xi + 2\eta_1 - \xi_0 \eta_0)\}}{c\xi}. \quad (17.10)$$

If the source is at the focus ($x_0 = y_0 = 0, z_0 = -\frac{1}{2}d$) and the observation point is on the z -axis:

$$V_{g.o.}^s = - \frac{1 - \eta_1}{1 + \eta_1} \frac{\exp \{ic(1 + 2\eta_1 - \xi \eta)\}}{c(1 - \xi \eta)}, \quad (17.11)$$

and in the far field ($\eta = -1, \xi \rightarrow \infty$):

$$V_{g.o.}^s = - \frac{1 - \eta_1}{1 + \eta_1} \frac{\exp \{ic(\xi + 2\eta_1 + 1)\}}{c\xi}. \quad (17.12)$$

For a source located at the focus ($x_0 = y_0 = 0, z_0 = -\frac{1}{2}d$), the scattered field is given by the Luneburg-Kline expansion (Kline et al. [1956]):

$$V^* \sim \frac{\exp \{i[k(QP) + 2c\eta_1]\}}{k(QP)w} \sum_{n=0}^{\infty} (2ic\eta_1)^{-n} \sum_{j=0}^n \left[\frac{2c\eta_1}{k(QP)w} \right]^j \sum_{t=0}^{2n-j} a_{jtn} w^{-t}, \quad (17.13)$$

where (QP) is the distance between the focus Q at $z = \frac{1}{2}d$ and the observation point P (see Fig. 17.3),

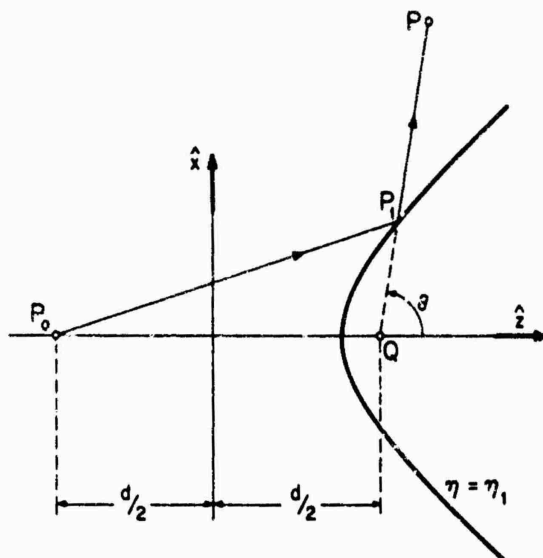


Fig. 17.3. Geometry for the reflected field with a point source at the focus $P_0 = (x_0 = y_0 = 0, z_0 = -\frac{1}{2}d)$

$$w = 1 + \frac{2\eta_1}{1-\eta_1^2} (\eta_1 - \cos \theta), \quad (17.14)$$

θ is the angle that the reflected ray P_1P forms with the positive z -axis,

$$a_{jtn} = \frac{1}{2j} \left[-(2j+t)(t+1)a_{j-1,t+1,n-1} + 2 \frac{1+\eta_1^2}{1-\eta_1^2} (j+t)^2 a_{j-1,t,n-1} - (j+t-1)(j+t)a_{j-1,t-1,n-1} \right], \quad (1 \leq j \leq n), \quad (17.15)$$

$$a_{0tn} = - \sum_{j=1}^n \sum_{s=0}^{2n-j} a_{jsn} \binom{j}{t-s} (-1)^{t-s}, \quad (0 \leq t \leq 2n; n \geq 1). \quad (17.16)$$

$$a_{000} = -1, \quad (17.17)$$

and the binomial coefficients $\binom{\alpha}{\beta}$ in eq. (17.16) are understood to be zero unless $0 \leq \beta \leq \alpha$. The first few terms of the expansion (17.13) are:

$$V^* \sim - \frac{\exp \{i[k(QP) + 2c\eta_1]\}}{k(QP)w} \left[1 + \frac{i}{2c\eta_1} \left(\frac{1+\eta_1^2-2w^{-1}}{1-\eta_1^2} + \frac{1}{w^2} \right) - \frac{i}{k(QP)w} \left(\frac{1+\eta_1^2}{1-\eta_1^2} - \frac{1}{w} \right) + \dots \right]. \quad (17.18)$$

For a source located at the focus $P_0 \equiv (x_0 = y_0, z_0 = \frac{1}{2}d; \xi_0 = \eta_0 = 1)$ on the *concave* side of the hyperboloid, the geometric optics scattered field is:

$$V_{g.o.}^s = - \frac{\exp \{ik[(P_0 P_1) + (P_1 P)]\}}{k(P_0 P_1)} \left\{ \left[1 + \frac{(P_1 P)}{(P_0 P_1)} - \frac{2(P_1 P)}{a_1 \cos \psi_1} \right] \times \left[i + \frac{(P_1 P)}{(P_0 P_1)} - \frac{2(P_1 P) \cos \psi_1}{b_1} \right] \right\}^{-\frac{1}{2}}, \quad (17.19)$$

where the geometry is shown in Fig. 17.4, a_1 and b_1 are given by eqs. (17.5) and (17.6), ξ_1 by eq. (17.7), and

$$\cos \psi_1 = \frac{d}{2(P_0 P_1)} \sqrt{\frac{\xi_1 - \eta_1}{\xi_1 + \eta_1} (1 - \eta_1^2)}. \quad (17.20)$$

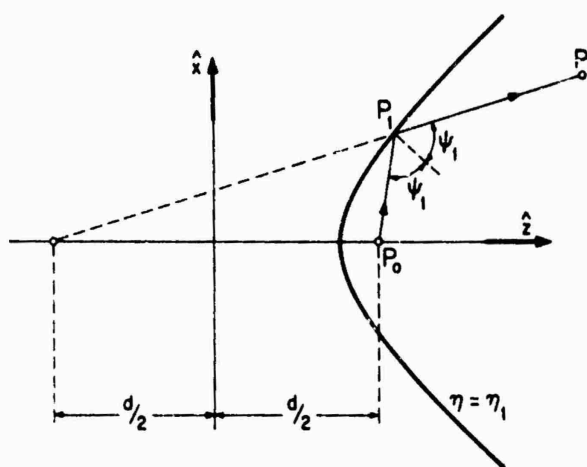


Fig. 17.4. Geometry for the reflected field with a point source at the focus $P_0 = (x_0 = y_0 = 0, z_0 = \frac{1}{2}d)$.

The result (17.19) is applicable if $kb_1 \gg 1$, and this is certainly the case if eq. (17.8) is satisfied.

In particular, if also the observation point is on the z -axis,

$$V_{g.o.}^s = - \frac{1 + \eta_1}{1 - \eta_1} \frac{\exp \{ic(1 - 2\eta_1 + \xi\eta)\}}{c(1 + \xi\eta)}, \quad (17.21)$$

where either $\xi = 1$ if $z < \frac{1}{2}d$, or $\eta = 1$ if $z > \frac{1}{2}d$; in the far field ($\eta = 1, \xi \rightarrow \infty$):

$$V_{g.o.}^s = - \frac{1 + \eta_1}{1 - \eta_1} \frac{\exp \{ic(\xi - 2\eta_1 + 1)\}}{c\xi}. \quad (17.22)$$

17.2.2. Plane wave incidence

For incidence from the half-plane $\phi_0 = 0$ at an angle ζ with respect to the negative z -axis (see Fig. 17.5), such that

$$V^i = \exp \{-ik(x \sin \zeta + z \cos \zeta)\}, \quad (17.23)$$

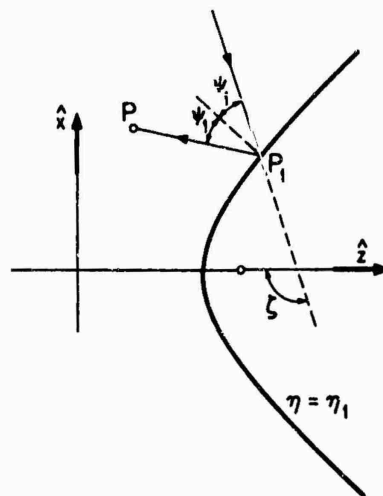


Fig. 17.5. Geometry for the reflected field with plane wave incidence.

the geometric optics scattered field at a point $P = (\xi, \eta, \phi = 0 \text{ or } \pi)$ located in the illuminated region is:

$$V_{\text{g.o.}}^s = - \left\{ \left[1 + \frac{2(P_1 P)}{a_1 \cos \psi_1} \right] \left[1 + \frac{2(P_1 P) \cos \psi_1}{b_1} \right] \right\}^{-1} \times \exp \{ ik[(P_1 P) - x_1 \sin \zeta - z_1 \cos \zeta] \}, \quad (17.24)$$

where $(P_1 P)$ is the distance between the reflection point $P_1 \equiv (x_1, 0, z_1) \equiv (\xi_1, \eta_1, \phi_1 = 0 \text{ or } \pi)$ and the observation point P , a_1 and b_1 are given by eqs. (17.5) and (17.6),

$$\cos \psi_1 = \frac{1}{\sqrt{(\xi_1^2 - \eta_1^2)}} (\pm \eta_1 \sqrt{\xi_1^2 - 1} \sin \zeta - \xi_1 \sqrt{1 - \eta_1^2} \cos \zeta),$$

(+ if $\phi_1 = 0$; - if $\phi_1 = \pi$), (17.25)

and ξ_1 is the root of

$$\frac{d}{2(P_1 P)} = \frac{\alpha \eta_1 \sqrt{\xi_1^2 - 1} \sin \zeta - \xi_1 \sqrt{1 - \eta_1^2} \cos \zeta}{\beta \eta_1 \sqrt{(\xi_1^2 - 1)(\xi^2 - 1)(1 - \eta^2)} - (\xi_1 \xi \eta - \eta_1) \sqrt{(1 - \eta_1^2)}},$$

($x = +1$ if $\phi_1 = 0$, $x = -1$ if $\phi_1 = \pi$;
 $\beta = +1$ if $\phi = \phi_1$, $\beta = -1$ if $\phi \neq \phi_1$). (17.26)

In the shadowed region, $V_{\text{g.o.}}^s = 0$.

In particular, for axial incidence ($\zeta = \pi$) and observation point on the z -axis:

$$V_{\text{g.o.}}^s = - \frac{1 - \eta_1^2}{1 + \eta_1^2 - 2\xi\eta\eta_1} \exp \{ ic(2\eta_1 - \xi\eta) \}, \quad (17.27)$$

where either $\xi = 1$ if $z > \frac{1}{2}d$, or $\xi = -1$ if $z < -\frac{1}{2}d$.

The geometric optics back scattering cross section is

$$\sigma_{g.o.} = \frac{\pi c^2}{k^2} (\eta_1 - \xi_1^2/\eta_1)^2; \quad (17.28)$$

in particular, for axial incidence ($\zeta = \pi$):

$$\sigma_{g.o.} = \frac{\pi c^2}{k^2} (\eta_1 - \eta_1^{-1})^2. \quad (17.29)$$

17.3. Acoustically hard hyperboloid

17.3.1. Point sources

For a point source at $P_0 = (\xi_0, \eta_0, \phi_0 = 0)$, such that

$$V^i = \frac{e^{ikR}}{kR}, \quad (17.30)$$

the geometric optics scattered field at a point $P = (\xi, \eta, \phi = 0 \text{ or } \pi)$ located in the illuminated region is:

$$V_{g.o.}^s = \frac{\exp \{ik[(P_0 P_1) + (P_1 P)]\}}{k(P_0 P_1)} \times \left\{ \left[1 + \frac{(P_1 P)}{(P_0 P_1)} + \frac{2(P_1 P)}{a_1 \cos \psi_1} \right] \left[1 + \frac{(P_1 P)}{(P_0 P_1)} + \frac{2(P_1 P) \cos \psi_1}{b_1} \right] \right\}^{-1}, \quad (17.31)$$

where $(P_0 P_1)$ and $(P_1 P)$ are, respectively, the distances between the source P_0 and the reflection point P_1 , and between P_1 and the observation point P (see Fig. 17.2); $\cos \psi_1$, a_1 , b_1 and ξ_1 are given by eqs. (17.4) to (17.7). This result is certainly valid if eq. (17.8) is satisfied.

In the shadowed region, $V_{g.o.} = 0$.

In particular, when both source and observation points are on the z -axis:

$$V_{g.o.}^s = \frac{(1 - \eta_1^2) \exp \{ic(2\eta_1 - \xi_0 \eta_0 - \xi \eta)\}}{c[2\eta_1(1 + \xi \eta \xi_0 \eta_0) - (1 + \eta_1^2)(\xi_0 \eta_0 + \xi \eta)]}, \quad (17.32)$$

where either $\xi_0 = 1$ if $z_0 > -\frac{1}{2}d$ or $\eta_0 = -1$ if $z_0 < -\frac{1}{2}d$, and either $\xi = 1$ if $z > -\frac{1}{2}d$ or $\eta = -1$ if $z < -\frac{1}{2}d$; in the far field ($\eta = -1$, $\xi \rightarrow \infty$):

$$V_{g.o.}^s = \frac{1 - \eta_1^2}{1 + \eta_1^2 - 2\eta_1 \xi_0 \eta_0} \frac{\exp \{ic(\xi + 2\eta_1 - \xi_0 \eta_0)\}}{c\xi}. \quad (17.33)$$

If the source is at the focus ($x_0 = y_0 = 0$, $z_0 = -\frac{1}{2}d$) and the observation point is on the z -axis:

$$V_{g.o.}^s = \frac{1 - \eta_1}{1 + \eta_1} \frac{\exp \{ic(1 + 2\eta_1 - \xi \eta)\}}{c(1 - \xi \eta)}. \quad (17.34)$$

and in the far field ($\eta = -1$, $\xi \rightarrow \infty$):

$$V_{g.o.}^s = \frac{1-\eta_1}{1+\eta_1} \frac{\exp\{ic(\xi+2\eta_1+1)\}}{c\xi}. \quad (17.35)$$

For a source located at the focus ($x_0 = y_0 = 0$; $z_0 = -\frac{1}{2}d$), the scattered field is given by the Luneburg-Kline expansion (KELLER et al. [1956]):

$$V^s \sim \frac{\exp\{i[k(QP)+2c\eta_1]\}}{k(QP)w} \sum_{n=0}^{\infty} (2ic\eta_1)^{-n} \sum_{j=0}^n \left[\frac{2c\eta_1}{k(QP)w} \right]^j \sum_{t=0}^{2n-j} a_{jtn} w^{-t}, \quad (17.36)$$

where (QP) is the distance between the focus Q at $z = \frac{1}{2}d$ and the field point P (see Fig. 17.3), w is given by eq. (17.14), a_{jtn} with $j \neq 0$ is given by eq. (17.15),

$$a_{0tn} = - \sum_{j=1}^{\infty} \sum_{s=0}^{2n-j} a_{jsn} \binom{j}{t-s} (-1)^{t-s} + \sum_{j=0}^{n-1} \sum_{s=0}^{2n-j-2} a_{j,s,n-1} (-1)^{t-s+1} \\ \times \left\{ (1+j) \binom{1+j}{t-s+1} - 2(j+s+1) \left[\binom{j}{t-s+1} + \frac{1+\eta_1^2}{1-\eta_1^2} \binom{j}{t-s} \right] \right\}, \\ (0 \leq t \leq 2n; n \geq 1), \quad (17.37)$$

$$a_{000} = +1, \quad (17.38)$$

and the binomial coefficients $\binom{\beta}{\alpha}$ in eq. (17.37) are understood to be zero unless $0 \leq \beta \leq \alpha$. The first few terms of the expansion (17.36) are:

$$V^s \sim \frac{\exp\{i[k(QP)+2c\eta_1]\}}{k(QP)w} \left[1 + \frac{i}{2c\eta_1} \left(\frac{1-3\eta_1^2-2w^{-1}}{1-\eta_1^2} + \frac{1}{w^2} \right) - \right. \\ \left. - \frac{i}{k(QP)w} \left(\frac{1+\eta_1^2}{1-\eta_1^2} - \frac{1}{w} \right) + \dots \right]. \quad (17.39)$$

For a source located at the focus $P_0 \equiv (x_0 = y_0 = 0, z_0 = \frac{1}{2}d; \xi_0 = \eta_0 = 1)$ on the *concave* side of the hyperboloid, the geometric optics scattered field is

$$V_{g.o.}^s = \frac{\exp\{ik[(P_0P_1)+(P_1P)]\}}{k(P_0P_1)} \left\{ \left[1 + \frac{(P_1P)}{(P_0P_1)} - \frac{2(P_1P)}{a_1 \cos \psi_1} \right] \right. \\ \left. \times \left[1 + \frac{(P_1P)}{(P_0P_1)} - \frac{2(P_1P) \cos \psi_1}{b_1} \right] \right\}^{-\frac{1}{2}}, \quad (17.40)$$

where a_1 , b_1 , ξ_1 and $\cos \psi_1$ are given by eqs. (17.5), (17.6), (17.7) and (17.20), respectively (see Fig. 17.4). The result (17.40) is applicable if $kb_1 \gg 1$, and this is certainly the case if eq. (17.8) is satisfied.

In particular, if the observation point is also on the z -axis,

$$V_{g.o.}^s = \frac{1+\eta_1}{1-\eta_1} \frac{\exp\{ic(1-2\eta_1+\xi\eta)\}}{c(1+\xi\eta)}, \quad (17.41)$$

where either $\xi = 1$ if $z < \frac{1}{2}d$, or $\eta = 1$ if $z > \frac{1}{2}d$; in the far field ($\eta = 1, \xi \rightarrow \infty$):

$$V_{g.o.}^s = \frac{1 + \eta_1}{1 - \eta_1} \frac{\exp \{ic(\xi - 2\eta_1 + 1)\}}{c\xi}. \quad (17.42)$$

17.3.2. Plane wave incidence

For incidence from the half-plane $\phi_0 = 0$ at an angle ζ with respect to the negative z -axis (see Fig. 17.5), such that

$$V^i = \exp \{-ik(x \sin \zeta + z \cos \zeta)\}, \quad (17.43)$$

the geometric optics scattered field at a point $P = (\xi, \eta, \phi = 0 \text{ or } \pi)$ located in the illuminated region is

$$V_{g.o.}^s = \left\{ \left[1 + \frac{2(P_1 P)}{a_1 \cos \psi_1} \right] \left[1 + \frac{2(P_1 P) \cos \psi_1}{b_1} \right] \right\}^{-\frac{1}{2}} \times \exp \{ik[(P_1 P) - x_1 \sin \zeta - z_1 \cos \zeta]\}, \quad (17.44)$$

where $(P_1 P)$ is the distance between the reflection point $P_1 \equiv (x_1, 0, z_1) \equiv (\xi_1, \eta_1, \phi_1 = 0 \text{ or } \pi)$ and the observation point P , and $a_1, b_1, \cos \psi_1$ and ξ_1 are given by eqs. (17.5), (17.6), (17.25) and (17.26) respectively. This result is certainly valid if eq. (17.8) is satisfied.

In the shadowed region, $V_{g.o.}^s = 0$.

In particular, for axial incidence ($\zeta = \pi$) and observation point on the z -axis:

$$V_{g.o.}^s = \frac{1 - \eta_1^2}{1 + \eta_1^2 - 2\xi\eta\eta_1} e^{ic(2\eta_1 - \xi\eta)}, \quad (17.45)$$

where either $\xi = 1$ if $z > -\frac{1}{2}d$, or $\eta = -1$ if $z < -\frac{1}{2}d$.

The geometric optics back scattering cross section is still given by eq. (17.28) and, in the particular case of axial incidence ($\zeta = \pi$), by eq. (17.29).

A more refined approximation based on the Luneburg-Kline method is available only for axial incidence ($\zeta = \pi$). The incident field

$$V^i = e^{ikz} \quad (17.46)$$

originates the scattered field (SCHENSTED [1955]):

$$V^s \sim \exp \{ik[z_1 + (P_1 P)]\} [V_0 + V_1 c^{-1} + O(c^{-2})], \quad (17.47)$$

where

$$V_0 = \sqrt{\frac{\rho_1}{h_1 h_2}}, \quad (17.48)$$

$$V_1 = -\frac{1}{2}i \sqrt{\frac{\rho_1}{h_1 h_2}} \left\{ \frac{1 - h_1^{-1}}{B} \left(\frac{1 + A^2}{8\rho_1^2} - \frac{AC}{h_1} \right) + (1 + h_1^{-1}) \left(\frac{A}{\rho_1} + B \right) + \frac{1}{2}(1 + A^2) \left[\frac{1}{4Ah_2} - \frac{1}{4\rho_1} + (1 - h_1^{-1})^2 \left(\frac{2C}{B^2\rho_1} + \frac{D}{B^2} \right) - \frac{5C^2}{3B^3} (1 - h_1^{-1})^3 \right] \right\}, \quad (17.49)$$

$$h_1 = 1 + \frac{4(\mathbf{P}_1 \mathbf{P})B}{(1+A^2)d}, \quad h_2 = \rho_1 + \frac{4(\mathbf{P}_1 \mathbf{P})A}{(1+A^2)d}, \quad (17.50)$$

$$A = \frac{\eta_1}{\xi_1} \sqrt{\frac{\xi_1^2 - 1}{1 - \eta_1^2}}, \quad (17.51)$$

$$B = \frac{\eta_1}{\xi_1^3(1 - \eta_1^2)}, \quad (17.52)$$

$$C = -\frac{3\eta_1}{\xi_1^5(1 - \eta_1^2)^{\frac{3}{2}}} \sqrt{(\xi_1^2 - 1)}, \quad (17.53)$$

$$D = -\frac{3\eta_1}{\xi_1^7(1 - \eta_1^2)^2} (5 - 4\xi_1^2), \quad (17.54)$$

$$\rho_1 = \sqrt{\{(\xi_1^2 - 1)(1 - \eta_1^2)\}}, \quad (17.55)$$

$(\mathbf{P}_1 \mathbf{P})$ is the distance between the reflection point $\mathbf{P}_1 \equiv (x_1, y_1 = 0, z_1) \equiv (\xi_1, \eta_1, \phi_1 = 0)$ and the observation point $\mathbf{P} \equiv (x, y = 0, z) \equiv (\xi, \eta, \phi = 0)$, and ξ_1 is a root of the equation:

$$\frac{2(\mathbf{P}_1 \mathbf{P})}{d} = \frac{\eta_1}{\xi_1} - \xi\eta + \frac{\eta_1}{\xi_1} \sqrt{\{(\xi_1^2 - 1)(\xi^2 - 1) \frac{1 - \eta^2}{1 - \eta_1^2}\}}. \quad (17.56)$$

A comparison of result (17.47) with the physical optics approximation is found in SCHENSTED [1955].

17.4. Perfectly conducting hyperboloid

17.4.1 Dipole sources

Geometrical and physical optics approximations are easily obtained in the case of a dipole on the z -axis and axially oriented; the considerations of this section are limited to this simple case.

For an electric dipole at $\mathbf{P}_0 \equiv (x_0 = y_0 = 0, z_0 \leq \frac{1}{2}d\eta_1)$ with moment $(4\pi\epsilon/k)\hat{z}$ corresponding to an incident electric Hertz vector $\hat{z}e^{ikR}/(kR)$, the incident field is

$$H_\phi^i = -k^2 cY \frac{e^{ikR}}{kR} \left(1 + \frac{i}{kR}\right) \frac{1}{kR} \sqrt{\{(\xi^2 - 1)(1 - \eta^2)\}},$$

$$H_\xi^i = H_\eta^i = E_\phi^i = 0. \quad (17.57)$$

In the physical optics approximation, the total magnetic field tangential to the surface $\eta = \eta_1$ at the point $\mathbf{P}_1 = (\xi_1, \eta_1, \phi_1)$ is:

$$(H_\phi)_{\text{p.o.}} = -2k^2 Y \frac{\exp\{ik(\mathbf{P}_0 \mathbf{P}_1)\}}{k(\mathbf{P}_0 \mathbf{P}_1)} \sqrt{\{(\xi_1^2 - 1)(1 - \eta_1^2)\}} \left[1 + \frac{i}{k(\mathbf{P}_0 \mathbf{P}_1)}\right], \quad (17.58)$$

where $(\mathbf{P}_0 \mathbf{P}_1)$ is the distance between the source point \mathbf{P}_0 and the observation point $\mathbf{P} = \mathbf{P}_1$.

If the dipole is far from the reflection point P_1 (i.e. $k(P_0 P_1) \gg 1$), such that

$$H_\phi^i \sim -k^2 Y \frac{\exp \{ik(P_0 P_1)\}}{k(P_0 P_1)} \frac{c\sqrt{(\xi_1^2 - 1)(1 - \eta_1^2)}}{k(P_0 P_1)}, \quad (17.59)$$

the geometrical optics scattered field is:

$$(H_\phi^s)_{g.o.} \sim -k^2 Y \frac{c\sqrt{(\xi_1^2 - 1)(1 - \eta_1^2)}}{k(P_0 P_1)} \frac{\exp \{ik[(P_0 P_1) + (P_1 P)]\}}{k(P_0 P_1)} \\ \times \left\{ \left[1 + \frac{(P_1 P)}{(P_0 P_1)} + \frac{2(P_1 P)}{a_1 \cos \psi_1} \right] \left[1 + \frac{(P_1 P)}{(P_0 P_1)} + \frac{2(P_1 P) \cos \psi_1}{b_1} \right] \right\}^{-1}, \quad (17.60)$$

where (P, P) is the distance between the reflection point $P_1 = (\xi_1, \eta_1, \phi_1 = \phi)$ and the observation point $P = (\xi, \eta, \phi)$, and ψ_1 is the angle of incidence; $\cos \psi_1$, a_1 , b_1 and ξ_1 are given by eqs. (17.4) to (17.7). The result (17.60) is valid if $kb_1 \gg 1$, and this is always the case if eq (17.8) is satisfied.

If the observation point is on the z -axis, the field is zero.

For a magnetic dipole at $P_0 \equiv (x_0 = y_0 = 0, z_0 \leq \frac{1}{2}d\eta_1)$ with moment $(4\pi/k)\hat{z}$ corresponding to an incident magnetic Hertz vector $\hat{z}e^{ikR}/(kR)$, the incident field is:

$$E_\phi^i = k^2 c Z \frac{e^{ikR}}{kR} \left(1 + \frac{i}{kR} \right) \frac{1}{kR} \sqrt{(\xi^2 - 1)(1 - \eta^2)}, \\ E_\xi^i = E_\eta^i = H_\phi^i = 0. \quad (17.61)$$

In the physical optics approximation, the total magnetic field tangential to the surface $\eta = \eta_1$ at the point $P_1 = (\xi_1, \eta_1, \phi_1)$ is:

$$(H_\xi)_{p.o.} = 2k^2 \sqrt{\frac{\xi_1^2 - 1}{\xi_1^2 - \eta_1^2}} \frac{\exp \{ik(P_0 P_1)\}}{k(P_0 P_1)} \\ \times \left\{ \frac{i\eta_1}{k(P_0 P_1)} \left[1 + \frac{i}{k(P_0 P_1)} \right] \left[1 - \frac{3c^2(\xi_1 \eta_1 - \xi_0 \eta_0)^2}{k^2(P_0 P_1)^2} \right] + \right. \\ \left. + \frac{c^2(1 - \eta_1^2)}{k^2(P_0 P_1)^2} \left[\eta_1(\xi_1^2 - 1) - \xi_1(\xi_1 \eta_1 - \xi_0 \eta_0) \left\{ 1 + \frac{3i}{k(P_0 P_1)} - \frac{3}{k^2(P_0 P_1)^2} \right\} \right] \right\}, \quad (17.62)$$

where $(P_0 P_1)$ is the distance between the source point P_0 and the observation point $P \equiv P_1$.

If the dipole is far from the reflection point P_1 (i.e. $k(P_0 P_1) \gg 1$), such that

$$E_\phi^i \sim k^2 Z \frac{\exp \{ik(P_0 P_1)\}}{k(P_0 P_1)} \frac{c\sqrt{(\xi_1^2 - 1)(1 - \eta_1^2)}}{k(P_0 P_1)}, \quad (17.63)$$

the geometrical optics scattered field is:

$$(E_{\phi}^s)_{\text{g.o.}} \sim -k^2 Z \frac{c\sqrt{(\xi_1^2-1)(1-\eta_1^2)}}{k(\mathbf{P}_0\mathbf{P}_1)} \frac{\exp\{ik[(\mathbf{P}_0\mathbf{P}_1)+(\mathbf{P}_1\mathbf{P})]\}}{k(\mathbf{P}_0\mathbf{P}_1)} \\ \times \left\{ \left[1 + \frac{(\mathbf{P}_1\mathbf{P})}{(\mathbf{P}_0\mathbf{P}_1)} + \frac{2(\mathbf{P}_1\mathbf{P})}{a_1 \cos \psi_1} \right] \left[1 + \frac{(\mathbf{P}_1\mathbf{P})}{(\mathbf{P}_0\mathbf{P}_1)} + \frac{2(\mathbf{P}_1\mathbf{P}) \cos \psi_1}{b_1} \right] \right\}^{-\frac{1}{2}}, \quad (17.64)$$

where (\mathbf{P}, \mathbf{P}) is the distance between the reflection point $\mathbf{P}_1 = (\xi_1, \eta_1, \phi_1 = \phi)$ and the observation point $\mathbf{P} = (\xi, \eta, \phi)$, and ψ_1 is the angle of incidence; $\cos \psi_1$, a_1 , b_1 and ξ_1 are given by eqs. (17.4) to (17.7). The result (17.64) is valid if $kb_1 \gg 1$, and this is always the case if eq. (17.8) is satisfied.

If the observation point is on the z -axis, the field is zero.

If the magnetic dipole is on the surface ($\xi_0 = 1, \eta_0 = \eta_1$), the exact electromagnetic field components are identically zero everywhere.

If the electric or magnetic dipole is oriented along the z -axis and located at the focus $\mathbf{P}_0 \equiv (x_0 = y_0 = 0, z_0 = \frac{1}{2}d)$ on the *concave* side of the hyperboloid, and if $k(\mathbf{P}_0\mathbf{P}_1) \gg 1$ and $kb_1 \gg 1$, then the geometrical optics scattered field is given by eqs. (17.60) and (17.64) respectively, in which a_1 is replaced by $(-a_1)$ and b_1 by $(-b_1)$.

17.4.2. Plane wave incidence

For a wave of arbitrary polarization incident at an angle ζ with respect to the negative z -axis, the geometrical optics back scattering cross section is:

$$\sigma_{\text{g.o.}} = \frac{\pi c^2}{k^2} (\eta_1 - \xi_1^2/\eta_1)^2, \quad (17.65)$$

where ξ_1 satisfies the relation

$$\tan \zeta = -\frac{\eta_1}{\xi_1} \sqrt{\frac{\xi_1^2-1}{1-\eta_1^2}}; \quad (17.66)$$

formula (17.65) is a good approximation if

$$\frac{c}{\eta_1} \sqrt{(\xi_1^2-\eta_1^2)(1-\eta_1^2)} \gg 1. \quad (17.67)$$

For axial incidence ($\zeta = \pi$),

$$\sigma_{\text{g.o.}} = \frac{\pi c^2}{k^2} (\eta_1 - \eta_1^{-1})^2, \quad (17.68)$$

and this is a good approximation if

$$\frac{c}{\eta_1} (1-\eta_1^2)^{-\frac{1}{2}} \gg 1. \quad (17.69)$$

A more refined approximation based on the Luneburg-Kline method is available only for axial incidence ($\zeta = \pi$). The incident field

$$\mathbf{E}^i = \hat{x}e^{ikz}, \quad \mathbf{H}^i = \hat{y}Ye^{ikz} \quad (17.70)$$

originates the scattered field (SCHENSTED [1955]):

$$E^s \sim \exp \{ik[z_1 + (\mathbf{P}_1 \mathbf{P})]\} [E_0 + E_1 c^{-1} + O(c^{-2})], \quad (17.71)$$

where

$$E_0 = \sqrt{\frac{\rho_1}{h_1 h_2}} (-\cos \phi \hat{\rho}_1 + \sin \phi \hat{\phi}), \quad (17.72)$$

$$\begin{aligned} E_1 = \frac{1}{2i} \sqrt{\frac{\rho_1}{h_1 h_2}} \left\{ \left[\frac{1-h_1^{-1}}{B} \left(\frac{1}{8\rho_1^2} - \frac{AC}{(1+A)h_1} \right) + \frac{2C+D\rho_1}{8\rho_1 B^2} (1-h_1^{-1})^2 - \frac{1}{8A\rho} - \right. \right. \\ \left. \left. - \frac{5C^2}{24B^3} (1-h_1^{-1})^3 \right] (1+A^2)(\cos \phi \hat{\rho}_1 - \sin \phi \hat{\phi}) + \right. \\ \left. + \left[B \left(1 + \frac{A^2-1}{A^2+1} h_1^{-1} \right) - \frac{A}{\rho_1} (1-h_1^{-1}) - \frac{(5A^2+1)(3A^2-1)}{8A(1+A^2)h_2} \right] \cos \phi \hat{\rho}_1 + \right. \\ \left. + \left[B(1-h_1^{-1}) - \frac{A}{\rho_1} (1+h_1^{-1}) + \frac{15A^2-1}{8Ah_2} \right] \sin \phi \hat{\phi} + \left[\frac{C}{Bh_1} (1-h_1^{-1}) - \right. \right. \\ \left. \left. - \left(\frac{1}{\rho_1} + \frac{2AB}{1+A^2} \right) h_1^{-1} + \frac{1+3A^2}{2(1+A^2)h_2} \right] \cos \phi \hat{s} \right\}, \quad (17.73) \end{aligned}$$

$$\hat{\rho}_1 = \frac{1-A^2}{1+A^2} (\cos \phi \hat{x} + \sin \phi \hat{y}) + \frac{2A}{1+A^2} \hat{z}, \quad (17.74)$$

$$\hat{\phi} = -\sin \phi \hat{x} + \cos \phi \hat{y}, \quad (17.75)$$

$$\hat{s} = \frac{2A}{1+A^2} (\cos \phi \hat{x} + \sin \phi \hat{y}) + \frac{A^2-1}{A^2+1} \hat{z}. \quad (17.76)$$

h_1 , h_2 , A , B , C , D and ρ_1 are given by eqs. (17.50) to (17.55), ξ_1 is a root of eq. (17.56), and $(\mathbf{P}_1 \mathbf{P})$ is the distance between the reflection point $\mathbf{P}_1 \equiv (x_1, y_1, z_1) \equiv (\xi_1, \eta_1, \phi_1 = \phi)$ and the observation point $\mathbf{P} \equiv (x, y, z) \equiv (\xi, \eta, \phi)$.

A comparison of result (17.71) with the physical optics approximation is found in SCHENSTED [1955].

For the axially incident field of eq. (17.70), the bistatic physical optics cross section in a direction parallel to the (x, z) plane and forming the angle $\theta = \arccos \eta$ with the positive z -axis is (SHUET et al. [1955]):

$$\sigma(\theta)_{\text{p.o.}} = \frac{\pi c^2}{k^2} (\eta_1 - \eta_1^{-1})^2 \left(1 - \frac{1 + \cos \theta}{2\eta_1^2} \right)^{-2}; \quad (17.77)$$

this formula is valid for

$$\theta > \pi - 2 \arctan \sqrt{\frac{1 - \eta_1^2}{\eta_1}}. \quad (17.78)$$

In particular, in the back scattering direction ($\theta = \pi$) formula (17.77) gives the geometric optics result of eq. (17.68).

Bibliography

- BLOOM, C. O. [1964], Diffraction by a Hyperbola, Doctoral Dissertation, New York University, New York. (Also available through University Microfilms, Inc., Ann Arbor, Michigan.)
- KELLER, J. B., R. M. LEWIS and B. D. SECTIER [1956], Asymptotic Solution of Some Diffraction Problems, *Comm. Pure Appl. Math.* **9**, 267-265.
- SCHENSTED, C. E. [1955], Electromagnetic and Acoustic Scattering by a Semi-Infinite Body of Revolution, *J. Appl. Phys.* **26**, 306-308.
- SIEGEL, K. M., H. A. ALPERIN, R. R. BONKOWSKI, J. W. CRISPIN, A. L. MAFFETT, C. E. SCHENSTED and I. V. SCHENSTED [1955], Bistatic Radar Cross Sections of Surfaces of Revolution, *J. Appl. Phys.* **26**, 297-305.

CHAPTER 18

THE CONE

J. J. BOWMAN

The cone is the limit of a hyperboloid as the interfocal distance shrinks to zero; however, the prolate spheroidal coordinates appropriate to a hyperboloid prove to be of little use in the analysis of the boundary value problem for the cone. An exact solution in spherical coordinates, on the other hand, has been intensively studied and has yielded important information concerning diffraction at a tip. Nevertheless, many features of the asymptotic behavior of the exact solution remain to be explored.

18.1. Cone geometry and preliminary considerations

In terms of the spherical polar coordinates (r, θ, ϕ) , which are related to the Cartesian coordinates (x, y, z) by the equations

$$\begin{aligned}x &= r \sin \theta \cos \phi, \\y &= r \sin \theta \sin \phi, \\z &= r \cos \theta,\end{aligned}\tag{18.1}$$

the surface of the cone is defined as $\theta = \theta_1$, where $\frac{1}{2}\pi \leq \theta_1 \leq \pi$. The exterior half-angle is therefore θ_1 , and the (interior) semivertex angle is $\delta = \pi - \theta_1$.

The primary source is a point or dipole source located at (r_0, θ_0, ϕ_0) with $0 \leq \theta_0 \leq \theta_1$, or a plane scalar wave or a plane electromagnetic wave incident from the direction θ_0, ϕ_0 . These configurations are illustrated in Fig. 18.1. The plane electromagnetic wave has arbitrary polarization as shown in Fig. 18.1c, and, in addition, the dipole source may be of arbitrary orientation. Although the considerations of this chapter are confined to the exterior problem with $\theta_1 \geq \frac{1}{2}\pi$, the exact point or dipole solutions are also applicable when $\theta_1 < \frac{1}{2}\pi$.

Most of the approximate analytical results for the cone consist of asymptotic field evaluations in the quasi-optic range (wave number $k \rightarrow \infty$). The quasi-optic effects are expected to comprise (Frisen [1959]) geometrical-optics (primary and reflected) contributions, a diffracted wave due to the cone tip, creeping waves around the cone body, and transition phenomena at the boundaries of the domains of existence of the various wave types. The geometrical-optics boundaries for the cone are the following: For $\theta_1 + \theta_0 > \pi - \theta_1$, such that a geometric shadow region exists, the optics boundaries are at $\theta = \pi - \theta_0$ (shadow boundary) and $\theta = |2\theta_1 - \pi + \theta_0|$ (reflection boundary); and for $\theta_0 < \pi - \theta_1$, such that no geometric shadow exists, the reflection boundaries are $\theta = 2\theta_1 - \pi + \theta_0$ and $\theta = |2\theta_1 - \pi - \theta_0|$.

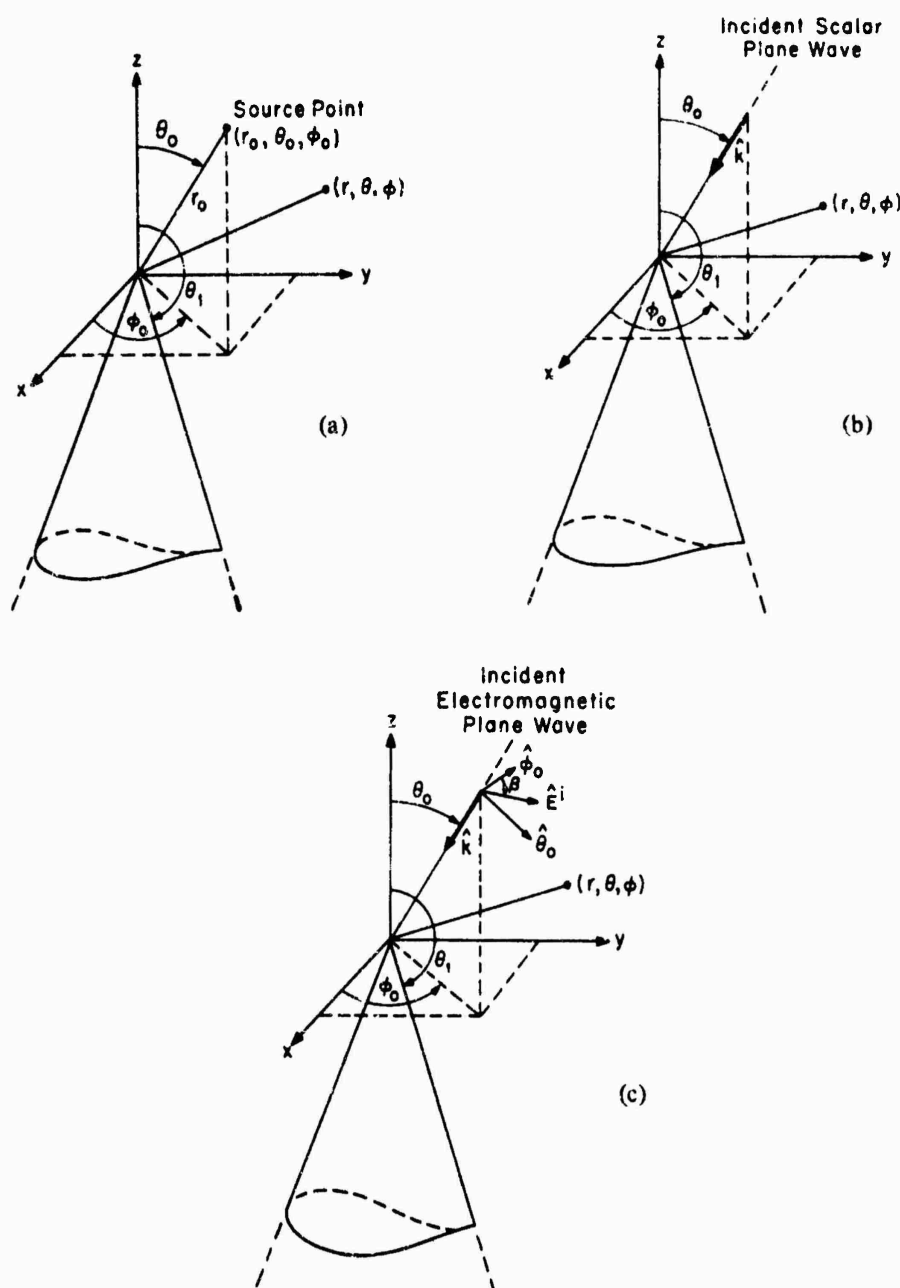


Fig. 18.1. Geometry for (a) point sources, (b) scalar plane wave illumination and (c) electromagnetic plane wave illumination.

Fundamental to the eigenfunction expansions in the sequel are the positive roots (or eigenvalues) p and q defined by the equations

$$P_p^{-m}(\cos \theta_1) = 0 \quad (18.2)$$

and

$$(\partial/\partial \theta_1) P_q^{-m}(\cos \theta_1) = 0, \quad (18.3)$$

respectively, with $m = 0, 1, 2, \dots$. All the roots of eqs. (18.2) and (18.3) are real and

simple (MACDONALD [1900], HOBSON [1931], ROBIN [1957-1959]); detailed bibliographical references to numerical calculations are given in Section 18.5. The notation $(\partial/\partial p)P_p^m(\cos \theta_1)$ and $(\partial^2/\partial q \partial \theta_1)P_q^m(\cos \theta_1)$ will be understood to mean $[(\partial/\partial v)P_v^m(\cos \theta_1)]_{v=p}$ and $[(\partial^2/\partial v \partial \theta_1)P_v^m(\cos \theta_1)]_{v=q}$, respectively. Also frequently occurring are the MEHLER [1881] conical functions $K_x^m(\cos \theta)$ defined as

$$K_x^m(\cos \theta) = P_{ix-\frac{1}{2}}^m(\cos \theta). \quad (18.4)$$

The properties of these functions are outlined in Section 18.5, where, in addition, other special functions that arise are discussed. Finally, we make use of the Heaviside step function $\eta(x)$, where

$$\eta(x) = \begin{cases} 1 & \text{for } x > 0 \\ 0 & \text{for } x < 0 \end{cases}$$

and the signum function $\text{sgn}(x) = \pm 1$ for $x \gtrless 0$.

Because of the practical interest in cone-like structures, a considerable body of experimental data is now in existence; however, due to the great difficulty in sorting out the effects of various base terminations, no attempt has been made to cite experimental results. For a review of available data, see KLEINMAN and SENIOR [1963]. Many of the theoretical results contained in this chapter are based upon unpublished memoranda written by the author (BOWMAN [1963]).

18.2. Acoustically soft cone

18.2.1. Point sources

For a point source at (r_0, θ_0, ϕ_0) , such that

$$V^i = \frac{e^{ikR}}{4R}, \quad (18.5)$$

the total field is (FELSEN [1957a]):

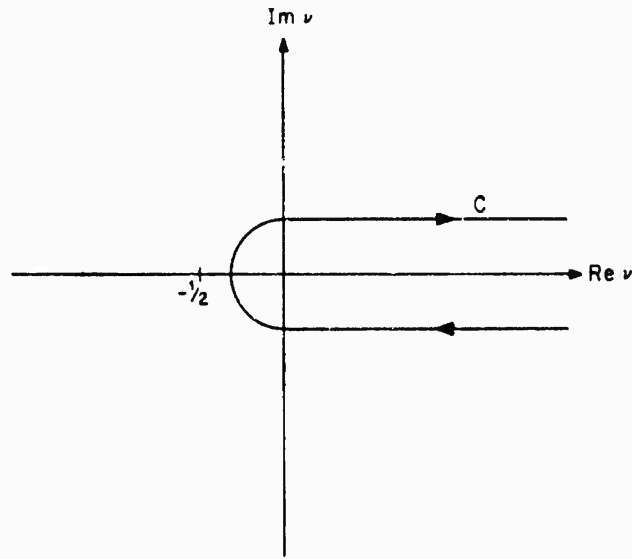
$$V^i + V^s = \frac{1}{\pi} \sum_{m=0}^{\infty} \varepsilon_m \cos m(\phi - \phi_0) \int_C dv (2v+1) j_v(kr_<) h_v^{(1)}(kr_>) G_1, \quad (18.6)$$

where

$$G_1 = -\frac{1}{2}\pi \frac{\Gamma(v+m+1)P_v^{-m}(\cos \theta_<)}{\Gamma(v-m+1)\sin(v-m)\pi} \left[P_v^{-m}(-\cos \theta_>) - \frac{P_v^{-m}(-\cos \theta_1)}{P_v^{-m}(\cos \theta_1)} P_v^{-m}(\cos \theta_>) \right] \quad (18.7)$$

and C is the contour shown in Fig. 18.2. An alternative representation of the total field as an eigenfunction expansion is (FELSEN [1957a]):

$$V^i + V^s = \frac{2i}{\sin \theta_1} \sum_{m=0}^{\infty} \varepsilon_m \cos m(\phi - \phi_0) \sum_{p=0}^{\infty} (2p+1) j_p(kr_<) h_p^{(1)}(kr_>) \times \frac{P_p^m(\cos \theta) P_p^m(\cos \theta_0)}{(\partial/\partial \theta_1) P_p^m(\cos \theta_1) (\partial/\partial p) P_p^m(\cos \theta_1)}, \quad (18.8)$$

Fig. 18.2. Contour of integration C in the v -plane.

which may be written as

$$V^i + V^s = 2i \sum_{m=0}^{\infty} \varepsilon_m \cos m(\phi - \phi_0) \sum_{p>0} j_p(kr_0) h_p^{(1)}(kr_0) \frac{P_p^m(\cos \theta) P_p^m(\cos \theta_0)}{\int_0^{\theta_1} [P_p^m(\cos \alpha)]^2 \sin \alpha d\alpha}. \quad (18.9)$$

The summations in p extend over all positive roots of the equation

$$P_p^{-m}(\cos \theta_1) = 0. \quad (18.10)$$

Expressions for the surface field $\partial(V^i + V^s)/\partial\theta$ are trivially obtainable from eqs. (18.8) and (18.9).

If $kr \ll 1$ and $kr_0 \gg 1$, the representation in eq. (18.8) is rapidly convergent and the dominant term leads to

$$V^i + V^s \sim \frac{e^{ikr_0 - 1/2 p_1 \pi}}{kr_0 \sin \theta_1} \frac{\sqrt{\pi} (kr)^{p_1}}{2^{p_1 - 1} \Gamma(p_1 + 1/2)} \frac{P_{p_1}(\cos \theta) P_{p_1}(\cos \theta_0)}{(\partial/\partial \theta_1) P_{p_1}(\cos \theta_1) (\partial/\partial p_1) P_{p_1}(\cos \theta_1)}, \quad (18.11)$$

where p_1 denotes the first zero of $P_p(\cos \theta_1)$ and $0 < p_1 < 1$ for $90^\circ < \theta_1 < 180^\circ$. The above equation makes explicit the behavior of the field near the tip.

In the region $\theta + \theta_0 < 2\theta_1 - \pi$, which excludes the domain of reflected waves, the scattered field is (FUSSEN [1957a]):

$$V^s = \frac{\pi^2}{2k_\infty r r_0} \sum_{m=0}^{\infty} \varepsilon_m \cos m(\phi - \phi_0) \int_0^{\infty} dx x \frac{\tanh \pi x}{\cosh \pi x} e^{-\pi x} H_{ix}^{(1)}(kr) H_{ix}^{(1)}(kr_0) \\ \times \frac{K_x^m(\cos \theta) K_x^m(\cos \theta_0) K_x^m(-\cos \theta_1)}{\Gamma(\frac{1}{2} + m + ix) \Gamma(\frac{1}{2} + m - ix) K_x^m(\cos \theta_1)}. \quad (18.12)$$

and for $kr_0 \ll kr_1 \ll 1$ with $\theta + \theta_0$ not too close to $2\theta_1 - \pi$ (see e.g. FELSEN [1957b] and KELLER et al. [1956], example 8):

$$V^s \sim \frac{e^{ik(r+r_0)}}{k^2 r r_0} \left[1 + \sum_{n=1}^{\infty} \frac{1}{(2ikr_0)^n n!} \prod_{s=1}^n \{s(s-1) + B\} \right] S, \quad (18.13)$$

where

$$S = -i\pi \sum_{m=0}^{\infty} \epsilon_m \cos m(\phi - \phi_0) \int_0^{\infty} dx x \frac{\tanh \pi x}{\cosh \pi x} \frac{K_x^m(\cos \theta) K_x^m(\cos \theta_0) K_x^m(-\cos \theta_1)}{\Gamma(\frac{1}{2} + m + ix) \Gamma(\frac{1}{2} + m - ix) K_x^m(\cos \theta_1)}, \quad (18.14)$$

and B is the Beltrami operator

$$B = \frac{1}{\sin \theta} \frac{\partial}{\partial \theta} \sin \theta \frac{\partial}{\partial \theta} + \frac{1}{\sin^2 \theta} \frac{\partial^2}{\partial \phi^2}. \quad (18.15)$$

The field in eq. (18.13) has the appearance of a spherical wave emanating from the cone tip. In the case of a thin cone ($\theta_1 \approx \pi$), a first order approximation to S is (FELSEN [1957a]):

$$S \approx \frac{i}{\log [\sin^2 \frac{1}{2} \delta]} \frac{1}{\cos \theta + \cos \theta_0}. \quad (18.16)$$

For a point source on the axis of symmetry ($\theta_0 = 0$), eq. (18.6) reduces to (FELSEN [1955]):

$$V^i + V^s = -\frac{1}{2\epsilon} \int_{\epsilon}^{\infty} dv \frac{2v+1}{\sin v\pi} j_v(kr_0) h_v^{(1)}(kr_1) \left[P_v(-\cos \theta) - \frac{P_v(-\cos \theta_1)}{P_v(\cos \theta_1)} P_v(\cos \theta) \right], \quad (18.17)$$

while eqs. (18.8) and (18.9) simplify respectively to

$$V^i + V^s = \frac{-2i}{\sin \theta_1} \sum_{p>0} \frac{(2p+1) j_p(kr_0) h_p^{(1)}(kr_1) P_p(\cos \theta)}{P_p^1(\cos \theta_1) (\partial/\partial p) P_p(\cos \theta_1)}, \quad (18.18)$$

$$V^i + V^s = 2i \sum_{p>0} \frac{j_p(kr_0) h_p^{(1)}(kr_1) P_p(\cos \theta)}{\int_0^{\theta_1} [P_p(\cos \alpha)]^2 \sin \alpha d\alpha}, \quad (18.19)$$

where the summations extend over the positive zeros p of $P_p(\cos \theta_1)$. The series expansion of eq. (18.18) dates back to CARSLAW [1910] and is also related to the solution presented by MACDONALD [1902] for an axial (or vertical) electric dipole.

For $\theta_0 = 0$, in the region $\theta \ll 2\theta_1 - \pi$, the scattered field is:

$$V^s = \frac{-\pi}{2k_0 r r_0} \int_0^{\infty} dx x \tanh \pi x e^{-ix} H_{ix}^{(1)}(kr) H_{ix}^{(1)}(kr_0) K_{ix}(\cos \theta) \frac{K_{ix}(-\cos \theta_1)}{K_{ix}(\cos \theta_1)}, \quad (18.20)$$

and the quantity S appearing in eq. (18.13), which determines the diffracted field due to the cone tip, becomes

$$S = -i \int_0^x dx x \tanh \pi x K_x(\cos \vartheta) \frac{K_x(-\cos \theta_1)}{K_x'(\cos \theta_1)}. \quad (18.21)$$

The approximation to S in eq. (18.16) remains valid for $\vartheta_0 = 0$.

FELSEN [1959] has treated the two-dimensional problem of a radiating ring source coaxial with the cone axis (see Fig. 18.3). The total field \dot{V} due to a source distributed

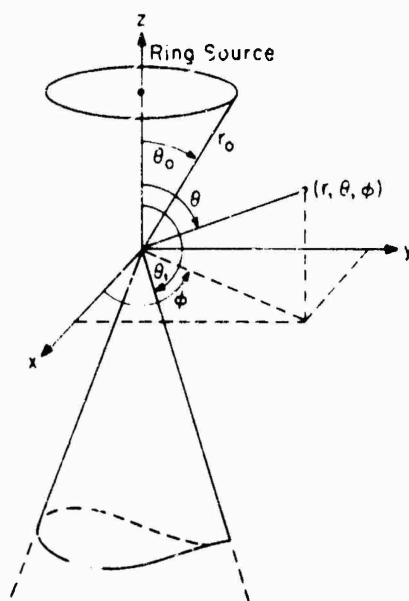


Fig. 18.3. Geometry for ring source excitation.

around a circle of radius a with an angular variation $f(\phi_0)$ is obtained from an integration of V as

$$\dot{V} = a \int_0^{2\pi} f(\phi_0) V d\phi_0 \quad (18.22)$$

with $a = r_0 \sin \theta_0$. If the source function is sinusoidal, i.e.

$$f(\phi_0) = \begin{cases} \cos m\phi_0 \\ \sin m\phi_0 \end{cases}, \quad m = 0, 1, 2, \dots, \quad (18.23)$$

then the total field \dot{V} is given by

$$\dot{V} = 2a \begin{cases} \cos m\phi \\ \sin m\phi \end{cases} \int_C dv (2v+1) j_v(kr_0) h_v^{(1)}(kr_0) G_1, \quad (18.24)$$

where C is the contour shown in Fig. 18.2 and G_1 is defined as in eq. (18.7).

For $kr_0 = kr_0 - 1$, a convenient decomposition of the total field is

$$\dot{V} = \dot{V}_d + \dot{V}_{g.o.} + \dot{V}_{tr.} \quad (18.25)$$

where \dot{V}_d is the field diffracted by the cone tip and $\dot{V}_{g.o.}$ is the total geometrical optics field. The remaining term $\dot{V}_{tr.}$ represents a transition field that provides a continuous field behavior across the various geometrical optics boundaries where the diffracted wave becomes singular and the reflected waves undergo finite jump discontinuities. A creeping wave contribution to the far field is absent as a consequence of the special ring source excitation. In the region $\theta + \theta_0 < 2\theta_1 - \pi$ outside the domain of specular reflections, the diffracted field in the far zone is (FELSEN [1959]):

$$\dot{V}_d \sim 2\pi^2 a \begin{Bmatrix} \cos m\phi \\ \sin m\phi \end{Bmatrix} \frac{e^{ik(r+r_0)}}{ik^2 r r_0} \int_0^\infty dx x \frac{\tanh \pi x}{\cosh \pi x} \frac{K_x^m(\cos \theta) K_x^m(\cos \theta_0) K_x^m(-\cos \theta_1)}{\Gamma(\frac{1}{2} + m + ix) \Gamma(\frac{1}{2} + m - ix) K_x^m(\cos \theta_1)}. \quad (18.26)$$

Although the above integral is convergent only for $\theta + \theta_0 < 2\theta_1 - \pi$, FELSEN [1959] has shown that the angular dependence of the far-zone diffracted field must be the same for all angles in $0 \leq (\theta, \theta_0) \leq \theta_1$. In principle, therefore, one may calculate the diffracted field from its integral representation (18.26) valid for the restricted range of angles and then employ the resulting closed form expression everywhere. The advantage accrued from this conclusion, however, is diminished by the fact that the integral is difficult to evaluate (even approximately) in terms of known functions, and a closed form expression valid for all angles is not available. For $(\sin \theta, \sin \theta_0, \sin \theta_1) \neq 0$ the geometrical optics and transition fields are given by (FELSEN [1959]):

$$\begin{aligned} \dot{V}_{g.o.} + \dot{V}_{tr.} \sim & \frac{-ae^{i(kr - \frac{1}{2}\pi)}}{kr\sqrt{2\pi kr_0 \sin \theta \sin \theta_0}} \begin{Bmatrix} \cos m\phi \\ \sin m\phi \end{Bmatrix} \\ & \times [I(r_0, \pi - |\theta - \theta_0|) - I(r_0, \pi - 2\theta_1 + \theta + \theta_0) - \\ & - i(-1)^m \{I(r_0, \pi - \theta - \theta_0) - I(r_0, \pi - 2\theta_1 + \theta - \theta_0) - I(r_0, \pi - 2\theta_1 + \theta_0 - \theta)\}]. \end{aligned} \quad (18.27)$$

with

$$I(r_0, x) = I_{g.o.}(r_0, x) + I_{tr.}(r_0, x), \quad (18.28)$$

$$I_{g.o.}(r_0, x) = -2\pi i \eta(x) e^{ikr_0 \cos x}, \quad (18.29)$$

$$I_{tr.}(r_0, x) = i\pi \operatorname{sgn}(x) \left[G(w) - \frac{e^{\frac{1}{2}i\pi}}{w\sqrt{2\pi}} \right] e^{ikr_0}, \quad (18.30)$$

$$w = \sqrt{k r_0} \sin \frac{1}{2}|x|, \quad G(w) = \frac{2}{\sqrt{\pi}} e^{-2iw^2} \int_0^\infty \frac{e^{-\mu^2}}{(1-iw)\mu} d\mu. \quad (18.31)$$

The properties of $G(w)$ along with $I(r_0, x)$ are discussed in Section 18.5. It should be emphasized that the above results for $\dot{V}_{g.o.}$ and $\dot{V}_{tr.}$ are valid only if both source and observer are located away from the axis of the cone and provided the cone apex angle is not small. If any of these restrictions are relaxed, different asymptotic expansions of the field must be obtained; for example, if $\theta \approx 0$ the dominant geometrical optics result is (FELSEN [1959]):

$$\begin{aligned}
 V_{\text{r.o.}} \sim & \frac{2\pi a}{kr} e^{i(kr - \frac{1}{2}m\pi)} \left\{ \frac{\cos m\phi}{\sin m\phi} \right\} \left\{ \exp \{ -ikr_0 \cos \theta \cos \theta_0 \} J_m(kr_0 \sin \theta \sin \theta_0) - \right. \\
 & - \int \frac{\sin(2\theta_1 - \theta_0)}{\sin \theta_0} \exp \{ -ikr_0 \cos \theta \cos(2\theta_1 - \pi) \} \\
 & \left. \times J_m[kr_0 \sin \theta \sin(2\theta_1 - \pi)] \eta(\pi - 2\theta_1 + \theta_0) \right\}. \quad (18.32)
 \end{aligned}$$

18.2.2. Plane wave incidence

For a plane wave incident from the direction θ_0, ϕ_0 such that

$$V^i = \exp \{ -ikr[\sin \theta \sin \theta_0 \cos(\phi - \phi_0) + \cos \theta \cos \theta_0] \}, \quad (18.33)$$

the total field is (FELSEN [1957a]):

$$V^i + V^s = \frac{1}{i\pi} \sum_{m=0}^{\infty} \varepsilon_m \cos m(\phi - \phi_0) \int_C dv (2v+1) e^{-\frac{1}{2}iv\pi} j_v(kr) G_1, \quad (18.34)$$

where

$$G_1 = -\frac{1}{2}\pi \frac{\Gamma(v+m+1)P_v^{-m}(\cos \theta_0)}{\Gamma(v-m+1)\sin(v-m)\pi} \left[\frac{P_v^{-m}(-\cos \theta_0)}{P_v^{-m}(\cos \theta_1)} - \frac{P_v^{-m}(-\cos \theta_1)}{P_v^{-m}(\cos \theta_0)} \right] \quad (18.35)$$

and C is the contour shown in Fig. 18.2. An alternative representation of the total field as an eigenfunction expansion is (FELSEN [1957a]):

$$\begin{aligned}
 V^i + V^s = & \frac{2}{\sin \theta_1} \sum_{m=0}^{\infty} \varepsilon_m \cos m(\phi - \phi_0) \sum_{p>0} (2p+1) e^{-\frac{1}{2}ip\pi} j_p(kr) \\
 & \times \frac{P_p^m(\cos \theta) P_p^m(\cos \theta_0)}{(\partial/\partial \theta_1) P_p^m(\cos \theta_1) (\partial/\partial p) P_p^m(\cos \theta_1)}, \quad (18.36)
 \end{aligned}$$

which may be written as

$$V^i + V^s = 2 \sum_{m=0}^{\infty} \varepsilon_m \cos m(\phi - \phi_0) \sum_{p>0} \frac{e^{-\frac{1}{2}ip\pi} j_p(kr) P_p^m(\cos \theta) P_p^m(\cos \theta_0)}{\int_0^{\theta_1} [P_p^m(\cos x)]^2 \sin x dx}. \quad (18.37)$$

The summations in p extend over all positive roots of the equation

$$P_p^{-m}(\cos \theta_1) = 0. \quad (18.38)$$

Expressions for the surface field $\partial(V^i + V^s)/\partial \theta$ are trivially obtainable from eqs. (18.36) and (18.37).

If $kr \ll 1$, the representation in eq. (18.36) is rapidly convergent and the dominant term leads to

$$V^i + V^s \sim \frac{e^{-\frac{1}{2}ip_1\pi}}{\sin \theta_1} \sqrt{\pi(kr)^{p_1}} \frac{P_{p_1}(\cos \theta) P_{p_1}(\cos \theta_0)}{2^{p_1-1} \Gamma(p_1 + \frac{1}{2}) (\partial/\partial \theta_1) P_{p_1}(\cos \theta_1) (\partial/\partial p_1) P_{p_1}(\cos \theta_1)}, \quad (18.39)$$

where p_1 denotes the first zero of $P_p(\cos \theta_1)$, and $0 < p_1 < 1$ for $90^\circ < \theta_1 < 180^\circ$. The above equation makes explicit the behavior of the field near the tip.

In the region $\theta + \theta_0 < 2\theta_1 - \pi$, which excludes the domain of reflected waves, the scattered field is (FELSEN [1957a]):

$$V^s = \pi \sqrt{\frac{\pi}{2kr}} e^{-\frac{1}{2}i\pi} \sum_{m=0}^{\infty} \varepsilon_m \cos m(\phi - \phi_0) \int_0^{\infty} dx x \frac{\tanh \pi x}{\cosh \pi x} e^{-\frac{1}{2}ix\pi} H_{ix}^{(1)}(kr) \\ \times \frac{K_x^m(\cos \theta) K_x^m(\cos \theta_0) K_x^m(-\cos \theta_1)}{\Gamma(\frac{1}{2} + m + ix) \Gamma(\frac{1}{2} + m - ix) K_x^m(\cos \theta_1)}; \quad (18.40)$$

and for $kr \gg 1$ with $\theta + \theta_0$ not too close to $2\theta_1 - \pi$ (see e.g. FELSEN [1957b] and KELLER et al. [1956], example 8):

$$V^s \sim \frac{e^{ikr}}{kr} \left[1 + \sum_{n=1}^{\infty} \frac{1}{(2ikr)^n n!} \prod_{s=1}^n \{s(s-1) + B\} \right] S, \quad (18.41)$$

where S is defined as in eq. (18.14), namely

$$S = -i\pi \sum_{m=0}^{\infty} \varepsilon_m \cos m(\phi - \phi_0) \int_0^{\infty} dx x \frac{\tanh \pi x}{\cosh \pi x} \frac{K_x^m(\cos \theta) K_x^m(\cos \theta_0) K_x^m(-\cos \theta_1)}{\Gamma(\frac{1}{2} + m + ix) \Gamma(\frac{1}{2} + m - ix) K_x^m(\cos \theta_1)}, \quad (18.42)$$

and B is the Beltrami operator

$$B = \frac{1}{\sin \theta} \frac{\partial}{\partial \theta} \sin \theta \frac{\partial}{\partial \theta} + \frac{1}{\sin^2 \theta} \frac{\partial^2}{\partial \phi^2}.$$

The field in eq. (18.42) has the appearance of a spherical wave emanating from the cone tip. In the case of a thin cone ($\theta_1 \approx \pi$), a first order approximation to S is (FELSEN [1957a]):

$$S \approx \frac{i}{\log [\sin^2 \frac{1}{2} \delta]} \frac{1}{\cos \theta + \cos \theta_0}. \quad (18.43)$$

Equation (18.43) does not account for the singularity in V^s as $\theta + \theta_0 \rightarrow \pi$; in this case, it is necessary to include the accompanying geometrical optics and transition fields. In particular, for a thin cone ($\theta_1 \approx \pi$) and $kr \gg 1$, the scattered field may be decomposed as

$$V^s = V_d + V_{\text{refl.}} + V_{\text{tr.}}, \quad (18.44)$$

where V_d is the diffracted field due to the cone tip, $V_{\text{refl.}}$ is the field reflected from the surface of the cone according to the laws of geometrical optics, and $V_{\text{tr.}}$ is a transition field that provides a continuous field behavior across the geometrical optics boundary $\theta = \pi - \theta_0$. The diffracted field to first order is obtained from eqs. (18.41) and (18.43):

$$V_d \sim \frac{e^{ikr}}{kr} \frac{i}{\log [\sin^2 \frac{1}{2} \delta]} \frac{1}{\cos \theta + \cos \theta_0}; \quad (18.45)$$

and, provided $kr \sin^2 \frac{1}{2}\delta \ll 1$ and $(\sin \theta, \sin \theta_0) \neq 0$, the reflected and transition fields are given by:

$$V_{\text{refl.}} + V_{\text{tr.}} \sim - \frac{e^{-\frac{1}{2}i\pi} I(r, \alpha)}{(2\pi kr \sin \theta \sin \theta_0)^{\frac{1}{2}} \log [\sin^2 \frac{1}{2}\delta]}, \quad (18.46)$$

with $\alpha = \theta + \theta_0 - \pi$ and

$$I(r, \alpha) = I_{\text{g.o.}}(r, \alpha) + I_{\text{tr.}}(r, \alpha), \quad (18.47)$$

$$I_{\text{g.o.}}(r, \alpha) = -2i\pi\eta(\alpha)e^{ikr \cos \alpha}, \quad (18.48)$$

$$I_{\text{tr.}}(r, \alpha) = i\pi \operatorname{sgn}(\alpha) \left[G(w) - \frac{e^{\frac{1}{2}i\pi}}{w\sqrt{2\pi}} \right] e^{ikr}, \quad (18.49)$$

$$w = \sqrt{kr} \sin \frac{1}{2}|\alpha|, \quad G(w) = \frac{2}{\sqrt{\pi}} e^{-2iw^2} \int_{(1-i)w}^{\infty} e^{-\mu^2} d\mu. \quad (18.50)$$

The properties of $G(w)$ along with $I(r, \alpha)$ are discussed in Section 18.5. Equation (18.46) is valid provided both source and observer are away from the cone axis. Such a restriction is no problem if both source and observer are located within the backward cone because in this instance only the diffraction term contributes significantly to the far field. If, on the other hand, either the source or observer is near the surface of the cone itself, eq. (18.46) is not valid. On the boundary $\theta = \pi - \theta_0$:

$$V^s \sim \frac{\sqrt{\pi} e^{ikr + \frac{1}{2}i\pi}}{(2kr)^{\frac{1}{2}} \sin \theta_0 \log [\sin^2 \frac{1}{2}\delta]}. \quad (18.51)$$

For a plane wave incident along the axis of symmetry $\theta_0 = 0$, such that

$$V^i = e^{-ikr \cos \theta}, \quad (18.52)$$

eq. (18.34) reduces to (FELSEN [1955]):

$$V^i + V^s = \frac{1}{2}i \int_0^{\infty} \frac{2\nu+1}{\sin \nu\pi} e^{-\frac{1}{2}i\nu\pi} j_\nu(kr) \left[P_\nu(-\cos \theta) - \frac{P_\nu(-\cos \theta_1)}{P_\nu(\cos \theta_1)} P_\nu(\cos \theta) \right], \quad (18.53)$$

while eqs. (18.36) and (18.37) simplify respectively to

$$V^i + V^s = \frac{-2}{\sin \theta_1} \sum_{p>0} (2p+1) e^{-\frac{1}{2}i p \pi} j_p(kr) \frac{P_p(\cos \theta)}{P_p^1(\cos \theta_1) (d^2/dp^2) P_p(\cos \theta_1)}, \quad (18.54)$$

$$V^i + V^s = 2 \sum_{p>0} \frac{e^{-\frac{1}{2}i p \pi} j_p(kr) P_p(\cos \theta)}{\int_0^{\theta_1} [P_p(\cos x)]^2 \sin x dx}, \quad (18.55)$$

where the summations extend over the positive zeros p of $P_p(\cos \theta_1)$.

For $\theta_0 = 0$, in the region $\theta < 2\theta_1 - \pi$, the scattered field is:

$$V^s = \int \frac{\pi}{2kr} e^{-\frac{1}{2}i\pi} \int_0^{\theta_1} dx x \tanh \pi x e^{-\frac{1}{2}i\pi} H_{ix}^{(1)}(kr) K_x(\cos \theta) \frac{K_x(-\cos \theta_1)}{K_x(\cos \theta_1)}, \quad (18.56)$$

and the quantity S appearing in eq. (18.41), which determines the diffracted field due to the cone tip, becomes

$$S = -i \int_0^\infty dx x \tanh \pi x F_x(\cos \theta) \frac{K_x(-\cos \theta_1)}{K_x(\cos \theta_1)}. \quad (18.57)$$

The approximation to S in eq. (18.43) remains valid for $\theta_0 = 0$.

For $\theta_0 = 0$ and $kr \gg 1$, the scattered field may be decomposed as in eq. (18.44) with the diffracted field given by:

$$V_d \sim \frac{e^{ikr}}{kr} S \quad (18.58)$$

where S is obtained from eq. (18.57). Although the integral in eq. (18.57) is convergent only for $\theta < 2\theta_1 - \pi$, it can be shown by a proof paralleling FELSEN [1959] that the angular dependence of the far-zone diffracted field must be the same for all angles in $0 \leq \theta \leq \theta_1$. In principle, therefore, one may calculate the diffracted field from the integral in eq. (18.57) valid for the restricted range of angles and then employ the resulting closed form expression everywhere. In practice, however, the integral is difficult to evaluate in terms of known functions, and a closed form expression valid for all angles is not available. For $(\sin \theta, \sin \theta_1) \neq 0$, the reflected and transition fields are given by:

$$V_{\text{refl.}} + V_{\text{tr.}} \sim \frac{-i}{\sqrt{\sin \theta}} \left(\frac{\partial}{\partial \alpha} - \frac{1}{4} \cot \theta_1 + \frac{1}{8} \cot \theta \right) T(r, \alpha), \quad (18.59)$$

where $\alpha = \pi - 2\theta_1 + \theta$ and

$$T(r, \alpha) = T_{\text{refl.}}(r, \alpha) + T_{\text{tr.}}(r, \alpha), \quad (18.60)$$

$$T_{\text{refl.}}(r, \alpha) = \eta(\alpha) \sqrt{\frac{\tan \frac{\alpha}{2}}{2\pi kr}} \exp \left\{ i(kr \cos \alpha + \frac{1}{4}\pi) + \frac{1}{4}ikr \frac{\sin^2 \alpha}{\cos \alpha} \right\} K_{\frac{1}{2}} \left(\frac{1}{4}ikr \frac{\sin^2 \alpha}{\cos \alpha} \right), \quad (18.61)$$

$$T_{\text{tr.}}(r, \alpha) = -[\eta(\alpha) + i\eta(-\alpha)] \sqrt{\frac{\tan \frac{1}{2}|\alpha|}{2\pi kr}} e^{i(kr + \frac{1}{4}\pi)} \left[e^{-iw^2} K_1(-iw^2) - \sqrt{\frac{1}{2}\pi} \frac{e^{\frac{1}{2}i\pi}}{w} \right], \quad (18.62)$$

with

$$w = \sqrt{\frac{1}{2}kr \sin \frac{1}{2}|\alpha|}. \quad (18.63)$$

The function K_1 is the modified Bessel function of the third kind and of order $\frac{1}{2}$. Properties of the function $T(r, \alpha)$ are discussed in Section 18.5. The transition function not only cancels the singularity at $\theta = 2\theta_1 - \pi$ in the diffracted wave term, but also properly compensates for the jump discontinuity in the reflected wave. Away from the geometrical optics boundary $\theta = 2\theta_1 - \pi$, such that $kr \sin^2 \alpha \gg 1$, the reflected field is

$$V_{\text{refl.}} \sim -\eta(\alpha) \sqrt{\frac{\sin \alpha}{\sin \theta}} e^{ikr \cos \alpha} \left\{ 1 - \frac{i}{kr} \left(\frac{\cot \theta_1}{4 \sin \alpha} - \frac{\cot \theta}{8 \sin \alpha} + \frac{\cot \alpha}{8 \sin \alpha} \right) + O \left[\frac{1}{(kr)^2} \right] \right\}, \quad (18.64)$$

which becomes, for $\theta = \theta_1$ (observer on the cone surface):

$$V_{\text{refl.}} \sim -e^{-ikr \cos \theta_1}. \quad (18.65)$$

The incident field (18.52) is thereby cancelled as required. It should be emphasized that the above results are valid only if the observer is located away from the axis of the cone and provided the cone apex angle is not small.

For $\theta_0 = 0$, $\theta = 0$, the back scattered far field is

$$V^{\text{ns}} = \frac{e^{ikr}}{ikr} \int_0^\infty dx x \tanh \pi x \frac{K_x(-\cos \theta_1)}{K_x(\cos \theta_1)} + \frac{e^{-\frac{1}{2}i\pi}}{\sqrt{2\pi kr}} \left(\frac{\partial}{\partial \alpha} - \frac{1}{4} \cot \theta_1 \right) I(r, \alpha), \quad (18.66)$$

where $\alpha = \pi - 2\theta$ and $I(r, \alpha)$ is defined by eqs. (18.47) through (18.50). The term involving $I(r, \alpha)$ is important only for a wide cone $\theta_1 \approx \frac{1}{2}\pi$, in which case both source

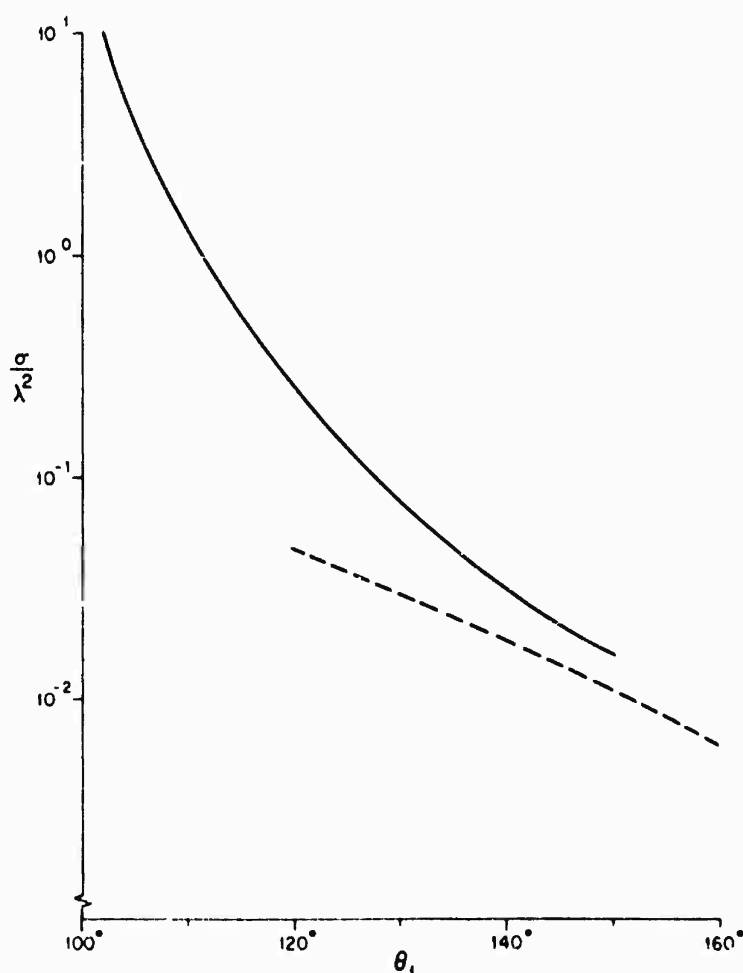


Fig. 18.4. Normalized nose-on back scattering cross section σ/λ^2 as a function of θ_1 for a soft cone: (—) wide cone and (---) thin cone.

and observer lie in a transition region. For $\theta_1 \approx \frac{1}{2}\pi$, a first order result is given by (FELSEN [1955], see also FELSEN [1953]):

$$\begin{aligned} V^{\text{BS}} &\sim -e^{ikr} \sin \theta_1 [1 - \sqrt{2\pi} e^{-\frac{1}{2}i\pi} w G(w)], & w < 4 \\ V^{\text{BS}} &\sim \frac{e^{ikr}}{ikr} \frac{1}{(2\theta_1 - \pi)^2}, & w \geq 4 \end{aligned} \quad (18.67)$$

where $w = -\sqrt{kr} \cos \theta_1$ and $G(w)$ is as defined in eq. (18.50). A plot of the magnitude and phase of the quantity in brackets in eq. (18.67) is provided in Section 18.5, Fig. 18.17b. It may be noted that when $\theta_1 = \frac{1}{2}\pi$, eq. (18.67) yields a back scattered plane wave appropriate to reflection from an infinite flat plane. For a thin cone ($\theta_1 \approx \pi$), eq. (18.43) remains valid for $\theta_0 = 0$, $\theta = 0$.

For $\theta_0 = 0$ and for a wide cone $\theta_1 \approx \frac{1}{2}\pi$, the back scattering cross section is, from eq. (18.67):

$$\sigma \approx \frac{\lambda^2}{\pi(2\theta_1 - \pi)^4}, \quad (18.68)$$

whereas, for a thin cone $\theta_1 \approx \pi$, eq. (18.43) leads to:

$$\sigma \approx \frac{\lambda^2}{16\pi [\log \frac{1}{2}(\pi - \theta_1)]^2}. \quad (18.69)$$

The cross sections given in eqs. (18.68) and (18.69) are plotted in Fig. 18.4 as functions of θ_1 .

18.3. Acoustically hard cone

18.3.1. Point sources

For a point source at (r_0, θ_0, ϕ_0) , such that

$$V^i = \frac{e^{ikR}}{kR}, \quad (18.70)$$

the total field is (CARSLAW [1914], FELSEN [1957a]):

$$V^i + V^s = \frac{1}{\pi} \sum_{m=0}^{\infty} \epsilon_m \cos m(\phi - \phi_0) \int_C dv (2v+1) j_v(kr_<) h_v^{(1)}(kr_>) G_2, \quad (18.71)$$

where

$$\begin{aligned} G_2 &= -\frac{1}{2}\pi \frac{\Gamma(v+m+1) P_v^{-m}(\cos \theta_<)}{\Gamma(v-m+1) \sin(v-m)\pi} \\ &\times \left[P_v^{-m}(-\cos \theta_>) - \frac{(d/d\theta_1) P_v^{-m}(-\cos \theta_>)}{(d/d\theta_1) P_v^{-m}(\cos \theta_1)} P_v^{-m}(\cos \theta_>) \right] \end{aligned} \quad (18.72)$$

and C is the contour shown in Fig. 18.2. An alternative representation of the total field as an eigenfunction expansion is (CARSLAW [1914], FELSEN [1957a]):

$$V^i + V^s = \frac{-2i}{\sin \theta_1} \sum_{m=0}^{\infty} \varepsilon_m \cos m(\phi - \phi_0) \sum_{q \geq 0} (2q+1) j_q(kr_<) h_q^{(1)}(kr_>) \times \frac{P_q^m(\cos \theta) P_q^m(\cos \theta_0)}{P_q^m(\cos \theta_1) (\partial^2 / \partial q \partial \theta_1) P_q^m(\cos \theta_1)}, \quad (18.73)$$

which may be written as

$$V^i + V^s = 2i \sum_{m=0}^{\infty} \varepsilon_m \cos m(\phi - \phi_0) \sum_{q \geq 0} \frac{j_q(kr_<) h_q^{(1)}(kr_>) P_q^m(\cos \theta) P_q^m(\cos \theta_0)}{\int_0^{\theta_1} [P_q^m(\cos \alpha)]^2 \sin \alpha d\alpha}. \quad (18.74)$$

The summations in q extend over all non-negative roots of the equation

$$(\partial / \partial \theta_1) P_q^{-m}(\cos \theta_1) = 0. \quad (18.75)$$

The root $q = 0$ occurs only for $m = 0$ and leads to a term $j_0(kr_<) h_0^{(1)}(kr_>) \operatorname{cosec}^2 \frac{1}{2} \theta$, in the eigenfunction representation of $V^i + V^s$; the remaining roots in q are positive.

Expressions for the total field on the surface are trivially obtainable from eqs. (18.73) and (18.74).

If $kr \ll 1$ and $kr_0 \gg 1$, the representation in eq. (18.73) is rapidly convergent and the dominant terms lead to

$$V^i + V^s \sim \frac{e^{ikr_0}}{kr_0} \left[\frac{-\sqrt{\pi} e^{-\frac{1}{2} i q_1 \pi} \cos(\phi - \phi_0) (kr)^{q_1}}{\sin \theta_1 2^{q_1-2} \Gamma(q_1 + \frac{1}{2})} \times \frac{P_{q_1}^1(\cos \theta) P_{q_1}^1(\cos \theta_0)}{P_{q_1}^1(\cos \theta_1) (\partial^2 / \partial q_1 \partial \theta_1) P_{q_1}^1(\cos \theta_1)} + 1 \right], \quad (18.76)$$

where q_1 denotes the first zero of $(\partial / \partial \theta_1) P_q^1(\cos \theta_1)$ and $0 < q_1 < 1$ for $90^\circ < \theta_1 < 180^\circ$. The above equation makes explicit the behavior of the field near the tip.

In the region $\theta + \theta_0 < 2\theta_1 - \pi$, which excludes the domain of reflected waves, the scattered field is (FELSEN [1957a]):

$$V^s = \frac{\pi^2}{2k \sqrt{rr_0}} \sum_{m=0}^{\infty} \varepsilon_m \cos m(\phi - \phi_0) \int_0^{\infty} dx x \frac{\tanh \pi x}{\cosh \pi x} e^{-x\pi} H_{ix}^{(1)}(kr) H_{ix}^{(1)}(kr_0) \times \frac{K_x^m(\cos \theta) K_x^m(\cos \theta_0) (d/d\theta_1) K_x^m(-\cos \theta_1)}{\Gamma(\frac{1}{2} + m + ix) \Gamma(\frac{1}{2} + m - ix) (d/d\theta_1) K_x^m(\cos \theta_1)}; \quad (18.77)$$

and for $kr_> \gg kr_< \gg 1$ with $\theta + \theta_0$ not too close to $2\theta_1 - \pi$ (FELSEN [1957b], see also KETTER et al. [1956], example 8):

$$V^s \sim \frac{e^{ik(r+r_0)}}{k^2 rr_0} \left[1 + \sum_{n=1}^{\infty} \frac{1}{(2ikr_<)^n n!} \prod_{s=1}^n \{s(s-1) + B\} \right] S, \quad (18.78)$$

where

$$S = -i\pi \sum_{m=0}^{\infty} \varepsilon_m \cos m(\phi - \phi_0) \times \int_0^{\infty} dx x \frac{\tanh \pi x}{\cosh \pi x} \frac{K_x^m(\cos \theta) K_x^m(\cos \theta_0) (d/d\theta_1) K_x^m(-\cos \theta_1)}{\Gamma(\frac{1}{2} + m + ix) \Gamma(\frac{1}{2} + m - ix) (d/d\theta_1) K_x^m(\cos \theta_1)}, \quad (18.79)$$

and B is the Beltrami operator

$$B = \frac{1}{\sin \theta} \frac{\partial}{\partial \theta} \sin \theta \frac{\partial}{\partial \theta} + \frac{1}{\sin^2 \theta} \frac{\partial^2}{\partial \phi^2}.$$

The field in eq. (18.78) has the appearance of a spherical wave emanating from the cone tip. For a thin cone ($\theta_1 \approx \pi$):

$$\begin{aligned} S \approx & \frac{2i \sin^2 \frac{1}{2} \delta}{(\cos \theta + \cos \theta_0)^3} [1 + \cos \theta \cos \theta_0 + 2 \cos(\phi - \phi_0) \sin \theta \sin \theta_0] (1 + \sin^2 \frac{1}{2} \delta) + \\ & + \frac{4i \sin^4 \frac{1}{2} \delta}{(\cos \theta + \cos \theta_0)^3} \left[\cos \theta \cos \theta_0 - 3 - \frac{6 \sin^2 \theta \sin^2 \theta_0}{(\cos \theta + \cos \theta_0)^2} \right] [\log(\sin^2 \frac{1}{2} \delta) - \frac{1}{2}] + \\ & + \frac{8i \sin^4 \frac{1}{2} \delta}{(\cos \theta + \cos \theta_0)^5} \cos(\phi - \phi_0) \sin \theta \sin \theta_0 [4(1 + \cos \theta \cos \theta_0) + \\ & + \sin^2 \theta + \sin^2 \theta_0] [\log(\sin^2 \frac{1}{2} \delta) + \frac{1}{2}] - \\ & - \pi i \sin^4 \frac{1}{2} \delta \int_0^{\infty} dx x \frac{\tanh \pi x}{\cosh \pi x} (x^2 + \frac{1}{4})^2 K_x(\cos \theta) K_x(\cos \theta_0) f(x) + \\ & + 2i\pi \sin^4 \frac{1}{2} \delta \cos(\phi - \phi_0) \int_0^{\infty} dx x \frac{\tanh \pi x}{\cosh \pi x} (x^2 + \frac{1}{4}) K_x^1(\cos \theta) K_x^1(\cos \theta_0) f(x) + \\ & + \frac{24i \sin^4 \frac{1}{2} \delta}{(\cos \theta + \cos \theta_0)^5} \cos 2(\phi - \phi_0) \sin^2 \theta \sin^2 \theta_0, \end{aligned} \quad (18.80)$$

where $f(x)$ is defined by

$$\begin{aligned} f(x) &= 4(1 - \log 2) + 2x^2 F(x), \\ F(x) &= \sum_{n=1}^{\infty} (n + \frac{1}{2})^{-1} [(n + \frac{1}{2})^2 + x^2]^{-1}. \end{aligned} \quad (18.81)$$

The definite integrals appearing in eq. (18.80) have not been evaluated in terms of known functions. However, they are amenable to numerical calculation since the integrands are positive real functions of x that decay exponentially for large x . In addition, upper and lower bounds may be placed on the integrals since

$$0 \leq f(x) - f(0) \leq 2x^2 F(0),$$

where $F(0) = 0.4144 \dots$. If δ is sufficiently small to warrant the omission of higher

order terms, eq. (18.80) reduces to the first order approximation given by FELSEN [1957a, b]:

$$S \approx \frac{2i \sin^2 \frac{1}{2}\delta}{(\cos \theta + \cos \theta_0)^3} [1 + \cos \theta \cos \theta_0 + 2 \cos (\phi - \phi_0) \sin \theta \sin \theta_0]. \quad (18.82)$$

If, on the other hand, $\theta \approx 0$ and $\theta_0 \approx 0$, eq. (18.80) may be approximated by

$$S \approx \frac{1}{2}i \sin^2 \frac{1}{2}\delta [1 + 2 \sin^2 \frac{1}{2}\theta + 2 \sin^2 \frac{1}{2}\theta_0 + 4 \sin^2 \frac{1}{2}\delta (1 - \log \sin \frac{1}{2}\delta) + 4 \cos (\phi - \phi_0) \sin \frac{1}{2}\theta \sin \frac{1}{2}\theta_0] - i\pi \sin^4 \frac{1}{2}\delta \int_0^\infty dx x \frac{\tanh \pi x}{\cosh \pi x} (x^2 + \frac{1}{4})^2 f(x). \quad (18.83)$$

For a point source on the axis of symmetry ($\theta_0 = 0$), eq. (18.71) reduces to (CARSLAW [1914], FELSEN [1955]):

$$V^i + V^s = -\frac{1}{2} \int_C dv \frac{2v+1}{\sin v\pi} j_v(kr_<) h_v^{(1)}(kr_>) \left[P_v(-\cos \theta) + \frac{P_v^1(-\cos \theta_1)}{P_v^1(\cos \theta_1)} P_v(\cos \theta) \right], \quad (18.84)$$

while eqs. (18.73) and (18.74) simplify respectively to

$$V^i + V^s = -\frac{2i}{\sin \theta_1} \sum_{q=0}^\infty \frac{(2q+1) j_q(kr_<) h_q^{(1)}(kr_>) P_q(\cos \theta)}{P_q(\cos \theta_1) (\partial/\partial q) P_q^1(\cos \theta_1)}, \quad (18.85)$$

$$V^i + V^s = 2i \sum_{q=0}^\infty \frac{j_q(kr_<) h_q^{(1)}(kr_>) P_q(\cos \theta)}{\int_0^{\theta_1} [P_q(\cos \alpha)]^2 \sin \alpha d\alpha}, \quad (18.86)$$

where the summations extend over the non-negative zeros q of $P_q^1(\cos \theta_1)$. The series expansion of eq. (18.85) dates back to CARSLAW [1914].

For $\theta_0 = 0$, in the region $\theta < 2\theta_1 - \pi$, the scattered field is:

$$V^s = \frac{-\pi}{2k\sqrt{rr_0}} \int_0^\infty dx x \tanh \pi x e^{-x\pi} H_{ix}^{(1)}(kr) H_{ix}^{(1)}(kr_0) K_x(\cos \theta) \frac{K_x^1(-\cos \theta_1)}{K_x^1(\cos \theta_1)}, \quad (18.87)$$

and the quantity S appearing in eq. (18.78), which determines the diffracted field due to the cone tip, becomes

$$S = i \int_0^\infty dx x \tanh \pi x K_x(\cos \theta) \frac{K_x^1(-\cos \theta_1)}{K_x^1(\cos \theta_1)}. \quad (18.88)$$

The approximations to S in eqs. (18.80), (18.82) and (18.83) remain valid for $\theta_0 = 0$. In particular, for a thin cone ($\theta_1 \approx \pi$), eq. (18.82) becomes

$$S \approx \frac{1}{2}i \sin^2 \frac{1}{2}\delta \sec^4 \frac{1}{2}\theta. \quad (18.89)$$

FELSEN [1959] has treated the two dimensional problem of a radiating ring source coaxial with the cone axis (see Fig. 18.3). The total field \tilde{U} due to a sinusoidal ring

source of radius $a = r_0 \sin \theta_0$ is given by eqs. (18.22) and (18.23) and by eq. (18.24) in which G_1 is replaced by G_2 . Explicitly,

$$\dot{V} = 2a \begin{Bmatrix} \cos m\phi \\ \sin m\phi \end{Bmatrix} \int_C dv (2v+1) j_v(kr_<) h_v^{(1)}(kr_>) G_2, \quad (18.90)$$

where C is the contour shown in Fig. 18.2 and G_2 is defined as in eq. (18.72).

For $kr \gg kr_0 \gg 1$, a convenient decomposition of the total field is

$$\dot{V} = \dot{V}_d + \dot{V}_{g.o.} + \dot{V}_{tr.} \quad (18.91)$$

where \dot{V}_d is the diffracted field due to the cone tip and $\dot{V}_{g.o.}$ is the total geometrical optics field. The remaining term $\dot{V}_{tr.}$ is a transition field that provides a continuous field behavior across the various geometrical optics boundaries where the diffracted wave becomes singular and the reflected waves undergo finite jump discontinuities. A creeping wave contribution to the far field is absent as a consequence of the special ring source excitation. In the region $\theta + \theta_0 < 2\theta_1 - \pi$ outside the domain of specular reflections, the diffracted field in the far zone is (FELSEN, [1959]):

$$\begin{aligned} \dot{V}_d \sim 2\pi^2 a \begin{Bmatrix} \cos m\phi \\ \sin m\phi \end{Bmatrix} \frac{e^{ik(r+r_0)}}{ik^2 r r_0} \\ \times \int_0^{\infty} dx x \frac{\tanh \pi x}{\cosh \pi x} \frac{K_x^m(\cos \theta) K_x^m(\cos \theta_0) (d/d\theta_1) K_x^m(-\cos \theta_1)}{\Gamma(\frac{1}{2} + m + ix) \Gamma(\frac{1}{2} + m - ix) (d/d\theta_1) K_x^m(\cos \theta_1)}. \end{aligned} \quad (18.92)$$

Although the above integral is convergent only for $\theta + \theta_0 < 2\theta_1 - \pi$, FELSEN [1959] has shown that the angular dependence of the far-zone diffracted field must be the same for all angles in $0 \leq (\theta, \theta_0) \leq \theta_1$. In principle, therefore, one may calculate the diffracted field from its integral representation (18.92) valid for the restricted range of angles and then employ the resulting closed form expression everywhere. In practice, however, the integral is difficult to evaluate (even approximately) in terms of known functions, and a closed form expression valid for all angles is not available. For $(\sin \theta, \sin \theta_0, \sin \theta_1) \neq 0$ the geometrical optics and transition fields are given by (FELSEN [1959]):

$$\begin{aligned} \dot{V}_{g.o.} + \dot{V}_{tr.} \sim \frac{-ae^{i(kr - \frac{1}{2}\pi)}}{kr \sqrt{2\pi k r_0 \sin \theta \sin \theta_0}} \begin{Bmatrix} \cos m\phi \\ \sin m\phi \end{Bmatrix} \\ \times [I(r_0, \pi - |\theta - \theta_0|) + I(r_0, \pi - 2\theta_1 + \theta + \theta_0) - \\ - i(-1)^m \{I(r_0, \pi - \theta - \theta_0) + I(r_0, \pi - 2\theta_1 + \theta - \theta_0) + I(r_0, \pi - 2\theta_1 + \theta_0 - \theta)\}], \end{aligned} \quad (18.93)$$

where $I(r_0, x)$ is defined by eqs. (18.28) through (18.31). This result is valid only if both source and observer are located away from the axis of the cone and provided the cone apex angle is not small. If any of these restrictions are relaxed, different asymptotic expansions of the field must be obtained; for example, if $\theta \approx 0$ the dominant geometrical optics result is (FELSEN [1959]):

$$\begin{aligned}
 V_{\text{g.o.}} \sim & \frac{2\pi a}{kr} e^{i(kr - \frac{1}{2}\pi m)} \left\{ \frac{\cos m\phi}{\sin m\phi} \right\} \left\{ \exp \{-ikr_0 \cos \theta \cos \theta_0\} J_m(kr_0 \sin \theta \sin \theta_0) + \right. \\
 & + \left. \sqrt{\frac{\sin(2\theta_1 - \theta_0)}{\sin \theta_0}} \exp \{-ikr_0 \cos \theta \cos(2\theta_1 - \theta_0)\} \right. \\
 & \left. \times J_m[kr_0 \sin \theta \sin(2\theta_1 - \theta_0)] \eta(\pi - 2\theta_1 + \theta_0) \right\}. \quad (18.94)
 \end{aligned}$$

18.3.2. Plane wave incidence

For a plane wave incident from the direction θ_0, ϕ_0 , such that

$$V^i = \exp \{-ikr[\sin \theta \sin \theta_0 \cos(\phi - \phi_0) + \cos \theta \cos \theta_0]\}, \quad (18.95)$$

the total field is (FELSEN [1957a]):

$$V^i + V^s = \frac{1}{i\pi} \sum_{m=0}^{\infty} \varepsilon_m \cos m(\phi - \phi_0) \int_C dv (2v+1) e^{-\frac{1}{2}iv\pi} j_v(kr) G_2, \quad (18.96)$$

where

$$\begin{aligned}
 G_2 = & -\frac{1}{2}\pi \frac{\Gamma(v+m+1)P_v^{-m}(\cos \theta_0)}{\Gamma(v-m+1)\sin(v-m)\pi} \\
 & \times \left[P_v^{-m}(-\cos \theta_0) - \frac{(d/d\theta_1)P_v^{-m}(-\cos \theta_1)}{(d/d\theta_1)P_v^{-m}(\cos \theta_1)} P_v^{-m}(\cos \theta_0) \right] \quad (18.97)
 \end{aligned}$$

and C is the contour shown in Fig. 18.2. An alternative representation of the total field as an eigenfunction expansion is (FELSEN [1957a]):

$$\begin{aligned}
 V^i + V^s = & \frac{-2}{\sin \theta_1} \sum_{m=0}^{\infty} \varepsilon_m \cos m(\phi - \phi_0) \sum_{q=0}^{\infty} (2q+1) e^{-\frac{1}{2}iq\pi} j_q(kr) \\
 & \times \frac{P_q^m(\cos \theta) P_q^m(\cos \theta_0)}{P_q^m(\cos \theta_1) (\partial/\partial \theta_1) P_q^m(\cos \theta_1)}, \quad (18.98)
 \end{aligned}$$

which may be written as

$$V^i + V^s = 2 \sum_{m=0}^{\infty} \varepsilon_m \cos m(\phi - \phi_0) \sum_{q=0}^{\infty} \frac{e^{-\frac{1}{2}iq\pi} j_q(kr) P_q^m(\cos \theta) P_q^m(\cos \theta_0)}{\int_0^{\theta_1} [P_q^m(\cos \alpha)]^2 \sin \alpha d\alpha}. \quad (18.99)$$

The summations in q extend over all non-negative roots of the equation

$$(\partial/\partial \theta_1) P_q^{-m}(\cos \theta_1) = 0. \quad (18.100)$$

The root $q = 0$ occurs only for $m = 0$ and leads to a term $j_0(kr) \operatorname{cosec}^2 \frac{1}{2}\theta_1$ in the eigenfunction representation of $V^i + V^s$; the remaining roots in q are positive.

Expressions for the total field on the surface are trivially obtainable from eqs. (18.98) and (18.99).

If $kr \ll 1$, the representation in eq. (18.98) is rapidly convergent and the dominant terms lead to

$$V^i + V^s \sim -\frac{\sqrt{\pi} e^{-\frac{1}{2} i q_1 \pi} \cos(\phi - \phi_0) (kr)^{q_1}}{\sin \theta_1 2^{q_1-2} \Gamma(q_1 + \frac{1}{2})} \frac{P_{q_1}^1(\cos \theta) P_{q_1}^1(\cos \theta_0)}{P_{q_1}^1(\cos \theta_1) (\partial^2 / \partial q_1 \partial \theta_1) P_{q_1}^1(\cos \theta_1)} + 1, \quad (18.101)$$

where q_1 denotes the first zero of $(\partial / \partial \theta_1) P_{q_1}^1(\cos \theta_1)$ and $0 < q_1 < 1$ for $90^\circ < \theta_1 < 180^\circ$. The above equation makes explicit the behavior of the field near the tip.

In the region $\theta + \theta_0 < 2\theta_1 - \pi$, which excludes the domain of reflected waves, the scattered field is (FELSEN [1957a]):

$$V^s = \pi \sqrt{\frac{\pi}{2kr}} e^{-\frac{1}{2} i \pi} \sum_{m=0}^{\infty} \varepsilon_m \cos m(\phi - \phi_0) \int_0^{\infty} dx x \frac{\tanh \pi x}{\cosh \pi x} e^{-\frac{1}{2} x \pi} H_{ix}^{(1)}(kr) \\ \times \frac{K_x^m(\cos \theta) K_x^m(\cos \theta_0) (d/d\theta_1) K_x^m(-\cos \theta_1)}{\Gamma(\frac{1}{2} + m + ix) \Gamma(\frac{1}{2} + m - ix) (d/d\theta_1) K_x^m(\cos \theta_1)}; \quad (18.102)$$

and for $kr \gg 1$ with $\theta + \theta_0$ not too close to $2\theta_1 - \pi$ (FELSEN [1957b], see also KELLER et al. [1956], example 8):

$$V^s \sim \frac{e^{i kr}}{kr} \left[1 + \sum_{n=1}^{\infty} \frac{1}{(2ikr)^n n!} \prod_{s=1}^n \{s(s-1) + B\} \right] S, \quad (18.103)$$

where S is defined as in eq. (18.79), namely

$$S = -i\pi \sum_{m=0}^{\infty} \varepsilon_m \cos m(\phi - \phi_0) \int_0^{\infty} dx x \frac{\tanh \pi x}{\cosh \pi x} \\ \times \frac{K_x^m(\cos \theta) K_x^m(\cos \theta_0) (d/d\theta_1) K_x^m(-\cos \theta_1)}{\Gamma(\frac{1}{2} + m + ix) \Gamma(\frac{1}{2} + m - ix) (d/d\theta_1) K_x^m(\cos \theta_1)}, \quad (18.104)$$

and B is the Beltrami operator

$$B = \frac{1}{\sin \theta} \frac{\partial}{\partial \theta} \sin \theta \frac{\partial}{\partial \theta} + \frac{1}{\sin^2 \theta} \frac{\partial^2}{\partial \phi^2}.$$

The field in eq. (18.103) has the appearance of a spherical wave emanating from the cone tip. For a thin cone ($\theta_1 \approx \pi$), approximations to S are given by eqs. (18.80) through (18.83); in particular, the first order approximation is (FELSEN [1957a, b]):

$$S \approx \frac{2i \sin^2 \frac{1}{2} \delta}{(\cos \theta + \cos \theta_0)^3} [1 + \cos \theta \cos \theta_0 + 2 \cos(\phi - \phi_0) \sin \theta \sin \theta_0]. \quad (18.105)$$

Equation (18.105) does not account for the singularity in V^s as $(\theta + \theta_0) \rightarrow \pi$; in this case it is necessary to include the accompanying geometrical optics and transition fields. For a thin cone ($\theta_1 \approx \pi$) and $kr \gg 1$, the scattered field may be decomposed as

$$V^s = V_d + V_{\text{refl.}} + V_{\text{tr.}}, \quad (18.106)$$

where V_d is the diffracted field due to the cone tip, $V_{\text{refl.}}$ is the field reflected from the surface of the cone according to the laws of geometrical optics, and $V_{\text{tr.}}$ is a transition field that provides a continuous field behavior across the geometrical optics boundary $\theta = \pi - \theta_0$. The diffracted field to first order is obtained from eqs. (18.103) and (18.105):

$$V_d \sim \frac{e^{ikr}}{kr} \frac{2i \sin^2 \frac{1}{2}\delta}{(\cos \theta + \cos \theta_0)^3} [1 + \cos \theta \cos \theta_0 + 2 \cos(\phi - \phi_1) \sin \theta \sin \theta_0]; \quad (18.107)$$

and, provided $kr \sin^2 \frac{1}{2}\delta \ll 1$ and $(\sin \theta, \sin \theta_0) \neq 0$, the reflected and transition fields are given by:

$$\begin{aligned} V_{\text{refl.}} + V_{\text{tr.}} \sim & \frac{-e^{-\frac{1}{2}i\pi} \sin^2 \frac{1}{2}\delta}{(2\pi kr \sin \theta \sin \theta_0)^{\frac{1}{2}}} \left[\frac{\partial^2}{\partial \alpha^2} + \frac{1}{8}(\cot \theta + \cot \theta_0) \frac{\partial}{\partial \alpha} + \right. \\ & \left. + \frac{3}{8}(1 + \frac{3}{16} \cot^2 \theta + \frac{3}{16} \cot^2 \theta_0) + \frac{1}{64} \cot \theta \cot \theta_0 \right] I(r, \alpha) - \\ & - \frac{2e^{-\frac{1}{2}i\pi} \sin^2 \frac{1}{2}\delta \cos(\phi - \phi_0)}{(2\pi kr \sin \theta \sin \theta_0)^{\frac{1}{2}}} \left[\frac{\partial^2}{\partial \alpha^2} - \frac{3}{8}(\cot \theta + \cot \theta_0) \frac{\partial}{\partial \alpha} - \right. \\ & \left. - \frac{1}{8}(1 + \frac{5}{16} \cot^2 \theta + \frac{5}{16} \cot^2 \theta_0) + \frac{9}{64} \cot \theta \cot \theta_0 \right] I(r, \alpha), \end{aligned} \quad (18.108)$$

where $\alpha = \theta + \theta_0 - \pi$ and $I(r, \alpha)$ is defined by eqs. (18.47) through (18.50). Equation (18.108) is valid provided both source and observer are away from the cone axis. Such a restriction is no problem if both source and observer are located within the backward cone because in this instance only the diffraction term contributes significantly to the far field. If, on the other hand, either the source or observer is near the surface of the cone itself, eq. (18.108) is not valid. On the boundary $\theta = \pi - \theta_0$:

$$\begin{aligned} V^s \sim & \sqrt{\frac{\pi}{2kr}} e^{ikr - \frac{1}{2}i\pi} \frac{kr \sin^2 \frac{1}{2}\delta}{\sin \theta_0} \left\{ 1 + \frac{i}{8kr} (3 + \cot^2 \theta_0) + \right. \\ & \left. + 2 \cos(\phi - \phi_0) \left[1 - \frac{i}{8kr} (1 + 3 \cot^2 \theta_0) \right] \right\}. \end{aligned} \quad (18.109)$$

For a plane wave incident along the axis of symmetry $\theta_0 = 0$, such that

$$V^i = e^{-ikr \cos \theta}, \quad (18.110)$$

eq. (18.96) reduces to (FELSEN [1955]):

$$V^i + V^s = \frac{1}{2} i \int_C dv \frac{2v+1}{\sin v\pi} e^{-\frac{1}{2}i\pi} j_v(kr) \left[P_v(-\cos \theta) + \frac{P_v^1(-\cos \theta_1)}{P_v^1(\cos \theta_1)} P_v(\cos \theta) \right], \quad (18.111)$$

while eqs. (18.98) and (18.99) simplify respectively to (SIEGEL and ALPERIN [1952], FELSEN [1955]):

$$V^i + V^s = \frac{2}{\sin \theta_1} \sum_{q=0}^{\infty} (2q+1) e^{-\frac{1}{2}iq\pi} j_q(kr) \frac{P_q(\cos \theta)}{P_q(\cos \theta_1) (\partial/\partial q) P_q^1(\cos \theta_1)}, \quad (18.112)$$

$$V^i + V^s = 2 \sum_{q=0}^{\infty} \frac{e^{-\frac{1}{2}iq\pi} j_q(kr) P_q(\cos \theta)}{\int_0^{\theta_1} [P_q(\cos \alpha)]^2 \sin \alpha d\alpha}, \quad (18.113)$$

where the summations extend over the non-negative zeros q of $P_q^1(\cos \theta_1)$.

For $\theta_0 = 0$, in the region $\theta < 2\theta_1 - \pi$, the scattered field is

$$V^s = - \sqrt{\frac{\pi}{2kr}} e^{-\frac{1}{2}i\pi} \int_0^{\infty} dx x \tanh \pi x e^{-\frac{1}{2}ix\pi} H_{ix}^{(1)}(kr) K_x(\cos \theta) \frac{K_x^1(-\cos \theta_1)}{K_x^1(\cos \theta_1)}, \quad (18.114)$$

and the quantity S appearing in eq. (18.103), which determines the diffracted field due to the cone tip, becomes

$$S = i \int_0^{\infty} dx x \tanh \pi x K_x(\cos \theta) \frac{K_x^1(-\cos \theta_1)}{K_x^1(\cos \theta_1)}. \quad (18.115)$$

The approximations to S in eqs. (18.80), (18.82) and (18.83) remain valid for $\theta_0 = 0$. In particular, for a thin cone ($\theta_1 \approx \pi$), eq. (18.82) becomes

$$S \approx \frac{1}{2}i \sin^2 \frac{1}{2}\delta \sec^4 \frac{1}{2}\theta. \quad (18.116)$$

For $\theta_0 = 0$ and $kr \gg 1$, the scattered field may be decomposed as in eq. (18.106) with the diffracted field given by:

$$V_d \sim \frac{e^{ikr}}{kr} S \quad (18.117)$$

where S is obtained from eq. (18.115). Although the integral in eq. (18.115) is convergent only for $\theta < 2\theta_1 - \pi$, it can be shown by a proof paralleling FELSEN [1959] that the angular dependence of the far zone diffracted field must be the same for all angles in $0 \leq \theta \leq \theta_1$. In principle, therefore, one may calculate the diffracted field from the integral in eq. (18.115) valid for the restricted range of angles and then employ the resulting closed form expression everywhere. In practice, however, the integral is difficult to evaluate in terms of known functions, and a closed form expression valid for all angles is not available. For $(\sin \theta, \sin \theta_1) \neq 0$, the reflected and transition fields are given by:

$$V_{\text{refl.}} + V_{\text{tr.}} \sim \frac{i}{\sin \theta} \left(\frac{\partial}{\partial \alpha} + \frac{1}{4} \cot \theta_1 + \frac{1}{8} \cot \theta \right) T(r, \alpha), \quad (18.118)$$

where $\alpha = \pi - 2\theta_1 + \theta$ and $T(r, \alpha)$ is defined by eqs. (18.60) through (18.63). The transition function properly compensates for the singularity at $\theta = 2\theta_1 - \pi$ in the

diffracted wave term and for the jump discontinuity in the reflected wave. Away from the geometrical optics boundary $\theta = 2\theta_1 - \pi$, such that $(kr \sin^2 \alpha) \gg 1$, the reflected field is

$$V_{\text{refl.}} \sim \eta(\alpha) \sqrt{\frac{\sin \alpha}{\sin \theta}} e^{ikr \cos \alpha} \left\{ 1 + \frac{i}{kr} \left(\frac{3 \cot \theta_1}{4 \sin \alpha} + \frac{\cot \theta}{8 \sin \alpha} - \frac{\cot \alpha}{8 \sin \alpha} \right) + O \left[\frac{1}{(kr)^2} \right] \right\}, \quad (18.119)$$

and for $\theta = \theta_1$ (observer on the cone surface):

$$V^i + V_{\text{refl.}} \sim e^{-ikr \cos \theta_1} \left\{ 2 + \frac{i}{kr} \frac{\cot \theta_1}{\sin \theta_1} + O \left[\frac{1}{(kr)^2} \right] \right\}. \quad (18.120)$$

It should be emphasized that the above results are valid only if the observer is located away from the axis of the cone and provided the cone apex angle is not small.

For $\theta_0 = 0$, $\theta = 0$, the backscattered far field is (see also, FELSEN [1958]):

$$V^{\text{BS}} = -\frac{e^{ikr}}{ikr} \int_0^\pi dx x \tanh \pi x \frac{K_x^1(-\cos \theta_1)}{K_x^1(\cos \theta_1)} - \frac{e^{-\frac{1}{2}i\pi}}{\sqrt{2\pi kr}} \left(\frac{\partial}{\partial \alpha} + \frac{1}{4} \cot \theta_1 \right) I(r, \alpha), \quad (18.121)$$

where $\alpha = \pi - 2\theta_1$ and $I(r, \alpha)$ is defined by eqs. (18.47) through (18.50). The term involving $I(r, \alpha)$ is important only for a wide cone $\theta_1 \approx \frac{1}{2}\pi$, in which case both source and observer lie in a transition region. For $\theta_1 \approx \frac{1}{2}\pi$, a first order result is given by (FELSEN [1955], see also FELSEN [1953]):

$$\begin{aligned} V^{\text{BS}} &\sim e^{ikr \sin \theta_1} [1 - \sqrt{2\pi} e^{-\frac{1}{2}i\pi} w G(w)], & w < 4 \\ V^{\text{BS}} &\sim -\frac{e^{ikr}}{ikr} \frac{1}{(2\theta_1 - \pi)^2}, & w \geq 4 \end{aligned} \quad (18.122)$$

where $w = -\sqrt{kr \cos \theta_1}$ and $G(w)$ is as defined in eq. (18.50). A plot of the magnitude and phase of the quantity in brackets in eq. (18.122) is provided in Section 18.5, Fig. 18.17b. It may be noted that when $\theta_1 = \frac{1}{2}\pi$, eq. (18.122) yields a back scattered plane wave appropriate to reflection from an infinite plane. For a thin cone ($\theta_1 \approx \pi$), eqs. (18.80), (18.82) and (18.83) remain valid for $\theta_0 = 0$, $\theta = 0$.

For $\theta_0 = 0$ and for a wide cone $\theta_1 \approx \frac{1}{2}\pi$, the back scattering cross section is, from eq. (18.122) (FELSEN [1953, 1955]):

$$\sigma \approx \frac{\lambda^2}{\pi(2\theta_1 - \pi)^4}, \quad (18.123)$$

whereas, for a thin cone $\theta_1 \approx \pi$, eq. (18.116) leads to (FELSEN [1953, 1955]):

$$\sigma \approx \frac{\lambda^2(\pi - \theta_1)^2}{64\pi}. \quad (18.124)$$

A more general expression for the back scattering cross section is given by (SCHENSTED [1953], SINGH et al. [1953a], SINGH et al. [1955b]):

$$\sigma = \frac{\lambda^2}{\pi} \left| \sum_q \frac{e^{-iq\pi}}{\int_0^{\delta_1} [P_q(\cos \alpha)]^2 \sin \alpha d\alpha} \right|^2, \quad (18.125)$$

where the summation is over the non-negative zeros of $P_q^1(\cos \theta_1)$, but only a finite number of terms must be included since the infinite series diverges. Despite this drawback, special summation techniques have been employed (SCHENSTED [1953], SIEGEL et al. [1953a], SIEGEL et al. [1955b]) to yield second order results in the wide cone and thin cone approximations: for a wide cone $\theta_1 \approx \frac{1}{2}\pi$,

$$\sigma \approx \frac{\lambda^2(1 - 4 \cos^2 \theta_1)}{16\pi \cos^4 \theta_1} \quad (18.126)$$

and for a thin cone ($\theta_1 \approx \pi$),

$$\sigma \approx \frac{\lambda^2}{4\pi} \sin^4 \frac{1}{2}\delta [1 - 2 \sin^2 \frac{1}{2}\delta (1 + 4 \log \sin \frac{1}{2}\delta)]. \quad (18.127)$$

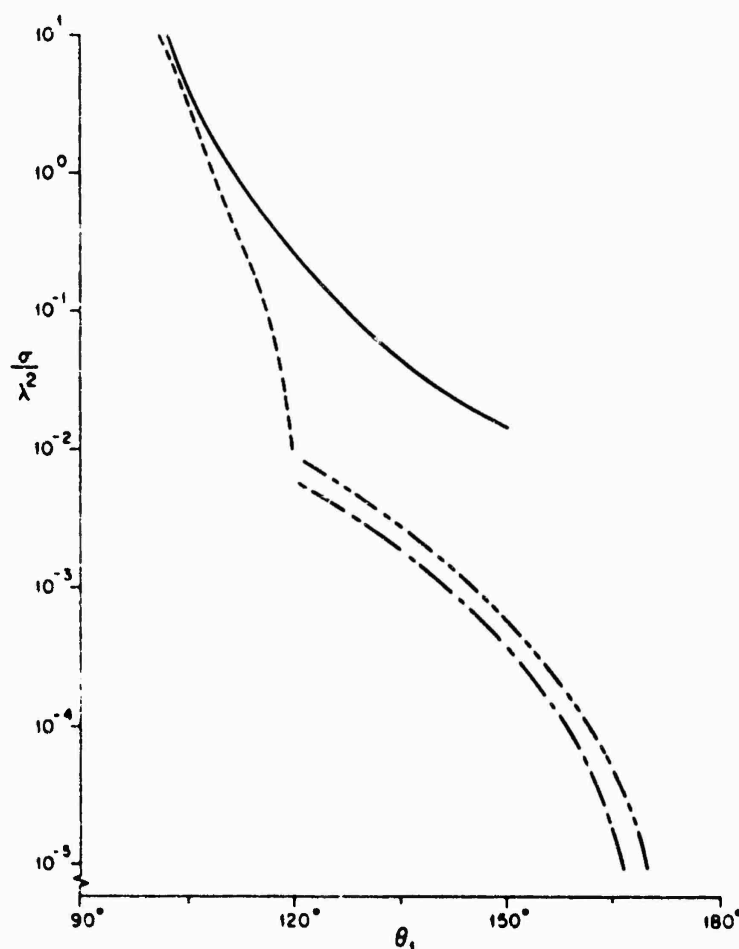


Fig. 18.5. Normalized nose-on back scattering cross section $\sigma \lambda^2$ as a function of θ_1 for a hard cone: (—) first order and (---) second order theory for wide cone, (-.-) first order and (----) second order theory for thin cone.

In the case of a thin cone, however, eq. (18.83) leads to

$$\sigma \approx \frac{\lambda^2}{4\pi} \sin^4 \frac{1}{2}\delta \left[1 + 8 \sin^2 \frac{1}{2}\delta (1 - \log \sin \frac{1}{2}\delta) - 4\pi \sin^2 \frac{1}{2}\delta \int_0^\infty dx x \frac{\tanh \pi x}{\cosh \pi x} (x^2 + \frac{1}{4})^2 f(x) \right], \quad (18.128)$$

where $f(x)$ is defined in eq. (18.81). Equations (18.127) and (18.128) have not been shown to be in agreement; the difficulty lies in evaluating the definite integral in eq. (18.128). The cross sections given in eqs. (18.126) and (18.127), as well as the first order approximations of eqs. (18.123) and (18.124) are plotted in Fig. 18.5 as functions of θ_1 .

18.4. Perfectly conducting cone

18.4.1. Electric dipole sources

For an arbitrarily oriented electric dipole at (r_0, θ_0, ϕ_0) with moment $(4\pi\epsilon/k)\hat{e}$, the total electromagnetic field is

$$\begin{aligned} E^i(\mathbf{r}) + E^s(\mathbf{r}) &= 4\pi k \mathcal{G}_e(\mathbf{r}|\mathbf{r}_0) \cdot \hat{e}, \\ H^i(\mathbf{r}) + H^s(\mathbf{r}) &= -4\pi i Y \nabla \wedge \mathcal{G}_e(\mathbf{r}|\mathbf{r}_0) \cdot \hat{e}, \end{aligned} \quad (18.129)$$

where \hat{e} is an arbitrary unit vector and $\mathcal{G}_e(\mathbf{r}|\mathbf{r}_0)$ is the electric dyadic Green function for the cone:

$$\begin{aligned} \frac{4\pi}{k} \mathcal{G}_e(\mathbf{r}|\mathbf{r}_0) &= \left\{ \frac{\hat{\theta}}{\sin \theta} \frac{\partial}{\partial \phi} - \hat{\phi} \frac{\partial}{\partial \theta} \right\} \left\{ \frac{\hat{\theta}_0}{\sin \theta_0} \frac{\partial}{\partial \phi_0} - \hat{\phi}_0 \frac{\partial}{\partial \theta_0} \right\} U_2 + \\ &+ \left\{ \rho \left(\frac{\partial^2}{\partial r^2} + k^2 \right) + \frac{\hat{\theta}}{r} \frac{\partial^2}{\partial r \partial \theta} + \frac{\hat{\phi}}{r \sin \theta} \frac{\partial^2}{\partial r \partial \phi} \right\} \left\{ \rho_0 \left(\frac{\partial^2}{\partial r_0^2} + k^2 \right) + \right. \\ &+ \left. \frac{\hat{\theta}_0}{r_0} \frac{\partial^2}{\partial r_0 \partial \theta_0} + \frac{\hat{\phi}_0}{r_0 \sin \theta_0} \frac{\partial^2}{\partial r_0 \partial \phi_0} \right\} \frac{r r_0 U_1}{k^2}, \end{aligned} \quad (18.130)$$

and where $\nabla \wedge \mathcal{G}_e(\mathbf{r}|\mathbf{r}_0)$ is given by:

$$\begin{aligned} \frac{4\pi}{k^2} \nabla \wedge \mathcal{G}_e(\mathbf{r}|\mathbf{r}_0) &= \left\{ \rho \left(\frac{\partial^2}{\partial r^2} + k^2 \right) + \frac{\hat{\theta}}{r} \frac{\partial^2}{\partial r \partial \theta} + \frac{\hat{\phi}}{r \sin \theta} \frac{\partial^2}{\partial r \partial \phi} \right\} \left\{ \frac{\hat{\theta}_0}{\sin \theta_0} \frac{\partial}{\partial \phi_0} - \right. \\ &- \left. \hat{\phi}_0 \frac{\partial}{\partial \theta_0} \right\} \frac{r U_1}{k} + \left\{ \frac{\hat{\theta}}{\sin \theta} \frac{\partial}{\partial \phi} - \hat{\phi} \frac{\partial}{\partial \theta} \right\} \left\{ \rho_0 \left(\frac{\partial^2}{\partial r_0^2} + k^2 \right) + \right. \\ &+ \left. \frac{\hat{\theta}_0}{r_0} \frac{\partial^2}{\partial r_0 \partial \theta_0} + \frac{\hat{\phi}_0}{r_0 \sin \theta_0} \frac{\partial^2}{\partial r_0 \partial \phi_0} \right\} \frac{r_0 U_1}{k}. \end{aligned} \quad (18.131)$$

In eqs. (18.130) and (18.131) the scalar functions U_1 and U_2 are (FELSEN [1957a]):

$$U_{1,2} = \frac{i}{\pi} \sum_{m=0}^{\infty} \epsilon_m \cos m(\phi - \phi_0) \int_C dv \frac{2v+1}{v(v+1)} J_v(kr_<) h_v^{(1)}(kr_>) G_{1,2}, \quad (18.132)$$

where

$$G_1 = -\frac{1}{2}\pi \frac{\Gamma(\nu+m+1)P_\nu^{-m}(\cos \theta_<)}{\Gamma(\nu-m+1)\sin(\nu-m)\pi} \times \left[P_\nu^{-m}(-\cos \theta_>) - \frac{P_\nu^{-m}(-\cos \theta_1)}{P_\nu^{-m}(\cos \theta_1)} P_\nu^{-m}(\cos \theta_>) \right], \quad (18.133)$$

$$G_2 = -\frac{1}{2}\pi \frac{\Gamma(\nu+m+1)P_\nu^{-m}(\cos \theta_<)}{\Gamma(\nu-m+1)\sin(\nu-m)\pi} \times \left[P_\nu^{-m}(-\cos \theta_>) - \frac{\frac{d}{d\theta_1} P_\nu^{-m}(-\cos \theta_1)}{\frac{d}{d\theta_1} P_\nu^{-m}(\cos \theta_1)} P_\nu^{-m}(\cos \theta_>) \right], \quad (18.134)$$

and C' is the contour shown in Fig. 18.6. Alternative representations of U_1 and U_2

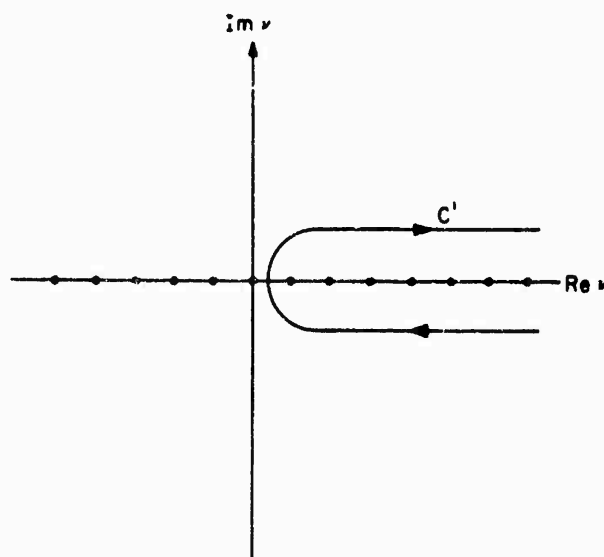


Fig. 18.6. Contour of integration C' encircling the positive poles in the ν -plane.

as eigenfunction expansions are (BAILIN and SILVER [1956]):

$$U_1 = \frac{2i}{\sin \theta_1} \sum_{m=0}^{\infty} \epsilon_m \cos m(\phi - \phi_0) \sum_{p>0} \frac{2p+1}{p(p+1)} j_p(kr_<) h_p^{(1)}(kr_>) \times \frac{P_p^m(\cos \theta) P_p^m(\cos \theta_0)}{(\partial/\partial \theta_1) P_p^m(\cos \theta_1) (\partial/\partial p) P_p^m(\cos \theta_1)}, \quad (18.135)$$

$$U_2 = \frac{-2i}{\sin \theta_1} \sum_{m=0}^{\infty} \epsilon_m \cos m(\phi - \phi_0) \sum_{q>0} \frac{2q+1}{q(q+1)} j_q(kr_<) h_q^{(1)}(kr_>) \times \frac{P_q^m(\cos \theta) P_q^m(\cos \theta_0)}{P_q^m(\cos \theta_1) (\partial^2/\partial q \partial \theta_1) P_q^m(\cos \theta_1)}, \quad (18.136)$$

which may also be written as (TAI [1954], BAILIN and SILVER [1956]):

$$U_1 = 2i \sum_{m=0}^{\infty} \varepsilon_m \cos m(\phi - \phi_0) \sum_{p>0} \frac{j_p(kr_<)h_p^{(1)}(kr_>)P_p^m(\cos \theta)P_p^m(\cos \theta_0)}{p(p+1) \int_0^{\theta_1} [P_p^m(\cos x)]^2 \sin x dx}, \quad (18.137)$$

$$U_2 = 2i \sum_{m=0}^{\infty} \varepsilon_m \cos m(\phi - \phi_0) \sum_{q>0} \frac{j_q(kr_<)h_q^{(1)}(kr_>)P_q^m(\cos \theta)P_q^m(\cos \theta_0)}{q(q+1) \int_0^{\theta_1} [P_q^m(\cos x)]^2 \sin x dx}. \quad (18.138)$$

The summations in p and q extend over all positive roots, respectively, of the equations

$$\begin{aligned} P_p^{-m}(\cos \theta_1) &= 0, \\ (\partial/\partial \theta_1)P_q^{-m}(\cos \theta_1) &= 0. \end{aligned} \quad (18.139)$$

If $kr \ll 1$ and $kr_0 \gg 1$, the representations in eqs. (18.135) and (18.136) are rapidly convergent and the dominant terms lead to

$$E^i + E^s \sim \frac{ike^{ikr_0 - \frac{1}{2}ip_1\pi}}{r_0 \sin \theta_1} \frac{\sqrt{\pi}(kr)^{p_1-1}}{2^{p_1-1}\Gamma(p_1 + \frac{1}{2})} \frac{(\hat{p} + (\hat{\theta}/p_1)\partial/\partial \theta)P_{p_1}^1(\cos \theta)P_{p_1}^1(\cos \theta_0)(\hat{\theta}_0 \cdot \hat{e})}{P_{p_1}^1(\cos \theta_1)(\partial/\partial p_1)P_{p_1}^1(\cos \theta_1)}, \quad (18.140)$$

$$\begin{aligned} H^i + H^s &\sim \frac{ikYe^{ikr_0 - \frac{1}{2}iq_1\pi}}{r_0 \sin \theta_1} \frac{\sqrt{\pi}(kr)^{q_1-1}}{2^{q_1-2}\Gamma(q_1 + \frac{1}{2})} \left[P_{q_1}^1(\cos \theta_1) \frac{\partial^2}{\partial q_1 \partial \theta_1} P_{q_1}^1(\cos \theta_1) \right]^{-1} \\ &\times \left[\hat{p} + \frac{\hat{\theta}}{q_1} \frac{\partial}{\partial \theta} + \frac{\hat{\phi}}{q_1 \sin \theta} \frac{\partial}{\partial \phi} \right] \left[\frac{(\hat{\theta}_0 \cdot \hat{e})}{\sin \theta_0} \frac{\partial}{\partial \phi_0} - (\hat{\phi}_0 \cdot \hat{e}) \frac{\partial}{\partial \theta_0} \right] \\ &\times P_{q_1}^1(\cos \theta)P_{q_1}^1(\cos \theta_0) \cos(\phi - \phi_0) \end{aligned} \quad (18.141)$$

where p_1, q_1 denote the first zeros of $P_p(\cos \theta_1)$ and $(\partial/\partial \theta_1)P_q(\cos \theta_1)$, respectively, and $0 < p_1 < 1, 0 < q_1 < 1$ for $90^\circ < \theta_1 < 180^\circ$. The above equations make explicit the behavior of the electromagnetic field near the tip.

For $r \neq r_0$, in the region $(\theta + \theta_0) < (2\theta_1 - \pi)$ which excludes the domain of reflected waves, the scattered portions of the functions U_1 and U_2 may be written as (FELSEN [1957a]):

$$\begin{aligned} U_1 &= -ih_0^{(1)}(kr)h_0^{(1)}(kr_0) \sum_{m=1}^{\infty} \frac{\cos m(\phi - \phi_0)}{m} [\tan \frac{1}{2}\theta \tan \frac{1}{2}\theta_0 \tan^2 \frac{1}{2}(\pi - \theta_1)]^m - \\ &- \frac{\pi^2}{2k\sqrt{rr_0}} \sum_{m=0}^{\infty} \varepsilon_m \cos m(\phi - \phi_0) \int_0^{\infty} \frac{dx x \tanh \pi x}{x^2 + \frac{1}{4} \cosh \pi x} e^{-\lambda x} H_{ix}^{(1)}(kr)H_{ix}^{(1)}(kr_0) \\ &\times \frac{K_x^m(\cos \theta)K_x^m(\cos \theta_0)K_x^m(-\cos \theta_1)}{\Gamma(\frac{1}{2} + m + ix)\Gamma(\frac{1}{2} + m - ix)K_x^m(\cos \theta_1)}. \end{aligned} \quad (18.142)$$

$$\begin{aligned}
U_2 = & i h_0^{(1)}(kr) h_0^{(1)}(kr_0) \sum_{m=1}^{\infty} \frac{\cos m(\phi - \phi_0)}{m} [\tan \frac{1}{2}\theta \tan \frac{1}{2}\theta_0 \tan^2 \frac{1}{2}(\pi - \theta_1)]^m - \\
& - \frac{\pi^2}{2k\sqrt{rr_0}} \sum_{m=0}^{\infty} \varepsilon_m \cos m(\phi - \phi_0) \int_0^{\infty} \frac{dx x}{x^2 + \frac{1}{4}} \frac{\tanh \pi x}{\cosh \pi x} e^{-x^2} H_{ix}^{(1)}(kr) H_{ix}^{(1)}(kr_0) \\
& \times \frac{K_x^m(\cos \theta) K_x^m(\cos \theta_0) (d/d\theta_1) K_x^m(-\cos \theta_1)}{\Gamma(\frac{1}{2} + m + ix) \Gamma(\frac{1}{2} + m - ix) (d/d\theta_1) K_x^m(\cos \theta_1)}; \quad (18.143)
\end{aligned}$$

and for $kr_+ \gg kr_- \gg 1$, with $(\theta + \theta_0)$ not too close to $(2\theta_1 - \pi)$ (FELSEN [1957b]):

$$U_{1,2} \sim \frac{e^{ik(r+r_0)}}{k^2 r r_0} \left[1 + \sum_{n=1}^{\infty} \frac{1}{(2ikr_-)^n n!} \prod_{s=1}^n \{s(s-1) + B\} \right] R_{1,2}, \quad (18.144)$$

where

$$\begin{aligned}
R_1 = & i \sum_{m=1}^{\infty} \frac{\cos m(\phi - \phi_0)}{m} [\tan \frac{1}{2}\theta \tan \frac{1}{2}\theta_0 \tan^2 \frac{1}{2}(\pi - \theta_1)]^m + \\
& + \pi i \sum_{m=0}^{\infty} \varepsilon_m \cos m(\phi - \phi_0) \int_0^{\infty} \frac{dx x}{x^2 + \frac{1}{4}} \frac{\tanh \pi x}{\cosh \pi x} \\
& \times \frac{K_x^m(\cos \theta) K_x^m(\cos \theta_0) K_x^m(-\cos \theta_1)}{\Gamma(\frac{1}{2} + m + ix) \Gamma(\frac{1}{2} + m - ix) K_x^m(\cos \theta_1)}, \quad (18.145)
\end{aligned}$$

$$\begin{aligned}
R_2 = & -i \sum_{m=1}^{\infty} \frac{\cos m(\phi - \phi_0)}{m} [\tan \frac{1}{2}\theta \tan \frac{1}{2}\theta_0 \tan^2 \frac{1}{2}(\pi - \theta_1)]^m + \\
& + \pi i \sum_{m=1}^{\infty} \varepsilon_m \cos m(\phi - \phi_0) \int_0^{\infty} \frac{dx x}{x^2 + \frac{1}{4}} \frac{\tanh \pi x}{\cosh \pi x} \\
& \times \frac{K_x^m(\cos \theta) K_x^m(\cos \theta_0) (d/d\theta_1) K_x^m(-\cos \theta_1)}{\Gamma(\frac{1}{2} + m + ix) \Gamma(\frac{1}{2} + m - ix) (d/d\theta_1) K_x^m(\cos \theta_1)}, \quad (18.146)
\end{aligned}$$

and B is the Beltrami operator

$$B = \frac{1}{\sin \theta} \frac{\partial}{\partial \theta} \sin \theta \frac{\partial}{\partial \theta} + \frac{1}{\sin^2 \theta} \frac{\partial^2}{\partial \phi^2}.$$

Equation (18.144) leads to an electromagnetic field that has the appearance of a spherical wave emanating from the cone tip. Since

$$\left[\frac{1}{\sin \theta} \frac{\partial}{\partial \theta} \sin \theta \frac{\partial}{\partial \theta} - \frac{m^2}{\sin^2 \theta} \right] \tan^m \frac{1}{2}\theta = 0, \quad (18.147)$$

the summations involving $\tan^m \frac{1}{2}\theta$ in eqs. (18.145) and (18.146) contribute only to the leading order term in eq. (18.144). In the case of a thin cone ($\theta_1 \approx \pi$), a first order approximation to R_1 and R_2 is (FELSEN [1957a, b]):

$$R_1 \approx i \sin^2 \frac{1}{2} \delta \tan \frac{1}{2} \theta \tan \frac{1}{2} \theta_0 \left(1 + \frac{2}{\cos \theta + \cos \theta_0} \right) \cos (\phi - \phi_0), \quad (18.148)$$

$$R_2 \approx -i \sin^2 \frac{1}{2} \delta \left\{ \frac{1}{\cos \theta + \cos \theta_0} + \tan \frac{1}{2} \theta \tan \frac{1}{2} \theta_0 \left(1 + \frac{2}{\cos \theta + \cos \theta_0} \right) \cos (\phi - \phi_0) \right\}.$$

For a radial electric dipole at (r_0, θ_0, ϕ_0) with moment $(4\pi\epsilon/k)\hat{r}_0$, the total field is

$$\begin{aligned} E^i + E^s &= \left\{ \hat{r} \left(\frac{\partial^2}{\partial r^2} + k^2 \right) + \frac{\hat{\theta}}{r} \frac{\partial^2}{\partial r \partial \theta} + \frac{\hat{\phi}}{r \sin \theta} \frac{\partial^2}{\partial r \partial \phi} \right\} \frac{r(V^i + V^s)}{r_0}, \\ H^i + H^s &= -ikY \left\{ \frac{\hat{\theta}}{\sin \theta} \frac{\partial}{\partial \phi} - \hat{\phi} \frac{\partial}{\partial \theta} \right\} \frac{V^i + V^s}{r_0}, \end{aligned} \quad (18.149)$$

where $V^i + V^s$ is the point source solution for an acoustically soft cone (see Section 18.2.1). The particular case of a radial dipole located on the axis of symmetry ($\theta_0 = 0$) was treated by MACDONALD [1902]. If the radial dipole is on the surface ($\theta_0 = \theta_1$), the total field is zero everywhere.

For a dipole on the surface ($\theta_0 = \theta_1$) with $\hat{e} = \hat{\theta}_1$, the non-zero components of the total far field are

$$\begin{aligned} E_\theta = ZH_\phi &= \frac{2ie^{ikr}}{rr_0 \sin \theta_1} \sum_{m=0}^{\infty} \epsilon_m \cos m(\phi - \phi_0) \sum_{p>0} \frac{2p+1}{p(p+1)} e^{-\frac{1}{2}ip\pi} \frac{\partial}{\partial r_0} [r_0 j_p(kr_0)] \\ &\times \frac{(\partial/\partial \theta)P_p^m(\cos \theta)}{(\partial/\partial p)P_p^m(\cos \theta_1)} - \frac{4ke^{ikr}}{r \sin \theta \sin^2 \theta_1} \sum_{m=1}^{\infty} m^2 \cos m(\phi - \phi_0) \\ &\times \sum_{q>0} \frac{2q+1}{q(q+1)} e^{-\frac{1}{2}iq\pi} j_q(kr_0) \frac{P_q^m(\cos \theta)}{(\partial^2/\partial q \partial \theta_1)P_q^m(\cos \theta_1)}, \end{aligned} \quad (18.150)$$

$$\begin{aligned} E_\phi = -ZH_\theta &= \frac{-4ie^{ikr}}{rr_0 \sin \theta \sin \theta_1} \sum_{m=1}^{\infty} m \sin m(\phi - \phi_0) \sum_{p>0} \frac{2p+1}{p(p+1)} e^{-\frac{1}{2}ip\pi} \\ &\times \frac{\partial}{\partial r_0} [r_0 j_p(kr_0)] \frac{P_p^m(\cos \theta)}{(\partial/\partial p)P_p^m(\cos \theta_1)} + \frac{4ke^{ikr}}{r \sin^2 \theta_1} \sum_{m=1}^{\infty} m \sin m(\phi - \phi_0) \\ &\times \sum_{q>0} \frac{2q+1}{q(q+1)} e^{-\frac{1}{2}iq\pi} j_q(kr_0) \frac{(\partial/\partial \theta)P_q^m(\cos \theta)}{(\partial^2/\partial q \partial \theta_1)P_q^m(\cos \theta_1)}. \end{aligned} \quad (18.151)$$

If a circumferential dipole (that is, $\hat{e} = \hat{\phi}_0$) is on the surface, the total field is zero everywhere.

For an x -directed dipole of moment $(4\pi\epsilon/k)\hat{x}$ located on the axis of symmetry at $(r_0, 0, 0)$, the incident field is

$$\begin{aligned} E_r^i &= \frac{e^{ikR}}{kR} \left[\frac{r(r-r_0 \cos \theta)}{R} \left(\frac{3}{R^3} - \frac{3ik}{R^2} - \frac{k^2}{R} \right) + \frac{ik}{R} - \frac{1}{R^2} + k^2 \right] \sin \theta \cos \phi, \\ E_\theta^i &= \frac{e^{ikR}}{kR} \left[\frac{rr_0 \sin \theta}{R} \left(\frac{3}{R^3} - \frac{3ik}{R^2} - \frac{k^2}{R} \right) \sin \theta + \left(\frac{ik}{R} - \frac{1}{R^2} + k^2 \right) \cos \theta \right] \cos \phi, \\ E_\phi^i &= -\frac{e^{ikR}}{kR} \left(\frac{ik}{R} - \frac{1}{R^2} + k^2 \right) \sin \phi, \end{aligned} \quad (18.152)$$

$$H_r^i = ikY \frac{e^{ikR}}{kR} \left(\frac{ik}{R} - \frac{1}{R^2} \right) r_0 \sin \theta \sin \phi,$$

$$H_\theta^i = -ikY \frac{e^{ikR}}{kR} \left(\frac{ik}{R} - \frac{1}{R^2} \right) (r \cos \theta - r_0) \sin \phi,$$

$$H_\phi^i = -ikY \frac{e^{ikR}}{kR} \left(\frac{ik}{R} - \frac{1}{R^2} \right) (r \cos \theta - r_0) \cos \phi,$$

and the total field is

$$\begin{aligned} E^i + E^s = & \left\{ \hat{\theta} \frac{\cos \phi}{\sin \theta} - \hat{\phi} \sin \phi \frac{\partial}{\partial \theta} \right\} k^2 A_2 + \\ & + \left\{ \hat{r} \cos \phi \left(\frac{\partial^2}{\partial r^2} + k^2 \right) + \hat{\theta} \frac{\cos \phi}{r} \frac{\partial^2}{\partial r \partial \theta} - \hat{\phi} \frac{\sin \phi}{r \sin \theta} \frac{\partial}{\partial r} \right\} \frac{r}{r_0} \frac{\partial}{\partial r_0} (r_0 A_1), \end{aligned} \quad (18.153)$$

$$\begin{aligned} H^i + H^s = & -ikY \left\{ \hat{r} \sin \phi \left(\frac{\partial^2}{\partial r^2} + k^2 \right) + \hat{\theta} \frac{\sin \phi}{r} \frac{\partial^2}{\partial r \partial \phi} + \hat{\phi} \frac{\cos \phi}{r \sin \theta} \frac{\partial}{\partial r} \right\} (r A_2) + \\ & + ikY \left\{ \hat{\theta} \frac{\sin \phi}{\sin \theta} + \hat{\phi} \cos \phi \frac{\partial}{\partial \theta} \right\} \frac{1}{r_0} \frac{\partial}{\partial r_0} (r_0 A_1), \end{aligned}$$

where

$$A_1 = \frac{1}{2} \int_{C'} dv \frac{2v+1}{v(v+1)} \frac{j_v(kr_<) h_v^{(1)}(kr_>)}{\sin v\pi} \left[P_v^1(-\cos \theta) - \frac{P_v^1(-\cos \theta_1)}{P_v^1(\cos \theta_1)} P_v^1(\cos \theta) \right], \quad (18.154)$$

$$\begin{aligned} A_2 = & \frac{1}{2} \int_{C'} dv \frac{2v+1}{v(v+1)} \frac{j_v(kr_<) h_v^{(1)}(kr_>)}{\sin v\pi} \\ & \times \left[P_v^1(-\cos \theta) - \frac{(d/d\theta_1) P_v^1(-\cos \theta_1)}{(d/d\theta_1) P_v^1(\cos \theta_1)} P_v^1(\cos \theta) \right], \end{aligned} \quad (18.155)$$

and C' is the contour shown in Fig. 18.6. Alternative representations of A_1 and A_2 as eigenfunction expansions are

$$A_1 = \frac{2i}{\sin \theta_1} \sum_{p>0} (2p+1) j_p(kr_<) h_p^{(1)}(kr_>) \frac{P_p^1(\cos \theta)}{(\partial/\partial \theta_1) P_p^1(\cos \theta_1) (\partial/\partial p) P_p^1(\cos \theta_1)}, \quad (18.156)$$

$$A_2 = \frac{-2i}{\sin \theta_1} \sum_{q>0} (2q+1) j_q(kr_<) h_q^{(1)}(kr_>) \frac{P_q^1(\cos \theta_1)}{P_q^1(\cos \theta_1) (\partial^2/\partial q \partial \theta_1) P_q^1(\cos \theta_1)}, \quad (18.157)$$

which may also be written as

$$A_1 = 2i \sum_{p>0} \frac{j_p(kr_<) h_p^{(1)}(kr_>) P_p^1(\cos \theta)}{\int_0^{\theta_1} [P_p^1(\cos \alpha)]^2 \sin \alpha d\alpha}, \quad (18.158)$$

$$A_2 = 2i \sum_{q>0} \frac{j_q(kr_<)h_q^{(1)}(kr_>)P_q^1(\cos \theta)}{\int_0^{\theta_1} [P_q^1(\cos \alpha)]^2 \sin \alpha d\alpha}. \quad (18.159)$$

The summations in p and q extend over the positive zeros of $P_p^1(\cos \theta_1)$ and $(\partial/\partial \theta_1)P_q^1(\cos \theta_1)$, respectively.

For $r \neq r_0$, in the region $\theta < 2\theta_1 - \pi$, the scattered portions of A_1 and A_2 may be written as:

$$A_1^s = -\frac{1}{2}ih_0^{(1)}(kr)h_0^{(1)}(kr_0) \tan \frac{1}{2}\theta \tan^2 \frac{1}{2}(\pi - \theta_1) + \\ + \frac{\pi}{2k\sqrt{rr_0}} \int_0^\infty \frac{dx x}{x^2 + \frac{1}{4}} \tanh \pi x e^{-x\pi} H_{ix}^{(1)}(kr) H_{ix}^{(1)}(kr_0) K_x^1(\cos \theta) \frac{K_x^1(-\cos \theta_1)}{K_x^1(\cos \theta_1)}, \quad (18.160)$$

$$A_2^s = \frac{1}{2}ih_0^{(1)}(kr)h_0^{(1)}(kr_0) \tan \frac{1}{2}\theta \tan^2 \frac{1}{2}(\pi - \theta_1) + \\ + \frac{\pi}{2k\sqrt{rr_0}} \int_0^\infty \frac{dx x}{x^2 + \frac{1}{4}} \tanh \pi x e^{-x\pi} H_{ix}^{(1)}(kr) H_{ix}^{(1)}(kr_0) K_x^1(\cos \theta) \\ \times \frac{(d/d\theta_1)K_x^1(-\cos \theta_1)}{(d/d\theta_1)K_x^1(\cos \theta_1)}; \quad (18.161)$$

and for $kr_> \gg kr_< \gg 1$, with $\theta + \theta_0$ not too close to $2\theta_1 - \pi$:

$$A_{1,2}^s \sim \frac{e^{ik(r+r_0)}}{k^2 rr_0} \left[1 + \sum_{n=1}^\infty \frac{1}{(2ikr_<)^n n!} \prod_{s=1}^n \{s(s-1) + B(1)\} \right] \Gamma_{1,2}, \quad (18.162)$$

where

$$\Gamma_1 = \frac{1}{2}i \tan \frac{1}{2}\theta \tan^2 \frac{1}{2}(\pi - \theta_1) - i \int_0^\infty \frac{dx x}{x^2 + \frac{1}{4}} \tanh \pi x K_x^1(\cos \theta) \frac{K_x^1(-\cos \theta_1)}{K_x^1(\cos \theta_1)}, \quad (18.163)$$

$$\Gamma_2 = -\frac{1}{2}i \tan \frac{1}{2}\theta \tan^2 \frac{1}{2}(\pi - \theta_1) - i \int_0^\infty \frac{dx x}{x^2 + \frac{1}{4}} \tanh \pi x K_x^1(\cos \theta) \frac{(d/d\theta_1)K_x^1(-\cos \theta_1)}{(d/d\theta_1)K_x^1(\cos \theta_1)}. \quad (18.164)$$

and $B(1)$ is the operator

$$B(1) = \frac{1}{\sin \theta} \frac{\partial}{\partial \theta} \sin \theta \frac{\partial}{\partial \theta} - \frac{1}{\sin^2 \theta}. \quad (18.165)$$

Equation (18.162) again leads to an electromagnetic field that has the appearance of a spherical wave emanating from the cone tip. For a thin cone ($\theta_1 \approx \pi$), a first order approximation to Γ_1 and Γ_2 is

$$\Gamma_1 \approx -\Gamma_2 \approx \frac{1}{2}i \sin^2 \frac{1}{2}\delta \tan \frac{1}{2}\theta (2 + \tan^2 \frac{1}{2}\theta). \quad (18.166)$$

18.4.2. Magnetic dipole sources

For an arbitrarily oriented magnetic dipole at (r_0, θ_0, ϕ_0) with moment $(4\pi/k)\hat{c}$, the total electromagnetic field is

$$\begin{aligned} H^i(r) + H^s(r) &= 4\pi k \mathcal{G}_m(r|r_0) \cdot \hat{c}, \\ E^i(r) + E^s(r) &= 4\pi i Z \nabla \wedge \mathcal{G}_m(r|r_0) \cdot \hat{c}, \end{aligned} \quad (18.167)$$

where \hat{c} is an arbitrary unit vector and $\mathcal{G}_m(r|r_0)$ is the magnetic dyadic Green function for the cone:

$$\begin{aligned} \frac{4\pi}{k} \mathcal{G}_m(r|r_0) &= \left\{ \frac{\hat{\theta}}{\sin \theta} \frac{\partial}{\partial \phi} - \hat{\phi} \frac{\partial}{\partial \theta} \right\} \left\{ \frac{\hat{\theta}_0}{\sin \theta_0} \frac{\partial}{\partial \phi_0} - \hat{\phi}_0 \frac{\partial}{\partial \theta_0} \right\} U_1 + \\ &+ \left\{ \hat{r} \left(\frac{\partial^2}{\partial r^2} + k^2 \right) + \frac{\hat{\theta}}{r} \frac{\partial^2}{\partial r \partial \theta} + \frac{\hat{\phi}}{r \sin \theta} \frac{\partial^2}{\partial r \partial \phi} \right\} \left\{ \hat{r}_0 \left(\frac{\partial^2}{\partial r_0^2} + k^2 \right) + \right. \\ &+ \left. \frac{\hat{\theta}_0}{r_0} \frac{\partial^2}{\partial r_0 \partial \theta_0} + \frac{\hat{\phi}_0}{r_0 \sin \theta_0} \frac{\partial^2}{\partial r_0 \partial \phi_0} \right\} \frac{r r_0 U_2}{k^2}, \end{aligned} \quad (18.168)$$

and where $\nabla \wedge \mathcal{G}_m(r|r_0)$ is given by:

$$\begin{aligned} \frac{4\pi}{k^2} \nabla \wedge \mathcal{G}_m(r|r_0) &= \left\{ \hat{r} \left(\frac{\partial^2}{\partial r^2} + k^2 \right) + \frac{\hat{\theta}}{r} \frac{\partial^2}{\partial r \partial \theta} + \right. \\ &+ \left. \frac{\hat{\phi}}{r \sin \theta} \frac{\partial^2}{\partial r \partial \phi} \right\} \left\{ \frac{\hat{\theta}_0}{\sin \theta_0} \frac{\partial}{\partial \phi_0} - \hat{\phi}_0 \frac{\partial}{\partial \theta_0} \right\} \frac{r U_1}{k} + \\ &+ \left\{ \frac{\hat{\theta}}{\sin \theta} \frac{\partial}{\partial \phi} - \hat{\phi} \frac{\partial}{\partial \theta} \right\} \left\{ \hat{r}_0 \left(\frac{\partial^2}{\partial r_0^2} + k^2 \right) + \frac{\hat{\theta}_0}{r_0} \frac{\partial^2}{\partial r_0 \partial \theta_0} + \frac{\hat{\phi}_0}{r_0 \sin \theta_0} \frac{\partial^2}{\partial r_0 \partial \phi_0} \right\} \frac{r_0 U_2}{k}. \end{aligned} \quad (18.169)$$

The scalar functions U_1 and U_2 are defined in eqs. (18.132) through (18.138).

If $kr \ll 1$ and $kr_0 \ll 1$, the representations in eqs. (18.135) and (18.136) are rapidly convergent and the dominant terms lead to

$$\begin{aligned} H^i + H^s &\sim \frac{-ike^{ikr_0 - i q_1 \pi}}{r_0 \sin \theta_1} \frac{\sqrt{\pi}(kr)^{q_1 - 1}}{2^{q_1 - 1} \Gamma(q_1 + \frac{1}{2})} [P_{q_1}^1(\cos \theta_1) (\partial^2 / \partial q_1 \partial \theta_1) P_{q_1}^1(\cos \theta_1)]^{-1} \\ &\times \left[\hat{r} + \frac{\hat{\theta}}{q_1} \frac{\partial}{\partial \theta} + \frac{\hat{\phi}}{q_1 \sin \theta} \frac{\partial}{\partial \phi} \right] \left[(\hat{\theta}_0 \cdot \hat{c}) \frac{\partial}{\partial \theta_0} + \frac{\hat{\phi}_0 \cdot \hat{c}}{\sin \theta_0} \frac{\partial}{\partial \phi_0} \right] \\ &\times P_{q_1}^1(\cos \theta) P_{q_1}^1(\cos \theta_0) \cos(\phi - \phi_0), \end{aligned} \quad (18.170)$$

$$\begin{aligned} E^i + E^s &\sim \frac{-ikZ e^{ikr_0 - i p_1 \pi}}{r_0 \sin \theta_1} \frac{\sqrt{\pi}(kr)^{p_1 - 1}}{2^{p_1 - 1} \Gamma(p_1 + \frac{1}{2})} \\ &\times \frac{[\hat{r} + (\hat{\theta}/p_1) \partial/\partial \theta] P_{p_1}(\cos \theta) P_{p_1}^1(\cos \theta_0) (\hat{\phi}_0 \cdot \hat{c})}{P_{p_1}^1(\cos \theta_1) (\partial/\partial p_1) P_{p_1}(\cos \theta_1)}, \end{aligned} \quad (18.171)$$

where p_1 and q_1 denote the first zeros of $P_p(\cos \theta_1)$ and $(\partial/\partial \theta_1)P_q^1(\cos \theta_1)$, respectively, and $0 < p_1 < 1$, $0 < q_1 < 1$ for $90^\circ < \theta_0 < 180^\circ$. The above equations make explicit the behavior of the electromagnetic field near the tip.

For the region $\theta + \theta_0 < 2\theta_1 - \pi$ which excludes the domain of reflected waves, exact and approximate expressions for the scattered portions of U_1 and U_2 are given in eqs. (18.142) through (18.148).

For a radial magnetic dipole at (r_0, θ_0, ϕ_0) with moment $(4\pi/k)\hat{p}_0$, the total field is

$$\begin{aligned} H^i + H^s &= \left\{ \hat{p} \left(\frac{\partial^2}{\partial r^2} + k^2 \right) + \frac{\hat{\theta}}{r} \frac{\partial^2}{\partial r \partial \theta} + \frac{\hat{\phi}}{r \sin \theta} \frac{\partial^2}{\partial r \partial \phi} \right\} \frac{r(V^i + V^s)}{r_0}, \\ E^i + E^s &= ikZ \left\{ \frac{\hat{\theta}}{\sin \theta} \frac{\partial}{\partial \phi} - \hat{\phi} \frac{\partial}{\partial \theta} \right\} \frac{V^i + V^s}{r_0}, \end{aligned} \quad (18.172)$$

where $V^i + V^s$ is the point source solution for an acoustically hard cone (see Section 18.3.1.).

For a radial dipole ($\hat{e} = \hat{p}_0$) on the surface ($\theta_0 = \theta_1$), the field components in the far zone are

$$\begin{aligned} H_\theta &= -YE_\phi = \frac{-2ie^{ikr}}{rr_0 \sin \theta_1} \sum_{m=0}^{\infty} \varepsilon_m \cos m(\phi - \phi_0) \sum_{q>0} (2q+1) e^{-\frac{1}{2}iq\pi} j_q(kr_0) \\ &\quad \times \frac{(\partial/\partial \theta)P_q^m(\cos \theta)}{(\partial^2/\partial \theta \partial \theta_1)P_q^m(\cos \theta_1)}, \\ H_\phi &= YE_\theta = \frac{4ie^{ikr}}{rr_0 \sin \theta \sin \theta_1} \sum_{m=1}^{\infty} m \sin m(\phi - \phi_0) \sum_{q>0} (2q+1) e^{-\frac{1}{2}iq\pi} j_q(kr_0) \\ &\quad \times \frac{P_q^m(\cos \theta)}{(\partial^2/\partial \theta \partial \theta_1)P_q^m(\cos \theta_1)}, \end{aligned} \quad (18.173)$$

where the summations in q extend over the positive zeros of $(\partial/\partial \theta_1)P_q^m(\cos \theta_1)$.

For a circumferential dipole ($\hat{e} = \hat{\phi}_0$) on the surface ($\theta_0 = \theta_1$), the field components in the far zone are

$$\begin{aligned} H_\theta &= -YE_\phi = \frac{4ke^{ikr}}{r \sin \theta \sin \theta_1} \sum_{m=1}^{\infty} m \sin m(\phi - \phi_0) \sum_{p>0} \frac{2p+1}{p(p+1)} e^{-\frac{1}{2}ip\pi} j_p(kr_0) \\ &\quad \times \frac{P_p^m(\cos \theta)}{(\partial/\partial \theta)P_p^m(\cos \theta_1)} - \frac{4ie^{ikr}}{rr_0 \sin^2 \theta_1} \sum_{m=1}^{\infty} m \sin m(\phi - \phi_0) \\ &\quad \times \sum_{q>0} \frac{2q+1}{q(q+1)} e^{-\frac{1}{2}iq\pi} \frac{\partial}{\partial r_0} [r_0 j_q(kr_0)] \frac{(\partial/\partial \theta)P_q^m(\cos \theta)}{(\partial^2/\partial \theta \partial \theta_1)P_q^m(\cos \theta_1)}, \end{aligned} \quad (18.174)$$

$$\begin{aligned} H_\phi &= YE_\theta = \frac{2ke^{ikr}}{r \sin \theta_1} \sum_{m=0}^{\infty} \varepsilon_m \cos m(\phi - \phi_0) \sum_{p>0} \frac{2p+1}{p(p+1)} e^{-\frac{1}{2}ip\pi} j_p(kr_0) \\ &\quad \times \frac{(\partial/\partial \theta)P_p^m(\cos \theta)}{(\partial/\partial \theta)P_p^m(\cos \theta_1)} - \frac{4ie^{ikr}}{rr_0 \sin^2 \theta_1 \sin \theta} \sum_{m=1}^{\infty} m^2 \cos m(\phi - \phi_0) \\ &\quad \times \sum_{q>0} \frac{2q+1}{q(q+1)} e^{-\frac{1}{2}iq\pi} \frac{\partial}{\partial r_0} [r_0 j_q(kr_0)] \frac{P_q^m(\cos \theta)}{(\partial^2/\partial \theta \partial \theta_1)P_q^m(\cos \theta_1)}, \end{aligned} \quad (18.175)$$

where the summations in p and q extend over the positive zeros of $P_p^{-m}(\cos \theta_1)$ and $(\partial/\partial \theta_1)P_q^{-m}(\cos \theta_1)$, respectively.

FELSEN [1959] has treated the problem of radiation from a narrow, axially symmetric, circumferential slot (see Fig. 18.7) located on the cone surface far from the

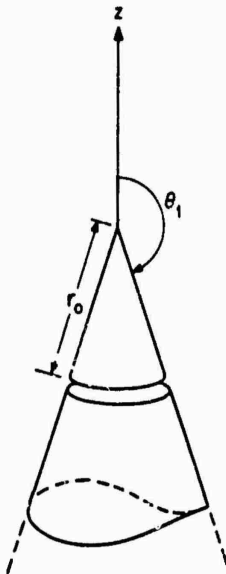


Fig. 18.7. Geometry for radiation from circumferential slot.

tip and excited with an azimuthal electric field distribution E_ϕ whose amplitude varies as $\cos m\phi_0$ or $\sin m\phi_0$. In this case the source distribution may be thought of as a ring of radially directed magnetic dipoles on the cone. Expressions for the dominant geometrical-optics field, including the transition behavior at $\theta \approx \pi - \theta_1$, are presented for $kr \gg kr_0 \gg 1$. The related problem in which the slot is excited with a radial electric aperture field distribution E_r , corresponding to a ring of circumferential dipoles, is also treated. Explicit results are given only for the special case of uniform field excitation ($E_r = 1$), although both the diffracted field (see especially, FELSEN [1957c]) and the geometrical optics contribution, including transition behavior, are considered. For this case of uniform field excitation, BAILIN and SILVER [1956] have computed the field patterns from the exact series representation of the normalized far field component given as (see also VAN BLADEL [1964]):

$$\frac{\hat{E}_\theta}{A} = \sum_{p>0} \frac{2p+1}{p(p+1)} e^{-1/2 p \pi} J_{p+1/2}(kr_0) \frac{(\partial/\partial \theta)P_p(\cos \theta)}{(\partial/\partial \theta_1)P_p(\cos \theta_1)}, \quad (18.176)$$

where the summation extends over the positive zeros of $P_p(\cos \theta_1)$ and

$$A = ikr_0 V_0 \left(\frac{\pi}{2kr_0} \right)^{1/2} \frac{e^{ikr}}{r}, \quad (18.177)$$

with V_0 denoting the constant voltage across the narrow circumferential slot. The field patterns of $|\hat{E}_\theta/A|$ presented by BAILIN and SILVER [1956] for $\theta_1 = 165^\circ$ with

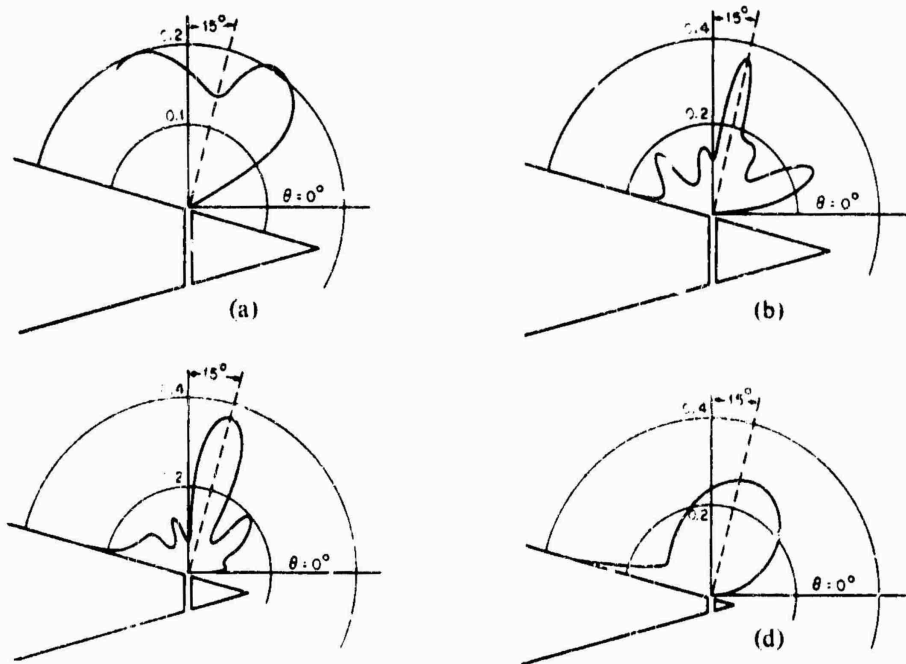


Fig. 18.8. Normalized far-field amplitude $|E_\theta/A|$ for $\theta_1 = 165^\circ$, and (a) $kr_0 = 50\pi$, (b) $kr_0 = 5\pi$, (c) $kr_0 = 3\pi$ and (d) $kr_0 = \pi$ (BAILIN and SILVER [1956]).

$kr_0 = 50\pi, 5\pi, 3\pi$ and π are reproduced in Fig. 18.8. For the case $\theta_1 = 165^\circ$, $kr_0 = 50\pi$ in which the series representation of eq. (18.176) is slowly convergent, the results of BAILIN and SILVER [1956] were found by GOODRICH et al. [1958] to be in good agreement with the simple geometrical optics result:

$$[E_\theta]_{\text{g.o.}} = V_0 \frac{e^{ikr}}{r} \sqrt{\frac{kr_0 \sin \theta_1}{2\pi \sin \theta}} \exp \{-ikr_0 \cos(\theta_1 - \theta) - \frac{1}{4}i\pi\}, \quad \theta > \pi - \theta_0. \quad (18.178)$$

Radiation patterns for other slot excitations and/or configurations located far from the tip are given in GOODRICH et al. [1958] and GOODRICH et al. [1959]. These last references contain refinements to the geometrical-optics approximation based upon an application of Fock theory to the surface of the cone (GOODRICH [1958]) and physical optics for the tip diffraction contribution. Transition phenomena are not taken into account by these methods.

For an x -directed dipole of moment $(4\pi/k)\mathcal{E}$ located on the axis of symmetry at $(r_0, 0, 0)$ the incident field is

$$\begin{aligned} H_r^i &= \frac{e^{ikR}}{kR} \left[\frac{r(r-r_0 \cos \theta)}{R} \left(\frac{3}{R^3} - \frac{3ik}{R^2} - \frac{k^2}{R} \right) + \frac{ik}{R} - \frac{1}{R^2} + k^2 \right] \sin \theta \cos \phi, \\ H_\theta^i &= \frac{e^{ikR}}{kR} \left[\frac{rr_0 \sin \theta}{R} \left(\frac{3}{R^3} - \frac{3ik}{R^2} - \frac{k^2}{R} \right) \sin \theta + \left(\frac{ik}{R} - \frac{1}{R^2} + k^2 \right) \cos \theta \right] \cos \phi, \\ H_\phi^i &= -\frac{e^{ikR}}{kR} \left(\frac{ik}{R} - \frac{1}{R^2} + k^2 \right) \sin \phi, \end{aligned} \quad (18.179)$$

$$E_r^i = -ikZ \frac{e^{ikR}}{kR} \left(\frac{ik}{R} - \frac{1}{R^2} \right) r_0 \sin \theta \sin \phi,$$

$$E_\theta^i = ikZ \frac{e^{ikR}}{kR} \left(\frac{ik}{R} - \frac{1}{R^2} \right) (r - r_0 \cos \theta) \sin \phi,$$

$$E_\phi^i = ikZ \frac{e^{ikR}}{kR} \left(\frac{ik}{R} - \frac{1}{R^2} \right) (r \cos \theta - r_0) \cos \phi,$$

and the total field is

$$\begin{aligned} H^i + H^s &= \left\{ \hat{\theta} \frac{\cos \phi}{\sin \theta} - \hat{\phi} \sin \phi \frac{\partial}{\partial \theta} \right\} k^2 A_1 + \left\{ \hat{r} \cos \phi \left(\frac{\partial^2}{\partial r^2} + k^2 \right) + \right. \\ &\quad \left. + \hat{\theta} \frac{\cos \phi}{r} \frac{\partial^2}{\partial r \partial \theta} - \hat{\phi} \frac{\sin \phi}{r \sin \theta} \frac{\partial}{\partial r} \right\} \frac{r}{r_0} \frac{\partial}{\partial r_0} (r_0 A_2), \\ E^i + E^s &= ikZ \left\{ \hat{r} \sin \phi \left(\frac{\partial^2}{\partial r^2} + k^2 \right) + \hat{\theta} \frac{\sin \phi}{r} \frac{\partial^2}{\partial r \partial \theta} + \hat{\phi} \frac{\cos \phi}{r \sin \theta} \frac{\partial}{\partial r} \right\} (r A_1) - \\ &\quad - ikZ \left\{ \hat{\theta} \frac{\sin \phi}{\sin \theta} + \hat{\phi} \cos \phi \frac{\partial}{\partial \theta} \right\} \frac{1}{r_0} \frac{\partial}{\partial r_0} (r_0 A_2), \end{aligned} \quad (18.180)$$

where the scalar functions A_1 and A_2 are as defined in eqs. (18.154) through (18.159).

For the region $\theta < 2\theta_1 - \pi$ which excludes the domain of reflected waves, exact and approximate expressions for the scattered portions of A_1 and A_2 are given in eqs. (18.160) through (18.166).

18.4.3. Plane wave incidence

For a plane wave of arbitrary polarization incident from the direction θ_0, ϕ_0 , such that (see Fig. 18.1c)

$$\begin{aligned} E^i &= (\hat{\theta}_0 \sin \beta + \hat{\phi}_0 \cos \beta) \exp \{ -ikr[\sin \theta \sin \theta_0 \cos(\phi - \phi_0) + \cos \theta \cos \theta_0] \}, \\ H^i &= Y(\hat{\theta}_0 \cos \beta - \hat{\phi}_0 \sin \beta) \exp \{ -ikr[\sin \theta \sin \theta_0 \cos(\phi - \phi_0) + \cos \theta \cos \theta_0] \}, \end{aligned} \quad (18.181)$$

where

$$\begin{aligned} \hat{\theta}_0 &= \hat{x} \cos \theta_0 \cos \phi_0 + \hat{y} \cos \theta_0 \sin \phi_0 - \hat{z} \sin \theta_0, \\ \hat{\phi}_0 &= -\hat{x} \sin \phi_0 + \hat{y} \cos \phi_0, \end{aligned} \quad (18.182)$$

the total field may be written in terms of the Debye potentials (u, v) as:

$$\begin{aligned} E^i + E^s &= ikZ \left\{ \frac{\hat{\theta}}{\sin \theta} \frac{\partial}{\partial \phi} - \hat{\phi} \frac{\partial}{\partial \theta} \right\} v + \left\{ \hat{r} \left(\frac{\partial^2}{\partial r^2} + k^2 \right) + \frac{\hat{\theta}}{r} \frac{\partial^2}{\partial r \partial \theta} + \frac{\hat{\phi}}{r \sin \theta} \frac{\partial^2}{\partial r \partial \phi} \right\} (ru), \\ H^i + H^s &= \left\{ \hat{r} \left(\frac{\partial^2}{\partial r^2} + k^2 \right) + \frac{\hat{\theta}}{r} \frac{\partial^2}{\partial r \partial \theta} + \frac{\hat{\phi}}{r \sin \theta} \frac{\partial^2}{\partial r \partial \phi} \right\} (rv) - ikY \left\{ \frac{\hat{\theta}}{\sin \theta} - \hat{\phi} \frac{\partial}{\partial \theta} \right\} u. \end{aligned} \quad (18.183)$$

For the cone, the Debye potentials (u, v) are

$$u = \frac{1}{\pi k} \sum_{m=0}^{\infty} \varepsilon_m \int_{C'} dv \frac{2v+1}{v(v+1)} j_v(kr) e^{-\frac{1}{2}iv\pi} \left[m \sin m(\phi - \phi_0) \cos \beta \left(\frac{G_1}{\sin \theta_0} \right) + \cos m(\phi - \phi_0) \sin \beta \left(\frac{\partial G_1}{\partial \theta_0} \right) \right], \quad (18.184)$$

$$v = \frac{Y}{\pi k} \sum_{m=0}^{\infty} \varepsilon_m \int_{C'} dv \frac{2v+1}{v(v+1)} j_v(kr) e^{-\frac{1}{2}iv\pi} \left[\cos m(\phi - \phi_0) \cos \beta \left(\frac{\partial G_2}{\partial \theta_0} \right) - m \sin m(\phi - \phi_0) \sin \beta \left(\frac{G_2}{\sin \theta_0} \right) \right], \quad (18.185)$$

where

$$G_1 = -\frac{1}{2}\pi \frac{\Gamma(v+m+1)P_v^{-m}(\cos \theta_<)}{\Gamma(v-m+1) \sin(v-m)\pi} \times \left[P_v^{-m}(-\cos \theta_>) - \frac{P_v^{-m}(-\cos \theta_1)}{P_v^{-m}(\cos \theta_1)} P_v^{-m}(\cos \theta_>) \right], \quad (18.186)$$

$$G_2 = -\frac{1}{2}\pi \frac{\Gamma(v+m+1)P_v^{-m}(\cos \theta_<)}{\Gamma(v-m+1) \sin(v-m)\pi} \times \left[P_v^{-m}(-\cos \theta_>) - \frac{(d/d\theta_1)P_v^{-m}(-\cos \theta_1)}{(d/d\theta_1)P_v^{-m}(\cos \theta_1)} P_v^{-m}(\cos \theta_>) \right], \quad (18.187)$$

and C' is the contour shown in Fig. 18.6. Alternative representations of (u, v) as eigenfunction expansions are

$$u = \frac{2i}{k \sin \theta_1} \sum_{m=0}^{\infty} \varepsilon_m \sum_{p>0} \frac{2p+1}{p(p+1)} \frac{e^{-\frac{1}{2}ip\pi} j_p(kr) P_p^m(\cos \theta)}{(\partial/\partial \theta_1) P_p^m(\cos \theta_1) (\partial/\partial p) P_p^m(\cos \theta_1)} \times \left[m \sin m(\phi - \phi_0) \cos \beta \frac{P_p^m(\cos \theta_0)}{\sin \theta_0} + \cos m(\phi - \phi_0) \sin \beta \frac{\partial}{\partial \theta_0} P_p^m(\cos \theta_0) \right], \quad (18.188)$$

$$v = \frac{-2iY}{k \sin \theta_1} \sum_{m=0}^{\infty} \varepsilon_m \sum_{q>0} \frac{2q+1}{q(q+1)} \frac{e^{-\frac{1}{2}iq\pi} j_q(kr) P_q^m(\cos \theta)}{P_q^m(\cos \theta_1) (\partial^2/\partial q \partial \theta_1) P_q^m(\cos \theta_1)} \times \left[\cos m(\phi - \phi_0) \cos \beta \frac{\partial}{\partial \theta_0} P_q^m(\cos \theta_0) - m \sin m(\phi - \phi_0) \sin \beta \frac{P_q^m(\cos \theta_0)}{\sin \theta_0} \right], \quad (18.189)$$

which may be written as

$$u = \frac{2i}{k} \sum_{m=0}^{\infty} \varepsilon_m \sum_{p>0} \frac{e^{-\frac{1}{2}ip\pi} j_p(kr) P_p^m(\cos \theta)}{p(p+1) \int_0^{\theta} [P_p^m(\cos \alpha)]^2 \sin \alpha d\alpha} \times \left[m \sin m(\phi - \phi_0) \cos \beta \frac{P_p^m(\cos \theta_0)}{\sin \theta_0} + \cos m(\phi - \phi_0) \sin \beta \frac{\partial}{\partial \theta_0} P_p^m(\cos \theta_0) \right], \quad (18.190)$$

$$v = \frac{2iY}{k} \sum_{m=0}^{\infty} \varepsilon_m \sum_{q>0} \frac{e^{-\frac{1}{2}iq\pi} j_q(kr) P_q^m(\cos \theta)}{q(q+1) \int_0^{\theta_1} [P_q^m(\cos \alpha)]^2 \sin \alpha d\alpha} \\ \times \left[\cos m(\phi - \phi_0) \cos \beta \frac{\partial}{\partial \theta_0} P_q^m(\cos \theta_0) - m \sin m(\phi - \phi_0) \sin \beta \frac{P_q^m(\cos \theta_0)}{\sin \theta_0} \right]. \quad (18.191)$$

The summations in p and q extend over all positive roots, respectively, of the equations

$$P_p^{-m}(\cos \theta_1) = 0, \\ (\partial/\partial \theta_1) P_q^{-m}(\cos \theta_1) = 0. \quad (18.192)$$

On the surface $\theta = \theta_1$:

$$E_{\theta}^i + E_{\theta}^s = \frac{ikZ}{\sin \theta_1} \frac{\partial \Lambda'}{\partial \phi} + \frac{1}{r} \frac{\partial}{\partial r} (r\Lambda), \\ H_{\phi}^i + H_{\phi}^s = \frac{1}{r \sin \theta_1} \frac{\partial^2}{\partial r \partial \phi} (r\Lambda') + ikY\Lambda, \\ H_r^i + H_r^s = \left(\frac{\partial^2}{\partial r^2} + k^2 \right) (r\Lambda'), \quad (18.193)$$

where

$$\Lambda = \frac{2i}{k \sin \theta_1} \sum_{m=0}^{\infty} \varepsilon_m \sum_{p>0} \frac{2p+1}{p(p+1)} \frac{e^{-\frac{1}{2}ip\pi} j_p(kr)}{(\partial/\partial p) P_p^m(\cos \theta_1)} \\ \times \left[m \sin m(\phi - \phi_0) \cos \beta \frac{P_p^m(\cos \theta_0)}{\sin \theta_0} + \cos m(\phi - \phi_0) \sin \beta \frac{\partial}{\partial \theta_0} P_p^m(\cos \theta_0) \right], \\ \Lambda' = \frac{-2iY}{k \sin \theta_1} \sum_{m=0}^{\infty} \varepsilon_m \sum_{q>0} \frac{2q+1}{q(q+1)} \frac{e^{-\frac{1}{2}iq\pi} j_q(kr)}{(\partial^2/\partial q \partial \theta_1) P_q^m(\cos \theta_1)} \\ \times \left[\cos m(\phi - \phi_0) \cos \beta \frac{\partial}{\partial \theta_0} P_q^m(\cos \theta_0) - m \sin m(\phi - \phi_0) \sin \beta \frac{P_q^m(\cos \theta_0)}{\sin \theta_0} \right]. \quad (18.194)$$

If $kr \ll 1$, the representations in eqs. (18.188) and (18.189) are rapidly convergent and the dominant terms lead to

$$E^i + E^s \sim \frac{ie^{-\frac{1}{2}ip_1\pi}}{\sin \theta_1} \frac{\sqrt{\pi}(kr)^{p_1-1}}{2^{p_1-1} \Gamma(p_1 + \frac{1}{2})} \frac{[\hat{p} + (\partial/p_1) \partial/\partial \theta] P_{p_1}(\cos \theta) P_{p_1}^1(\cos \theta_0) \sin \beta}{P_{p_1}^1(\cos \theta_1) (\partial/\partial p_1) P_{p_1}(\cos \theta_1)}, \quad (18.195) \\ H^i + H^s \sim \frac{iY e^{-\frac{1}{2}iq_1\pi}}{\sin \theta_1} \frac{\sqrt{\pi}(kr)^{q_1-1}}{2^{q_1-2} \Gamma(q_1 + \frac{1}{2})} \frac{[P_{q_1}^1(\cos \theta_1) (\partial^2/\partial q_1 \partial \theta_1) P_{q_1}^1(\cos \theta_1)]^{-1}}{\times \left(\hat{p} + \frac{\partial}{q_1} \frac{\partial}{\partial \theta_1} + \frac{\hat{\phi}}{q_1 \sin \theta_1} \frac{\partial}{\partial \phi} \right) \left(\sin \beta \frac{\partial}{\sin \theta_0} \frac{\partial}{\partial \phi_0} - \cos \beta \frac{\partial}{\partial \theta_0} \right)} \\ \times P_{q_1}^1(\cos \theta) P_{q_1}^1(\cos \theta_0) \cos(\phi - \phi_0). \quad (18.196)$$

where p_1, q_1 denote the first zeros of $P_p(\cos \theta_1)$ and $(\partial/\partial \theta_1)P_q^1(\cos \theta_1)$, respectively, and $0 < p_1 < 1, 0 < q_1 < 1$ for $90^\circ < \theta_1 < 180^\circ$. The above equations make explicit the behavior of the electromagnetic field near the tip.

In the region $\theta + \theta_0 < 2\theta_1 - \pi$, which excludes the domain of reflected waves, the scattered portions of (u, v) may be written as:

$$u^s = - \frac{e^{ikr}}{k^2 r \sin \theta_0} \sum_{m=1}^{\infty} \sin \{m(\phi - \phi_0) + \beta\} [\tan \frac{1}{2}\theta \tan \frac{1}{2}\theta_0 \tan^2 \frac{1}{2}(\pi - \theta_1)]^m -$$

$$- \frac{\pi}{k} \sqrt{\frac{\pi}{2kr}} e^{i\pi} \sum_{m=0}^{\infty} \epsilon_m \int_0^{\infty} \frac{dx x \tanh \pi x}{x^2 + \frac{1}{4} \cosh \pi x}$$

$$\times \frac{e^{-\frac{1}{2}\pi} H_{ix}^{(1)}(kr) K_x^m(\cos \theta) K_x^m(-\cos \theta_1)}{\Gamma(\frac{1}{2} + m + ix) \Gamma(\frac{1}{2} + m - ix) K_x^m(\cos \theta_1)}$$

$$\times \left[m \sin m(\phi - \phi_0) \cos \beta \frac{K_x^m(\cos \theta_0)}{\sin \theta_0} + \cos m(\phi - \phi_0) \sin \beta \frac{d}{d\theta_0} K_x^m(\cos \theta_0) \right], \quad (18.197)$$

$$v^s = \frac{Y e^{ikr}}{k^2 r \sin \theta_0} \sum_{m=1}^{\infty} \cos \{m(\phi - \phi_0) + \beta\} [\tan \frac{1}{2}\theta \tan \frac{1}{2}\theta_0 \tan^2 \frac{1}{2}(\pi - \theta_1)]^m -$$

$$- \frac{\pi Y}{k} \sqrt{\frac{\pi}{2kr}} e^{i\pi} \sum_{m=0}^{\infty} \epsilon_m \int_0^{\infty} \frac{dx x \tanh \pi x}{x^2 + \frac{1}{4} \cosh \pi x}$$

$$\times \frac{e^{-\frac{1}{2}\pi} H_{ix}^{(1)}(kr) K_x^m(\cos \theta) (d/d\theta_1) K_x^m(-\cos \theta_1)}{\Gamma(\frac{1}{2} + m + ix) \Gamma(\frac{1}{2} + m - ix) (d/d\theta_1) K_x^m(\cos \theta_1)}$$

$$\times \left[\cos m(\phi - \phi_0) \cos \beta \frac{d}{d\theta_0} K_x^m(\cos \theta_0) - m \sin m(\phi - \phi_0) \sin \beta \frac{K_x^m(\cos \theta_0)}{\sin \theta_0} \right]; \quad (18.198)$$

and for $kr \rightarrow 1$ with $\theta + \theta_0$ not too close to $2\theta_1 - \pi$:

$$(u^s, v^s) \sim \frac{e^{ikr}}{k^2 r} \left[1 + \sum_{n=1}^{\infty} \frac{1}{(2ikr)^n n!} \prod_{s=1}^n \{s(s-1) + B\} \right] (U, V), \quad (18.199)$$

where

$$U = - \frac{1}{\sin \theta_0} \sum_{m=1}^{\infty} \sin \{m(\phi - \phi_0) + \beta\} [\tan \frac{1}{2}\theta \tan \frac{1}{2}\theta_0 \tan^2 \frac{1}{2}(\pi - \theta_1)]^m -$$

$$- \pi \sum_{m=0}^{\infty} \epsilon_m \int_0^{\infty} \frac{dx x \tanh \pi x}{x^2 + \frac{1}{4} \cosh \pi x} \frac{K_x^m(\cos \theta) K_x^m(-\cos \theta_1)}{\Gamma(\frac{1}{2} + m + ix) \Gamma(\frac{1}{2} + m - ix) K_x^m(\cos \theta_1)}$$

$$\times \left[m \sin m(\phi - \phi_0) \cos \beta \frac{K_x^m(\cos \theta_0)}{\sin \theta_0} + \cos m(\phi - \phi_0) \sin \beta \frac{d}{d\theta_0} K_x^m(\cos \theta_0) \right], \quad (18.200)$$

$$\begin{aligned} \mathfrak{Z} = & \frac{Y}{\sin \theta_0} \sum_{m=1}^{\infty} \cos \{m(\phi - \phi_0) + \beta\} [\tan \frac{1}{2}\theta \tan \frac{1}{2}\theta_0 \tan^2 \frac{1}{2}(\pi - \theta_1)]^m - \\ & - \pi Y \sum_{m=0}^{\infty} \varepsilon_m \int_0^{\infty} \frac{dx x}{x^2 + \frac{1}{4}} \frac{\tanh \pi x}{\cosh \pi x} \frac{K_x^m(\cos \theta)(d/d\theta_1)K_x^m(-\cos \theta_1)}{\Gamma(\frac{1}{2} + m + ix)\Gamma(\frac{1}{2} + m - ix)(d/d\theta_1)K_x^m(\cos \theta_1)} \\ & \times \left[\cos m(\phi - \phi_0) \cos \beta \frac{d}{d\theta_0} K_x^m(\cos \theta_0) - m \sin m(\phi - \phi_0) \sin \beta \frac{K_x^m(\cos \theta_0)}{\sin \theta_0} \right], \end{aligned} \quad (18.201)$$

and B is the Beltrami operator

$$B = \frac{1}{\sin \theta} \frac{\partial}{\partial \theta} \sin \theta \frac{\partial}{\partial \theta} + \frac{1}{\sin^2 \theta} \frac{\partial^2}{\partial \phi^2}.$$

Equation (18.199) leads to an electromagnetic field that has the appearance of a spherical wave emanating from the cone tip. Since

$$\left[\frac{1}{\sin \theta} \frac{\partial}{\partial \theta} \sin \theta \frac{\partial}{\partial \theta} - \frac{m^2}{\sin^2 \theta} \right] \tan^m \frac{1}{2}\theta = 0, \quad (18.202)$$

the summations involving $\tan^m \frac{1}{2}\theta$ in eqs. (18.200) and (18.201) contribute only to the leading order term in eq. (18.199).

For $\theta + \theta_0 < 2\theta_1 - \pi$, the non-zero components of the scattered field in the far zone are

$$\begin{aligned} E_{\theta}^s &= ZH_{\phi}^s = \frac{e^{ikr}}{kr} S_1, \\ E_{\phi}^s &= -ZH_{\theta}^s = \frac{e^{ikr}}{kr} S_2, \end{aligned} \quad (18.203)$$

where

$$\begin{aligned} S_1 &= i \frac{\partial}{\partial \theta} \Pi + \frac{iZ}{\sin \theta} \frac{\partial}{\partial \phi} \mathfrak{Z}, \\ S_2 &= i \frac{\partial}{\sin \theta} \Pi - iZ \frac{\partial}{\partial \theta} \mathfrak{Z}, \end{aligned} \quad (18.204)$$

with (Π, \mathfrak{Z}) defined as in eqs. (18.200) and (18.201). For $\beta = \frac{1}{2}\pi$ (incident magnetic field perpendicular to the cone axis) and $\theta_1 \approx \pi$ (thin cone):

$$\begin{aligned} S_1 &\approx \frac{\pi i}{\log(\sin^2 \frac{1}{2}\delta)} \int_0^{\infty} \frac{dx x}{x^2 + \frac{1}{4}} \frac{\tanh \pi x}{\cosh \pi x} \frac{K_x^1(\cos \theta)K_x^1(\cos \theta_0)}{1 + g(x)/\log(\sin^2 \frac{1}{2}\delta)} \\ &\quad - \frac{4i \sin^2 \frac{1}{2}\delta}{(\cos \theta + \cos \theta_0)^3} \cos(\phi - \phi_0)(1 + \cos \theta \cos \theta_0), \\ S_2 &\approx \frac{4i \sin^2 \frac{1}{2}\delta \sin(\phi - \phi_0)}{(\cos \theta + \cos \theta_0)^2}, \end{aligned} \quad (18.205)$$

where $g(x)$ is

$$g(x) = f(x) - (x^2 + \frac{1}{4})^{-1} \quad (18.206)$$

with $f(x)$ defined as in eq. (18.81). The definite integral in eq. (18.205) has not been evaluated in terms of known functions. However, if δ is sufficiently small to warrant the omission of higher order terms, eq. (18.205) reduces to the first order approximation (compare with eq. (18.43)):

$$S_1 \approx \frac{i}{\log(\sin^2 \frac{1}{2}\delta)} \frac{\tan \frac{1}{2}\theta \tan \frac{1}{2}\theta_0}{\cos \theta + \cos \theta_0},$$

$$S_2 \approx 0. \quad (18.207)$$

On the other hand, for $\beta = 0$ (incident electric field perpendicular to the cone axis) and $\theta_1 \approx \pi$ (thin cone):

$$S_1 \approx -i \sin^2 \frac{1}{2}\delta \sin(\phi - \phi_0) \left\{ \frac{4}{(\cos \theta + \cos \theta_0)^2} + \frac{24 \sin^2 \frac{1}{2}\delta}{(\cos \theta + \cos \theta_0)^4} \right. \\ \times (1 + \cos \theta \cos \theta_0 + \sin^2 \theta_0) + \frac{8 \sin^2 \frac{1}{2}\delta [1 - \log(\sin^2 \frac{1}{2}\delta)]}{(\cos \theta + \cos \theta_0)^4} (\sin^2 \theta - \sin^2 \theta_0) + \\ \left. + 2\pi \sin^2 \frac{1}{2}\delta \left(\frac{1}{\sin \theta} \frac{\partial}{\partial \theta_0} - \frac{1}{\sin \theta_0} \frac{\partial}{\partial \theta} \right) \int_0^\infty dx x \frac{\tanh \pi x}{\cosh \pi x} K_x^1(\cos \theta) K_x^1(\cos \theta_0) f(x) \right\} - \\ - i \sin^4 \frac{1}{2}\delta \sin 2(\phi - \phi_0) \frac{24 \sin \theta \sin \theta_0}{(\cos \theta + \cos \theta_0)^4}, \quad (18.208)$$

$$S_2 \approx -i \sin^2 \frac{1}{2}\delta \left\{ \frac{2 \sin \theta \sin \theta_0}{(\cos \theta + \cos \theta_0)^3} + \frac{12 \sin^2 \frac{1}{2}\delta}{(\cos \theta + \cos \theta_0)^5} \sin \theta \sin \theta_0 (1 + \cos \theta \cos \theta_0) + \right. \\ \left. + \frac{4 \sin^2 \frac{1}{2}\delta [1 - \log(\sin^2 \frac{1}{2}\delta)]}{(\cos \theta + \cos \theta_0)^5} \sin \theta \sin \theta_0 [4(1 + \cos \theta \cos \theta_0) + \sin^2 \theta + \sin^2 \theta_0] - \right. \\ \left. - \pi \sin^2 \frac{1}{2}\delta \int_0^\infty dx x \frac{\tanh \pi x}{\cosh \pi x} (x^2 + \frac{1}{4}) K_x^1(\cos \theta) K_x^1(\cos \theta_0) f(x) \right\} - \\ - i \sin^2 \frac{1}{2}\delta \cos(\phi - \phi_0) \left\{ \frac{4(1 + \cos \theta \cos \theta_0)}{(\cos \theta + \cos \theta_0)^3} + \frac{24 \sin^2 \frac{1}{2}\delta}{(\cos \theta + \cos \theta_0)^5} \right. \\ \times [2(1 + \cos \theta \cos \theta_0) + (\sin^2 \theta + \sin^2 \theta_0) \cos \theta \cos \theta_0 + 5 \sin^2 \theta \sin^2 \theta_0] - \\ - \frac{8 \sin^2 \frac{1}{2}\delta [1 - \log(\sin^2 \frac{1}{2}\delta)]}{(\cos \theta + \cos \theta_0)^5} [(\sin^2 \theta + \sin^2 \theta_0)(1 + \cos \theta \cos \theta_0) + 4 \sin^2 \theta \sin^2 \theta_0] + \\ \left. + 2\pi \sin^2 \frac{1}{2}\delta \left(\frac{\partial^2}{\partial \theta \partial \theta_0} - \frac{1}{\sin \theta \sin \theta_0} \right) \int_0^\infty dx x \frac{\tanh \pi x}{\cosh \pi x} K_x^1(\cos \theta) K_x^1(\cos \theta_0) f(x) \right\} - \\ - i \sin^4 \frac{1}{2}\delta \cos 2(\phi - \phi_0) \frac{24 \sin \theta \sin \theta_0}{(\cos \theta + \cos \theta_0)^4} \left\{ \frac{1 + \cos \theta \cos \theta_0}{\cos \theta + \cos \theta_0} + \right. \\ \left. + \frac{1}{4} \tan^2 \frac{1}{2}\theta \tan^2 \frac{1}{2}\theta_0 (2 + \cos \theta + \cos \theta_0) \right\}, \quad (18.209)$$

where $f(x)$ is as defined in eq. (18.81). Again, the definite integrals appearing in eqs. (18.208) and (18.209) have not been evaluated in terms of known functions. If, however, δ is sufficiently small to ignore higher order terms, eqs. (18.208) and (18.209) reduce to the first order approximation

$$\begin{aligned} S_1 &\approx \frac{-4i \sin^2 \frac{1}{2} \delta \sin(\phi - \phi_0)}{(\cos \theta + \cos \theta_0)^2}, \\ S_2 &\approx \frac{-2i \sin^2 \frac{1}{2} \delta}{(\cos \theta + \cos \theta_0)^3} [\sin \theta \sin \theta_0 + 2 \cos(\phi - \phi_0)(1 + \cos \theta \cos \theta_0)]. \end{aligned} \quad (18.210)$$

FELSEN's [1957a] first order approximation, after some trigonometric reduction, is identical to that in eq. (18.210). For $\theta \approx 0$, $\theta_0 \approx 0$, eqs. (18.208) and (18.209) may be approximated by

$$\begin{aligned} S_1 &\approx -i \sin^2 \frac{1}{2} \delta \sin(\phi - \phi_0) [1 + 3 \sin^2 \frac{1}{2} \delta + 2 \sin^2 \frac{1}{2} \theta + 2 \sin^2 \frac{1}{2} \theta_0], \\ S_2 &\approx -i \sin^2 \frac{1}{2} \delta [\sin \frac{1}{2} \theta \sin \frac{1}{2} \theta_0 + \cos(\phi - \phi_0)(1 + 3 \sin^2 \frac{1}{2} \delta + 2 \sin^2 \frac{1}{2} \theta + 2 \sin^2 \frac{1}{2} \theta_0)]. \end{aligned} \quad (18.211)$$

Equations (18.207) and (18.210) do not account for the singularity in E^s as $(\theta + \theta_0) \rightarrow \pi$; in this case it is necessary to include the accompanying geometrical optics and transition fields. For a thin cone ($\theta_1 \approx \pi$) and $kr \gg 1$, the scattered field may be decomposed as

$$E^s = E_d + E_{\text{refl.}} + E_{\text{tr.}}, \quad (18.212)$$

where E_d is the diffracted field due to the cone tip, $E_{\text{refl.}}$ is the field reflected from the surface of the cone according to the laws of geometrical optics, and $E_{\text{tr.}}$ is a transition field that provides a continuous behavior across the geometrical optics boundary $\theta = \pi - \theta_0$. For $\beta = \frac{1}{2}\pi$, the diffracted field to first order is obtained from eqs. (18.203) and (18.207):

$$E_d \sim \hat{\theta} \frac{e^{ikr}}{kr} \frac{i}{\log(\sin^2 \frac{1}{2} \delta)} \frac{\tan \frac{1}{2} \theta \tan \frac{1}{2} \theta_0}{\cos \theta + \cos \theta_0}; \quad (18.213)$$

and, provided $kr \sin^2 \frac{1}{2} \delta \ll 1$ and $(\sin \theta, \sin \theta_0) \neq 0$, the reflected and transition fields are given by:

$$\begin{aligned} E_{\text{refl.}} + E_{\text{tr.}} &\sim -\hat{\rho} \frac{e^{i\pi}}{(kr)^2 \sqrt{(\sin \theta \sin \theta_0) \log(\sin^2 \frac{1}{2} \delta)}} \frac{1}{\partial \alpha} \left(\frac{\partial}{\partial \alpha} + \frac{1}{8} \cot \theta - \frac{1}{8} \cot \theta_0 \right) \\ &\times \sqrt{\frac{kr}{2\pi}} I(r, \alpha) + \hat{\theta} \frac{e^{i\pi}}{k^2 r \sqrt{(\sin \theta \sin \theta_0) \log(\sin^2 \frac{1}{2} \delta)}} \frac{1}{\partial r} \sqrt{\frac{kr}{2\pi}} I(r, \alpha), \end{aligned} \quad (18.214)$$

where $\alpha = \theta + \theta_0 - \pi$ and $I(r, \alpha)$ is defined by eqs. (18.47) through (18.50). On the boundary $\theta = \pi - \theta_0$:

$$E^s \sim \hat{r} \frac{e^{ikr}}{kr \sin \theta_0} \frac{i}{\log(\sin^2 \frac{1}{2}\delta)} \left\{ 1 - \frac{1}{2} \sqrt{\frac{\pi}{2kr}} e^{\pm i\pi} \cot \theta_0 \right\} + \\ + \hat{\theta} \frac{\sqrt{\pi} e^{ikr + \frac{1}{2}i\pi}}{2kr \sin \theta_0 \log(\sin^2 \frac{1}{2}\delta)} \left\{ 1 - \sqrt{\frac{2}{\pi kr}} e^{\pm i\pi} \operatorname{cosec} \theta_0 - \frac{i}{2kr} \right\}. \quad (18.215)$$

For $\beta = 0$, on the other hand, the diffracted field to first order is obtained from eqs. (18.203) and (18.210):

$$E_d \sim \hat{\theta} \frac{e^{ikr}}{ikr} \frac{4 \sin^2 \frac{1}{2}\delta \sin(\phi - \phi_0)}{(\cos \theta + \cos \theta_0)^2} + \\ + \hat{\phi} \frac{e^{ikr}}{ikr} \frac{2 \sin^2 \frac{1}{2}\delta}{(\cos \theta + \cos \theta_0)^3} [\sin \theta \sin \theta_0 + 2 \cos(\phi - \phi_0)(1 + \cos \theta \cos \theta_0)]; \quad (18.216)$$

and, provided $kr \sin^2 \frac{1}{2}\delta \ll 1$ and $(\sin \theta, \sin \theta_0) \neq 0$, the reflected and transition fields are given by:

$$E_{\text{refl.}} + E_{\text{tr.}} \sim \hat{r} \frac{2e^{\pm i\pi} \sin^2 \frac{1}{2}\delta}{(kr)^2 \sqrt{(\sin \theta \sin \theta_0)}} \tilde{A} \sin(\phi - \phi_0) \sqrt{\frac{kr}{2\pi}} I(r, \alpha) + \\ + \hat{\theta} \frac{2e^{\pm i\pi} \sin^2 \frac{1}{2}\delta}{ikr \sqrt{(\sin \theta \sin \theta_0)}} \tilde{B} \sin(\phi - \phi_0) \sqrt{\frac{kr}{2\pi}} I(r, \alpha) + \\ + \hat{\phi} \frac{2e^{\pm i\pi} \sin^2 \frac{1}{2}\delta}{ikr \sqrt{(\sin \theta \sin \theta_0)}} \{ \frac{1}{2} \tilde{C}_0 + \tilde{C}_1 \cos(\phi - \phi_0) \} \sqrt{\frac{kr}{2\pi}} I(r, \alpha), \quad (18.217)$$

where $\alpha = \theta + \theta_0 - \pi$, $I(r, \alpha)$ is defined by eqs. (18.47) through (18.50), and

$$\tilde{A} = \frac{1}{\sin \theta_0} \left(\frac{\partial^2}{\partial x^2} - \frac{7}{8} \cot \theta \frac{\partial}{\partial x} - \frac{7}{8} \cot \theta_0 \frac{\partial}{\partial \alpha} \right), \\ \tilde{B} = \frac{1}{ik \sin \theta_0} \frac{\partial}{\partial r} \left(\frac{\partial}{\partial x} - \frac{7}{8} \cot \theta - \frac{7}{8} \cot \theta_0 \right) + \frac{1}{\sin \theta} \left(\frac{\partial}{\partial \alpha} - \frac{7}{8} \cot \theta_0 - \frac{7}{8} \cot \theta \right), \\ \tilde{C}_0 = \frac{\partial^2}{\partial x^2} - \frac{7}{8} \cot \theta \frac{\partial}{\partial x} - \frac{7}{8} \cot \theta_0 \frac{\partial}{\partial \alpha} - \\ - \frac{1}{8} \left(\frac{15}{6} \cot^2 \theta + \frac{15}{6} \cot^2 \theta_0 - \frac{9}{8} \cot \theta \cot \theta_0 + 1 \right), \\ \tilde{C}_1 = \frac{\partial^2}{\partial x^2} - \frac{7}{8} \cot \theta \frac{\partial}{\partial x} - \frac{7}{8} \cot \theta_0 \frac{\partial}{\partial \alpha} + \frac{1}{\sin \theta \sin \theta_0} \frac{1}{ik} \frac{\partial}{\partial r} + \\ + \frac{1}{16} \left(\frac{57}{8} \cot^2 \theta + \frac{57}{8} \cot^2 \theta_0 + \frac{9}{4} \cot \theta \cot \theta_0 + 6 \right). \quad (18.218)$$

On the boundary $\theta = \pi - \theta_0$:

$$E^s \sim \hat{r} \frac{e^{ikr}}{ikr} \int \frac{2\pi}{kr} \frac{e^{-\frac{1}{2}i\pi} \sin^2 \frac{1}{2}\delta}{\sin^2 \theta_0} \sin(\phi - \phi_0) - \hat{\theta} \frac{e^{ikr}}{kr} \frac{4kr \sin^2 \frac{1}{2}\delta}{\sin^2 \theta_0} \sin(\phi - \phi_0) -$$

$$\begin{aligned}
& -\phi \frac{\sqrt{\pi} e^{ikr - \frac{1}{2}i\pi} k r \sin^2 \frac{1}{2}\delta}{\sqrt{2kr \sin \theta}} \left\{ 1 - \frac{i}{8kr} (3 \cot^2 \theta_0 + 1) + \right. \\
& \left. + 2 \cos(\phi - \phi_0) \left[1 + \frac{i}{8kr} (9 \cot^2 \theta_0 + 11) \right] \right\}. \quad (18.219)
\end{aligned}$$

The above expressions for the reflected and transition fields are valid provided both source and observer are away from the cone axis. Such a restriction is no problem if both source and observer are located with the backward cone because in this instance only the diffraction term contributes significantly to the far field. If, on the other hand, either the source or observer is near the surface of the cone itself, the above results are not valid.

For $\theta_0 < \pi - \theta_1$, so that the entire cone is illuminated, and $\beta = 0$ (incident electric field perpendicular to the cone axis), the physical optics bistatic scattering cross section is

$$\begin{aligned}
& \sigma_{p.o.}(\theta, \phi; \theta_0, \phi_0) = \\
& = \frac{\lambda^2}{\pi} \frac{\tan^4 \delta [(1 + \cos \theta \cos \theta_0) + \cos(\phi - \phi_0) \sin \theta \sin \theta_0]^2}{[(\cos \theta + \cos \theta_0)^2 - \tan^2 \delta \{\sin^2 \theta + \sin^2 \theta_0 + 2 \cos(\phi - \phi_0) \sin \theta \sin \theta_0\}]^3}, \quad (18.220)
\end{aligned}$$

provided $\theta + \theta_0 < 2\theta_1 - \pi$, which excludes the region of specular reflections. It is interesting to compare the physical optics cross section with the cross section obtained from the exact theory, i.e.

$$\sigma(\theta, \phi; \theta_0, \phi_0) = \frac{\lambda^2}{\pi} (|S_1|^2 + |S_2|^2), \quad (18.221)$$

where $S_{1,2}$ are defined in eq. (18.204). For a thin cone ($\theta_1 \approx \pi$) and $\beta = 0$, the approximation in eq. (18.211) with $\theta \approx 0$, $\theta_0 \approx 0$ leads to

$$\begin{aligned}
& \sigma(\theta, \phi; \theta_0, \phi_0) \approx \\
& \approx \frac{\lambda^2}{\pi} \sin^4 \frac{1}{2}\delta [1 + 6 \sin^2 \frac{1}{2}\delta + 4 \sin^2 \frac{1}{2}\theta + 4 \sin^2 \frac{1}{2}\theta_0 + 2 \cos(\phi - \phi_0) \sin \frac{1}{2}\theta \sin \frac{1}{2}\theta_0], \quad (18.222)
\end{aligned}$$

whereas, for $\theta_1 \approx \pi$, $\theta \approx 0$ and $\theta_0 \approx 0$, eq. (18.220) becomes

$$\begin{aligned}
& \sigma_{p.o.}(\theta, \phi; \theta_0, \phi_0) \approx \\
& \approx \frac{\lambda^2}{\pi} \sin^4 \frac{1}{2}\delta [1 + 6 \sin^2 \frac{1}{2}\delta + 4 \sin^2 \frac{1}{2}\theta + 4 \sin^2 \frac{1}{2}\theta_0 + 4 \cos(\phi - \phi_0) \sin \frac{1}{2}\theta \sin \frac{1}{2}\theta_0]. \quad (18.223)
\end{aligned}$$

These two approximations differ only in the term involving $\cos(\phi - \phi_0)$, and for axial incidence ($\theta_0 = 0$) the two results are in complete agreement to this order of ap-

proximation. For back scattering $\theta = \theta_0$, $\phi = \phi_0$, eq. (18.220) reduces to (SPENCER [1951])

$$\sigma_{p.o.} = \frac{\lambda^2}{16\pi} \tan^4 \delta \left(1 - \frac{\sin^2 \theta}{\cos^2 \delta} \right)^{-3}. \quad (18.224)$$

The back scattering cross section given in eq. (18.224) is plotted in Fig. 18.9 as a function of θ for various cone angles.

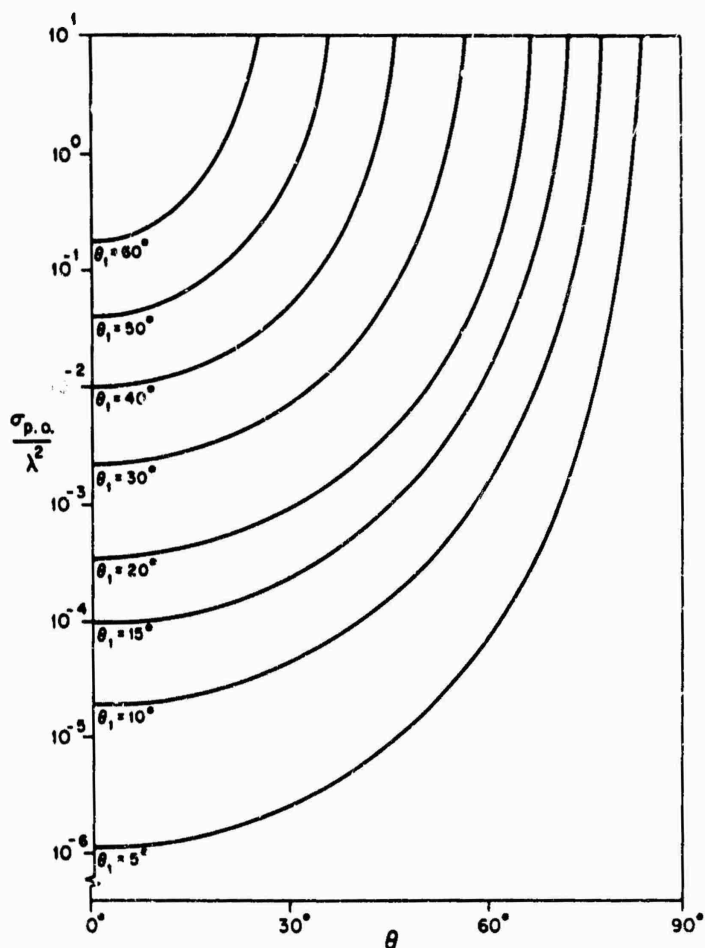


Fig. 18.9. Normalized physical optics back scattering cross section $\sigma_{p.o.}/\lambda^2$ as a function of θ for various cone angles θ_1 (SPENCER[1951]).

For $\beta = \frac{1}{2}\pi$ (incident magnetic field perpendicular to the cone axis), and $\theta_1 \approx \pi$ (thin cone), with $\theta + \theta_0$ not too close to π , eq. (18.207) leads to

$$\sigma(\theta, \phi; \theta_0, \phi_0) \approx \frac{\lambda^2}{4\pi} \frac{\tan^2 \frac{1}{2}\theta \tan^2 \frac{1}{2}\theta_0}{[\log \frac{1}{2}(\pi - \theta_1)]^2 (\cos \theta + \cos \theta_0)^2}, \quad (18.225)$$

which becomes, for back scattering [compare with eq. (18.69)]:

$$\sigma \approx \frac{\lambda^2}{16\pi} \frac{\tan^4 \frac{1}{2}\theta}{[\log \frac{1}{2}(\pi - \theta_1)]^2 \cos^2 \theta}. \quad (18.226)$$

It is interesting to note that for this polarization ($\beta = \frac{1}{2}\pi$), a result analogous to eq. (18.225) is also rigorously obtained in the case of scattering by a semi-infinite cylinder whose circumference $2\pi a$ is small compared to the wavelength; indeed, the corresponding half-cylinder result is obtained upon replacing $\frac{1}{2}(\pi - \theta_1)$ in eq. (18.225) with ka , where $ka \ll 1$. An attempt to regard the thin cone as an approximation to a thin semi-infinite wire dates back to MACDONALD [1902], who treated the case of a radial electric dipole located on the axis of symmetry (see eq. (18.149)).

For a plane wave incident along the axis of symmetry $\theta_0 = 0$, such that

$$E^i = \hat{x}e^{-ikr \cos \theta}, \quad (18.227)$$

eqs. (18.184) and (18.185) for the Debye potentials reduce to (GORYANOV [1961])

$$\begin{aligned} u &= \frac{\cos \phi}{2k} \int_{C'} dv \frac{2v+1}{v(v+1)} \frac{e^{-\frac{1}{2}iv\pi} j_v(kr)}{\sin v\pi} \left[P_v^1(-\cos \theta) - \frac{P_v^1(-\cos \theta_1)}{P_v^1(\cos \theta_1)} P_v^1(\cos \theta) \right], \\ v &= -Y \frac{\sin \phi}{2k} \int_{C'} dv \frac{2v+1}{v(v+1)} \frac{e^{-\frac{1}{2}iv\pi} j_v(kr)}{\sin v\pi} \\ &\quad \times \left[P_v^1(-\cos \theta) - \frac{(d/d\theta_1)P_v^1(-\cos \theta_1)}{(d/d\theta_1)P_v^1(\cos \theta_1)} P_v^1(\cos \theta) \right], \end{aligned} \quad (18.228)$$

while eqs. (18.188) through (18.191) simplify to

$$\begin{aligned} u &= \frac{2i \cos \phi}{k \sin \theta_1} \sum_{p>0} (2p+1) e^{-\frac{1}{2}ip\pi} j_p(kr) \frac{P_p^1(\cos \theta)}{(\partial/\partial \theta_1)P_p^1(\cos \theta_1)(\partial/\partial p)P_p^1(\cos \theta_1)}, \\ v &= \frac{2iY \sin \phi}{k \sin \theta_1} \sum_{q>0} (2q+1) e^{-\frac{1}{2}iq\pi} j_q(kr) \frac{P_q^1(\cos \theta)}{P_q^1(\cos \theta_1)(\partial^2/\partial q \partial \theta_1)P_q^1(\cos \theta_1)}, \end{aligned} \quad (18.229)$$

and

$$\begin{aligned} u &= \frac{2i \cos \phi}{k} \sum_{p>0} \frac{e^{-\frac{1}{2}ip\pi} j_p(kr) P_p^1(\cos \theta)}{\int_0^{\theta_1} [P_p^1(\cos \alpha)]^2 \sin \alpha d\alpha}, \\ v &= -\frac{2iY \sin \phi}{k} \sum_{q>0} \frac{e^{-\frac{1}{2}iq\pi} j_q(kr) P_q^1(\cos \theta)}{\int_0^{\theta_1} [P_q^1(\cos \alpha)]^2 \sin \alpha d\alpha}, \end{aligned} \quad (18.230)$$

where the summations in p and q extend over the positive roots, respectively, of $P_p^1(\cos \theta_1)$ and $(\partial/\partial \theta_1)P_q^1(\cos \theta_1)$.

On the surface $\theta = \beta$ (SENIOR and WILCOX [1967]):

$$\begin{aligned} E_\theta^i + E_\theta^s &= \cos \phi \left[\frac{i}{kr} \frac{\partial}{\partial r} (rA) + \frac{A'}{\sin \theta_1} \right], \\ H_\phi^i + H_\phi^s &= -Y \cos \phi \left[\frac{i}{kr \sin \theta_1} \frac{\partial}{\partial r} (rA') + A \right], \\ H_r^i + H_r^s &= -\frac{iY}{k} \sin \phi \left(\frac{\partial^2}{\partial r^2} + k^2 \right) (rA'). \end{aligned} \quad (18.231)$$

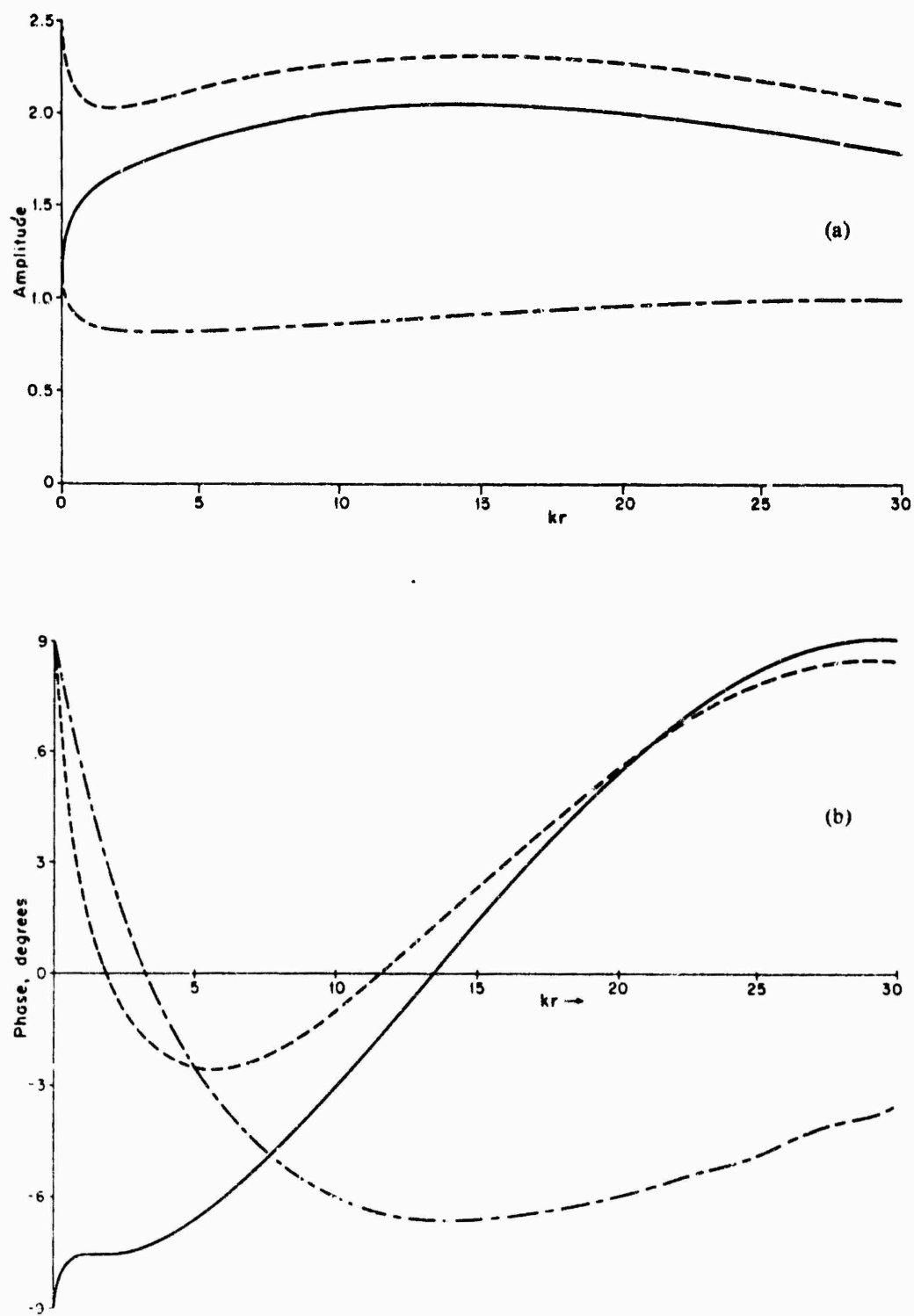


Fig. 18.10. Amplitudes (a) and phases (b) of surface field components \hat{U}_θ (—), \hat{U}_ϕ (---) and \hat{U}_r (- · -) for $\theta_1 = 150^\circ$ (SENIOR AND WILCOX [1967]).

where

$$\begin{aligned} A &= \frac{2}{\sin \theta_1} \sum_{p>0} \frac{(2p+1)e^{-\frac{1}{2}p\pi} j_p(kr)}{(\partial/\partial p)P_p^1(\cos \theta_1)}, \\ A' &= \frac{-2}{\sin \theta_1} \sum_{q>0} \frac{(2q+1)e^{-\frac{1}{2}q\pi} j_q(kr)}{(\partial^2/\partial q \partial \theta_1)P_q^1(\cos \theta_1)}. \end{aligned} \quad (18.232)$$

SENIOR and WILCOX [1967] have computed the surface field components \mathcal{E}_θ , \mathcal{H}_ϕ , \mathcal{H}_r defined by

$$\begin{aligned} E_\theta^i + E_\theta^s &= \cos \phi \mathcal{E}_\theta, \\ H_\phi^i + H_\phi^s &= Y \cos \phi \mathcal{H}_\phi, \\ H_r^i + H_r^s &= Y \sin \phi \mathcal{H}_r, \end{aligned} \quad (18.233)$$

where the actual formulae for \mathcal{E}_θ , \mathcal{H}_ϕ and \mathcal{H}_r are evident from eq. (18.231). The components were computed in real and imaginary parts, amplitude and phase, as functions of kr , $0 < kr \leq 30$, for a sequence of values of θ_1 spanning the range $150^\circ \leq \theta_1 \leq 172\frac{1}{2}^\circ$. Their results for the amplitudes and phases, with the phases relative to those of the physical optics approximation,

$$\begin{aligned} [\mathcal{E}_\theta]_{\text{p.o.}} &= 2 \cos \theta_1 e^{-ikr \cos \theta_1}, \\ [\mathcal{H}_\phi]_{\text{p.o.}} &= -2e^{-ikr \cos \theta_1}, \\ [\mathcal{H}_r]_{\text{p.o.}} &= -2 \sin \theta_1 e^{-ikr \cos \theta_1}, \end{aligned} \quad (18.234)$$

are plotted in Figs. 18.10 through 18.12 for $\theta_1 = 150^\circ$, 165° and $172\frac{1}{2}^\circ$, corresponding to cones of half-angle $\delta = 30^\circ$, 15° and $7\frac{1}{2}^\circ$, respectively.

For $\theta_0 = 0$, in the region $\theta < 2\theta_1 - \pi$, the scattered portions of (u, v) are

$$\begin{aligned} u^s &= -\frac{\cos \phi e^{ikr}}{2k^2 r} \tan \frac{1}{2}\theta \tan^2 \frac{1}{2}(\pi - \theta_1) + \frac{\cos \phi}{k} \sqrt{\frac{\pi}{2kr}} e^{i\frac{1}{2}\pi} \\ &\quad \times \int_0^\infty \frac{dx x}{x^2 + \frac{1}{4}} \tanh \pi x e^{-\frac{1}{2}\pi x} H_{ix}^{(1)}(kr) K_x^1(\cos \theta) \frac{K_x^1(-\cos \theta_1)}{K_x^1(\cos \theta_1)}, \end{aligned} \quad (18.235)$$

$$\begin{aligned} v^s &= -\frac{Y \sin \phi e^{ikr}}{2k^2 r} \tan \frac{1}{2}\theta \tan^2 \frac{1}{2}(\pi - \theta_1) - \frac{Y \sin \phi}{k} \sqrt{\frac{\pi}{2kr}} e^{i\frac{1}{2}\pi} \\ &\quad \times \int_0^\infty \frac{dx x}{x^2 + \frac{1}{4}} \tanh \pi x e^{-\frac{1}{2}\pi x} H_{ix}^{(1)}(kr) K_x^1(\cos \theta) \frac{(d/d\theta_1)K_x^1(-\cos \theta_1)}{(d/d\theta_1)K_x^1(\cos \theta_1)}, \end{aligned} \quad (18.236)$$

and the scattered field in the far zone is (GOR'YANOV [1961]):

$$\begin{aligned} E_\theta^s &= ZH_\phi^s = \cos \phi \frac{e^{ikr}}{ikr} L_1(\theta), \\ E_\phi^s &= -ZH_\theta^s = -\sin \phi \frac{e^{ikr}}{ikr} L_2(\theta), \end{aligned} \quad (18.237)$$

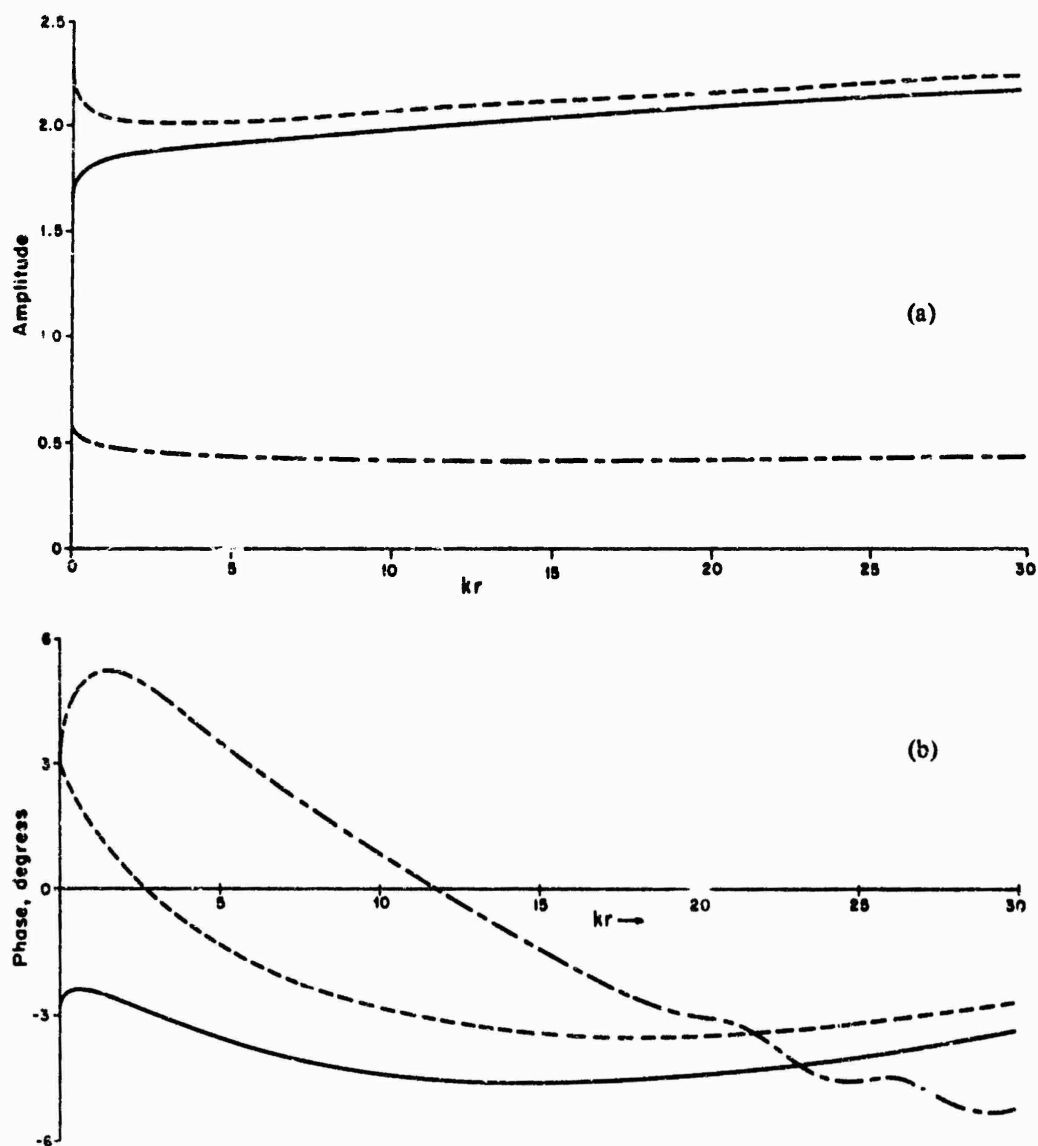


Fig. 18.11. Amplitudes (a) and phases (b) of surface field components E_θ (—), H_ϕ (---) and H_r (- · - ·) for $\theta_1 = 165^\circ$ (SENIOR and WILCOX [1967]).

where

$$L_1(\theta) = \frac{\Gamma'}{\sin \theta} - \frac{\partial \Gamma}{\partial \theta} + \frac{1}{2} \sec^2 \frac{1}{2} \theta \tan^2 \frac{1}{2} (\pi - \theta_1), \quad (18.238)$$

$$L_2(\theta) = \frac{\partial \Gamma'}{\partial \theta} - \frac{\Gamma}{\sin \theta} + \frac{1}{2} \sec^2 \frac{1}{2} \theta \tan^2 \frac{1}{2} (\pi - \theta_1),$$

in which

$$\Gamma = \int_0^\infty \frac{dx}{x^2 + \frac{1}{4}} \tanh \pi x K_x^1(\cos \theta) \frac{K_x^1(-\cos \theta_1)}{K_x^1(\cos \theta_1)},$$

$$\Gamma' = \int_0^\infty \frac{dx}{x^2 + \frac{1}{4}} \tanh \pi x K_x^1(\cos \theta) \frac{(d/d\theta_1) K_x^1(-\cos \theta_1)}{(d/d\theta_1) K_x^1(\cos \theta_1)}. \quad (18.239)$$

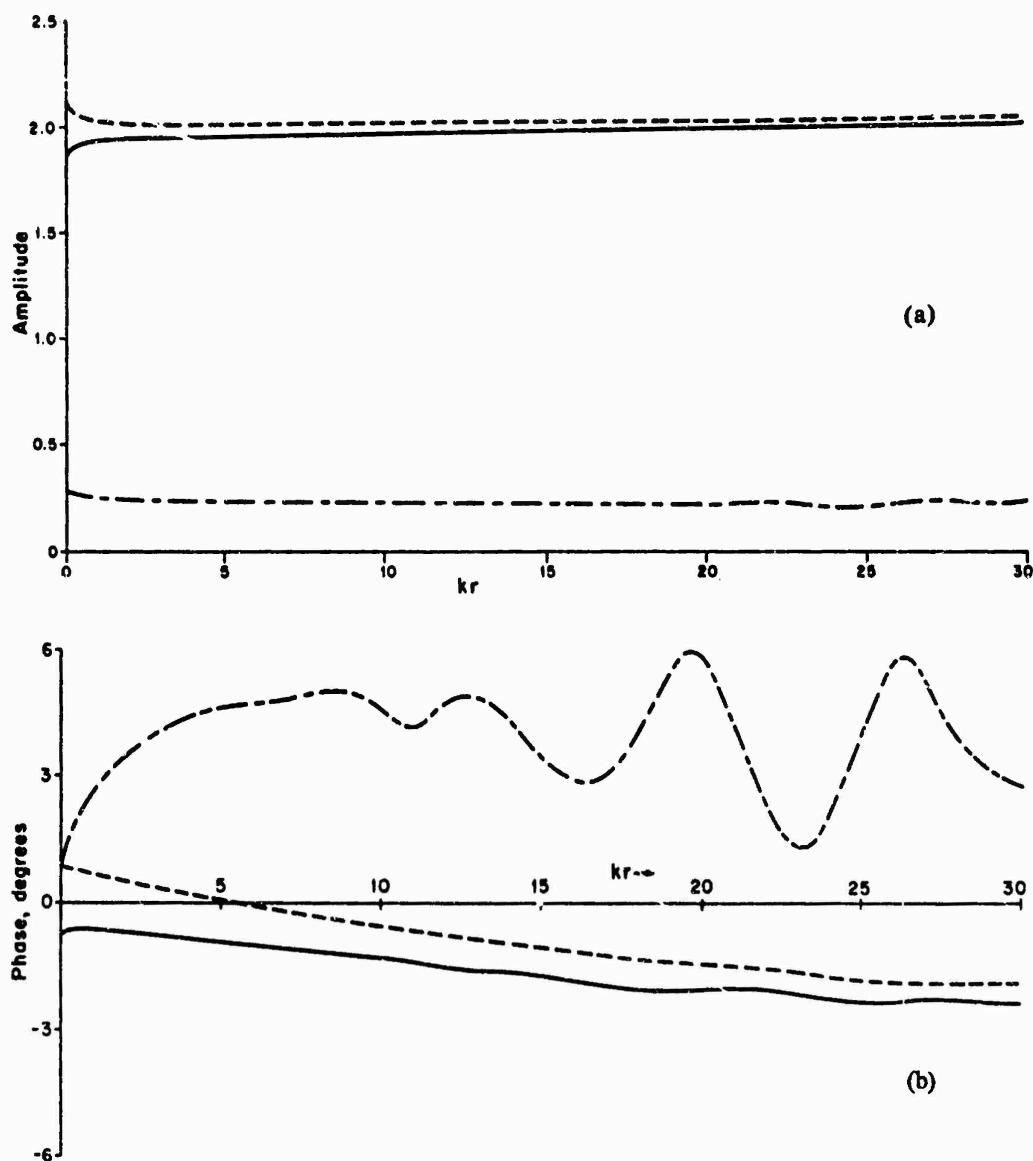


Fig. 18.12. Amplitudes (a) and phases (b) of surface field components E_θ (—), H_ϕ (---) and H_r (— · —) for $\theta_1 = 172\frac{1}{2}^\circ$ (SENIOR and WILCOX [1967]).

The functions $L_{1,2}(\theta)$ are real, positive, and increase monotonically with increasing θ in the interval $0 \leq \theta < 2\theta_1 - \pi$. GORYANOV [1961] reports of extensive numerical calculations of $L_{1,2}(\theta)$ for $0 \leq \theta \leq 2\theta_1 - \pi - 2^\circ$, $96^\circ \leq \theta_1 \leq 178^\circ$, $\Delta\theta = 2^\circ$, $\Delta\theta_1 = 2^\circ$, and a reproduction of his data appears in Fig. 18.13. The far fields according to physical optics are also presented in the form

$$\begin{aligned}
 [E_\theta^s]_{p.o.} &= Z[H_\phi^s]_{p.o.} = \cos \phi \frac{e^{ikr}}{ikr} L_{p.o.}(\theta), \\
 [E_\phi^s]_{p.o.} &= -Z[H_\theta^s]_{p.o.} = -\sin \phi \frac{e^{ikr}}{ikr} L_{p.o.}(\theta),
 \end{aligned}
 \tag{18.240}$$

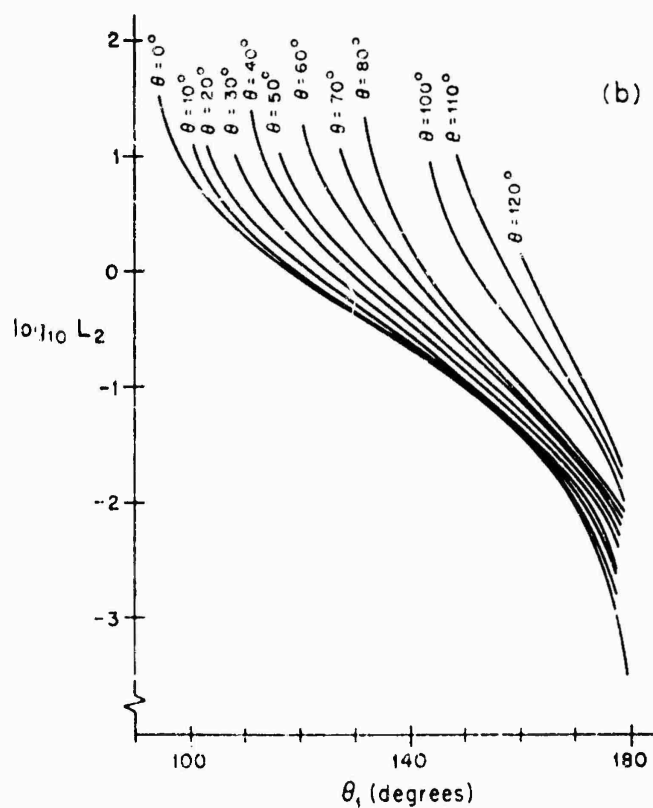
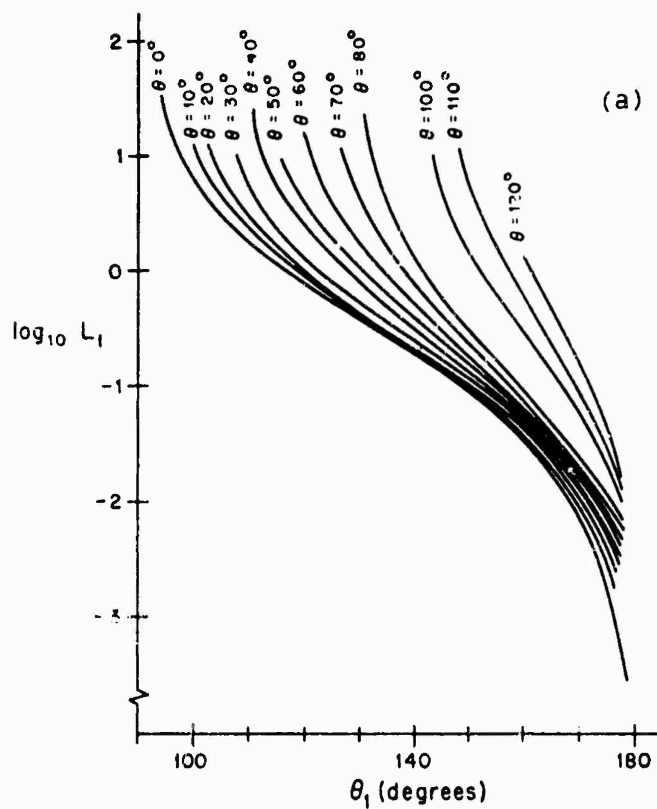


Fig. 18.13. Angular distributions (a) $\log_{10} L_1(\theta)$ and (b) $\log_{10} L_2(\theta)$ as functions of θ_1 for various angles θ (GOR'YANOV [1961]).

where

$$L_{p.o.}(\theta) = \frac{-\sin^2 \theta_1 \cos \theta_1}{4 \cos \frac{1}{2} \theta [\cos (\theta_1 - \frac{1}{2} \theta) \cos (\theta_1 + \frac{1}{2} \theta)]^{\frac{1}{2}}}, \quad (18.241)$$

and graphs of the quantities $(L_{1,2}/L_{p.o.}) - 1$ plotted as functions of θ_1 are reproduced in Fig. 18.14. GORYANOV [1961] concludes that the difference between the true far field and that predicted by physical optics increases uniformly with angle away from the back scattered direction and that the difference never exceeds 10 percent of the value computed with eq. (18.237) for $\theta \leq 2\theta_1 - \pi - \pi/90$.

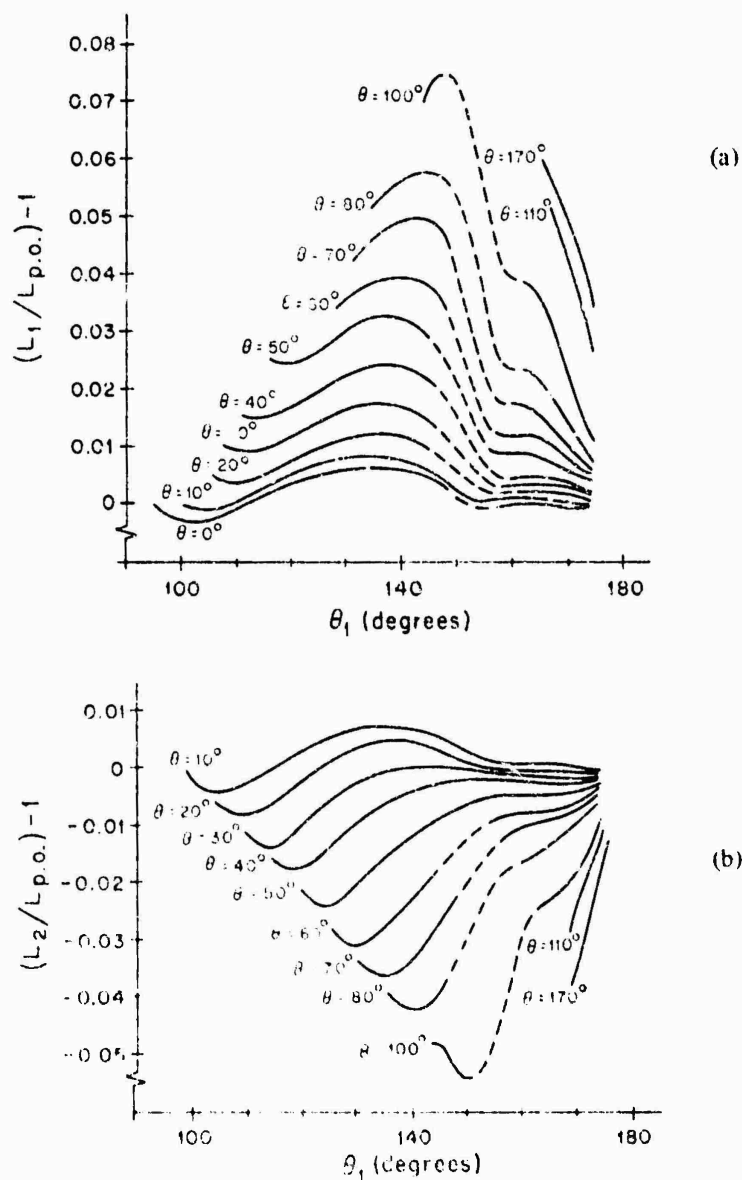


Fig. 18.14. The quantities (a) $[L_1/L_{p.o.}] - 1$ and (b) $[L_2/L_{p.o.}] - 1$ as functions of θ_1 for various angles θ (GORYANOV [1961]).

For $\theta_0 = 0$ and $kr \gg 1$, the scattered field may be decomposed as in eq. (18.212) with the diffracted field given by:

$$E_d \sim \frac{e^{ikr}}{ikr} [\hat{\theta} \cos \phi L_1(\theta) - \hat{\phi} \sin \phi L_2(\theta)] \quad (18.242)$$

where $L_1(\theta)$ and $L_2(\theta)$ are obtained from eq. (18.238). Although the integrals in eq. (18.239) are convergent only for $\theta < 2\theta_1 - \pi$, it can be shown by a proof paralleling FELSEN [1959] that the angular dependence of the far-zone diffracted field must be the same for all angles in $0 \leq \theta \leq \theta_1$. In principle, therefore, one may calculate the diffracted field by means of the integrals in eq. (18.239) valid for the restricted range of angles and then employ the resulting closed form expressions everywhere. In practice, however, the integrals are difficult to evaluate in terms of known functions, and closed form expressions valid for all angles are not available. For $(\sin \theta, \sin \theta_1) \neq 0$, the reflected and transition fields are given by:

$$\begin{aligned} E_{\text{refl.}} + E_{\text{tr.}} \sim & \hat{r} \frac{\cos \phi}{kr \sqrt{\sin \theta}} \left(\frac{\partial^2}{\partial \alpha^2} - \frac{7}{8} \cot \theta \frac{\partial}{\partial \alpha} + \frac{3}{4} \cot \theta_1 \frac{\partial}{\partial \alpha} \right) T(r, \alpha) - \\ & - \hat{\theta} \frac{\cos \phi}{kr \sqrt{\sin \theta}} \left[\left(\frac{\partial}{\partial \alpha} - \frac{7}{8} \cot \theta + \frac{3}{4} \cot \theta_1 \right) \frac{\partial}{\partial r} + \frac{ik}{\sin \theta} \right] r T(r, \alpha) - \\ & - \hat{\phi} \frac{\sin \phi}{ir \sqrt{\sin \theta}} \left[\left(\frac{\partial}{\partial \alpha} - \frac{7}{8} \cot \theta + \frac{7}{4} \cot \theta_1 \right) - \frac{i}{k \sin \theta} \frac{\partial}{\partial r} \right] r T(r, \alpha), \end{aligned} \quad (18.243)$$

where $\alpha = \pi - 2\theta_1 + \theta$ and $T(r, \alpha)$ is defined by eqs. (18.60) through (18.63). The transition function properly compensates for the singularities at $\theta = 2\theta_1 - \pi$ in the diffracted wave and for the jump discontinuities in the reflected wave. Away from the geometrical optics boundary $\theta = 2\theta_1 - \pi$, such that $kr \sin^2 \alpha \gg 1$, the reflected field is

$$\begin{aligned} E_{\text{refl.}} \sim & \eta(\alpha) \sqrt{\frac{\sin \alpha}{\sin \theta}} e^{ikr \cos \alpha} \\ & \times \left\{ -\hat{r} \sin \alpha \cos \phi \left[1 + \frac{i}{kr} \left(\frac{3 \cot \theta_1}{4 \sin \alpha} - \frac{3 \cot \theta}{8 \sin \alpha} + \frac{3 \cot \alpha}{8 \sin \alpha} \right) \right] - \right. \\ & - \hat{\theta} \cos \alpha \cos \phi \left[1 + \frac{i}{kr} \left(\frac{3 \cot \theta_1}{4 \sin \alpha} - \frac{7 \cot \theta}{8 \sin \alpha} - \frac{1 \cot \alpha}{8 \sin \alpha} + \frac{1 - \sin \theta \sin \alpha}{\sin \theta \sin \alpha \cos \alpha} \right) \right] + \\ & \left. + \hat{\phi} \sin \phi \left[1 + \frac{i}{kr} \left(\frac{7 \cot \theta_1}{4 \sin \alpha} - \frac{7 \cot \theta}{8 \sin \alpha} - \frac{1 \cot \alpha}{8 \sin \alpha} + \frac{\cot \alpha}{\sin \theta} \right) \right] + O \left[\frac{1}{(kr)^2} \right] \right\}, \end{aligned} \quad (18.244)$$

and for $\theta = \theta_1$ (observer on the cone surface):

$$E + E_{\text{refl.}} \sim \hat{\theta} e^{-ikr \cos \theta_1} \cos \theta_1 \cos \phi \left\{ 2 - \frac{i \cot \theta_1}{kr \sin \theta_1} + O \left[\frac{1}{(kr)^2} \right] \right\}, \quad (18.245)$$

with the tangential components equal to zero as required. It should be emphasized that the above results are valid only if the observer is located away from the axis of the cone and provided the cone apex angle is not small.

For $\theta_0 = 0$, the total field along the axis $\theta = 0$ is (FELSEN [1955]):

$$E^i + E^s = \hat{x} \frac{\pi i}{kr} \frac{\partial}{\partial r} \left[\sum_{p>0} (p + \frac{1}{2}) e^{-\frac{1}{2}ip\pi} \frac{r j_p(kr) P_p^1(-\cos \theta_1)}{\sin p\pi (\partial/\partial n) P_p^1(\cos \theta_1)} \right] + \\ + \hat{x} \left[\sum_{q>0} (q + \frac{1}{2}) e^{-\frac{1}{2}iq\pi} \frac{j_q(kr) (\partial/\partial \theta_1) P_q^1(-\cos \theta_1)}{\sin q\pi (\partial^2/\partial q \partial \theta_1) P_q^1(\cos \theta_1)} \right], \quad (18.246)$$

which may also be written as

$$E^i + E^s = \hat{x} \frac{i}{kr} \frac{\partial}{\partial r} \left[\sum_{p>0} \frac{p(p+1) e^{-\frac{1}{2}ip\pi} r j_p(kr)}{\int_0^{\theta_1} [P_p^1(\cos \alpha)]^2 \sin \alpha d\alpha} \right] + \\ + \hat{x} \left[\sum_{q>0} \frac{q(q+1) e^{-\frac{1}{2}iq\pi} j_q(kr)}{\int_0^{\theta_1} [P_q^1(\cos \alpha)]^2 \sin \alpha d\alpha} \right], \quad (18.247)$$

and the summations in p and q extend over the positive zeros, respectively, of $P_p^1(\cos \theta_1)$ and $(\partial/\partial \theta_1) P_q^1(\cos \theta_1)$. The back scattered far field is (see also, FELSEN [1958]):

$$E^{BS} = \hat{x} \frac{e^{ikr}}{2ikr} \left\{ \cot^2 \frac{1}{2}\theta_1 - \frac{4}{\pi} \int_0^\infty dx x (x^2 + \frac{1}{4}) \frac{\sinh \pi x}{(d/d\theta_1) [K_x^1(\cos \theta_1)]^2} \right\} - \\ - \hat{x} \frac{e^{\frac{1}{2}i\pi}}{2k^2 r} \left(\frac{\partial}{\partial \alpha} + \frac{1}{4} \cot \theta_1 \right) \frac{\partial}{\partial r} \sqrt{\frac{kr}{2\pi}} I(r, \alpha) + \\ + \hat{x} \frac{e^{-\frac{1}{2}i\pi}}{2kr} \left(\frac{\partial}{\partial \alpha} + \frac{7}{4} \cot \theta_1 \right) \sqrt{\frac{kr}{2\pi}} I(r, \alpha), \quad (18.248)$$

where $\alpha = \pi - 2\theta_1$ and $I(r, \alpha)$ is defined by eqs. (18.47) through (18.50). The terms involving $I(r, \alpha)$ are important only for a wide cone $\theta_1 \approx \frac{1}{2}\pi$, in which case both source and observer lie in a transition region. For $\theta_1 \approx \frac{1}{2}\pi$, a first order result is given by (FELSEN [1955], see also FELSEN [1953]):

$$E^{BS} \sim -\hat{x} e^{ikr} \sin \theta_1 [1 - \sqrt{2\pi} e^{-\frac{1}{2}i\pi} w G(w)], \quad w < 4 \\ E^{BS} \sim \hat{x} \frac{e^{ikr}}{ikr (2\theta_1 - \pi)^2}, \quad w \geq 4 \quad (18.249)$$

where $w = -\sqrt{kr} \cos \theta_1$ and $G(w)$ is as defined in eq. (18.50). A plot of the magnitude and phase of the quantity in brackets in eq. (18.249) is provided in Section 18.5, Fig. 18.17b. It may be noted that when $\theta_1 = \frac{1}{2}\pi$, eq. (18.249) yields a back scattered plane wave appropriate to reflection from an infinite flat plane. For a thin cone ($\theta_1 \approx \pi$), eqs. (18.208) through (18.211) remain valid for $\theta_0 = 0$, $\theta = 0$.

For $\theta_0 = 0$, the physical optics bistatic scattering cross section in eq. (18.220) reduces to

$$\sigma_{p.o.}(\theta, \phi) = \frac{\lambda^2}{\pi} \frac{\tan^4 \delta (1 + \cos \theta)^2}{[(1 + \cos \theta)^2 - \tan^2 \delta \sin^2 \theta]^3}, \quad (18.250)$$

and by some trigonometric transformation, eq. (18.250) can be shown to be in agreement with SIEGEL et al. [1955a] and with the result of GORYANOV [1961] (see eq. (18.240)). For $\theta = 0$, eq. (18.250) reduces to the widely quoted nose-on back scattering cross section (SPENCER [1951]):

$$\sigma_{p.o.} = \frac{\lambda^2}{16\pi} \tan^4 \delta. \quad (18.251)$$

For a wide cone $\theta_1 \approx \frac{1}{2}\pi$, the back scattering cross section is, from eq. (18.249):

$$\sigma \approx \frac{\lambda^2}{\pi(2\theta_1 - \pi)^4}, \quad (18.252)$$

whereas, for a thin cone $\theta_1 \approx \pi$, eq. (18.210) yields the first order expression:

$$\sigma \approx \frac{\lambda^2(\pi - \theta_1)^4}{16\pi}. \quad (18.253)$$

A more general expression for the back scattering cross section is given by (HANSEN and SCHIFF [1948], SCHENSTED [1953], SIEGEL et al. [1953a, 1955b], MENTZER [1955]):

$$\sigma = \frac{\lambda^2}{4\pi} \left| \sum_{p>0} \frac{p(p+1)e^{-ip\pi}}{\int_0^{\theta_1} [P_p^1(\cos \alpha)]^2 \sin \alpha d\alpha} - \sum_{q>0} \frac{q(q+1)e^{-iq\pi}}{\int_0^{\theta_1} [P_q^1(\cos \alpha)]^2 \sin \alpha d\alpha} \right|^2, \quad (18.254)$$

where the summations are over the positive zeros of $P_p^1(\cos \theta_1)$ and $(\partial/\partial \theta_1)P_q^1(\cos \theta_1)$, but only a finite number of terms must be included since the infinite series diverges. Despite this drawback, special summation techniques have been employed (SCHENSTED [1953], SIEGEL et al. [1953a, 1955b]) to yield second order results in the wide cone and thin cone approximations: For a wide cone $\theta_1 \approx \frac{1}{2}\pi$,

$$\sigma \approx \frac{\lambda^2(1 - 2 \cos^2 \theta_1)}{16\pi \cos^4 \theta_1}, \quad (18.255)$$

and for a thin cone ($\theta_1 \approx \pi$),

$$\sigma \approx \frac{\lambda^2}{\pi} \sin^2 \frac{1}{2}\delta [1 + 6 \sin^2 \frac{1}{2}\delta] \quad (18.256)$$

in agreement with eq. (18.222). It should be noted that the physical optics result in eq. (18.251) is in agreement with the exact theory for both wide cones:

$$\sigma_{p.o.} \approx \frac{\lambda^2}{16\pi \cos^2 \theta_1} [1 - 2 \cos^2 \theta_1 + \cos^4 \theta_1 + \dots] \quad (18.257)$$

and for thin cones:

$$\sigma_{p.o.} \approx \frac{\lambda^2}{\pi} \sin^2 \frac{1}{2} \delta [1 + 6 \sin^2 \frac{1}{2} \delta + 25 \sin^4 \frac{1}{2} \delta + \dots]. \quad (18.258)$$

The cross sections given by eqs. (18.251), (18.252), (18.253), (18.255) and (18.256) are plotted in Fig. 18.15 as functions of θ_1 .

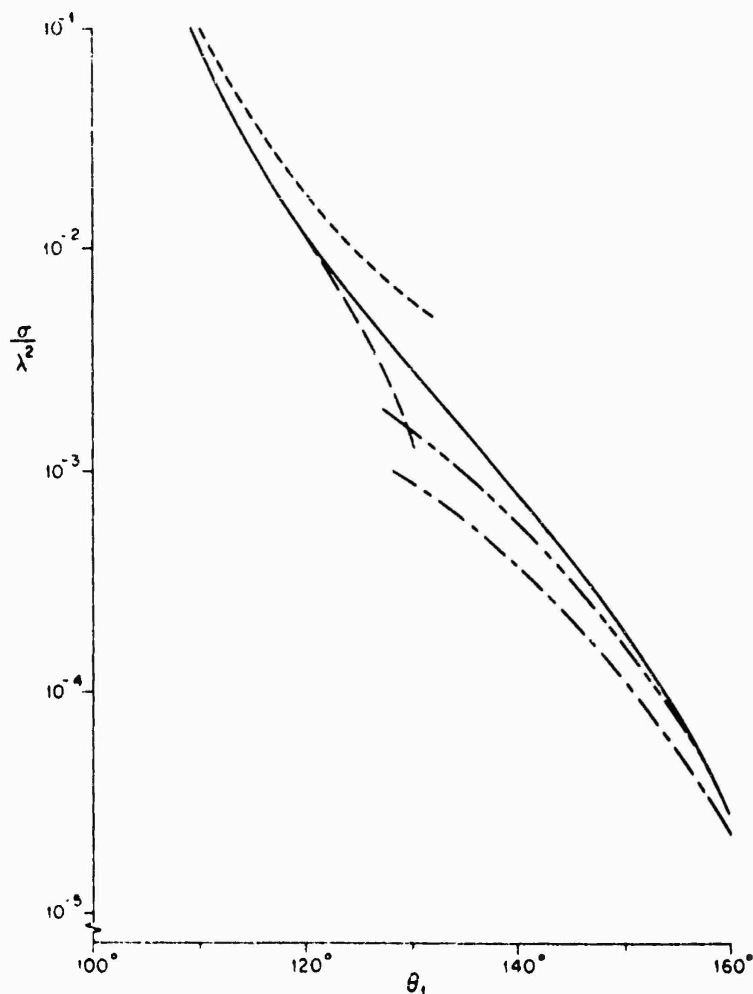


Fig. 18.15. Normalized nose-on back scattering cross section σ/λ^2 as a function of θ_1 for a perfectly conducting cone: (—) physical optics, (---) first order and (---) second order theory for wide cone, (- · -) first order and (- · -) second order theory for thin cone.

18.5. Special functions

The Legendre function $P_\nu^\mu(\cos \theta_1)$ is an entire function of ν . For μ real and $\mu < 1$, or for μ an integer, the zeros of $P_\nu^\mu(\cos \theta_1)$ in the ν -plane are all real and simple (ROBIN [1959], see also MACDONALD [1900] and HOBSON [1931] who take μ real and $\mu > 0$). The positive zeros p and q defined, respectively, as roots of the equations

$$P_p^m(\cos \theta_1) = 0, \quad (18.259)$$

$$(\hat{c} \hat{c} \theta_1) P_q^m(\cos \theta_1) = 0, \quad (18.260)$$

with $m = 0, 1, 2, \dots$, are fundamental to eigenfunction expansions involving conical boundaries. Because of the relation

$$P_v^m(\cos \theta_1) = (-)^m \frac{\Gamma(v+m+1)}{\Gamma(v-m+1)} P_v^{-m}(\cos \theta_1), \quad (18.261)$$

the functions $P_v^m(\cos \theta_1)$ and $(\partial/\partial \theta_1)P_v^m(\cos \theta_1)$ possess the same zeros as $P_v^{-m}(\cos \theta_1)$ and $(\partial/\partial \theta_1)P_v^{-m}(\cos \theta_1)$, respectively, along with the $2m$ zeros $v = -m, -m+1, \dots, m-1$ of $\Gamma(v+m+1)/\Gamma(v-m+1)$. Since

$$P_v^m(\cos \theta_1) = P_{-v-1}^m(\cos \theta_1), \quad (18.262)$$

the positive and negative zeros are related: For each zero v we also have $-v-1$ as a zero. Various analytical approximations to p and q for arbitrary m may be found scattered in the references, but for a general review, see ROBIN [1959].

From the Wronskian relation

$$\begin{aligned} P_v^m(\cos \theta_1) \frac{d}{d\theta_1} P_v^m(-\cos \theta_1) - P_v^m(-\cos \theta_1) \frac{d}{d\theta_1} P_v^m(\cos \theta_1) = \\ = \frac{2}{\pi} \frac{\sin(v-m)\pi}{\sin \theta_1} \frac{\Gamma(v+m+1)}{\Gamma(v-m+1)}, \end{aligned} \quad (18.263)$$

it follows that

$$P_p^m(-\cos \theta_1) = -\frac{2}{\pi} \frac{\sin(p-m)\pi}{\sin \theta_1} \frac{\Gamma(p+m+1)}{\Gamma(p-m+1)} \left[\frac{\partial}{\partial \theta_1} P_p^m(\cos \theta_1) \right]^{-1}, \quad (18.264)$$

$$\frac{\partial}{\partial \theta_1} P_q^m(-\cos \theta_1) = \frac{2}{\pi} \frac{\sin(q-m)\pi}{\sin \theta_1} \frac{\Gamma(q+m+1)}{\Gamma(q-m+1)} [P_q^m(\cos \theta_1)]^{-1}. \quad (18.265)$$

It may also be demonstrated that (see, e.g., BAILIN and SILVER [1956])

$$\int_0^{\theta_1} [P_p^m(\cos \alpha)]^2 \sin \alpha d\alpha = \frac{\sin \theta_1}{2p+1} \frac{\partial P_p^m(\cos \theta_1)}{\partial \theta_1} \frac{\partial P_p^m(\cos \theta_1)}{\partial p}, \quad (18.266)$$

$$\int_0^{\theta_1} [P_q^m(\cos \alpha)]^2 \sin \alpha d\alpha = -\frac{\sin \theta_1}{2q+1} \frac{\partial^2 P_q^m(\cos \theta_1)}{\partial q \partial \theta_1} P_q^m(\cos \theta_1). \quad (18.267)$$

Equations (18.263) through (18.267) have been employed in deriving alternative expressions for the eigenfunctions expansions for the cone.

Some numerical tables for the roots p or q are available and are based upon different computational methods, including asymptotic analysis (PAL [1918, 1919], HORTON [1947], CARRUS and TREUENFELS [1950]), power series in the argument θ_1 (HALL [1949]), power series in the index v (SIEGEL et al. [1951, 1952, 1953b]), numerical integration of the Mehler-Dirichlet integral representation (WATERMAN [1963]), and trigonometric series expansion for the Legendre function (WILCOX [1968]). PAL [1918, 1919] calculated the first five values of p and q for $\theta_1 = 15^\circ, 30^\circ, 45^\circ$ and

$m = 0, 1, 2$; his tables were later corrected by HORTON [1947]. For $m = 0$, HALL [1949] presents the first three roots p for $1 + \cos \theta_1 = 10^{-2}$ and the five first roots p for $1 + \cos \theta_1 = 10^{-3}, 10^{-4}, 10^{-5}$; in addition, the corresponding values of the normalization integral in eq. (18.266) are given. For $m = 1$, CARRUS and TREUENFELS [1950] tabulated the first fifty zeros p every 5° for $90^\circ \leq \theta_1 \leq 175^\circ$ and the first fifty zeros q every 5° for $90^\circ \leq \theta_1 \leq 130^\circ$. Also tabulated were the normalization integrals in eqs. (18.266) and (18.267). Errors in the Carrus-Treuenfels tables were noted by SIEGEL et al. [1951]. For the special value $\theta_1 = 165^\circ$ with $m = 1$, the first nineteen zeros p and the first fifteen zeros q , along with the normalization integrals, were re-computed by SIEGEL et al. [1952, 1953b]. These were again recomputed with even more accuracy by the Institute of Numerical Analysis, University of California, Los Angeles (see SIEGEL et al. [1953a]). For this same value of $\theta_1 = 165^\circ$ and $m = 1$, the first thirty zeros p and q were later presented with a stated accuracy of seven significant figures by WATERMAN [1963], and to the same accuracy, the first fifty zeros were provided by WILCOX [1968]. Comparison of the results in these last two references shows agreement in the values of p to six and usually seven significant figures. However, for q the values in WATERMAN [1963] are consistently lower than those in WILCOX [1968], with the difference showing up in the fifth decimal place for the higher order zeros. No explanation for the discrepancy has been found, although on the basis of re-evaluating the Legendre function at each of the two proposed values for the zero, WILCOX [1968] concludes that his values are more accurate. The first five zeros of $P_p(\cos \theta_1)$, $P_q^1(\cos \theta_1)$ and $(\partial/\partial \theta_1)P_q^1(\cos \theta_1)$ are plotted in Fig. 18.16 as functions of θ_1 for $90^\circ \leq \theta_1 \leq 180^\circ$.

The MEHLER [1881] conical functions $K_x^m(\cos \theta)$ are defined in terms of Legendre functions by the equation

$$K_x^m(\cos \theta) = P_{1x-1/2}^m(\cos \theta), \quad (18.268)$$

where x is a real parameter and $m = 0, 1, 2, \dots$. The principal properties of these functions can be deduced from the general results concerning the Legendre functions (see e.g. ROBIN [1957-1959]); in particular, from eq. (18.262) we observe

$$K_x^m(\cos \theta) = K_{-x}^m(\cos \theta), \quad (18.269)$$

implying that $K_x^m(\cos \theta)$ is an even function of x , and from eq. (18.261) we obtain

$$K_x^{-m}(\cos \theta) = \frac{K_x^m(\cos \theta)}{(x^2 + \frac{1}{4})(x^2 + \frac{9}{4}) \dots [x^2 + \frac{1}{4}(2m-1)^2]}. \quad (18.270)$$

For $0 \leq \theta < \pi$:

$$\begin{aligned} K_x^{-m}(\cos \theta) &= \frac{(-1)^m}{m!} \tan^m \frac{1}{2}\theta {}_2F_1\left(\frac{1}{2}+ix, \frac{1}{2}-ix; m+1; \sin^2 \frac{1}{2}\theta\right) = \\ &= \frac{(-1)^m}{m!} \tan^m \frac{1}{2}\theta \left[1 + \frac{4x^2+1^2}{1!2^2(m+1)} \sin^2 \frac{1}{2}\theta + \frac{(4x^2+1^2)(4x^2+3^2)}{2!2^4(m+1)(m+2)} \sin^4 \frac{1}{2}\theta + \dots \right]. \end{aligned} \quad (18.271)$$

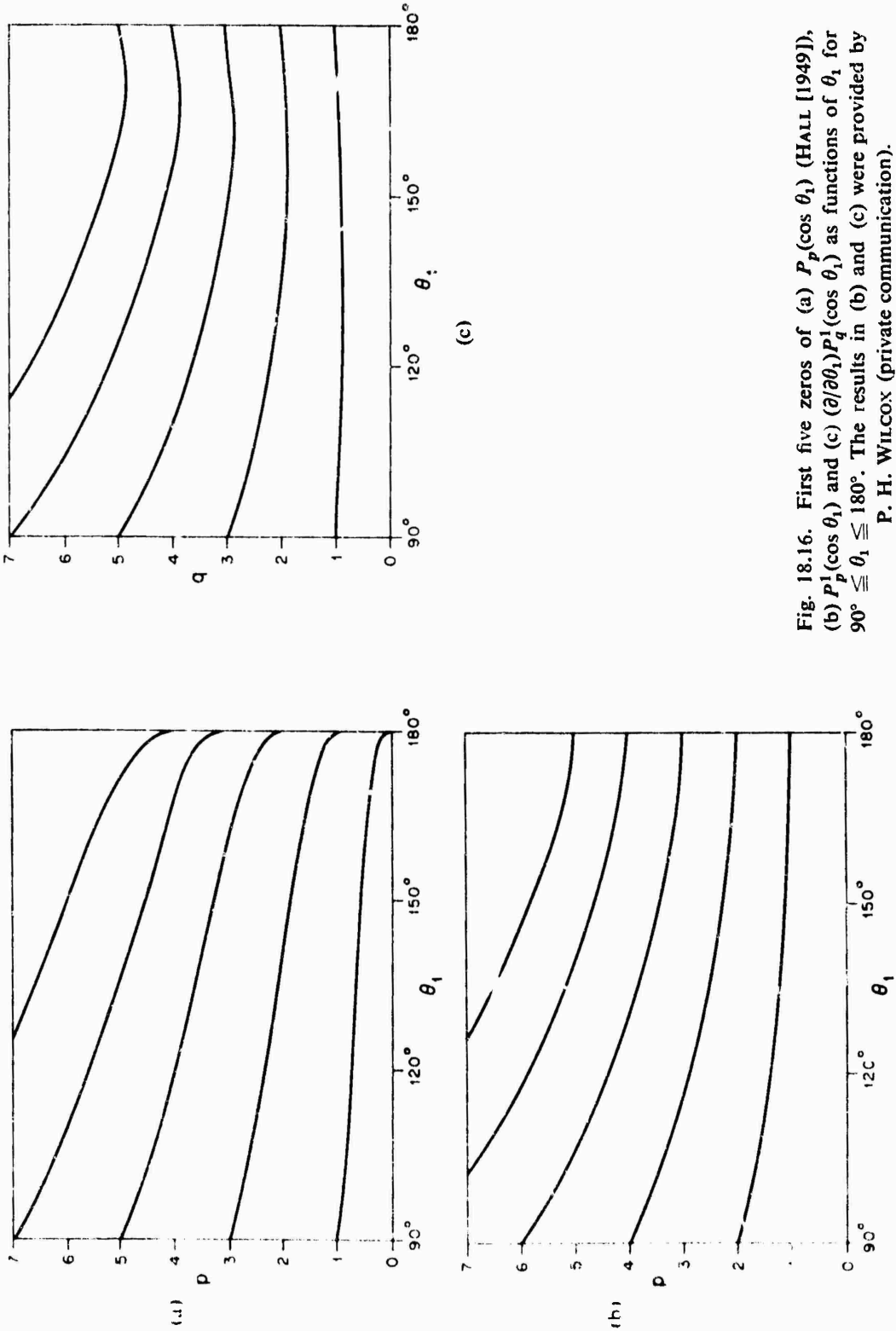


Fig. 18.16. First five zeros of (a) $P_p(\cos \theta_1)$ (Hall [1949]), (b) $P_q^1(\cos \theta_1)$ and (c) $(\partial/\partial \theta_1)P_q^1(\cos \theta_1)$ as functions of θ_1 for $90^\circ \leq \theta_1 \leq 180^\circ$. The results in (b) and (c) were provided by P. H. Wilcox (private communication).

where ${}_2F_1$ is the Gauss hypergeometric function; in particular, for $m = 0$:

$$K_x(\cos \theta) = 1 + \sum_{n=1}^{\infty} \frac{(4x^2+1^2)(4x^2+3^2) \dots [4x^2+(2n-1)^2]}{2^{2n}(n!)^2} \sin^{2n} \frac{1}{2}\theta. \quad (18.272)$$

It is clear from eqs. (18.270) through (18.272) that $K_x^m(\cos \theta)$ is real and that $K_x(\cos \theta) > 0$. For $\theta = \pi$, $K_x(\cos \theta)$ displays a logarithmic singularity, and an expansion suitable for $\theta \approx \pi$ is

$$K_x(\cos \theta) = \frac{1}{\pi} \cosh \pi x \left\{ \log \tan^2 \frac{1}{2}\theta - g(x) + \sum_{n=1}^{\infty} \frac{(4x^2+1^2)(4x^2+3^2) \dots [4x^2+(2n-1)^2]}{2^{2n}(n!)^2} \cos^{2n} \frac{1}{2}\theta \left[\log \tan^2 \frac{1}{2}\theta - g(x) + \sum_{s=1}^n \frac{2}{s} \right] \right\} \quad (18.273)$$

where

$$g(x) = 2 \sum_{n=1}^{\infty} \frac{4x^2-2n+1}{n[4x^2+(2n-1)^2]} \quad (18.274)$$

is the quantity that appears in eqs. (18.205) and (18.206). For $x \sin \theta \gg 1$:

$$K_x^m(\cos \theta) \sim \frac{(-x)^m e^{x\theta}}{(2\pi x \sin \theta)^{\frac{1}{2}}} \left[1 - \frac{4m^2-1}{8x} \cot \theta + O\left(\frac{1}{x^2}\right) \right]. \quad (18.275)$$

For $\theta + \theta_0 < \pi$, an integral of particular importance for diffraction by thin cones is

$$\int_0^{\frac{1}{2}\pi} dx x \frac{\tanh \pi x}{\cosh \pi x} K_x^m(\cos \theta) K_x^m(\cos \theta_0) = \frac{(2m)!}{\pi} \frac{\sin^m \theta \sin^m \theta_0}{(\cos \theta + \cos \theta_0)^{2m+1}}, \quad (18.276)$$

which is a generalization of the result given by MEHLER [1881] for $m = 0$. Other pertinent integrals are given by FELSEN [1956]; in particular, for $\theta + \theta_0 < \pi$:

$$\int_0^{\frac{1}{2}\pi} dx x \frac{\tanh \pi x}{\cosh \pi x} (x^2 + \frac{1}{4}) K_x(\cos \theta) K_x(\cos \theta_0) = \frac{2}{\pi} \frac{1 + \cos \theta \cos \theta_0}{(\cos \theta + \cos \theta_0)^3}, \quad (18.277)$$

$$\begin{aligned} \int_0^{\frac{1}{2}\pi} dx x \frac{\tanh \pi x}{\cosh \pi x} (x^2 + \frac{1}{4}) K_x^1(\cos \theta) K_x^1(\cos \theta_0) &= \\ &= \frac{4}{\pi} \frac{\sin \theta \sin \theta_0}{(\cos \theta + \cos \theta_0)^5} [4(1 + \cos \theta \cos \theta_0) + \sin^2 \theta + \sin^2 \theta_0], \end{aligned} \quad (18.278)$$

$$\int_0^{\frac{1}{2}\pi} dx x \frac{\tanh \pi x}{x^2 + \frac{1}{4} \cosh \pi x} K_x^1(\cos \theta) K_x^1(\cos \theta_0) = \frac{1}{\pi} \frac{\tan \frac{1}{2}\theta \tan \frac{1}{2}\theta_0}{\cos \theta + \cos \theta_0}, \quad (18.279)$$

to which may be added

$$\begin{aligned} \int_0^{\frac{1}{2}\pi} dx x \frac{\tanh \pi x}{x^2 + \frac{1}{4} \cosh \pi x} K_x^2(\cos \theta) K_x^2(\cos \theta_0) &= \\ &= \frac{2}{\pi} \frac{\tan^2 \frac{1}{2}\theta \tan^2 \frac{1}{2}\theta_0}{\cos \theta + \cos \theta_0} \left[1 + \frac{2}{\cos \theta + \cos \theta_0} + \frac{1 + \cos \theta \cos \theta_0}{(\cos \theta + \cos \theta_0)^2} \right]; \end{aligned} \quad (18.280)$$

$$\int_0^\infty dx x \frac{\tanh \pi x}{\cosh \pi x} (x^2 + \frac{1}{4})^2 K_x(\cos \theta) K_x(\cos \theta_0) =$$

$$= \frac{24}{\pi} \frac{\sin^2 \theta \sin^2 \theta_0}{(\cos \theta + \cos \theta_0)^2} - \frac{3 - \cos \theta \cos \theta_0}{\pi (\cos \theta + \cos \theta_0)^3}. \quad (18.281)$$

Still further similar integrals can be obtained by employing the recurrence formulas

$$\left(\frac{d}{d\theta} - m \cot \theta \right) K_x^m = -K_x^{m+1},$$

$$\left(\frac{d}{d\theta} + m \cot \theta \right) K_x^m = -[(x^2 + \frac{1}{4}) + m(m-1)] K_x^{m-1}, \quad (18.282)$$

or integral equation

$$\left[\frac{1}{\sin \theta} \frac{d}{d\theta} \sin \theta \frac{d}{d\theta} - \frac{m^2}{\sin^2 \theta} \right] K_x^m = (x^2 + \frac{1}{4}) K_x^m. \quad (18.283)$$

The function $I(r, \alpha)$ governing certain geometrical optics and transition phenomena is defined by the following equations:

$$I(r, \alpha) = I_{g.o.}(r, \alpha) + I_{tr.}(r, \alpha), \quad (18.284)$$

$$I_{g.o.}(r, \alpha) = -2\pi i \eta(\alpha) e^{ikr \cos \alpha}, \quad (18.285)$$

$$I_{tr.}(r, \alpha) = \pi i \operatorname{sgn}(\alpha) \left[G(w) - \frac{e^{4i\pi}}{w\sqrt{2\pi}} \right] e^{ikr}, \quad (18.286)$$

$$w = \sqrt{kr \sin \frac{1}{2}|\alpha|}, \quad G(w) = \frac{2}{\sqrt{\pi}} e^{-2iw^2} \int_{(1-i)w}^\infty e^{-\mu^2} d\mu. \quad (18.287)$$

Physically, the angle α determines some geometrical optics boundary at $\alpha = 0$. The function $G(w)$ is related to the Fresnel integral discussed in the Introduction by

$$G(w) = \frac{2}{\sqrt{\pi}} e^{-2iw^2 - \frac{1}{2}i\pi} F(w\sqrt{2}) \quad (18.288)$$

so that its principal properties may be deduced from the general results concerning the Fresnel integral. In particular, for $w \gg 1$ (away from the geometrical optics boundary):

$$G(w) \sim \frac{e^{4i\pi}}{w\sqrt{2\pi}} \left[1 + \sum_{n=1}^{\infty} \frac{1 \cdot 3 \cdots (2n-1)}{(4iw^2)^n} \right], \quad (18.289)$$

and the transition function $I_{tr.}(r, \alpha)$ in eq. (18.286) is therefore very small for points well away from the geometrical optics boundary; i.e. for $kr \sin^2 \frac{1}{2}\alpha \gg 1$:

$$I_{tr.}(r, \alpha) \sim -\frac{\pi e^{i(kr - \frac{1}{2}\pi)}}{\sqrt{2kr \sin \frac{1}{2}\alpha}} \sum_{n=1}^{\infty} \frac{1 \cdot 3 \cdots (2n-1)}{[4ikr \sin^2 \frac{1}{2}\alpha]^n}. \quad (18.290)$$

On the other hand, an expansion suitable for $w \approx 0$ is

$$G(w) = e^{-2iw^2} - 2 \sqrt{\frac{2}{\pi}} e^{-\frac{1}{2}i\pi} w \sum_{n=0}^{\infty} \frac{(-4iw^2)^n}{1 \cdot 3 \cdots (2n+1)}; \quad (18.291)$$

thus, for points close to the geometrical optics boundary, i.e. for $kr \sin^2 \frac{1}{2}\alpha \ll 1$ the total function $I(r, \alpha)$ behaves as

$$I(r, \alpha) = \frac{\sqrt{\pi} e^{i(kr - \frac{1}{2}\pi)}}{\sqrt{2kr \sin \frac{1}{2}\alpha}} - \pi i e^{ikr \cos \alpha} - 2e^{\frac{1}{2}i\pi} \sqrt{2\pi kr \sin \frac{1}{2}\alpha} \sum_{n=0}^{\infty} \frac{[-4ikr \sin^2 \frac{1}{2}\alpha]^n}{1 \cdot 3 \cdots (2n+1)}. \quad (18.292)$$

The singular part in $I(r, \alpha)$, represented by the first term in eq. (18.292), yields a field contribution that is exactly cancelled by a corresponding singularity in the diffracted field due to the cone tip. The remaining terms in eq. (18.292) are regular and free of jump discontinuities on the geometrical optics boundary $\alpha = 0$. The phase and amplitude of both $G(w)$ and

$$-\frac{1}{2} \sqrt{\frac{2}{\pi}} e^{\frac{1}{2}i\pi} \frac{dG(w)}{dw} = [1 - \sqrt{2\pi} e^{-\frac{1}{2}i\pi} w G(w)] \quad (18.293)$$

have been plotted by FELSEN [1955, 1957c, 1958, 1959] and his results are reproduced in Fig. 18.17. Also shown in Fig. 18.17 are the amplitudes of the leading asymptotic approximations to $G(w)$ and $[1 - \sqrt{2\pi} \exp(-\frac{1}{2}i\pi) w G(w)]$ for $w \gg 1$ as determined from eq. (18.289). On the basis of these plots Felsen concludes that transition effects are appreciable only for $w < 4$.

The function $T(r, \alpha)$ governing geometrical optics and transition phenomena for axial incidence (except when $\theta_1 \rightarrow \frac{1}{2}\pi$) is defined by the following equations:

$$T(r, \alpha) = T_{\text{refl.}}(r, \alpha) + T_{\text{tr.}}(r, \alpha), \quad (18.294)$$

$$T_{\text{refl.}}(r, \alpha) = \eta(x) \sqrt{\frac{\tan \alpha}{2\pi kr}} \exp \{i(kr \cos \alpha + \frac{1}{4}\pi)\} \\ \times \exp \left\{ \frac{1}{2} ikr \frac{\sin^2 \alpha}{\cos \alpha} \right\} K_{\frac{1}{2}} \left(\frac{1}{2} ikr \frac{\sin^2 \alpha}{\cos \alpha} \right), \quad (18.295)$$

$$T_{\text{tr.}}(r, \alpha) = -[\eta(x) + i\eta(-x)] \sqrt{\frac{\tan \frac{1}{2}|\alpha|}{2\pi kr}} e^{i(kr + \frac{1}{2}\pi)} \left[e^{-iw^2} K_{\frac{1}{2}}(-iw^2) - \sqrt{\frac{\pi}{2}} \frac{e^{\frac{1}{2}i\pi}}{w} \right], \quad (18.296)$$

with

$$w = \sqrt{kr \sin \frac{1}{2}|\alpha|}. \quad (18.297)$$

The function $K_{\frac{1}{2}}$ represents the modified Bessel (or Macdonald) function of order $\frac{1}{2}$. The angle α determines the geometrical optics boundary at $\alpha = 0$, and for axial plane-wave incidence, $\alpha = \pi - 2\theta_1 + \theta$. In the region $kr \sin^2 \frac{1}{2}\alpha \gg 1$ well away from the optics boundary, the transition function yields a negligible contribution to the field since it behaves as

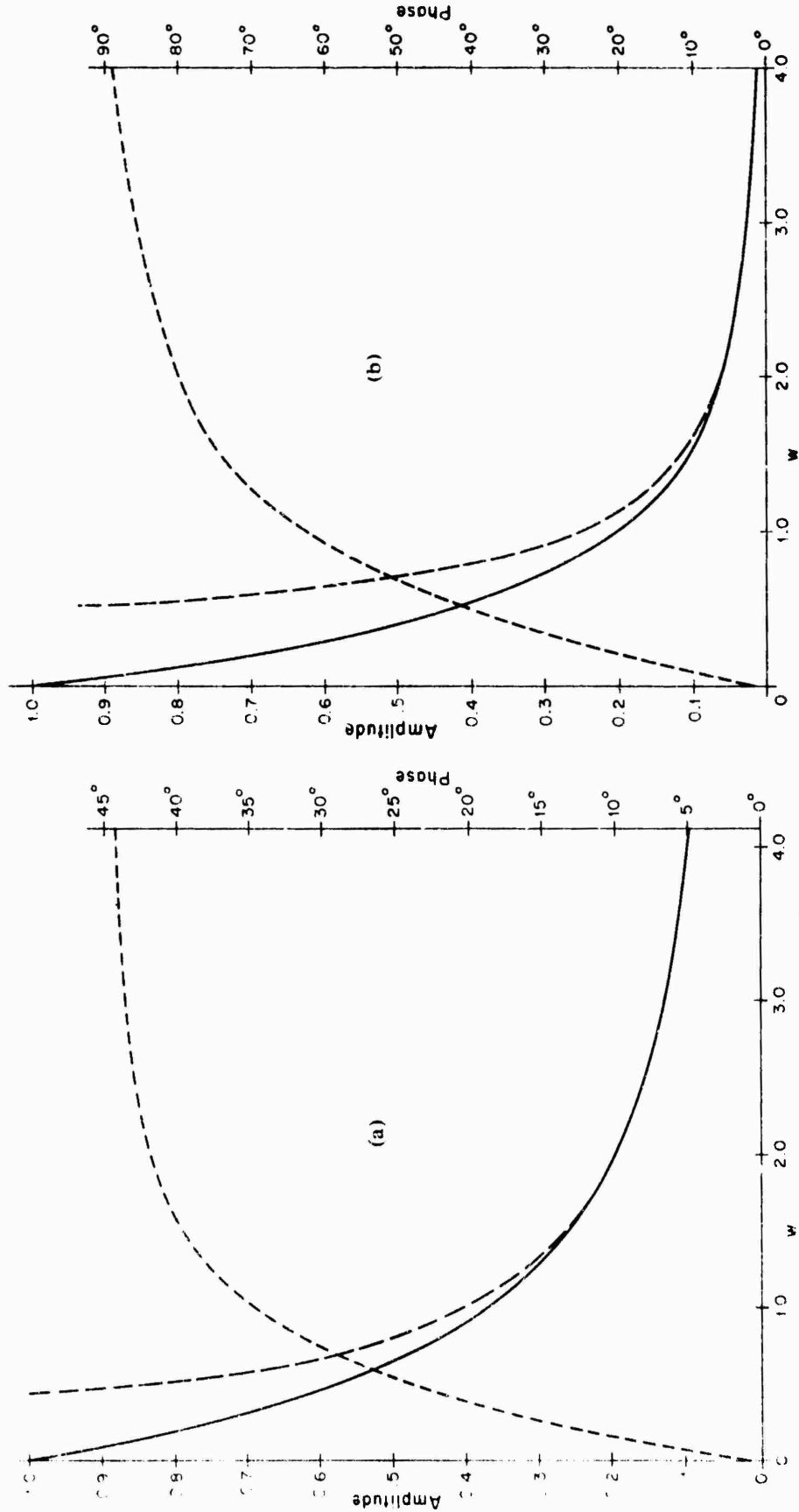


Fig. 18.17. Amplitude (—) and phase (---) of (a) $G(w)$ and (b) $[1 - \sqrt{2/7} \exp(-\frac{1}{2} i \pi) w G(w)]$; also, amplitude (---) of the corresponding asymptotic approximations (a) $[i/(4w^2)]$ and (b) $[i/(4w^2)]$.

$$T_{\text{tr.}}(r, \alpha) \sim -[\eta(\alpha) + i\eta(-\alpha)] \frac{3e^{ikr}}{2^{\frac{1}{2}}(2kr)^2(\sin|\alpha|)^{\frac{1}{2}}\sin^2\frac{1}{2}\alpha} + O\left[\frac{1}{(kr)^3}\right]. \quad (18.298)$$

In this same region, $kr \sin^2 \frac{1}{2}\alpha \gg 1$, we have

$$T_{\text{refl.}}(r, \alpha) \sim \frac{\eta(\alpha)e^{ikr \cos \alpha}}{kr(\sin \alpha)^{\frac{1}{2}}} \left\{ 1 + \frac{3i}{8kr} \frac{\cot \alpha}{\sin \alpha} + O\left[\frac{1}{(kr)^2}\right] \right\}. \quad (18.299)$$

On the other hand, for points close to the optics boundary, i.e. for $kr \sin^2 \frac{1}{2}\alpha \ll 1$ and $kr \gg 1$, the total function $T(r, \alpha)$ behaves as

$$T(r, \alpha) \approx \frac{i[\eta(\alpha) + i\eta(-\alpha)]e^{ikr}}{kr(2 \sin|\alpha|)^{\frac{1}{2}}} + \frac{\sqrt{\pi}e^{i(kr - \frac{1}{2}\pi)}}{(2kr)^{\frac{1}{2}}[\cos \frac{1}{2}\alpha]^{\frac{1}{2}}} \left\{ \frac{1}{\Gamma(\frac{3}{4})} + \frac{e^{-\frac{1}{2}i\pi}}{\Gamma(\frac{5}{4})} \left(\frac{1}{2}kr \right)^{\frac{1}{2}} \sin \frac{1}{2}\alpha - \frac{ikr}{\Gamma(\frac{3}{4})} \sin^2 \frac{1}{2}\alpha + \dots \right\}. \quad (18.300)$$

The singular part in $T(r, \alpha)$ represented by the first term in eq. (18.300), leads to a field contribution that is cancelled by a corresponding singularity in the diffraction field due to the cone tip. The remaining terms, to this order of approximation, are regular and free of jump discontinuities on the geometrical optics boundary $\alpha = 0$; however, the higher order terms do contain jump discontinuities at $\alpha = 0$, so that for smaller kr the function $T(r, \alpha)$ would have to be modified in order to obtain an appropriate uniform asymptotic expansion for the field.

Bibliography

- BAILIN, L. L. and S. SILVER [1956], Exterior Electromagnetic Boundary Value Problems for Spheres and Cones, IRE Trans. AP-4, 5-16; see corrections in IRE Trans. AP-5 (1957) 313.
- BOWMAN, J. J. [1963], Far-Zone Scattering of Plane Sound Waves by a Rigid Semi-Infinite Cone (Nose-on Incidence), Memorandum D0620-109-M; Far-Zone Scattering of Plane Electromagnetic waves by a Perfectly Conducting Semi-Infinite Cone (Nose-on Incidence), Memorandum D0620-112-M; Plane-Wave Scattering by Small-Angle Cones, Memorandum D0620-149-M, P0047-18; Plane-Wave Scattering by Small-Angle Cones II, Memorandum D0620-152-M, P004721; Far Scattered Fields Due to Thin Semi-Infinite Cones and Cylinders, Memorandum D0620-162-M, P0047-23; Plane-Wave Scattering by Small-Angle Cones III, Memorandum D0620-164-M, P0047-24; Plane-Wave Scattering by Small-Angle Cones IV, Geometrical-Optics and Transition Phenomena, Memorandum D0620-169-M. Conductron Corporation, Ann Arbor, Michigan.
- CARRUS, P. A. and C. G. TREUENIELS [1950], Tables of Roots and Incomplete Integrals of Associated Legendre Functions of Fractional Orders, J. Math. and Phys. 29, 282-299.
- CARSLAW, H. S. [1910], The Scattering of Waves by a Cone, Phil. Mag. 6, 690-691. In the expressions for u multiply the summands by $n + \frac{1}{2}$.
- CARSLAW, H. S. [1914], The Scattering of Sound Waves by a Cone, Math. Ann. 75, 133-147.
- ELISEN, L. B. [1953], Back Scattering from Wide-Angle and Narrow-Angle Cones, presented at McGill Symp. on Microwave Optics, Air Force Cambridge Research Center Report No. TR-59-118(II) (1959).
- ELISEN, L. B. [1955], Back Scattering from Wide-Angle and Narrow-Angle Cones, J. Appl. Phys. 26, 138-151. In eqs. (2.28a) and (3.15a) replace $64\pi^2$ by 16π , and in eq. (3.14a) replace $\sin^2 \theta_n$ by $\sin \theta_n$.

- FELSEN, L. B. [1956], Some Definite Integrals Involving Conical Functions, *J. Math. and Phys.* **35**, 177-178.
- FELSEN, L. B. [1957a], Plane-Wave Scattering by Small-Angle Cones, *IRE Trans. AP-5*, 121-129. See corrections in *IRE Trans. AP-5*, 402-404.
- FELSEN, L. B. [1957b], Asymptotic Expansion of the Diffracted Wave For a Semi-Infinite Cone, *IRE Trans. AP-5*, 402-404.
- FELSEN, L. B. [1957c], Radiation from Source Distributions on Cones and Wedges, Polytechnic Institute of Brooklyn Microwave Research Institute Report No. R-574-57, PIB-512.
- FELSEN, L. B. [1958], Back Scattering from a Semi-Infinite Cone, Polytechnic Institute of Brooklyn Microwave Research Institute Memorandum No. 43-R675-58, PIB-603.
- FELSEN, L. B. [1959], Radiation from Ring Sources in the Presence of a Semi-Infinite Cone, *IRE Trans. AP-7*, 168-180. See correction in *IRE Trans. AP-7*, 251. In eq. (24c) replace $4/\sqrt{\pi}$ by $2(2/\pi)^{1/2}$. The right-hand ordinate in fig. 5 should be labelled: Phase, χ . In the line immediately following eq. (31) replace $w > 4$ by $w < 4$ and in the line preceding eq. (35a) replace $u \approx 0$ by $0 \neq 0$. Multiply right-hand sides of eqs. (34a) and (34b) by $E(r')$.
- GOODRICH, R. F. [1958], Studies in Radar Cross Sections XXVI - Fock Theory, The University of Michigan Radiation Laboratory Report No. 2591-3-T.
- GOODRICH, R. F., R. E. KLEINMAN, A. L. MAFFETT, N. E. REITLINGER, C. E. SCHENSTED and K. M. SIEGEL [1958], Radiation and Scattering from Simple Shapes II, *L'Onde Elect.* **1**, 49-57.
- GOODRICH, R. F., R. E. KLEINMAN, A. L. MAFFETT, C. E. SCHENSTED, K. M. SIEGEL, M. G. CHERNIN, H. E. SHANKS and R. E. PLUMMER [1959], Radiation from Slot Arrays on Cones, *IRE Trans. AP-7*, 213-222.
- GORYANOV, A. S. [1961], Diffraction of a Plane Electromagnetic Wave Propagated Along the Axis of a Cone, *Radio Eng. Electron.* **6**, 65-81 (English translation of *Radiotekhnika i Elektronika* **6** [1961] 47-57).
- HALL, R. N. [1949], The Application of Non-Integral Legendre Functions to Potential Problems, *J. Appl. Phys.* **20**, 925-931.
- HANSEN, W. W. and L. I. SCHIFF [1948], Theoretical Study of Electromagnetic Waves Scattered from Shaped Metal Surfaces, Stanford University Microwave Laboratory Quarterly Reports 1 to 4, Contract W28-099-333.
- HOBSON, E. W. [1931], *The Theory of Spherical and Ellipsoidal Harmonics*, Cambridge University Press, Cambridge, England.
- HORTON, C. W. [1947], Note on the Zeros of $P_n^m(\cos \theta)$ and $dP_n^m(\cos \theta)/d\theta$ considered as Functions of n , *Bull. Am. Math. Soc.* **53**, 153-155.
- KETTER, J. B., R. M. LEWIS and B. D. SECKLER [1956], Asymptotic Solutions of Some Diffraction Problems, *Comm. Pure Appl. Math.* **9**, 207-265.
- KLEINMAN, R. E. and T. B. A. SENIOR [1963], Studies in Radar Cross Sections XLVIII - Diffraction and Scattering by Regular Bodies II: the Cone, The University of Michigan Radiation Laboratory Report No. 3648-2-T.
- MACDONALD, H. M. [1900], Zeros of the Spherical Harmonic $P_n^m(\mu)$ considered as a Function of n , *Proc. London Math. Soc.* **31**, 264-278.
- MACDONALD, H. M. [1902], *Electric Waves*, Cambridge University Press, Cambridge, England.
- MEHLER, F. G. [1881], Ueber eine mit den Kugel- und Cylinderfunktionen verwandte und ihre Anwendung in der Theorie der Elektrizitäts-vertheilung, *Math. Ann.* **18**, 161-194.
- MENZIE, J. R. [1955], *Scattering and Diffraction of Radio Waves*, Pergamon Press, New York.
- PAL, B. [1918], On the Numerical Calculation of the Roots of the Equations $P_n^m(\mu) = 0$ and $(d/d\mu)P_n^m(\mu) = 0$ regarded as Equations in n , *Bull. Calcutta Math. Soc.* **9**, 85-95.
- PAL, B. [1919], On the Numerical Calculation of the Roots of the Equations $P_n^m(\mu) = 0$ and $(d/d\mu)P_n^m(\mu) = 0$ regarded as Equations in n - Part II, *Bull. Calcutta Math. Soc.* **10**, 187-194.
- ROUS, L. [1957-1959], *Fonctions Sphériques de Legendre et Fonctions Sphéroïdales*, Tome I, II, III, Gauthier-Villars, Paris, France.

- SCHENSTED, C. E. [1953], Application of Summation Techniques to the Radar Cross Section of a Cone, Presented at McGill Symp. on Microwave Optics. Air Force Cambridge Research Center Report No. TR-59-118(II) (1959).
- SENIOR, T. B. A. and P. H. WILCOX [1967], Travelling Waves in Relation to the Surface Fields on a Semi-Infinite Cone, *Radio Science* **2**, 479-487. In the expression for E_θ in eq. (11), replace $\partial A / \partial \theta_0$ by $\partial A / \partial \rho$.
- SIEGEL, K. M., D. M. BROWN, H. E. HUNTER, H. A. ALPERIN and C. W. QUILLEN [1951], Studies in Radar Cross sections II - The Zeros of the Associated Legendre Functions $P_n^m(\mu)$ of Non-Integral Degree, The University of Michigan Willow Run Research Center Report No. UMM-82.
- SIEGEL, K. M. and H. A. ALPERIN [1952], Studies in Radar Cross Sections III - Scattering by a Cone, The University of Michigan Willow Run Research Center Report No. UMM-87.
- SIEGEL, K. M., J. W. CRISPIN Jr., R. E. KLEINMAN and H. E. HUNTER [1952], The Zeros of $P'_{n_i}(x_0)$ of Non-Integral Degree, *J. Math. and Phys.* **31**, 170-179. Throughout this article $P'_{n_i}(x)$ should read $P'_{n_i}(x)$. On p. 172 in the line directly above eq. (2.4) the quantity $\frac{1}{2}(1-x_0)$ should read $\sqrt{\frac{1}{2}(1-x_0)}$.
- SIEGEL, K. M., H. A. ALPERIN, J. W. CRISPIN Jr., H. E. HUNTER, R. E. KLEINMAN, W. C. ORTHWEIN and C. E. SCHENSTED [1953a], Studies in Radar Cross Sections IV - Comparison between Theory and Experiment of the Cross Section of a Cone, The University of Michigan Willow Run Research Center Report No. UMM-92.
- SIEGEL, K. M., J. W. CRISPIN Jr., R. E. KLEINMAN and H. E. HUNTER [1953b], Note on the Zeros of $(dP_{m_i}(x)/dx)|_{x=x_0}$, *J. Math. and Phys.* **32**, 193-196.
- SIEGEL, K. M., H. A. ALPERIN, R. R. BONKOWSKI, J. W. CRISPIN Jr., A. L. MAFFETT, C. E. SCHENSTED and I. V. SCHENSTED [1955a], Bistatic Radar Cross Sections of Surfaces of Revolution, *J. Appl. Phys.* **26**, 297-305.
- SIEGEL, K. M., J. W. CRISPIN Jr. and C. E. SCHENSTED [1955b], Electromagnetic and Acoustical Scattering from a Semi-Infinite Cone, *J. Appl. Phys.* **26**, 309-313.
- SPENCER, R. C. [1951], Back Scattering from Conducting Surfaces, Air Force Cambridge Research Center Report No. E5070.
- TAI, C. T. [1954], A Glossary of Dyadic Green's Functions, Technical Report No. 46, Stanford Research Institute, Stanford, California.
- VAN BLADEL, J. [1964], *Electromagnetic Fields*, McGraw-Hill Book Co., New York.
- WATERMAN, P. C. [1963], Roots of Legendre Functions of Variable Index, *J. Math. Phys.* **42**, 323-328.
- WILCOX, P. H. [1968], The Zeros of $P_v^1(\cos \theta)$ and $(\partial/\partial \theta)P_v^1(\cos \theta)$, *Math. Comp.* **22**, 205-208.

APPENDICES

PRECEDING PAGE BLANK

A. SELECTED BIBLIOGRAPHY

I Books of general interest

On electromagnetic theory:

- [1] COLLIN, R. E. (1960), *Field Theory of Guided Waves* (McGraw-Hill).
- [2] JONES, D. S. (1964), *The Theory of Electromagnetism* (Macmillan).
- [3] LANDAU, L. D. and E. M. LIFSHITZ (1962), *The Classical Theory of Fields*, 2nd edition, (Addison-Wesley).
- [4] LANDAU, L. D. and E. M. LIFSHITZ (1960), *Electrodynamics of Continuous Media* (Addison-Wesley).
- [5] PANOFKY, K. H. and M. PHILLIPS (1962), *Classical Electricity and Magnetism*, 2nd edition, (Addison-Wesley).
- [6] SCHELKUNOFF, S. A. (1943), *Electromagnetic Waves* (Van Nostrand).
- [7] SMYTHE, W. R. (1950), *Static and Dynamic Electricity*, 2nd edition (McGraw-Hill).
- [8] SOMMERFELD, A. (1952), *Electrodynamics* (Academic Press).
- [9] STRATTON, J. A. (1941), *Electromagnetic Theory* (McGraw-Hill).
- [10] VAN BLADEL, J. (1964), *Electromagnetic Fields* (McGraw-Hill).
- [11] *Handbuch der Physik*, Vol. 16 (1958), *Electric Fields and Waves* (Springer).

On sound:

- [12] MORSE, P. M. (1948), *Vibration and Sound*, 2nd edition (McGraw-Hill).
- [13] MORSE, P. M. and K. UNGER (1968), *Theoretical Acoustics* (McGraw-Hill) [this book contains a good, up-to-date bibliography on the subject].
- [14] STRUTT, J. W., Lord Rayleigh (1945), *The Theory of Sound* (Dover).

On the connection between electromagnetism and optics:

- [15] BORN, M. and E. WOLF (1959), *Principles of Optics* (Pergamon Press).
- [16] KLEIN, M. and L. W. KAY (1965), *Electromagnetic Theory and Geometrical Optics* (Interscience).
- [17] LUNBERG, R. K. (1964), *Mathematical Theory of Optics* (University of California Press).
- [18] SOMMERFELD, A. (1964), *Optics* (Academic Press).

On antennas:

- [19] FRADIN, A. Z. (1961), *Microwave Antennas* (Pergamon Press).
- [20] JASIK, H. (1961), *Antenna Engineering Handbook* (McGraw-Hill).
- [21] KING, R. W. P. (1956), *The Theory of Linear Antennas* (Harvard University Press).
- [22] KRAUS, J. D. (1950), *Antennas* (McGraw-Hill).
- [23] SCHELKUNOFF, S. A. (1952), *Advanced Antenna Theory* (John Wiley).
- [24] SILVER, S. (1963), *Microwave Antenna Theory and Design* (Boston Technical Lithographers).

On asymptotic expansions (see also Section I.3 of the Introduction):

- [25] COPSON, E. T. (1965), *Asymptotic Expansions* (Cambridge).
- [26] DE BRUIJN, N. G. (1958), *Asymptotic Methods in Analysis* (North-Holland).
- [27] ERDÉLYI, A. (1956), *Asymptotic Expansions* (Dover).
- [28] FOCKE, J. (1954), *Asymptotische Entwicklungen Mittels der Methode der stationären Phase* (Akademie Verlag, Berlin) (in German).
- [29] JEFFREYS, H. (1962), *Asymptotic Approximations* (Oxford).
- [30] TITCHMARSH, E. C. (1946/1958), *Eigenfunction Expansions Associated with Second-Order Differential Equations* (Oxford) (in two volumes).

II Books on scattering theory

- [31] BAKER, B. B. and E. T. COPSON (1950), *The Mathematical Theory of Huygens' Principle*, 2nd. edition (Oxford).
- [32] BARLOW, H. M. and J. BROWN (1962), *Radio Surface Waves* (Oxford).
- [33] BECKMANN, P. (1968), *The Depolarization of Electromagnetic Waves* (The Golem Press, Boulder, Colorado).
- [34] BECKMANN, P. and A. SPIZZICHINO (1963), *The Scattering of Electromagnetic Waves from Rough Surfaces* (Pergamon Press).
- [35] BOROVIKOV, V. A. (1966), *Diffraction by Polygons and Polyhedrons* (Nauka, Moscow) (in Russian).
- [36] BREMMER, H. (1949), *Terrestrial Radio Waves* (Elsevier).
- [37] CRISPIN JR., J. W. and K. M. SIEGEL (1968), editors, *Radar Cross Section Analysis* (Academic Press).
- [38] FOCK, V. A. (1965), *Electromagnetic Diffraction and Propagation Problems* (Pergamon Press).
- [39] FRIEDLANDER, F. G. (1958), *Sound Pulses* (Cambridge).
- [40] HANSEN, E. B. (1964), *Studier i asymptotisk diffraktionsteori* (Akademisk Forlag, Copenhagen) (in Danish).
- [41] LAX, P. D. and R. S. PHILLIPS (1967), *Scattering Theory* (Academic Press).
- [42] KING, R. W. P. and T. T. WU (1959), *The Scattering and Diffraction of Waves* (Harvard University Press).

- [43] MENTZER, J. R. (1955), *Scattering and Diffraction of Radio Waves* (Pergamon Press).
- [44] RUBINOWICZ, A. (1966), *Die Beugungswelle in der Kirchhoffschen Theorie der Beugung* (Springer) (in German).
- [45] RUCK, G., D. BARRICK and W. STUART (1969), *Radar Cross Section Handbook* (Plenum Press, New York).
- [46] VAN DE HULST, H. C. (1957), *Light Scattering by Small Particles* (John Wiley).
- [47] WAIT, J. R. (1959), *Electromagnetic Radiation from Cylindrical Structures* (Pergamon Press).
- [48] *Handbuch der Physik*, Vol. 25/1 (1961), *Theorie der Beugung* by H. Hönl, A. W. Maue and K. Westpfahl (Springer) (in German).

See also the following two reports:

- [49] LOGAN, N. A. (1959), *General Research in Diffraction Theory*, Vols. 1 and 2, Lockheed Missiles and Space Division Technical Reports Nos. LMSD-288087/8 (ASTIA Nos. AD 241228 and AD 243182), Sunnyvale, California.

On propagation in various media:

- [50] AL'PERT, YA. L., E. G. GUSEVA and D. S. FLIGEL (1967), *Propagation of Low Frequency Electromagnetic Waves in the Earth Ionosphere Waveguide* (Academy of Sciences of the U.S.S.R.) [in Russian; an English translation by H. Needler is available from the Federal Clearinghouse for Scientific Information, Springfield, Virginia 22151 (ASTIA No. AD 665-698)].
- [51] BREKHOVSKIKH, L. M. (1960), *Waves in Layered Media* (Academic Press).
- [52] BUDDEN, K. G. (1961), *Radio Waves in the Ionosphere* (Cambridge).
- [53] CHERNOV, L. A. (1960), *Wave Propagation in a Random Medium* (McGraw-Hill).
- [54] DAVIES, K. (1965), *Ionospheric Radio Propagation*, N.B.S. Monograph No. 80 (U.S. Government Printing Office, Washington).
- [55] GINZBURG, V. L. (1961), *Propagation of Electromagnetic Waves in Plasma* (Gordon and Breach, New York).
- [56] TATARSKI, V. I. (1961), *Wave Propagation in a Turbulent Medium* (McGraw-Hill).
- [57] WAIT, J. R. (1962), *Electromagnetic Waves in Stratified Media* (Pergamon Press).

III Proceedings of symposia

- [58] *The Theory of Electromagnetic Waves* (1951), edited by M. Kline (Interscience; reprinted by Dover (1965)); see also *Comm. Pure Appl. Math.* 3 (1950) 355-449 and 4 (1951) 33-160 (Symposium at New York University, June 1950).
- [59] *Symposium on Microwave Optics* (1953), edited by B. S. Karasik, Air Force Cambridge Research Center Report No. AFCRC-TR-59-118 (in two volumes, ASTIA No. AD 211499) (URSI Symposium at McGill University, Montreal, June 1953).

- [60] Symposium on Electromagnetic Wave Theory (July 1956) IRE Trans. **AP-4** (URSI Symposium at The University of Michigan, Ann Arbor, June 1955).
- [61] Electromagnetic Wave Propagation (1960), edited by M. Desirant and J. L. Michiels (Academic Press) (Symposium at the 1958 Brussels International Exhibition).
- [62] Symposium on Electromagnetic Theory (December 1959) IRE Trans. **AP-7** (URSI Conference at University of Toronto, June 1959).
- [63] Radio Waves and Circuits (1963), edited by S. Silver (Elsevier) (Commission 6 of URSI, 13th General Assembly, London, September 1960).
- [64] Electromagnetic Waves (1961), edited by R. E. Langer (University of Wisconsin Press) (Symposium at the Mathematics Research Center, U.S. Army, University of Wisconsin, April 1961).
- [65] Electromagnetic Theory and Antennas (1963), edited by E. C. Jordan (Pergamon Press) (in two volumes) (URSI International Symposium, Copenhagen, June 1962).
- [66] Electromagnetic Scattering (1963), edited by M. Kerker (Pergamon Press) (Interdisciplinary Conference, Clarkson College, Potsdam, N.Y., August 1962).
- [67] Quasi-Optics (1964), edited by J. Fox (Polytechnic Press, Brooklyn) (14th Symposium of the P.I.B. Microwave Research Institute, June 1964).
- [68] Electromagnetic Scattering (1968), edited by R. L. Rowell and R. S. Stein (Gordon and Breach, New York) (Second Interdisciplinary Conference, University of Massachusetts, Amherst, June 1965).
- [69] Electromagnetic Wave Theory (1967), edited by J. Brown (Pergamon Press) (URSI International Symposium, Delft, September 1965).
- [70] Electromagnetic Waves (1969), edited by F. Carassa and P. J. B. Clarricoats, *Alta Frequenza*, **38**, special issue (URSI International Symposium, Stresa, Italy, June 1968).

See also the special issue on:

- [71] Radar Reflectivity (August 1965), edited by P. C. Fritsch, *Proc. IEEF* **53**.

IV Reviews and bibliographies

Many survey articles with extensive bibliographies may be found in the Symposia Proceedings listed above. See also the following:

- [72] BOUWKAMP, C. J. (1954), Diffraction Theory, *Rep. Progr. Phys.* **17**, 35-100.
- [73] CORRIHER, H. A. and B. O. PYRON (1965), A Bibliography of Articles on Radar Reflectivity and Related Subjects: 1957-1964, *Proc. IEEE* **53**, 1025-1064.
- [74] KELLER, J. B. and E. B. HANSEN (1965), Survey of the Theory of Diffraction of Short Waves by Edges, *Acta Phys. Polon.* **27**, 217-234.
- [75] LOGAN, N. A. and R. FLYNN (July 1957), Bibliography of Soviet Research on Radiowave Propagation and Antennas, Air Force Cambridge Research Center Report No. AFCRC-TR-57-113 (ASTIA No. AD 133638).

- [76] TWERSKY, V. (1964), Rayleigh Scattering, Appl. Opt. **3**, 1150-1162.
- [77] Onde Superficiali, lectures held at the Centro Internazionale Matematico Estivo (C.I.M.E.), Italy; Edizioni Cremonese, Rome (1961).
- [78] Radio Science, J. Res. NBS **68D**, 435-517, (1964). (This report on electromagnetics covers the contributions made by workers in the United States during the years 1960-1963.)
- [79] Radio Science **4**, 575-666 (1969) (U.S. National Committee Report to the 16th General Assembly of URSI).

B. VECTOR RELATIONS

A, B, C, D are arbitrary vector fields; f and g are arbitrary scalar fields.

General formulas:

- (1) $A \cdot B \wedge C = B \cdot C \wedge A = C \cdot A \wedge B$
- (2) $A \wedge (B \wedge C) = (A \cdot C)B - (A \cdot B)C$
- (3) $A \wedge (B \wedge C) + B \wedge (C \wedge A) + C \wedge (A \wedge B) = 0$
- (4) $(A \wedge B) \cdot (C \wedge D) = A \cdot [B \wedge (C \wedge D)] = (A \cdot C)(B \cdot D) - (A \cdot D)(B \cdot C)$
- (5) $(A \wedge B) \wedge (C \wedge D) = (A \wedge B \cdot D)C - (A \wedge B \cdot C)D$
- (6) $\nabla(fg) = f\nabla g + g\nabla f$
- (7) $\nabla \cdot (fA) = A \cdot \nabla f + f\nabla \cdot A$
- (8) $\nabla \wedge (fA) = \nabla f \wedge A + f\nabla \wedge A$
- (9) $\nabla(A \cdot B) = (A \cdot \nabla)B + (B \cdot \nabla)A + A \wedge (\nabla \wedge B) + B \wedge (\nabla \wedge A)$
- (10) $\nabla \cdot (A \wedge B) = B \cdot \nabla \wedge A - A \cdot \nabla \wedge B$
- (11) $\nabla \wedge (A \wedge B) = A\nabla \cdot B - B\nabla \cdot A + (B \cdot \nabla)A - (A \cdot \nabla)B$
- (12) $\nabla \wedge \nabla f = 0$
- (13) $\nabla \cdot \nabla \wedge A = 0$
- (14) $\nabla \wedge \nabla \wedge A = \nabla \nabla \cdot A - \nabla^2 A$
- (15) $\nabla^2 f = \nabla \cdot \nabla f$
- (16) $\nabla f(g) = \frac{\partial f}{\partial g} \nabla g$
- (17) $\nabla^2(fg) = f\nabla^2 g + g\nabla^2 f + \nabla f \cdot \nabla g$
- (18) $\nabla^2(fA) = f\nabla^2 A + A\nabla^2 f + 2(\nabla f \cdot \nabla)A$
- (19) $\nabla \nabla \cdot (fA) = (\nabla f)\nabla \cdot A + f\nabla \nabla \cdot A + (\nabla f \cdot \nabla)A + (A \cdot \nabla)\nabla f + \nabla f \wedge (\nabla \wedge A)$
- (20) $\nabla \wedge \nabla \wedge (fA) = f\nabla \wedge \nabla \wedge A - A\nabla^2 f + (\nabla f)\nabla \cdot A +$
 $+ \nabla f \wedge (\nabla \wedge A) + (A \cdot \nabla)\nabla f - (\nabla f \cdot \nabla)A$

Special formulas:

If $\mathbf{r} = r\hat{\mathbf{r}}$ is the radius vector from a fixed origin and \mathbf{F} is any constant vector, then

$$(21) \quad \nabla r = \hat{\mathbf{r}}$$

$$(22) \quad \nabla \cdot \mathbf{r} = 3$$

$$(23) \quad \nabla \wedge \mathbf{r} = 0$$

$$(24) \quad \nabla(1/r) = -\hat{\mathbf{r}}/r^2$$

$$(25) \quad \nabla \cdot (\hat{\mathbf{r}}/r^2) = -\nabla^2(1/r) = -4\pi\delta(\mathbf{r}),$$

$$\text{where } \delta(\mathbf{r}) = 0 \text{ if } \mathbf{r} \neq 0, \text{ and } \int_{\text{all space}} \delta(\mathbf{r}) d\mathbf{r} = 1$$

$$(26) \quad \nabla \cdot (\mathbf{F}/r) = -\mathbf{F} \cdot \hat{\mathbf{r}}/r^2$$

$$(27) \quad \nabla \wedge [\mathbf{F} \wedge \hat{\mathbf{r}}/r^2] = -\nabla[\mathbf{F} \cdot \hat{\mathbf{r}}/r^2], \quad \text{if } \mathbf{r} \neq 0$$

$$(28) \quad \nabla^2(\mathbf{F}/r) = 0, \quad \text{if } \mathbf{r} \neq 0$$

$$(29) \quad \nabla \wedge (\mathbf{F} \wedge \mathbf{A}) = \mathbf{F}(\nabla \cdot \mathbf{A}) + \mathbf{F} \wedge (\nabla \wedge \mathbf{A}) - \nabla(\mathbf{F} \cdot \mathbf{A})$$

Integral relations:

Gauss' theorems:

$$(30) \quad \int_v \nabla f \, dv = \int_S f \hat{\mathbf{n}} dS$$

$$(31) \quad \int_v \nabla \cdot \mathbf{A} \, dv = \int_S \mathbf{A} \cdot \hat{\mathbf{n}} dS$$

$$(32) \quad \int_v \nabla \wedge \mathbf{A} \, dv = \int_S \hat{\mathbf{n}} \wedge \mathbf{A} dS,$$

where the volume v is bounded by the closed regular surface S with unit normal $\hat{\mathbf{n}}$ pointing outward from v , and the partial derivatives which appear in the integrands are continuous in the interiors of a finite number of regular regions of which v is the sum.

Substitution of special vectors in Gauss' theorems yields various Green's theorems, such as

$$(33) \quad \int_v (f \nabla^2 g + \nabla f \cdot \nabla g) dv = \int_S f \frac{\partial g}{\partial n} dS,$$

$$(34) \quad \int_v (f \nabla^2 g - g \nabla^2 f) dv = \int_S \left(f \frac{\partial g}{\partial n} - g \frac{\partial f}{\partial n} \right) dS;$$

for other Green's theorems, see Appendix 1 in VAN BLADEL (reference [10] of Appendix A).

Stokes' theorems:

$$(35) \quad \int_S \hat{n} \wedge \nabla f \, dS = \oint_l f \, dl$$

$$(36) \quad \int_S \nabla \wedge A \cdot \hat{n} \, dS = \oint_l A \cdot dl$$

$$(37) \quad \int_S [(\hat{n} \wedge \nabla) \wedge A] \, dS = - \oint_l A \wedge dl$$

$$(38) \quad \int_S (\nabla f \wedge \nabla g) \cdot \hat{n} \, dS = \oint_l f \nabla g \cdot dl \\ = - \oint_l g \nabla f \cdot dl,$$

where the open regular surface S is bounded by the contour l whose line element dl is oriented in the positive sense with respect to the normal \hat{n} to S , and where the various partial derivatives in the integrands are continuous in a region containing S in its interior.

Dyadics:

The formal multiplication AB of two vectors A and B is called a dyad; by definition:

$$(39) \quad AB \cdot C = A(B \cdot C), \quad C \cdot AB = (C \cdot A)B.$$

If $B = B_x \hat{x} + B_y \hat{y} + B_z \hat{z}$ is a linear vector function of $A = A_x \hat{x} + A_y \hat{y} + A_z \hat{z}$, then the relation

$$(40) \quad \begin{pmatrix} B_x \\ B_y \\ B_z \end{pmatrix} = \begin{pmatrix} g_{xx} & g_{xy} & g_{xz} \\ g_{yx} & g_{yy} & g_{yz} \\ g_{zx} & g_{zy} & g_{zz} \end{pmatrix} \begin{pmatrix} A_x \\ A_y \\ A_z \end{pmatrix}$$

may be written as

$$(41) \quad B = \mathcal{G} \cdot A,$$

with the dyadic operator \mathcal{G} given by

$$(42) \quad \mathcal{G} = g_{xx} \hat{x} \hat{x} + g_{xy} \hat{x} \hat{y} + g_{xz} \hat{x} \hat{z} + \\ + g_{yx} \hat{y} \hat{x} + g_{yy} \hat{y} \hat{y} + g_{yz} \hat{y} \hat{z} + \\ + g_{zx} \hat{z} \hat{x} + g_{zy} \hat{z} \hat{y} + g_{zz} \hat{z} \hat{z};$$

thus, \mathcal{G} represents a tensor of rank two.

We may also write (42) in the forms:

$$(43) \quad \mathcal{G} = \hat{x} G_x + \hat{y} G_y + \hat{z} G_z \\ + G'_x \hat{x} + G'_y \hat{y} + G'_z \hat{z},$$

where the G are the row vectors and the G' the column vectors of the matrix $\{g_{ij}\}$ of (40). In particular, the identity dyadic is given by

$$(44) \quad \mathcal{I} = \hat{x} \hat{x} + \hat{y} \hat{y} + \hat{z} \hat{z}.$$

A list of useful relationships for dyadics may be found, for example, in reference [10] of Appendix A; here we only give a few differential operators.

In rectangular Cartesian coordinates (x, y, z) :

$$(45) \quad \nabla A = \left(\hat{x} \frac{\partial}{\partial x} + \hat{y} \frac{\partial}{\partial y} + \hat{z} \frac{\partial}{\partial z} \right) A \\ = \nabla(A_x \hat{x}) + \nabla(A_y \hat{y}) + \nabla(A_z \hat{z})$$

$$(46) \quad A \nabla = \frac{\partial A}{\partial x} \hat{x} + \frac{\partial A}{\partial y} \hat{y} + \frac{\partial A}{\partial z} \hat{z}$$

$$(47) \quad \nabla \cdot \mathcal{G} = \frac{\partial}{\partial x} G_x + \frac{\partial}{\partial y} G_y + \frac{\partial}{\partial z} G_z \\ = (\nabla \cdot \mathbf{G}'_x) \hat{x} + (\nabla \cdot \mathbf{G}'_y) \hat{y} + (\nabla \cdot \mathbf{G}'_z) \hat{z}$$

$$(48) \quad \mathcal{G} \cdot \nabla = \hat{x} \nabla \cdot \mathbf{G}_x + \hat{y} \nabla \cdot \mathbf{G}_y + \hat{z} \nabla \cdot \mathbf{G}_z$$

$$(49) \quad \nabla \wedge \mathcal{G} = \hat{x} \left(\frac{\partial G_z}{\partial y} - \frac{\partial G_y}{\partial z} \right) + \hat{y} \left(\frac{\partial G_x}{\partial z} - \frac{\partial G_z}{\partial x} \right) + \hat{z} \left(\frac{\partial G_y}{\partial x} - \frac{\partial G_x}{\partial y} \right) \\ = (\nabla \wedge \mathbf{G}'_x) \hat{x} + (\nabla \wedge \mathbf{G}'_y) \hat{y} + (\nabla \wedge \mathbf{G}'_z) \hat{z}.$$

In circular cylindrical coordinates (ρ, ϕ, z) we may write, in analogy to (43):

$$(50) \quad \mathcal{G} = \hat{\rho} G_\rho + \hat{\phi} G_\phi + \hat{z} G_z \\ = G'_\rho \hat{\rho} + G'_\phi \hat{\phi} + G'_z \hat{z};$$

then:

$$(51) \quad \nabla A = \left(\hat{\rho} \frac{\partial}{\partial \rho} + \frac{\hat{\phi}}{\rho} \frac{\partial}{\partial \phi} + \hat{z} \frac{\partial}{\partial z} \right) A \\ = \left(\nabla A_\rho - \frac{A_\phi}{\rho} \hat{\phi} \right) \hat{\rho} + \left(\nabla A_\phi + \frac{A_\rho}{\rho} \hat{\phi} \right) \hat{\phi} + \nabla A_z \hat{z}$$

$$(52) \quad \nabla \cdot \mathcal{G} = \left(\frac{1}{\rho} + \frac{\partial}{\partial \rho} \right) G_\rho + \frac{1}{\rho} \frac{\partial G_\phi}{\partial \phi} + \frac{\partial G_z}{\partial z} \\ = \left(\nabla \cdot \mathbf{G}'_\rho - \frac{g_{\phi\phi}}{\rho} \right) \hat{\rho} + \left(\nabla \cdot \mathbf{G}'_\phi + \frac{g_{\rho\rho}}{\rho} \right) \hat{\phi} + (\nabla \cdot \mathbf{G}'_z) \hat{z}$$

$$(53) \quad \nabla \wedge \mathcal{G} = \hat{\rho} \left(\frac{1}{\rho} \frac{\partial G_z}{\partial \phi} - \frac{\partial G_\phi}{\partial z} \right) + \hat{\phi} \left(\frac{\partial G_\rho}{\partial z} - \frac{\partial G_z}{\partial \rho} \right) + \hat{z} \left(\frac{G_\phi}{\rho} + \frac{\partial G_\phi}{\partial \rho} - \frac{1}{\rho} \frac{\partial G_\rho}{\partial \phi} \right) \\ = \left(\nabla \wedge \mathbf{G}'_\rho + \frac{1}{\rho} \mathbf{G}'_\phi \wedge \hat{\phi} \right) \hat{\rho} + \left(\nabla \wedge \mathbf{G}'_\phi - \frac{1}{\rho} \mathbf{G}'_\rho \wedge \hat{\phi} \right) \hat{\phi} + \nabla \wedge \mathbf{G}'_z \hat{z}$$

and in particular

$$(54) \quad \nabla \hat{\rho} = \frac{1}{\rho} \hat{\phi} \hat{\phi}, \quad \nabla \hat{\phi} = \frac{1}{\rho} \hat{\phi} \hat{\rho}, \quad \nabla \hat{z} = 0.$$

In spherical polar coordinates (r, θ, ϕ) we may write, in analogy to (43):

$$(55) \quad \mathcal{G} = \hat{r}G_r + \hat{\theta}G_\theta + \hat{\phi}G_\phi \\ = G'_r\hat{r} + G'_\theta\hat{\theta} + G'_\phi\hat{\phi};$$

then:

$$(56) \quad \nabla A = \left(\hat{r} \frac{\partial}{\partial r} + \frac{\hat{\theta}}{r} \frac{\partial}{\partial \theta} + \frac{\hat{\phi}}{r \sin \theta} \frac{\partial}{\partial \phi} \right) A \\ = \left[\nabla A_r - \frac{1}{r} (A_\theta \hat{\theta} + A_\phi \hat{\phi}) \right] \hat{r} + \left[\nabla A_\theta + \frac{1}{r} (A_r \hat{r} - A_\phi \cot \theta \hat{\phi}) \right] \hat{\theta} + \\ + \left[\nabla A_\phi + \frac{1}{r} (A_r + A_\theta \cot \theta) \hat{\phi} \right] \hat{\phi}$$

$$(57) \quad \nabla \cdot \mathcal{G} = \left(\frac{2}{r} + \frac{\partial}{\partial r} \right) G_r + \frac{1}{r} \left(\frac{\partial}{\partial \theta} + \cot \theta \right) G_\theta + \frac{1}{r \sin \theta} \frac{\partial G_\phi}{\partial \phi} \\ = \left(\nabla \cdot G'_r - \frac{g_{\theta\theta} + g_{\phi\phi}}{r} \right) \hat{r} + \left[\nabla \cdot G'_\theta + \frac{1}{r} (g_{\theta r} - g_{\phi\phi} \cot \theta) \right] \hat{\theta} + \\ + \left[\nabla \cdot G'_\phi + \frac{1}{r} (g_{\phi r} + g_{\theta\theta} \cot \theta) \right] \hat{\phi}$$

$$(58) \quad \nabla \wedge \mathcal{G} = \frac{\hat{r}}{r} \left[\left(\frac{\partial}{\partial \theta} + \cot \theta \right) G_\phi - \frac{1}{\sin \theta} \frac{\partial G_\theta}{\partial \phi} \right] + \\ + \hat{\theta} \left[\frac{1}{r \sin \theta} \frac{\partial G_r}{\partial \phi} - \left(\frac{\partial}{\partial r} + \frac{1}{r} \right) G_\phi \right] + \\ + \hat{\phi} \left[\left(\frac{\partial}{\partial r} + \frac{1}{r} \right) G_\theta - \frac{1}{r} \frac{\partial G_r}{\partial \theta} \right] \\ = \left[\nabla \wedge G'_r + \frac{1}{r} (G'_\theta \wedge \hat{\theta} + G'_\phi \wedge \hat{\phi}) \right] \hat{r} + \\ + \left[\nabla \wedge G'_\theta + \frac{1}{r} (G'_\phi \wedge \hat{\phi} \cot \theta - G'_r \wedge \hat{\theta}) \right] \hat{\theta} + \\ + \left[\nabla \wedge G'_\phi - \frac{1}{r} (G'_r + G'_\theta) \wedge \hat{\phi} \right] \hat{\phi}$$

and in particular

$$(59) \quad \nabla \hat{r} = \frac{\hat{\theta}\hat{\theta} + \hat{\phi}\hat{\phi}}{r}, \quad \nabla \hat{\theta} = \frac{1}{r} (\hat{\phi}\hat{\phi} \cot \theta - \hat{\theta}\hat{r}), \quad \nabla \hat{\phi} = -\frac{1}{r} (\hat{\phi}\hat{r} + \hat{\phi}\hat{\theta} \cot \theta).$$

C. ORTHOGONAL CURVILINEAR COORDINATES

Let $u_1(x, y, z)$, $u_2(x, y, z)$, $u_3(x, y, z)$ be a right-handed system of orthogonal curvilinear coordinates, and let \hat{u}_i be a unit vector tangent to the coordinate line u_i , oriented toward increasing u_i , and such that $\hat{u}_1 \wedge \hat{u}_2 = \hat{u}_3$. The metric coefficients h_1, h_2, h_3 are given by

$$(1) \quad h_i^2 = \left(\frac{\partial x}{\partial u_i} \right)^2 + \left(\frac{\partial y}{\partial u_i} \right)^2 + \left(\frac{\partial z}{\partial u_i} \right)^2, \quad i = 1, 2, 3,$$

the line element ds by

$$(2) \quad (ds)^2 = \sum_{i=1}^3 h_i^2 (du_i)^2$$

and the volume element dv by

$$(3) \quad dv = h_1 h_2 h_3 du_1 du_2 du_3.$$

If f is a scalar field and A is a vector field with components $A_i = A \cdot \hat{u}_i$:

$$(4) \quad \nabla f = \sum_{i=1}^3 \frac{1}{h_i} \frac{\partial f}{\partial u_i} \hat{u}_i,$$

$$(5) \quad \nabla \cdot A = \frac{1}{h_1 h_2 h_3} \left[\frac{\partial}{\partial u_1} (h_2 h_3 A_1) + \frac{\partial}{\partial u_2} (h_3 h_1 A_2) + \frac{\partial}{\partial u_3} (h_1 h_2 A_3) \right],$$

$$(6) \quad \nabla \wedge A = \frac{1}{h_2 h_3} \left[\frac{\partial}{\partial u_2} (h_3 A_3) - \frac{\partial}{\partial u_3} (h_2 A_2) \right] \hat{u}_1 + \\ + \frac{1}{h_3 h_1} \left[\frac{\partial}{\partial u_3} (h_1 A_1) - \frac{\partial}{\partial u_1} (h_3 A_3) \right] \hat{u}_2 + \\ + \frac{1}{h_1 h_2} \left[\frac{\partial}{\partial u_1} (h_2 A_2) - \frac{\partial}{\partial u_2} (h_1 A_1) \right] \hat{u}_3,$$

$$(7) \quad \nabla^2 f = \frac{1}{h_1 h_2 h_3} \left[\frac{\partial}{\partial u_1} \left(\frac{h_2 h_3}{h_1} \frac{\partial f}{\partial u_1} \right) + \frac{\partial}{\partial u_2} \left(\frac{h_3 h_1}{h_2} \frac{\partial f}{\partial u_2} \right) + \frac{\partial}{\partial u_3} \left(\frac{h_1 h_2}{h_3} \frac{\partial f}{\partial u_3} \right) \right].$$

Formula (6) is valid only if the coordinate systems (x, y, z) and (u_1, u_2, u_3) are either both right-handed or both left-handed. Otherwise, the right-hand side of eq. (6) must be multiplied by minus one.

Particular formulas for the eight coordinate systems adopted in this book are given in the following; for other coordinate systems see, for example, MOON and SPENCER (1961), Field Theory Handbook (Springer); MORSE and FESHBACH (1953), Methods

of Theoretical Physics, chapter 5 (McGraw-Hill); MARGENAU and MURPHY (1943), The Mathematics of Physics and Chemistry (Van Nostrand).

1. *Rectangular Cartesian coordinates:*

$$(8) \quad u_1 = x, \quad u_2 = y, \quad u_3 = z; \quad -\infty < x, y, z < \infty$$

$$(9) \quad h_x = h_y = h_z = 1$$

$$(10) \quad \nabla f = \frac{\partial f}{\partial x} \hat{x} + \frac{\partial f}{\partial y} \hat{y} + \frac{\partial f}{\partial z} \hat{z}$$

$$(11) \quad \nabla \cdot \mathbf{A} = \frac{\partial A_x}{\partial x} + \frac{\partial A_y}{\partial y} + \frac{\partial A_z}{\partial z}$$

$$(12) \quad \nabla \wedge \mathbf{A} = \left(\frac{\partial A_z}{\partial y} - \frac{\partial A_y}{\partial z} \right) \hat{x} + \left(\frac{\partial A_x}{\partial z} - \frac{\partial A_z}{\partial x} \right) \hat{y} + \left(\frac{\partial A_y}{\partial x} - \frac{\partial A_x}{\partial y} \right) \hat{z}$$

$$(13) \quad \nabla^2 f = \frac{\partial^2 f}{\partial x^2} + \frac{\partial^2 f}{\partial y^2} + \frac{\partial^2 f}{\partial z^2}$$

$$(14) \quad \nabla^2 \mathbf{A} = (\nabla^2 A_x) \hat{x} + (\nabla^2 A_y) \hat{y} + (\nabla^2 A_z) \hat{z}.$$

2. *Circular cylinder coordinates:*

$$(15) \quad u_1 = \rho, \quad u_2 = \phi, \quad u_3 = z; \quad 0 \leq \rho < \infty, \quad 0 \leq \phi < 2\pi, \quad -\infty < z < \infty$$

$$x = \rho \cos \phi, \quad y = \rho \sin \phi, \quad z = z; \quad \rho = \sqrt{(x^2 + y^2)}$$

$$(16) \quad h_\rho = 1, \quad h_\phi = \rho, \quad h_z = 1$$

$$(17) \quad A_\rho = A_x \cos \phi + A_y \sin \phi, \quad A_\phi = A_y \cos \phi - A_x \sin \phi, \quad A_z = A_z$$

$$A_x = A_\rho \cos \phi - A_\phi \sin \phi, \quad A_y = A_\rho \sin \phi + A_\phi \cos \phi,$$

$$(18) \quad \frac{\partial}{\partial \rho} = \frac{x}{\rho} \frac{\partial}{\partial x} + \frac{y}{\rho} \frac{\partial}{\partial y}, \quad \frac{\partial}{\partial \phi} = x \frac{\partial}{\partial y} - y \frac{\partial}{\partial x}$$

$$\frac{\partial}{\partial x} = \cos \phi \frac{\partial}{\partial \rho} - \frac{\sin \phi}{\rho} \frac{\partial}{\partial \phi}, \quad \frac{\partial}{\partial y} = \sin \phi \frac{\partial}{\partial \rho} + \frac{\cos \phi}{\rho} \frac{\partial}{\partial \phi}$$

$$(19) \quad \nabla f = \frac{\partial f}{\partial \rho} \hat{\rho} + \frac{1}{\rho} \frac{\partial f}{\partial \phi} \hat{\phi} + \frac{\partial f}{\partial z} \hat{z}$$

$$(20) \quad \nabla \cdot \mathbf{A} = \frac{1}{\rho} \frac{\partial}{\partial \rho} (\rho A_\rho) + \frac{1}{\rho} \frac{\partial A_\phi}{\partial \phi} + \frac{\partial A_z}{\partial z}$$

$$(21) \quad \nabla \wedge \mathbf{A} = \left[\frac{1}{\rho} \frac{\partial A_z}{\partial \phi} - \frac{\partial A_\phi}{\partial z} \right] \hat{\rho} + \left[\frac{\partial A_\rho}{\partial z} - \frac{\partial A_z}{\partial \rho} \right] \hat{\phi} + \left[\frac{1}{\rho} \frac{\partial}{\partial \rho} (\rho A_\phi) - \frac{1}{\rho} \frac{\partial A_\rho}{\partial \phi} \right] \hat{z}$$

$$(22) \quad \nabla^2 f = \frac{1}{\rho} \frac{\partial}{\partial \rho} \left(\rho \frac{\partial f}{\partial \rho} \right) + \frac{1}{\rho^2} \frac{\partial^2 f}{\partial \phi^2} + \frac{\partial^2 f}{\partial z^2}$$

$$(23) \quad \nabla^2 A = \left(\nabla^2 A_\rho - \frac{A_\rho}{\rho^2} - \frac{2}{\rho^2} \frac{\partial A_\phi}{\partial \phi} \right) \hat{\rho} + \\ + \left(\nabla^2 A_\phi - \frac{A_\phi}{\rho^2} + \frac{2}{\rho^2} \frac{\partial A_\rho}{\partial \phi} \right) \hat{\phi} + (\nabla^2 A_z) \hat{z}$$

$$(24) \quad \nabla \cdot \hat{\rho} = \frac{1}{\rho}, \quad \nabla \cdot \hat{\phi} = \nabla \cdot \hat{z} = 0 \\ \nabla \wedge \hat{\phi} = \frac{\hat{z}}{\rho}, \quad \nabla \wedge \hat{\rho} = \nabla \wedge \hat{z} = 0.$$

3. Elliptic cylinder coordinates:

$$(25) \quad u_1 = u, \quad u_2 = v, \quad u_3 = z; \quad 0 \leq u < \infty, \quad 0 \leq v < 2\pi, \quad -\infty < z < \infty \\ x = \frac{1}{2}d \cosh u \cos v, \quad y = \frac{1}{2}d \sinh u \sin v, \quad z = z \\ d = \text{interfocal distance} \\ \text{also: } \xi = \cosh u, \quad \eta = \cos v; \quad 1 \leq \xi < \infty, \quad -1 \leq \eta \leq 1$$

$$(26) \quad h_u = h_v = \frac{1}{2}d(\cosh^2 u - \cos^2 v)^{\frac{1}{2}}, \quad h_z = 1$$

$$(27) \quad \nabla f = \frac{2}{d} (\cosh^2 u - \cos^2 v)^{-\frac{1}{2}} \left(\frac{\partial f}{\partial u} \hat{u} + \frac{\partial f}{\partial v} \hat{v} \right) + \frac{\partial f}{\partial z} \hat{z}$$

$$(28) \quad \nabla \cdot A = \frac{2}{d} (\cosh^2 u - \cos^2 v)^{-\frac{1}{2}} \left\{ \frac{\partial}{\partial u} [(\cosh^2 u - \cos^2 v)^{\frac{1}{2}} A_u] + \right. \\ \left. + \frac{\partial}{\partial v} [(\cosh^2 u - \cos^2 v)^{\frac{1}{2}} A_v] \right\} + \frac{\partial A_z}{\partial z}$$

$$(29) \quad \nabla \wedge A = \left[\frac{2}{d} (\cosh^2 u - \cos^2 v)^{-\frac{1}{2}} \frac{\partial A_z}{\partial v} - \frac{\partial A_v}{\partial z} \right] \hat{u} + \\ + \left[\frac{\partial A_u}{\partial z} - \frac{2}{d} (\cosh^2 u - \cos^2 v)^{-\frac{1}{2}} \frac{\partial A_z}{\partial u} \right] \hat{v} + \\ + \frac{2}{d} (\cosh^2 u - \cos^2 v)^{-\frac{1}{2}} \\ \times \left[\frac{\partial A_v}{\partial u} - \frac{A_u}{\partial v} + \frac{A_v \sinh u \cosh u - A_u \sin v \cos v}{\cosh^2 u - \cos^2 v} \right] \hat{z}$$

$$(30) \quad \nabla^2 f = \frac{4}{d^2} (\cosh^2 u - \cos^2 v)^{-\frac{1}{2}} \left(\frac{\partial^2 f}{\partial u^2} + \frac{\partial^2 f}{\partial v^2} \right) + \frac{\partial^2 f}{\partial z^2}.$$

4. Parabolic cylinder coordinates:

$$(31) \quad u_1 = \xi, \quad u_2 = \eta, \quad u_3 = z; \quad -\infty < \xi < \infty, \quad 0 \leq \eta < \infty, \quad -\infty < z < \infty \\ x = \frac{1}{2}(\xi^2 - \eta^2), \quad y = \xi\eta, \quad z = z$$

$$(32) \quad h_\xi = h_\eta = (\xi^2 + \eta^2)^{\frac{1}{2}}, \quad h_z = 1$$

$$(33) \quad \nabla f = (\xi^2 + \eta^2)^{-\frac{1}{2}} \left(\frac{\partial f}{\partial \xi} \hat{\xi} + \frac{\partial f}{\partial \eta} \hat{\eta} \right) + \frac{\partial f}{\partial z} \hat{z}$$

$$(34) \quad \nabla \cdot A = (\xi^2 + \eta^2)^{-1} \left\{ \frac{\partial}{\partial \xi} [(\xi^2 + \eta^2)^{\frac{1}{2}} A_\xi] + \frac{\partial}{\partial \eta} [(\xi^2 + \eta^2)^{\frac{1}{2}} A_\eta] \right\} + \frac{\partial A_z}{\partial z}$$

$$(35) \quad \nabla \wedge A = \left[(\xi^2 + \eta^2)^{-\frac{1}{2}} \frac{\partial A_z}{\partial \eta} - \frac{\partial A_\eta}{\partial z} \right] \hat{\xi} + \left[\frac{\partial A_\xi}{\partial z} - (\xi^2 + \eta^2)^{-\frac{1}{2}} \frac{\partial A_z}{\partial \xi} \right] \hat{\eta} + (\xi^2 + \eta^2)^{-\frac{1}{2}} \left[\frac{\partial A_\eta}{\partial \xi} - \frac{\partial A_\xi}{\partial \eta} + \frac{\xi A_\eta - \eta A_\xi}{\xi^2 + \eta^2} \right] \hat{z}$$

$$(36) \quad \nabla^2 f = (\xi^2 + \eta^2)^{-1} \left(\frac{\partial^2 f}{\partial \xi^2} + \frac{\partial^2 f}{\partial \eta^2} \right) + \frac{\partial^2 f}{\partial z^2}$$

5. Spherical coordinates:

$$(37) \quad u_1 = r, \quad u_2 = \theta, \quad u_3 = \phi; \quad 0 \leq r < \infty, \quad 0 \leq \theta \leq \pi, \quad 0 \leq \phi < 2\pi$$

$$x = r \sin \theta \cos \phi, \quad y = r \sin \theta \sin \phi, \quad z = r \cos \theta; \quad r = \sqrt{(x^2 + y^2 + z^2)}$$

$$(38) \quad h_r = 1, \quad h_\theta = r, \quad h_\phi = r \sin \theta$$

$$(39) \quad A_r = A_x \sin \theta \cos \phi + A_y \sin \theta \sin \phi + A_z \cos \theta$$

$$A_\theta = A_x \cos \theta \cos \phi + A_y \cos \theta \sin \phi - A_z \sin \theta$$

$$A_\phi = A_y \cos \phi - A_x \sin \phi$$

$$A_x = A_r \sin \theta \cos \phi + A_\theta \cos \theta \cos \phi - A_\phi \sin \phi$$

$$A_y = A_r \sin \theta \sin \phi + A_\theta \cos \theta \sin \phi + A_\phi \cos \phi$$

$$A_z = A_r \cos \theta - A_\theta \sin \theta$$

$$(40) \quad \frac{\partial}{\partial r} = \frac{x}{r} \frac{\partial}{\partial x} + \frac{y}{r} \frac{\partial}{\partial y} + \frac{z}{r} \frac{\partial}{\partial z}$$

$$\frac{\partial}{\partial \theta} = \frac{xz}{\rho} \frac{\partial}{\partial x} + \frac{yz}{\rho} \frac{\partial}{\partial y} - \rho \frac{\partial}{\partial z}; \quad \rho = \sqrt{(x^2 + y^2)}$$

$$\frac{\partial}{\partial \phi} = x \frac{\partial}{\partial y} - y \frac{\partial}{\partial x}$$

$$\frac{\partial}{\partial x} = \sin \theta \cos \phi \frac{\partial}{\partial r} + \frac{1}{r} \cos \theta \cos \phi \frac{\partial}{\partial \theta} - \frac{\sin \phi}{r \sin \theta} \frac{\partial}{\partial \phi}$$

$$\frac{\partial}{\partial y} = \sin \theta \sin \phi \frac{\partial}{\partial r} + \frac{1}{r} \cos \theta \sin \phi \frac{\partial}{\partial \theta} + \frac{\cos \phi}{r \sin \theta} \frac{\partial}{\partial \phi}$$

$$\frac{\partial}{\partial z} = \cos \theta \frac{\partial}{\partial r} - \frac{\sin \theta}{r} \frac{\partial}{\partial \theta}$$

$$(41) \quad \nabla f = \frac{\partial f}{\partial r} \hat{r} + \frac{1}{r} \frac{\partial f}{\partial \theta} \hat{\theta} + \frac{1}{r \sin \theta} \frac{\partial f}{\partial \phi} \hat{\phi}$$

$$(42) \quad \nabla \cdot \mathbf{A} = \frac{1}{r^2} \frac{\partial}{\partial r} (r^2 A_r) + \frac{1}{r \sin \theta} \frac{\partial}{\partial \theta} (\sin \theta A_\theta) + \frac{1}{r \sin \theta} \frac{\partial A_\phi}{\partial \phi}$$

$$(43) \quad \nabla \wedge \mathbf{A} = \frac{1}{r \sin \theta} \left[\frac{\partial}{\partial \theta} (\sin \theta A_\phi) - \frac{\partial A_\theta}{\partial \phi} \right] \hat{\rho} + \frac{1}{r} \left[\frac{1}{\sin \theta} \frac{\partial A_r}{\partial \phi} - \frac{\partial}{\partial r} (r A_\phi) \right] \hat{\theta} + \\ + \frac{1}{r} \left[\frac{\partial}{\partial r} (r A_\theta) - \frac{\partial A_r}{\partial \theta} \right] \hat{\phi}$$

$$(44) \quad \nabla^2 f = \frac{1}{r^2} \frac{\partial}{\partial r} \left(r^2 \frac{\partial f}{\partial r} \right) + \frac{1}{r^2 \sin \theta} \frac{\partial}{\partial \theta} \left(\sin \theta \frac{\partial f}{\partial \theta} \right) + \frac{1}{r^2 \sin^2 \theta} \frac{\partial^2 f}{\partial \phi^2}$$

$$(45) \quad \nabla^2 \mathbf{A} = \left(\nabla^2 A_r - \frac{2}{r^2} A_r - \frac{2 \cot \theta}{r^2} A_\theta - \frac{2}{r^2} \frac{\partial A_\theta}{\partial \theta} - \frac{2}{r^2 \sin \theta} \frac{\partial A_\phi}{\partial \phi} \right) \hat{\rho} + \\ + \left(\nabla^2 A_\theta + \frac{2}{r^2} \frac{\partial A_r}{\partial \theta} - \frac{1}{r^2 \sin^2 \theta} A_\theta - \frac{2 \cot \theta}{r^2 \sin \theta} \frac{\partial A_\phi}{\partial \phi} \right) \hat{\theta} + \\ + \left(\nabla^2 A_\phi + \frac{2}{r^2 \sin \theta} \frac{\partial A_r}{\partial \phi} - \frac{1}{r^2 \sin^2 \theta} A_\phi + \frac{2 \cot \theta}{r^2 \sin \theta} \frac{\partial A_\theta}{\partial \phi} \right) \hat{\phi}$$

$$(46) \quad \nabla \cdot \hat{\rho} = \frac{2}{r}, \quad \nabla \cdot \hat{\theta} = \frac{\cot \theta}{r}, \quad \nabla \cdot \hat{\phi} = 0$$

$$\nabla \wedge \hat{\rho} = 0, \quad \nabla \wedge \hat{\theta} = \frac{\hat{\phi}}{r}, \quad \nabla \wedge \hat{\phi} = \frac{\cot \theta}{r} \hat{\rho} - \frac{\hat{\theta}}{r}$$

6. Prolate spheroidal coordinates:

$$(47) \quad u_1 = u, \quad u_2 = v, \quad u_3 = \phi; \quad 0 \leq u < \infty, \quad 0 \leq v \leq \pi, \quad 0 \leq \phi < 2\pi$$

$$x = \frac{1}{2}d \sinh u \sin v \cos \phi, \quad y = \frac{1}{2}d \sinh u \sin v \sin \phi, \quad z = \frac{1}{2}d \cosh u \cos v$$

d = interfocal distance

$$\text{also: } \xi = \cosh u, \quad \eta = \cos v; \quad 1 \leq \xi < \infty, \quad -1 \leq \eta \leq 1$$

$$(48) \quad h_\xi = \frac{1}{2}d \left(\frac{\xi^2 - \eta^2}{\xi^2 - 1} \right)^{\frac{1}{2}}, \quad h_\eta = \frac{1}{2}d \left(\frac{\xi^2 - \eta^2}{1 - \eta^2} \right)^{\frac{1}{2}}, \quad h_\phi = \frac{1}{2}d [(\xi^2 - 1)(1 - \eta^2)]^{\frac{1}{2}}$$

$$(49) \quad \nabla f = \frac{2}{d} (\xi^2 - \eta^2)^{-\frac{1}{2}} \left[(\xi^2 - 1)^{\frac{1}{2}} \frac{\partial f}{\partial \xi} \hat{\xi} + (1 - \eta^2)^{\frac{1}{2}} \frac{\partial f}{\partial \eta} \hat{\eta} \right] + \\ + \frac{2}{d} [(\xi^2 - 1)(1 - \eta^2)]^{-\frac{1}{2}} \frac{\partial f}{\partial \phi} \hat{\phi}$$

$$(50) \quad \nabla \cdot \mathbf{A} = \frac{2}{d} \left(\frac{\xi^2 - 1}{\xi^2 - \eta^2} \right)^{\frac{1}{2}} \left[\frac{\partial}{\partial \xi} + \frac{\xi}{\xi^2 - \eta^2} + \frac{\xi}{\xi^2 - 1} \right] A_\xi + \\ + \frac{2}{d} \left(\frac{1 - \eta^2}{\xi^2 - \eta^2} \right)^{\frac{1}{2}} \left[\frac{\partial}{\partial \eta} - \frac{\eta}{\xi^2 - \eta^2} - \frac{\eta}{1 - \eta^2} \right] A_\eta + \frac{2}{d} [(\xi^2 - 1)(1 - \eta^2)]^{-\frac{1}{2}} \frac{\partial A_\phi}{\partial \phi}$$

$$\begin{aligned}
 (51) \quad -\nabla \wedge A = & \frac{2}{d} \left(\frac{1-\eta^2}{\xi^2-\eta^2} \right)^{\frac{1}{2}} \left(\frac{\partial}{\partial \eta} - \frac{\eta}{1-\eta^2} \right) A_\phi - [(\xi^2-1)(1-\eta^2)]^{-\frac{1}{2}} \frac{\partial A_\eta}{\partial \phi} \xi + \\
 & + \frac{2}{d} \left\{ [(\xi^2-1)(1-\eta^2)]^{-\frac{1}{2}} \frac{\partial A_\xi}{\partial \phi} - \left(\frac{\xi^2-1}{\xi^2-\eta^2} \right)^{\frac{1}{2}} \left(\frac{\partial}{\partial \xi} + \frac{\xi}{\xi^2-1} \right) A_\phi \right\} \hat{\eta} + \\
 & + \frac{2}{d} (\xi^2-\eta^2)^{-\frac{1}{2}} \left[(\xi^2-1)^{\frac{1}{2}} \left(\frac{\partial}{\partial \xi} + \frac{\xi}{\xi^2-\eta^2} \right) A_\eta - \right. \\
 & \left. - (1-\eta^2)^{\frac{1}{2}} \left(\frac{\partial}{\partial \eta} - \frac{\eta}{\xi^2-\eta^2} \right) A_\xi \right] \hat{\phi}
 \end{aligned}$$

$$\begin{aligned}
 (52) \quad \nabla^2 f = & \frac{4}{d^2} (\xi^2-\eta^2)^{-1} \left\{ \frac{\partial}{\partial \xi} \left[(\xi^2-1) \frac{\partial f}{\partial \xi} \right] + \frac{\partial}{\partial \eta} \left[(1-\eta^2) \frac{\partial f}{\partial \eta} \right] \right\} + \\
 & + \frac{4}{d^2} [(\xi^2-1)(1-\eta^2)]^{-1} \frac{\partial^2 f}{\partial \phi^2}.
 \end{aligned}$$

7. Oblate spheroidal coordinates:

$$\begin{aligned}
 (53) \quad u_1 = u, \quad u_2 = v, \quad u_3 = \phi; \quad 0 \leq u < \infty, \quad 0 \leq v \leq \pi, \quad 0 \leq \phi < 2\pi \\
 x = \frac{1}{2}d \cosh u \sin v \cos \phi, \quad y = \frac{1}{2}d \cosh u \sin v \sin \phi, \quad z = \frac{1}{2}d \sinh u \cos v \\
 d = \text{interfocal distance}
 \end{aligned}$$

$$\text{also: } \xi = \sinh u, \quad \eta = \cos v; \quad 0 \leq \xi < \infty, \quad -1 \leq \eta \leq 1$$

$$(54) \quad h_\xi = \frac{1}{2}d \left(\frac{\xi^2+\eta^2}{\xi^2+1} \right)^{\frac{1}{2}}, \quad h_\eta = \frac{1}{2}d \left(\frac{\xi^2+\eta^2}{1-\eta^2} \right)^{\frac{1}{2}}, \quad h_\phi = \frac{1}{2}d [(\xi^2+1)(1-\eta^2)]^{\frac{1}{2}}$$

$$\begin{aligned}
 (55) \quad \nabla f = & \frac{2}{d} (\xi^2+\eta^2)^{-\frac{1}{2}} \left[(\xi^2+1)^{\frac{1}{2}} \frac{\partial f}{\partial \xi} \xi + (1-\eta^2)^{\frac{1}{2}} \frac{\partial f}{\partial \eta} \hat{\eta} \right] + \\
 & + \frac{2}{d} [(\xi^2+1)(1-\eta^2)]^{-\frac{1}{2}} \frac{\partial f}{\partial \phi} \hat{\phi}
 \end{aligned}$$

$$\begin{aligned}
 (56) \quad \nabla \cdot A = & \frac{2}{d} \left(\frac{\xi^2+1}{\xi^2+\eta^2} \right)^{\frac{1}{2}} \left[\frac{\partial}{\partial \xi} + \frac{\xi}{\xi^2+\eta^2} + \frac{\xi}{\xi^2+1} \right] A_\xi + \frac{2}{d} \left(\frac{1-\eta^2}{\xi^2+\eta^2} \right)^{\frac{1}{2}} \\
 & \times \left[\frac{\partial}{\partial \eta} + \frac{\eta}{\xi^2+\eta^2} - \frac{\eta}{1-\eta^2} \right] A_\eta + \frac{2}{d} [(\xi^2+1)(1-\eta^2)]^{-\frac{1}{2}} \frac{\partial A_\phi}{\partial \phi}
 \end{aligned}$$

$$\begin{aligned}
 (57) \quad -\nabla \wedge A = & \frac{2}{d} \left(\frac{1-\eta^2}{\xi^2+\eta^2} \right)^{\frac{1}{2}} \left(\frac{\partial}{\partial \eta} - \frac{\eta}{1-\eta^2} \right) A_\phi - [(\xi^2+1)(1-\eta^2)]^{-\frac{1}{2}} \frac{\partial A_\eta}{\partial \phi} \xi + \\
 & + \frac{2}{d} \left\{ [(\xi^2+1)(1-\eta^2)]^{-\frac{1}{2}} \frac{\partial A_\xi}{\partial \phi} - \left(\frac{\xi^2+1}{\xi^2+\eta^2} \right)^{\frac{1}{2}} \left(\frac{\partial}{\partial \xi} + \frac{\xi}{\xi^2+1} \right) A_\phi \right\} \hat{\eta} + \\
 & + \frac{2}{d} (\xi^2+\eta^2)^{-\frac{1}{2}} \left[(\xi^2+1)^{\frac{1}{2}} \left(\frac{\partial}{\partial \xi} + \frac{\xi}{\xi^2+\eta^2} \right) A_\eta - (1-\eta^2)^{\frac{1}{2}} \right. \\
 & \left. \times \left(\frac{\partial}{\partial \eta} + \frac{\eta}{\xi^2+\eta^2} \right) A_\xi \right] \hat{\phi}
 \end{aligned}$$

$$(58) \quad \nabla^2 f = \frac{4}{d^2} (\xi^2 + \eta^2)^{-1} \left\{ \frac{\partial}{\partial \xi} \left[(\xi^2 + 1) \frac{\partial f}{\partial \xi} \right] + \frac{\partial}{\partial \eta} \left[(1 - \eta^2) \frac{\partial f}{\partial \eta} \right] \right\} + \frac{4}{d^2} [(\xi^2 + 1)(1 - \eta^2)]^{-1} \frac{\partial^2 f}{\partial \phi^2}.$$

8. *Parabolic coordinates:*

$$(59) \quad u_1 = \xi, \quad u_2 = \eta, \quad u_3 = \phi; \quad 0 \leq \xi < \infty, \quad 0 \leq \eta < \infty, \quad 0 \leq \phi < 2\pi$$

$$x = 2\sqrt{\xi\eta} \cos \phi, \quad y = 2\sqrt{\xi\eta} \sin \phi, \quad z = \xi - \eta$$

$$\text{also: } \xi_1 = \sqrt{2\xi}, \quad \xi_2 = \sqrt{2\eta}; \quad 0 \leq \xi_1 < \infty, \quad 0 \leq \xi_2 < \infty$$

$$(60) \quad h_\xi = \left(\frac{\xi + \eta}{\xi} \right)^{\frac{1}{2}}, \quad h_\eta = \left(\frac{\xi + \eta}{\eta} \right)^{\frac{1}{2}}, \quad h_\phi = 2(\xi\eta)^{\frac{1}{2}}$$

$$(61) \quad \nabla f = (\xi + \eta)^{-\frac{1}{2}} \left(\xi^{\frac{1}{2}} \frac{\partial f}{\partial \xi} \hat{\xi} + \eta^{\frac{1}{2}} \frac{\partial f}{\partial \eta} \hat{\eta} \right) + \frac{1}{2} (\xi\eta)^{-\frac{1}{2}} \frac{\partial f}{\partial \phi} \hat{\phi}$$

$$(62) \quad \nabla \cdot \mathbf{A} = \left(\frac{\xi}{\xi + \eta} \right)^{\frac{1}{2}} \left[\frac{\partial}{\partial \xi} + \frac{2\xi + \eta}{2\xi(\xi + \eta)} \right] A_\xi + \left(\frac{\eta}{\xi + \eta} \right)^{\frac{1}{2}} \left[\frac{\partial}{\partial \eta} + \frac{2\eta + \xi}{2\eta(\xi + \eta)} \right] A_\eta + \frac{1}{2\xi\eta} \frac{\partial A_\phi}{\partial \phi}$$

$$(63) \quad \nabla \wedge \mathbf{A} = \left[\left(\frac{\eta}{\xi + \eta} \right)^{\frac{1}{2}} \left(\frac{\partial}{\partial \eta} + \frac{1}{2\eta} \right) A_\phi - \frac{1}{2} (\xi\eta)^{-\frac{1}{2}} \frac{\partial A_\eta}{\partial \phi} \right] \hat{\xi} + \left[\frac{1}{2} (\xi\eta)^{-\frac{1}{2}} \frac{\partial A_\xi}{\partial \phi} - \left(\frac{\xi}{\xi + \eta} \right)^{\frac{1}{2}} \left(\frac{\partial}{\partial \xi} + \frac{1}{2\xi} \right) A_\phi \right] \hat{\eta} + (\xi + \eta)^{-\frac{1}{2}} \left\{ \xi^{\frac{1}{2}} \left[\frac{\partial}{\partial \xi} + \frac{1}{2(\xi + \eta)} \right] A_\eta - \eta^{\frac{1}{2}} \left[\frac{\partial}{\partial \eta} + \frac{1}{2(\xi + \eta)} \right] A_\xi \right\} \hat{\phi}$$

$$(64) \quad \nabla^2 f = (\xi + \eta)^{-1} \left[\frac{\partial}{\partial \xi} \left(\xi \frac{\partial f}{\partial \xi} \right) + \frac{\partial}{\partial \eta} \left(\eta \frac{\partial f}{\partial \eta} \right) \right] + \frac{1}{4\xi\eta} \frac{\partial^2 f}{\partial \phi^2}.$$

AUTHOR INDEX

The following listing is confined to those authors whose work is referenced within the body of the text.

- ABRAMOWITZ, M.: 50, 62, 68, 285
 ADACHI, S.: 31
 ADEY, A. W.: 93, 94
 AIRY, G. B.: 62
 ALPERIN, H. A.: 466, 524, 591, 635, 657-659, 690, 692, 693
 ALISHULER, S.: 38
 ANDREASEN, M. G.: 50
 ANDREJEWSKI, W.: 564, 569, 570
 ANDREWS, C. L.: 582, 583
 ANGELAKOS, D. J.: 50
 AR, E.: 1, 20, 351, 352, 438, 512
 ÅS, B. O.: 484, 485
 ASVESTAS, J. S.: 430, 433, 434, 446, 455, 456, 508, 515, 536, 546
 BAGHDASARIAN, A.: 50
 BAILIN, L. L.: 661, 662, 669, 670, 692
 BAIN, J. D.: 121, 122
 BAKER, B. B.: 21
 BARAKAT, R.: 132-134, 147-149, 185, 186, 188, 208
 BATEMAN, H.: 21
 BAZER, J.: 49, 529, 538, 551
 BECHTEL, M. E.: 25, 400, 579, 581
 BECKMANN, P.: 369, 379, 380, 414
 BEKEH, G.: 530, 531, 582, 584
 BELKINA, M. G.: 381-383, 385, 386, 390-395, 407, 409, 459, 460, 582
 BEVENSEE, R. M.: 39
 BLANCH, G.: 130
 BLASS, J.: 48
 BLEISTEIN, N.: 26
 BLOCK, F.: 474-476
 BLOOM, C. O.: 244, 247-249, 623
 BLORE, W. E.: 30
 BOERNER, W. M.: 351
 BOERSMA, J.: 210, 213, 537, 550, 576, 577
 BOLLJAHN, J. T.: 523
 BONKOWSKI, R. R.: 466, 524, 591, 635, 690
 BORN, M.: 7, 10, 20, 21, 395
 BOUWKAMP, C. J.: 11, 14, 31, 41, 181, 188, 208, 530, 531, 539, 549, 551, 577
 BOWMAN, J. J.: 25, 47-49, 336, 341, 351, 352, 639
 BRAUNBEK, W.: 317, 319, 320, 546, 547, 553
 BRICK, D. B.: 160
 BROWN, A.: 529, 538, 551
 BROWN, D. M.: 692, 693
 BROWN JR., W. P.: 26, 34
 BRUNDELL, P. O.: 495
 BRUNDRIT, G. B.: 442, 446, 515
 BRYSK, H.: 501
 BUCHAL, R. N.: 26, 541
 BUCHHOLZ, H.: 594-596, 601, 605, 609, 614, 620, 621
 BURKE, J. E.: 134-139, 141, 150-155, 157, 188, 190-192, 194, 195, 208, 210-213, 431, 453, 509, 516
 CAIRO, L.: 39
 CAMPOPIANO, C. N.: 57
 CARLSON, J. F.: 41, 45
 CARRUS, P. A.: 692, 693
 CARLSLAW, H. S.: 255, 260, 264, 267, 270, 272, 311, 316, 323, 327, 330, 333, 641, 649, 650, 652
 CARTER, P. S.: 121
 CASE, K. M.: 49, 540
 CASIMIR, H. B. G.: 11
 CHANG, H. H. C.: 584
 CHANG, S.: 482, 485
 CHEN, Y. M.: 25
 CHERNIN, M. G.: 670
 CHERRY, T. M.: 57
 CHESTER, W.: 45
 CHRISTENSEN, E. J.: 134, 136-138, 150, 154, 155, 188, 190, 194, 195, 208, 210, 213
 CHU, L. J.: 130
 CLEMMOW, P. C.: 37, 44, 45, 49, 146, 311, 312, 317, 323, 325, 327, 329
 COCHRAN, J. A.: 36
 COHEN, D. S.: 36
 COPSON, E. T.: 21, 41, 44, 45
 CORNU, A.: 68
 CRISPIN JR., J. W.: 31, 457, 466, 524, 591, 635, 658, 659, 690, 692, 693
 CULLEN, J. A.: 32, 33
 DARLING, D. A.: 21
 DAVIS, J.: 113, 116

- DEBETENCOURT, J. T.: 480, 481, 486, 488, 489, 491-493
DEBYE, P.: 54
DEHOOP, A. T.: 13, 188, 208, 551
DEPPERMAN, K.: 25
DIKE, S. H.: 475
DINGLE, R. B.: 130
DOLPH, C. L.: 38
DUCMANIS, J. A.: 397-399
DUNHAM, R. W.: 584
EGGIMANN, W. H.: 561, 575-577
EINARSSON, O.: 48, 120, 123, 472, 478, 480-481, 487-489, 491-494, 496, 498, 591
EPSTEIN, D. I.: 304
ERDELYI, A.: 50, 67, 68, 285, 595
FARAN, J. J.: 116
FAULKNER, T. R.: 49
FEDOROV, A. A.: 143, 144, 158, 159, 164, 169, 411, 614, 617-619
FELSEN, L. B.: 22, 25, 36, 47, 277, 340, 637, 639-647, 649, 650, 652, 658, 660, 662, 663, 669, 677, 688, 689, 695, 697
FESHBACH, H.: 6, 12, 17, 19, 39, 41, 48, 361, 417, 418, 438, 505, 512
FIALKOVSKII, A. T.: 49, 199, 486
FISCHER, E.: 36
FLAMMER, C.: 39, 417, 473, 504, 528, 565
FOCK, V.: 23, 26, 31-33, 41, 43, 49, 57, 62, 63, 594, 595, 614, 617-620
FRAHN, W. E.: 581, 583, 584
FRANZ, W.: 25, 31, 101, 102, 110, 111, 114, 117, 244, 251, 355, 356, 369, 370, 374, 379, 380, 414
FRESNEL, A. J.: 67
FRIEDLANDER, F. G.: 593
FRIEDMAN, B.: 36
FRITZE, U.: 546, 548
GAKHOV, F. D.: 43
GAILE, R.: 101, 102, 110, 111
GARABEDIAN, D. R.: 37, 38, 40
GERF, B. H.: 461
GERMAN, J. P.: 473
GORLICK, T. J.: 39
GOLDSTEIN, M.: 36
GOODRICH, R. F.: 32, 35-37, 145, 146, 159, 165, 167, 170, 171, 224, 270, 411, 413, 421, 422, 440, 466, 507, 513, 514, 524, 670
GORJAINOV, A. S.: 102, 103, 111, 112, 681, 683, 685-687, 690
GRADSHTEYN, I. S.: 50, 68
GRANNEMANN, W. W.: 254
GRINBERG, J. M.: 39
GRINBERG, G. A.: 183, 198, 203, 204, 216, 220, 221, 226, 227, 230, 303, 563
GROSCWITZ, E.: 208
GRÜNBERG, G. A.: 49
GUTMAN, A. L.: 19
HALL, R. N.: 692-694
HALLÉN, E.: 472, 473, 495, 498
HAMERMESH, M.: 474-476
HANSEN, E. B.: 25, 181, 224, 229, 526, 532, 533, 539, 540, 544, 553, 554
HANSEN, W. W.: 19, 690
HARDEN, B. N.: 313
HARRINGTON, R. F.: 50
HASSERJIAN, G.: 117
HASTINGS, C.: 496
HATCHER, E. C.: 460
HEDGECOCK, N. E.: 255
HEINS, A.: 41, 45, 538
HENSMAN, R.: 68
HEY, J. S.: 400, 568, 569
HOBSON, E. W.: 68, 71, 74, 639, 691
HOCHSTADT, H.: 288, 302, 304, 306, 538, 595, 620
HONG, S.: 33, 37, 146
HÖNL, H.: 41, 45, 57, 181, 188, 208
HOPF, E.: 41
HORTON, C. W.: 255, 260, 261, 595, 602, 609-611, 618, 692, 693
HSU, H. P.: 205, 206
HU, Y. Y.: 483
HUANG, C.: 396, 397, 574
HUNTER, H. E.: 417, 658, 659, 690, 692, 693
HURD, R. A.: 539
HUTNER, R. A.: 130
IGARASHI, A.: 45
IJIMA, T.: 48
INAWASHIRO, S.: 557, 560, 561, 563
ISHIMARU, A.: 117
IVANOV, V. I.: 286, 288-291, 293-295, 597-601, 607, 608
JENKINS, D. P.: 68
JONES, D. S.: 37, 38, 45, 48, 49, 188, 336, 381, 436, 457, 467, 510, 517, 524, 539, 540, 543, 554, 583
KAHAN, T.: 39
KARAL JR., F. C.: 25, 602, 609, 611, 618
KARP, S. N.: 41, 45, 49, 195, 196, 201, 213, 214, 218, 541
KATSURA, S.: 557, 558, 566, 569, 571-573
KAY, L.: 21, 22, 27
KAZARINOFF, N. D.: 35, 165, 167, 169, 171, 224, 230, 421, 422, 440, 507, 513, 514

- KELLER, J. B.: 22, 24-27, 34, 36, 37, 47, 99, 101, 109, 110, 142, 143, 157, 158, 165, 170, 181, 195, 196, 200, 201, 213, 214, 218, 242-246, 250, 251, 287, 288, 292, 293, 298, 301, 304, 306, 349, 355, 356, 362-364, 367, 369, 370, 376-379, 420, 421, 435, 439, 457, 467, 526, 539, 541, 545, 553, 564, 602-605, 611, 613, 620, 625, 630, 641, 645, 650, 655
 KELLOGG, O. D.: 15
 KENNAUGH, E. M.: 462
 KHASKIND, M. D.: 49, 216
 KIEBURTZ, R. B.: 219, 220
 KING, F. D.: 475
 KING, M. J.: 130
 KING, R. W. P.: 93, 99, 103, 108, 145, 159, 160, 203, 219, 361, 375, 402-405, 472, 475
 KIRK, D. B.: 417
 KLANTÉ, K.: 244, 251, 597, 607
 KLEINMAN, R. E.: 20, 21, 48, 120, 123, 401, 430, 433, 434, 438, 446, 455, 456, 470, 508, 512, 515, 536, 546, 591, 639, 658, 659, 670, 690, 692, 693
 KLINE, M.: 21, 27
 KOCHERZHEVSKI, G. N.: 173, 174, 232, 233
 KODIS, R. D.: 38, 39, 93, 396, 397, 574
 KOHN, W.: 38
 KONTOROVICH, M. J.: 49
 KORBANSKIY, I. N.: 614
 KORNHAUSER, E. T.: 39
 KOHN, L.: 36
 KOPYOUMJIAN, R. G.: 22, 29, 31, 484, 485
 KRAMP, C.: 67
 KRANZER, H. C.: 49
 KRAUS, L.: 1, 591
 KRAVISOV, YU. A.: 26
 LAMB, H.: 286, 292, 602, 611
 LANGER, R. E.: 57
 LAUKIEN, G.: 317, 319, 320
 LAURIN, P.: 48, 120, 123, 591
 LAX, M.: 6
 LIBEDIV, N. N.: 49, 256, 303
 LEINER, A.: 460, 546
 LEVINE, H.: 1, 38, 39, 48, 539, 541, 552, 554, 572, 574, 591
 LEVIS, C. A.: 123
 LIVY, B. R.: 25, 34, 143, 158, 164, 169, 170, 243, 244, 246, 251, 292, 355, 356, 363-364, 369, 370, 376, 378, 420, 421, 435, 439, 457, 467
 LEWIS, R. M.: 25, 27, 99, 101, 109, 110, 245, 250, 287, 288, 292, 293, 304, 306, 349, 363, 364, 367, 377, 379, 602, 605, 611, 613, 620, 625, 630, 641, 645, 650, 655
 LIEPA, V. V.: 397-399, 482, 485
 LINDROTH, K.: 475, 484, 485
 LOGAN, N. A.: 32, 33, 36, 62-66, 410, 412, 413
 LOMMEL, E.: 530
 LOWAN, A. N.: 417, 504
 LUCKE, W. S.: 121, 173, 174, 232
 LUDWIG, D.: 26, 34
 LÜNEBERG, E.: 196, 197, 199, 202
 LUNEBURG, R. K.: 21, 26
 LUR'E, K. A.: 565, 575
 LYTTLÉ, S. B.: 134, 136-138, 150, 154, 155, 188, 190, 194, 195, 208, 210, 213
 MACCAMY, R. C.: 538
 MACDONALD, H. M.: 255, 260, 264, 265, 267, 270, 272, 273, 311, 323, 324, 328, 331-333, 335, 340, 344, 639, 641, 664, 681, 691
 MACFARLANE, G.: 38
 MACROBERT, T. M.: 68
 MAFFETT, A. L.: 466, 524, 591, 635, 670, 690
 MAGNUS, W.: 36, 50, 67, 68, 285, 304
 MALYUZHNETS, G. D.: 48, 49, 275, 335, 336
 MANDRAZH, V. P.: 132, 133, 163, 185, 188, 221, 222
 MARCINKOWSKI, C. J.: 48, 315, 316, 322
 MARCUVITZ, N.: 19, 36
 MATSUI, E.: 48
 MAUE, A. W.: 16, 41, 45, 57, 181
 MCCREA, W. H.: 10
 MCCAY, A. B.: 255
 MEHLER, F. G.: 639, 693, 695
 MEI, K. K.: 50
 MEIJER, C. S.: 53
 MEIXNER, J.: 4, 546, 548, 554, 564, 569
 MENTZER, J. R.: 690
 MILES, J. W.: 188
 MILLAR, R. F.: 188, 189, 191-195, 198, 200, 202, 208, 209, 212, 213, 215, 217, 220, 223, 229, 583-585
 MILLER, J. C. P.: 60, 62, 63
 MIRIMANOV, R. G.: 595
 MITZNER, K. M.: 17
 MIYAZAKI, Y.: 37, 146
 MOFFATT, D. L.: 462, 463
 MÖGLICH, F.: 1
 MONTEROLLI, F. W.: 39
 MOON, P. H.: 17
 MORSE, P. M.: 12, 17, 19, 39, 41, 48, 130, 185, 192, 207, 361, 417, 418, 438, 505, 512
 MOULTIN, L. B.: 324-326
 MÜLLER, C.: 16
 MÜLLER, H. J. W.: 130, 417, 504

- MÜLLER, R.: 188, 208
MULLIN, C. R.: 50
MUSAL JR., H. M.: 30
MUSHIAKE, Y.: 468, 469, 473, 525
MUSKHELISHVILI, N. I.: 41, 43
National Bureau of Standards: 130
NEUGEBAUER, H. E. J.: 14, 581, 582
NEWTON, R. G.: 36
NICHOLSON, J. W.: 34
NISBET, A.: 10
NOBLE, B.: 20, 41, 45, 48, 96, 109, 134, 150, 163, 169, 185, 223, 229, 418, 438, 505, 512
NOMURA, Y.: 557, 558, 566, 569, 571-573
NUSSENZVEIG, H. M.: 57, 362-368
OBERHETTINGER, F.: 50, 67, 68, 120, 121, 257, 258, 262, 270, 272, 285
OKASHIMO, K.: 121, 122
OLVER, F. W. J.: 57
ORTHWEIN, W. C.: 658, 659, 690, 693
PAL, B.: 692
PALEY, R. E. A. C.: 41
PANOFSKY, K. H.: 10
PAPAS, C. H.: 38
PAULI, W.: 258, 262
PEARSON, J. D.: 48
PETERS, A. S.: 49
PELUMM, E.: 36
PHILLIPS, M.: 10
PIMENOV, YU. V.: 188, 208, 223, 229, 563
PINNEY, E.: 594, 595, 620
PINSON, J. T.: 400, 568, 569
PLUMMER, R. E.: 670
POGORZELSKI, W.: 43
POINCARÉ, H.: 34
POLEKHIN, A. I.: 591
PRINCE, P. F. V.: 400, 568, 569
QUITTEN, C. W.: 692, 693
RADLOW, J.: 1, 49, 591
REGGI, T.: 36
REICH, F.: 259, 264
REITINGER, N.: 461, 670
RIEHNSTEIN, J.: 400
RICE, S. O.: 287, 292
RICHMOND, J. H.: 50, 484, 485, 494
RIEL, R. K.: 169
ROBIN, L.: 68, 76, 145, 160, 296, 301, 639, 691-693
ROSS, R. A.: 25
ROSSI, B.: 68
ROW, R. V.: 265
RUBINSSTEIN, P. J.: 185, 192, 207
RUBINOW, S. I.: 36, 365, 366
RULF, B.: 26
RUMSEY, V. H.: 13
RUSSEK, A.: 214
RYAN, C. E.: 568
RYZHIK, I. W.: 50, 60
SANDBURG, R.: 50
SAVORNIN, J.: 315, 322
SCHELKUNOFF, S. A.: 31
SCHENSTED, C. E.: 27, 28, 30, 31, 466, 524, 591, 610, 612, 618, 631, 632, 635, 658, 659, 670, 690, 693
SCHENSTED, I. V.: 466, 524, 591, 635, 690
SCHIFF, L. I.: 690
SCHIFFER, M. M.: 21
SCHMITT, H. J.: 484, 485, 569
SCHÖBE, W.: 57
SCHULTZ, F. V.: 461
SCHWINGER, J.: 38, 48, 572
SCOTT, J. M. C.: 412
SECKLER, B. D.: 26, 27, 99, 101, 109, 110, 245, 250, 287, 288, 292, 293, 304, 306, 349, 363, 364, 367, 377, 379, 602-605, 611, 613, 620, 625, 630, 641, 645, 650, 655
SENIOR, T. B. A.: 5, 19, 21, 31, 48, 49, 91, 336, 341, 360, 361, 367, 375, 378, 379, 411, 413, 417, 422-432, 441, 443-454, 464, 521, 639, 681-685
SENSIPER, S.: 117
SESHADRI, S. R.: 202, 219, 584
SEVERIN, H.: 531, 532, 535, 539, 540, 546-548
SEVICK, J.: 484, 485
SHANKS, H. E.: 670
SHARPLES, A.: 130
SHENDEROV, E. L.: 116
SIEGEL, K. M.: 20, 31, 457, 461, 466, 523, 524, 591, 635, 657-659, 670, 685, 690, 692, 693
SILVER, S.: 661, 662, 669, 670, 692
SINCLAIR, G.: 174, 176
SKALSKAYA, I. P.: 49, 256, 303, 620
SKAVEM, S.: 193
SLEATOR, F. B.: 457, 461
STEPHAN, D.: 417
SOMMERFELD, A.: 12, 21, 36, 68, 188, 208, 254, 311, 316, 317, 381
SONI, R. P.: 50, 68
SONNENBUCK, F.: 417
SPARENBERG, J. A.: 41
SPENCE, R. D.: 441, 442, 535
SPENCER, D. E.: 17
SPENCER, R. C.: 680, 690
STAKGOUD, L.: 39

- STARKE, C.: 531, 532
 STEGUN, I.: 50, 62, 68, 285
 STEVENSON, A. F.: 21, 460, 462-464, 520, 521
 STEWART, G. S.: 400, 568, 569
 STONE, S. E.: 620
 STRATTON, J. A.: 10, 16, 19, 68, 130, 354, 380, 395
 STREIFER, W.: 36
 STROMGREN, L.: 495
 STRUTT, J. W. (Lord Rayleigh): 1, 20, 96, 99, 109, 134, 150, 188, 361, 376, 401, 465, 466, 523
 SU, C. W. H.: 473
 SWANSON, C. A.: 595
 SZEGÖ, G.: 76
 TAI, C. T.: 13, 19, 123, 171, 230, 233, 275, 279, 337-339, 342, 380, 472, 476, 478, 479, 484, 485, 491, 523, 662
 TANG, C. L.: 564
 TAO, L. N.: 39
 TARTAKOVSKII, L. B.: 591
 TAVENNER, M. S.: 315, 322
 TEISSEYRE, R.: 275, 279
 THORNE, R. C.: 76
 TILSTON, W. V.: 276, 280, 339, 343
 TITCHMARSH, E. C.: 41, 42
 TRANTER, C. J.: 208
 TREUENFELS, C. G.: 692, 693
 TRICOMI, F. G.: 50, 67, 68, 285
 TUZHILIN, A. A.: 254, 257, 262, 265, 266, 268, 270, 271, 273-275, 278, 279, 281, 310, 324, 331, 340, 344, 345
 TWERSKY, V.: 20, 134-139, 141, 150-155, 157, 188, 190-192, 208, 210-212
 ÜBERALL, H.: 31
 UDA, S.: 473
 UDAGAWA, K.: 37, 146
 UFIMTSEV, P. Ia.: 199, 217, 481, 483, 486, 487, 578-580, 582
 UFLYAND, YA. S.: 303
 URSELL, F.: 35
 USLENGHI, P. L. E.: 30, 48, 91, 120, 123, 591
 VAINSHTEIN, L. A.: see Weinstein, L. A.
 VAN BLADEL, J.: 4, 9-11, 13, 21, 50, 96, 109, 134, 150, 669
 VANDAKUROV, Y. V.: 331, 336, 337, 342
 VAN DE HULST, H. C.: 395, 405
 VAN VLECK, J. H.: 474-476
 VELLINE, L. O.: 50
 VOLTERRA, V.: 37
 WAGNER, R. J.: 39
 WAINSTAIN, L. A.: see Weinstein, L. A.
 WALT, J. R.: 117, 120-122, 124, 176
 WARSHAWSKI, S. E.: 37
 WATERMAN, P. C.: 50, 183, 184, 187, 188, 692, 693
 WATSON, G. N.: 34, 35, 50, 53, 54, 365, 575
 WATSON, R. B.: 254, 255, 260, 261
 WEINSTEIN, L. A.: 1, 26, 45, 46, 48, 49, 143, 144, 158, 159, 164, 169, 216, 381-383, 385, 386, 390-395, 407, 409
 WELCH, W. J.: 13
 WERNER, P.: 20
 WESTON, V. H.: 1, 5, 33, 37, 47, 146, 351, 352, 410, 507, 513, 514
 WESTPFAHL, K.: 41-45, 49, 57, 181, 188, 196, 197, 199, 202, 208, 552, 553
 WETZEL, L.: 38, 145, 159, 160
 WHITE, F. P.: 35
 WIEGREBE, A.: 255, 260, 264, 267, 270, 272
 WIENER, N.: 41
 WILCOX, C. H.: 6, 10, 350, 351, 681-685, 692, 693
 WILLIAMS, W. E.: 48, 336, 472, 537, 550
 WILISE, J. C.: 130
 WITTE, H. H.: 49, 552, 553
 WILLENBERG, E. R.: 417
 WOLF, E.: 7, 10, 20, 21, 395
 WOLFE, P.: 26
 WOODS, B. D.: 336
 WOONTON, G. A.: 582
 WU, T. T.: 93, 99, 103, 108, 112, 141, 145, 157, 159, 160, 202, 203, 219, 361, 365, 366, 368, 369, 375, 380, 402, 405, 414, 484, 485, 539, 541, 552, 554, 584
 YEE, H. Y.: 25, 32, 33, 36, 47, 63
 ZANDERER, E.: 26, 34
 ZIMMER, F.: 188, 208
 ZITRON, N.: 113, 116

SUBJECT INDEX

- Babinet's principle: 14-15, 182, 528
- Beltrami's operator: 350, 641
- Boundary conditions: 1, 4-6
- Cone circular: 637-701
 - , elliptic: 1
- Conformal mapping: 36-37
- Convergence, of eigenfunction expansions: 34, 93, 136, 417, 504
 - , radius of: 432, 454
- Coordinates, orthogonal curvilinear: 715-721
- Creeping waves: 33-36
- Cylinder, circular: 92-128
 - , elliptic: 129-180
 - , hyperbolic: 240-251
 - , parabolic: 284-307
- Disc: 528-588
- Dyadic Green's functions: 13, 119, 123, 171, 174, 230-231, 233, 275-276, 279-280, 337-339, 342-343, 380, 387, 660, 667
- Dyadics: 712-714
- Ellipsoid, triaxial: 1
- Equations, differential
 - , -, acoustical: 2-3
 - , -, Airy: 60
 - , -, associated Mathieu: 248
 - , -, Bessel: 50
 - , -, Legendre: 68
 - , -, Maxwell: 2
 - , -, spherical Bessel: 58
 - , -, wave: 3-4
- Equations, integral: 15-17, 41-45, 49-50
 - , -, Cauchy: 42-43
 - , -, dual: 42
 - , -, Maue: 16
 - , -, Wiener-Hopf: 41-42
- Far field coefficients: 6
- Fock's theory: 31-34
- Function-theoretic methods: 41-49
- Functions
 - , Airy: VII, 57, 60-63
 - , Bessel: 50-60, 354
 - , cosine integral: 494, 602
 - , dilogarithm: 498-499
 - , Fock: 63-67
 - , Fresnel: 67-68, 310
 - , Heaviside: 253, 310, 639
 - , Legendre: 68-76, 691-694
 - , Lommel: 365
 - , MacDonald: 697
 - , Mathieu: 130, 182, 240
 - , Mehler: 693, 695-696
 - , oblate spheroidal: 504, 528
 - , prolate spheroidal: 417
 - , Riccati-Bessel: 60, 354
 - , signum: 253, 310, 639
 - , sine integral: 494, 602
 - , trilogarithm: 498-499, 501
 - , Weber-Hermite: 285
 - , Whittaker: 594-595
- Geometrical theory of diffraction: 24-26
- Green's functions: 11-13; *see also* Dyadic - -
- Half plane: 308-345
- High-frequency methods: 21-36
- Hyperboloid: 623-636
- Inverse scattering: 349-352
- Keller's theory: 24-26
- Low-frequency methods: 20-21
- Luneburg-Kline expansions: 26-29, 99-101, 109-110, 245-246, 250, 288, 293, 304, 306, 364, 367, 374, 378, 379, 604-605, 613, 620, 625-626, 630, 631-632, 634-635
- Numerical methods: 49-50
- Oblique incidence on infinite cylinder: 89-91
- Ogive: 1
- Optics, geometrical: 22-24
 - , physical: 29-31
- Paraboloid: 593-622
- Potentials: 8-11
 - , Debye: 10-11
- , Hertz: 9-10
- , scalar: 8
- , vector: 8
- Quarter plane: 1
- Radar cross sections: 7-8, 349
 - , -, of semi-infinite bodies: 591
- Radiation condition: 5-6
- Reciprocity: 13
- Schwinger's principle: 38

- Separation of variables: 1, 17-20, 41
Shape approximation: 145-146, 161, 436-437,
458-459, 468-469, 510-511, 517-518, 524-525
Sphere: 353-415
Spheroid, oblate: 503-527
-, prolate: 416-471
Strip: 181-239
Torus: 1
Variational methods: 37-41
Vector calculus: 710-714
Velocity potential: 3
Watson's transformation: 34-36
Wedge: 252-283
Wiener-Hopf technique: 41-42
Wire: 472-502
Wronskian determinants: 52
-- -, Airy: 62
-- -, Bessel: 52
-- -, Legendre: 69, 73, 692
-- -, spherical Bessel: 59
-- -, Whittaker: 595
Zeros of functions
-- -, Airy: VII, 62, 367, 379
-- -, Bessel: 36
-- -, Legendre: 691-694

UNCLASSIFIED

Security Classification		DOCUMENT CONTROL DATA - R & D	
(Security classification of title, body of abstract and indexing annotation must be entered when the overall report is classified)			
1. ORIGINATING ACTIVITY (Corporate author) The University of Michigan Radiation Laboratory, Dept. of Electrical Engineering, 201 Catherine Street, Ann Arbor, Michigan 48108		2a. REPORT SECURITY CLASSIFICATION UNCLASSIFIED	
		2b. GROUP	
3. REPORT TITLE ELECTROMAGNETIC AND ACOUSTIC SCATTERING BY SIMPLE SHAPES			
4. DESCRIPTIVE NOTES (Type of report and inclusive dates) Scientific. Final February 1965 - February 1969 Approved 22 January 1970			
5. AUTHOR(S) (First name, middle initial, last name) Edited by: John J. Bowman Thomas B.A. Senior Piergiorgio L. E. Uslenghi			
6. REPORT DATE 15 January 1970		7a. TOTAL NO. OF PAGES 727	7b. NO. OF REFS 397
8a. CONTRACT OR GRANT NO. AF19(628)-4328		9a. ORIGINATOR'S REPORT NUMBER(S) 7133-6-F	
b. PROJECT NO. 5635-02-01		9b. OTHER REPORT NO(S) (Any other numbers that may be assigned this report) AFCRL-70-0047	
c. DoD Element 51445014			
d. DoD Subelement 681305			
10. DISTRIBUTION STATEMENT 1 - This document has been approved for public release and sale; its distribution is unlimited.			
11. SUPPLEMENTARY NOTES TECH, OTHER		12. SPONSORING MILITARY ACTIVITY Air Force Cambridge Research Laboratories (CRD) L.G. Hanscom Field, Bedford, MA, 01730	
13. ABSTRACT This book represents an exhaustive study of the scattering properties of acoustically soft and hard bodies and of perfect conductors, presented for 15 geometrically-simple shapes. Such shapes are important in their own right and as a basis for synthesizing the radiation and scattering properties of more complex configurations. Each shape is treated in a separate chapter whose contents are presented in stylized format for easy reference. Emphasis is placed on results in the form of formulae and diagrams. Although no detailed derivation are included, an outline of methods in scattering theory is given in the Introduction.			

DD FORM 1 NOV 61 1473

UNCLASSIFIED

Security Classification

14	KEY WORDS	LINK A		LINK B		LINK C	
		ROLE	WT	ROLE	WT	ROLE	WT
	Electromagnetic Waves						
	Acoustic Waves						
	Scattering						
	Diffraction						
	Theoretical						
	Experimental						